

UNCLASSIFIED

AD NUMBER

ADB160550

LIMITATION CHANGES

TO:

Approved for public release; distribution is unlimited.

FROM:

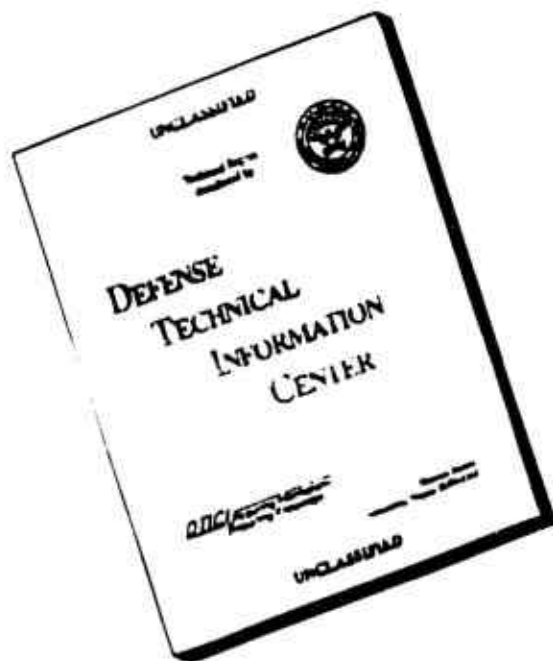
Distribution authorized to U.S. Gov't. agencies and their contractors;
Administrative/Operational Use; OCT 1991. Other requests shall be referred to Aviation Applied Technology Directorate, U.S. Army Aviation Systems Command, Fort Eustis, VA 33604-5577.

AUTHORITY

EUSIS VA-AMSAT-R-TMS - 27 Mar 1995, via Memo
dtd 27 Mar 1995

THIS PAGE IS UNCLASSIFIED

DISCLAIMER NOTICE



THIS DOCUMENT IS BEST QUALITY AVAILABLE. THE COPY FURNISHED TO DTIC CONTAINED A SIGNIFICANT NUMBER OF PAGES WHICH DO NOT REPRODUCE LEGIBLY.

AD-B160 550



STBIN

✓

2

USAAVSCOM TR 91-D-3



US ARMY
AVIATION
SYSTEMS COMMAND

**HELICOPTER MANEUVERABILITY AND AGILITY DESIGN
SENSITIVITY AND AIR COMBAT MANEUVER DATA
CORRELATION STUDY**

Thomas H. Lawrence, Sherman Corning, and Frank Wharburton

**Sikorsky Aircraft Division
United Technologies Corporation
6900 Main Street
Stratford, CT 06601-1381**



October 1991

Final Report for Period October 1988 - December 1990

Distribution authorized to U.S. Government agencies and their contractors.
Administrative/Operational Use, October 1991. Other requests for this
document shall be referred to the Aviation Applied Technology Directorate,
U.S. Army Aviation Systems Command, Fort Eustis, VA 23604-5577.

Prepared for

**AVIATION APPLIED TECHNOLOGY DIRECTORATE
US ARMY AVIATION SYSTEMS COMMAND
FORT EUSTIS, VA 23604-5577**

91-16710

91 10 29 015

AVIATION APPLIED TECHNOLOGY DIRECTORATE POSITION STATEMENT

This report presents an assessment of the maneuverability and agility (M&A) characteristics of several helicopters including a maneuver simulation evaluation, analysis of data from the U.S. Army's Air-to-Air Combat Tests (AACT), and a correlation of the two results. The results, relative to the subject helicopters and their available AACT data base, provide a limited verification of simulation predictions of M&A capability as well as a scoring and M&A rating scheme for subsequent preliminary design applications. The design sensitivities presented herein will contribute to the development of future attack rotorcraft requirements.

Mr. G. Thomas White of the Systems Integration Technical Area, Aeronautical Systems & Technology Division, served as project engineer for this investigation.

Trade names cited in this report do not constitute an official endorsement or approval of the use of such commercial hardware or software.

DESTRUCTION NOTICE

For classified documents, follow the procedures in DOD 5200.22-M, Industrial Security Manual, Section 11-1B. OOO
5200.1-A, Information Security Program Regulation, Chapter IX. For unclassified, limited documents, destroy
method that will prevent disclosure of contents or reconstruction of the document. ny

REPORT DOCUMENTATION PAGE

Form Approved
OMB No. 0704-0188

Public reporting burden for this collection of information is estimated to average 1 hour per response, including the time for reviewing instructions, searching existing data sources, gathering and maintaining the data needed, and completing and reviewing the collection of information. Send comments regarding this burden estimate or any other aspect of this collection of information, including suggestions for reducing this burden, to Washington Headquarters Services, Directorate for Information Operations and Reports, 1215 Jefferson Davis Highway, Suite 1204, Arlington, VA 22202-4302, and to the Office of Management and Budget, Paperwork Reduction Project (0704-0188), Washington, DC 20503.

1. AGENCY USE ONLY (Leave blank)		2. REPORT DATE October 1991	3. REPORT TYPE AND DATES COVERED Final October 1988 - December 1990	
4. TITLE AND SUBTITLE Helicopter Maneuverability and Agility Design Sensitivity and Air Combat Maneuver Data Correlation Study			5. FUNDING NUMBERS Contract DAAJ02-88-C-001	
6. AUTHOR(S) Lawrence, Thomas H., Corning, Sherman and Wharburton, Frank				
7. PERFORMING ORGANIZATION NAME(S) AND ADDRESS(ES) Sikorsky Aircraft Division United Technologies Corporation 6900 Main Street Stratford, CT 06601-1381			8. PERFORMING ORGANIZATION REPORT NUMBER	
9. SPONSORING/MONITORING AGENCY NAME(S) AND ADDRESS(ES) Aviation Applied Technology Directorate U. S. Army Aviation Systems Command Fort Eustis, VA 23604-5577			10. SPONSORING/MONITORING AGENCY REPORT NUMBER USAAVSCOM TR 91-D-3	
11. SUPPLEMENTARY NOTES				
12a. DISTRIBUTION/AVAILABILITY STATEMENT Distribution authorized to U.S. Government agencies and their contractors, Administrative/Operational Use, October 1991. Other requests for this document shall be referred to the Aviation Applied Technology Directorate, U.S. Army Aviation Systems Command, Fort Eustis, VA 23604-5577.			12b. DISTRIBUTION CODE	
13. ABSTRACT (Maximum 200 words) A helicopter maneuverability and agility (M/A) study has been conducted to determine the characteristics of eight different helicopters. This study included a simulation evaluation, analysis of data from the U.S. Army's Air-to-Air Combat Tests (AACT) and a correlation of the two. The results validated previously developed M/A design guidelines and design parameter sensitivities. The helicopters evaluated were the UH-60A, S-76A, AH-64A, AH-1S, OH-58A and SA-365N-1. The CH-53E and Soviet Mi-28 (unclassified) were also analyzed although no AACT data were available for them. The M/A characteristics of these vehicles were assessed by "flying" detailed, blade element General Helicopter Flight Dynamics Simulation (GenHel) computer models through a series of nine discrete maneuvers. Selected flight test data from AACT II, III and IV were analyzed using a workstation to replay the data and generate synthetic out-of-cockpit views. A method for scoring the simulated maneuvers and the AACT engagements was devised. M/A ratings for all of the subject aircraft were determined using the simulated maneuver scores. Correlation of the M/A ratings to the AACT scores was very good with the winning air combat aircraft having the highest M/A rating in four of the five engagement pairs analyzed. This study also produced a unique database employing a common simulation technology and evaluation methodology for all of the subject helicopters.				
14. SUBJECT TERMS Maneuverability, Agility, Helicopter, Flight Test Correlation, Design Sensitivity			15. NUMBER OF PAGES 563	
			16. PRICE CODE	
17. SECURITY CLASSIFICATION OF REPORT Unclassified	18. SECURITY CLASSIFICATION OF THIS PAGE Unclassified	19. SECURITY CLASSIFICATION OF ABSTRACT Unclassified	20. LIMITATION OF ABSTRACT	

PREFACE

The work reported herein was performed by the Sikorsky Aircraft Division of United Technologies Corporation, Stratford, Connecticut during the period from October 1988 to August 1990 under contract DAAJ02-88-C-0017 to the Aviation Applied Technology Directorate (AATD), U.S. Army Aviation Research and Technology Activity (AVSCOM), Ft. Eustis, Virginia.

Mr. T.H. Lawrence was Sikorsky Project Manager. Mr. G.T. White of AATD was Program Technical Monitor.

Others who made major contributions to the study include Messrs. S. Corning, J. Occhisto, F. Wharburton, T. Lauder and N. Lappos.

Accession For	
NTIS GRA&I	<input type="checkbox"/>
DTIC TAB	<input checked="" type="checkbox"/>
Unannounced	<input type="checkbox"/>
Justification	
By	
Distribution/	
Availability Codes	
Dist	Special

C2



TABLE OF CONTENTS

	<u>Page</u>
PREFACE.....	iii
LIST OF FIGURES.....	vi
LIST OF TABLES.....	xxii
INTRODUCTION.....	1
Background.....	1
Overview of this Correlation Study.....	7
Simulation Models.....	10
SIMULATION RESULTS.....	41
Discussion of Results for Each Maneuver.....	41
Discussion of Results for Each Aircraft.....	69
AACT DATA ANALYSIS.....	72
Introduction.....	72
Software Development.....	73
Engagement Analysis.....	77
SCORING AND RATING METHODOLOGY.....	90
Introduction.....	90
Scoring of Simulated Maneuvers.....	90
Scoring of AACT Encounters.....	107
CORRELATION OF M/A ANALYSIS TO AACT DATA.....	117
Discussion of Correlation Method.....	117
Results of Correlation.....	118
CONCLUSIONS.....	127
RECOMMENDATIONS.....	128
REFERENCES.....	130
LIST OF SYMBOLS/ABBREVIATIONS/ACRONYMS.....	132
APPENDIXES	
A. UH-60A Model Data.....	137
B. S-76A Model Data.....	176
C. CH-53E Model Data.....	216
D. AH-64A Model Data.....	253
E. OH-58A Model Data.....	295
F. AH-1S Model Data.....	331
G. SA-365N Model Data.....	370
H. MI-28 Model Data.....	427
I. AACT Maneuver Time History Data.....	472
J. AACT Maneuver Analyses.....	507
K. MI-28 Design Analysis.....	521
L. Mathematical Curve Fits to Maneuver Data.....	538
M. Aerodynamic Scaling Method.....	559
N. Aircraft Drag Data.....	561

LIST OF FIGURES

<u>Figure</u>		<u>Page</u>
1	M/A Correlation Study Overview.....	2
2	Example Fundamental Parameter Chart.....	5
3	Example Weight Sensitivity Chart.....	6
4	Summary of M/A Phase I Results.....	8
5	GenHsl Library System.....	11
6	GenHsl Modular Architecture.....	12
7	GenHel Overview.....	13
8	Gross Weight Comparison Chart.....	25
9	Main Rotor Radius Comparison Chart.....	26
10	Reference SHP Comparison Chart.....	27
11	Main Rotor Tip Spssd Comparison Chart.....	28
12	Main Rotor Hinge Offsst Comparison Chart.....	29
13	Disk Loading Comparison Chart.....	30
14	Blads Loading Comparison Chart.....	31
15	Power Loading Comparison Chart	32
16	Main Rotor Solidity Comparison Chart.....	33
17	Main Rotor Lock Numbar Comparison Chsrt.....	35
18	Pitch Control Sensitivity Comparison Chart.....	36
19	Roll Control Sensitivity Comparison Chart.....	37
20	Yaw Control Sensitivity Comparison Chart.....	38
21	Manauver Controllar Schematic.....	40
22	Hover Bob-Up Summary Chart.....	46
23	Effect of Increased Power on M1-28 Hover Bob-Up.....	47

LIST OF FIGURES

<u>Figure</u>		<u>Page</u>
24	Acceleration from Hover to 80 Knots Summary Chart.....	49
25	Effect of Increased Power on Mi-28 Acceleration from Hover to 80 Knots.....	51
26	Deceleration from 80 knots to Hover Summary Chart.....	53
27	80-Knot Climb Summary Chart.....	56
28	Effect of Increased Power on Mi-28 80-Knot Steady Climb.....	57
29	80-Knot Steady Turn Summary Chart.....	59
30	Effect of Increased Power on Mi-28 80-Knot Steady Turn.....	60
31	80-Knot Decelerating Turn Summary Chart.....	61
32	Effect of Increased Rotor Speed on Mi-28 80-Knot Decelerating Turn.....	63
33	130-Knot Decelerating Turn Summary Chart.....	64
34	Effect of Increased Rotor Speed on Mi-28 130-Knot Decelerating Turn.....	65
35	140-Knot Pull-Up Summary Chart.....	67
36	Effect of Increased Rotor Speed on Mi-28 140-Knot Pull-Up...	68
37	180-Degree Hover Turn Summary Chart.....	70
38	Effect of Yaw Inertia on Mi-28 180-Degree Hover Turn.....	71
39	AACT Data Processing Chart.....	74
40	Coordinate Axes Definitions.....	75
41	Cockpit Displays, Counter 208019.....	83
42	Cockpit Displays, Counter 302014.....	84
43	Cockpit Displays, Counter 417003.....	85
44	Cockpit Displays, Counter 411011.....	86
45	Cockpit Displays, Counter 23038.....	87

LIST OF FIGURES

<u>Figure</u>		<u>Page</u>
46	Cockpit Displays, Counter 27026.....	88
47	Overlaid Data Block, Out-of-Cockpit Views.....	89
48	Overlaid Data Block, External Views.....	89
49	Maneuver Scoring Methodology.....	91
50	M/A Weighting Factors Chart.....	94
51	AACT Scoring Methodology.....	110
52	AACT Points Chart.....	111
53	AACT Correlation - OH-58A vs. S-76A.....	120
54	AACT Correlation - OH-58A vs. U-60A.....	121
55	AACT Correlation - UH-60A vs. S-76A.....	123
56	AACT Correlation - AH-1S vs. OH-58A.....	124
57	AACT Correlation - AH-64A vs. SA-365N.....	125
A-1	UH-60A Three-View Drawing.....	151
A-2	UH-60A Main Rotor Blade Twist Map.....	152
A-3	UH-60A Fuselage Lift Map.....	153
A-4	UH-60A Fuselage Drag Map.....	154
A-5	UH-60A Fuselage Pitching Moment Map.....	155
A-6	UH-60A Fuselage Delta Lift Map.....	156
A-7	UH-60A Fuselage Delta Drag Map.....	157
A-8	UH-60A Fuselage Delta Pitching Moment Map.....	158
A-9	UH-60A Fuselage Sideforce Map.....	159
A-10	UH-60A Fuselage Rolling Moment Map.....	160
A-11	UH-60A Fuselage Yawing Moment Map.....	161

LIST OF FIGURES

<u>Figure</u>		<u>Page</u>
A-12	UH-60A Main Rotor Downwash on Fuselage Map..... (x-direction)	162
A-13	UH-60A Main Rotor Downwash on Fuselage Map..... (z-direction)	163
A-14	UH-60A Horizontal Stabilizer Lift Map.....	164
A-15	UH-60A Horizontal Stabilizer Drag Map.....	165
A-16	UH-60A Horizontal Stabilizer Moment..... Map	166
A-17	UH-60A Main Rotor Downwash on Horizontal..... Stabilizer Map (x-direction)	167
A-18	UH-60A Main Rotor Downwash on Horizontal..... Stabilizer Map (z-direction)	168
A-19	UH-60A Fuselage Downwash on Horizontal Stabilizer Map.....	169
A-20	UH-60A Dynamic Pressure Ratio at Horizontal Stabilizer Map...	170
A-21	UH-60A Vertical Stabilizer Lift Map.....	171
A-22	UH-60A Vertical Stabilizer Drag Map.....	172
A-23	UH-60A Vertical Stabilizer Moment Map.....	173
A-24	UH-60A Fuselage Sidewash on Vertical Stabilizer Map.....	174
A-25	UH-60A Dynamic Pressure Ratio at Vertical..... Stabilizer Map	175
B-1	S-76A Three-View Drawing.....	191
B-2	S-76A Main Rotor Blade Twist Map.....	192
B-3	S-76A Fuselage Lift Map.....	193
B-4	S-76A Fuselage Drag Map.....	194
B-5	S-76A Fuselage Pitching Moment Map.....	195
B-6	S-76A Fuselage Delta Lift Map.....	196

LIST OF FIGURES

<u>Figure</u>		<u>Page</u>
B-7	S-76A Fuselage Delta Drag Map.....	197
B-8	S-76A Fuselage Delta Pitching Moment Map.....	198
B-9	S-76A Fuselage Sideforce Map.....	199
B-10	S-76A Fuselage Rolling Moment Map.....	200
B-11	S-76A Fuselage Yawing Moment Map.....	201
B-12	S-76A Main Rotor Downwash on Fuselage Map..... (x-direction)	202
B-13	S-76A Main Rotor Downwash on Fuselage Map..... (z-direction)	203
B-14	S-76A Horizontal Tail Lift Map.....	204
B-15	S-76A Horizontal Tail Drag Map.....	205
B-16	S-76A Main Rotor Downwash on Horizontal Tail Map..... (x-direction)	206
B-17	S-76A Main Rotor Downwash on Horizontal..... Tail Map (z-direction)	207
B-18	S-76A Fuselage Downwash on Horizontal Tail Map.....	208
B-19	S-76A Dynamic Pressure Ratio at Horizontal..... Tail Map	209
B-20	S-76A Vertical Tail Lift Map.....	210
B-21	S-76A Vertical Tail Drag Map.....	211
B-22	S-76A Fuselage Sidewash on Vertical Tail Map.....	212
B-23	S-76A Dynamic Pressure Ratio at Vertical Tail Map.....	213
B-24	S-76A Main Rotor Downwash on Vertical Tail Map..... (x-direction)	214
B-25	S-76A Main Rotor Downwash on Vertical Tail Map..... (z-direction)	215

LIST OF FIGURES

<u>Figure</u>		<u>Page</u>
C-1	CH-53E Three-View Drawing.....	229
C-2	CH-53E Main Rotor Blade Twist Map.....	230
C-3	CH-53E Fuselage Lift Map.....	231
C-4	CH-53E Fuselage Drag Map.....	232
C-5	CH-53E Fuselage Pitching Moment Map.....	233
C-6	CH-53E Fuselage Delta Lift Map.....	234
C-7	CH-53E Fuselage Delta Drag Map.....	235
C-8	CH-53E Fuselage Delta Pitching Moment Map.....	236
C-9	CH-53E Fuselage Sideforce Map.....	237
C-10	CH-53E Fuselage Rolling Moment Map.....	238
C-11	CH-53E Fuselage Yawing Moment Map.....	239
C-12	CH-53E Main Rotor Downwash on Fuselage Map..... (x-direction)	240
C-13	CH-53E Main Rotor Downwash on Fuselage Map..... (z-direction)	241
C-14	CH-53E Horizontal Tail Lift Map.....	242
C-15	CH-53E Horizontal Tail Drag Map.....	243
C-16	CH-53E Main Rotor Downwash on Horizontal Tail..... Map (x-direction)	244
C-17	CH-53E Main Rotor Downwash on Horizontal Tail..... Map (z-direction)	245
C-18	CH-53E Fuselage Downwash on Horizontal Tail Map.....	246
C-19	CH-53E Vertical Tail Lift Map.....	247
C-20	CH-53E Vertical Tail Drag Map.....	248
C-21	CH-53E Main Rotor Downwash on Vertical Tail Map..... (x-direction)	249

LIST OF FIGURES

<u>Figure</u>		<u>Page</u>
C-22	CH-53E Main Rotor Downwash on Vertical Tail Map..... (z-direction)	250
C-23	CH-53E Main Rotor Downwash on Tail Rotor Map..... (x-direction)	251
C-24	CH-53E Main Rotor Downwash on Tail Rotor Map..... (z-direction)	252
D-1	AH-64A Three-View Drawing.....	268
D-2	AH-64A Pitch Attitude Correlation.....	269
D-3	AH-64A Longitudinal Stick Correlation.....	270
D-4	AH-64A Lateral Stick Correlation.....	271
D-5	AH-64A Collective Stick Correlation.....	272
D-6	AH-64A Pedal Correlation.....	273
D-7	AH-64A Stabilator Position Correlation.....	274
D-8	AH-64A Power Required Correlation.....	275
D-9	AH-64A Longitudinal Stick Pulse Correlation.....	276
D-10	AH-64A Main Rotor Blade Twist Map.....	277
D-11	AH-64A Fuselage Lift Map.....	278
D-12	AH-64A Fuselage Drag Map.....	279
D-13	AH-64A Fuselage Pitching Moment Map.....	280
D-14	AH-64A Fuselage Sideforce Map.....	281
D-15	AH-64A Fuselage Yawing Moment Map.....	282
D-16	AH-64A Main Rotor Downwash on Fuselage Map..... (x-direction)	283
D-17	AH-64A Main Rotor Downwash on Fuselage Map..... (z-direction)	284
D-18	AH-64A Horizontal Stabilizer Lift Map.....	285

LIST OF FIGURES

<u>Figure</u>		<u>Page</u>
D-19	AH-64A Horizontal Stabilizer Drag Map.....	286
D-20	AH-64A Main Rotor Downwash on Horizontal Stabilizer (x-direction)	287
D-21	AH-64A Main Rotor Downwash on Horizontal Stabilizer Map..... (z-direction)	288
D-22	AH-64A Fuselage Downwash on Horizontal Stabilizer Map.....	289
D-23	AH-64A Vertical Stabilizer Lift Map.....	290
D-24	AH-64A Vertical Stabilizer Drag Map.....	291
D-25	AH-64A Fuselage Sidewash on Vertical Stabilizer Map.....	292
D-26	AH-64A Wing Lift Map.....	293
D-27	AH-64A Wing Drag Map.....	294
E-1	OH-58A Three-View Drawing.....	306
E-2	OH-58A Pitch Attitude Correlation.....	307
E-3	OH-58A Longitudinal Stick Correlation.....	308
E-4	OH-58A Lateral Stick Correlation.....	309
E-5	OH-58A Collective Stick Correlation..	310
E-6	OH-58A Pedal Correlation.....	311
E-7	OH-58A Main Rotor Blade Tiplet Map.....	312
E-8	OH-58A Fuselage Lift Map.....	313
E-9	OH-58A Fuselage Drag Map.....	314
E-10	OH-58A Fuselage Pitching Moment Map.....	315
E-11	OH-58A Fuselage Delta Drag Map.....	316
E-12	OH-58A Fuselage Delta Pitching Moment Map.....	317
E-13	OH-58A Fuselage Sideforce Map.....	318

LIST OF FIGURES

<u>Figure</u>		<u>Page</u>
E-14	OH-58A Fuselage Rolling Moment Map.....	319
E-15	OH-58A Fuselage Yawing Moment Map.....	320
E-16	OH-58A Main Rotor Downwash on Fuselaga Map..... (x-direction)	321
E-17	OH-58A Main Rotor Downwash on Fuselaga Map..... (z-diraction)	322
E-18	OH-58A Horizontal Stabilizer Lift Map.....	323
E-19	OH-58A Horizontal Stabilizer Drag Map.....	324
E-20	OH-58A Main Rotor Downwash on Horizontal Stabilizer Map..... (x-direction)	325
E-21	OH-58A Main Rotor Downwash on Horizontal Stabilizer Map..... (z-direction)	326
E-22	OH-58A Vartical Stabilizer Lift Map.....	327
E-23	OH-58A Verticel Stabilizer Drag Map.....	328
E-24	OH-58A Main Rotor Downwash on Vertical..... Stabilizer Map (x-direction)	329
E-25	OH-58A Main Rotor Downwash on Vertical..... Stabilizer Map (z-direction)	330
F-1	AH-1S Thraa-View Drawing.....	343
F-2	AH-1S Pitch Attitude Correlation.....	344
F-3	AH-1S Longitudinal Stick Corralation.....	345
F-4	AH-1S Lateral Stick Correlation.....	346
F-5	AH-1S Collectiva Stick Correlation.....	347
F-6	AH-1S Pedal Corralation.....	348
F-7	AH-1S Power Required Corralation.....	349
F-8	AH-1S Fuselage Lift Map.....	350

LIST OF FIGURES

<u>Figure</u>		<u>Page</u>
F-9	AH-1S Fuselage Drag Map.....	351
F-10	AH-1S Fuselage Pitching Moment Map.....	352
F-11	AH-1S Fuselage Delta Lift Map.....	353
F-12	AH-1S Fuselage Delta Drag Map.....	354
F-13	AH-1S Fuselage Sideforce Map.....	355
F-14	AH-1S Fuselage Rolling Moment Map.....	356
F-15	AH-1S Fuselage Yawing Moment Map.....	357
F-16	AH-1S Main Rotor Downwash on Fuselage Map..... (x-direction)	358
F-17	AH-1S Main Rotor Downwash on Fuselage Map..... (z-direction)	359
F-18	AH-1S Horizontal Stabilizer Lift Map.....	360
F-19	AH-1S Horizontal Stabilizer Drag Map.....	361
F-20	AH-1S Main Rotor Downwash on Horizontal Stabilizer Map..... (x-direction)	362
F-21	AH-1S Main Rotor Downwash on Horizontal Stabilizer Map..... (z-direction)	363
F-22	AH-1S Vertical Stabilizer Lift Map.....	364
F-23	AH-1S Vertical Stabilizer Drag Map.....	365
F-24	AH-1S Main Rotor Downwash on Vertical Stabilizer Map..... (x-direction)	366
F-25	AH-1S Main Rotor Downwash on Vertical Stabilizer Map..... (z-direction)	367
F-26	AH-1S Wing Lift Map.....	368
F-27	AH-1S Wing Drag Map.....	369

LIST OF FIGURES

<u>Figure</u>		<u>Page</u>
G-1	SA-365N Threa-View Drawing.....	388
G-2	SA-365N Longitudinal Stick Correlation.....	389
G-3	SA-365N Lateral Stick Correlation.....	390
G-4	SA-365N Collective Stick Correlation.....	391
G-5	SA-365N Pedal Correlation.....	392
G-6	SA-365N Main Rotor Power Correlation.....	393
G-7	SA-365N Fenestron Power Correlation.....	394
G-8	SA-365N Main Rotor Blade Twist Map.....	395
G-9	SA-365N Fuselage Lift Map.....	396
G-10	SA-365N Fuselage Drag Map.....	397
G-11	SA-365N Fuselage Pitching Moment Map.....	398
G-12	SA-365N Fuselage Delta Lift Map.....	399
G-13	SA-365N Fuselage Delta Drag Map.....	400
G-14	SA-365N Fuselage Delta Pitching Moment Map.....	401
G-15	SA-365N Fuselage Sideforce Map.....	402
G-16	SA-365N Fuselage Rolling Moment Map.....	403
G-17	SA-365N Fuselage Yawing Moment Map.....	404
G-18	SA-365N Main Rotor Downwash on Fuselage Map..... (x-direction)	405
G-19	SA-365N Main Rotor Downwash on Fuselage Map..... (z-direction)	406
G-20	SA-365N Horizontal Stabilizer Lift Map.....	407
G-21	SA-365N Horizontal Stabilizer Drag Map.....	408

LIST OF FIGURES

<u>Figure</u>		<u>Page</u>
G-22	SA-365N Main Rotor Downwash on Horizontal Stabilizer..... Map (x-direction)	409
G-23	SA-365N Main Rotor Downwash on Horizontal Stabilizer..... Map (z-direction)	410
G-24	SA-365N Fuselage Downwash on Horizontal Stabilizer Map.....	411
G-25	SA-365N Dynamic Pressure Ratio at Horizontal Stabilizer Map..	412
G-26	SA-365N Vertical Stabilizer Lift Map.....	413
G-27	SA-365N Vertical Stabilizer Drag Map.....	414
G-28	SA-365N Main Rotor Downwash on Vertical Stabilizer..... Map (x-direction)	415
G-29	SA-365N Main Rotor Downwash on Vertical Stabilizer..... Map (z-direction)	416
G-30	SA-365N Dynamic Pressure Ratio at Vertical Stabilizer Map....	417
G-31	SA-365N Fan Shroud Lift Map.....	418
G-32	SA-365N Fan Shroud Drag Map.....	419
G-33	SA-365N Main Rotor Downwash on Fan Shroud Map..... (x-direction)	420
G-34	SA-365N Main Rotor Downwash on Fan Shroud Map..... (z-direction)	421
G-35	SA-365N Dynamic Pressure Ratio on Fan Shroud Map.....	422
G-36	SA-365N Endplate Lift Map.....	423
G-37	SA-365N Endplate Drag Map.....	424
G-38	SA-365N Dynamic Pressure Ratio at Left Endplate Map.....	425
G-39	SA-365N Dynamic Pressure Ratio at Right Endplate Map.....	426
H-1	M1-28 Three-View Drawing.....	442
H-2	M1-28/AH-64A Profile Comparison.....	443

LIST OF FIGURES

<u>Figure</u>		<u>Page</u>
H-3	Mi-28 Pitch Attitude Comparison.....	444
H-4	Mi-28 Longitudinal Stick Comparison.....	445
H-5	Mi-28 Lateral Stick Comparison.....	446
H-6	Mi-28 Collective Stick Comparison.....	447
H-7	Mi-28 Pedal Comparison.....	448
H-8	Mi-28 Stabilator Comparison.....	449
H-9	Mi-28 Power Required Comparison.....	450
H-10	Mi-28 Main Rotor Blade Twist Map..	451
H-11	Mi-28 Fuselage Lift Map.....	452
H-12	Mi-28 Fuselage Drag Map.....	453
H-13	Mi-28 Fuselage Pitching Moment Map.....	454
H-14	Mi-28 Fuselage Sideforce Map.....	455
H-15	Mi-28 Fuselage Yawing Moment Map.....	456
H-16	Mi-28 Main Rotor Downwash on Fuselage Map..... (x-direction)	457
H-17	Mi-28 Main Rotor Downwash on Fuselage Map..... (z-direction)	458
H-18	Mi-28 Horizontal Stabilizer Lift Map.....	459
H-19	Mi-28 Horizontal Stabilizer Drag Map.....	460
H-20	Mi-28 Main Rotor Downwash on Horizontal Stabilizer Map..... (x-direction)	461
H-21	Mi-28 Main Rotor Downwash on Horizontal Stabilizer Map..... (z-direction)	462
H-22	Mi-28 Vertical Stabilizer Lift Map.....	463

LIST OF FIGURES

<u>Figure</u>		<u>Page</u>
H-23	Mi-28 Vertical Stabilizer Drag Map.....	464
H-24	Mi-28 Main Rotor Downwash on Vertical Stabilizer Map..... (x-direction)	465
H-25	Mi-28 Main Rotor Downwash on Vertical Stabilizer Map..... (z-direction)	466
H-26	Mi-28 Fuselage Sidewash on Vertical Stabilizer Map.....	467
H-27	Mi-28 Main Rotor Downwash on Tail Rotor Map..... (x-direction)	468
H-28	Mi-28 Main Rotor Downwash on Tail Rotor Map..... (z-direction)	469
H-29	Mi-28 Wing Lift Map.....	470
H-30	Mi-28 Wing Drag Map.....	471
I-1	Time History Data, Counter 208019.....	473
I-2	Time History Data, Counter 208025.....	474
I-3	Time History Data, Counter 208026.....	475
I-4	Time History Data, Counter 208027.....	476
I-5	Time History Data, Counter 302014.....	477
I-6	Time History Data, Counter 302018.....	478
I-7	Time History Data, Counter 302019.....	479
I-8	Time History Data, Counter 417003.....	480
I-9	Time History Data, Counter 417005.....	481
I-10	Time History Data, Counter 417005.....	482
I-11	Time History Data, Counter 417008.....	483
I-12	Time History Data, Counter 417009.....	484

LIST OF FIGURES

<u>Figure</u>		<u>Page</u>
I-13	Time History Data, Counter 411011.....	485
I-14	Time History Data, Counter 411013.....	486
I-15	Time History Data, Counter 411023.....	487
I-16	Time History Data, Counter 23020.....	488
I-17	Time History Data, Counter 23021.....	489
I-18	Time History Data, Counter 23025.....	490
I-19	Time History Data, Counter 23026.....	491
I-20	Time History Data, Counter 23032.....	492
I-21	Time History Data, Counter 23034.....	493
I-22	Time History Data, Counter 23035.....	494
I-23	Time History Data, Counter 23037.....	495
I-24	Time History Data, Counter 23038.....	496
I-25	Time History Data, Counter 27026.....	497
I-26	Time History Data, Counter 27027.....	498
I-27	Time History Data, Counter 27029.....	499
I-28	Time History Data, Counter 27031.....	500
I-29	Time History Data, Counter 27034.....	501
I-30	Time History Data, Counter 27036.....	502
I-31	Time History Data, Counter 27037.....	503
I-32	Time History Data, Counter 27038.....	504
I-33	Time History Data, Counter 27041.....	505
I-34	Time History Data, Counter 27043.....	506

LIST OF FIGURES

<u>Figure</u>		<u>Page</u>
K-1	Mi-28 OGE Hover Gross Weight Capability with..... Two 2650 SHP Engines	532
K-2	Mi-28 OGE Hover Gross Weight Capability with..... Two 2200 SHP Engines	533
K-3	Mi-28 Power Required, SLS Conditions, Clean.....	534
K-4	Mi-28 Power Required, SLS Conditions, with External Stores...	535
K-5	Mi-28 Power Required, 4K/95 Conditions, Clean.....	536
K-6	Mi-28 Power Required, 4K/95 Conditions, with External Stores.	537
L-1	Empirical Manuever Prediction Equations.....	539
L-2	Empirical Hover Bob-up Comparison.....	540
L-3	Empirical Acceleration from Hover to 80 Knots Comparison....	542
L-4	Empirical Deceleration from 80 Knots to Hover Comparison....	543
L-5	Empirical 80-Knot Climb Comparison.....	544
L-6	Empirical 80-Knot Steady Turn Comparison.....	545
L-7	Empirical 80-Knot Decelerating Turn Comparison.....	546
L-8	Empirical 130-Knot Decelerating Turn Comparison.....	547
L-9	Empirical 140-Knot Pull-up Comparison.....	548
L-10	Empirical 180-Degree Hover Turn Comparison.....	549
L-11	Comparison of CanHel and Empirical M/A Basic Ratings.....	550
L-12	Comparison of CanHel and Empirical M/A ATA Ratings.....	551
L-13	Comparison of CanHel and Empirical M/A ATC Ratings.....	552
L-14	Comparison of CanHel and Empirical M/A NOE Ratings.....	553
L-15	Comparison of CanHel and Empirical M/A Contour Ratings.....	554
M-1	Aerodynamic Scaling Method.....	560

LIST OF TABLES

<u>Table</u>		<u>Page</u>
1	Input Data List for M/A Aircraft.....	15
2	Derived Parameter Summary.....	20
3	Main Rotor Power Available Summary.....	23
4	Static Parameter Data List.....	42
5	Maneuver Results Summary.....	44
6	AACT Firing Window Analysis Summary.....	80
7	Maneuver Scoring Equations.....	92
8	M/A Weighting Factors Derivation.....	93
9	UH-60A M/A Scoring and Rating Summary (AACT).....	97
10	UH-60A M/A Scoring and Rating Summary (BDGW).....	98
11	S-76A M/A Scoring and Rating Summary.....	98
12	CH-53E M/A Scoring and Rating Summary.....	99
13	AH-64A M/A Scoring and Rating Summary (AACT).....	99
14	AH-64A M/A Scoring and Rating Summary (BDGW).....	100
15	OH-58A M/A Scoring and Rating Summary.....	100
16	AH-1S M/A Scoring and Rating Summary.....	103
17	SA-365N M/A Scoring and Rating Summary.....	103
18	M1-28 M/A Scoring and Rating Summary (Baseline).....	104
19	M1-28 M/A Scoring and Rating Summary (400 shp increase).....	104
20	M1-28 M/A Scoring and Rating Summary (900 shp increase).....	105
21	M1-28 M/A Scoring and Rating Summary (105 percent Nr).....	105
22	M1-28 M/A Scoring and Rating Summary (+10% Izz).....	106
23	M1-28 M/A Scoring and Rating Summary (-10% Izz).....	106
24	AACT Scoring Summary, S-76A versus OH-58A.....	112

LIST OF TABLES

<u>Table</u>		<u>Page</u>
25	AACT Scoring Summary, UH-60A vases OH-58A.....	114
26	AACT Scoring Summary, UH-60A vases S-76A.....	115
27	AACT Scoring Summary, AH-1S versas OH-58A.....	115
28	AACT Scoring Summary, AH-64A verses SA-365N..... (Fixed Gun)	116
29	AACT Scoring Summary, AH-64A vases SA-365N..... (Turratad Gun)	116
30	Correlation Data Summary.....	119
A-1	UH-60A Specific Fila Data.....	138
B-1	S-76A Specific File Data.....	177
G-1	GH-53E Specific Fila Data.....	217
D-1	AH-64A Specific File Data.....	255
E-1	OH-58A Specific File Data.....	297
F-1	AH-1S Specific Fila Data.....	331
G-1	SA-365N Specific File Data.....	373
H-1	Mi-28 Specific File Data.....	429
J-1	AACT Engagemant Initial Conditions.....	518
K-1	Mi-28 Power Availabla Summary.....	528
K-2	Mi-28 Waight Braakdown.....	529
K-3	Mi-28 OGE Hover Gross Weight Capability.....	530
K-4	Mi-28 IGE Hovar Gross Weight Capability.....	531
L-1	20K Mi-28 Manauver Pradictions.....	556
L-2	20K Mi-28 Scores snd Ratings.....	557
N-1	Drag Braakdown Summary.....	562

INTRODUCTION

This report documents a helicopter maneuverability and agility (M/A) study conducted by Sikorsky Aircraft for the U.S. Army Aviation Applied Technology Directorate (AATD). Four major activities were undertaken in this effort.

First, detailed, free-flying GenHel computer simulation models of eight helicopters were created and flown through nine different maneuvers to assess their capabilities. Six of these aircraft (UH-60A, AH-64A, AH-1S, OH-58A, S-76A, SA-365N) had participated in U.S. Army Air-to-Air Combat Tests while two (Mi-28, CH-53E) were included because of relevance to this study. The nine maneuvers investigated were a hover bob-up, acceleration from hover to 80 knots, deceleration from 80 knots to hover, 80 knot steady turn, 80 knot steady climb, decelerating turns at 80 and 130 knots, 140 knot symmetrical pull-up and a 180 degree hover turn. These data were analyzed to show the sensitivities of various design attributes on maneuverability and agility and to see if previously defined guidelines were appropriate.

Second, selected encounters from the AACT tests were analyzed to determine how the pilots maneuvered to gain advantage during the engagements and when firing opportunities were achieved.

The third task was the development of a scoring and M/A rating scheme for the simulation maneuvers and a scoring scheme for the AACT engagements.

The final activity was a correlation of the GenHel simulation results and AACT data to determine if the simulation predictions of M/A capability were verified by the AACT flight test data.

An overview of this correlation study is presented schematically in Figure 1.

BACKGROUND

Historically, helicopters have been used for transport and general utility by the armed services. In the Vietnam era, helicopter usage expanded greatly to include armed reconnaissance and ground attack missions. Current rotorcraft operations involve flight in Nap-of-the-Earth (NOE) conditions and involvement in both air-to-ground and air-to-air combat. As a result, the requirements for helicopter maneuverability and agility (M/A) have significantly increased. There is a need therefore, to have a methodology which both defines the M/A characteristics of existing helicopters and predicts those of new designs.

Definition of Maneuverability and Agility (M/A)

Before proceeding any further it is appropriate to define the terms maneuverability and agility as used in this report. Maneuverability is defined as the ability to change the aircraft flight path by application of forces from the main rotor, tail rotor or other control devices. Agility is defined as how quickly the aircraft flight path can be changed.

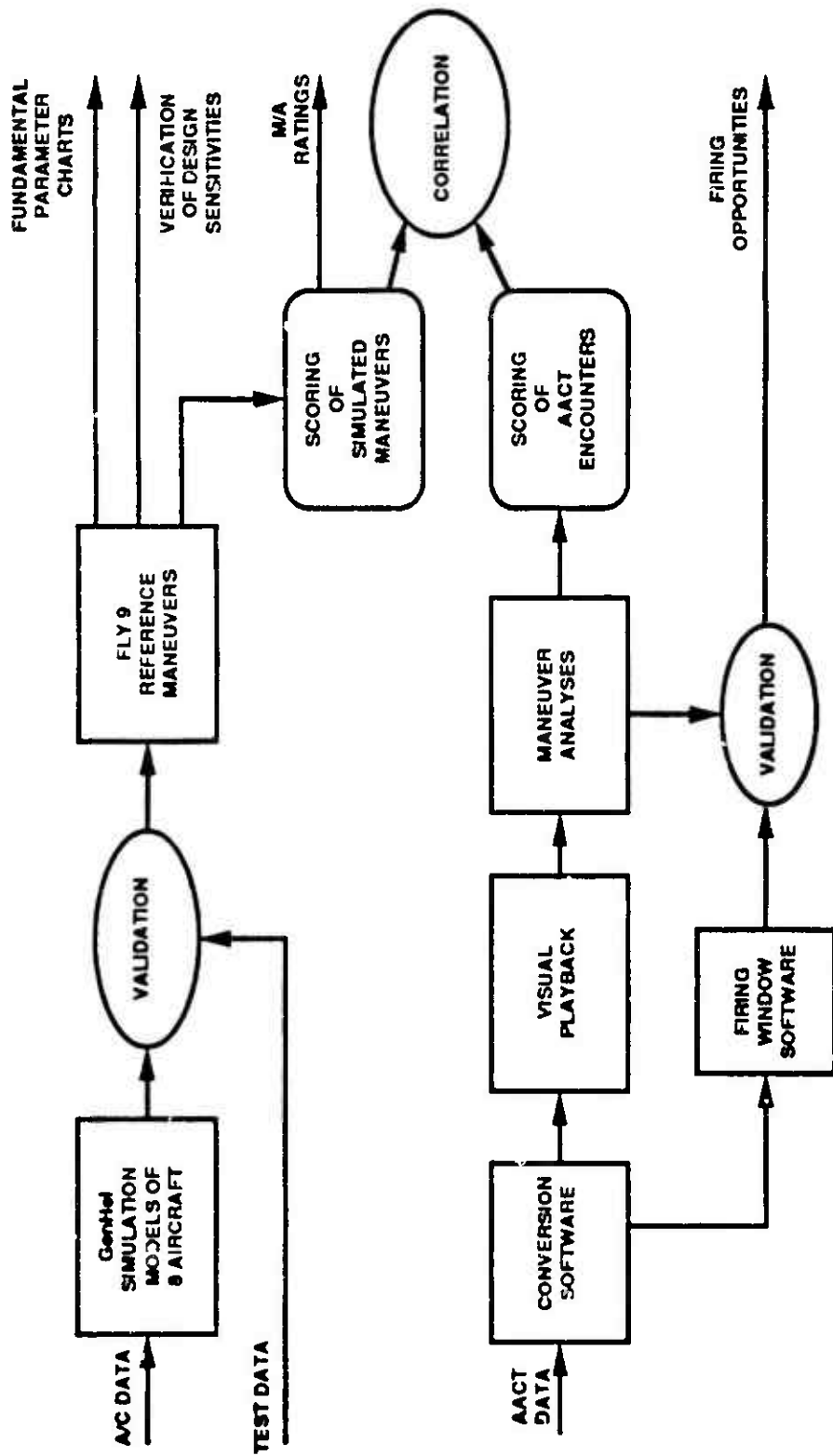


Figure 1. M/A Correlation Study Overview

For our purposes, such broad definitions need to be quantified in an easily measurable way. This is done by flying computer simulation models of various aircraft through a set of predefined maneuvers. This then relates M/A to parameters such as load factor or turn rate that are easily measured. It should be noted that maneuverability and agility are to some extent complementary. That is, those things which improve maneuverability such as more blade area or increased disk area tend to increase the size and weight of the helicopter and degrade agility. This is not to say, however, that changes which improve maneuverability always degrade agility. For example, engine power can frequently be increased without any change to the size or weight of the engine. In this case, both agility and maneuverability have been improved.

Importance of M/A in Modern Rotorcraft

In the past, helicopter design has focused on such attributes as hover climb performance and gross weight capability, maximum level flight speed, payload/range and other such performance measures. Maneuverability and agility was a fallout of the design process. This was due to two factors. The first was a lack of requirements or specifications for M/A and the second was lack of any industry standard metrics for defining these characteristics

However, there are many activities in which the helicopter is engaged which depend critically on M/A for success. After Vietnam, the value of the helicopter as a gun platform and its use in ground attack were well established. In addition, the requirement to repulse large armor attacks in the European theater led to the development of specialized anti-tank missions. And since no tactical commander would allow his armor to be attacked with impunity, air-to-air missions were developed. The widespread use of helicopters in the battlefield and their importance to the overall effort insure that air-to-air combat will be a significant part of future helicopter operations.

Intelligence gathering continues to be a major activity, and the armed scout helicopter is an important asset. The advent of sophisticated airborne sensors and availability of satellite communication and navigation have expanded the capabilities of the scout helicopter enormously. Even the mundane but important process of providing helicopter transport for supplies and troops has become more difficult due to the availability of lightweight, shoulder-fired anti-aircraft missiles. All of these activities point out the need for increased levels of M/A in modern rotorcraft. The questions this report will address are how maneuverability and agility can be measured and what are the values for current U.S. Army helicopters.

Review of M/A Design Sensitivity Analysis

In 1988, Sikorsky conducted, under contract to AATD, a Helicopter Maneuverability and Agility Design Sensitivity Analysis covering Design Guidelines, Air-to-Air Simulation Methodology, and Weight Methodology. These were subsequently documented in References 1, 2 and 3, respectively. Hereafter, that effort will be designated as the M/A Phase I Study.

The M/A Phase I Study quantified the measurement of maneuverability and agility for helicopters. The approach taken in that study was as follows:

A baseline aircraft of 10,000 pounds gross weight was selected. Sikorsky's GenHel computer simulation model of the aircraft was then flown through a series of maneuvers. Parameters such as tip speed, disk loading, blade loading, power available, hinge-offset and gross weight were varied individually and the maneuvers reflight. These data were then analyzed to determine two metrics. The first was a reasonable measure-of-effectiveness (MOE) for each maneuver. The second was a normalizing or "fundamental" parameter that would collapse the parametric results onto a single line. This activity led to the creation of the fundamental parameter charts, an example of which is shown in Figure 2. This chart is for a 130-knot decelerating turn. The MOE is turn rate, in degrees-per-second. The fundamental parameter is the normalized blade loading margin. This is defined as the maximum CT/σ available at 130 knots minus the trim value, the resultant normalized by the trim value. As can be seen, variations in blade loading (BL), disk loading (DL), tip speed (TS), Lock number (LN) and twist (TW) all have the same effect on trim or maximum CT/σ and therefore all can be normalized by this fundamental parameter.

The second part of that study addressed the weight sensitivity associated with the parametric variations discussed above. The purpose was to determine the impact of improved M/A on aircraft empty weight. These variations in weight were then plotted against the changes in the MOE as shown in Figure 3. Of importance is the slopes of these lines; i.e., which parameter change would produce the greatest improvement in the MOE for the least weight. In the example shown, it can be seen that increased disk loading both reduces weight and increases the turn rate. However, disk loading is bounded by other constraints, so decreased blade loading is another way to improve turn rate.

The third part of the M/A Phase I study involved analyzing Air-to-Air Combat Test (AACT) data to determine when firing windows occurred. This task was done using a computer program to define when firing windows were achieved. The AACT data were analyzed to determine the range between the two aircraft and the angle between the attack aircraft boresight and the center of the victim aircraft. If the range was less than 1500 meters and the angle less than three degrees, the attack aircraft was considered to have a firing "window". The time that these conditions were maintained was also recorded. It was clear after the study was completed that some method of visualizing the encounters was required. This was subsequently addressed during the Phase II Study. The central issue was what maneuvering capability was responsible for achievement of a firing opportunity.

The conclusion of the Phase I study was that the design approach for improving maneuverability and agility depends on the relative importance of the individual maneuvers investigated. There is no generalized design method that will maximize all maneuvers. Specific design guidelines can be formulated for each maneuver independently, but these will not be the same for all maneuvers and will frequently conflict. Increased power, lower blade loading and reduced Lock number are the most weight effective options for improving overall maneuverability and agility characteristics.

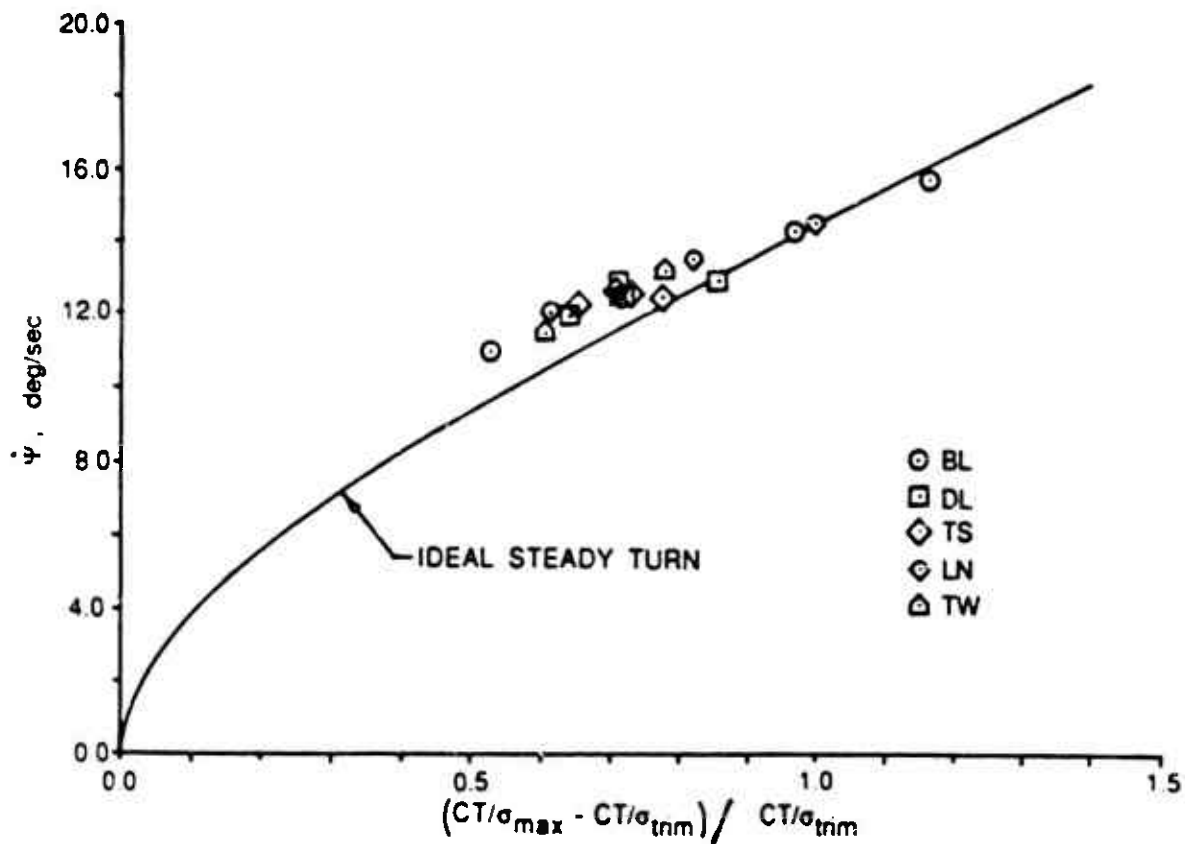


Figure 2. Example Fundamental Parameter Chart

BASELINE = 29.8 DEG/SEC

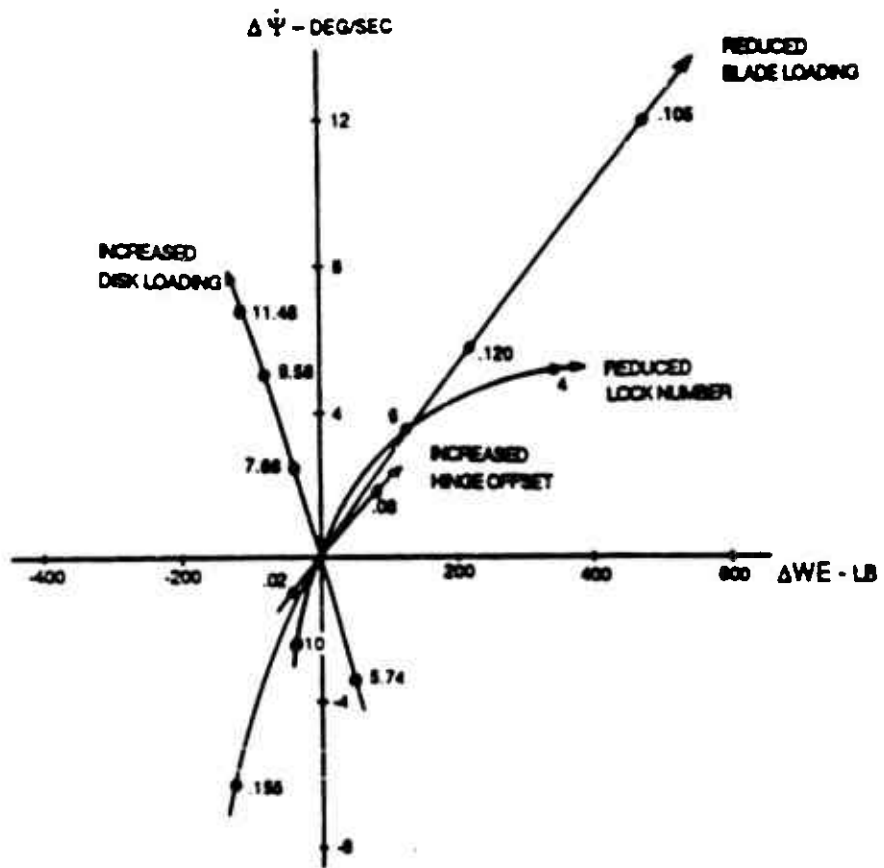


Figure 3. Example Weight Sensitivity Chart

Figure 4 shows a summary chart extracted from Reference 1. It shows that improving maneuverability in the low-speed range emphasizes different design parameters than those required for high-speed improvement. Low-speed maneuverability is primarily dependent on those parameters that affect power while high speed is dominated by rotor thrust capability. In the mid-speed (power bucket) regime, both power-limited and thrust-limited capabilities need to be matched.

At the end of the M/A Phase I study it was concluded that a number of other issues needed to be addressed. One was whether or not this methodology was applicable to a wide variety of rotorcraft, rather than parametric variations of a single design. Another issue was the correlation between these analytical results and flight test data. Finding answers to these questions formulated the basis for the M/A correlation study documented in this report.

OVERVIEW OF THIS CORRELATION STUDY

The Helicopter Maneuverability and Agility Design Sensitivity and AACT Data Correlation Analysis documented in this report is a follow-on to the M/A Phase I Study and will be denoted herein as the M/A Phase II Study. This effort was aimed at expanding the Phase I activities. The overall goal was to devise a quantitative M/A rating scheme and then verify its correctness by using the AACT data.

The first part involved creating GenHel Simulation models of the various aircraft that participated in the AACT tests and flying them through the Phase I maneuvers. These included the UH-60A, AH-64A, AH-1S, OH-58A, S-76A and SA-365N. Since the GenHel simulation of the CH-53E already existed, it was added to the study to evaluate heavy lift helicopter M/A. A contract modification was exercised to add the Soviet Mi-28 HAVOC to the study, drawing on unclassified data from various sources, to create a GenHel simulation. The results were plotted on the fundamental parameter charts to see if the fundamental (or normalizing) parameter would "collapse" the data for a wide variety of aircraft types along the already established Phase I trend curves.

The second part involved automation of the firing window analysis so that data from the AACT activities could be presented graphically. The third major part was the development of a scoring scheme for the simulation results and a scoring schema for the AACT encounters.

The last part was a correlation of the first two using the scoring methodology.

Each part of this study represented a significant effort. Detailed and comprehensive free-flight computer simulation models of all the non-Sikorsky aircraft were created and validated against available flight test data. For most aircraft, the modeling data were taken from C-81 input listings provided as government furnished information (CFI). These data had to be reorganized to fit the GenHel input format. After validation, the simulations were flown through the previously defined nine M/A maneuvers using a software maneuver controller. This assured consistency in the way maneuvers were performed amongst the various helicopters. In addition, the maneuvers were constrained

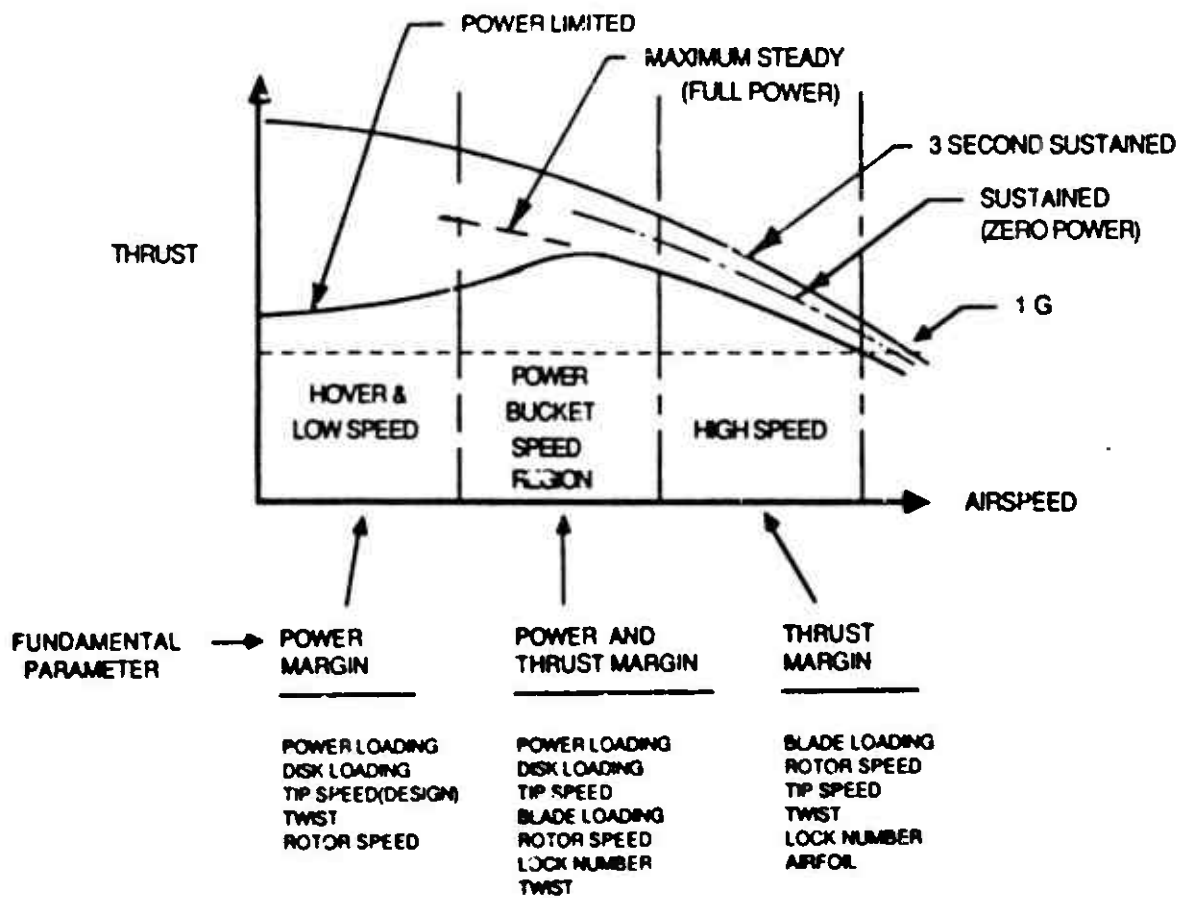


Figure 4. Summary of M/A Phase I Results

by variety of realistic operational limitations to add fidelity to the results. Next, the fundamental parameters had to be calculated and the fundamental parameter charts created. These fundamental parameter charts are then really quite profound. Each point, representing one helicopter, is the culmination of an extensive modeling, validation and evaluation process.

In the second major part of this study, the AACT data were processed through a variety of axis transformations and then through a firing window analysis code. In addition to predicting when one aircraft was within the firing window of the other, the specific parameters (range, angular error, time in window) were also available. Finally, a display driver was set up to operate in the work station environment. This allowed graphical display playback of any of the AACT data. The data could be viewed in real time, slowed down, speeded up, or stopped. Views out of either cockpit, from above, or from an arbitrary point in combat space could be displayed. This allowed analysis of the maneuvering sequence prior to gaining a firing window.

The third part of this study was the development of scoring schemes for the simulated maneuvers and the AACT engagements. For the simulated maneuvers, the result for each maneuver was converted to a numerical score. The average score for the nine maneuvers was taken to be the basic M/A rating. However, different mission elements emphasize different maneuvers. For example, NOE flight would be dominated by the characteristics found in the hover bob-up, hover turn, and accelerations to and decelerations from 80 knots. On the other hand, air-to-air combat would be affected most by the characteristics shown in the 140 knot pull-up or the 130 and 80 knot decelerating turn. Therefore, to account for this, scores for each maneuver were multiplied by weighing factors for air-to-air (ATA), air-to-ground (ATG), nap-of-the-earth (NOE), and contour (CON) mission types. The average of the scores in each category was taken as the M/A rating for that mission type.

Scoring of the AACT tests was based on using the available data from the firing window analysis program - time in window, angular error and range. A scheme was devised to award points to the attack aircraft based on these parameters and calculate an overall score as the sum of each aircraft's points.

The fourth part of this study was a correlation of the simulated maneuver results and the AACT flight tests using the scores generated in the manner disclosed above. The estimated ATA capability was calculated by taking the percentage ratio of each helicopter's M/A ATA rating to the total for the two aircraft. For example, the UH-60A has an ATA M/A rating of 79.0 while the S-76 has a rating of 34.8. The estimated results of air-to-air combat would be 69.4 percent ($79.0 / (79.0 + 34.8)$) for the UH-60A and 30.6 percent ($34.8 / (79.0 + 34.8)$) for the S-76A. In a like manner, the actual ATA capability was calculated by taking the percentage ratio of each helicopter's AACT scores to the total for the two aircraft. In this case the UH-60A had scored 121 points and the S-76 6.3 points for percentage ratios of 95.1 and 4.9, respectively. Correlation was judged by comparing the two sets of percentages.

Detailed, substantiating data for these activities is provided in Appendixes A through N.

SIMULATION MODELS

Overview of GenHel

Sikorsky's General Helicopter Flight Dynamics Simulation (GenHel) is a simulation environment that allows the user to easily create models of any rotorcraft for which sufficient data are available. It is important to note that GenHel is not merely a computer code but a simulation environment. The major features of GenHel are:

- 1) Free-flight, total force, large angle mathematical model. GenHel is not a perturbational model, but a complete free-flying analysis. Wind tunnel and trim modes are also available.
- 2) Generic, reusable software coded in modules and maintained in a library. GenHel code is available to the user through selection of a series of modules. These modules are coded symbolically and contain no numbers. They can be used to model any rotorcraft. These modules are maintained in libraries so that the users can not modify them and so that all users get the same model. Data for each specific aircraft/configuration are maintained in separate data (or "specific") files created by the user. The library has provisions for prototype modules accessible to the user. These are maintained in a separate prototype area. The library system is shown schematically in Figure 5. A typical module breakdown is shown in Figure 6, while an overview is presented graphically in Figure 7.
- 3) A large array of auxiliary and utility modules are available. In addition to the basic aircraft model, modules are available for external loads, flexible airframe, deck/slope landing and maneuver loads. Interfaces are available for CRT terminal, line printer and strip chart recorder outputs. The resulting simulations can be interfaced with Sikorsky's fixed base and moving base simulators for piloted evaluation.
- 4) Extensive validation of existing simulations (UH-60A, S-76A, GH-53E) against a wide variety of flight test data.

An example of the mathematical modeling used in GenHel is documented in Reference 4.

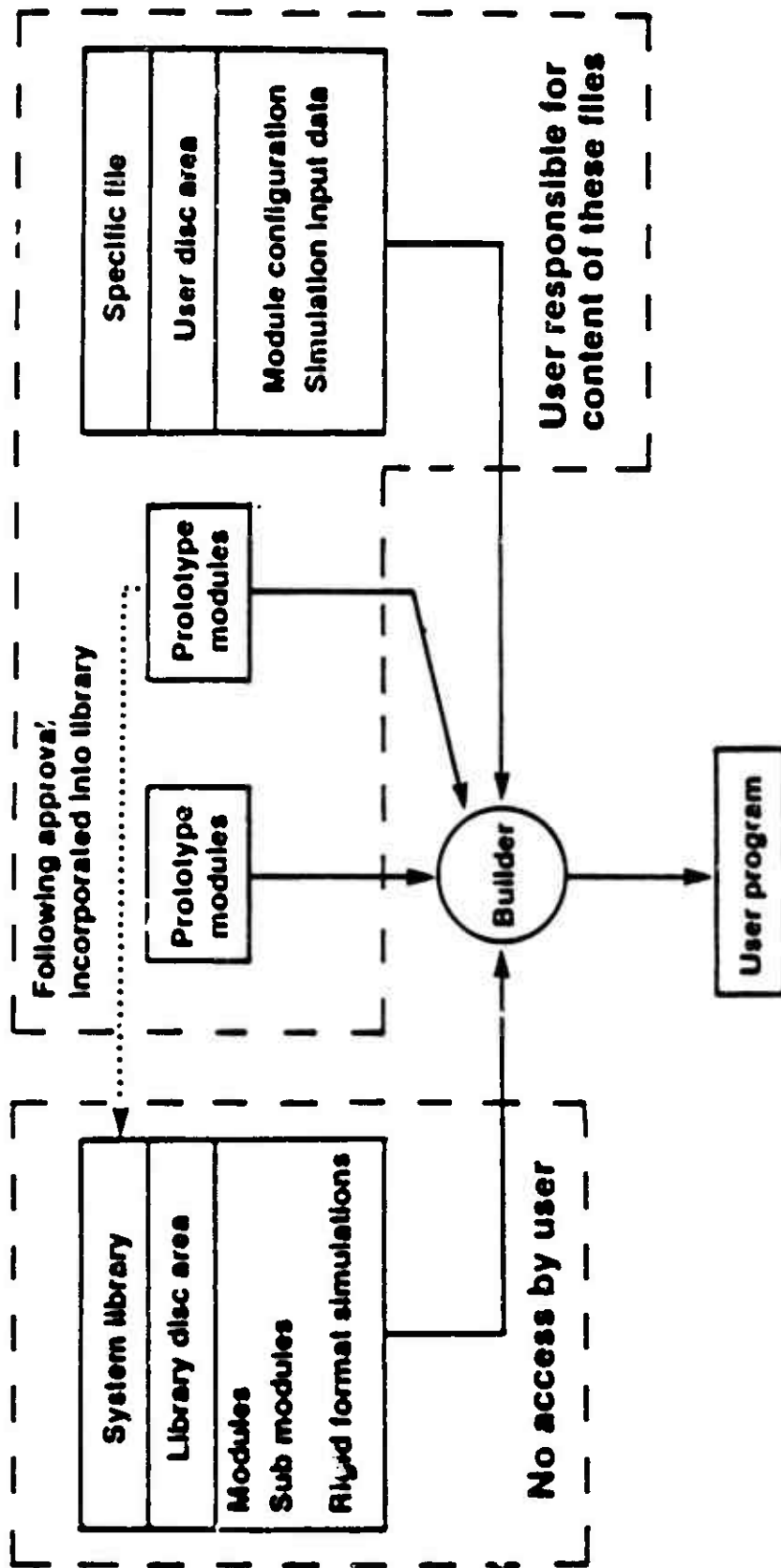


Figure 5. GENHEL Library System

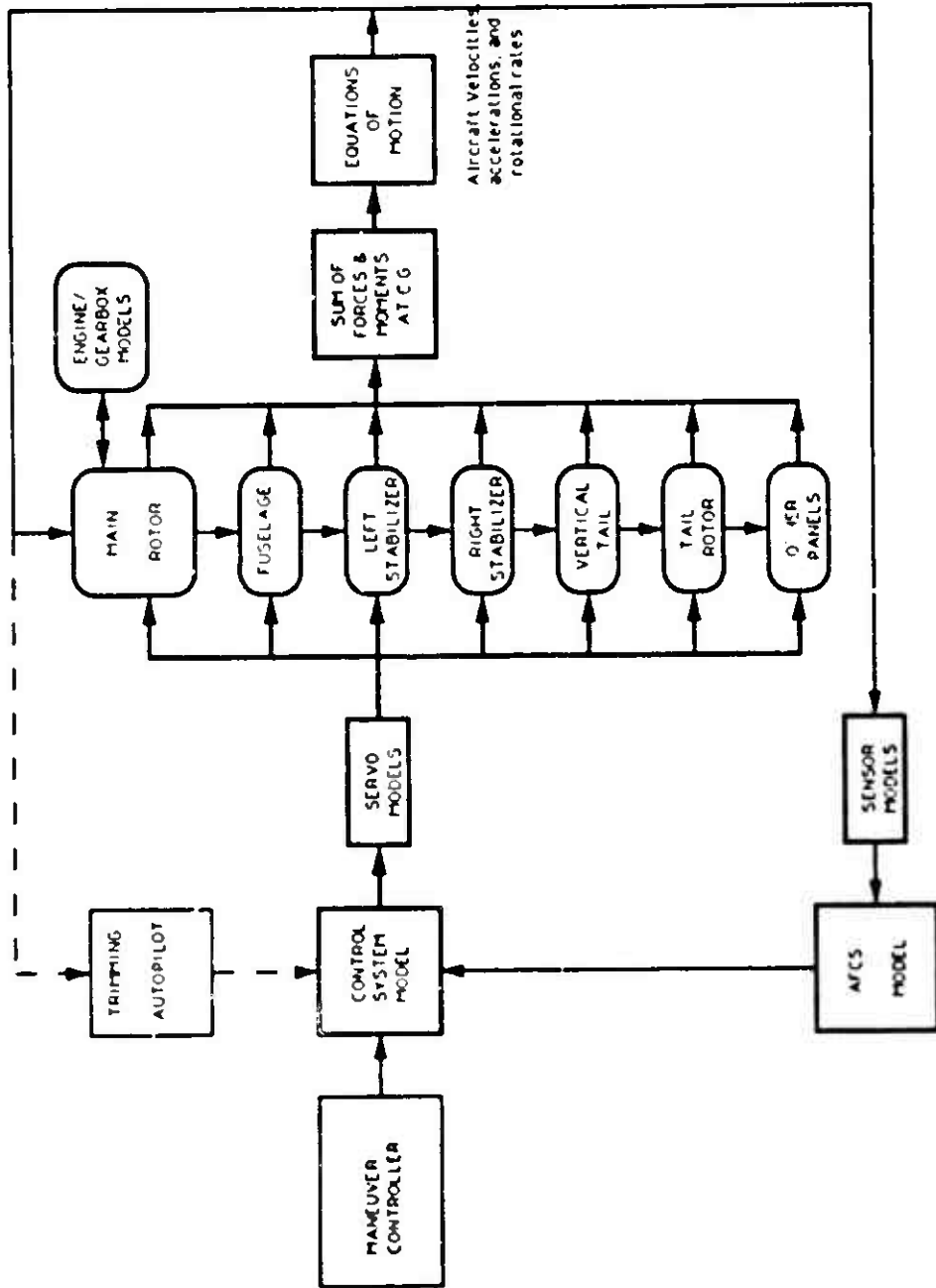


Figure 6. GENHEL Modular Architecture

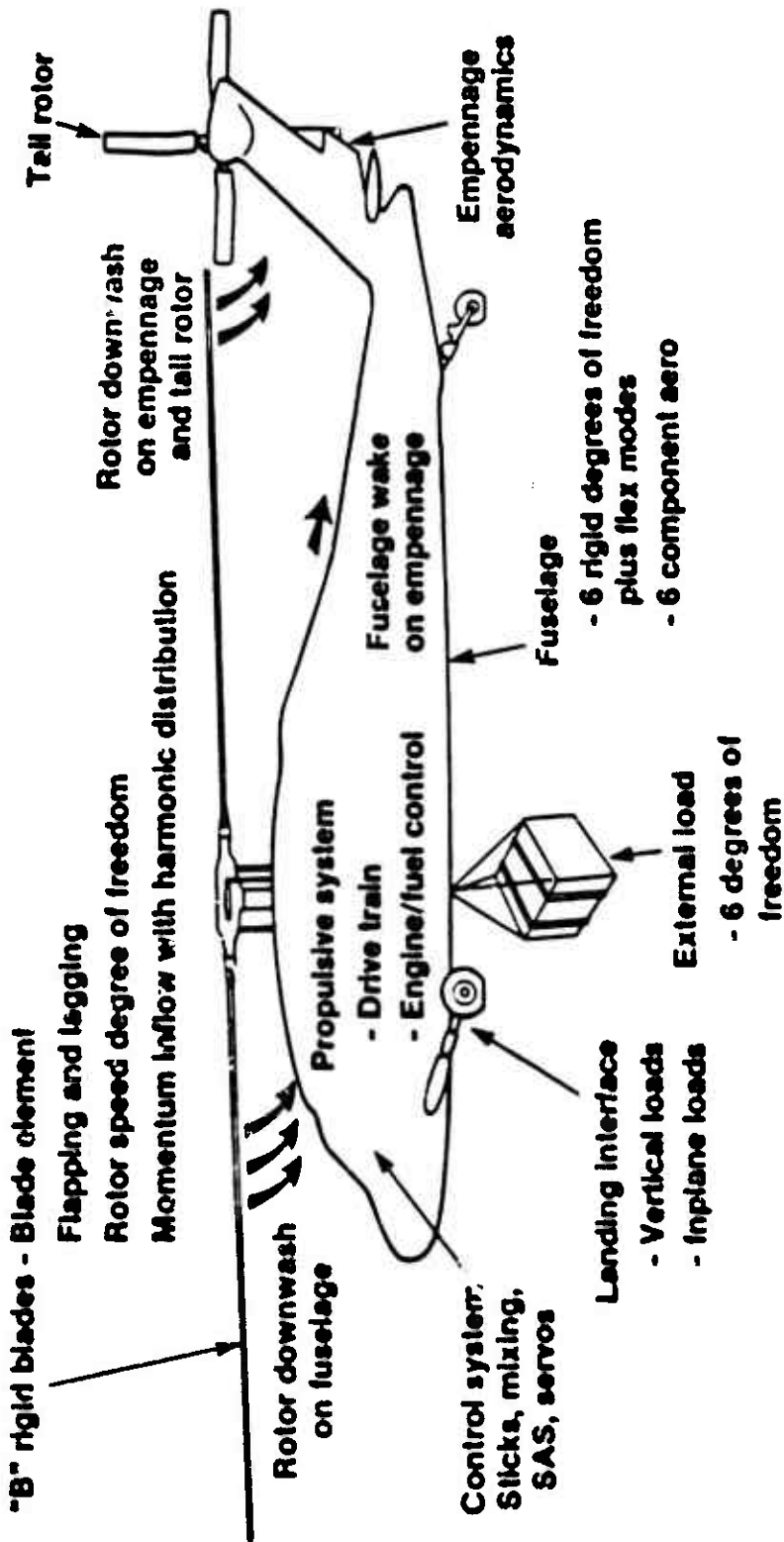


Figure 7. GENHEL Overview

Discussion of Aircraft Models

Introduction

The aircraft selected for this M/A correlation study were:

- 1) Sikorsky UH-60A BLACK HAWK
- 2) Sikorsky S-76A
- 3) Sikorsky CH-53E Super Stallion
- 4) McDonnell-Douglas AH-64A Apache
- 5) Bell AH-1S Cobra
- 6) Bell OH-58A Kiowa
- 7) Aerospatiale SA-365N1 Dauphin
- 8) Mil Mi-26 HAVOC

All of these aircraft except the Super Stallion and HAVOC were involved in the AACT flight evaluations. The CH-53E was added to represent the heavy weight category and since a GenHel simulation model of it already existed, this was easy to implement. The Mi-28 simulation was created after that helicopter was shown at the 1989 Paris Air show. Photographs of the aircraft were available along with other information from the Soviet delegates. A contract modification was implemented to include the HAVOC in this study.

Detailed discussions of each of the simulation models are provided in Appendixes A to H. These include a brief history and description of each aircraft, discussion of data sources, correlation of GenHel with flight test data and detailed numerical GenHel input data used in each helicopter model. One important output of this study is a comprehensive and consistent data base for all these helicopters.

For convenience the basic data for the study aircraft are summarized in Table 1. This provides data on geometry, rotor speeds and mass properties. Derived parameters such as disk loading, blade loading, control power, etc., are provided in Table 2. Note that the UH-60A was evaluated at both its AACT test weight of 14,685 pounds and its Basic Design Gross Weight (BDGW) of 16,825 pounds. The AH-64A was handled in a similar manner for its AACT (16,222 pounds) and BDGW (14,770 pounds) configurations. Data on the Mi-28 at both 22,984 pounds and 20,000 pounds are provided, but only the heavier case was evaluated in this study. Power available data are provided in Table 3. This shows the intermediate rated power (IRP) for each engine, the total IRP power for the aircraft, the main gearbox limits on power, and the power available to the main rotor at different airspeeds. Note that for the sea level standard conditions of this study, many of the modern helicopters were main gearbox limited and could not use all of the engine power available. A drag breakdown for the aircraft is provided in Appendix N.

TABLE 1. INPUT DATA LIST FOR M/A AIRCRAFT

AIRCRAFT	UH-60A	S-76A	CH-53E	AH-64A	OH-58A	AH-1S	SA-365M	MI-28
.....
RAIN ROTOR PARAMETERS								
FUSELAGE STATION, IN.	341.2	200.0	336.5	198.6	106.9	200.0	300.0	400.0
WATERLINE STATION, IN.	315.0	157.0	259.0	215.9	120.0	152.8	200.0	300.0
BUTTLINE STATION, IN. (+PORT)	0.0	0.0	0.0	0.0	0.0	0.0	0.0	0.0
RADIUS, FT	26.83	22.0	39.5	24.0	17.7	22.0	19.57	28.21
ROTATIONAL RATE, RAD/SEC	27.01	30.7	19.7	30.26	37.1	33.9	36.62	25.34
NUMBER OF BLADES	4	4	7	4	2	2	4	5
LONG SHAFT TILT (+REAR), DEG	-3.0	-5.0	-5.0	-5.0	-5.0	0.0	-4.0	-5.0
SWASHPLATE PHASE ANGLE, DEG	-9.7	-25.0	-10.0	-5.0	0.0	0.0	0.0	-5.0
FLAPPING HINGE OFFSET, DEG	0.0	16.7	0.0	0.0	0.0	0.0	0.0	0.0
LAGGING HINGE OFFSET COEF.								
FUNC(LG)	0.0	-0.05	0.0	0.0	0.0	0.0	0.0	0.0
LAGGING HINGE OFFSET COEF.								
FUNC(LG**2)	0.0	-0.005	0.0	0.0	0.0	0.0	0.0	0.0
BLADE TIP CHORD, FT	1.73	1.29	2.42	1.75	1.08	1.6	1.263	2.0
BLADE CHORD AT ROOT, FT	1.73	1.29	2.42	1.75	1.08	3.09	1.263	2.0
HINGE OFFSET, FT	1.25	.833	2.50	.917	0.0	0.0	0.75	1.552
HINGE TO START OF BLADE, FT	3.83	3.53	9.33	2.42	4.363	4.004	2.531	6.04
WEIGHT OF ONE BLADE, LBS	256.9	125.1	652.0	156.6	137.4	475.6	123.9	244.1
BLADE MOMENT OF INERTIA								
ABOUT HINGE, SLUG-FT**2	1512.6	459.0	5914.0	1060.4	335.9	1385.1	322.5	1336.0
BLADE MASS MOMENT ABOUT								
HINGE, SLUG-FT	86.7	32.5	249.0	64.36	28.42	100.55	28.88	77.08
PRECOME FOR GINBAL ROTOR	2.5	2.75
BLADE TIP CUT-OFF RATIO	.97	.97	.97	.97	.97	.97	.97	.97
DEL-DRAW COEF FOR EACH SEG	.002	.002	.002	.002	.002	.002	.002	.002
EFFECTIVE TWIST, DEG								
SEGMENT#1 AIRFOIL	S195U	81095	0012	HM02	0012	VR78C	S1095	S195U
SEGMENT#2 AIRFOIL	S4R8U	SC4R8	0012	HM02	0012	VR78C	S1095	S195U
SEGMENT#3 AIRFOIL	S4R8U	SC4R8	0012	HM02	0012	VR78C	S1095	S195U
SEGMENT#4 AIRFOIL	8195U	S1095	0012	HM02	0012	VR88C	81095	S195U
SEGMENT#5 AIRFOIL	S195U	S1095	0012	HM02	0012	VR88C	81095	S195U
RAIN ROTOR HORSEPOWER	2828.	1300.	13174.	2784.	420.	1290.	1372.	

TABLE 1. INPUT DATA LIST FOR M/A AIRCRAFT (Cont'd)

FLAPPING/LAGGING DAMPER PARAMETERS										

FLAPPING HINGE SPRING CONST,	0.0	0.0	0.0	0.0	0.0	0.0	0.0	0.0	8053.	0.0
FLAPPING HINGE DAMPER CONST,	0.0	0.0	0.0	0.0	0.0	0.0	0.0	0.0	0.0	0.0
FT-LBS/RAD										
ALIGNMENT OFFSET IN	7.0	-7.5	0.0	7.0	0.0	0.0	0.0	0.0	0.0	7.0
RELATION TO LAG, DEG										
FIXED BLADE PITCH RELATIONSHIP	17.48	2.0	0.0	17.48	0.0	0.0	0.0	0.0	0.0	2.0
BET. ARM AND THCUFF										17.481

FUSELAGE PARAMETERS										

FUSELAGE STATION, IN.	345.5	200.0	336.4	208.0	114.2	199.3	300.0	400.0		
WATERLINE STATION, IN.	234.0	90.0	161.4	142.0	58.2	71.2	140.0	205.8		
BUTTLINE STATION, IN. (+ PORT)	0.0	0.0	0.0	0.0	0.0	0.0	0.0	0.0		

RIGHT STABILIZER PARAMETERS										

FUSELAGE STATION, IN.	700.1	473.8	879.4	552.5	258.2	397.5	494.0	825.0		
WATERLINE STATION, IN.	244.0	100.8	302.7	147.2	72.9	55.66	126.0	312.5		
BUTTLINE STATION, IN. (+PORT)	-36.6	-25.0	-48.0	-22.3	0.0	0.0	-30.0	25.6		
SURFACE AREA OF PANEL, FT**2	22.5	9.25	58.0	16.68	9.65	15.14	8.0	14.0		
PANEL ORIENTATION, DEG	0.0	0.0	0.0	0.0	0.0	0.0	0.0	0.0		
PANEL INCIDENCE, DEG	0.0	2.0	0.0	0.0	0.0	6.97	0.0	0.0		

LEFT STABILIZER PARAMETERS										

FUSELAGE STATION, IN.	700.1	473.8	0.0	552.5	0.0	0.0	494.0	0.0		
WATERLINE STATION, IN.	244.0	100.8	0.0	147.2	0.0	0.0	126.0	0.0		
BUTTLINE STATION, IN. (+PORT)	36.6	25.0	0.0	22.3	0.0	0.0	30.0	0.0		
SURFACE AREA OF PANEL, FT**2	22.5	9.25	0.0	16.7	0.0	0.0	8.0	0.0		
PANEL ORIENTATION, DEG	0.0	0.0	0.0	0.0	0.0	0.0	0.0	0.0		
PANEL INCIDENCE, DEG	0.0	2.0	0.0	0.0	0.0	0.0	0.0	0.0		

TABLE 1. INPUT DATA LIST FOR N/A AIRCRAFT (Cont'd)

***** VERTICAL STABILIZER PARAMETERS *****									
FUSELAGE STATION, IN.	695.0	490.0	861.2	544.4	354.6	501.1	550.0	790.0	*****
WATERLINE STATION, IN.	273.0	141.3	247.0	189.2	85.9	97.18	184.0	267.5	*****
BUTTLINE STATION, IN.	0.0	0.0	0.0	0.0	-8.0	0.0	0.0	0.0	*****
SURFACE AREA OF PANEL, FT**2	32.3	19.7	74.0	32.2	9.18	18.87	15.8	21.88	*****
PANEL ORIENTATION, DEG	-90.0	-90.0	*****	90.0	90.0	-90.0	-90.0	90.0	*****
PANLZ INCIDENCE, DEG	0.0	0.0	0.0	0.0	4.0	4.5	0.0	0.0	*****
***** RIGHT WING/ENDPLATE PARAMETERS *****									
FUSELAGE STATION, IN.	*****	*****	*****	201.9	*****	189.7	495.0	417.5	*****
WATERLINE STATION, IN.	*****	*****	*****	137.5	*****	68.28	126.0	228.8	*****
BUTTLINE STATION, IN.	*****	*****	*****	-46.3	*****	0.0	-63.2	-73.8	*****
AREA OF PANEL, FT**2	*****	*****	*****	30.95	*****	28.15	8.2	16.41	*****
PANEL ORIENTATION, DEG	*****	*****	*****	0.0	*****	0.0	90.0	0.0	*****
PANEL INCIDENCE, DEG	*****	*****	*****	6.0	*****	17.0	5.0	10.0	*****
***** LEFT WING/ENDPLATE PARAMETERS *****									
FUSELAGE STATION, IN.	*****	*****	*****	201.9	*****	*****	495.0	417.5	*****
WATERLINE STATION, IN.	*****	*****	*****	137.5	*****	*****	126.0	228.8	*****
BUTTLINE STATION, IN.	*****	*****	*****	46.3	*****	*****	63.2	73.8	*****
AREA OF PANEL, FT**2	*****	*****	*****	30.95	*****	*****	8.2	16.41	*****
PANEL ORIENTATION, DEG	*****	*****	*****	0.0	*****	*****	90.0	0.0	*****
PANEL INCIDENCE, DEG	*****	*****	*****	6.0	*****	*****	5.0	10.0	*****
***** TAIL ROTOR/PAN BASE PARAMETERS *****									
PAN BASE AREA, FT**2	*****	*****	*****	*****	*****	*****	17.13	*****	*****
RADIUS, FT	5.5	4.0	10.0	4.58	2.58	4.25	1.805	6.3	*****
ROTATIONAL RATE, RAD/SEC	124.62	168.75	76.86	146.9	272.3	175.6	383.8	113.5	*****
NUMBER OF BLADES	4	4	4	4	2	2	11	4	*****
FUSELAGE STATION, IN.	732.0	518.0	930.7	554.7	352.2	520.7	554.7	217.5	*****
WATERLINE STATION, IN.	324.7	162.9	289.0	216.2	87.18	118.3	136.1	308.7	*****
BUTTLINE STATION, IN. (+POINT)	-14.0	20.0	80.36	-33.05	10.0	14.1	0.0	-32.5	*****
BLADE TWIST, DEG	-18.0	-8.0	-8.0	-8.8	0.0	0.0	-13.2	-10.0	*****

TABLE 1. INPUT DATA LIST FOR M/A AIRCRAFT (Cont'd)

***** CONTROL SYSTEM PARAMETERS *****										
ALS UPPER LIMIT	8.0	9.2	10.2	7.0	7.0	5.87	9.2	7.0	7.0	7.0
ALS LOWER LIMIT	-8.0	-7.6	-9.8	-10.5	-7.0	-11.0	-7.6	-10.5	-7.6	-10.5
BIS UPPER LIMIT	16.3	19.25	18.0	20.0	12.75	15.0	19.25	20.0	19.25	20.0
BIS LOWER LIMIT	-12.5	-14.75	-8.0	-10.0	-11.75	-15.6	-14.75	-10.0	-14.75	-10.0
THETA0 UPPER LIMIT	25.9	22.7	22.047	25.9	27.03	27.6	22.7	25.9	22.7	25.9
THETA0 LOWER LIMIT	9.9	4.0	4.447	9.9	9.033	7.80	4.0	9.9	4.0	9.9
THETTA UPPER LIMIT	36.5	14.5	24.0	36.5	12.0	10.0	14.5	36.5	12.0	36.5
THETTA LOWER LIMIT	4.5	-14.2	-10.0	4.5	-19.0	-18.17	-14.2	4.5	-14.2	4.5
LAT STICK UPPER LIMIT	10.0	12.0	9.25	9.0	9.1	8.5	7.7	9.0	9.1	9.0
LAT STICK LOWER LIMIT	0.0	0.0	0.0	0.0	0.0	0.0	0.0	0.0	0.0	0.0
LONG STICK UPPER LIMIT	10.0	8.5	8.96	10.0	11.36	10.1	9.8	10.0	11.36	10.0
LONG STICK LOWER LIMIT	0.0	0.0	0.0	0.0	0.0	0.0	0.0	0.0	0.0	0.0
COLL STICK UPPER LIMIT	10.0	8.8	11.0	12.0	10.65	8.9	6.6	12.0	10.65	12.0
COLL STICK LOWER LIMIT	0.0	0.0	0.0	0.0	0.0	0.0	0.0	0.0	0.0	0.0
PEDAL UPPER LIMIT	5.38	4.7	4.17	4.8	6.34	6.0	5.4	4.8	6.34	4.8
PEDAL LOWER LIMIT	0.0	0.0	0.0	0.0	0.0	0.0	0.0	0.0	0.0	0.0

TABLE 2. DERIVED PARAMETER SUMMARY

ITEM	AIRCRAFT			
	UH-60A (AACT)	S-76A	CH-53E	AH-64A (AACT)
Gross Weight, lbs	14685	8925	56000	16222
Reference shp	2828	1300	12339	2784
Disk Loading, lb/ft ²	6.49	5.87	11.42	8.96
Blade Loading, lb/ft ²	79.1	78.6	83.7	96.6
Power Loading, lb/shp (total)	5.19	6.86	4.54	5.83
MR Tip Speed, fps	724	675	778	726
MR Solidity	.0821	.0747	.1365	.0928
Hinge Offset, %	4.66	3.79	6.33	3.82
Lock Number	8.08	8.97	13.57	7.46
Thrust Coefficient	.00521	.00541	.00793	.00715
Roll Control Sensitivity, rad/sec ² /deg	.937	.760	.416	1.607
Pitch Control Sensitivity, rad/sec ² /deg	.113	.135	.071	.128
Yaw Sensitivity, rad/sec ² /deg	.0659	.0874	.0449	.069

TABLE 2. DERIVED PARAMETER SUMMARY (Cont'd)

ITEM	AIRCRAFT			
	OH-58A	AH-1S	SA-365N	Mi-28
Gross Weight, lbs	2790	9620	8750	22984
Reference shp	420	1290	1372	4400
Disk Loading, lb/ft ²	2.83	6.33	7.27	9.15
Blade Loading, lb/ft ²	73.0	87.5	88.5	81.5
Power Loading, lb/shp (total)	6.64	7.46	6.38	5.22
MR Tip Speed, fps	657	746	717	715
MR Solidity	.0388	.0723	.0822	.1128
Hinge Offset, %	0	0	3.83	5.50
Lock Number	4.30	5.76	7.83	12.92
Thrust Coefficient	.00276	.00478	.00596	.00757
Roll Control Sensitivity, rad/sec ² /deg	.501	.409	.749	.455
Pitch Control Sensitivity, rad/sec ² /deg	.107	.100	.133	.090
Yaw Control Sensitivity, rad/sec ² /deg	.1035	.0802	.106	.0489

TABLE 2. DERIVED PARAMETER SUMMARY (Cont'd)

ITEM	AIRCRAFT		
	UH-60A (BDGW)	AH-64A (BDGW)	MI-28 (A/A)
Gross Weight, lbs	16825	14770	20000
Reference shp	2828	2784	4400
Disk Loading, lb/ft ²	7.44	8.16	7.96
Blade Loading, lb/ft ²	90.6	87.9	70.9
Power Loading, lb/shp (total)	5.95	5.31	4.55
MR Tip speed, fps	724	726	715
MR Solidity	.0821	.0928	.1128
Hinge Offset, %	4.66	3.82	5.50
Lock Number	8.0	7.46	12.92
Thrust Coefficient	.00596	.00651	.00658
Roll Control Sensitivity, rad/sec/deg	.825	2.064	.481
Pitch Control Sensitivity, rad/sec ²	.105	.135	.0936
Yaw Control Sensitivity, rad/sec ² /deg	.0583	.0775	.0546

TABLE 3. MAIN ROTOR POWER AVAILABLE SUMMARY

ITEM	UH-60A	AH-64A	S-76A	AH-1S
Engine	T700-GE-700	T700-GE-701	T250-C30	T53-L-703
IRP Power Available (30 min)	1622	1698	650	1800
Times No. of Engines	3244	3396	1300	1800
MGB Limit (30 min)	2828	2784	1352	1290
Ref. SHP	2828	2784	1300	1290
MR SHP Available				
Hover (0.840)	2376	2339	1092	1084
40 kts (0.887)	2508	2469	1153	1144
80 kts (0.920)	2602	2561	1196	1187
140 kts (0.927)	2622	2581	1205	1196

ITEM	CH-53E	OH-58A	SA-365N-1	MI-28
Engine	T64-GE-416	T63-A-700	Arrival 1-C	Isotov TV3-117
IRP Power Available (30 min)	4113	420	686	2650
Times No. of Engines	12,339	420	1332	5300
MGB Limit (30 min)	13,174	----	----	4400
Ref SHP	12,339	420	1372	4400
MR SHP Available				
Hover (0.840)	10,281	353	1152	3696
40 kts (0.887)	10,856	373	1217	3903
80 kts (0.920)	11,260	386	1262	4048
140 kts (0.927)	11,346	389	1272	4079

Aircraft Comparisons

In order to study the M/A characteristics of these eight helicopters, it is necessary to understand how the aircraft compare to one another, not only in their basic attributes such as gross weight or rotor radius but also in their classical design parameters such as disk loading, solidity and control power.

The aircraft studied were all single-rotor helicopters which are in current use. They range in gross weight from 2790 pounds for the OH-58A to 56,000 pounds for the CH-53E (Figure 8). In spite of a factor of 20 difference in gross weight, rotor radii only varied by a factor of 2.2 when the 17.7 feet of the Kiowa is compared to the 39.5 feet of the Super Stallion (Figure 9). Available horsepower, on the other hand, varied by a factor of 30 (420 shp OH-58, 12339 shp CH-53E) as shown in Figure 10. Main rotor tip speeds (Figure 11) are all around 700 feet per second (657 for OH-58A, 778 for CH-53E at 105 percent). Several types of rotors are represented, ranging from the teetering types of the Bell aircraft to the starflex rotor on the Dauphin. The Sikorsky, McDonnell Douglas, and Mil designs employ conventional articulated hub designs. Flapping hinge offsets are illustrated in Figure 12 and vary from zero for the teetering rotors to 6.33 percent for the large Super Stallion.

When considering such a diverse array of vehicles, more appropriate comparisons can be achieved by reviewing the classical nondimensional parameters shown in Figures 13 through 17. One of the most important of these parameters is disk loading (Figure 13), which is very significant in hover and at low speeds. The OH-58A has a very low disk loading of 2.83 pounds/square foot. Most of the other aircraft have more typical values, between 6 and 9 pounds/square foot but the CH-53E is 11.42 at the 56,000 pounds of this study. Blade loading, on the other hand, is remarkably similar for such a wide range of types. The average value is about 83 pounds/square (Figure 14) foot with the OH-58A on the bottom end at 73.0 and the AH-64A on the high end at 96.6 psf (at its AACT GW of 16,222 pounds). Since the previous M/A Phase I study showed the importance of power at low speeds, the power loading (pounds/shp) is another parameter of interest. As seen in Figure 15, power loadings average about 5.81 pounds/shp. The CH-53E and ATA Mi-28 (20,000 pound GW) have the best values of 4.55, while the AH-1S is the worst at 7.46. The Cobra's main gearbox (MCB) is limited to 1290 shp. If the full 1800 shp of the T53 engine were available, its power loading would fall to a much better 5.31 pounds/square foot. The UH-60A and AH-64A are also main gearbox limited, but not to as great an extent as the Cobra. At its BDGW, the BLACK HAWK would improve its power loading by going to 5.19 from 5.95. Similarly, the Apache would move from 5.31 to 4.35, better than the lightweight Mi-28 and CH-53E.

Main rotor solidity (blade area/disk area) varies greatly for the eight helicopters (Figure 16). The seven-bladed Super Stallion has a solidity of 13.7 percent and the five-bladed HAVOC has 11.3 percent. The Kiowa is lowest at 3.9 percent, but the Cobra (also two-bladed) has a more typical value of 7.2 percent.

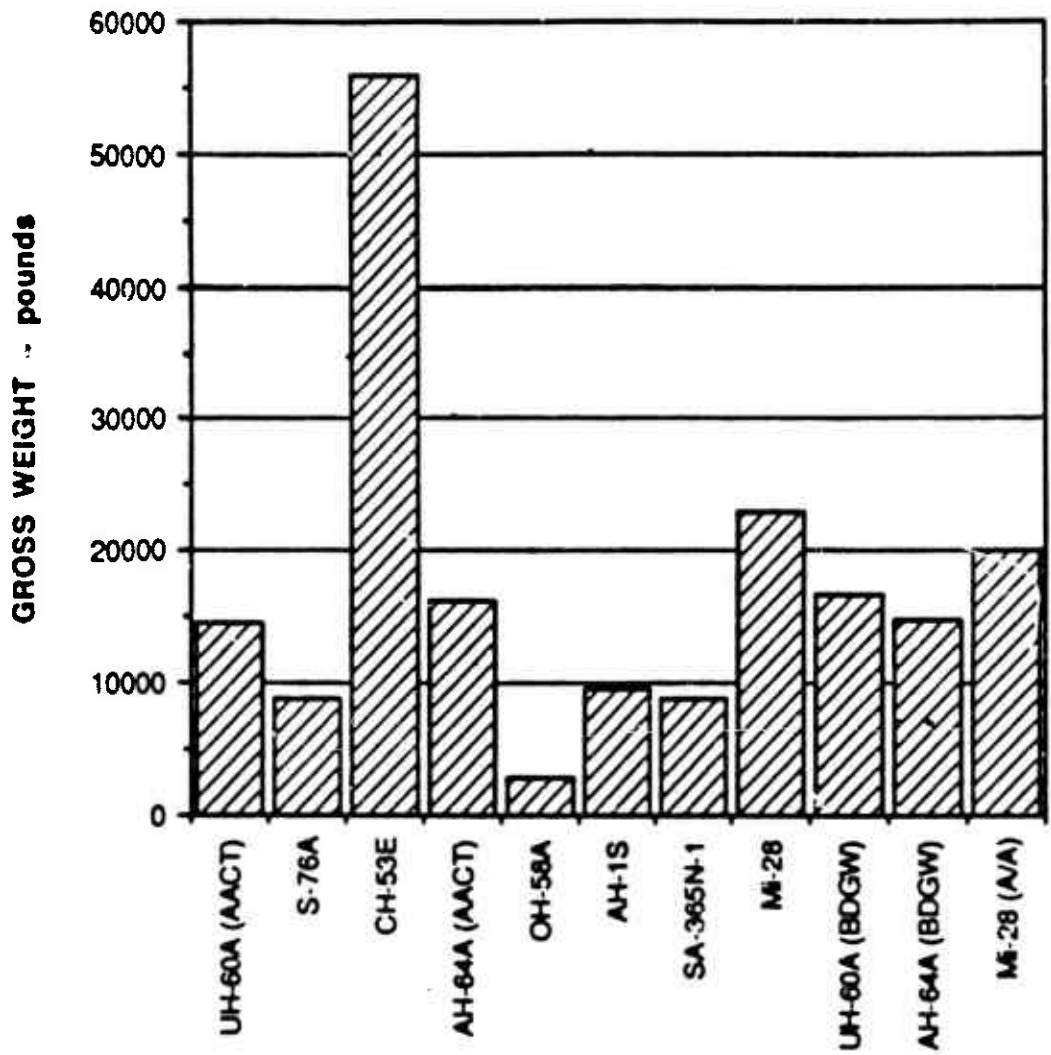


Figure 8. Gross Weight Comparison Chart

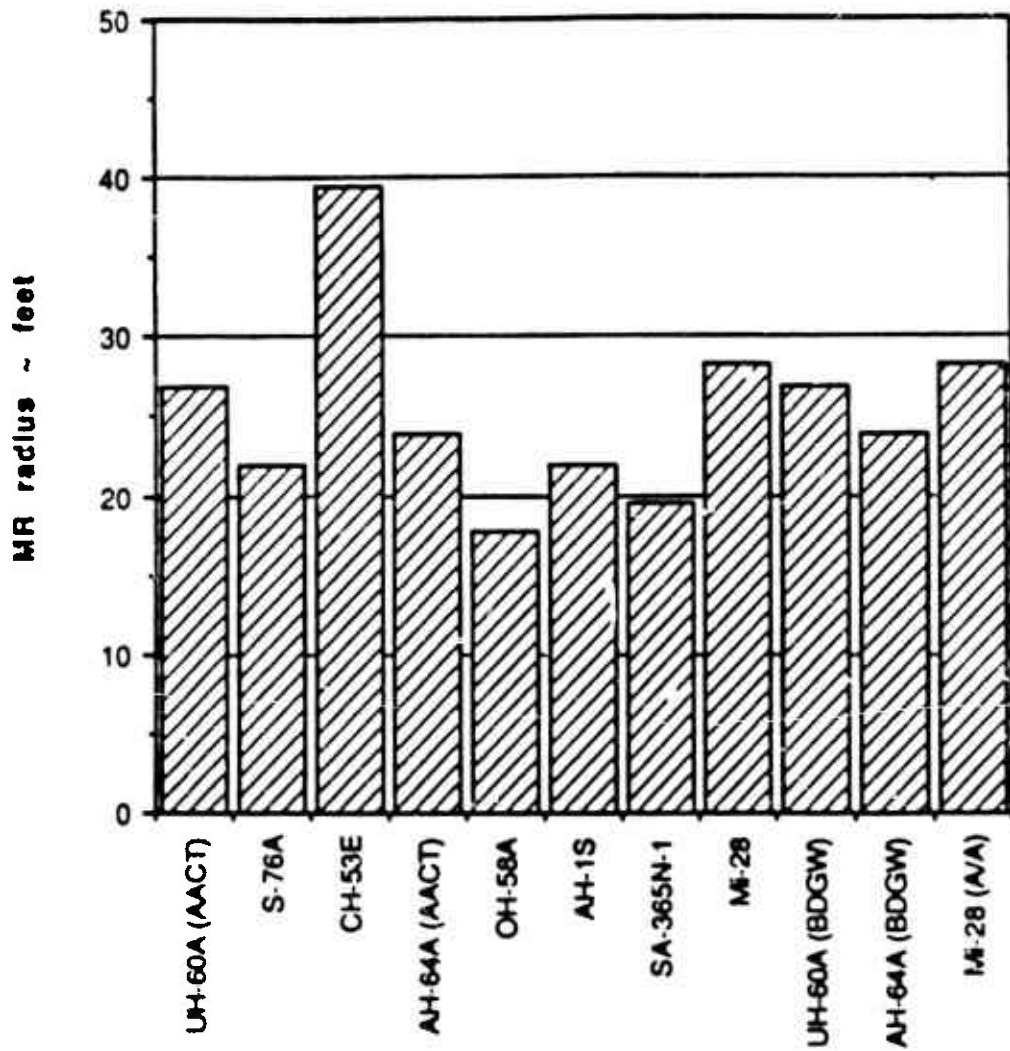


Figure 9. Main Rotor Radius Comparison Chart

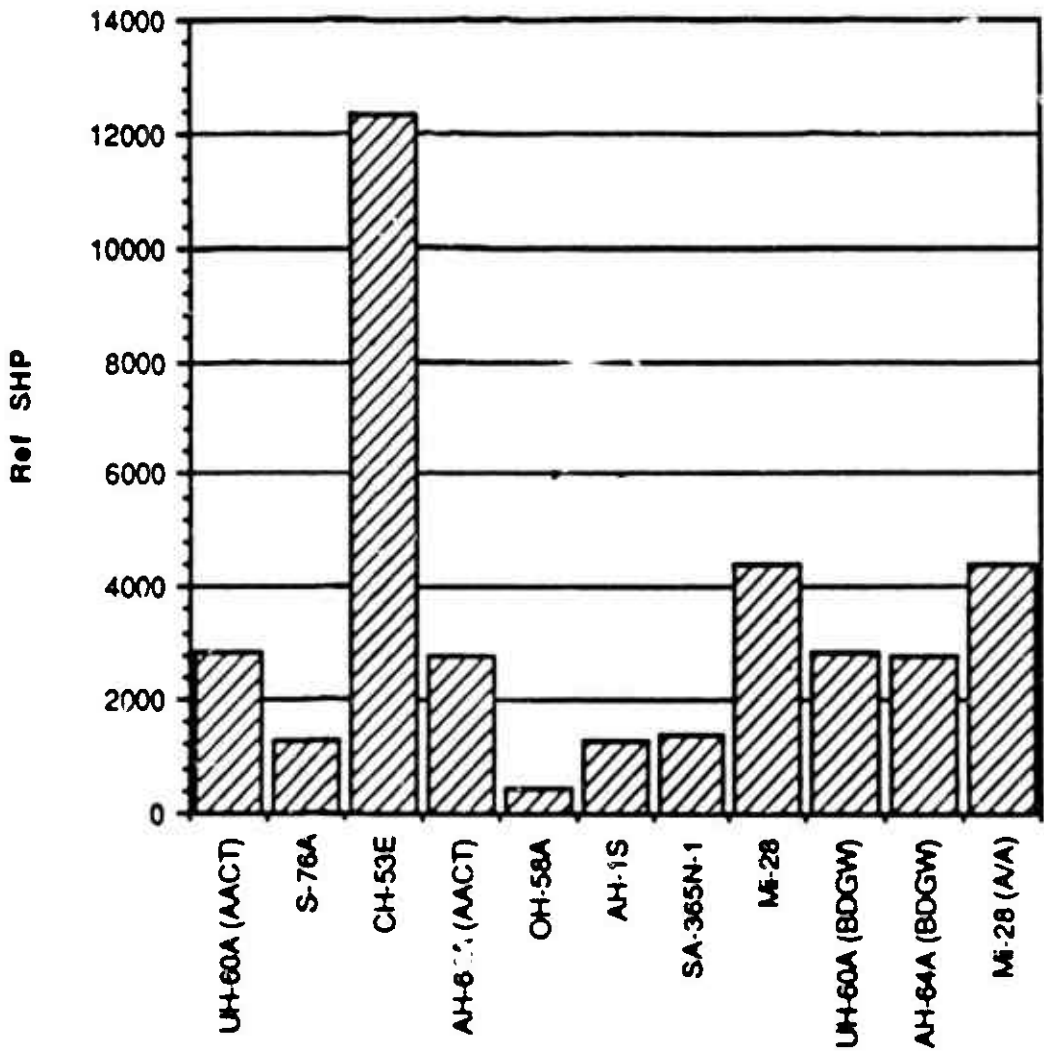


Figure 10. Reference SHP Comparison Chart

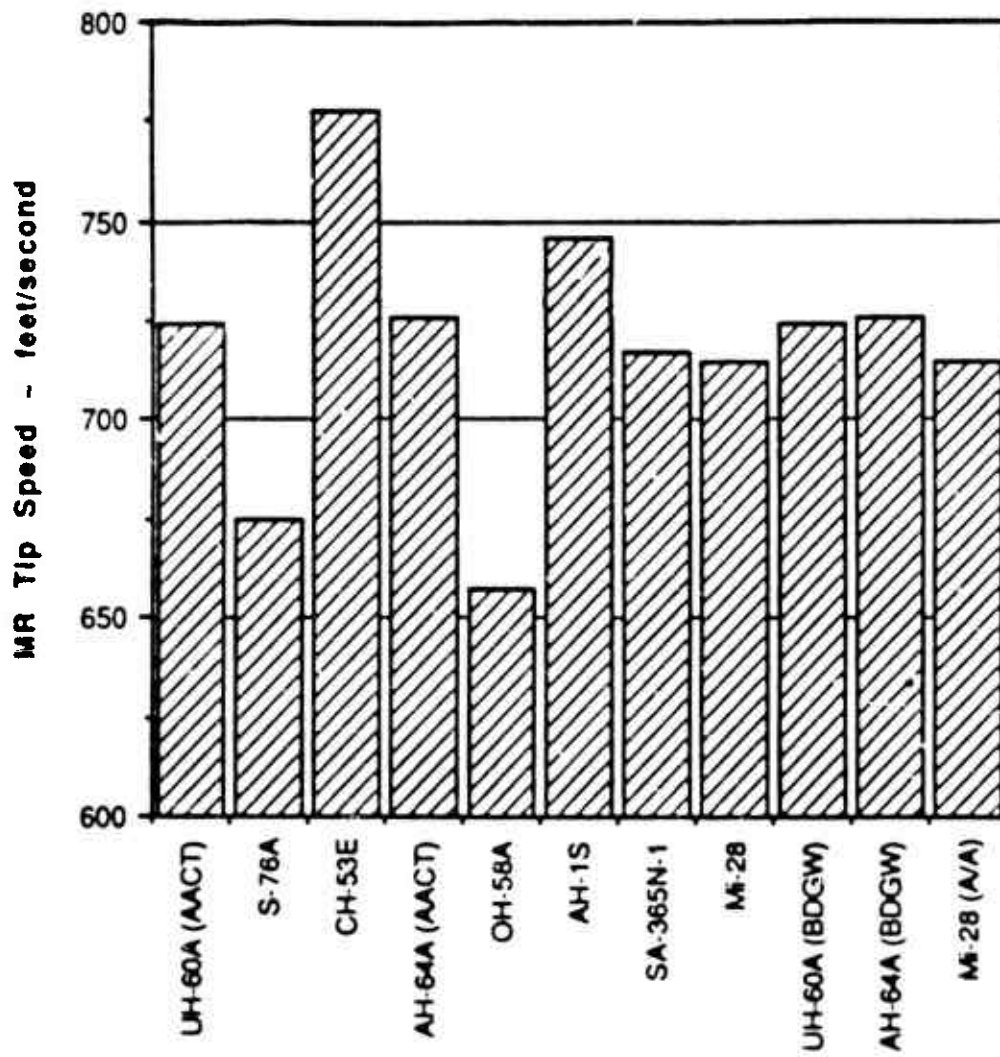
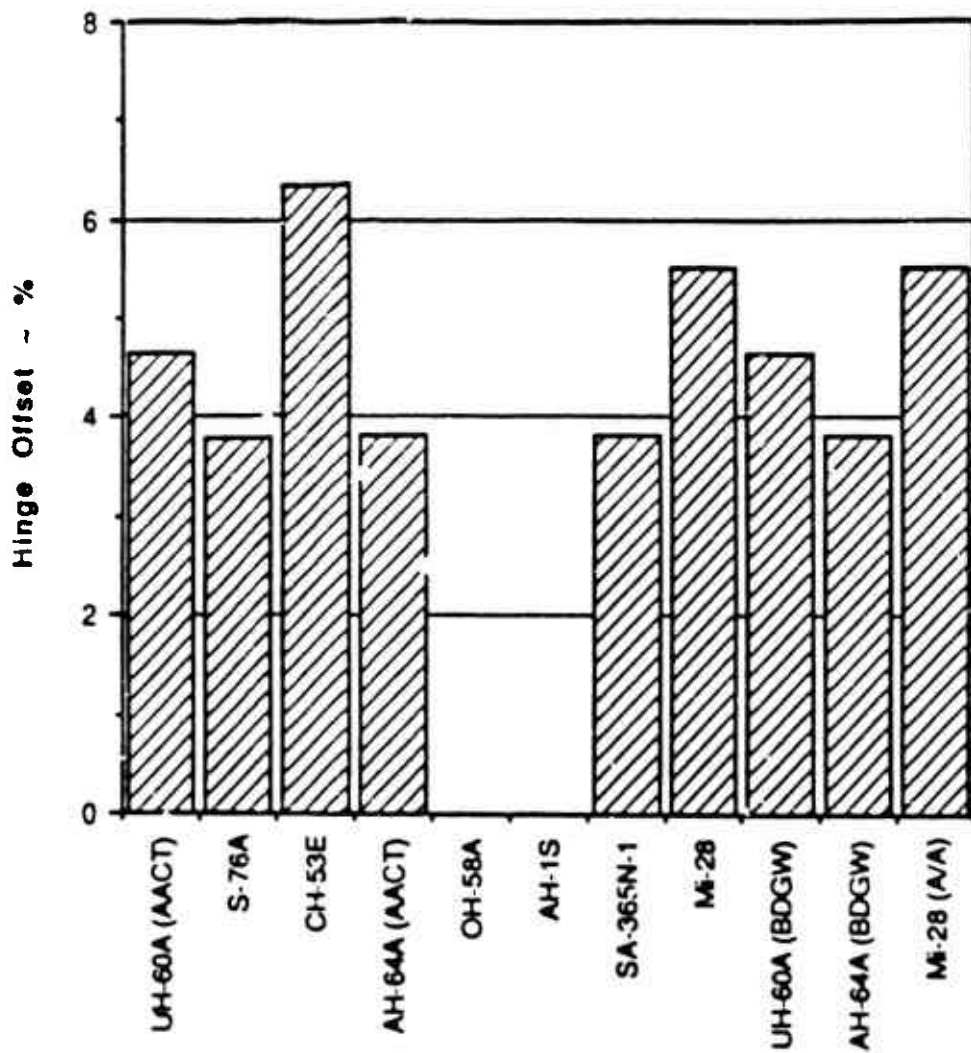


Figure 11. Main Rotor Tip Speed Comparison Chart



Figures 12. Main Rotor Hinge Offset Comparison Chart

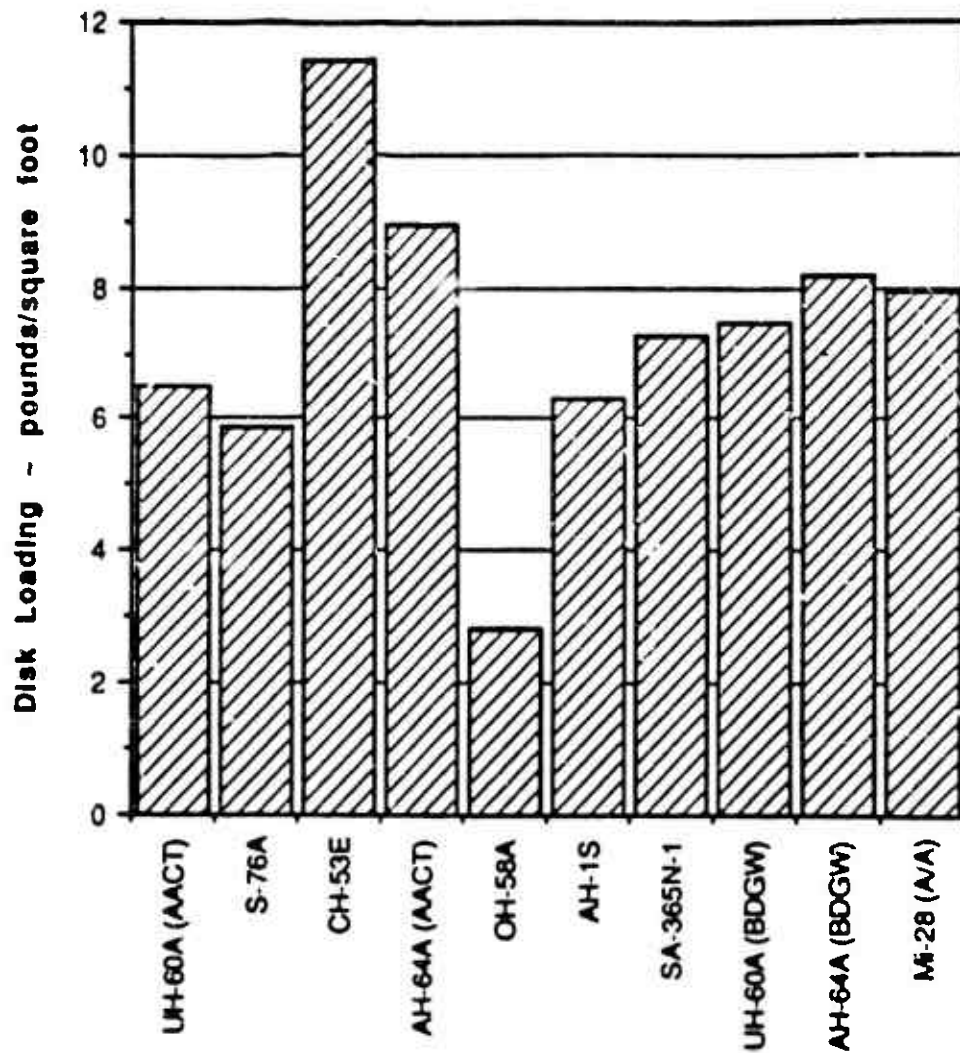


Figure 13. Disk Loading Comparison Chart

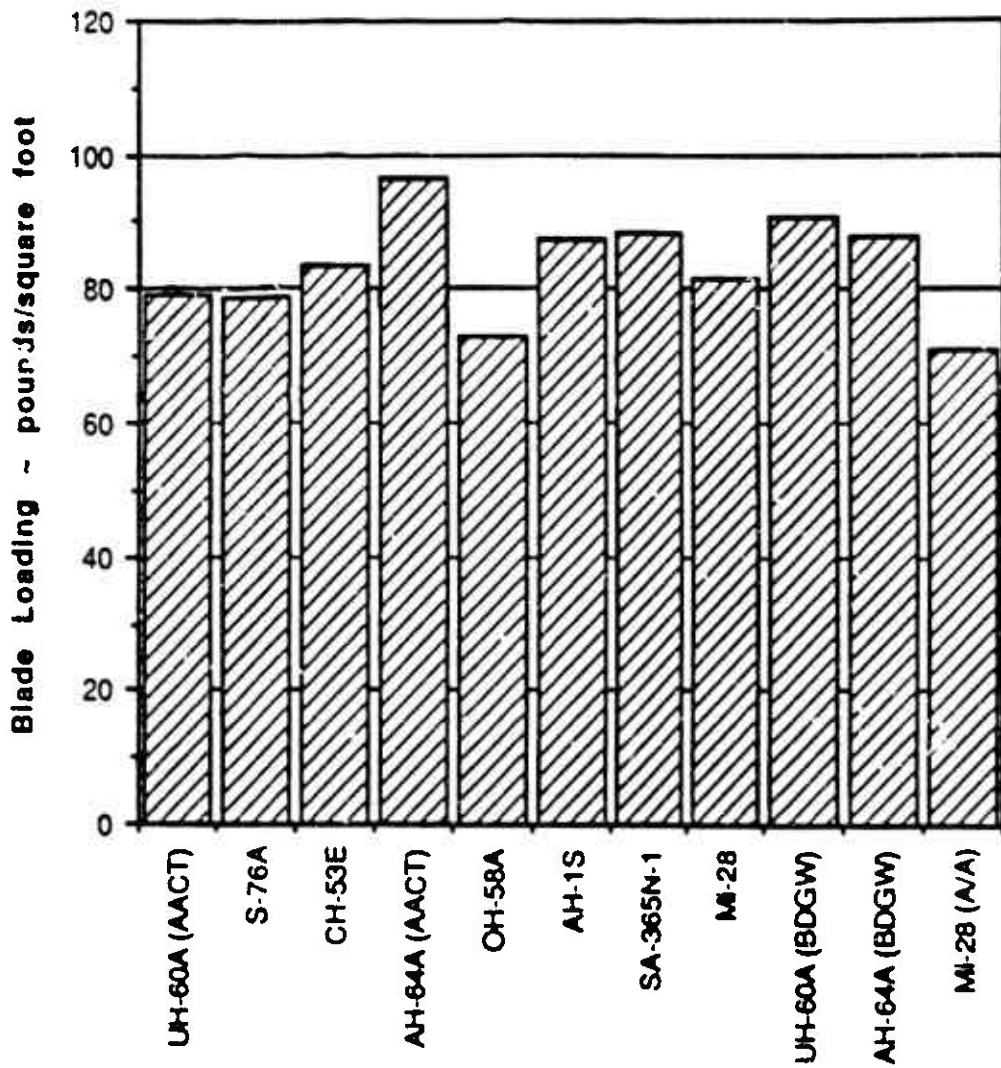


Figure 14. Blade Loading Comparison Chart

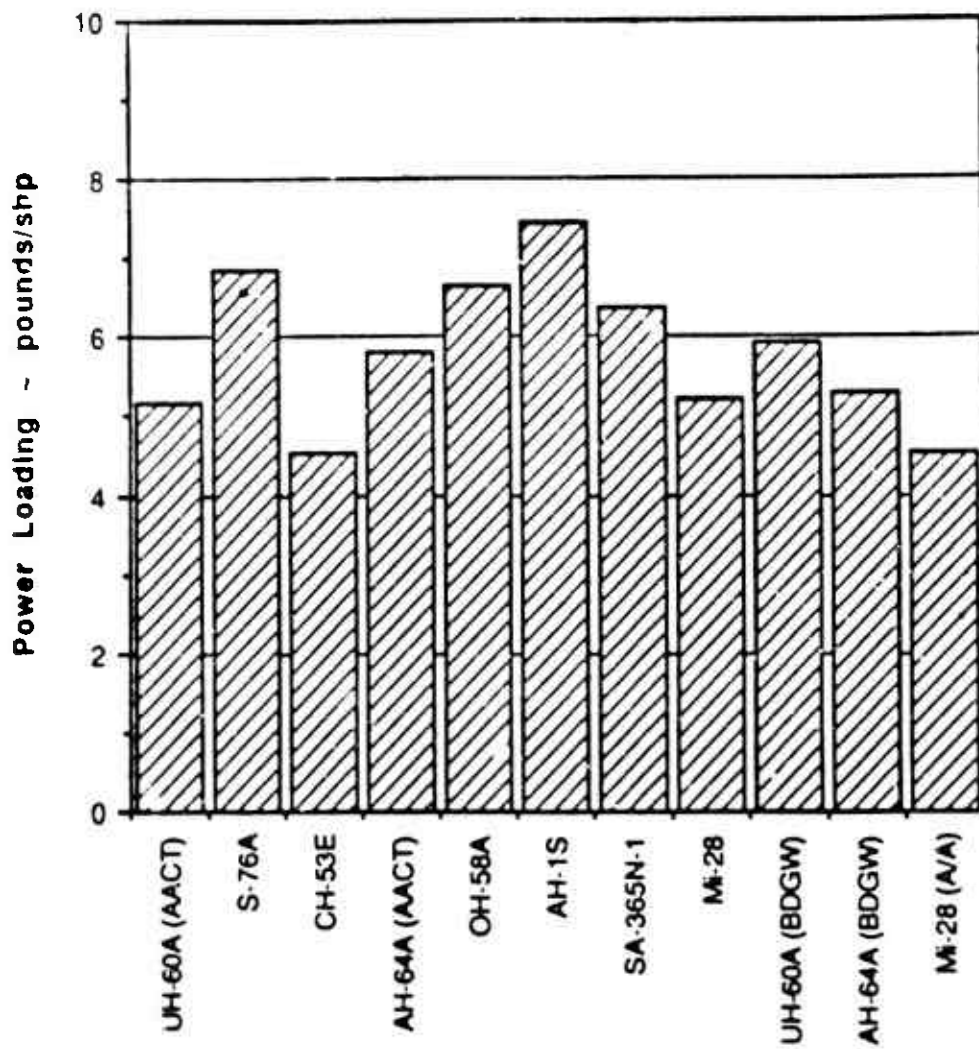


Figure 15. Power Loading Comparison Chart

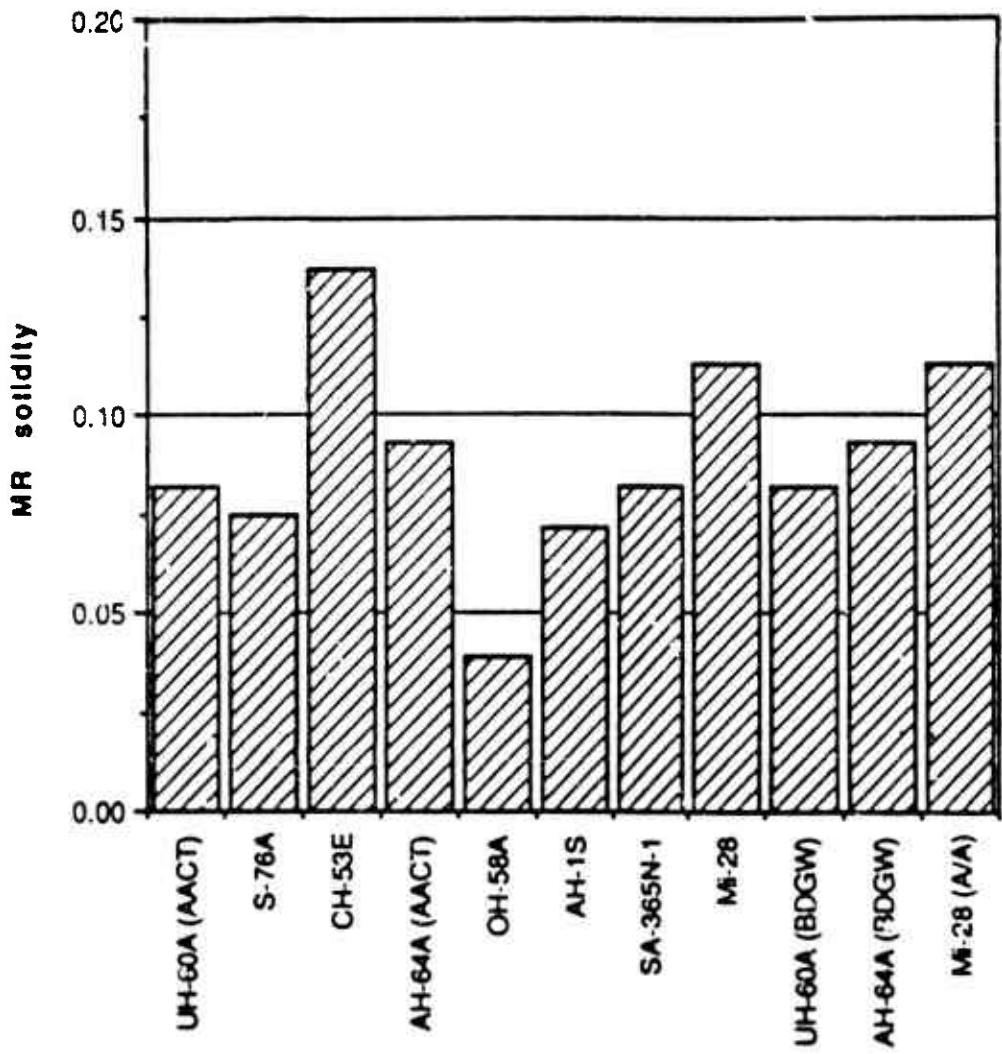


Figure 16. Main Rotor Solidity Comparison Chart

The Lock number (ratio of blade air loading to inertial loading) also displays a wide range of values, but this is expected because rotor blades do not scale directly with gross weight. Most of the aircraft have values around eight, but the CH-53E is highest at 13.57 (Figure 17) followed by the HI-28 at 12.92. The OH-58A is lowest at 4.30 with the AH-1S just ahead at 5.76.

The effect of tip speed, solidity, hinge-offset and Lock number on maneuverability and agility can be assessed by looking at the normalized pitch and roll control sensitivities (Figures 18 and 19). The moment capabilities were calculated using the hub moment calculations of Reference 6. If these values are divided by the pitch and roll inertias, the normalized pitch and roll control sensitivities in radians-per-second-squared-per-degree result. A better measure would have been the classical control powers of radians-per-second-squared-per-inch of stick deflection. Because the heel limits in degrees were not always known, the sensitivities are provided rather than the control powers.

A review of Figure 18 shows that the Apache, Dauphin and S-76A have the highest values of pitch control sensitivity, around 0.13, while the CH-53E is worst at 0.07 radian-per-second-squared-per-degree.

The roll control sensitivities illustrated in Figure 19 are much larger than the pitch values and also show a much greater spread of values. The generally higher values simply reflect the higher pitch inertias of all helicopters (typically, 5x times of the roll value). The extreme spread is dominated by the very high values of the Apache. This is due to the low roll inertia of this configuration. Estimates of the yaw control power were also made. In this case the tail rotor was assumed to have a maximum thrust coefficient/solidity of 0.14. For the fenestron of the SA-365N, the thrust of the fan was based on the annular area and the thrust augmentation due to the duct was set at the classical value of 2.0. The results are plotted in Figure 20. About a two-to-one variation between highest and lowest values is present. The OH-58A and Dauphin were the best while the Super Stallion and HAVOC were the worst.

As the above discussion shows, the helicopters used in this study cover a broad range of characteristics. Yet each aircraft has its own distinct profile or "signature" of attributes. Thus, they provide an excellent test for the M/A methodology developed in the Phase I Study. Because most of these helicopters participated in the AACT activity, the analytical results can be compared to actual flight test data. The fact that these are all contemporary designs ensures that the results are relevant.

The M/A Phase I study showed that the classical design parameters affect M/A in different ways. For example, in some maneuvers low disk loading may be a virtue and in others it may be a liability. Thus, knowledge of these parameters does not allow one to assess the relative maneuverability and agility of a given design. In this report a methodology for assessing M/A capability is developed.

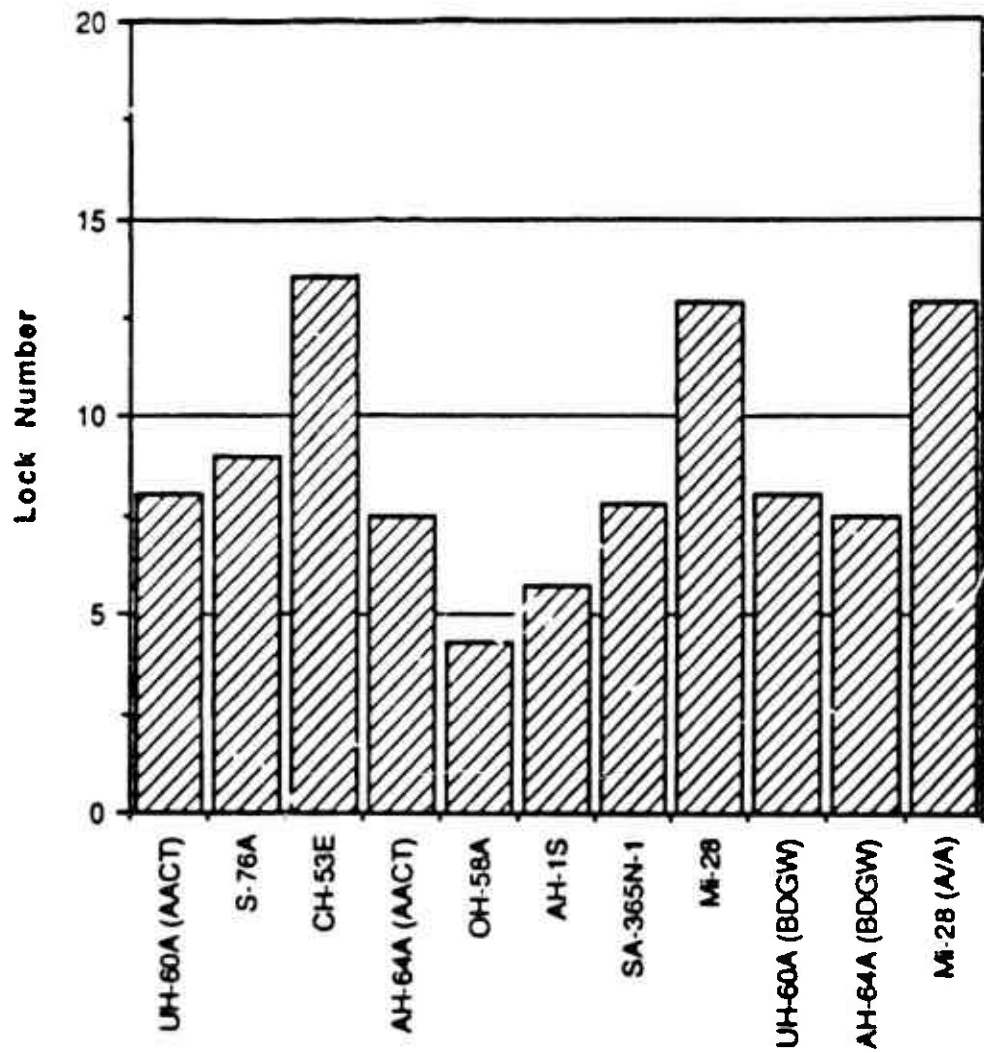


Figure 17. Main Rotor Lock Number Comparison Chart

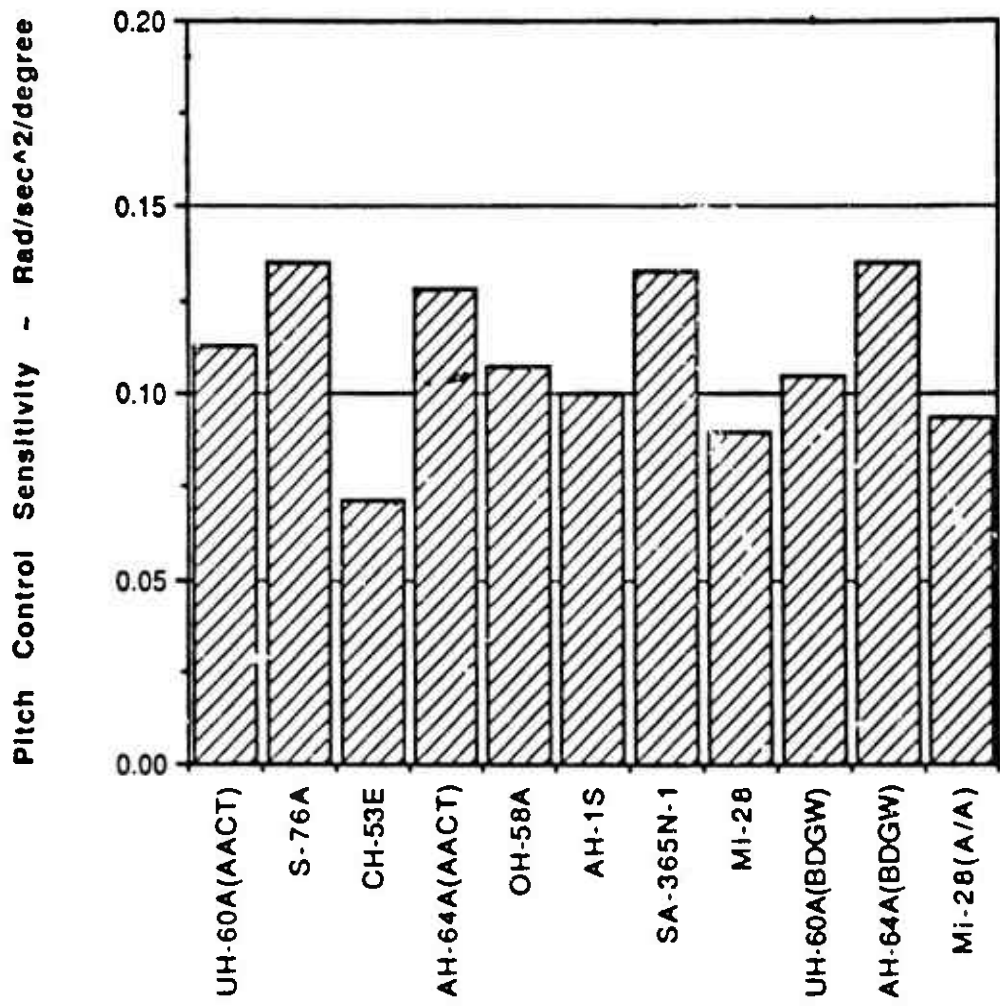


Figure 18. Pitch Control Sensitivity Comparison Chart

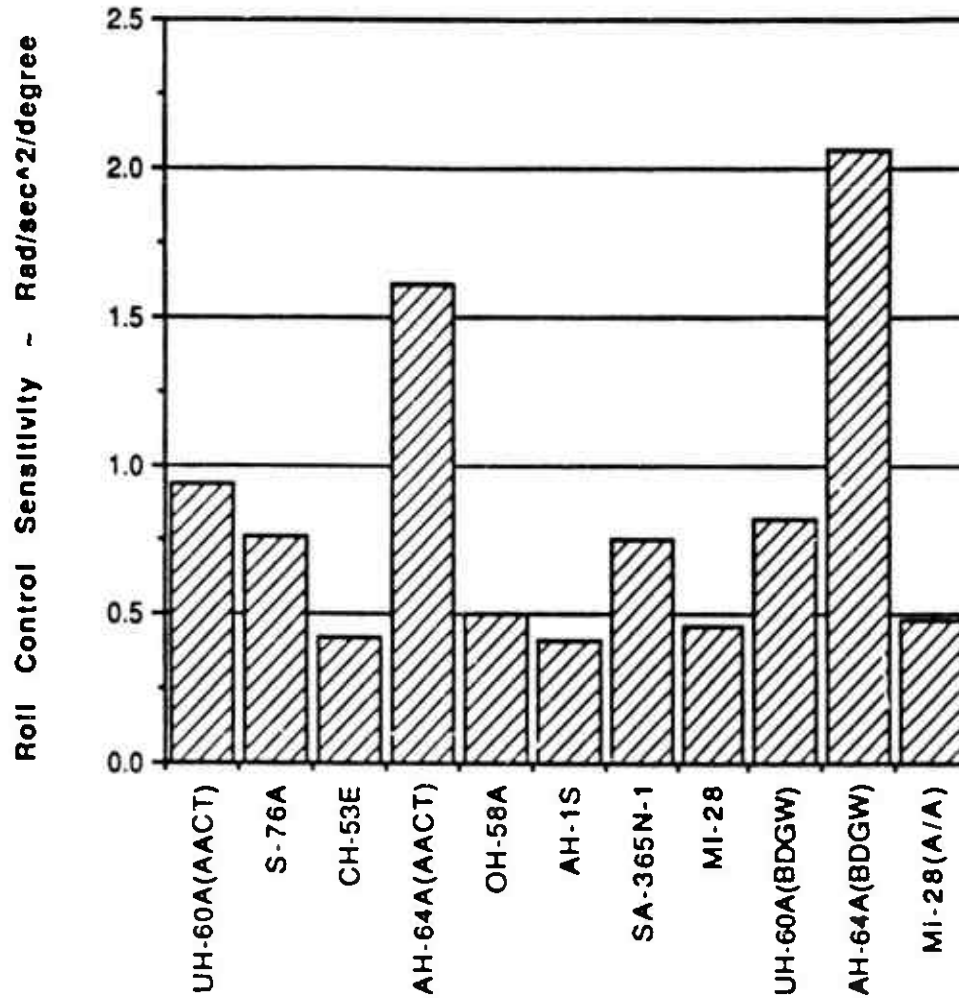


Figure 19. Roll Control Sensitivity Comparison Chart

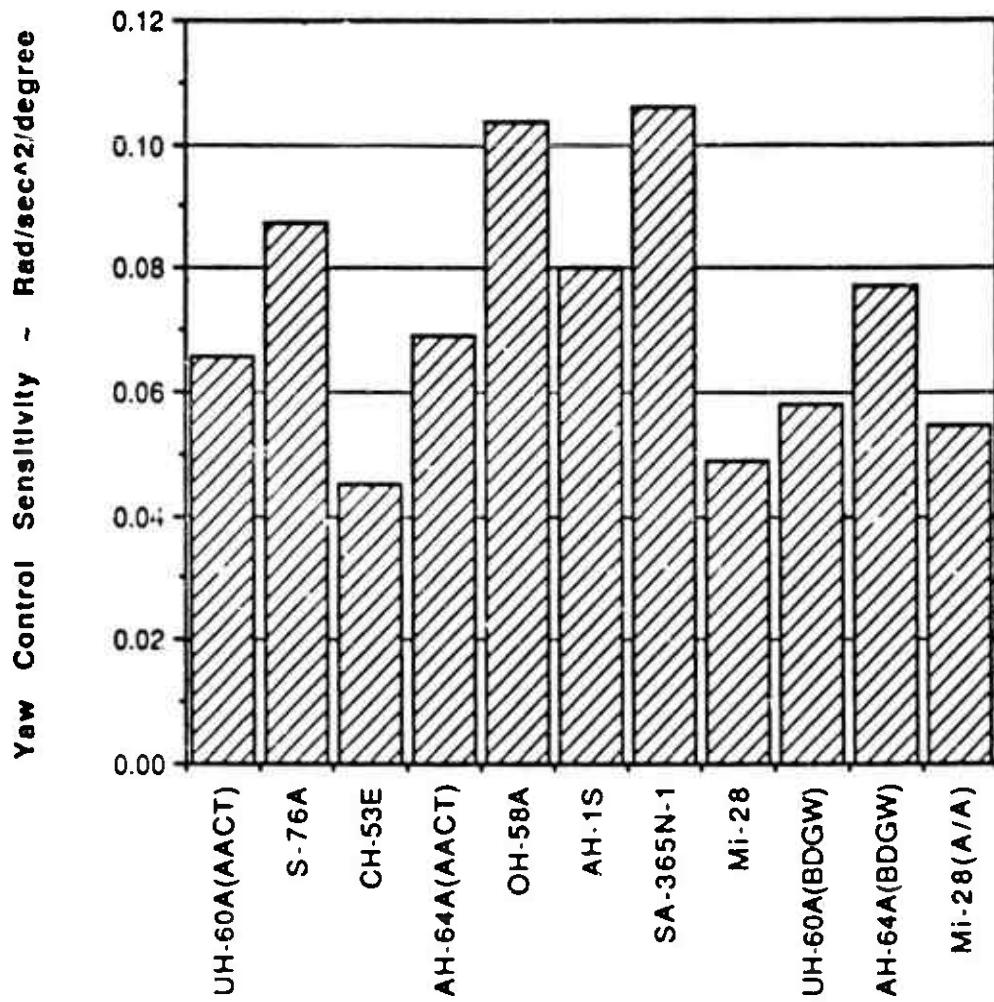


Figure 20. Yaw Control Sensitivity Comparison Chart

Maneuver Controller Description

While the GenHel simulation environment provides the user with a detailed, free-flying model of the helicopter, the process of actually "flying" a maneuver manually is difficult (in an analysis mode and not linked to a cockpit). The engineer must find the control time histories that will result in a specified maneuver. For example, in a symmetrical pull-up, the controls need to be manipulated not only to achieve the desired load factor but also to retain heading and maintain zero roll angle. In order to ease the burden of this task, two auxiliary modules are available in GenHel. One is a trimming autopilot, the other is a maneuver controller.

The trimming autopilot is used to generate "static" data. The trimmer will find the control positions that give the aircraft a specified set of accelerations (typically zero, but not necessarily) and prescribed turn rates, climb rates and velocity. This module was used for maneuvers like the 80 knot steady turn. In this case, the engineer would let the trimmer find the solution for a given bank angle then increase that value and retrim iterating until the power available limit was reached.

The maneuver controller was used for "dynamic" maneuvers like the acceleration from hover to 80 knots. The user specified a desired maneuver profile and the controller would fly the aircraft through the maneuver. The design of this controller is shown in Figure 21. The basic scheme is explicit model following. The commanded profile is sent to shaping filters which define the desired aircraft response. These signals then go to a model-following control system. This contains an inverse model of the aircraft which converts the desired responses into control commands. The inverse model is linear, with the matrix coefficients based on derivatives generated in the GenHel simulation model of that aircraft. The commands are then fed to the GenHel simulation model. Since the simulation, like the aircraft, is nonlinear, the actual responses are compared to the commands and the error used to update the control positions. The controller, then, regulates the error to zero so the resulting aircraft response matches the command profile.

The maneuver controllers do not impose limits on the command response. When flying the maneuvers, the engineer has to inspect the time histories to see if the appropriate limits (power available, pitch attitude, rotor stall boundaries, etc.) have been exceeded. If so, the command profiles are altered and the maneuvers reflown until the appropriate limits are not violated.

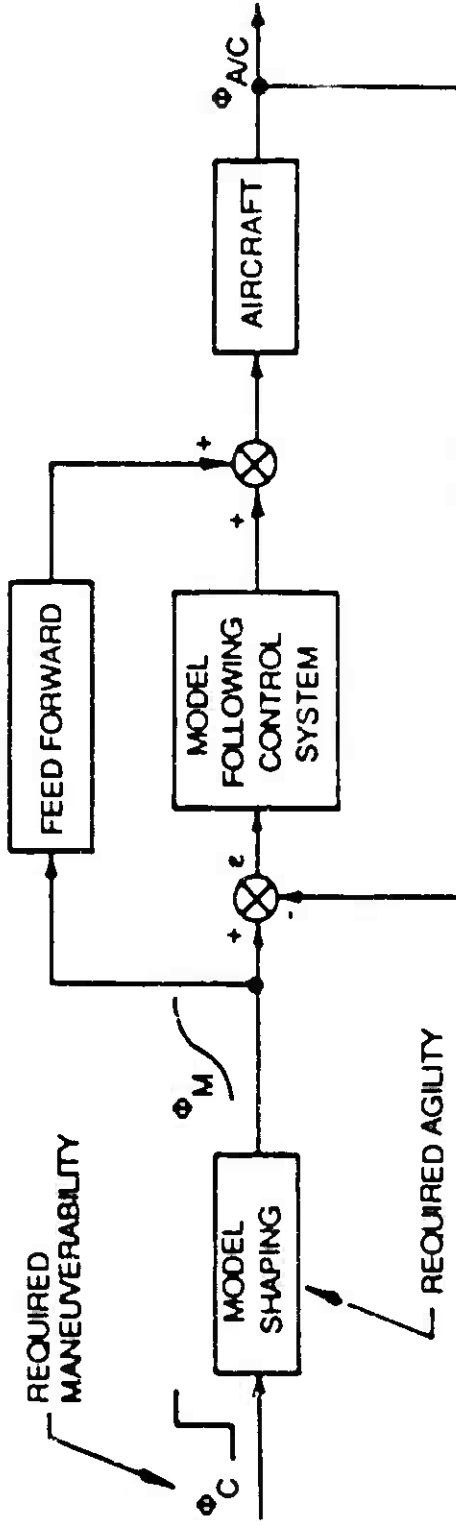


Figure 21. Maneuver Controller Schematic

SIMULATION RESULTS

This section of the report discusses the results of the simulated maneuvers. It is divided into two major parts. The first reviews the results on a maneuver-by-maneuver basis. The second discusses the overall results on an aircraft-by-aircraft basis.

DISCUSSION OF RESULTS FOR EACH MANEUVER

In order to structure this discussion, the fundamental parameter plots for each maneuver will be reviewed individually. The maneuver results will be presented in four parts - a description of the maneuver itself, a listing of the constraints imposed on it, a review of the fundamental parameter and measure-of-effectiveness (MOE) for the maneuver, and a detailed discussion of the simulation results. These detailed discussions will include the Mi-28 parametric study. All of the static data used to calculate the fundamental parameters is provided in Table 4. The fundamental parameters and the maneuver results are summarized in Table 5.

Hover Bob-Up

Maneuver: The hover bob-up/bob-down is used in a threat environment to provide masking. The helicopter climbs vertically, hovers momentarily to activate sensors or weapons, then rapidly descends to remask. Time was not available to analyze both bob-up and bob-down. Since the bob-up and bob-down are really separate maneuvers, sensitive to different parameters, the results of this bob-up study should not be used to imply any bob-down characteristics.

Constraints: This is a "dynamic" maneuver done with the maneuver controller. The helicopter must maintain its position over the ground, must maintain its heading and must stop at 100 feet.

Fundamental Parameter and MOE: The fundamental parameter for this maneuver is the hover maximum thrust to gross weight ratio. The simulation was hovered at increasing gross weights until the main rotor hover power available of Table 3 was reached. This defined the maximum thrust available. Since low speed maneuvers are typically power constrained, the maximum thrust-to-weight ratio was found to be the best normalizing factor. The MOE was defined as the maximum rate-of-climb (ROC) achieved during the maneuver. This is not necessarily the maximum ROC capability of the aircraft since the maneuver requires the aircraft to climb, then slow down and stop at exactly 100 feet.

TABLE 4. STATIC PARAMETER DATA LIST

Static Parameter	UH-60A	B0GW	S-78A	AH-64A	B0GW	OH-58A	AH-1S	CH-53E	SA-366N-1	MB-28
Max ROC (ft/min)	1,710.0	1,327.0	1,020.0	1,140.0	1,450.0	1,650.0	776.0	1,244.0	649.0	1,400.0
Max Thrust (lbs)	23,125.0	23,125.0	11,250.0	20,950.0	20,050.0	3,944.0	11,500.0	76,800.0	10,600.0	31,900.0
Weight (lbs)	14,885.0	18,825.0	8,925.0	16,222.0	14,770.0	2,790.0	9,620.0	56,000.0	6,575.0	22,984.0
MFR-Payload hover (ft)	2,376.0	2,376.0	1,092.0	2,339.0	2,339.0	353.0	1,084.0	10,261.0	1,152.0	3,698.0
Time (sec) hover to 80 lbs	8.3	9.6	11.1	12.25	10.3	11.5	12.0	9.6	11.2	10.5
MFR-Payload 60 lbs (ft)	2,508.0	2,508.0	1,153.0	2,469.0	2,469.0	373.0	1,144.0	10,856.0	1,217.0	3,903.0
MFR-Payload (ft)	1,377.0	1,607.0	611.0	1,675.0	1,497.0	190.0	652.0	6,647.0	696.0	2,451.0
Time (sec) 80 lbs to hover	14.7	13.6	15.0	13.7	13.4	16.0	13.5	12.6	12.7	11.05
ROC (ft/min) 80 lb steady	3,682.0	3,022.0	2,564.0	2,622.0	2,946.0	2,195.0	2,127.0	3,433.0	2,432.0	2,467.0
MFR-Payload 80 lbs (ft)	2,602.0	2,602.0	1,196.0	2,561.0	2,561.0	366.0	1,187.0	11,260.0	1,262.0	4,048.0
MFR-Payload 80 lbs (ft)	954.0	1,031.0	439.0	1,035.0	959.0	139.0	457.0	4,465.0	500.0	1,721.0
MZ (g's) 80 lb steady turn	2.30	1.96	1.60	1.88	2.08	1.67	1.69	1.91	1.71	1.63
Christma hover (non-dm)	0.0587	0.0679	0.0716	0.0759	0.0689	0.0861	0.076	0.0527	0.0721	0.0644

TABLE 4. STATIC PARAMETER DATA LIST (Cont'd)

Static Parameter	UH-60A	BOGW	S-76A	AH-64A	BOGW	OH-58A	AH-1S	CH-53E	SA-365N-1	MH-28
Yaw rate 80 lbs (deg/sec)	33.3	26.8	23.0	30.4	35.1	26.0	27.0	36.5	23.5	27.3
Chignra 80 lb turn	0.1289	0.1318	0.1282	0.1536	0.1570	0.1305	0.158	0.1103	0.1280	0.1288
Chignra 80 lbs (non-dir)	0.0588	0.0687	0.0700	0.0735	0.0665	0.0690	0.0713	0.0541	0.0716	0.0869
Yaw rate 130 lbs (deg/sec)	18.34	15.1	18.2	15.7	18.1	---	12.15	18.25	10.6	14.31
Chignra 130 lb turn	0.1289	0.1269	0.1258	0.1312	0.1338	---	.1161	0.1038	0.1068	0.1114
Chignra 130 lbs (non-dir)	0.0812	0.0712	0.1029	0.0717	0.0853	---	0.0832	0.0550	0.0742	0.0725
NZ mass (lb) 140 lb pull-up	2.48	2.05	1.6	1.95	2.2	---	2.15	2.0	1.5	1.7
Chignra max 140 lb pull-up	0.1325	0.1300	0.1050	0.1300	0.1350	---	0.145	0.1000	0.1050	0.1100
Chignra 140 lbs (non-dir)	0.0422	0.0723	0.0725	0.0723	0.0884	---	0.0627	0.0559	0.0750	0.0751
Time (sec) 180 deg hover turn	4.2	4.5	4.5	4.7	4.8	4.6	4.7	6.8	4.8	5.0
TFluctdy (non-dir)	0.1875	0.1675	0.1719	0.2318	0.2316	0.1216	0.1438	0.1634	0.4003	0.1601

TABLE 5. MANEUVER RESULTS SUMMARY

	BOB UP		ACCEL		DECEL		STEADY CLIMB		STEADY TURN	
	T/W	Max ROC	(avail hover)/hover	Time to Accel	hover/W	Time to Decel	(avail 80 cts)/W	ROC	PU/BL	NE
UH 60A	1.57	1710	0.9214	6.3	0.0936	14.7	0.1122	3662	1.5093	2.3
UH 60A 60GW	1.37	1327	0.5607	9.6	0.0955	13.6	0.0934	3022	1.1386	1.96
AH 64A	1.26	1140	0.4740	12.25	0.1033	13.7	0.0941	2622	1.0400	1.66
AH 64A 60GW	1.42	1450	0.6493	10.3	0.1014	13.4	0.1085	2948	1.2563	2.08
CH 53E	1.41	1244	0.6332	9.6	0.1167	12.6	0.1213	3433	1.9077	1.91
S. 78A	1.26	1020	0.4217	11.1	0.0909	15	0.0648	2564	0.9356	1.6
OH 58A	1.41	1650	0.9632	11.5	0.0881	16	0.0685	2195	1.0465	1.67
AH 15	1.20	776	0.3427	12	0.0866	13.5	0.0750	2127	0.7910	1.69
SA 365N 1	1.21	849	0.3552	11.2	0.1026	12.7	0.0671	2432	1.0002	1.71
Mt 28 6 machine	1.39	1400	0.5924	10.5	0.1086	11.05	0.1012	2467	1.3674	1.63
Mt 28 hp 2400	1.47	1566	0.7173	10.23			0.1173	2664	1.4917	1.67
Mt 28 hp 2850	1.56	1753	0.9160				0.1373	3417	1.6471	1.9
Mt 28 CMR 1.05										
Mt 28 IZ 61.124										
Mt 28 IZ 74.707										

80 DECEL TURN (CTmax 80 CT 80)CT 80	130 DECEL TURN (CTmax 130 CT 130)CT 130		140 PULL UP (CTmax 140 CT 140)CT 140		HOVER TURN	
	Passdot 80	Passdot 130	Passdot 130	Max f/z	Max f/z	Time to Turn
1.1997	33.3	1.1062	19.34	1.1302	2.45	1.705
0.9165	26.9	0.7623	15.1	0.7981	2.05	1.394
1.0696	30.4	0.8298	15.7	0.7981	1.95	1.317
1.3609	35.1	1.0490	16.1	1.0331	2.2	1.437
1.0388	36.5	0.6673	16.25	0.7889	2.0	1.061
0.6029	23	0.2224	10.2	0.4683	1.6	1.770
0.6910	26					2.270
1.1879	27	0.6667	12.15	1.3126	2.15	1.479
0.7877	23.6	0.4367	10.6	0.4000	1.5	0.942
0.6924	27.3	0.5366	14.31	0.4647	1.7	
1.0296	30.6	0.7035	16.5	0.6365	1.92	1.047
						0.657
						4.75
						6.23

Simulation Results: The hover bob-up fundamental parameter plot is shown in Figure 22. This shows the maximum rate-of-climb achieved during the bob-up to 100 feet versus the maximum hover thrust to gross weight ratio. Ten data points are shown, one for each of the study aircraft plus the UH-60A and AH-64A at their BDGW. In addition, the trend line from the M/A Phase I study is also presented. Note that all these data are for sea level standard conditions. Significantly this plot shows that the fundamental parameter of thrust/weight does indeed collapse the data from this wide variety of aircraft onto a single line. The only two exceptions are the CH-53E and the OH-58A, the largest and smallest, respectively, of the helicopters evaluated. In addition, the maximum thrust available was limited by power available in all cases. The trend line from the M/A Phase I study is somewhat higher than the current data, due to the differences in the way the available power was handled. In the Phase I study, all the available power was utilized by the rotor, while in this study appropriate tail rotor and accessory losses were accounted for.

In examining these data more closely, it can be seen that the CH-53E is below the trend line, the AH-64A at its BDGW is on the line and the OH-58A is above, yet all have about the same thrust/weight ratio. The reason for this is explainable in the dynamic nature of the maneuver.

Review of the time history data shows that the high disk loading Super Stallion reaches its power limit quickly in the maneuver and is still increasing its ROC when the collective has to be lowered to stop at 100 feet. The Kiowa, on the other hand, has a very low disk loading. It takes longer to reach its power limit and is in a steady climb by the time the collective is lowered. The disk loading and power loading differences of these two helicopters result in a similar thrust/weight ratio, so their steady rate-of-climb would be about the same, but the dynamic effects of the lower disk loading gives the Kiowa a quickness advantage in this maneuver.

The effect of additional power on the Mi-28 hover bob-up is shown in Figure 23. Total aircraft power available was evaluated at values of 4400, 4800 and 5300 shp. The resulting powers available to the main rotor were 3696, 4032 and 4452 shp, respectively. The Mi-28 improvement in ROC falls along the basic trend line established by the other aircraft. The 4032 shp point represents a 9-percent increase in power available and provides a 13-percent improvement in ROC. The 4452 shp case shows that a 20-percent power increase yields a 25-percent higher ROC.

Acceleration from Hover to 80 Knots

Maneuver: Since the best maneuvering speed for a helicopter is in the power bucket (typically 70 to 80 knots), it is important for an aircraft to be able to accelerate rapidly from low NOE speeds to this maneuvering speed. This maneuver is done by lowering the nose and applying power. The time to accelerate is basically limited by power absorbed by the rotor.

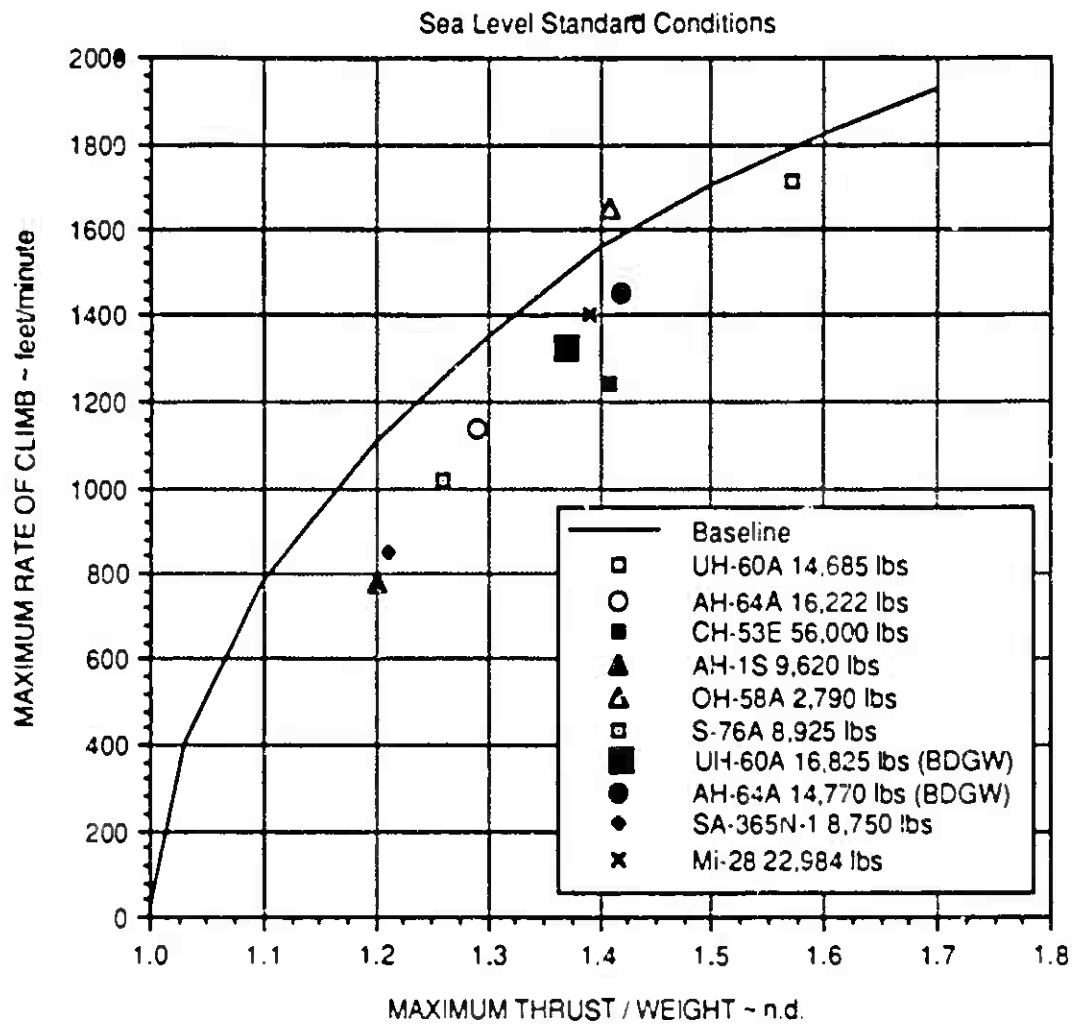


Figure 22. Hover Bob-Up Summary Chart

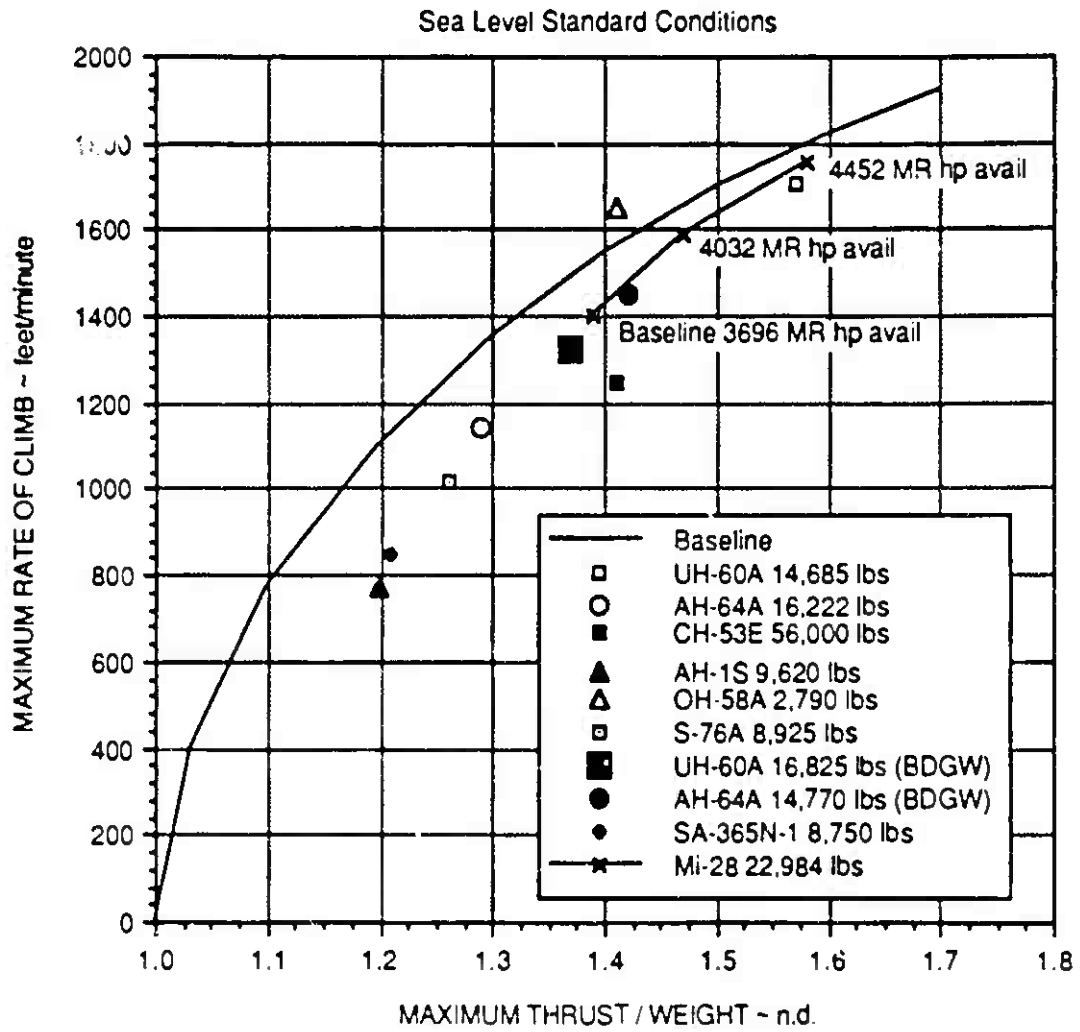


Figure 23. Effect of Increased Power on Mi-28 Hover Bob-Up

Constraints: In GenHel, this is also a "dynamic" maneuver done with the maneuver controller. Limitations imposed included the following:

- a) Altitude must be held constant.
- b) Heading must be held constant.
- c) Power available to the rotor could not exceed the amount available at 40 knots.
- d) Nose down pitch altitude could not exceed 25 degrees.

The first two constraints are obvious. The third one was imposed to limit the power utilized at higher speeds. Since the power available varies with airspeed, the value at 40 knots was selected. The last constraint was based on realistic piloting constraints. Typically, excessive nose down attitudes are not used by pilots because of lack of visibility and physical discomfort. In order to treat all the helicopters fairly, a 25-degree nose down limit was imposed on all of them.

Fundamental Parameter and MOE: Being a low speed maneuver and hence dominated by power available, the acceleration to 80 knots uses the normalized power margin as the fundamental parameter. This is the main rotor power available in hover minus the hover power required, divided by the hover power required. While the performance is obviously a function of the power available over the whole speed range of the maneuver, the M/A Phase I study showed that the data collapsed well using the hover power margin. The MOE was the time to get to 80 knots.

Simulation Results: Figure 24 shows the hover acceleration to 80 knots fundamental parameter plot. This shows the time to get to 80 knots versus the normalized hover power margin. The same ten data points are shown as for the hover bob-up along with the trend line from the Phase I study.

For this maneuver, the fundamental parameter collapses the data, but not as well as the hover bob-up. The reason for this is that more constraints are applied.

Review of the time history data shows that all the aircraft except the heavy-weight Apache are restricted initially by the 25-degree nose-down pitch attitude limit. At the end of the maneuver, the nose comes up as the power limit is reached for each helicopter. Because of the impact of individual aircraft encountering constraints at different times, it is instructive to examine the maneuver histories on an individual basis.

QH-58A - This helicopter rapidly rotates down to the pitch attitude limit and stays there for about two-thirds of the acceleration interval. The nose comes up and the Kiowa is on its power limit for the remaining one-third of the maneuver.

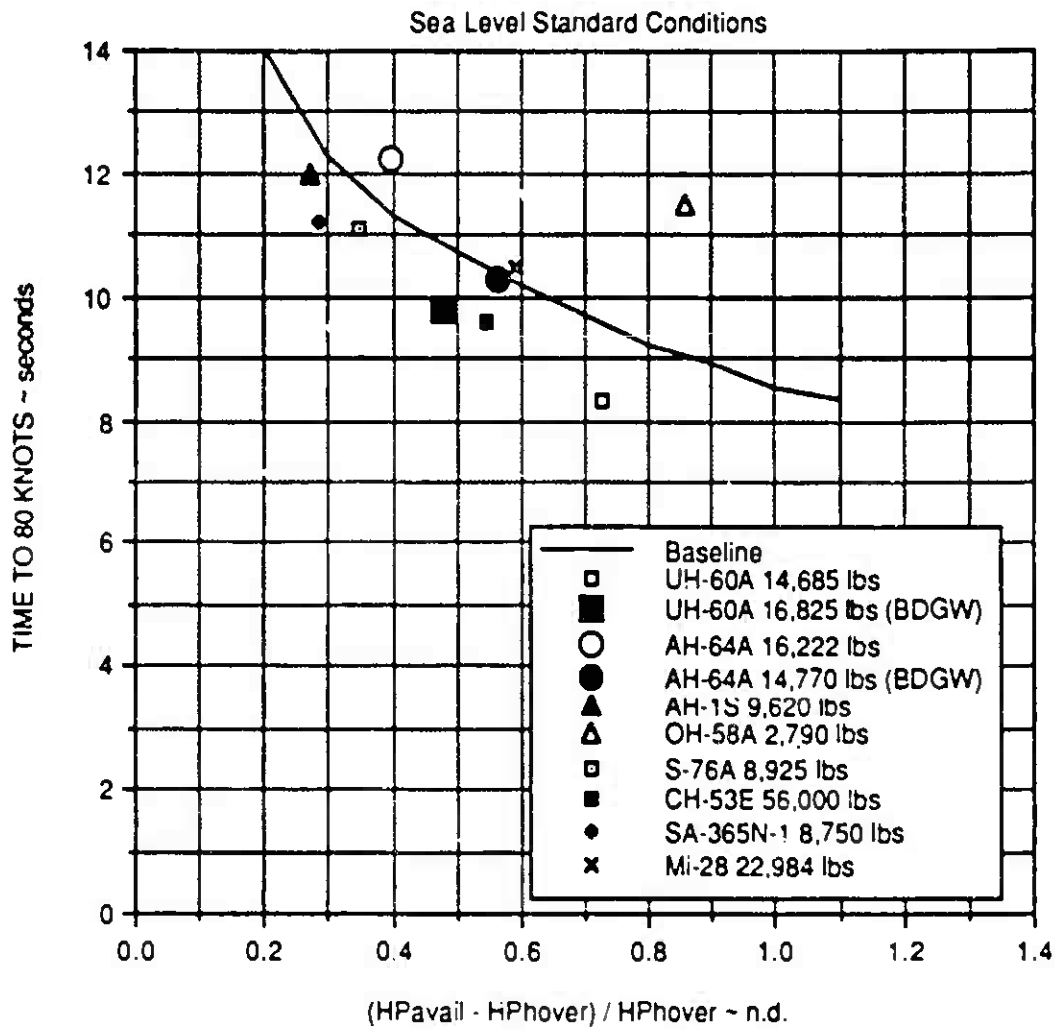


Figure 24. Acceleration from Hover to 80 Knots Summary Chart

SA-365N - The Dauphin noses over and sits on the pitch attitude limit for the first one-third of the maneuver. It reaches its power limit in this nose-down state and the nose comes up for the remainder of the acceleration. The SA-365N is power-limited for the last three-fourths of the maneuver.

S-76A - The S-76 noses down but is on the 25 degree attitude limit for only a short time before it becomes power limited. The nose comes up and the aircraft remains power limited for about 80 percent of the acceleration interval.

AH-1S - The Cobra noses over and stays on the -25 degree limit for about one-half of the acceleration interval and is power limited for the other half.

UH-60A - The lightweight (14,685 pounds) AACT BLACK HAWK rotates quickly to the nose-down attitude limit and stays there for approximately one-half of the maneuver. As velocity increases, the aircraft reaches its power limit and the nose begins to migrate upward with increasing airspeed to stay on that limit for the rest of the acceleration. The heavier (16,825 pounds) BDCW helicopter follows a similar profile, but it is slower in rotating to the nose-down limit and reaches the power limit sooner. At this point, the BDCW aircraft nose migrates upward with increasing airspeed to stay on the power limit.

AH-64A - The lightweight (BDCW) Apache gets to the -25 degree pitch attitude limit and stays there for about one-third of the maneuver. The remainder of the acceleration is power limited, with lower pitch attitudes. Longitudinal flapping as high as -10 degrees is achieved. The heavier (AACT) aircraft never gets to the pitch attitude limit, but gets down to -12 degrees. It is power limited for the last 60 percent of the maneuver.

Mi-28 - The HAVOC rotates down to the -25 degree limit and stays there for most of the maneuver, with the nose coming up to -20 degrees as the power limit is reached at the end of the acceleration. The results of the power available parametric study are illustrated in Figure 25. The same total aircraft powers were used as before, yielding values of main rotor power available of 3903, 4257 and 4701 shp at 40 knots. This study was very instructive in the effect of maneuver constraints. The 4257 shp case improved the acceleration time by only 0.27 second. This was due to the -25 degree pitch attitude limit, which prevented the aircraft from using all of the power available. As a consequence, the 4701 shp configuration had no improvement in the acceleration time compared to the 4257 shp case. The nose-down attitude constraint limits the maneuver capability, regardless of the power available.

CH-53E - The Super Stallion rotates down to the attitude limit and stays there for about one-half of the maneuver. During the last half the power limit is reached and the nose comes up.

Examination of the Figure 25 Fundamental Parameter Chart shows that the data are well collapsed except for the OH-58A. The excessive time for the OH-58A acceleration may be due in part to the poor longitudinal trim correlation discussed in Appendix E. While a basic trend exists, the inherent differences between the aircraft and the effects of the imposed operational constraints result in more scatter than the Phase I data.

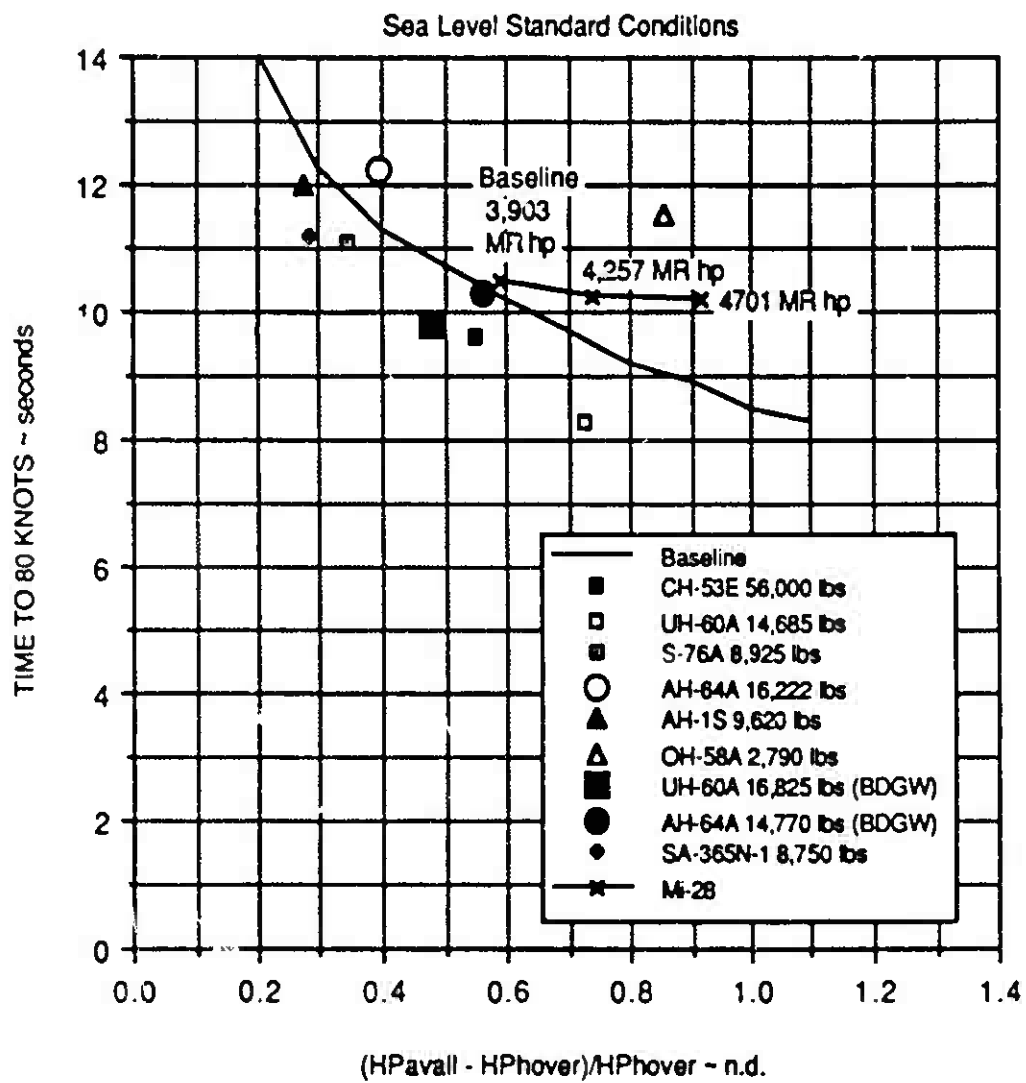


Figure 25. Effect of Increased Power of Mi-28 Acceleration from Hover to 30 Knots

Deceleration from 80 Knots to Hover

Maneuver: This maneuver is basically a masking one in which the helicopter decelerates airspeed quickly from 80 knots to hover. Typically, this maneuver is flown aggressively to mask the helicopter from potential threats or to position it for an air-to-air encounter with a crossing threat. This maneuver is performed by pitching the aircraft up and using the aft-directed rotor thrust to produce deceleration. To avoid ballooning to a higher altitude, the collective pitch must be reduced.

Constraints: This is also a "dynamic" maneuver using the GenHel maneuver controller.

Realistic constraints applied to this maneuver were:

- a) Altitude must be held constant.
- b) Rotor could not be over-speeded - only driven to zero-torque autorotation.
- c) Nose-up pitch attitude could not exceed 25 degrees.
- d) Rotor power required could not exceed the hover power available as shown in Table 3. This was done because some of the aircraft continued to decelerate at low speed using high power.

The first constraint avoids the natural tendency of the aircraft to gain altitude when rotated to nose-up attitudes. The second one was imposed because it is unlikely that the pilot will want to decouple the rotor from the engines by over-speeding it when he is in the tactical environment. The pitch attitude limit was added because of visibility and comfort reasons as was done in the previous acceleration maneuver. The power limit was added to avoid having the helicopters reach hover with large nose-up attitudes.

Fundamental Parameter and MOE: For this maneuver, the fundamental parameter is the hover power required divided by the gross weight. This did not normalize the data as well as the previous maneuvers, but a definite trend was present. The MOE was the time to do the maneuver.

Simulation Results: This maneuver showed more variety in how the eight different helicopters responded than the previous two. In general, the helicopters would nose-up until autorotation limited. As the aircraft slowed down, the nose-up attitude would increase until the 25-degree limit was reached. At the end of the maneuver, the nose would come down, sometimes forced by the hover power available limit. As a consequence the data is more scattered, as shown in Figure 26. Review of the time history data for each aircraft highlights the individual "signature" each type has for this maneuver.

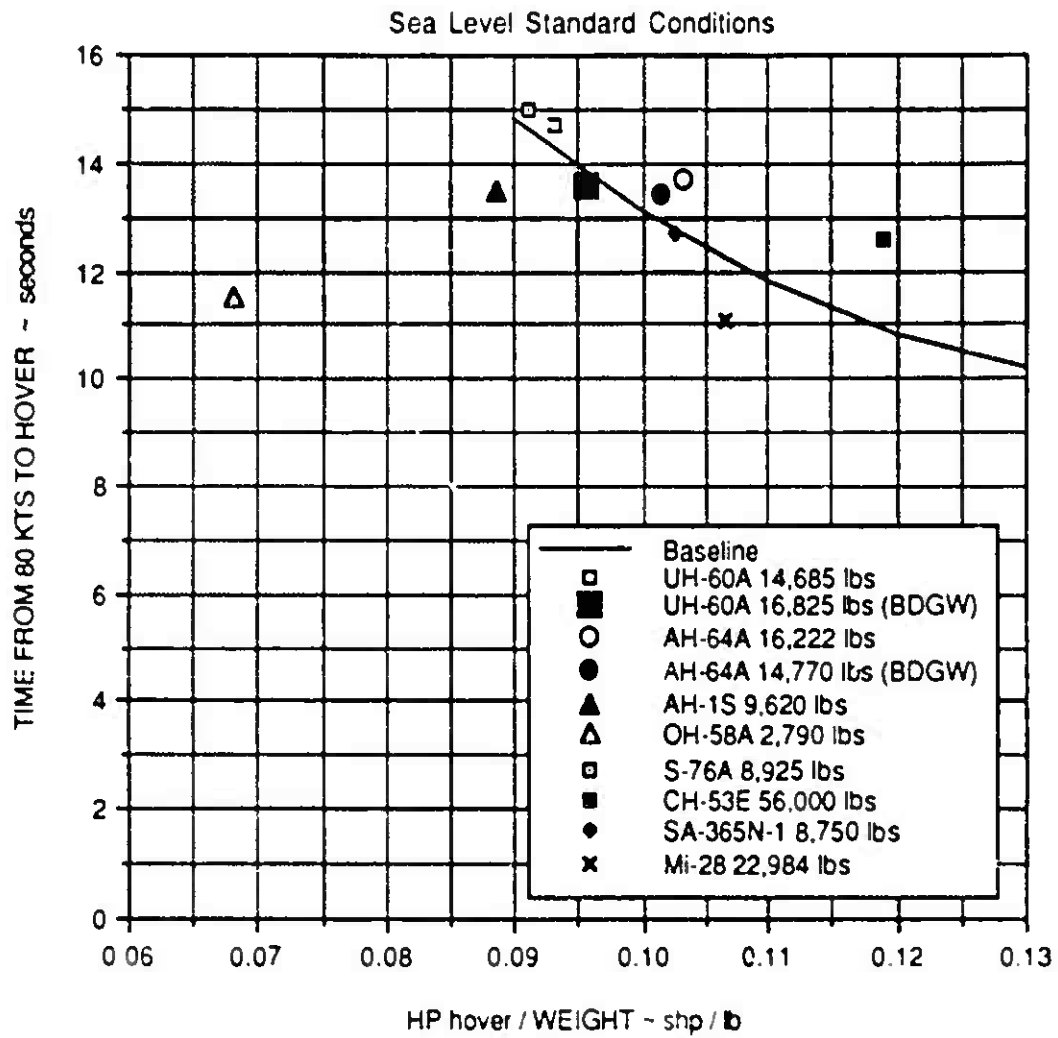


Figure 26. Deceleration from 80 Knots to Hover Summary Chart

OH-58A - The Kiowa is autorotation limited for most of the maneuver, never getting to the 25-degree nose-up pitch attitude limit. At the end of the maneuver, the nose is forced down by the hover power available limitation.

SA-365N - For this French helicopter, the initial pitch-up is limited by autorotation for about 25 percent of the maneuver time. The attitude then increases to the attitude limit until the end of the maneuver. This aircraft is not limited by the hover power constraint.

S-76A - The S-76A behavior is similar to the Dauphin. The initial pitch-up is autorotation limited for 15 percent of the maneuver. The nose comes up as the aircraft slows and is at the limit until hover is reached. The hover power available was not a limiting factor.

AH-1S - The Cobra is restricted by all of the limitations. In the initial part of the flare, the nose pitches up and is limited by autorotation for about one-third of the deceleration time. As the AH-1S slows, the nose comes up further and hits the 25-degree attitude limit for about ten percent of the maneuver time. At the end, the nose is driven down by the requirement to not exceed the hover power available.

UH-60A - The UH-60A at its AACT weight was on the autorotation limit initially for about ten percent of the maneuver time. As the helicopter slowed, it was able to gradually increase its nose-up attitude until the limit was reached. The hover power limit was not encountered at the end of the maneuver. The BDGW case was very similar. The helicopter was on the autorotation limit a little longer (15 percent of the maneuver) and all of the maneuver was somewhat more gradual. Again, the hover power available was not a limitation.

AH-64A - With similar disk and blade loadings compared to the S-76A and UH-60A, the Apache (both AACT and BDGW) performed the deceleration in a like manner. The initial flare was autorotation limited for about 10-15 percent of the maneuver time, then attitude limited in the middle of the deceleration. The hover power available did not constrain the pitch attitude at the end of the maneuver for either weight.

MI-28 - The higher disk loading of the Soviet vehicle results in it only touching the autorotation limit and then staying on the pitch attitude limit for most of the deceleration until the end when the nose drops to achieve hover. The hover power available constraint was not a limiting factor.

No parametric evaluation of this maneuver was done since engine power available was not a factor.

CH-53E - The big Super Stallion simply noses-up to 25 degrees and stays there for most of the maneuver with the nose coming down at the end. It was not restricted by either the autorotation boundary or the hover power available constraint.

This maneuver is a good illustration of the interaction between the individual helicopter characteristics and the realistic constraints. The low disk loading OH-58A is autorotation limited for most of the deceleration and never has a pitch attitude higher than 22 degrees. Aircraft with higher disk loading are only autorotation limited initially, then pitch attitude constrained. The higher disk loading CH-53E never gets to the autorotation boundary. At the end of the maneuver, some of the helicopters are constrained by the hover power available limit, but others are not. This interaction between the vehicles' intrinsic design features and reasonable operational limits results in the scatter shown in Figure 26.

80-Knot Steady Climb

Maneuver: Good bucket-speed climb performance is very important for scout/attack helicopters, especially in air-to-air encounters. The ability to quickly climb to catch an enemy or, alternatively, to be able to climb quickly to avoid an engagement is one of the most important attributes that a combat helicopter could have.

Constraints: This is a static maneuver done using the trimming autopilot. No particular constraints are applied except that the helicopter is trimmed wings level in a steady climb.

Fundamental Parameter and MOE: The fundamental parameter is the normalized power margin. This is the power available at 80 knots minus the level flight trim power required, divided by the trim power. The MOE is the maximum rate-of-climb achieved. For this study, the main rotor power available and power required were used, as shown in Table 3.

Simulation Results: The fundamental parameter plot is shown in Figure 27. Although this is a "static" maneuver, the data shows some scatter but compares well to the baseline from the M/A Phase I study. The BLACK HAWK and S-76A do slightly better than the trend while the OH-58A and Mi-28 are worse. The OH-58A is beyond its bucket speed at 80 knots while the Mi-28 was evaluated in a high-drag, ATG configuration.

The effect of increased power available on Mi-28 performance is shown in Figure 28. The improvement in ROC is just as expected, matching the basic trend of the other aircraft and the baseline Phase I study. However, an offset still remains, indicating a lower climb efficiency than most of the other helicopters.

80-Knot Steady Turn

Maneuver: The bucket-speed level turn is a critical tactical maneuver, both for air-to-air and air-to-ground missions, and should be a critical design parameter.

Constraints: This is a "static" maneuver, flown coordinated at both constant altitude and constant airspeed.

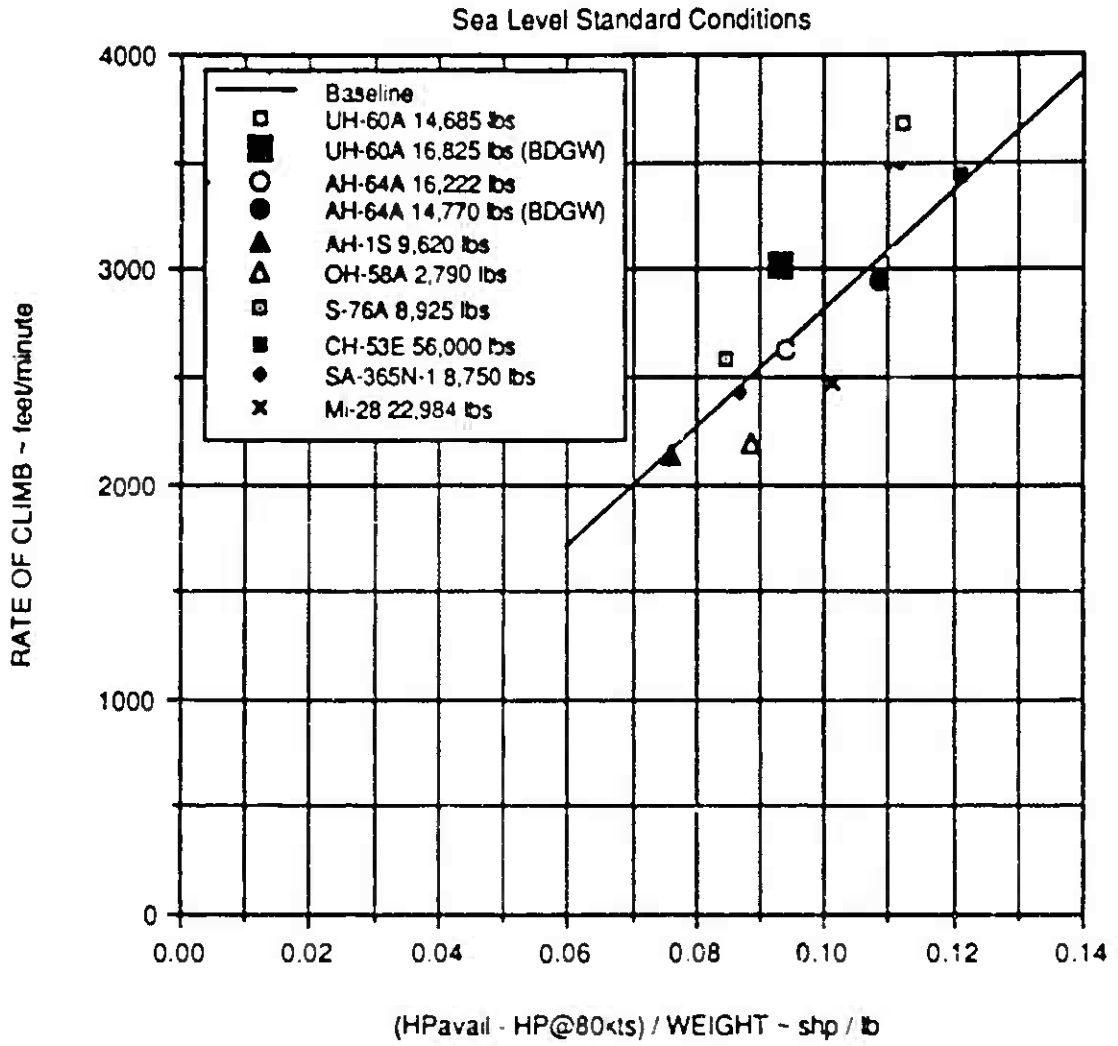


Figure 27. 80-Knot Climb Summary Chart

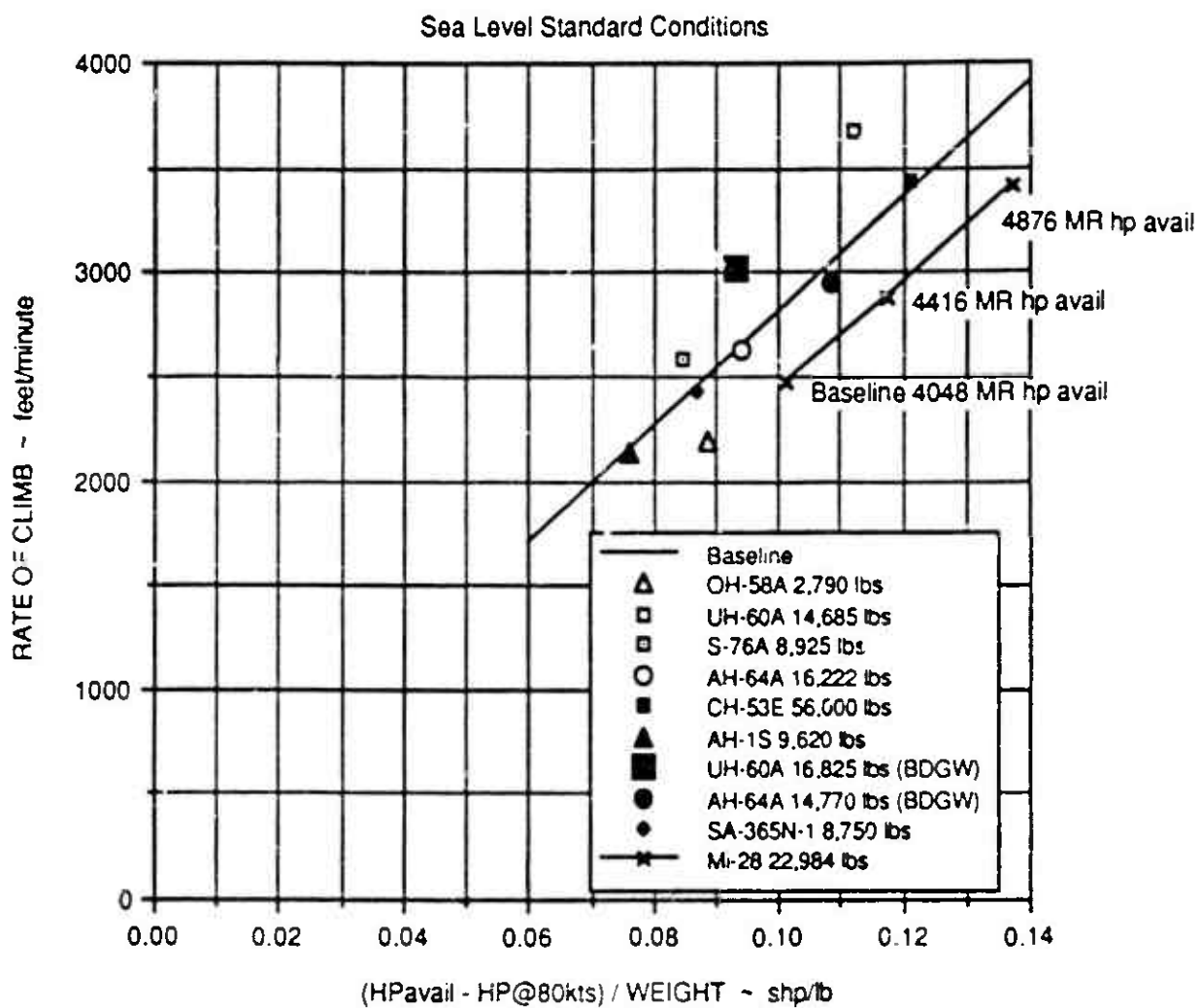


Figure 28. Effect of Increased Power on Mi-28 80-Knot Steady Climb

Fundamental Parameter and MOE: This mid-speed steady turn is dependent on both rotor thrust capability and on excess power available. The fundamental parameter is power loading over blade loading. Power loading was defined as main rotor power available at 80 knots divided by gross weight while the blade loading was defined non-dimensionally as $2 C_T/\sigma$ in hover. The MOE was maximum load factor achieved.

Simulation Results: The simulation results are shown in Figure 29. Five of the ten aircraft trend well and match the M/A Phase I baseline data. The AH-1S and AACT BLACK HAWK are somewhat better while the Dauphin, Mi-28, and CH-53E are worse. In all cases, the load factor capability was power limited.

The results of the Mi-28 parametric study (Figure 30) are very revealing. A 9-percent increase in power available only improves the load factor capability by 0.04g, while a 20-percent increase produces only 0.07g. This is clearly an indication of rotor stall and shows that at 80 knots rotor thrust capability begins to have a significant effect on the maneuvers. In other words, the thrust capability and power available need to match. An excess of either is not beneficial to this maneuver.

80-Knot Decelerating Turn

Maneuver: The decelerating turn is very important in air-to-air combat. Basically, it utilizes the kinetic energy of the aircraft to improve turn capability. The maneuver is entered at mid to high speeds with the objective of turning as quickly as possible, without regard for the exit speed. Once the turn is entered, the rotor angle-of-attack is increased while collective pitch is lowered, putting the rotor in an autorotative state to capitalize on the higher thrust that this permits.

Constraints: This is a "static" maneuver, done using the trimming autopilot. The helicopter was trimmed in a coordinated turn at 80 knots. The nose was raised to provide deceleration until it reached a zero torque autorotation. Then the bank angle was increased and the process repeated until the rotor reached incipient stall, defined as having a rotor stall parameter, bC_{Qd}/σ , of 0.004. Thus, the trimmer generated the highest turn rate/deceleration possible with the rotor simultaneously in autorotation and at its stall boundary.

Fundamental Parameter and MOE: The fundamental parameter is the nondimensional thrust margin, defined as the maximum C_T/σ available minus the level flight trim value, divided by the trim value. Turn rate was used as the MOE.

Simulation Results: The 80-knot decelerating turn results are plotted in Figure 31. No baseline trend line was available from the M/A Phase I Study. The data are well collapsed, showing that the fundamental parameter normalizes the results properly. The CH-53E does better than expected while the AH-1S is worse. The high disk loading of the Super Stallion requires a higher rotor angle-of-attack to produce autorotation which improves its deceleration capability while the AH-1S shows the opposite effect due to its low disk loading. The OH-58A should also be below the trend, but 80 knots is well above its bucket speed, so it suffers a disproportionate loss in maximum C_T/σ capability.

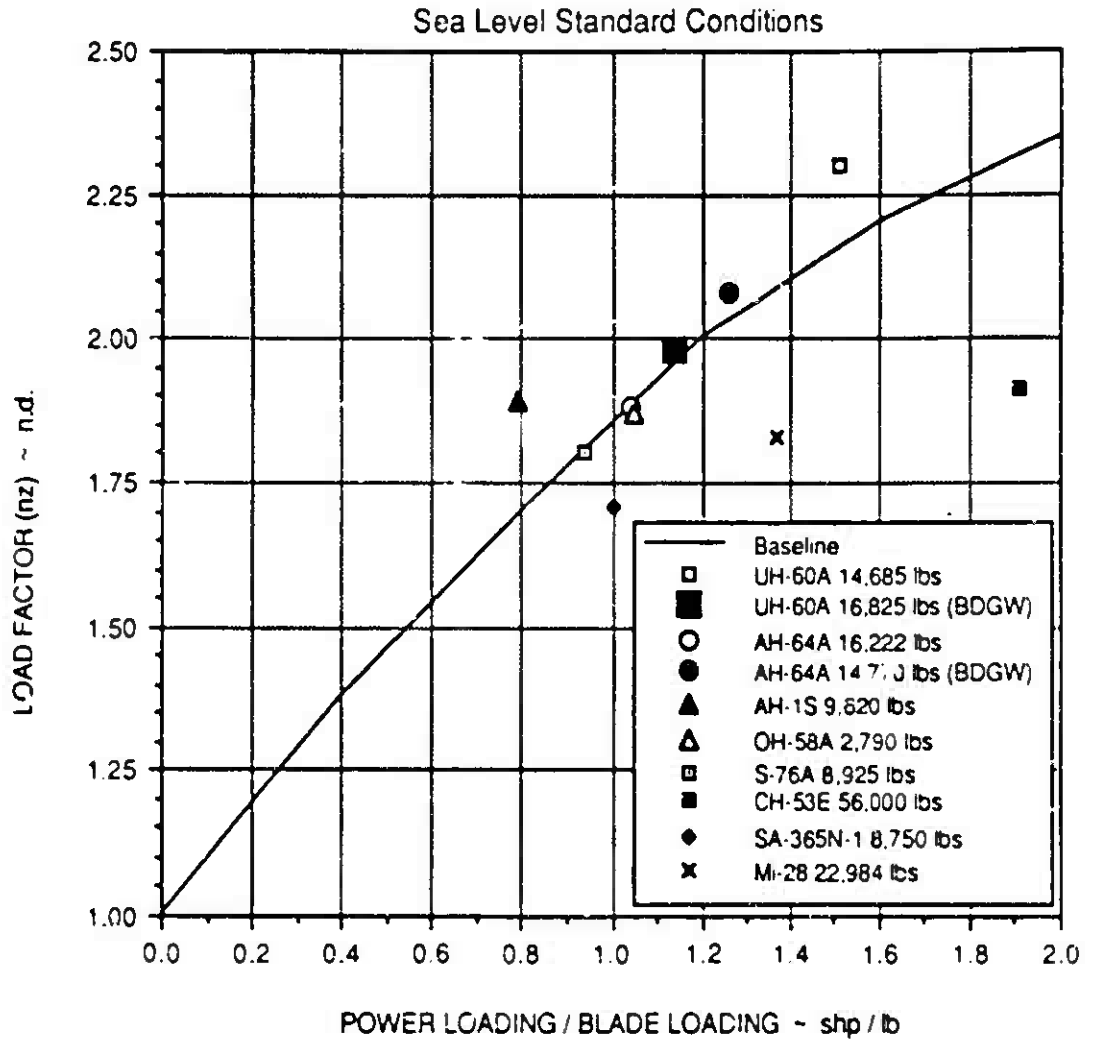


Figure 29. 80-Knot Steady Turn Summary Chart

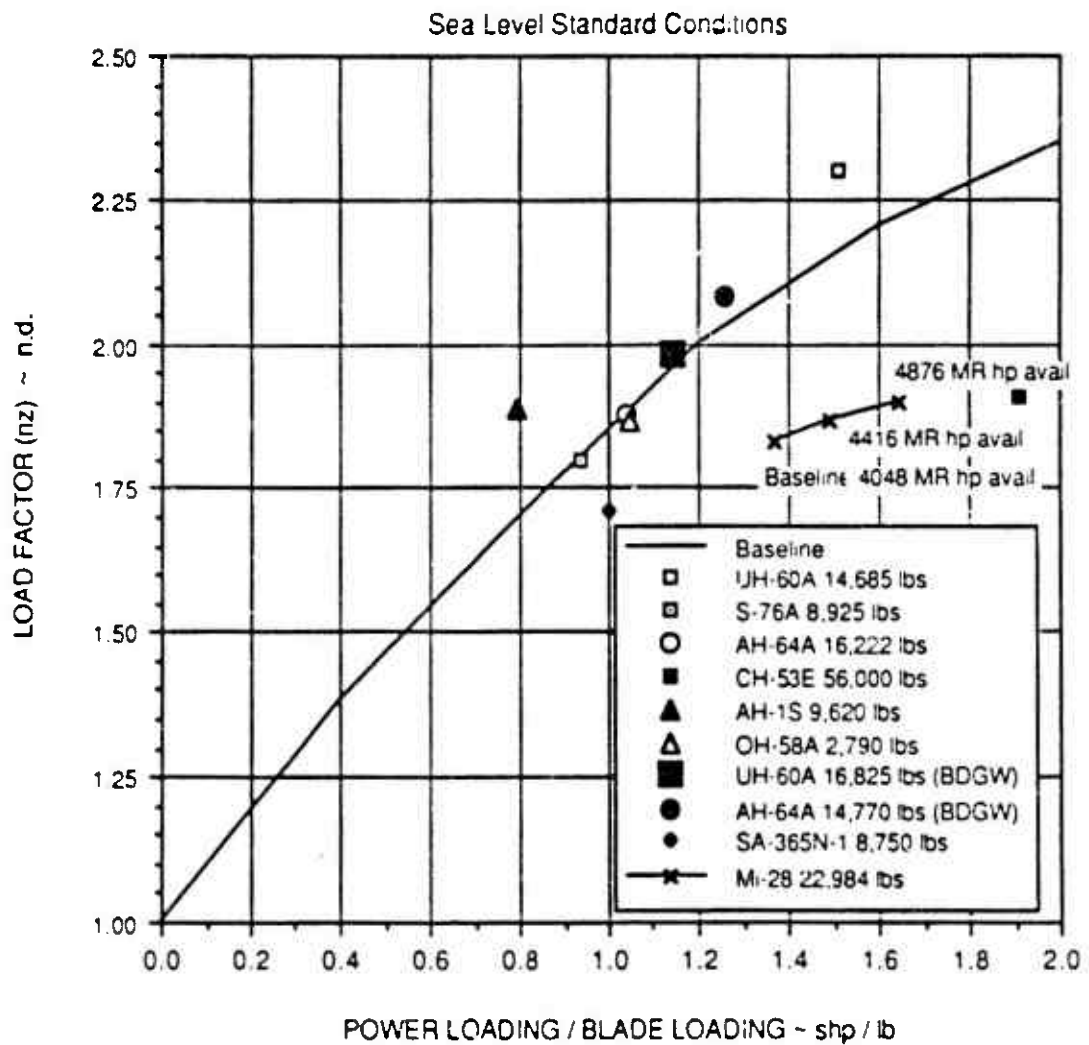


Figure 30. Effect of Increased Power on Mi-28 80-Knot Steady Turn

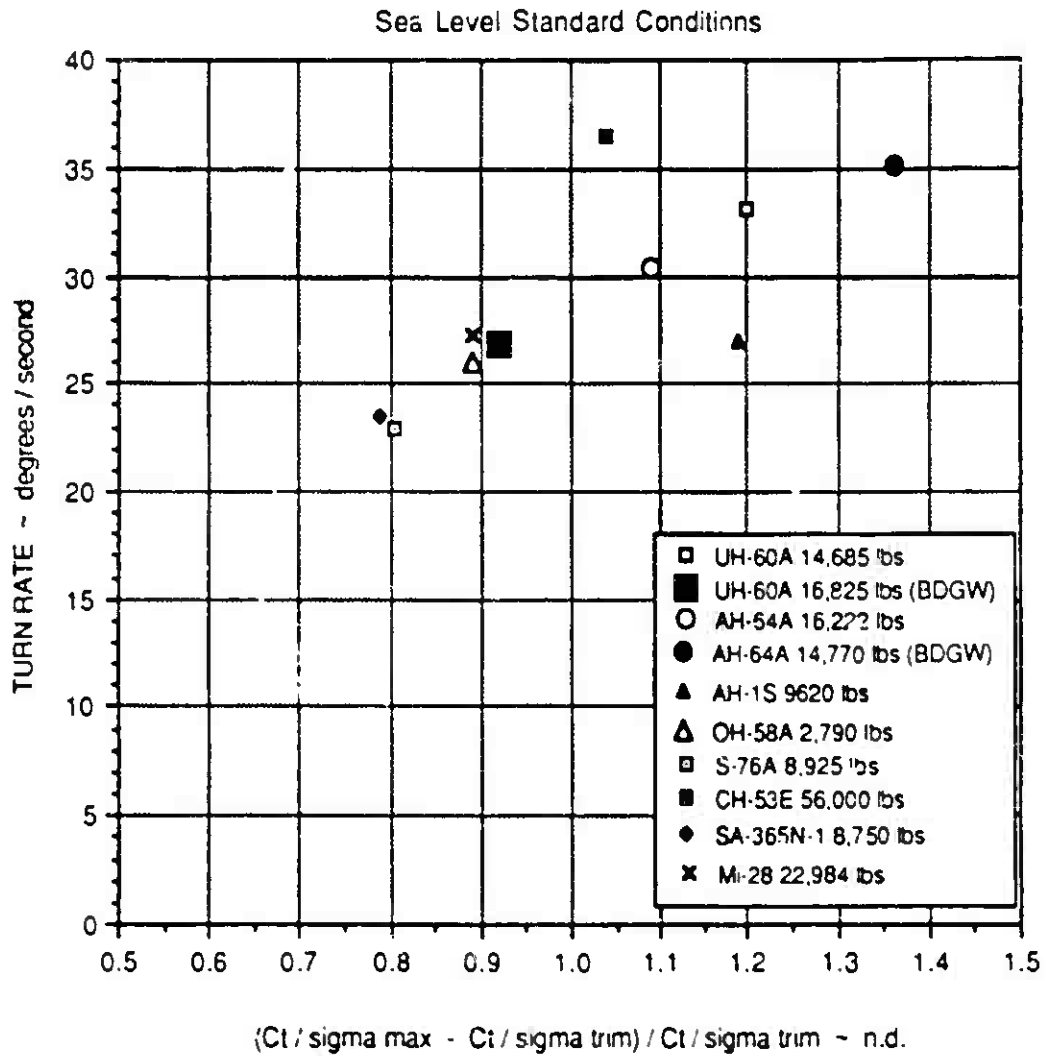


Figure 31. 80-Knot Decelerating Turn Summary Chart

The Mi-28 parametric results are shown in Figure 32. In this maneuver, the rotor thrust capability was enhanced by operation at 105 percent rotor speed. The resulting increase in turn rate matches well with the basic trend of the other helicopters.

130-Knot Decelerating Turn

Maneuver: This maneuver is identical to the 80 knot version except it is done at 130 knots.

Constraints: This "static" maneuver was done in the same manner as the 80 knot case.

Fundamental Parameter and MOE: These are the same as the 80-knot decelerating turn.

Simulation Results: The GenHel data for the 130-knot decelerating turn are shown in Figure 33. Note that the OH-58A is absent because it cannot perform this maneuver. Its maximum design level flight speed is about 120 knots.

These data show a well defined trend line, though not as collapsed as the 80 knot data. Again, the CH-53E is somewhat above the basic trend and the AH-1S below. The turn rates are much lower, typically one-half of the 80 knot values. This is due to the decrease in rotor thrust capability at higher advance ratios.

Operation of the HAVOC at 105 percent rotor speed (Figure 34) improves its capabilities somewhat more than expected. The increased rotor speed has two effects. First it increases the maximum C_T/σ and decreases the trim C_T/σ . Secondly, it slightly reduces the advance ratio and allows a higher C_T/σ to be reached before the stall limit is encountered.

140-Knot Pull-up

Maneuver: The high-speed symmetrical pull-up is tactically important for situations where a rapid change in altitude is required, such as obstacle avoidance or escape from a tailing threat. The maneuver is limited by the rotor thrust capability and, because of its transient nature, not restricted by power available.

Constraints: This maneuver was performed dynamically with the maneuver controller. The aircraft had to remain wings-level, maintain heading and not exceed a rotor stall parameter of 0.0125, representing deep stall. Power required could not exceed power available, but for all aircraft this power limitation was never imposed.

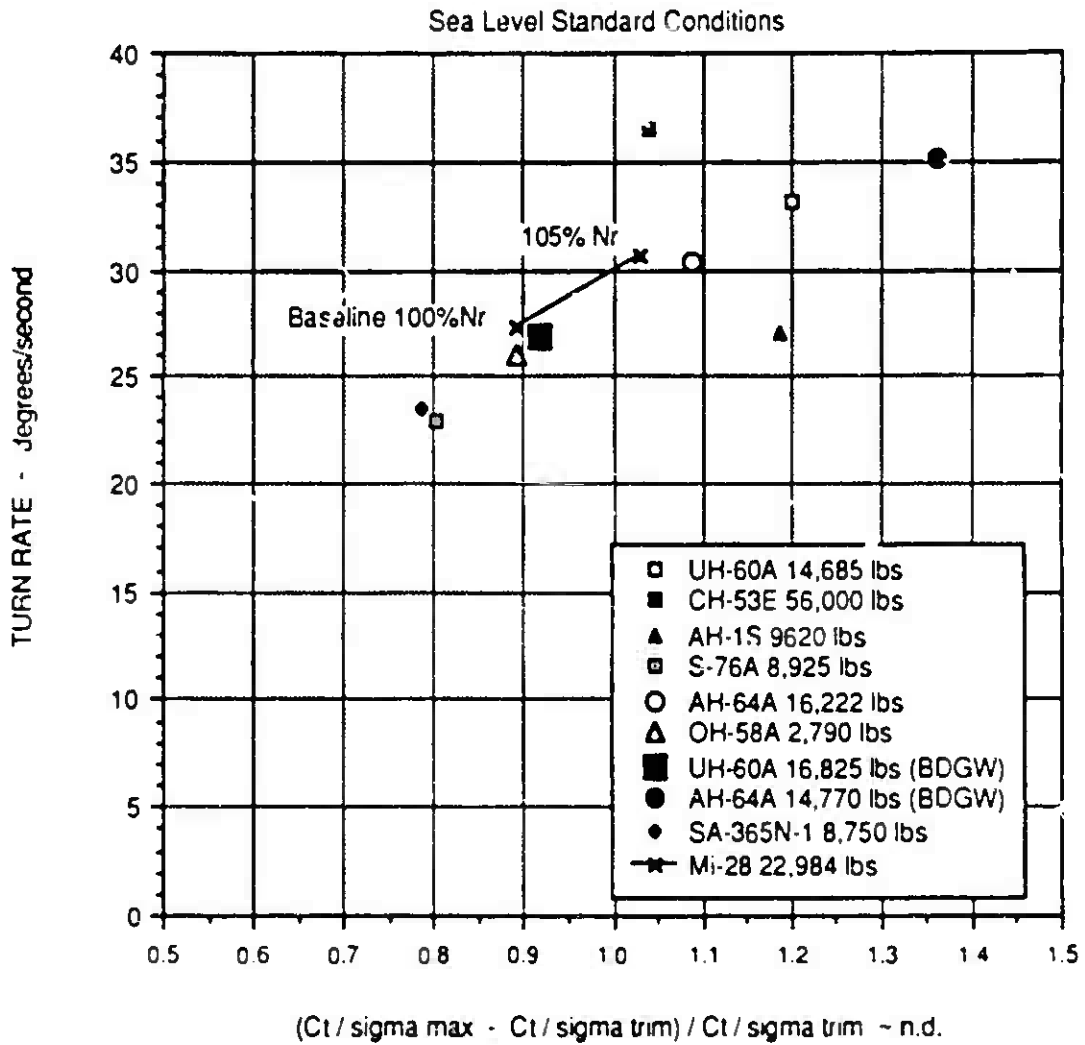


Figure 32. Effect of Increased Rotor Speed on Mi-28 80-Knot Decelerating Turn

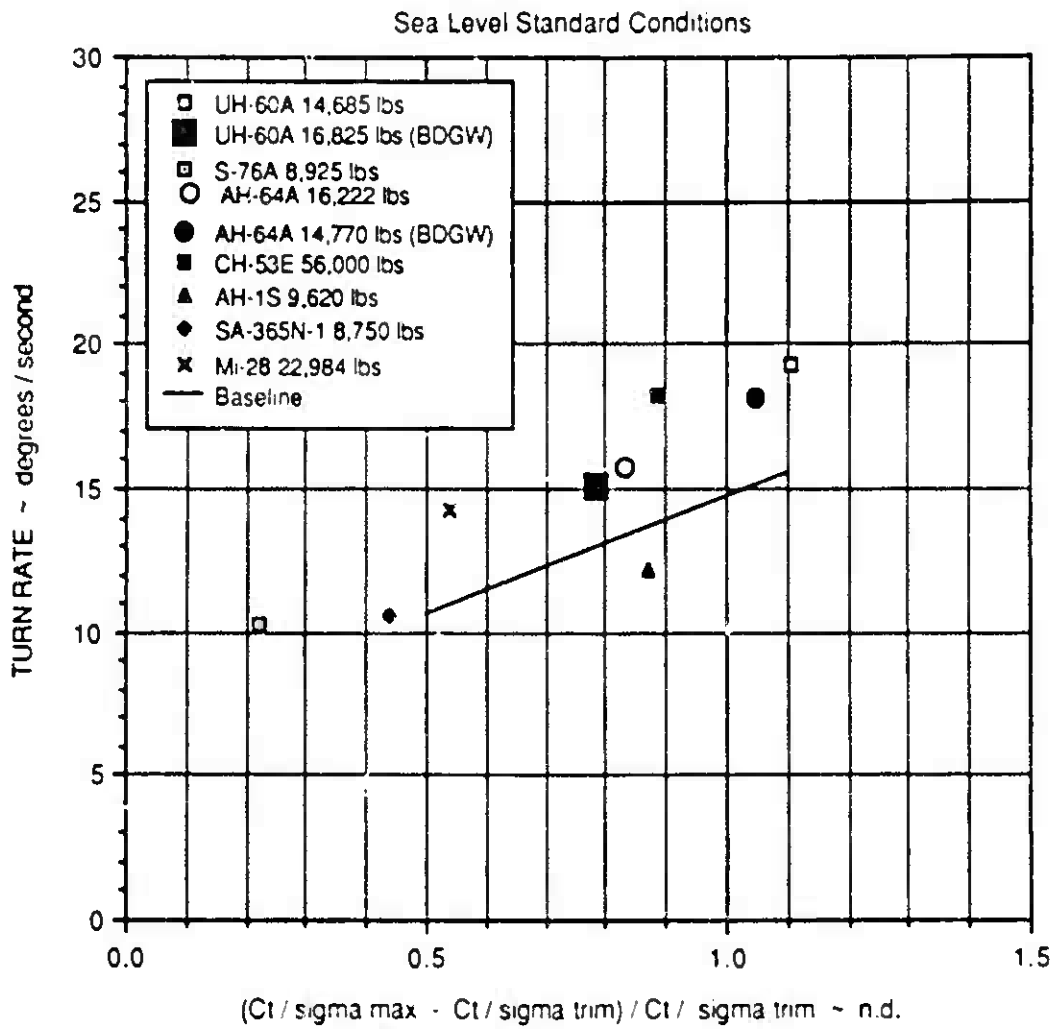


Figure 33. 130-Knot Decelerating Turn Summary Chart

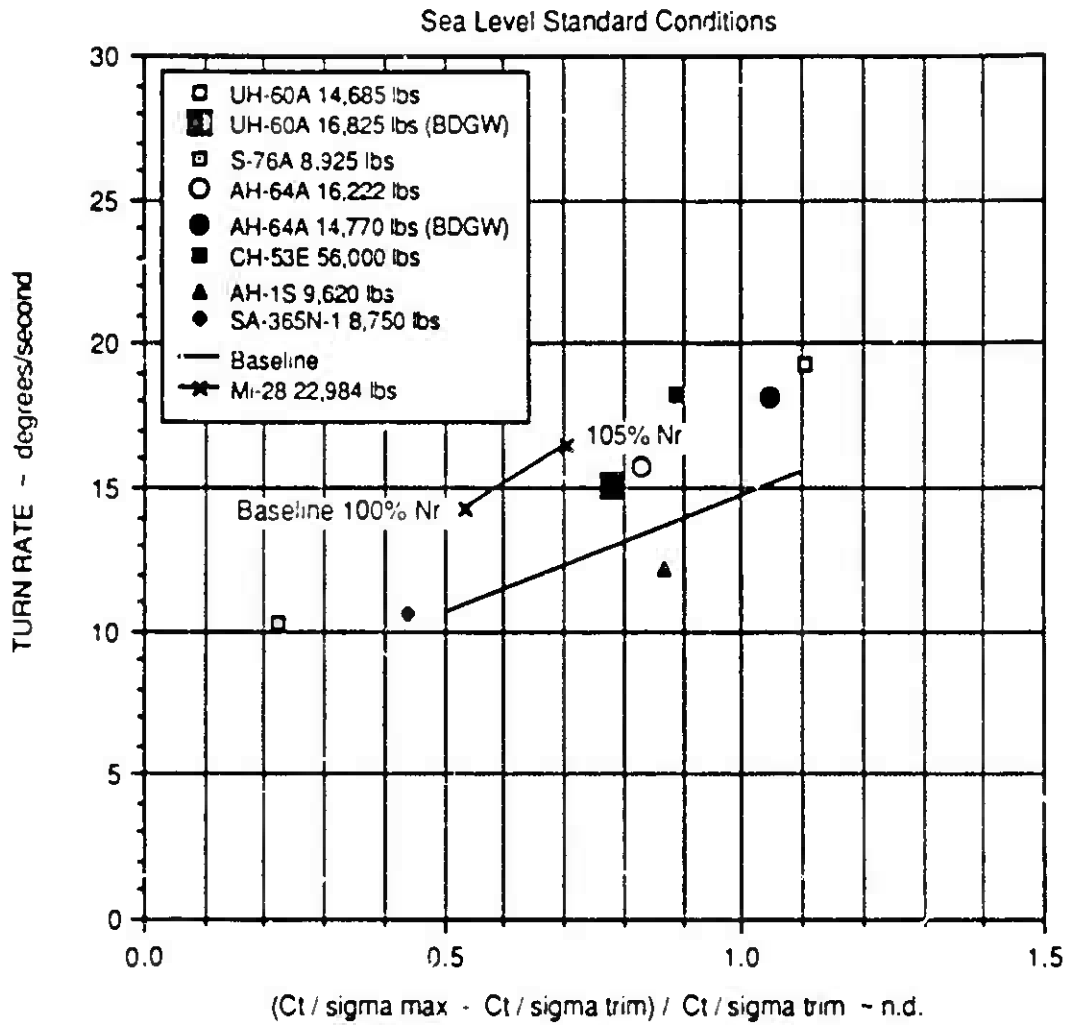


Figure 34. Effect of Increased Rotor Speed on Mi-28 130-Knot Decelerating Turn

Fundamental Parameter and MOE: The fundamental parameter for the high-speed pull-up was the normalized thrust margin, the same parameter used for the decelerating turns. In this case, of course, the C_T/σ values were calculated for 140 knots. The maximum load factor achieved was the obvious MOE.

Simulation Results: The results of the 140-knot pull-up are shown in Figure 35. Again, the OH-58A is not present because it cannot do this maneuver. The data points are well trended and closely match the M/A Phase I study result. The AH-1S, however, is well below the expected value because it hits the rotor stall boundary sooner than expected.

The Mi-28 does slightly better than expected at 105 percent rotor speed (Figure 36). This is due to the reduction in advance ratio and consequent improvement in rotor stall capability as noted in the decelerating turn discussion.

180-Degree Hover Turn

Maneuver: The ability to perform a hover turn quickly and to come to a desired heading with little overshoot is very important for both targeting and attack. It requires both high control power (acceleration) and high damping. This maneuver is made with the pedals and is essentially independent of main rotor attributes.

Constraints: This was a "dynamic" maneuver. The helicopter had to remain in position at constant altitude and turn exactly 180 degrees with no overshoot. Pilot experience dictated a limit on yaw rate of 60 degrees per second, since values above this limit make it difficult to stop on a desired heading without excessive overshoot. Since CenHel uses a Bailey-type tail rotor model, the tail rotor C_r/σ was arbitrarily limited to 0.14. For the Dauphin, the Fenestron thrust was calculated using Sikorsky's existing Fan Tail model which properly accounts for the augmentation due to the duct.

Fundamental Parameter and MOE: In the original Phase I Study, the fundamental parameter was tail rotor solidity. For the wide variety of aircraft in this effort, the fundamental parameter was defined as the theoretical yaw acceleration capability. This was calculated by assuming a maximum C_r/σ capability of 0.14, calculating the maximum static thrust available, subtracting the thrust required for hover, and calculating the residual yaw acceleration available. The measure-of-effectiveness was the time required to make the 180-degree turn.

Sea Level Standard Conditions

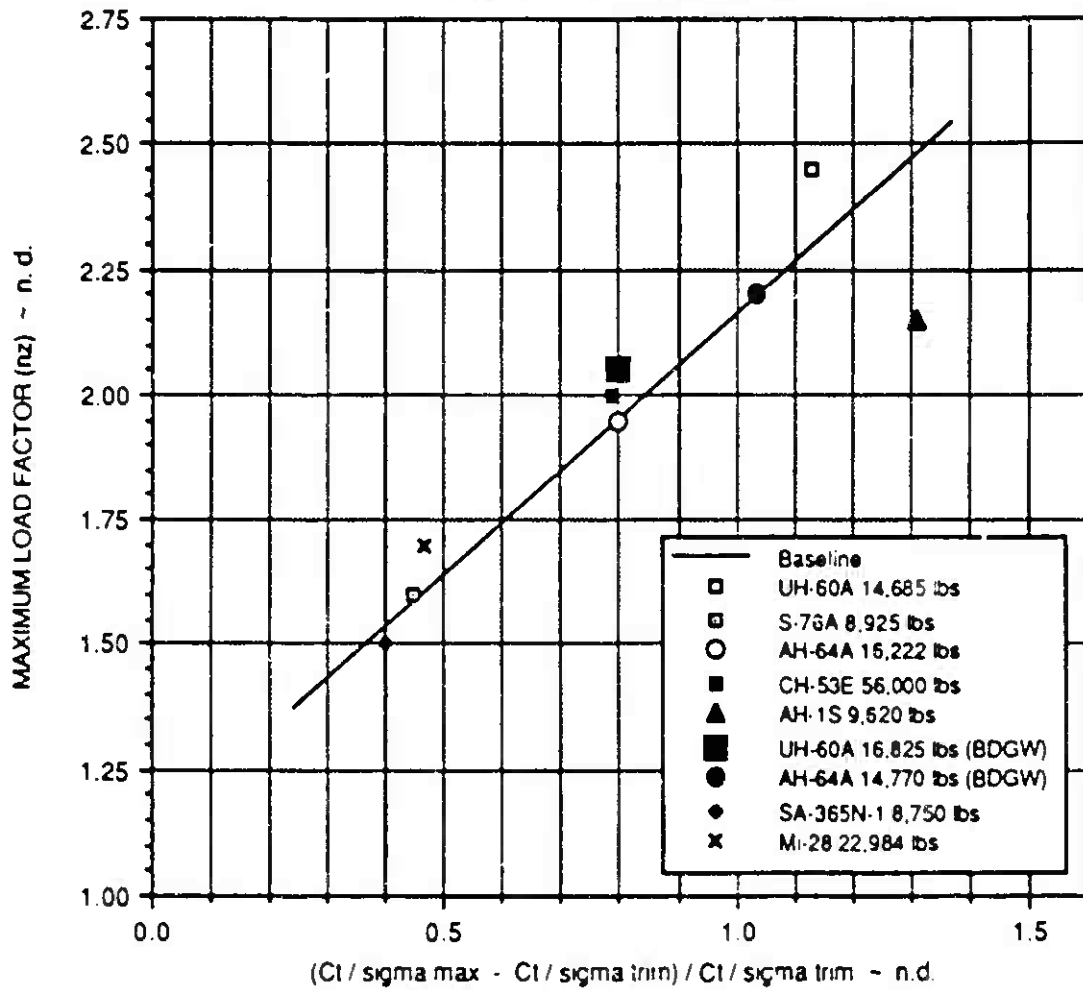


Figure 35. 140-Knot Pull-Up Summary Chart

Sea Level Standard Conditions

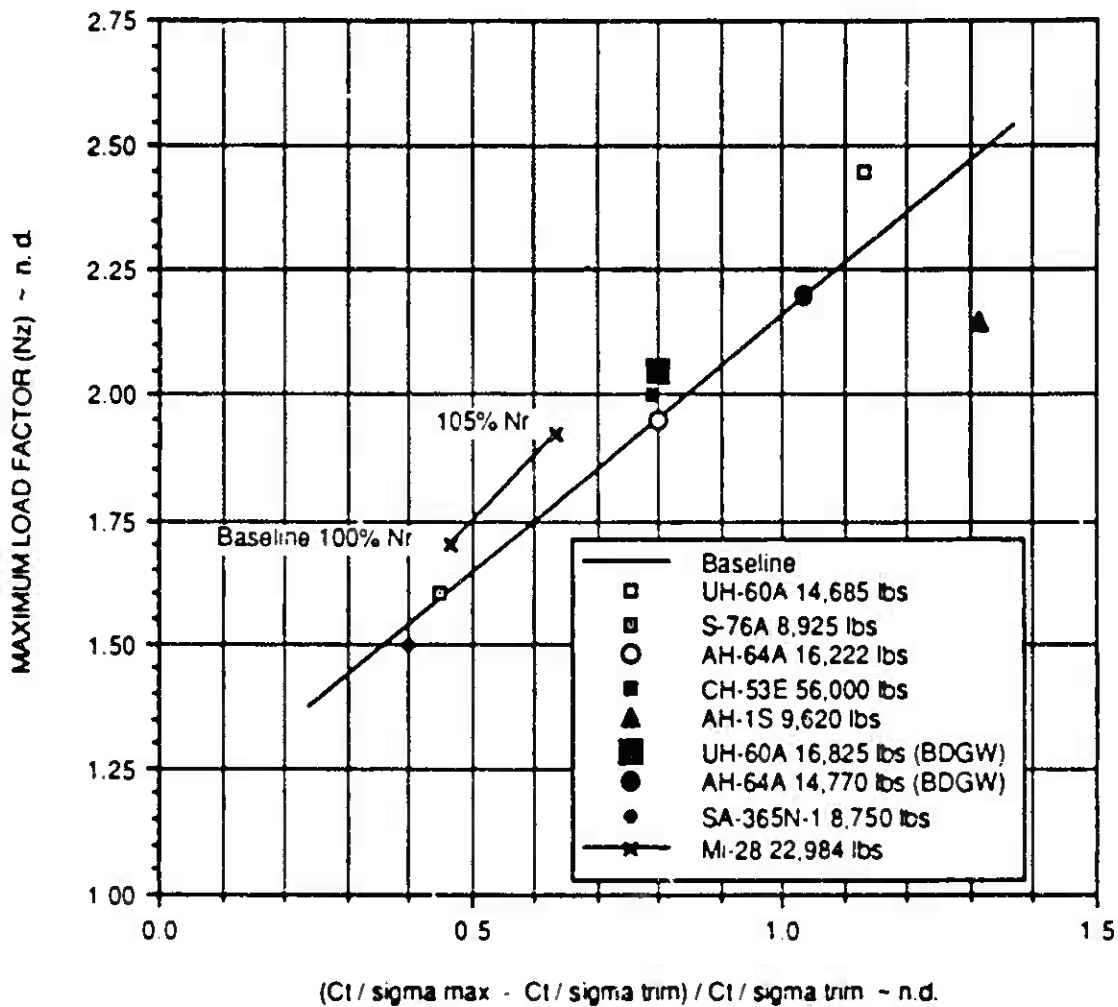


Figure 36. Effect of Increased Rotor Speed on Mi-28 140-Knot Pull-Up

Simulation Results: Figure 37 shows the simulation results. Surprisingly, the times to turn were all very similar and relatively insensitive to the fundamental parameter. The reason for this was the presence of the yaw rate limit. Helicopters with more acceleration capability could not use it since they simply ran into the rate limit sooner. The excessive time for the CH-53E reflects a thrust limit on the tail rotor below the $0.14 C_T/\sigma$ assumed by the fundamental parameter.

The effect of yaw inertia on the HAVOC hover turn is presented in Figure 38. Inertia was varied by 10 percent above and below the baseline value. This resulted in a change in the hover turn time of about 1/4 second in each case.

DISCUSSION OF RESULTS FOR EACH AIRCRAFT

Overall, the UH-60A and AH-64A at their light weights had the most consistently good maneuvers. Adding a ton to each helicopter to bring them to their high gross weight configurations significantly reduced the maneuver results. The CH-53E did surprisingly well for such a large aircraft, but recall that it was flown at a mid-weight and at 105 percent rotor speed. The two civil aircraft, the SA-365N and S-76, in general did poorly. Both have high power loadings which significantly affected the maneuver results. The older generation military helicopters, AH-1S and OH-58A, tended to fall between the civil aircraft and the modern military ones. The Mi-28 did not do as well as expected. This is due basically to the high weight/high drag configuration that was evaluated. The analytical study in Appendix L shows that a lighter weight HAVOC could have maneuver capabilities comparable to the AH-64A and UH-60A.

Overall, the fundamental parameter charts worked very well. They collapsed the maneuver results from this wide variety of aircraft and are useful in predicting the effect of parametric changes on the maneuver results. It is clear, however, that the presence of reasonable operational limitations can have a strong effect on the maneuvers. While the fundamental parameter plots provide a useful guide to the capability of an aircraft or design, the actual maneuver results can only be determined by flying the GenHel simulation (or an equivalent simulation) through the maneuver.

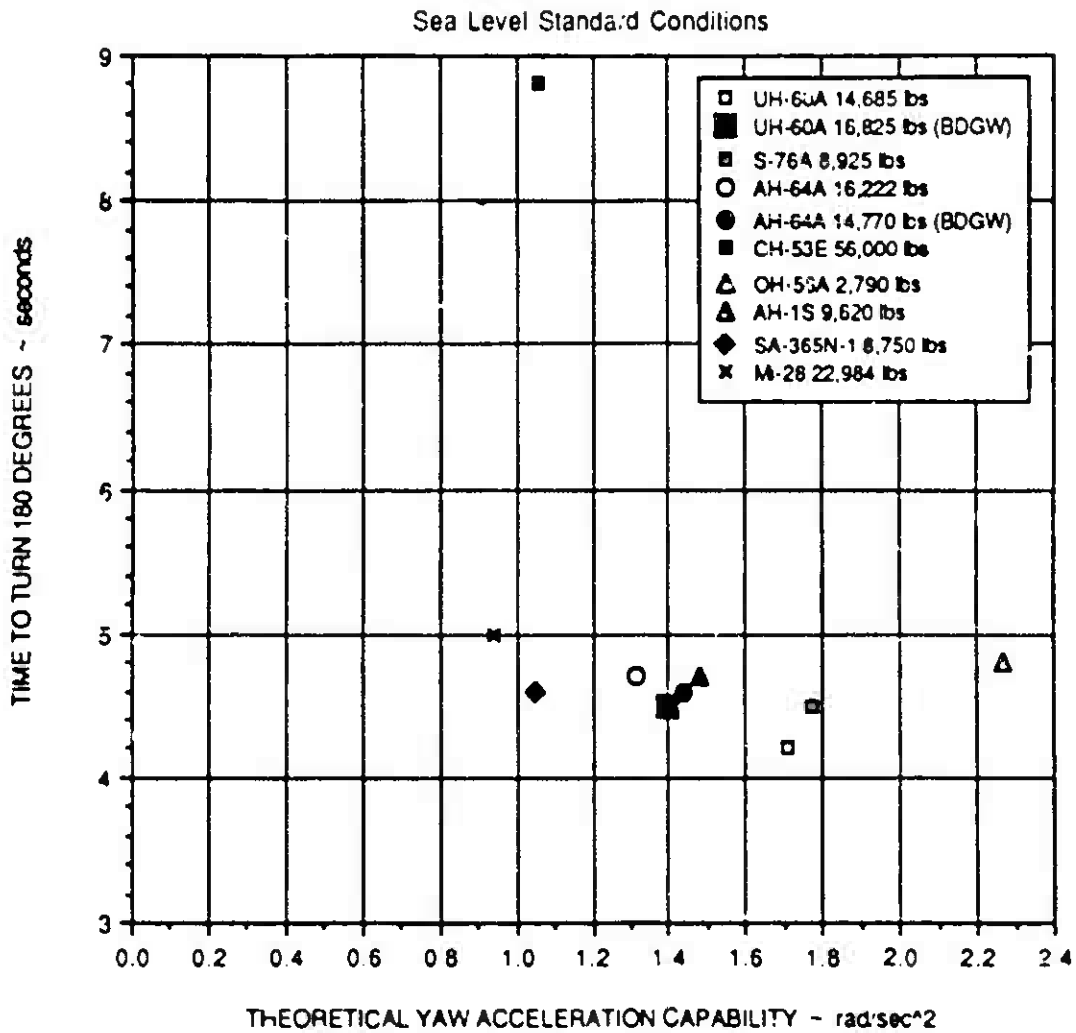


Figure 37. 180-Degree Hover Turn Summary Chart

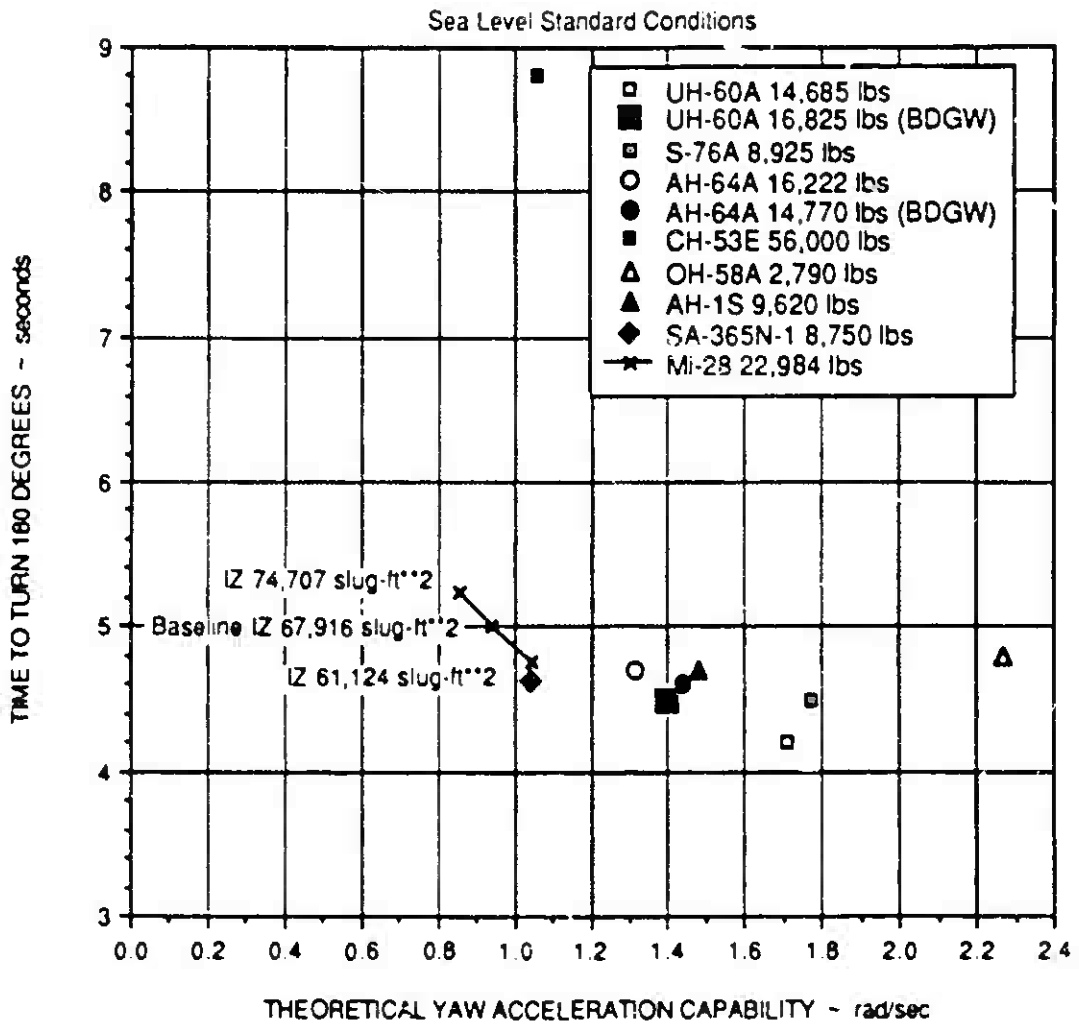


Figure 38. Effect of Yaw Inertia on Mi-28 180-Degree Hover Turn

AACT DATA ANALYSIS

INTRODUCTION

This section of the report discusses the analysis of the air-to-air combat flight test data. These data were supplied by the U.S. Army and covered one-on-one engagements between a variety of helicopters. Sikorsky conducted an analysis to determine when firing opportunities occurred and an evaluation of the maneuvering that took place in each engagement relevant to these firing opportunities. The basic methodology was to develop software which would synthesize the view out of each cockpit during the engagements. This was coupled with a firing window analysis code which calculated the range and boresight angular error between the aircraft. These firing window data were superimposed on the cockpit views. The user could then replay the engagement, note what maneuvering took place, and define the times and durations of the firing opportunities. Although the contract statement of work only required analysis of six engagements for each pair of aircraft, the procedure was so efficient that all 59 of the engagements provided by the Army were analyzed, providing a very comprehensive data base.

Overview of Air Combat Tests

Realizing the increasing threat posed by armed helicopters, the U.S. Army has been involved for many years in a program to assess the requirements for air-to-air combat. One phase of this program has been conducting dissimilar air combat tests between various state-of-the-art helicopters (Reference 5). These tests simulated the air-to-air combat that could arise from a chance encounter between two helicopters. Initial activities focused on fixed-gun engagements (no missiles or rockets) but later studies evaluated turreted guns. These one-on-one engagements were flown at the Naval Air Test Center (NATC) at Patuxent River, Maryland, and were intended both to evaluate the maneuverability and agility of current helicopters and to assess future requirements for this type of mission.

The first series of tests, designated Air-to-Air Combat Tests I (AACT I), was flown in April 1983 using a Bell OH-58A and a Bell AH-1S. This AACT developed and validated the techniques for obtaining and processing air combat data. These flights demonstrated that tests of this nature could be safely performed and generate useful data.

A second series of tests, AACT II, was flown in July 1983. Three aircraft were involved: a Sikorsky UH-60A, a Sikorsky S-76A (in its armed utility version designated AUH-76) and a Bell OH-58A. The main objective of AACT II was to establish a data base of helicopter M/A characteristics for a variety of different designs.

AACT III, the third series of flight tests, was flown in December 1984. The following helicopters participated: Hughes H-530F, Bell OH-58A, Bell AH-1S and Messerschmidt-Bolkow-Blohm/Kawasaki BK-117. For this series of tests, laser weapon simulators were fitted to the BK-117 and H-530F to represent fixed-forward 20mm guns.

The success of the first three flight tests resulted in AACT IV being conducted in April 1987. Aircraft utilized for this activity included: Aerospatiale SA-365N1, McDonnell Douglas AH-64A, Bell Model 406 Combat Scout and Bell AH-1S. The B-406 is similar to the OH-58D Advanced Helicopter Improvement Program (AHIP) aircraft in having a four-bladed hingeless rotor and upgraded engine. In these flight tests, the laser weapon simulators were mounted on the turrets of the Apache and Cobra to allow evaluation of turreted guns in air-to-air combat.

Background

Once data from the AACT flight tests were available, a significant data analysis effort was required. In the M/A Phase I study, several encounters were analyzed to evaluate maximum maneuvering while achieving firing opportunities. The process of examining the AACT encounter time histories was very laborious. A computer code was available to calculate the distance between the helicopters and the relative azimuth and elevation angles. The time steps where one aircraft was within the firing window of the other could be determined from these data. But, analysis of the maneuvering before, during and after the firing opportunity was performed manually. The engineer had to inspect time history plots of positions, attitudes, velocities, angular rates and control inputs to determine what each helicopter was doing. An automated method for this analysis was clearly needed.

The approach taken in this study was to develop software which would allow playback of the AACT data on a workstation-based simulator. This allowed the engineer to recreate the view out of each cockpit during the engagements. To aid in this analysis, a mode was available to show the overhead view of the engagement or, in fact, the view of the engagement from any fixed point in combat space. The analysis of the maneuvers was significantly enhanced by this approach.

SOFTWARE DEVELOPMENT

The software developed for analysis of the AACT data is shown schematically in Figure 39. The original data were supplied to Sikorsky by AACT in the form of floppy disks. These data were then read into a conversion module. This module broke the data into separate files arranged by counter number. A counter number had been assigned to each engagement. The firing window analysis code and simulation software use different earth referenced coordinates than the AACT data, so two coordinate transformations were employed as illustrated in Figure 40. The output of the conversion module was restructured data files. These files, one per counter, contained the data in each of the new axes systems and the firing window analysis data. This restructured data file was then used to drive the synthesized replay of the AACT engagements. In addition, a plotting routine was also available.

One of the most important aspects of this effort was the validation of the results because of the extensive manipulation of the data required. Within the simulation module itself, evaluations were conducted to assure that the views out of each cockpit and from overhead were compatible. More importantly, the firing window data which were separately derived from the original

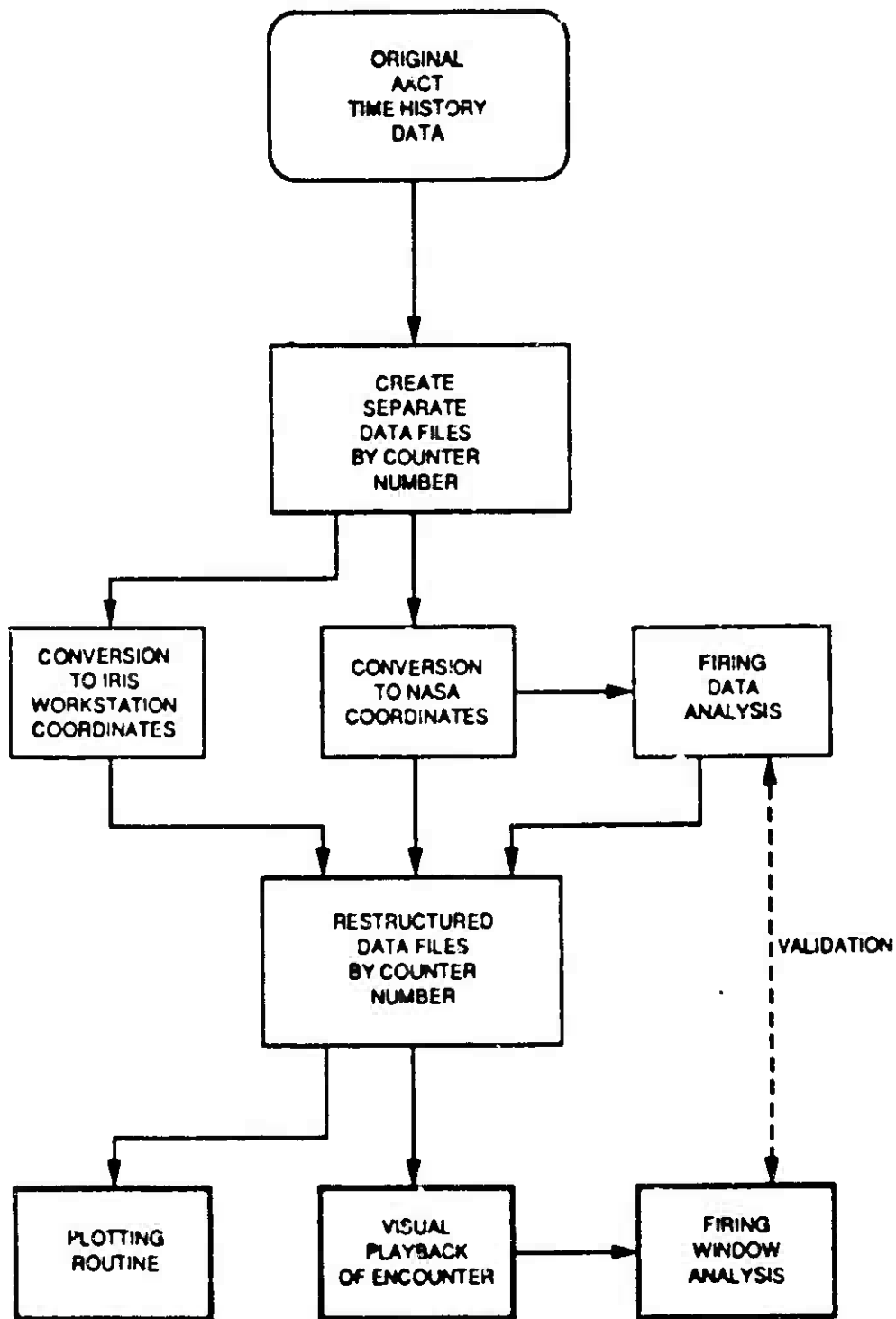
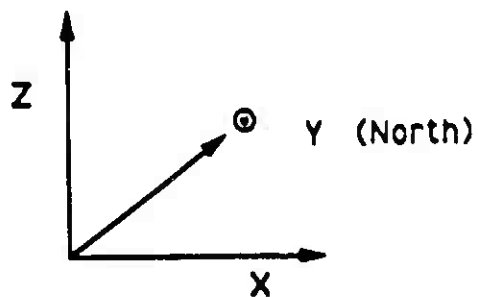
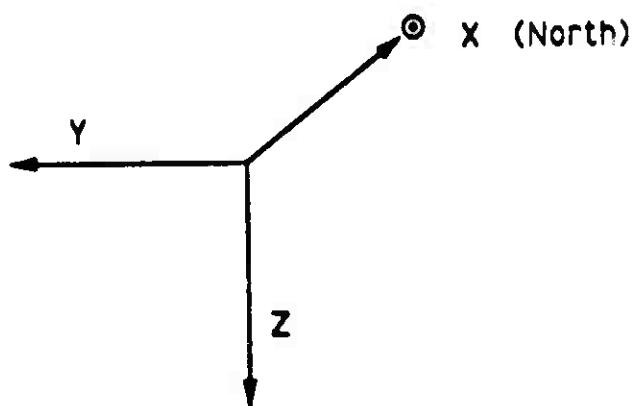


Figure 39. AACT Data Processing Chart

DATAMAP



NASA TRANSFORM



SILICON GRAPHICS
IRIS

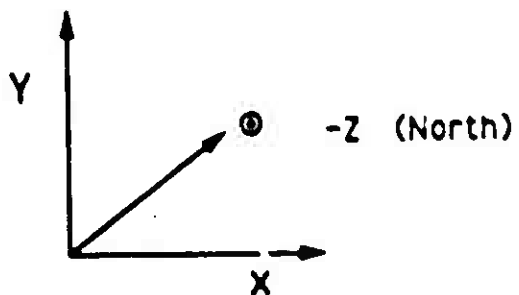


Figure 40. Coordinate Axes Definitions

AACT information were compared with the out-of-cockpit views. The user could easily confirm that the view out of the cockpit and the range, azimuth and elevation to target data superimposed on it were compatible. Extensive verification work of this kind was performed to assure that the flight test conditions were properly replicated.

A detailed discussion of the software modules is given below.

Conversion Module

The conversion module has three functions. The first is a reconfiguration program that reads the data files supplied by the Army and separates them into distinct files by counter number. The second is a coordinate axis transformation program to make the AACT data compatible with the NASA coordinate system used by the firing window analysis and compatible with the earth-referenced coordinate system of simulation modules. Care had to be exercised in these transformations because of the large number of 360-degree shifts in the angle data. The third function of the conversion module was to exercise a firing opportunity analysis code. This program was originally developed in the M/A Phase I study (Reference 2) in the Speakeasy language. For this application, it was converted to the C programming language. This program reads the test data and calculates the range in meters and the azimuth and elevation angles in degrees between one helicopter and the other in the body axes of the first. The final output of the conversion module is a restructured data file for each counter that contains the transformed data and the firing window data.

Simulation Module

The simulation module creates a visual representation of the engagement. This Silicon Graphics 3130 software utilizes high resolution, solid-color, polygonal computer-generated imagery. In addition to display of the other helicopter, the terrain around the Patuxent River Naval Air Test Center (the AACT test site) was also modeled. Two simulation playback modes were available. The basic software for these modes had been developed previously under IR&D funds but extensive customizing was required for this M/A study. Both modes read the restructured data file and can replay the AACT engagement in slow, real, or fast time, or frame by frame. One mode displays the view out of the cockpit and can be toggled from one cockpit to the other.

Digital data superimposed on the cockpit display includes:

Own Ship - airspeed, altitude, heading, sideslip, bank angle

Other Ship - relative azimuth and elevation angles, resultant angle, airspeed

Information - time, which cockpit this view, type of view (slow, real, fast, frame)

The other mode allows a view of both helicopters from any fixed point in the combat space. Digital data superimposed on this display includes time, firing window data, and each helicopter's altitude, airspeed and sideslip angle.

Plotting Module

The plotting software was a modification of an existing program. The modifications allowed plotting of multiple parameters per page and addition of parameter titles.

ENGAGEMENT ANALYSIS

With the engagement playback available, analysis of the firing opportunities was easily achieved. Each encounter was viewed and as the aircraft moved into position, the results of the firing window computation could be inspected. The firing window for this study was defined as a range less than 1500 meters and azimuth and elevation angles less than plus or minus three degrees. No minimum time in the firing window was required before "activation" of the duration counter. Detailed discussion of each of the 59 encounters is presented in Appendix J along with a table of the initial conditions. The encounters analyzed were divided among the AACT data as follows:

AACT II	UH-60A vs S-76A Counters 208018 to 208028
	S-76A vs OH-58A Counters 23020 to 23038
	UH-60A vs OH-58A Counters 27026 to 27043
AACT III	AH-1S vs OH-58A Counters 302013 to 302021
AACT IV	AH-64A vs SA-356N (AH-64A fixed gun) Counters 411009 to 411023
	AH-64A vs SA-365N (AH-64A turreted gun) Counters 417001 to 417012

The engagement counter numbers are principally used for AACT data base access. They are five or six digit numbers encoded with the following information:

First Digit	-	AACT number 27027 - AACT II 417001 - AACT IV
Second, Third Digit	-	Flight number 27027 - Flight #7 417001 - Flight #17
Last Three Digits	-	Engagement number 27027 - Engagement #27 417001 - Engagement #1

While the details of the individual engagements are presented in Appendix J, some overall comments on the engagements can be made and are presented below.

UH-60A vs S-76A

These tests were distinguished by very extensive maneuvering of each aircraft. Bank angles of over 90 degrees were achieved by both helicopters. Unbanked, or pedal turns were also used frequently. The BLACK HAWK had the most firing opportunities due to its lower power loading.

UH-60A vs OH-58A

These tests consisted mainly of tail chases and S-turns with the UH-60A in the dominant position most of the time. The BLACK HAWK frequently has bank angles of near 90 degrees and in one encounter makes a 92-degree left bank angle to gain position on the Kiowa. The OH-58A maneuvers were restricted to bank angles of 60 degrees or less. The lower power loading and higher maneuverability of the UH-60A allowed it to dominate the engagements.

S-76A vs OH-58A

These encounters featured tight turns and short ranges. Neither aircraft had bank angles over 60 degrees, but the S-76A made extensive use of pedal turns. The S-76 had the largest number of valid firing windows.

AH-1S vs OH-58A

The engagements of these two helicopters do not show the very aggressive maneuvering seen in the previous pairs. Several of the encounters had one aircraft remain in hover while the other targeted it, so these are not really representative of air-to-air combat. Both helicopters made use of pedal turns to try and gain an advantage.

SA-365N vs AH-64A (fixed gun)

The Dauphin frequently made use of mid-speed pedal turns to target the Apache. The Apache was able to use its lower power loading to gain altitude over the SA-365N, but this did not necessarily give it firing opportunities on the Dauphin. In one case the encounter was initialized with the Apache on the tail of the Dauphin, but neither aircraft achieved any firing opportunities. On the other hand, when the scenario was initialized with the SA-365N on the tail of the AH-64A, the Dauphin got a firing window as the Apache tried to turn in on it.

The original AH-64A/SA-365N data supplied by the Army inadvertently covered engagements where the AH-64A was simulating use of a turreted gun in air-to-air combat. These data were analyzed for fixed gun firing opportunities before the error was discovered. A review of the maneuvering sequences shows that they were similar to the fixed gun engagements with the SA-365N using

pedal turns to gain advantage and the Apache making use of its better climb capability. However, since the Apache was simulating the use of a turreted gun, there was no requirement for the pilot to aggressively drive his attitude toward boresight alignment with the Dauphin. Data for these cases are provided since the analysis was done, but they were not used in the correlation study and no conclusions should be drawn from them.

Firing Opportunities Analysis

The mathematical firing opportunities that occurred in the 59 encounters analyzed are summarized in Table 6. The columns in Table 6 are numbered at the bottom for the purpose of identifying the data as explained in the following paragraphs:

Column 1 lists the helicopters involved and counter numbers of the AACT flight test data files for each scenario where the helicopter number is used for identification in subsequent data entries of the table. Column 2 is the length of the encounter to the nearest second.

Column 3.1 lists the minimum vector value of the azimuth and elevation angles from the body reference axis of helicopter 1 to the center of helicopter 2. The azimuth and elevation angles are tabulated in column 3.2. All angles are in degrees. Column 3.3 is the range between the two helicopters in meters at the same time step as the data of columns 3.1 and 3.2.

Columns 4.1, 4.2 and 4.3 are the same data definitions as 3.1, 3.2 and 3.3 except that the frame of reference is from the body reference axis of helicopter 2 to the center of helicopter 1.

Columns 5.1, 5.2, 5.3, and 5.4 list data for the geometric firing windows that are less than or equal to ± 3 degrees in both azimuth and elevation angles. The minimum azimuth and elevation angles for the less than or equal to ± 3 degree azimuth and elevation burets are listed in column 5.2. The first entry of column 5.3 is the number of time steps that the azimuth and elevation angles are less than or equal to ± 3 degrees. One time step is equal to .1 second for all the data evaluated. The second data entry of column 5.3 is the starting time of the firing window.

Column 6 is the minimum range for the entire flight sequence. Columns 7.1 and 7.2 are the maximum bank angles for helicopters 1 and 2, respectively.

Out-Of-Cockpit Views

Figures 41 through 46 present out-of-cockpit views of selected engagements from each of the 5 helicopter pairs. Each of these views had pertinent information superimposed over the display as shown in Figure 47. For views from other locations in combat space, data on both aircraft were provided as shown in Figure 48.

The criteria for choosing the engagement presented was, in order of preference, a scenario with the most accurate 3-degree firing window, a sequence which had the longest 3-degree firing window duration, or the scenario with the closest range during its firing window. Thus the engagement chosen represents the best firing opportunities for each helicopter pair.

The flight scenario counters chosen were 208019, 302014, 417003, 411011, 23038, and 27026.

For the S-76 versus the UH-60A scenarios, flight sequence counter 208019 was the clear choice. The only other possible candidate, counter 20827, had a firing window of only .1 second in duration (Figure 41).

For the AH-1S versus the OH-58A set of scenarios, the flight sequence choice was counter 302014. Although this flight sequence only had a .2-second 3-degree duration firing window, the only other possible candidate flight sequence, counter 302018, did not include a 3-degree firing window during the maneuvering segment of the engagement (Figure 42).

The AH-64A versus the SA-365N turreted gun encounters had several candidate flight sequences. Flight scenario counter 417005 was not chosen since the AH-64A for reasons unknown did not maneuver while the SA-365N-1 scored its 13-degree firing window, and flight sequence counter 417009 was not chosen since the 13-degree firing window was scored before the initial pass of the two helicopters. Consequently, the final choice was flight scenario counter 417003 (Figure 43).

For the AH-64A versus SA-365N fixed gun engagements, the selected cockpit view was counter 411011. This shows the two helicopters trying to turn in on each other. The Apache is making a banked turn while the Dauphin has pedal turned to achieve a firing window (Figure 44).

The choice for the best flight sequence with a 13-degree firing window for the S-76 versus OH-58A flight scenarios was straight forward since the chosen flight sequence, counter 23038, had a very accurate firing window. The 13 degree firing window was .0 degree in azimuth and .2 degree in elevation and was held for 1.8 seconds (Figure 45).

For the UH-60A versus OH-58A flight scenarios, the best flight sequence counter was 27026. It represented the most accurate, longest duration, and closest range combination 13-degree firing window score. Several of the other encounters had more accurate and longer duration 3-degree firing windows but they occurred before the initial pass of the two helicopters, and so while they were calculated, they were not valid engagements (Figure 46).

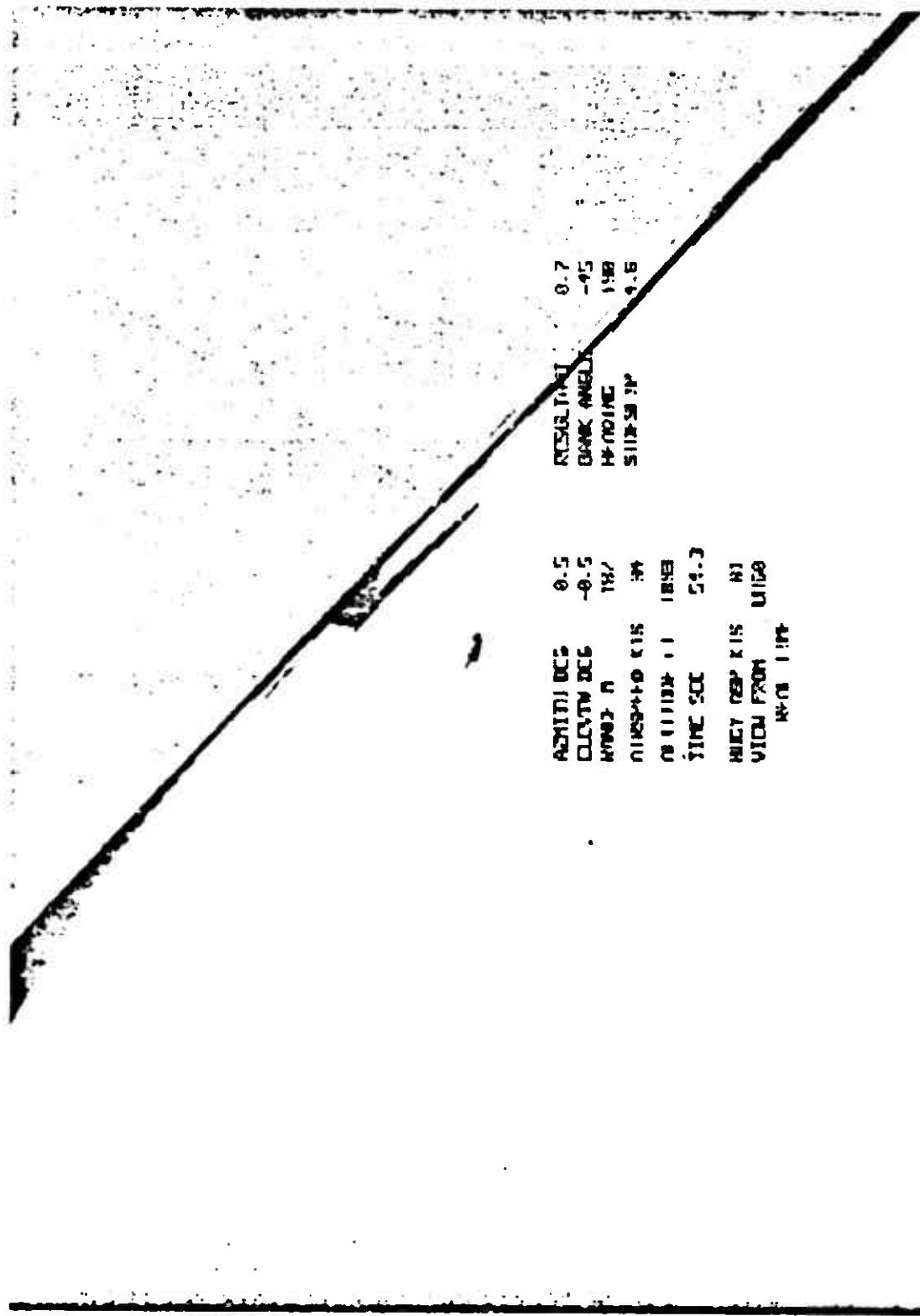


Figure 41. Cockpit Display, Counter 208019

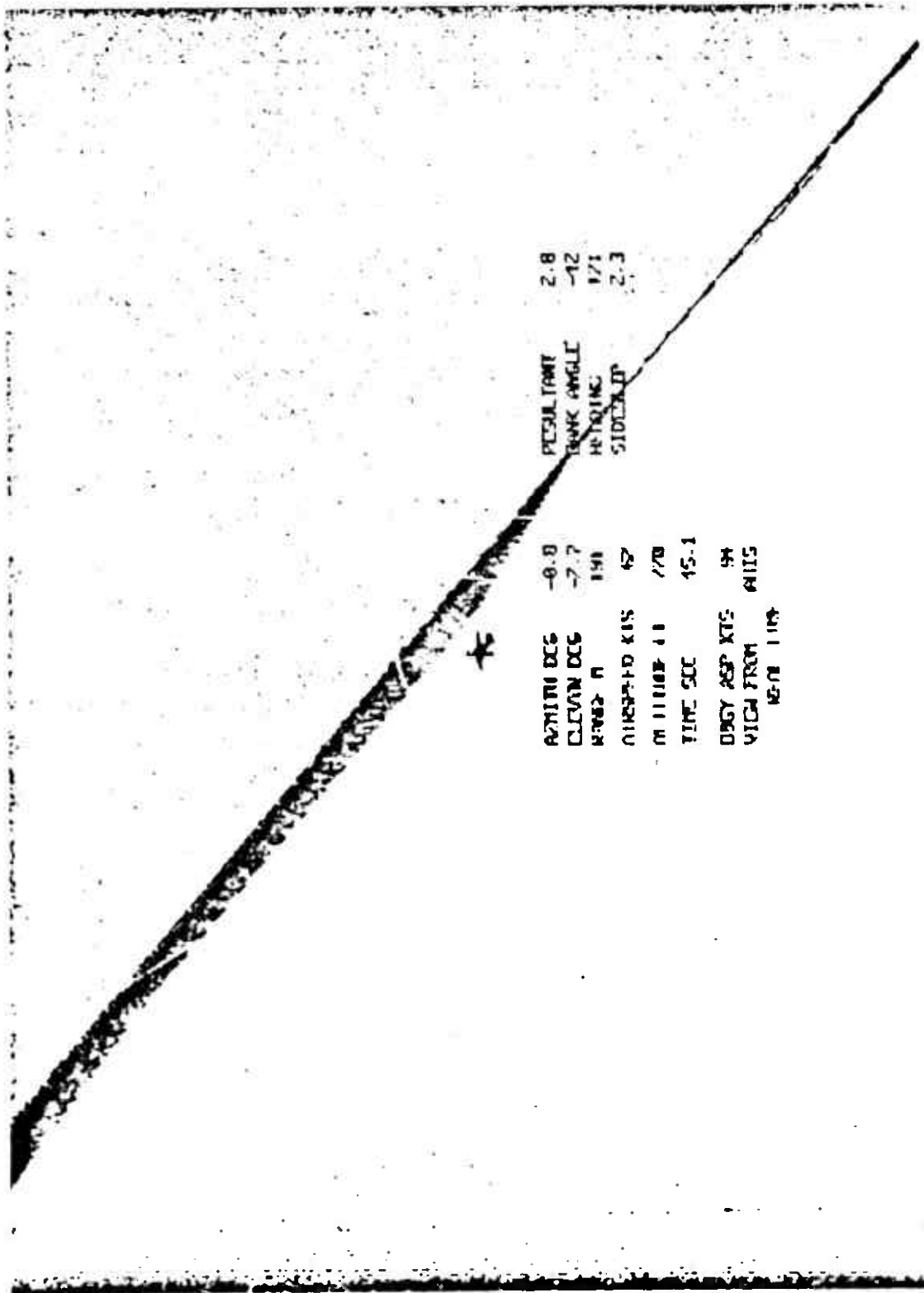


Figure 42. Cockpit Display, Counter 302014

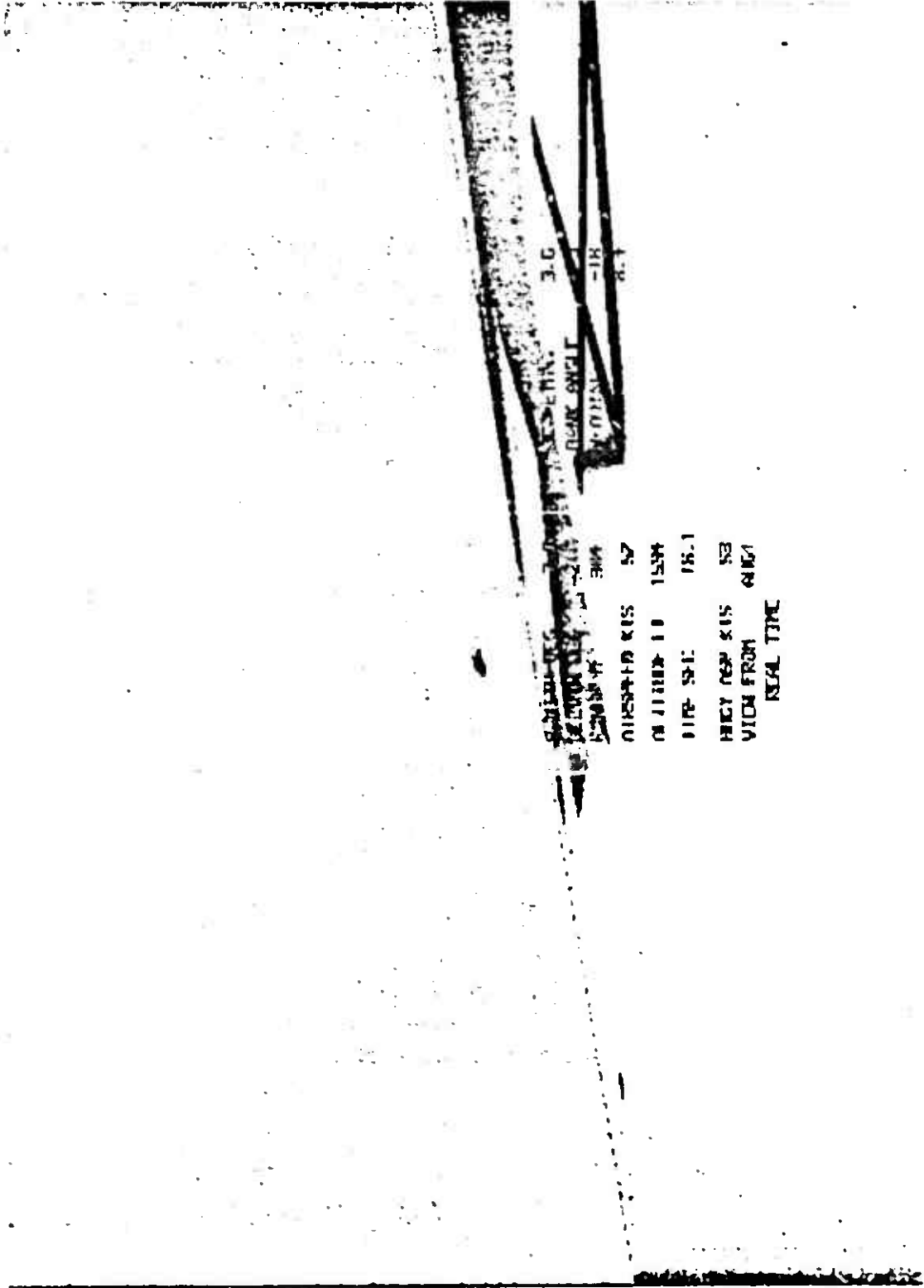


Figure 43. Cockpit Display, Counter 417003

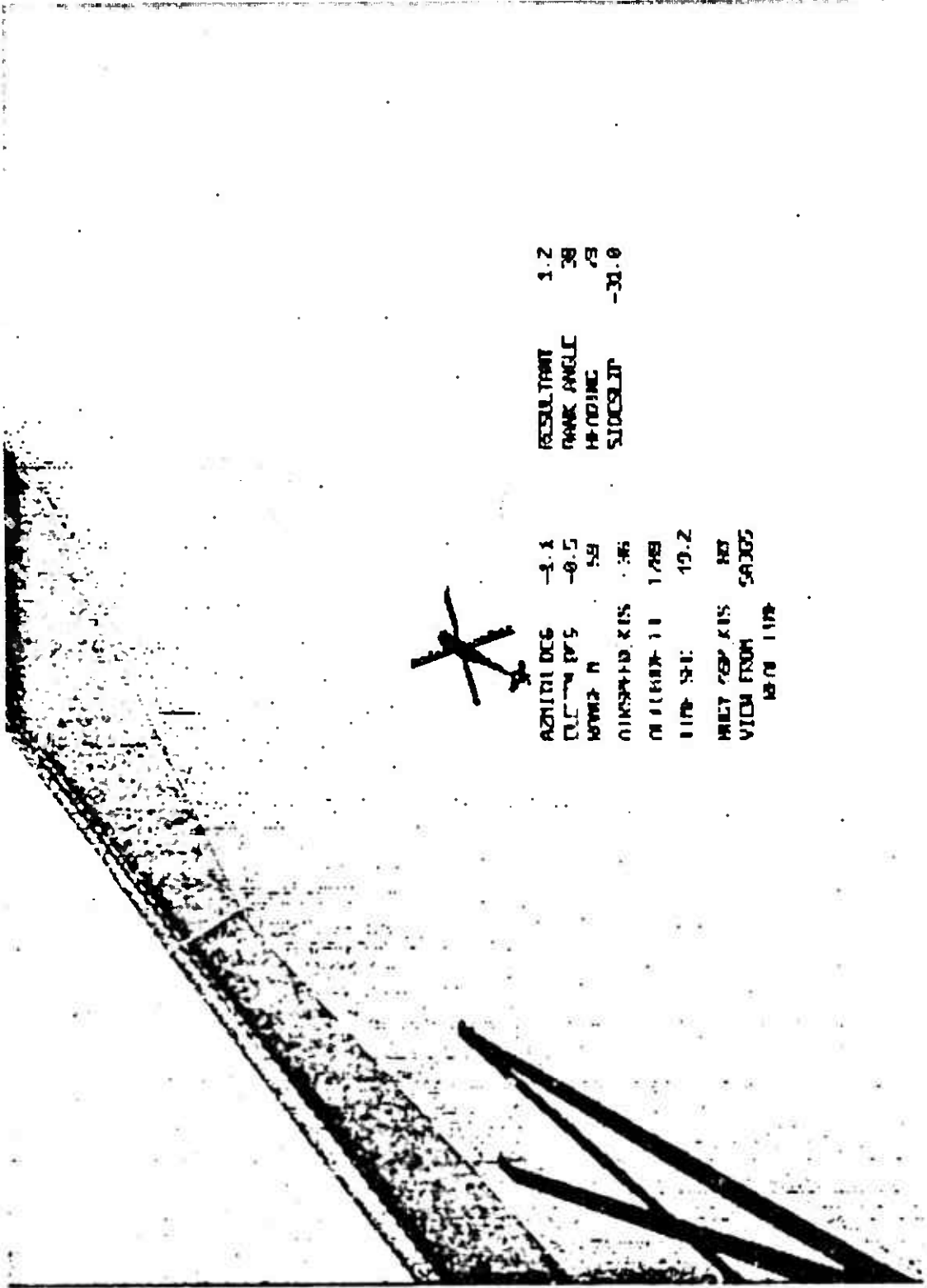
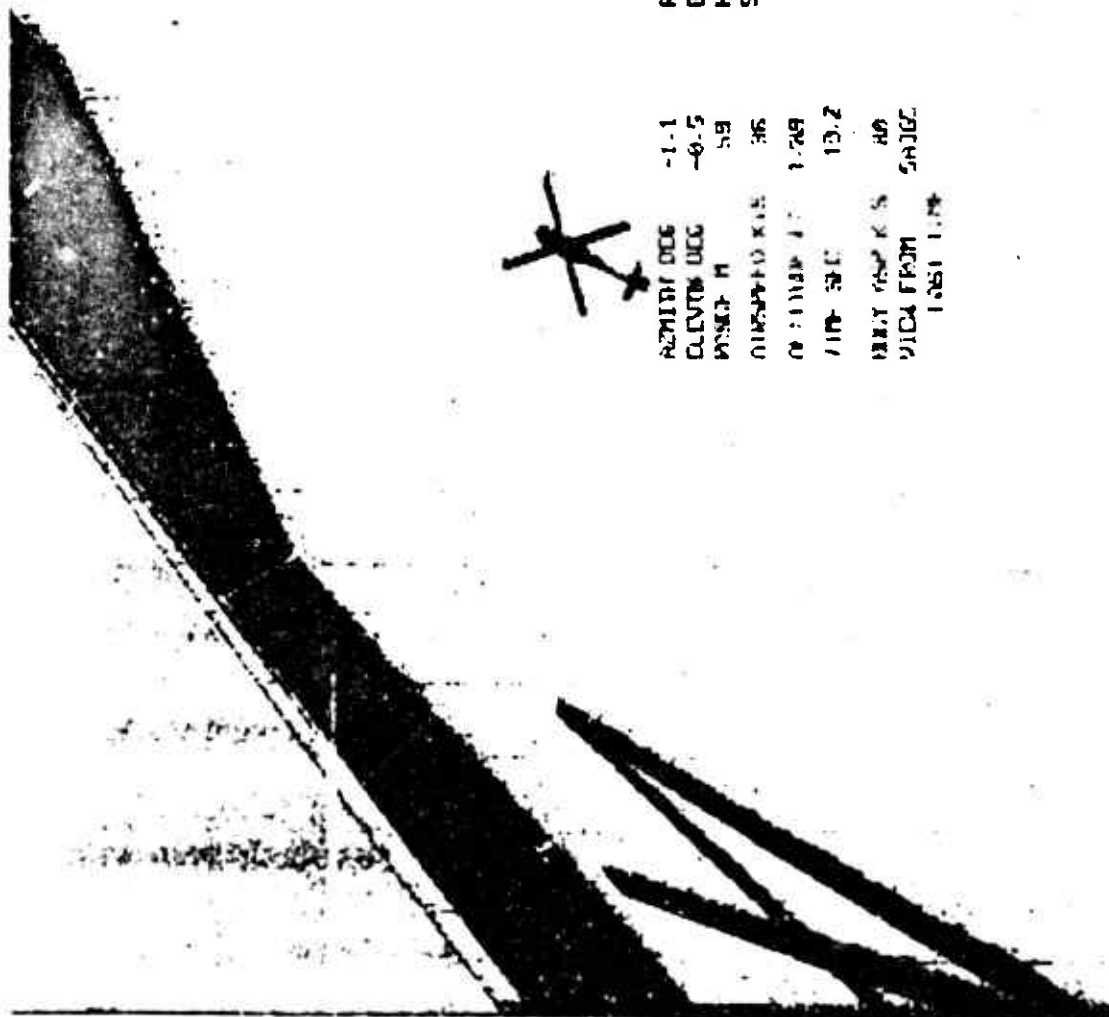


Figure 44. Cockpit Display, Counter 411011



RESULTANT 2-2
 BANK ANGLE 30
 ROLLING 12
 SIDE SLIP -25.0

AZIMUTH DEG -1.1
 CLIMB DEG -0.5
 PITCH DEG 59
 AIRSPEED KTS 36
 ALTITUDE FT 1789
 AIR SPEED 13.2
 WING AREA SQ FT 80
 WING FROM SAGE
 1051 1.4



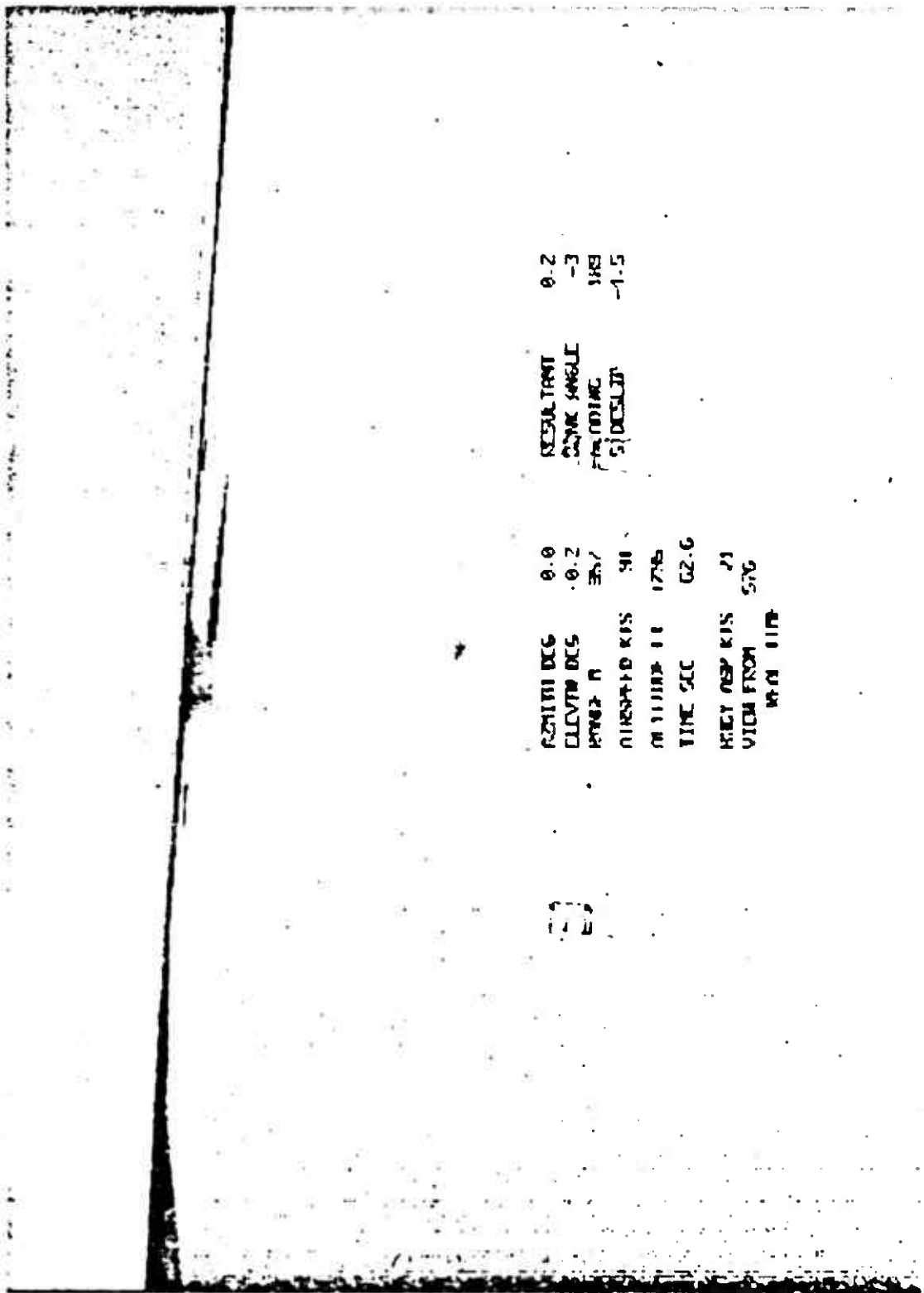
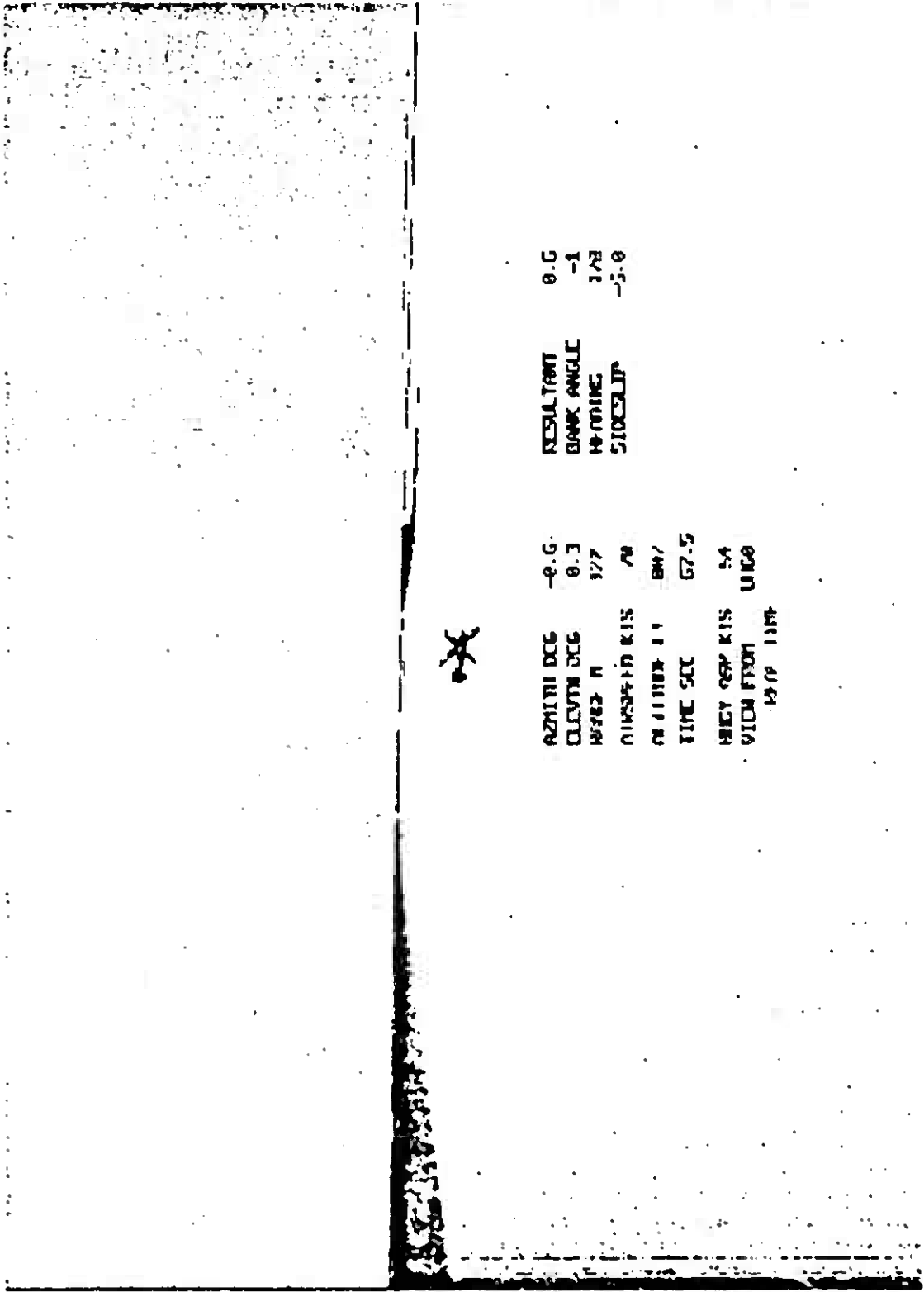


Figure 45. Cockpit Display, Counter 23038



AZIMUTH DEG	-0.0	RESALTANT	0.0
ELEVATION DEG	0.3	BANK ANGLE	-1
WIND N	177	HEADING	178
AIRSPEED KTS	70	SPEEDUP	-5.0
CRUISE F	807		
TIME SEC	67.5		
HEAT COP KTS	54		
VICIN FROM	UNCG		
WIND DIR	130		

Figure 46. Cockpit Display, Counter 27026

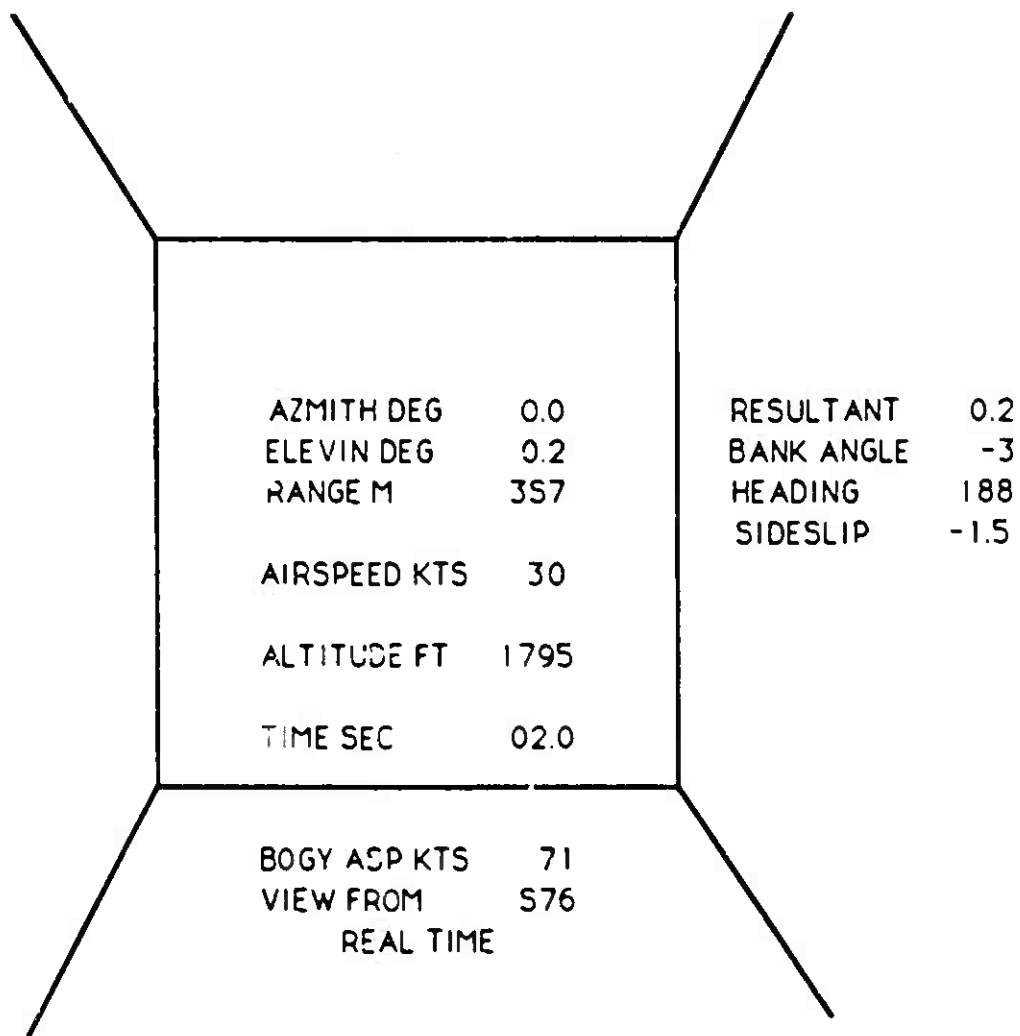


Figure 47. Overlaid Data Blocks, Cut-of-Cockpit Views

DATA FOR BROWN HELO		DATA FOR OD HELO	
S-76	TIME SEC S 4	UH-60	
	SLOW TIME		
AZMITH DEG	0.6	AZMITH DEG	6.8
ELEVIN DEG	1.9	ELEVIN DEG	2.0
RANGE FT	459	RANGE FT	459
AIRSPEED KTS	73	AIRSPEED KTS	89
ALTITUDE FT	1202	ALTITUDE FT	704
SIDESLIP DEG	1.7	SIDESLIP DEG	0.3

Figure 48. Overlaid Data Blocks, External Views

SCORING AND RATING METHODOLOGY

INTRODUCTION

This section of the report discusses the scoring systems devised for the simulated maneuvers and for the AACT engagements. The first part of this section will deal with scoring of the simulated maneuver results. This will include derivation of weighting factors for air-to-air (ATA), air-to-ground (ATG), nap-of-the-earth (NOE), and contours (CON) flight regimes. With the score for each maneuver available, a M/A rating could be obtained by taking the average of the scores for all nine maneuvers. The second part of this section will cover the scoring for AACT engagements where a firing opportunity occurred. This scheme used the time in the firing window, range and angular error to calculate points for each engagement. The final score was the sum of the points for that aircraft.

These M/A air-to-air ratings and the AACT scores were used as the basis for the correlation covered in the next section of this report.

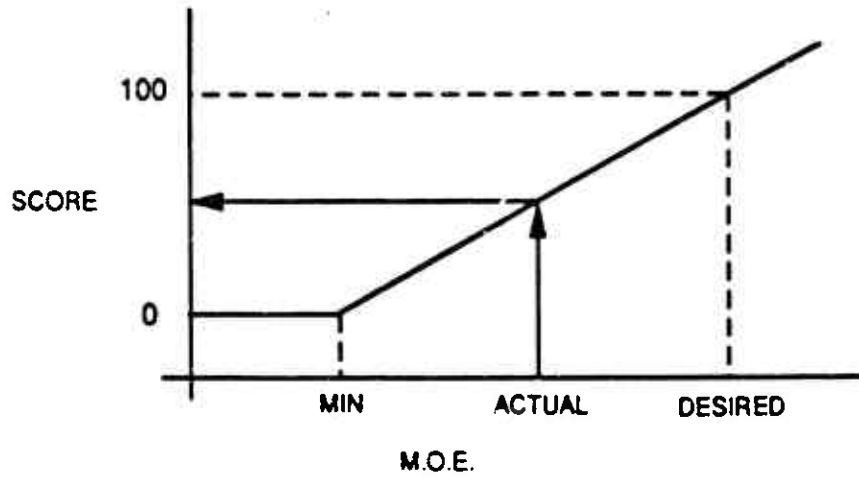
SCORING OF SIMULATED MANEUVERS

Methodology

The method for calculating the score for each maneuver is shown in Figure 49. For the hover bob-up, 80-knot steady turn, 80-knot steady climb, 80- and 130-knot decelerating turns and 140-knot pull-up, the MOE is better when it is numerically higher. For these cases a minimum acceptable maneuver result and a desired result for a highly agile and maneuverable helicopter were defined. These minimum and desired results were based on discussions with Sikorsky pilots and by reviewing the GenHel maneuver results themselves. The intent was to scale the scores so that most of the helicopters would fall between the minimum and desired results and so that the desired value would represent future requirements. The minimal value was assigned a score of zero while the desired value had a score of 100. The score for the maneuver was linearly interpolated between these two values based on the maneuver result. If the maneuver MOE was less than the minimal value, it was given a zero score, not a negative one. On the other hand, if the maneuver result was better than the desired value, a score greater than 100 was allowed.

For the zero to 80-knot accelerations, the corresponding decelerations and the hover turn, the MOE was time to complete the maneuver, so a numerically lower MOE is a better result. In this case a maximum value for the maneuver was defined and given a zero score with the desired value again having a score of 100. Again, the scores were a linear interpolation between the desired and maximum values. Times higher than the maximum value were assigned a zero score, but ones lower than the desired value were allowed their interpolated scores. The values for minimum or maximum and desired results for each maneuver are shown in Table 7. In addition, the scoring equation for each maneuver is also presented.

HIGHER M.O.E. IS BETTER (Turn Rate, Load Factor, etc.)



LOWER M.O.E. IS BETTER (time)

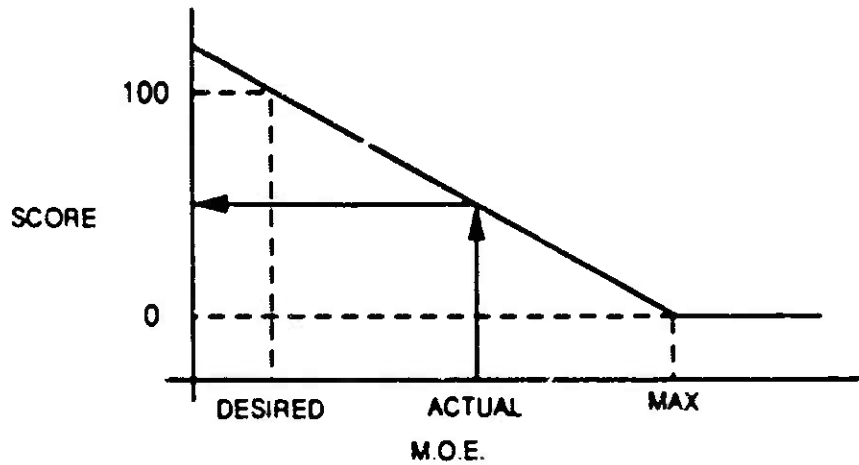


Figure 49. Maneuver Scoring Methodology

TABLE 7. MANEUVER SCORING EQUATIONS

MANEUVER	MINIMUM	DESIRED	MAXIMUM	SCORING EQUATION
1. HOVER BOB-UP	500 fpm	2000 fpm	- - -	$S = [(ROC - 500) / 1500] * 100$
2. 0 TO 80 KT ACCEL	- - -	9 eecs	14 secs	$S = 100 - [(T - 8) / 6] * 100$
3. 80 TO 0 KT DECEL	- - -	12 secs	13 eecs	$S = 100 - [(T - 12) / 6] * 100$
4. 80 KT STEADY CLIMB	1000 fpm	4000 fpm	- - -	$S = [(ROC - 1000) / 3000] * 100$
5. 80 KT STEADY TURN	1.6 g'e	2.6 g'e	- - -	$S = [(Nz - 1.6) / 1.0] * 100$
6. 80 KT DECEL TURN	20 deg/eec	45 deg/eec	- - -	$S = [(PSID - 20) / 25] * 100$
7. 130 KT DECEL TURN	8 deg/sec	20 deg/sec	- - -	$S = [(PSID - 8) / 12] * 100$
8. 140 KT PULL-UP	1.5 g's	2.75 g's	- - -	$S = [(Nz - 1.5) / 1.25] * 100$
9. HOVER TURN	- - -	3.5 secs	8.0 eecs	$S = 100 - [(T - 3.5) / 4.5] * 100$

Weighting Factors

It is clear that different maneuvers have different levels of importance, depending on the mission. For example, the hover bob-up is not very important in air-to-air combat, but it is critical in NOE flight. The M/A Phase I study (Reference 1) contained pilot ratings of each of the nine maneuvers for four different mission elements - air-to-air combat, air-to-ground combat, nap-of-the-earth and contour flying. These ratings were based on a poll of 13 pilots and assigned a value of 1 for most critical, 2 for moderately critical and 3 for least critical. The results are shown in Table 8 along with a conversion equation which changed these pilot ratings into weighting factors. The weighting factor was scaled from zero to 1.0, with 1.0 being most beneficial and 0.0 being not important.

Overall, the results look very reasonable. A bar graph chart of the resulting weighting factors is shown in Figure 50. The hover bob-up, for example, got a weighting factor of 0.1 for ATA combat, but 1.0 for NOE flying. Conversely, the 140-knot pull up has a weighting factor of 0.9 in ATA combat but only 0.05 in NOE flight.

By taking the maneuver scores and filtering them through the weighting factors, an assessment of the overall M/A characteristics of the helicopter can be made together with its capability in various flight modes.

TABLE 8. M/A WEIGHTING FACTORS DERIVATION

MANEUVER	MISSION							
	ATA		ATG		NOE		CONTOUR	
	PR	WF	PR	WF	PR	WF	PR	WF
1. HOVER BOB-UP	2.8	0.10	1.8	0.60	1.0	1.00	2.1	0.45
2. 0 TO 80 KT ACCEL	1.2	0.90	1.7	0.65	1.4	0.80	1.7	0.65
3. 80 TO 0 KT DECEL	1.6	0.70	1.9	0.55	1.4	0.80	1.7	0.65
4. 80 KT CLIMB	1.3	0.85	2.1	0.45	2.3	0.35	1.5	0.75
5. 80 KT STEADY TURN	1.6	0.70	2.1	0.45	2.5	0.25	1.6	0.70
6. 80 KT DECEL TURN	1.9	0.55	1.5	0.75	1.7	0.65	1.7	0.65
7. 130 KT DECEL TURN	1.2	0.90	2.0	0.50	2.8	0.10	1.8	0.60
8. 140 KT PULL-UP	1.2	0.90	2.0	0.50	2.9	0.05	1.9	0.55
9. HOVER TURN	1.9	0.55	1.5	0.75	1.0	1.00	2.4	0.30

PR - pilot rating

WF - weighting factor

WF = 1.00 - [(PR-1) * 0.50]

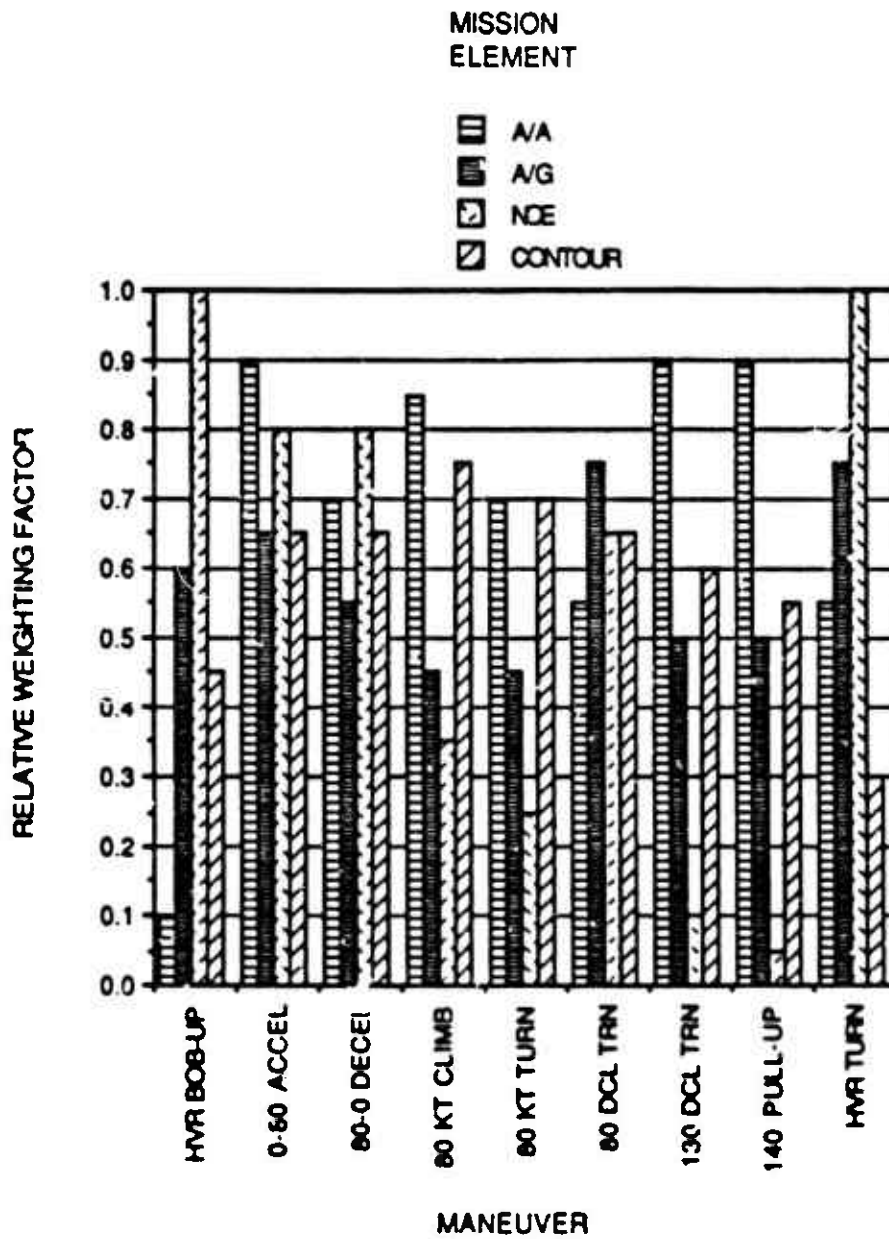


Figure 50. M/A Weighting Factors Chart

Aircraft Scores and Ratings

The resulting M/A scores and ratings are presented in Tables 9 to 23. The first ten tables cover the eight aircraft studied with the UH-60A and AH-64A evaluated at both their AACT weights and their BDGW. The next five tables cover the Mi-28 parametric study.

Each table provides a list of the nine maneuvers, the maneuver MGE result the basic score for that maneuver based on the scoring equations of Table 7 and the scores for each of the four mission elements calculated by using weighting factors of Table 8. For example, in Table 9, the UH-60A at its AACT gross weight achieved 2.45 g's in the 140-knot pull-up. The scoring equation for this maneuver is:

$$S = [(Nz - 1.5)/1.25] * 100$$

In this case the UH-60A gets a score of 76.00 for this maneuver.

The weighting factors for the four mission elements are:

ATA - 0.90
ATC - 0.50
NOE - 0.05
CON - 0.55

As a consequence, the scores for each of these elements is the basic score of 76.0 times the weighting factor, or:

ATA 0.76 * 0.90 = 68.40
ATC = 0.76 * 0.50 = 38.00
NOE = 0.76 * 0.05 = 3.80
CON = 0.76 * 0.55 = 41.80

After the scores for basic maneuver and the four mission elements are available, the ratings can be calculated by taking the sum of the scores for a mission element and dividing by the sum of the weighting factors. For example, the AACT UH-60A has a total score of 400.45 for the ATA element, the sum of the ATA weighting factors is 5.20, so the ATA M/A rating is (400.45/5.20) or 77.01. The same procedure is followed for the basic data and for the other mission elements. Thus, the resulting M/A rating for the AACT UH-60A are:

BASIC - 77.54
ATA - 79.01
ATC - 77.01
NOE - 76.36
CON - 76.99

Before proceeding further, it should be noted that the M/A ratings reflect the results of the simulation maneuvers and are intended to be estimators of each aircraft intrinsic maneuverability and agility characteristics. These ratings are the result of nine discrete maneuvers flown with an automatic controller. If any one of the aircraft studied were to be flown through these same maneuvers, the results could be better or worse. The computer simulation models

are good replicas of the helicopters, but not exact. A pilot flying one of the maneuvers might not control the aircraft as precisely as the automatic controllers in the computer simulation, but he would also not be tightly limited by the constraints. The actual flight test results might be slightly better or worse than these predictions. In addition, the intrinsic M/A characteristics of the helicopter make only a partial contribution to mission success. Obviously, pilot training, sensor capability and weapon lethality are also very important parts of mission capability.

The simulation results will be discussed below on an aircraft-by-aircraft basis.

UH-60A BLACK HAWK

The AACT weight BLACK HAWK (Table 9) had the best overall results, with a basic M/A rating of 77.5 and ratings for the other flight regimes that varied from 79.0 for ATA to 76.3 in NOE flight. This helicopter did not necessarily have the best results for each maneuver. Rather, its capabilities were consistently good for all nine maneuvers. This result can be attributed primarily to the light AACT test weight. When the BLACK HAWK was evaluated at its more typical BDCW of 16,825 pounds, the basic M/A rating dropped to 56.9 with a variation between 55.9 and 61.3 for the various mission elements as shown in Table 10. The BLACK HAWK basically has both ample power and an excellent rotor, so it does well at low, mid, and high speeds. Its M/A ratings are very similar for all of the four mission elements.

S-76A

Being a civil aircraft, the S-76A ended up with a 35.8 basic M/A rating. This helicopter performed best in hover and at low speeds. For example, the ATA rating was 34.8 while the NOE rating was 44.9 as shown in Table 11. The S-76 does fairly well at low speeds since its high power loading is compensated for by the relatively low disk loading. At high speeds, however, the rotor thrust capability is inadequate to allow good maneuver results. The rotor was optimized for the cruise condition of a civil transport, not for high maneuverability.

CH-53E Super Stallion

For this evaluation, the CH-53E was flown at its BDCW weight of 56,000 pounds and at 105 percent rotor speed. For this configuration, the Super Stallion had a M/A rating of 57.4. In the contour regime, the score went up to 61.3 while it dropped to 54.0 in NOE conditions as shown in Table 12. These are remarkably good ratings for such a large aircraft. However, if flown at 100 percent rotor speed and higher gross weights, one would expect the scores to be significantly reduced. The Super Stallion has both a low power loading and high solidity. The large amount of power compensates for the high disk loading at low speeds while the high solidity provides good thrust margin at high speeds. The reasonably good scores achieved by this large helicopter indicate that the 9 maneuvers chosen tend to emphasize maneuverability rather than agility.

AH-64A Apache

The AH-64A (AACT) scores and ratings are shown in Table 13. For the heavy AACT weight of 16,222 pounds, the basic M/A rating was 48.9, with the best flight condition being NOE where the rating went up to 51.4 and the worst for contour flying where the rating dropped slightly to 47.5. When flown at the BDGW of 14,770 pounds, the maneuver results, scores and ratings all improved considerably. The ratings were very consistent, with a basic value of 65.6 and an NOE rating of 67.0 while the rating was 64.9 for contour flight. (Table 14). Like the BLACK HAWK, the Apache features both ample power and an excellent rotor designed to provide good maneuverability. Thus, the maneuver results are good over low, mid, and high speed regimes. As expected, the addition of about 1500 pounds (almost 10 percent of the gross weight) degrades the M/A ratings significantly.

OH-58A Kiowa

The OH-58A (Table 15) was hampered by a maximum design level flight speed limit of 120 knots. Thus it could not perform either the 130-knot decelerating turn or the 140-knot pull-up and got a zero score for them. On the other hand, it did very well in the hover bob-up. Overall, the M/A rating was 34.9, but the variation with mission element was significant. The NOE rating was a very good 48.81 while ATG was 37.1. In contour flying, the rating dropped to 31.9 and it was a lower 28.2 in ATA as might be expected. The Kiowa has a very low disk loading and good power loading (with 420-shp) so it does well in the low speed regime. Performance at mid-speeds is hampered by low solidity and high speeds are beyond its capabilities. Thus, it generates a 20-point spread in its M/A ratings.

TABLE 9. UH-60A M/A SCORING AND RATING SUMMARY (AACT)

UH-60A GW=14,685 lbs (AACT)						
Ref. HP=2928						
	Maneuver	BASIC	A/A	A/G	NOE	CONTOUR
	Result	Score	Score	Score	Score	Score
Maneuver						
1. Hover Bob-up: Max ROC (ft/min)	1710	80.67	8.07	48.40	80.67	36.30
2. Accel Hover to 80 kts Time (sec)	8.3	95.00	85.50	61.75	76.00	61.75
3. Decel 80 kts to Hover: Time (sec)	14.7	55.00	38.50	30.25	44.00	35.75
4. 80 kt Steady Climb: ROC (ft/min)	3682	89.40	75.99	40.23	31.29	67.05
5. 80 kt Steady Turn: Nz (g's)	2.3	70.00	49.00	31.50	17.50	49.00
6. 80 kt Decel Turn: Turn Rate (deg/sec)	33.3	53.20	29.26	39.90	34.58	34.58
7. 130 kt Decel Turn: Turn Rate (deg/sec)	19.3	94.17	84.75	47.08	42	56.50
8. 140 kt Pull-up: Max Nz (g's)	2.45	76.00	68.40	38.00	3.80	41.80
9. Hover Turn: Time (sec)	4.2	84.44	46.44	63.33	84.44	25.33
	Total	697.88	485.91	400.45	381.70	408.96
	Avg Factor	9.00	6.15	5.20	5.00	5.30
	Rating	77.54	79.01	77.01	76.34	76.99

TABLE 10. UH-60A M/A SCORING AND RATING SUMMARY (BDGW)

UH-60A GW=16,825 lbs (BDGW)						
Ref. HP=2828						
	Maneuver	BASIC	A/A	A/G	NDE	CONTOUR
	Results	Score	Score	Score	Score	Score
Maneuver						
1. Hover Bob-up: Max ROC (ft/min)	1327	55.13	5.51	33.08	55.13	24.81
2. Accel Hover to 00 kts: Time (sec)	9.8	70.00	63.00	45.50	56.00	45.50
3. Decel 80 kts to Hover: Time (sec)	13.6	73.33	51.33	40.33	58.67	47.67
4. 80 kt Steady Climb: ROC (ft/min)	3022	67.40	57.29	30.33	23.59	50.55
5. 80 kt Steady Turn: Nz (g's)	1.98	38.00	26.60	17.10	9.50	26.60
6. 80 kt Decel Turn: Turn Rate (deg/sec)	26.9	27.60	15.18	20.70	17.94	17.94
7. 130 kt Decel Turn: Turn Rate (deg/sec)	15.1	59.17	53.25	29.58	5.92	35.50
8. 140 kt Pull-up: Max Nz (g's)	2.05	44.00	39.60	22.00	2.20	24.20
9. Hover Turn: Time (sec)	4.5	77.78	42.78	58.33	77.78	23.33
	Total	512.41	354.54	296.96	306.72	295.10
	Avg. Factor	9.00	6.15	5.20	5.00	5.30
	Rating	56.93	57.65	57.11	61.34	55.87

TABLE 11. S-76A M/A SCORING AND RATING SUMMARY

S-76A GW=8,925 lbs						
Ref. HP=1300						
	Maneuver	BASIC	A/A	A/G	NDE	CONTOUR
	Result	Score	Score	Score	Score	Score
Maneuver						
1. Hover Bob-up: Max ROC (ft/min)	1020	34.67	3.47	20.80	34.67	15.60
2. Accel Hover to 80 kts: Time (sec)	11.1	48.33	43.50	31.42	38.67	31.42
3. Decel 80 kts to Hover: Time (sec)	15	50.00	35.00	27.50	40.00	32.50
4. 80 kt Steady Climb: ROC (ft/min)	2584	52.80	44.88	23.76	18.48	39.60
5. 60 kt Steady Turn: Nz (g's)	1.8	20.00	14.00	9.00	5.00	14.00
6. 60 kt Decel Turn: Turn Rate (deg/sec)	23	12.00	6.60	9.00	7.80	7.60
7. 130 kt Decel Turn: Turn Rate (deg/sec)	10.2	18.33	16.50	9.17	1.83	11.00
8. 140 kt Pull-up: Max Nz (g's)	1.6	6.00	7.20	4.00	0.40	4.40
9. Hover Turn: Time (sec)	4.5	77.78	42.78	56.33	77.78	23.33
	Total	321.91	213.92	192.98	224.62	179.65
	Avg. Factor	9.00	6.15	5.20	5.00	5.30
	Rating	35.77	34.78	37.11	44.92	33.90

TABLE 12. CH-53E M/A SCORING AND RATING SUMMARY

CH-53E GW=56,000 lbs						
Ref. HP=12339						
	Maneuver	BASIC	A/A	A/G	NCE	CONTOUR
	Result	Score	Score	Score	Score	Score
Maneuver						
1. Hover Bob-up: Max ROC (ft/min)	1244	49.60	4.96	29.76	49.60	22.32
2. Accel Hover to 80 kts: Time (sec)	9.6	73.33	66.00	47.67	58.67	47.67
3. Decel 80 kts to Hover: Time (sec)	12.6	90.00	63.00	49.50	72.00	58.50
4. 80 kt Steady Climb: ROC (ft/min)	3433	81.10	68.94	36.50	28.39	60.83
5. 80 kt Steady Turn: Nz (g's)	1.91	31.00	21.70	13.95	7.75	21.70
6. 80 kt Decel Turn: Turn Rate (deg/sec)	36.5	66.00	36.30	49.50	42.90	42.90
7. 130 kt Decel Turn: Turn Rate (deg/sec)	18.3	65.83	77.25	42.92	8.58	51.50
8. 140 kt Pull-up: Max Nz (g's)	2	40.00	36.00	20.00	2.00	22.00
9. Hover Turn: Time (sec)	8.8	0.00	0.00	0.00	0.00	0.00
	Total	516.87	374.15	289.79	269.89	327.41
	Avg. Factor	9.00	6.15	5.20	5.00	5.30
	Rating	57.43	60.84	55.73	53.98	61.78

TABLE 13. AH-64A M/A SCORING AND RATING SUMMARY (AACT)

AH-64A GW=16,222 lbs (AACT)						
Ref. HP=2784						
	Maneuver	BASIC	A/A	A/G	NCE	CONTOUR
	Result	Score	Score	Score	Score	Score
Maneuver						
1. Hover Bob-up: Max ROC (ft/min)	1140	42.67	4.27	25.60	42.67	19.20
2. Accel Hover to 80 kts: Time (sec)	12.3	28.33	25.50	18.42	22.67	18.42
3. Decel 80 kts to Hover: Time (sec)	13.7	71.67	50.17	39.42	57.33	46.58
4. 80 kt Steady Climb: ROC (ft/min)	2622	54.07	45.96	24.33	18.92	40.55
5. 80 kt Steady Turn: Nz (g's)	1.88	28.00	19.60	12.60	7.00	19.60
6. 80 kt Decel Turn: Turn Rate (deg/sec)	30.4	41.60	22.88	31.20	27.04	27.04
7. 130 kt Decel Turn: Turn Rate (deg/sec)	15.7	64.17	57.75	32.08	6.42	38.50
8. 140 kt Pull-up: Max Nz (g's)	1.95	36.00	32.40	15.00	1.80	19.80
9. Hover Turn: Time (sec)	4.7	73.33	40.33	5.00	73.33	22.00
	Total	439.83	298.85	256.65	257.18	251.69
	Avg. Factor	9.00	6.15	5.20	5.00	5.30
	Rating	48.87	48.59	49.36	51.44	47.49

TABLE 14. AH-64A M/A SCORING AND RATING SUMMARY (BDGW)

AH-64A GW=14,770 lbs (BDGW)						
Ref. HP=2784						
	Maneuver	BASIC	A/A	A/G	NDE	CONTOUR
	Result	Score	Score	Score	Score	Score
Maneuver						
1. Hover Bob-up: Max ROC (ft/min)	1450	63.33	6.33	38.00	63.33	28.50
2. Accel Hover to 80 kts: Time (sec)	10.3	61.67	55.50	40.08	49.33	40.08
3. Decel 80 kts to Hover: Time (sec)	13.4	76.67	53.67	42.17	61.33	49.83
4. 80 kt Steady Climb: ROC (ft/min)	2948	64.93	55.19	29.22	22.73	48.70
5. 80 kt Steady Turn: Nz (g's)	2.08	48.00	33.60	21.60	12.00	33.60
6. 80 kt Decel Turn: Turn Rate (deg/sec)	35.1	60.40	33.22	45.30	39.26	39.26
7. 130 kt Decel Turn: Turn Rate (deg/sec)	18.1	84.17	75.75	42.08	8.42	50.50
8. 140 kt Pull-up: Max Nz (g's)	2.2	56.00	50.40	28.00	2.80	30.80
9. Hover Turn: Time (sec)	4.6	75.56	41.56	56.67	75.56	22.67
	Total	590.72	405.22	343.12	334.76	343.94
	Avg Factor	9.00	6.15	5.20	5.00	5.30
	Rating	65.64	65.89	65.98	66.95	64.89

TABLE 15. OH-58A M/A SCORING AND RATING SUMMARY

OH-58A GW=2,790 lbs						
Ref HP=420						
	Maneuver	BASIC	A/A	A/G	NDE	CONTOUR
	Result	Score	Score	Score	Score	Score
Maneuver						
1. Hover Bob-up: Max ROC (ft/min)	1650	76.67	7.67	46.00	76.67	34.50
2. Accel Hover to 80 kts: Time (sec)	11.5	41.67	37.50	27.08	33.33	27.06
3. Decel 60 kts to Hover: Time (sec)	16	33.33	23.33	18.33	26.67	21.67
4. 60 kt Steady Climb: ROC (ft/min)	2195	39.93	33.86	17.93	13.94	29.68
5. 80 kt Steady Turn: Nz (g's)	1.87	27.00	18.90	12.15	6.75	18.90
6. 80 kt Decel Turn: Turn Rate (deg/sec)	26	24.00	13.20	18.00	15.60	15.60
7. 130 kt Decel Turn: Turn Rate (deg/sec)	0	0.00	0.00	0.00	0.00	0.00
8. 140 kt Pull-up: Max Nz (g's)	0	0.00	0.00	0.00	0.00	0.00
9. Hover Turn: Time (sec)	4.8	71.11	39.11	53.33	71.11	21.33
	Total	313.61	173.57	192.83	244.07	138.96
	Avg Factor	9.00	6.15	5.20	6.00	5.30
	Rating	34.85	26.22	37.08	48.81	31.88

AH-1S Cobra

The AH-1S performance was average, hampered by a high power loading. The results, as shown in Table 16, are reasonably consistent for the various flight conditions. NOE is best with a rating of 44.6 while contour is worst at 40.9. A basic rating of 42.4 was achieved. In the low speed regime, the Cobra's low disk loading was compromised by its high power loading so the maneuver results were lackluster. At high speeds, the low solidity and somewhat high blade-loading reduce its ability to do well in the maneuvers.

SA-365N Dauphin

The Dauphin, designed as a civil aircraft, did not receive very good scores in comparison to the other aircraft in the study. Its overall M/A rating was 36.5, although the NOE rating was 47.5 as shown in Table 17. The lowest score, 35.2, was obtained for contour flying. However, in AACT IV the SA-365N did very well by making use of its large sideslip envelope. This allowed it to make very quick mid-speed pedal turns. None of the nine maneuvers of this study evaluated that capability. This suggests that a large sideslip turn should be added to the maneuver list. Overall, the Dauphin was much like the S-76. As a civil aircraft, it is optimized for the high-speed cruise condition. As a consequence, it has both high disk loading and high blade loading while its power loading is only average. The unique attribute of the Fenestron to allow high sideslip angles at high speed should be noted, however.

Mi-28 HAVOC

The baseline HAVOC (Table 18) was flown at a gross weight of 22,894 pounds. This weight was provided by Soviet delegates at the 1989 Paris Air Show and validated using existing Sikorsky parametric methods as noted in Appendix K. The rotor tip speed, also provided by the Soviets, is a typically modern 715 feet per second. Yaw inertia was estimated using the methodology outlined in Appendix G. The HAVOC was a solid mid-pack aircraft with an overall M/A rating of 52.3. The NOE rating was higher at 62.8 while the ATA rating was only 50.7.

Parametrically, increasing power improved the ratings as shown in Tables 19 and 20. Increases of 400 and 900 shp were evaluated for the hover bob-up, acceleration from hover to 80 knots, the 80-knot steady climb and 80-knot steady turn. The 900 shp increase resulted in an improvement in basic M/A rating from 52.3 to 59.2. The NOE M/A rating improved by almost eight points to 70.1 while the ATA value improved by six points to 56.2. The intermediate case of a 400 shp increase resulted in ratings between the baseline and the 900 shp case. The hover bob-up showed a fairly linear variation with increased power, as did the 80-knot climb. However, the 80-knot turn showed clear evidence of rotor stall, so the increased power was not usable.

Rotor speed increase to 105 percent (Table 21) was evaluated in the 80- and 130-knot decelerating turns and the 140-knot pull-up. As might be expected, this improved the ATA score by 6.4 points. The ATG score showed less improvement, 5.4 points, while the NOE and contour scores increased by 2.2 and 5.5 points, respectively.

Varying yaw inertia by plus and minus 10 percent changed the hover turn scores significantly. The increased inertia case (Table 22) took 0.23 second longer to complete the 180-degree turn and decreased the hover score from 66.7 points to 61. For a decrease in yaw inertia, the maneuver score improved to 72.2 points as a result of a .25 second improvement in the time to turn (Table 23). However, since the M/A rating is the average of all nine maneuvers, these significant changes in the hover turn score only change the M/A rating slightly. The increased inertia case reduces the basic rating by 0.6 point and the decreased yaw inertia case only increases it by the same amount.

The baseline HAVOC at 22,894 pounds is average in its disk loading, blade loading and power loading. As a consequence it tends to get good scores over the whole speed range, but not high ones. The only exception was the deceleration from 80 knots to hover where its high drag and relatively high disk loading gave it a score of 115.

After the parametric study was completed, Sikorsky pilots reviewed a copy of the data. They noted that the weight of 22,984 pounds represented a high weight, air-to-ground configuration for the HAVOC and that it could fly an air-to-air mission at a much lighter weight. A weight analysis, discussed in Appendix K, indicated that an air-to-air configuration would have a gross weight of around 20,000 pounds. Time was not available to run a full set of GenHel maneuvers at this lighter weight, but an empirically based estimate of M/A ratings was made and is presented in Appendix L.

Concluding Observations

Overall, the first observation to emerge from these results is that each aircraft possesses its own "signature" of characteristics. Secondly, the use of simple parameters like disk loading or blade loading can give insight to the maneuver results, but not predict them. The modern Army helicopters (UH-60A, AH-64A) designed with ample power to provide altitude capability and with good maneuverability do very well in this study, as expected. The civil aircraft (S-76A, SA-365N) do very poorly as they were optimized for high speed cruise and not for maneuverability. The older generation of Army helicopters (OH-58A, AH-1S) tended to fall between the first two. The CH-53E does surprisingly well but it was flown at a moderate weight and at 105 percent rotor speed. The fact that the Super Stallion does well is an indication that the 9 selected maneuvers emphasize maneuverability over agility. The Mi-28 at 22,984 pounds is only a fair performer. In all cases, a significant reduction in gross weight leads to significant improvement in the M/A scores.

TABLE 16. AH-1S M/A SCORING AND RATING SUMMARY

AH-1S GW=9,620 lbs						
Ref. HP=1290						
	Maneuver	BASIC	A/A	A/G	NCE	CONTOUR
	Result	Score	Score	Score	Score	Score
Maneuver						
1. Hover Bob-up: Max ROC (ft/min)	776	18.40	1.84	11.04	18.40	8.28
2. Accel Hover to 80 kts: Time (sec)	12	33.33	30.00	21.67	26.67	21.67
3. Decel 80 kts to Hover: Time (sec)	13.5	75.00	52.50	41.25	60.00	48.75
4. 80 kt Steady Climb: ROC (ft/min)	2127	37.57	31.93	16.91	13.15	28.18
5. 80 kt Steady Turn: Nz (g's)	1.89	29.00	20.30	13.05	7.25	20.30
6. 80 kt Decel Turn: Turn Rate (deg/sec)	27	28.00	15.40	21.00	18.20	18.20
7. 130 kt Decel Turn: Turn Rate (deg/sec)	12.15	34.58	31.13	17.29	3.46	20.75
8. 140 kt Pull-up: Max Nz (g's)	2.15	52.00	46.80	26.00	2.60	28.60
9. Hover Turn: Time (sec)	4.7	73.33	40.33	55.00	73.33	22.00
	Total	381.22	270.23	223.20	223.06	216.72
	Avg. Factor	9.00	6.15	5.20	5.00	5.30
	Rating	42.36	43.94	42.92	44.61	40.89

TABLE 17. SA-365N M/A SCORING AND RATING SUMMARY

SA-365N-1 GW=8,750 lbs						
Ref. HP=1372						
	Maneuver	BASIC	A/A	A/G	NCE	CONTOUR
	Result	Score	Score	Score	Score	Score
Maneuver						
1. Hover Bob-up: Max ROC (ft/min)	849	23.27	2.33	13.96	23.27	10.47
2. Accel Hover to 80 kts: Time (sec)	11.2	46.67	42.00	30.33	37.33	30.33
3. Decel 80 kts to Hover: Time (sec)	12.7	88.33	61.83	48.58	70.67	57.42
4. 80 kt Steady Climb: ROC (ft/min)	2432	47.73	40.57	21.48	16.71	35.80
5. 80 kt Steady Turn: Nz (g's)	1.71	11.00	7.70	4.95	2.75	7.70
6. 80 kt Decel Turn: Turn Rate (deg/sec)	23.5	14.00	7.70	10.50	9.10	9.10
7. 130 kt Decel Turn: Turn Rate (deg/sec)	11.6	21.67	19.50	10.83	2.17	13.00
8. 140 kt Pull-up: Max Nz (g's)	1.5	0.00	0.00	0.00	0.00	0.00
9. Hover Turn: Time (sec)	4.6	75.56	41.56	56.67	75.56	22.67
	Total	328.22	223.19	197.31	237.55	186.49
	Avg. Factor	9.00	6.15	5.20	5.00	5.30
	Rating	36.47	36.29	37.94	47.51	35.19

TABLE 18. MI-28 M/A SCORING AND RATING SUMMARY (BASELINE)

MI-28 GW=22,984 lbs (Baseline)						
Ref. HP= 4400						
	Maneuver	BASIC	A/A	A/G	NCE	CONTOUR
	Result	Score	Score	Score	Score	Score
Maneuver						
1. Hover Bob-up: Max ROC (ft/min)	1400	60.00	6.00	36.00	60.00	27.00
2. Accel Hover to 80 kts: Time (sec)	10.5	58.33	52.50	37.92	46.67	37.92
3. Decel 80 kts to Hover: Time (sec)	11.05	115.83	81.08	63.71	92.67	75.29
4. 80 kt Steady Climb: ROC (ft/min)	2467	48.90	41.57	22.01	17.12	36.63
5. 80 kt Steady Turn: Nz (g's)	1.83	23.00	16.10	10.35	5.75	16.10
6. 80 kt Decel Turn: Turn Rate (deg/sec)	27.3	29.20	16.06	21.90	18.98	18.98
7. 130 kt Decel Turn: Turn Rate (deg/sec)	14.31	52.58	47.33	26.29	5.26	31.55
8. 140 kt Pull-up: Max Nz (g's)	1.7	16.00	14.40	8.00	0.80	8.80
9. Hover Turn: Time (sec)	5	66.67	36.67	50.00	66.67	20.00
	Total	470.52	311.70	276.17	313.90	272.31
	Avg. Factor	9.00	6.15	5.20	5.00	5.30
	Rating	52.28	50.68	53.11	62.78	51.38

TABLE 19. MI-28 M/A SCORING AND RATING SUMMARY (400 shp increase)

MI-28 GW=22,984 lbs (+400 shp)						
Ref. HP= 4800						
	Maneuver	BASIC	A/A	A/G	NCE	CONTOUR
	Result	Score	Score	Score	Score	Score
Maneuver						
1. Hover Bob-up: Max ROC (ft/min)	1588	72.53	7.25	43.52	72.53	32.64
2. Accel Hover to 80 kts: Time (sec)	10.23	62.83	56.55	40.84	50.27	40.84
3. Decel 80 kts to Hover: Time (sec)	11.05	115.83	81.08	63.71	92.67	75.29
4. 80 kt Steady Climb: ROC (ft/min)	2884	62.80	53.38	28.26	21.98	47.10
5. 80 kt Steady Turn: Nz (g's)	1.87	27.00	18.90	12.15	6.75	18.90
6. 80 kt Decel Turn: Turn Rate (deg/sec)	27.3	29.20	16.06	21.90	18.98	18.98
7. 130 kt Decel Turn: Turn Rate (deg/sec)	14.31	52.58	47.33	26.29	5.26	31.55
8. 140 kt Pull-up: Max Nz (g's)	1.7	16.00	14.40	8.00	0.80	8.80
9. Hover Turn: Time (sec)	5	66.67	36.67	50.00	66.67	20.00
	Total	505.45	331.62	294.67	335.90	284.10
	Avg. Factor	9.00	6.15	5.20	5.00	5.30
	Rating	56.16	53.92	56.67	67.18	55.49

TABLE 20. MI-28 M/A SCORING AND RATING SUMMARY (900 shp increase)

MI-28 GW=22,984 lbs (+900 shp)							
Ref. HP= 5300							
	Maneuver	BASIC	A/A	A/G	NCE	CONTOUR	
	Result	Score	Score	Score	Score	Score	
Maneuver							
1	Hover Bob-up: Max ROC (ft/min)	1753	83.53	8.35	50.12	83.53	37.59
2	Accel Hover to 80 kts: Time (sec)	10.5	58.33	52.50	37.92	46.67	37.92
3	Decel 80 kts to Hover: Time (sec)	11.05	115.83	81.08	63.71	92.67	75.29
4	80 kt Steady Climb: ROC (ft/min)	3417	80.57	68.48	36.26	28.20	60.43
5	80 kt Steady Turn: Nz (g's)	1.9	21.00	21.00	13.50	7.50	21.00
6	80 kt Decel Turn: Turn Rate (deg/sec)	27.3	29.20	16.06	21.90	18.98	18.98
7	130 kt Decel Turn: Turn Rate (deg/sec)	14.31	52.58	47.33	26.29	5.26	31.55
8	140 kt Pull-up: Max Nz (g's)	1.7	16.00	14.40	8.00	0.80	8.80
9	Hover Turn: Time (sec)	5	66.67	36.67	50.00	66.67	20.00
	Total		532.72	345.87	307.69	350.27	311.55
	Avg. Factor		9.00	6.15	5.20	5.00	5.30
	Rating		59.19	56.24	59.17	70.05	58.78

TABLE 21. MI-28 M/A SCORING AND RATING SUMMARY (105% Nr)

MI-28 GW=22,984 lbs Nr=105%							
Ref. HP= 4400							
	Maneuver	BASIC	A/A	A/G	NCE	CONTOUR	
	Result	Score	Score	Score	Score	Score	
Maneuver							
1	Hover Bob-up: Max ROC (ft/min)	1400	60.00	6.00	36.00	60.00	27.00
2	Accel Hover to 80 kts: Time (sec)	10.5	58.33	52.50	37.92	46.67	37.92
3	Decel 80 kts to Hover: Time (sec)	11.05	115.83	81.08	63.71	92.67	75.29
4	80 kt Steady Climb: ROC (ft/min)	2467	48.90	41.57	22.01	17.12	36.68
5	80 kt Steady Turn: Nz (g's)	1.83	23.00	16.10	10.35	5.75	16.10
6	80 kt Decel Turn: Turn Rate (deg/sec)	30.6	42.40	23.32	31.80	27.55	27.56
7	130 kt Decel Turn: Turn Rate (deg/sec)	16.5	70.83	63.75	35.42	7.08	42.50
8	140 kt Pull-up: Max Nz (g's)	1.92	33.60	30.24	16.80	1.68	18.48
9	Hover Turn: Time (sec)	5	66.67	36.67	50.00	66.67	20.00
	Total		519.57	351.23	304.00	325.19	301.52
	Avg. Factor		9.00	6.15	5.20	5.00	5.30
	Rating		57.73	57.11	58.46	65.04	56.89

TABLE 22. M1-28 M/A SCORING AND RATING SUMMARY (+10X Izz)

M1-28 GW=22,984 lb (IZ=74707 slug-ft ²)							
Ref. HP= 4400							
	Maneuver	BASIC	A/A	A/G	NCE	CONTOUR	
	Result	Score	Score	Score	Score	Score	
Maneuver							
1.	Hover Bob-up: Max ROC (ft/min)	1400	60.00	6.00	36.00	60.00	27.00
2.	Accel Hover to 80 kts: Time (sec)	10.5	58.33	52.50	37.92	46.67	37.92
3.	Decel 80 kts to Hover: Time (sec)	11.05	115.83	81.08	63.71	92.67	75.29
4.	80 kt Steady Climb: ROC (ft/min)	2467	48.90	41.57	22.01	17.12	36.68
5.	60 kt Steady Turn: Nz (g's)	1.83	23.00	16.10	10.35	5.75	16.10
6.	80 kt Decel Turn: Turn Rate (deg/sec)	27.3	29.20	16.06	21.90	18.98	18.98
7.	130 kt Decel Turn: Turn Rate (deg/sec)	14.31	52.58	47.33	26.29	5.26	31.55
8.	140 kt Pull-up: Max Nz (g's)	1.7	16.00	14.40	6.00	0.80	6.80
9.	Hover Turn: Time (sec)	5.23	61.56	33.86	46.17	61.56	18.47
	Total		465.41	308.89	272.34	308.79	270.78
	Avg. Factor		9.00	6.15	5.20	5.00	5.30
	Rating		51.71	50.23	52.37	61.76	51.09

TABLE 23. M1-28 M/A SCORING AND RATING SUMMARY (-10X Izz)

M1-28 GW=22,984 lb (IZ=61124 slug-ft ²)							
Ref. HP= 4400							
	Maneuver	BASIC	A/A	A/G	NCE	CONTOUR	
	Result	Score	Score	Score	Score	Score	
Maneuver							
1.	Hover Bob-up: Max ROC (ft/min)	1400	60.00	6.00	36.00	60.00	27.00
2.	Accel Hover to 80 kts: Time (sec)	10.5	58.33	52.50	37.92	46.67	37.92
3.	Decel 80 kts to Hover: Time (sec)	11.05	115.83	81.08	63.71	92.67	75.29
4.	80 kt Steady Climb: ROC (ft/min)	2467	46.90	41.57	22.01	17.12	36.66
5.	80 kt Steady Turn: Nz (g's)	1.83	23.00	16.10	10.35	5.75	16.10
6.	60 kt Decel Turn: Turn Rate (deg/sec)	27.3	29.20	16.06	21.90	18.98	18.98
7.	130 kt Decel Turn: Turn Rate (deg/sec)	14.31	52.58	47.33	26.29	5.26	31.55
8.	140 kt Pull-up: Max Nz (g's)	1.7	16.00	14.40	6.00	0.80	6.80
9.	Hover Turn: Time (sec)	4.75	72.22	39.72	54.17	72.22	21.67
	Total		476.07	314.76	260.34	319.46	273.96
	Avg. Factor		9.00	6.15	5.20	5.00	5.30
	Rating		52.90	51.18	53.81	63.84	51.69

SCORING OF AACT ENCOUNTERS

In order to correlate the results of the simulated maneuvers to the AACT data, a method for scoring the AACT engagements was required. The methodology adopted consisted of the following:

- 1) Use the data of Table 6 to select those engagements where a firing opportunity occurred.
- 2) Review these engagements to determine if the firing opportunities were valid. As discussed below, there were many engagements where the mathematical criteria for a firing opportunity were achieved but the encounter was not really valid.
- 3) Assign points to each valid firing opportunity based on range, angular error and time in the firing window.
- 4) Calculate a final score by summing of all points achieved by each aircraft during a test.

Selection of Valid Firing Opportunities

A careful review of the engagement descriptions provided in Appendix J shows that many of the mathematical firing opportunities were not really valid. For example, many engagements were initialized with the two helicopters approaching one another on parallel, but offset, courses. Frequently, this would result in one or even both of the aircraft meeting the firing window criteria (range less than 1500 meters, angular error less than ± 3 degrees) before the actual engagement began. This, for example, is the case in counters 208019, 208025, 302019 and 417008 of Table 6. Other non-valid cases include 208026 where the S-76 never maneuvered after passing the UH-60A and the BLACK HAWK turned and achieved an easy firing window, and 302018 where the engagement had the AH-1S in a hover and the Apache simply approached while the Cobra remained stationary. All of these types of scenarios were deleted from the AACT scoring database. Of the 59 mathematical firing windows shown in Table 6, 27 were judged valid. With these limited firing opportunities available for analysis, the database was searched to find engagements where valid firing opportunities occurred with a five degree window. Only four such cases were found. Another concern was that all of the mathematical firing windows were very short, typically a few tenths of a second. Pilot comments indicated a feeling that the windows were much longer. However, since there were no gunfights in these aircraft, a pilot may have been in an excellent firing position and had the capability of staying in the window, but the target may have been in the mathematical window for only a short time. Future AACT activities should include gunsights and weapon emulators so the pilots can precisely position themselves and get feedback on their maneuvering, as was done in AACT IV.

It should be noted at this point that the data originally supplied by the Government for the AH-64A versus SA-365N were for engagements where the Apache was simulating use of a turreted gun (counters 417001 to 417012). These data were analyzed before the mistake was discovered. The correct data for fixed gun engagements (counters 411009 to 411023) were subsequently provided by the Government and also analyzed. The resulting analyses for both data sets will be provided herein for completeness, but only the fixed-gun data were used in the correlation effort.

The final result was 31 valid mathematical firing opportunities distributed as follows:

AACT II

S-76A vs OH-58A
6 cases

UH-60A vs OH-58A
9 cases

UH-60A vs S-76A
4 cases + 3 cases for a 5-degree window

AACT III

AH-1S vs OH-58A
1 case + 1 case for a 5-degree window

AACT IV

SA-365N vs AH-64A (fixed gun)
4 cases

SA-365N vs AH-64A (turreted gun)
3 cases

Method of Assigning Points

Points were awarded to the attack aircraft in each valid firing opportunity. The method for assigning points is shown in Figure 51. The three major factors in the calculation are minimum range, minimum angular error and time in the firing window. It is clear that a large angular error at long ranges is much worse than the same error at short ranges. To assign points, the "dispersion" of the boresight was calculated by taking the range times the angular error in radians. A dispersion coefficient was calculated as one minus the logarithm of the dispersion divided by 8.73. This scaling factor was set to give a value of one for a range of 500 meters and an angular error of one degree. A time coefficient was defined as the time in the firing window divided by two. The point allocation is the dispersion coefficient times the time coefficient times 100. Thus, a firing window for two seconds at a range of 500 meters with an angular error of one degree would achieve 100 points. Shorter range, smaller angular error or longer time in the window would increase the points and visa-versa. A points chart is shown in Figure 52.

The aircraft score for each test was the total of its points for all of the valid firing opportunities.

AACT Scores

The AACT scores are summarized in Tables 24 to 29. Each table is for one helicopter pair and lists the counter numbers, attack aircraft, victim aircraft, time in firing window, minimum range and minimum angle in firing window and points achieved by the attacking helicopter. It should be noted that the initial conditions for the encounters could have an impact on the scoring. Most of the engagements were "neutral", with the aircraft flying towards one another on parallel, offset courses. However, in some cases, one helicopter or the other was given an "advantage" position, with the encounter initialized with aircraft on the tail of the other or one aircraft in hover while the other attacked. A table showing the initial conditions for each encounter is provided in Appendix J, as are detailed discussions of each encounter.

Some aircraft pairs had many "valid" encounters, some had few. No effort was made to normalize the scores amongst all of the pairs. However, in the correlation effort discussed below the scores of each aircraft in a pair were normalized by the total of both aircraft scores.

The results of the AACT analysis are reviewed below:

S-76A vs OH-58A (Table 24)

A very uneven match. The Kiowa had one good window, getting 29.7 points, but the S-76 had five, including a long well-aimed one that netted 221.9 points. Final score was 330 for the S-76A and 29.7 for the OH-58A. Notable are the close ranges and generally short times of the firing opportunities.

EQUATIONS

Dispersion:	$D = \text{Range (m)} * \text{Angle (deg)} / 57.3$
Dispersion Coefficient:	$Dc = 1.0 - \text{Log (D/8.73)}$
Time Coefficient:	$Tc = \text{Time (secs)} / 2$
Score (points)	$S = Dc * Tc * 100$

EXAMPLE

Range -	870 meters
Angle -	1.73 degrees
Time -	0.5 seconds
D -	$870 * 1.73 / 57.3 = 26.267$
Dc -	$1.0 - \text{Log (26.267/8.73)} = 0.5216$
Tc -	$0.5 / 2 = 0.25$
S -	$0.5216 * 0.25 * 100 = \underline{13.04 \text{ points}}$

Figure 51. AACT Scoring Methodology

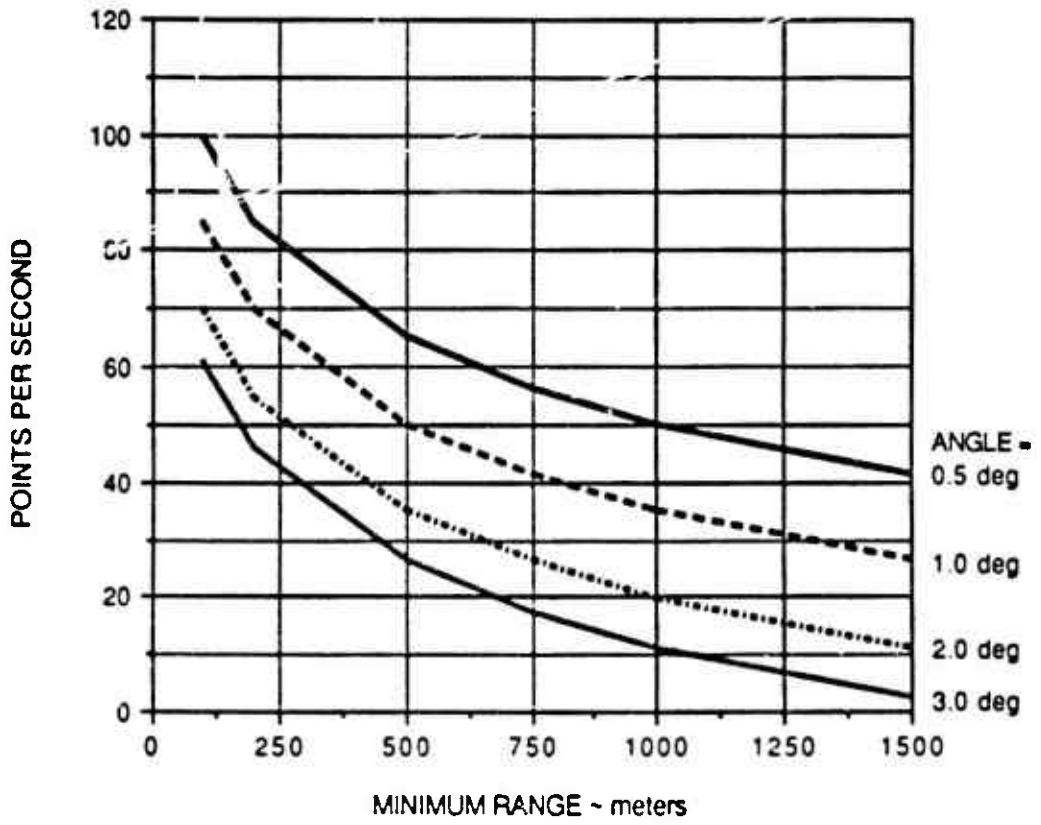


Figure 52. AACT Points Chart

TABLE 24. AACT SCORING SUMMARY

(S-76A versus OH-58A)

Counter	Attack Aircraft	Victim Aircraft	Time (Secs)	Range (m)	Angle (Degs)	Score (Points)
23020	S-76A	OH-58A	0.8	69	1.70	65.2
23020	OH-58A	S-76A	0.4	147	1.11	29.7
23021	S-76A	OH-58A	0.6	357	2.21	24.1
23021	S-76A	OH-58A	0.1	200	2.45	5.1
23032	S-76A	OH-58A	0.2	86	2.47	13.7
23038	S-76A	OH-58A	1.8	340	0.20	221.9

OH-58A TOTAL POINTS 29.7 S-76A TOTAL POINTS 330

UH-60A vs OH-58A (Table 25)

Another very uneven match. Of nine windows, the Kiowa only got one. The UH-60A final score of 265.4 represents consistent wins over the 30.6 of the OH-58A. There was one engagement with a range of only 60 meters. The OH-58A firing window was 1.8 seconds long but at a long range (1139 meters) so the points count was small.

UH-60A vs S-76A (Table 26)

In this case, the BLACK HAWK completely dominated the S-76A. There were four original firing windows plus three more that were just outside the criteria. The UH-60A was the attacker in five of these, getting 121 total points. The S-76A only managed to get 6.3 points. One of its windows was at very long range (1508 meters), the other had a large angular error (5 degrees). Note that if the three additional data sets had not been added, the S-76 score would have been zero.

AH-1S vs OH-58A (Table 27)

Only one regular firing opportunity was achieved by this pair. Another case with a 5.2-degree angular error was added. Both involved the Cobra as the attacking helicopter. The AH-1S received 17.8 points and the OH-58A received none.

SA-365N vs AH-64A (AH-64A fixed gun) (Table 28)

This pair had four valid encounters, three won by the Dauphin, giving it a score of 68.7 points while the single Apache firing opportunity netted it 34.3 points. However, the Apache points happened in an engagement where the SA-365N also scored points. In fact, the aircraft turned into each other and the Dauphin got a 0.5 second window at 334 meters two seconds before the Apache got a 0.4 second window at 194 meters. Both were counted for this study, but it could be argued that since the Dauphin "shot" first, the AH-64A firing opportunity should not be considered valid.

SA-365N vs AH-64A (AH-64A turreted gun) (Table 29)

Data for these cases should not really be considered since they were analyzed as fixed-gun engagements but were flown with the Apache in a turreted-gun configuration. Three firing windows were achieved, two by the AH-64A and one by the SA-365N. However, one Apache case was at long range and the other had a large angular error so the Dauphin got more points, a score of 30.6, compared to the AH-64A with 14.1 points.

TABLE 25. AACT SCORING SUMMARY

(UH-60A versus OH-58A)

Counter	Attack Aircraft	Victim Aircraft	Time (Secs)	Range (m)	Angle (Degs)	Score (Points)
27026	UH-60A	OH-58A	0.5	115	0.67	45.3
27026	UH-60A	OH-58A	0.4	139	2.14	24.5
27027	OH-58A	UH-60A	1.8	1139	2.01	30.6
27027	UH-60A	OH-58A	0.2	100	2.24	13.5
27027	UH-60A	OH-58A	0.4	107	1.10	32.6
27034	UH-60A	OH-58A	2.9	589	1.91	94.0
27036	UH-60A	OH-58A	0.2	60	0.54	21.9
27037	UH-60A	OH-58A	0.3	128	3.18	16.3
26038	UH-60A	OH-58A	0.3	160	2.20	17.3

UH-60A TOTAL POINTS 265.4OH-58A TOTAL POINTS 30.6

TABLE 26. AACT SCORING SUMMARY

(UH-60A versus S-76A)

Counter	Attack Aircraft	Victim Aircraft	Time (Secs)	Range (m)	Angle (Degs)	Score (Points)
208027	UH-60A	S-76A	0.8	1242	0.89	26.2
208027	UH-60A	S-76A	0.1	139	3.44	8.35
208019	UH-60A	S-76A	0.4	1467	1.70	6.0
208028	UH-60A	S-76A	0.7	89	3.4	42.6
208020*	S-76A	UH-60A	0.9	1508	2.70	4.0
208028*	UH-60A	S-76A	0.7	80	4.20	41.1
208028*	S-76A	UH-60A	0.5	810	5.0	2.3

*Did not meet firing window criteria, but close to boundaries

UH-60A TOTAL POINTS 121.0S-76A TOTAL POINTS 6.3

TABLE 27. AACT SCORING SUMMARY

(AH-1S versus OH-58A)

Counter	Attack Aircraft	Victim Aircraft	Time (Secs)	Range (m)	Angle (Degs)	Score (Points)
302013*	AH-1S	OH-58A	0.4	377	5.2	8.1
302013	AH-1S	OH-58A	0.2	191	2.8	9.7

*Did not meet firing window criteria, but close to boundaries

AH-1S TOTAL POINTS 17.8OH-58A TOTAL POINTS 0

TABLE 28. AACT SCORING SUMMARY
(AH-64A (fixed gun) versus SA-365N)

Counter	Attack Aircraft	Victim Aircraft	Time (Secs)	Range (m)	Angle (Degs)	Score (Points)
411011	SA-365N	AH-64A	0.2	59	1.21	18.5
411013	AH-64A	SA-365N	0.4	194	0.5	34.3
411013	SA-365N	AH-64A	0.5	339	0.67	33.6
411023	SA-365N	AH-64A	0.3	287	1.34	16.7

AH-64A TOTAL POINTS 34.3 SA-365N TOTAL POINTS 68.8

TABLE 29. AACT SCORING SUMMARY
(AH-64A (turreted gun) versus SA-365N)

Counter	Attack Aircraft	Victim Aircraft	Time (Secs)	Range (m)	Angle (Degs)	Score (Points)
417003	AH-64A	SA-365N	0.3	304	3.7	9.7
417003	SA-365N	AH-64A	0.6	251	1.9	30.6
417003	AH-64A	SA-365N	0.4	1162	2.6	4.4

NOTE: Firing windows based on assumption of a fixed gun, however, tests flown simulating turreted gun on the AH-64A.

AH-64A TOTAL POINTS 14.1 SA-365N TOTAL POINTS 30.6

CORRELATION OF M/A ANALYSIS TO AACT DATA

DISCUSSION OF CORRELATION METHOD

The objective of this part of the study is to compare results achieved by each helicopter in the AACT tests with the analytically derived M/A ratings. This is done in two ways. First, the AACT derived scoring is compared directly with the derived M/A ratings. Where the two ratings are vastly different explanations are offered. Secondly, the AACT test results are rationalized based on a comparison of each aircraft's level of the fundamental design parameter.

The methodology used here is to compare the predicted ratio of successful engagements to the actual. These successful engagement ratios are estimated as follows:

1. For the predicted ATA performance, the M/A ratings of the two combating helicopters are simply added and the success of each is taken as its percentage of the total. For example, in the case of the UH-60A vs the S-76 (AACT II) the M/A rating of each is

UH-60A	-	79.0
S-76A	-	<u>34.8</u>
		113.8

This methodology implies that the UH-60A would be expected to win 79 out of 113.8 encounters or 69.4%. The S-76A would be expected to win 34.8 out of 113.8 or 30.6%.

2. Similarly for the AACT tests, the total score of each of the two combating helicopters is added to establish a total potential score and the percentage of points each achieved of that total is the percentage of winning engagement expected. For example, as was noted previously in the S-76A vs the OH-58A combat, the S-76A received 330 points whereas the OH-58A received 89.7. Therefore, based on these results, the S-76A was successful 330 times out of 330 + 89.7 encounters or 78.6% of the time, and conversely the OH-58A was successful 21.4% of the encounters.

The actual winning engagement ratios are compared to the predicted winning engagement ratios to form the basis of the correlation. These ratios from both the M/A ratings and the AACT scores are presented graphically in Figures 53 to 57.

However, while the M/A rating is based on a direct comparison of each helicopter's physical capability, the AACT tests included other factors which may have influenced the results. For example, pilot proficiency or piloting choices of maneuvers may have had some effect on the firing window opportunities. Cockpit visibility differences between combating helicopters could also have been a factor. Specific aircraft maneuvering limits which are peculiar to each design, such as attitude rate limit which do not enter into the M/A ratings, could also have influenced the outcome. The engagement initial conditions, the number of engagements analyzed with either neutral, advantaged or disadvantaged set-ups, and the "fights on" positions could

influence the results. Finally, the requirements for safety and boundaries of the combat airspace may also have influenced the piloting techniques used. These factors are noted here as a reminder that the AACT test results contain more than just the maneuverability difference between each helicopter.

RESULTS OF THE CORRELATION

The following paragraphs detail the individual AACT test results and correlate those results with the M/A air-to-air (ATA) ratings.

AACT II

There were three combinations of combating pairs during AACT II testing. The UH-60A vs the OH-58A, the S-76A vs the UH-60A, and the S-76A vs the OH-58A.

S-76A vs OH-58A (Figure 53): The M/A ratings of these aircraft were similar, with the S-76A having a slightly better rating, yielding a ratio of M/A ATA ratings of 55 to 45 as shown in Table 30. This similarity results because both aircraft (see Table 2) have similar power and blade loadings and achieve similar climb and load factor performance.

The AACT firing window scoring for these aircraft was quite different, however. Of the six valid firing opportunities, the S-76A got five and the OH-58A got one, which resulted in a score of 330 for the S-76A and 29.7 for the OH-58A. The lopsided scoring was dominated by one very long well-aimed engagement of the S-76A on the OH-58A which alone netted 221.9 points.

The correlation between the M/A predictions and the actual AACT tests is shown in Table 30. There are two possible explanations for such poor correlation of the results. First, the S-76A pilot flew more aggressively than the OH-58A pilot, despite similar performance, as evidenced by the summary performance usage charts shown in Reference 5. Secondly, the S-76A has significantly more maneuverability which is not adequately factored into the M/A ratings. For example, the S-76A can fly to zero 'g' and below whereas the OH-58A with its teetering rotor is limited to +.5g. Thirdly, the ability to outclimb an opponent was determined to be a big factor in achieving winning engagements, or moreover to defeat the adversary's ability to attain a firing opportunity, and even the small advantage enjoyed by the S-76A may have been the determining factor for the consistent wins.

UH-60A vs OH-58A (Figure 54): The M/A rating of the UH-60A is very different from that of the OH-58A - 79 for the BLACK HAWK and 28 for the OH-58A. This is due to several factors. The UH-60A has superior power loading which resulted in better climb and acceleration performance. It also had lower blade loading so it has a higher N_z capability which results in superior mid to high speed turn rate.

The AACT scoring for the two aircraft was also quite different - the UH-60A ended up with 265.4 points and the OH-58A with 30.6 points. As mentioned in the AACT scoring section, the UH-60A was the successful combatant in eight out of nine valid firing opportunities.

TABLE 30 CORRELATION DATA SUMMARY

AIRCRAFT PAIR	M/A ATA RATINGS	AACT SCORES	M/A ATA PERCENTAGE	AACT PERCENTAGE
OH-58A	28.2	29.7	44.8	8.3
S-76A	34.8	330.0	55.2	91.7
OH-58A	28.2	30.6	26.3	10.3
UH-60A	79.0	265.4	73.7	89.7
UH-60A	79.0	121.0	69.4	95.1
S-76A	34.8	6.3	30.6	4.9
OH-58A	28.2	0.0	39.1	0.0
AH-1S	43.9	17.8	60.9	100.0
AH-64A	48.6	34.3	57.2	33.3
SA-365N (fixed gun)	36.3	68.8	43.8	66.7

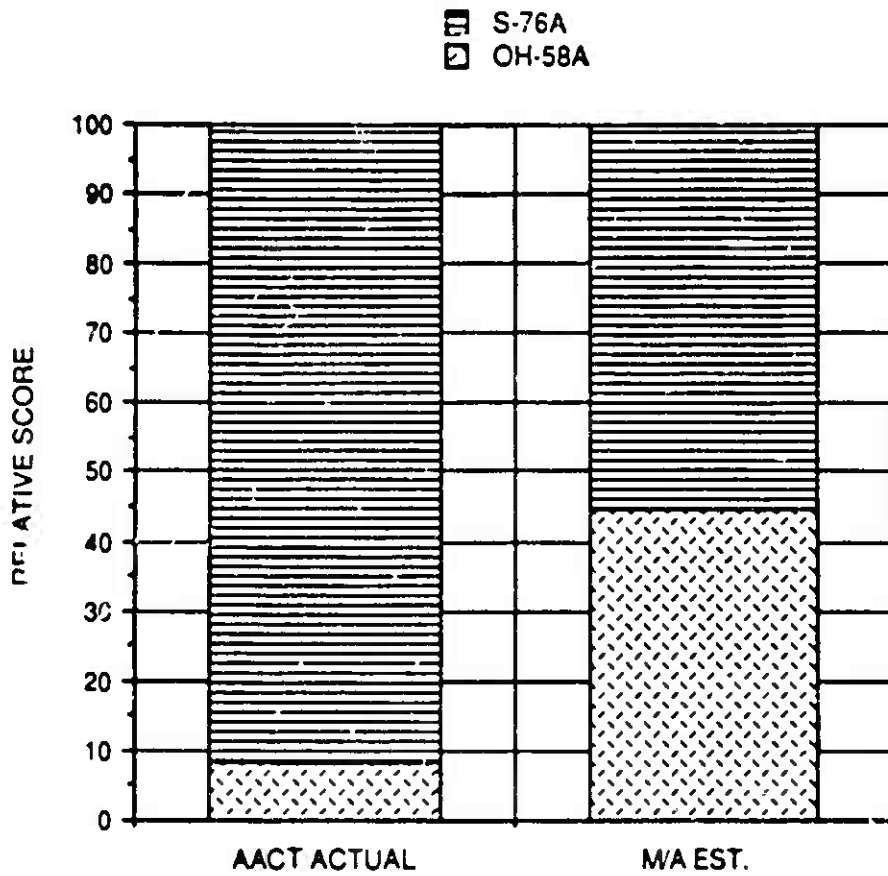


Figure 53. AACT Correlation - S-76A vs OH-58A

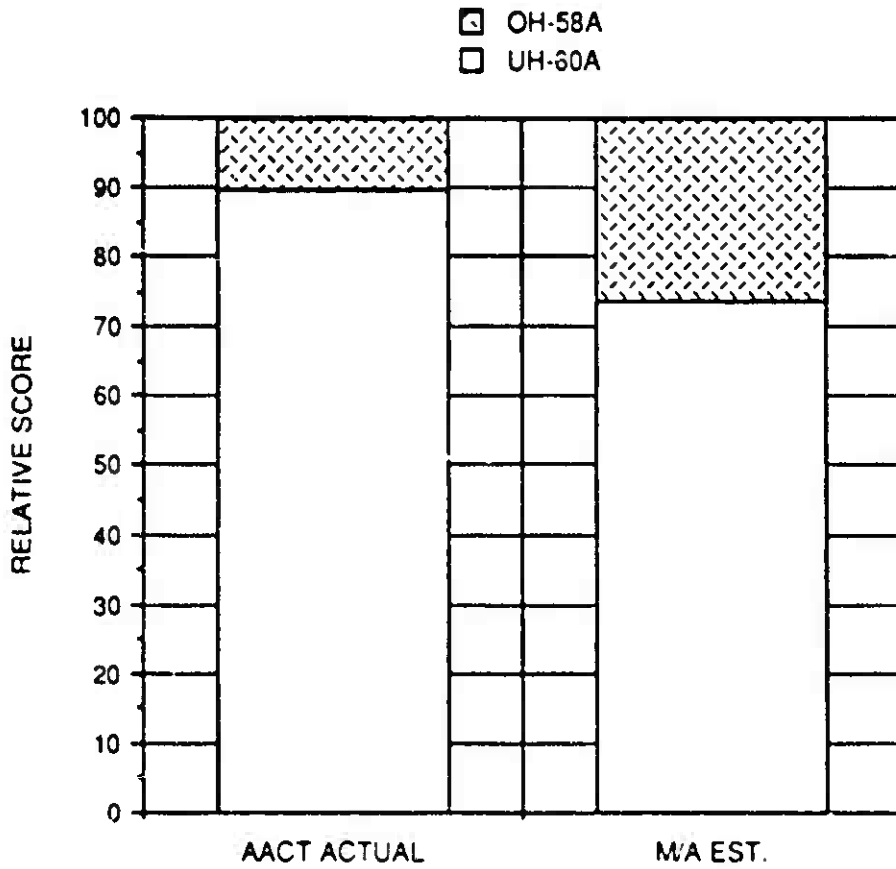


Figure 54. AACT Correlation - UH-60A vs OH-58A

The scoring ratio comparison for these two combating helicopters is shown in Table 30. The M/A ATA ratio correlates well with the AACT test results. The AACT score ratio actually shows the UH-60A to be more dominant over the OH-58A than does the M/A ATA scoring. One explanation could be the maneuver advantage that the UH-60A enjoys over the OH-58A. Like the S-76A the UH-60A has an advantage in attitude quickness and low 'g' capability.

S-76A vs UH-60A (Figure 55): The M/A rating of the UH-60A is quite a bit higher than the S-76A - 79 for the UH-60A and 35 for the S-76A. This is due to the improved power loading and the lower blade loading of the BLACK HAWK. The resulting ratios give the BLACK HAWK a 69 to 31 advantage.

The AACT scoring shows the UH-60A to be even more dominant than the M/A predictions. The UH-60A received a total of 121 points while the S-76A obtained only 6.3. It appears that a maneuvering advantage can result in total to dominance in air-to-air combat. If one helicopter has an advantage over another (e.g., better climb rate, higher turn rate), the pilot uses that advantage all of the time and this can result in consistent wins. The M/A ratings reflect more of a relative maneuvering index.

OH-58A vs AH-1S (Figure 56): The air-to-air M/A rating for the Cobra is significantly higher than that of the Kiowa, 43.9 to 28.2. This results from the low design speed of the OH-58, which prevents it from doing either the 140-knot pull-up or the 130-knot decelerating turn.

Unfortunately, the AACT data analysis yielded only two firing windows, one case 2 degrees outside the 3-degree criteria. Both of these were won by the AH-1S. However, review of the AACT data shows that the engagements were more balanced than the firing window data would indicate. Thus the correlation in this case is indeterminate.

SA-365N vs AH-64A (fixed gun) (Figure 57): The M/A ratings for this pair are also split but not as much as some of the other cases. The AH-64A (AACT) has a 48.6 rating while the Dauphin is 36.3. The primary reason for this is the lower power loading of the Apache.

The AACT firing window analysis generated four cases, one won by the AH-64A and three by the SA-365N. The Dauphin achieved twice the score of the Apache (68.8 to 34.3). The reason for the discrepancy lies in the extensive use by the Dauphin of pedal (flat) turns which generated large sideslip angles at bucket speeds. The large sideslip capability of the Fenestron allowed the SA-365N to regularly out turn the AH-64A. The Apache's lower power loading allowed it to out climb the Dauphin, but this only allowed the AH-64A to avoid the Dauphin, not to target it in these fixed gun encounters. Since this large slip capability was not evaluated in the simulated maneuvers, the Dauphin's M/A rating does not reflect this capability.

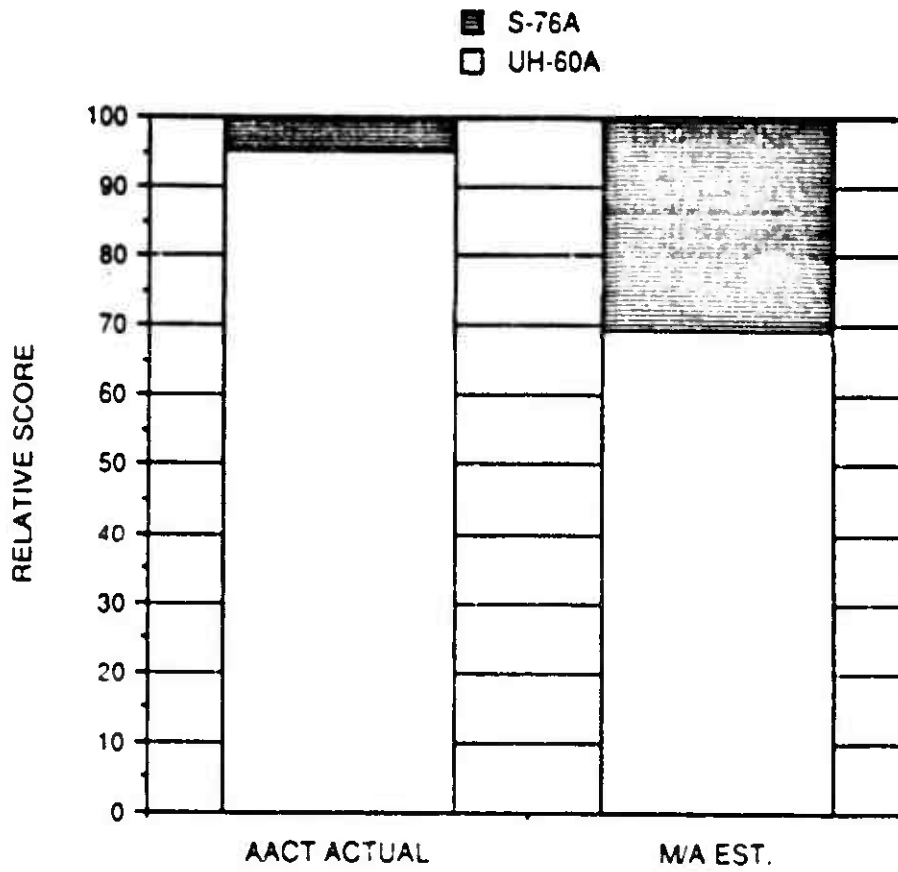


Figure 55. AACT Correlation - S-76A vs UH-60A

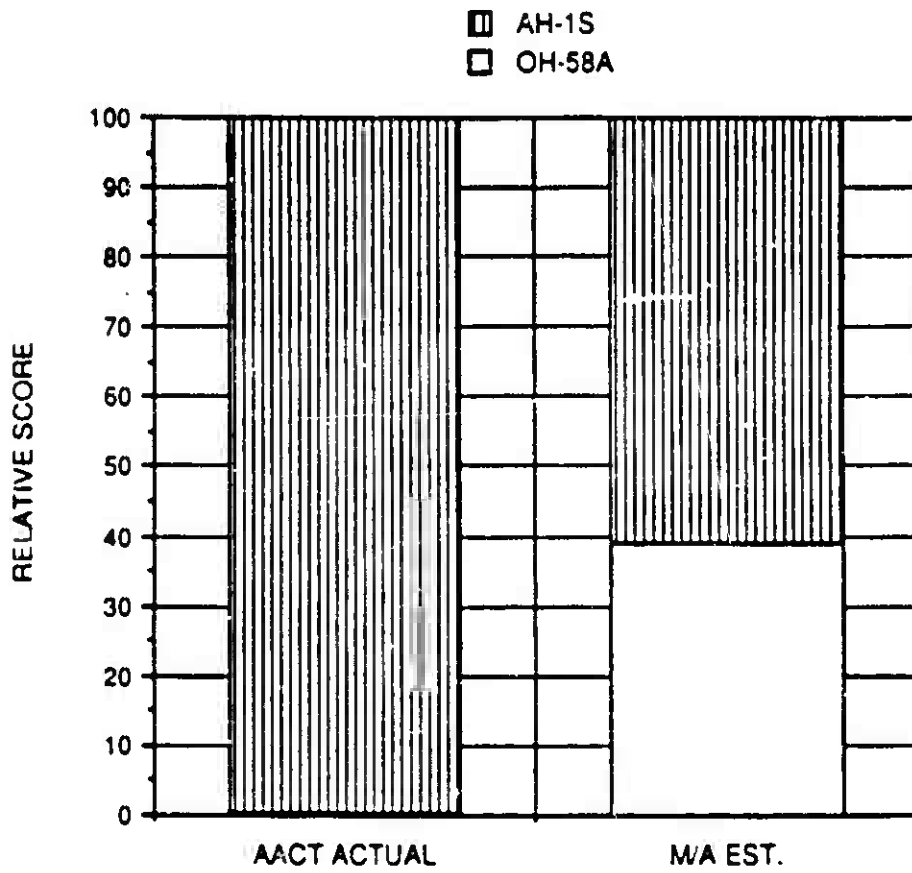


Figure 56. AACT Correlation - OH-58A vs AH-1S

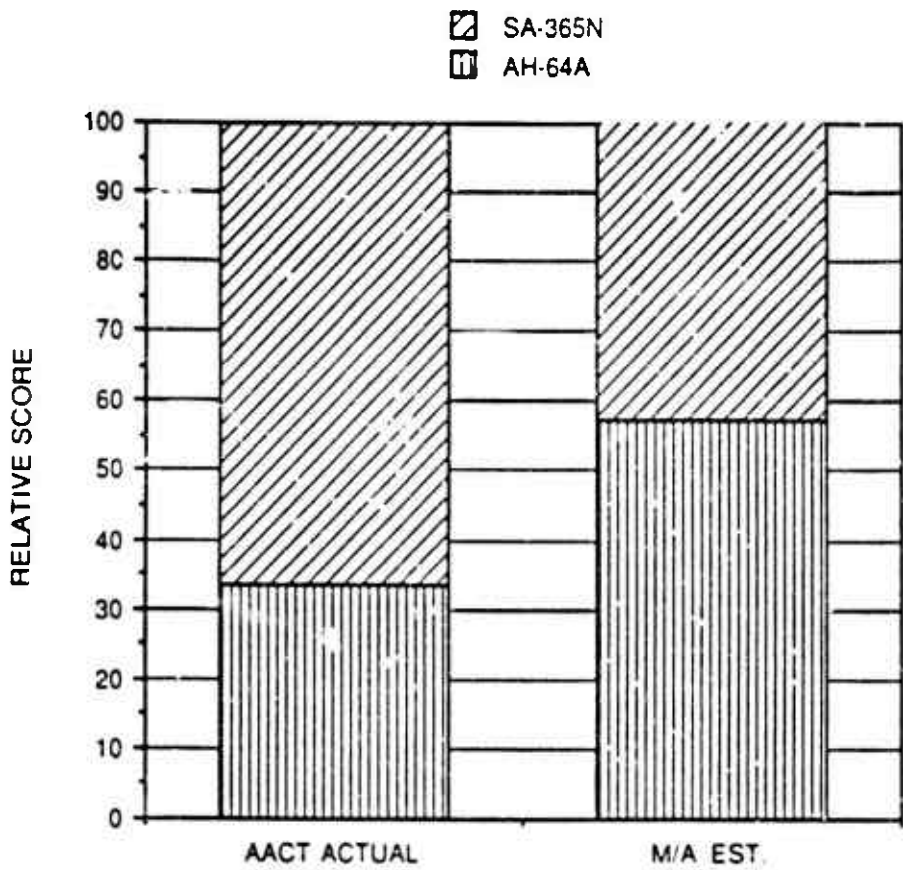


Figure 57. AACT Correlation - SA-365N vs AH-64A (fixed gun)

Two major conclusions emerge from this correlation. First, if an aircraft has an advantage over another, it can use that advantage to win consistently even though the overall M/A characteristics of the two aircraft may be similar. Thus small differences in the M/A ratings or even in maneuver scores may be more significant than they appear. Secondly, certain attributes important to the AACT results were not evaluated in the simulated maneuvers. One of these was the ability to make mid-speed pedal turns. This maneuver was used to some extent by all of the helicopters and resulted in many of the valid firing opportunities. The other attribute was quickness, or pure agility. The AACT results showed the importance of this capability, but none of the nine simulated maneuvers evaluated pure agility.

In addition, the paucity of valid firing windows reduces the correlation validity. Since the helicopters did not have gunsights, frequent cases existed where the attacking helicopter was in good position and had ample control and maneuver capability to achieve the firing window, but did not actually get in the window.

CONCLUSIONS

1. Fundamental parameter charts developed in M/A Phase I are applicable to a wide variety of helicopters. The only exception is the hover turn where the fundamental parameter was changed from tail rotor solidity to yaw acceleration capability.
2. Modern combat helicopters, such as UH-60A and AH-64A, had better M/A than either current civil aircraft, like S-76A and SA-365N, or older military aircraft such as AH-1S and OH-58A.
3. A methodology has been developed to allow visual playback of AACT time history data and provide views out of each cockpit or from any other point in the combat space. This methodology also calculates when firing opportunities occur and is efficient enough that all 59 encounters available were analyzed.
4. Relatively few encounters, even at close range, resulted in fixed gun firing opportunities. Five aircraft pairs were evaluated for a total of 59 one-on-one engagements. Only 23 legitimate firing opportunities occurred in all of these data.
5. A methodology has been developed to score the M/A maneuvers and to calculate an M/A rating based on those scores. M/A ratings can be calculated for the basic aircraft and for ATA, ATC, NOE and contour mission elements. This methodology not only allows comparisons of existing aircraft, but provides quantitative evaluations of the effects of changes to new designs or existing helicopters.
6. A methodology for scoring the AACT firing opportunities has been developed. This takes into account the range, angular error and time in the firing window. It allows a quantitative comparison of the firing opportunities.
7. Correlation of the M/A ratings and AACT scores was very good. For four of the five aircraft pairs, the aircraft with the higher M/A rating had the highest AACT score. In the case of the AH-64A versus SA-365N, the Dauphin had a higher AACT score even though it had a lower M/A rating. Review of the data indicates that the SA-365N had a very large sideslip envelope which allowed it to make flat turns and get more firing opportunities.
8. Detailed and comprehensive free flight CenHel simulation models of the UH-60A, S-76A, CH-53E, AH-64A, AH-1S, OH-58A, SA-365N and Mi-28 are available.
9. Mi-28 has only fair M/A characteristics when flown in its ATC configuration at a weight of 22,984 pounds. If evaluated in a ATA configuration at a weight of 20,000 pounds (a 13-percent reduction in GW), the M/A rating could be significantly better.

RECOMMENDATIONS

1. The maneuver simulation, scoring and rating analyses should be extended to cover different density altitudes. All of the modern helicopters studied employed flat-rated engines to provide them with improved performance at altitude. This study, conducted at sea level standard conditions, to coincide with the AACT data, does not show the benefits of such flat-rating.
2. Additional helicopters should be added to the study both to increase the analytical database and to provide more data for correlation. Candidate helicopters are:
 - a) UH-60L - Current production variant of the BLACK HAWK, essentially identical to the UH-60A except for increase in power and upgraded main gearbox.
 - b) Mil-24 HIND - Current Soviet attack helicopter. Analytical comparison of this aircraft to current U.S. Army inventory helicopters would be valuable.
 - c) Bell 406 Combat Scout - Tested in AACT IV; evaluation of this helicopter would broaden the correlation database. In addition, it provides a good comparison with the OH-58A, showing the effect of a new rotor and increased power on basically the same airframe.
 - d) MBB/Kawasaki, BK-117 - Also tested in AACT IV; analysis of this helicopter would not only broaden the correlation but also provide data on a small, modern hingeless rotor helicopter.
 - e) Other candidate aircraft include the MH-60K and SH-60B/F since GenHel simulation models of these helicopters already exist at Sikorsky. In addition, the Mi-28 should be reevaluated in a lighter weight air-to-air configuration and the CH-53E could be evaluated at more typical operational gross weights. The rotor speed should be set following current operational procedures - 100-percent for gross weights less than 60,000 pounds and 105 percent for higher weights.
3. Additional maneuvers should be added to the evaluation. One of these would be a large sideslip turn where the helicopter uses its elip capability to slow down and turn more quickly. For this maneuver, the sideslip envelopes for each aircraft would have to be specified. Another maneuver to be added would be a level flight roll-reversal. This would be a good measure of pure agility.
4. The AACT fixed gun data should be reanalyzed using larger angles to define the firing window. The reason for this is that the existing analysis shows very few firing opportunities were achieved within the arbitrary ± 3 -degree window and they were all of short duration. This is probably due to the lack of gunights on the competing aircraft. A pilot can not really judge a three-degree error in pointing. Therefore, there

were probably many instances where the pilot had an excellent firing opportunity and the control authority to stay within the firing window but in fact was just outside the mathematical criteria. In addition, normal instrumentation errors may result in indication that the pointing angle was too large when, in fact, it was inside the firing window.

5. The firing window criteria should be modified to specify a dispersion distance rather than an angle. For example, at 1500 meters, a ten meter scoring box implies an angular error of 0.38 degree, but at 100 meters the angular error is 5.73 degrees. At high ranges, even small pointing errors result in missing the target while at very close ranges, much larger pointing angles simply result in targeting of different parts of the helicopter.
6. Future AACT activities should employ gunsights. It would also be desirable to use some form of weapons emulator, as was done in AACT IV, to give the pilot feedback on his or her targeting accuracy.
7. Piloted simulation should be used to evaluate the maneuver results predicted by the maneuver controllers. The maneuver controller is very precise but it also had the operational limitations rigidly enforced. A human pilot might not be as precise but he would also not be able to impose the operational limits as tightly.
8. Future AACT activities should include the M/A rating maneuvers as part of the workup to air-to-air combat. This would allow a direct correlation with the GenHel predictions.
9. An air-to-air combat study should be conducted using piloted simulators. Several important activities would be:
 - a) Emulation of ATA combat between AACT pairs to compare results of simulators to actual combat.
 - b) Evaluation of engagements between pairs of aircraft not already involved in AACT. This would be a very cost-efficient method for evaluating combat maneuvering given the use of an ATA validated simulation facility. In addition, aircraft pairs not readily testable (e.g., UH-60A versus Mi-28) could be analyzed via simulation.
 - c) The effect of design parameter changes on ATA combat could be assessed quickly and directly. For example, fly a series of engagements, then change the hinge offset or blade chord or power available on one aircraft and re-fly the engagements to quantify the effects. Such instantaneous back-to-back comparisons would be invaluable.
 - d) The simulator would also allow for direct evaluation of weapons, something that can not be realistically done in the AACT test environment. Thus, engagements could be flown with a variety of different weapons or with parametric variations of a single weapon. Similar activities could be pursued for sensors, displays and control systems.

REFERENCES

1. Occhiato, John J., Kaplita, Thaddeus T., and Olsen, John R., Helicopter Maneuverability and Agility Design Sensitivity Analysis Volume I - Design Guidelines, USA AVSCOM TR-87-D-6A, January 1989
2. Kershner, Stuart D. and McVicar, Keith L., Helicopter Maneuverability and Agility Design Sensitivity Analysis Volume II - Air-to-Air Simulation Methodology, USA AVSCOM TR-87-D-6B, January 1989.
3. Cuppernull, Michael J., Helicopter Maneuverability and Agility Design Sensitivity Analysis Volume III - Weight Methodology, USA AVSCOM TR-87-D-6C, January 1989
4. Mowlett, James J., UH-60A Black Hawk Engineering Simulation Program. Volume I - Mathematical Model, NASA CR166309, December 1981
5. Wolfrom, Joseph A., Findings from Fixed-Gun Air-to-Air Combat Tests Involving Both Foreign and U.S. Helicopters, USA AVSCOM TR-86-D-24, December 1986.
6. Johnson, Wayne, Helicopter Theory, Princeton University Press, 1980.
7. Anonymous, "C-81 Computer Program Input Data List for AH-64A".
8. Morris, Patrick, M., et al, Airworthiness and Flight Characteristics Test - Part 1, YAH-64 Attack Helicopter, USAAEFA Project No. 80-17-1, September, 1981.
9. Picasso, Bartholomew D., et al, Airworthiness and Flight Characteristics Test of YAH-64 Advanced Attack Helicopter - Prototype Qualification Test Government, Part 3 and Production Validation Test - Government for Handbook Verification, USAAEFA Project No. 80-17-3, October 1982.
10. Bender, Gary L., et al, First Article Preproduction Tests of the AH-64A Helicopter, USAAEFA Project No. 84-10, November 1984.
11. Anonymous, "C-81 Computer Program Input Data List for OH-58A".
12. Smith, Raymond B., Benson, Tom P. and Smith, John R., Handling Qualities Evaluation of the OH-58A Helicopter Incorporating the Model 5708 Three-Axis Stability and Control Augmentation System, USA AVSCOM Project No. 72-30, February 1973.
13. Yamakaw, George M. and Watts, Joseph C., Airworthiness and Flight Characteristics Tests, Production OH-58A Helicopter Unarmed and Armed with XM27E1 Weapons System, USAAVSCOM Project No. 68-30, September 1970.

REFERENCES - (Cont'd)

14. Anonymous, "C-81 Computer Program Input Data List for AH-1G".
15. Diekmann Vernon L., et al. Production Validation Test - Government Kaman K747 Improved Main Rotor Blade, USAAEFA Project No. 77-38, October 1979.
16. Bill, F. A., Test Results of a Flying Qualities Demonstration on a UAH-1R/S Helicopter Configured with K747-001 Improved Main Rotor Blades, Kaman Aerospace Corporation Report T-579-1, February 3, 1977.
17. Fitzpatrick, J.E., Technical Description Data for the K717 Improved Main Rotor Blade for the AH-1Q Helicopter, Kaman Aerospace Corporation Report P-83, Revision B, October 1979.
18. Anonymous, SA-365N Operators Manual, Aerospatiale Document 365 02.101.01A.

LIST OF SYMBOLS/ABBREVIATIONS/ACRONYMS

AATD	-	U. S. Army Aviation Applied Technology Directorate
ADGW	-	Alternate Design Gross Weight
ATA	-	Air-to-Air
ATG	-	Air-to-Ground
AACT	-	Air-to-Air Combat Tests
AOA	-	Angle-of-Attack
BDGW	-	Basic Design Gross Weight
BL	-	Blade Loading
CG	-	Center-of-Gravity
CON	-	Contour Flight Regime
C _T	-	Thrust Coefficient
C _T /σ	-	Thrust Coefficient divided by Solidity
D	-	Dispersion
D _c	-	Dispersion Coefficient
DL	-	Disk Loading
FPM	-	Feet per minute
FP	-	Fundamental Parameter
FPS	-	Feet per Second
GenHel	-	General Helicopter Flight Dynamics Simulation
GFI	-	Government Furnished Information
GW	-	Gross Weight
H _d	-	Density Altitude
HIRSS	-	Hover Infrared Suppression System
HP	-	Horsepower
h _{rotor}	-	Rotor Height above the Ground
H _l	-	Height of Reference Fuselage in Aerodynamic Scaling Equation

LIST OF SYMBOLS/ABBREVIATIONS/ACRONYMS (Cont'd)

H2	-	Height of Modeled Fuselage in Aerodynamic Scaling Equation
IGE	-	In-Ground-Effect
ISA	-	International Standard Atmosphere
L1	-	Length of Reference Fuselage in Aerodynamic Scaling Equation
L2	-	Length of Modeled Fuselage in Aerodynamic Scaling Equation
M	-	Pitching Moment
M/A	-	Maneuverability and Agility
MGB	-	Main Gearbox (Transmission)
mm	-	millimeter
MOE	-	Measure of Effectiveness
N	-	Yawing Moment
NOE	-	Nap-of-the-Earth
Nz	-	Normal Load Factor
P	-	Roll Rate
PSID	-	Psi dot, Yaw Rate
Q	-	Pitch Rate
q	-	Dynamic Pressure
ROC	-	Rate-of-Climb
ROD	-	Rate-of-Descent
RPM	-	Revolutions per minute, Rounds per Minute (Gun)
S	-	Score
shp	-	Shaft Horsepower
SLS	-	Sea Level Standard
T	-	Time
Tc	-	Time Coefficient
TS	-	Tip Speed
TW	-	Twist
T/W	-	Thrust to Weight Ratio

LIST OF SYMBOLS/ABBREVIATIONS/ACRONYMS (Cont'd)

WE	-	Weight Empty
W1	-	Width of Reference Fuselage in Aerodynamic Scaling Equation
W2	-	Width of Modeled Fuselage in Aerodynamic Scaling Equation
Y	-	Sideforce
σ	-	Rotor Solidity
$\dot{\psi}$	-	Yaw Rate

GenHel Program SYMBOLS

		Units
AFAPPn	-	Absolute Value of ALFPPn deg
ALFWF	-	Fuselage Angle-of-Attack deg
ALFPPn	-	Panel n Angle-of-Attack deg
ALF1MR	-	Pitch-Lag Coupling Coefficient deg/deg
BCQDOS	-	Rotor Stall Parameter n.d.
BLCG	-	Buttline of the Center-of-Gravity inches
BLMR	-	Buttline of the Main Rotor inches
BLPn	-	Buttline of Panel n inches
BLTR	-	Buttline of the Tail Rotor inches
CDPn	-	Panel n Drag Coefficient n.d.
CHDTMR	-	Main Rotor Blade Tip Chord feet
CHD1MR	-	Main Rotor Blade Root Chord feet
CHIPMR	-	Rotor Wake Skew Angle deg
CLPn	-	Panel n Lift Coefficient n.d.
CMPn	-	Panel n Pitching Moment Coefficient n.d.
DDQF	-	Fuselage Delta Drag/q square ft.
DELT3MR	-	Pitch-Flap Coupling Coefficient deg/deg
DLQF	-	Fuselage Delta Lift/q square ft.
DMQF	-	Fuselage Delta Pitching Moment/q cubic feet
DQF	-	Fuselage Drag/q square ft.

LIST OF SYMBOLS/ABBREVIATIONS/ACRONYMS (Cont'd)

GenHel Program SYMBOLS

		<u>Units</u>
EKXPn	- Rotor Interference Velocity Ratio on Panel n in the x-direction	n.d.
EKXTR	- Rotor Interference Velocity Ratio on Tail Rotor in the x-direction	n.d.
EKXWF	- Rotor Interference Velocity Ratio on Fuselage in the x-direction	n.d.
EKZPn	- Rotor Interference Velocity Ratio on Panel n in the z-direction	n.d.
EKZTR	- Rotor Interference Velocity Ratio on Tail Rotor in the z-direction	n.d.
EKZWF	- Rotor Interference Velocity Ratio on Fuselage in the z-direction	n.d.
EPSPn	- Fuselage Downwash Angle on Panel n	deg
EPSTR	- Fuselage Downwash Angle on Tail Rotor	deg
FSCG	- Fuselage Station of the Center-of-Gravity	inches
HPMR	- Main Rotor Horsepower	Horsepower
LQF	- Fuselage Lift/q	square ft.
MQF	- Fuselage Pitching Moment/q	cubic feet
NQF	- Fuselage Yawing Moment/q	cubic feet
OMEGMR	- Actual Main Rotor Rotational Speed	rad/sec
OMEGTR	- Tail Rotor Rotational Speed	rad/sec
OMGTMR	- Main Rotor Trim Rotational Speed	rad/sec
PDEG	- Aircraft Roll Rate	deg/sec
PDOT	- Aircraft Roll Acceleration	rad/sec ²
PHIB	- Aircraft Roll Angle	deg
PSABWF	- Absolute Value of PSIWF	deg
PSIB	- Aircraft Heading Angle	deg
PSIWF	- Fuselage Yaw Angle (= -sideslip)	deg
QDEG	- Aircraft Pitch Rate	deg/sec
QDOT	- Aircraft Pitch Acceleration	rad/sec ²

LIST OF SYMBOLS/ABBREVIATIONS/ACRONYMS (Cont'd)

GenHel Program SYMBOLS

		<u>Units</u>
QPnQWF	- Dynamic Pressure Ratio at Panel n	n.d.
RDEG	- Aircraft Yaw Rate	deg/sec
RDOT	- Aircraft Yaw Acccleration	rad/sec ²
RHO	- Atmospheric Density	slugs/ft ³
RMR	- Main Rotor Radius	feet
RQF	- Fuselage Rolling Moment/q	cubic feet
RTR	- Tail Rotor Radius	feet
SIGPn	- Fuseiage Sidewash Angle on Panel n	deg
SIGTR	- Fuselage Sidewash Angle on Tail Rotor	deg
THETAB	- Fuselage Pitch Attitude	deg
TWSTMR	- Blade Preformed Twist Angle	deg
VXBDOT	- Aircraft Longitudinal Acceleration	ft/sec ²
VXBIKT	- Indicated Airspeed	knots
WLCCG	- Waterline of the Center-of-Gravity	inches
XSEGMR	- Non-dimensional distance from center of rotation to center of blade element	n.d.
YQF	- Fuselage Sideforce/q	square ft.

APPENDIX A

UH-60A MODEL DATA

The UH-60A (Figure A-1) is a medium-size, single-rotor assault transport helicopter designed to meet stringent U.S. Army specifications. Approximately 1200 UH-60A are in service with the U.S. Army. A large number of derivatives of this helicopter have been produced for the U.S. Navy (SH-60B, SH-60F, HH-60H), U.S. Air Force (MH-60G, HH-60A), U.S. Coast Guard (HH-60J) and foreign military use. The BLACK HAWK has a Basic Design Gross Weight (BDGW) of 16,825 pounds, a rotor diameter of 53 feet 8 inches, and is powered by two General Electric T700-GE-700 turboshaft engines with a intermediate rated power (IRP) of 1622 shp each.

The four-bladed main rotor is of conventional articulated design using electromeric bearings. Flapping and lagging hinges are coincident with a 4.66 percent hinge offset. The Sikorsky SC1095 airfoil is utilized inboard and outboard while a drooped-nose SC1095R8 airfoil is employed on the mid-span of the main rotor blades. The four-bladed tail rotor is 11-feet in diameter, is a bearingless rotor design, and employs the SC1095 airfoils. A continuous composite span connects each pair of blades. The tail rotor is a tractor configuration and is canted 20 degrees from the vertical. The BLACK HAWK has a 45-square-foot all-moving horizontal tail (stabilator).

The BLACK HAWK GenHel simulation was already operational at Sikorsky and had been extensively validated against flight test data, both in-house and at NASA Ames.

All of the numerical data used to model the UH-60A are provided in this appendix. The first section is a tabular listing of all the input data (Table A-1). The second section is plots of the map data for fuselage, vertical tail and horizontal tail aerodynamics along with plots of the rotor interference and fuselage interference data (Figures A-2 through A-25). The tabular data are provided with appropriate labels. Map data are identified with GenHel variable names provided in the List of Symbols.

For the UH-60A model, the panel allocation was as follows:

1. Right horizontal tail
2. Left horizontal tail
3. Vertical tail

TABLE A-1. UH-60A SPECIFIC FILE

;***** INPT PARAMETERS FOR MAIN ROTOR MODULES (#A.) *****

FSMR:: 341.215 ; FUSELAGE STATION, INCHES
 WLNR:: 315.0 ; WATERLINE STATION, INCHES
 BLNR:: 0.0 ; BUTTLINE STATION, INCHES (+IVE TO PORT)
 RMR:: 26.83 ; RADIUS, FT.
 OMTMR:: 27.0063 ; TRIM ROTATIONAL SPEED, RAD/SEC
 BMR:: 4.0 ; ACTUAL NUMBER OF BLADES
 ISMR:: -3.0 ; LONGITUDINAL SHAFT TILT, (POS. BACKWARDS), DEG
 ILMR:: 0.0 ; LATERAL SHAFT TILT, (POS. STARBOARD), DEG
 OELSMR:: -9.7 ; SWASHPLATE PHASE ANGLE, DEG
 DEL3MR:: 0.0 ; FLAPPING HINGE OFFSET ANGLE, DEG.
 KAF1MR:: 0.0 ; LAGGING HINGE OFFSET COEF. (PUNC(LG))
 KAF2MR:: 0.0 ; LAGGING HINGE OFFSET COEF. (PUNC(LG**2))
 CHOTMR:: 1.73 ; BLADE CHORD AT TIP, FT.
 CHDRMR:: 1.73 ; BLADE CHORD AT ROOT, FT.
 OPSTMR:: 1.25 ; HINGE OFFSET, FT.
 SPRLMR:: 3.83 ; HINGE TO START OF BLADE, FT.
 WTBOMR:: 256.91 ; WEIGHT OF ONE BLADE, LBS.
 IBMR:: 1512.6 ; BLADE MOMENT OF INERTIA ABOUT HINGE, SLUG-FT**2
 MBMR:: 86.7 ; BLADE MASS MOMENT ABOUT HINGE, SLUG-FT**2
 IRMR:: 943.9 ; ROTATING INERTIA OF DRIVE TRAIN ROTDR
 ; (DUAL ENGINE FAILURE), SLUG-FT**2
 BTLMR:: .97 ; BLADE TIP CUT OFF RATIO
 DCDMR:: .002 ; DELTA DRAG COEF. FOR EACH SEGMENT
 NBSMR:: 4 ; NUMBER OF BLADES SIMULATED, FIX POINT
 NSSMR:: 5 ; NUMBER OF SEGMENTS SIMULATED, FIX POINT

; ** MAIN ROTOR NON-LINEAR TWIST MAP **

TWRMP:: UVR## ; MAP ARGUMENT: LOOK UP ROUTINE
 XSEGM## ; INPUT VARIABLE
 TWSTMR## ; OUTPUT VARIABLE
 TWRLO ; MAP NAME
 EXP 0.0, 1.0, 0.05 ; LOWER LIMIT, UPPER LIMIT, DELTA

TWRLO:	EXP	0.0,	0.0,	0.0,	0.0,	-0.15
	EXP	-0.95,	-1.8,	-2.75,	-3.55,	-4.4
	EXP	-5.3,	-6.15,	-7.1,	-7.9,	-8.8
	EXP	-9.65,	-10.3,	-10.75,	-12.3,	-13.1
		-10.9				

;***** MAIN ROTOR DYNAMIC TWIST SUBMODULE (#A) *****

KOTWMP:: UVR##
 VKT##
 KOTWMR##
 KOTWLO
 EXP 100.0, 150.0, 50.0
 KOTWLO: EXP -0.0003, -0.00052

;***** MAIN ROTOR DOWNWASH SUBMODULE (#A) *****

RCTMR:: 1.0 ; TRUST GAIN FOR UNIFORM DOWNWASH
 KCMR:: 0.0 ; PITCH MOM. GAIN FOR DOWNWASH SIN. HARMONIC
 KSLMR:: 0.0 ; ROLL MOM. GAIN FOR DOWNWASH COS. HARMONIC
 TDWOMR:: 0.01038 ; TIME CONST. FOR UNIFORM DOWNWASH FILTER, SEC
 TDWCHR:: 0.0 ; TIME CONST. FOR DOWNWASH SIN. HARMON. FILTER, SEC.
 TDWSMR:: 0.0 ; TIME CONST. FOR DOWNWASH COS. HARMON. FILTER, SEC.

TABLE A-1. UH-60A SPECIFIC FILE (Cont'd)

```

***** FLAPPING/LAGGING DAMPER CALCULATIONS (8C) *****

KBRMR:: 0.0      ; FLAPPING HINGE SPRING CONST, FT-LBS/RAD
KBR.MR::0.0     ; FLAPPING HINGE DAMPER CONST, FT-LBS-SEC/RAD

; **SET OF MOUNTING DIMENSIONS FOR LAG DAMPER, INCHES**
ALDMR:: 0.227   ;
BLDMR:: 3.242   ;
CLDMR:: 12.040  ;
DLDMR:: 10.0102 ;
RLDMR:: 6.898   ;
LGODMR::7.0     ; ALIGNMENT OFFSET IN RELATION TO LAG, DEG
THLDMR::17.481  ; FIXED BLADE PITCH RELATIONSHIP BET. ARM AND THCUFF

; ** BLACK HAWK LAG DAMPER FORCE VS LAG DAMPER ARM RATE
LDMRMP:::UVSUVS## ;MAP ARGUMENT:LDDK UP RDUTINE
      LD.MR##(A16) ;INPUT VARIABLE
      PD.MR##(A16) ;DUTPUT VARIABLE
      LDMRLO      ;LDW RANGE MAP NAME
      EXP 0.0,2.0,0.1 ;LDWER LIMIT,UPPER LIMIT,DELTA
      LDMRHI      ;HIGH RANGE MAP NAME
      EXP 2.0,7.0,1.0 ;LOWER LIMIT,UPPER LIMIT,DELTA

; LOW ANGLE MAP: LD.MR 0 TO 2.0 , DELTA = .1
LDMRLO: EXP 0.0, 30.0, 90.0, 160.0, 280.0
        EXP 490.0, 720.0, 950.0, 1190.0, 1400.0
        EXP 1630.0, 1860.0, 2090.0, 2310.0, 2530.0
        EXP 2770.0, 2980.0, 3200.0, 3310.0, 3370.0
        EXP 3410.0

; HIGH ANGLE MAP: LD.MR 2.0 TO 7.0 , DELTA=1.0
LDMRHI: EXP 3410.0, 3550.0, 3615.0, 3680.0, 3745.0
        EXP 3815.0

***** INPUT PARAMETERS PDR FUSELAGE/WING (8A) *****
***** MOUNTING POINT FOR MDEL IN WIND TUNNEL *****
FSWF:: 345.5      ; FUSELAGE STATION, IN.
WLWF:: 234.0     ; WATERLINE STATIDN, IN.
BLWF:: 0.0       ; BUTTLINE STATION, IN. (+IVE TO PORT)
IWF:: 0.0        ; WING INCIDENCE, DEG.

; ** BLACK HAWK FUSELAGE LIFT (TAIL OFF IRS DFF) VS ALPWF
LOFMP:::UVRUVR## ;MAP ARGUMENT:LDDK UP RDUTINE
      ALPWF##     ;INPUT VARIABLE
      LOF##       ;DUTPUT VARIABLE
      LOFLO      ;LOW ANGLE MAP NAME
      EXP -30.0,30.0,5.0 ;LOWER LIMIT,UPPER LIMIT,DELTA-LDW ANGLE
      LOFHI      ;HIGH ANGLE MAP NAME
      EXP -90.0,90.0,10.0 ;LOWER LIMIT,UPPER LIMIT,DELTA-HIGH ANGLE

; LDW ANGLE MAP: ALPWF -30 TD 30 , DELTA=5
LOFLD: EXP -70.0, -52.0, -35.0, -25.0, -13.0
        EXP -5.0, 1.0, 10.0, 20.0, 25.0
        EXP 30.0, 34.0, 37.0

; HIGH ANGLE MAP: ALPWF -90 TD 90 , DELTA=10
LOFHI: EXP -24.0, -54.0, -72.0, -81.0, -85.0
        EXP -83.0, -70.0, -35.0, -13.0, 1.0
        EXP 20.0, 30.0, 37.0, 43.0, 48.0
        EXP 50.0, 48.0, 39.0, 22.0
    
```

TABLE A-1. UH-60A SPECIFIC FILE (Cont'd)

```

; ** BLACK HAWK FUSELAGE DRAG (TAIL OFF IRS OFF) VS ALPWF
; REVISD TO INCLUDE FUSELAGE HARDPOINTS 3/87
DQFMP::UVRUVR## ;MAP ARGUMENT:LOOK UP ROUTINE
ALPWF## ;INPUT VARIABLE
DQF## ;OUTPUT VARIABLE
DQFLO ;LOW ANGLE MAP NAME
EXP -30.0,30.0,5.0 ;LOWER LIMIT,UPPER LIMIT,DELTA-LOW ANGLE
DQFHI ;HIGH ANGLE MAP NAME
EXP -90.0,90.0,10.0 ;LOWER LIMIT,UPPER LIMIT,DELTA-HIGH ANGLE

; LOW ANGLE MAP: ALPWF -30 TO 30 , DELTA=5
DQFLO: EXP 46.99, 39.49, 33.59, 29.39, 26.97
EXP 25.49, 25.49, 26.99, 29.49, 33.19
EXP 38.49, 44.99, 52.99

; HIGH ANGLE MAP: ALPWF -90 TO 90 , DELTA=10
DQFHI: EXP 151.91, 146.91, 134.91, 115.91, 89.91
EXP 62.91, 46.99, 33.59, 26.97, 25.49
EXP 29.49, 38.49, 52.99, 67.91, 85.91
EXP 111.91, 133.91, 146.91, 151.91

; ** BLACK HAWK FUSELAGE PITCH MOMENT(TAIL OFF) VS ALPWF
MQFMP::UVRUVR## ;MAP ARGUMENT:LOOK UP ROUTINE
ALPWF## ;INPUT VARIABLE
MQF## ;OUTPUT VARIABLE
MQFLO ;LOW ANGLE MAP NAME
EXP -30.0,30.0,5.0 ;LOWER LIMIT,UPPER LIMIT,DELTA-LOW ANGLE
MQFHI ;HIGH ANGLE MAP NAME
EXP -90.0,90.0,10.0 ;LOWER LIMIT,UPPER LIMIT,DELTA-HIGH ANGLE

; LOW ANGLE MAP: ALPWF -30 TO 30 , DELTA=5
MQFLO: EXP -740.0, -700.0, -630.0, -520.0, -380.0
EXP -230.0, -90.0, 10.0, 100.0, 290.0
EXP 450.0, 600.0, 750.0

; HIGH ANGLE MAP: ALPWF -90 TO 90 , DELTA=10
MQFHI: EXP -200.0, -470.0, -645.0, -730.0, -760.0
EXP -760.0, -740.0, -630.0, -380.0, -90.0
EXP 100.0, 450.0, 750.0, 810.0, 825.0
EXP 780.0, 650.0, 470.0, 200.0

; ** BLACK HAWK FUSELAGE DELTA LIFT VS PSIMF
DLQFMP::UVR## ;MAP ARGUMENT:LOOK UP ROUTINE
PSIMF## ;INPUT VARIABLE
DLQF## ;OUTPUT VARIABLE
DLQFLO ;LOW ANGLE MAP NAME
EXP -30.0,30.0,5.0 ;LOWER LIMIT,UPPER LIMIT,DELTA-LOW ANGLE

; LOW ANGLE MAP: PSIMF -30 TO 30, DELTA=5
DLQFLO: EXP 30.0, 20.0, 12.0, 7.0, 3.0
EXP 2.0, 0.0, 2.0, 5.0, 10.0
EXP 15.0, 22.0, 30.0

; ** BLACK HAWK FUSELAGE DELTA DRAG VS PSIMF(ABS)
DDOFMP::UVRUV## ;MAP ARGUMENT:LOOK UP ROUTINE
PSABWF## ;INPUT VARIABLE
DDQF## ;OUTPUT VARIABLE
DDOFLO ;LOW ANGLE MAP NAME
EXP 0.0,30.0,5.0 ;LOWER LIMIT,UPPER LIMIT,DELTA-LOW ANGLE
DDQFHI ;HIGH ANGLE MAP NAME
EXP 30.0,90.0,10.0 ;LOWER LIMIT,UPPER LIMIT,DELTA-HIGH ANGLE

```

TABLE A-1. UH-60A SPECIFIC FILE (Cont'd)

```

; LOW ANGLE MAP: PSI(ABS) 0 TO 30, DELTA=5
DDQFLO: EXP 0.0, 1.0, 4.0, 9.0, 16.3
EXP 28.0, 38.5

; HIGH ANGLE MAP: PSI(ABS) 30 TO 90, DELTA=10
DDQFHI: EXP 38.5, 76.5, 113.5, 141.5, 164.5
EXP 169.5, 170.5

; ** BLACK HAWK FUSELAGE DEL PITCH MOM VS PSIWF(ABS)
DQFMP: :UVR## ;MAP ARGUMENT:LOOR UP ROUTINE
PSABWF## ;INPUT VARIABLE
DQF## ;OUTPUT VARIABLE
DQFLO ;LOW ANGLE MAP NAME
EXP 0.0,30.0,5.0 ;LOWER LIMIT,UPPER LIMIT,DELTA-LOW ANGLE MAP

; LOW ANGLE MAP: PSI(ABS) 0 TO 30, DELTA=5
DQFLO:EXP 0.0, 10.0, 20.0, 50.0, 90.0
EXP 130.0, 180.0

; ** BLACK HAWK FUSELAGE SIDE FORCE (TAIL OFF) VS PSIWF
YQFMP: :UVSUVS## ;MAP ARGUMENT:LOOR UP ROUTINE
PSIWF## ;INPUT VARIABLE
YQF## ;OUTPUT VARIABLE
YQFLO ;LOW ANGLE MAP NAME
EXP 0.0,30.0,5.0 ;LOWER LIMIT,UPPER LIMIT,DELTA-LOW ANGLE
YQFHI ;HIGH ANGLE MAP NAME
EXP 30.0,90.0,10.0 ;LOWER LIMIT,UPPER LIMIT,DELTA-HIGH ANGLE

; LOW ANGLE MAP: PSIWF 0 TO 30, DELTA=5 Y(PSI)--Y(-PSI)
YQFLO: EXP 0.0, 11.0, 23.0, 35.0, 50.0
EXP 65.0, 72.0

; HIGH ANGLE MAP: PSIWF 30 TO 90, DELTA=10 Y(PSI)--Y(-PSI)
YQFHI: EXP 72.0, 92.0, 103.0, 100.0, 84.0
EXP 64.0, 37.0

; ** BLACK HAWK FUSELAGE ROLLING MOMENT (TAIL OFF) VS PSIWF
RQFMP: :UVSUVS## ;MAP ARGUMENT:LOOR UP ROUTINE
PSIWF## ;INPUT VARIABLE
RQF## ;OUTPUT VARIABLE
RQFLO ;LOW ANGLE MAP NAME
EXP 0.0,30.0,5.0 ;LOWER LIMIT,UPPER LIMIT,DELTA-LOW ANGLE
RQFHI ;HIGH ANGLE MAP NAME
EXP 30.0,90.0,10.0 ;LOWER LIMIT,UPPER LIMIT,DELTA-HIGH ANGLE

; LOW ANGLE MAP: PSIWF 0 TO 30, DELTA=5 R(PSI)--R(-PSI)
RQFLO: EXP 0.0, 0.0, 0.0, -30.0, -75.0
EXP -120.0, -110.0

; HIGH ANGLE MAP: PSIWF 30 TO 90, DELTA=10 R(PSI)--R(-PSI)
RQFHI: EXP -110.0, -106.0, -103.0, -101.0, -100.0
EXP -100.0, -100.0

; ** BLACK HAWK FUSELAGE YAWING MOMENT (TAIL OFF) VS PSIWF
NQFMP: :UVRUVR## ;MAP ARGUMENT:LOOK UP ROUTINE
PSIWF## ;INPUT VARIABLE
NQF## ;OUTPUT VARIABLE
NQFLO ;LOW ANGLE MAP NAME
EXP -30.0,30.0,5.0 ;LOWER LIMIT,UPPER LIMIT,DELTA-LOW ANGLE
NQFHI ;HIGH ANGLE MAP NAME
EXP -90.0,90.0,10.0 ;LOWER LIMIT,UPPER LIMIT,DELTA-HIGH ANGLE

; LOW ANGLE MAP: PSIWF -30 TO 30, DELTA=5
NQFLO: EXP -140.0, -190.0, -240.0, -220.0, -180.0
EXP -100.0, 0.0, 100.0, 180.0, 220.0
EXP 240.0, 190.0, 140.0

```

TABLE A-1. UH-60A SPECIFIC FILE (Cont'd)

```

; HIGH ANGLE MAP: PSIWF -90 TO 90, DELTA=10
NOFHI: EXP 440.0, 392.0, 332.0, 259.0, 160.0
EXP 40.0, -140.0, -240.0, -180.0, 0.0
EXP 180.0, 240.0, 140.0, 59.0, -30.0
EXP -125.0, -220.0, -320.0, -420.0

;***** ROTOR INTERFERENCE ON THE FUSLEAGE (MRPA) *****

; ** BLACK HAWK FORE/AFT M.R. DOWNWASH AT FUSELAGE
EXWFMP::BIV## ;MAP ARGUMENT:LOOK UP ROUTINE
EXP CHIPMR##,AA1FMR## ;INPUT VARIABLE #1, INPUT VARIABLE #2
ERXWF## ;OUTPUT VARIABLE
EXWFLO ;LOW ANGLE MAP NAME

EXP 0.0,100.0,10.0,13 ;LOW LIM,UPPER LIM,DELTA,#ENTRYS(OCT)-CHIPMR
EXP -6.0,6.0,6.0 ;LOW LIM,UPPER LIM,DELTA-AA1FMR

; LOW ANGLE MAP CHIPMR 0 TO 100 (DEL=10) AA1FMR -6,0,6
; AA1FMR=-6
EXWFLO:EXP 0.08, 0.18, 0.3, 0.43, 0.55
EXP 0.66, 0.79, 0.9, 1.03, 0.55
0.0

; AA1FMR=0
EXP 0.0, 0.1, 0.21, 0.32, 0.42
EXP 0.54, 0.66, 0.8, 0.94, 0.5
0.0

; AA1FMR=6
EXP -0.12, 0.02, 0.08, 0.18, 0.28
EXP 0.4, 0.53, 0.67, 0.82, 0.8
0.0

; ** BLACK HAWK VERTICAL M.R. DOWNWASH AT FUSELAGE
EZWFMP::BIV## ;MAP ARGUMENT:LOOK UP ROUTINE
EXP CHIPMR##,AA1FMR## ;INPUT VARIABLE #1, INPUT VARIABLE #2
ERZWF## ;OUTPUT VARIABLE
EZWFLO ;LOW ANGLE MAP NAME
EXP 0.0,100.0,10.0,13 ;LOW LIM,UPPER LIM,DELTA,#ENTRYS(OCT)-CHIPMR
EXP -6.0,6.0,6.0 ;LOW LIM,UPPER LIM,DELTA-AA1FMR

; LOW ANGLE MAP CHIPMR 0 TO 100 (DEL=10) AA1FMR -6,0,6
; AA1FMR=-6
EZWFLO:EXP 1.11, 1.09, 1.08, 1.065, 1.05
EXP 1.04, 1.02, 1.01, 1.0, 0.88
0.6

; AA1FMR=0
EXP 1.12, 1.12, 1.12, 1.12, 1.12
EXP 1.12, 1.12, 1.12, 1.11, 0.96
0.6

; AA1FMR=6
EXP 1.15, 1.15, 1.15, 1.15, 1.16
EXP 1.17, 1.18, 1.22, 1.16, 0.98
0.6

;***** INPUT PARAMETERS FOR PANEL #1 (8A) *****
FSP1:: 700.1 ; FUSELAGE STATION,INCH
WLP1:: 244.0 ; WATERLINE STATION,INCH
BLP1:: -36.6 ; BUFTLINE STATION,INCH (+IVE TO PORT)
SAP1:: 22.5 ; SURFACE AREA OF PANEL IF NOT INCLUDE IN MAP
GAMP1:: 0.0 ; PANEL ORIENTATION, DEG
IOP1:: 2 ; PANEL INCIDENCE,DEG
CPI1:: 1.0 ; PANEL MEAN AERO CHORD,FT

```


TABLE A-1. UH-60A SPECIFIC FILE (Cont'd)

```

; ** BLACK HAWK HORIZONTAL STABILIZER (RT PANEL) LIFT COEFFICIENT VS ALFPP1

; S=22.5 FT**2 ,ASPECT RATIO=4.6 ,0014 AIRFOIL
CLPIMP::UVSUVS00 ;MAP ARGUMENT:LOOK UP ROUTINE
        ALFPP100 ;INPUT VARIABLE
        CLP100 ;OUTPUT VARIABLE
        CLP1LO ;LOW ANGLE MAP NAME
        EXP 0.0,30.0,5.0 ;LOWER LIMIT,UPPER LIMIT,DELTA-LOW ANGLE
        CLP1HI ;HIGH ANGLE MAP NAME
        EXP 30.0,90.0,10.0 ;LOWER LIMIT,UPPER LIMIT,DELTA-HIGH ANGLE

; LOW ANGLE MAP ALFPP1 0 TO 30,DELTA=5 CL(ALF)--CL(-ALF)
CLP1LO: EXP 0.0, 0.356, 0.71, 0.92, 1.02
        EXP 1.02, 0.99

; HIGH ANGLE MAP ALFPP1 30 TO 90,DELTA=10 CL(ALF)--CL(-ALF)
CLP1HI: EXP 0.99, 0.847, 0.847, 0.745, 0.556
        EXP 0.254, 0.0

; ** BLACK HAWK HORIZONTAL STABILIZER DRAG VS ALFPP1 (ABS)
CDPIMP::UVRUVR00 ;MAP ARGUMENT:LOOK UP ROUTINE
        AFAPP100 ;INPUT VARIABLE
        CDP100 ;OUTPUT VARIABLE
        CDP1LO ;LOW ANGLE MAP NAME
        EXP 0.0,30.0,5.0 ;LOWER LIMIT,UPPER LIMIT,DELTA
        CDP1HI ;HIGH ANGLE MAP NAME
        EXP 30.0,90.0,10.0 ;LOWER LIMIT,UPPER LIMIT,DELTA

; LOW ANGLE MAP ALFPP1 0 TO 30,DELTA=5 CD(ALF)=CD(-ALF)
CDP1LO: EXP 0.01, 0.022, 0.04, 0.19, 0.36
        EXP 0.37, 0.43

; HIGH ANGLE MAP ALFPP1 30 TO 90,DELTA=10 CD(ALF)=CD(-ALF)
CDP1HI: EXP 0.43, 0.531, 0.702, 0.888, 1.05
        EXP 1.161, 1.2

; ** BLACK HAWK HORIZONTAL STABILIZER MOMENT @C/4 VS ALFPP1
CMPIMP::UVSUVS00 ;MAP ARGUMENT:LOOK UP ROUTINE
        ALFPP100 ;INPUT VARIABLE
        CMP100 ;OUTPUT VARIABLE
        CMP1LO ;LOW ANGLE MAP NAME
        EXP 0.0,30.0,5.0 ;LOWER LIMIT,UPPER LIMIT,DELTA-LOW ANGLE
        CMP1HI ;HIGH ANGLE MAP NAME
        EXP 30.0,90.0,10.0 ;LOWER LIMIT,UPPER LIMIT,DELTA-HIGH ANGLE

; LOW ANGLE MAP ALFPP1 0 TO 30, DELTA=5
CMP1LO: EXP 0.0, 0.00125, 0.0025, 0.005, -0.045
        EXP -0.105, -0.125

; HIGH ANGLE MAP ALFPP1 30 TO 90, DELTA=10
CMP1HI: EXP -0.125, -0.125, -0.125, -0.125, -0.125
        EXP -0.125, -0.125

;***** INPUT PARAMETERS FOR ROTOR INTERFERENCE ON THE HORIZ.TAIL #1 (MRPA)

; ** BLACK HAWK FORE/AFT M.R. DOWNWASH AT HORIZONTAL TAIL
EXPIMP::BIV00 ;MAP ARGUMENT:LOOK UP ROUTINE
        EXP CHIPMR00,AA1PMR00 ;INPUT VARIABLE #1, INPUT VARIABLE #2
        EKXP100 ;OUTPUT VARIABLE
        EXP1LO ;LOW ANGLE MAP NAME
        EXP 0.0,100.0,10.0,13 ;LOW LIM,UPPER LIM,DELTA,#ENTRYS(OCT)-CHIPMR
        EXP -6.0,6.0,6.0 ;LOW LIM,UPPER LIM,DELTA-AA1PMR

```

TABLE A-1. UH-60A SPECIFIC FILE (Cont'd)

```

; LOW ANGLE MAP CHIPMR 0 TO 100 (DEL-10) AALFMR -6,0,6
; AALFMR--6
EXP1LO:EXP 0.0, -0.2, 0.05, 0.3, 0.54
EXP 0.8, 1.04, 1.3, 1.55, 0.8
0.0

; AALFMR=0
EXP -0.4, -0.6, -0.2, 0.12, 0.36
EXP 0.6, 0.83, 1.06, 1.3, 0.66
0.0

; AALFMR=6
EXP -0.56, -0.8, -0.74, -0.32, 0.04
EXP 0.32, 0.6, 0.86, 1.12, 0.54
0.0

; ** BLACK HAWK VERTICAL H.R. DOWNWASH AT HORIZONTAL TAIL

EZPIMP::BIV## ;MAP ARGUMENT:LOOK UP ROUTINE
EXP CHIPMR##,AALFMR## ;INPUT VARIABLE #1, INPUT VARIABLE #2
FKZP1## ;OUTPUT VARIABLE
EZP1LO ;LOW ANGLE MAP NAME
EXP 0.0,100.0,10.0,13 ;LOW LIM,UPPER LIM,DELTA,#ENTRYS(OCT)-CHIPMR
EXP -6.0,6.0,6.0 ;LOW LIM,UPPER LIM,DELTA-AALFMR

; LOW ANGLE MAP CHIPMR 0 TO 100 (DEL-10) AALFMR -6,0,6
; AALFMR--6
EZP1LO:EXP -0.13, 0.8, 1.8, 1.82, 1.86
EXP 1.88, 1.91, 1.94, 1.69, 1.42
1.14

; AALFMR=0
EXP 0.4, 0.94, 1.84, 1.91, 1.98
EXP 2.04, 2.08, 2.14, 1.89, 1.62
1.35

; AALFMR=6
EXP 0.78, 1.36, 1.91, 1.98, 2.06
EXP 2.14, 2.21, 2.28, 2.16, 1.96
1.56

;***** FUSELAGE INTERFERENCE ON THE HORIZ.TAIL #1 (WPPA) *****

; ** BLACK HAWK DYNAMIC PRESSURE RATIO AT HORIZONTAL TAIL VS ALFWF
QPIMP::UVR## ;MAP ARGUMENT:LOOK UP ROUTINE
ALFWF## ;INPUT VARIABLE
QP1QWF## ;OUTPUT VARIABLE
QP1LO ;LOW ANGLE MAP NAME
EXP -30.0,30.0,5.0 ;LOWER LIMIT, UPPER LIMIT, DELTA

; LOW ANGLE MAP ALFPP1 -30 TO 30 DELTA=5
QP1LO: EXP 1.0, 0.875, 0.762, 0.76, 0.76
EXP 0.76, 0.76, 0.76, 0.76, 0.82
EXP 0.90, 1.0, 1.0

; ** BLACK HAWK DOWNWASH ON HORIZONTAL TAIL VS ALFWF DUE TO BODY
EPPIMP::UVRUVR## ;MAP ARGUMENT:LOOK UP ROUTINE
ALFWF## ;INPUT VARIABLE
EPSP1## ;OUTPUT VARIABLE
EPP1LO ;LOW ANGLE MAP NAME
EXP -30.0,30.0,5.0 ;LOWER LIMIT,UPPER LIMIT,DELTA-LOW ANGLE
EPP1HI ;HIGH ANGLE MAP NAME
EXP -90.0,90.0,10.0 ;LOWER LIMIT,UPPER LIMIT,DELTA-HIGH ANGLE

```

TABLE A-1. UH-60A SPECIFIC FILE (Cont'd)

```

; LOW ANGLE MAP ALPPP1 -30 TO 30 DELTA=5
EPP1LO: EXP 1.8, 1.4, 1.1, 0.8, 0.55
EXP 0.5, 0.45, 0.40, 0.38, 0.33
EXP 0.19, -0.12, -0.40

```

```

; HIGH ANGLE MAP ALPPP1 -90 TO 90 DELTA=10
EPP1HI: EXP 0.0, 0.25, 0.7, 1.2, 1.6
EXP 1.9, 1.8, 1.1, 0.55, 0.45
EXP 0.38, 0.19, -0.4, -0.7, -0.75
EXP -0.65, -0.45, -0.15, 0.0

```

***** INPUT PARAMETERS FOR PANEL #2 (#A) *****

```

FSP2:: 700.1 ; FUSELAGE STATION, INCH
WLP2:: 244.0 ; WATERLINE STATION, INCH
BLP2:: 36.6 ; BUTTLINE STATION, INCH (+IVE TO PORT)
SAP2:: 22.5 ; SURFACE AREA OF PANEL IF NOT INCLUCD IN MAP
GAMP2:: 0.0 ; PANEL ORIENTATION, DEG
IOP2:: 2 ; PANEL INCIDENCE, DEG
CP2:: 1.0 ; PANEL MEAN AERO CHORD, FT

```

** BLACK HAWK HORIZONTAL STABILIZER (LT PANEL) LIFT COEFFICIENT VS ALPPP2
; S=22.5 FT**2 ,ASPECT RATIO=4.6 ,0014 AIRPOIL

```

CLP2MP: UVSUVS00 ;MAP ARGUMENT:LOOK UP ROUTINE
ALPPP200 ;INPUT VARIABLE
CLP200 ;OUTPUT VARIABLE
CLP2LO ;LOW ANGLE MAP NAME
EXP 0.0,30.0,5.0 ;LOWER LIMIT,UPPER LIMIT,DELTA-LOW ANGLE
CLP2HI ;HIGH ANGLE MAP NAME
EXP 30.0,90.0,10.0 ;LOWER LIMIT,UPPER LIMIT,DELTA-HIGH ANGLE

```

```

; LOW ANGLE MAP ALPPP2 0 TO 30,DELTA=5 CL(ALP)=-CL(-ALP)
CLP2LO: EXP 0.0, 0.356, 0.71, 0.92, 1.02
EXP 1.02, 0.99

```

```

; HIGH ANGLE MAP ALPPP2 30 TO 90,DELTA=10 CL(ALP)=-CL(-ALP)
CLP2HI: EXP 0.99, 0.847, 0.847, 0.745, 0.558
EXP 0.294, 0.0

```

** BLACK HAWK HORIZONTAL STABILIZER DRAG VS ALPPP2 (ABS)

```

CDP2MP: UVRUVR00 ;MAP ARGUMENT:LOOK UP ROUTINE
AFAPP200 ;INPUT VARIABLE
CDP200 ;OUTPUT VARIABLE
CDP2LO ;LOW ANGLE MAP NAME
EXP 0.0,30.0,5.0 ;LOWER LIMIT,UPPER LIMIT,DELTA
CDP2HI ;HIGH ANGLE MAP NAME
EXP 30.0,90.0,10.0 ;LOWER LIMIT,UPPER LIMIT,DELTA

```

```

; LOW ANGLE MAP ALPPP2 0 TO 30,DELTA=5 CD(ALP)=-CD(-ALP)
CDP2LO: EXP 0.01, 0.022, 0.04, 0.19, 0.36
EXP 0.37, 0.43

```

```

; HIGH ANGLE MAP ALPPP2 30 TO 90,DELTA=10 CD(ALP)=-CD(-ALP)
CDP2HI: EXP 0.43, 0.531, 0.702, 0.888, 1.05
EXP 1.161, 1.2

```

** BLACK HAWK HORIZONTAL STABILIZER MOMENT @C/4 VS ALPPP2

```

CMP2MP: UVSUVS00 ;MAP ARGUMENT:LOOK UP ROUTINE
ALPPP200 ;INPUT VARIABLE
CMP200 ;OUTPUT VARIABLE
CMP2LO ;LOW ANGLE MAP NAME
EXP 0.0,30.0,5.0 ;LOWER LIMIT,UPPER LIMIT,DELTA-LOW ANGLE
CMP2HI ;HIGH ANGLE MAP NAME
EXP 30.0,90.0,10.0 ;LOWER LIMIT,UPPER LIMIT,DELTA-HIGH ANGLE

```

TABLE A-1. UH-60A SPECIFIC FILE (Cont'd)

CMP2LO: EXP ; LOW ANGLE MAP ALFPP2 0 TO 30, DELTA=5
 EXP 0.0, 0.00125, 0.0025, 0.005, -0.045
 EXP -0.105, -0.125

CMP2HI: EXP ; HIGH ANGLE MAP ALFPP2 30 TO 90, DELTA=10
 EXP -0.125, -0.125, -0.125, -0.125, -0.125
 EXP -0.125, -0.125

;***** INPUT PARAMETERS FOR ROTOR INTERFERENCE ON THE HORIZ.TAIL #2 (MRPA)

; ** BLACK HAWK FORE/AFT H.R. DOWNWASH AT HORIZONTAL TAIL
 EXP2MP::BIV#0 ;MAP ARGUMENT:LOOK UP ROUTINE
 EXP CHIPMR#0,AA1FMR#0 ;INPUT VARIABLE #1, INPUT VARIABLE #2
 EKXP2#0 ;OUTPUT VARIABLE
 EXP2LO ;LOW ANGLE MAP NAME
 EXP 0.0,100.0,10.0,13 ;LOW LIM,UPPER LIM,DELTA,#ENTRYS(OCT)-CHIPMR
 EXP -6.0,6.0,6.0 ;LOW LIM,UPPER LIM,DELTA-AA1FMR

; LOW ANGLE MAP CHIPMR 0 TO 100 (DEL=10) AA1FMR -6,0,6
 ; AA1FMR=-6
 EXP2LO:EXP 0.0, -0.2, 0.05, 0.3, 0.54
 EXP 0.8, 1.04, 1.3, 1.55, 0.8
 0.0

; AA1FMR=0
 EXP -0.4, -0.6, -0.2, 0.12, 0.36
 EXP 0.6, 0.83, 1.06, 1.3, 0.6
 0.0

; AA1FMR=6
 EXP -0.56, -0.8, -0.74, -0.32, 0.04
 EXP 0.32, 0.6, 0.86, 1.12, 0.54
 0.0

; ** BLACK HAWK VERTICAL H.R. DOWNWASH AT HORIZONTAL TAIL
 EXP2MP::BIV#0 ;MAP ARGUMENT:LOOK UP ROUTINE
 EXP CHIPMR#0,AA1FMR#0 ;INPUT VARIABLE #1, INPUT VARIABLE #2
 ERZP2#0 ;OUTPUT VARIABLE
 EXP2LO ;LOW ANGLE MAP NAME
 EXP 0.0,100.0,10.0,13 ;LOW LIM,UPPER LIM,DELTA,#ENTRYS(OCT)-CHIPMR
 EXP -6.0,6.0,6.0 ;LOW LIM,UPPER LIM,DELTA-AA1FMR

; LOW ANGLE MAP CHIPMR 0 TO 100 (DEL=10) AA1FMR -6,0,6
 ; AA1FMR=-6
 EXP2LO:EXP -0.13, 0.8, 1.8, 1.82, 1.85
 EXP 1.88, 1.91, 1.94, 1.69, 1.42
 1.14

; AA1FMR=0
 EXP 0.4, 0.94, 1.84, 1.91, 1.98
 EXP 2.04, 2.08, 2.14, 1.89, 1.62
 1.35

; AA1FMR=6
 EXP 0.78, 1.36, 1.91, 1.98, 2.06
 EXP 2.14, 2.21, 2.28, 2.16, 1.96
 1.56

;***** FUSELAGE INTERFERENCE ON THE HORIZ.TAIL #2 (MPPA) *****

; ** BLACK HAWK DYNAMIC PRESSURE RATIO AT HORIZONTAL TAIL VS ALFPP
 OP2MP::UVR#0 ;MAP ARGUMENT:LOOK UP ROUTINE
 ALFPP#0 ;INPUT VARIABLE
 OP2QV#0 ;OUTPUT VARIABLE
 OP2LO ;LOW ANGLE MAP NAME
 EXP -30.0,30.0,5.0 ;LOWER LIMIT, UPPER LIMIT, DELTA

TABLE A-1. UH-60A SPECIFIC FILE (Cont'd)

```

; LOW ANGLE MAP ALPPP2 -30 TO 30 DELTA-5
QP2LO: EXP 1.0, 0.875, 0.762, 0.76, 0.76
      EXP 0.76, 0.76, 0.76, 0.76, 0.82
      EXP 0.90, 1.0, 1.0

; ** BLACK HAWK DOWNWASH ON HORIZDNTAL TAIL VS ALFWF DUE TO BODY
EPP2MP: UVRUVR00 ;MAP ARGUMENT:LOOK UP ROUTINE
      ALFWF00 ;INPUT VARIABLE
      EPSP200 ;OUTPUT VARIABLE
      EPP2LO ;LOW ANGLE MAP NAME
      EXP -30.0,30.0,5.0 ;LOWER LIMIT,UPPER LIMIT,DELTA-LOW ANGLE
      EPP2HI ;HIGH ANGLE MAP NAME
      EXP -90.0,90.0,10.0 ;LOWER LIMIT,UPPER LIMIT,DELTA-HIGH ANGLE

; LOW ANGLE MAP ALPPP2 -30 TO 30 DELTA-5
EPP2LO: EXP 1.8, 1.4, 1.1, 0.8, 0.55
      EXP 0.5, 0.45, 0.40, 0.38, 0.33
      EXP 0.19, -0.12, -0.40

; HIGH ANGLE MAP ALPPP2 -90 TO 90 DELTA-10
EPP2HI: EXP 0.0, 0.25, 0.7, 1.2, 1.6
      EXP 1.9, 1.8, 1.1, 0.55, 0.45
      EXP 0.38, 0.19, -0.4, -0.7, -0.75
      EXP -0.65, -0.45, -0.15, 0.0

;***** INPUT PARAMETERS FOR PANEL #3 (#A) *****
FSP3:: 695.0 ; FUSELAGE STATION,INCH
WLP3:: 273.0 ; WATERLINE STATION,INCH
BLP3:: 0.0 ; BUTTLINE STATION,INCH
SAP3:: 32.3 ; SURFACE AREA OF PANEL IF NOT INCLUDE IN MAP
GANF3:: -90.0 ; PANEL ORIENTATION, DEG
IOP3:: 0.0 ; PANEL INCIDENCE,DEG
CP3:: 1.0 ; PANEL MEAN ARCO CHORD,FT

; ** BLACK HAWK VERTICAL STABILIZER LIFT COEFFICIENT VS ALPPP3
; S=32.3 FT**2 ,ASPECT RATIO =1.92 ,0021 NDD AIRFOIL
CLP3MP: UVRUVR00 ;MAP ARGUMENT:LOOK UP ROUTINE
      ALPPP300 ;INPUT VARIABLE
      CLP300 ;OUTPUT VARIABLE
      CLP3LO ;LOW ANGLE MAP NAME
      EXP -30.0,30.0,5.0 ;LOWER LIMIT,UPPER LIMIT,DELTA-LOW ANGLE
      CLP3HI ;HIGH ANGLE MAP NAME
      EXP -90.0,90.0,10.0 ;LOWER LIMIT,UPPER LIMIT,DELTA-HIGH ANGLE

; LOW ANGLE MAP ALPPP3 -30 TO 30,DELTA-5
CLP3LO:EXP -1.00, -1.00, -0.93, -0.73, -0.5
      EXP -0.28, -0.06, 0.16, 0.38, 0.61
      EXP 0.82, 0.89, 0.89

; HIGH ANGLE MAP ALPPP3 -90 TO 90,DELTA-10
CLP3HI:EXP -0.0, -0.12, -0.28, -0.46, -0.65
      EXP -0.88, -1.00, -0.93, -0.5, -0.06
      EXP 0.38, 0.82, 0.89, 0.8, 0.63
      EXP 0.48, 0.32, 0.17, 0.0

; ** BLACK HAWK VERTICAL STABILIZER DRAG COEFFICIENT VS ALPPP3
CDP3MP: UVRUVR00 ;MAP ARGUMENT:LOOK UP ROUTINE
      ALPPP300 ;INPUT VARIABLE
      CDP300 ;OUTPUT VARIABLE
      CDP3LD ;LOW ANGLE MAP NAME
      EXP -30.0,30.0,5.0 ;LOWER LIMIT,UPPER LIMIT,DELTA-LOW ANGLE
      CDP3HI ;HIGH ANGLE MAP NAME
      EXP -90.0,90.0,10.0 ;LOWER LIMIT,UPPER LIMIT,DELTA-HIGH ANGLE

```

TABLE A-1. UH-60A SPECIFIC FILE (Cont'd)

```

; LOW ANGLE MAP ALPPP3 -30 TO 30, DELTA=5
COP3LO: EXP 0.36, 0.265, 0.174, 0.118, 0.066
        EXP 0.033, 0.018, 0.021, 0.044, 0.092
        EXP 0.162, 0.248, 0.355

; HIGH ANGLE MAP ALPPP3 -90 TO 90, DELTA=10
CDP3HI: EXP 1.1, 1.025, 0.965, 0.875, 0.745
        EXP 0.575, 0.36, 0.174, 0.066, 0.018
        EXP 0.044, 0.162, 0.355, 0.58, -0.75
        EXP 0.875, 0.965, 1.02, 1.08

; ** BLACK HAWK VERTICAL STABILIZER MOMENT @C/4 VS ALPPP3(ABS)
CMP3MP: UVRUVR00 ;MAP ARGUMENT:LOOK UP ROUTINE
        ALPPP300 ;INPUT VARIABLE
        CMP300 ;OUTPUT VARIABLE
        CMP3LO ;LOW ANGLE MAP NAME
        EXP -30.0,30.0,5.0 ;LOWER LIMIT,UPPER LIMIT,DELTA-LOW ANGLE
        CMP3HI ;HIGH ANGLE MAP NAME
        EXP -90.0,90.0,30.0 ;LOWER LIMIT,UPPER LIMIT,DELTA-HIGH ANGLE

; LOW ANGLE MAP ALPPP3 -30 TO 30, DELTA=5
CMP3LO: EXP -0.051, -0.051, -0.051, -0.051, -0.051
        EXP -0.051, -0.051, -0.051, -0.051, -0.051
        EXP -0.051, -0.051, -0.051

; HIGH ANGLE MAP ALPPP3 -90 TO 90, DELTA=30
CMP3HI: EXP -0.051, -0.051, -0.051, -0.051, -0.051
        EXP -0.051, -0.051

;***** ROTOR INTERFERENCE ON THE VERTICAL TAIL (MRPA) *****

; ** ROTOR ERX-FACTOR ON VERTICAL TAIL MAP **
EXP3MP: CONST00 ;MAP ARGUMENT:LOOK UP ROUTINE
        ERXP100 ;INPUT VARIABLE
        ERXP300 ;OUTPUT VARIABLE

; ** ROTOR ERZ-FACTOR ON VERTICAL TAIL MAP **
EXP3MP: CONST00 ;MAP ARGUMENT:LOOK UP ROUTINE
        ERZP100 ;INPUT VARIABLE
        ERZP300 ;OUTPUT VARIABLE

;***** FUSELAGE INTERFERENCE ON THE VERTICAL TAIL (MPPA) *****

; ** BLACK HAWK DYNAMIC PRESSURE RATIO AT VERTICAL TAIL VS PSINP
QP3MP: RIV00 ;MAP ARGUMENT:LOOK UP ROUTINE
        EXP PSABWF00,ALPWF00 ;INPUT VARIABLE #1, INPUT VARIABLE #2
        QP3QWF00 ;OUTPUT VARIABLE
        QP3LO ;LOW ANGLE MAP NAME
        EXP 0.0,30.0,5.0,7 ;LOWER LIM,UPPER LIM,DELTA,#ITEMS(GCT)-PSABWF
        EXP -10.0,10.0,10.0 ;LOWER LIM,UPPER LIM,DELTA-ALPWF

; LOW ANGLE MAP PSI(ABS) 0 TO 30 DELTA=5
QP3LO: EXP ;ALPWF= -10 DEG
        EXP 0.62, 0.64, 0.66, 0.72, 0.79
        EXP 0.86, 1.00
        EXP ;ALPWF= 0 DEG
        EXP 0.62, 0.64, 0.66, 0.72, 0.79
        EXP 0.88, 1.00
        EXP ;ALPWF= 10 DEG
        EXP 0.62, 0.64, 0.66, 0.72, 0.79
        EXP 0.88, 1.00
    
```

TABLE A-1. UH-60A SPECIFIC FILE (Cont'd)

```

; ** BLACK HAWK SIDEWASH ON VERTICAL TAIL VS PSIWF DUE TO BODY
SGP3MP: UVSUVS00 ;MAP ARGUMENT:LOOK UP ROUTINE
        PSIWF00 ;INPUT VARIABLE
        SIGP300 ;OUTPUT VARIABLE
        SGP3LO ;LOW ANGLE MAP NAME
EXP 0.0,30.0,5.0 ;LOWER LIMIT, UPPER LIMIT, DELTA-LOW ANGLE
        SGP3HI ;HIGH ANGLE MAP NAME
EXP 0.0,90.0,30.0 ;LOWER LIMIT, UPPER LIMIT, DELTA-HIGH ANGLE

; LOW ANGLE MAP PSIWF 0 TO 30 DELTA-5
SGP3LO: EXP 0.0, -0.4, -0.6, 0.8, 1
        EXP 0.6, 0.2

; HIGH ANGLE MAP PSIWF 0 TO 90 DELTA-30
SGP3HI: EXP 0.0, 0.2, 0.0, 0.0
        PAGE

;***** INPUT PARAMETERS FOR TAIL ROTOR (8A) - (BAILEY) <*****
RTR: 5.5 ;RADIUS,FT
OMEGTR:124.62 ;TRIM ROTATIONAL RATE, RAD/SEC
BTR: 4.0 ;ACTUAL NUMBER OF BLADES
YSTR: 732.0 ;FUSELAGE STATION,IN
WLTR: 324.7 ;WATERLINE STATION,IN
BLTR: -14.0 ;BUTTLINE STATION,IN (+IVE TO PORT)
TWSTR: -18.0 ;BLADE TWIST,DATUM CENTER OF ROTATION,DEG
BIASR: 6.0 ;BLADE PITCH CORRECTION FOR N.L.TWIST(NEG REDUCES PITCH)
GAMTR: 70.0 ;TAIL ROTOR CANT ANGLE,DEG
DEL3TR: 35.0 ;FLAPPING HINGE OFFSET ANGLE,DEG
DELTR: .001455 ;RATE OF CHANGE OF COMA ANGLE WITH THRUST,DEG/LB
CHRDR: .81 ;BLADE CHORD,FT
ATR: 5.73 ;BLADE LIFT CURVE SLOPE,1/RAD
BTLR: .92 ;BLADE TIP LOSS FACTOR
CDTR: 0.0 ;TAIL ROTOR HEAD DRAG,FT**2
IBTR: 3.0996 ;T.R. BLADE SECOND MOMENT SLUGS-FT**2
DRD0TR: 0.0087 ;T.R. BLADE SECTION DRAG COEFF,CD0
DRD1TR: -0.0216 ;T.R. BLADE SECTION DRAG COEFF,CD1
DRD2TR: 0.4 ;T.R. BLADE SECTION DRAG COEFF,CD2
DROTTR: -1.0 ;T.R. ROTATION +1.0 MEANS COUNTER CLOCKWISE
; WHEN VIEWED FROM PORT SIDE

;***** ROTOR INTERFERENCE ON TAIL ROTOR (MRPA) *****

; ** ROTOR X-FACTOR ON TAIL ROTOR MAP **
EXTRMP: CONST00 ;MAP ARGUMENT:LOOK UP ROUTINE
        ERXP300 ;INPUT VARIABLE
        ERXTR00 ;OUTPUT VARIABLE

; ** ROTOR Z-FACTOR ON TAIL ROTOR MAP **
EZTRMP: CONST00 ;MAP ARGUMENT:LOOK UP ROUTINE
        EZXP300 ;INPUT VARIABLE
        EZXTR00 ;OUTPUT VARIABLE

;***** FUSELAGE INTERFERENCE ON THE TAIL ROTOR (MPPA) *****

; ** TAIL ROTOR DYNAMIC PRESSURE RATIO MAP **
OTRMP: CONST00 ;MAP ARGUMENT:LOOK UP ROUTINE
        OP3QW ;INPUT VARIABLE
        OTROWP00 ;OUTPUT VARIABLE

; ** BODY DOWNWASH ON TAIL ROTOR MAP **
EPTRMP: CONST00 ;MAP ARGUMENT:LOOK UP ROUTINE
        EPSP100 ;INPUT VARIABLE
        EPSTR00 ;OUTPUT VARIABLE

```

TABLE A-1. UH-60A SPECIFIC FILE (Cont'd)

```

; ** BODY SIDEWASH ON TAIL ROTOR MAP **
SGTRMP::CONST#0 ;MAP ARGUMENT:LOOK UP ROUTINE
          SIGP3#0 ;INPUT VARIABLE
          SIGTR#0 ;OUTPUT VARIABLE

;***** VERTICAL TAIL INTERPERNCE ON TAIL ROTOR INFLOW *****

VBVTTR::30.0 ; AIRSPEED BREAK FT. - NO BLOCKAGE ABOVE,KT.
KBVTTR::0.796 ; TAIL ROTOR BLOCKAGE COEF. AT HOVER

;***** INPUT PARAMETERS FOR EQUATIONS OF MOTION (#B) *****

PSCG:: 355.9 ; FUSELAGE STATION,OF C.G.,INCH
WLCG:: 248.2 ; WATERLINE STATION OF C.G.,INCH
BLCG:: 0.0 ; BUTTLINE STATION OF C.G.,INCH (+IVE TO PORT)

WEIGHT::16638.0 ; AIRCRAFT GROSS WEIGHT,IBS.
IX:: 4659.0 ; INERTIA ABOUT BOOY X-AXIS,SLUG-FT**2
IY:: 38512.0 ; INERTIA ABOUT BOOY Y-AXIS,SLUG-FT**2
IZ:: 36796.0 ; INERTIA ABOUT BOOY Z-AXIS,SLUG-FT**2
IXZ:: 1882.0 ; CROSS COUPLING INERTIA,SLUG-FT**2
IXY:: 0.0
IYZ:: 0.0

AISUL:: 8.0 ; A1S UPPER LIMIT
AISLL:: -8.0 ; A1S LOWER LIMIT
BISUL:: 16.3 ; B1S UPPER LIMIT
BISLL:: -12.5 ; B1S LOWER LIMIT
THOUL:: 25.9 ; THETA0 UPPER LIMIT
THOLL:: 9.9 ; TBETA0 LOWER LIMIT
THKUL:: 36.5 ; THETTR UPPER LIMIT
THKLL:: 4.5 ; THETTR LOWER LIMIT

XAUL:: 10.0 ; LAT STICK UPPER LIMIT
XALL:: 0.0 ; LAT STICK LOWER LIMIT
XBUL:: 10.0 ; LONG STCK UPPER LIMIT
XBLL:: 0.0 ; LONG STCK LOWER LIMIT
XCUL:: 10.0 ; COLL STCK UPPER LIMIT
XCLL:: 0. ; COLL STCK LOWER LIMIT
XPUL:: 5.28 ; PEDAL UPPER LIMIT
XPLL:: 0.0 ; PEDAL LOWER LIMIT

```

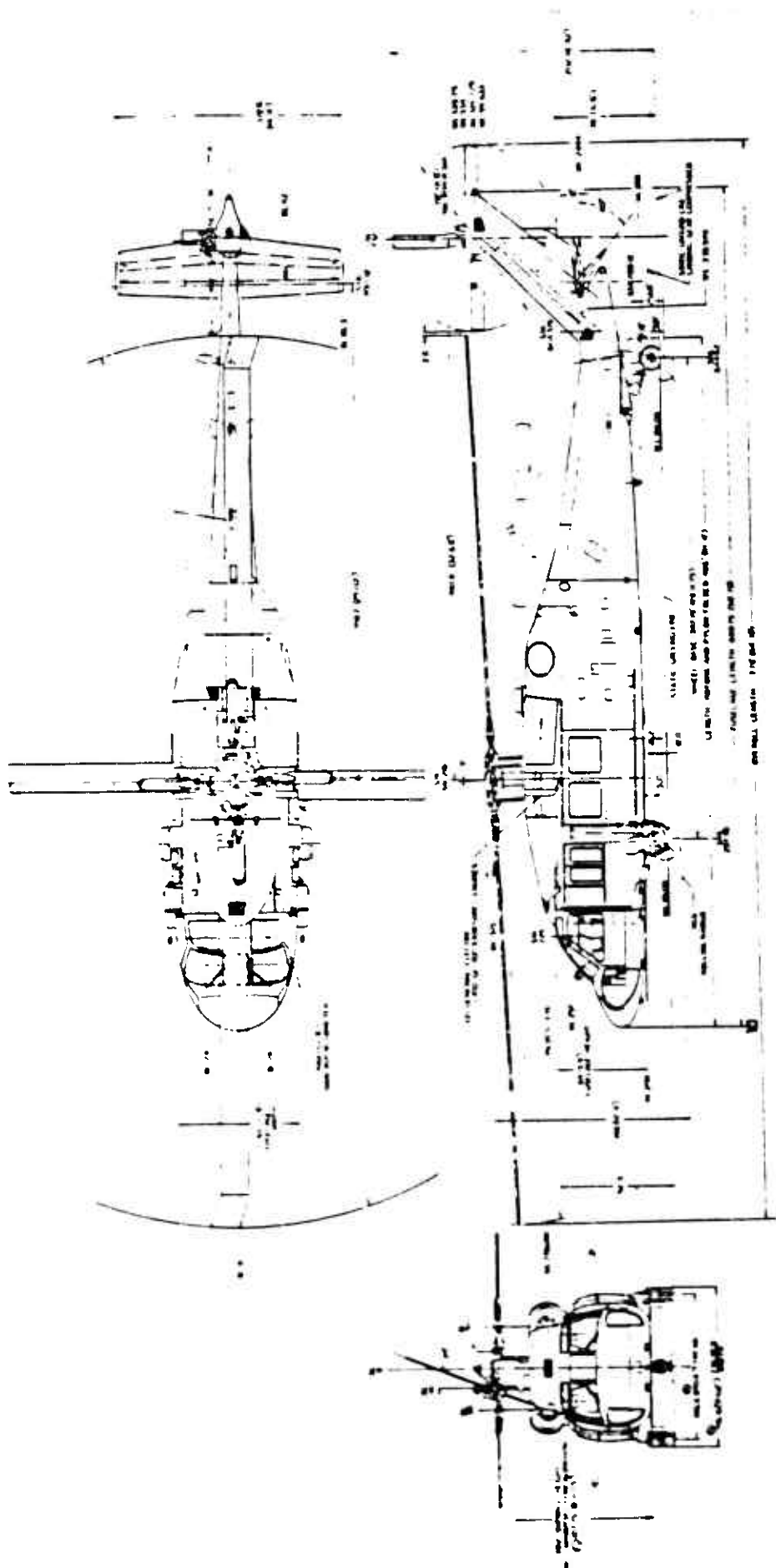



Figure A-1. UH-60A Three-View Drawing

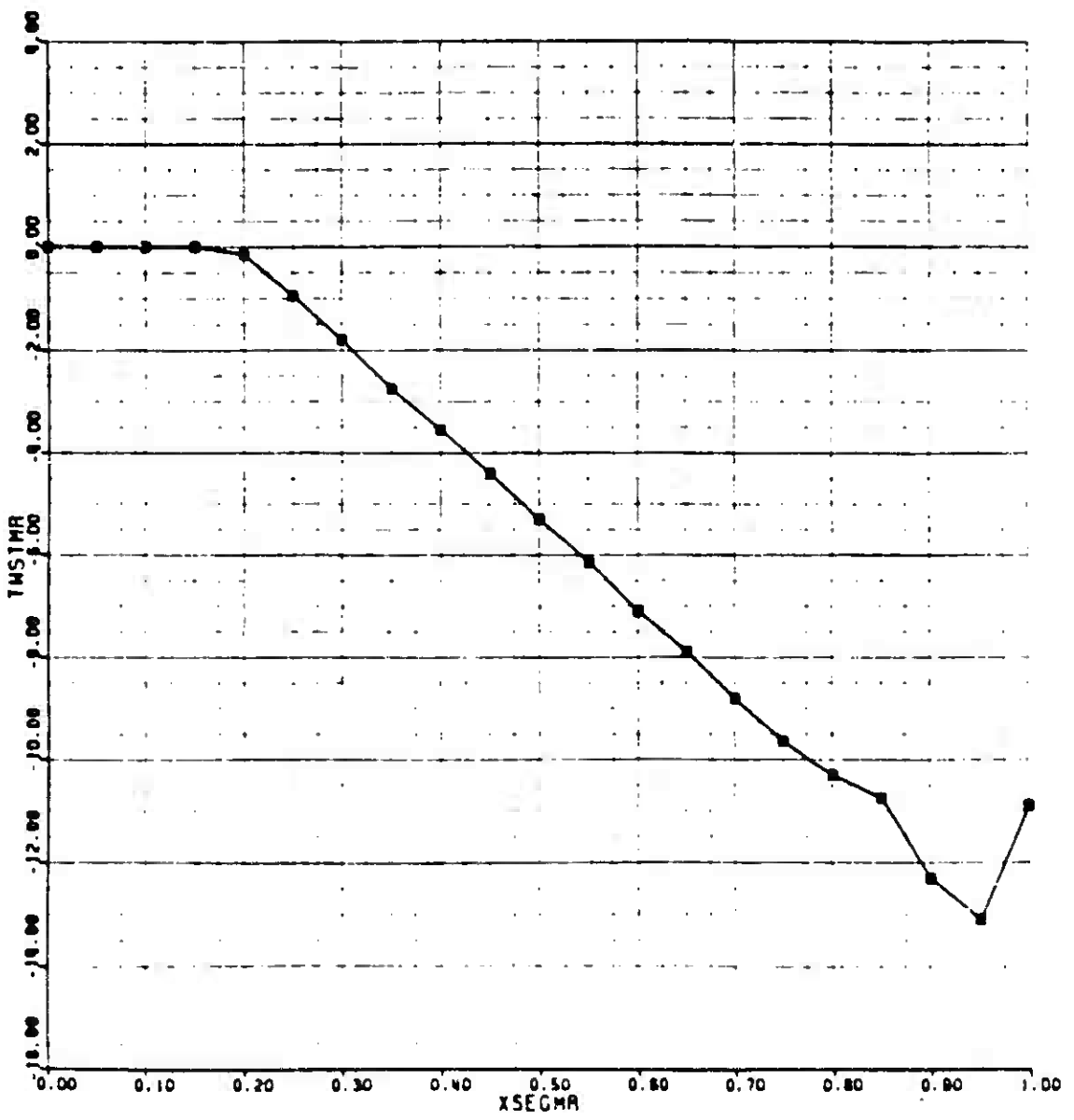


Figure A-2. UH-60A Main Rotor Blade Twist Map

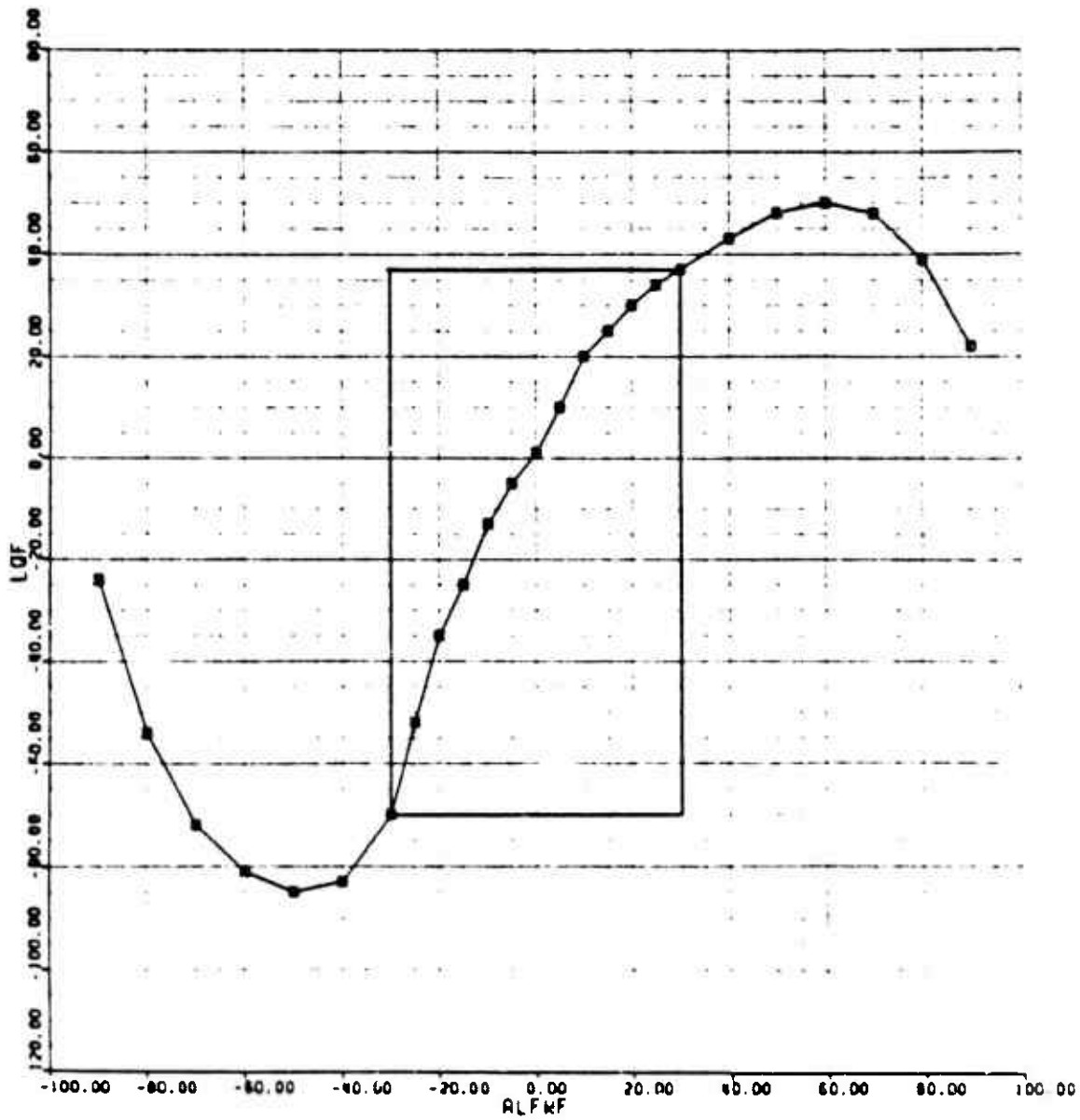


Figure A-3. UH-60A Fuselage Lift Map

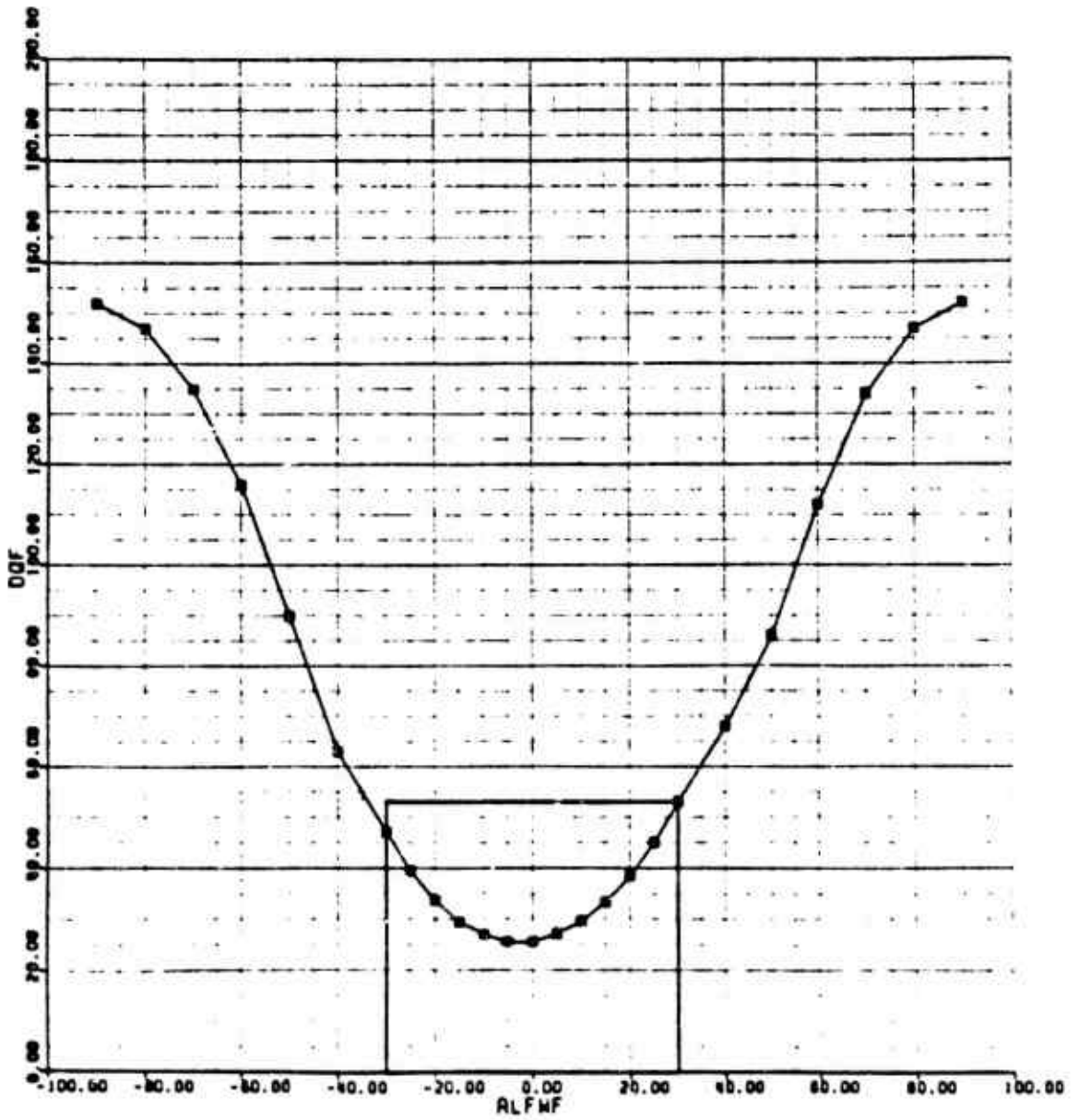


Figure A-4. UE-60A Fuselage Drag Map

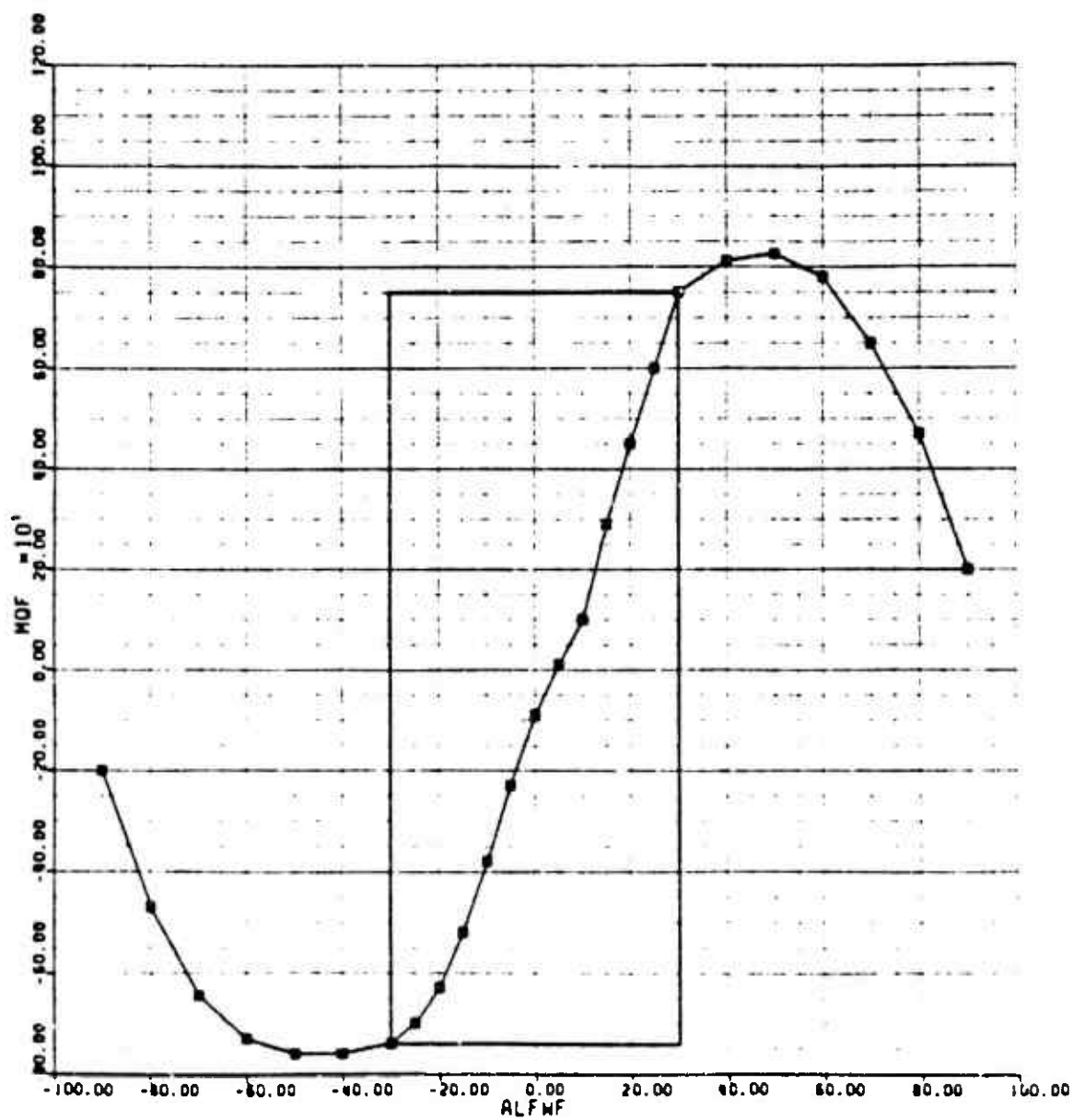


Figure A-5. UH-60A Fuselage Pitching Moment Map

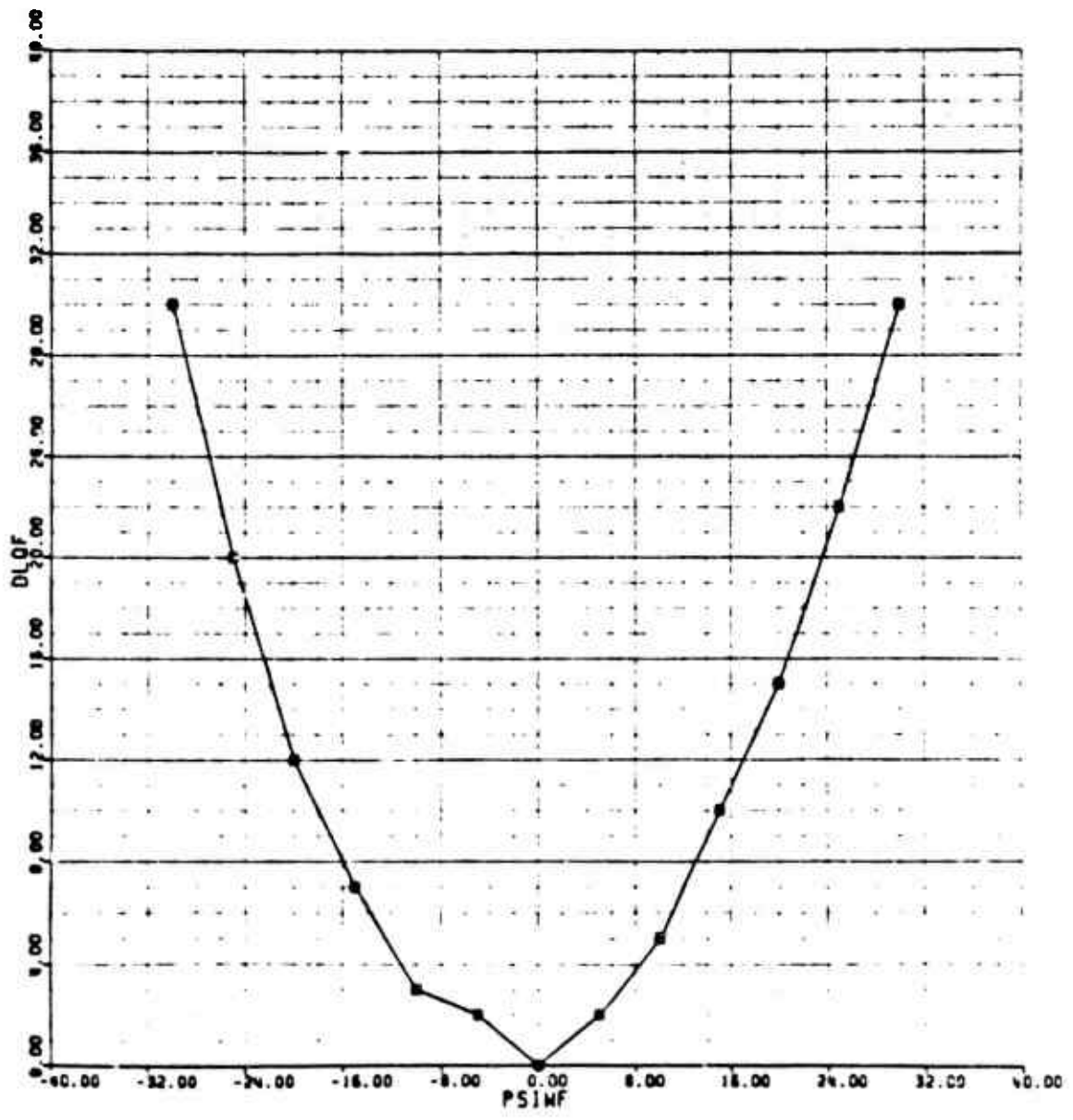


Figure A-6. UH-60A Fuselage Delta Lift Map

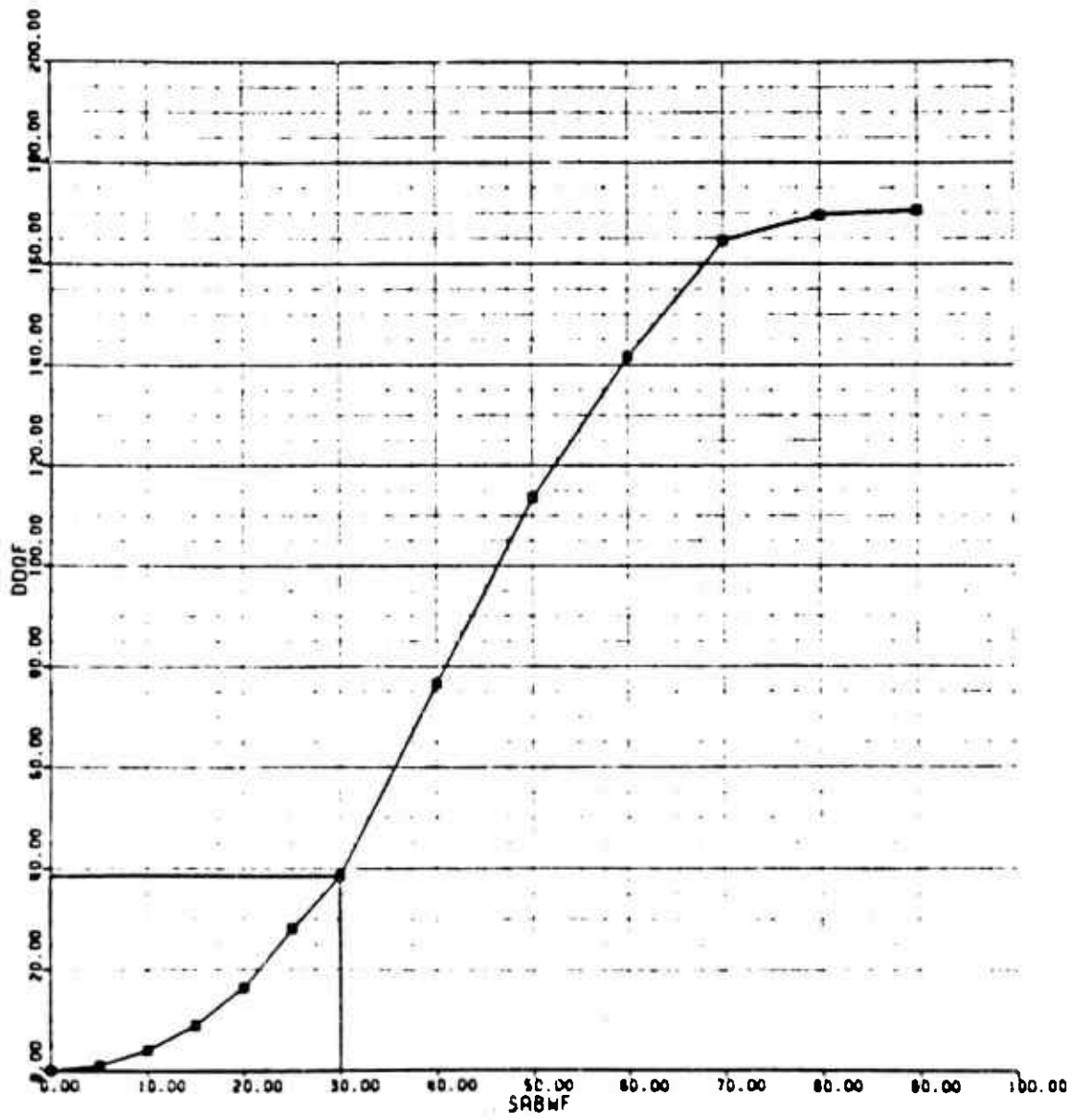


Figure A-7. UH-60A Fuselage Delta Drag Map

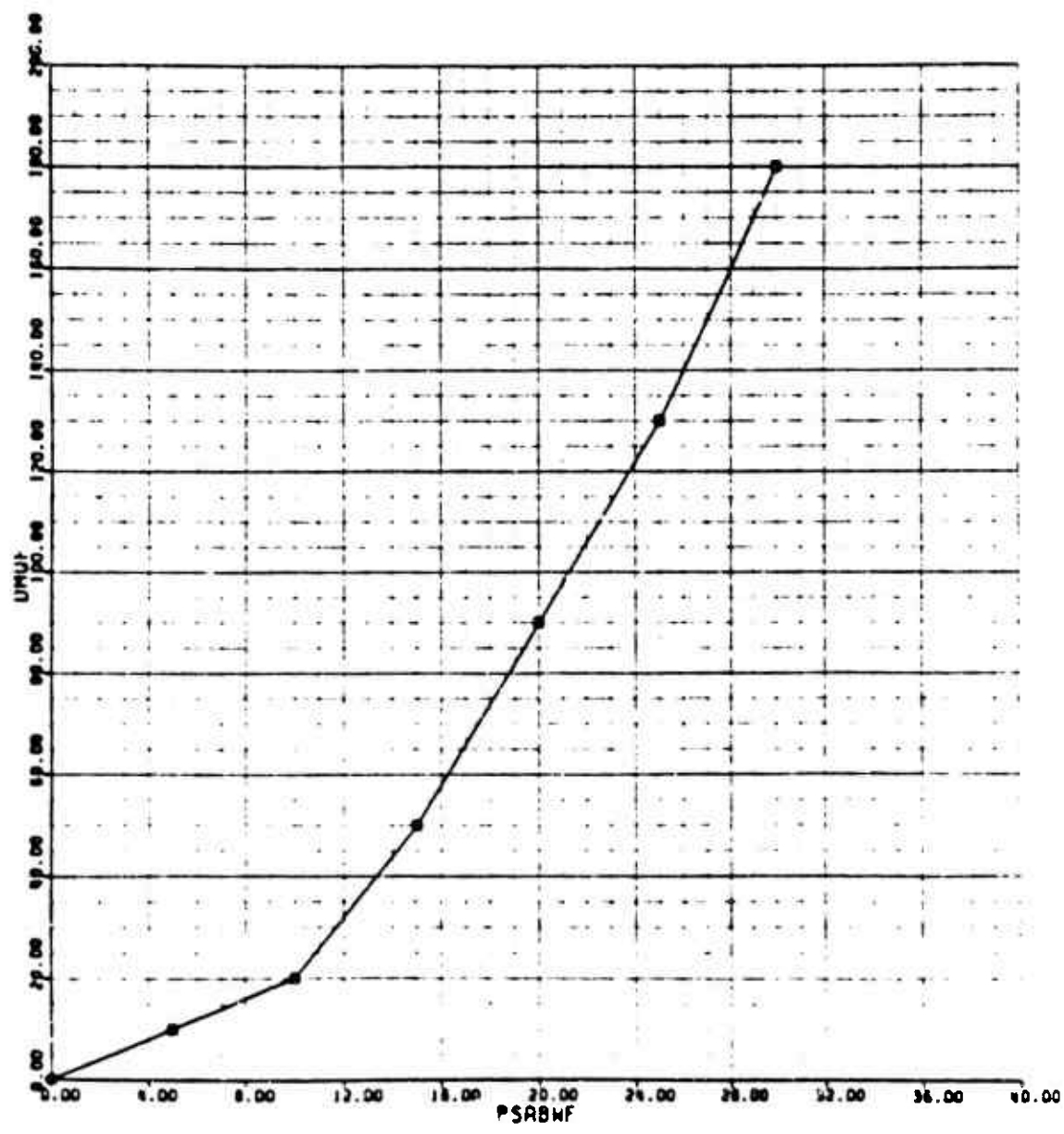


Figure A-8. UH-60A Fuselage Delta Pitching Moment Map

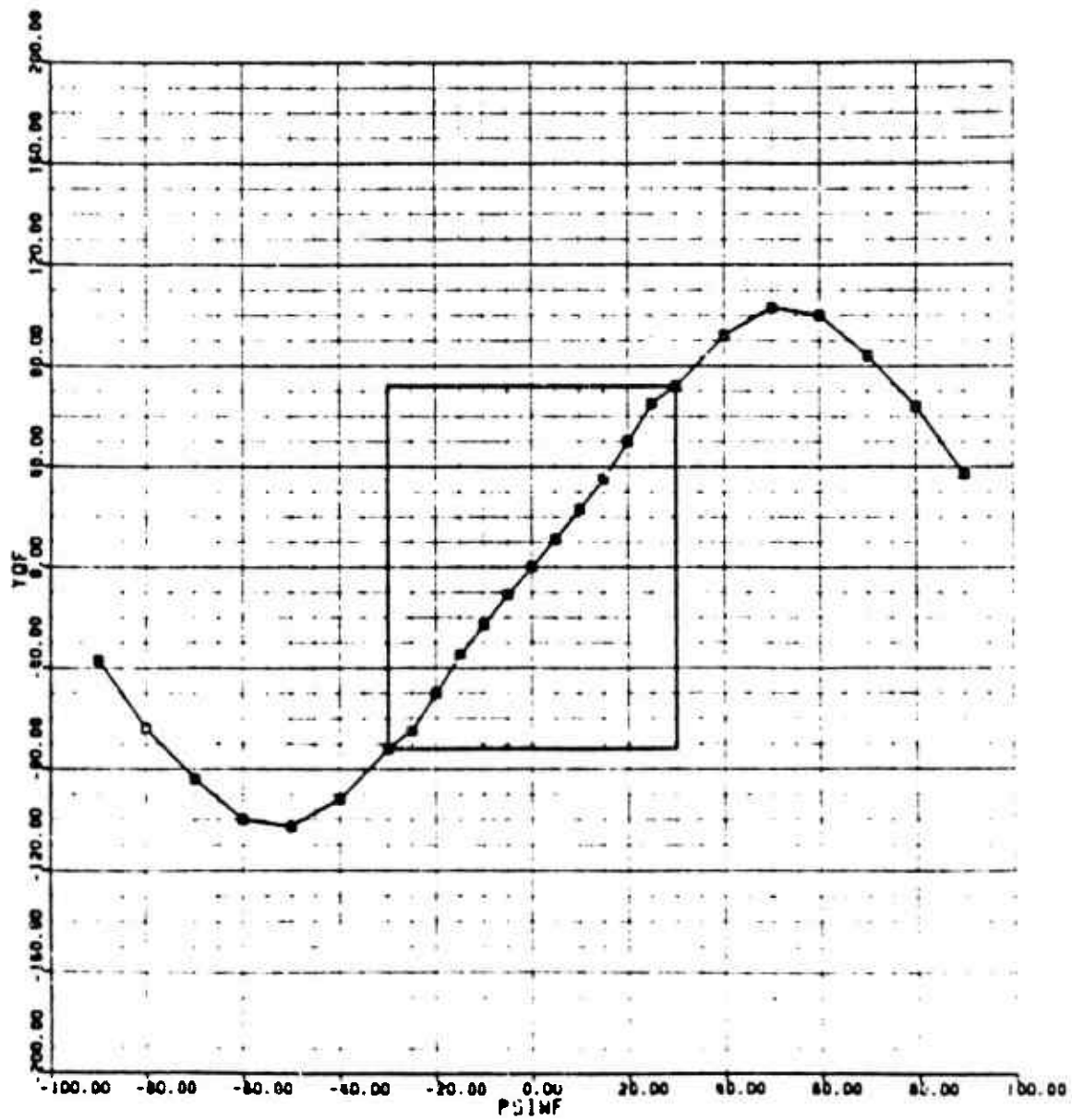


Figure A-9. U2-60A Fuselage Sideforce Map

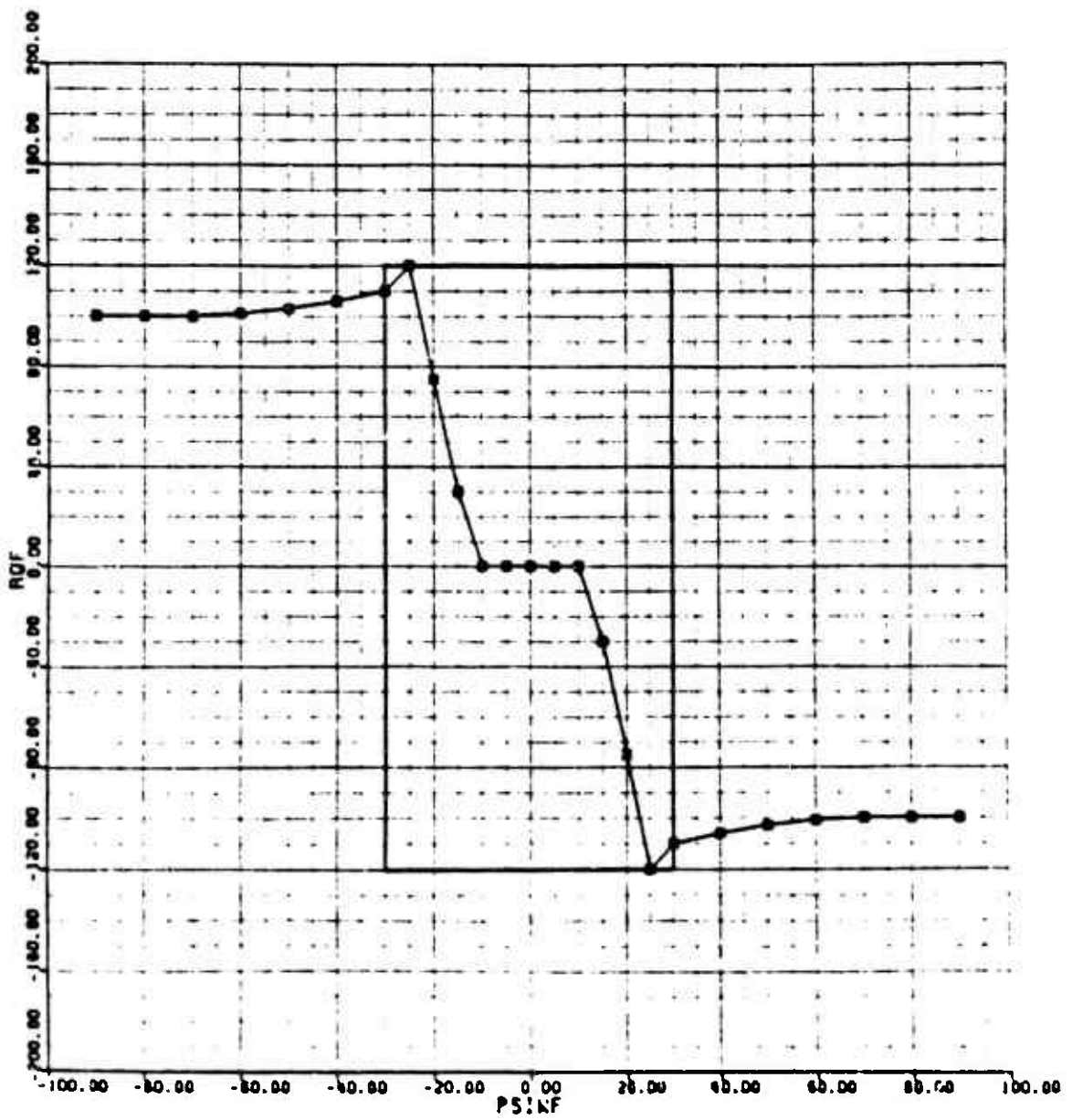


Figure A-10. UH-60A Fuselage Rolling Moment Map

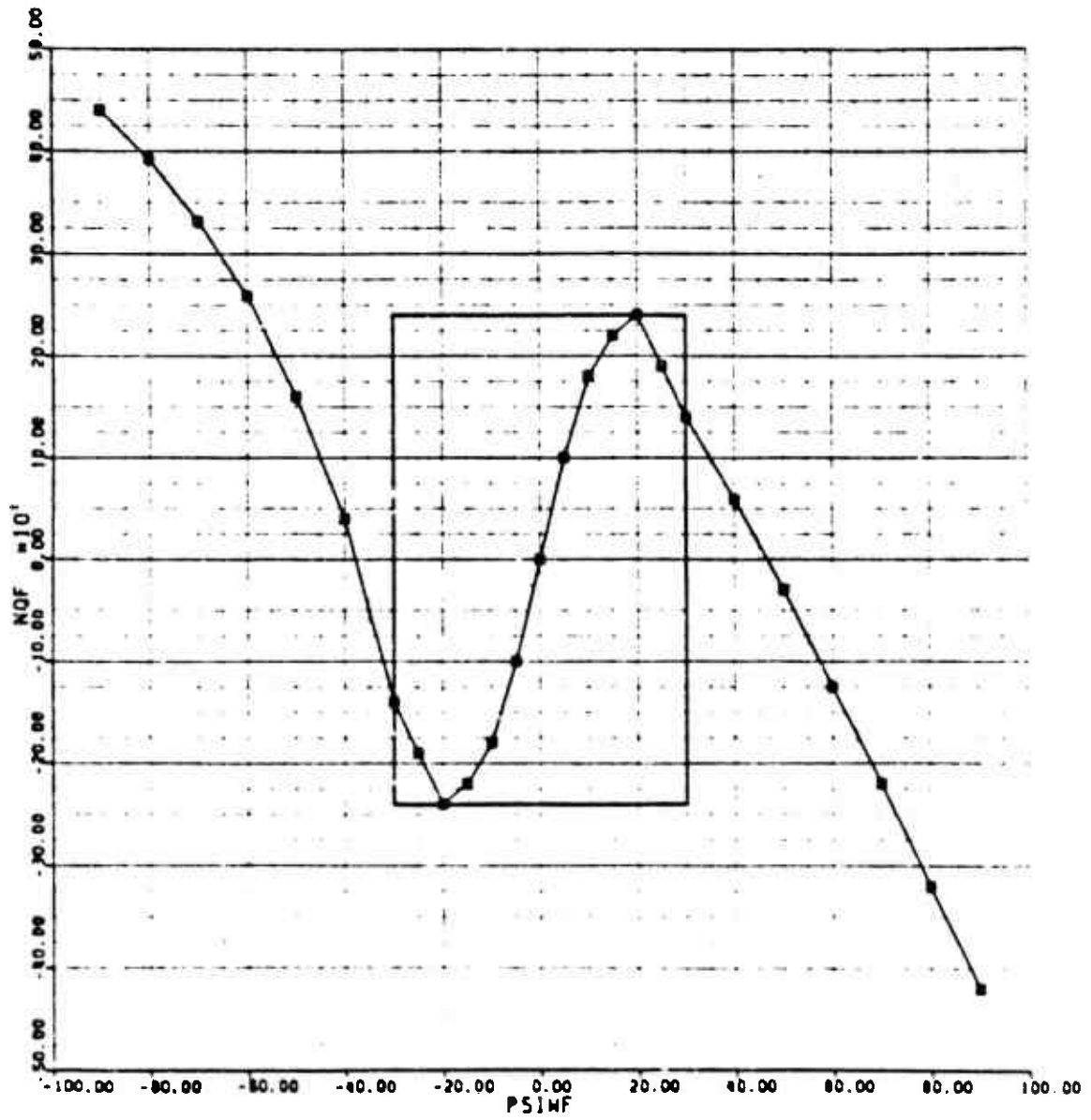


Figure A-11. UH-60A Fuselage Yawing Moment Map

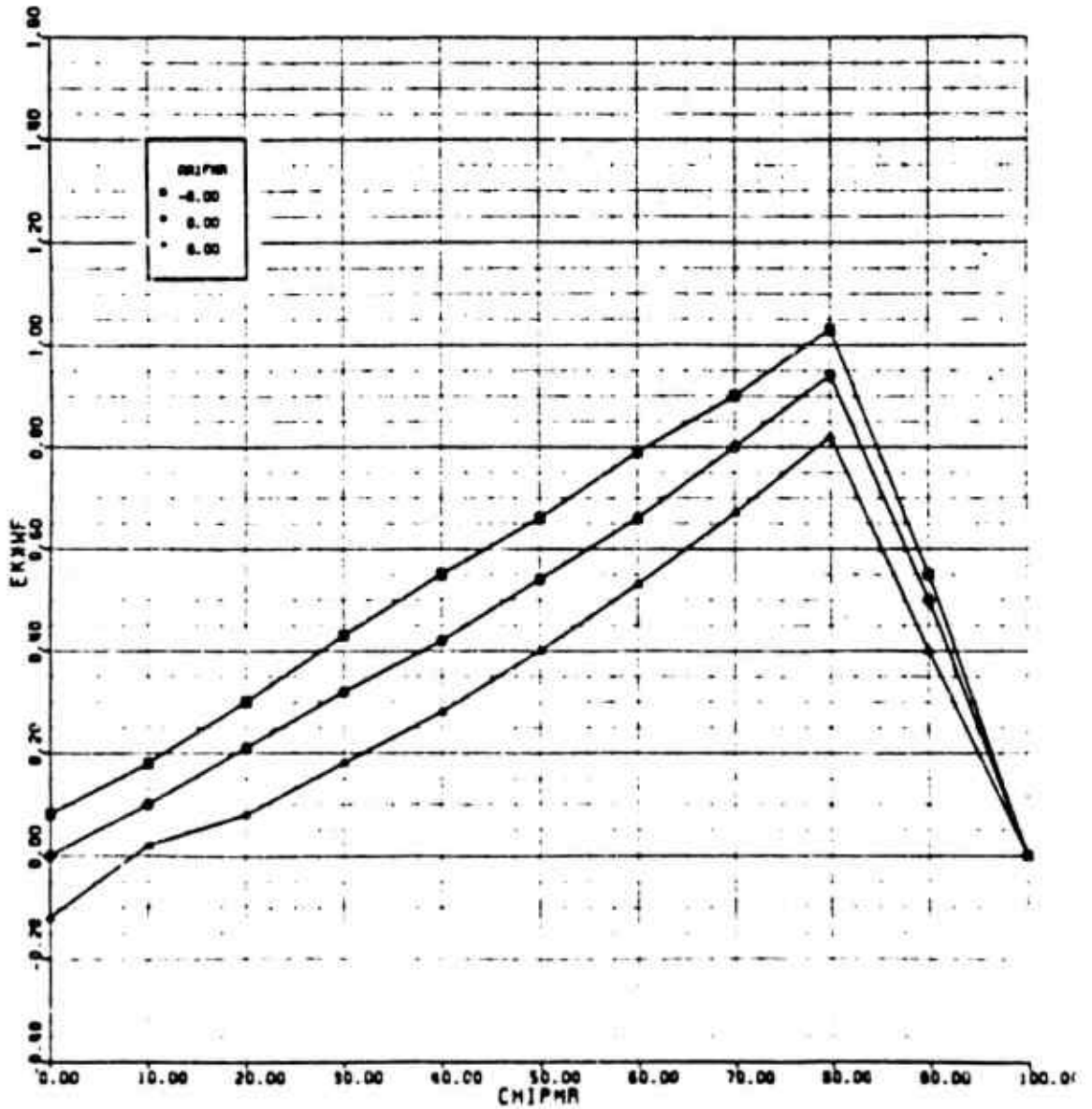


Figure A-12. UH-60A Main Rotor Downwash on Fuselage Map (x-direction)

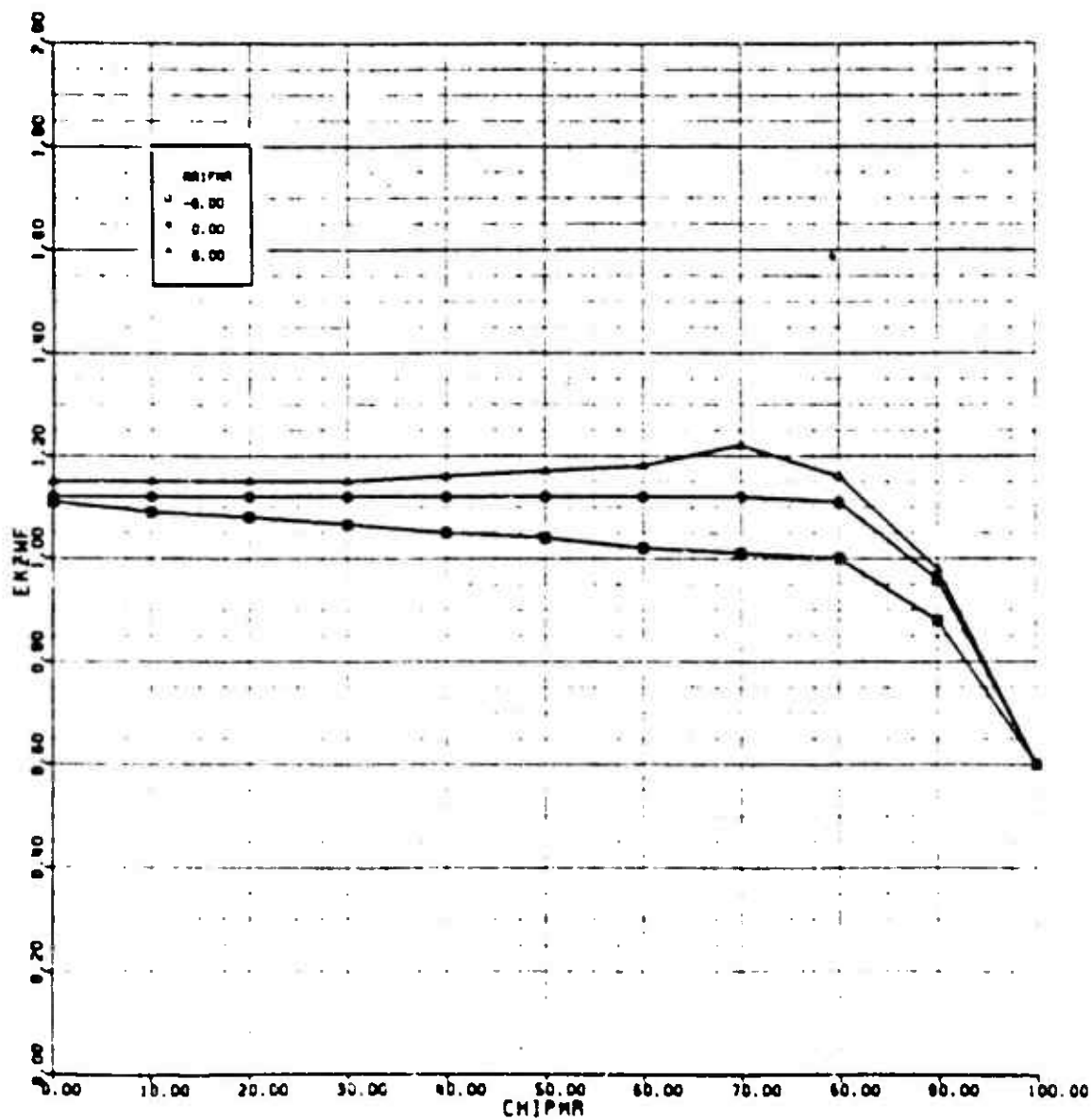


Figure A-13. UH-60A Main Rotor Downwash on Fuselage Map (z-direction)

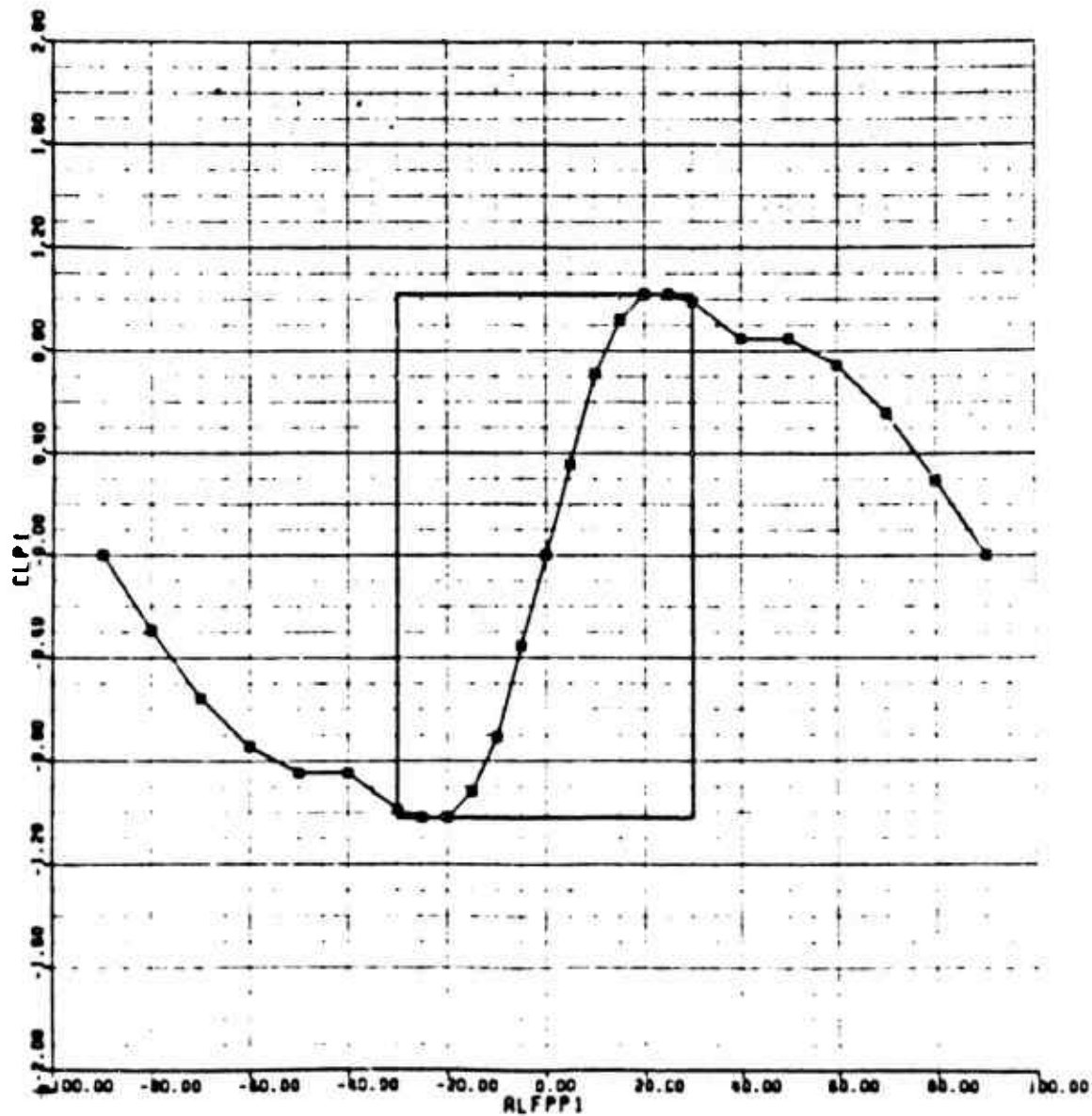


Figure A-14. UH-60A Horizontal Stabilizer Lift Map

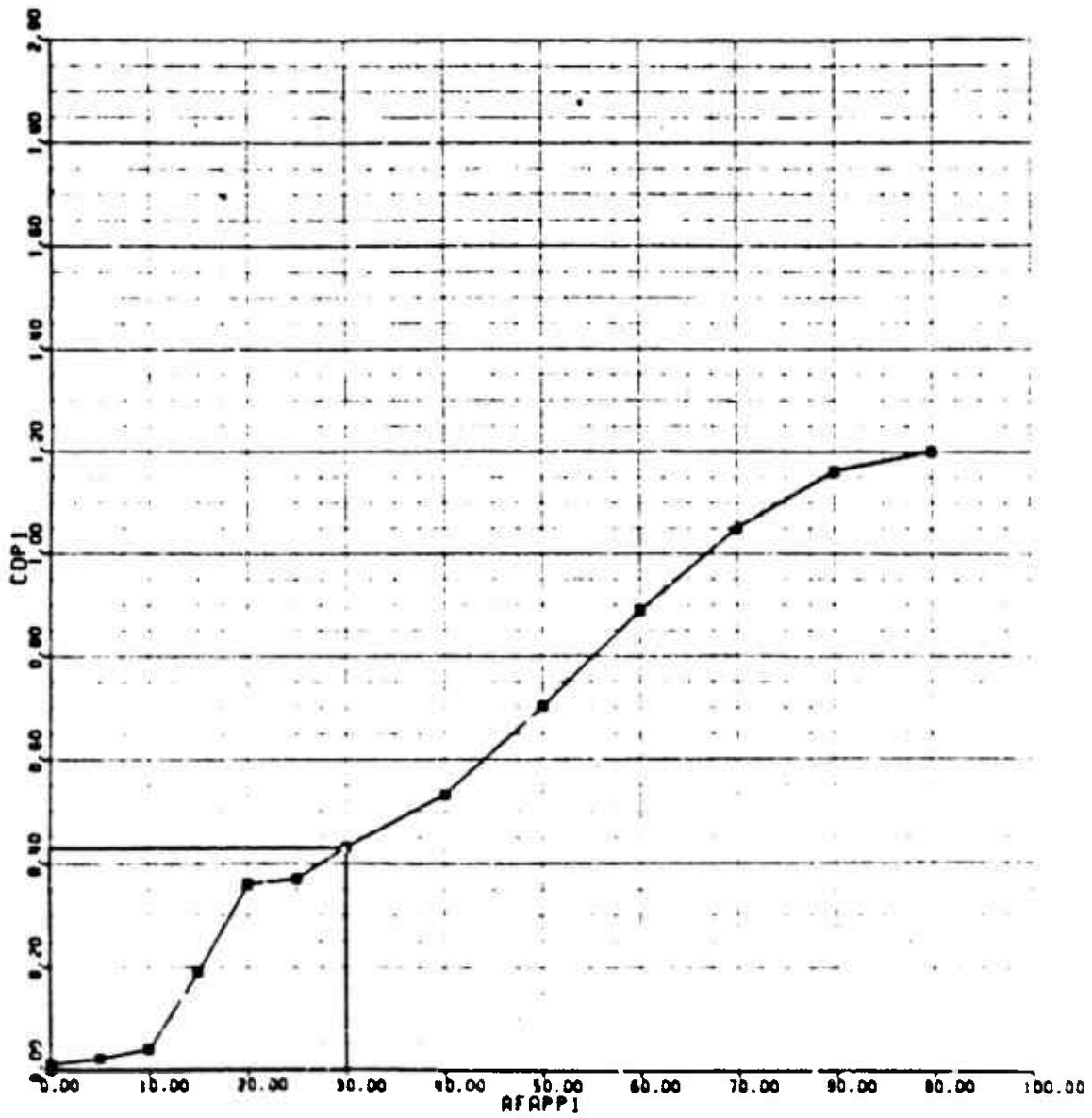


Figure A-15. UH-60A Horizontal Stabilizer Drag Map

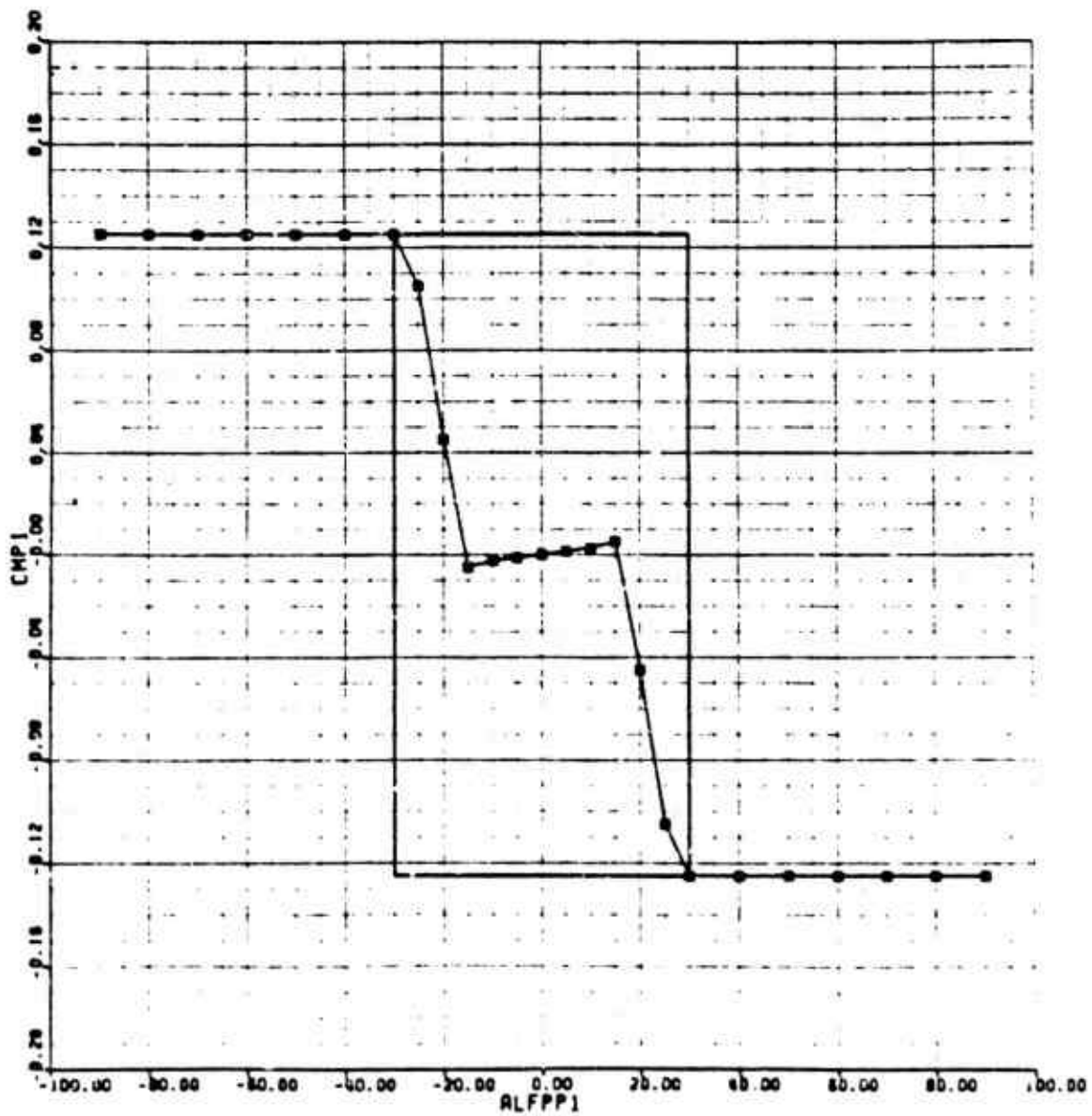


Figure A-16. UH-60A Horizontal Stabilizer Moment Map

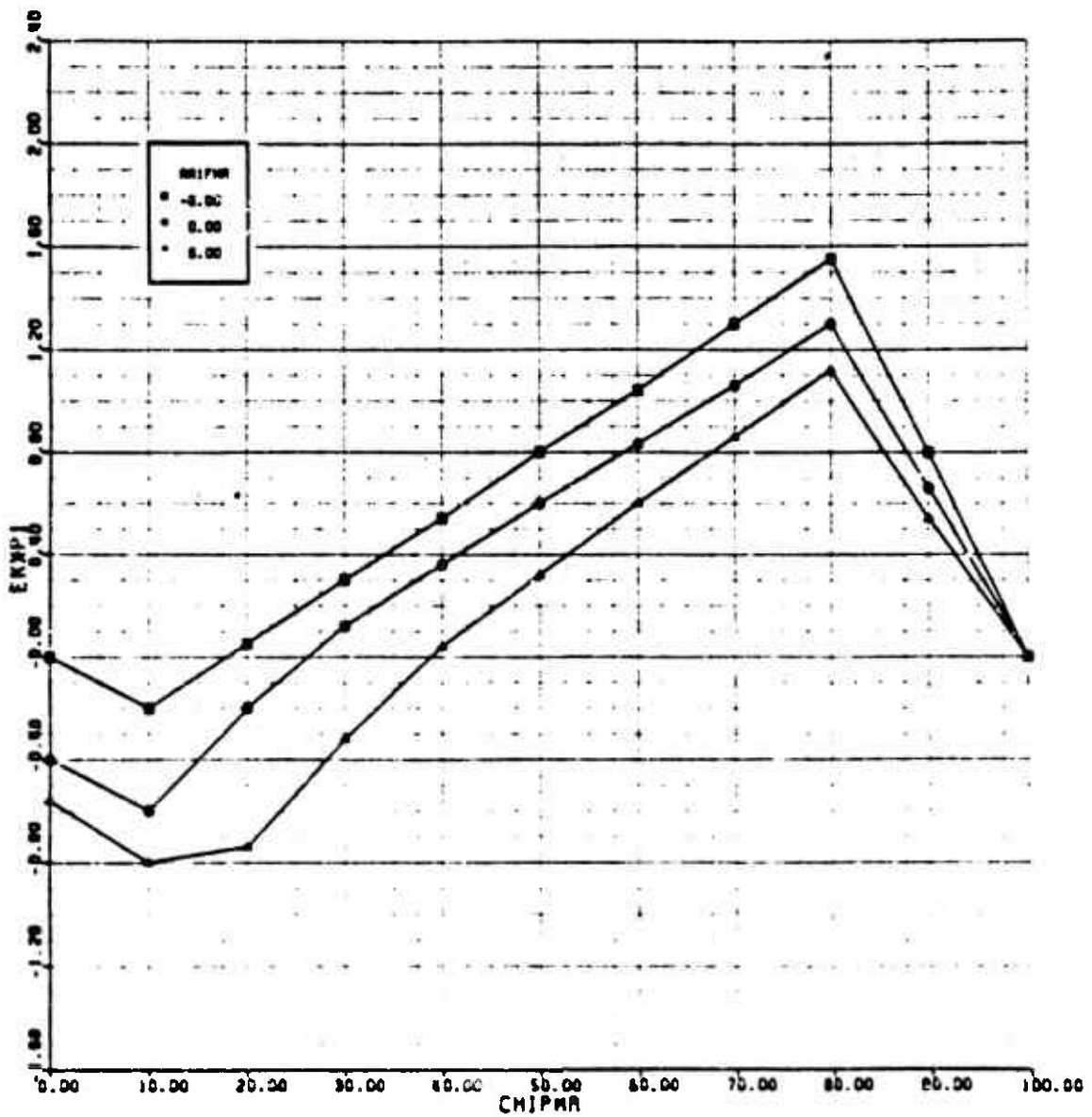


Figure A-17. UH-60A Main Rotor Downwash on Horizontal Stabilizer Map (x-direction)

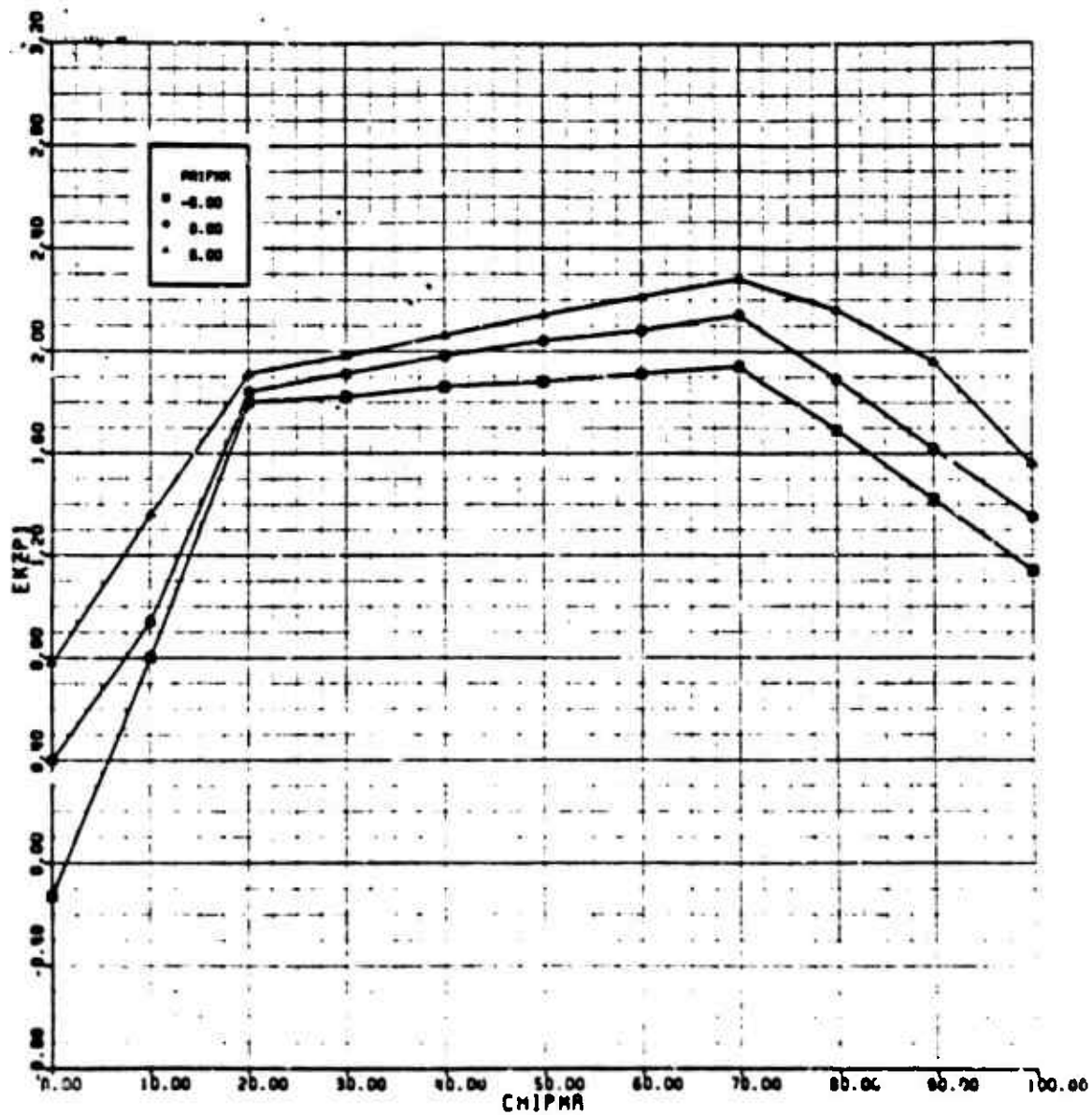


Figure A-18. UH-60A Main Rotor Downwash on Horizontal Stabilizer Map (z-direction)

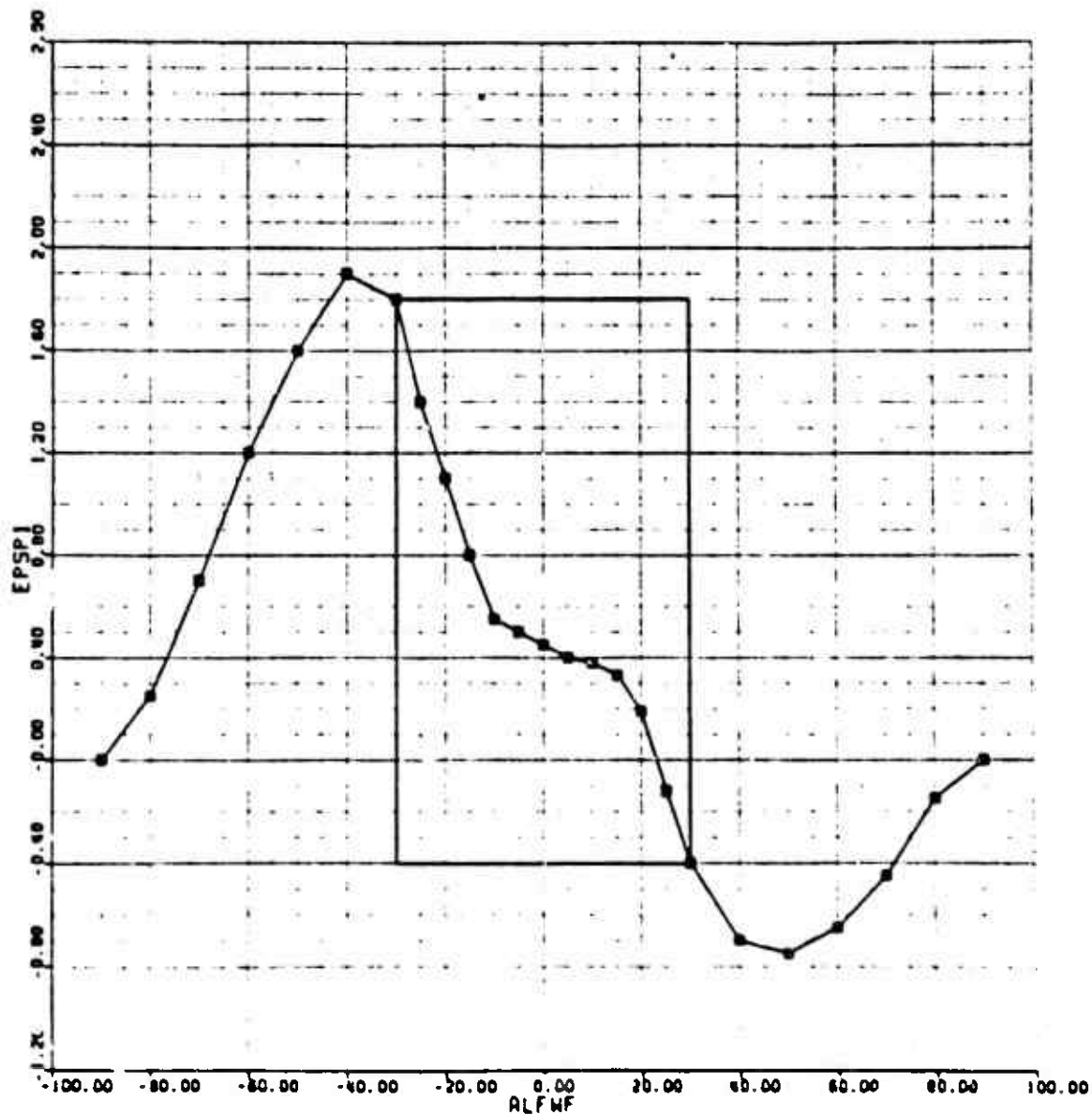


Figure A-19. UH-60A Fuselage Driftwash on Horizontal Stabilizer Map

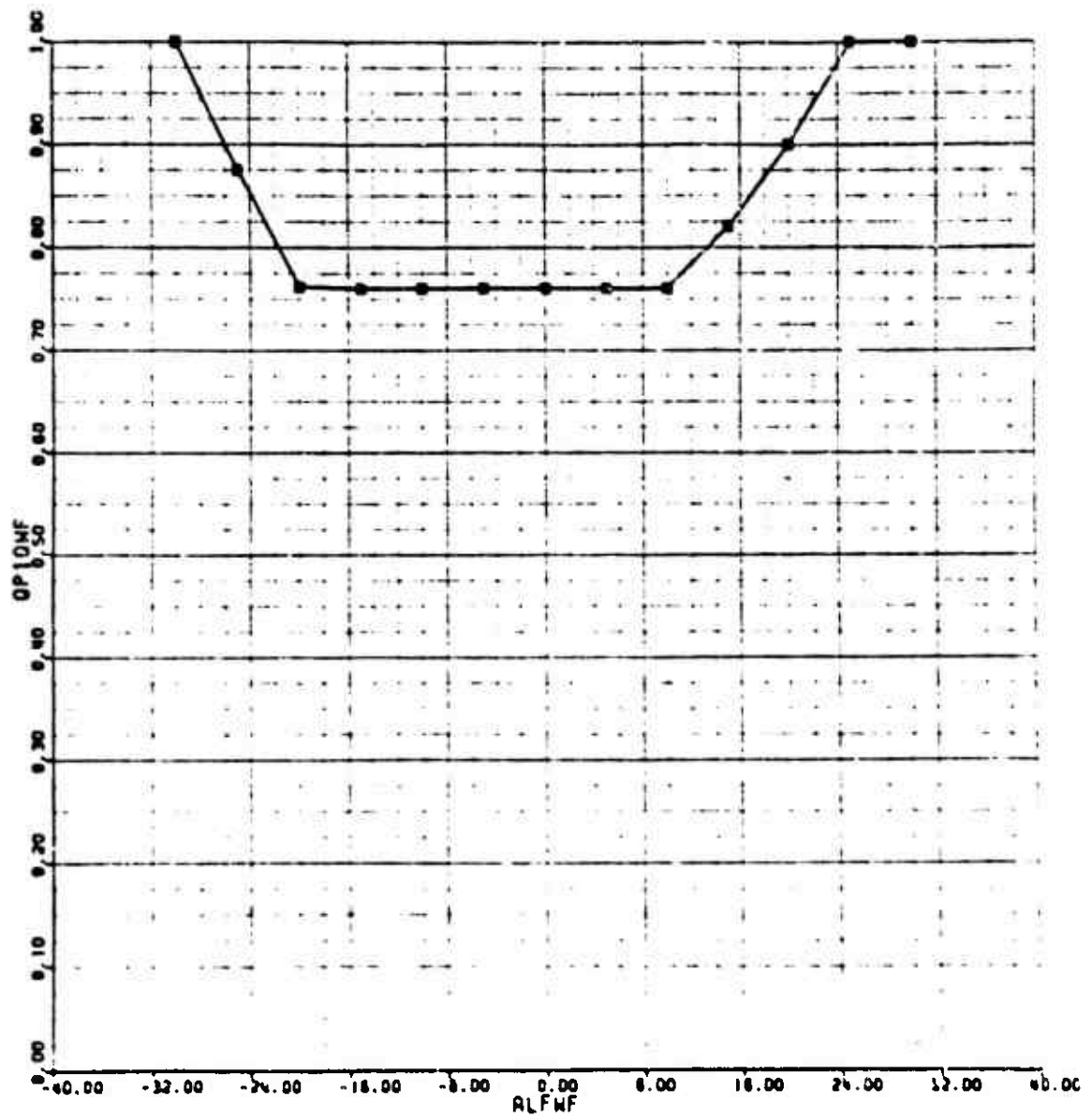


Figure A-20. UH-60A Dynamic Pressure Ratio at Horizontal Stabilizer Map

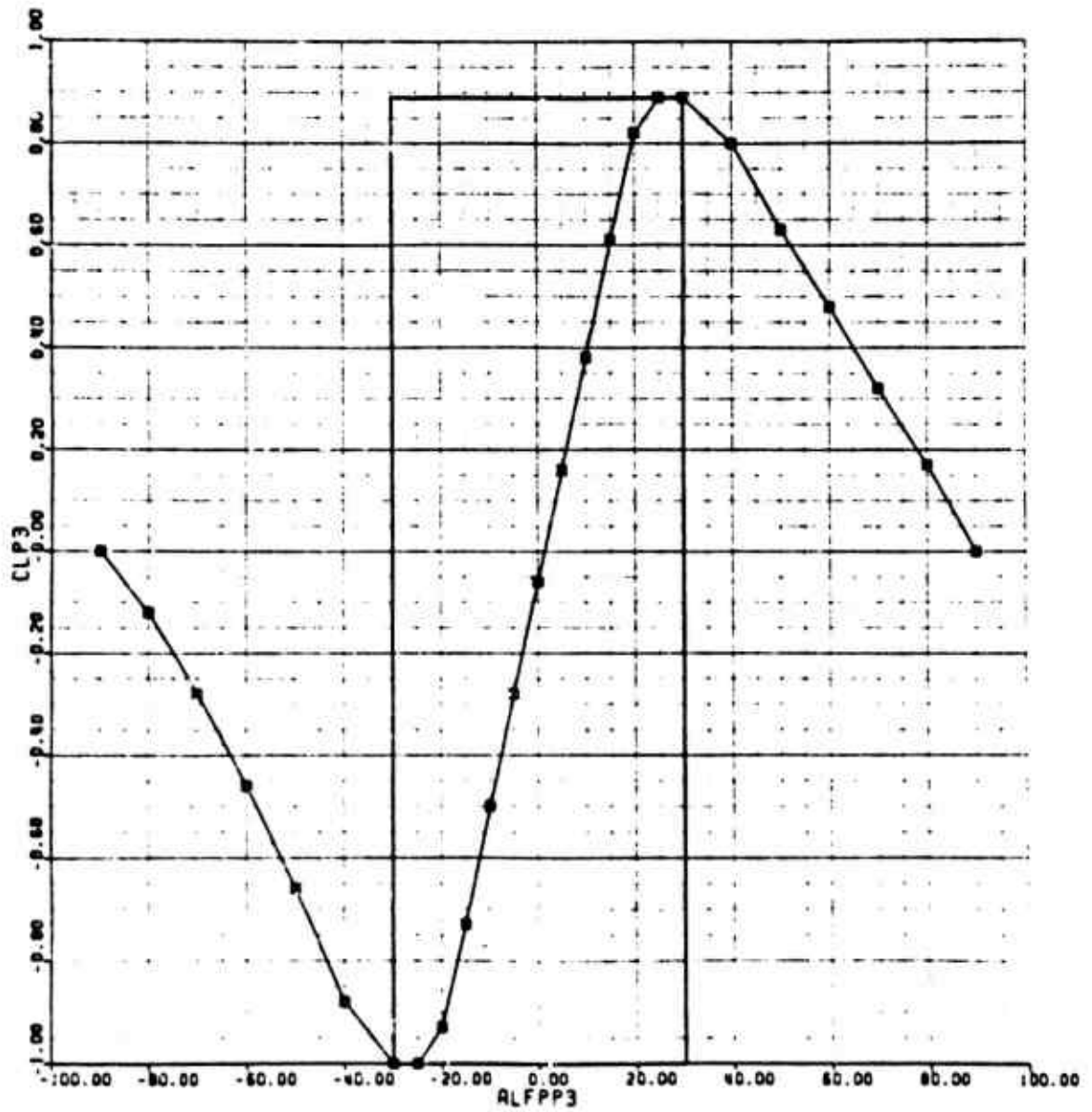


Figure A-21. UH-60A Vertical Stabilizer Lift Map

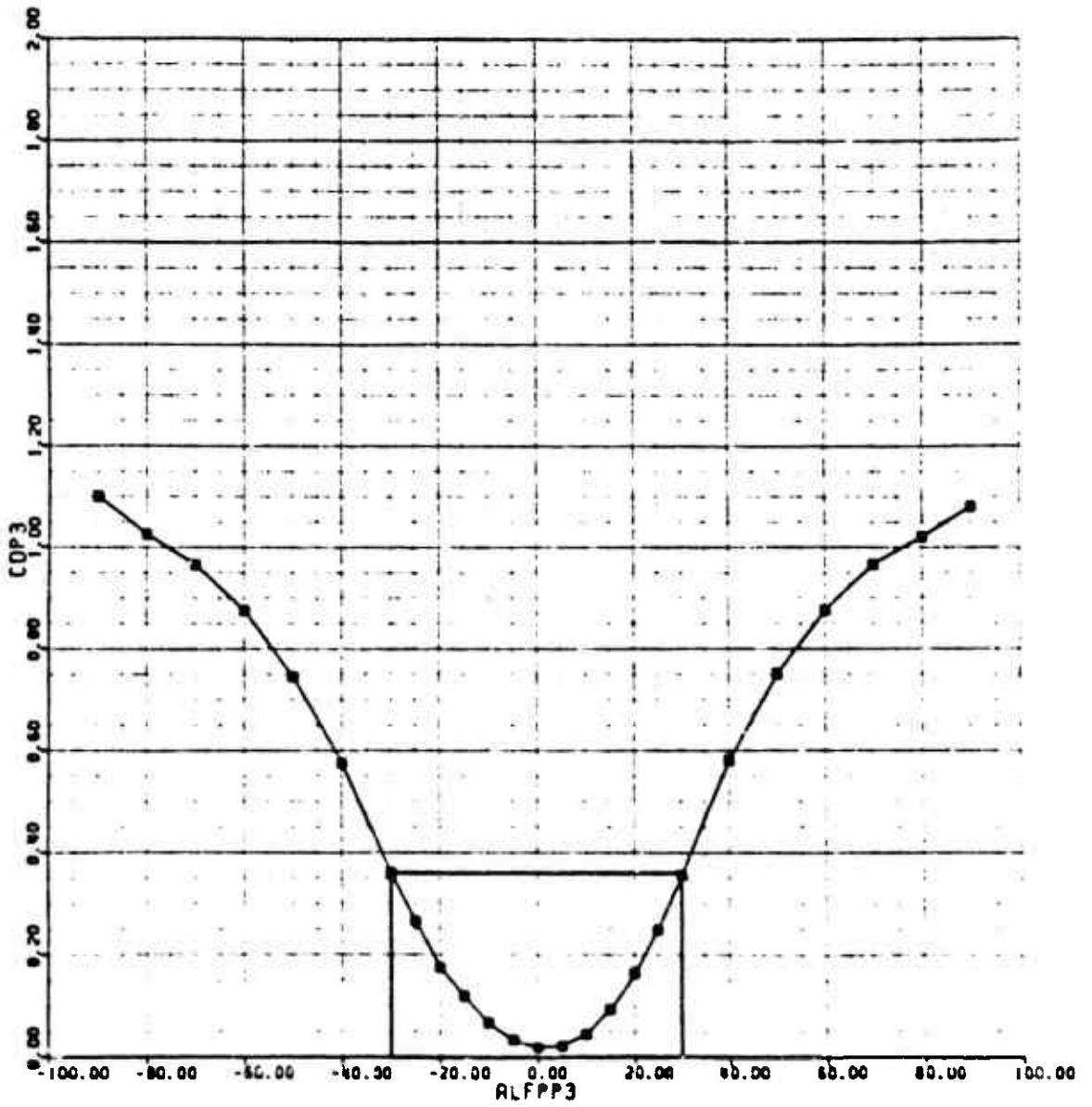


Figure A-22. UH-60A Vertical Stabilizer Drag Map

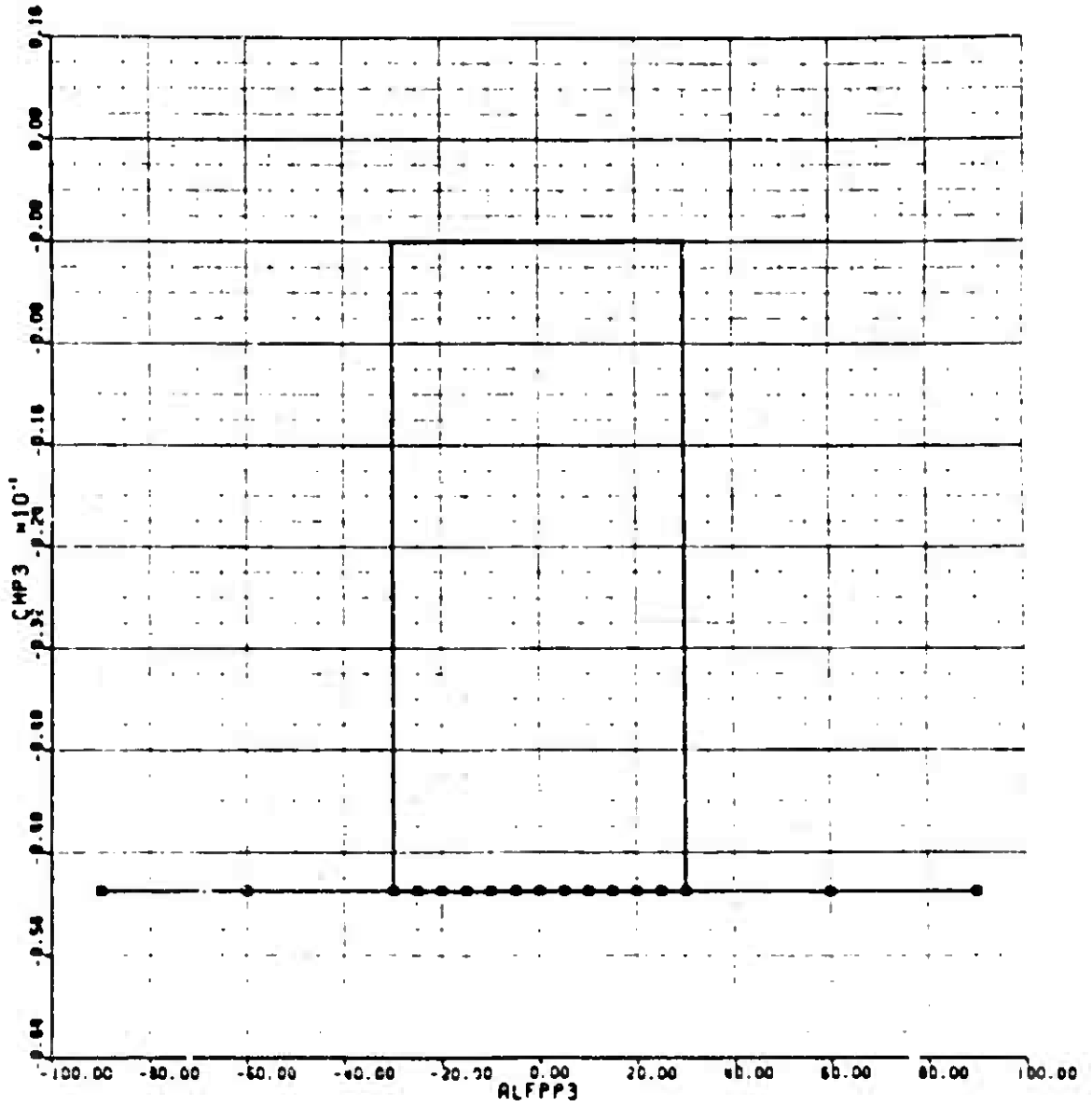


Figure A-23. UH-60A Vertical Stabilizer Moment Map

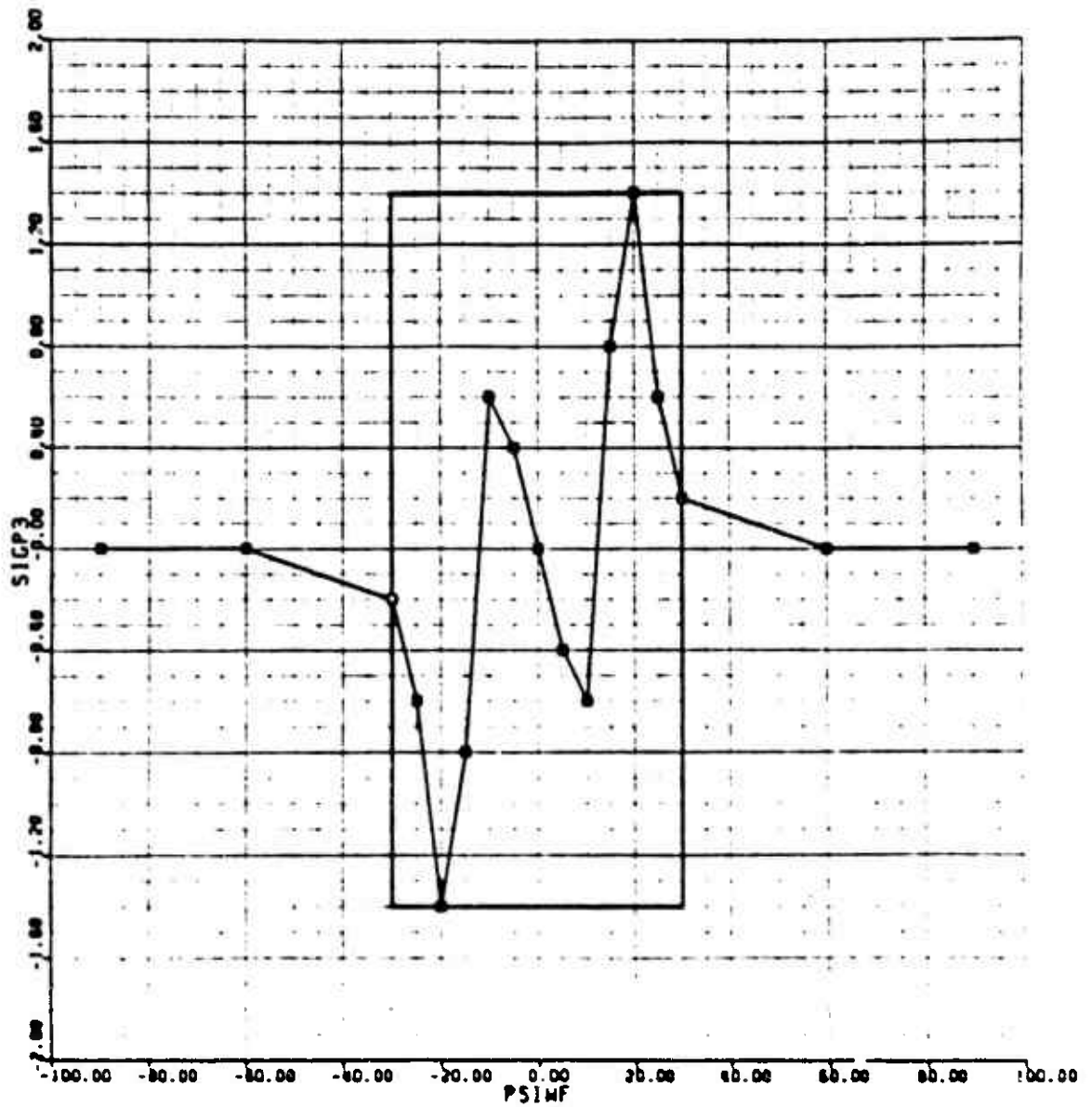


Figure A-24. UH-60A Fuselage Sidewash on Vertical Stabilizer Map

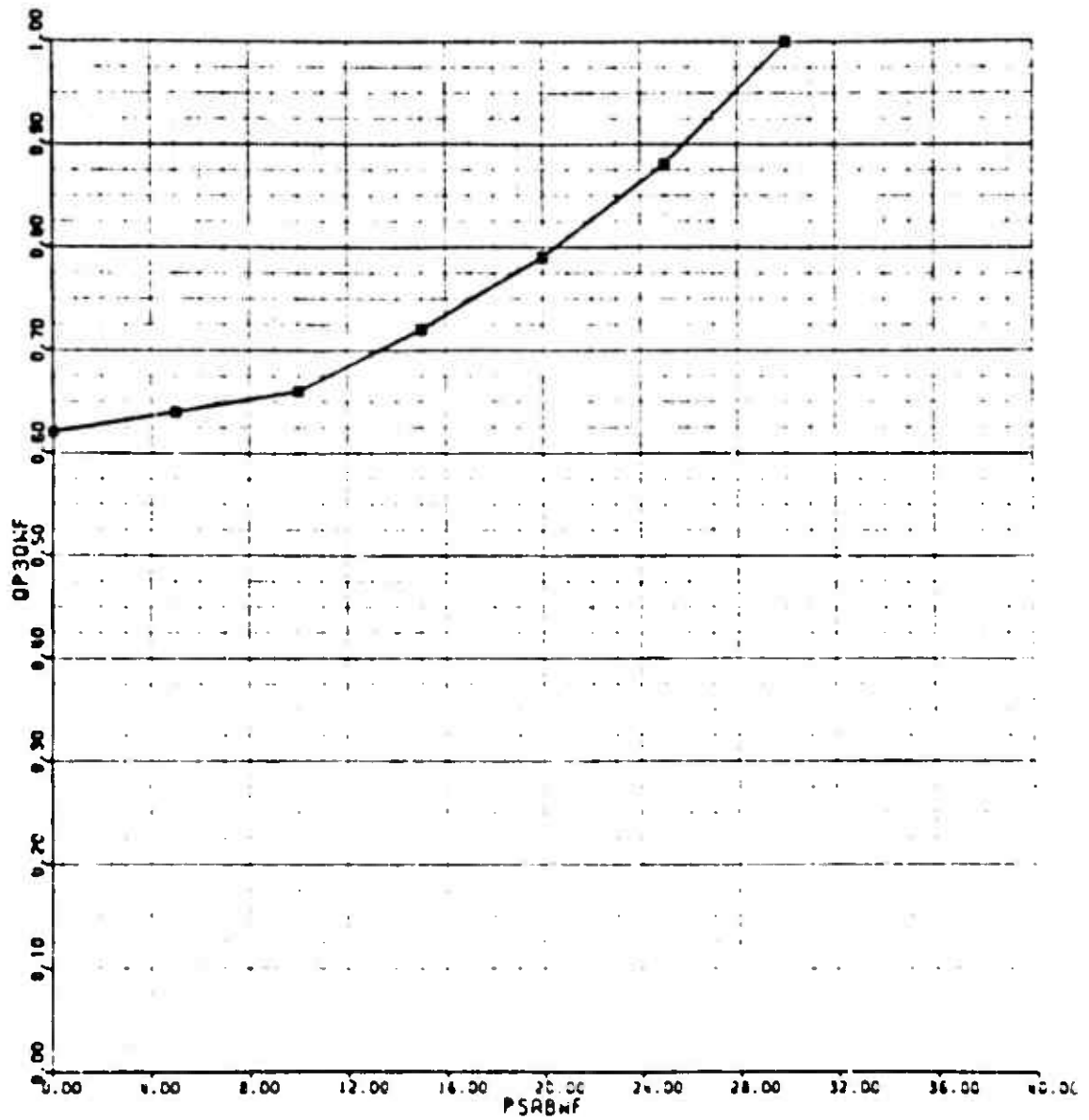


Figure A-25. UH-60A Dynamic Pressure Ratio at Vertical Stabilizer Map

APPENDIX B

S-76A MODEL DATA

The S-76A (Figure B-1) is a middle-weight commercial transport helicopter. The airframe makes extensive use of composite and is extremely clean aerodynamically. The basic design gross weight is 10,000 pounds and a 44-foot-diameter main rotor is employed. Two Allison T250-C30 turboshaft engines with a rating of 650 shp each power the S-76A. Approximately 300 S-76s have been sold. Most of these have been for commercial use, but military variants are also available.

The S-76 main rotor is a four-bladed unit utilizing SC1095 airfoils. The rotor is of conventional articulated design with coincident flap and lag hinges. Hinge offset is 3.79 percent. The 8-foot-diameter tail rotor has four blades and is of a bearingless design similar to that of the BLACK HAWK. Unlike the BLACK HAWK, the tail rotor is not canted and a fixed horizontal stabilizer of 18.5 square feet is mounted at the base of the vertical fin. The tail rotor also employs SC1095 airfoils while the horizontal stabilizer uses an inverted 4412 section.

A S-76A GenHel simulation was already operational at Sikorsky and has been extensively validated against flight test data. All of the numerical data used to model the S-76A are provided in this appendix. The first section is a listing of all the input data (Table B-1). The second section includes plots of the map data for fuselage, vertical tail and horizontal tail aerodynamics along with plots of the rotor interference and fuselage interference data (Figures B-2 through B-25). The tabular data are provided with appropriate labels. Map data are identified with GenHel variable names provided in the List of Symbols.

For the S-76A model, the panel allocation was as follows:

1. Right horizontal tail
2. Left horizontal tail
3. Vertical tail

TABLE B-1. S-76A SPECIFIC FILE

```

***** INPUT PARAMETERS FOR MAIN ROTOR MODULES (0A.) *****

FSMR:: 200.0 ; FUSELAGE STATION, INCHES
MLMR:: 157.0 ; WATERLINE STATION, INCHES
BLMR:: 0.0 ; BUTTLINE STATION, INCHES (+IVE TO FORT)
RMR:: 22.0 ; RADIUS, FT.
ONGTMR:: 30.6818 ; TRIM ROTATIONAL SPEED, RAD/SEC
BMR:: 4.0 ; ACTUAL NUMBER OF BLADES
ISMRR:: -5.0 ; LONGITUDINAL SHAFT TILT, (POS. BACKWARDS), DEG
ILMRR:: 0.0 ; LATERAL SHAFT TILT, (POS. STARBOARD), DEG
DELSMR:: -25.0 ; SWASHPLATE PHASE ANGLE, DEG
DEL3MR:: 16.7 ; FLAPPING HINGE OFFSET ANGLE, DEG.
KAF1MR:: -0.05 ; LAGGING HINGE OFFSET COEF. (FUNC(LG))
KAF2MR:: -0.005 ; LAGGING HINGE OFFSET COEF. (FUNC(LG**2))
CMDTMR:: 1.2917 ; BLADE CHORD AT TIP, FT.
CHDRMR:: 1.2917 ; BLADE CHORD AT ROOT, FT.
OPSTRR:: .833 ; HINGE OFFSET, FT.
SPRLRR:: 3.53 ; HINGE TO START OF BLADE, FT.
MTBDMR:: 125.15 ; WEIGHT OF ONE BLADE, LBS.
IBMR:: 459.0 ; BLADE MOMENT OF INERTIA ABOUT HINGE, SLUG-FT**2
MBMR:: 32.5 ; BLADE MASS MOMENT ABOUT HINGE, SLUG-FT**2
IRMR:: 164.0 ; ROTOR POLAR MOMENT OF INERTIA (LESS BLADES), SLUG-FT**2
BTLMR:: .97 ; BLADE TIP CUT OFF RATIO
DCDMR:: .002 ; DELTA DRAG COEF. FOR EACH SEGMENT
NBSMR:: 4 ; NUMBER OF BLADES SIMULATED, FIX POINT
NSSMR:: 5 ; NUMBER OF SEGMENTS SIMULATED, FIX POINT

; ** MAIN ROTOR NON LINEAR TWIST MAP **
TWRMRP:: UVR00 ; MAP LOOK UP NAME
          XSEGMR00 ; INPUT VARIABLE NAME
          TWSTMR00 ; OUTPUT VARIABLE NAME
          TWRLO ; MAP NAME
          EXP 0.0, 1.0, .05 ; LOWER LIMIT, UPPER LIMIT, DELTA

TWRLO: EXP 0.0, 0.0, 0.0, 0.0, 1.0
        EXP 2.5, 2.6, 2.1, 1.6, 1.1
        EXP -6, -1, -4, -9, -1.4
        EXP -2.0, -2.4, -3.0, -3.5, -4.0
        EXP -4.5

***** MAIN ROTOR DOWNWASH SUBMODULE (0A) *****

RCTMR:: 1.0 ; THRUST GAIN FOR UNIFORM DOWNWASH
KCMR:: 0.0 ; PITCH MOD. GAIN FOR DOWNWASH SIN. HARMONIC
RSLMR:: 0.0 ; ROLL MOD. GAIN FOR DOWNWASH COS. HARMONIC
TDWOMR:: .01038 ; TIME CONST. FOR UNIFORM DOWNWASH FILTER, SEC.
TDWCMR:: 0.0 ; TIME CONST. FOR DOWNWASH SIN. HARMON. FILTER, SEC.
TDWSMR:: 0.0 ; TIME CONST. FOR DOWNWASH COS. HARMON. FILTER, SEC.

***** FLAPPING/LAGGING DAMPER (0C) *****

RBRMR:: 0.0 ; FLAPPING HINGE SPRING CONST, FT-LBS/RAD
RBR.MR:: 0.0 ; FLAPPING HINGE DAMPER CONST, FT-LBS-SEC/RAD

; **SET OF MOUNTING DIMENSIONS FOR LAG DAMPER, INCHES**
ALDMR:: 0.0 ;
BLDMR:: 0.0 ;
CLDMR:: 15.6 ;
DLDMR:: 6.64 ;
RLDMR:: 5.0 ;
LGDMR:: -7.5 ; ALIGNMENT OFFSET IN RELATION TO LAG, DEG
TLDMR:: 2.0 ; FIXED BLADE PITCH RELATIONSHIP BET. ARM AND THRUFF

```

TABLE B-1. S-76A SPECIFIC FILE (Cont'd)

```

; **LAG DAMPER FORCE VS DAMPER ARM RATE **
LOMRP: UVRYS88 ; MAP LOOK UP NAME
        LO.MR00(16) ; INPUT VARIABLE NAME
        PLD.MR00(A16) ; OUTPUT VARIABLE NAME
        L.MRLO ; MAP NAME
        EXP 0.0,2.0,.05 ; LOWER LIMIT,UPPER LIMIT,DELTA

L.MRLO: EXP 0.0, 15.0, 35.0, 60.0, 100.0
        EXP 145.0, 215.0, 315.0, 435.0, 580.0
        EXP 735.0, 905.0, 1055.0, 1180.0, 1290.0
        EXP 1345.0, 1385.0, 1410.0, 1425.0, 1440.0
        EXP 1450.0, 1455.0, 1460.0, 1462.2, 1464.4
        EXP 1466.6, 1468.8, 1471.0, 1473.2, 1475.4
        EXP 1477.6, 1479.8, 1482.0, 1484.2, 1486.4
        EXP 1488.6, 1490.8, 1493.8, 1495.2, 1497.4
        1499.6

;***** INPUT PARAMETERS FOR FUSELAGE/WING (8A) *****
;***** MOUNTING POINT FOR MODEL IN WIND TUNNEL
FSWF: 200.0 ; FUSELAGE STATION,IN.
WLWF: 90.0 ; WATERLINE STATION,IN.
BLWF: 0.0 ; BUTTLINE STATION,IN. (+IVE TO PORT)
INWF: 0.0 ; WING INCIDENCE,DEG.

; ** FUSELAGE LIFT (TAIL-OFF) VS ALPWF MAP **
LOFNP: UVRUVR00 ;MAP ARGUMENT:LOOK UP ROUTINE
        ALPWF00 ;INPUT VARIABLE
        LOF00 ;OUTPUT VARIABLE
        LOFLO ;PRIMARY (BASIC) MAP NAME
        EXP -20.0,20.0,2.0 ;LOWER LIMIT,UPPER LIMIT,DELTA - PRIMARY MAP
        LOFHI ;SECONDARY (HIGH ANGLE) MAP NAME
        EXP -100.0,100.0,20.0 ;LOWER LIMIT,UPPER LIMIT,DELTA - HIGH ANGLE MAP

; LOW ANGLE MAP:ALPWF -20 TO 20, DELTA = 2
LOFLO: EXP -12.5, -11.7, -10.1, -8.1, -6.3
        EXP -4.7, -3.2, -2.0, -0.8, -0.1
        EXP 0.4, 0.7, 1.1, 1.4, 1.7
        EXP 1.9, 2.3, 2.8, 3.8, 5.2
        6.8

; HIGH ANGLE MAP:ALPWF -100 TO 100, DELTA = 20
LOFHI: EXP 1.0, -1.0, -4.9, -10.1, -12.5
        EXP 0.4, 8.8, 7.0, 3.5, 1.0
        -1.0

; ** FUSELAGE DRAG (TAIL-OFF) VS ALPWF MAP **
DOFNP: UVRUVR00 ;MAP ARGUMENT:LOOK UP ROUTINE
        ALPWF00 ;INPUT VARIABLE
        DOF00 ;OUTPUT VARIABLE
        DOFLO ;PRIMARY (BASIC) MAP NAME
        EXP -20.0,20.0,2.0 ;LOWER LIMIT,UPPER LIMIT,DELTA - PRIMARY MAP
        DOFHI ;SECONDARY (HIGH ANGLE) MAP NAME
        EXP -100.0,100.0,20.0 ;LOWER LIMIT,UPPER LIMIT,DELTA - HIGH ANGLE MAP

; LOW ANGLE MAP:ALPWF -20 TO 20, DELTA = 2
DOFLO: EXP 12.5, 11.2, 10.2, 9.4, 9.0
        EXP 8.6, 8.5, 8.4, 8.3, 8.1
        EXP 8.4, 8.5, 8.65, 8.8, 8.0
        EXP 9.1, 9.6, 9.9, 10.2, 10.5
        10.9

; HIGH ANGLE MAP. ALPHA FROM -100 DEG TO 100 DEG, DEL=20
DOFHI: EXP 186.0, 174.0, 116.0, 45.0, 12.5
        EXP 8.4, 10.9, 43.0, 115.0, 171.0
        187.0

```

TABLE B-1. S-76A SPECIFIC FILE (Cont'd)

```

; **FUSELAGE PITCH MOM (TAIL-OFF) VS ALPWF MAP**
MQPMP:: UVRUVR00 ;MAP ARGUMENT:LOOK UP ROUTINE
        ALPWF00 ;INPUT VARIABLE
        MQP00 ;OUTPUT VARIABLE
        MQPFO ;PRIMARY (BASIC) MAP NAME
EXP -20.0,20.0,2.0 ;LOWER LIMIT,UPPER LIMIT,DELTA - PRIMARY MAP
        MQPFI ;SECONDARY (HIGH ANGLE) MAP NAME
EXP -100.0,100.0,20.0 ;LOWER LIMIT,UPPER LIMIT,DELTA - HIGH ANGLE MAP

; PRIMARY MAP, ALPHA FROM -20 DEG TO 20 DEG, OELTA = 2
MQPFO: EXP -365.0, -357.0, -345.0, -330.0, -310.0
        EXP -287.0, -260.0, -232.5, -195.0, -157.5
        EXP -120.0, -82.5, -45.0, -7.5, 30.0
        EXP 67.5, 105.0, 140.0, 173.0, 200.0
        225.0

; HIGH ANGLE MAP, ALPHA FROM -100 DEG TO 100 DEG, DEL=20
MQPFI: EXP 18.0, -18.0, -142.0, -296.0, -365.0
        EXP -120.0, 225.0, 183.0, 87.0, 11.0
        -11.0

; **FUSELAGE DELTA LIFT (TAIL-OFF) VS PSINF MAP**
DLQFMP:: BIV00 ;MAP ARGUMENT:LOOK UP ROUTINE
        EXP PSINF00,ALPWF00 ;INPUT VARIABLE #1,INPUT VARIABLE #2
        DLQF00 ;OUTPUT VARIABLE
        DLQFLO ;PRIMARY (BASIC) MAP NAME
EXP -20.0,20.0,2.0,25 ;LDW LIM,UP LIM,DELTA,#ENTRIES(OCTAL) PSINF
EXP -10.0,10.0,10.0 ;LOW LIM,UP LIM,DELTA ALPWF

; PRIMARY MAP PSINF -20 TO 20 DEG FOR ALPWF -10.0,10 DEG
; ALPWF = -10 DEG
DLQFLO: EXP -14.04, -12.87, -11.18, -9.84, -6.76
        EXP -4.81, -3.12, -1.82, -0.78, -0.13
        EXP 0.0, -0.13, -0.78, -1.82, -3.12
        EXP -4.81, -6.76, -8.84, -11.18, -12.87
        -14.04

; ALPWF = 0 DEG
        EXP -5.4, -4.95, -4.3, -3.4, -2.6
        EXP -1.85, -1.2, -0.7, -0.3, -0.05
        EXP 0.0, -0.05, -0.3, -0.7, -1.2
        EXP -1.85, -2.6, -3.4, -4.3, -4.95
        -5.4

; ALPWF = 10 DEG
        EXP -7.02, -6.35, -5.59, -4.42, -3.38
        EXP -2.405, -1.56, -0.91, -0.39, -0.065
        EXP 0.0, -0.065, -0.39, -0.91, -1.56
        EXP -2.405, -3.38, -4.42, -5.59, -6.435
        -7.02

; ** FUSELAGE DELTA DRAG VS PSINF MAP **
DDQFMP:: UVRUVR00 ;MAP ARGUMENT:LOOK UP ROUTINE
        PSINF00 ;INPUT VARIABLE
        DDQF00 ;OUTPUT VARIABLE
        DDQFLO ;PRIMARY (BASIC) MAP NAME
EXP -20.0,20.0,2.0 ;LOWER LIMIT, UPPER LIMIT, DELTA - PRIMARY MAP
        DDQFHI ;SECONDARY (HIGH ANGLE) MAP NAME
EXP -100.0,100.0,20.0 ;LOW. LIMIT, UP. LIMIT, DELTA - HIGH ANGLE MAP

; PRIMARY MAP - PSINF FROM -20 TO 20 DEGREES, DELTA = 2
DDQFLO: EXP 18.8, 14.8, 11.5, 8.8, 6.5
        EXP 4.5, 3.0, 1.9, 1.0, 0.5
        EXP 0.0, 0.5, 1.0, 1.9, 3.0
        EXP 4.5, 6.5, 8.8, 11.5, 14.8 18.8

; HIGH ANGLE MAP: PSI -100 TO 100 DEGREES, DELTA = 20
DDQFHI: EXP 169.0, 163.0, 123.0, 62.0, 18.8
        EXP 0.0, 18.8, 62.0, 123.0, 163.0
        169.0

```

TABLE B-1. S-76A SPECIFIC FILE (Cont'd)

```

; ** FUS. DELTA PITCH MOMENT VS PSIMF MAP **
DMQFMP: BIVBIV00 ;MAP ARGUMENT:LOOK UP ROUTINE
EXP PSIMF00,ALFWF00 ;INPUT VARIABLE #1, INPUT VARIABLE #2
DMQF00 ;OUTPUT VARIABLE
OMQFLO ;PRIMARY (BASIC) MAP NAME
EXP -20.0,20.0,2.0,25 ;LOW. LIM., UP. LIM., DELTA, # ITEMS(OCTAL),PSI
EXP -10.0,10.0,10.0 ;LOW. LIM., UP. LIM., DELTA, ALFWF
DMQFHI ;SECONDARY (HIGH ANGLE) MAP NAME
EXP -100.0,100.0,20.0,13 ;LOW. LIM., UP. LIM., DELTA, # ITEMS(OCTAL),PSI
EXP -10.0,10.0,10.0 ;LOW. LIM., UP. LIM., DELTA, ALFWF

;PRIMARY MAP - PSIMF -20 TO 20 DEG FOR ALFWF -10,0,10
;ALFWF = -10 DEG
OMQFLO: EXP 180.4, 165.0, 145.2, 115.5, 88.0
EXP 61.59, 39.6, 24.2, 12.1, 4.4
EXP 0.0, 4.4, 12.1, 24.2, 39.6
EXP 61.59, 88.0, 115.5, 145.2, 165.0
180.4

;ALFWF = 0 DEG
EXP 82.0, 75.0, 66.0, 52.5, 40.0
EXP 28.0, 18.0, 11.0, 5.5, 2.0
EXP 0.0, 2.0, 5.5, 11.0, 18.0
EXP 28.0, 40.0, 52.5, 66.0, 75.0
82.0

;ALFWF = +10 DEG
EXP 57.4, 52.5, 46.2, 36.75, 28.0
EXP 19.6, 12.6, 7.7, 3.84, 1.4
EXP 0.0, 1.4, 3.84, 7.7, 12.6
EXP 19.6, 28.0, 36.75, 46.2, 52.5
57.4

;HIGH ANGLE MAP PSIMF -100 TO 100 DEG FOR ALF -10,0,10
;ALFWF = -10 DEG
OMQFHI: EXP -9.0, 9.0, 70.0, 146.0, 180.4
EXP 0.0, 180.4, 146.0, 70.0, 9.0
-9.0

;ALFWF = 0 DEG
EXP -4.0, 4.0, 32.0, 67.0, 82.0
EXP 0.0, 82.0, 67.0, 32.0, 4.0
-4.0

;ALFWF = 10 DEG
EXP -3.0, 3.0, 22.0, 47.0, 57.4
EXP 0.0, 57.4, 47.0, 22.0, 3.0
-3.0

; ** FUSELAGE SIDEFORCE VS PSIMF MAP **
;MAP ARGUMENT:LOOK UP ROUTINE
YQFAP: BIVBIV40
EXP PSIMF00,ALFWF44 ;INPUT VARIABLE #1, INPUT VARIABLE #2
YQF44 ;OUTPUT VARIABLE
YQFLO ;PRIMARY (BASIC) MAP NAME
EXP -20.0,20.0,2.0,25 ;LOW. LIM., UP. LIM., DELTA, # ITEMS(OCTAL) PSI
EXP -10.0,10.0,10.0 ;LOW. LIM., UP. LIM., DELTA, ALFWF
YQFHI ;SECONDARY (HIGH ANGLE) MAP NAME
EXP -100.0,100.0,20.0,13 ;LOW. LIM., UP. LIM., DELTA, # ITEMS(OCTAL) PSI
EXP -10.0,10.0,10.0 ;LOW. LIM., UP. LIM., DELTA, ALFWF

;LOW ANGLE MAP;PSI -20 TO 20 DEG, ALF -10, 0, 10 DEG
;ALFWF = -10.0 DEG
YQFLO: EXP -44.0, -37.0, -31.0, -25.0, -20.0
EXP -15.0, -10.5, -7.0, -4.0, -2.0
EXP 0.0, 2.0, 4.0, 7.0, 10.5
EXP 15.0, 20.0, 25.0, 31.0, 37.0
44.0

```

TABLE B-1. S-76A SPECIFIC FILE (Cont'd)

```

;ALFWF = 0 OEG
EXP -44.0, -37.5, -32.5, -27.5, -22.5
EXP -18.5, -14.5, -10.5, -7.0, -3.5
EXP 0.0, 3.5, 7.0, 10.5, 14.5
EXP 18.5, 22.5, 27.5, 32.5, 37.5
EXP 44.0

;ALFWF = 10.0 DEG
EXP -57.0, -51.0, -43.0, -39.0, -33.0
EXP -27.5, -21.5, -16.0, -10.5, -5.5
EXP 0.0, 5.5, 10.5, 16.0, 21.5
EXP 27.5, 33.0, 39.0, 43.0, 51.0
EXP 57.0

; HIGH ANGLE MAP PSI -100 TO 100 DEG, ALF -10.0,10 OEG
;ALFWF = -10 OEG
YQPHI: EXP -5.0, -70.0, -130.0, -100.0, -44.0
EXP 0.0, 44.0, 100.0, 130.0, 70.0
EXP 5.0

;ALFWF = 0 OEG
EXP -5.0, -70.0, -130.0, -100.0, -44.0
EXP 0.0, 44.0, 100.0, 130.0, 70.0
EXP 5.0

;ALFWF = 10 OEG
EXP -5.0, -70.0, -130.0, -100.0, -57.0
EXP 0.0, 57.0, 100.0, 130.0, 70.0
EXP 5.0

; ** FUSELAGE ROLLING MOMENT VS PSIWF MAP **
RQFMP: BIVBIV00 ;MAP ARGUMENT:LOOK UP ROUTINE
EXP PSIWF00,ALFWF00 ;INPUT VARIABLE #1, INPUT VARIABLE #2
RQF00 ;OUTPUT VARIABLE
RQFLO ;PRIMARY (BASIC) MAP NAME
EXP -20.0,20.0,2.0,25 ;LOW LIMIT, UP LIMIT, DELTA, # ITEMS(OCTAL) PSI
EXP -10.0,10.0,10.0 ;LOW LIMIT, UP LIMIT, DELTA ALFWF
RQPHI ;SECONDARY (HIGH ANGLE) MAP NAME
EXP -100.0,100.0,20.0,13 ;LOW LIMIT, UP LIMIT, DELTA, # ITEMS(OCTAL) PSI
EXP -10.0,10.0,10.0 ;LOW LIMIT, UP LIMIT, DELTA ALFWF

;LOW ANGLE MAP:PSIWF FROM -20 TO 20 OEG FOR ALFWF-10.0,10
;ALFWF = -10.0 OEG
RQFLO: EXP -36.5, -30.0, -24.0, -19.5, -14.5
EXP -10.0, -6.5, -4.0, 2.0, -0.5
EXP 0.0, 0.5, 2.0, 4.0, 6.5
EXP 10.0, 14.5, 19.5, 24.0, 30.0
EXP 36.5

;ALFWF = 0.0 DEG
EXP -19.0, -18.0, -16.5, -14.6, -13.0
EXP -11.3, -9.0, -7.0, -5.0, -2.5
EXP 0.0, 2.5, 5.0, 7.0, 9.0
EXP 11.3, 13.0, 14.6, 16.5, 18.0
EXP 19.0

;ALFWF = 10.0 OEG
EXP 22.5, 19.0, 15.8, 12.7, 10.0
EXP 7.5, 5.2, 3.6, 2.0, 1.0
EXP 0.0, -1.0, -2.0, -3.6, -5.2
EXP -7.5, -10.0, -12.7, -15.8, -19.0
EXP -22.5

;HIGH ANGLE MAP:PSIWF FROM -100 TO 100 DEG,ALFWF -10.0,10
;ALFWF =-10 DEG
RQPHI: EXP 400.0, 400.0, 300.0, -120.0, -36.5
EXP 0.0, 36.5, 120.0, -300.0, -400.0
EXP -400.0

```

TABLE B-1. S-76A SPECIFIC FILE (Cont'd)

```

;ALFWP = 0 DEG
EXP 400.0, 400.0, 300.0, 0.0, -19.0
EXP 0.0, 19.0, 0.0, -300.0, -400.0
-400.0

;ALFWP = 10 DEG
EXP 400.0, 400.0, 300.0, 60.0, 22.5
EXP 0.0, -22.5, -60.0, -300.0, -400.0
-400.0

NQFNP: BIVBIV00 ;** FUSELAGE YAWING MOMENT VS PSWIF MAP **
EXP PSWIF00,ALFWP00 ;MAP ARGUMENT:LOOK UP ROUTINE
NQF00 ;INPUT VARIABLE #1, INPUT VARIABLE #2
NQFLO ;OUTPUT VARIABLE
;PRIMARY (BASIC) MAP NAME
EXP -20.0,20.0,2.0,25 ;LOW LIMIT, UP LIMIT, DELTA, # ITEMS(OCTAL) PSI
EXP -10.0,10.0,10.0 ;LOW LIMIT, UP LIMIT, DELTA ALFWP
NQPHI ;SECONDARY (HIGH ANGLE) MAP NAME
EXP-100.0,100.0,20.0,13 ;LOW LIMIT, UP LIMIT, DELTA, # ITEMS(OCTAL) PSI
EXP -10.0,10.0,10.0 ;LOW LIMIT, UP LIMIT, DELTA ALFWP

;LOW ANGLE MAP:PSWIF -20 TO 20 DEG FOR ALFWP = -10.0,10
;ALFWP = -10 DEG
NQFLO: EXP -80.0, -117.0, -141.0, -155.0, -160.0
EXP -156.0, -144.0, -122.0, -90.0, -48.0
EXP 0.0, 48.0, 90.0, 122.0, 144.0
EXP 156.0, 160.0, 155.0, 141.0, 117.0
80.0

;ALFWP = 0 DEG
EXP -122.0, -145.0, -154.0, -153.0, -149.0
EXP -136.0, -116.0, -90.0, -60.0, -31.0
EXP 0.0, 31.0, 60.0, 90.0, 116.0
EXP 136.0, 149.0, 153.0, 154.0, 145.0
122.0

;ALFWP = 10 DEG
EXP -90.0, -89.0, -84.0, -76.0, -67.0
EXP -57.0, -47.0, -36.0, -24.0, -12.0
EXP 0.0, 12.0, 24.0, 36.0, 47.0
EXP 57.0, 67.0, 76.0, 84.0, 89.0
90.0

;HIGH ANGLE MAP:PSWIF -100 TO 100 DEG FOR ALFWP = -10.0,10
;ALFWP = -10 DEG
NQPHI: EXP 1100.0, 600.0, 400.0, 300.0, -80.0
EXP 0.0, 80.0, -300.0, -400.0, -600.0
-1100.0

;ALFWP = 0 DEG
EXP 1100.0, 600.0, 400.0, 300.0, -122.0
EXP 0.0, 122.0, -300.0, -400.0, -600.0
-1100.0

;ALFWP = 10 DEG
EXP 1100.0, 600.0, 400.0, 0.0, -90.0
EXP 0.0, 90.0, 0.0, -400.0, -600.0
-1100.0

NQFPNP: UVR00 ;** FUSELAGE PITCHING MOMENTS VS H.R. THRUST **
PSWIF00 ;MAP ARGUMENTS: LOOK UP ROUTINE
NQFPNP00 ; INPUT VARIABLE NAME
NQFPLO ; OUTPUT VARIABLE NAME
; NAME OF MAP
EXP -20.0,20.0,2.0 ; LOWER LIMIT,UPPER LIMIT,DELTA

```


TABLE B-1. S-76A SPECIFIC FILE (Cont'd)

```

; ** PSIWT= -20.0 TO 20.0 IN 2 DEG INCREMENTS
MQFPLO: EXP    65.0,    65.0,    65.0,    65.0,    63.0
          EXP    61.0,    56.0,    50.0,    31.0,    15.0
          EXP     0.0,   -15.0,   -25.0,   -35.0,   -44.0
          EXP   -49.0,   -51.0,   -50.0,   -45.0,   -40.0
          EXP   -35.0
    
```

***** ROTOR INTERFERENCE ON THE FUSLEAGE (MRPA) *****

```

; ** ROTOR X-FACTOR ON FUSELAGE MAP **
EXWFMP: UVR44 ;MAP ARGUMENT:LOOK UP ROUTINE
        CHIPMR04 ;INPUT VARIABLE
        ERXWF04 ;OUTPUT VARIABLE
        EXWFLO ;PRIMARY (BASIC) MAP NAME
        EXP -20.0,100.0,10.0 ;LOWER LIMIT, UPPER LIMIT, DELTA

EXWFLO: EXP    -0.15,    -0.04,    0.09,    0.20,    0.33
          EXP     0.46,    0.60,    0.74,    0.89,    1.00
          EXP     0.20,    -0.50,    -0.55
    
```

```

; ** ROTOR Z-FACTOR ON FUSELAGE MAP **
EZWFMP: UVR04 ;MAP ARGUMENT:LOOK UP ROUTINE
        CNIPMR04 ;INPUT VARIABLE
        EKZWF00 ;OUTPUT VARIABLE
        EZWFLO ;PRIMARY (BASIC) MAP NAME
        EXP -20.0,100.0,10.0 ;LOWER LIMIT, UPPER LIMIT, DELTA

EZWFLO: EXP     1.20,    1.21,    1.22,    1.23,    1.24
          EXP     1.25,    1.26,    1.27,    1.28,    1.29
          EXP     1.15,    1.00,    1.05
    
```

***** INPUT PARAMETERS FOR PANEL #1 (RT HORIZONTAL) *****

```

FSP1: 473.0 ; FUSELAGE STATION, INCH
WLP1: 100.0 ; WATERLINE STATION, INCH
BLP1: -25.0 ; BUTTLINE STATION, INCH (+IVE TO PORT)
SAP1: 9.25 ; SURFACE AREA, FT**2
GAMP1: 0.0 ; PANEL ORIENTATION, DEG
IOP1: 2.0 ; PANEL INCIDENCE, DEG
CPI: 1.0 ; PANEL MEAN AERO CHORD, FT
    
```

```

; ** HORIZONTAL STABILIZER (RT PANEL) LIFT VS ALFPP1 MAP **
CLPIMP: UVRUVR00 ;MAP ARGUMENT:LOOK UP ROUTINE
        ALFPP100 ;INPUT VARIABLE
        CLP100 ;OUTPUT VARIABLE
        CLP1LO ;PRIMARY (BASIC) MAP NAME
        EXP -24.0,24.0,2.0 ;LOWER LIMIT, UPPER LIMIT, DELTA - LOW ANGLE MAP
        CLP1MI ;SECONDARY (BIG ANGLE) MAP NAME
        EXP -90.0,90.0,15.0 ;LOWER LIMIT, UPPER LIMIT, DELTA - BI ANGLE MAP
    
```

```

;LOW ANGLE MAP:ALFPP1 -24 TO 24 DEG, DELTA = 2 DEG
CLP1LO: EXP    -0.76,    -0.90,    -1.15,    -1.19,    -1.17
          EXP    -1.13,    -1.07,    -1.00,    -0.86,    -0.71
          EXP    -0.57,    -0.42,    -0.27,    -0.12,    0.03
          EXP     0.17,    0.30,    0.39,    0.45,    0.49
          EXP     0.51,    0.46,    0.50,    0.55,    0.60
    
```

```

;RIGR ANGLE MAP:ALFPP1 -90 TO 90 DEG, DELTA = 15 DEG
CLP1MI: EXP     0.0,    -0.35,    -0.70,    -0.80,    -0.75
          EXP    -0.775,    -0.27,    0.45,    0.70,    0.80
          EXP     0.70,    0.35,    0.0
    
```

```

; ** HORIZONTAL STABILIZER (RT PANEL) DRAG VS ALFPP1 MAP **
CDPIMP: UVRUVR00 ;MAP ARGUMENT:LOOK UP ROUTINE
        ALFPP100 ;INPUT VARIABLE
        CDP100 ;OUTPUT VARIABLE
        CDP1LO ;PRIMARY (BASIC) MAP NAME
        EXP -24.0,24.0,2.0 ;LOWER LIMIT, UPPER LIMIT, DELTA - LOW ANGLE MAP
        CDP1MI ;SECONDARY (BIG ANGLE) MAP NAME
    
```

TABLE B-1. S-76A SPECIFIC FILE (Cont'd)

```

;LOW ANGLE MAP:ALPPP1 -24 TO 24 DEG, DELTA = 2 DEG
CDPILO: EXP    0.36,    0.35,    0.34,    0.32,    0.29
          EXP    0.21,    0.13,    0.08,    0.06,    0.045
          EXP    0.03,    0.02,    0.013,   0.009,   0.009
          EXP    0.012,   0.016,   0.022,   0.03,    0.065
          EXP    0.11,    0.15,    0.18,    0.22,    0.26

;HIGH ANGLE MAP:ALPPP1 -90 TO 90 DEG, DELTA = 15 DEG
CDPHI:  EXP    1.20,    1.12,    0.91,    0.65,    0.41
          EXP    0.285,   0.013,   0.185,   0.31,    0.58
          EXP    0.89,    1.12,    1.20
    
```

***** INPUT PARAMETER FOR ROTOR INTERFERENCE ON THE HORIZ.TAIL #1 (RRPA)

```

; ** ROTOR X-FACTOR ON HORIZONTAL TAIL MAP **
EXP1RP::BIV00 ;MAP ARGUMENT:LOOK UP ROUTINE
EXP CHIPR00,AA1PR00 ;INPUT VARIABLE #1, INPUT VARIABLE #2
EKXP100 ;OUTPUT VARIABLE
EXP1LO ;MAP NAME
EXP -20.0,100.0,10.0,15 ;LOW LIM, UP LIM, DELTA, #ITERS(OCTAL) CHI
EXP -3.0,3.0,3.0 ;LOWER LIRIT, UPPER LIMIT, DELTA - AA1PRR
    
```

```

;CHIPR -20 TO 100 DEG FOR AA1PRR -3,0,3 DEG
;AA1PRR = -3 DEG
EXP1LO: EXP    0.0,    0.0,    -0.42,    0.05,    0.24
          EXP    0.42,    0.62,    0.84,    1.08,    1.34
          EXP    1.80,    0.09,    0.50
    
```

```

;AA1PRR = 0 DEG
EXP    0.0,    0.0,    -0.40,    -0.19,    0.20
EXP    0.40,    0.60,    0.82,    1.07,    1.34
EXP    1.50,    -0.05,    0.50
    
```

```

;AA1PRR = 3 DEG
EXP    0.0,    0.0,    -0.45,    -0.62,    0.02
EXP    0.23,    0.45,    0.67,    0.92,    1.19
EXP    1.51,    0.16,    0.50
    
```

```

; ** ROTOR Z-FACTOR ON HORIZONTAL TAIL MAP **
EXP2RP::BIV00 ;MAP ARGUMENT:LOOK UP ROUTINE
EXP CHIPR00,AA1PR00 ;INPUT VARIABLE #1, INPUT VARIABLE #2
EKXP100 ;OUTPUT VARIABLE
EXP2ILO ;PRIMARY (BASIC) MAP NAME
EXP -20.0,100.0,10.0,15 ;LOW LIM, UP LIM, DELTA, #ITERS(OCTAL) CRI
EXP -3.0,3.0,3.0 ;LOWER LIMIT, UPPER LIRIT, DELTA - AA1PRR
    
```

```

;CHIPR -20 TO 100 DEG FOR AA1PRR -3,0,3 DEG
;AA1PRR = -3 DEG
EXP2ILO: EXP    -0.30,   -0.80,   -0.50,    1.76,    1.80
          EXP    1.83,    1.85,    1.87,    1.88,    1.89
          EXP    1.85,    1.47,    0.90
    
```

```

;AA1PRR = 0 DEG
EXP    -0.30,   -0.40,   -0.50,    1.15,    1.83
EXP    1.86,    1.88,    1.90,    1.92,    1.92
EXP    1.90,    1.60,    1.00
    
```

```

;AA1PRR = 3 DEG
EXP    -0.30,   -0.30,   -0.30,   -1.80,    1.82
EXP    1.91,    1.95,    2.00,    2.03,    2.05
EXP    2.07,    1.78,    1.15
    
```

***** FUSELAGE INTERFERENCE ON THE HORIZ.TAIL #1 (WPPA) *****

```

; ** HORIZONTAL TAIL DYNAMIC PRESSURE RATIO MAP **
QPIMP:: UVR00 ;MAP ARGUMENT:LOOK UP ROUTINE
        ALPWP00 ;INPUT VARIABLE
        QP1QWP00 ;OUTPUT VARIABLE
        QPILO ;PRIMARY (BASIC) MAP NAME
    
```

TABLE B-1. S-76A SPECIFIC FILE (Cont'd)

```

EXP -20.0,20.0,4.0 ;LOWER LIMIT, UPPER LIMIT, DELTA

;ALFWF -20 TO 20 DEG, DELTA = 4 DEG
QPILO: EXP 1.00, .96, .82, .74, .74
      EXP .74, .79, .79, .85, .96
      1.00

; ** BODY DOWNWASH ON HORIZONTAL TAIL MAP **
EPP1MP::UVR00 ;MAP ARGUMENT:LOOK UP ROUTINE
      ALFWF00 ;INPUT VARIABLE
      EPSF100 ;OUTPUT VARIABLE
      EPP1LO ;PRIMARY (BASIC) MAP NAME
EXP -40.0,40.0,5.0 ;LOWER LIMIT, UPPER LIMIT, DELTA

;LOW ANGLE MAP:ALFWF -40 TO 40 DEG, DELTA = 5 DEG
EPP1LO: EXP 0.0, 1.0, 2.0, 3.0, 4.0
      EXP 3.6, 3.1, 2.6, 2.1, 1.55
      EXP 1.0, 0.5, 0.0, 0.0, 0.0
      EXP 0.0, 0.0

; ** BODY SIDEWASH ON HORIZONTAL TAIL MAP **
SGP1MP::BIV00 ;MAP ARGUMENT:LOOK UP ROUTINE
      EXP PSIW00,ALFW00 ;INPUT VARIABLE #1, INPUT VARIABLE #2
      SIGF100 ;OUTPUT VARIABLE
      SGP1LO ;PRIMARY (BASIC) MAP NAME
EXP -24.0,24.0,4.0,15 ;LOW LIMIT, UP LIMIT, DELTA, #ITEMS(OCTAL),PSI
EXP -10.0,10.0,10.0 ;LOW LIMIT, UP LIMIT, DELTA, ALFWF

;LOW ANGLE MAP:PSIW0 -24 TO 24 DEG FOR ALFWF -10.0,10
;ALFWF = -10 DEG
SGP1LO: EXP 0.0, -2.4, -4.8, -3.6, -2.4
      EXP -1.2, 0.0, 1.2, 2.4, 3.6
      EXP 4.8, 2.4, 0.0

;ALFWF = 0 DEG
      EXP 0.0, -1.5, -3.0, -1.7, -0.4
      EXP -0.2, 0.0, 0.2, 0.4, 1.7
      EXP 3.0, 1.5, 0.0

;ALFWF = 10 DEG
      EXP 0.0, 1.6, 3.2, 4.8, 3.2
      EXP 1.6, 0.0, -1.6, -3.2, -4.8
      EXP -3.2, -1.6, 0.0

;***** INPUT PARAMETERS FOR PANEL #2 (LT HORIZONTAL) *****
FSP2:: 473.8 ; FUSELAGE STATION,INCH
WLP2:: 100.8 ; WATERLINE STATION,INCH
BLP2:: 25.0 ; BUTTLINE STATION,INCH (+IVE TO PORT)
SAP2:: 9.25 ; SURFACE AREA FT**2
GAMP2:: 0.0 ; PANEL ORIENTATION,DEG
IOP2:: 2.0 ; TAIL INCIDENCE,DEG
CP2:: 1.0 ; PANEL MEAN AERO CHORD,FT

; ** HORIZONTAL STAB... (LT PANEL) LIFT VS ALFWP2 MAP **
CLP2MP::UVR(UVR00 ;MAP ARGUMENT:LOOK UP ROUTINE
      ALFWP200 ;INPUT VARIABLE
      CLP200 ;OUTPUT VARIABLE
      CLP2LO ;PRIMARY (BASIC) MAP NAME
EXP -24.0,24.0,2.0 ;LOWER LIMIT, UPPER LIMIT,DELTA - LOW ANGLE MAP
      CLP2HI ;SECONDARY (HIGH ANGLE) MAP NAME
EXP -90.0,90.0,15.0 ;LOWER LIMIT, UPPER LIMIT, DELTA - HI ANGLE MAP

;LOW ANGLE MAP:ALFWP2 -24 TO 24 DEG, DELTA = 2 DEG
CLP2LO: EXP -0.76, -0.90, -1.15, -1.19, -1.17
      EXP -1.13, -1.07, -1.00, -0.86, -0.71
      EXP -0.57, -0.42, -0.27, -0.12, 0.03
      EXP 0.17, 0.30, 0.39, 0.45, 0.49
      EXP 0.51, 0.46, 0.50, 0.55, 0.60

```

TABLE B-1. S-76A SPECIFIC FILE (Cont'd)

```

;HIGH ANGLE MAP:ALPPP2 -90 TO 90 DEG, DELTA = 15 DEG
CLP2HI: EXP      0.0,      -0.35,     -0.70,     -0.80,     -0.75
        EXP      -0.775,   -0.27,     0.45,      0.70,      0.60
        EXP      0.70,     0.35,      0.0

; ** HORIZONTAL STABILIZER (LT PANEL) DMAG VS ALPPP2 MAP **
CDP2MP::UVRUVR00 ;MAP ARGUMENT:LOOK UP ROUTINE
        ALPPP200 ;INPUT VARIABLE
        COP200 ;OUTPUT VARIABLE
        CDP2LO ;PRIMARY (BASIC) MAP NAME
        EXP -24.0,24.0,2.0 ;LOWER LIMIT, UPPER LIMIT, DELTA - LOW ANGLE MAP
        CDP2HI ;SECONDARY (HIGH ANGLE) MAP NAME
        EXP -90.0,90.0,15.0 ;LOWER LIMIT, UPPER LIMIT, DELTA - HI ANGLE MAP

;LOW ANGLE MAP:ALPPP2 -24 TO 24 DEG, DELTA = 2 DEG
CDP2LO: EXP      0.36,     0.35,      0.34,      0.32,      0.29
        EXP      0.21,     0.13,      0.08,      0.06,      0.045
        EXP      0.03,     0.02,      0.013,     0.009,     0.009
        EXP      0.012,    0.016,     0.022,     0.03,      0.065
        EXP      0.11,     0.15,      0.18,      0.22,      0.26

;HIGH ANGLE MAP:ALPPP2 -90 TO 90 DEG, DELTA = 15 DEG
CDP2HI: EXP      1.20,     1.12,      0.91,      0.65,      0.41
        EXP      0.285,    0.013,     0.185,     0.31,      0.58
        EXP      0.89,     1.12,      1.20

;***** INPUT PARAMETER FOR ROTOR INTERFERENCE ON THE HORIZ.TAIL 02 (RRPA)

; ** ROTOR X-FACTOR ON HORIZONTAL TAIL MAP **
EXP2MP::BIV00 ;MAP ARGUMENT:LOOK UP ROUTINE
        EXP CHIPRR00,AAIPRR00 ;INPUT VARIABLE #1, INPUT VARIABLE #2
        EKXP200 ;OUTPUT VARIABLE
        EXP2LO ;MAP NAME
        EXP -20.0,100.0,10.0,15 ;LOW LIM, UP LIM, DELTA, #ITEMS(OCTAL) CHI
        EXP -3.0,3.0,3.0 ;LOWER LIMIT, UPPER LIMIT, DELTA - AAIPRR

;CHIPRR -20 TO 100 DEG FOR AAIPRR -3,0,3 DEG
;AAIPRR = -3 DEG
EXP2LO: EXP      0.0,      0.0,      -0.42,     0.05,      0.24
        EXP      0.42,     0.62,     0.84,      1.06,      1.34
        EXP      1.40,     0.09,     0.50

;AAIPRR = 0 DEG
        EXP      0.0,      0.0,      -0.40,     -0.19,     0.20
        EXP      0.40,     0.60,     0.82,      1.07,      1.34
        EXP      1.50,     -0.05,    0.50

;AAIPRR = 3 DEG
        EXP      0.0,      0.0,      -0.45,     -0.62,     0.02
        EXP      0.23,     0.45,     0.67,      0.92,      1.19
        EXP      1.51,     0.16,     0.50

; ** ROTOR Z-FACTOR ON HORIZONTAL TAIL MAP **
EIP2RP::BIV00 ;MAP ARGUMENT:LOOK UP ROUTINE
        EXP CHIPRR00,AAIPRR00 ;INPUT VARIABLE #1, INPUT VARIABLE #2
        EKIP200 ;OUTPUT VARIABLE
        EIP2LO ;PRIMARY (BASIC) MAP NAME
        EXP -20.0,100.0,10.0,15 ;LOW LIM, UP LIM, DELTA, #ITEMS(OCTAL) CHI
        EXP -3.0,3.0,3.0 ;LOWER LIMIT, UPPER LIMIT, DELTA - AAIPRR

;CHIPRR -20 TO 100 DEG FOR AAIPRR -3,0,3 DEG
;AAIPRR = -3 DEG
EIP2LO: EXP      -0.30,    -0.40,     -0.50,     1.76,      1.80
        EXP      1.83,     1.85,     1.87,      1.88,      1.89
        EXP      1.85,     1.47,     0.90

;AAIPRR = 0 DEG
        EXP      -0.30,    -0.40,     -0.50,     1.15,      1.93
        EXP      1.86,     1.88,     1.90,      1.92,      1.92
    
```

TABLE B-1. S-76A SPECIFIC FILE (Cont'd)

```

EXP          1.90,      1.60,      1.00

;AALFRR = 3 DEG
EXP          -0.30,    -0.30,    -0.30,    -1.40,    1.82
EXP          1.91,      1.95,      2.00,      2.03,    2.05
EXP          2.07,      1.74,      1.15

;***** FUSELAGE INTERFERENCE ON THE HORIZ.TAIL #2 (WPPA) *****

QP2RP:: UVR00          ;** HORIZONTAL TAIL DYNAMIC PRESSURE RATIO MAP**
        ALFWF00        ;MAP ARGUMENT:LOOK UP ROUTINE
        QP2QWF00       ;INPUT VARIABLE
        QP2LO          ;OUTPUT VARIABLE
        EXP -20.0,20.0,4.0 ;PRIMARY (BASIC) MAP NAME
                        ;LOWER LIMIT, UPPER LIMIT, DELTA

QP2LO: EXP          ;ALFWF -20 TO 20 DEG, DELTA = 4 DEG
        EXP          1.00,      .96,      .82,      .74,      .74
        EXP          .74,      .79,      .79,      .85,      .96
        EXP          1.00

EPP2MP::UVR00          ;** BODY DOWNWASH ON HORIZONTAL TAIL MAP **
        ALFWF00        ;MAP ARGUMENT:LOOK UP ROUTINE
        EPSP200        ;INPUT VARIABLE
        EPP2LO         ;OUTPUT VARIABLE
        EXP -40.0,40.0,5.0 ;PRIMARY (BASIC) MAP NAME
                        ;LOWER LIMIT, UPPER LIMIT, DELTA

EPP2LO: EXP          ;LOW ANGLE MAP:ALFWF -40 TO 40 DEG, DELTA = 5 DEG
        EXP          0.0,      1.0,      2.0,      3.0,      4.0
        EXP          3.6,      3.1,      2.6,      2.1,      1.55
        EXP          1.0,      0.5,      0.0,      0.0,      0
        EXP          0.0,      0.0

SGP2RP::BIV00          ;** BODY SIDEWASH ON HORIZONTAL TAIL MAP **
        EXP PSINWF00,ALFWF00 ;MAP ARGUMENT:LOOK UP ROUTINE
        SIGP200        ;INPUT VARIABLE #1, INPUT VARIABLE #2
        SGP2LO         ;OUTPUT VARIABLE
        EXP -24.0,24.0,4.0,15 ;PRIMARY (BASIC) MAP NAME
        EXP -10.0,10.0,10.0 ;LOW LIMIT, UP LIMIT, DELTA, #ITEMS(OCTAL),PSI
                        ;LOW LIMIT, UP LIMIT, DELTA, ALFWF

SGP2LO: EXP          ;LOW ANGLE MAP:PSINWF -24 TO 24 DEG FOR ALFWF -10,0,10
        EXP          ;ALFWF = -10 DEG
        EXP          0.0,      -2.4,      -4.8,      -3.6,      -2.4
        EXP          -1.2,      0.0,      1.2,      2.4,      3.6
        EXP          4.8,      2.4,      0.0

        EXP          ;ALFWF = 0 DEG
        EXP          0.0,      -1.5,      -3.0,      -1.7,      -0.4
        EXP          -0.2,      0.0,      0.2,      0.4,      1.7
        EXP          3.0,      1.5,      0.0

        EXP          ;ALFWF = 10 DEG
        EXP          0.0,      1.6,      3.2,      4.8,      3.2
        EXP          1.6,      0.0,      -1.6,      -3.2,      -4.8
        EXP          -3.2,      -1.6,      0.0

;***** INPUT PARAMETERS FOR PANEL #3 (VERTICAL TAIL) *****

INFP3:: MRP3AV00,,RRFA00 ; **INTERFERENCE SUBMODULE DEFINITION**
        MFP3AV00,,MPPA00 ; (VAR.BLK.,SUBMOD) R.R. - PANEL #3
        GP3AVK00,,GPA00 ; (VAR.BLK.,SUBMOD.NAME) GUST(A0) - PANEL #3
        Z                ; TERMINATE INTERFERENCE SUBMODULE LIST

FSP3:: 490.0            ; FUSELAGE STATION, INCH
WLP3:: 141.3           ; WATERLINE STATION, INCH
BLP3:: 0.0             ; BUTTLINE STATION, INCH (+IVE TO PORT)

```

TABLE B-1. S-76A SPECIFIC FILE (Cont'd)

```

SAP3:: 19.7 ; SURFACE AREA, FT**2
GAMP3:: -90.0 ; PANEL ORIENTATION, DEG
IOP3:: Z ; PANEL INCIDENCE, DEG
CP3:: 1.0 ; PANEL MEAN AERO CHORD, FT

; ** VERTICAL STABILIZER LIFT VS ALPPP3 MAP **
CLP3MP::UVRUVR00 ; MAP ARGUMENT: LOOK UP ROUTINE
ALPPP300 ; INPUT VARIABLE
CLP300 ; OUTPUT VARIABLE
CLP3LO ; PRIMARY (BASIC) MAP NAME
EXP -24.0, 24.0, 2.0 ; LOWER LIMIT, UPPER LIMIT, DELTA - LOW ANGLE MAP
CLP3HI ; SECONDARY (HIGH ANGLE) MAP NAME
EXP -90.0, 90.0, 15.0 ; LOWER LIMIT, UPPER LIMIT, DELTA - HI ANGLE MAP

; LOW ANGLE MAP: ALPPP3 -24 TO 24 DEG, DELTA = 2 DEG
CLP3LO: EXP -0.76, -0.95, -0.89, -0.82, -0.75
EXP -0.68, -0.60, -0.52, -0.44, -0.36
EXP -0.28, -0.20, -0.12, -0.04, 0.04
EXP 0.12, 0.195, 0.27, 0.35, 0.43
EXP 0.51, 0.59, 0.66, 0.73, 0.66

; HIGH ANGLE MAP: ALPPP3 -90 TO 90 DEG, DELTA = 15 DEG
CLP3HI: EXP 0.0, -0.35, -0.70, -0.77, -0.70
EXP -0.85, -0.12, 0.60, 0.70, 0.77
EXP 0.70, 0.35, 0.0

; ** VERTICAL STABILIZER DRAG VS ALPPP3 MAP **
CDP3MP::UVRUVR00 ; MAP ARGUMENT: LOOK UP ROUTINE
ALPPP300 ; INPUT VARIABLE
CDP300 ; OUTPUT VARIABLE
CDP3LO ; PRIMARY (BASIC) MAP NAME
EXP -24.0, 24.0, 2.0 ; LOWER LIMIT, UPPER LIMIT, DELTA - LOW ANGLE MAP
CDP3HI ; SECONDARY (HIGH ANGLE) MAP NAME
EXP -90.0, 90.0, 15.0 ; LOWER LIMIT, UPPER LIMIT, DELTA - HI ANGLE MAP

; LOW ANGLE MAP: ALPPP3 -24 TO 24 DEG, DELTA = 2 DEG
CDP3LO: EXP 0.260, 0.215, 0.175, 0.145, 0.119
EXP 0.097, 0.077, 0.061, 0.048, 0.034
EXP 0.023, 0.016, 0.011, 0.009, 0.009
EXP 0.012, 0.017, 0.024, 0.034, 0.047
EXP 0.063, 0.080, 0.110, 0.150, 0.210

; HIGH ANGLE MAP: ALPPP3 -90 TO 90 DEG, DELTA = 15 DEG
CDP3HI: EXP 1.20, 1.12, 0.89, 0.58, 0.31
EXP 0.185, 0.011, 0.135, 0.26, 0.54
EXP 0.86, 1.12, 1.20

; ***** ROTOR INTERFERENCE ON THE VERTICAL TAIL 01 (NRPA) *****

; ** ROTOR X-FACTOR ON VERTICAL TAIL MAP **
EXP3MP::RIV00 ; MAP ARGUMENT: LOOK UP ROUTINE
EXP CRIPMR00, AAIFMR00 ; INPUT VARIABLE 01, INPUT VARIABLE 02
EKXP300 ; OUTPUT VARIABLE
EXP3 ; PRIMARY (BASIC) MAP NAME
EXP -20.0, 100.0, 10.0, 15 ; LOW LIM, UP LIM, DELTA, #ITEMS (OCTAL) CMI
EXP -3.0, 3.0, 3.0 ; LOWER LIMIT, UPPER LIMIT, DELTA - AAIFMR

; CRIPMR -20 TO 100 DEG FOR AAIFMR -3, 0, 3 DEG
; AAIFMR = -3 DEG
EXP3: EXP -0.20, -0.10, -0.25, -0.50, -0.40
EXP -0.10, 3.59, 0.83, 1.09, 1.37
EXP 1.69, 0.03, 0.0

; AAIFMR = 0 DEG
EXP -0.20, -0.10, -0.25, -0.50, -0.50
EXP -0.50, -0.25, 0.45, 1.10, 1.39
EXP 1.73, 0.08, 0.0

```

TABLE B-1. S-76A SPECIFIC FILE (Cont'd)

```

;AALPMR = 3 DEG
EXP -0.20, -0.10, -0.25, -0.50, -0.50
EXP -0.50, -0.50, -0.35, -0.20, 0.80
EXP 1.63, 3.01, 0.0

; ** ROTOR Z-FACTOR ON VERTICAL TAIL MAP **
EZP3MP::BIV00 ;MAP ARGUMENT:LOOR UP ROUTINE
EXP CHIPMR00,AALPMR00 ;INPUT VARIABLE #1, INPUT VARIABLE #2
EKZP300 ;OUTPUT VARIABLE
EZP3LO ;PRIMARY (BASIC) MAP NAME
EXP -20.0,100.0,10.0,15 ;LOW LIM, UP LIM, DELTA, #ITEMS(OCTAL) CHI
EXP -5.0,3.0,3.0 ;LOWER LIMIT, UPPER LIMIT, DELTA - AALPMR

;CHIPMR 0 TO 100 DEG FOR AALPMR -3, 0, 3 DEG
;AALPMR = -3 DEG
EZP3LO: EXP 0.0, 0.0, -0.12, -0.04, 0.95
EXP 1.45, 1.97, 1.99, 2.00, 1.99
EXP 2.01, 1.86, 1.05

;AALPMR = 0 DEG
EXP 0.0, 0.0, -0.05, 0.0, 0.20
EXP 1.03, 1.53, 2.07, 2.06, 2.07
EXP 2.07, 2.00, 1.25

;AALPMR = 3 DEG
EXP 0.0, 0.0, -0.04, 0.04, 0.20
EXP 0.45, 1.05, 1.47, 1.77, 2.08
EXP 2.24, 2.21, 1.50

;***** FUSELAGE INTERPERENCE ON THE VERTICAL TAIL #1 (WPPA) *****

OP3MP:: BIV00 ; ** VERTICAL TAIL DYNAMIC PRESSURE RATIO MAP **
EXP PSIMF00,ALFMP00 ;MAP ARGUMENT:LOOR UP ROUTINE
OP3OWF00 ;INPUT VARIABLE #1, INPUT VARIABLE #2
OP3LO ;OUTPUT VARIABLE
EXP -20.0,20.0,4.0,13 ;PRIMARY (BASIC) MAP NAME
EXP -10.0,10.0,5.0 ;LOW LIMIT, UP LIM, DELTA, #ITEMS(OCTAL), PSI
;LOW ANGLE MAP:PSIMF -20 TO 20 DEG FOR ALFMP -10,0,10
;ALFMP = -10 DEG
QP3LO: EXP 1.00, 0.97, 0.92, 0.89, 0.84
EXP 0.75, 0.84, 0.89, 0.92, 0.97
EXP 1.00

;ALFMP = -5 DEG
EXP 1.00, 0.96, 0.88, 0.85, 0.77
EXP 0.72, 0.77, 0.85, 0.88, 0.96
EXP 1.00

;ALFMP = 0 DEG
EXP 1.00, 0.95, 0.85, 0.82, 0.71
EXP 0.70, 0.71, 0.82, 0.85, 0.95
EXP 1.00

;ALFMP = 5 DEG
EXP 1.00, 0.93, 0.83, 0.76, 0.68
EXP 0.66, 0.68, 0.76, 0.83, 0.93
EXP 1.00

;ALFMP = 10 DEG
EXP 1.00, 0.90, 0.80, 0.70, 0.64
EXP 0.62, 0.64, 0.70, 0.80, 0.90
EXP 1.00

EPP3MP::CONST00 ; ** BODY DOWNWASH ON VERTICAL TAIL MAP **
EPSP100 ;MAP ARGUMENT:LOOR UP ROUTINE
EPSP300 ;INPUT VARIABLE
;OUTPUT VARIABLE

```

TABLE B-1. S-76A SPECIFIC FILE (Cont'd)

```

***** INPUT PARAMETERS FOR TAIL ROTOR (8A) - (BAILEY) *****

RTR:: 4.0 ;RADIUS,FT
OMEGTR::168.75 ;TRIM ROTATIONAL RATE,RAD/SEC
BTR:: 4.0 ;ACTUAL NUMBER OF BLADES
FSTR:: 518.046 ;FUSELAGE STATION,IN
WLTR:: 162.879 ;WATERLINE STATION,IN
BLTR:: 20.0 ;BUTTLINE STATION,IN (+IVE TO PORT)
TWSTR::-8.0 ;BLADE TWIST,DATUM CENTER OF ROTATION,OEG
BIASR::14.0 ;BLADE PITCH CORRECTION FOR N.L.TWIST(NEG REDUCES PITCH)
GAMTR:: 90.0 ;TAIL ROTOR CANT ANGLE,OEG
DEL3TR::45.0 ;FLAPPING HINGE OFFSET ANGLE,OEG
OELTR::.002 ;RATE OF CHANGE OF CONE ANGLE WITH THRUST,DEG/LB
CHROTR::.540 ;BLADE CHORD,FT
ATR:: 5.73 ;BLADE LIFT CURVE SLOPE,1/RAD
BTLTR:: .92 ;BLADE TIP LOSS FACTOR
COTR:: 2.0 ;TAIL ROTOR HEAD DRAG,FT**2

*****TAIL ROTOR B PARAMETERS*****
IBTR::0.67 ;BLADE MOMENT OF INERTIA ABOUT HINGE, SLUG-FT**2
OROOTR::0.0087 ;BLADE SECTION DRAG COEFFICIENT, WHERE
ORO1TR::-0.0216 ;CD = DRDOTR + ORO1TR*ALPHA + DRD2TR*ALPHA**2
DRD2TR::0.4 ;
OROTR::-1.0 ;COEF FOR DIRECTION OF ROTATION
TAUDTR::0.1 ;DOWNWASH LAG TIME CONSTANT

***** ROTOR INTERFERENCE ON TAIL ROTOR (MRPA) *****

EXTRMP::CONST00 ;** ROTOR X-FACTOR ON TAIL ROTOR MAP **
ERXP300 ;MAP ARGUMENT:LOOR UP ROUTINE
ERXTR00 ;INPUT VARIABLE
;OUTPUT VARIABLE

EZTRMP::CONST00 ;** ROTOR Z-FACTOR ON TAIL ROTOR MAP **
ERZP300 ;MAP ARGUMENT:LOOR UP ROUTINE
ERZTR00 ;INPUT VARIABLE
;OUTPUT VARIABLE

***** VERTICAL TAIL INTERFERENCE ON TAIL ROTOR INFLOW *****

VBVTR::30.0 ; AIRSPEED BREAK PT. - NO BLOCKAGE ABOVE,RT.
RBVTR::.895 ; TAIL ROTOR BLOCKAGE COEF. AT NOVER

***** INPUT PARAMETERS FOR EQUATIONS OF MOTION (8A) *****

FSCG:: 210.0 ; FUSELAGE STATION OF C.G., INCH
WLCCG:: 95.4 ; WATERLINE STATION OF C.G., INCH
BLCCG:: 0.0 ; BUTTLINE STATION OF C.G., INCH (+IVE TO PORT)

WEIGHT::8750.0 ; AIRCRAFT GROSS WEIGHT,LBS.
IX:: 2225.0 ; INERTIA ABOUT BODY X-AXIS,SLUG-FT**2
IY:: 12500.0 ; INERTIA ABOUT BODY Y-AXIS,SLUG-FT**2
IZ:: 11041.0 ; INERTIA ABOUT BODY Z-AXIS,SLUG-FT**2
IX2:: 1294.0 ; CROSS COUPLING INERTIA,SLUG-FT**2
IYZ:: 0.0
IXY:: 0.0

```

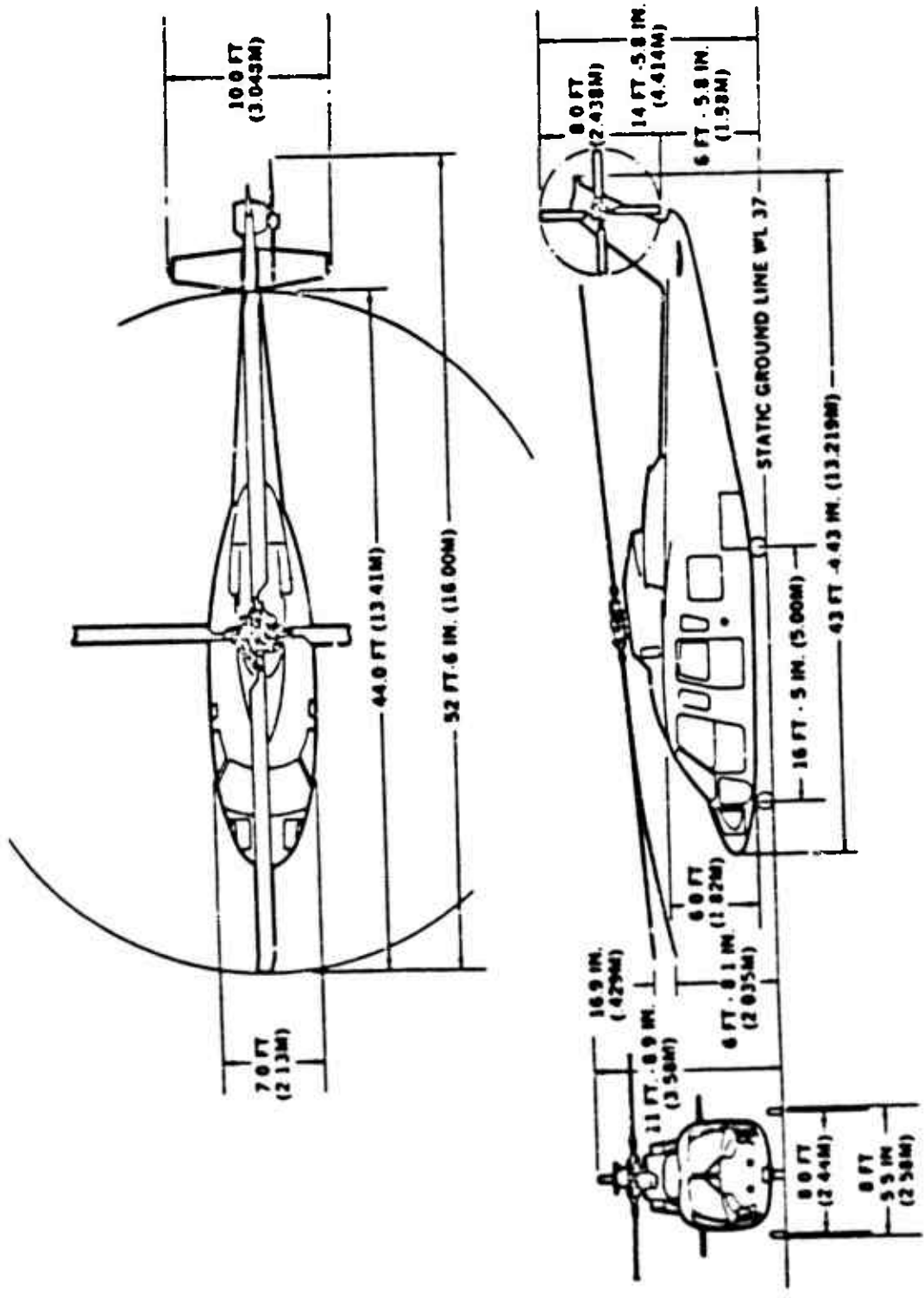



Figure B-1. S-76A Three-View Drawing

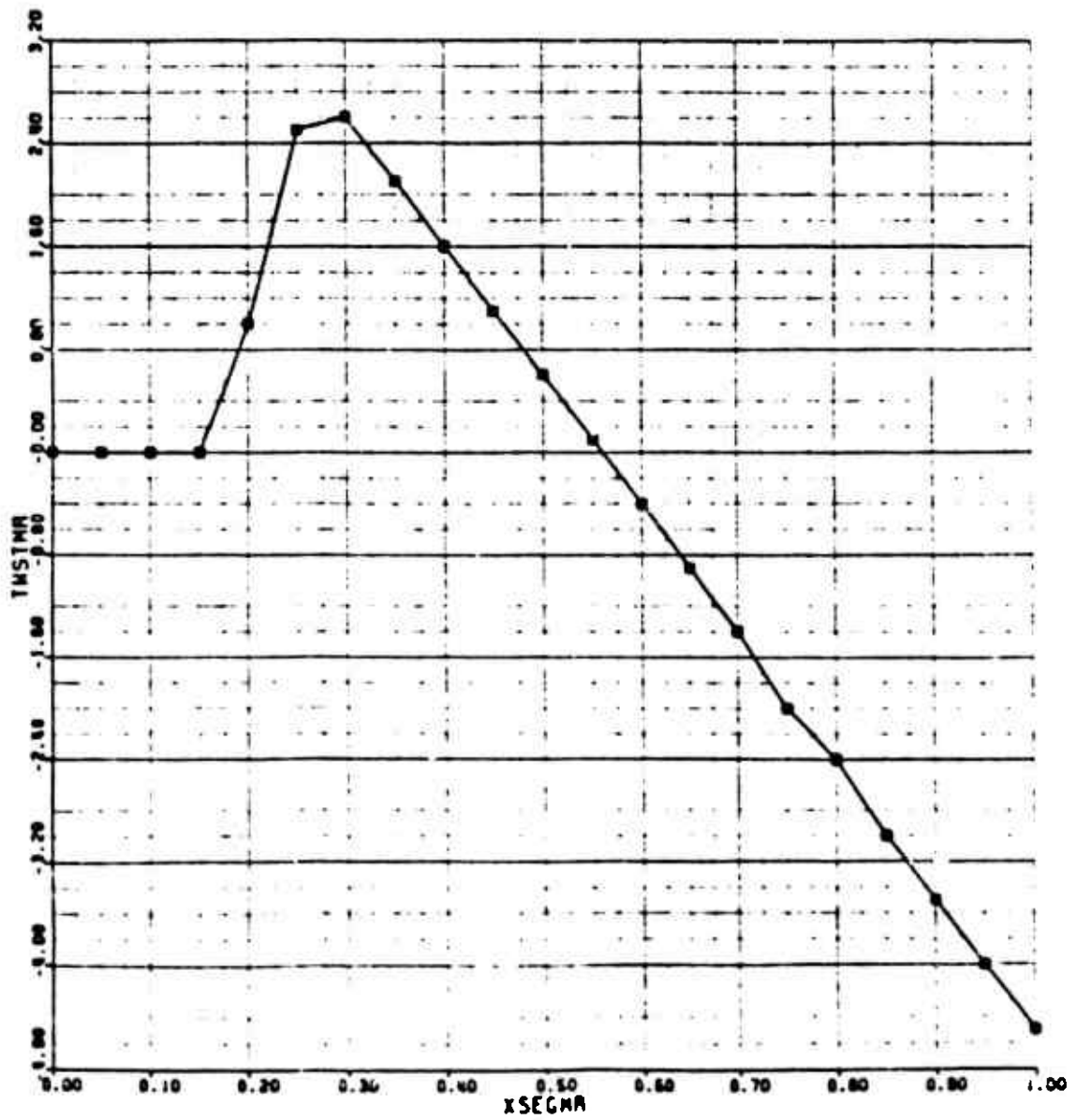


Figure B-2. S-76A Main Rotor Blade Twist Map

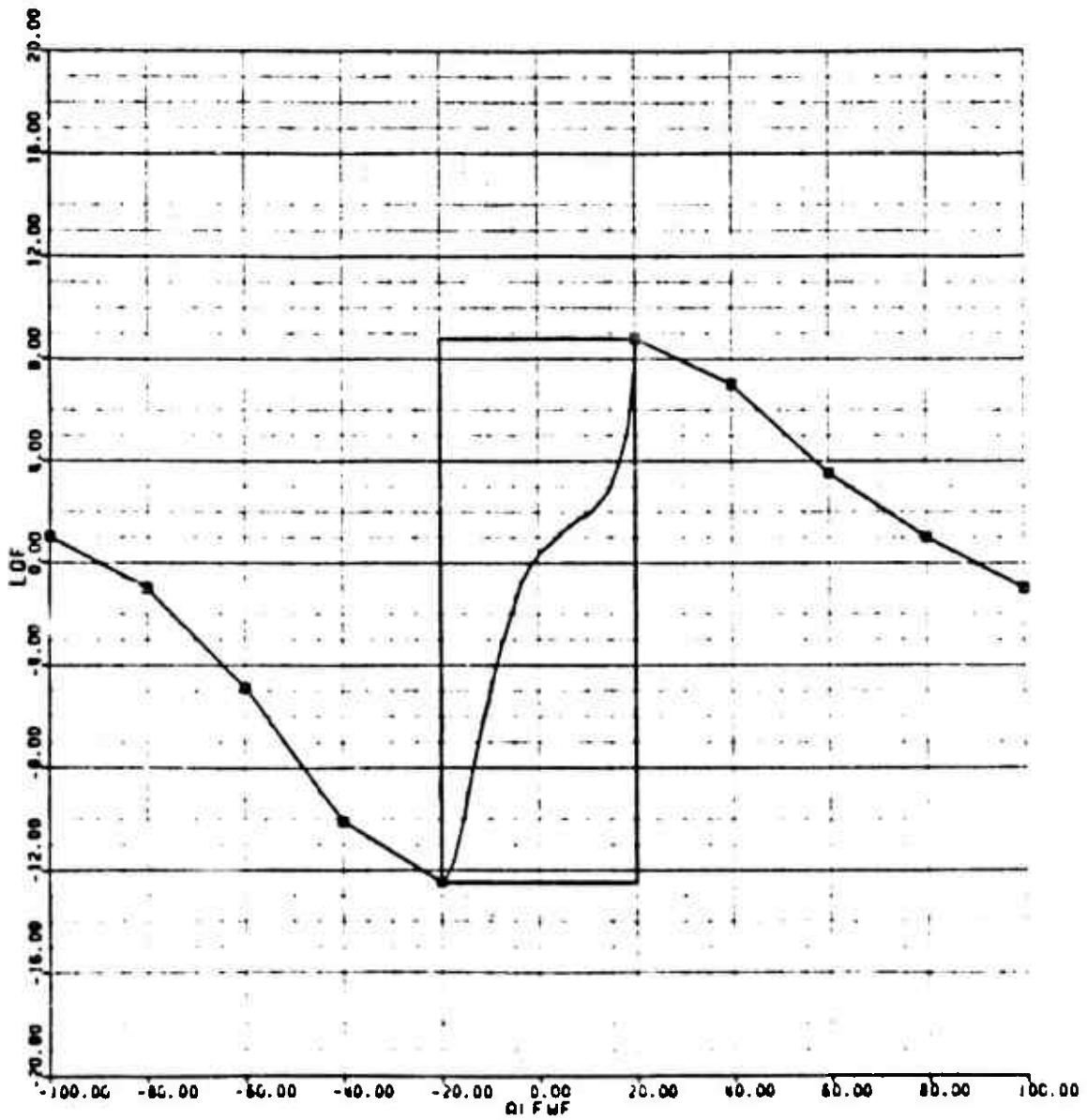


Figure B-3. S-76A Fuselage Lift Map

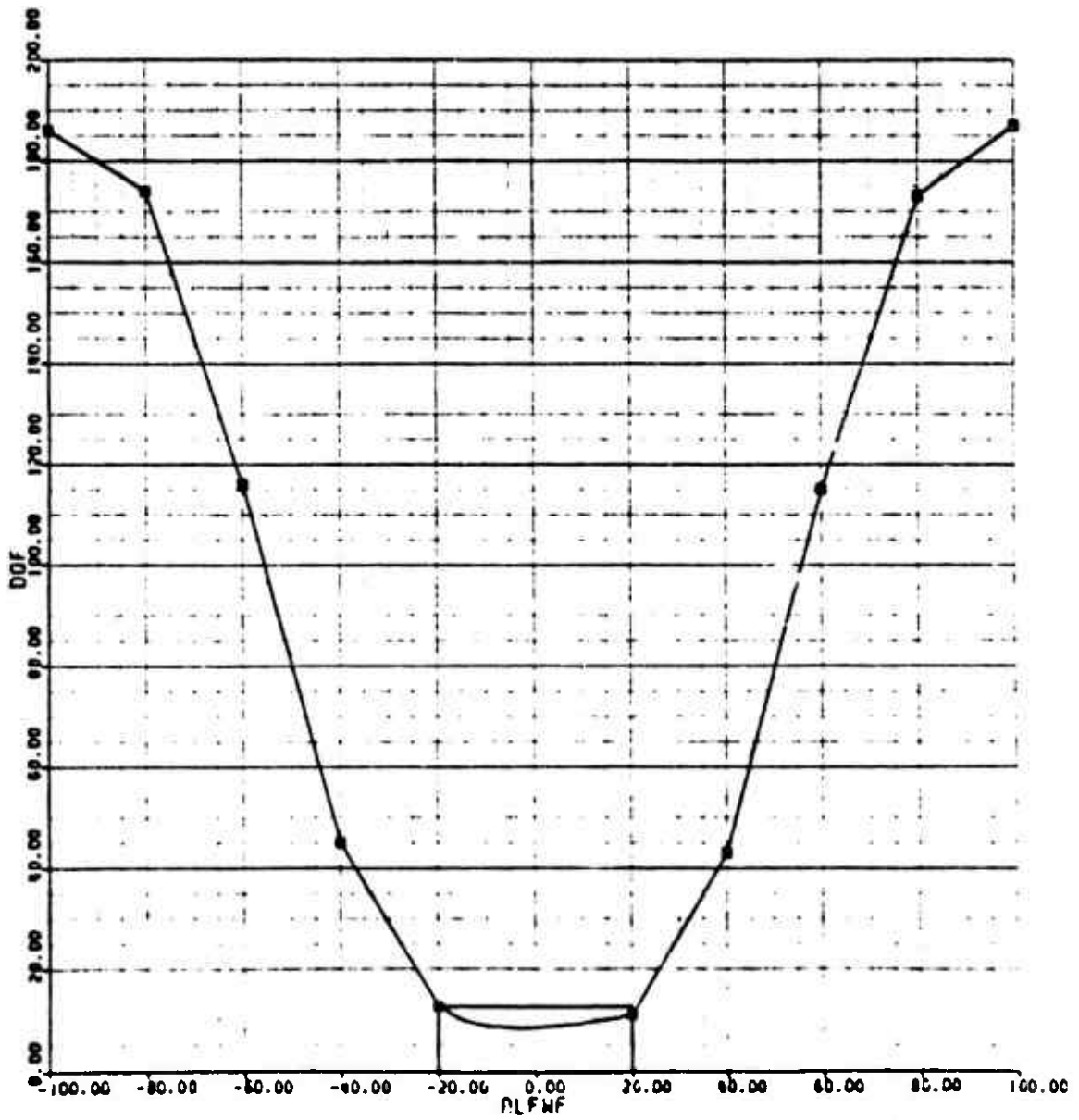


Figure B-4. S-76A Fuselage Drag Map

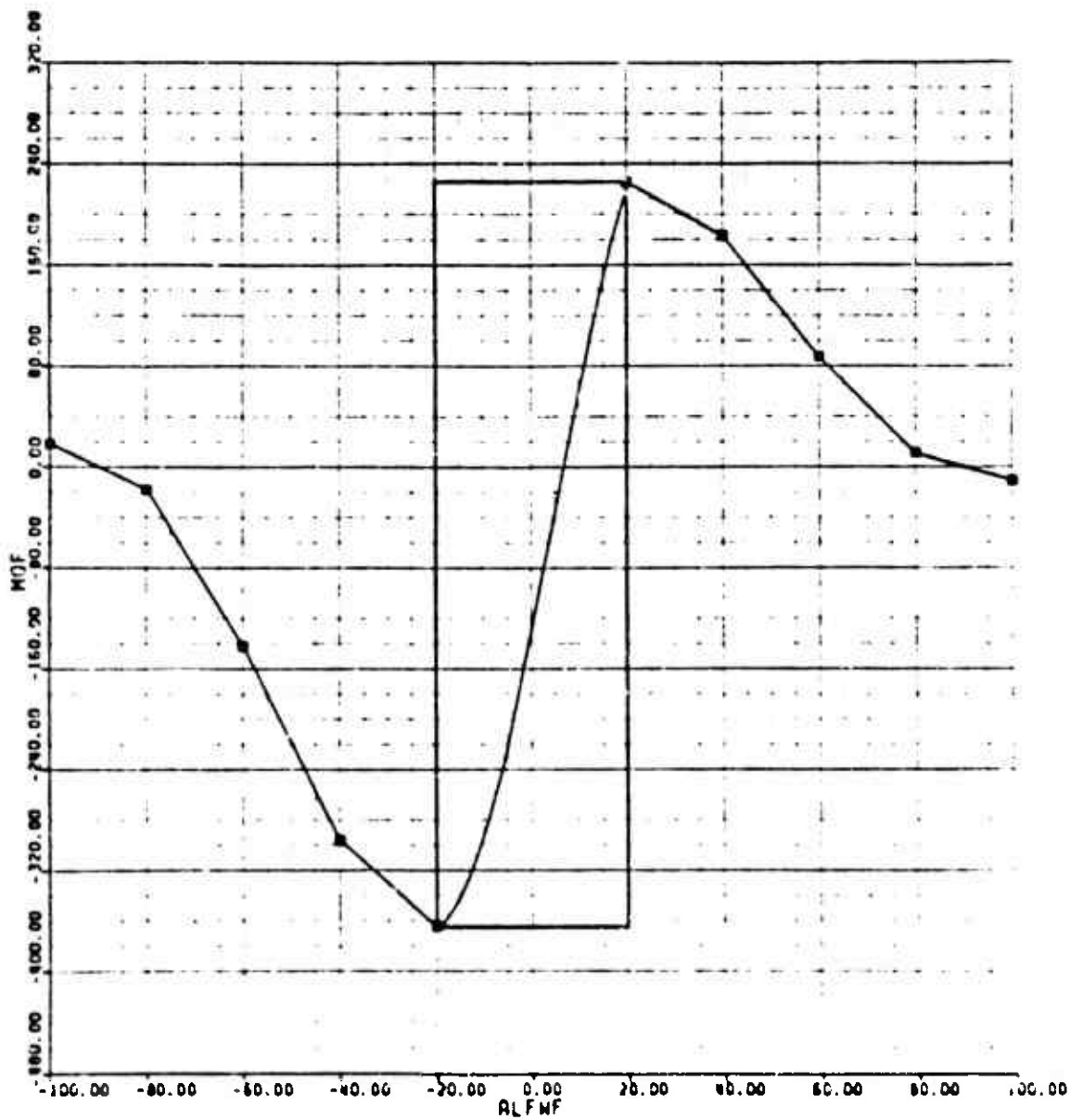


Figure B-5. S-76A Fuselage Pitching Moment Map

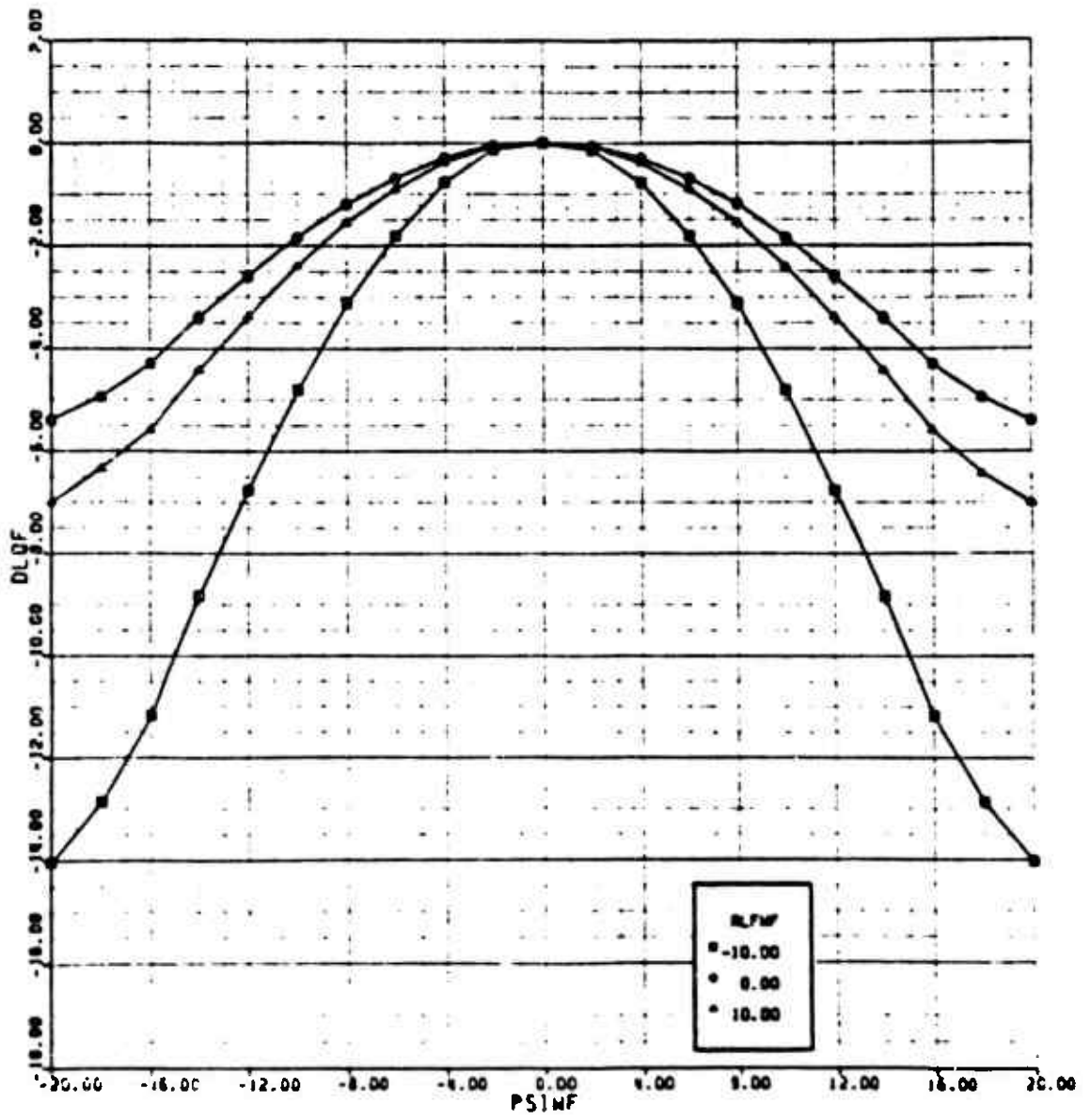


Figure B-6. S-76A Fuselage Delta Lift Map

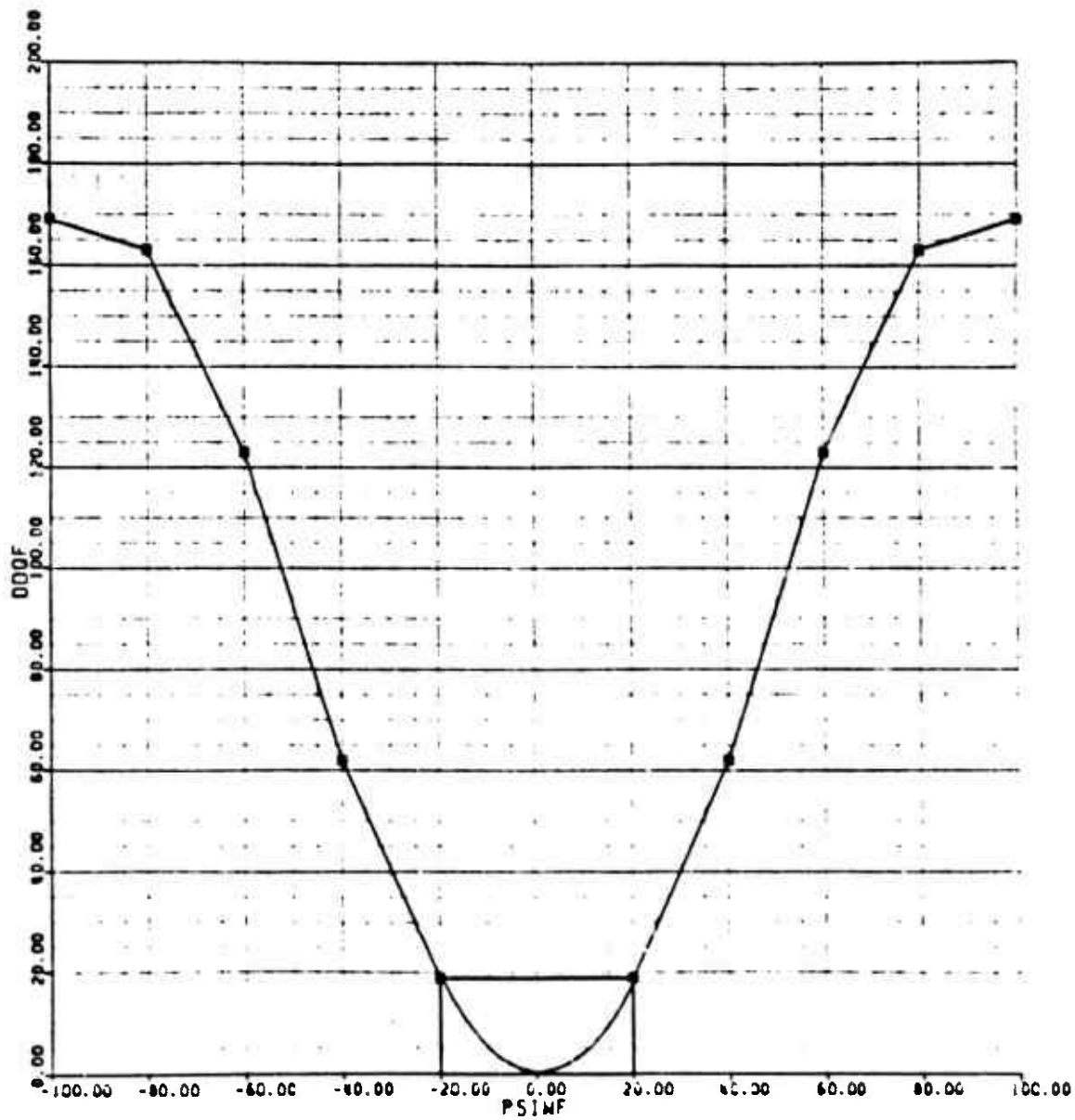


Figure B-7. S-76A Fuselage Delta Drag Map

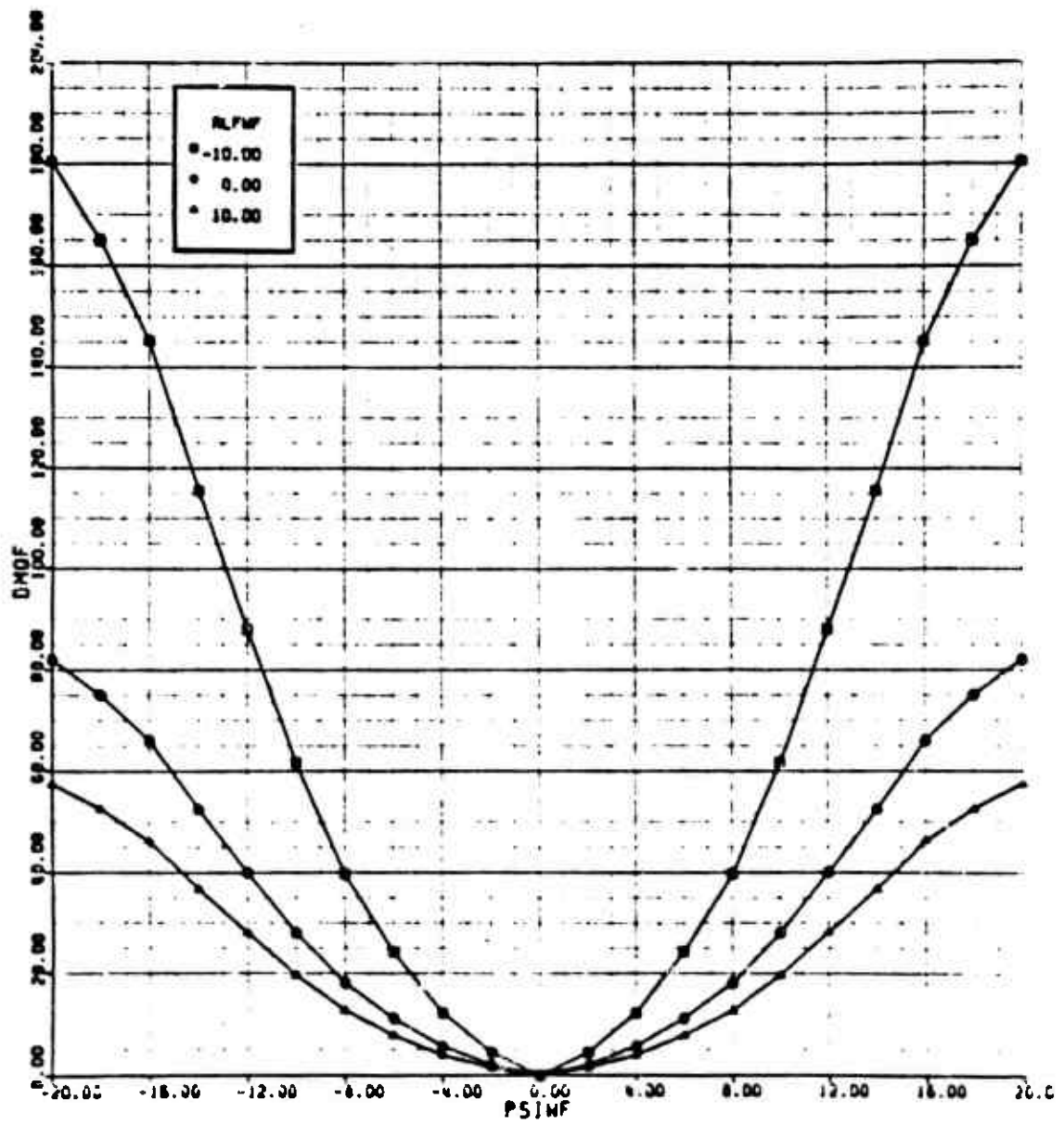


Figure B-8. S-76A Fuselage Delta Pitching Moment Map

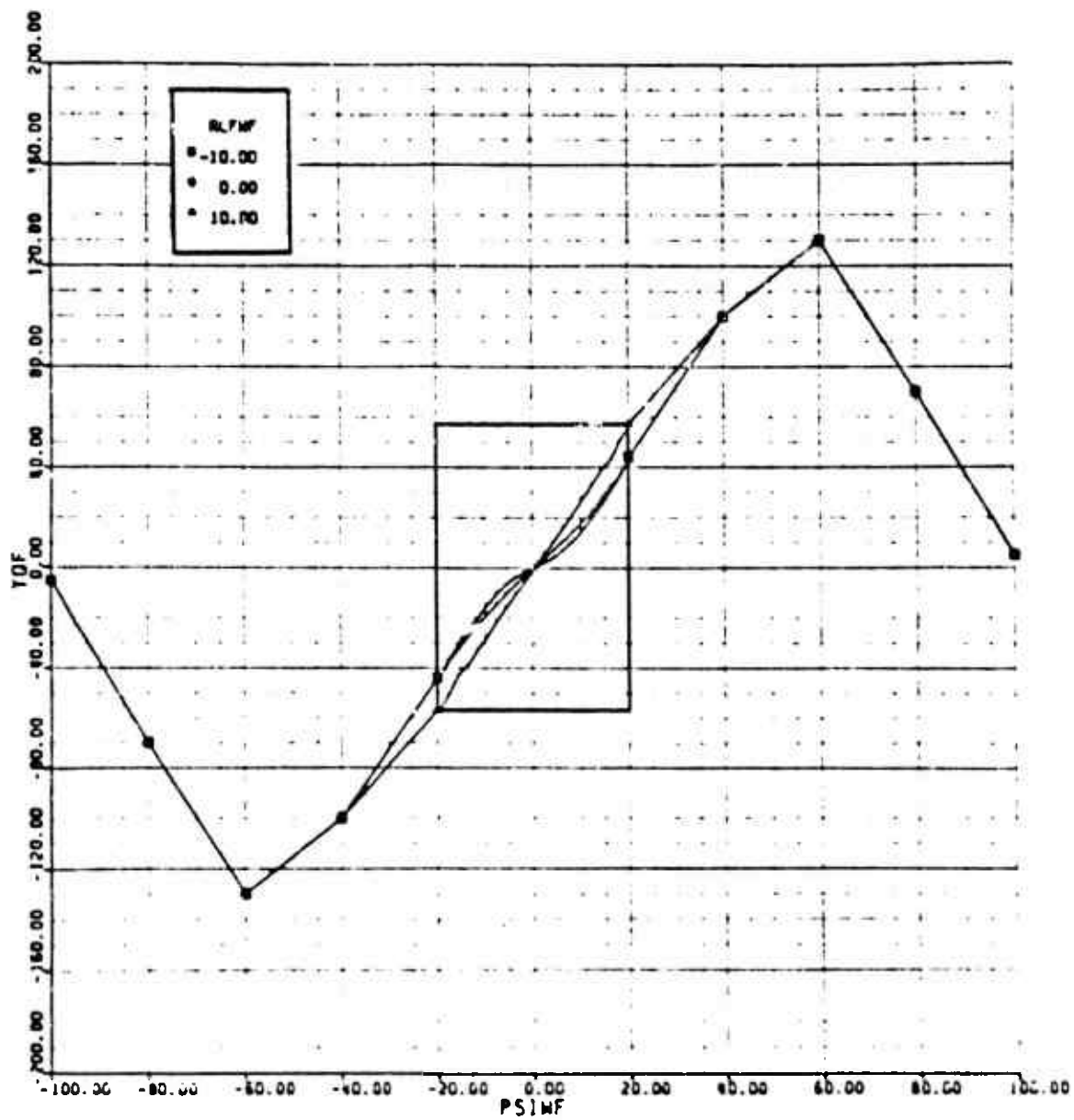


Figure B-9. S-76A Fuselage Sideforce Map

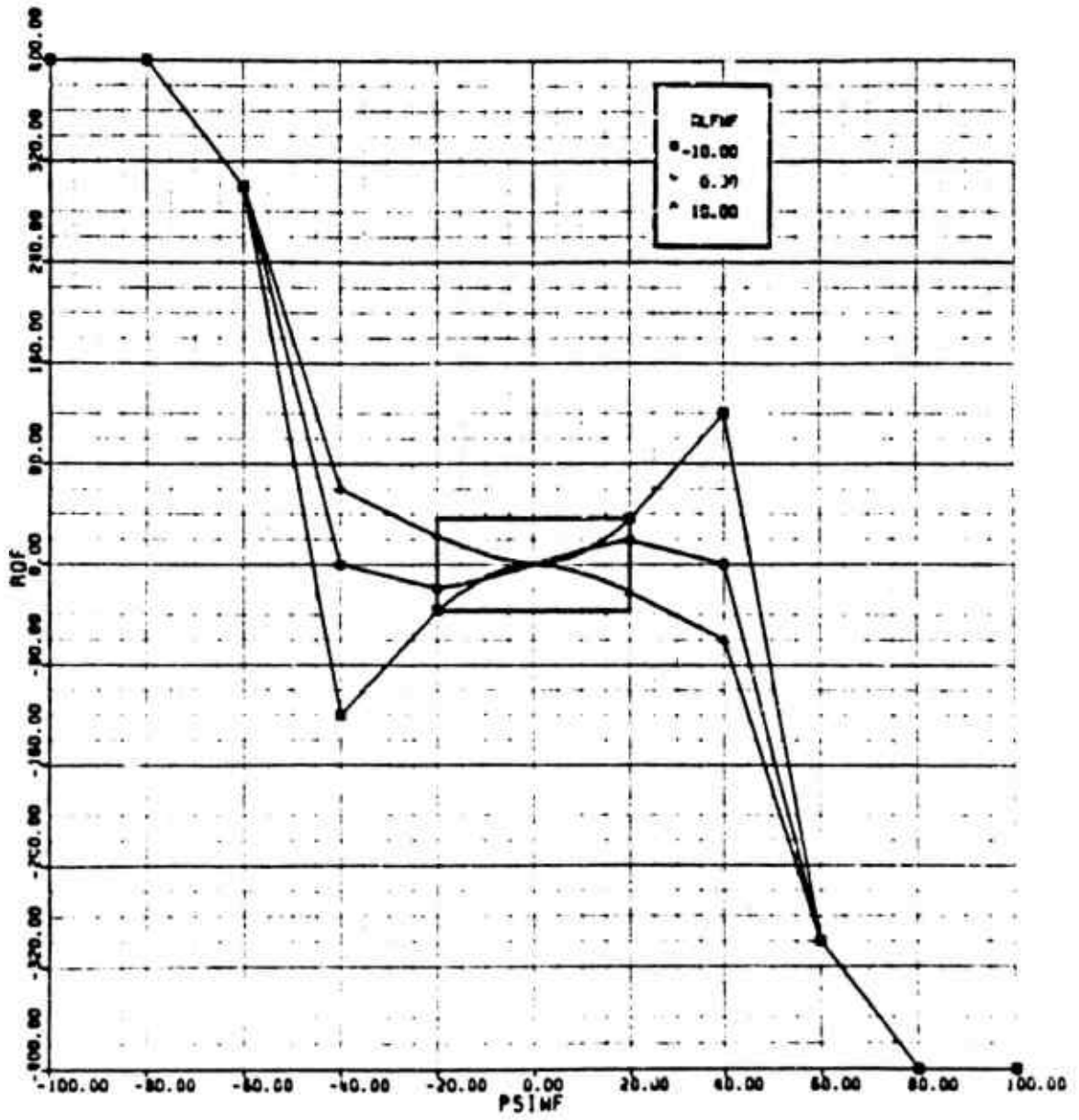


Figure B-10. S-76A Fuselage Rolling Moment Map

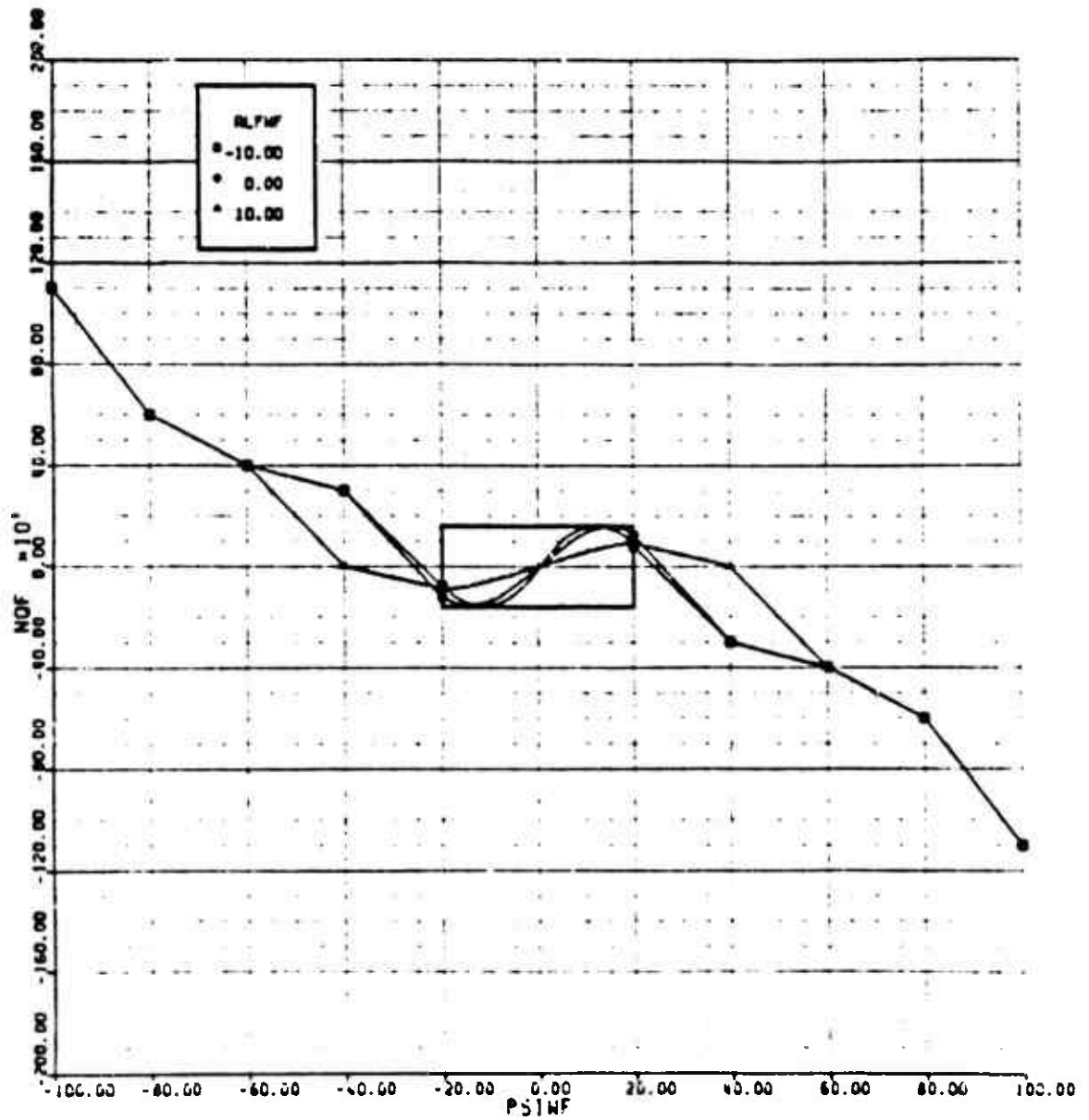


Figure B-11. S-76A Fuselage Yawing Moment Map

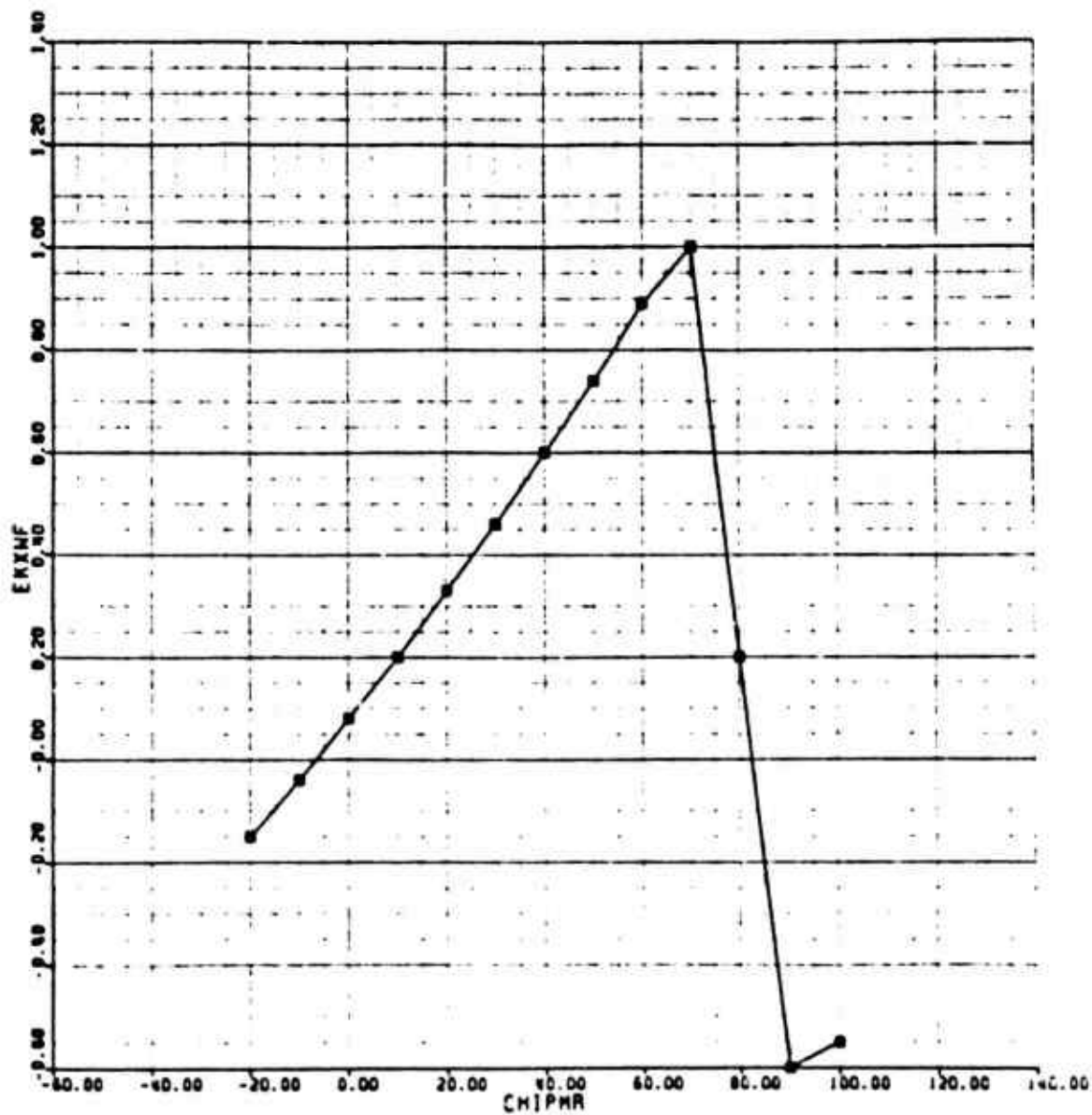


Figure B-12. S-76A Main Rotor Downwash on Fuselage Map (y-direction)

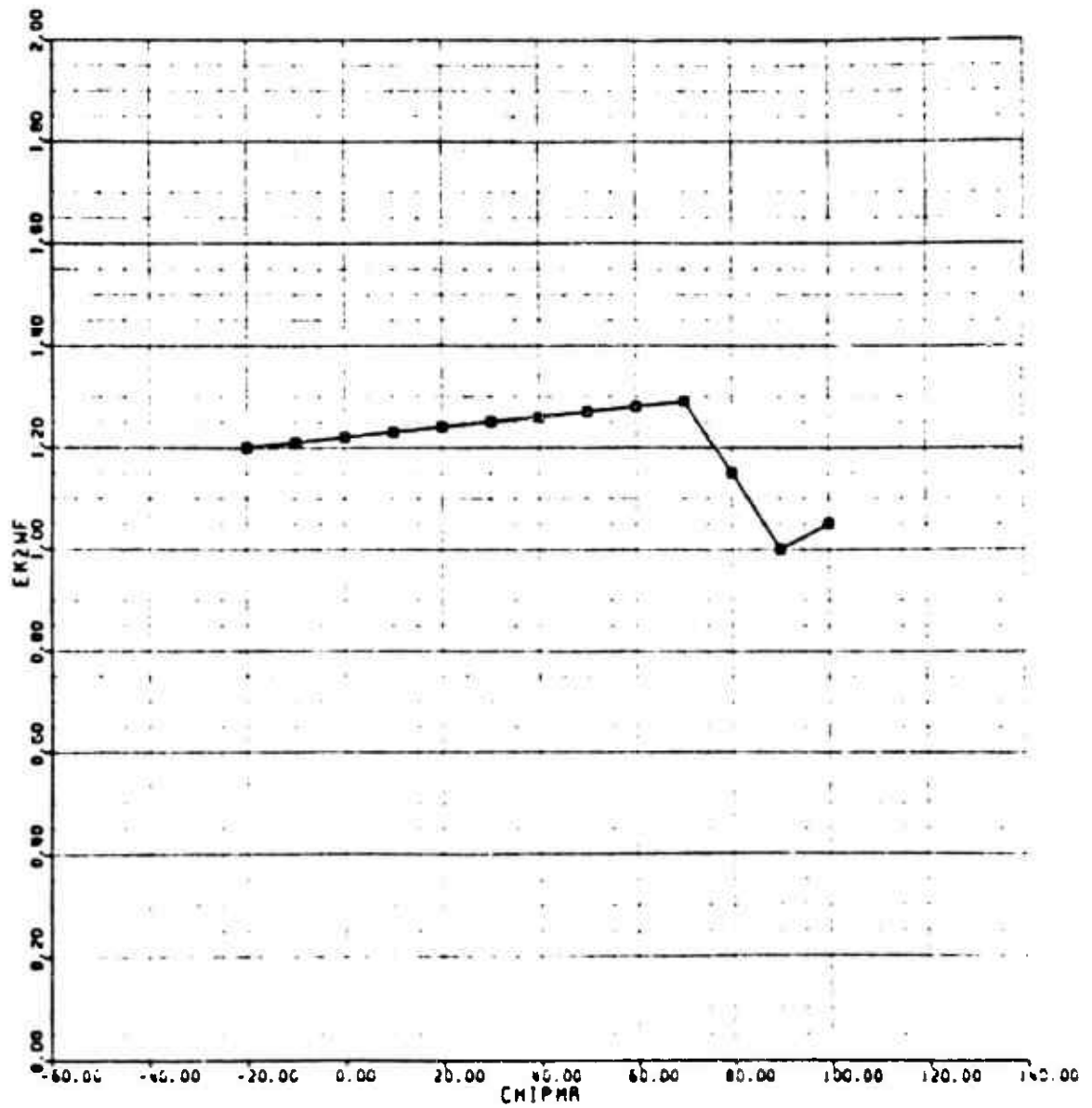


Figure B-13. S-76A Main Rotor Downwash on Fuselage Map (x-direction)

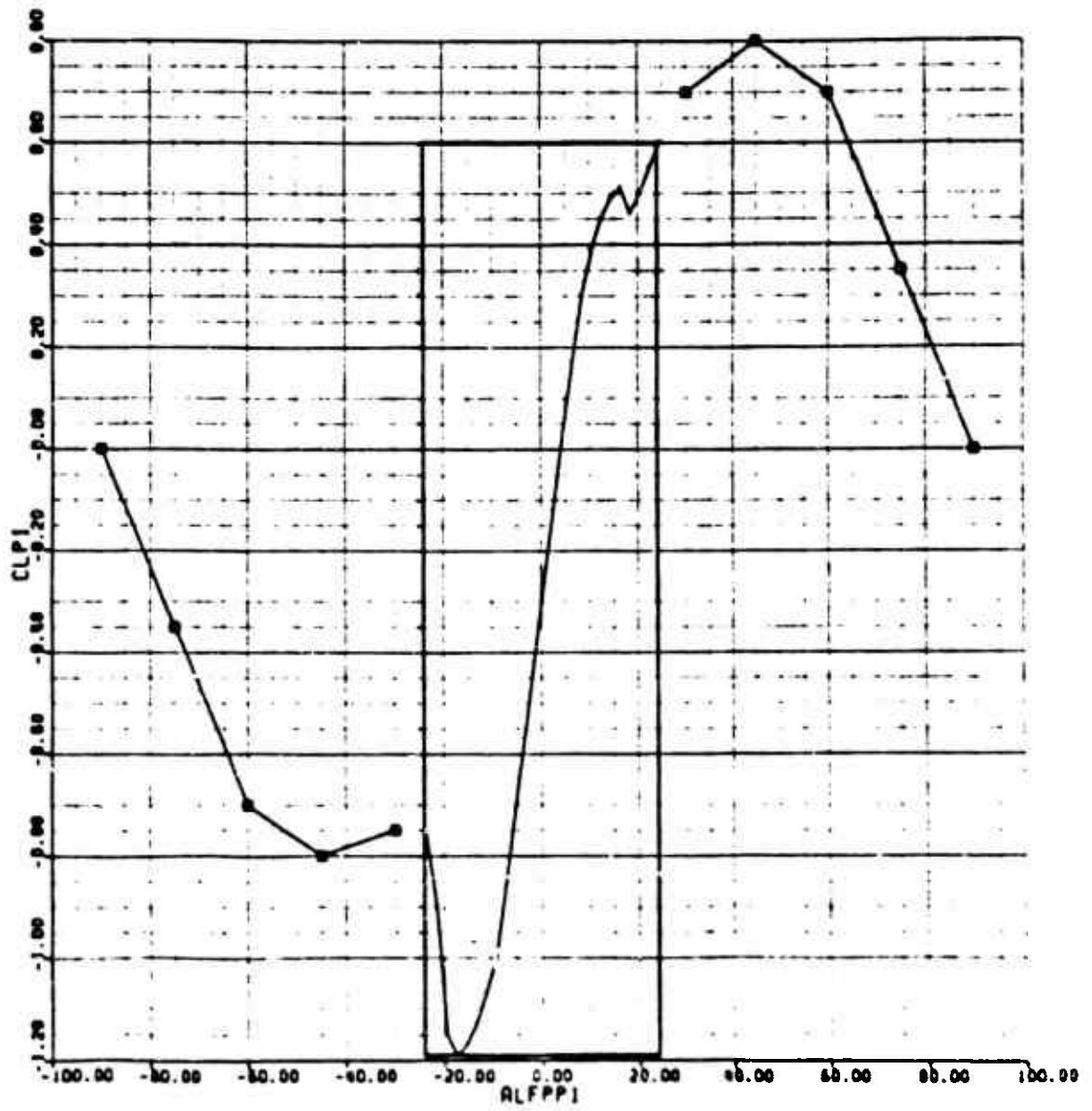


Figure B-14. S-76A Horizontal Tail Lift Map

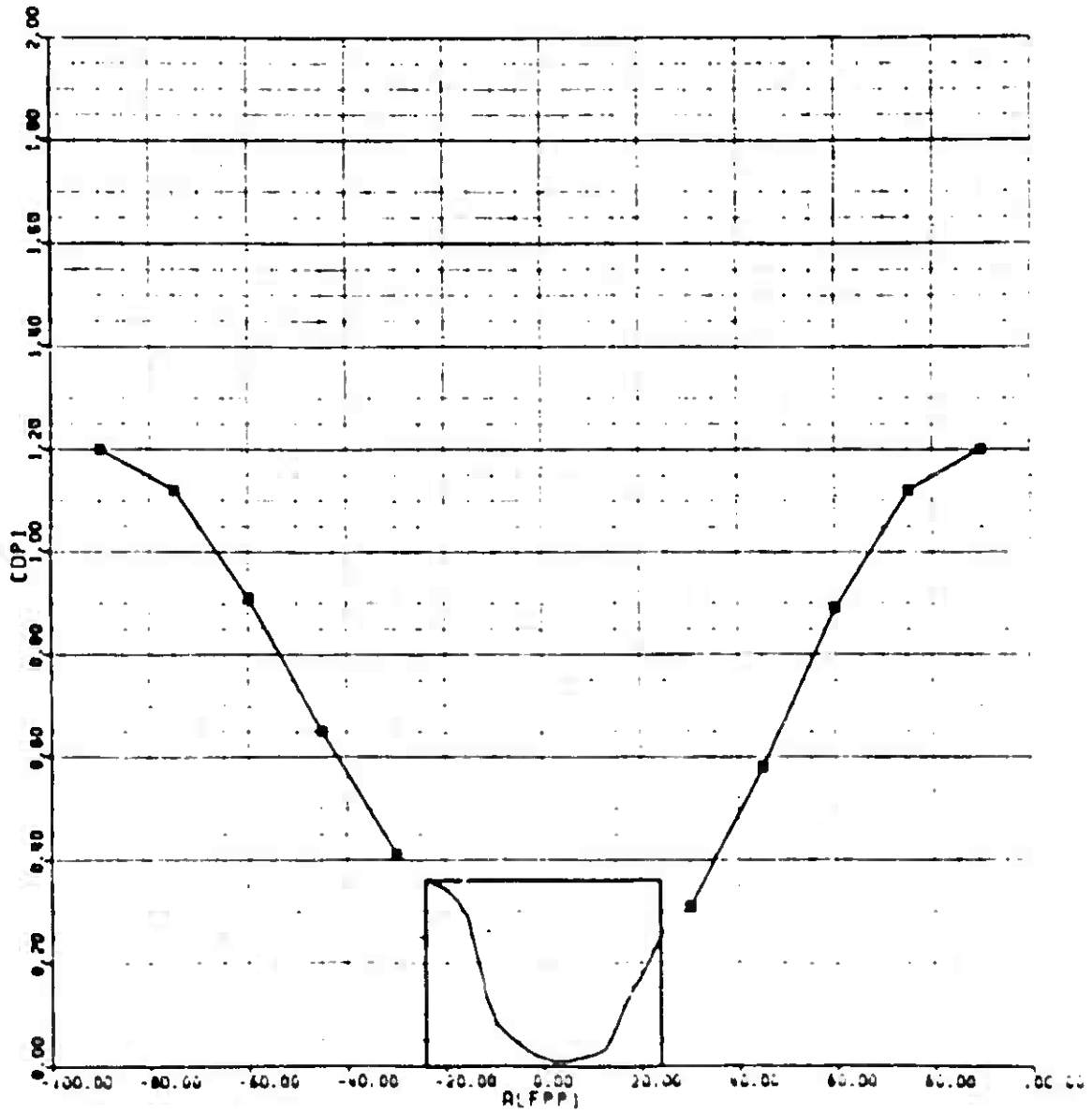


Figure B-15. S-76A Horizontal Tail Drag Map

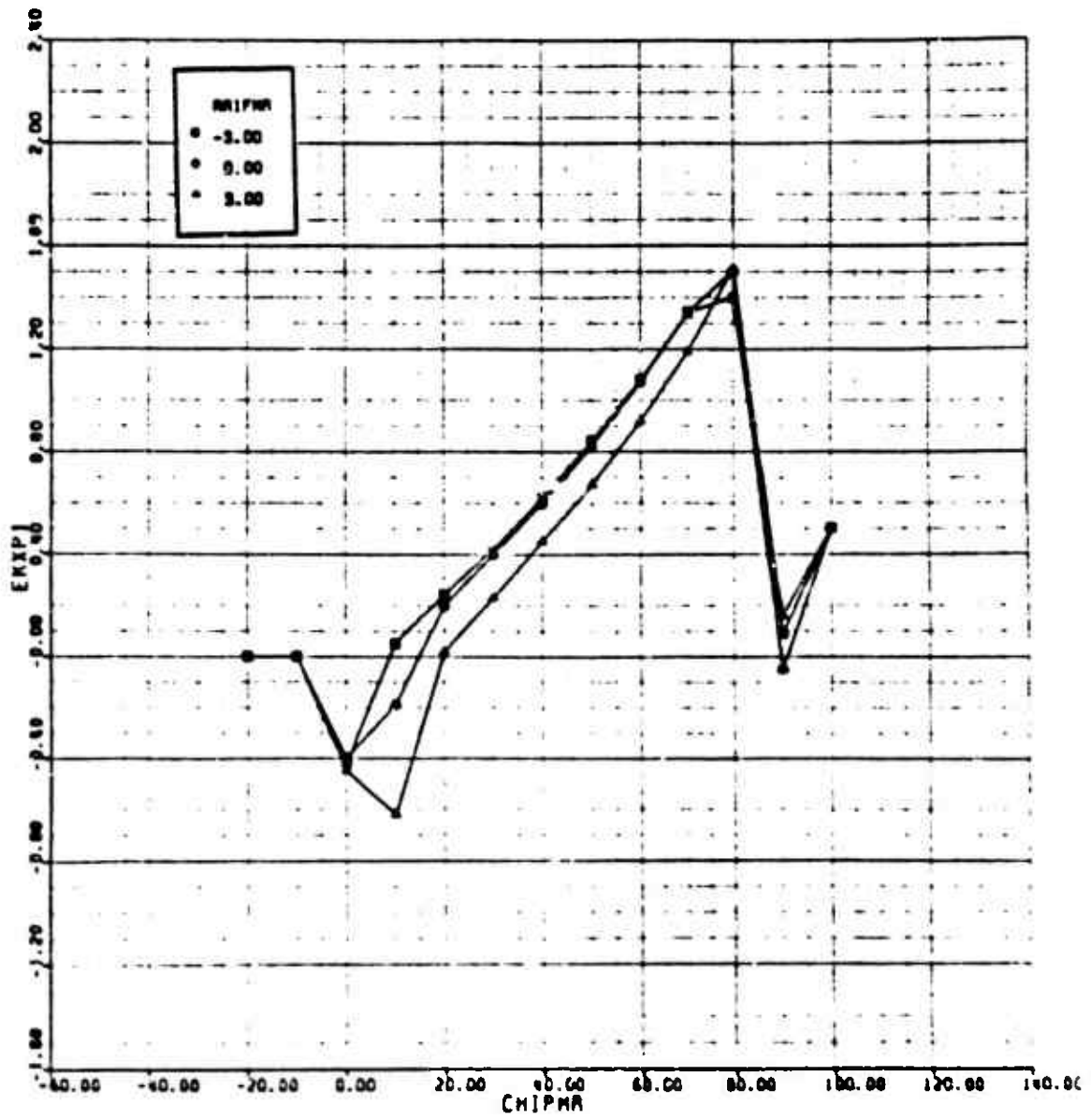


Figure B-16. S-76A Main Rotor Downwash on Horizontal Tail Map (x-direction)

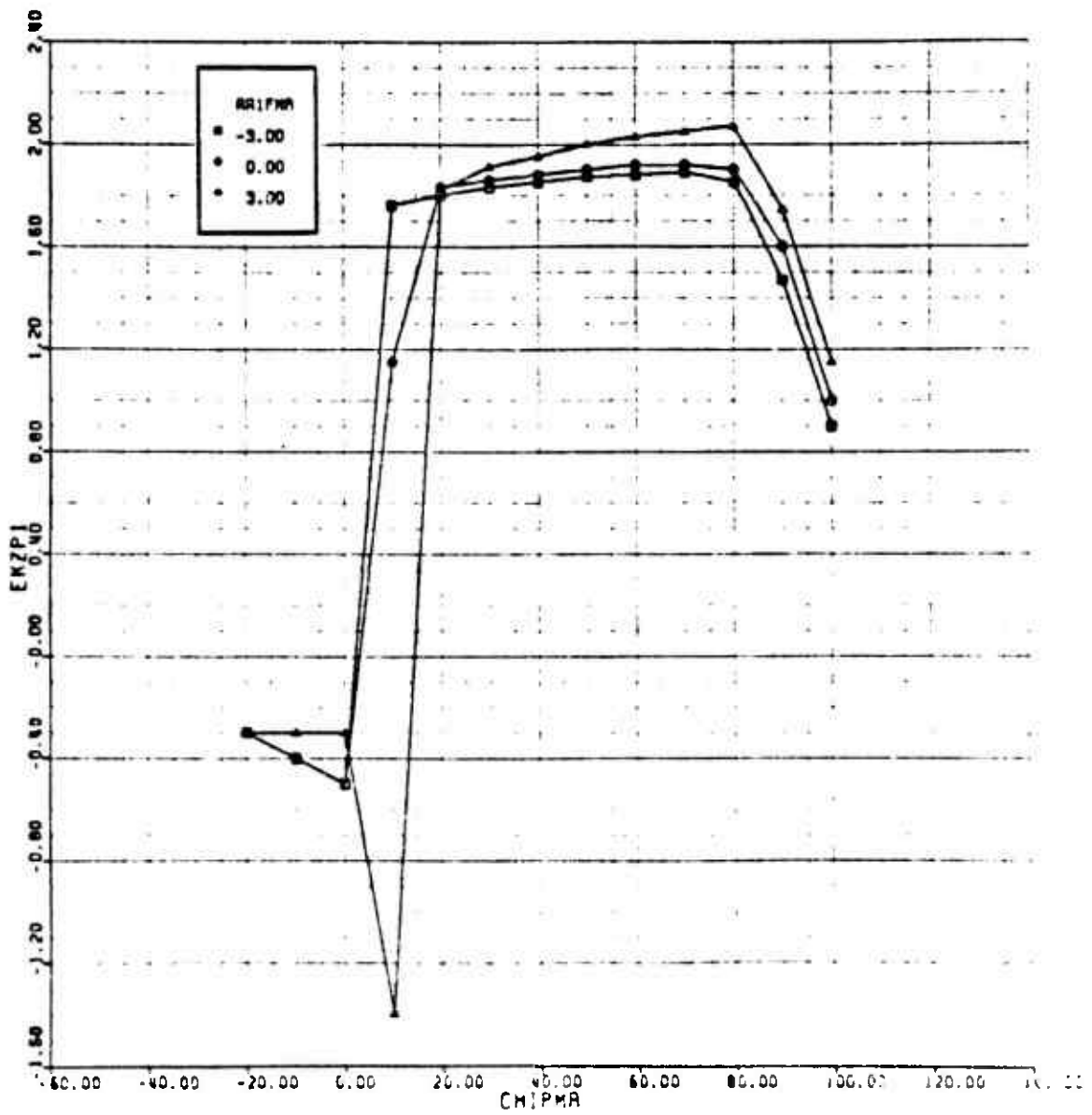


Figure B-17. S-764 Main Rotor Downwash on Horizontal Tail Map (z-direction)

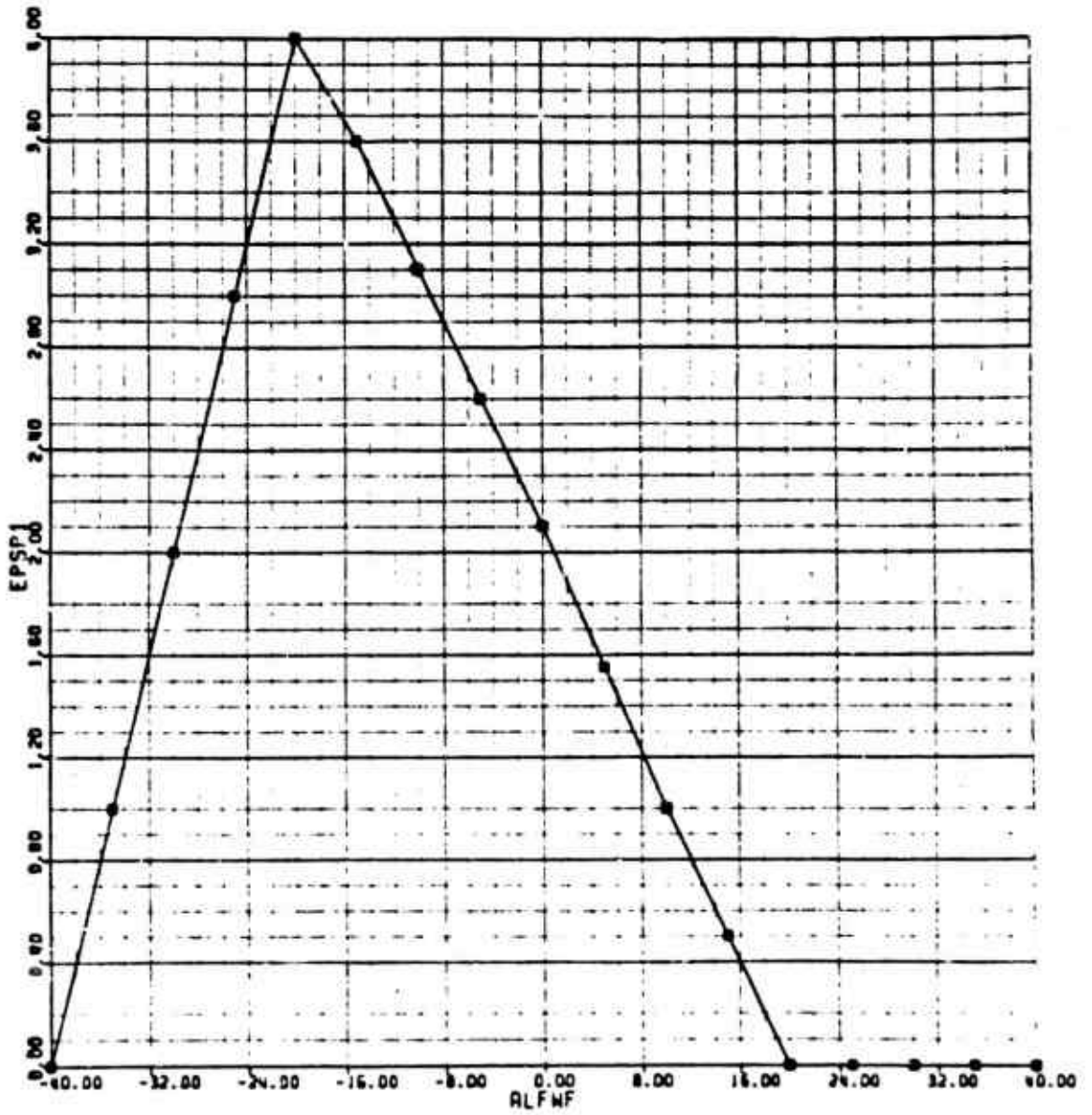


Figure B-18. S-76A Fuselage Downwash on Horizontal Tail Map

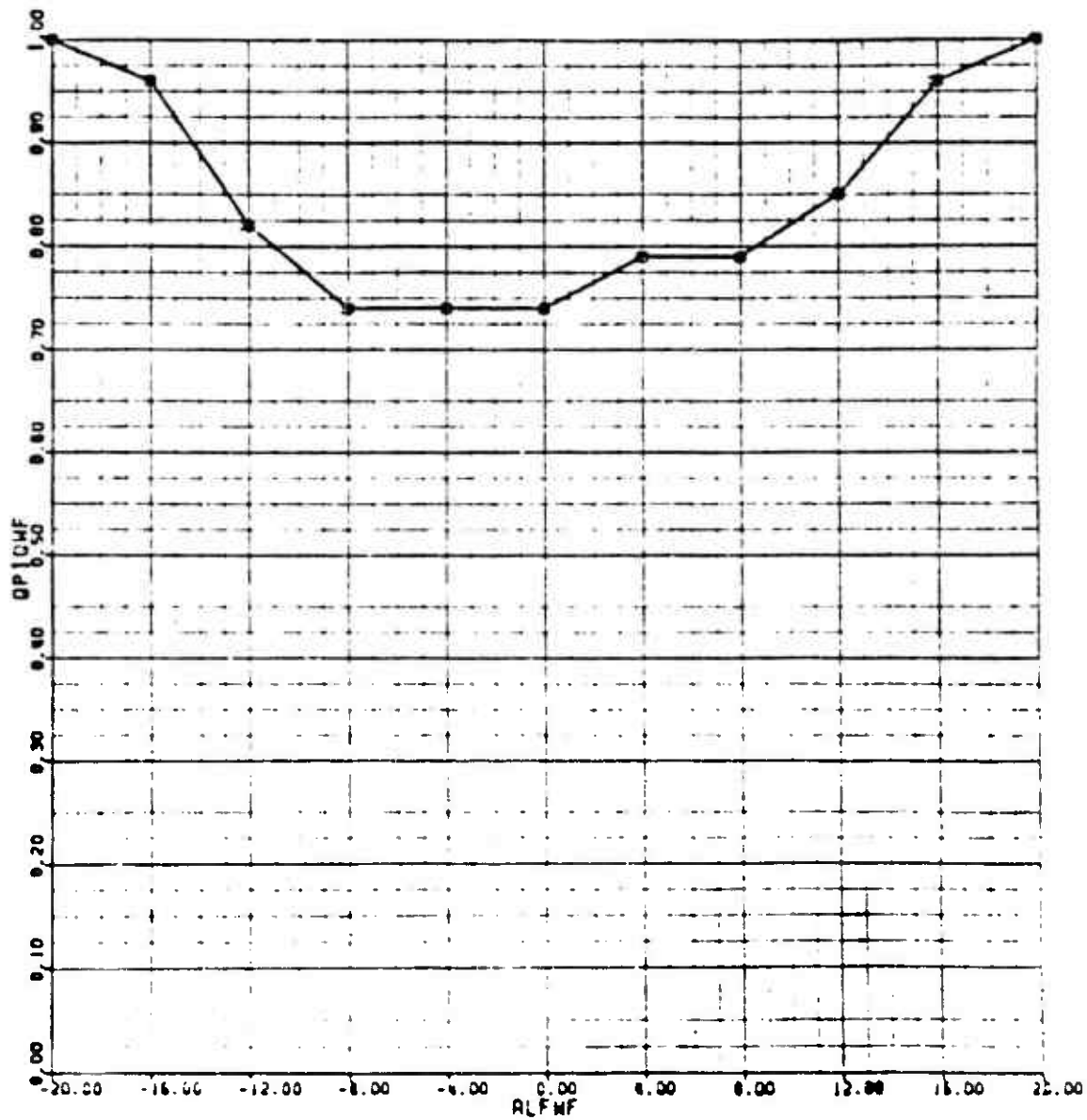


Figure B-19. S-76A Dynamic Pressure Ratio at Horizontal Tail Map

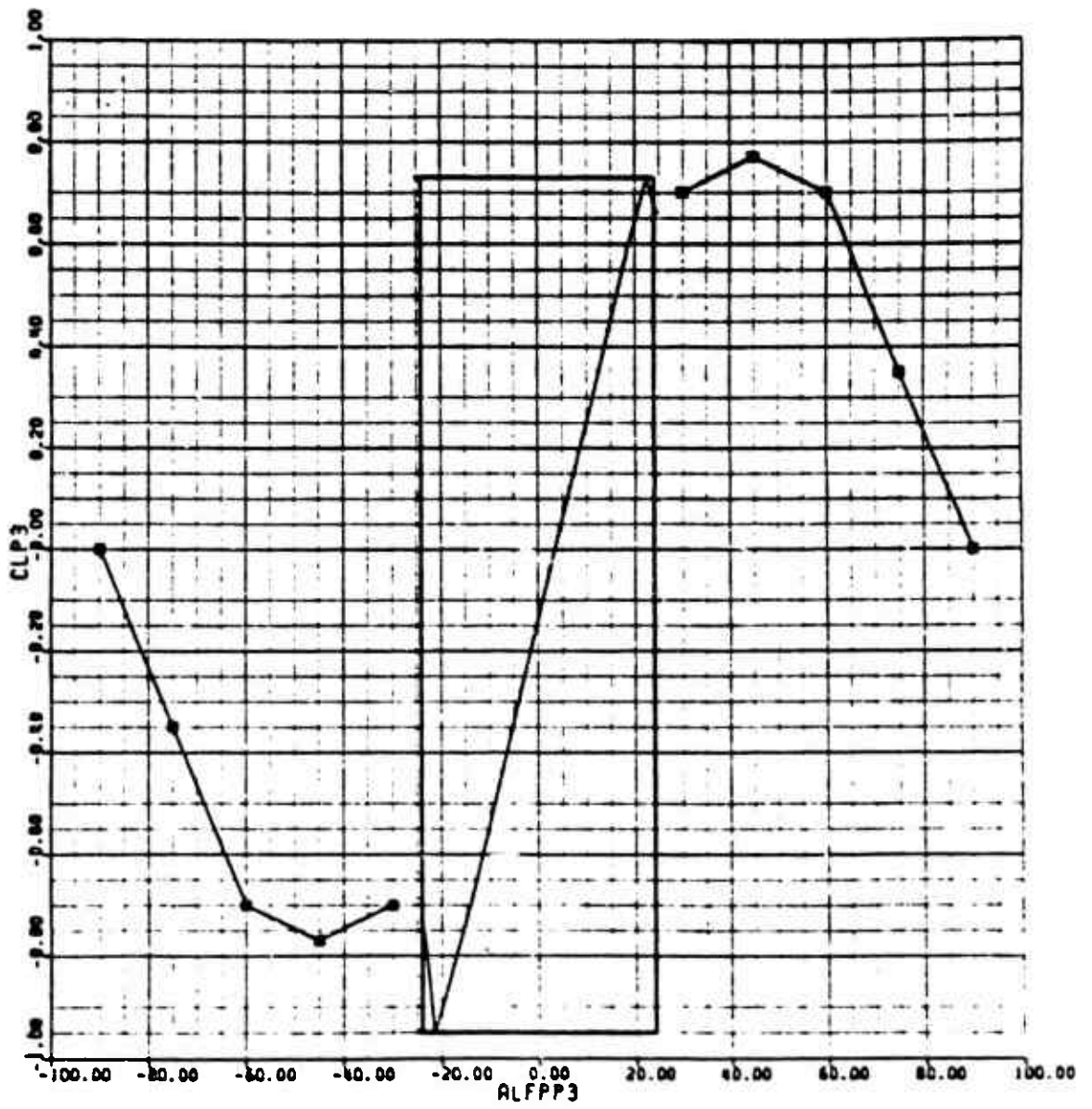


Figure B-20. S-76A Vertical Tail Lift Map

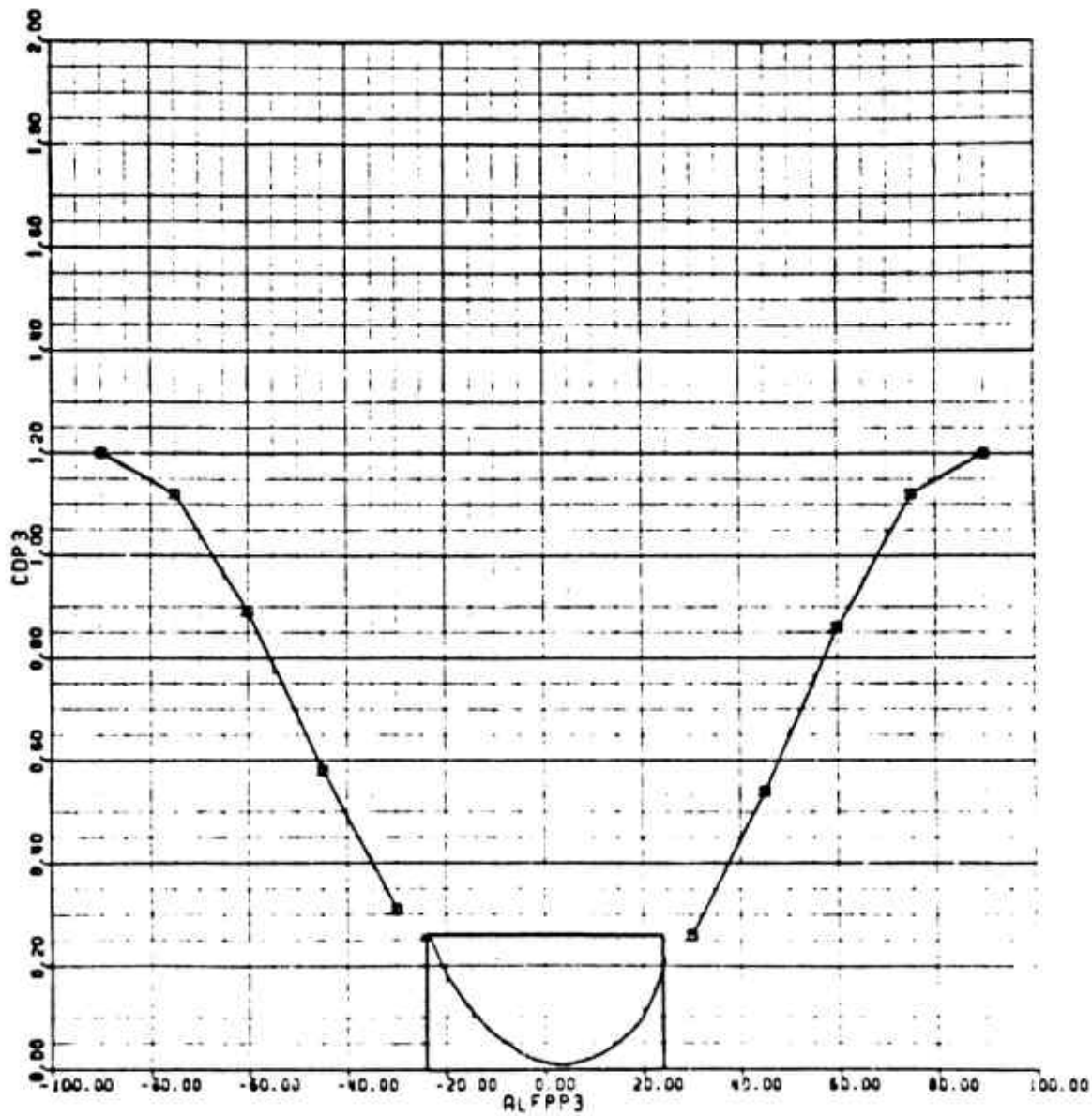


Figure B-21. S-76A Vertical Tail Drag Map

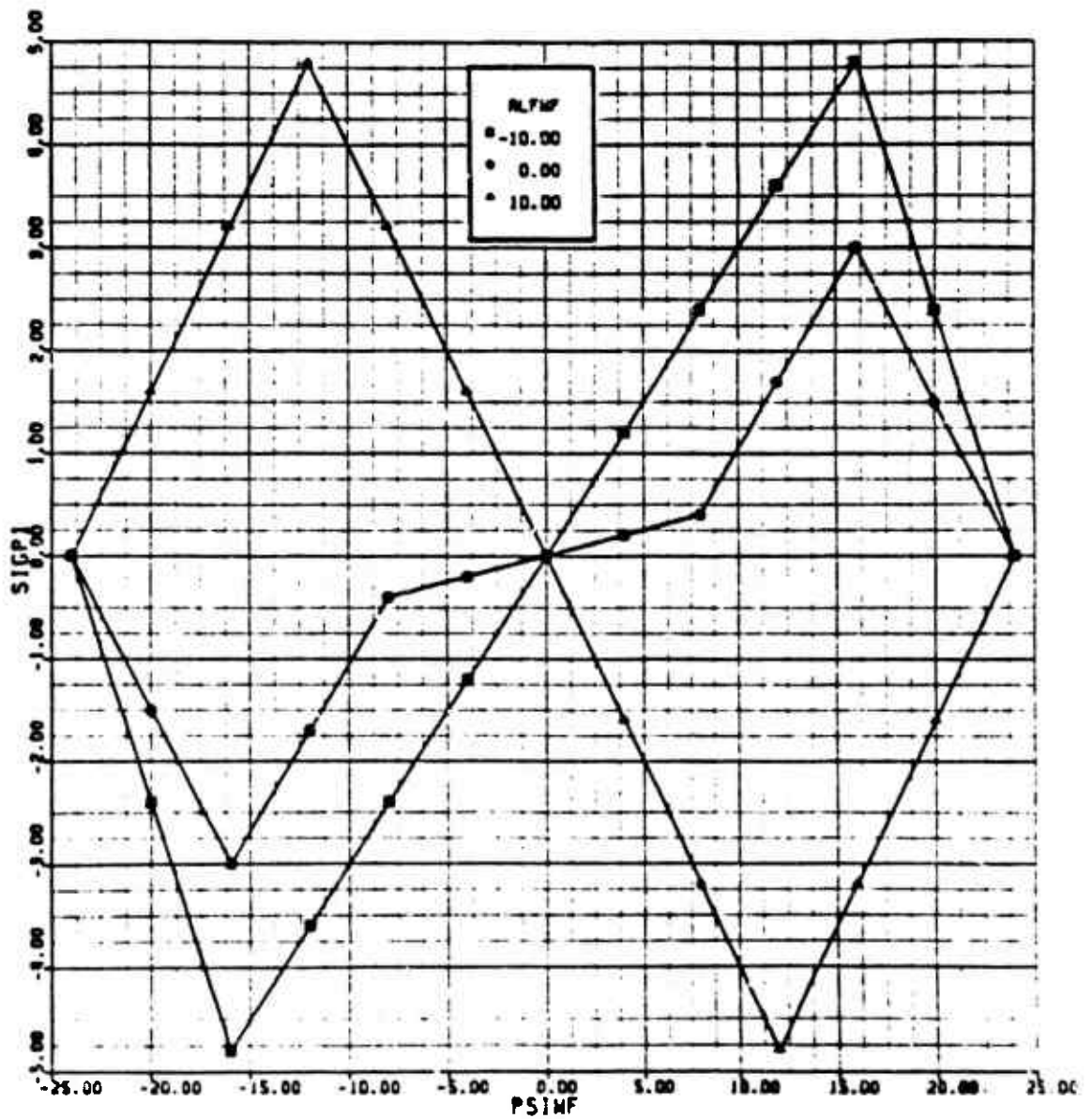


Figure B-22. S-76A Fuselage Sidewash on Vertical Tail Map

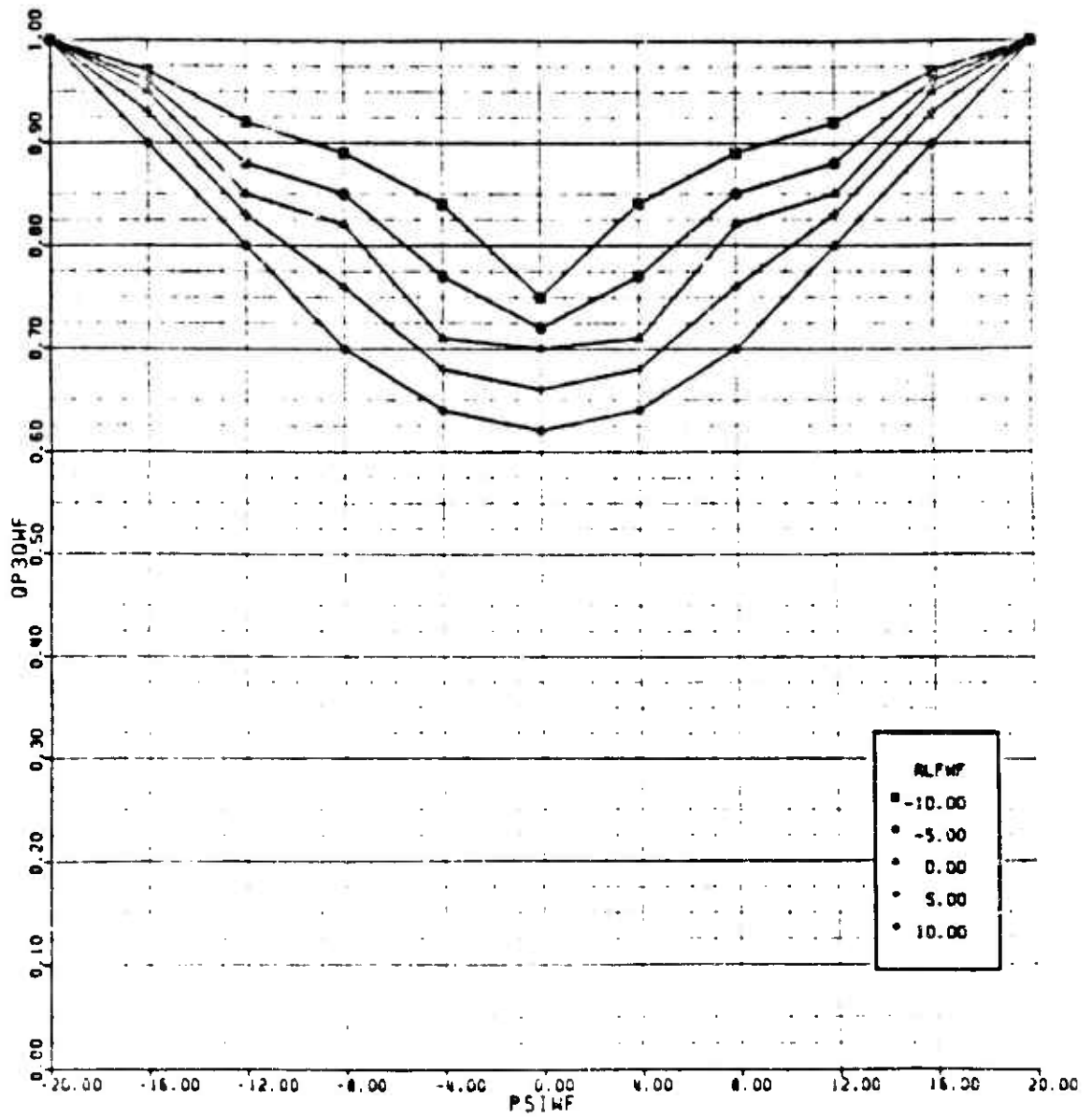


Figure B-23. S-76A Dynamic Pressure Ratio at Vertical Tail Map

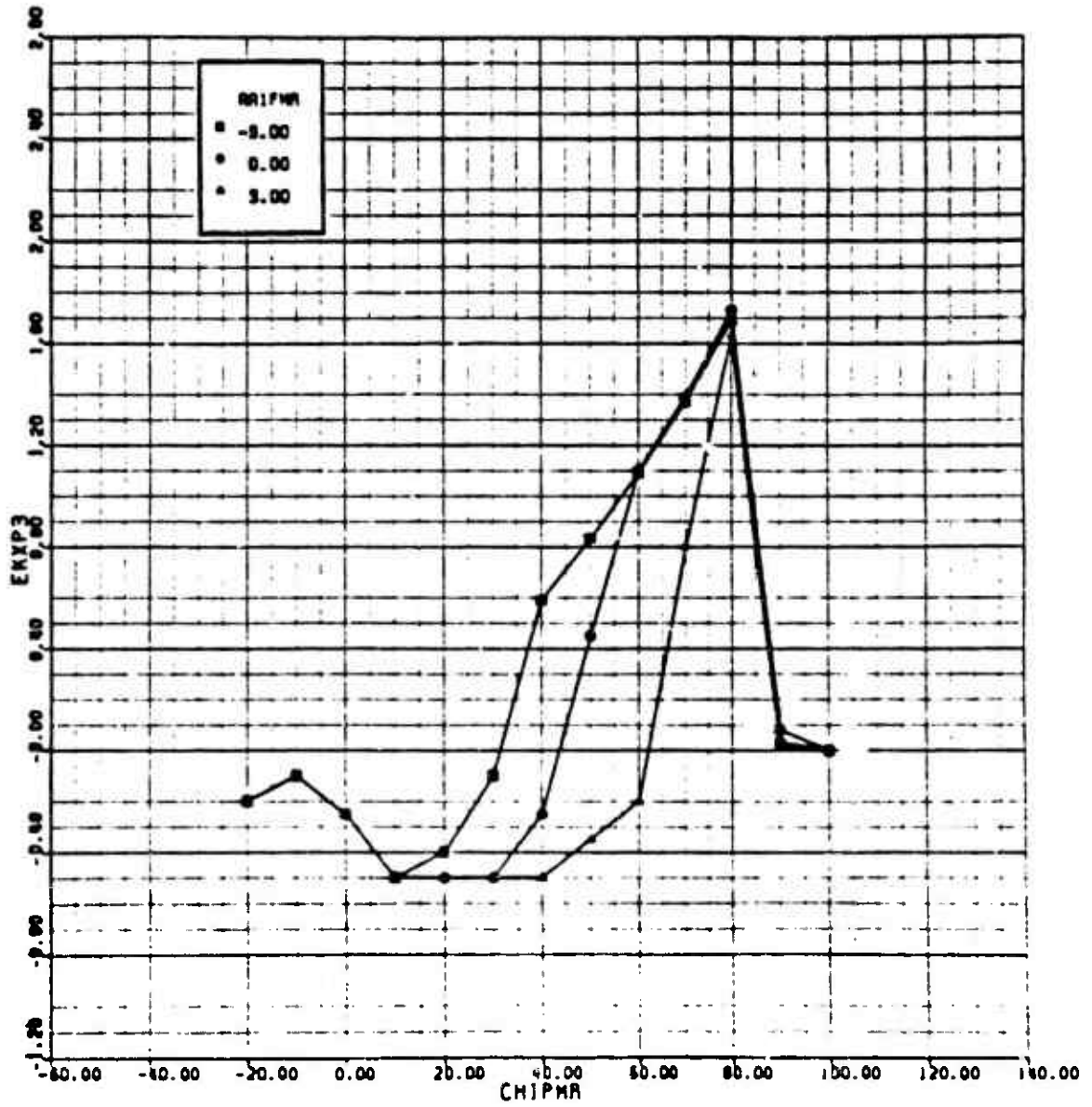


Figure B-24. S-76A Main Rotor Downwash on Vertical Tail Map (x-direction)

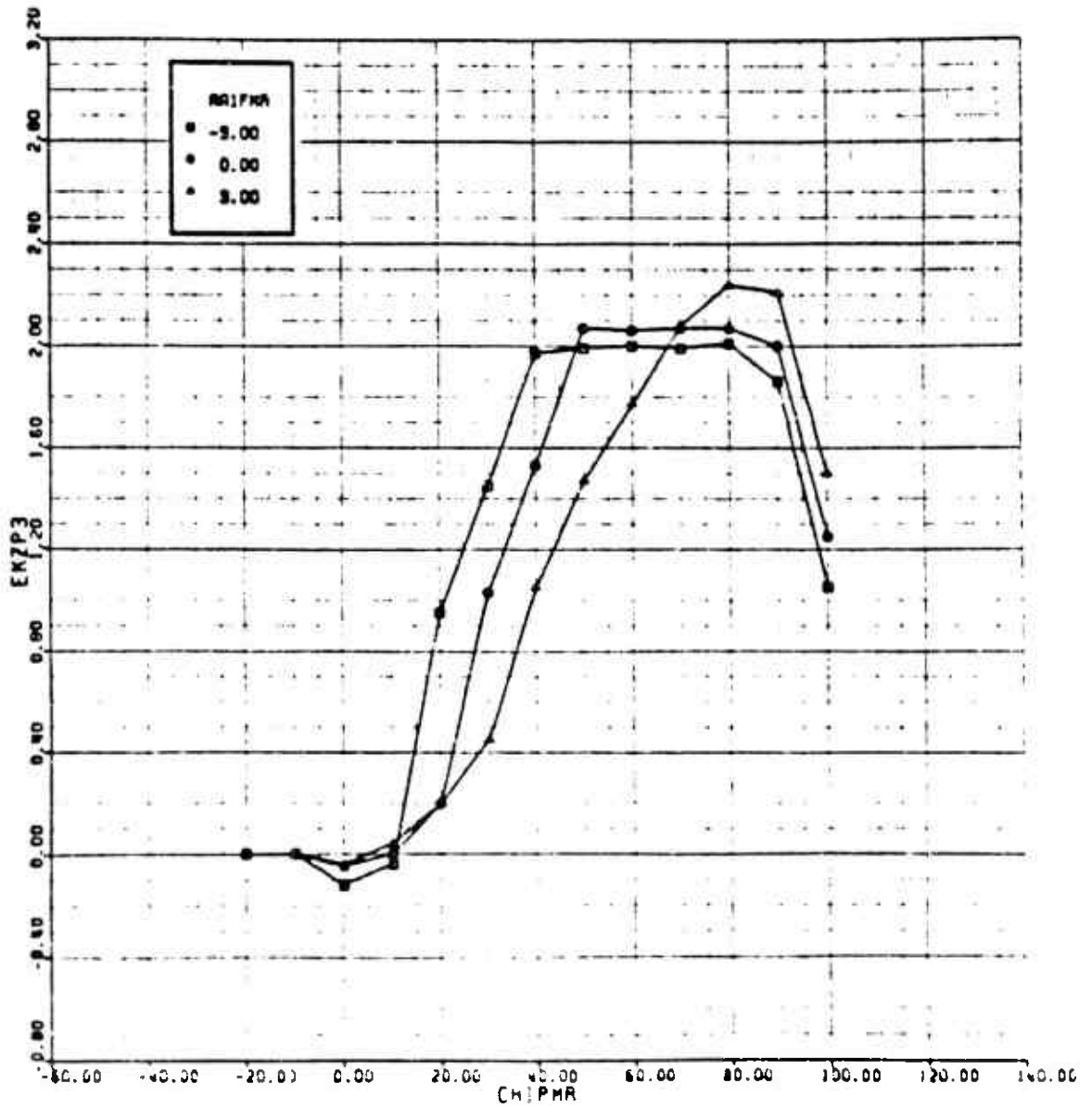


Figure B-25. S-76A Main Rotor Downwash on Vertical Tail Map (z-direction)

APPENDIX C

CH-53E MODEL DATA

The CH-53E (Figure C-1) is the largest assault transport helicopter in the free world. It is an extensively modified derivative of the CH-53D Sea Stallion. Its basic Design Gross Weight is 46,500 pounds, and with internal loads its maximum gross weight is 69,750 pounds. The main rotor is 79 feet in diameter and features seven blades. Three General Electric T64-6E-416 turbo-shaft engines power the CH-53E. These have an IRP rating of 4,113 shp each. Approximately 400 CH-53E helicopters have been produced in two basic variants. CH-53Es are used as assault transports by the U.S. Marine Corps while MH-53Es are used primarily as aerial mine sweepers by the U.S. Navy.

The main rotor is of conventional articulated design with coincident flap and lag hinges. The hinge offset is 6.33 percent. The Super Stallion main rotor blades also employ SC1095 airfoil sections.

The tail rotor is a four-bladed unit 20 feet in diameter. It is of conventional semi-articulated design with flapping hinges but no lag hinges. The fixed horizontal tail is mounted to the top of the vertical fin and has an area of 58 square feet. Both the vertical fin and tail rotor are canted 20 degrees from the vertical. The tail rotor is a pusher type, and the horizontal tail is a gull-wing configuration so most of the surface is horizontal, even though it is attached to the canted fin.

The CH-53E GenHel simulation was already operational at Sikorsky and has been extensively validated against flight test data. Since the CH-53E is a heavy lift transport, its evaluation in this M/A study was made at a medium gross weight of 56,000 pounds and with 105 percent rotor speed. The up-speeded rotor is used operationally for some heavy-lift missions.

All of the numerical data used to model the CH-53E are provided in this appendix. Table C-1 is a listing of all the input data. Figures C-2 through C-24 are plots of the map data for fuselage, vertical tail and horizontal tail aerodynamics along with plots of the rotor interference and fuselage interference data. The tabular data are provided with appropriate labels. Map data are identified with GenHel variable names provided in the List of Symbols.

For the CH-53E model, the panel allocation was as follows:

H1 Horizontal tail
V1 Vertical tail

TABLE C-1. CH-53E SPECIFIC FILE

TITLE CH53E WITH TIP TANKS,EAPS, FLEXIBLE FUSELAGE AND ENGINES

;***** INPUT PARAMETERS FOR MAIN ROTOR MODULES (#A) *****

FSRR:: 336.5 ; FUSELAGE STATION,INCHES
 WLRR:: 259.0 ; WATERLINE STATION,INCHES
 BLMR:: 0.0 ; BUTTLINE STATION,INCHES,(+VE TO PORT)
 RMR:: 39.5 ; RADIUS,FT.
 OMTMR::18.732 ; TRIM ROTATIONAL SPEED (100%)
 BRR:: 7.0 ; ACTUAL NUMBER OF BLADES
 ISRR:: -5.0 ; LONGITUDINAL SHAFT TILT,(POS.BACKWARDS),DEG
 ILMR:: 0.0 ; LATERAL SHAFT TILT,(POS.STARBOARD),DEG
 DELSRR::-10.0 ; SWASHPLATE PHASE ANGLE,DEG
 DEL3MR::0.0 ; FLAPPING HINGE OFFSET ANGLE,DEG.
 KAF1MR::0.0 ; LAGGING HINGE OFFSET COEF.(FUNC(LG))
 KAF2RR::0.0 ; LAGGING HINGE OFFSET COEF.(FUNC(LG**2))
 CHDTRR::2.42 ; BLADE CHORD AT TIP,FT.
 CHDRRR::2.42 ; BLADE CHORD AT ROOT,FT.
 OFSTMR::2.5043 ; HINGE OFFSET,FT.
 SPRLMR::9.33 ; HINGE TO START OF BLADE,FT.
 WTBDRR::652.0 ; WEIGHT OF ONE BLADE,LBS.
 IBMR:: 5918.0 ; BLADE MOMENT OF INERTIA ABOUT HINGE,SLUG-FT**2
 MBMR:: 249.0 ; BLADE MASS MOMENT ABOUT HINGE,SLUG-FT**2
 BTLMM:: .97 ; BLADE TIP CUT OFF RATIO
 DCDMM:: .002 ; DELTA DRAG COEF. FOR EACH SEGMENT
 NBSRR:: 7 ; NUMBER OF BLADES SIMULATED,PIX POINT
 NSSRR:: 5 ; NUMBER OF SEGMENTS SIMULATED,PIX POINT
 DELTHO::.25 ; MAIN ROTOR TWIST DELTA

; *** MAIN ROTOR NON-LINEAR TWIST MAP ***

TWRRMP::UVR00 ;MAP ARGUMENT LOOK-UP ROUTINE
 XSEGR00 ;INPUT - X FROM CENTER OF ROTATION
 TWSTR00 ;OUTPUT - TWIST AT BLADE SEGMENT
 TWRLO ;MAP NAME
 EXP 0.0,1.0,0.05 ;LOWER LIMIT,UPPER LIRIT,DELTA

TWRLO:	EXP	0.0,	0.0,	0.0,	0.0,	0.0
	EXP	0.0,	0.0,	-0.098,	-0.625,	-1.553
	EXP	-2.582,	-3.530,	-8.516,	-5.508,	-6.497
	EXP	-7.447,	-8.242,	-8.823,	-9.372,	-9.830
		-10.667				

;***** MAIN ROTOR DOWNWASH SUBMODULE (#A) *****

KCTRM:: 1.0 ; TBRUST GAIN FOR UNIFORM DOWNWASH
 KCMR:: 0.0 ; PITCH.MOR.GAIN FOR DOWNWASH SIN.HARMONIC
 KSLRR:: 0.0 ; ROLL ROR.GAIN FOR DOWNWASH COS.HARMONIC
 TDW0RR::.01038 ; TIME CONST.FOR UNIFORM DOWNWASH FILTER,SEC
 TDWCHR:: 0.0 ; TIME CONST.FOR DOWNWASH SIN.HARMON.FILTER,SEC.
 TDWSMR:: 0.0 ; TIME CONST.FOR DOWNWASH COS.HARMON.FILTER,SEC.

;***** FLAPPING/LAGGING DAMPER CALCULATIONS (#C) *****

KBPMR:: 0.0 ; FLAPPING HINGE SPRING CONST.FT-LBS/RAD
 KBR.MR::0.0 ; FLAPPING HINGE DAMPER CONST. FT-LBS-SEC/RAD

; **SET OF ROUNDING DIMENSIONS FOR LAG DAMPER,INCHES**
 ALDMR:: 2.40 ; DATA WERE REVISED TO MATCH C/MH-53E DAMPERS
 BLDMP:: 27.983 ; DAMPER RATE IS FUNCTION ONLY OF LAG RATE
 CLEMP:: 0.0 ; ALSO INTRODUCED AIR-SPRING PRE-LOAD (TENSION)
 DLDMP:: 8.835 ; ALL THIS ON 13 JUNE 1988
 RLDMP:: 9.312 ;

TABLE C-1. CH-53E SPECIFIC FILE (Cont'd)

LGOONR::0.0 ; ALIGNMENT OFFSET IN RELATION TO LAG,OEG
 TOLONR::0.0 ; FIXED BLADE PITCH RELATIONSHIP BET. ARM AND THRUFF
 ILOMR:: 4550.0 ; INTERCEPT OF PRE-LOAD FUNCTION, LBS
 SLOMR:: 5730.0 ; SLOPE OF PRE-LOAD (100 LN/DEG), LBS/RAD
 ; TENSION PRODUCES A NEGATIVE LAG NOTION

; *** LAG DAMPER FORCE VS DAMPER ARM RATE ***

LONRMP::UVSUVS66 ;MAP ARGUMENT - LOOK-UP ROUTINE
 LO.NR00(A16) ;INPUT - DAMPER AXIAL VEL IN/SEC
 FLO.NR05(A16) ;OUTPUT - DAMPER FORCE LBS
 LDNRLO ;LOW RANGE MAP NAME
 EXP 0.0,1.0,0.1 ;LOWER LIMIT,UPPER LIMIT, DELTA
 LONRH1 ;HIGH RANGE MAP NAME
 EXP 1.0,8.0,1.0 ;LOWER LIMIT,UPPER LIMIT,DELTA

; REVISED PRODUCTION DAMPER DATA INSERTED 10 FEB 1988

; LOW RA. - MAP
 LONRLO: EXP 0.0, 230.0, 500.0, 1140.0, 1800.0
 EXP 2500.0, 3050.0, 3600.0, 3840.0, 3870.0
 3900.0

; HIGH RANGE MAP
 LONRH1: EXP 3900.0, 4100.0, 4240.0, 4380.0, 4500.0
 EXP 4600.0, 4670.0, 4700.0

;***** INPUT PARAMETERS FOR FUSELAGE/WING (#A) *****
 ;***** MOUNTING POINT OF MODEL IN WIND TUNNEL *****

FSWF:: 336.4 ; FUSELAGE STATION, IN.
 WLWF:: 161.4 ; WATERLINE STATION, IN.
 MLWF:: 0.0 ; MIDLIN STATION, IN. (+VE TO PORT)
 IW:: 0.0 ; WING INCIDENCE, OEG.

;**CH-53E TAIL-OFF TANKS-ON EAPS-ON BODY DATA**
 ; UPDATED 8-21-87

;**FUSELAGE LIFT VS ALPHA MAP CH-53E**

;UPDATED WITH SER-13491 INFO 8-21-87

LQFMP::UVR00 ;UNIVARIATE
 ALPWF00 ;WING- US ANGLE OF ATTACK, INPUT
 LQF00 ;FUSELAGE LIFT, FT SQ, OUTPUT
 LQFLO ;NAME OF PRIMARY SET OF MAP DATA
 EXP -25.0,25.0,5.0 ;ALFA RANGE AND DELTA ALFA
 ;(PSINT = 0)
 LQFLD: EXP -304.5, -250.7, -177.4, -94.65, -45.0, 0.0
 EXP 42.5, 100.0, 172.5, 240.00, 304.5

;**FUSELAGE DRAG VS ALPHA MAP CH-53E**

; UPDATE WITH SER-13491 INFO 8-21-87

DQFMP::UVR00 ;UNIVARIATE
 ALPWF00 ;IN ALFA W-P
 DQF00
 DQFLO
 EXP -25.0,25.0,5.0 ;ALFA RANGE AND DELTA ALFA
 ;(PSINT = 0)
 DQFLO: EXP 152.0, 116.0, 92.00, 72.0, 62.0, 55.0
 EXP 62.0, 72.0, 90.00, 116.0, 154.5

TABLE G-1. CH-53E SPECIFIC FILE (Cont'd)

```

; **FUSELAGE PITCH MOMENT VS ALPHA MAP CH-53E**
; UPDATED WITH SER-13491 INFO 8-21-87
; UNIVARIATE
; IN ALPHA W-F
MOFMP: :UVR00
        ALFMP00
        MOF00
        MOFLO
        EXP -25.0,25.0,5.0 ;ALPHA RANGE AND DELTA ALPHA
; (PSINT = 0)
MOFLO: EXP -1175.2, -1162.6, -1126.2, - 937.8, - 502.0, 80.0
        EXP 603.0, 1200.0, 1622.9, 2227.2, 2354.0

; **FUSELAGE LIPT VS PSI MAP CH-53E**
; UPDATED WITH SER-13491 INFO 8-21-87
; BIVARIATE
; IN PSI AND ALPHA
DLOFMP: :BIV00
        EXP PSIMF00,ALFMP00
        DLOF00
        DLOFLO
        EXP -25.0,25.0,5.0,13 ;PSI RANGE WITH OEL PSI AND 13 POINTS(OCT)
        EXP -10.0,10.0,10.0 ;ALPHA RANGE WITH DEL ALPHA
; (ALP=-10)
DLOFLO: EXP -60.4, -49.0, -36.0, -22.8, - 7.4, 0.0
        EXP - 6.8, -20.5, -34.4, -44.4, -54.7
; (ALP= 0 )
        EXP -37.3, -24.0, -12.7, - 5.4, - 1.0, 0.0
        EXP 2.0, 3.4, 2.7, - 2.8, -18.9
; (ALP= 10)
        EXP - 4.7, 7.4, 6.9, 5.7, 3.8, 0.0
        EXP 15.0, 16.5, 11.2, 9.5, -7.7

; **FUSELAGE DRAG VS PSI MAP CH-53E**
; UPDATED WITH SER-13491 INFO 8-21-87
; BIVARIATE
; IN PSI AND ALPHA
ODOFMP: :BIV00
        EXP PSIMF00,ALFMP00
        ODOF00
        ODOFLO
        EXP -25.0,25.0,5.0,13 ;PSI RANGE,OEL PSI,13 PTS (OCT)
        EXP -10.0,10.0,10.0 ;ALPHA RANGE,DEL ALP
; (ALP=-10)
ODOFLO: EXP 78.3, 47.0, 27.8, 12.5, 3.5, 0.0
        EXP 5.3, 13.8, 29.6, 49.7, 82.0
; (ALP= 0 )
        EXP 65.9, 41.4, 23.8, 12.4, 4.2, 0.0
        EXP 2.5, 9.0, 20.0, 38.3, 68.8
; (ALP= 10)
        EXP 60.2, 35.7, 18.5, 8.0, 2.5, 0.0
        EXP 3.5, 9.5, 20.9, 36.4, 58.7

```

TABLE C-1. CH-53E SPECIFIC FILE (Cont'd)

```

; **FUSELAGE PITCH MOMENT WITH PSI CH-53E**
; UPDATED WITH SER-13491 INFO 8-21-87
; BIVARIATE
; IN PSI AND ALFA
DMQFMP::RIV00
EXP PSIMP00,ALPMP00
DMQF00
DMQFLO
EXP -25.0,25.0,5.0,13 ; PSI RANGE,DEL PSI,13 PTS (OCT)
EXP -10.0,10.0,10.0 ; ALF RANGE,DEL ALF
; (ALF=-10)
DMQFLO: EXP 500.0, 545.0, 460.0, 305.0, 95.0, 0.0
EXP 110.0, 410.0, 730.0, 670.0, 830.0
; (ALF= 0 )
EXP 420.0, 255.0, 105.0, 35.0, 5.0, 0.0
EXP 5.0, 25.0, 75.0, 210.0, 420.0
; (ALF= 10)
EXP 315.0, 210.0, 115.0, 45.0, 20.0, 0.0
EXP 20.0, 75.0, 180.0, 215.0, 460.0

; **FUSELAGE SIDE FORCE WITH PSI CH-53E**
; UPDATED WITH SER-13491 INFO 8-21-87
; BIVARIATE
; IN PSI AND ALFA
TOPMP::RIV00
EXP PSIMP00,ALPMP00
TOP00
TOPFLD
EXP -25.0,25.0,5.0,13 ; PSI RANGE,DEL PSI,13 PTS(OCT)
EXP -10.0,10.0,10.0 ; ALF RANGE,DEL ALF
; (ALF=-10)
TOPFLD: EXP -124.0, - 91.0, - 58.0, - 30.0, - 11.0, 0.0
EXP 13.0, 31.0, 60.0, 86.0, 116.0
; (ALF= 0 )
EXP -152.0, -134.0, -105.0, - 75.0, - 36.0, 0.0
EXP 25.0, 50.0, 76.0, 112.0, 144.0
; (ALF= 10)
EXP -164.0, -157.0, -120.0, - 85.0, - 46.0, 0.0
EXP 36.0, 75.0, 105.0, 136.0, 166.0

; **FUSELAGE ROLL MOMENT WITH PSI CH-53E**
; **UPDATED ALF=0 DATA WITH SER 13491 INFO**
; BIVARIATE
; IN PSI AND ALFA
ROFMP::RIV00
EXP PSIMP00,ALPMP00
ROF00
ROFLD
EXP -25.0,25.0,5.0,13 ; PSI RANGE,DEL PSI,13 PTS(DCT)
EXP -10.0,10.0,10.0 ; ALF RANGE,DEL ALF
; (ALF=-10)
ROFLD: EXP 320.0, 245.0, 160.0, 115.0, 60.0, 0.0
EXP - 30.0, - 85.0, -155.0, -230.0, -300.0
; (ALF= 0 )
EXP -100.0, -160.0, -200.0, -190.0, -150.0, -40.0
EXP 90.0, 225.0, 340.0, 335.0, 275.0
; (ALF= 10)
EXP -165.0, -190.0, -115.0, - 60.0, - 20.0, 45.0
EXP 115.0, 175.0, 255.0, 240.0, 160.0

```

TABLE C-1. CH-53E SPECIFIC FILE (Cont'd)

```

; **FUSELAGE YAW MOMENT WITH PSI CH-53E**
; **UPDATED ALP=0 WITH SER-13491 INFO 8-21-87

NQFMP:;BIV## ;BIVARIATE
EXP PSIMP##,ALFWF## ;IN PSI AND ALFA
NQF##
NQFLO
EXP -25.0,25.0,5.0,13 ;PSI RANGE,DEL PSI,13 PTS(OCT)
EXP -10.0,10.0,10.0 ;ALF RANGE,DEL ALFA
; (ALP=-10)

NQFLO: EXP -1620.0,-1630.0,-1550.0,-1320.0,- 660.0, 0.0
EXP 690.0, 1200.0, 1510.0, 1640.0, 1660.0
; (ALP= 0 )
EXP -1240.0,-1140.0,- 980.0,- 760.0,- 460.0, -100.0
EXP 270.0, 660.0, 1040.0, 1200.0, 1200.0
; (ALP= 10)
EXP - 820.0,- 730.0,- 590.0,- 400.0,- 200.0, 0.0
EXP 200.0, 400.0, 590.0, 770.0, 850.0

;***** ROTOR INTERFERENCE ON THE FUSELAGE (MRPA) *****

; **ROTOR DOWNWASH ON FUS. ERKF CH-53E**
; **MAP CHANGED TO BIV AND NEW VALUES INSERTED
; 8-21-87. NEW WAKL MAP FROM IBM ANALYSIS PROGRAM
; UNIFORM DISTRIBUTION

EXWFP:;BIV## ;A UNIVARIATE
EXP CNIPMR##,AALFMR## ;IN CHI TIP PATH PLANE
ERXWF## ;OUTPUT
EXWFLO
EXP 0.0,100.0,10.0,13 ;WHICH VARIES FROM 0 TO 100 DEG IN STEPS OF 10
EXP -6.0,6.0,6.0
; AALFMR=-6 DEG
EXWFLO: EXP 0.22, 0.32, 0.42, 0.52, 0.63, 0.74, 0.86, 0.92, -0.85
EXP -0.85, -0.85
; AALFMR=0 DEG
EXP 0.09, 0.19, 0.29, 0.40, 0.49, 0.63, 0.76, 0.89, -0.9
EXP -0.8, -0.8
; AALFMR=6 DEG
EXP -0.06, 0.04, 0.15, 0.27, 0.38, 0.50, 0.63, -0.17
EXP -0.93, -0.87

; **ROTOR DOWNWASH ON FUS. ERKF CH-53E**
; **MAP WAS REVISED ON 8-21-87 BASED ON NEW RUNS
; OF IBM ANALYSIS USING UNIFORM DISTRIBUTION

EZWFMP:;BIV## ;A UNIVARIATE
EXP CNIPMR##,AALFMR## ;IN CHI TIP PATH PLANE
ERZWF##
EZWFLO
EXP 0.0,100.0,10.0,13 ;FROM 0 TO 100 DEG IN STEPS OF 10
EXP -6.0,6.0,6.0
; AALFMR=-6 DEG
EZWFLO: EXP 1.20, 1.20, 1.19, 1.18, 1.16, 1.15
EXP 1.13, 1.11, 0.91, 0.71, 0.71
; AALFMR=0 DEG
EXP 1.20, 1.22, 1.22, 1.23, 1.22, 1.23, 1.23
EXP 1.23, 0.93, 0.73, 0.73
; AALFMR=6 DEG
EXP 1.20, 1.22, 1.23, 1.23, 1.27, 1.29, 1.30
EXP 1.02, 0.90, 0.64, 0.64

```

TABLE C-1. CH-53E SPECIFIC FILE (Cont'd)

```

;***** INPUT PARAMETERS FOR HORIZONTAL TAIL H1 *****

PSN1:: 879.4 ; PUCELAGE STATION, INCH
WLMI:: 302.7 ; WATERLINE STATION, INCH
BLH1:: -48.0 ; BUTTLINE STATION, INCH(+VE TO PORT)
SAH1:: 58.0 ; SURFACE AREA OF PANEL IF NOT INCLUDE IN MAP
IH1:: 0.0 ; TAIL INCIDENCE, DEG

; **HORIZONTAL TAIL LIPT (CL) MAP CH-53E**
; LIPT UPDATED USING SER-13491 INPO 8-21-87

CLHIMP::UVR00 ; UNIVARIATE FOR TAIL ASSEMBLY
ALPHH100 ; IN ALFA HT
CLH100
CLH1LO
EXP -90.0,90.0,5.0 ; FROM -90 TO 90 DEG IN STEPS OF 5 DEG
; INT= 0 DEG
CLH1LO: EXP 0.0, -0.11, -0.22, -0.30, -0.38, -0.44, -0.49, -0.54, -0.58
EXP -0.59, -0.60, -0.59, -0.58, -0.57, -0.60, -0.86, -0.77, -0.41, -0.05
EXP 0.21, 0.48, 0.63, 0.57, 0.54, 0.56, 0.58, 0.59, 0.59
EXP 0.58, 0.54, 0.49, 0.44, 0.38, 0.30, 0.22, 0.11, 0.0

; **HORIZONTAL TAIL DRAG (CD) MAP CN-53E**
; UPDATED WITH SER-13491 INPO 8-21-87
CDHIMP::UVR00 ; UNIVARIATE FOR TAIL ASSEMBLY
ALPHH100 ; IN ALFA HT
CDH100
CDH1LO
EXP -90.0,90.0,5.0 . FROM -90 TO 90 DEG IN STEPS OF 5 DEG
; INT= 0 DEG
CDH1LO: EXP 1.30, 1.25, 1.20, 1.14, 1.08, 1.01, 0.94, 0.87, 0.80
EXP 0.72, 0.64, 0.56, 0.48, 0.39, 0.31, 0.22, 0.12, 0.07, 0.05
EXP 0.07, 0.12, 0.22, 0.31, 0.39, 0.48, 0.56, 0.64, 0.72
EXP 0.80, 0.87, 0.94, 1.01, 1.08, 1.14, 1.20, 1.25, 1.30

;***** ROTOR INTERPERENCE ON THE HORIZ TAIL H1 (MRPA) *****

; **ROTOR DOWNWASH ON H.T. ERXHT CH-53E**
; UPDATED 8-21-87
EXHIMP::BIV00 ; A BIVARIATE
EXP CHIPR00, AALPHR00 ; IN CHITPP AND AI PLAPPING
EXH100
EXH1LO
EXP 0.0,100.0,10.0,13 ; WITH CHITPP FROM 0 TO 100 DEG, DEL 10,13(8)PTS
EXP -6.0,6.0,6.0 ; AND AAIIF FROM -6 TO 6 , DEL 6 DEG
; AIP=-6 DEG
EXH1LO: EXP -0.70, -0.74, -0.78, -0.80, -0.79, -0.72
EXP -0.59, -0.37, 1.55, 1.85, 1.85
; AIP=0 DEG
EXP -0.64, -0.65, -0.66, -0.65, -0.62, -0.56
EXP -0.45, -0.28, -0.06, 0.15, 0.15
; AIP=6 DEG
EXP -0.48, -0.52, -0.52, -0.51, -0.45, -0.43
EXP -0.35, -0.23, -0.06, 0.14, 0.14

```


TABLE C-1. CH-53E SPECIFIC FILE (Cont'd)

```

; **ROTOR DOWNWASH ON H.T. EKZHT CH-53E**
; **UPDATED 8-21-87
EZHIMP::BIV66 ;A BIVARIATE
EXP CHIPMR00,AAIPMR00 ;IN CHITPP AND AI FLAPPING
EKZHI00
EZHILO
EXP 0.0,100.0,10.0,13 ;FOR CHITPP FROM 0 TO 100 DEG,DEL 10, 13(8)PTS
EXP -6.0,6.0,6.0 ;AND AI DF -6,0,6 DEG
;ALF=-6 DEG
EZHILO: EXP 0.00, 0.15, 0.32, 0.52, 0.74, 0.97
EXP 1.18, 1.31, 1.32, 1.18, 1.18
;ALF= 0 DEG
EXP 0.20, 0.28, 0.41, 0.56, 0.73, 0.91
EXP 1.09, 1.24, 1.27, 1.11, 1.10
;ALF= 6 DEG
EXP 0.18, 0.29, 0.40, 0.51, 0.63, 0.77
EXP 0.92, 1.06, 1.16, 1.16, 1.16

;***** FUSELAGE INTERFERENCE ON HDRIZ TAIL H1 (WPPA) *****

QHIMP::CONST00 ;**DYNAMIC PRESSURE RATIO AT H.T. CH-53E**
[0.9] ;A CONSTANT VALUE IS USED
CHIOWF00 ;EQUAL TO 0.9

; **FUSELAGE DOWNWASH DN HDRIZ. TAIL CH-53E**
EPHIMP::UVR00 ;UNIVARIATE
ALFWF00 ;ALFA DEG INPUT
EPSHI00 ;EPSILON DEG OUTPUT
EPHILD
EXP -30.0,30.0,5.0 ;ALFA RANGE AND DEL ALFA
;BDDY DOWNWASH DN HORIZONTAL TAIL
EPHILD: EXP 0.0, -6.5, -5.6, -4.7, -3.8, -2.9, -2.0
EXP -1.1, -0.2, 0.7, 1.6, 0.0, 0.0

; **FUSELAGE SIDEMASH ON HORIZ. TAIL CH-53E**
SGHIMP::CDNST00 ;A VALUE IS USED WHICH IS
SIGVI00 ;EQUAL TO THE VERTICAL TAIL
SIGHI00

```

TABLE C-1. CH-53E SPECIFIC FILE (Cont'd)

```

;***** INPUT PARAMETERS FOR VERTICAL TAIL V1 (A) *****
FSV1:: 861.2          ; FUSELAGE STATION, INCH
NLV1:: 247.0         ; WATERLINE STATION, INCH
BLV1:: 0.0           ; BUTTLINE STATION, INCH (+VE TO PORT)
SAV1:: 74.0         ; SURFACE AREA OF PANEL IF NOT INCLUDE IN MAP
IV1:: 2              ; TAIL INCIDENCE, DEG
                    ; 5 DEG L.E. RIGHT IS INHERENT IN W.T. DATA
                    ; **VERTICAL TAIL LIFT (CLVT) MAP CH-53E**
                    ; LIFT UPDATED PER SER 13491 INFO 8-21-87

CLVIMP::UVR00
        BETVV100     ; IN BETA (-PSI WT)
        CLV100
        CLV1LO
        EXP -90.0,90.0,5.0 ; FROM -90 TO 90 IN STEPS OF 5 DEG
                                ; IVT= 5 DEG
CLVILD: EXP 0.0, -0.13, -0.22, -0.30, -0.37, -0.43, -0.49, -0.53, -0.56
        EXP -0.59, -0.60, -0.61, -0.61, -0.66, -0.89, -0.77, -0.61, -0.43, -0.27
        EXP -0.11, 0.05, 0.22, 0.38, 0.54, 0.70, 0.89, 0.79, 0.65
        EXP 0.60, 0.55, 0.50, 0.44, 0.38, 0.31, 0.23, 0.13, 0.0
                    ; **VERTICAL TAIL DRAG (CDVT) MAP CH-53E**
                    ; DRAG UPDATED PER SER 13491 INFO 8-21-87
CDVIMP::UVR00
        BETVV100     ; IN BETA (-PSI WT)
        CDV100
        COVILD
        EXP -90.0,90.0,5.0 ; FROM -90 TO 90 IN STEPS OF 5 DEG
                                ; IVT= 5 DEG
CDVILD: EXP 1.30, 1.19, 1.10, 1.01, 0.93, 0.84, 0.76, 0.69, 0.61
        EXP 0.53, 0.47, 0.40, 0.34, 0.29, 0.24, 0.20, 0.16, 0.14, 0.11
        EXP 0.09, 0.10, 0.10, 0.11, 0.12, 0.15, 0.18, 0.23, 0.29
        EXP 0.36, 0.45, 0.55, 0.66, 0.80, 0.93, 1.05, 1.18, 1.30

;***** ROTOR INTERFERENCE ON THE VERTICAL TAIL H1 (MRPA) ***
                    ; **ROTOR DOWNWASH DN V.T. EXKVT CH-53E**
                    ; UPDATED 8-21-87

EXVIMP::BIV00
        EXP CH1PFR00, AA1PFR00
        EXKV100
        EXV1LO
        EXP 0.0,100.0,10.0,13
        EXP -6.0,6.0,6.0

                    ; ALF=-6
EXVILD: EXP -0.70, -0.77, -0.88, -0.93, 1.15, 1.36
        EXP 1.62, 1.52, 0.58, 0.0, 0.0

                    ; ALF=0 DEG
        EXP -0.65, -0.88, -0.94, -0.98, -0.97, -0.91
        EXP -0.78, -0.51, 2.84, 1.80, 1.80

                    ; ALF = 6 DEG
        EXP -0.73, -0.75, -0.77, -0.77, -0.73, -0.67
        EXP -0.55, -0.38, -0.15, 1.10, 1.10

```

TABLE C-1. CH-53E SPECIFIC FILE (Cont'd)

```

; **ROTOR DOWNWASH ON V.T. EKZVT CH-53E**
; UPDATED 8-21-87

EZVIMP::BIV00
      EXP CHIPMR00,AA1FMR00
      EKZV100
      EZV1LO
EX: 0.0, 100.0, 10.0, 13
EXP -6.0, 6.0, 6.0

      ;ALF = -6
EZV1LO:: EXP -0.26, -0.07, 0.12, 0.40, 2.65, 2.33, 2.00
      EXP 1.45, 0.64, 0.0, 0.0

      ;ALF=0 DEG
EX: -0.10, 0.08, 0.26, 0.48, 0.72, 0.97, 1.21
EXP 1.37, 1.80, 0.50, 0.50

      ;ALF = 6 DEG
EX: 0.12, 0.27, 0.42, 0.58, 0.76, 0.95, 1.14
EXP 1.29, 1.32, 1.18, 1.18

;***** FUSELAGE INTERFERENCE ON VERTICAL TAIL H1 (MPPA) ***

      ; **DYNAMIC PRESSURE RATIO AT V.T. CH-53E**

QVIMP::CONST00      ;A CONSTANT VALUE IS USED
      [0.9]          ;EQUAL TO 0.9 REV 6-15-79
      QV1QMP00

      ; **FUSELAGE DOWNWASH ON VERTICAL TAIL CH-53E**

EPVIMP::CONST00     ;A VALUE IS USED WHICH IS
      EPSH100        ;EQUAL TO THE HORIZONTAL TAIL
      EPSV100

      ; **FUSELAGE SIDEWASH ON VERTICAL TAIL CH-53E**

SGVIMP::CONST00     ;A CONSTANT VALUE IS USED (SG=SIGMA)
      [+1.00]        ;EQUAL TO +1.00 REV 8-21-87
      SIGV100

```

TABLE C-1. CH-53E SPECIFIC FILE (Cont'd)

```

***** INPUT PARAMETERS FOR TAIL ROTOR (#A) - (BAILEY) *****

RTR::      10.0      ;RADIUS,FT
OMEGTR::   73.205   ;TRIM ROTATIONAL RATE,RAD/SEC @ 100% MAIN ROTOR SPEED
BTR::      4.0       ;ACTUAL NUMBER OF BLADES
FSTR::     930.7    ;FUSELAGE STATION,IN
WLTR::     289.9    ;WATERLINE STATION ,IN
BLTR::     80.36    ;BUTTLINE STATION,IN(+VE TO PORT)
TWSTTR::   -8.0     ;BLADE TWIST,DATUM CENTER OF ROTATION,DEG
BIASTR::   0.0      ;BLADE PITCH CORRECTION, N.L.TWIST (NEG REDUCES PITCH)
GAMTR::    70.0     ;TAIL ROTOR CANT ANGLE,DEG
OEL3TR::   45.0     ;FLAPPING HINGE OFFSET ANGLE,DEG
DEL3TR::   0.0005   ;RATE OF CHANGE OF CONE ANGLE WITH THRUST,DEG/LB
CHROTR::   1.283    ;BLADE CHORO,FT
ATR::      5.73     ;BLADE LIFT CURVE SLOPE,1/RAD
BTLTR::    0.92     ;BLADE TIP LOSS FACTOR
COTR::     2.0      ;TAIL ROTOR HEAD DRAG,FT**2

                                ;FOR TRB
IBTR::     38.22    ;BLADE MOMENT OF INERTIA ABOUT HINGE,SLUG-FT**2
OROOTR::   0.0087   ;BLADE SECTION DRAG COEFFICIENT, WHERE
OROLTR::   -0.0216 ;CD-ORD0TR+OROLTR*ALFA+DRO2TR*ALFA**2
ORD2TR::   1.425    ;1.187 FOR 100% NR CH-53E
OROTR::    -1.0     ;OIRECTION OF ROTATION,(-)=UPPER TIP AFT

                                ;FOR TRCFAL.MAC
INTR::     183.43   ;FOR DRIVE LOSS
                                ; FOR DOWNWASH LAG
TAUDTR::   0.01038 ; TIME CONSTANT SAME AS MAIN ROTOR

***** MAIN ROTOR INTERFERENCE ON THE TAIL ROTOR (MRPA) *****

                                ;**MAIN ROTOR DOWNWASH ON TR  EXXTR CH-53E**
                                ;**UPOATEO 8-21-87

EXTRMP::BIV00
          EXP CHIPMR00,AA1PMR00
          EXXTR00
          EXTRLO
          EXP 0.0, 100.0,10.0,13
          EXP -6.0,6.0,6.0

                                ;ALF = -6
EXTRLO:  EXP  -0.48,  -0.53,  -0.58,  -0.62,  -0.63,  -0.61,  -0.52
          EXP  -0.34,   2.59,   1.85,   1.85

                                ;ALF = 0
          EXP  -0.46,  -0.50,  -0.54,  -0.56,  -0.56,  -0.54,  -0.47
          EXP  -0.34,  -0.15,   0.03,   0.03

                                ;ALF = 6
          EXP  -0.43,  -0.45,  -0.47,  -0.48,  -0.48,  -0.46,  -0.41
          EXP  -0.32,  -0.17,   0.03,   0.03

```

TABLE C-1. CH-53E SPECIFIC FILE (Cont'd)

```

;***MAIN ROTOR DOWNWASH ON TP ERZTR CH-53E**
;UPDATED 8-21-87

EZTRMP::BIV00
      EXP CHIPMR00,AAIPMR00
      ERZTR00
      EZTRLO

      EXP 0.0,100.0,10.0,13
      EXP -6.0,6.0,6.0

;ALF= -6
EZTRLO:  EXP 0.0, 0.09, 0.22, 0.38, 0.57, 0.86, 1.02
      EXP 1.16, 1.14, 0.90, 0.90

;ALF = 0
      EXP 0.0, 0.14, 0.25, 0.38, 0.54, 0.73, 0.92
      EXP 1.10, 1.14, 0.95, 0.95

;ALF= 6 DEG
      EXP 0.0, 0.17, 0.26, 0.37, 0.49, 0.64, 0.80
      EXP 0.97, 1.10, 0.98, 0.98

;***** FUSELAGE INTERFERENCE ON TAIL ROTOR (WPPA) *****

;***DYNAMIC PRESSURE RATIO AT T.R. CH-53E**

QTRMP::CONST00 ;A VALUE IS USED WHICH IS
      QV1QWF00 ;EQUAL TO THE VERTICAL TAIL
      QTRQWF00

;***FUSELAGE DOWNWASH ON TAIL ROTOR CH-53E**

EPTRMP::CONST00 ;A VALUE IS USED WHICH IS
      EPSV100 ;EQUAL TO THE VERTICAL TAIL
      EPSTR00

;***FUSELAGE SIDEWASH ON TAIL ROTOR CH-53E**

SGTRMP::CONST00 ;A VALUE IS USED WHICH IS
      SIGV100 ;EQUAL TO THE VERTICAL TAIL
      SIGTR00

;***** VERTICAL TAIL INTERFERENCE ON TAIL ROTOR INFLOW *****

VBVTR:: 40.0 ; AIRSPEED BREAK PT. - NO BLOCKAGE ABOVE,KT.
KBVTR:: 0.862 ; TAIL ROTOR BLOCKAGE COEF. AT HOVER

```

TABLE C-1. CH-53E SPECIFIC FILE (Cont'd)

***** INPUT PARAMETERS FOR EQUATIONS OF MOTION (#A) *****

FSCG:: 355.0 ; FUSELAGE STATION, OF C.G., INCH
 WLCG:: 162.3 ; WATERLINE STATION OF C.G., INCH
 BLCCG:: 0.0 ; BUTTLINE STATION OF C.G., INCH(+VE TO PORT)

WEIGHT:: 46000.0 ; AIRCRAFT GROSS WEIGHT, LBS.
 IX:: 60539.0 ; INERTIA ABOUT BODY X-AXIS, SLUG-FT**2
 IY:: 296694.0 ; INERTIA ABOUT BODY Y AXIS, SLUG-FT**2
 IZ:: 275834.0 ; INERTIA ABOUT BODY Z AXIS, SLUG-FT**2
 IXZ:: 23343.0 ; CROSS COUPLING INERTIA, SLUG-FT**2
 IXY:: 0.0
 IYZ:: 0.0

***** INPUT PARAMETERS FOR NOASE (#A) *****

; ** NO MIXING AND NO PBA **

AISUL:: 10.2 ; AIS UPPER LIMIT, RIG COLL AND PED
 AISLL:: -9.8 ; AIS LOWER LIMIT
 BISUL:: 18.0 ; B1S UPPER LIMIT, RIG COLL AND PED
 BISLL:: -8.0 ; B1S LOWER LIMIT
 THOUL:: 22.047 ; THETA0 UPPER LIMIT, THETA.75U = 14.6
 THOLL:: 4.447 ; THETA0 LOWER LIMIT, THETA.75L = -3.0
 THRUL:: 24.0 ; THETTR UPPER LIMIT, RIG COLL
 THRLL:: -10.0 ; THETTR LOWER LIMIT, RIG COLL

XAUL:: 9.25 ; LAT STICK UPPER LIMIT
 XALL:: 0.0 ; LAT STICK LOWER LIMIT
 XBUL:: 8.956 ; LONG STCR UPPER LIMIT, PBA CENTERED (0 AT 120 KN)
 XBLL:: 0.0 ; LONG STCR LOWER LIMIT
 XCUL:: 11.0 ; COLL STCK UPPER LIMIT, WITH INACTIVE 1 INCH
 XCLL:: 0.0 ; COLL STCK LOWER LIMIT
 XPUL:: 4.173 ; PEDAL UPPER LIMIT, NO OVERTRAVEL
 XPLL:: 0.0 ; PEDAL LOWER LIMIT

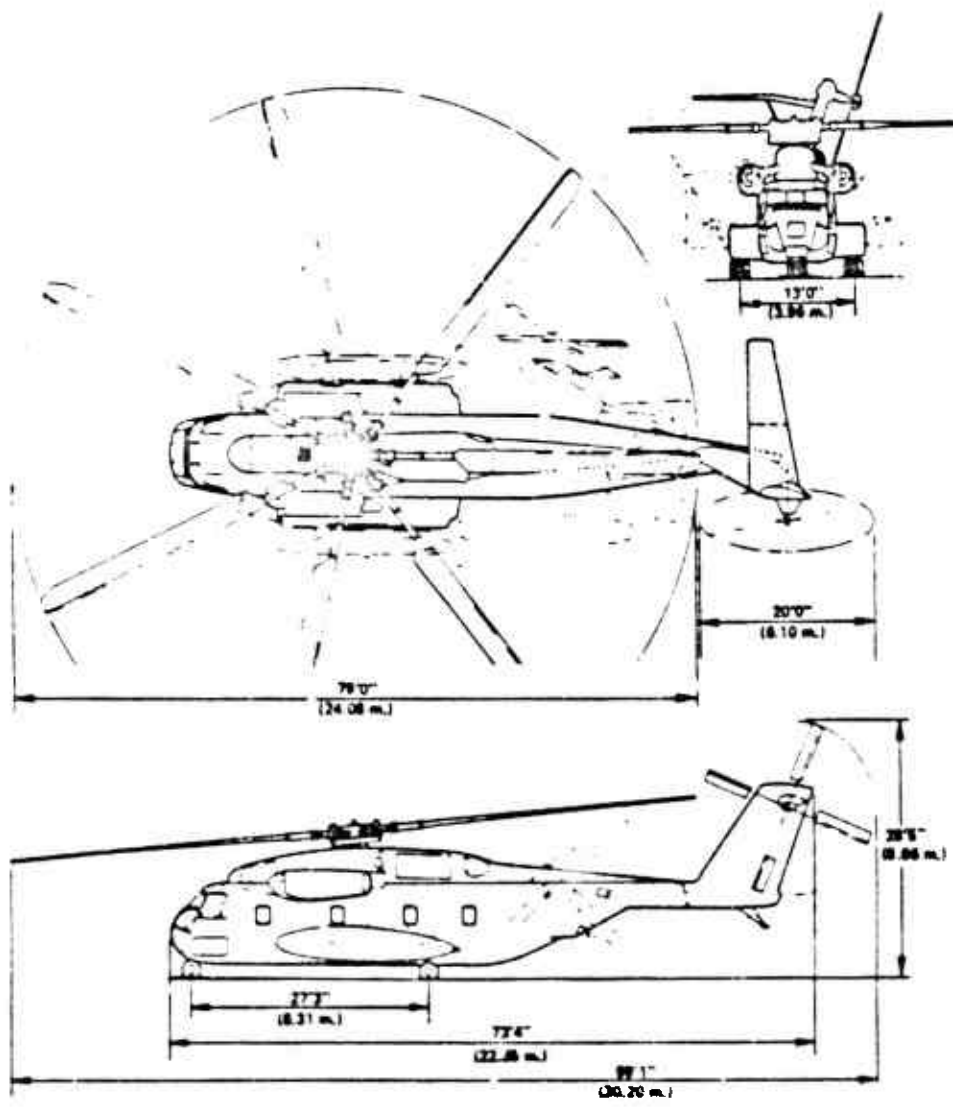


Figure C-1 CH-53E Three-View Drawing

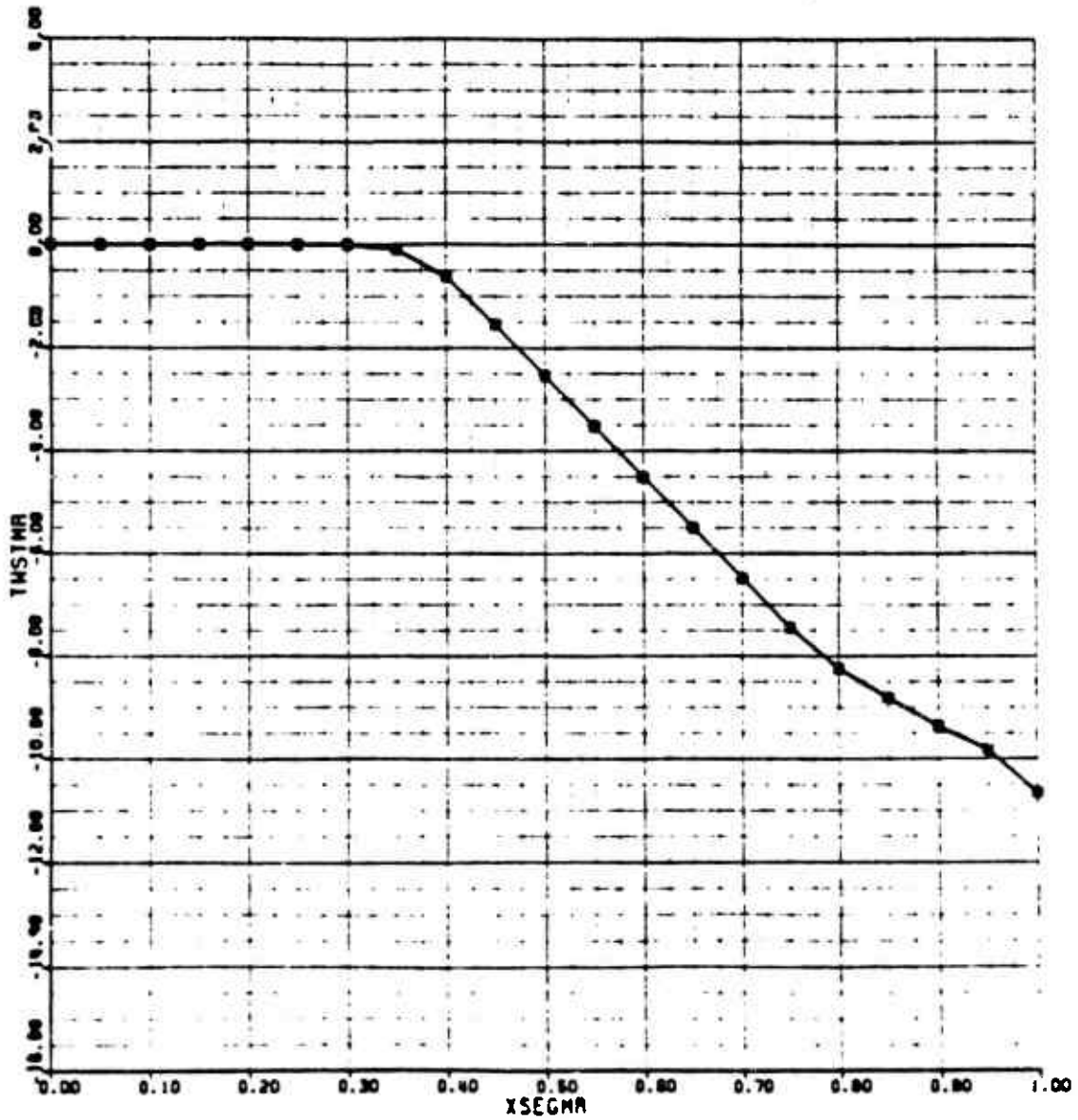


Figure C-2. CH-53E Main Rotor Blade Twist Map

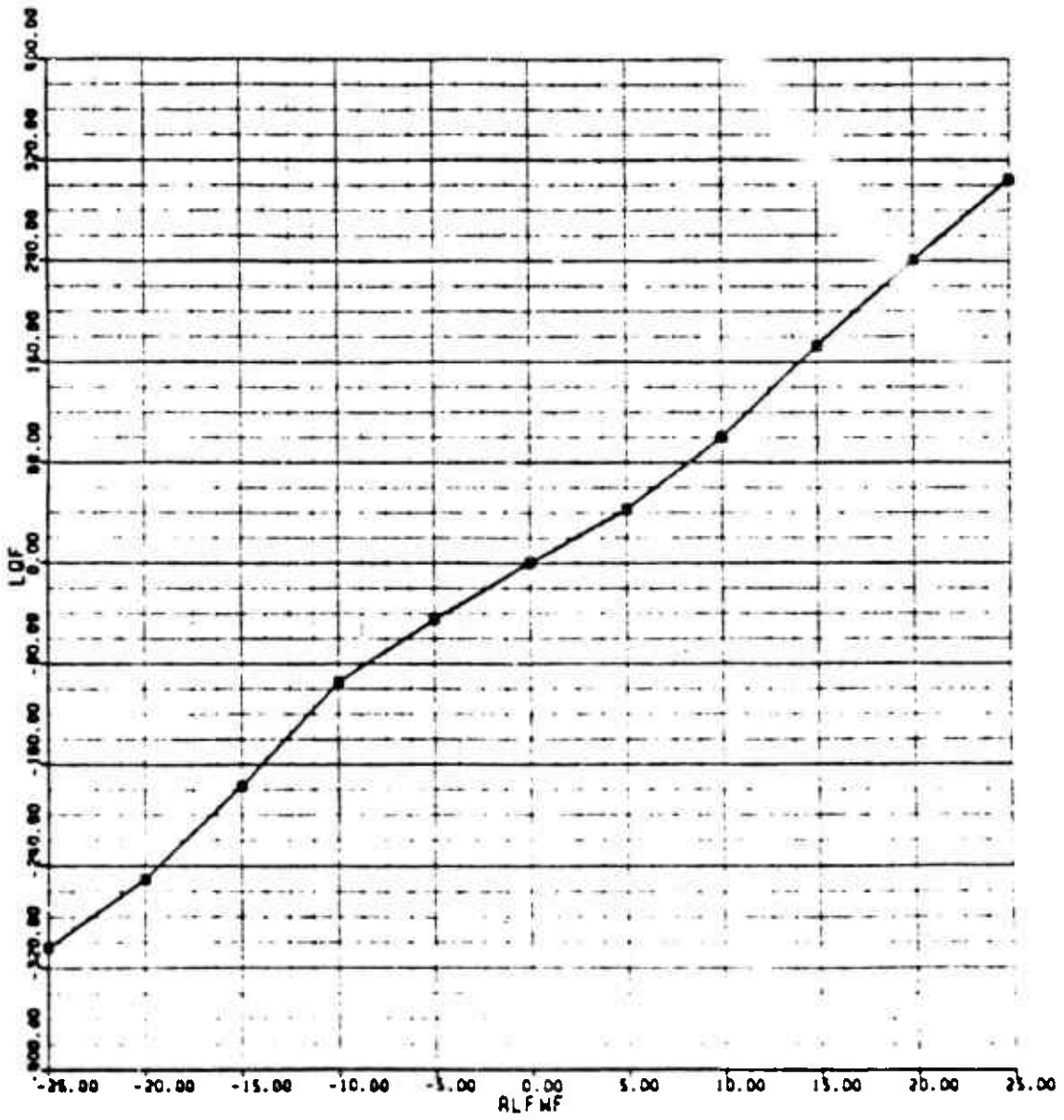


Figure C-3. CH-53E Fuselage Lift Map

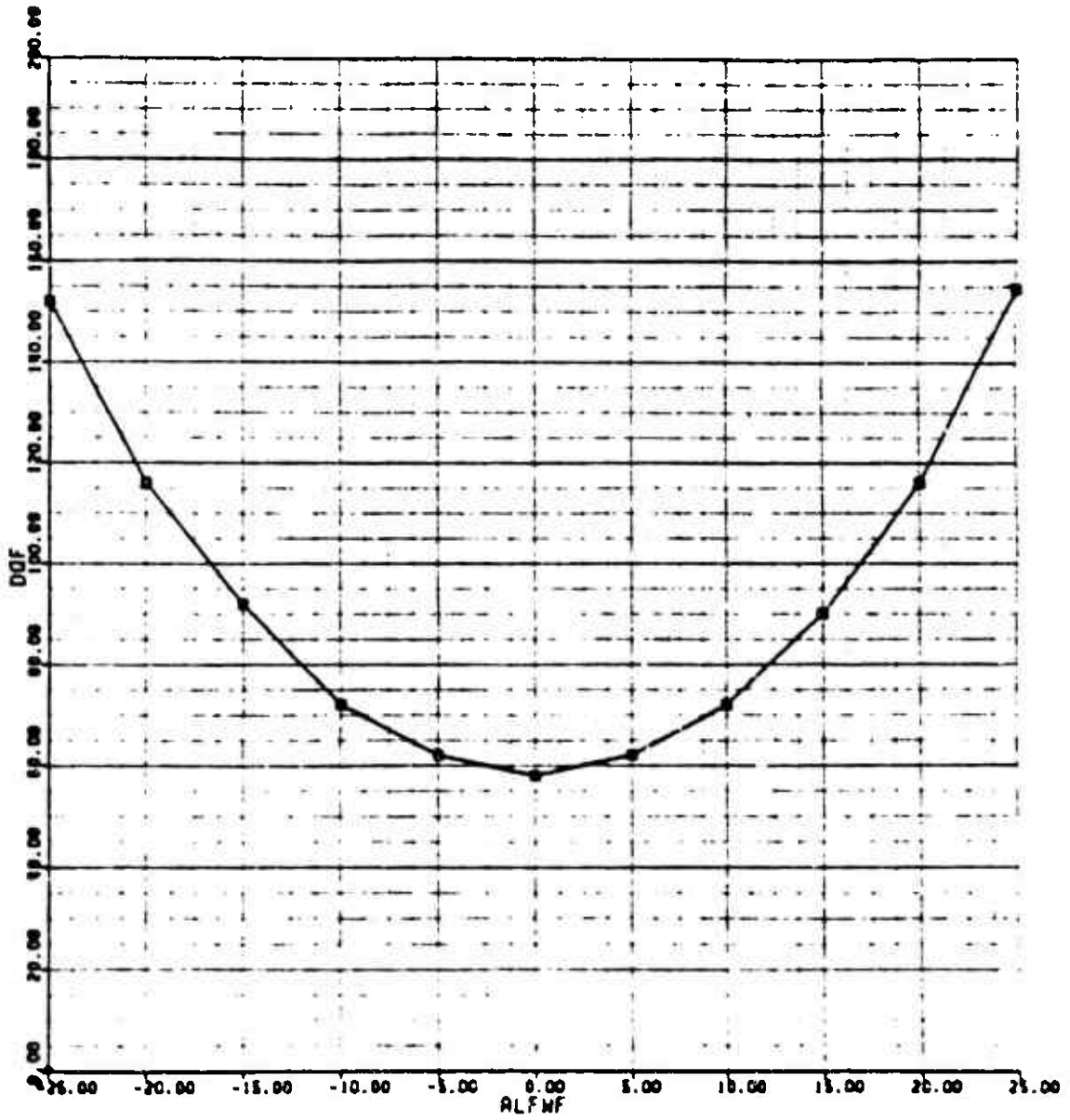


Figure C-4. CH-53E Fuselage Drag Map

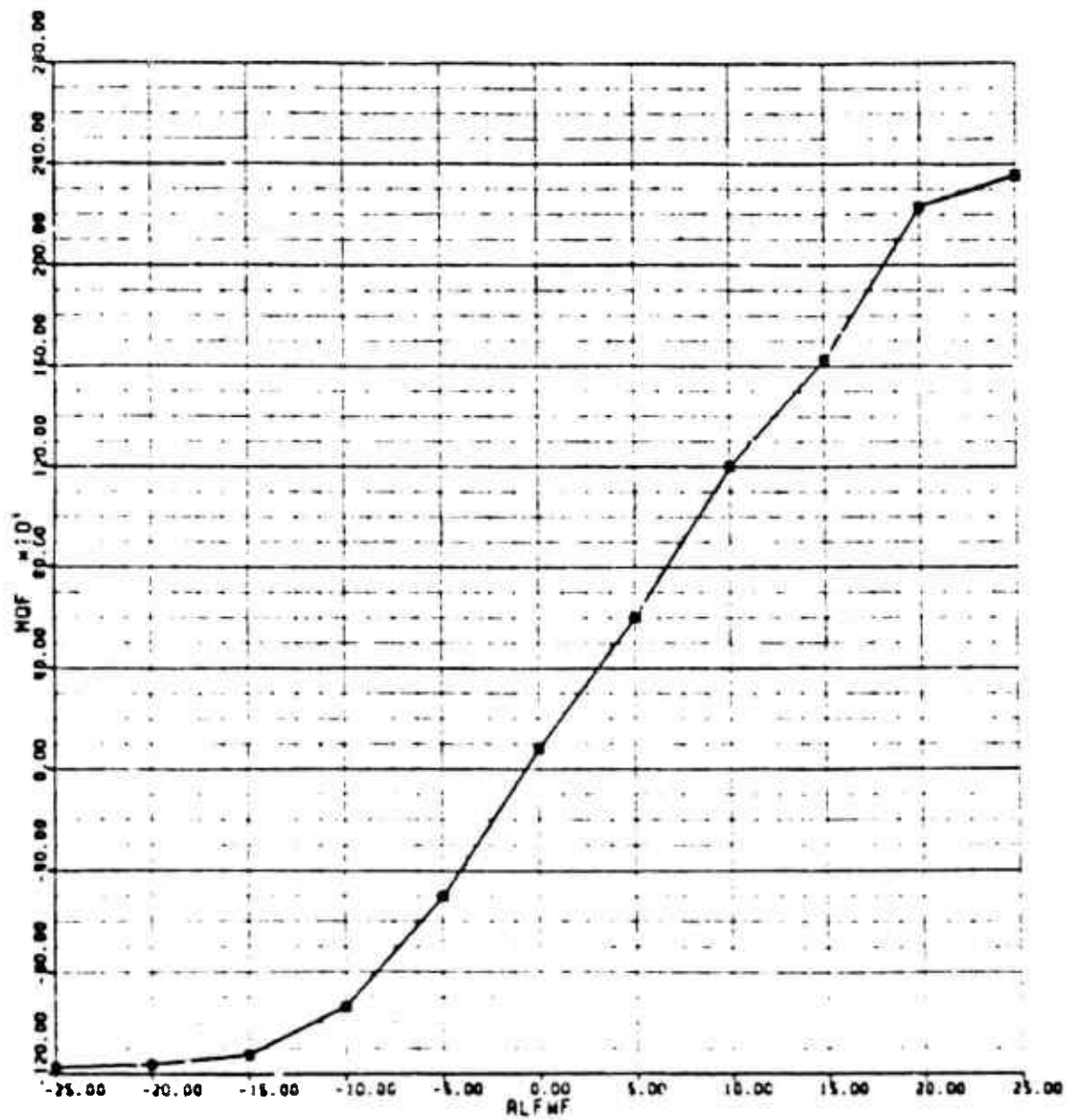


Figure C-5. CH-53E Fuselage Pitching Moment Map

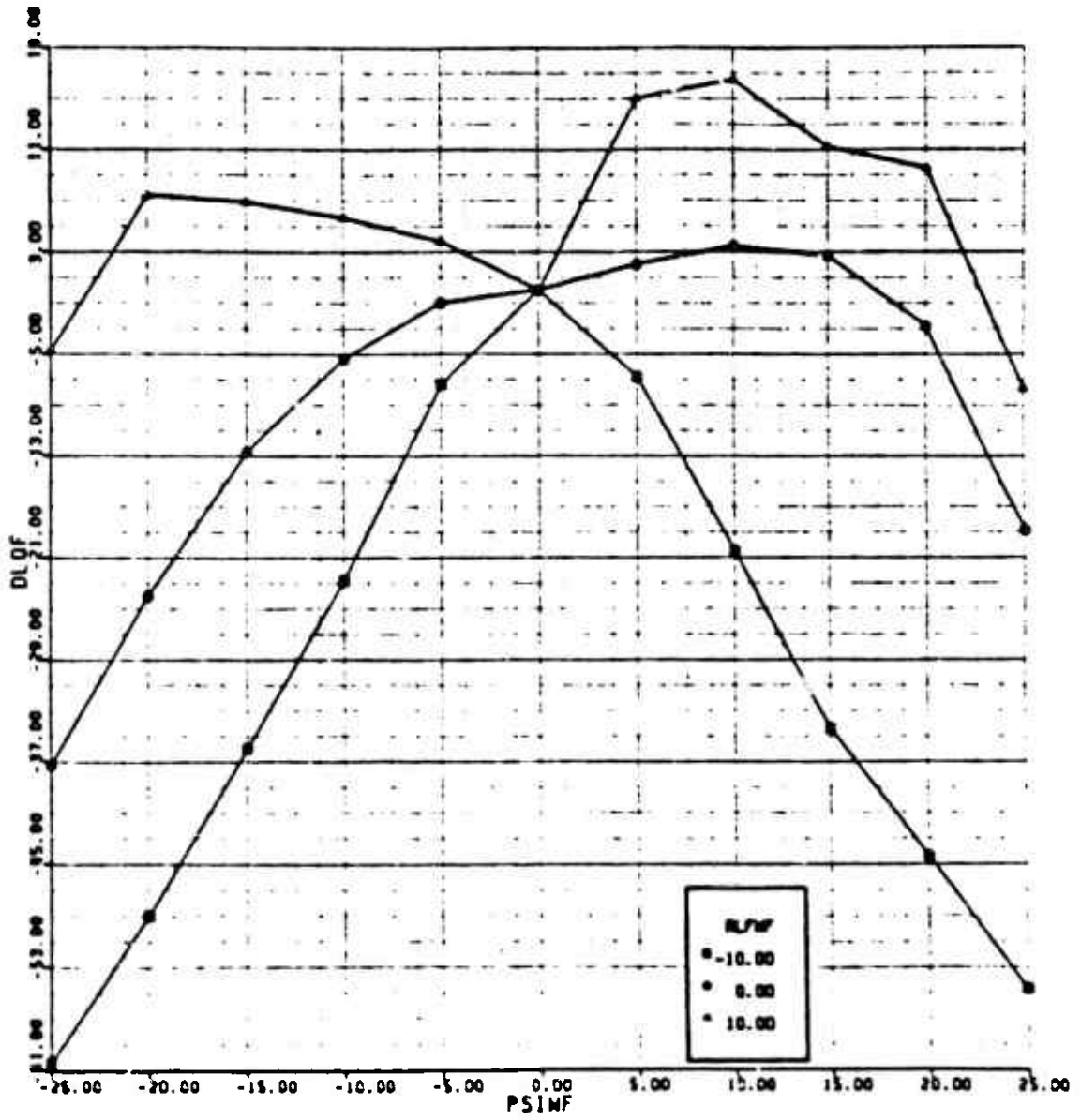


Figure C-6. CH-53E Fuselage Delta Lift Map

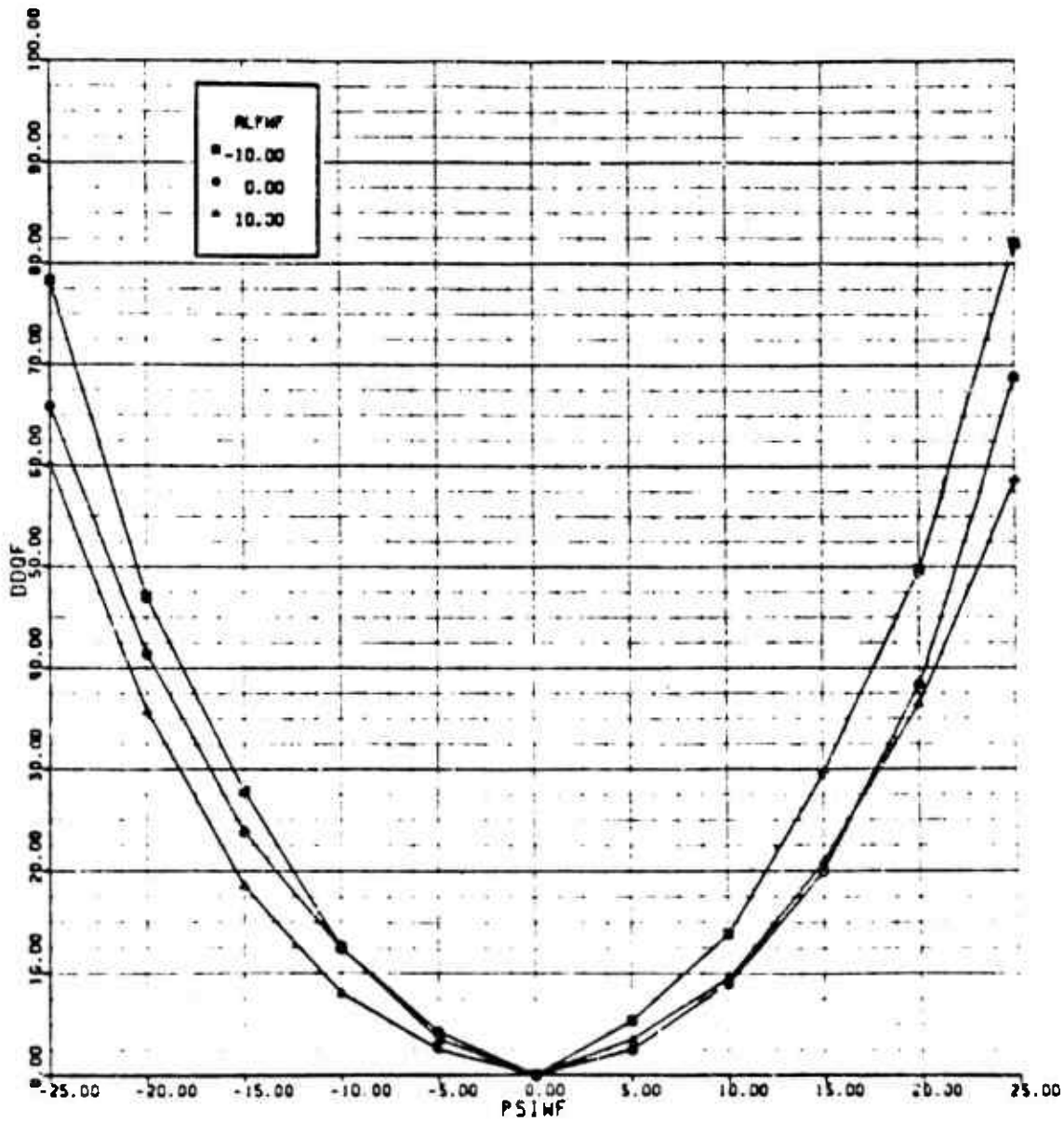


Figure C-7. CH-53E Fuselage Delta Drag Map

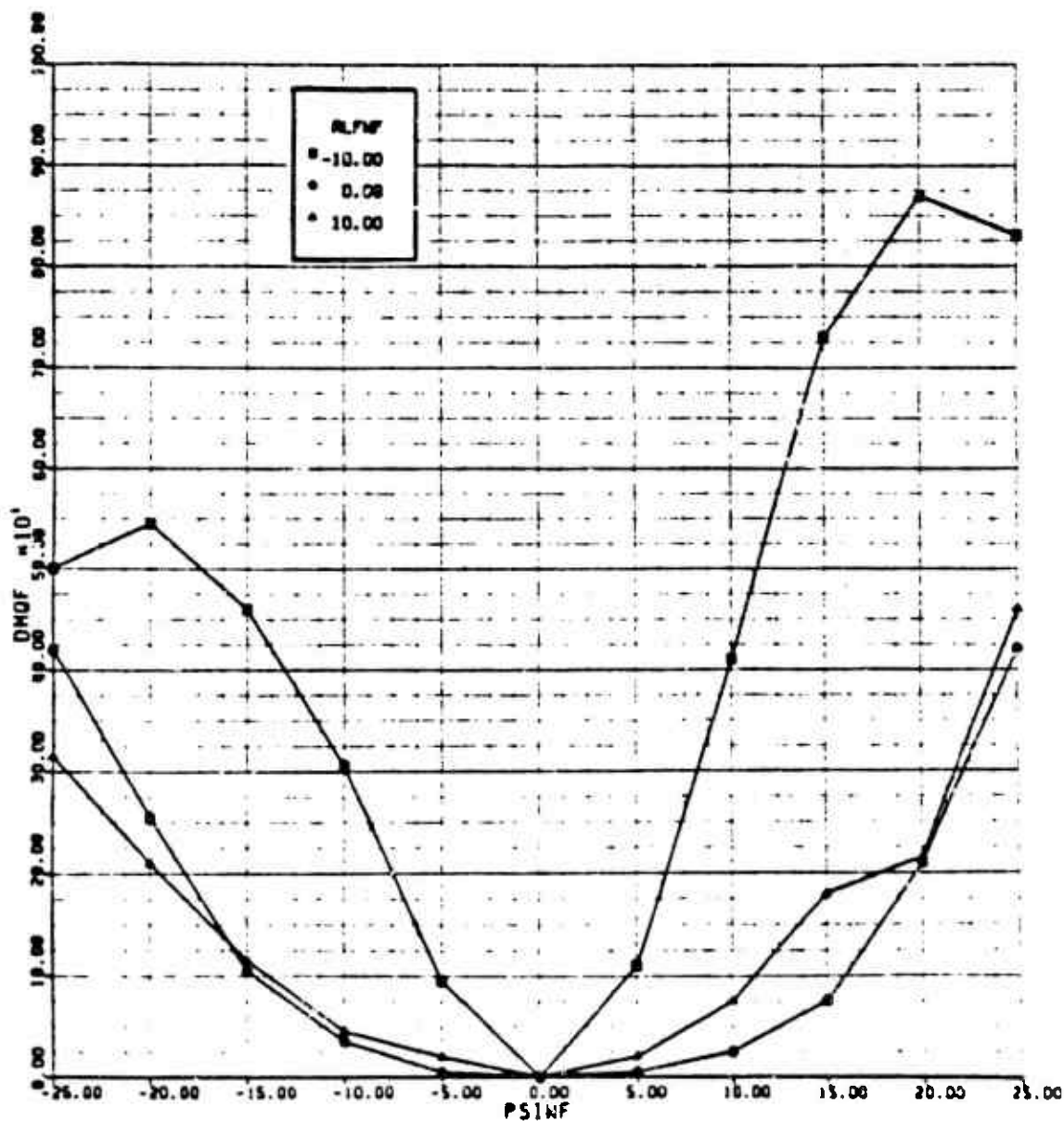


Figure C-8. CH-53E Fuselage Delta Pitching Moment Map

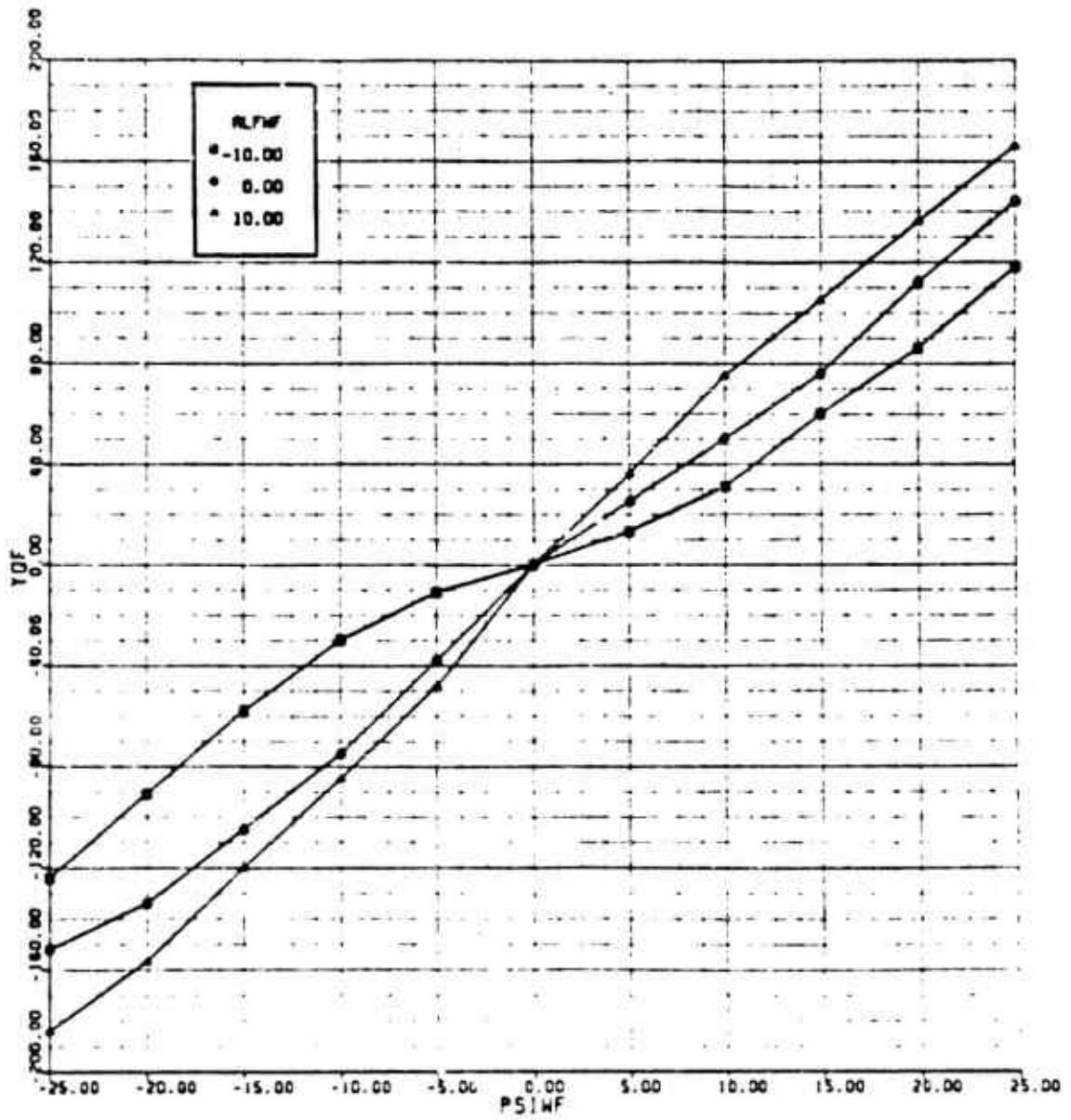


Figure C-9. CH-53E Fuselage Sideforce Map

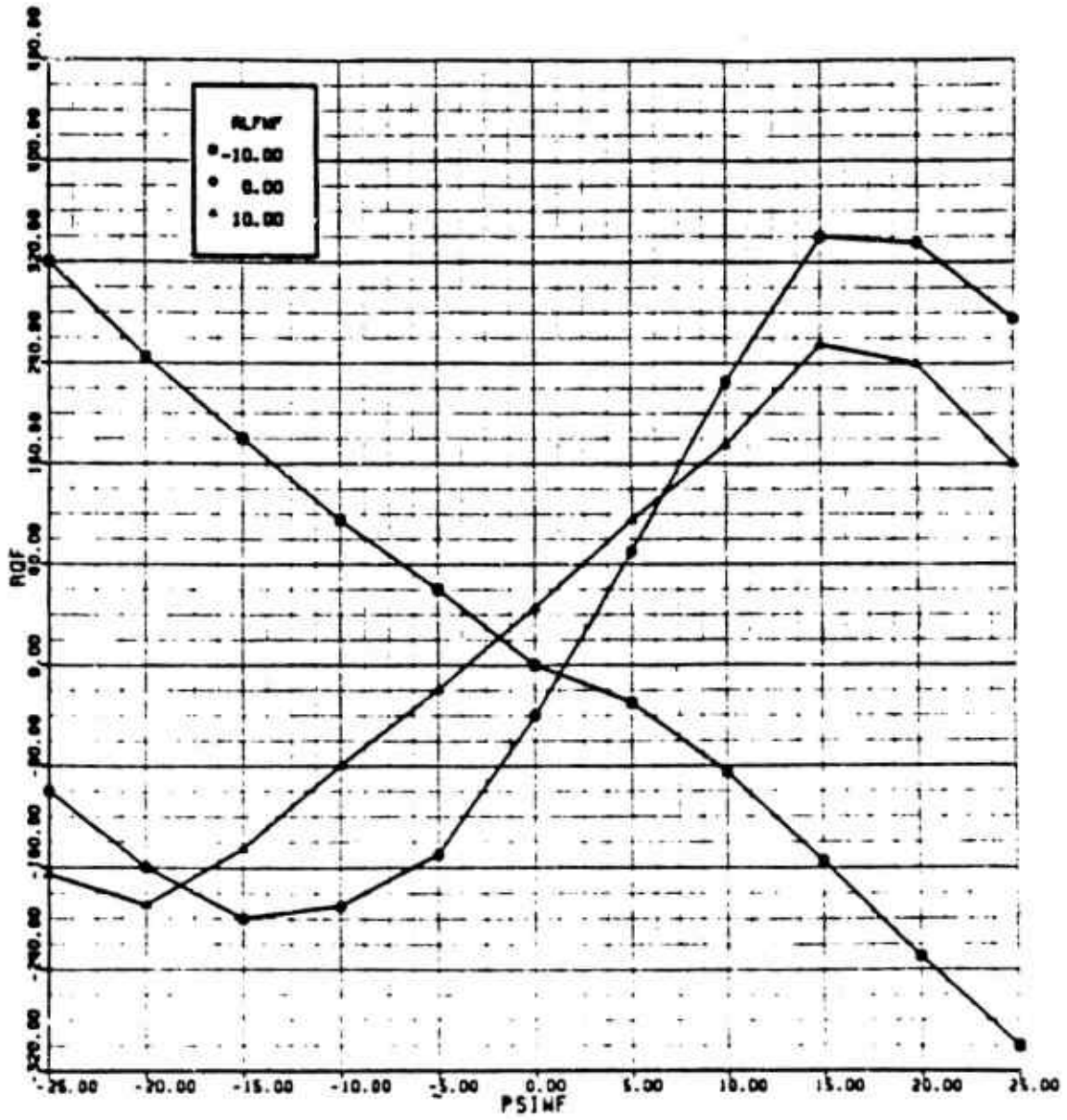


Figure C-10. CH-53E Fuselage Rolling Moment Map

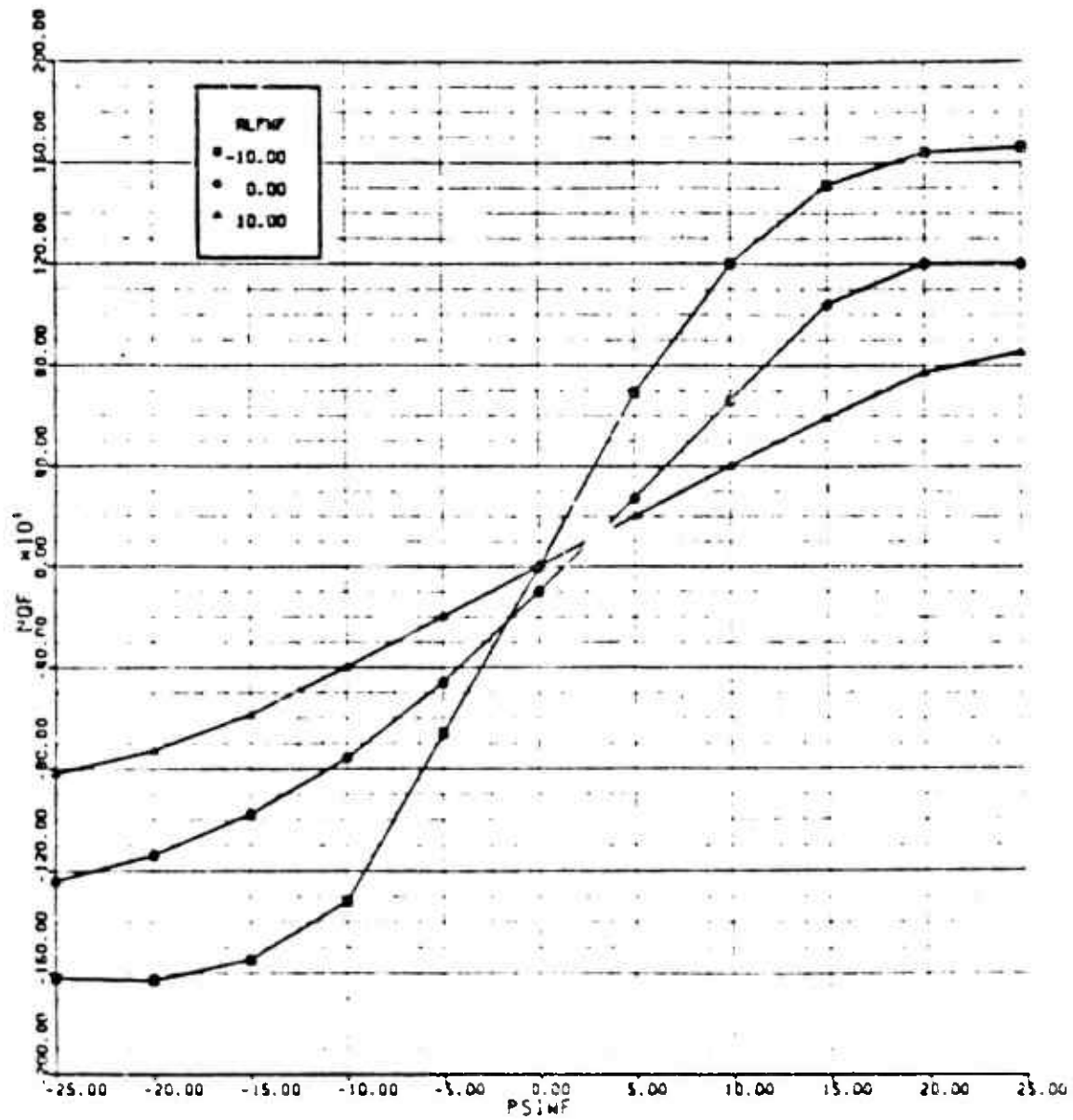


Figure C-11. CH-53E Fuselage Yawing Moment Map

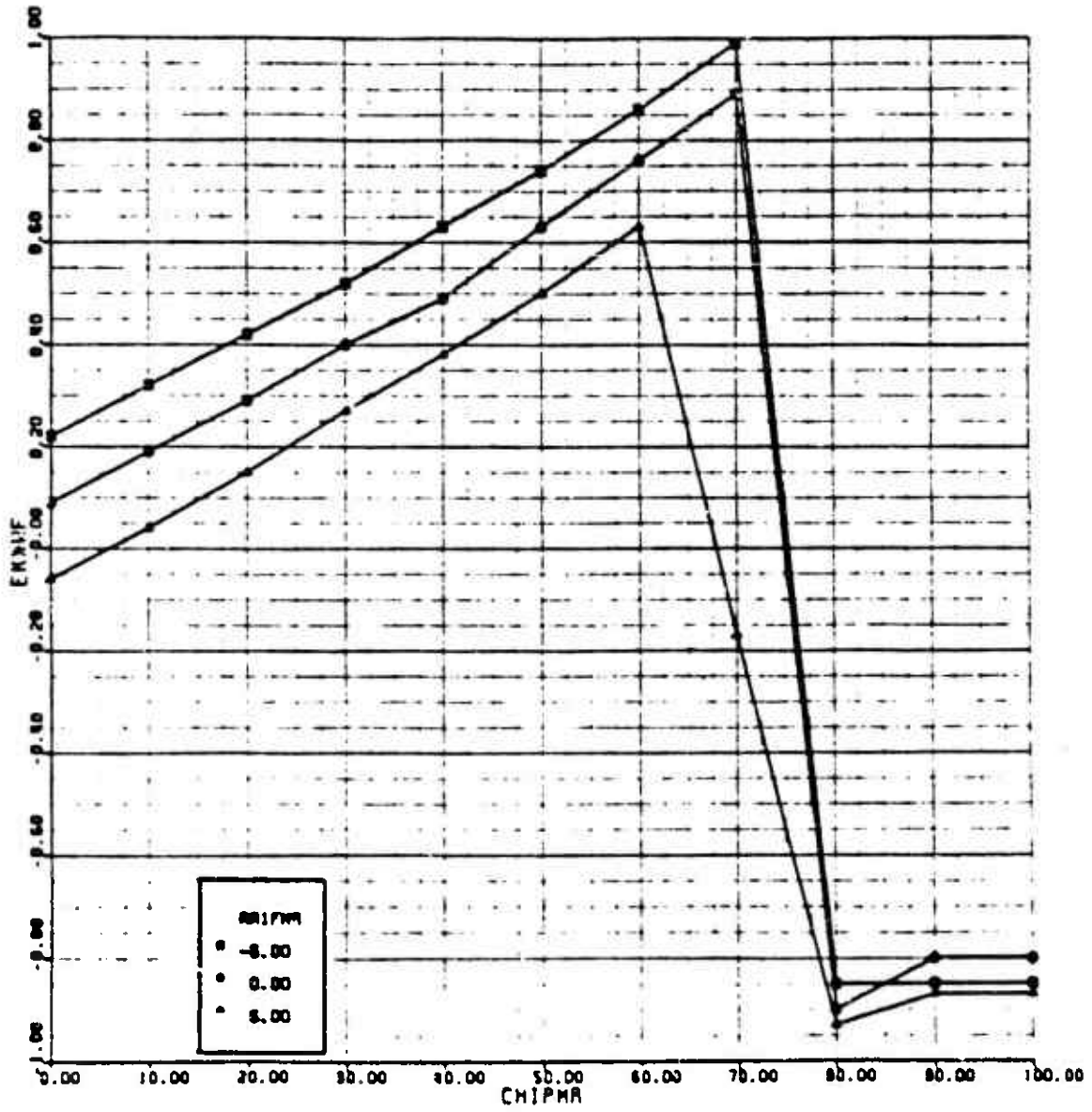


Figure C-12. CH-53E Main Rotor Downwash on Fuselage Map (x-direction)

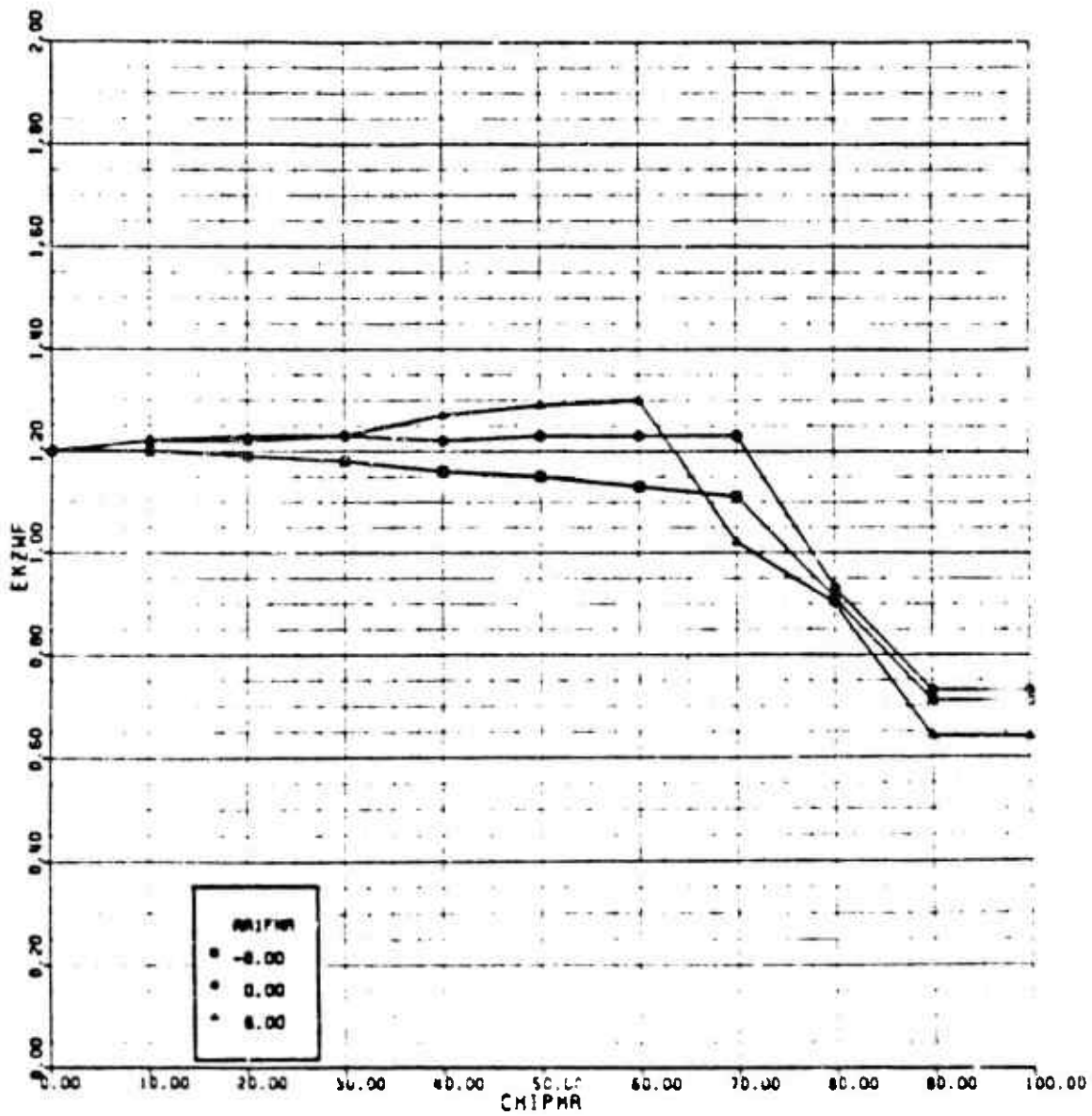


Figure C-13. CH-53E Main Rotor Downwash on Fuselage Map (z-direction)

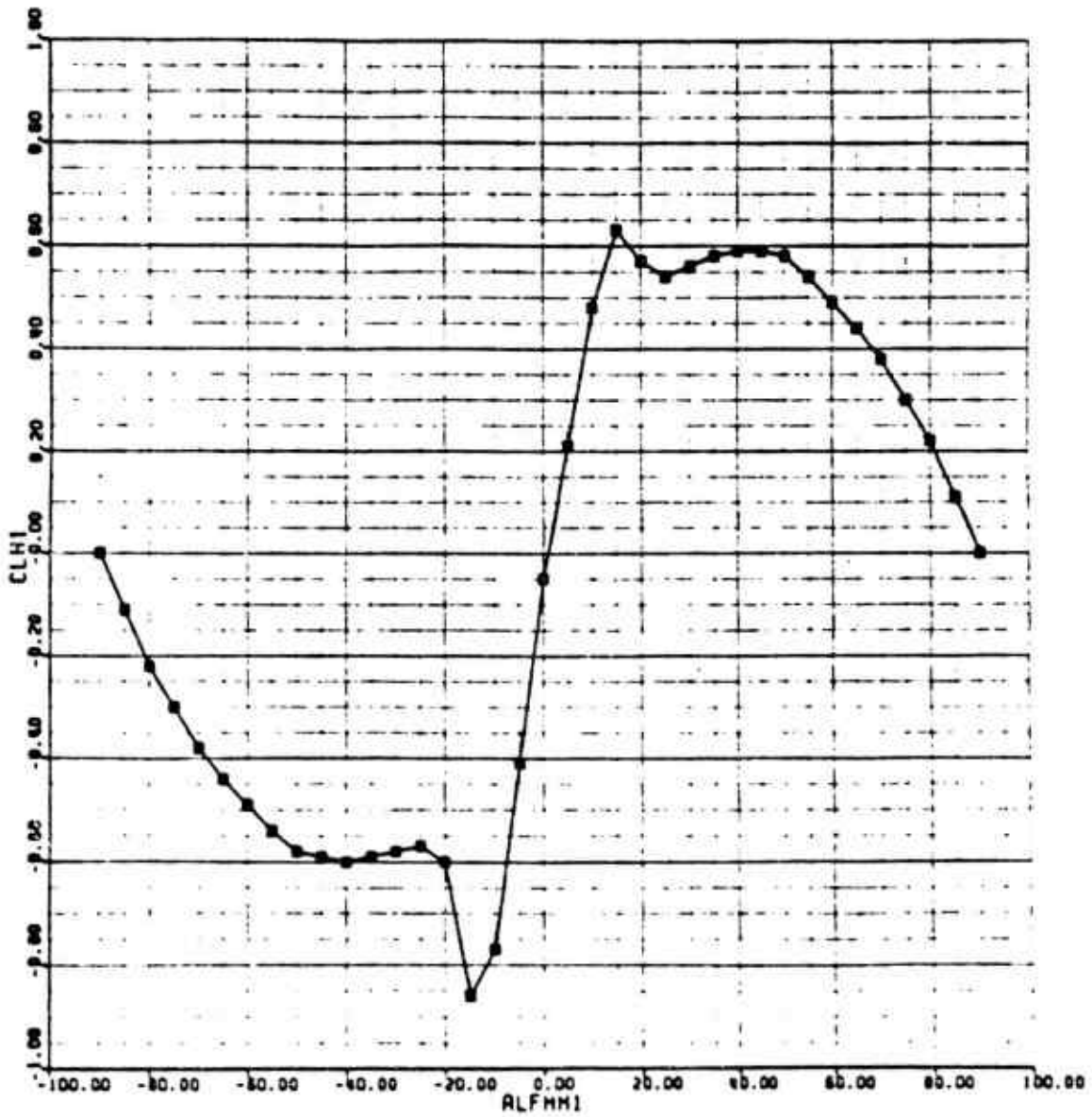


Figure C-14. CH-53E Horizontal Tail Lift Map

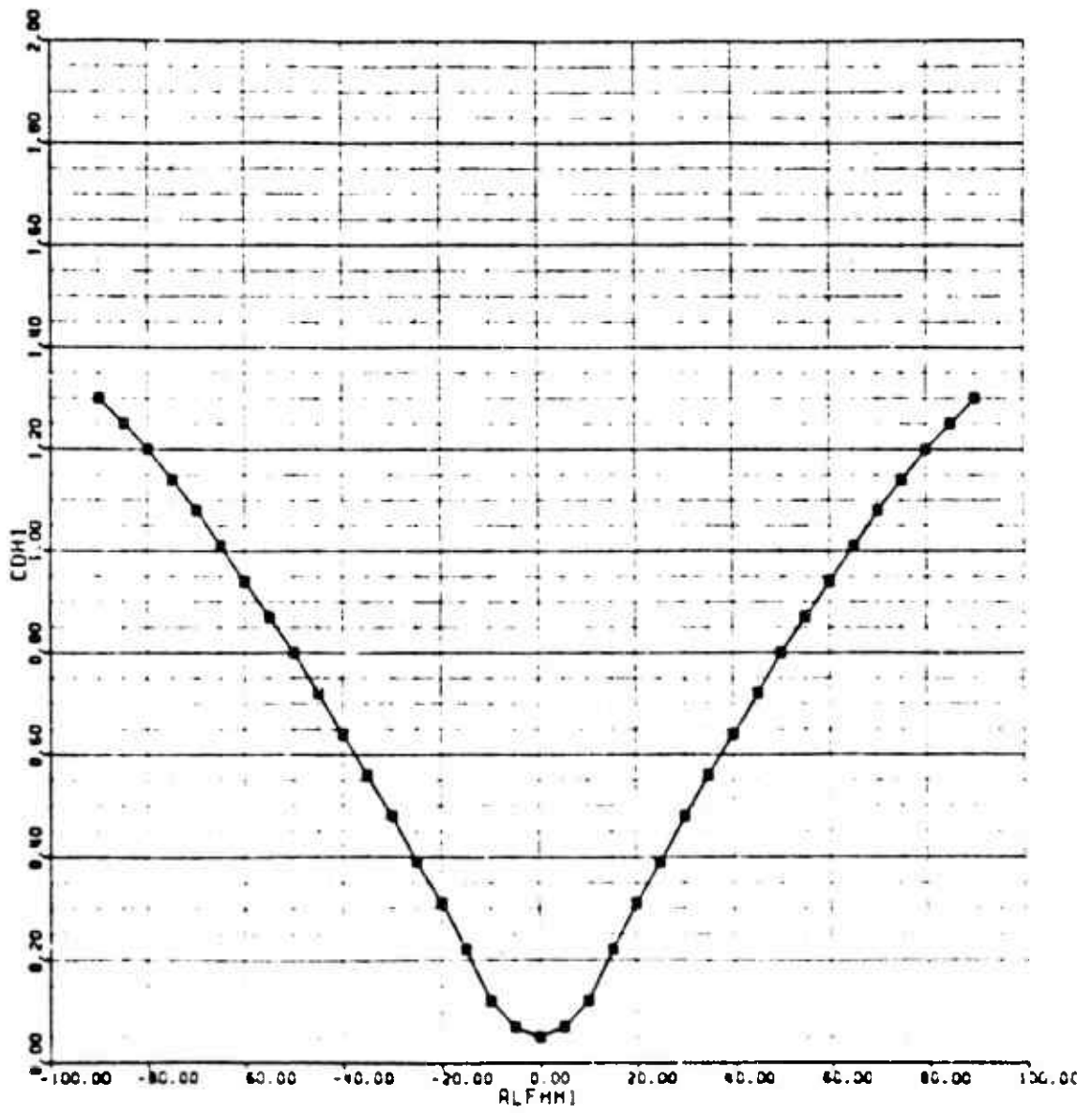


Figure C-15. CH-53E Horizontal Tail Drag Map

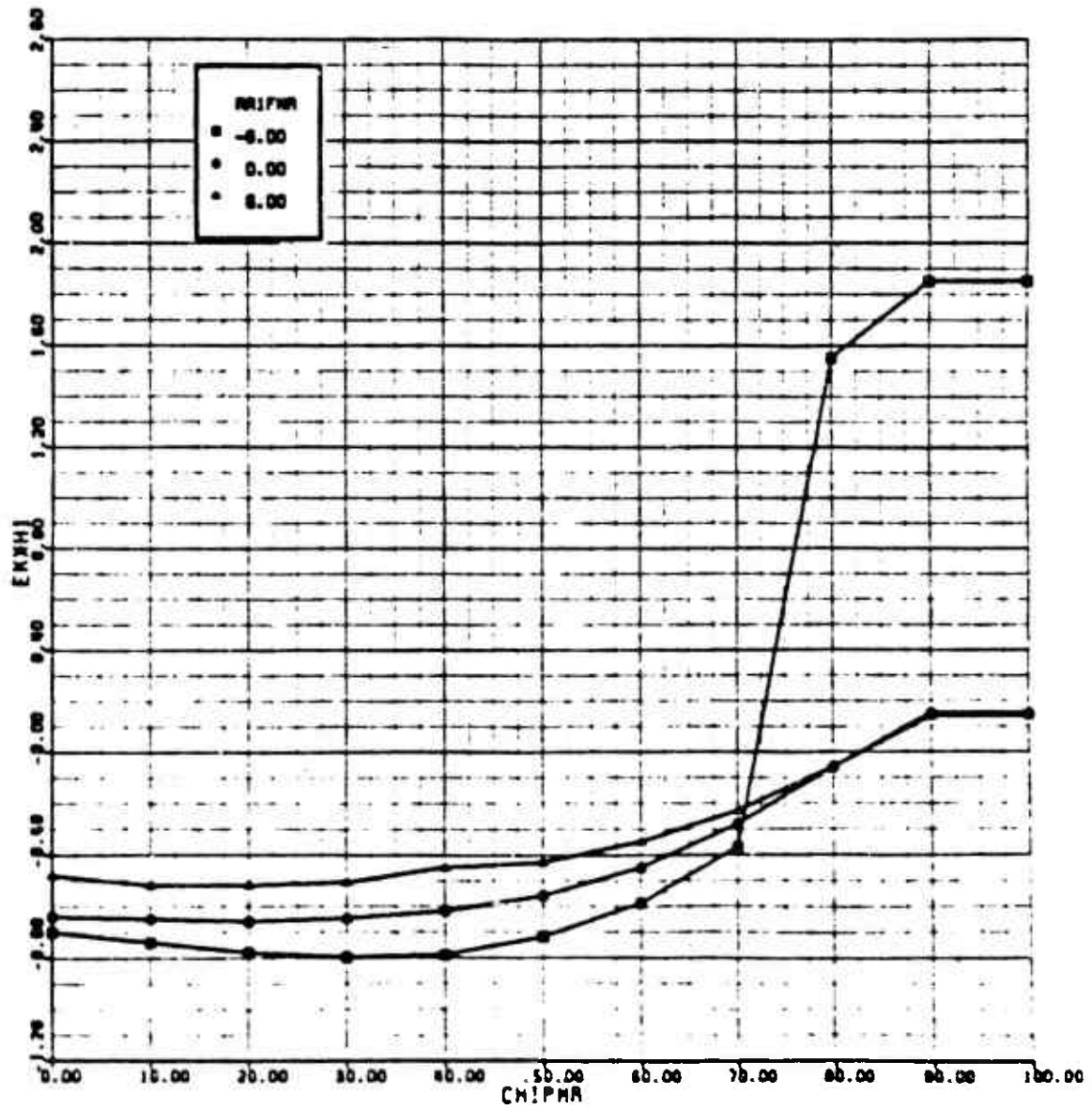


Figure C-16. CH-53E Main Rotor Downwash on Horizontal Tail Map (x-direction)

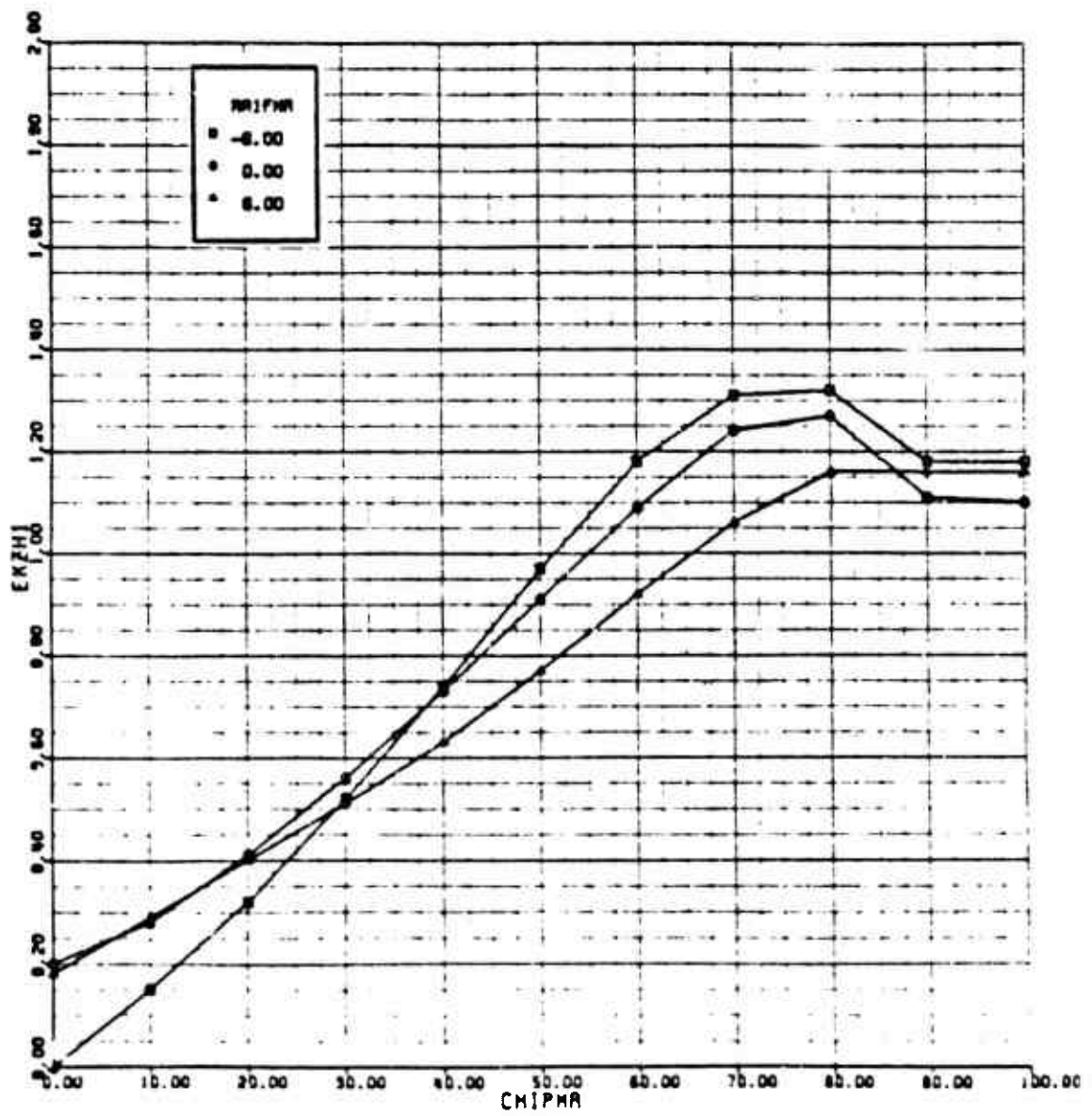


Figure C-17. CH-53E Main Rotor Downwash on Horizontal Tail Map (v-direction)

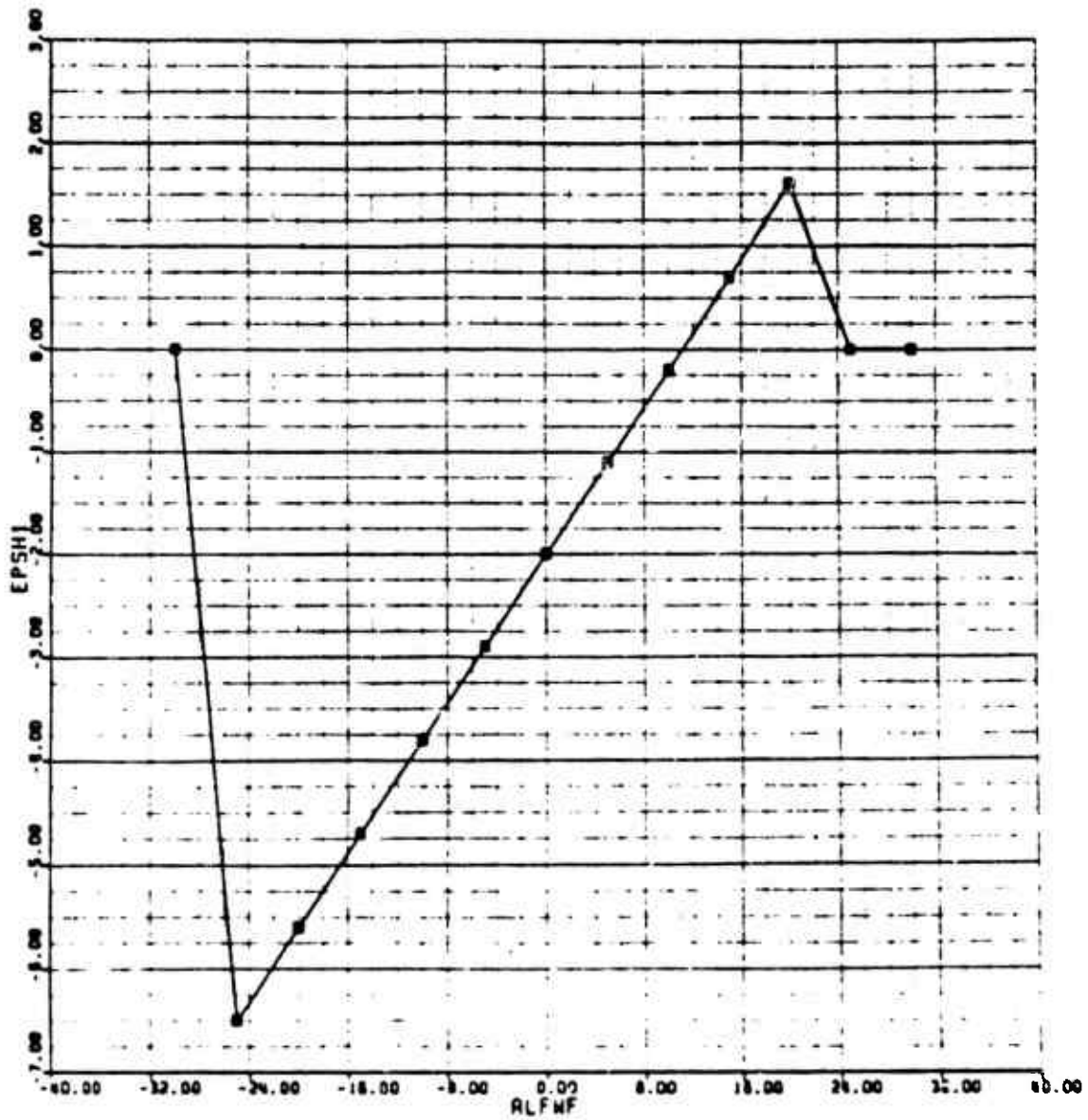


Figure C-18. CH-53E Fuselage Downwash on Horizontal Tail Map

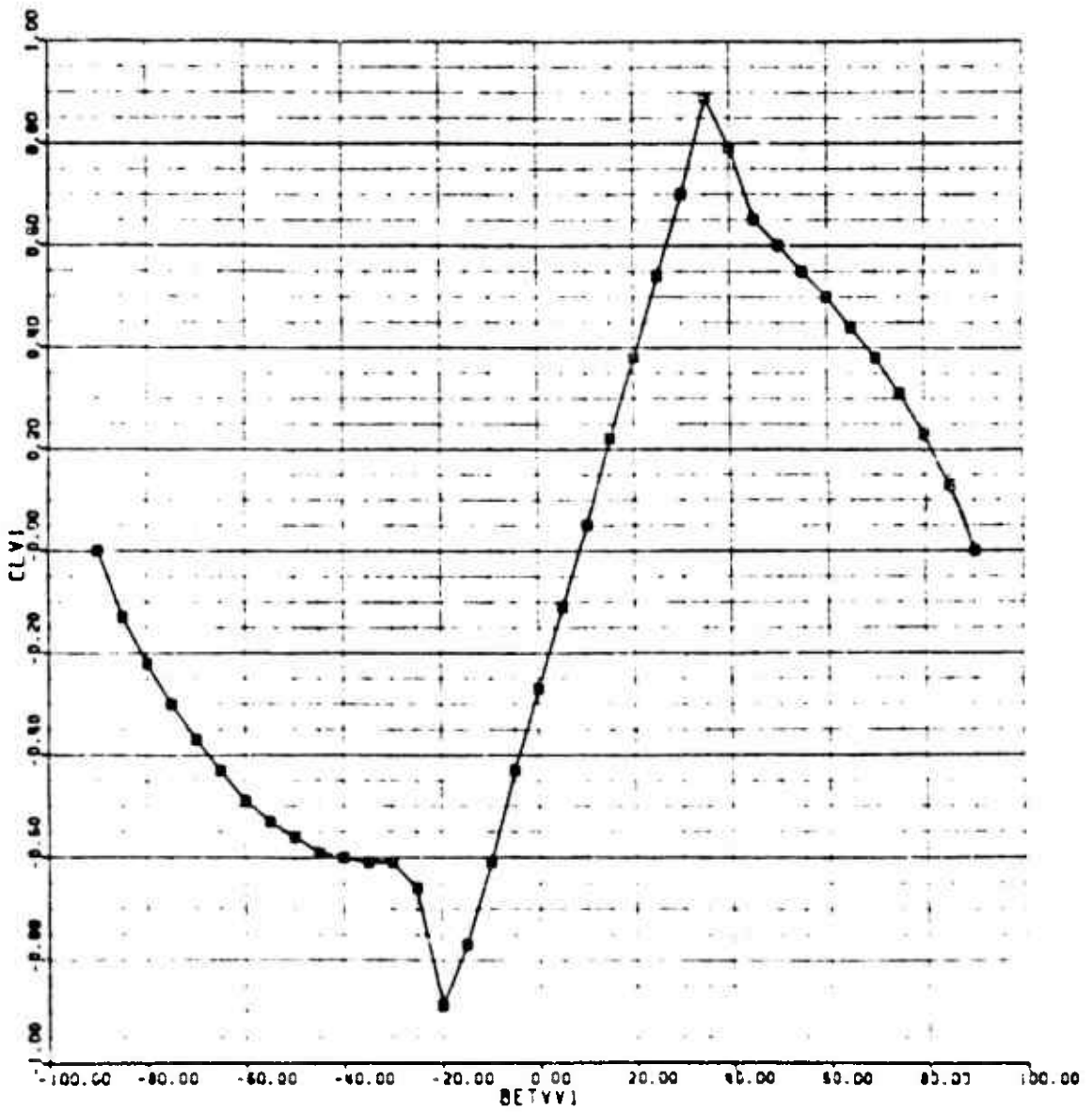


Figure C-19. CH-53E Vertical Tail Lift Map

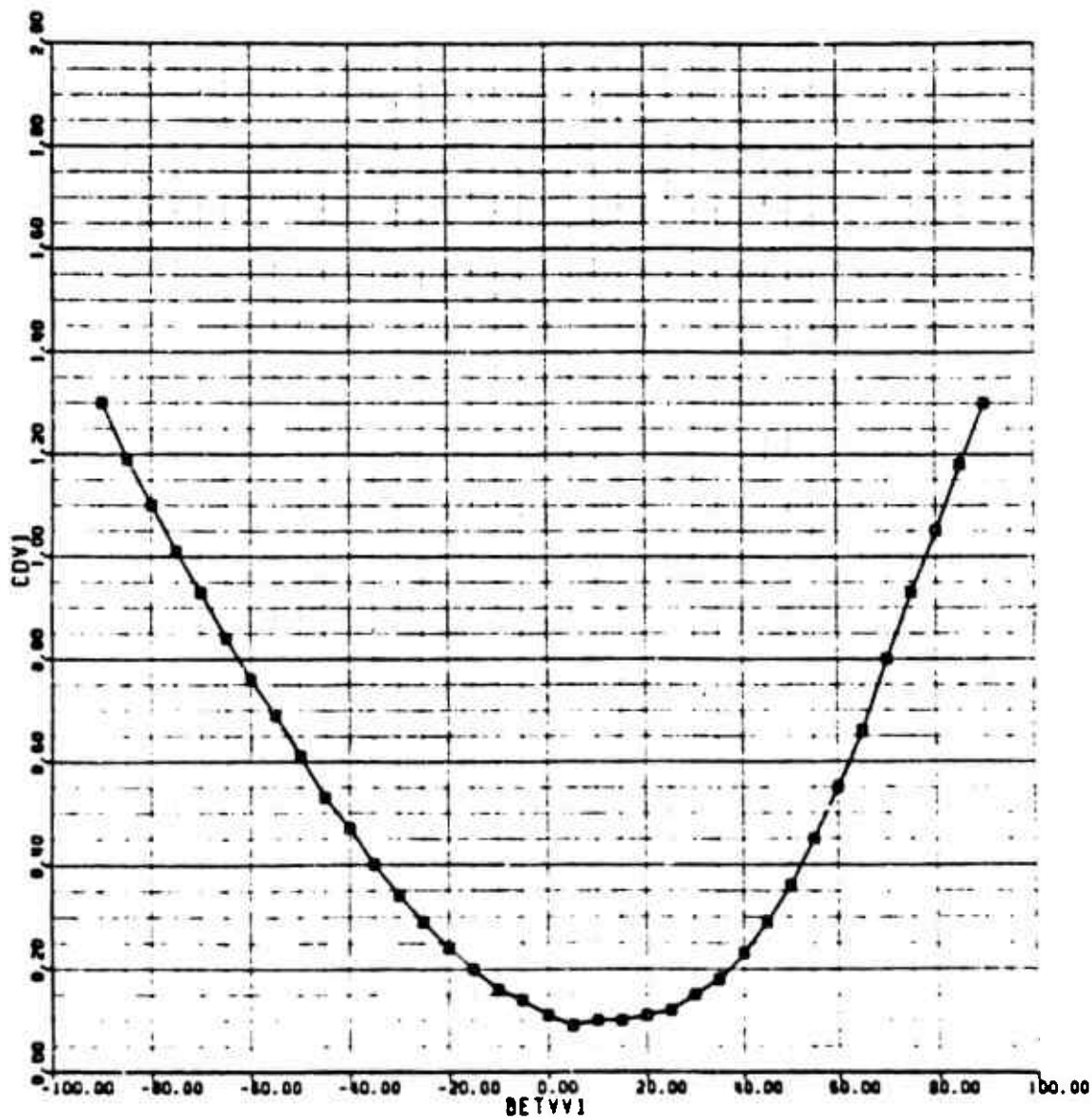


Figure C-20. CE-53E Vertical Tail Drag map

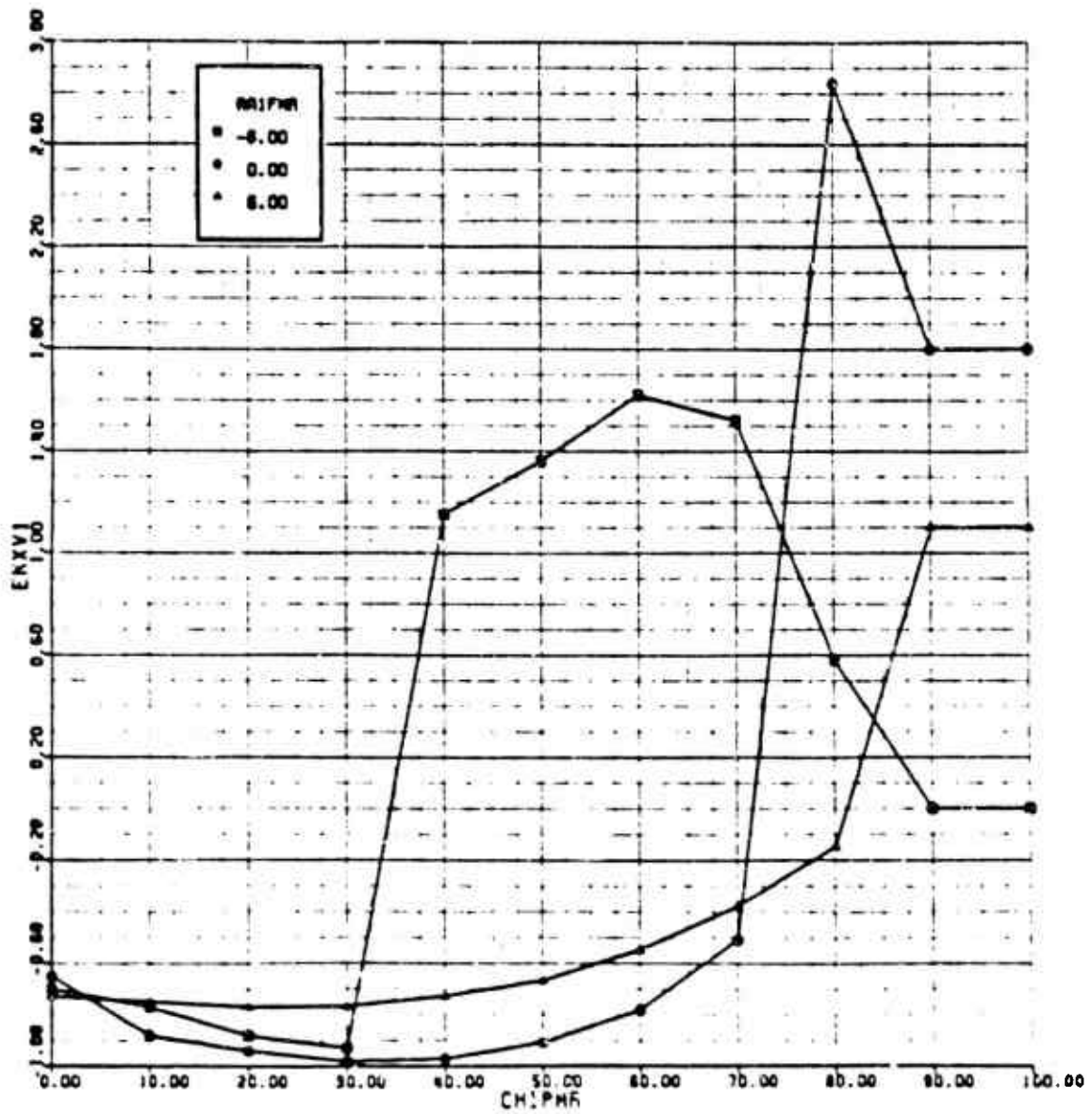


Figure C-21. CH-53E Main Rotor Downwash on Vertical Tail Map (x-direction)

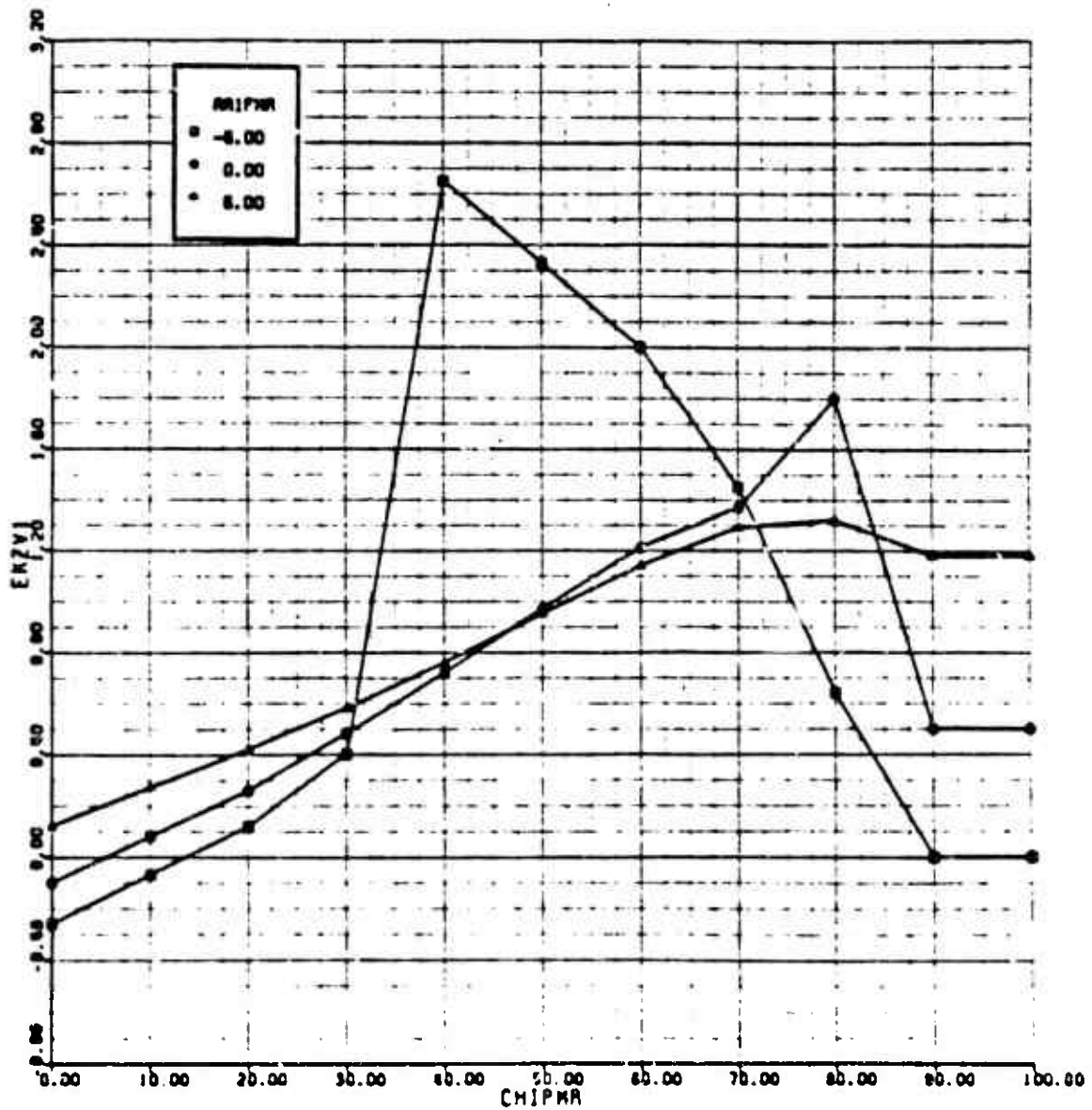


Figure C-22. CH-53E Main Rotor Downwash on Vertical Tail Map (z-direction)

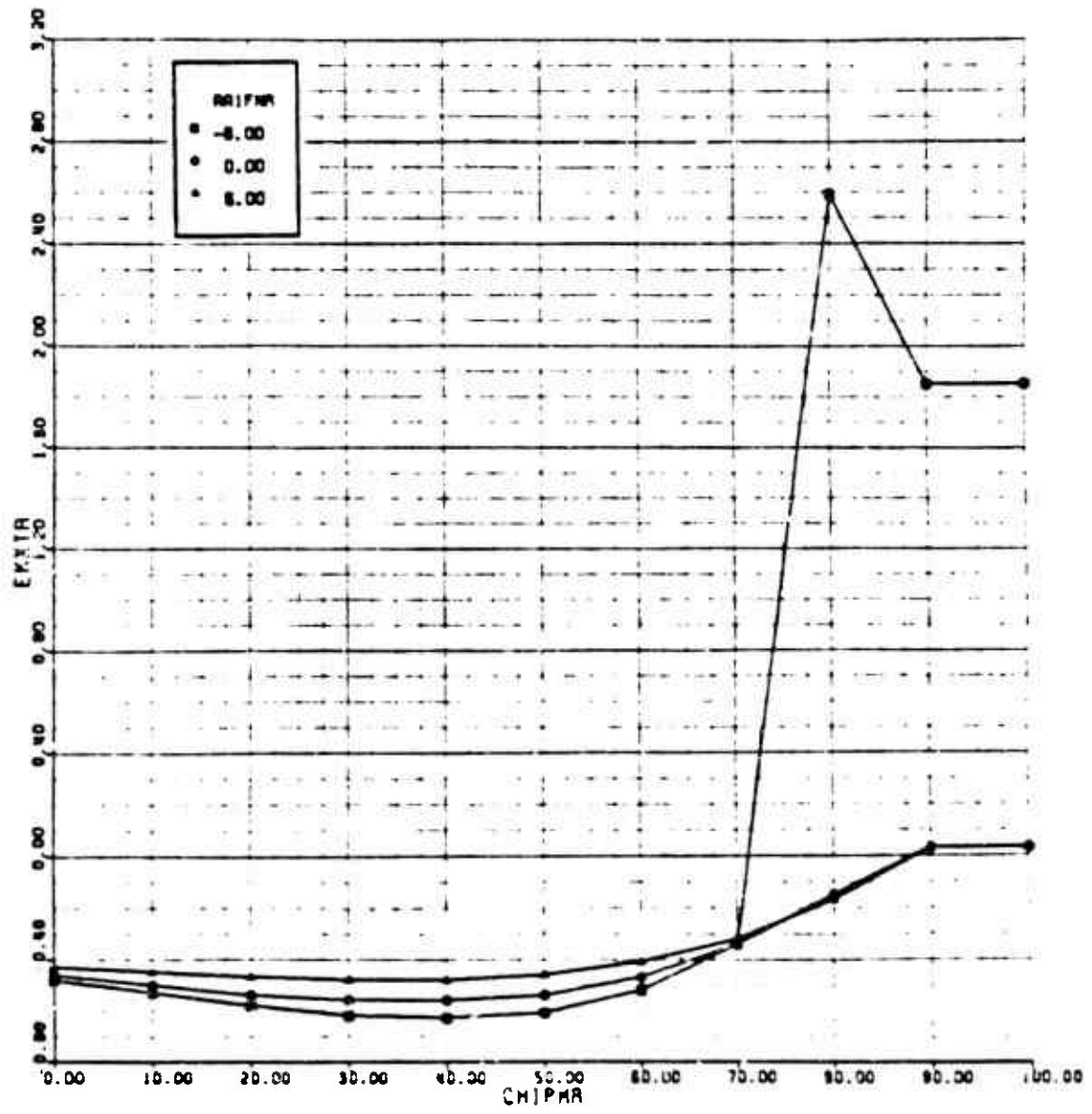


Figure C-23. CH-53E Main Rotor Downwash on Tail Rotor Map (x-direction)

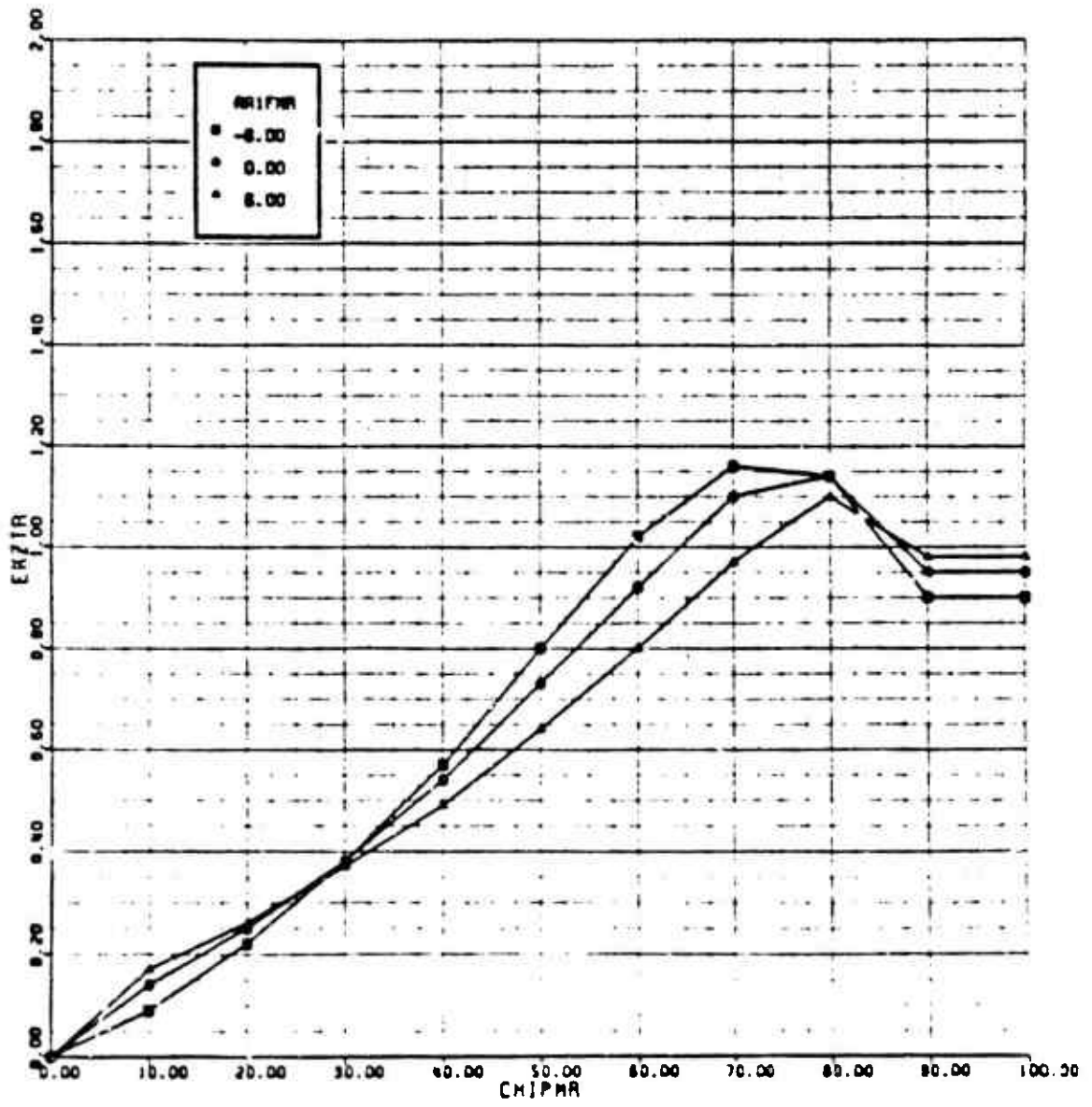


Figure C-24. CH-53E Main Rotor Downwash on Tail Rotor Map (z-direction)

APPENDIX D

AH-64A MODEL DATA

The AH-64A Apache (Figure D-1) is the U.S. Army's latest attack helicopter. It is a medium-size single-rotor helicopter designed to meet stringent U.S. Army specifications. It is fitted with an extensive avionics suite including a Target Acquisition Designation System and Pilot's Night Vision System (TADS/PNVIS) and employs a McDonnell Douglas M230 30mm turreted gun. The Apache was designed to have high levels of maneuverability and agility and to be survivable in the battlefield environment. Approximately 400 are in service with the U.S. Army. The Apache has a BDGW of 14,770 pounds, a rotor diameter of 48 feet and is powered by two General Electric T700-GE-701 turbo-shaft engines with an IRP of 1698 shp each.

The four-bladed main rotor is of articulated design. Flapping hinge offset is 3.8 percent of the rotor radius while the lag hinge is at 12 percent. Hughes HHO2 airfoil section is used for the main rotor. The four-bladed tail rotor is 9 feet 2 inches in diameter and of a scissored configuration. Blade spacing is 55/125 degrees to reduce noise. A 33.4-square-foot stabilator is mounted at the base of the vertical fin.

The fuselage is of conventional aluminum semimonocoque construction. It has a narrow width typical of attack helicopters and features tandem seating for the pilot and gunner. The copilot/gunner sits in the front seat while the pilot sits in the rear. Small, low aspect ratio wings/stores pylons are fitted to each side of the fuselage. These are detachable for transport and storage. Flight controls are of conventional hydromechanical design but with additional features to provide ballistic tolerance.

Since a GenHel simulation of the Apache did not exist at Sikorsky, the first task was to prepare the input data files. Most of the numerical data defining the AH-64A were available from Reference 7. These data were converted to fit the GenHel format. For example, the fuselage aerodynamics in C-81 are presented as a sum of coefficients times various trigonometric functions of angle-of-attack and sideslip angle. In GenHel, simple table look-ups or maps are used for these data. The GenHel maps are constructed to have even increments and to have a small angle region with fine increments and a large angle region with coarser increments.

While the C-81 approach is more compact, it has limitations. The wind tunnel test data must be fitted to the series representation available. In addition, the resulting coefficients have no physical significance. Any errors in them are not readily detectable by the user. Finally, knowing the coefficient does not enable one to know where the maximum lift point is or when the zero moment occurs. The GenHel maps, on the other hand, are derived directly from the wind tunnel data. All of the characteristics of that data are fully represented. No "smoothing" or "fitting" is required. More importantly, the input (angle-of-attack) and output (fuselage lift/q) data are in normal physical units. Any errors in the data are readily detectable by the user. The shape of the data, points of maximum value, or zero cross-over are readily available.

ables. In addition to the available C-81 data, other information was required. The effect of fuselage aerodynamic interference on the empennage needed to be modeled as well as the effect of rotor wake impingement on both the fuselage and empennage. Fuselage interference effects were based on BLACK HAWK data for downwash, sidewash and dynamic pressure loss. Rotor interference velocities were calculated using an existing Hayson-method computer code.

The AH-64A control system was modeled using data available in References 8, 9 and 10. Stick to head rigging was represented simply as a gain and a bias. The stabilator positioning logic was based on data provided in Reference D-10. Trim correlation with data from the same references are shown in Figures D-2 to D-9. These were evaluated for the conditions of Figures 16 of Reference 10:

GW - 14,770 pounds
FSCG - 206.7
Density Altitude - 10,000 feet
Rotor Speed - 100 percent

As can be seen, correlation was very good. Pitch attitude was generally within one degree and stick positions within one-half inch. Stabilator and power required data were also judged to have good correlation.

The SCAS system was not modeled as it was not really required for this M/A study and a detailed modeling of the system was beyond the scope of the current effort. Evaluation of the flight dynamics was difficult because most of the data were flown SCAS on. One SCAS-off longitudinal pulse was available in Reference 10. The GenHel correlation results are presented in Figures D-9. The simulation is somewhat more responsive than the aircraft, but the frequency and amplitudes of the responses are well matched.

All of the numerical data used to model the AH-64A are provided in this appendix. The first section is a listing of all the input data (Table D-1). The second section presents plots of the map data for fuselage, vertical tail, horizontal tail and wing/stores support aerodynamics along with plots of the rotor interference and fuselage interference data (D-9 to D-27). The tabular data are provided with appropriate labels. Map data are identified with GenHel variable names provided in the List of Symbols.

For the AH-64A model, the panel allocation was as follows:

1. Right horizontal tail
2. Left horizontal tail
3. Vertical tail
4. Right wing/stores support
5. Left wing/stores support

TABLE D-1. AH-64A SPECIFIC FILE

```

;***** INPUT PARAMETERS FOR MAIN ROTOR MODULES (#A.) *****

FSMR:: 198.61 ; FUSELAGE STATION, INCHES
WLNR:: 215.94 ; WATERLINE STATION, INCHES
BLNR:: 0.0 ; BUTTLINE STATION, INCHES (+IVE TO PORT)
RMR:: 24.0 ; RADIUS, FT.
OMGTR:: 30.2640 ; TRIM ROTATIONAL SPEED, RAD/SEC
BMR:: 4.0 ; ACTUAL NUMBER OF BLADES
ISMR:: -5.0 ; LONGITUDINAL SHAFT TILT, (POS. BACKWARDS), DEG
ILNR:: 0.0 ; LATERAL SHAFT TILT, (POS. STARBOARD), DEG
DELSMR:: -5.0 ; SWASHPLATE PHASE ANGLE, DEG
DEL3MR:: 0.0 ; FLAPPING HINGE OFFSET ANGLE, DEG.
KAP1MR:: 0.0 ; LAGGING HINGE OFFSET COEF. (FUNC(LG))
KAP2MR:: 0.0 ; LAGGING HINGE OFFSET COEF. (FUNC(LG**2))
CHDTMR:: 1.75 ; BLADE CHORD AT TIP, FT.
CHDRMR:: 1.75 ; BLADE CHORD AT ROOT, FT.
OPSTMR:: 0.917 ; HINGE OFFSET, FT.
SPRLMR:: 2.42 ; HINGE TO START OF BLADE, FT.
WTBDMR:: 156.6 ; WEIGHT OF ONE BLADE, LBS.
IBMR:: 1060.4 ; BLADE MOMENT OF INERTIA ABOUT HINGE, SLUG-FT**2
MBMR:: 64.36 ; BLADE MASS MOMENT ABOUT HINGE, SLUG-FT
IEMR:: 943.9 ; ROTATING INERTIA OF DRIVE TRAIN
; (DUAL ENGINE FAILURE), SLUG-FT**2
PTLMR:: .97 ; BLADE TIP CUT OFF RATIO
DCDMR:: .002 ; DELTA DRAG COEF. FOR EACH SEGMENT
NBSMR:: 4 ; NUMBER OF BLADES SIMULATED, FIX POINT
NSSMR:: 5 ; NUMBER OF SEGMENTS SIMULATED, FIX POINT

; ** MAIN ROTOR NON-LINEAR TWIST MAP **
; ** TWIST IS LINEAR ON AH-64A **
TWRMP:: UVR#0 ; MAP ARGUMENT: LOOR UP ROUTINE
; XSEGMR#0 ; INPUT VARIABLE
; TWSTMR#0 ; OUTPUT VARIABLE
; TWRLO ; MAP NAME
EXP 0.0, 1.0, 0.10 ; LOWER LIMIT, UPPER LIMIT, DELTA

TWRLO: EXP 0.00, 0.00, -1.80, -2.70, -3.60
EXP -4.50, -5.40, -6.30, -7.20, -8.10
EXP -9.00

;***** MAIN ROTOR DYNAMIC TWIST SUBMODULE (#A) *****

KOTWMP:: UVR#0
; VXT#0
; KOTWMR#0
; ROTWLO
EXP 100.0, 150.0, 50.0
ROTWLO: EXP -.0003, -.00052

;***** MAIN ROTOR DOWNWASH SUBMODULE (#A) *****

RCTMR:: 1.0 ; THRUST GAIN FOR UNIFORM DOWNWASH
KCMR:: 0.0 ; PITCH MOM. GAIN FOR DOWNWASH SIN. HARMONIC
RSLMR:: 0.0 ; ROLL MOM. GAIN FOR DOWNWASH COS. HARMONIC
TDWOMR:: 0.01038 ; TIME CONST. FOR UNIFORM DOWNWASH FILTER, SEC
TDWCMR:: 0.0 ; TIME CONST. FOR DOWNWASH SIN. HARMON. FILTER, SEC.
TDWSMR:: 0.0 ; TIME CONST. FOR DOWNWASH COS. HARMON. FILTER, SEC.

;***** FLAPPING/LAGGING DAMPER CALCULATIONS (#C) *****

RBRMR:: 0.0 ; FLAPPING HINGE SPRING CONST. FT-LBS/RAD
KBR.MR:: 0.0 ; FLAPPING HINGE DAMPER CONST. FT-LBS-SEC/RAD
; **SET OF MOUNTING DIMENSIONS FOR LAG DAMPER, INCHES**

```

TABLE D-1. AH-64A SPECIFIC FILE (Cont'd)

```

ALDMR:: 0.227 ;
BLDMR:: 3.242 ;
CLDMR:: 12.040 ;
DLDMR:: 10.0102 ;
RLDMR:: 6.898 ;
LGDMDR:: 7.0 ; ALIGNMENT OFFSET IN RELATION TO LAG, DEG
1BLDMR:: 17.481 ; FIXED BLADE PITCH RELATIONSHIP SET. ARM AND THCUFF

; ** BLACK HAWK LAG DAMPER FORCE VS LAG DAMPER ARM RATE
LDMRMP:: UVSVU00 ; MAP ARGUMENT: LOOK UP ROUTINE
LD.MR00(A16) ; INPUT VARIABLE
PLD.MR00(A16) ; OUTPUT VARIABLE
LDMRLO ; LOW RANGE MAP NAME
EXP 0.0, 2.0, 0.1 ; LOWER LIMIT, UPPER LIMIT, DELTA
LDMRHI ; HIGH RANGE MAP NAME
EXP 2.0, 7.0, 1.0 ; LOWER LIMIT, UPPER LIMIT, DELTA

; LOW ANGLE MAP: LD.MR 0 TO 2.0 , DELTA = .1
LDMRLO: EXP 0.0, 30.0, 90.0, 160.0, 280.0
EXP 490.0, 720.0, 950.0, 1190.0, 1400.0
EXP 1630.0, 1860.0, 2090.0, 2310.0, 2530.0
EXP 2770.0, 2980.0, 3200.0, 3310.0, 3370.0
EXP 3410.0

; HIGH ANGLE MAP: LD.MR 2.0 TO 7.0 , DELTA=1.0
LDMRHI: EXP 3410.0, 3550.0, 3615.0, 3680.0, 3745.0
EXP 3815.0

;***** INPUT PARAMETERS FOR FUSELAGE/WING (0A) *****
;***** MOUNTING POINT FOR MODEL IN WIND TUNNEL *****
FSWF:: 208.0 ; FUSELAGE STATION, IN.
WLWF:: 142.0 ; WATERLINE STATION, IN.
BLWF:: 0.0 ; BUTTLINE STATION, IN. (+IVE TO PORT)
IWF:: 0.0 ; WING INCIDENCE, DEG.

; ** AB-64A FUSELAGE LIFT (TAIL OFF) VS ALPWF
LQFMP:: UVUVR00 ; MAP ARGUMENT: LOOK UP ROUTINE
ALPWF00 ; INPUT VARIABLE
LQF00 ; OUTPUT VARIABLE
LQFLD ; LOW ANGLE MAP NAME
EXP -30.0, 30.0, 5.0 ; LOWER LIMIT, UPPER LIMIT, DELTA-LOW ANGLE
LQFHI ; HIGH ANGLE MAP NAME
EXP -90.0, 90.0, 10.0 ; LOWER LIMIT, UPPER LIMIT, DELTA-HIGH ANGLE

; LOW ANGLE MAP: ALPWF -30 TO 30 , DELTA=5
LQFLO: EXP -45.0, -40.0, -34.0, -28.0, -20.0
EXP -11.0, -1.0, 12.0, 25.0, 41.0
EXP 56.0, 65.0, 71.0

; HIGH ANGLE MAP: ALPWF -90 TO 90 , DELTA=10
LQFHI: EXP 0.0, -19.0, -34.0, -44.0, -50.0
EXP -51.0, -45.0, -34.0, -20.0, -1.0
EXP 25.0, 56.0, 71.0, 76.0, 74.0
EXP 64.0, 50.0, 30.0, 0.0

; ** AB-64A FUSELAGE DRAG (TAIL OFF) VS ALPWF
DQFMP:: BIVBIV00 ; MAP ARGUMENT: LOOK UP ROUTINE
EXP ALPWF00, PSINF00 ; INPUT VARIABLE #1, INPUT VARIABLE #2
DQF00 ; OUTPUT VARIABLE
DQFLD ; LOW ANGLE MAP NAME
EXP -30.0, 30.0, 5.0, 15 ; LOWER LIM, UPPER LIM, DELTA, #ITERS(OCTAL), ALPWF
EXP -20.0, 20.0, 10.0 ; LOWER LIMIT, UPPER LIMIT, DELTA, PSINF
DQFHI ; HIGH ANGLE MAP NAME
EXP -90.0, 90.0, 10.0, 23 ; LOWER LIM, UPPER LIM, DELTA, #ITERS(OCTAL), ALPWF
EXP -20.0, 20.0, 10.0 ; LOWER LIMIT, UPPER LIMIT, DELTA, PSINF

```

TABLE D-1. AH-64A SPECIFIC FILE (Cont'd)

```

; LOW ANGLE MAP: ALFWY -30 TO 30, DELTA=5, PSIMF--20 TO +20
; PSIMF = -20
DQFLO: EXP 71.0, 68.5, 66.0, 62.0, 58.5
      EXP 57.0, 56.0, 57.0, 58.5, 61.5
      EXP 65.0, 68.0, 70.0

; PSIMF = -10
      EXP 66.0, 62.0, 56.0, 45.0, 39.5
      EXP 36.0, 35.0, 35.0, 38.0, 43.0
      EXP 52.0, 60.0, 66.0

; PSIMF = 0
      EXP 61.0, 56.0, 45.0, 36.0, 31.0
      EXP 28.0, 27.0, 27.0, 29.0, 34.0
      EXP 45.0, 56.0, 62.0

; PSIMF = +10
      EXP 66.0, 62.0, 54.0, 45.0, 39.5
      EXP 36.0, 35.0, 35.0, 38.0, 43.0
      EXP 52.0, 60.0, 66.0

; PSIMF = +20
      EXP 71.0, 68.5, 66.0, 62.0, 58.5
      EXP 57.0, 56.0, 57.0, 58.5, 61.5
      EXP 65.0, 68.0, 70.0

; HIGH ANGLE MAP: ALFWY -90 TO 90, DELTA=10, PSIMF--20 TO +20
; PSIMF = -20
DQFHI: EXP 84.0, 82.0, 80.0, 79.0, 77.0
      EXP 74.5, 71.0, 66.0, 58.5, 56.0
      EXP 58.5, 65.0, 70.0, 74.0, 77.0
      EXP 79.0, 81.0, 82.0, 83.0

; PSIMF = -10
      EXP 84.0, 82.0, 80.0, 78.0, 75.0
      EXP 71.5, 66.0, 54.0, 39.5, 35.0
      EXP 36.0, 52.0, 66.0, 72.0, 76.0
      EXP 78.5, 81.0, 82.0, 83.0

; PSIMF = 0
      EXP 84.0, 82.0, 80.0, 77.0, 73.0
      EXP 69.0, 61.0, 45.0, 31.0, 27.0
      EXP 29.0, 45.0, 62.0, 70.5, 75.0
      EXP 78.0, 81.0, 82.0, 83.0

; PSIMF = +10
      EXP 84.0, 82.0, 80.0, 78.0, 75.0
      EXP 71.5, 66.0, 54.0, 39.5, 35.0
      EXP 38.0, 52.0, 66.0, 72.0, 76.0
      EXP 78.5, 81.0, 82.0, 83.0

; PSIMF = +20
      EXP 84.0, 82.0, 80.0, 79.0, 77.0
      EXP 74.5, 71.0, 66.0, 58.5, 56.0
      EXP 58.5, 65.0, 70.0, 74.0, 77.0
      EXP 79.0, 81.0, 82.0, 83.0

; ** AH-64A FUSELAGE PITCH MOMENT (TAIL OFF) VS ALFWY
NQPHF: :UVRUVR00 ;MAP ARGUMENT:LOOK UP ROUTINE
      ALFWF00 ;INPUT VARIABLE
      NQF00 ;OUTPUT VARIABLE
      NQFLO ;LOW ANGLE MAP NAME
      EXP -30.0,30.0,5.0 ;LOWER LIMIT,UPPER LIMIT,DELTA-LOW ANGLE
      NQPHI ;HIGH ANGLE MAP NAME
      EXP -90.0,90.0,10.0 ;LOWER LIMIT,UPPER LIMIT,DELTA-HIGH ANGLE

```

TABLE D-1. AH-64A SPECIFIC FILE (Cont'd)

```

; LOW ANGLE MAP: ALFNP -30 TO 30 , DELTA=5
MQPLO: EXP -305.0, -290.0, -262.0, -205.0, -152.0
        EXP -102.0, -62.0, -25.0, 7.0, 35.0
        EXP 62.0, 87.0, 110.0

; HIGH ANGLE MAP: ALFNP -90 TO 90 , DELTA=10
MQPHI: EXP 0.0, -95.0, -180.0, -285.0, -285.0
        EXP -307.0, -305.0, -262.0, -152.0, -62.0
        EXP 7.0, 62.0, 110.0, 153.0, 163.0
        EXP 150.0, 120.0, 60.0, 0.0

; ** AH-60A FUSELAGE SIDE FORCE (TAIL OFF) VS PSINP
YQFNP: :UVRUFR00 ;MAP ARGUMENT:LOOK UP ROUTINE
        PSINP00 ;INPUT VARIABLE
        YQF00 ;OUTPUT VARIABLE
        YQFLO ;LOW ANGLE MAP NAME
        EXP -30.0,30.0,5.0 ;LOWER LIMIT,UPPER LIMIT,DELTA-LOW ANGLE
        YQFHI ;HIGH ANGLE MAP NAME
        EXP -90.0,90.0,10.0 ;LOWER LIMIT,UPPER LIMIT,DELTA-HIGH ANGLE

; LOW ANGLE MAP: PSINP -30 TO 30, DELTA=5
TOPLO: EXP -84.0, -73.0, -60.0, -45.0, -30.0
        EXP -15.0, 0.0, 15.0, 30.0, 45.0
        EXP 60.0, 73.0, 88.0

; HIGH ANGLE MAP: PSINP -90 TO 90, DELTA=10
YQPHI: EXP 0.0, -39.0, -69.0, -88.0, -98.0
        EXP -98.0, -88.0, -60.0, -30.0, 0.0
        EXP 30.0, 60.0, 84.0, 98.0, 98.0
        EXP 91.0, 75.0, 48.0, 0.0

; ** AH-60A FUSELAGE TAWING MOMENT (TAIL OFF) VS PSINP
NQFNP: :UVRUVH00 ;MAP ARGUMENT:LOOK UP ROUTINE
        PSINP00 ;INPUT VARIABLE
        NQF00 ;OUTPUT VARIABLE
        NQFLO ;LOW ANGLE MAP NAME
        EXP -30.0,30.0,5.0 ;LOWER LIMIT,UPPER LIMIT,DELTA-LOW ANGLE
        NQFHI ;HIGH ANGLE MAP NAME
        EXP -90.0,90.0,10.0 ;LOWER LIMIT,UPPER LIMIT,DELTA-HIGH ANGLE

; LOW ANGLE MAP: PSINP -30 TO 30, DELTA=5
NQPLO: EXP -510.0, -460.0, -390.0, -325.0, -235.0
        EXP -125.0, -10.0, 90.0, 185.0, 262.0
        EXP 325.0, 380.0, 415.0

; HIGH ANGLE MAP: PSINP -90 TO 90, DELTA=10
NQPHI: EXP 0.0, -200.0, -365.0, -480.0, -580.0
        EXP -550.0, -510.0, -390.0, -235.0, -10.0
        EXP 105.0, 325.0, 415.0, 440.0, 440.0
        EXP 380.0, 280.0, 150.0, 0.0

;***** ROTOR INTERFERENCE ON THE FUSELAGE (RRPA) *****

; ** BLACK HAWK FUSE/APT N.R. DOWNWASH AT FUSELAGE
EKWFNP: :BIV00 ;MAP ARGUMENT:LOOK UP ROUTINE
        EXP CHIPNR00,AAIFNR00 ;INPUT VARIABLE 01, INPUT VARIABLE 02
        EKWF00 ;OUTPUT VARIABLE
        EKWFLO ;LOW ANGLE MAP NAME
        EXP 0.0,100.0,10.0,13 ;LOW LIM,UPPER LIM,DELTA,ENTRYS(OCT)-CHIPNR
        EXP -6.0,6.0,6.0 ;LOW LIM,UPPER LIM,DELTA-AAIFNR

; LOW ANGLE MAP CHIPNR 0 TO 100 (DEL=10) AAIFNR -6.0,6
EKWFLO: EXP 0.05, 0.15, 0.3, 0.63, 0.55
        EXP 0.66, 0.79, 0.9, 1.03, 0.55
        EXP 0.0
    
```

TABLE D-1. AH-64A SPECIFIC FILE (Cont'd)

```

; AALFMR=0
EXP 0.0, 0.1, 0.21, 0.32, 0.42
EXP 0.54, 0.66, 0.8, 0.94, 0.5
EXP 0.0

; AALFMR=6
EXP -0.12, 0.02, 0.08, 0.19, 0.28
EXP 0.4, 0.53, 0.67, 0.82, 0.4
EXP 0.0

; ** BLACK HAWK VERTICAL W.R. DOWNWASH AT FUSELAGE
EZWFMP::HIV00 ;MAP ARGUMENT:LOOK UP ROUTINE
EXP CHIPMR00,AALFMR00 ;INPUT VARIABLE #1, INPUT VARIABLE #2
EKZWF00 ;OUTPUT VARIABLE
ZIMFLO ;LOW ANGLE MAP NAME
EXP 0.0,100.0,10.0,13 ;LOW LIM,UPPER LIM,DELTA,#ENTRYS(OCT)-CHIPMR
EXP -6.0,6.0,6.0 ;LOW LIM,UPPER LIM,DELTA-AALFMR

; LOW ANGLE MAP CHIPMR 0 TO 100 (DEL=10) AALFMP -6,0,6
; AALFMR=-6
EZWFLO:EXP 1.11, 1.09, 1.08, 1.065, 1.05
EXP 1.04, 1.02, 1.01, 1.0, 0.88
EXP 0.6

; AALFMR=0
EXP 1.12, 1.12, 1.12, 1.12, 1.12
EXP 1.12, 1.12, 1.12, 1.11, 0.96
EXP 0.6

; AALFMR=6
EXP 1.15, 1.15, 1.15, 1.15, 1.16
EXP 1.17, 1.18, 1.22, 1.16, 0.98
EXP 0.6

;***** INPUT PARAMETERS FOR PANEL #1 (#A) *****
FSF1:: 552.5 ; FUSELAGE STATION,INCH
WLP1:: 147.2 ; WATERLINE STATION,INCH
HLP1:: -22.3 ; BUTTLINE STATION,INCH (+IVE TO PORT)
SAP1:: 16.68 ; SURFACE AREA OF PANEL IF NOT INCLUDE IN MAP
GAMP1:: 0.0 ; PANEL ORIENTATION, DEG
IOP1:: 2 ; PANEL INCIDENCE,DEG
CPI1:: 1.0 ; PANEL MEAN AERO CHORD,FT

; ** AH-64A HORIZONTAL STABILIZER (RT PANEL) LIFT COEFFICIENT VS ALFPP1
; ** S=16.68 FT**2 ,ASPECT RATIO=3.41,0018 AIRFOIL
CLP1MP::UVRVK00 ;MAP ARGUMENT:LOOK UP ROUTINE
ALFPP100 ;INPUT VARIABLE
CLP100 ;OUTPUT VARIABLE
CLP1LO ;LOW ANGLE MAP NAME
EXP -30.0,30.0,5.0 ;LOWER LIRIT,UPPER LIRIT,DELTA-LOW ANGLE
CLP1HI ;HIGH ANGLE MAP NAME
EXP -90.0,90.0,10.0 ;LOWER LIRIT,UPPER LIRIT,DELTA-HIGH ANGLE

; LOW ANGLE MAP ALFPP1 -30 TO 30,DELTA=5
CLP1LO:EXP -0.80, -0.87, -0.93, -0.88, -0.58
EXP -0.29, 0.00, 0.29, 0.58, 0.88
EXP 0.93, 0.87, 0.80

; HIGH ANGLE MAP ALFPP1 -90 TO 90,DELTA=10
CLP1HI:EXP 0.00, -0.14, -0.28, -0.40, -0.53
EXP -0.68, -0.80, -0.93, -0.58, 0.00
EXP 0.58, 0.93, 0.80, 0.68, 0.53
EXP 0.40, 0.28, 0.16, 0.00

```

TABLE D-1. AH-64A SPECIFIC FILE (Cont'd)

```

; ** AH-64A HORIZONTAL STABILIZER DRAG VS ALPPP1
CDP1RP:;UVRVVR00 ;MAP ARGUMENT:LOOK UP ROUTINE
        ALPPP100 ;INPUT VARIABLE
        CDP100 ;OUTPUT VARIABLE
        CDP1LO ;LOW ANGLX MAP NAME
        XXP -30.0,30.0,5.0 ;LDWER LIMIT,UPPER LIMIT,DELTA
        CDP1HI ;HIGH ANGLE MAP NAME
        EXP -90.0,90.0,10.0 ;LOWER LIMIT,UPPER LIMIT,DELTA

; LOW ANGLE MAP ALPPP1 -30 TO 30,DELTA=5
CDP1LD: EXP 0.343, 0.271, 0.200, 0.105, 0.050
        EXP 0.020, 0.010, 0.020, 0.050, 0.105
        EXP 0.200, 0.271, 0.343

; HIGH ANGLE MAP ALPPP1 -90 TO 90,DELTA=10
CDP1HI: EXP 1.200, 1.057, 0.914, 0.771, 0.629
        EXP 0.486, 0.343, 0.200, 0.050, 0.010
        XXP 0.050, 0.200, 0.343, 0.486, 0.629
        EXP 0.771, 0.914, 1.057, 1.200

;***** INPUT PARAMETERS FOR ROTOR INTERFERENCE ON THE HORIZ.TAIL 01 (MRPA)

; ** BLACK HAWK FORE/APT R.R. DOWNWASH AT HORIZTONTAL TAIL
XFP1RP:;BIV40 ;MAP ARGUMENT:LOOK UP ROUTINE
        EXP CHIPRR00,AA1PRR00 ;INPUT VARIABLE 01, INPUT VARIABLE 02
        XXP144 ;OUTPUT VARIABLE
        EXPILD ;LOW ANGLE MAP NAME
        EXP 0.0,100.0,10.0,13 ;LOW LIM,UPPER LIM,DELTA,#ENTRYS(OCT)-CHIPRR
        EXP -6.0,6.0,6.0 ;LOW LIM,UPPER LIM,DELTA-AA1PRR

; LOW ANGLE MAP CHIPRR 0 TO 100 (DEL=10) AA1PRR -6,0,6
; AA1PRR=-6
EXPILD:EXP 0.0, -0.2, 0.05, 0.3, 0.54
        XXP 0.8, 1.04, 1.3, 1.55, 0.8
        EXP 0.0

; AA1PRR=0
EXP -0.4, -0.6, -0.2, 0.12, 0.36
XPX 0.6, 0.83, 1.06, 1.3, 0.66
EXP 0.0

; AA1PRR=6
EXP -0.56, -0.8, -0.74, -0.32, 0.04
XPX 0.32, 0.6, 0.86, 1.12, 0.54
EXP 0.0

; ** BLACK HAWK VERTICAL R.R. DOWNWASH AT HORIZTONTAL TAIL
ZFP1RP:;BIV00 ;MAP ARGUMENT:LOOK UP ROUTINE
        XXP CHIPRR04,AA1PRR04 ;INPUT VARIABLE 01, INPUT VARIABLE 02
        XXP104 ;OUTPUT VARIABLE
        EXPILD ;LOW ANGLE MAP NAME
        EXP 0.0,100.0,10.0,13 ;LOW LIM,UPPER LIM,DELTA,#ENTRYS(DCT)-CHIPRR
        XXP -6.0,6.0,6.0 ;LOW LIM,UPPER LIM,DELTA-AA1PRR

; LOW ANGLE MAP CHIPRR 0 TO 100 (DEL=10) AA1PRR -6,0,0
; AA1PRR=-6
EXPILD:EXP -0.13, 0.8, 1.8, 1.82, 1.86
        EXP 1.88, 1.91, 1.94, 1.89, 1.42
        EXP 1.14

; AA1PRR=0
EXP 0.4, 0.94, 1.84, 1.9, 1.98
XPX 2.04, 2.08, 2.14, 1.89, 1.62
EXP 1.35

; AA1PRR=6

```

TABLE D-1. AH-64A SPECIFIC FILE (Cont'd)

EXP	0.78,	1.36,	1.91,	1.98,	2.06
EXP	2.14,	2.21,	2.28,	2.16,	1.96
	1.56				

***** FUSELAGE INTERFERENCE ON THE HORIZ.TAIL #1 (WPPA) *****

; ** AH-64A DYNAMIC PRESSURE RATIO AT HORIZONTAL TAIL VS ALFWP

QPIMP::CONST00 ;MAP ARGUMENT:LOOK UP ROUTINE
 [0.80]
 QPIQWF00 ;OUTPUT VARIABLE

; ** MODIFIED BLACK HAWK DOWNWASH ON HORIZONTAL TAIL VS ALFWP
 ; ** DUE TO BODY AND STORE SUPPORT WINGS

EPPIMP::UVRUVR00 ;MAP ARGUMENT:LOOK UP ROUTINE
 ALFWF00 ;INPUT VARIABLE
 EPSP100 ;OUTPUT VARIABLE
 EPP1LO ;LOW ANGLE MAP NAME
 EXP -30.0,30.0,5.0 ;LOWER LIMIT,UPPER LIMIT,DELTA-LOW ANGLE
 EPP1HI ;HIGH ANGLE MAP NAME
 EXP -90.0,90.0,10.0 ;LOWER LIMIT,UPPER LIMIT,DELTA-HIGH ANGLE

; LOW ANGLE MAP ALPPP1 -30 TO 30 DELTA-5

EPP1LO: EXP	1.30,	0.90,	0.50,	-0.80,	-2.00
EXP	-1.00,	2.00,	4.00,	3.60,	3.30
EXP	3.20,	2.90,	2.60		

; HIGH ANGLE MAP ALPPP1 -90 TO 90 DELTA-10

EPP1HI: EXP	0.00,	0.00,	0.00,	0.00,	0.43
EXP	0.86,	1.30,	0.60,	-2.00,	2.00
EXP	3.60,	3.20,	2.60,	1.72,	0.85
EXP	0.00,	0.00,	0.00,	0.00	

***** INPUT PARAMETERS FOR PANEL #2 (8A) *****

FSP2:: 552.5 ; FUSELAGE STATION, INCH
 WLP2:: 147.2 ; WATERLINE STATION, INCH
 BLP2:: 22.3 ; BUTTLINE STATION, INCH (+IVE TO PORT)
 SAP2:: 16.68 ; SURFACE AREA OF PANEL IF NOT INCLUDE IN MAP
 GAMP2:: 0.0 ; PANEL ORIENTATION, DEG
 IOP2:: 2 ; PANEL INCIDENCE, DEG
 CP2:: 1.0 ; PANEL MEAN AERO CHORD, FT

; ** AH-64A HORIZONTAL STABILIZER (LT PANEL) LIFT COEFFICIENT VS ALPPP2
 ; ** S-16.68 FT**2 ,ASPECT RATIO-3.41 ,0018 AIRFOIL

CLP2MP::UVRUVR00 ;MAP ARGUMENT:LOOK UP ROUTINE
 ALPPP200 ;INPUT VARIABLE
 CLP200 ;OUTPUT VARIABLE
 CLP1LO ;LOW ANGLE MAP NAME
 EXP -30.0,30.0,5.0 ;LOWER LIMIT,UPPER LIMIT,DELTA
 CLP1HI ;HIGH ANGLE MAP NAME
 EXP -90.0,90.0,10.0 ;LOWER LIMIT,UPPER LIMIT,DELTA

; ** AH-64A HORIZONTAL STABILIZER DRAG VS ALPPP2

CDP2MP::UVRUVR00 ;MAP ARGUMENT:LOOK UP ROUTINE
 ALPPP200 ;INPUT VARIABLE
 CDP200 ;OUTPUT VARIABLE
 CDP1LO ;LOW ANGLE MAP NAME
 EXP -30.0,30.0,5.0 ;LOWER LIMIT,UPPER LIMIT,DELTA
 CDP1HI ;HIGH ANGLE MAP NAME
 EXP -90.0,90.0,10.0 ;LOWER LIMIT,UPPER LIMIT,DELTA

***** INPUT PARAMETERS FOR ROTOR INTERFERENCE ON THE HORIZ.TAIL #2 (MRPA)

; ** BLACK HAWK FORE/AFT H.R. DOWNWASH AT HORIZONTAL TAIL

EXP2MP::CONST00 ;MAP ARGUMENT:LOOK UP ROUTINE
 EXXP100 ;INPUT VARIABLE

TABLE D-1. AH-64A SPECIFIC FILE (Cont'd)

```

EKXP200          ;OUTPUT VARIABLE
; ** BLACK RANK VERTICAL M.R. DOWNWASH AT HORIZONTAL TAIL
EZF2MP::CDNST00  ;MAP ARGUMENT:LOOK UP ROUTINE
EKZP100          ;INPUT VARIABLE
EKXP200          ;OUTPUT VARIABLE

;***** FUSELAGE INTERFERENCE ON THE HORIZ.TAIL #2 (WPPA) *****
; ** AH-64A DYNAMIC PRESSURE RATIO AT HORIZDNTAL TAIL VS ALFWP
QP2MP::CONST00  ;MAP ARGUMENT:LOOK UP ROUTINE
QP1QWF00        ;INPUT VARIABLE
QP2QWF00        ;OUTPUT VARIABLE
; ** MODIFIED BLACKRANK DOWNWASH ON HORIZONTAL TAIL VS ALFWP
; ** DUE TO BODY
EPP2MP::CONST00 ;MAP ARGUMENT:LOOK UP ROUTINE
EPSP100         ;INPUT VARIABLE
EPSP200         ;OUTPUT VARIABLE

;***** INPUT PARAMETERS FOR PANEL #3 (#A) *****
FSP3:: 544.4     ; FUSELAGE STATION,INCH
WLP3:: 189.2     ; WATERLINE STATION,INCH
HLP3:: 0.0       ; HUTTLINE STATION,INCH
SAP3:: 32.2     ; SURFACE AREA OF PANEL IF NDT INCLUDE IN MAP
GAMP3:: 90.0    ; PANEL ORIENTATION, DEG
IOP3:: 0.0      ; PANEL INCIDENCE,DEC
CP3:: 1.0       ; PANEL MEAN ARED CHORD,FT

; ** AH-64A VERTICAL STABILIZER LIFT COEFFICIENT VS ALPPP3
; ** S=32.2 FT**2 ,ASPECT RATIO =2.5 ,4415 WDD ROOT, 4416 TIP AIRFOIL
CLP3MP::UVRUVR00 ;MAP ARGUMENT:LOOK UP ROUTINE
ALPPP300        ;INPUT VARIABLE
CLP300         ;OUTPUT VARIABLE
CLP3LO        ;LOW ANGLE MAP NAME
EXP -30.0,30.0,5.0 ;LOWER LIMIT,UPPER LIMIT,DELTA-LOW ANGLE
CLP3HI        ;HIGH ANGLE MAP NAME
EXP -90.0,90.0,10.0 ;LOWER LIMIT,UPPER LIMIT,DELTA-HIGH ANGLE

; LOW ANGLE MAP ALPPP3 -30 TO 30,DELTA=5
CLP3LO:EXP      -1.06,   -0.81,   -0.57,   -0.31,   -0.05
EXP             0.20,    0.45,    0.71,    0.97,    1.19
EXP             1.34,    1.40,    1.34

; HIGH ANGLE MAP ALPPP3 -90 TO 90,DELTA=10
CLP3HI:EXP      0.00,   -0.22,   -0.45,   -0.68,   -0.90
EXP             -1.13,  -1.06,   -0.57,   -0.05,   0.45
EXP             0.97,   1.34,   1.34,   1.12,   0.93
EXP             0.68,   0.45,   0.23,   0.00

; ** AH-64A VERTICAL STABILIZER DRAG COEFFICIENT VS ALPPP3
CDP3MP::UVRUVR00 ;MAP ARGUMENT:LOOK UP ROUTINE
ALPPP300        ;INPUT VARIABLE
CDP300         ;OUTPUT VARIABLE
CDP3LO        ;LOW ANGLE MAP NAME
EXP -30.0,30.0,5.0 ;LOWER LIMIT,UPPER LIMIT,DELTA-LOW ANGLE
CDP3HI        ;HIGH ANGLE MAP NAME
EXP -90.0,90.0,10.0 ;LOWER LIMIT,UPPER LIMIT,DELTA-HIGH ANGLE

; LOW ANGLE MAP ALPPP3 -30 TO 30,DELTA=5
CDP3LO:EXP      0.559,   0.505,   0.310,   0.160,   0.130
EXP             0.100,   0.090,   0.100,   0.130,   0.180
EXP             0.310,   0.505,   0.559

; HIGH ANGLE MAP ALPPP3 -90 TO 90,DELTA=10

```


TABLE D-1. AH-64A SPECIFIC FILE (Cont'd)

```

CDP3B1: EXP    1.200,    1.093,    0.986,    0.879,    0.772
          EXP    0.665,    0.559,    0.310,    0.130,    0.090
          EXP    0.130,    0.310,    0.559,    0.665,    0.772
          EXP    0.879,    0.986,    1.093,    1.200

;***** ROTOR INTERFERENCE ON THE VERTICAL TAIL (MRPA) *****
          ; ** ROTOR EXX-FACTOR ON VERTICAL TAIL MAP **

EXP3RP::CONST##          ;MAP ARGUMENT:LOOK UP ROUTINE
          EKXP1##          ;INPUT VARIABLE
          EKXP3##          ;OUTPUT VARIABLE

          ; ** ROTOR EKZ-FACTOR ON VERTICAL TAIL MAP **

EZP3RP::CONST##          ;MAP ARGUMENT:LOOK UP ROUTINE
          EKZP1##          ;INPUT VARIABLE
          EKZP3##          ;OUTPUT VARIABLE

;***** FUSELAGE INTERFERENCE ON THE VERTICAL TAIL (MRPA) *****
          ; ** AH-64A DYNAMIC PRESSURE RATIO AT VERTICAL TAIL VS PS1WF

QP3MP:: CONST##          ;MAP ARGUMENT:LOOK UP ROUTINE
          [0.75]
          QP3QWF##          ;OUTPUT VARIABLE

          ; ** BLACK HAWK SIDEWASH ON VERTICAL TAIL VS PS1WF DUE TO BODY

SGP3MP::UVSUVS44          ;MAP ARGUMENT:LOOK UP ROUTINE
          PS1WF##          ;INPUT VARIABLE
          SIGP314          ;OUTPUT VARIABLE
          SGP3LO          ;LOW ANGLE MAP NAME
          EXP 0.0,30.0,5.0 ;LOWER LIMIT, UPPER LIMIT, DELTA-LOW ANGLE
          SG73HI          ;HIGH ANGLE MAP NAME
          EXP 0.0,90.0,30.0 ;LOWER LIMIT, UPPER LIMIT, DELTA-HIGH ANGLE

          ; LOW ANGLE MAP PS1WF 0 TO 30 DELTA=5
SGP3LO: EXP    0.0,    -0.4,    -0.6,    0.8,    1.4
          EXP    0.6,    0.2

          ; HIGH ANGLE MAP PS1WF 0 TO 90 DELTA=30
SG73HI: EXP    0.0,    0.2,    0.0,    0.0
          PAGE

;***** INPUT PARAMETERS FOR PANEL #4 (#A) *****

FSP4:: 201.93          ; FUSELAGE STATION, INCH
WLP4:: 137.5          ; WATERLINE STATION, INCH
BLP4:: -46.3          ; BUTLINE STATION, INCH (+IVE TO PORT)
SAP4:: 30.95          ; SURFACE AREA OF PANEL IF NOT INCLUDE IN MAP
GAMP4:: 0.0          ; PANEL ORIENTATION, DEG
10P4:: 6.0          ; PANEL INCIDENCE, DEG
CP4:: 1.0          ; PANEL MEAN AERO CHORD, FT

          ; ** AH-64A RIGHT WING LIFT COEFFICIENT ALPPP4
          ; ** 5=30.95 FT**2 ,ASPECT RATIO=4.6 ,4423 ROOT, 4470 TIP AIRFOIL
CLP4MP::UVRUVR44          ;MAP ARGUMENT:LOOK UP ROUTINE
          ALPPP4##          ;INPUT VARIABLE
          CLP4##          ;OUTPUT VARIABLE
          CLP4LO          ;LOW ANGLE MAP NAME
          EXP -30.0,30.0,5.0 ;LOWER LIMIT,UPPER LIMIT,DELTA-LOW ANGLE
          CLP4HI          ;HIGH ANGLE MAP NAME
          EXP -90.0,90.0,10.0 ;LOWER LIMIT,UPPER LIMIT,DELTA-HIGH ANGLE

          ; LOW ANGLE MAP ALPPP4 -30 TO 30,DELTA=5

```

TABLE D-1. AH-64A SPECIFIC FILE (Cont'd)

```

CLP4LO: EXP   -0.68,   -0.64,   -0.50,   -0.30,   -0.12
        EXP    0.07,    0.25,    0.43,    0.61,    0.76
        EXP    0.80,    0.76,    0.70

; HIGH ANGLE MAP ALPPP4 -90 TO 90,DELTA=10
CLP4HI: EXP    0.00,   -0.11,   -0.22,   -0.33,   -0.45
        EXP   -0.57,   -0.68,   -0.50,   -0.12,    0.25
        EXP    0.61,    0.80,    0.70,    0.58,    0.47
        EXP    0.35,    0.23,    0.11,    0.00

; ** AH-64A RIGHT WING DRAG VS ALPPP4
CDP4HP:;UVRUVR## ;MAP ARGUMENT:LOOK UP ROUTINE
        ALPPP4## ;INPUT VARIABLE
        CDP4## ;OUTPUT VARIABLE
        CDP4LO ;LOW ANGLE MAP NAME
        EXP -30.0,30.0,5.0 ;LOWER LIMIT,UPPER LIMIT,DELTA
        CDP4HI ;HIGH ANGLE MAP NAME
        EXP -90.0,90.0,10.0 ;LOWER LIMIT,UPPER LIMIT,DELTA

; LOW ANGLE MAP ALPPP4 -30 TO 30,DELTA=5
CDP4LO: EXP    0.428,   0.364,   0.300,   0.235,   0.171
        EXP    0.126,   0.100,   0.107,   0.128,   0.165
        EXP    0.254,   0.303,   0.372

; HIGH ANGLE MAP ALPPP4 -90 TO 90,DELTA=10
CDP4HI: EXP    1.200,   1.070,   0.943,   0.814,   0.696
        EXP    0.557,   0.428,   0.300,   0.171,   0.100
        EXP    0.128,   0.234,   0.372,   0.510,   0.648
        EXP    0.786,   0.924,   1.062,   1.200

;***** INPUT PARAMETERS FOR ROTOR INTERFERENCE ON THE RIGHT WING (MRPA)

; ** AH-64A PORE/AFT H.R. DOWNWASH AT RIGHT WING
EXP4HP:;CONST## ;MAP ARGUMENT:LOOK UP ROUTINE
        ERXP## ;INPUT VARIABLE
        ERXP4## ;OUTPUT VARIABLE

; ** AH-64A VERTICAL H.R. DOWNWASH AT RIGHT WING
EXP4HP:;CONST## ;MAP ARGUMENT:LOOK UP ROUTINE
        EK2WP## ;INPUT VARIABLE
        ERIP4## ;OUTPUT VARIABLE

;***** FUSELAGE INTERPERENCE ON THE RIGHT WING (MPPA) *****

; ** AH-64A DYNAMIC PRESSURE RATIO AT RIGHT WING VS ALPWT
QP4HP:;CONST## ;MAP ARGUMENT:LOOK UP ROUTINE
        (1.0)
        QP4(MP## ;OUTPUT VARIABLE

;***** INPUT PARAMETERS FOR PANEL #5 (#A) *****
PSP5: 201.93 ; FUSELAGE STATION,INCR
WLP5: 137.5 ; WATERLINE STATION,INCH
BLP5: 46.3 ; BUTTLINE STATION,INCH (-IVE TO PORT)
SAP5: 30.35 ; SURFACE AREA OF PANEL IF NOT INCLUDE IN MAP
GAMP5: 0.0 ; PANEL ORIENTATION, DEG
IOP5: 6.0 ; PANEL INCIDENCE,DEG
CP5: 1.0 ; PANEL MEAN AERO CHORD,PT

```

TABLE D-1. AH-64A SPECIFIC FILE (Cont'd)

```

; ** AH-64A LEFT WING LIFT COEFFICIENT VS ALPPP5
; ** S=30.95 FT**2 ,ASPECT RATIO=4.6 ,4423 ROOT, 4420 TIP AIRFOIL
CLP5MP::UVRUVR00 ;MAP ARGUMENT:LOOK UP ROUTINE
ALPPP500 ;INPUT VARIABLE
CLP500 ;OUTPUT VARIABLE
CLP4LO ;LOW ANGLE MAP NAME
EXP -30.0,30.0,5.0 ;LOWER LIMIT,UPPER LIMIT,DELTA-LOW ANGLE
CLP4HI ;HIGH ANGLE MAP NAME
EXP -90.0,90.0,10.0 ;LOWER LIMIT,UPPER LIMIT,DELTA-HIGH ANGLE

; ** AB-64A LEFT WING DRAG VS ALPPP5
CDP5MP::UVRUVR00 ;MAP ARGUMENT:LOOK UP ROUTINE
ALPPP500 ;INPUT VARIABLE
CDP500 ;OUTPUT VARIABLE
CDP4LO ;LOW ANGLE MAP NAME
EXP -30.0,30.0,5.0 ;LOWER LIMIT,UPPER LIMIT,DELTA
CDP4HI ;HIGH ANGLE MAP NAME
EXP -90.0,90.0,10.0 ;LOWER LIMIT,UPPER LIMIT,DELTA

;***** INPUT PARAMETERS FOR ROTOR INTERFERENCE ON THE LEFT WING (WRPA)

; ** AH-64A FORE/AFT H.R. DOWNWASH AT LEFT WING
EXP5MP::CONST00 ;MAP ARGUMENT:LOOK UP ROUTINE
EKXWF00 ;INPUT VARIABLE
EKXP500 ;OUTPUT VARIABLE

; ** AH-64A VERTICAL H.R. DOWNWASH AT LEFT WING
EZP5MP::CONST00 ;MAP ARGUMENT:LOOK UP ROUTINE
EKZWF00 ;INPUT VARIABLE
EKIP500 ;OUTPUT VARIABLE

;***** FUSELAGE INTERFERENCE ON THE LEFT WING (WPPA) *****

; ** AH-64A DYNAMIC PRESSURE RATIO AT LEFT WING VS ALPMF
QP5MP::CONST00 ;MAP ARGUMENT:LOOK UP ROUTINE
QP4QWF00 ;INPUT VARIABLE
QP5QWF00 ;OUTPUT VARIABLE

;***** INPUT PARAMETERS FOR TAIL ROTOR (RA) - (BAILEY) *****
RTR:: 4.58 ;RADIUS,FT
OMEGTR::146.9 ;TRIM ROTATIONAL RATE, RAD/SEC
RTR:: 4.0 ;ACTUAL NUMBER OF BLADES
FSTR:: 554.69 ;FUSELAGE STATION,IN
NLTR:: 216.25 ;NATERLINE STATION,IN
RLTR:: -33.05 ;RUTLINE STATION,IN (+IVE TO PORT)
TWSTTR:: -8.4 ;BLADE TWIST,DATUM CENTER OF ROTATION,DEG
RIASTR:: 1.5 ;BLADE PITCH CORRECTION FOR N.L.TWIST(NEG REDUCES PITCH)
GAMTR:: 90.0 ;TAIL ROTOR CANT ANGLE,DEG
DELJTR:: 35.0 ;FLAPPING HINGE OFFSET ANGLE,DEG
DELTR:: .001455 ;RATE OF CHANGE OF CONE ANGLE WITH THRUST,DEG/LB
CNRDTR:: .833 ;BLADE CRORD,FT
ATR:: 5.873 ;BLADE LIFT CURVE SLOPE,1/RAD
RTLTR:: .92 ;BLADE TIP LOSS FACTOR
CDTR:: 0.0 ;TAIL ROTOR HEAD DRAG,FT**2
IRTR:: 2.318 ;T.R.BLADE SECOND MOMENT SLUGS-FT**2
DRD0TR:: 0.0087 ;T.R. BLADE SECTION DRAG COEFF,CD0
DRD1TR:: -0.0216 ;T.R. BLADE SECTION DRAG COEFF,CD1
DRD2TR:: 0.4 ;T.R. BLADE SECTION DRAG COEFF,CD2
DROTTR:: -1.0 ;T.R. ROTATION +1.0 REAMS COUNTER CLOCKWISE
; WHEN VIEWED FROM PORT SIDE

```

TABLE D-1. AH-64A SPECIFIC FILE (Cont'd)

```

;***** ROTOR INTERPERNCE ON TAIL ROTOR (MRPA) *****

EXTRMP::CONST00      ;** ROTOR X-FACTOR ON TAIL ROTOR MAP **
EKXP300              ;MAP ARGUMENT:LOOK UP ROUTINE
EKXTR00              ;INPUT VARIABLE
                     ;OUTPUT VARIABLE

EZTRMP::CONST00      ;** ROTOR E-FACTOR ON TAIL ROTOR MAP **
EKZP300              ;MAP ARGUMENT:LOOK UP ROUTINE
EKZTR00              ;INPUT VARIABLE
                     ;OUTPUT VARIABLE

;***** FUSELAGE INTERPERNCE ON THE TAIL ROTOR (WFFA) *****

QTRMP::CONST00       ;** TAIL ROTOR DYNAMIC PRESSURE RATIO MAP **
QP3QWP              ;MAP ARGUMENT:LOOK UP ROUTINE
QTRQWP00            ;INPUT VARIABLE
                     ;OUTPUT VARIABLE

EPTRMP::CONST00      ;** BODY DOWNWASH ON TAIL ROTOR MAP **
EPSP100             ;MAP ARGUMENT:LOOK UP ROUTINE
EPSTR00             ;INPUT VARIABLE
                     ;OUTPUT VARIABLE

SGTRMP::CONST00      ;** BODY SIDWASH ON TAIL ROTOR MAP **
SIGP300             ;MAP ARGUMENT:LOOK UP ROUTINE
SIGTR00             ;INPUT VARIABLE
                     ;OUTPUT VARIABLE

;***** VERTICAL TAIL INTERPERNCE ON TAIL ROTOR INFLOW *****

VBVTTR::30.0         ; AIRSPEED BREAK PT. - NO BLOCKAGE ABOVE,KT.
KBVTTR::0.796        ; TAIL ROTOR BLOCKAGE COEF. AT ROVER

;***** INPUT PARAMETERS FOR EQUATIONS OF MOTION (6B) *****

PSCG:: 208.0          ; FUSELAGE STATION,OP C.G.,INCH
WLCG:: 142.3          ; WATERLINE STATION OF C.G.,INCH
RLCG:: 0.0            ; RUTLINE STATION OF C.G.,INCH (+IVE TO PORY)

WEIGHT::10222.0       ; AIRCRAFT GROSS WEIGHT,LBS.
IE:: 2336.6           ; INERTIA ABOUT BODY X-AXIS,SLUG-FT**2
IY:: 28444.8          ; INERTIA ABOUT BODY Y-AXIS,SLUG-FT**2
IE:: 26796.5          ; INERTIA ABOUT BODY E-AXIS,SLUG-FT**2
IXI:: 0.0             ; CROSS COUPLING INERTIA,SLUG-FT**2
IEY:: 0.0
IYI:: 0.0

```

TABLE D-1. AH-64A SPECIFIC FILE (Cont'd)

,***** INPUT PARAMETERS FOR MOASE (4A) *****

AISUL:: 7.0 ; AIS UPPER LIMIT
AISLL:: -10.5 ; AIS LOWER LIMIT
BISUL:: 20.0 ; BIS UPPER LIMIT
BISLL:: -10.0 ; BIS LOWER LIMIT
THOUL:: 25.9 ; THETAO UPPER LIMIT
THOLL:: 9.9 ; THETAO LOWER LIMIT
THRUL:: 36.5 ; THETTR UPPER LIMIT
THRLL:: 4.5 ; THETTR LOWER LIMIT

XAUL:: 9.0 ; LAT STICK UPPER LIMIT
YALL:: 0.0 ; LAT STICK LOWER LIMIT
XBUL:: 10.0 ; LONG STICK UPPER LIMIT
XBLL:: 0.0 ; LONG STICK LOWER LIMIT
XUL:: 12.0 ; COLL STICK UPPER LIMIT
XCLL:: 0.0 ; COLL STICK LOWER LIMIT
XPUL:: 4.8 ; PEDAL UPPER LIMIT
XPLL:: 0.0 ; PEDAL LOWER LIMIT

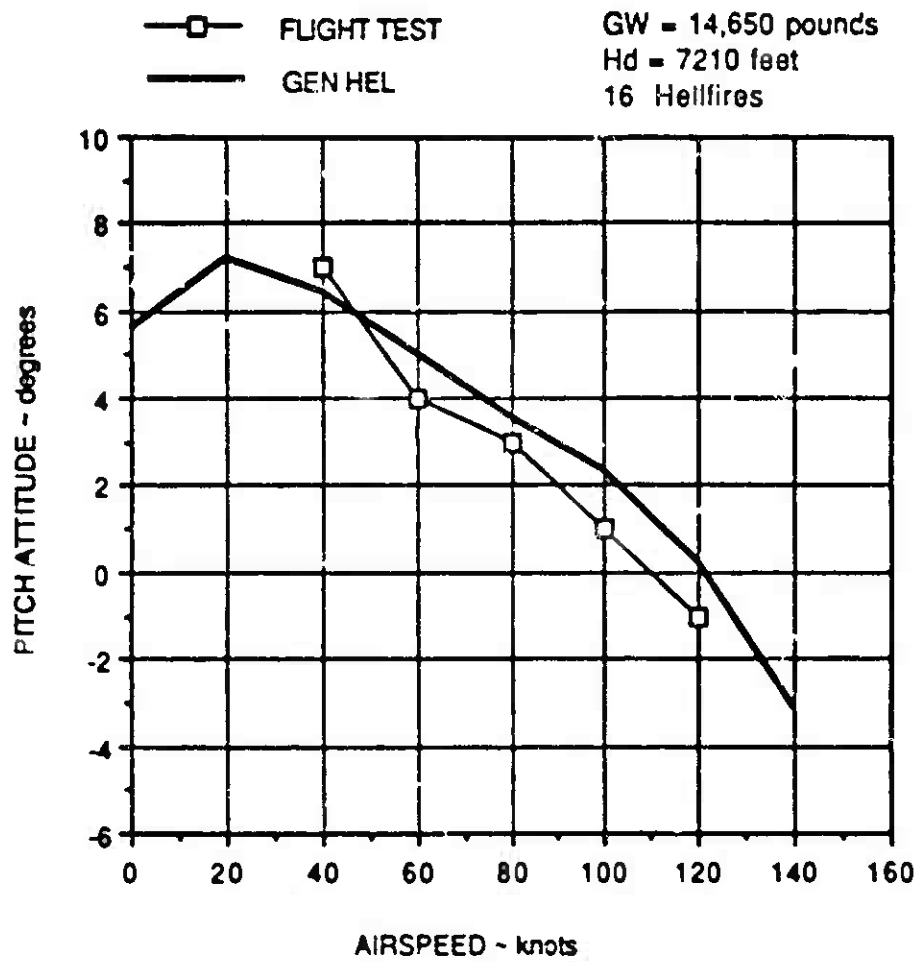


Figure D-2. AH-64A Pitch Attitude Correlation

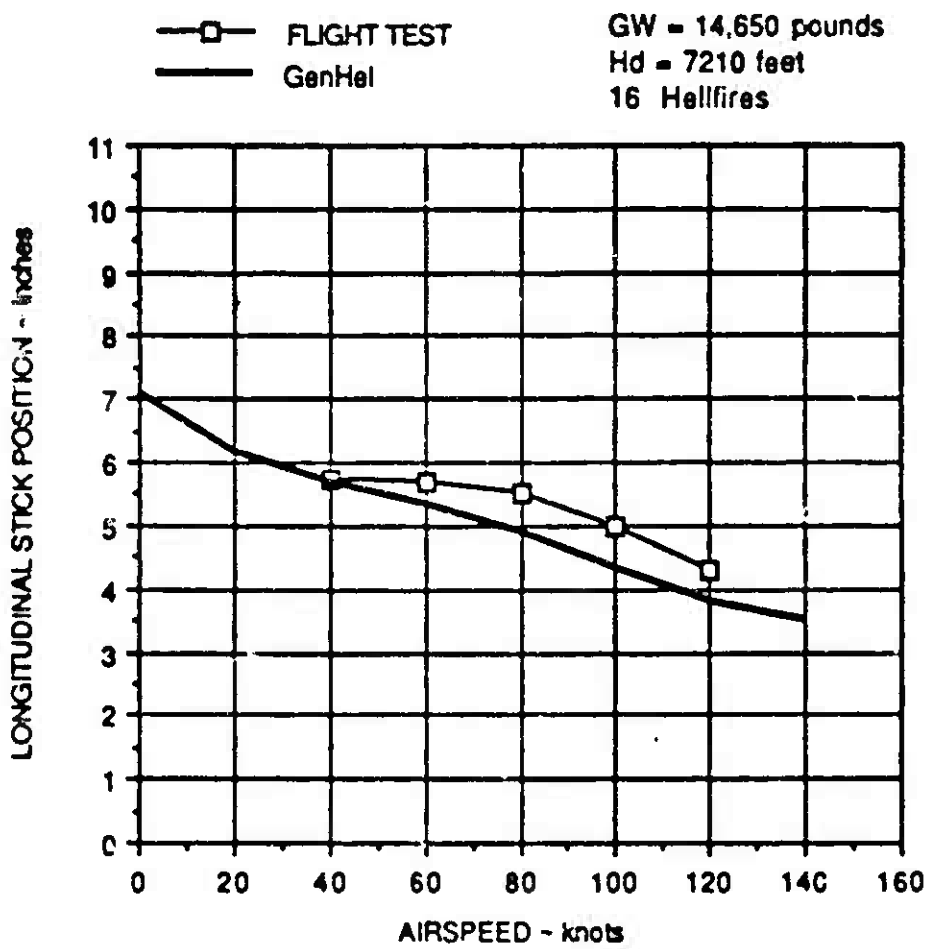


Figure D-3. A1-6AA Longitudinal Stick Correlation

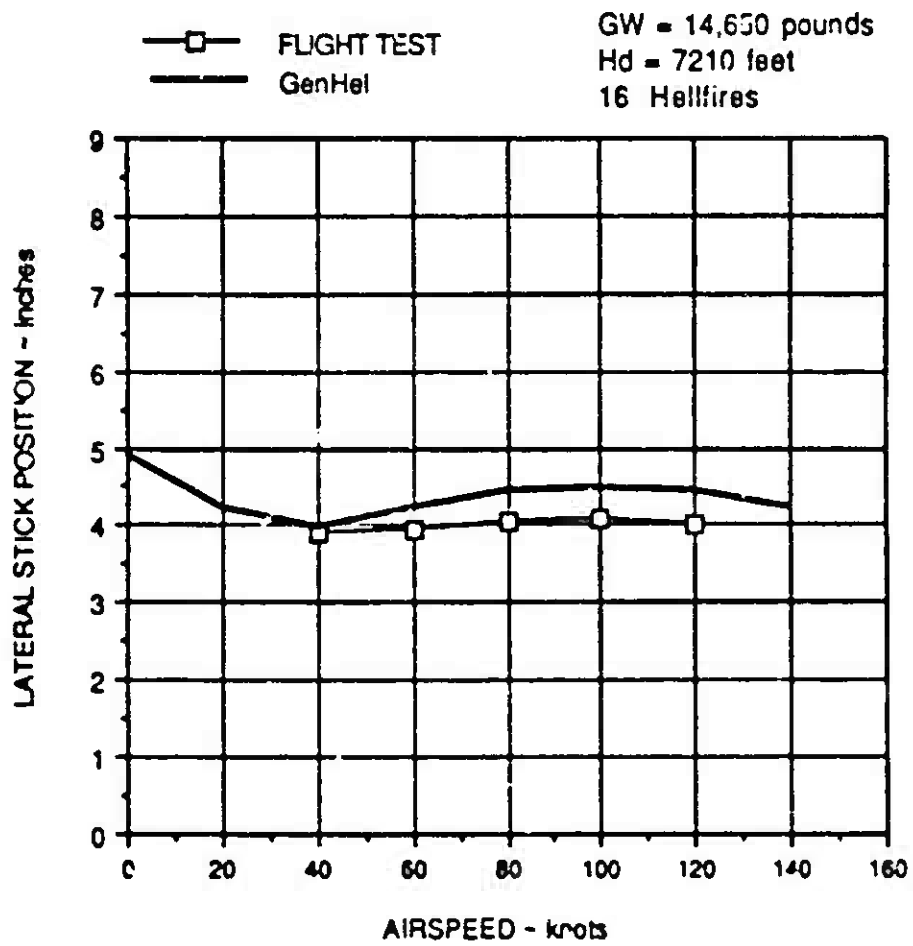


Figure D-4. AH-64A Lateral Stick Correlation

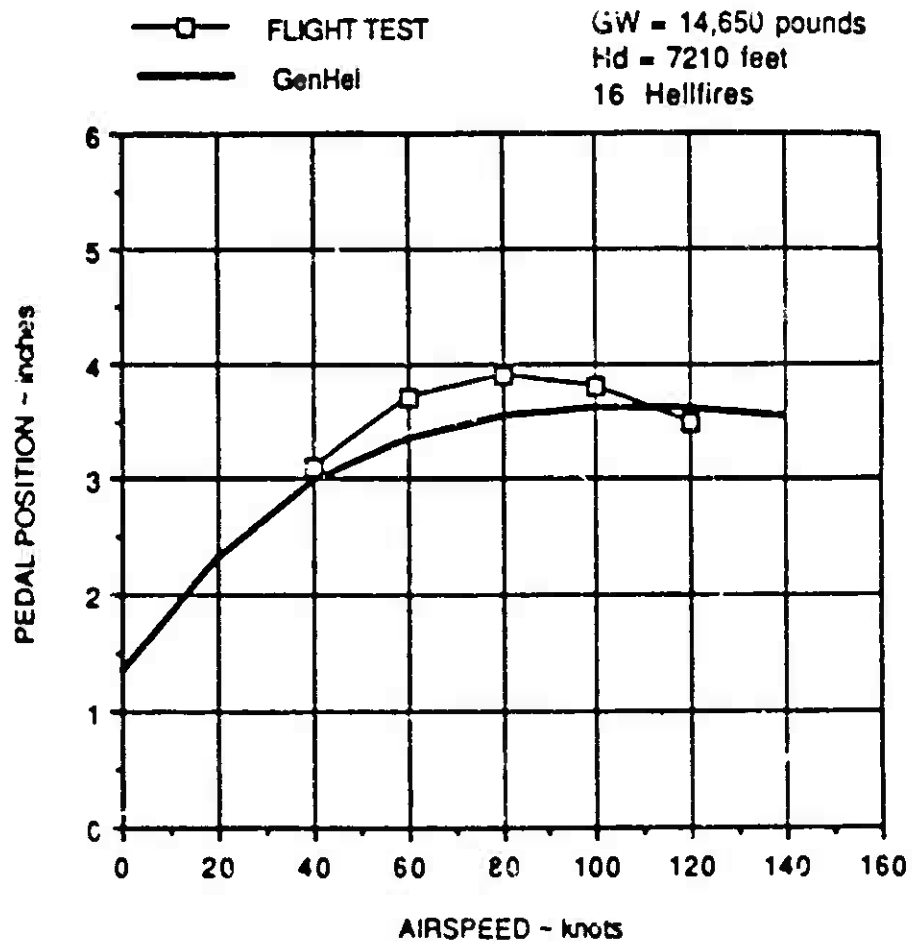


Figure D-6. AM-64A Pedal Correlation

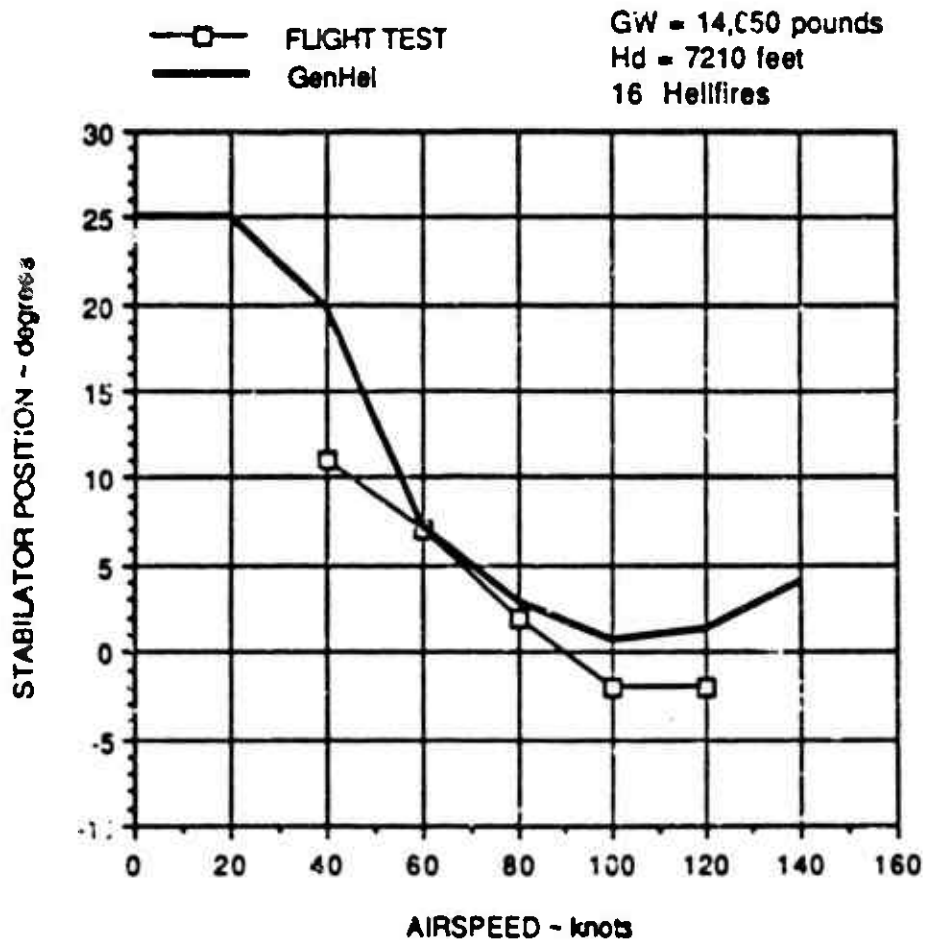


Figure D-7. AH-64A Stabilator Position Correlation

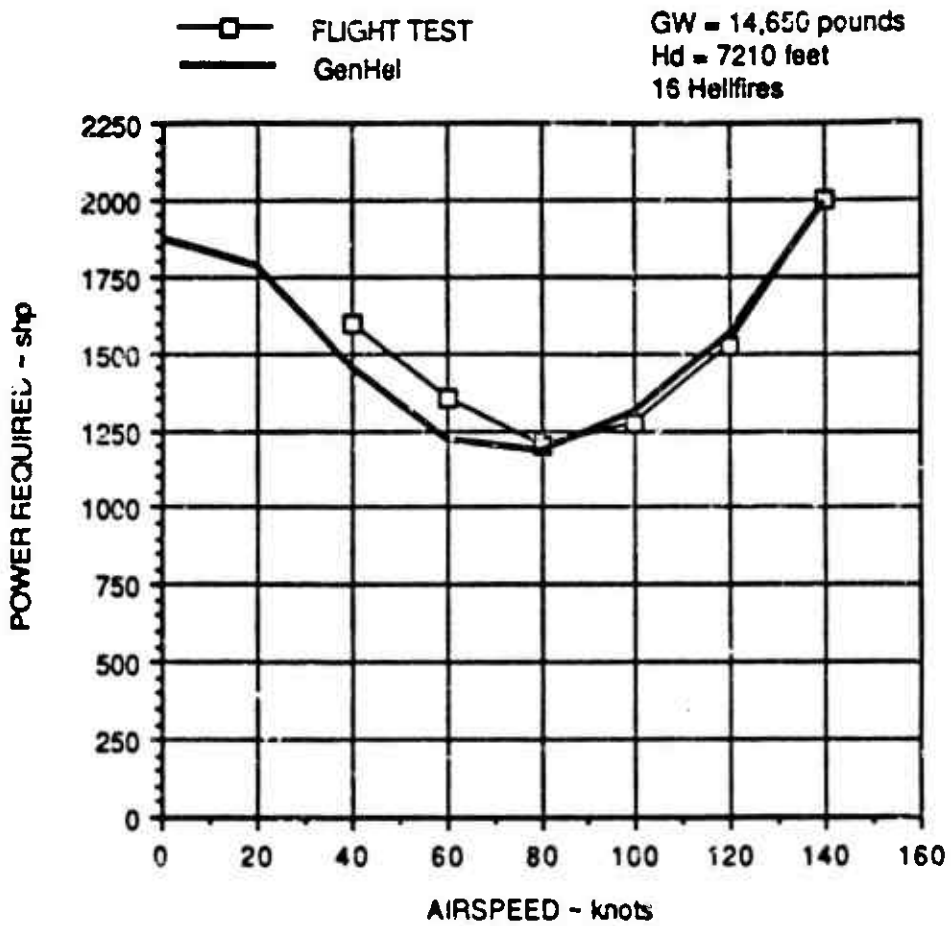


Figure D-8. AH-64A Power Required Correlation

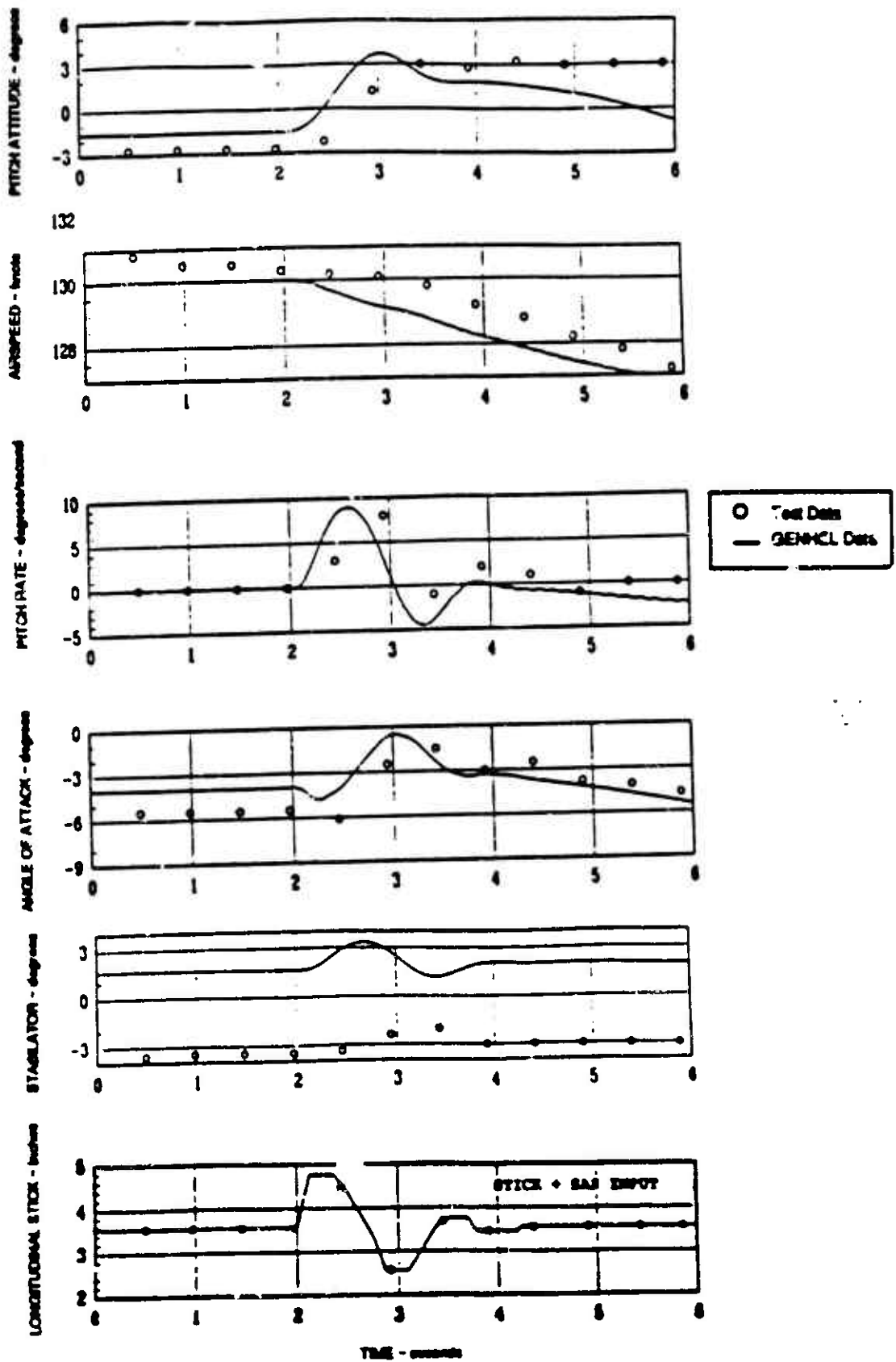


Figure D-9. AH-64A Longitudinal Stick Pulse Correlation

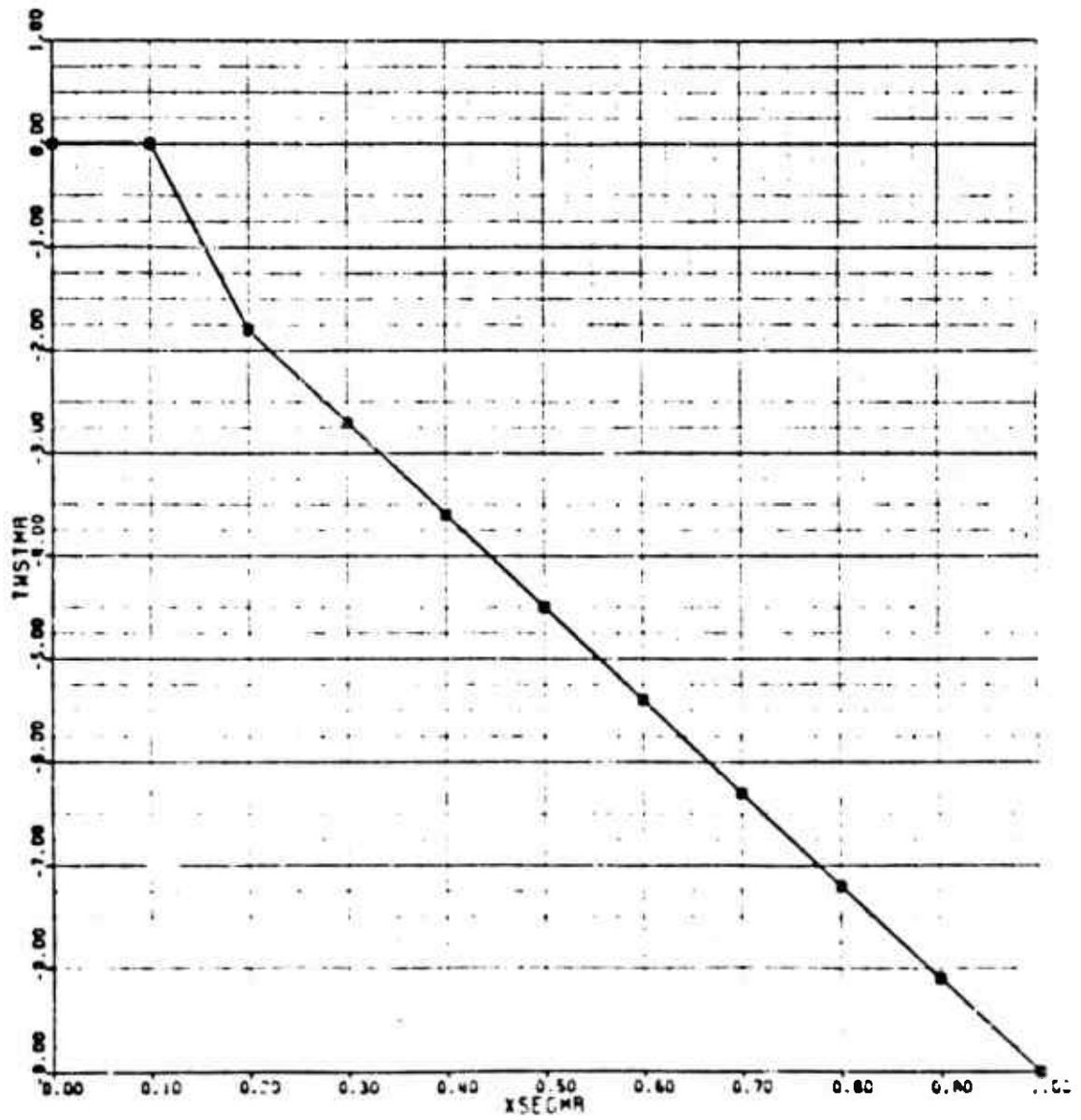


Figure D-10. AH-64A Main Rotor Blade Twist Map

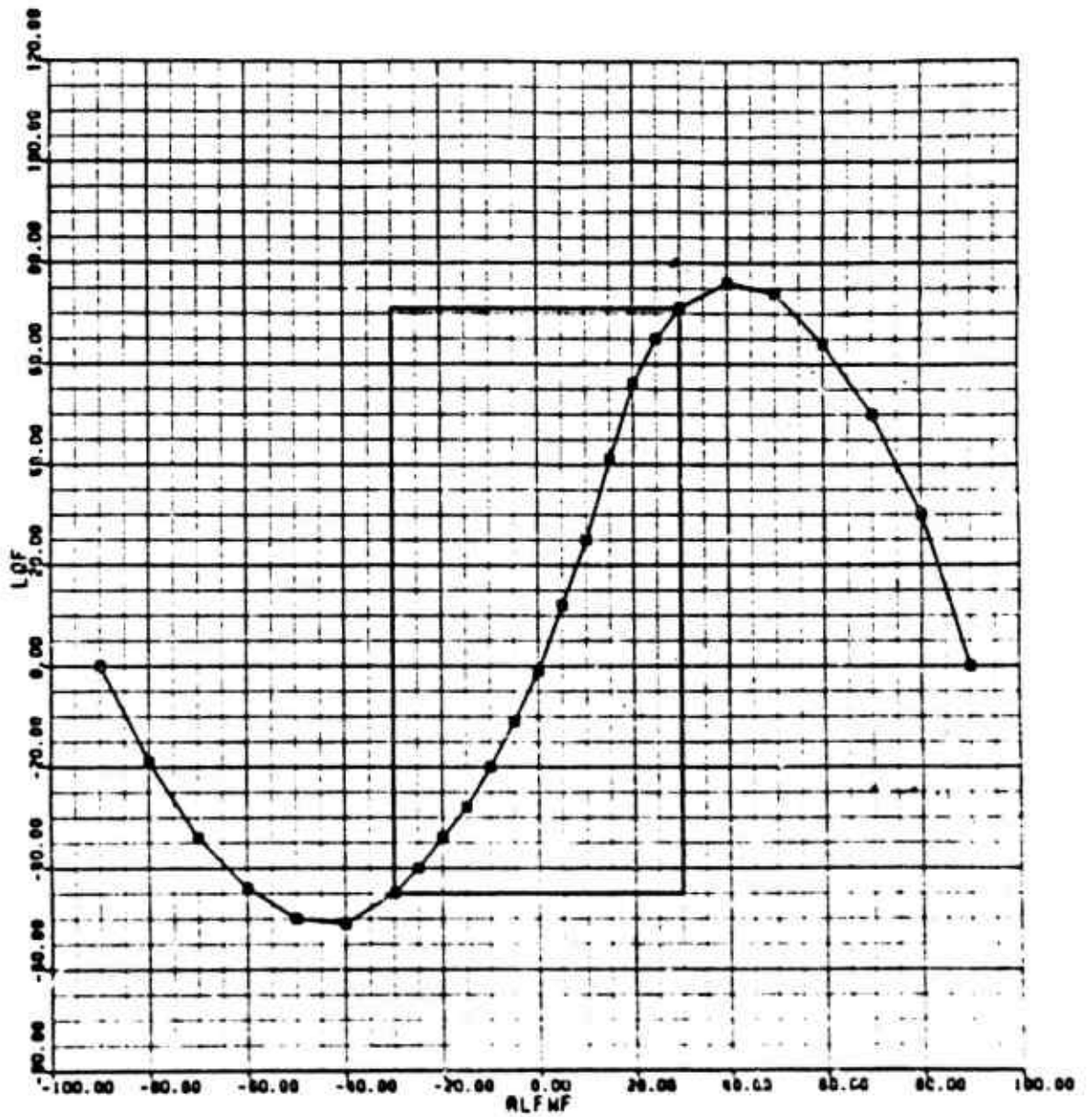


Figure D-11. AH-64A Fuselage Lift Map

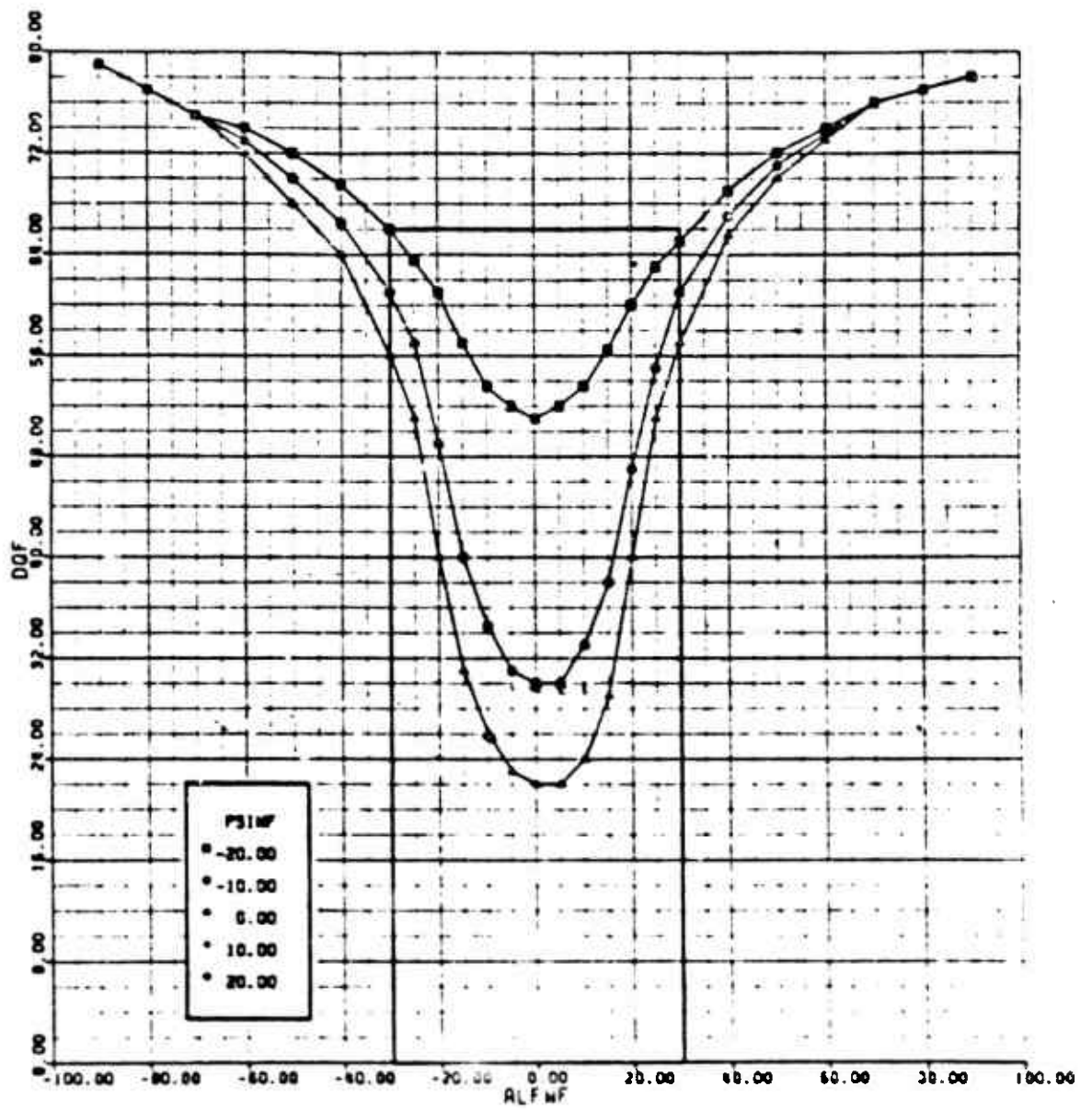


Figure D-12. AH-64A Fuselage Drag Map

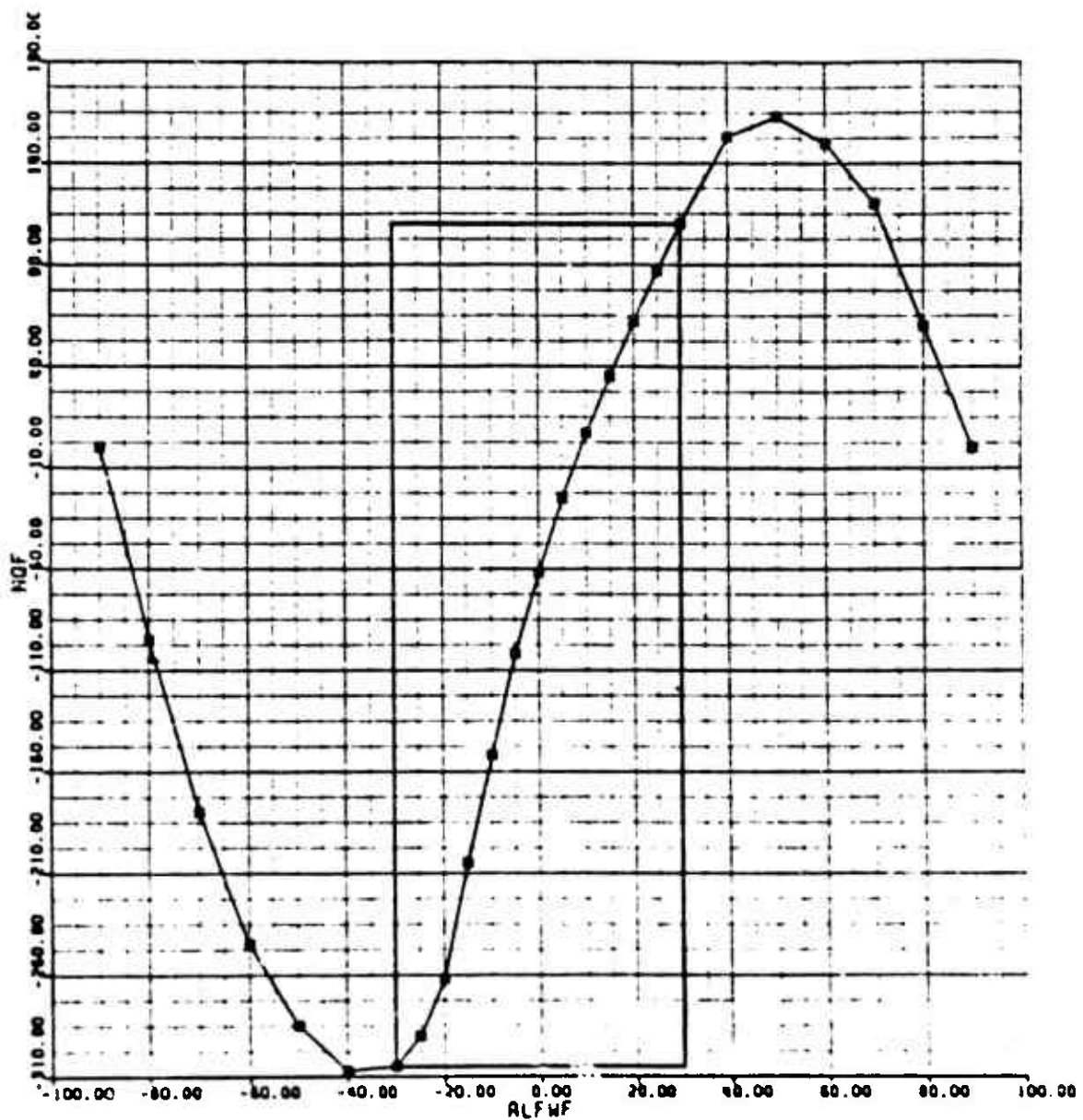


Figure D-13. AH-64A Fuselage Pitching Moment Map

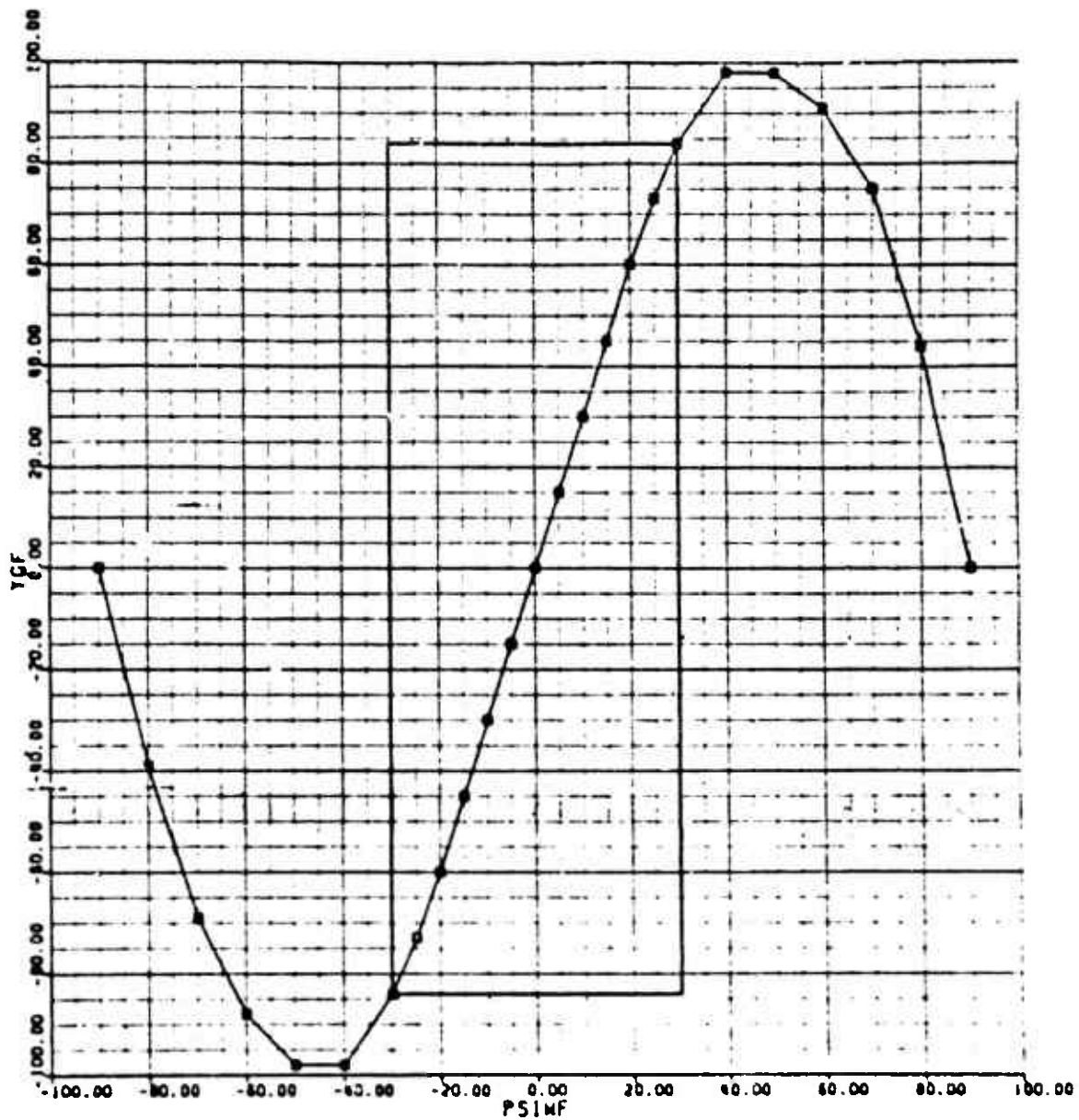


Figure D-14. AH-64A Fuselage Sideforce Map

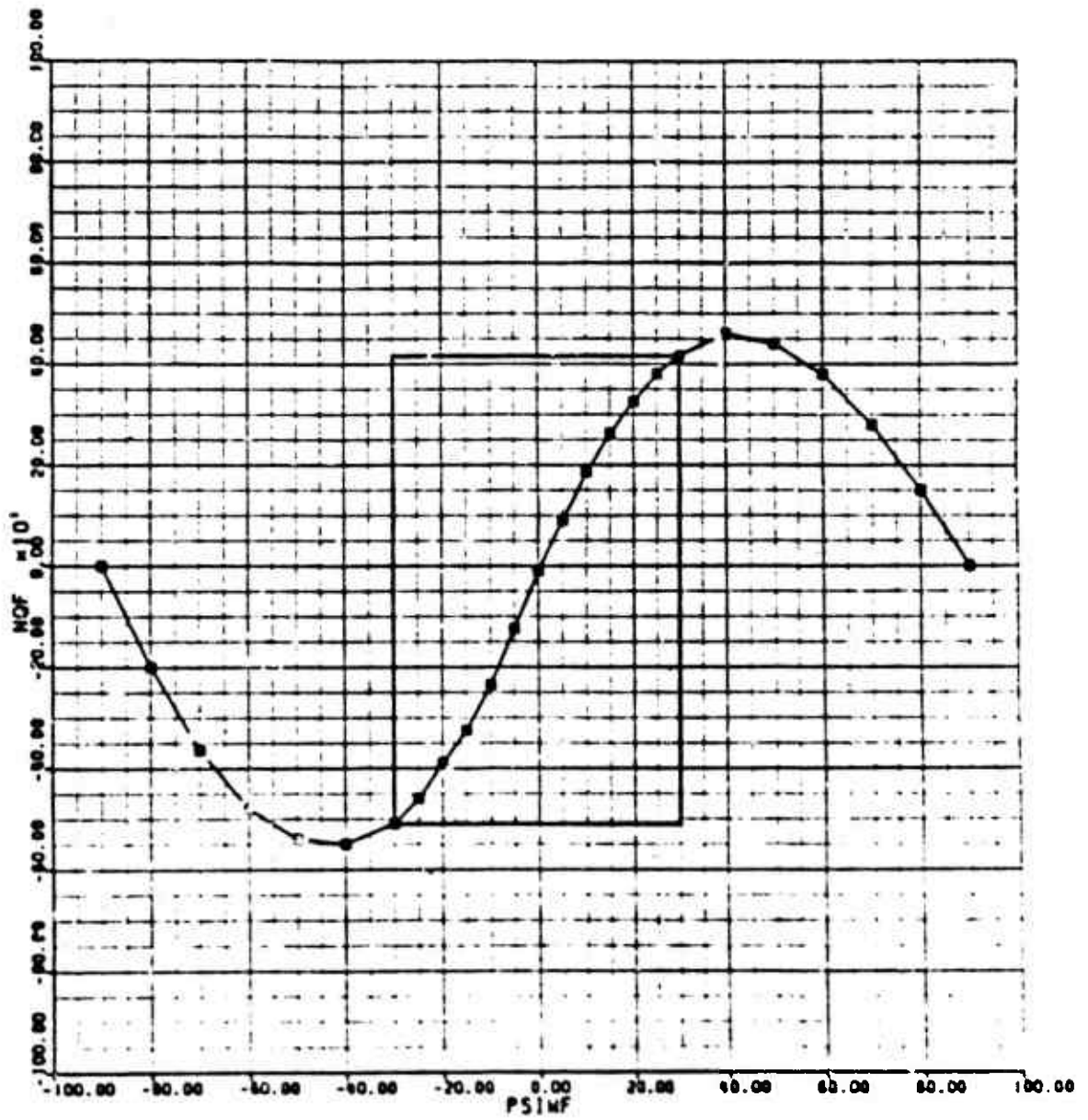


Figure D-15. AH-64A Fuselage Yawing Moment Map

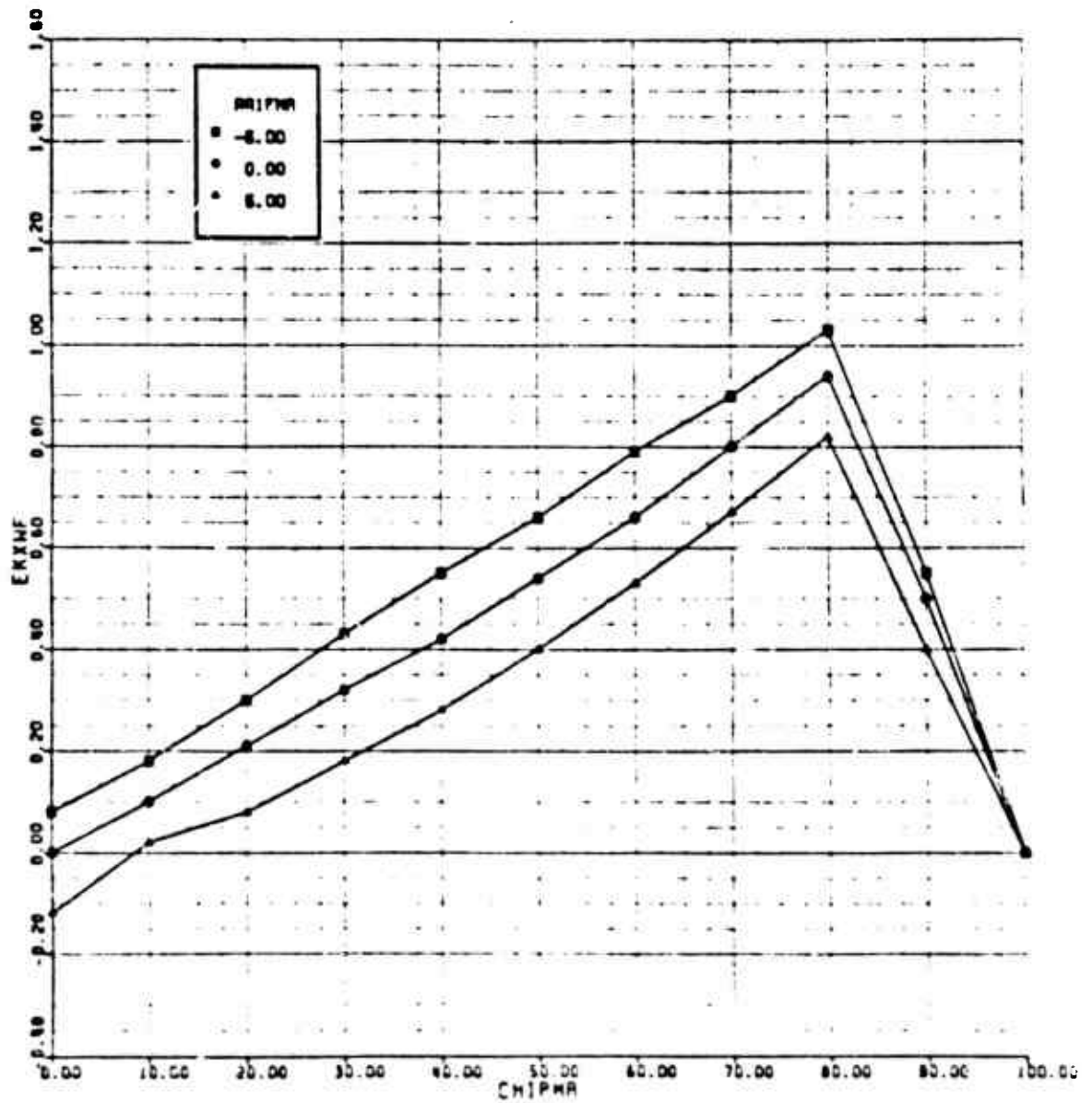


Figure D-16. AH-64A Main Rotor Downwash on Fuselage Map (x-direction)

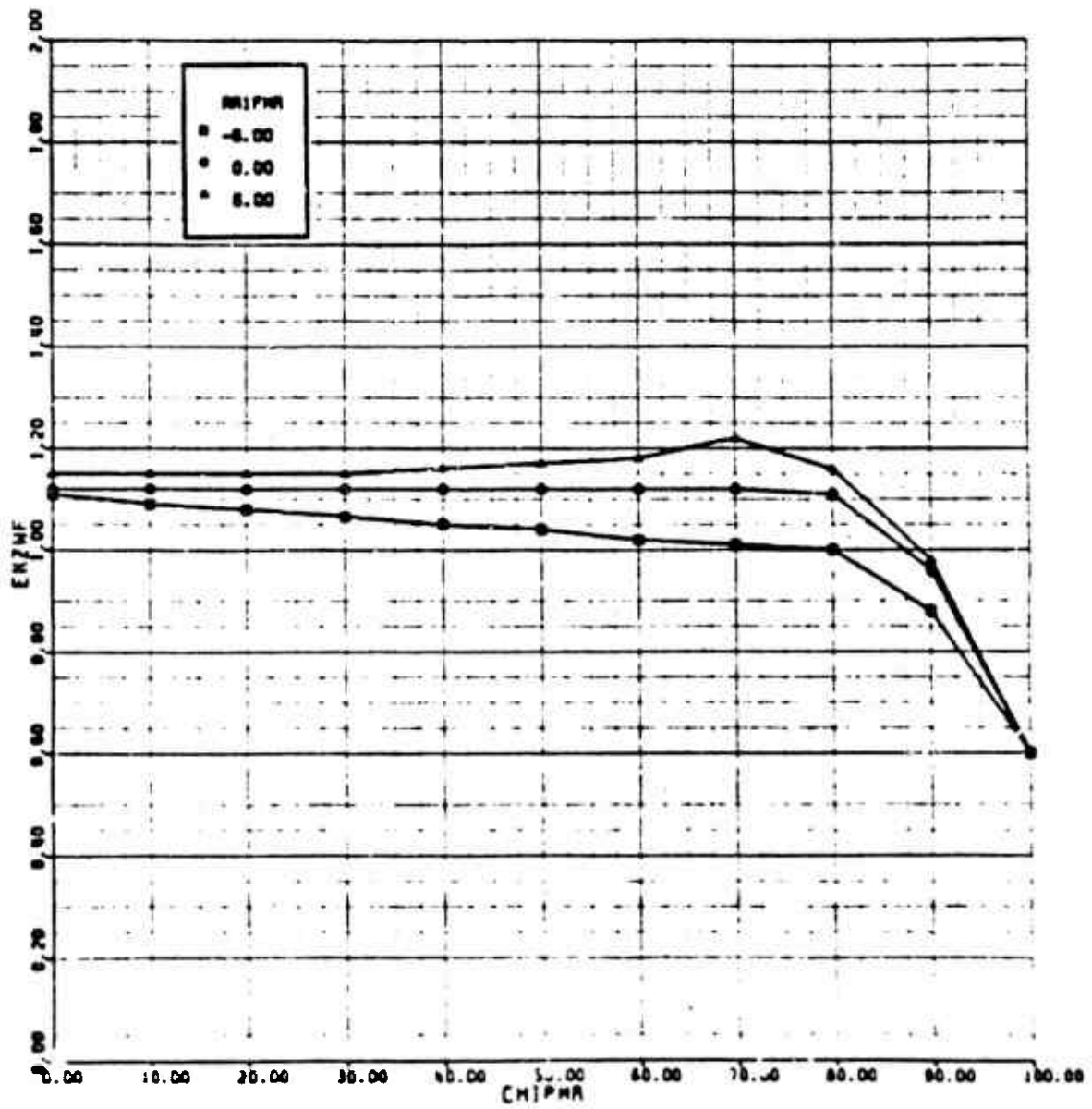


Figure D-17. AH-64A Main Rotor Downwash on Fuselage Map (z-direction)

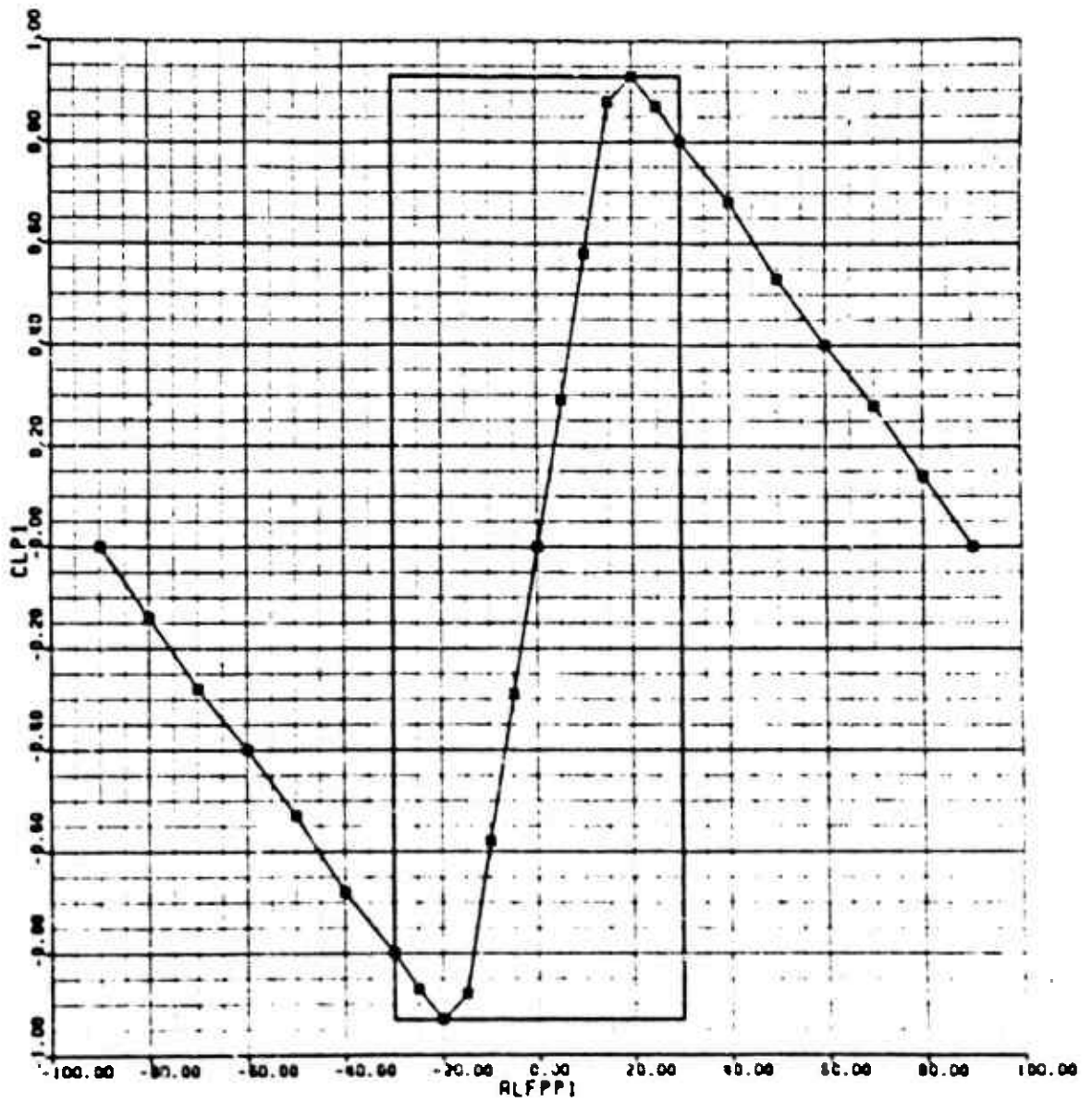


Figure D-18. AH-64A Horizontal Stabilizer Lift Map

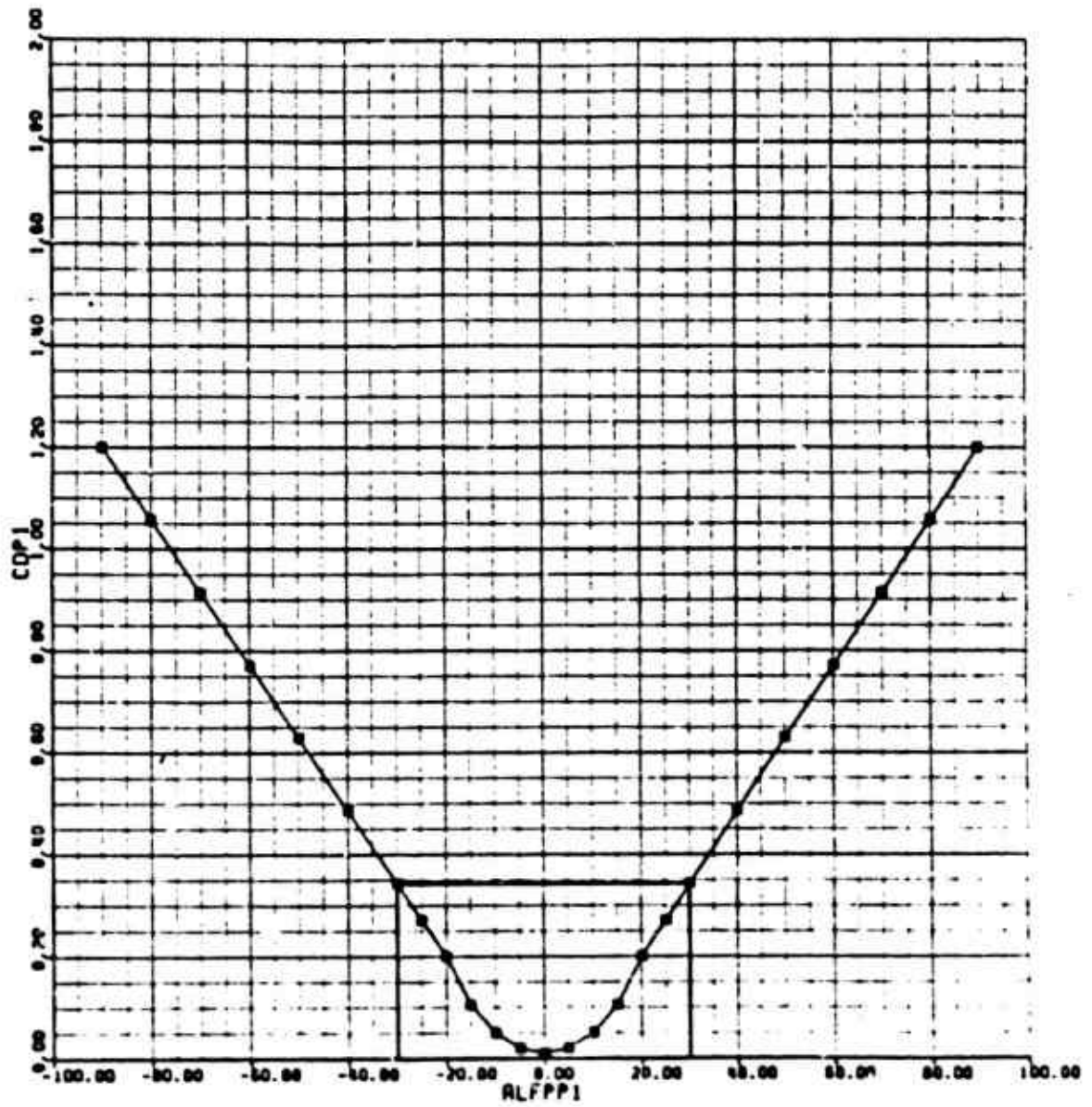


Figure D-19. AH-64A Horizontal Stabilizer Drag Map

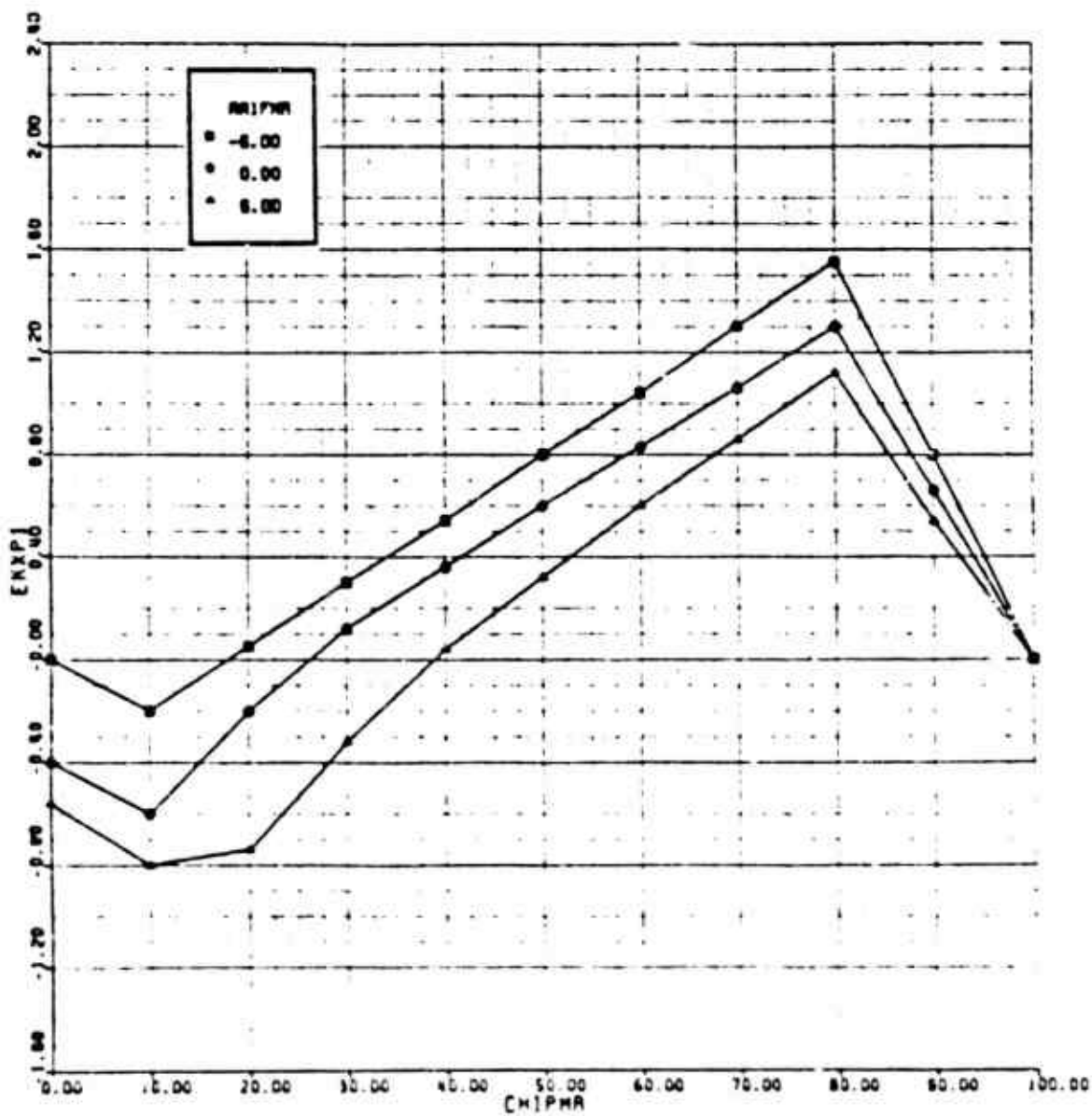


Figure D-20. AH-64A Main Motor Lowwash on Horizontal Stabilizer Map (x-direction)

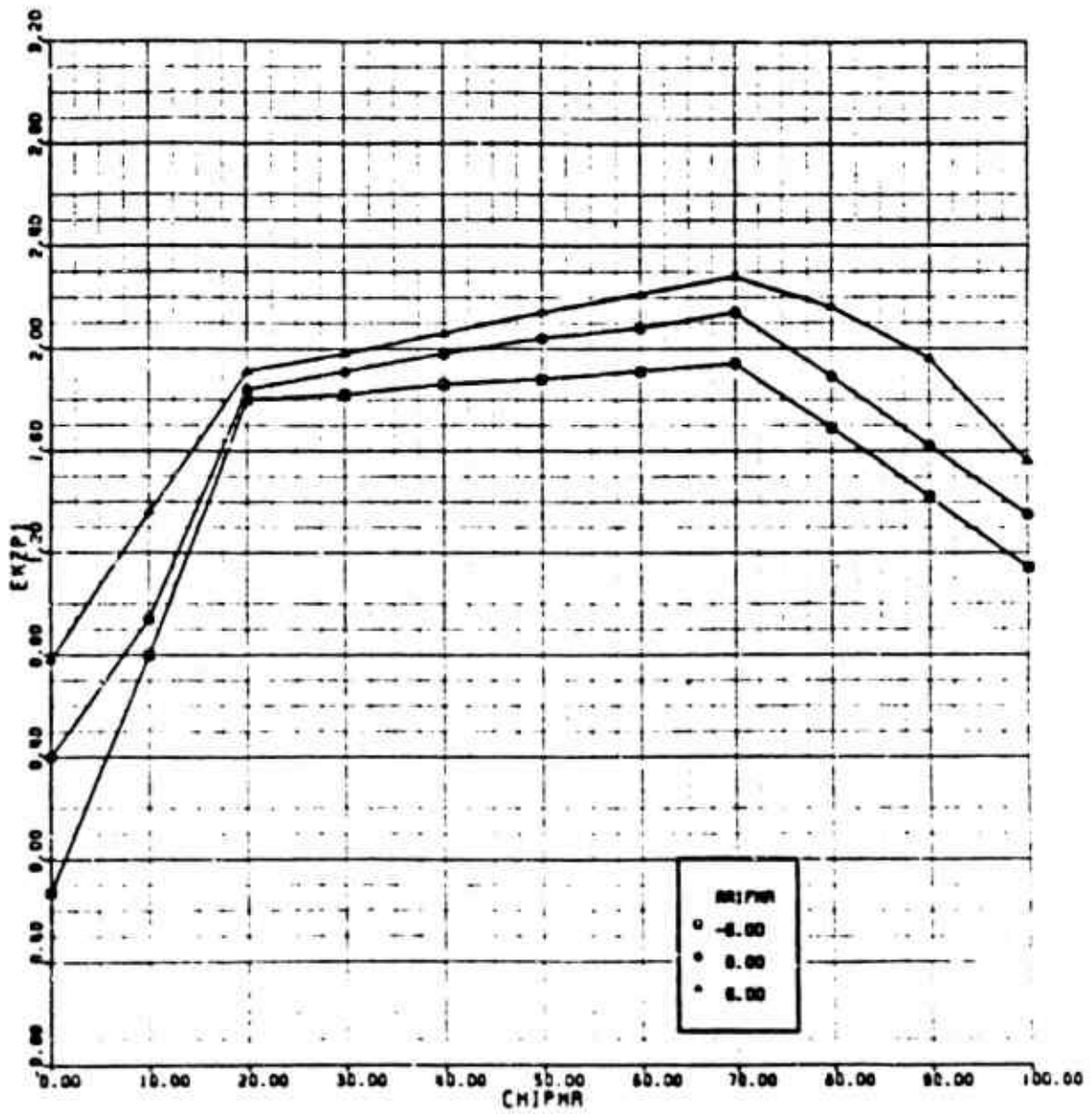


Figure D-21. AH-64A Main Rotor Downwash on Horizontal Stabilizer Map (z-direction)

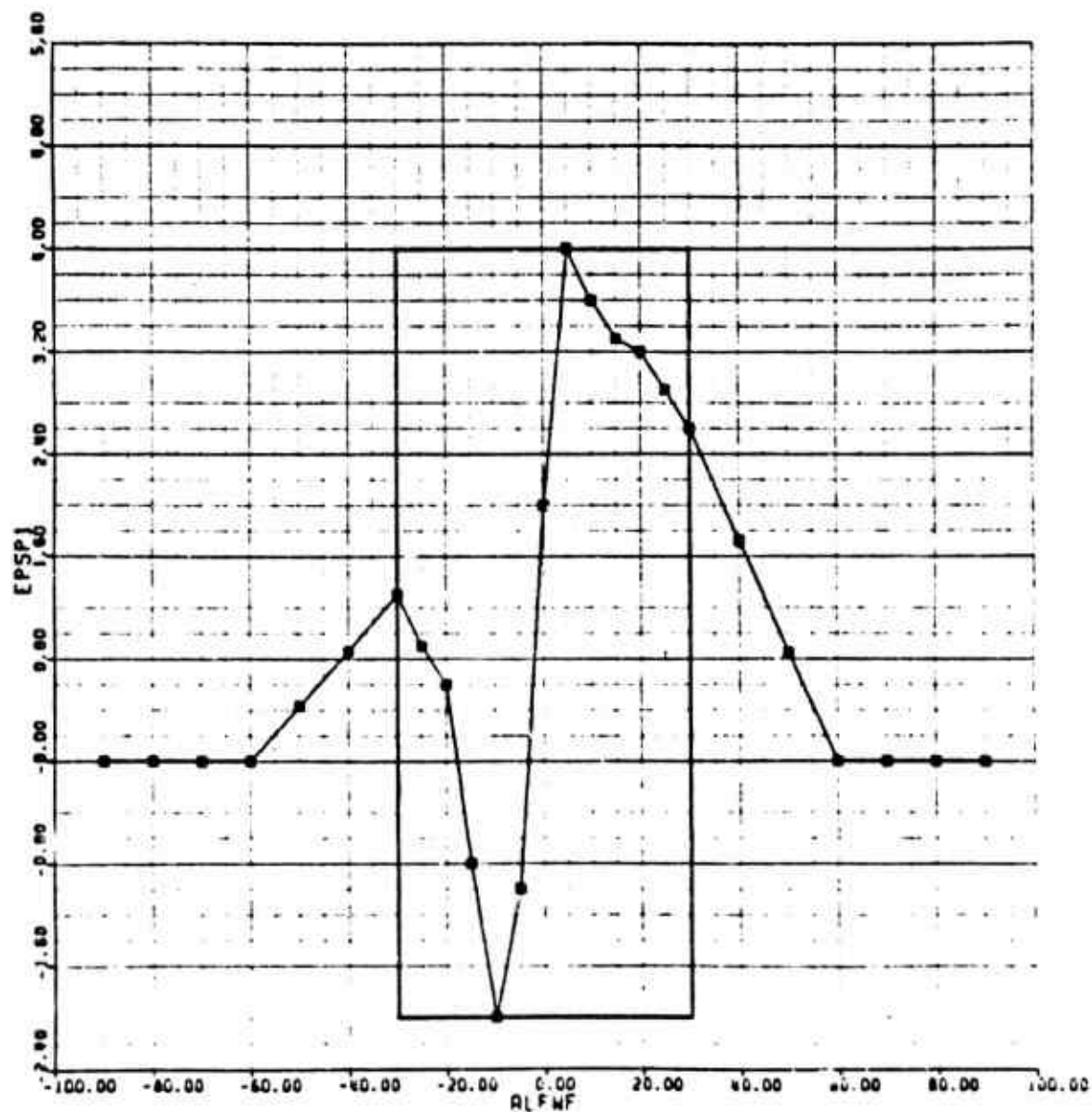


Figure D-22. AH-64A Fuselage Downwash on Horizontal Stabilizer Map

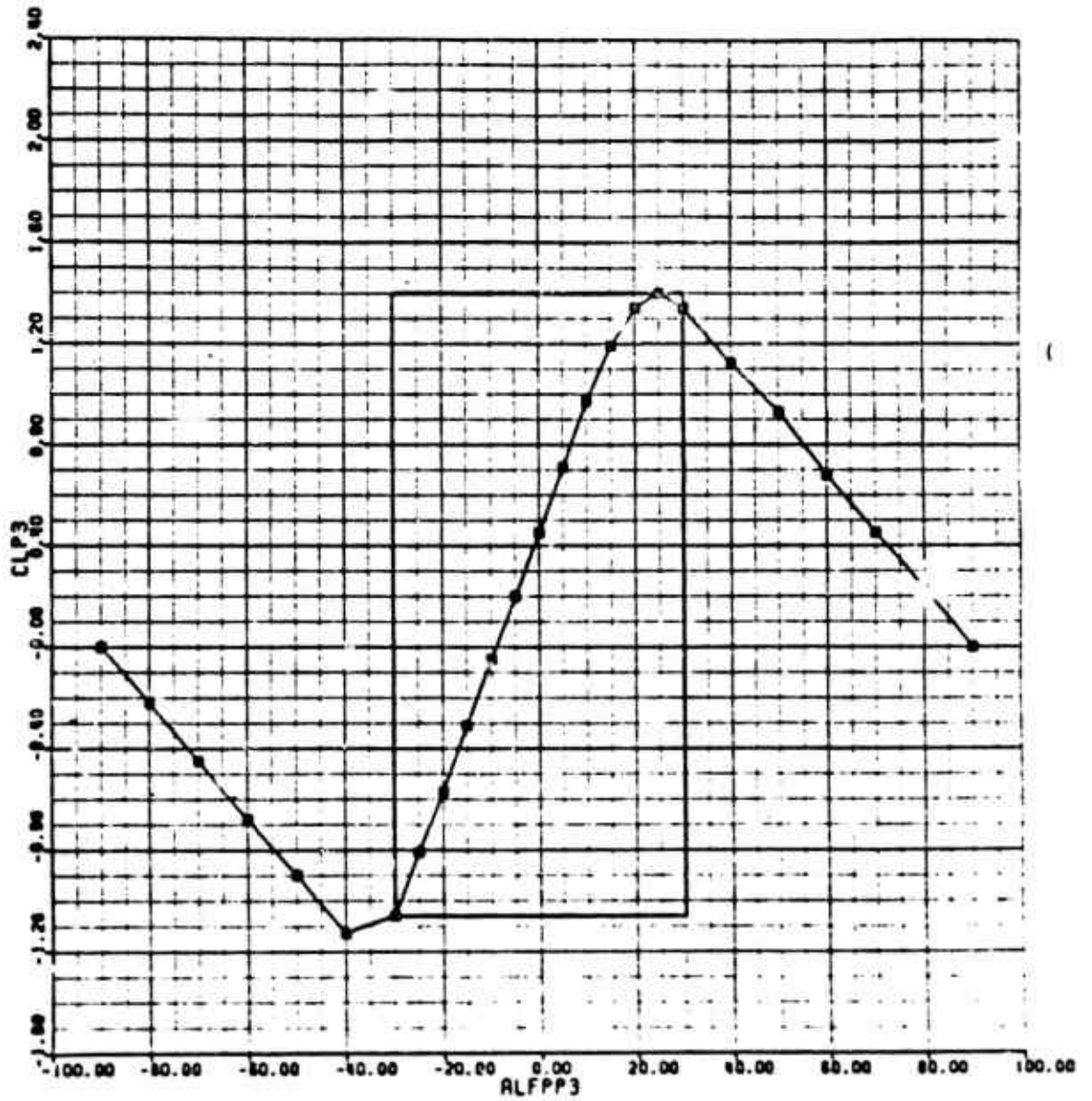


Figure D-23. AH-64A Vertical Stabilizer Lift Map

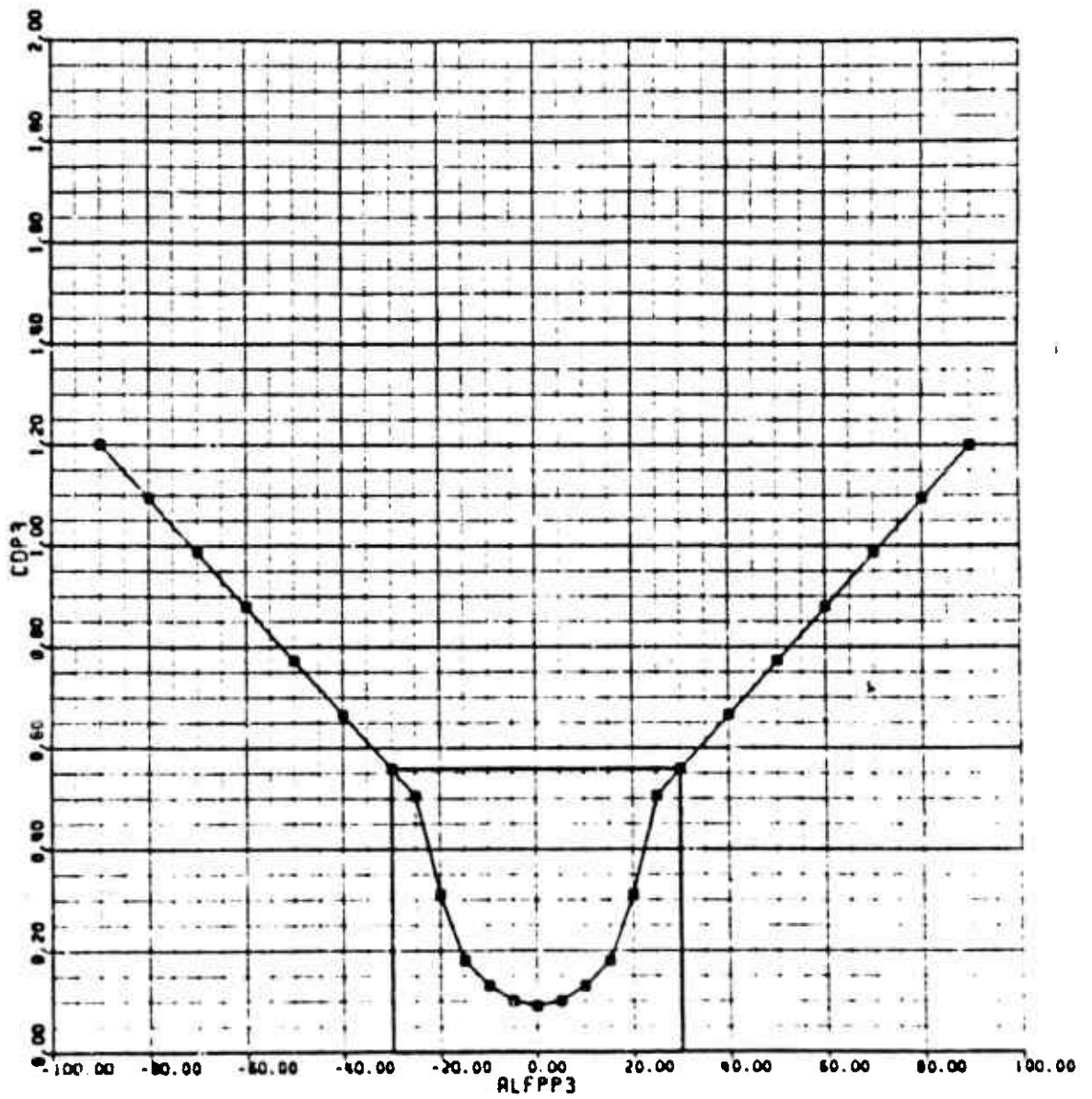


Figure D-24. UA-64A Vertical Stabilizer Drag Map

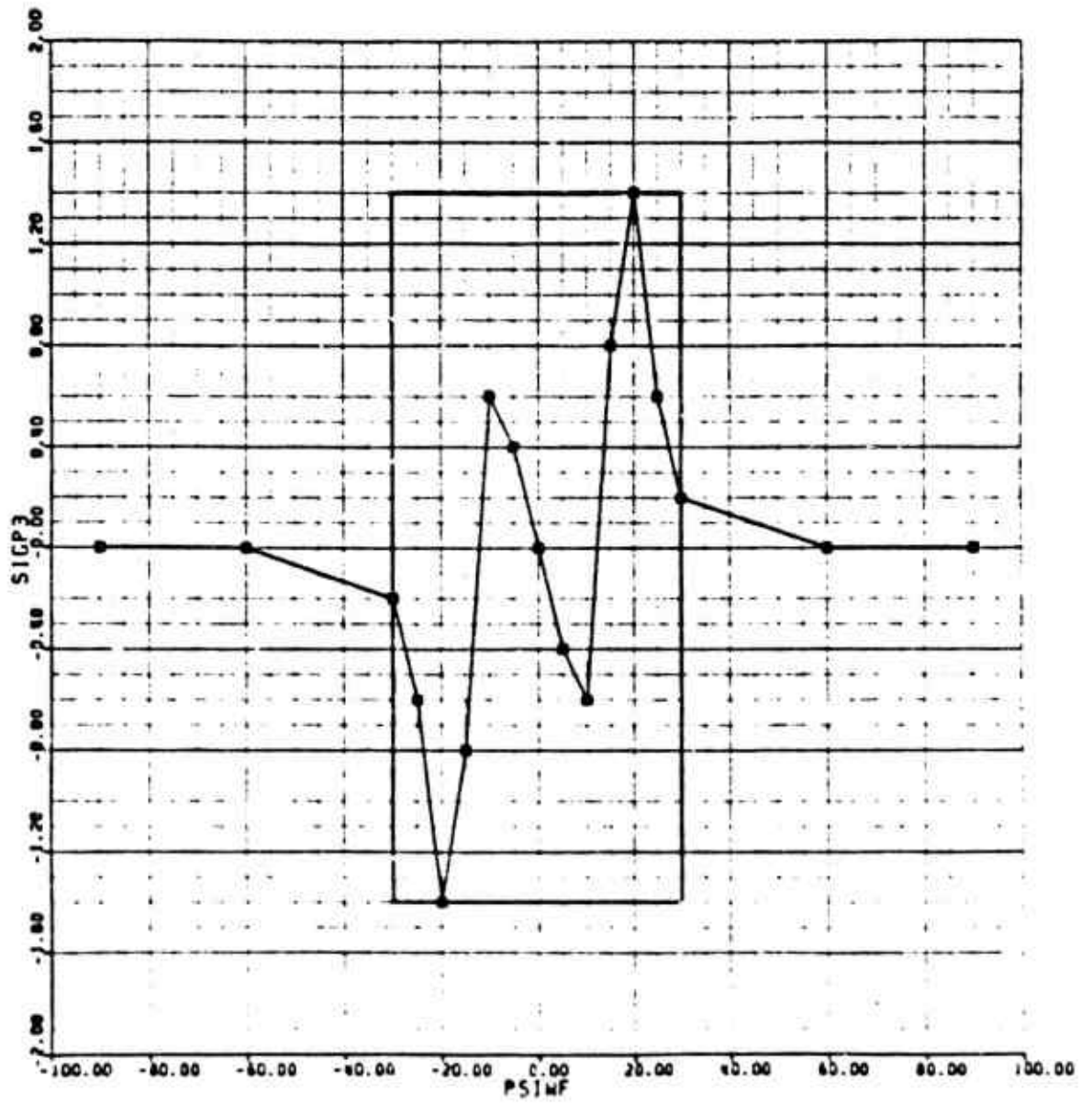


Figure D-25. AH-64A Fuselage Sidewash on Vertical Stabilizer Map

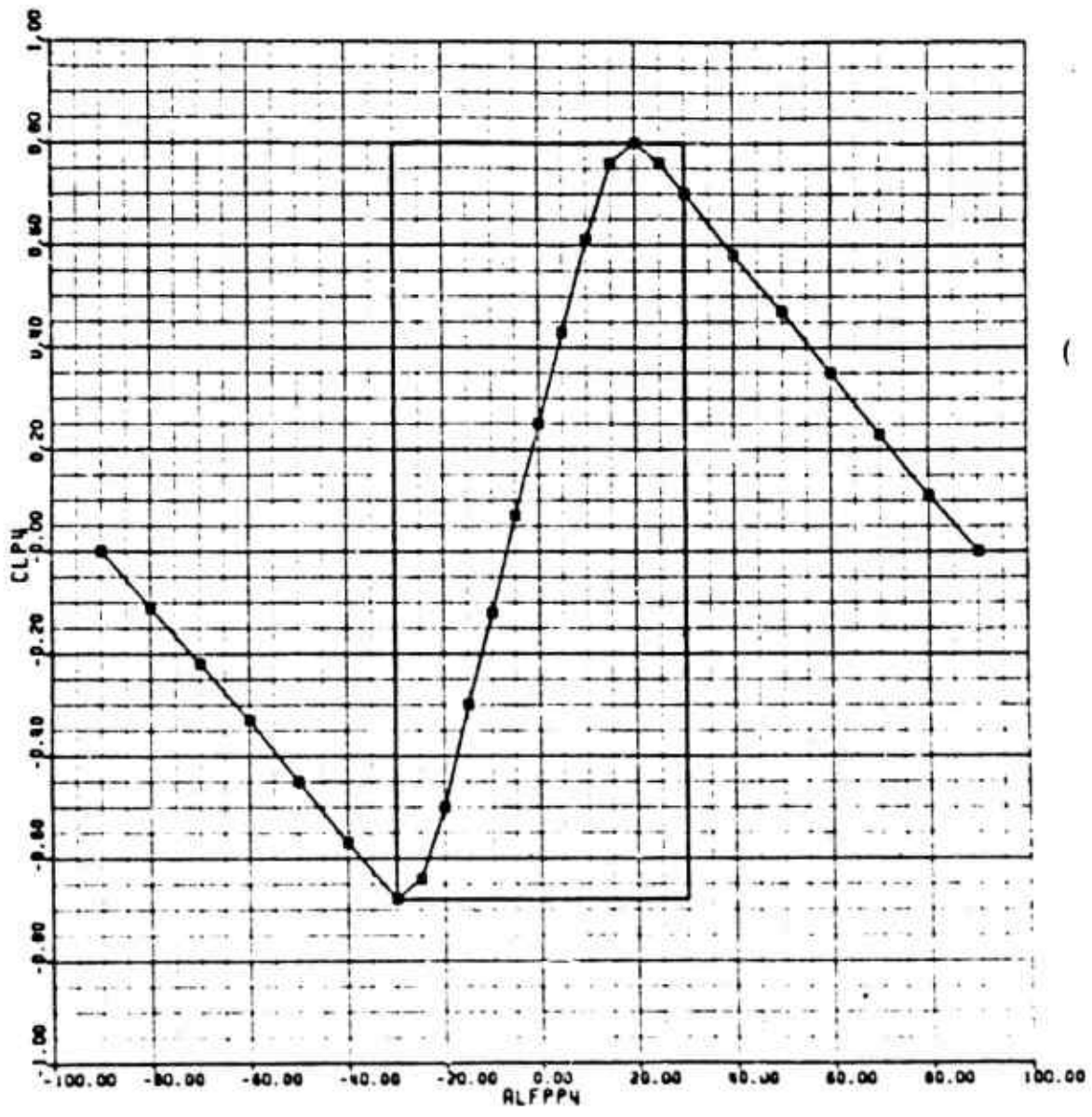


Figure D-26. AH-64A Wing Lift Map

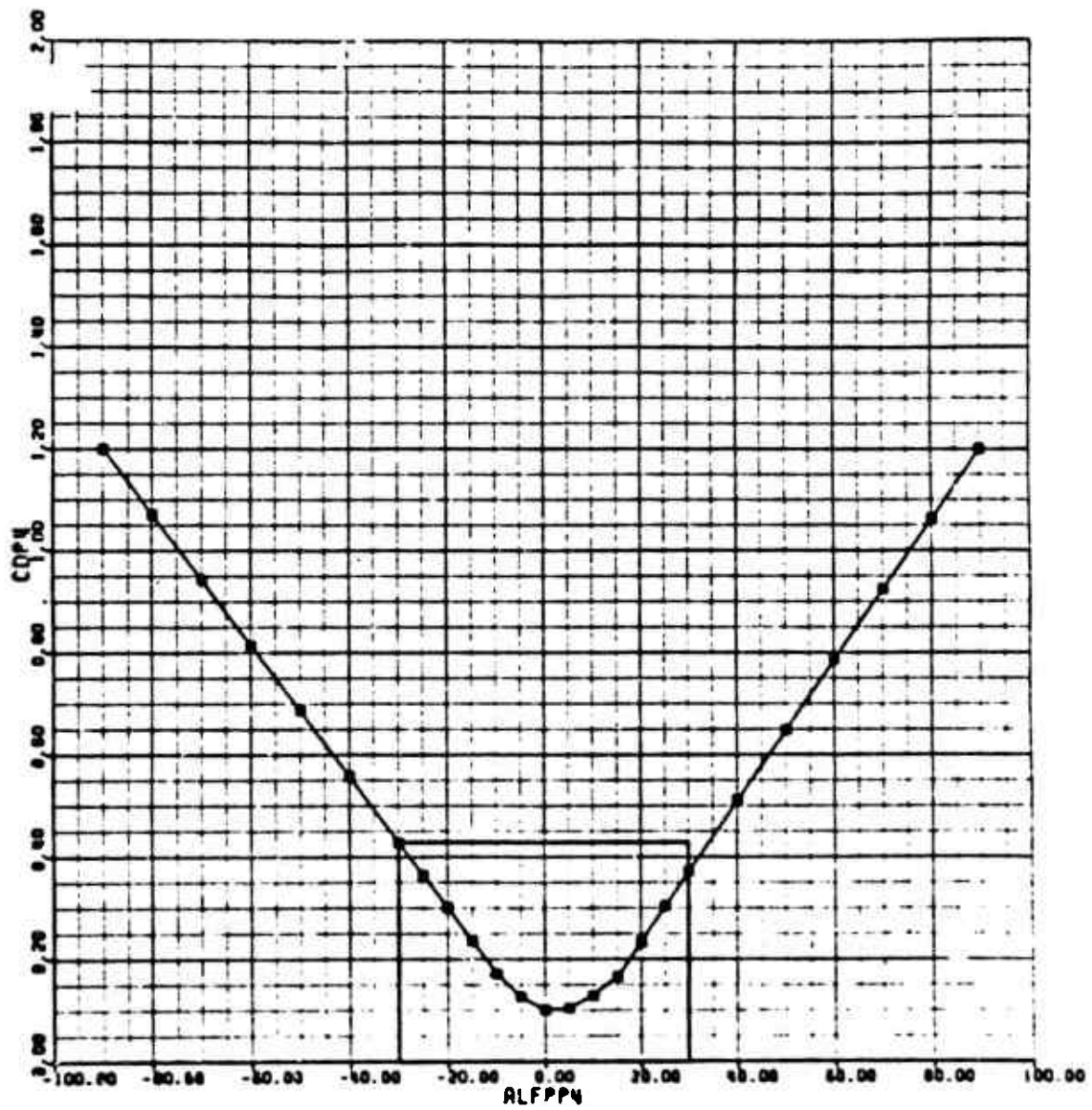


Figure D-27. AH-64A Wing Drag Map

APPENDIX E

OH-58A MODEL DATA

The OH-58A Kiowa (Figure E-1) is a small aircraft originally designed to meet the requirements of the Light Observation Helicopter (LOH) competition. This requirement arose from experience in Vietnam showing the need for a small, agile platform to perform combat surveillance and light utility missions. The Kiowa has a maximum takeoff gross weight of 3000 pounds and utilizes a two-bladed main rotor 35 feet 4 inches in diameter. Power is supplied by a single Allison T63-A-700 turboshaft engine with a takeoff rating of 317 shp.

The main rotor is a classical Bell teetering design, both precone and under-slung. The blades themselves are of conventional construction employing aluminum D-spars with aluminum skins over honeycomb. The GenHel simulation used O012 airfoils to model these blades. The tail rotor is also a two-bladed, teetering unit, 5 feet 2 inches in diameter. A 9.65-square-foot fixed horizontal stabilizer is mounted on the middle of the tail boom. The OH-58A airframe is of conventional aluminum semimonocoque design and has skid-type landing gear. The GenHel simulation model was created using data from Reference 11. Since the Kiowa employs a teetering rotor, the existing GenHel gimbaled rotor module was used instead of the articulated one. A Heyson downwash program was run with OH-58A parameters to obtain the rotor interference effects on the fuselage and empennage.

When the GenHel Oh-58A simulation was first flown, problems were encountered. These were traced to coding errors in the gimbaled rotor module. Some of the coding had been written assuming a four-bladed rotor. These were corrected. The model continued to exhibit high two-per-rev vibrations. This is true of the actual aircraft, but the mathematically rigid blades in GenHel and cantilever constraints for lag and collective bending make them more severe. On the actual helicopter the flexibility in the blades reduces these loads.

The correlation of GenHel to flight test data for level flight trim is shown in Figures E-2 to E-6. Flight test data were taken from Figure 7 of Reference 12. Test conditions were:

GW - 2770 pounds
FSCC - 111.9
Density Altitude - 6100 feet

Collective, lateral and pedal positions all show good correlation, but pitch attitude and longitudinal stick are poor. A significant effort was undertaken to improve these results. Data flown at a different c.g. were correlated. Variations in rotor and fuselage downwash were tried along with a change to stabilizer incidence. Data of Reference 13 were reviewed. None of these significantly changed the correlation. A decision was made to conduct the M/A study with the model as shown.

All of the numerical data used to model the OH-58A are provided in this appendix. The first section is a listing of all the input data (Table E-1). The second section presents plots of the map data for fuselage, vertical tail and horizontal tail aerodynamics along with plots of the rotor interference and fuselage interference data (Figures E-7 to E-25). The tabular data are provided with appropriate labels. Map data are identified with GenHel variables provided in the List of Symbols.

For the OH-58A model, the panel allocation was as follows:

1. Horizontal tail
2. None
3. Vertical tail

TABLE E-1. OH-58A SPECIFIC FILE

```

;***** INPUT PARAMETERS FOR MAIN ROTOR MODULES (JA) *****
FSRR:: 106.91 ; FUSELAGE STATION, INCHES
WLRR:: 120.00 ; ** WATERLINE STATION, INCHES
BLRR:: 0.0 ; BUTTLINE STATION, INCHES (+IVE TO PORT)
RMR:: 17.667 ; RADIUS, FT.
OROTRR:: 37.07 ; PRIR ROTATIONAL SPEED, RAD/SEC
SMR:: 2.0 ; ACTUAL NUMBER OF BLADES
ISMR:: -5.0 ; LONGITUDINAL SHAFT TILT, (POS. BACKWARDS), DEG
ILRR:: 0.0 ; LATERAL SHAFT TILT, (POS. STARBOARD), DEG
DELSRR:: 0.0 ; ** SHWASHPLATE PHASE ANGLE, DEG
DEL3RR:: 0.0 ; FLAPPING HINGE OFFSET ANGLE, DEG.
KAP1RR:: 0.0 ; ** LAGGING HINGE OFFSET COEF. (FUNC(LG))
KAP2RR:: 0.0 ; ** LAGGING HINGE OFFSET COEF. (FUNC(LG**2))
CHOTRR:: 1.08 ; BLADE CHORO AT TIP, FT.
CHORRR:: 1.08 ; BLADE CHORO AT ROOT, FT.
OPSTRR:: 0.0 ; ** HINGE OFFSET, FT.
SPRRR:: 4.363 ; ** HINGE TO START OF BLADE, FT.
WTSORR:: 137.43 ; WEIGHT OF ONE BLADE, LBS.
ISRR:: 335.8779 ; ** SLADE RORENT OF INERTIA ABOUT HINGE, SLUG-FT**2
RMRR:: 28.42 ; ** BLADE MASS RORENT ABOUT HINGE, SLUG-FT**2
IRMR:: 2750.4 ; ** ROTOR POLAR MOM OF INERTIA (LESS SLADES), SLUG-FT**2
BIBO:: 2.5 ; ** PRECONE FOR GIMBAL ROTOR
STLRR:: .97 ; SLADE TIP CUT OFF RATIO
OCORR:: .002 ; DELTA ORAG COEF. FOR EACH SEGMENT
NBSRR:: 2 ; NUMBER OF BLADES SIMULATED, FIX POINT
NSSRR:: 5 ; NUMBER OF SEGMENTS SIMULATED, FIX POINT

; ** RAIN ROTOR LINEAR TWIST MAP **
TWRMRP:: UVR00 ; MAP LOOK UP NAME
XSEGR00 ; INPUT VARIABLE NAME
TWSTR00 ; OUTPUT VARIABLE NAME
TWRLO ; MAP NAME
EXP 0.0, 1.0, .50 ; LOWER LIM, UPPER LIM, DELTA

TWRLO: EXP 0.0, -5.3, -10.6

;***** MAIN ROTOR DOWNWASH SUBROULE (6A) *****
KCTRR:: 1.0 ; THRUST GAIN FOR UNIFORM DOWNWASH
RCMRR:: 0.0 ; PITCH MOR. GAIN FOR DOWNWASH SIN. HARMONIC
ILRR:: 0.0 ; ROLL MOR. GAIN FOR DOWNWASH COS. HARMONIC
TOWORR:: .01038 ; TIME CONST. FOR UNIFORM DOWNWASH FILTER, SEC
TDNCRR:: 0.0 ; TIME CONST. FOR DOWNWASH SIN. HARMON. FILTER, SEC.
TOWSHR:: 0.0 ; TIME CONST. FOR DOWNWASH COS. HARMON. FILTER, SEC.

;***** INPUT PARAMETERS FOR FUSELAGE (6A) *****
;***** ROUTING POINT FOR ROOEL IN WIND TUNNEL *****
FSWF:: 114.2 ; FUSELAGE STATION, IN.
WLWF:: 58.2 ; WATERLINE STATION, IN.
BLWF:: 0.0 ; BUTTLINE STATION, IN. (+IVE TO PORT)
IWF:: 0.0 ; WING INCIDENCE, DEG.

; ** FUSELAGE LIFT (TAIL-OFF) VS ALPWF MAP **
LOFRP:: UVRUVR00 ; MAP LOOK UP ROUTINE
ALPWF00 ; INPUT VARIABLE
LOF00 ; OUTPUT VARIABLE
LOFLO ; LOW ANGLE MAP NAME
EXP -20.0, 20.0, 4.0 ; LOWER LIM, UPPER LIM, DELTA
LOFHI ; HIGH ANGLE MAP NAME
EXP -100.0, 100.0, 20.0 ; LOWER LIM, UPPER LIM, DELTA

LOFLO: EXP ; LOW ANGLE MAP ALPWF -20 TO 20, DELTA = 4
-9.16, -7.79, -6.27, -4.65, -2.95

```

TABLE E-1. OH-58A SPECIFIC FILE (Cont'd)

```

EXP      -1.20,    0.56,    2.30,    3.98,    5.57
EXP      7.04

; HIGH ANGLE MAP ALFWF -100 TO 100, DELTA = 20
LQPHI:  EXP      4.27,    -4.35,   -11.21,   -13.11,   -9.16
EXP      -1.20,    7.04,    11.70,    10.61,    4.27
EXP      -4.34

; ** FUSELAGE DRAG (TAIL-OFF) VS ALFWF **
DQFMP:: UVRUVR00 ;MAP LOOK UP ROUTINE
        ALFWF00 ;INPUT VARIABLE
        DQF00  ;OUTPUT VARIABLE
        DQFLO  ;LOW ANGLE MAP NAME
EXP      -20.0,20.0,2.0 ;LOWER LIM,UPPER LIM,DELTA
        DQPHI  ;HIGH ANGLE MAP NAME
EXP      -100.0,100.0,20.0 ;LOWER LIM,UPPER LIM,DELTA

; LOW ANGLE MAP ALFWF -20 TO 20, DELTA = 2 DEG
DQFLO:  EXP      11.1470,  10.2016,  9.3429,  8.5752,  7.9020
EXP      7.3268,  6.8522,  6.4808,  6.2141,  6.0536
EXP      6.0000,  6.0536,  6.2141,  6.4808,  6.8522
EXP      7.3268,  7.9020,  8.5752,  9.3429,  10.2016
        11.1470

; HIGH ANGLE MAP ALFWF -100 TO 100 , DEL = 20 DEG
DQPHI:  EXP      48.6732,  48.6732,  39.0000,  24.1797,  11.1470
EXP      6.0000,  11.1470,  24.1797,  39.0000,  48.6732
        48.6732

; ** FUSELAGE PITCH MOM (TAIL-OFF) VS ALFWF **
MQFMP:: UVRUVR00 ;MAP LOOK UP ROUTINE
        ALFWF00 ;INPUT VARIABLE
        MQF04  ;OUTPUT VARIABLE
        MQFLO  ;LOW ANGLE MAP NAME
EXP      -20.0,20.0,2.0 ;LOWER LIM,UPPER LIM,DELTA
        MQPHI  ;HIGH ANGLE MAP NAME
EXP      -100.0,100.0,20.0 ;LOWER LIM,UPPER LIM,DELTA

; LOW ANGLE MAP ALFWF FROM -20 TO 20, DELTA = 2 DEG
MQFLO:  EXP      -125.0000, -115.9500, -106.8900, -97.8400, -88.7900
EXP      -79.7330, -72.5064, -65.1337, -57.6507, -50.0938
EXP      -42.5000, -34.9062, -27.3493, -19.8663, -12.4936
EXP      -5.2670,  3.7860,  12.8400,  24.8900,  30.9500
        40.0000

; HIGH ANGLE MAP ALFWF FROM -100 TO 100, DELTA = 20 DEG
MQPHI:  EXP      -384.5000, -364.8400, -274.4800, -200.0000, -125.0000
EXP      -42.5000,  40.0000,  115.0000,  189.4768,  279.8393
        299.5054

; ** FUSELAGE DELTA DRAG VS PSIWF **
DDQFMP:: UVRUVR00 ;MAP LOOK UP ROUTINE
        PSIWF00 ;INPUT VARIABLE
        DDQF00 ;OUTPUT VARIABLE
        DDQFLO ;LOW ANGLE MAP NAME
EXP      -20.0,20.0,4.0 ;LOWER LIM,UPPER LIM,DELTA
        DDQPHI ;HIGH ANGLE MAP NAME
EXP      -100.0,100.0,20.0 ;LOWER LIM,UPPER LIM,DELTA

; LOW ANGLE MAP PSIWF FROM -20 TO 20, DELTA = 4 DEG
DDQFLD: EXP      6.31,  4.10,  2.33,  1.04,  0.26
EXP      0.00,  0.26,  1.04,  2.33,  4.10
EXP      6.31,

; HIGH ANGLE MAP PSIWF FROM -100 TO 100, DELTA = 20 DEG
DDQPHI: EXP      52.40,  52.40,  40.50,  22.30,  6.31

```

TABLE E-1. CH-58A SPECIFIC FILE (Cont'd)

EXP	0.00,	6.31,	22.30,	40.50,	52.40
EXP	52.40				
; ** FUS. DELTA PITCH MOMENT VS PSIMF **					
; MAP LOOK UP ROUTINE					
DRQFNF::	BIVBIV00				
EXP	PSIMF00,ALPWF00				
	ONCF00				
	DRQFLO				
EXP	-20.0,20.0,4.0,011				
EXP	-10.0,10.0,10.0				
	ORQFHI				
EXP	-100.0,100.0,20.0,011				
EXP	-10.0,10.0,10.0				
; LOW ANGLE MAP PSIMF -20 TO 20 FOR ALPWF -10,0,10 DEG					
; ALPWF = -10 DEG					
DRQFLO: EXP	6.67,	4.33,	2.46,	1.10,	0.27
EXP	0.00,	0.27,	1.10,	2.46,	4.33
EXP	6.67				
; ALPWF = 0 DEG					
EXP	5.00,	3.23,	1.84,	0.83,	0.21
EXP	0.00,	0.21,	0.83,	1.84,	3.23
EXP	5.00				
; ALPWF = +10 DEG					
EXP	0.85,	0.55,	0.31,	0.14,	0.03
EXP	0.00,	0.03,	0.14,	0.31,	0.55
EXP	0.85				
; HIGH ANGLE MAP PSIMF -100 TO 100 FOR ALPWF -10,0,10 DEG					
; ALPWF = -10 DEG					
DRQFHI: EXP	55.30,	55.30,	42.80,	23.60,	6.67
EXP	0.00,	6.67,	23.60,	42.80,	55.30
EXP	55.30				
; ALPWF = 0 DEG					
EXP	41.20,	41.20,	31.90,	17.60,	5.00
EXP	0.00,	5.00,	17.60,	31.90,	41.20
EXP	41.20				
; ALPWF = 10 DEG					
EXP	7.10,	7.10,	5.46,	3.01,	0.85
EXP	0.00,	0.85,	3.01,	5.46,	7.10
EXP	7.10				
; ** FUSELAGE SIDEFORCE VS PSIMF **					
; MAP LOOK UP ROUTINE					
YQFNF::	UVNUNV00				
EXP	PSIMF00				
	YQF00				
	YQFLO				
EXP	-20.0,20.0,2.0				
	YQFHI				
EXP	-100.0,100.0,20.0				
; LOW ANGLE MAP PSIMF -20 TO 20, DELTA = 2 DEG					
YQFLO: EXP	-3.57,	-3.13,	-2.72,	-2.33,	-1.96
EXP	-1.60,	-1.27,	-0.94,	-0.62,	-0.31
EXP	0.00,	0.31,	0.62,	0.94,	1.27
EXP	1.61,	1.96,	2.33,	2.72,	3.13
EXP	3.56,				
; HIGH ANGLE MAP PSIMF -100 TO 100, DELTA = 2 DEG					
YQFHI: EXP	-38.94,	-30.00,	-18.99,	-9.62,	-3.57
EXP	0.00,	3.57,	9.62,	18.99,	30.00
EXP	38.94,				

TABLE E-1. OH-58A SPECIFIC FILE (Cont'd)

```

; ** FUSELAGE ROLLING MOMENT VS PSIWF **
RQFMP: UVRUVR00 ;MAP LOOK UP ROUTINE
EXP PSIWF00 ;INPUT VARIABLE
RQP00 ;OUTPUT VARIABLE
RQFLO ;LOW ANGLE MAP NAME
EXP -20.0,20.0,2.0 ;LOWER LIM,UPPER LIM,DELTA
RQPHI ;HIGH ANGLE MAP NAME
EXP -100.0,100.0,20.0 ;LOWER LIM,UPPER LIM,DELTA

;LOW ANGLE MAP PSIWF FROM -20 TO 20 DEG, DELTA = 2
RQFLO: EXP -16.91, -15.47, -13.94, -12.35, -10.70
EXP -9.00, -7.25, -5.47, -3.66, -1.84
EXP 0.00, 1.84, 3.66, 5.47, 7.25
EXP 9.00, 10.70, 12.35, 13.94, 15.46
EXP 16.91

;HIGH ANGLE MAP:PSIWF FROM -100 TO 100 DEG, DELTA = 20
RQPHI: EXP 9.00, -9.00, -22.79, -25.91, -16.91
EXP 0.00, 16.91, 25.91, 22.79, 9.00
EXP -9.00

; ** FUSELAGE YAWING MOMENT VS PSIWF **
NQFMP: UVRUVR00 ;MAP LOOK UP ROUTINE
PSIWF00 ;INPUT VARIABLE
NQF00 ;OUTPUT VARIABLE
NQFLO ;LOW ANGLE MAP NAME
EXP -20.0,20.0,2.0 ;LOWER LIM,UPPER LIM,DELTA
NQPHI ;HIGH ANGLE MAP NAME
EXP -100.0,100.0,20.0 ;LOWER LIM,UPPER LIM,DELTA

;LOW ANGLE MAP PSIWF -20 TO 20, DELTA = 2 DEG
NQFLO: EXP -69.65, -64.43, -58.68, -52.44, -45.77
EXP -38.72, -31.36, -23.75, -15.94, -8.00
EXP 0.00, 8.00, 15.93, 23.75, 31.36
EXP 38.73, 45.77, 52.44, 58.68, 64.43
EXP 69.65

;HIGH ANGLE MAP:PSIWF -100 TO 100 DEG, DELTA = 20
NQPHI: EXP 270.41, 123.51, -12.79, -82.95, -69.65
EXP 0.00, 69.64, 82.95, 12.79, -123.51
EXP -270.41

;***** ROTOR INTERFERENCE ON THE FURLEAGE (MRPA) *****

; ** ROTOR X-FACTOR ON FURELAGE MAP **
EXWMP: UVR00 ;MAP ARGUMENT:LOOK UP ROUTINE
CHIPMR40 ;INPUT VARIABLE
EKXW40 ;OUTPUT VARIABLE
EXWFLO ;LOW ANGLE MAP NAME
EXP -20.0,100.0,10.0 ;LOWER LIM,UPPER LIM,DELTA

EXWFLO: EXP -0.15, -0.04, 0.08, 0.20, 0.33
EXP 0.46, 0.60, 0.74, 0.89, 1.00
EXP 0.20, -0.90, -0.55

; ** ROTOR Z-FACTOR ON FURELAGE MAP **
EZWMP: UVR00 ;MAP LOOK UP ROUTINE
CRIPMR40 ;INPUT VARIABLE
EKIWP00 ;OUTPUT VARIABLE
EZWFO ;LOW ANGLE MAP NAME
EXP -20.0,100.0,10.0 ;LOWER LIM,UPPER LIM,DELTA

EZWFLO: EXP 1.20, 1.21, 1.22, 1.23, 1.24
EXP 1.25, 1.26, 1.27, 1.28, 1.29
EXP 1.15, 1.00, 1.05

```

TABLE E-1. OH-58A SPECIFIC FILE (Cont'd)

```

;***** INPUT PARAMETERS FOR PANEL #1 (HORIZONTAL) *****
;***** (OH-58A DATA FROM C-81 LISTING) *****
;***** (E= 9.65 FT**2, AR= 4.29, TR= 1.0, SWEEP= 0, e= .9)

PSP1:: 258.213      ; FUSELAGE STATION, INCH
NLP1:: 72.98       ; WATERLINE STATIDN, INCH
SLP1:: 0.0         ; SUTLINE STATIDN, INCH (+IVE TO PORT)
SAP1:: 9.65        ; SURFACE AREA, FT**2
GAMP1:: 0.0        ; PANEL ORIENTATIDN, DEG
IOP1:: 0.0         ; PANEL INCIDENCE, DEG
CPI1:: 1.0         ; PANEL MEAN AERO CHDRD, PT

;** HORIZONTAL STABILIZER LIPT VS ALPPP1 **
CLPIMP::UVRUVR00   ;MAP LOOK UP ROUTINE
          ALPPP100   ;INPUT VARIABLE
          CLP100    ;OUTPUT VARIABLE
          CLP1LD    ;LOW ANGLE MAP NAME
EXP -30.0,30.0,5.0 ;LOWER LIM,UPPER LIM,DELTA
          CLP1HI    ;HIGH ANGLE MAP NAME
EXP -90.0,90.0,30.0 ;LOWER LIM,UPPER LIM,DELTA

;LOW ANGLE MAP:ALPPP1 -30 TO 30, DELTA = 5 DEG
CLP1LO: EXP      -0.880,   -0.950,   -1.140,   -1.050,   -0.790
          EXP      -0.500,   -0.265,   -0.125,   0.010,   0.100
          EXP      0.210,   0.310,   0.330

;HIGH ANGLE MAP:ALPPP1 -50 TO 90 DEG, DELTA = 10 DEG
CLP1HI: EXP      0.000,   -0.839,   -0.873,   -0.265,   0.330
          EXP      0.165,   0.000

;** HORIZONTAL STABILIZER DRAG VS ALPPP1 **
CDPIMP::UVRUVR00   ;MAP LOOK UP ROUTINE
          ALPPP100   ;INPUT VARIABLE
          CDP100    ;OUTPUT VARIABLE
          CDP1LO    ;LOW ANGLE MAP NAME
EXP -30.0,30.0,5.0 ;LOWER LIM,UPPER LIM,DELTA
          CDP1HI    ;HIGH ANGLE MAP NAME
EXP -90.0,90.0,30.0 ;LOWER LIM,UPPER LIM,DELTA

;LOW ANGLE MAP ALPPP1 -30 TO 30, DELTA = 5 DEG
CDP1LD: EXP      0.603,   0.870,   0.338,   0.225,   0.145
          EXP      0.105,   0.085,   0.077,   0.085,   0.110
          EXP      0.275,   0.409,   0.603

;HIGH ANGLE MAP:ALPPP1 -90 TO 90 DEG, DELTA = 30 DEG
CDP1HI: EXP      1.200,   1.040,   0.603,   0.085,   0.603
          EXP      0.940,   1.200

;***** INPUT PARAMETER FOR ROTOR INTERFERENCE ON THE HORIZ. TAIL #1 (MRPA)

EXPIMP::RIV00      ;** ROTOR X-FACTOR ON HORIZONTAL TAIL **
EXP  CRIPR00,AAIPR00 ;INPUT VAR#1,INPUT VAR#2
          EXXP100    ;OUTPUT VARIABLE
          EXP1LD    ;MAP NAME
EXP 0.0,90.0,10.0,010 ;LOWER LIM,UPPER LIM,DELTA
EXP -10.0,10.0,10.0 ;LOWER LIM,UPPER LIM,DELTA

;CRIPR 0 TO 90 DEG FOR AAIPR -10,0,10 DEG
;AAIPR = -10 DEG
EXP1LD: EXP      0.15,   0.28,   0.42,   0.58,   0.75
          EXP      0.93,   1.15,   1.35,   1.55,   1.75

;AAIPR = 0 DEG
EXP      -0.20,   -0.08,   0.06,   0.22,   0.38

```

TABLE E-1. OH-58A SPECIFIC FILE (Cont'd)

```

EXP      0.56,      0.76,      0.98,      1.21,      1.41

EXP      ;AALPHR = 3 DEG
EXP      -0.53,     -0.42,     -0.30,     -0.17,     -0.02
EXP      0.14,      0.32,      0.54,      0.79,      1.01

EZP1MP: :BIW00      ;** NOTDR 2-FACTOR ON HORIZONTAL TAIL MAP **
          CHIPR008   ;MAP LOOK UP ROUTINE
          AALPHR08   ;INPUT VARIABLE 81
          EKZP100    ;INPUT VARIABLE 82
          EZP1LO     ;OUTPUT VARIABLE
          EXP 0.0,90.0,10.0,^D10 ;LOW ANGLE MAP NAME
          EXP -10.0,10.0,10.0 ;LOWER LIM,UPPER LIM,DELTA,8ITEMS
          ;LOWER LIM,UPPER LIM,DELTA AALPHR

          ;CHIPR 0 TO 90 DEG FOR AALPHR -10,0,10 DEG
          ;AALPHR = -10 DEG
EZP1LD: EXP      1.49,      1.50,      1.50,      1.51,      1.50
          EXP      1.50,      1.49,      1.48,      1.47,      1.46

          ;AALPHR = 0 DEG
          EXP      1.42,      1.47,      1.51,      1.55,      1.60
          EXP      1.54,      1.68,      1.72,      1.76,      1.80

          ;AALPHR = -10 DEG
          EXP      1.23,      1.31,      1.39,      1.48,      1.56
          EXP      1.65,      1.74,      1.84,      1.95,      2.06

;***** FUSELAGE INTERPERNCE ON THE RDHIL.TAIL (MPPA) *****

OPI1MP: :CONST00   ;** HORIZONTAL TAIL DYNAMIC PRESSURE RATIO MAP**
          [0.80]    ;MAP LOOK UP ROUTINE
          OPI1QW00  ;DUTPUT VARIABLE

;***** INPUT PARAMETERS FOR PANEL 83 (VERTICAL TAIL) *****
;***** (R= 9.18 FT**2, AR= 4.67, alpha= 0.9) *****

FSP3:   354.6      ; FUSELAGE STATION, INCHES
MLP3:   85.9       ; WATERLINE STATION, INCHES
BLP3:   -8.0       ; BUTTLINE STATION, INCH (+IVE TO PORT)
SAP3:   9.18      ; SURFACE AREA, FT**2
GAMP3:  90.0      ; PANEL ORIENTATION, DEG
IOP3:   4.0       ; PANEL INCIDENCE, DEG
CP3:    1.0       ; PANEL MEAN AERO CBDRD, FT

CLP3MP: :UVRUVR00  ;** VERTICAL STABILIZER LIFT VS ALPPP3 MAP **
          ALPPP300  ;MAP LOOK UP ROUTINE
          CLP308    ;INPUT VARIABLE
          CLP3LO    ;DUTPUT VARIABLE
          EXP -30.0,30.0,5.0 ;LOW ANGLE MAP NAME
          CLP3HI    ;LOWER LIM,UPPER LIM,DELTA
          EXP -90.0,90.0,30.0 ;HIGH ANGLE MAP
          ;LOWER LIM,UPPER LIM,DELTA

          ;LOW ANGLE MAP ALPPP3 -30 TO 30. DELTA = 5 DEG
CLP3LD: EXP      -0.753,     -0.790,     -0.775,     -0.640,     -0.430
          EXP      -0.200,     0.000,     0.225,     0.445,     0.655
          EXP      0.775,     0.795,     0.753

          ;HIGH ANGLE MAP:ALPPP3 -90 TO 90 DEG, DELTA = 30 DEG
CLP3HI: EXP      0.000,     -0.350,     -0.753,     0.000,     0.753
          EXP      0.350,     0.000

;** VERTICAL STABILIZER DRAG VS ALPPP3 **
CDP3MP: :UVRUVR00  ;MAP LOOK UP ROUTINE

```


TABLE E-1. OH-58A SPECIFIC FILE (Cont'd)

```

ALFPP300 ;INPUT VARIABLE
CDP300 ;OUTPUT VARIABLE
CDP3LO ;LOW ANGLE MAP NAME
EXP -30.0,30.0,5.0 ;LOWER LIM,UPPER LIM,DELTA
CDP3HI ;HIGH ANGLE MAP
EXP -90.0,90.0,30.0 ;LOWER LIM,UPPER LIM,DELTA

;LOW ANGLE MAP ALFPP3 -30 TO 30, DELTA = 5 DEG
CDP3LO: EXP 0.352, 0.242, 0.160, 0.026, 0.051
EXP 0.022, 0.012, 0.022, 0.052, 0.098
EXP 0.160, 0.248, 0.352

;HIGH ANGLE MAP:ALFPP3 -90 TO 90 DEG, DELTA = 30 DEG
CDP3HI: EXP 1.200, 0.900, 0.352, 0.012, 0.352
EXP 0.900, 1.200

;***** ROTOR INTERFERENCE ON THE VERTICAL TAIL #1 (MRPA) *****

EXP3MP: BIV00 ;** ROTOR X-FACTOR ON VERTICAL TAIL MAP **
EXP CHIPR00, AALFMR00 ;MAP ARGUMENT:LOOK UP ROUTINE
EKXP300 ;INPUT VARIABLE #1, INPUT VARIABLE #2
EXP3 ;OUTPUT VARIABLE
EXP 0.0,90.0,10.0, D10 ;LOW ANGLE MAP NAME
EXP -10.0,10.0,10.0 ;LOWER LIM,UPPER LIM,DELTA, #ITEMS
;LOWER LIM,UPPER LIM,DELTA - AALFMR

;CHIPMR 0 TO 90 FOR AALFMR -10,0,10 DEG
;AALFMR = -10 DEG
EXP3: EXP -0.47, -0.03, 0.52, 0.71, 0.91
EXP 1.12, 1.35, 1.61, 0.86, 0.00

;AALFMR = 0 DEG
EXP -0.45, -0.57, -0.70, 0.30, 0.58
EXP 0.77, 1.02, 1.30, 1.61, 0.00

;AALFMR = 10 DEG
EXP -0.57, -0.65, -0.74, -0.82, -0.88
EXP -0.91, -0.89, -0.78, 1.33, 0.00

;** ROTOR Z-FACTOR ON VERTICAL TAIL MAP **
EXP3MP: BIV00 ;MAP ARGUMENT:LOOK UP ROUTINE
EXP CHIPR00, AALFMR00 ;INPUT VARIABLE #1, INPUT VARIABLE #2
EKZP300 ;OUTPUT VARIABLE
EXP3LO ;LOW ANGLE MAP NAME
EXP 0.0,100.0,10.0, D11 ;LOWER LIM,UPPER LIM,DELTA, #ITEMS
EXP -10.0,10.0,10.0 ;LOWER LIM,UPPER LIM,DELTA - AALFMR

;CHIPMR 0 TO 100 DEG FOR AALFMR -10,0,10 DEG
;AALFMR = -10 DEG
EXP3LO: EXP -0.15, 0.98, 1.77, 1.77, 1.76
EXP 1.74, 1.71, 1.68, , 1.15
EXP 0.70

;AALFMR = 0 DEG
EXP -0.17, -0.07, 0.09, 1.92, 1.98
EXP 2.01, 2.03, 2.04, 2.05, 0.34
EXP 0.25

;AALFMR = 3 DEG
EXP -0.11, -0.01, 0.13, 0.30, 0.53
EXP 0.82, 1.16, 1.56, 2.45, 2.26
EXP 0.50

;***** FUSELAGE INTERFERENCE ON THE VERTICAL TAIL #A (WPPA) *****

;** VERTICAL TAIL DYNAMIC PRESSURE RATIO MAP **

```

TABLE E-1. OH-58A SPECIFIC FILE (Cont'd)

```

QP3MP:: CONST00 ;MAP LOOK UP ROUTINE
EXP [1.0] ;INPUT VARIABLE
QP3QWF00 ;OUTPUT VARIABLE

; ** BOOY DOWNWASH ON VERTICAL TAIL MAP **
EPP3MP::CONST00 ;MAP LOOK UP ROUTINE
EPSP100 ;INPUT VARIABLE
EPSP300 ;OUTPUT VARIABLE

; **BOOY SIDEWASH ON VERTICAL TAIL MAP **
SGP3MP::CONST00 ;MAP LOOK UP ROUTINE
SIGP100 ;INPUT VARIABLE
SIGP300 ;OUTPUT VARIABLE

;***** INPUT PARAMETERS FOR TAIL ROTOR (0A) - (BAILEY) *****
RTR:: 2.58333 ;RADIUS, FT
OMEGTR::272.2712 ;TRIM ROTATIONAL RATE, RAD/SEC
BTR:: 2.0 ;ACTUAL NUMBER OF BLADES
FSTR:: 352.180 ;FUSELAGE STATION, IN
WLTR:: 87.177 ;WATERLINE STATION, IN
BLTR:: 10.0 ;BUTTLINE STATION, IN (+IVE TO PORT)
TWSTTR::0.0 ;BLADE TWIST, OATUM CENTER OF ROTATION, DEG
BIASTR::0.0 ;BLADE PITCH CORRECTION FOR N.L.TWIST(NEG REDUCES PITCH)
GAMTR::-90.0 ;TAIL ROTOR CANT ANGLE, DEG
OEL3TR::0.0 ;FLAPPING HINGE OFFSET ANGLE, DEG
OELTTR::0.0 ;RATE OF CHANGE CF CONE ANGLE WITE THRUST, DEG/LB
CHRDTR::.4333 ;BLADE CHORD, FT
ATR:: 5.73 ;BLADE LIFT CURVE SLOPE, 1/RAD
BTLTR:: .975 ;BLADE TIP LOSS FACTOR
COTR:: 1.0 ;TAIL ROTOR HEAD DRAG, FT**2

;***** ROTOR INTERFERENCE ON TAIL ROTOR (MRPA) *****
; ** ROTOR X-FACTOR ON TAIL ROTOR MAP **
EXTRMP::CONST00 ;MAP LOOK UP ROUTINE
EKXP300 ;INPUT VARIABLE
EKXTR00 ;OUTPUT VARIABLE

; ** ROTOR Z-FACTOR ON TAIL ROTOR MAP **
EZTRMP::CONST00 ;MAP LOOK UP ROUTINE
EKZP300 ;INPUT VARIABLE
EKZTR00 ;OUTPUT VARIABLE

;***** FUSELAGE INTERFERENCE ON TBE TAIL ROTOR (WPPA) *****
; ** TAIL ROTOR DYNAMIC PRESSURE RATIO MAP **
QTRMP:: CONST00 ;MAP LOOK UP ROUTINE
QP3QWP ;INPUT VARIABLE
OTRQWP00 ;OUTPUT VARIABLE

; ** BODY DOWNWASH ON TAIL ROTOR MAP **
EPTRMP::CONST00 ;MAP LOOK UP ROUTINE
EPSP100 ;INPUT VARIABLE
EPSTR00 ;OUTPUT VARIABLE

; ** BODY SIDEWASH ON TAIL ROTOR MAP **
SGTRMP::CONST00 ;MAP LOOK UP ROUTINE
SIGP100 ;INPUT VARIABLE
SIGTR00 ;OUTPUT VARIABLE

;***** VERTICAL TAIL INTERFERENCE ON TAIL ROTOR INFLOW *****
VBVTR::30.0 ; AIRSPEED BREAK PT. - NO BLOCKAGE ABOVE, KT.
KBVTR::.895 ; TAIL ROTOR BLOCKAGE CCEP. AT BOVER

```

TABLE E-1. OH-58A SPECIFIC FILE (Cont'd)

```
***** INPUT PARAMETERS FOR EQUATIONS OF MOTION (#A) *****  
PSCG:: 109.1      ; FUSELAGE STATION, OF C.G., INCH  
WLCG:: 55.0       ; WATERLINE STATION OF C.G., INCH  
BLCG:: 0.0        ; BUTTLINZ STATION OF C.G., INCH (+IVE TO PORT)  
  
WEIGHT:: 2790.0   ; AIRCRAFT GROSS WEIGHT, LBS.  
IX:: 526.0        ; INERTIA ABOUT BODY X-AXIS, SLUG-FT**2  
IY:: 2460.0       ; INERTIA ABOUT BODY Y-AXIS, SLUG-FT**2  
IZ:: 2029.0       ; INERTIA ABOUT BODY Z-AXIS, SLUG-FT**2  
IXZ:: 356.0       ; CROSS COUPLING INERTIA, SLUG-FT**2  
IYZ:: 0.0         ;  
IXY:: 0.0         ;
```

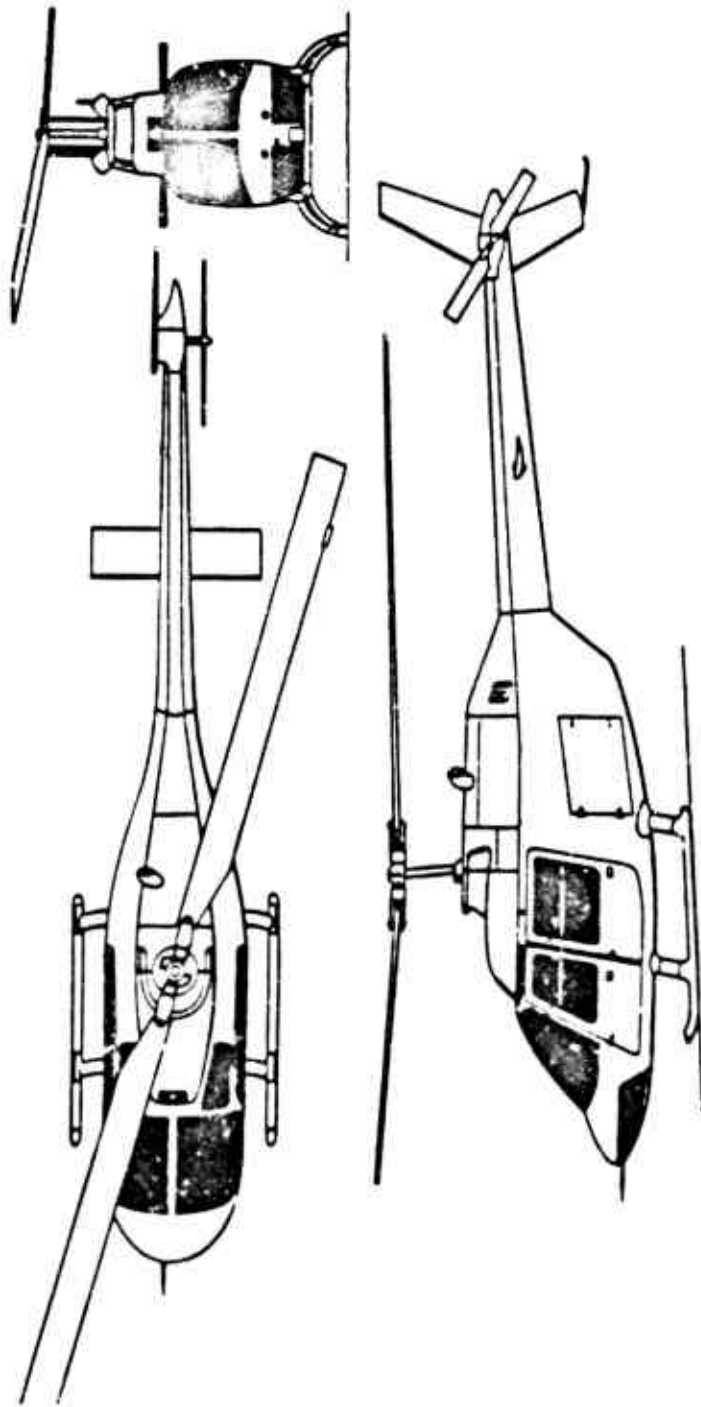


Figure E-1. OH-58A Three-View Drawing

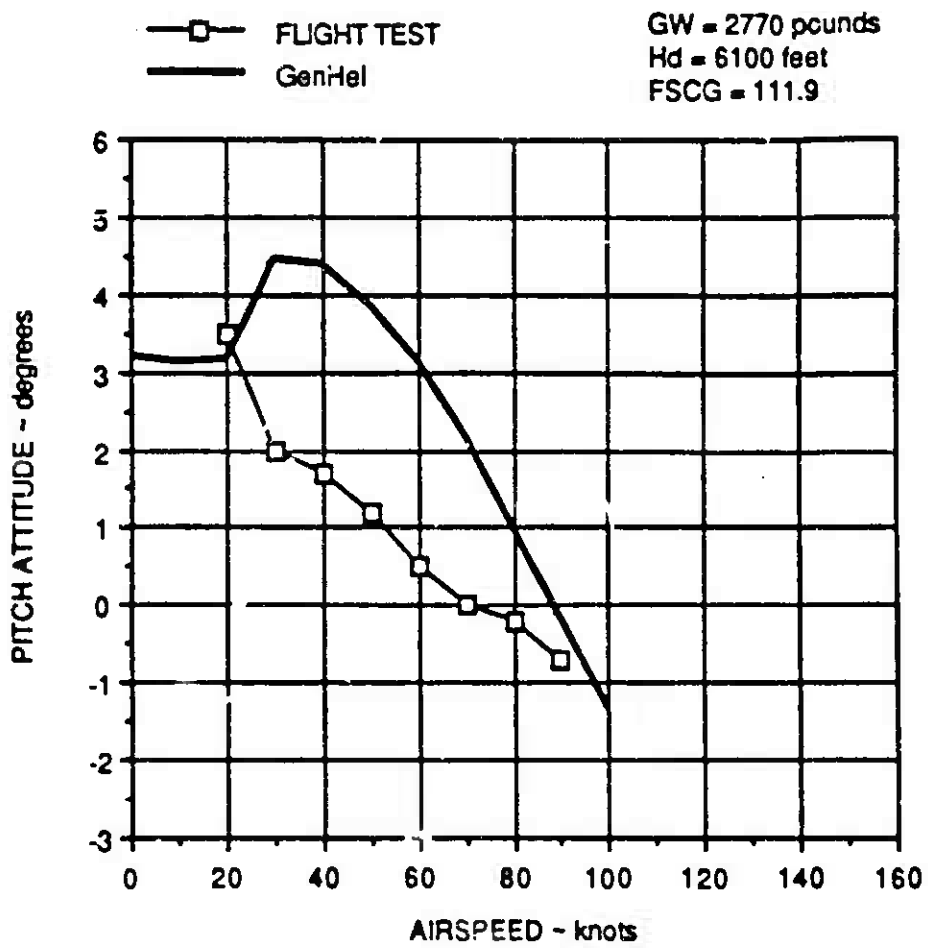


Figure E-2. OH-58a Pitch Attitude Correlation

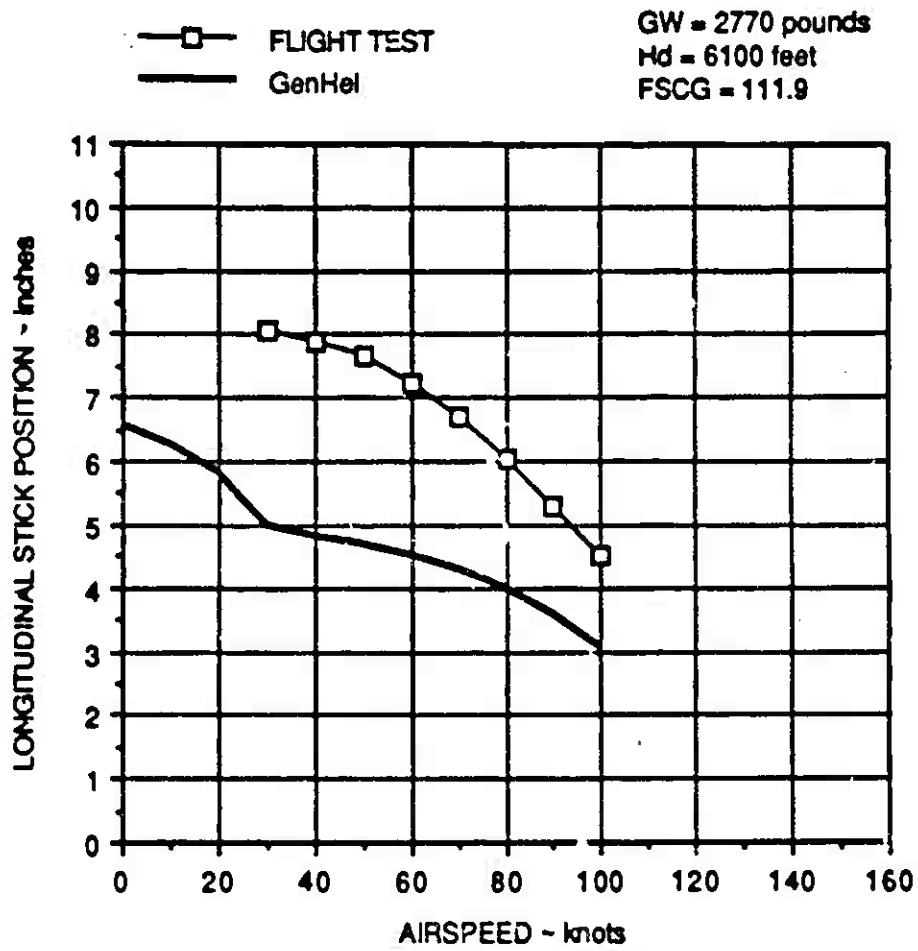


Figure E-3. OH-58A Longitudinal Stick Correlation

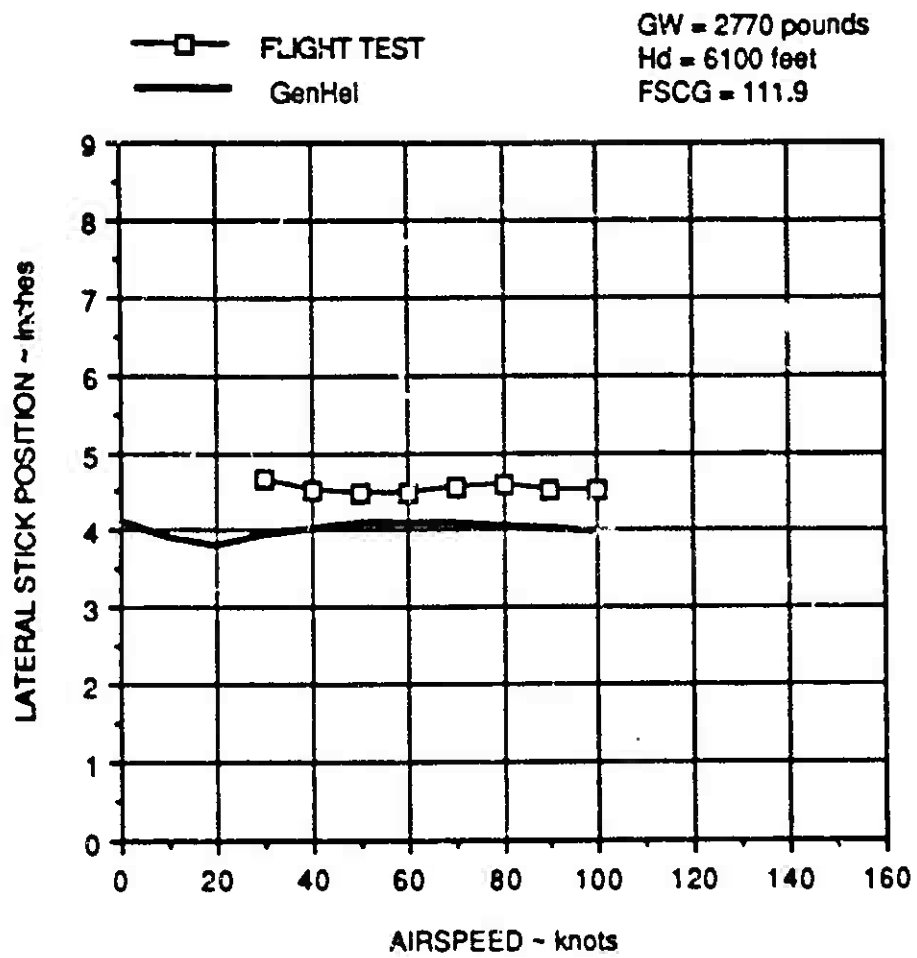


Figure E-4. OH-58A Lateral Stick Correlation

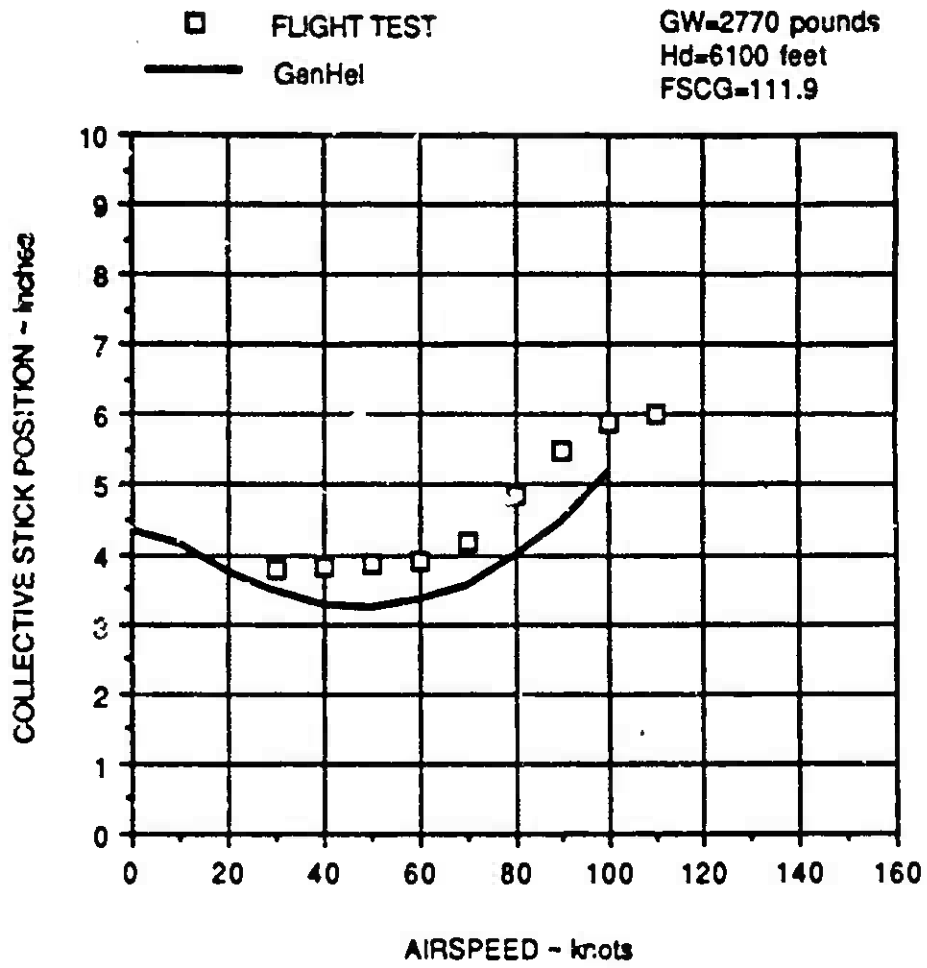


Figure E-5 OH-58A Collective Stick Correlation

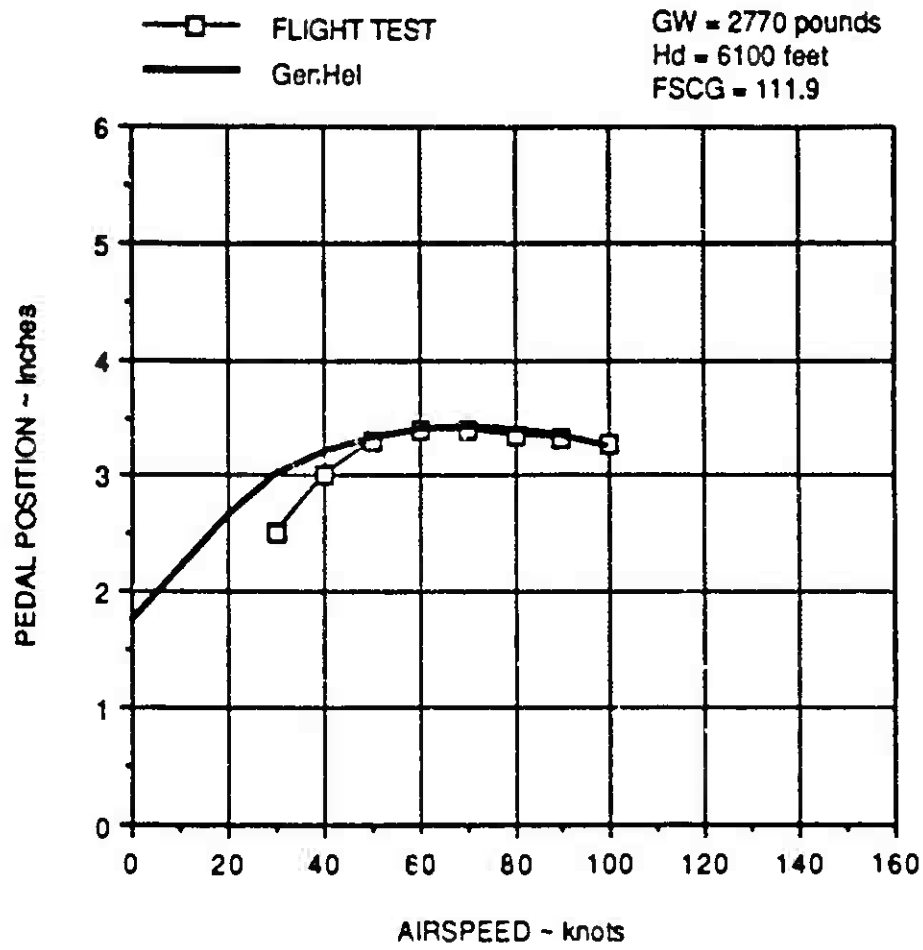


Figure E-6. OH-58A Pedal Correlation

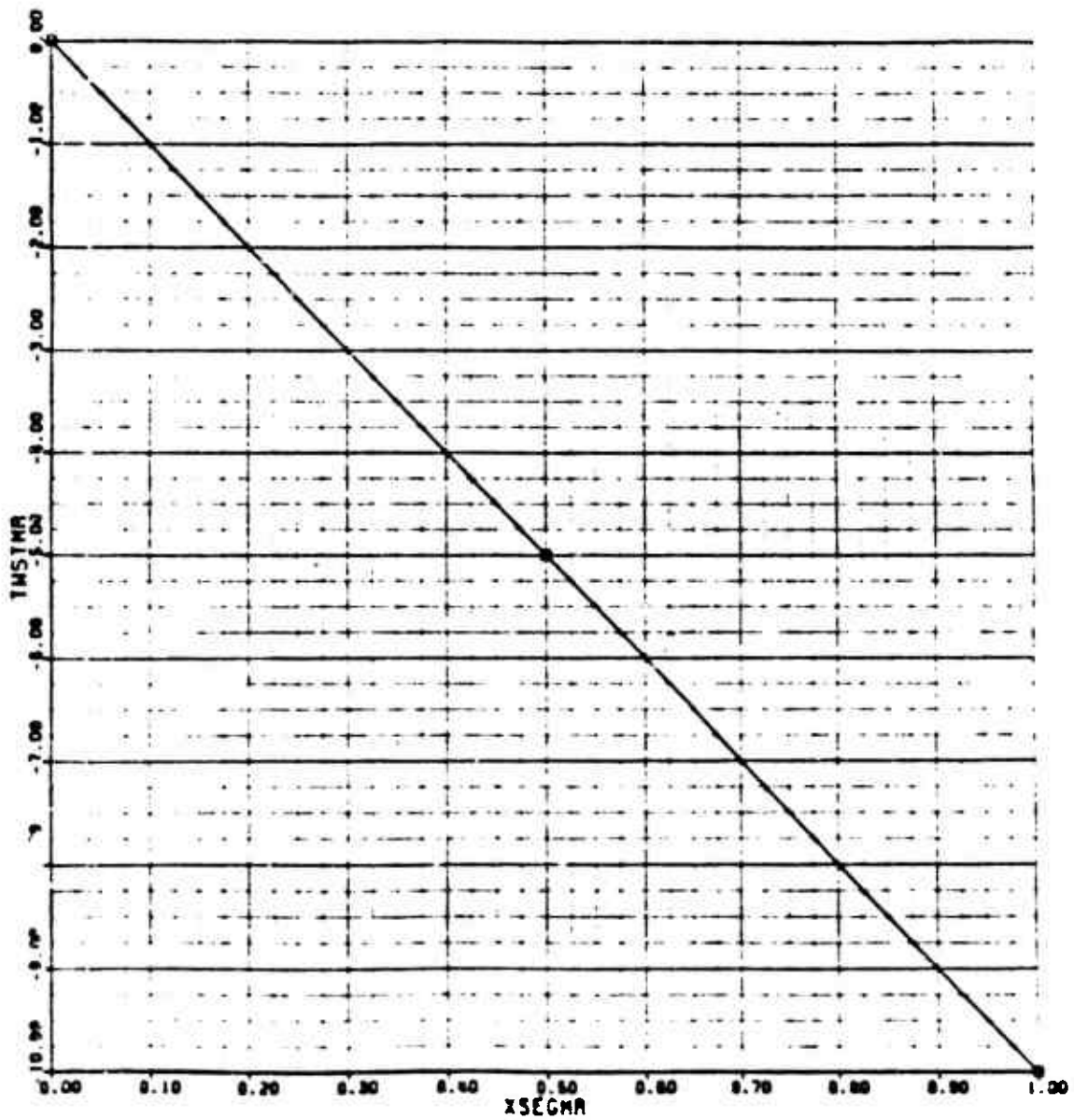


Figure E-7. OH-580 Main Rotor Blade Twist Map

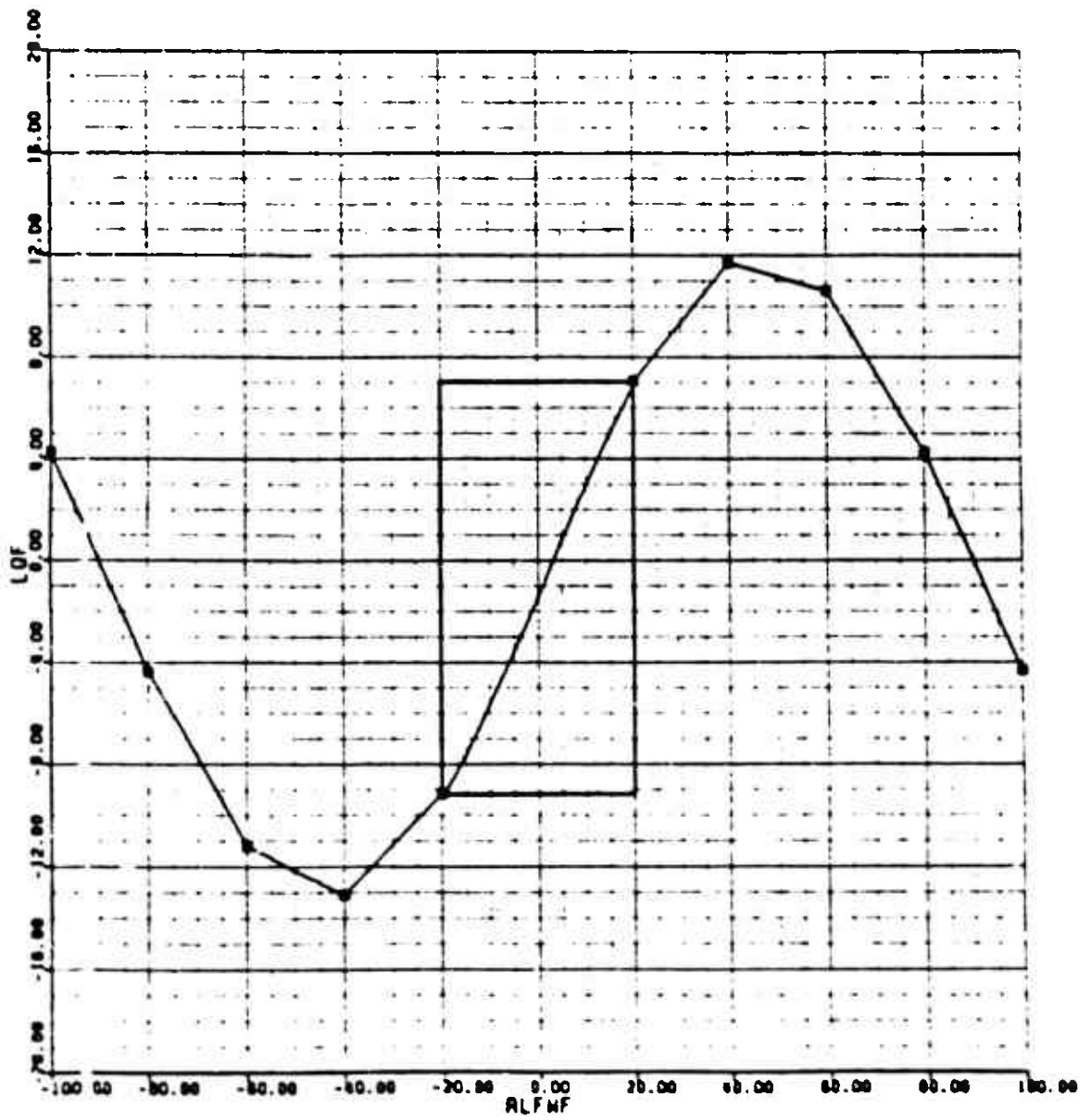


Figure E-8. F-5B Fuselage Lift Map

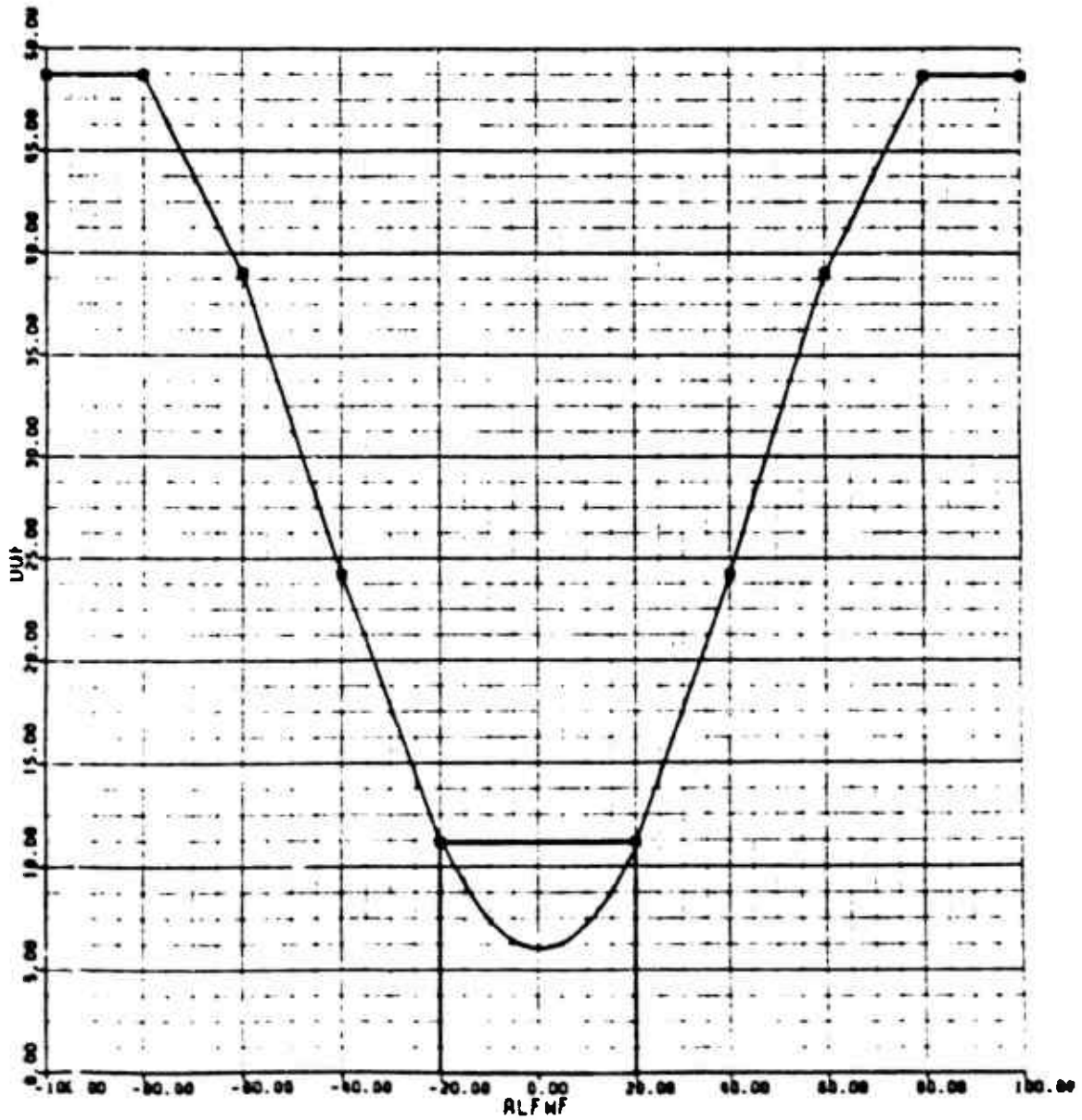


Figure K-9. OH-58A Fuselage Drag Map

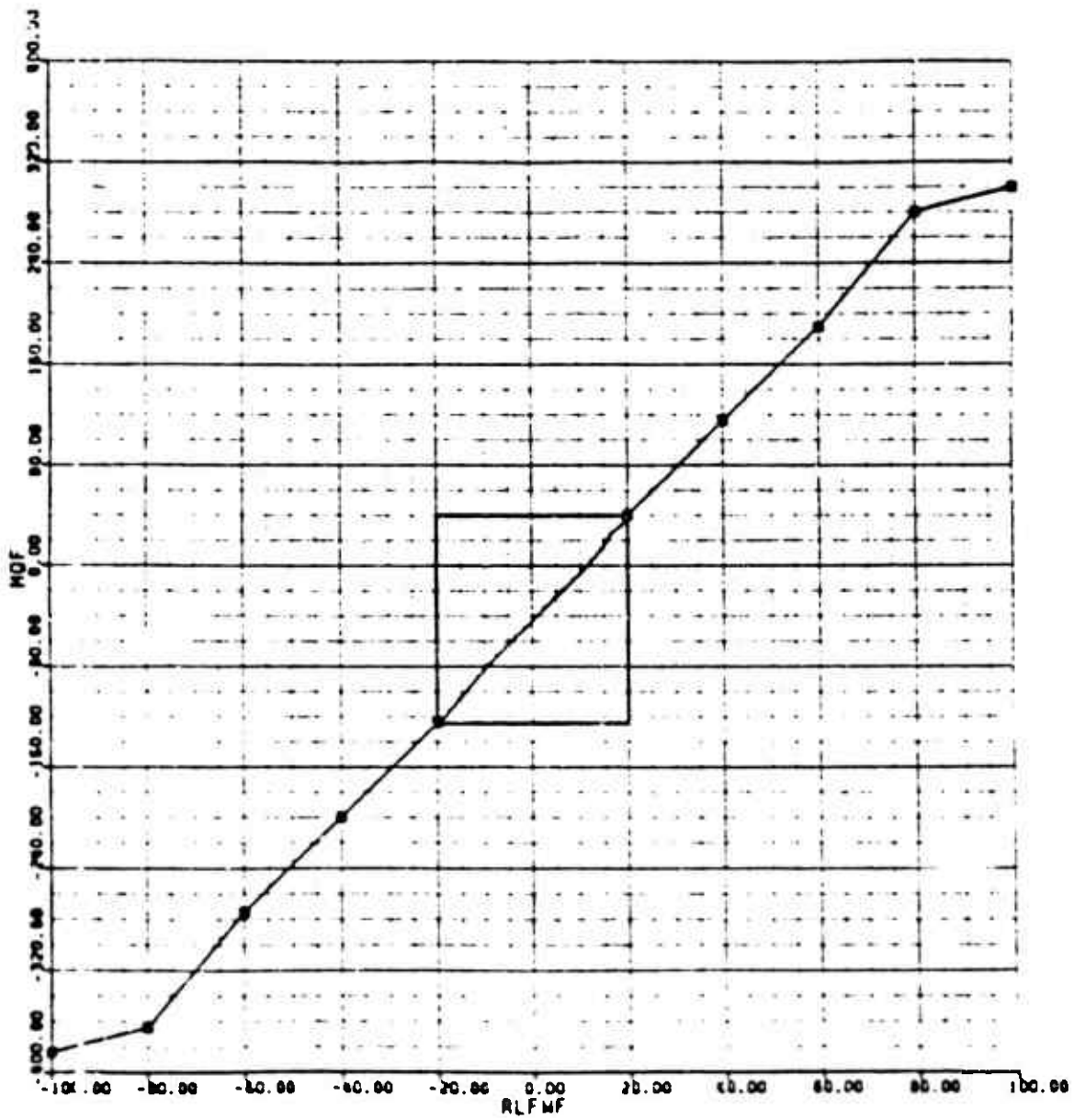


Figure E-10. OH-58A Fuselage Pitching Moment Map

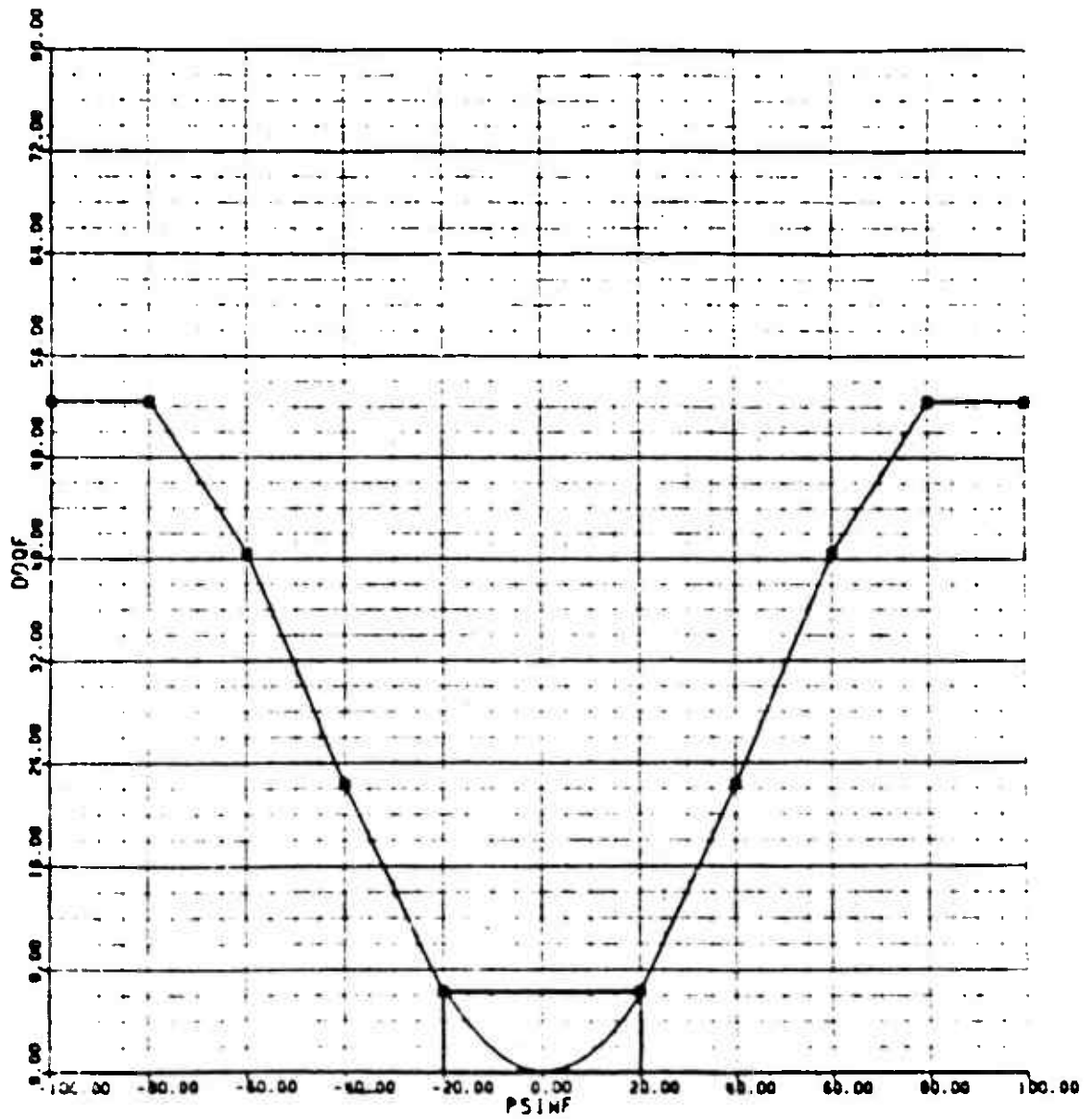


Figure E-11. OH-58A Fuselage Delta Drag Map

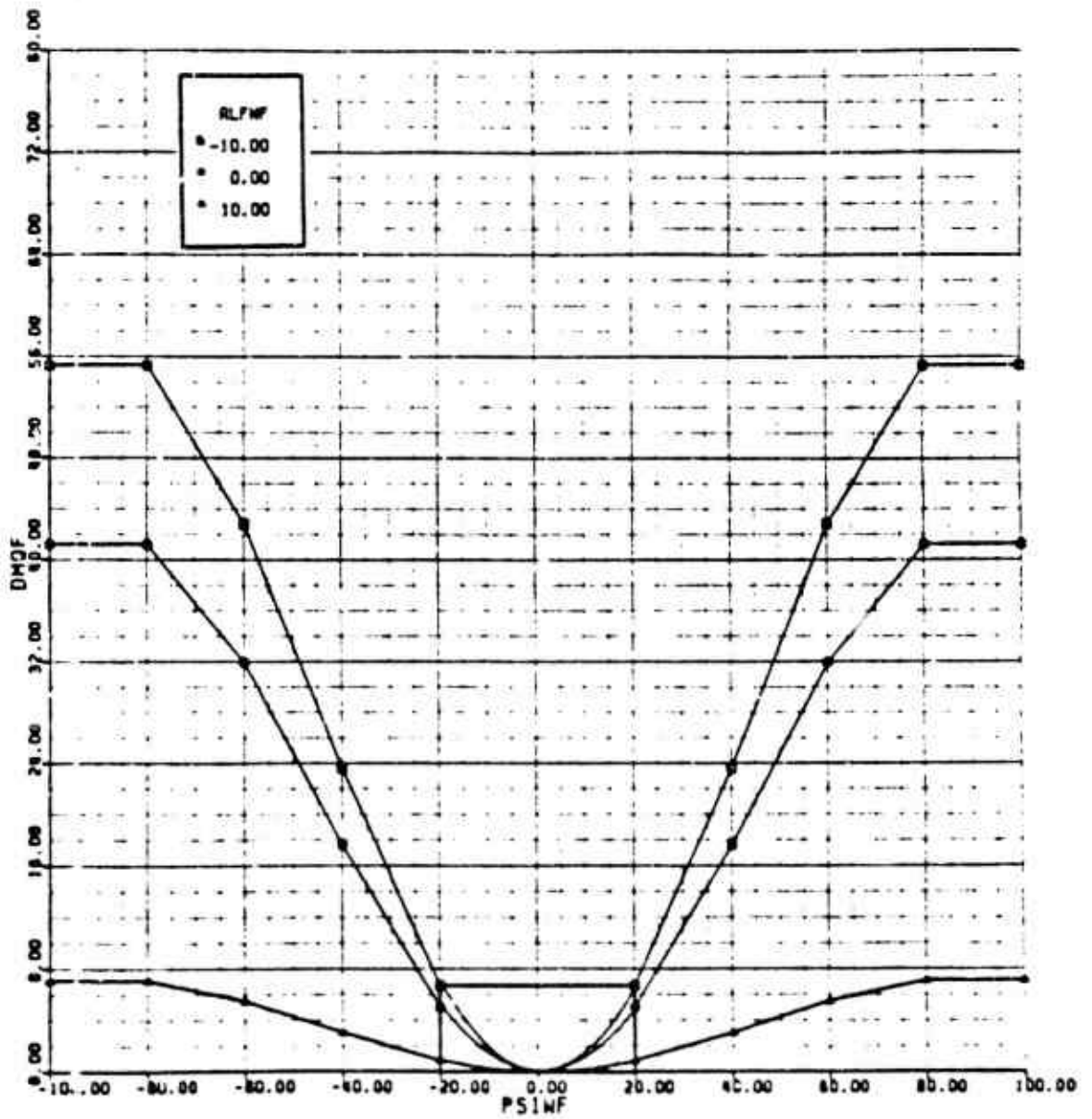


Figure E-12. OH-58A Fuselage Delta Pitching Moment Map

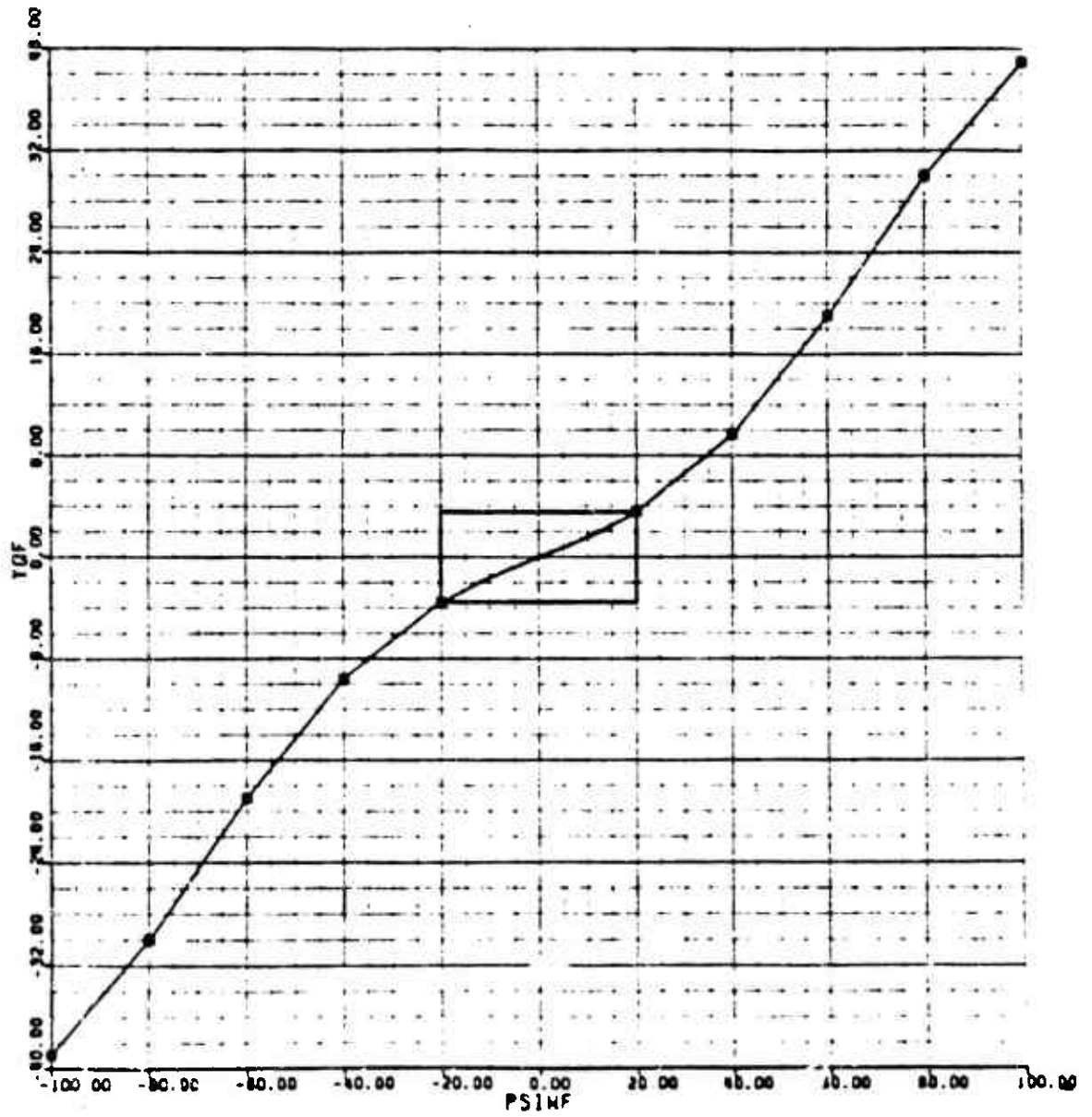


Figure E-13. OH-58A Fuselage Sideforce Map

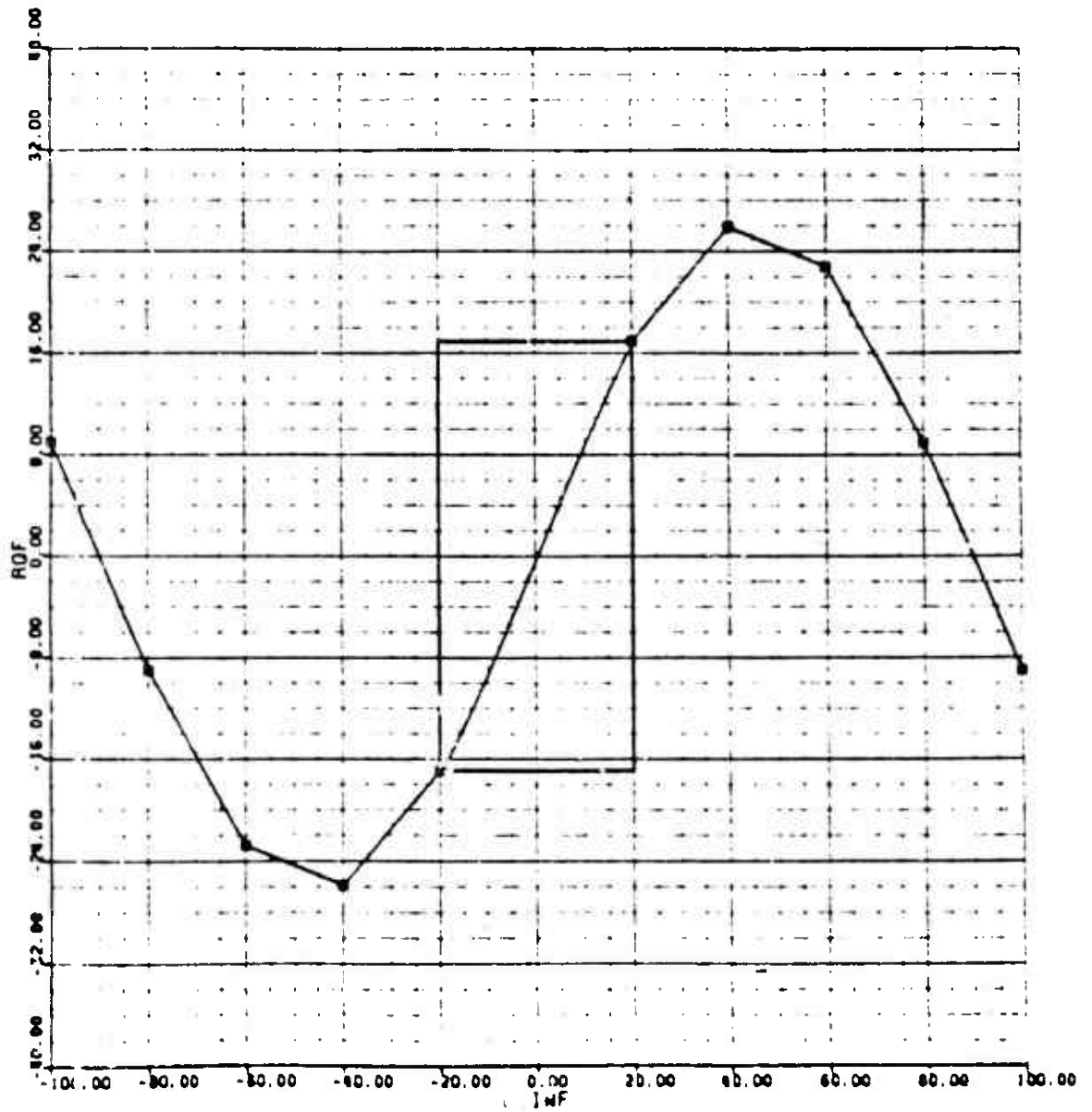


Figure E-14. OH-58A Fuselage Rolling Moment Map

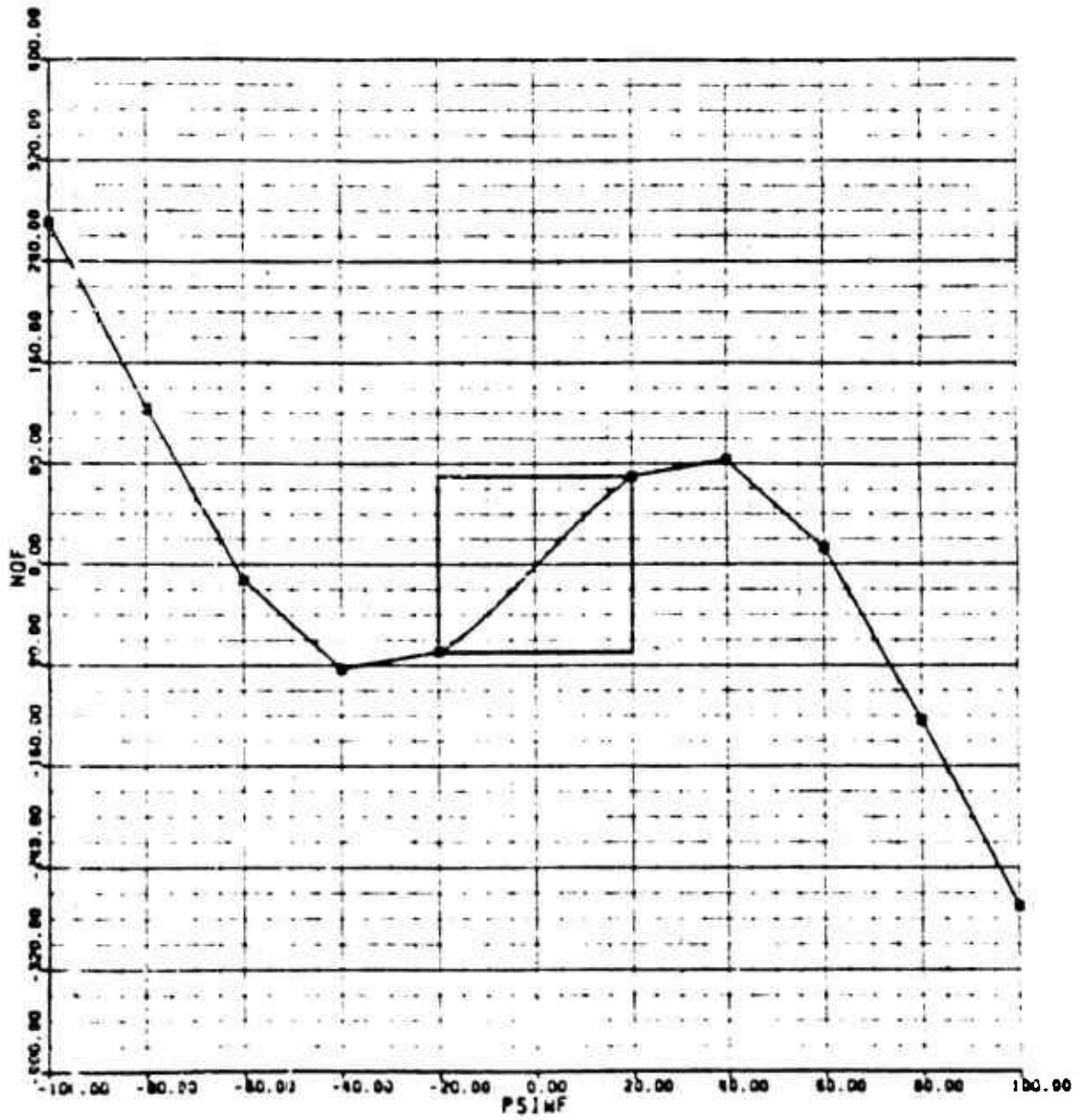


Figure E-15. OH-58A Fuselage Wing Moment Map

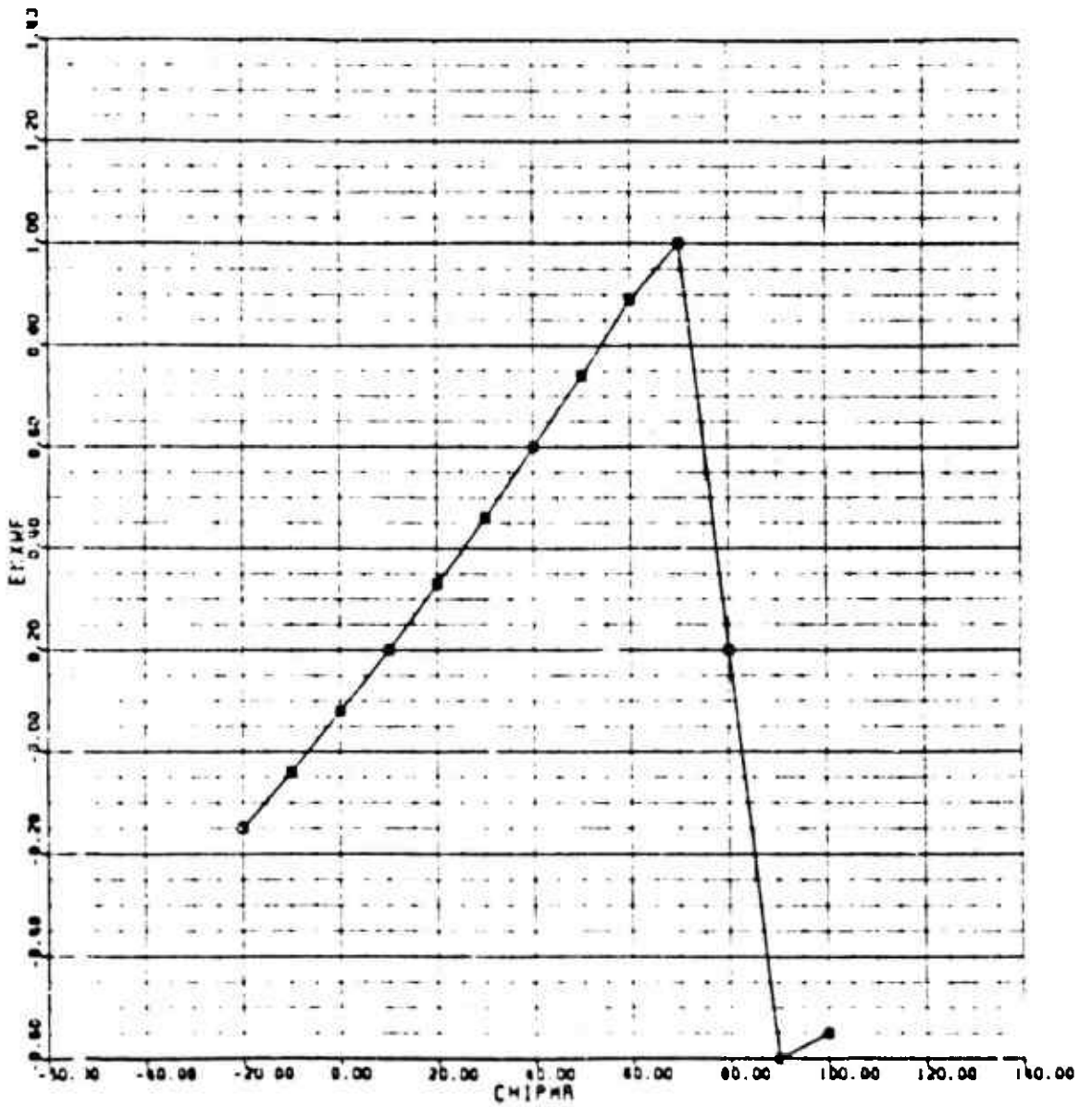


Figure E-16. OH-58A Main Rotor Downwash on Fuselage Map (x-direction)

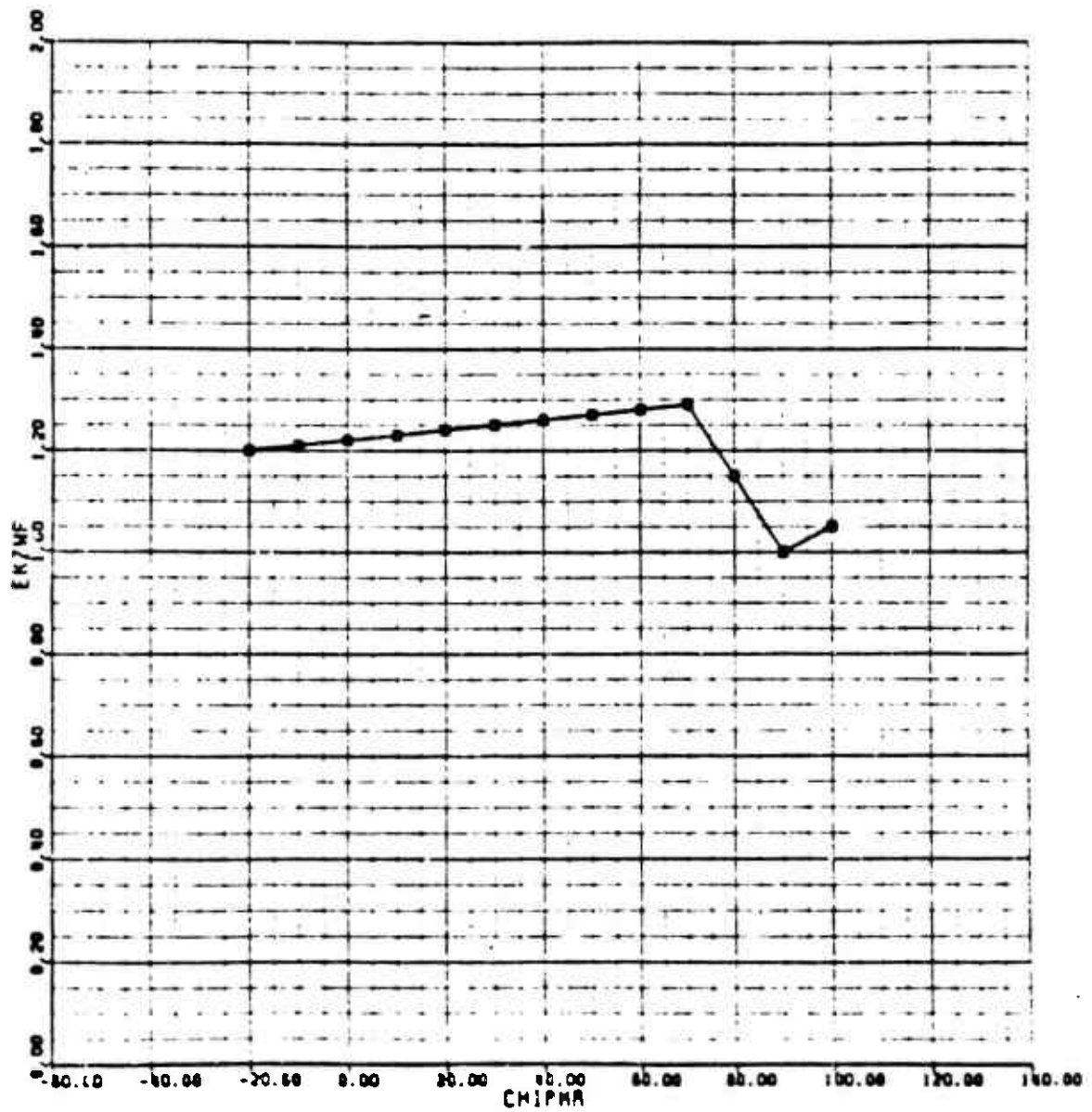


Figure E-17. OH-58A Main Rotor Downwash on Fuselage Map (z-direction)

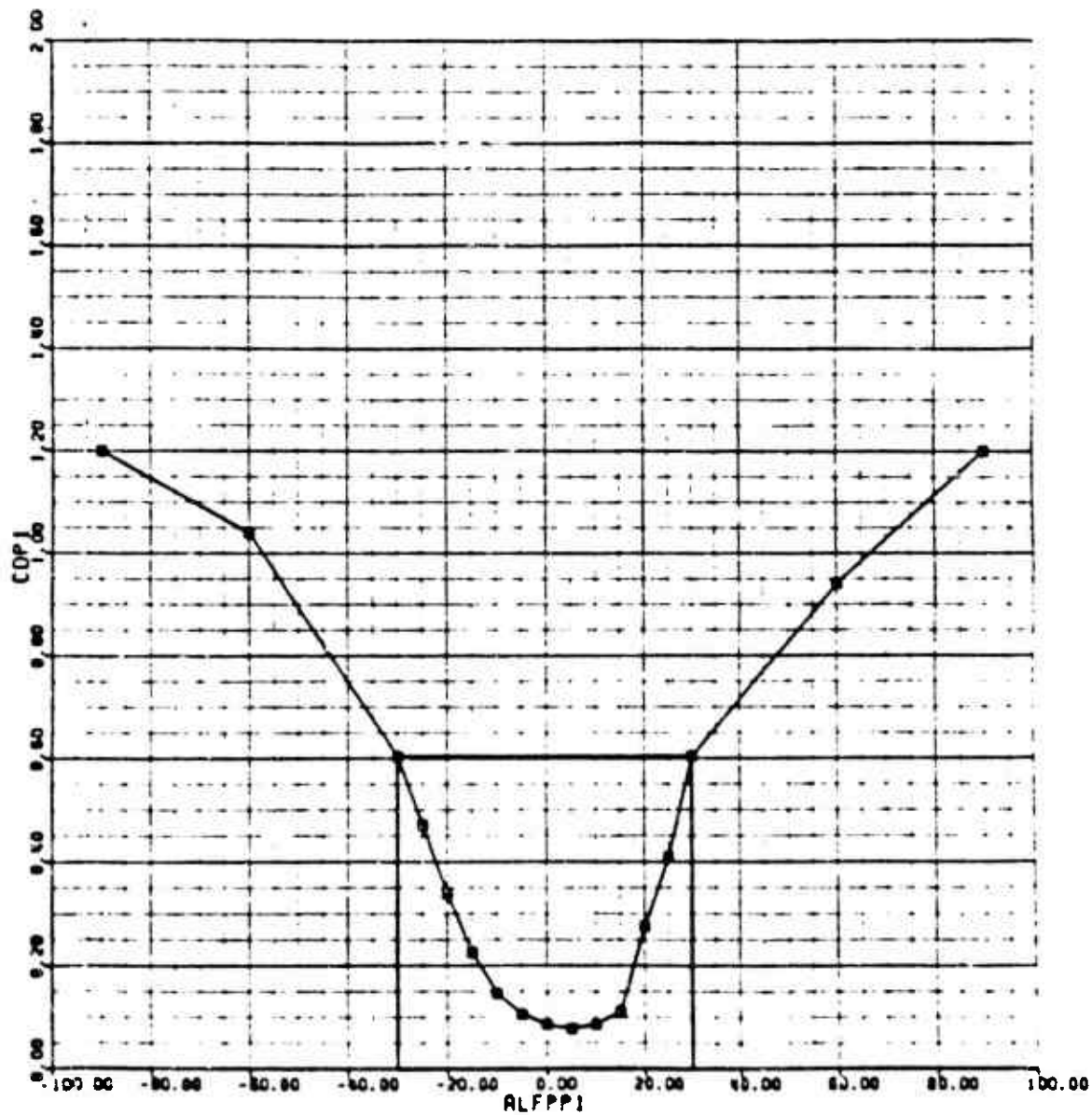


Figure K-19. OH-58A Horizontal Stabilizer Drag Map

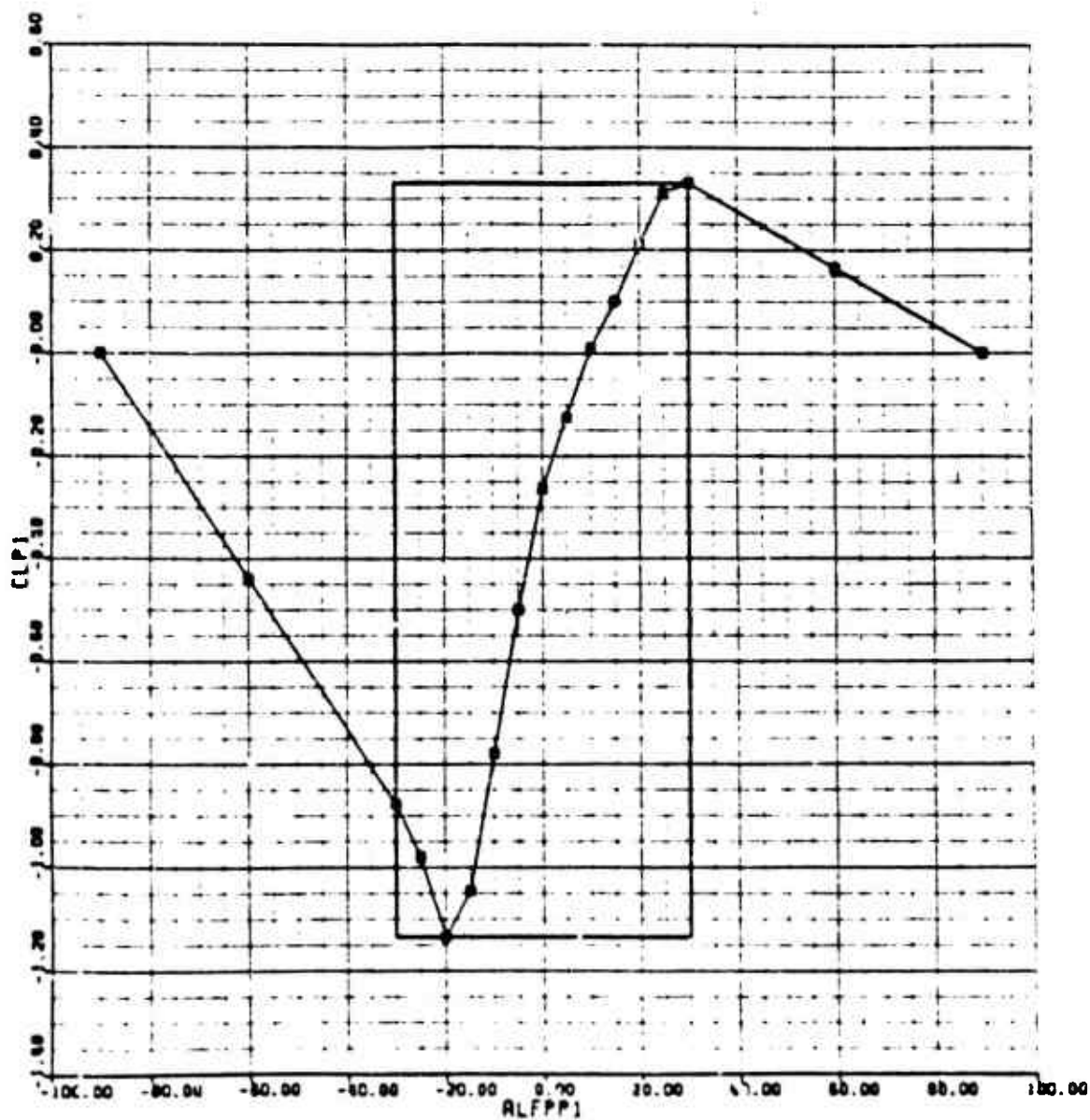


Figure E-18. OH-58A Horizontal Stabilizer Lift Map

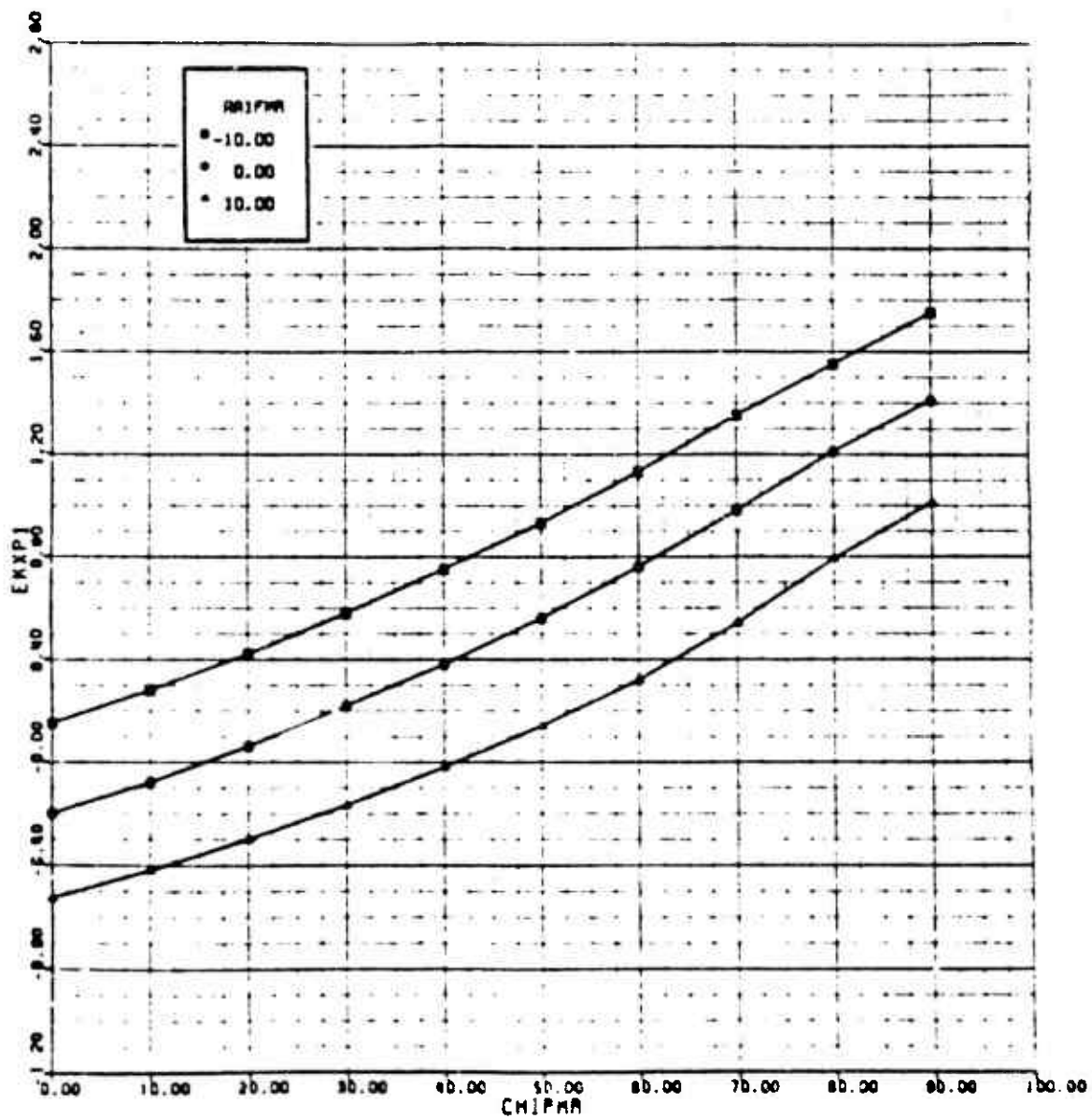


Figure E-20. OH-58A Main Rotor Downwash on Horizontal Stabilizer Map (x-direction)

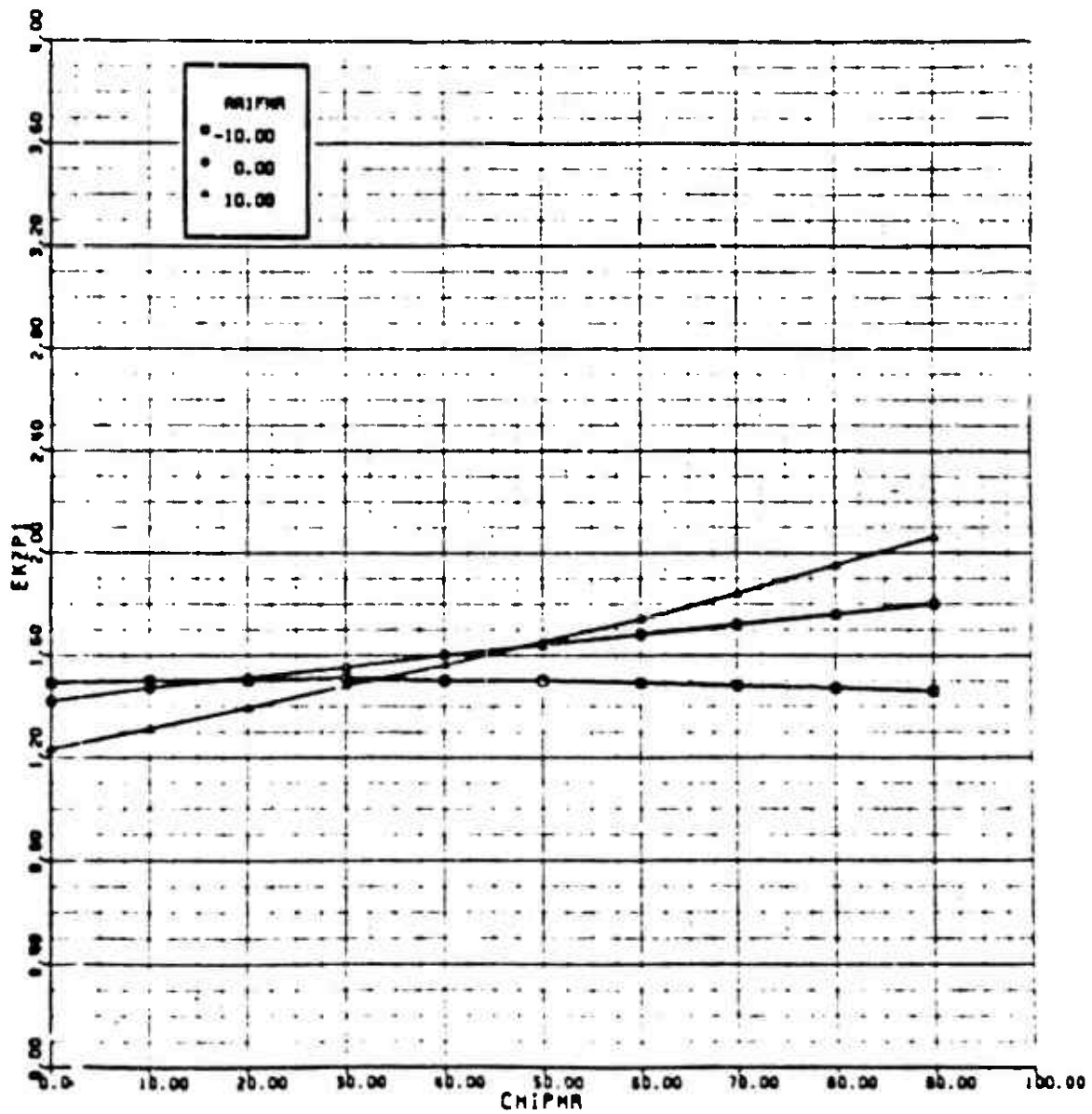


Figure E-21. OH-58A Main Rotor Downwash on Horizontal Stabilizer Map (z-direction)

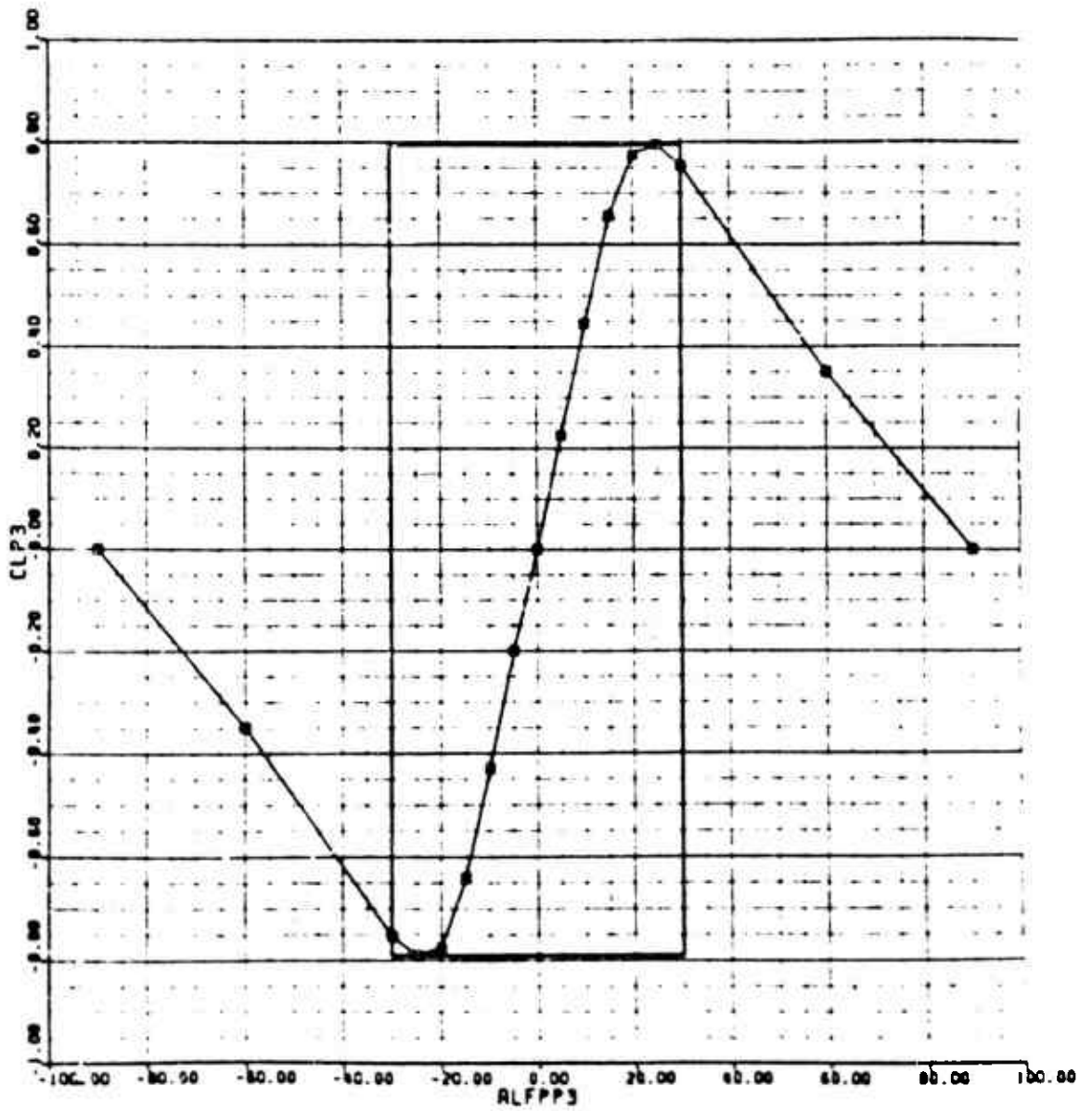


Figure E-22. OH-58A Vertical Stabilizer Lift Map

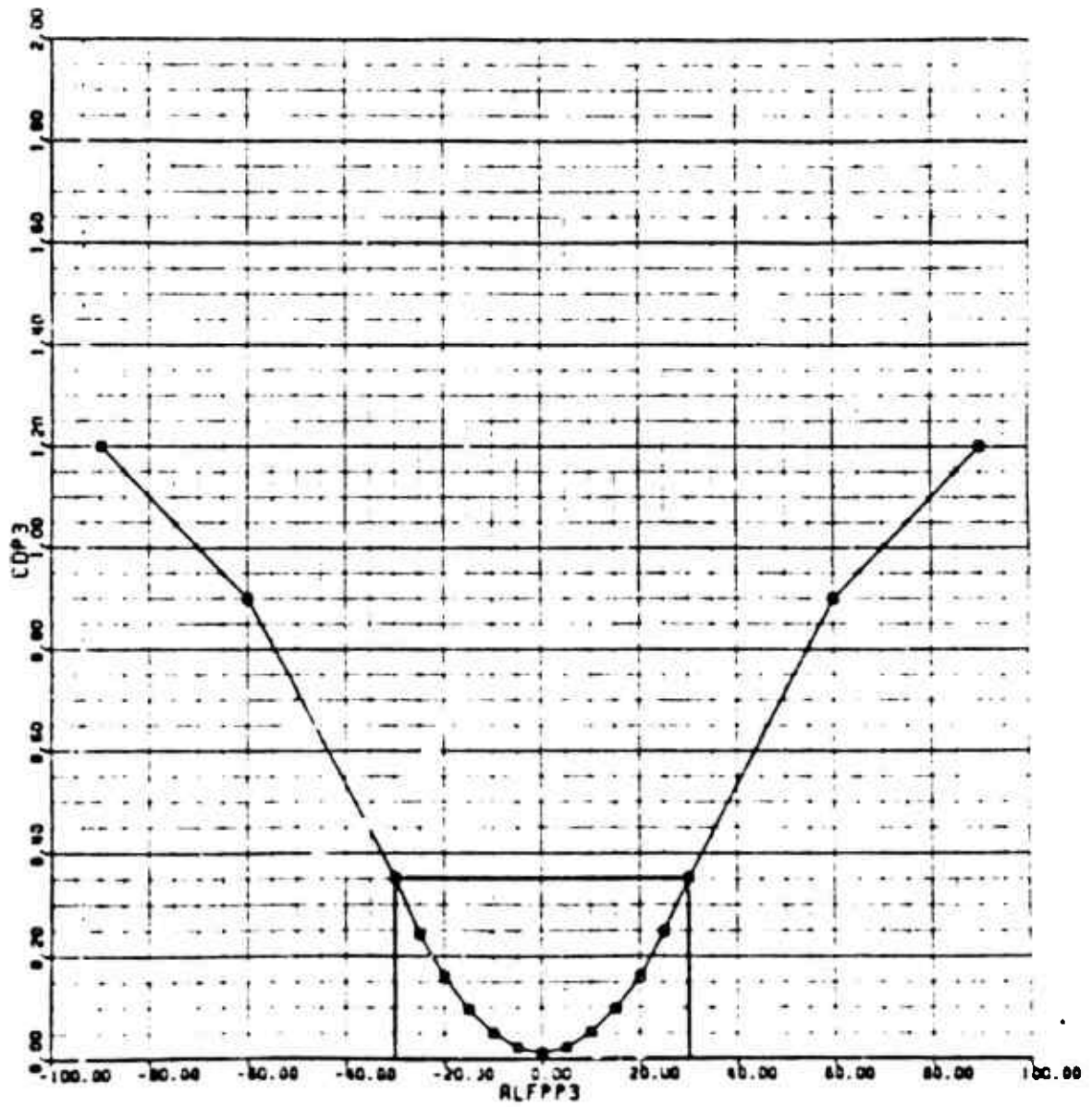


Figure E-23. OH-58A Vertical Stabilizer Drag Map

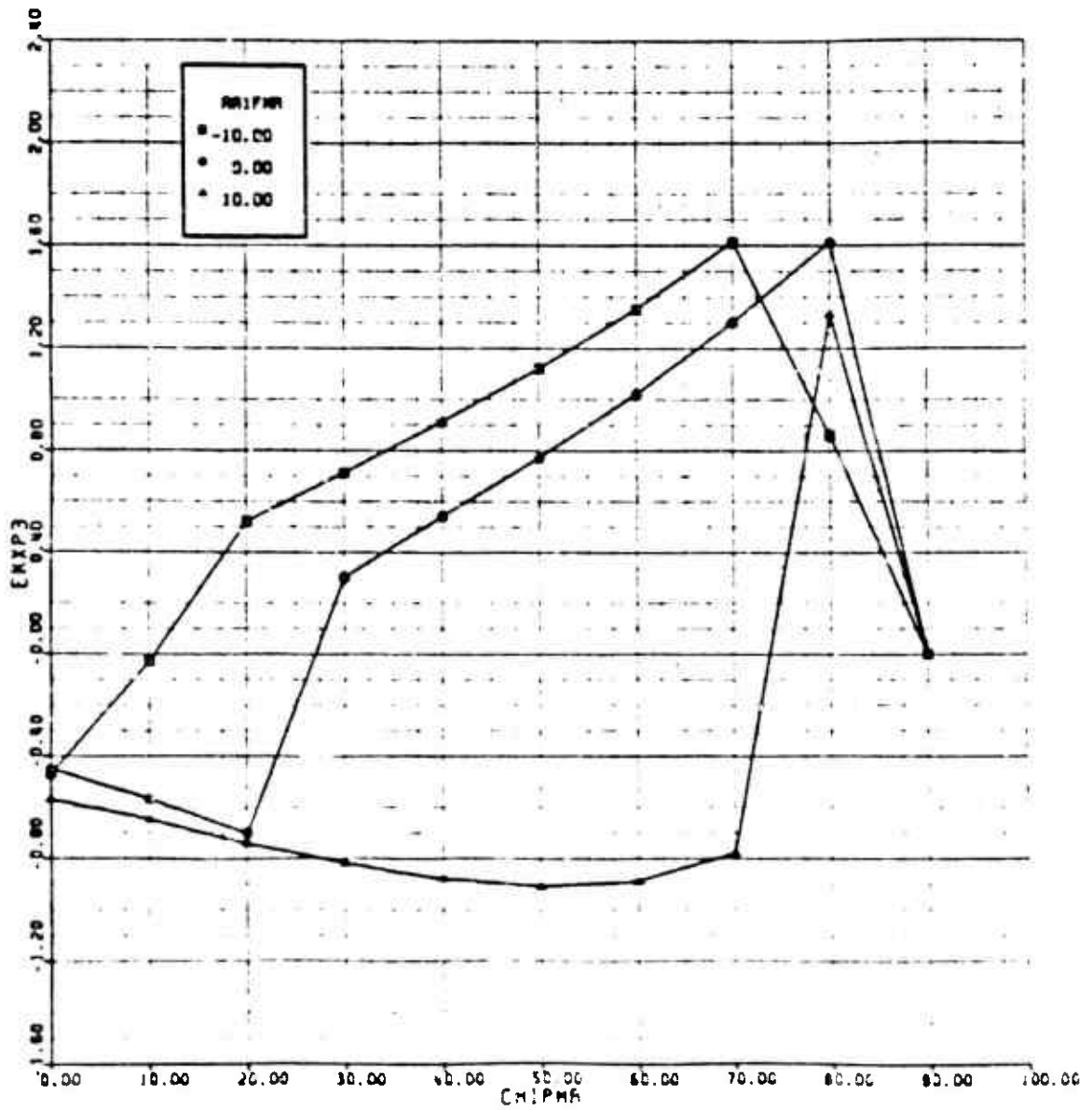


Figure E-24. UH-58A Main Rotor Downwash Vertical Stabilizer Map (x-direction)

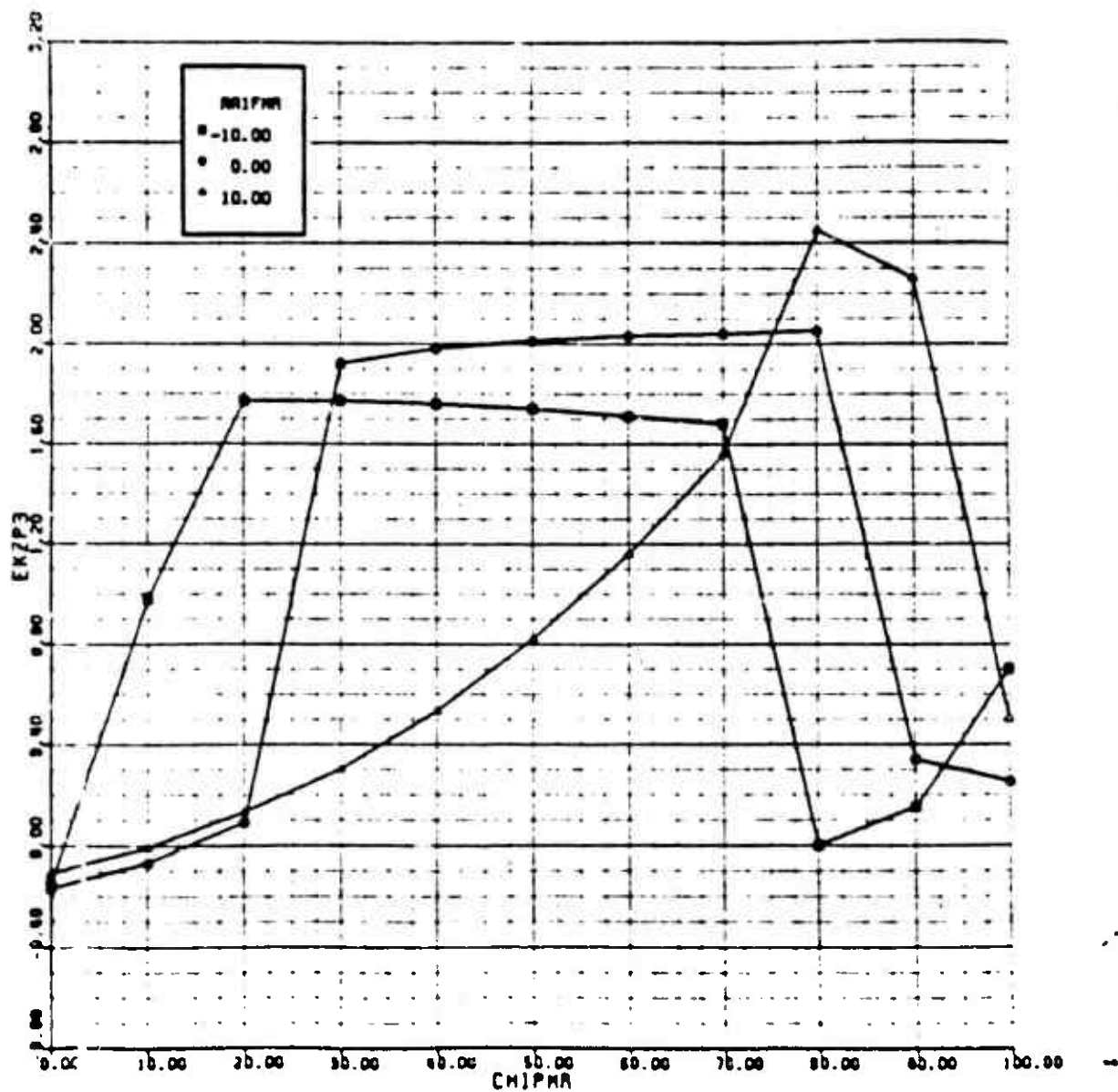


Figure E-25. OH-58A Main Rotor Downwash on Vertical Stabilizer Map (z-direction)

APPENDIX F

AH-1S MODEL DATA

The AH-1S Cobra (Figure F-1) is the latest version of this attack helicopter in service with the U.S. Army. The original Cobra was developed during Vietnam to provide a purpose-built ground attack aircraft. Since that time the design has been constantly upgraded and refined. Two basic versions exist. Single-engine variants using upgraded T53 engines for the U.S. Army and two-engine types for the U.S. Marine Corps. The AH-1S represents the current U.S. Army type and is fitted with a flat-plate canopy, an upgraded T53-L-703 engine, and new composite rotor blades built by Kaman Aerospace. The aircraft has improved avionics and systems over earlier versions. The Cobra has a maximum takeoff gross weight of 10,000 pounds, a rotor diameter of 44 feet, and is powered by a single Lycoming T53-L-703 turboshaft engine with an IRP of 1800 shp. However, the main gearbox is limited to 1290 shp.

The two-bladed main rotor is a classical Bell teetering design. The blades are built by Kaman Aerospace Corporation and are of composite construction with a multi-cell, ballistically tolerant spar. The chord is a constant 30 inches up to the 85 percent radius point where it has a linear taper to ten inches at the tip. Built-in twist is a linear ten degrees. A Boeing VR-7 airfoil is used over most of the blade transitioning to a VR-8 outboard. The AH-1S tail rotor is a two-bladed unit 8 feet 6 inches in diameter, mounted as a tractor. A 15.1-square-foot stabilizer is mounted in the middle of the tail boom and mechanically connected to the longitudinal stick.

The GenHel simulation model was created using the data from References 14 to 17. This model used the same corrected gimbal rotor file used for the OH-58A. Trim correlation data are shown in Figures F-2 to F-7. The flight test data were taken from Figure 26 of Reference 15. Test conditions were:

GW - 8120 pounds
FSCG - 193.9
Density Altitude - 2200 feet
Rotor Speed - 324 RPM

Overall, the correlation of GenHel to flight was very good. Longitudinal stick had a one-half inch forward bias and GenHel showed one-inch more pedal at 140 knots.

All of the numerical data used to model the AH-1S are provided in this appendix. The first section is a tabular listing of all the input data (Table F-1). The second section presents plots of the map data for fuselage, vertical tail, horizontal tail, and wing/stores support aerodynamics along with plots of the rotor interference and fuselage interference data (Figures F-8 to F-27). The tabular data are provided with appropriate labels. Map data are identified with GenHel variables provided in the List of Symbols.

For the AH-1S model, the panel allocation was as follows:

1. Horizontal tail
2. None
3. Vertical tail

TABLE F-1. AH-1S SPECIFIC FILE

```

***** INPUT PARAMETERS FOR MAIN ROTOR MODULES (#A) *****
***** DATA FROM C81 TO SUPPORT AH-1G AIRCRAFT USED FOR AH-1S ***

FSMR:: 200.00 ; FUSELAGE STATION, INCHES
WLMR:: 152.06 ; WATERLINE STATION, INCHES
BLMR:: 0.0 ; BUTTLINE STATION, INCHES (+IVE TO PORT)
RMR:: 22.00 ; RADIUS, FT.
OMGTMR:: 33.93 ; TRIM ROTATIONAL SPEED, RAD/SEC
BNR:: 2.0 ; ACTUAL NUMBER OF BLADES
ISMR:: 0.0 ; LONGITUDINAL SHAFT TILT, (POS. BACKWARDS), DEG
ILMR:: 0.0 ; LATERAL SHAFT TILT, (POS. STARBOARD), DEG
DELSMR:: 0.0 ; ** SHWASHPLATE PHASE ANGLE, DEG
DELJMR:: 0.0 ; FLAPPING HINGE OFFSET ANGLE, DEG.
KAF1MR:: 0.0 ; ** LAGGING HINGE OFFSET COEF. (FUNC(LG))
KAF2MR:: 0.0 ; ** LAGGING HINGE OFFSET COEF. (FUNC(LG**2))
CBDTMR:: 1.6 ; BLADE CHORD AT TIP, FT.
CBDRMR:: 3.09 ; BLADE CHORD AT ROOT, FT.
OPSTMR:: 0.0 ; ** HINGE OFFSET, FT.
SPRLMR:: 4.004 ; ** HINGE TO START OF BLADE, FT.
WIBDMR:: 475.6 ; WEIGHT OF ONE BLADE, LBS.
IBMP:: 1385.08 ; ** BLADE MOMENT OF INERTIA ABOUT HINGE, SLUG-FT**2
MBMP:: 100.55 ; ** BLADE MASS MOMENT ABOUT HINGE, SLUG-FT**2
IRMR:: 2750.4 ; ** ROTOR POLAR MOM OF INERTIA (LESS BLADES), SLUG-FT**2
BID0:: 2.75 ; ** PRECONE FOR GIMBAL ROTOR
BTLMR:: .57 ; BLADE TIP CUT OFF RATIO (C81 USES EQUATION FOR G)
DCDMR:: .002 ; DELTA DRAG COEF. FOR EACH SEGMENT
NBSMR:: 2 ; NUMBER OF BLADES SIMULATED, FIX POINT
NSSMR:: 5 ; NUMBER OF SEGMENTS SIMULATED, FIX POINT

TWMRMP: :UVR## ; ** MAIN ROTOR LINEAR TWIST MAP **
          XSEGM## ; MAP LOOK UP NAME
          TWSTMR## ; INPUT VARIABLE NAME
          TWMRLO ; OUTPUT VARIABLE NAME
          TWMRLO ; MAP NAME
          EXP 0.0, 1.0, .10 ; LOWER LIM, UPPER LIM, DELTA

TWMRLO: EXP 0.00, 0.00, -1.38, -2.38, -3.38
          EXP -4.38, -5.38, -6.38, -7.38, -8.38
          EXP -9.38

***** MAIN ROTOR DOWNWASH SUBMODULE (#A) *****

KCTR:: 1.0 ; TBRUST GAIN FOR UNIFORM DOWNWASH
KCMR:: 0.0 ; FITCH. MOM. GAIN FOR DOWNWASH SIN. HARMONIC
KSLMR:: 0.0 ; ROLL MOM. GAIN FOR DOWNWASH COS. HARMONIC
TDWOMR:: .01036 ; TIME CONST. FOR UNIFORM DOWNWASH FILTER, SEC
TDWCMR:: 0.0 ; TIME CONST. FOR DOWNWASH SIN. HARMON. FILTER, SEC.
TDWSMR:: 0.0 ; TIME CONST. FOR DOWNWASH COS. HARMON. FILTER, SEC.

***** INPUT PARAMETERS FOR FUSELAGE (#A) *****
***** MOUNTING POINT OF MODEL IN WIND TUNNEL *****

FSWF:: 199.3 ; FUSELAGE STATION, IN.
WLSWF:: 71.2 ; WATERLINE STATION, IN.
BLSWF:: 0.0 ; BUTTLINE STATION, IN. (+IVE TO PORT)
IWF:: 0.0 ; WING INCIDENCE, DEG.

LQFMP: :UVRUVR## ; ** FUSELAGE LIFT (TAIL-OFF) VS ALPWF MAP **
          ALPWF## ; MAP LOOK UP ROUTINE
          LQF## ; INPUT VARIABLE
          LQF## ; OUTPUT VARIABLE
          LQFLO ; LOW ANGLE MAP NAME
          EXP -20.0, 20.0, 2.0 ; LOWER LIM, UPPER LIM, DELTA
          LQFHI ; HIGH ANGLE MAP NAME

```

TABLE F-1. AH-1S SPECIFIC FILE (Cont'd)

```

EXP -100.0,100.0,20.0 ;LOWER LIM,UPPER LIM,DELTA

LQFLO: EXP ; LOW ANGLE MAP ALFWF -20 TO 20, DELTA = 2
        EXP -5.16, -4.91, -4.59, -4.19, -3.72
        EXP -3.18, -2.59, -1.96, -1.31, -0.65
        EXP 0.00, 0.62, 1.20, 1.72, 2.16
        EXP 2.52, 2.78, 2.94, 2.99, 2.95
        EXP 2.82

LQPHI: EXP ; HIGH ANGLE MAP ALFWF -100 TO 100, DELTA = 20
        EXP -0.70, -0.85, -2.35, -3.75, -5.16
        EXP 0.00, 2.82, 2.00, 1.20, 0.40
        EXP -0.45

DQFNP: UVRUVR## ;** FUSELAGE DRAG (TAIL-OFF) VS ALFWF **
        ALFWF## ;MAP LOOK UP ROUTINE
        DQF## ;INPUT VARIABLE
        DQFLO ;OUTPUT VARIABLE
        DQFLO ;LOW ANGLE MAP NAME
        EXP -20.0,20.0,2.0 ;LOWER LIM,UPPER LIM,DELTA
        DQPHI ;HIGH ANGLE MAP NAME
        EXP -100.0,100.0,20.0 ;LOWER LIM,UPPER LIM,DELTA

DQFLO: EXP ; LOW ANGLE MAP ALFWF -20 TO 20, DELTA = 2
        EXP 8.86, 8.16, 7.55, 7.01, 6.56
        EXP 6.18, 5.88, 5.67, 5.53, 5.48
        EXP 5.50, 5.60, 5.79, 5.05, 6.40
        EXP 6.82, 7.32, 7.91, 8.57, 9.32
        EXP 10.14

DQPHI: EXP ; HIGH ANGLE MAP ALFWF -100 TO 100, DELTA = 20
        EXP 102.30, 66.94, 39.58, 20.22, 8.86
        EXP 5.50, 10.14, 22.78, 43.42, 72.06
        EXP 108.70

MQFNP: UVRUVR## ;**FUSELAGE PITCH MOM (TAIL-OFF) VS ALFWF **
        ALFWF## ;MAP LOOK UP ROUTINE
        MQF## ;INPUT VARIABLE
        MQFLO ;OUTPUT VARIABLE
        MQFLO ;LOW ANGLE MAP NAME
        EXP -20.0,20.0,2.0 ;LOWER LIM,UPPER LIM,DELTA
        MQPHI ;HIGH ANGLE MAP NAME
        EXP -100.0,100.0,20.0 ;LOWER LIM,UPPER LIM,DELTA

MQFLO: EXP ; LOW ANGLE MAP ALPHA FROM -20 TO 20, DELTA = 2 DEG
        EXP -93.25, -90.63, -87.18, -82.92, -77.86
        EXP -72.05, -65.56, -58.50, -51.00, -43.18
        EXP -35.21, -27.23, -19.42, -11.91, -4.85
        EXP 1.63, 7.45, 12.51, 16.77, 20.21
        EXP 22.84

MQPHI: EXP ; HIGH ANGLE MAP ALPHA FROM -100 TO 100, DELTA = 20 DEG
        EXP 0.00, -48.00, -96.00, -100.00, -93.25
        EXP -35.21, 22.84, 30.00, 26.00, 10.00
        EXP -9.00

DLQFNP: BIV## ;**FUSELAGE DELTA LIFT (TAIL-OFF) VS PSIWF MAP**
        PSIWF## ;MAP LOOK UP ROUTINE
        ALFWF## ;INPUT VARIABLE #1
        ALFWF## ;INPUT VARIABLE #2
        DLQF## ;OUTPUT VARIABLE
        DLQFLO ;LOW ANGLE MAP NAME
        EXP -100.0,100.0,10.0,10.0,2.0 ;LOWER LIM,UPPER LIM,DELTA,#ITEMS
        EXP -10.0,10.0,20.0 ;LOWER LIM,UPPER LIM,DELTA - ALFWF

;PSIWF -100 TO 100 DEG FOR ALFWF -10,10 DEG

```


TABLE F-1. AH-1S SPECIFIC FILE (Cont'd)

```

;ALFWF = -10 DEG
DLQFLO: EXP 12.30, 11.07, 9.84, 8.61, 7.38
        EXP 6.15, 4.92, 3.69, 2.45, 1.23
        EXP 0.00, 1.23, 2.46, 3.69, 4.92
        EXP 6.15, 7.38, 8.61, 9.84, 11.07
        EXP 12.30

;ALFWF = 10 DEG
        EXP -10.35, -9.32, -8.28, -7.25, -6.21
        EXP -5.18, -4.14, -3.11, -2.07, -1.31
        EXP 0.00, -1.31, -2.07, -3.11, -4.14
        EXP -5.18, -6.21, -7.25, -8.28, -9.32
        EXP -10.35

; ** FUSELAGE DELTA DRAG VS PSIMF MAP **
DDQFMP: BIVBIV00 ;MAP LOOK UP ROUTINE
        PSIMF00 ;INPUT VARIABLE #1
        ALFWF00 ;INPUT VARIABLE #2
        DDQF00 ;OUTPUT VARIABLE
        DDQFLO ;LOW ANGLE MAP NAME
        EXP -20.0,20.0,2.0,"D21";LOWER LIM,UPPER LIM,DELTA,#ITEMS
        EXP -10.0,10.0,10.0 ;LOWER LIM,UPPER LIM,DELTA - ALFWF
        DDQFHI ;HIGH ANGLE MAP NAME
        EXP -100.0,100.0,20.0,"D11";LOWER LIM,UPPER LIM,DELTA,#ITEMS
        EXP -10.0,10.0,10.0 ;LOWER LIM,UPPER LIM,DELTA - ALFWF

;LOW ANGLE MAP PSIMF FROM -20 TO 20 DEG, DELTA = 2 DEG
;ALFWF= -10 DEG
DDQFLO: EXP 9.61, 7.84, 6.24, 4.81, 3.55
        EXP 2.47, 1.59, 0.89, 0.40, 0.10
        EXP 0.00, 0.10, 0.40, 0.89, 1.59
        EXP 2.47, 3.55, 4.81, 6.24, 7.84
        EXP 9.61

;ALFWF= 0 DEG
        EXP 11.52, 9.40, 7.48, 5.77, 4.26
        EXP 2.97, 1.91, 1.08, 0.48, 0.12
        EXP 0.00, 0.12, 0.48, 1.08, 1.91
        EXP 2.97, 4.26, 5.77, 7.48, 9.40
        EXP 11.52

;ALFWF= 10 DEG
        EXP 13.44, 10.97, 8.73, 6.72, 4.97
        EXP 3.46, 2.23, 1.26, 0.56, 0.14
        EXP 0.00, 0.14, 0.56, 1.26, 2.23
        EXP 3.46, 4.97, 6.72, 8.73, 10.97
        EXP 13.44

;HIGH ANGLE MAP PSIMF -100 TO 100 DEG, DELTA = 20 DEG
;ALFWF= -10 DEG
DDQFHI: EXP 79.68, 79.68, 61.61, 33.94, 9.61
        EXP 0.00, 9.61, 33.94, 61.61, 79.68
        EXP 79.68

;ALFWF= 0 DEG
        EXP 95.52, 95.52, 73.86, 40.69, 11.52
        EXP 0.00, 11.52, 40.69, 73.86, 95.52
        EXP 95.52

;ALFWF= 10 DEG
        EXP 111.36, 111.36, 86.11, 47.44, 13.44
        EXP 0.00, 13.44, 47.44, 86.11, 111.36
        EXP 111.36

; ** FUSELAGE SIDEFORCE VS PSIMF MAP **
YOFMP: : UVR00 ;MAP LOOK UP ROUTINE

```

TABLE F-1. AH-1S SPECIFIC FILE (Cont'd)

```

EXP      PSIMF##      ;INPUT VARIABLE
YQF##    ;OUTPUT VARIABLE
YQFLO    ;LOW ANGLE MAP NAME
EXP -100.0,100.0,10.0 ;LOWER LIM,UPPER LIM,DELTA

;LOW ANGLE MAP PSIMF -100 TO 100 DEG, DELTA = 10 DEG
YQFLO:  EXP      -12.00,  0.00,  -30.00,  -65.00,  -105.00
        EXP      -140.00, -175.00, -115.00, -65.00,  -25.00
        EXP       0.00,  28.00,   65.00,  115.00,  175.00
        EXP      140.00, 105.00,  65.00,  30.00,   0.00
        EXP       12.00

; ** FUSELAGE ROLLING MOMENT VS PSIMF MAP **
NQFMP:  UVR##      ;MAP LOOK UP ROUTINE
        PSIMF##    ;INPUT VARIABLE
        QF##      ;OUTPUT VARIABLE
        QFLO      ;LOW ANGLE MAP NAME
EXP -100.0,100.0,10.0 ;LOWER LIM,UPPER LIM,DELTA

;LOW ANGLE MAP PSIMF -100 TO 100 DEG, DELTA = 10 DEG
NQFLO:  EXP      -4.00,  0.00,  4.00,  7.00,  10.00
        EXP      10.60,  11.30,  9.40,  7.40,  4.00
        EXP       0.00,  -4.90,  -7.40,  -9.40,  -11.30
        EXP      -10.60, -10.00,  -7.00,  -4.00,  0.00
        EXP       4.00

; ** FUSELAGE YAWING MOMENT VS PSIMF **
NQFMP:  UVRUVR##  ;MAP LOOK UP ROUTINE
        PSIMF##    ;INPUT VARIABLE
        NQF##     ;OUTPUT VARIABLE
        NQFLO     ;LOW ANGLE MAP NAME
EXP -20.0,20.0,2.0 ;LOWER LIM,UPPER LIM,DELTA
        NQFHI     ;HIGH ANGLE MAP NAME
EXP-100.0,100.0,20.0 ;LOWER LIM,UPPER LIM,DELTA

;LOW ANGLE MAP PSIMF -20 TO 20, DELTA = 2 DEG
NQFLO:  EXP      -226.62, -222.22, -213.38, -199.97, -182.06
        EXP      -159.87, -133.80, -104.40, -72.35, -38.43
        EXP       -3.50,  31.55,  65.81,  98.44, 128.62
        EXP      155.66, 179.01, 198.23, 213.08, 223.46
        EXP      229.48

;HIGH ANGLE MAP PSIMF -100 TO 100, DELTA = 20 DEG
NQFHI:  EXP      155.66, -159.88, -196.92, -237.00, -226.62
        EXP       -3.50,  229.48,  240.00,  207.81,  155.67
        EXP      -159.87

;***** ROTOR INTERFERENCE ON THE FUSELAGE (MRPA) *****

; ** ROTOR X-FACTOR ON FUSELAGE MAP **
EXWFMP: UVR##     ;MAP ARGUMENT: LOOK UP ROUTINE
        CHIPR##   ;INPUT VARIABLE
        EXWF##    ;OUTPUT VARIABLE
        EXWFLO    ;LOW ANGLE MAP NAME
EXP -20.0,100.0,10.0 ;LOWER LIM,UPPER LIM,DELTA

EXWFLO: EXP      -0.15,  -0.04,  0.08,  0.20,  0.33
        EXP       0.46,  0.50,  0.74,  0.89,  1.00
        EXP       0.20,  -0.60,  -0.55

; ** ROTOR Z-FACTOR ON FUSELAGE MAP **
EZWFMP: UVR##     ;MAP LOOK UP ROUTINE
        CHIPR##   ;INPUT VARIABLE
        EZWF##    ;OUTPUT VARIABLE
        EZWFLO    ;LOW ANGLE MAP NAME
EXP -20.0,100.0,10.0 ;LOWER LIM,UPPER LIM,DELTA

```

TABLE F-1. AH-1S SPECIFIC FILE (Cont'd)

EZWFO: EXP 1.20, 1.21, 1.22, 1.23, 1.24
 EXP 1.25, 1.26, 1.27, 1.28, 1.29
 EXP 1.15, 1.00, 1.05

;***** INPUT PARAMETERS FOR PANEL #1 (RT HORIZONTAL) *****
 ;***** S=15.14 FT**2, AR= , e=.98

FSP1:: 397.5 ; FUSELAGE STATION, INCH
 WLP1:: 55.66 ; WATERLINE STATION, INCH
 BLP1:: 0.0 ; BUTTLINE STATION, INCH (+IVE TO PORT)
 SAPI:: 15.14 ; SURFACE AREA, FT**2
 GAMP1:: 0.0 ; PANEL ORIENTATION, DEG
 IOP1:: 6.97 ; PANEL INCIDENCE, DEG
 CPI:: 1.0 ; PANEL MEAN AERO CHORD, FT

;** HORIZONTAL STABILIZER LIFT VS ALFPP1 **
 CLPIMP::UVRUVR00 ;MAP LOOK UP ROUTINE
 ALFPP100 ;INPUT VARIABLE
 CLP100 ;OUTPUT VARIABLE
 CLP1LO ;LOW ANGLE MAP NAME
 EXP -30.0,30.0,2.0 ;LOWER LIM,UPPER LIM,DELTA
 CLP1HI ;HIGH ANGLE MAP NAME
 EXP -90.0,90.0,30.0 ;LOWER LIM,UPPER LIM,DELTA

;LOW ANGLE MAP ALFPP1 -32 TO 32, DELTA = 2 DEG
 CLP1LO: EXP -0.878, -0.920, -0.970, -1.020, -1.078
 EXP -1.135, -1.133, -1.095, -1.020, -0.915
 EXP -0.800, -0.695, -0.573, -0.460, -0.363
 EXP -0.265, -0.208, -0.150, -0.105, -0.060
 EXP -0.015, 0.030, 0.075, 0.120, 0.165
 EXP 0.210, 0.250, 0.290, 0.320, 0.345
 EXP 0.350

;HIGH ANGLE MAP ALFPP1 -90 TO 90, DELTA = 30 DEG
 CLP1HI: EXP 0.000, -0.440, -0.878, -0.265, -0.350
 EXP 0.160, 0.000

;** HORIZONTAL STABILIZER DRAG VS ALFPP1 **
 CDPIMP::UVRUVR00 ;MAP LOOK UP ROUTINE
 ALFPP100 ;INPUT VARIABLE
 CDP100 ;OUTPUT VARIABLE
 CDP1LO ;LOW ANGLE MAP NAME
 EXP -30.0,30.0,2.0 ;LOWER LIM,UPPER LIM,DELTA
 CDP1HI ;HIGH ANGLE MAP NAME
 EXP -90.0,90.0,30.0 ;LOWER LIM,UPPER LIM,DELTA

;LOW ANGLE MAP ALFPP1 -30 TO 30, DELTA = 2 DEG
 CDP1LO: EXP 0.603, 0.545, 0.493, 0.440, 0.389
 EXP 0.338, 0.289, 0.245, 0.202, 0.170
 EXP 0.147, 0.124, 0.113, 0.102, 0.094
 EXP 0.085, 0.081, 0.077, 0.077, 0.077
 EXP 0.064, 0.090, 0.107, 0.123, 0.149
 EXP 0.175, 0.212, 0.248, 0.293, 0.342
 EXP 0.402

;HIGH ANGLE MAP ALFPP1 -90 TO 90, DELTA = 30 DEG
 CDP1HI: EXP 1.200, 0.900, 0.603, 0.085, 0.402
 EXP 0.810, 1.200

;***** INPUT PARAMETER FOR ROTOR INTERFERENCE ON THE HORIZ.TAIL #1
 ;***** (MRPA)

;** ROTOR X-FACTOR ON HORIZONTAL TAIL **
 EXPIMP::BIV00 ;MAP LOOK UP ROUTINE
 EXP CRIPR00,ALFPR00 ;INPUT VAR01,INPUT VAR02

TABLE F-1. AH-1S SPECIFIC FILE (Cont'd)

```

EEXP100          ;OUTPUT VARIABLE
EXP10           ;MAP NAME
EXP 0.0,90.0,10.0,"D10 ;LOWER LIM,UPPER LIM,DELTA
EXP -10.0,10.0,10.0 ;LOWER LIM,UPPER LIM,DELTA

;CHIPMR 0 TO 90 DEG FOR AALPMR -10,0,10 DEG
;AALPMR = -10 DEG
EXP10: EXP      0.05, 0.19, 0.34, 0.50, 0.67
      EXP      0.86, 1.06, 1.29, 1.55, 1.85

;AALPMR = 0 DEG
EXP      -0.30, -0.18, -0.03, 0.13, 0.30
EXP      0.48, 0.69, 0.92, 1.18, 1.45

;AALPMR = 10 DEG
EXP      -0.66, -0.55, -0.42, -0.28, -0.12
EXP      0.05, 0.24, 0.47, 0.72, 1.00

EZP1MP::HIV00    ;** ROTOR 2-FACTOR ON HORIZONTAL TAIL MAP **
              ;MAP LOOK UP ROUTINE
CHIPMR00     ;INPUT VARIABLE #1
AALPMR00     ;INPUT VARIABLE #2
EKZP100     ;OUTPUT VARIABLE
EZP1LO      ;LOW ANGLE MAP NAME
EXP 0.0,90.0,10.0,"D10 ;LOWER LIM,UPPER LIM,DELTA,#ITEMS
EXP -10.0,10.0,10.0 ;LOWER LIM,UPPER LIM,DELTA AALPMR

;CHIPMR 0 TO 90 DEG FOR AALPMR -10,0,10 DEG
;AALPMR = -10 DEG
EZP1LO: EXP      1.58, 1.59, 1.60, 1.61, 1.62
      EXP      1.63, 1.63, 1.63, 1.62, 1.62

;AALPMR = 0 DEG
EXP      1.51, 1.56, 1.61, 1.66, 1.71
EXP      1.76, 1.81, 1.87, 1.94, 1.98

;AALPMR = 10 DEG
EXP      1.32, 1.41, 1.51, 1.60, 1.70
EXP      1.80, 1.90, 2.01, 2.13, 2.26

;***** FUSELAGE INTERPERNCE ON THE HORIZ.TAIL (MPPA) *****

QP1MP:: CONST00 ;** HORIZONTAL TAIL DYNAMIC PRESSURE RATIO MAP**
      (1.0)      ;MAP LOOK UP ROUTINE
QP1QMP00     ;OUTPUT VARIABLE

;***** INPUT PARAMETERS FOR PANEL #3 (VERTICAL TAIL) *****
;*****      8-18.87 FT**2, AR=1.62, e=-.99      *****

PS3:: 501.113 ; FUSELAGE STATION, INCHES
WLP3:: 97.18 ; WATERLINE STATION, INCHES
BLP3:: 0.0 ; BUTTLINE STATION, INCH (+IVE TO PORT)
SAP3:: 18.87 ; SURFACE AREA, FT**2
GAMP3:: -90.0 ; PANEL ORIENTATION, DEG
IOP3:: 4.5 ; PANEL INCIDENCE, DEG
CP3:: 1.0 ; PANEL MEAN AERO CHORD, FT

CLP3MP::UVRUVR00 ;** VERTICAL STABILIZER LIFT VS ALPPP3 MAP **
      ;MAP LOOK UP ROUTINE
ALPPP300     ;INPUT VARIABLE
CLP300      ;OUTPUT VARIABLE
CLP3LO      ;LOW ANGLE MAP NAME
EXP -30.0,70.0,2.0 ;LOWER LIM,UPPER LIM,DELTA
CLP3HI      ;HIGH ANGLE MAP NAME
EXP -90.0,90.0,30.0 ;LOWER LIM,UPPER LIM,DELTA

```

TABLE F-1. AH-1S SPECIFIC FILE (Cont'd)

```

;LOW ANGLE MAP ALPPP3 -30 TO 30, DELTA = 2 DEG
CLP3LO: EXP -0.750, -0.775, -0.790, -0.800, -0.790
        EXP -0.775, -0.735, -0.690, -0.620, -0.525
        EXP -0.450, -0.355, -0.260, -0.175, -0.085
        EXP 0.000, 0.085, 0.175, 0.260, 0.355
        EXP 0.450, 0.525, 0.620, 0.690, 0.735
        EXP 0.775, 0.790, 0.800, 0.790, 0.775
        EXP 0.750
    
```

```

;HIGH ANGLE MAP ALPPP3 -90 TO 90, DELTA = 30 DEG
CLP3HI: EXP 0.000, -0.380, -0.750, 0.000, 0.750
        EXP 0.380, 0.000
    
```

```

; ** VERTICAL STABILIZER DRAG VS ALPPP3 **
CDF3MP: :UVRUVR00 ;MAP LOOK UP ROUTINE
        ALPPP300 ;INPUT VARIABLE
        CDF300 ;OUTPUT VARIABLE
        CDF3LO ;LOW ANGLE MAP NAME
        EXP -30.0,30.0,2.0 ;LOWER LIM,UPPER LIM,DELTA
        CDF3HI ;HIGH ANGLE MAP NAME
        EXP -90.0,90.0,30.0 ;LOWER LIM,UPPER LIM,DELTA
    
```

```

;LOW ANGLE MAP ALPPP3 -30 TO 30, DELTA = 2 DEG
CDF3LO: EXP 0.360, 0.303, 0.265, 0.225, 0.190
        EXP 0.160, 0.135, 0.108, 0.090, 0.067
        EXP 0.051, 0.036, 0.026, 0.017, 0.013
        EXP 0.012, 0.013, 0.017, 0.026, 0.036
        EXP 0.051, 0.067, 0.090, 0.108, 0.135
        EXP 0.160, 0.190, 0.225, 0.265, 0.303
        EXP 0.360
    
```

```

;LOW ANGLE MAP ALPPP3 -90 TO 90, DELTA = 30 DEG
CDF3HI: EXP 1.200, 0.785, 0.360, 0.012, 0.360
        EXP 0.785, 1.200
    
```

***** ROTOR INTERFERENCE ON THE VERTICAL TAIL #1 (MRPA) *****

```

; ** ROTOR X-FACTOR ON VERTICAL TAIL MAP **
EXP3MP: :BIV00 ;MAP ARGUMENT:LOOK UP ROUTINE
        EXP CHIPMR00,AAIPMR00 ;INPUT VARIABLE #1, INPUT VARIABLE #2
        ERXP300 ;OUTPUT VARIABLE
        EXP3 ;LOW ANGLE MAP NAME
        EXP 0.0,90.0,10.0,"D10 ;LOWER LIM,UPPER LIM,DELTA,#ITEMS
        EXP -10.0,10.0,10.0 ;LOWER LIM,UPPER LIM,DELTA - AAIPMR
    
```

```

;CHIPMR 0 TO 90 FOR AAIPMR -10,0,10 DEG
;AAIPMR = -10 DEG
EXP3: EXP -0.39, -0.50, -0.52, 0.54, 0.76
        EXP 0.99, 1.23, 1.50, 0.75, 0.00
    
```

```

;AAIPMR = 0 DEG
EXP -0.47, -0.55, -0.64, -0.73, -0.80
EXP -0.84, 0.93, 1.20, 1.52, 0.00
    
```

```

;AAIPMR = 10 DEG
EXP -0.49, -0.54, -0.59, -0.64, -0.68
EXP -0.70, -0.70, -0.65, -0.52, 0.00
    
```

```

; ** ROTOR Z-FACTOR ON VERTICAL TAIL MAP **
EXP3MP: :BIV00 ;MAP ARGUMENT:LOOK UP ROUTINE
        EXP CHIPMR00,AAIPMR00 ;INPUT VARIABLE #1, INPUT VARIABLE #2
        ERXP300 ;OUTPUT VARIABLE
        EXP3LO ;LOW ANGLE MAP NAME
        EXP 0.0,90.0,10.0,"D10 ;LOWER LIM,UPPER LIM,DELTA,#ITEMS
    
```

TABLE F-1. AH-1S SPECIFIC FILE (Cont'd)

```

EXP -10.0,10.0,10.0 ;LOWER LIM,UPPER LIM,DELTA AALFMR

;CHIPMR 0 TO 90 DEG FOR AALFMR -10,0,10 DEG
;AALFMR = -10 DEG
EZP3LO: EXP -0.13, -0.03, 0.13, 1.87, 1.89
EXP 1.89, 1.89, 1.87, 1.94, 2.00

;AALFMR = 0 DEG
EXP -0.10, -0.01, 0.12, 0.29, 0.53
EXP 0.83, 2.20, 2.22, 2.24, 2.00

;AALFMR = 10 DEG
EXP 0.00, 0.07, 0.18, 0.31, 0.48
EXP 0.69, 0.95, 1.27, 1.65, 2.00

;***** FUSELAGE INTERFERENCE ON THE VERTICAL TAIL (WPPA) *****

QP3MP::CONST00 ;** VERTICAL TAIL DYNAMIC PRESSURE RATIO MAP **
EXP [1.0] ;MAP LOOK UP ROUTINE
QP3QWF00 ;INPUT VARIABLE
;OUTPUT VARIABLE

EPP3MP::CONST00 ;** BODY DOWNWASH ON VERTICAL TAIL MAP **
EPSP100 ;MAP LOOK UP ROUTINE
EPSP300 ;INPUT VARIABLE
;OUTPUT VARIABLE

SGP3MP::CDNST00 ;** HEDDY SIDEWASH DN VERTICAL TAIL MAP **
SIGP100 ;MAP LOOK UP ROUTINE
SIGP300 ;INPUT VARIABLE
;OUTPUT VARIABLE

;***** INPUT PARAMETERS FOR PANEL 00 (0A) *****

FSP4:: 189.73 ; FUSELAGE STATION,INCR
WLP4:: 63.28 ; WATERLINE STATION,INCH
BLP4:: 0.0 ; HUTLINE STATION,INCH (+IVE TO PORT)
SAP4:: 28.15 ; SURFACE AREA OF PANEL IF NOT INCLUDE IN MAP
GAMP4:: 0.0 ; PANEL ORIENTATION, DEG
IOP0:: 17.0 ; PANEL INCIDENCE,DEG
CP0:: 2.7 ; PANEL REAR AERO CHDRD,PT

; ** AH-1S WING LIFT COEFFICIENT VS ALPPP0
; ** S=30.95 FT**2,ASPECT RATIO=4.6,0023 ROOT,0420 TIP AIRFDIL
CLP4MP::UVRUVR00 ;MAP LOOK UP ROUTINE
ALPPP400 ;INPUT VARIABLE
CLP400 ;OUTPUT VARIABLE
CLP0LO ;LOW ANGLE MAP NAME
EXI -20 0,20.0,2.0 ;LOWER LIM,UPPER LIM,DELTA
CLP4HI ;HIGH ANGLE MAP NAME
EXP -90.0,90.0,10.0 ;LOWER LIM,UPPER LIM,DELTA

; LOW ANGLE MAP ALPPP4 -20 TO 20. DELTA = 2 DEG
CLP4LD: EXP -1.10, -1.16, -1.10, -1.20, -1.13
EXP -1.30, -0.85, -0.70, -0.55, -0.35
EXP -0.15, 0.05, 0.25, 0.45, 0.60
EXP 0.75, 0.90, 1.00, 0.98, 0.95
EXP 0.92

; HIGH ANGLE MAP ALPPP0 -90 TO 90 ,DELTA = 10 DEG
CLP0HI: EXP 0.00, -0.16, -0.31, -0.07, -0.63
EXP -0.79, -0.94, -1.10, -1.00, 0.15
EXP 0.75, 0.92, 0.79, 0.60, 0.53
EXP 0.39, 0.26, 0.13, 0.00

; ** AH-1S WING DRAG VS ALPPP0

```

TABLE F-1 AH-1S SPECIFIC FILE (Cont'd)

```

CDP4MP::UVRUVR00 ;MAP LOOK UP ROUTINE
          ALRPP400 ;INPUT VARIABLE
          CDP400 ;OUTPUT VARIABLE
          CDP4LO ;LOW ANGLE MAP NAME
EXP -20.0,20.0,2.0 ;LOWER LIM,UPPER LIM,DELTA
          CDP4HI ;HIGH ANGLE MAP NAME
EXP -90.0,90.0,10.0 ;LOWER LIM,UPPER LIM,DELTA

; LOW ANGLE MAP ALPPP4 -20 TO 20, DELTA = 2 DEG
CDP4LO: EXP 0.164, 0.134, 0.105, 0.075, 0.050
EXP 0.016, 0.013, 0.011, 0.010, 0.009
EXP 0.008, 0.008, 0.009, 0.010, 0.011
EXP 0.012, 0.015, 0.019, 0.050, 0.081
EXP 0.112

; HIGH ANGLE MAP ALPPP4 -90 TO 90, DELTA = 10 DEG
CDP4HI: EXP 1.200, 1.052, 0.904, 0.756 0.608
EXP 0.460, 0.312, 0.164, 0.010, 0.008
EXP 0.012, 0.112, 0.268, 0.123, 0.378
EXP 0.734, 0.889, 1.045, 1.200

;***** INPUT PARAMETERS FOR ROTOR INTERFERENCE ON WING (MPPA) *****
; ** AH-1S FORE/AFT M.R. DOWNWASH AT WING
EXP4MP::CONST00 ;MAP LOOK UP ROUTINE
          EKXWF00 ;INPUT VARIABLE
          EKXP400 ;OUTPUT VARIABLE

; ** AH-1S VERTICAL M.R. DOWNWASH AT WING
EVP4MP::CONST00 ;MAP LOOK UP ROUTINE
          ERZWF00 ;INPUT VARIABLE
          ERZP400 ;OUTPUT VARIABLE

;***** FUSELAGE INTERFERENCE ON WING (WPPA) *****
; ** AH-1S DYNAMIC PRESSURE RATIO AT WING VS ALPWF
QR4MP::CONST00 ;MAP LOOK UP ROUTINE
          [1.0]
          QP4QWF00 ;OUTPUT VARIABLE

;***** INPUT PARAMETERS FOR TAIL ROTOR (RA) - (BAILEY) *****
RTR:: 4.25 ;RADIUS,FT
OMEGTR::175.64 ;TRIM ROTATIONAL RATE,RAD/SEC
BTR:: 2.0 ;ACTUAL NUMBER OF BLADES
RSTR:: 520.67 ;FUSELAGE STATION,IN
WLTR:: 118.27 ;WATERLINE STATION,IN
BLTR:: 14.10 ;BUTTLINE STATION,IN (+IVE TO PORT)
TWSTR::0.0 ;BLADE TWIST,DATUM CENTER OF ROTATION,DEG
BIATR::0.0 ;BLADE RITCH CORRECTION FOR N.L.TWIST(NEG REDUCES PITCH)
GAMTR::-90.0 ;TAIL ROTOR CANT ANGLE,DEG
DFL3TR::0.0 ;FLARRING HINGE OFFSET ANGLE,DEG
DZL3TR::0.0 ;RATE OF CHANGE OF CONE ANGLE WITH THRUST,DEG/LB
CHRDR::.70 ;BLADE CHORD,FT
ATR:: 6.13 ;BLADE LIFT CURVE SLORE,1/RAD
BTLCR:: .975 ;BLADE TIP LOSS FACTOR (C31 USES EQN FOR G)
CDTR:: 2.0 ;TAIL ROTOR HEAD DRAG,FT**2

;***** ROTOR INTERFERENCE ON TAIL ROTOR (MRPA) *****
; ** ROTOR X-FACTOR ON TAIL ROTOR MAP **
EXTRR::CONST00 ;MAP LOOK UP ROUTINE
          EFXP300 ;INPUT VARIABLE
          EKXTR00 ;OUTPUT VARIABLE

; ** ROTOR Y-FACTOR ON TAIL ROTOR MAP **

```

TABLE F-1. AH-1S SPECIFIC FILES (Cont'd)

```

EZTRMP::CONST00      ;MAP LOOK UP ROUTINE
                  EKZP300      ;INPUT VARIABLE
                  EKZTR00      ;OUTPUT VARIABLE

;***** FUSELAGE INTERFERENCE ON THE TAIL ROTOR (WFFA) *****

QTRMP:: CONST00      ;** TAIL ROTOR DYNAMIC PRESSURE RATIO MAP **
                  ;MAP LOOK UP ROUTINE
                  QP3QW0      ;INPUT VARIABLE
                  QTRQW00     ;OUTPUT VARIABLE

EPTTRMP::CONST00     ;** BODY DOWNWASH ON TAIL ROTOR MAP **
                  ;MAP LOOK UP ROUTINE
                  EPSP100     ;INPUT VARIABLE
                  EPSTR00     ;OUTPUT VARIABLE

EGTRMP::CONST00     ;** BODY SIDEWASH ON TAIL ROTOR MAP **
                  ;MAP LOOK UP ROUTINE
                  SIGP100     ;INPUT VARIABLE
                  SIGTR00     ;OUTPUT VARIABLE

;***** VERTICAL TAIL INTERFERENCE ON TAIL ROTOR INFLOW *****

VBVTTR::30.0        ; AIRSPEED BREAK PT. - NO BLOCKAGE ABOVE,KT.
KBVTTR::.895        ; TAIL ROTOR BLOCKAGE COEF. AT HOVER

;***** INPUT PARAMETERS FOR EQUATIONS OF MOTION (#B) *****

PSCG:: 200.6        ; FUSELAGE STATION,OF C.G.,INCH
WLCG:: 68.0         ; WATERLINE STATION OF C.G.,INCH
BLCC:: 0.0          ; BUTLINE STATION OF C.G.,INCH (+IVE TO PORT)

WEIGHT:: 9000.0     ; AIRCRAFT GROSS WEIGHT,LBS.
IX:: 2904.0         ; INERTIA ABOUT BODY X-AXIS,SLUG-FT**2
IY:: 11883.4        ; INERTIA ABOUT BODY Y-AXIS,SLUG-FT**2
II:: 10233.5        ; INERTIA ABOUT BODY Z-AXIS,SLUG-FT**2
IXZ:: -585.0        ; CROSS COUPLING INERTIA,SLUG-FT**2
IYZ:: 0.0
IXY:: 0.0
    
```

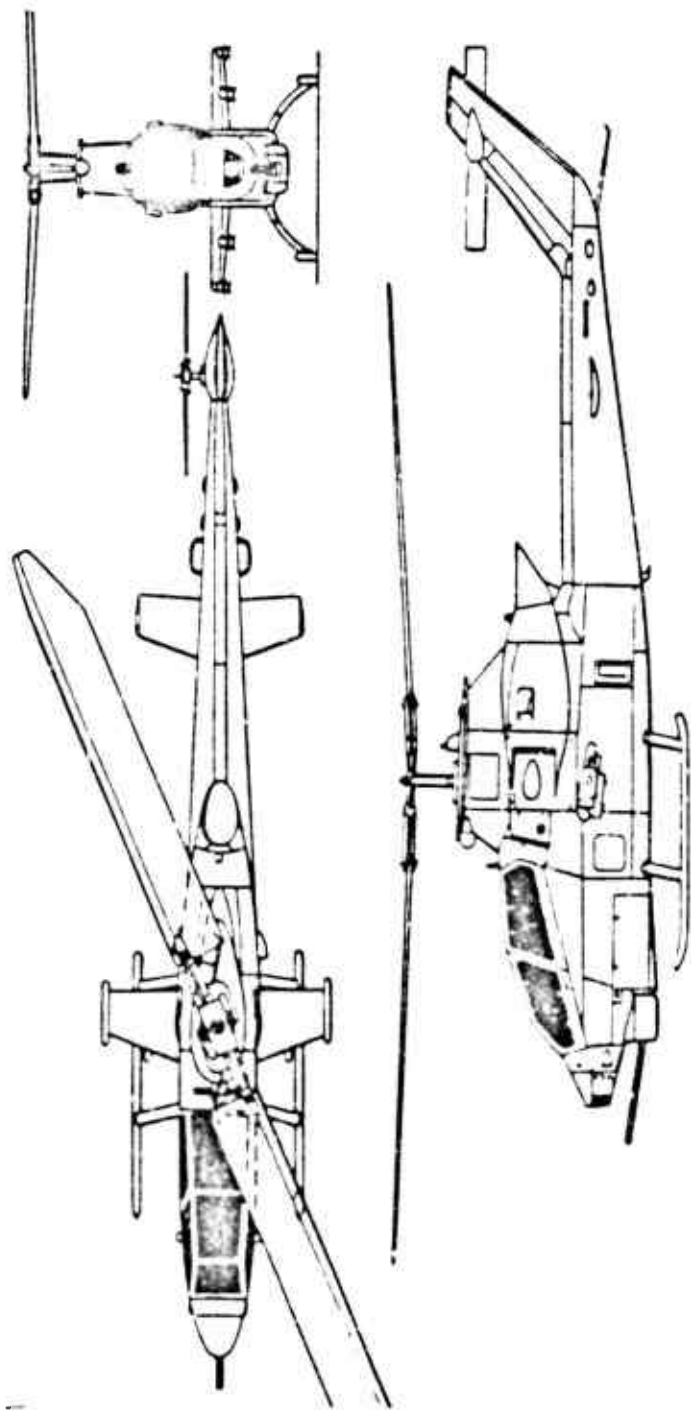



Figure P-1. AH-13 Three-View Drawing

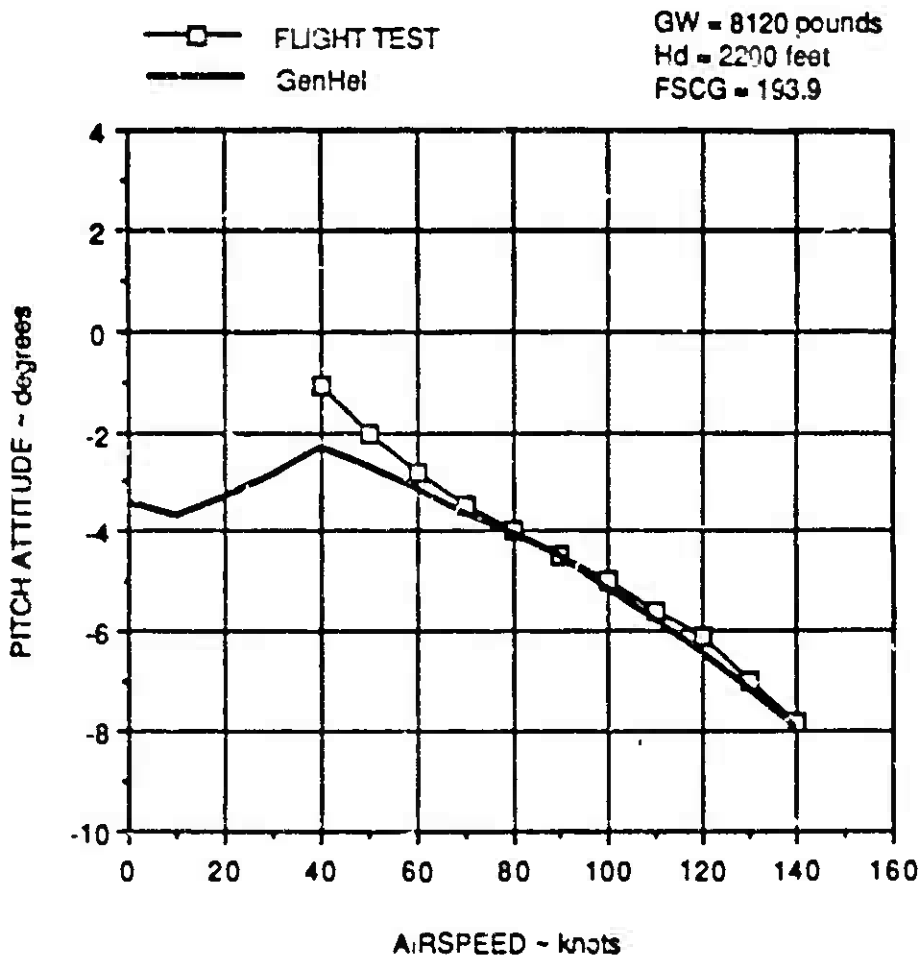


Figure F-2. AH-15 Pitch Attitude Correlation

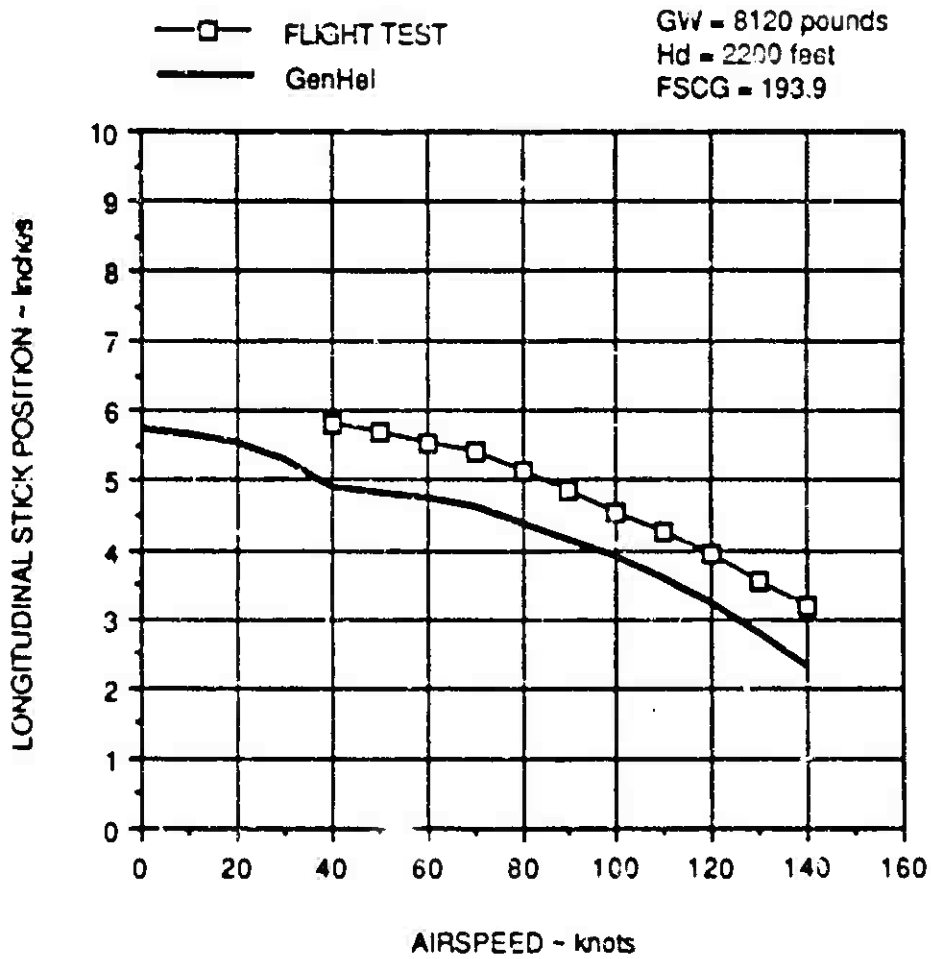


Figure F-3. AH-1S Longitudinal Stick Correlation

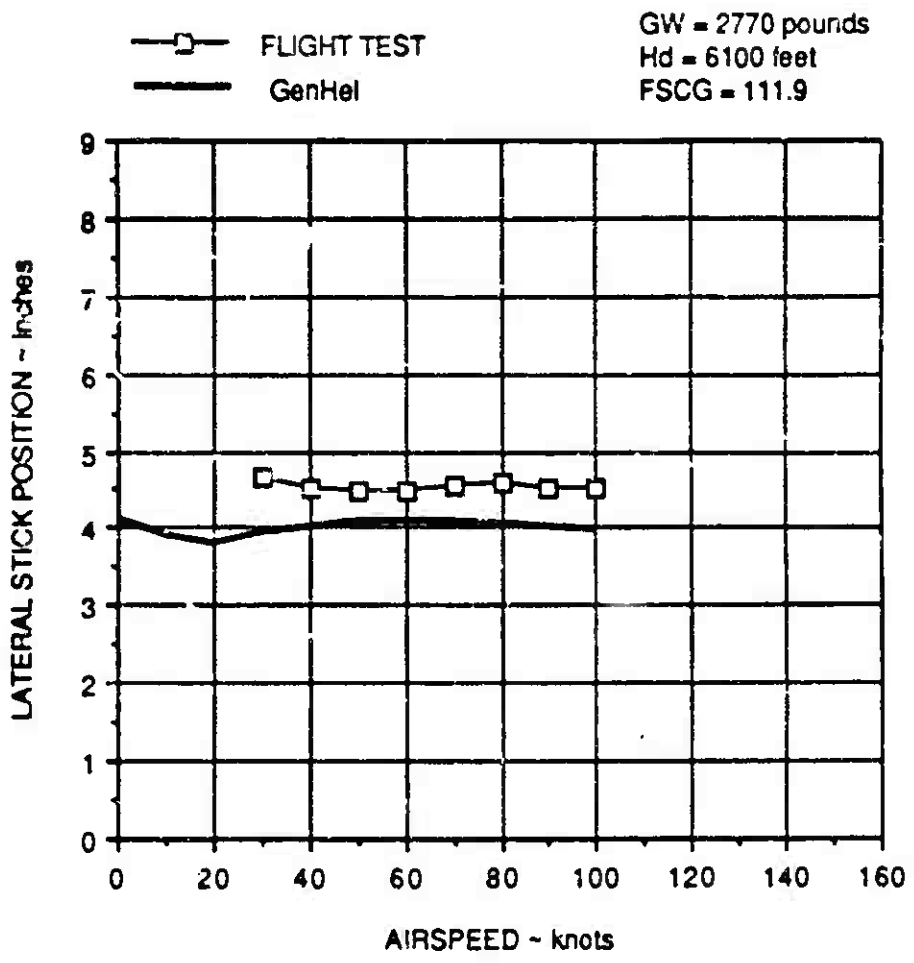


Figure F-4. AH-1S Lateral Stick Correlation

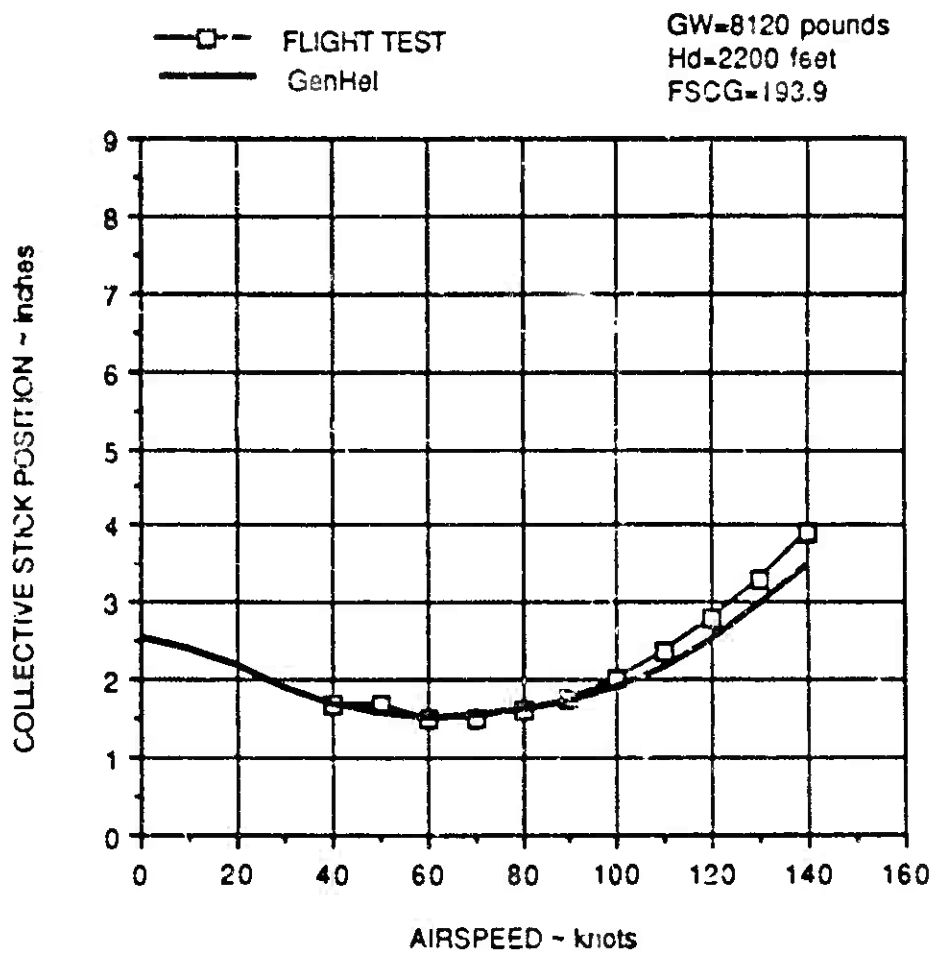


Figure F-5. AH-1S Collective Stick Correlation

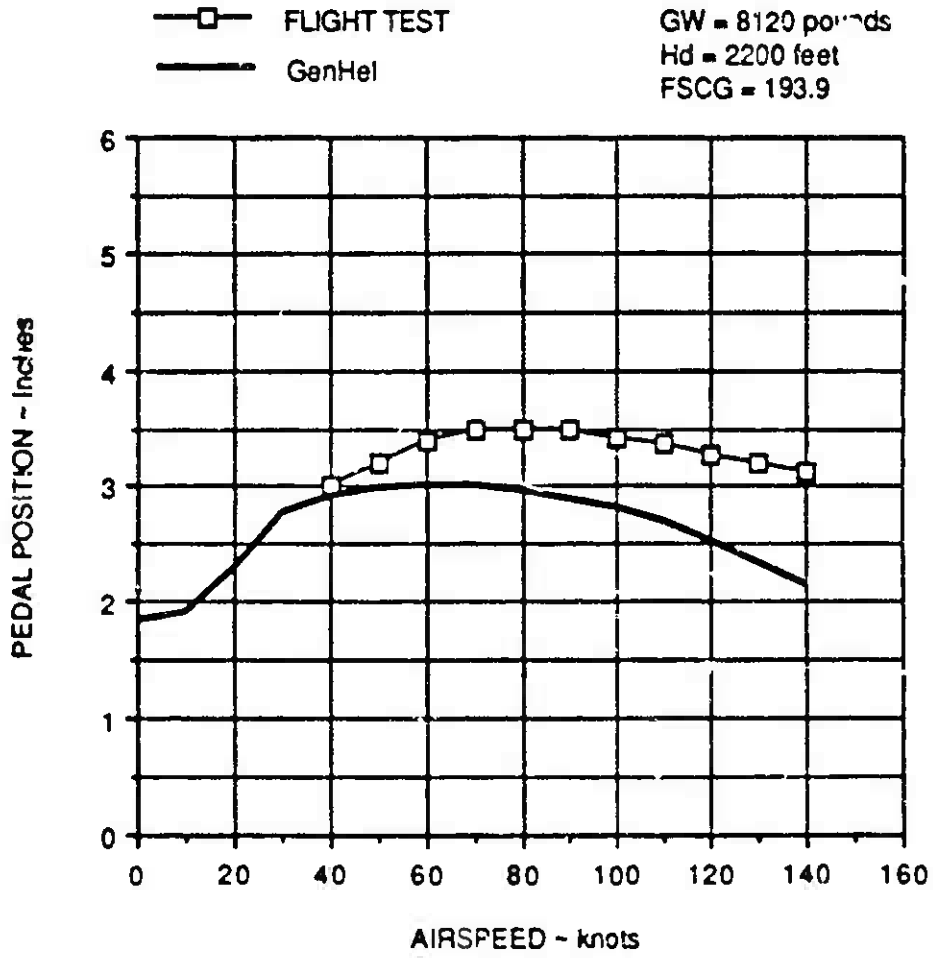


Figure F-6. AH-1S Pedal Correlation

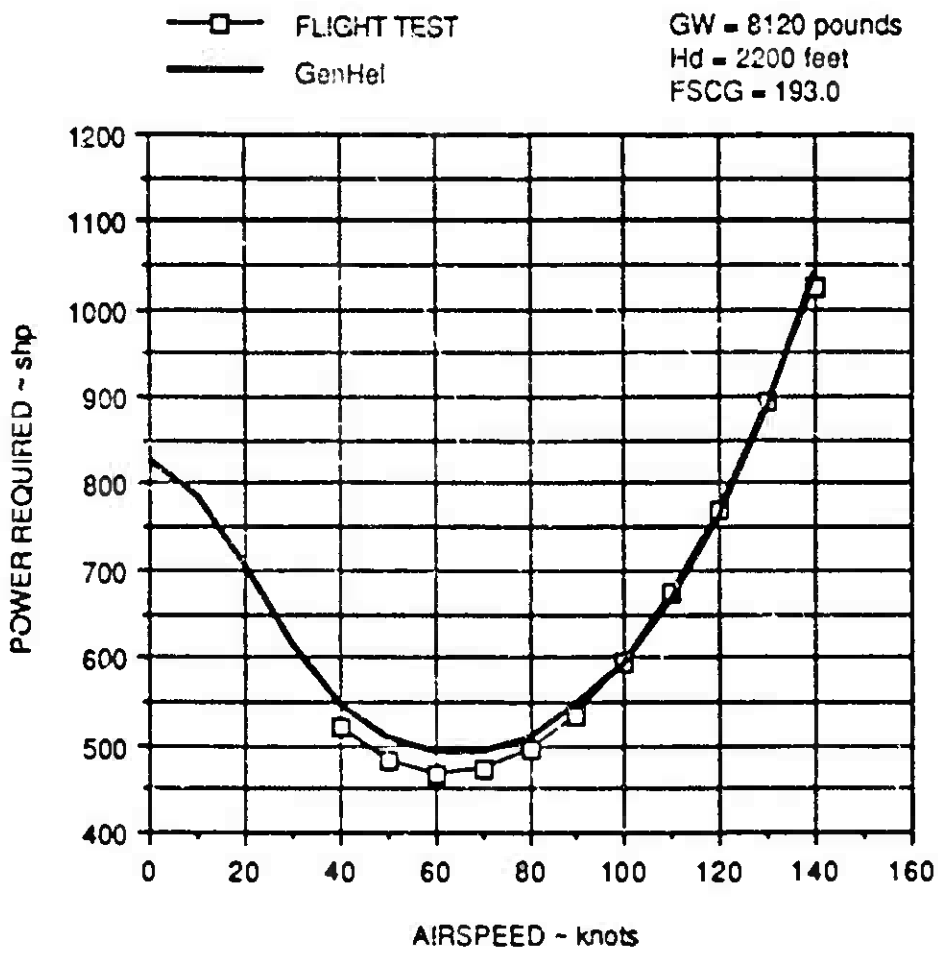


Figure -7. AH-1S Power Required Correlation

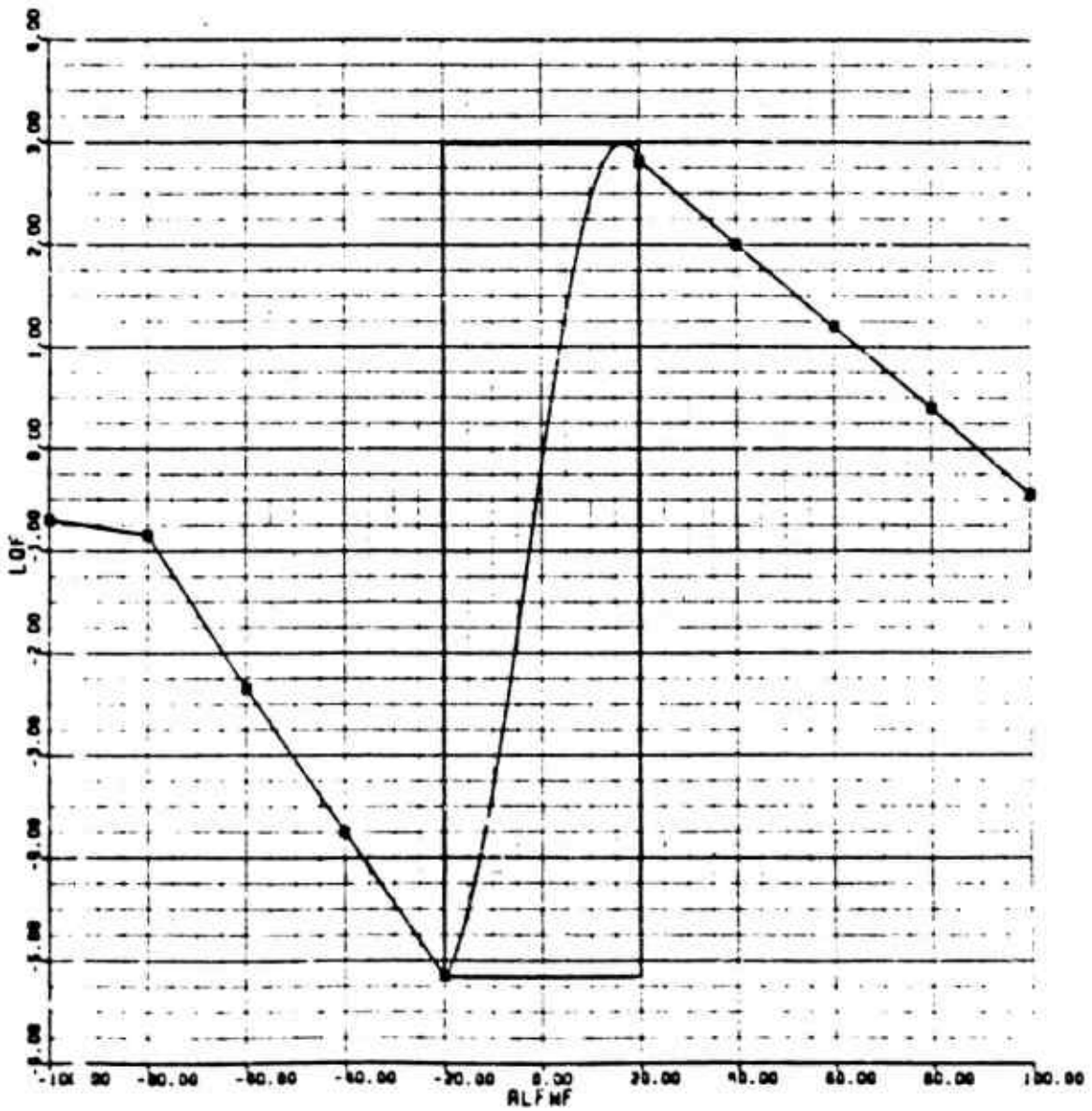


Figure F-8. AH-1S Fuselage Lift Map

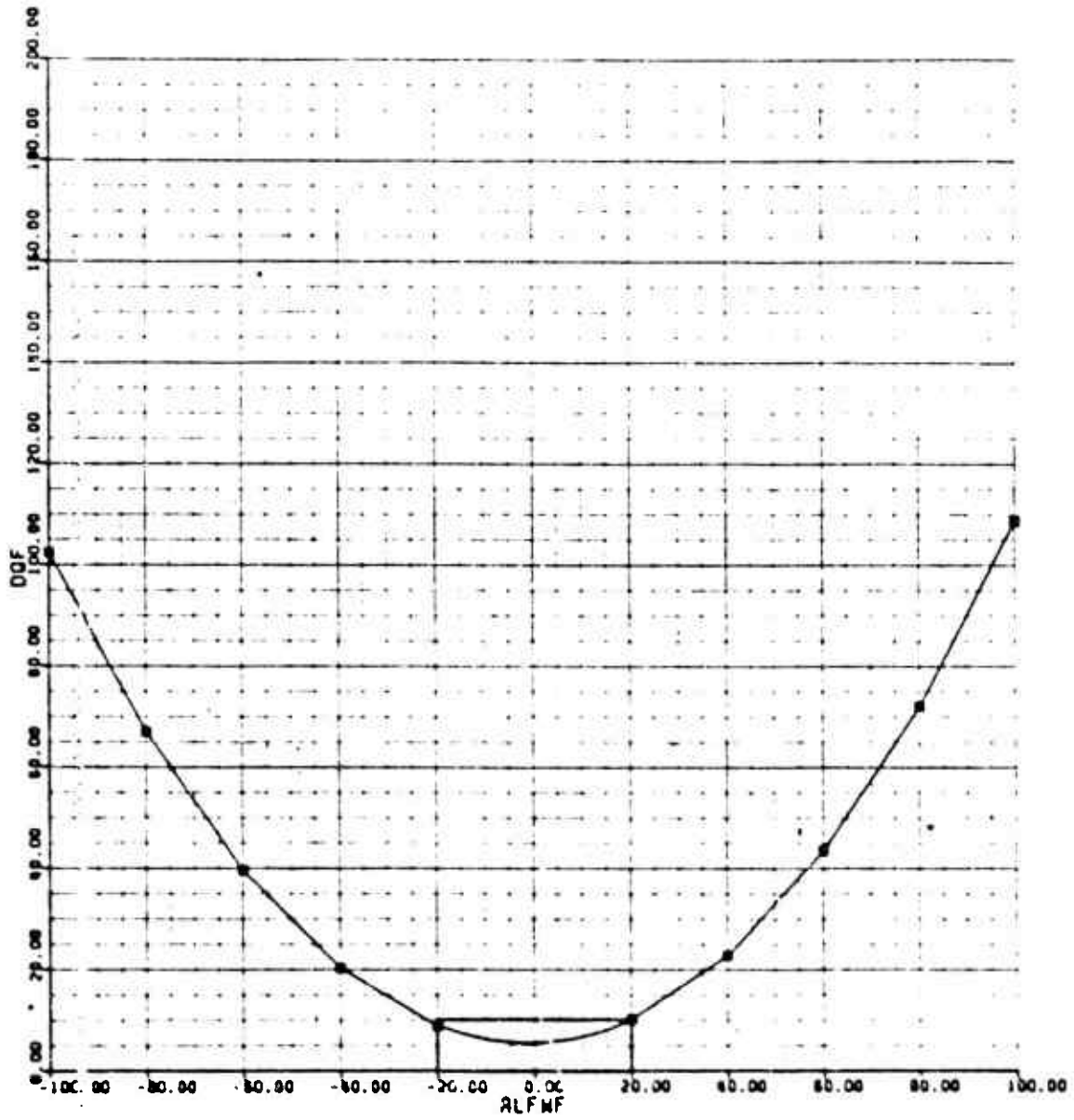


Figure F-9. AH-1S Fuselage Drag Map

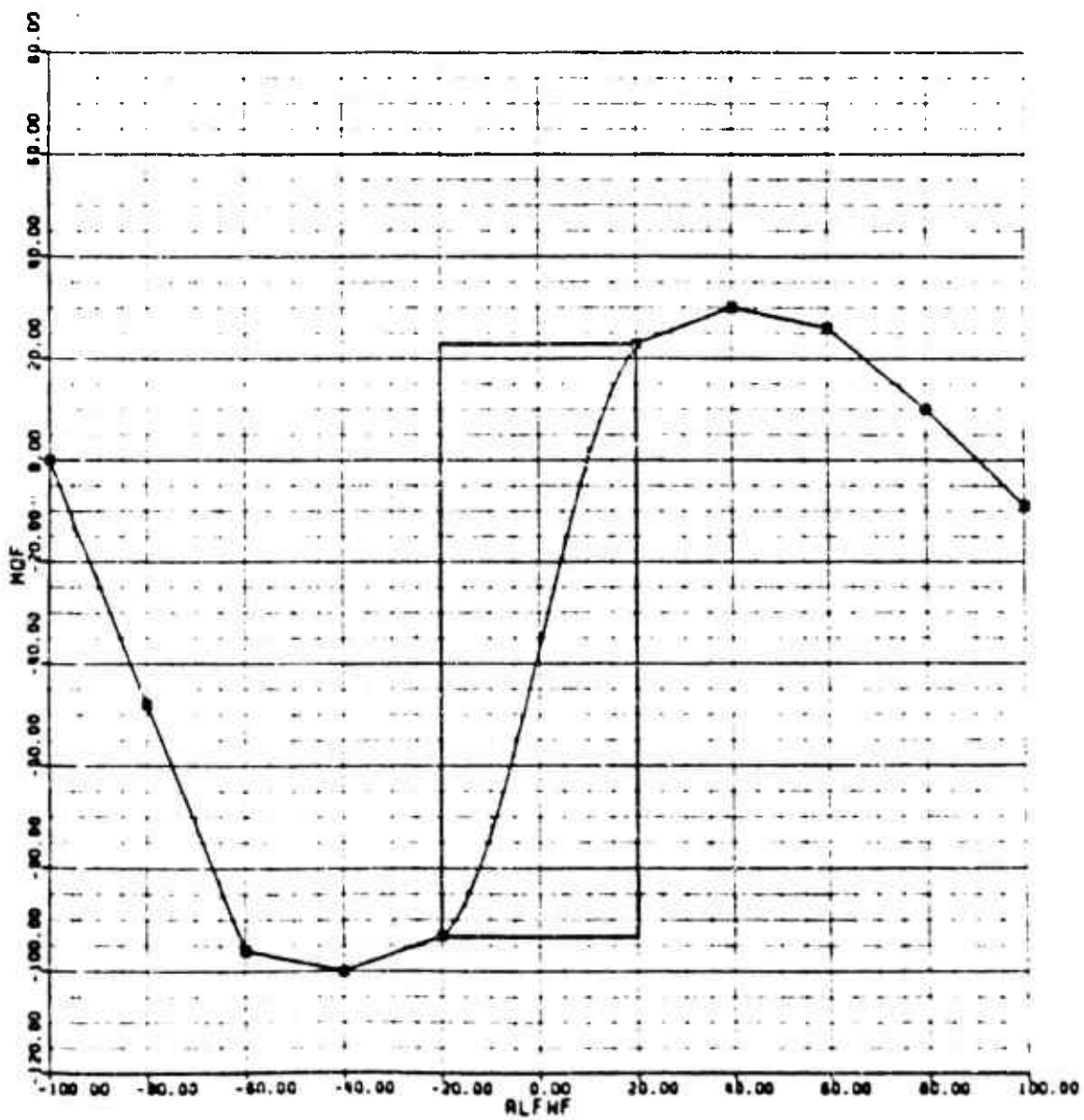


Figure F-10. AH-1S Fuselage Pitching Moment Map

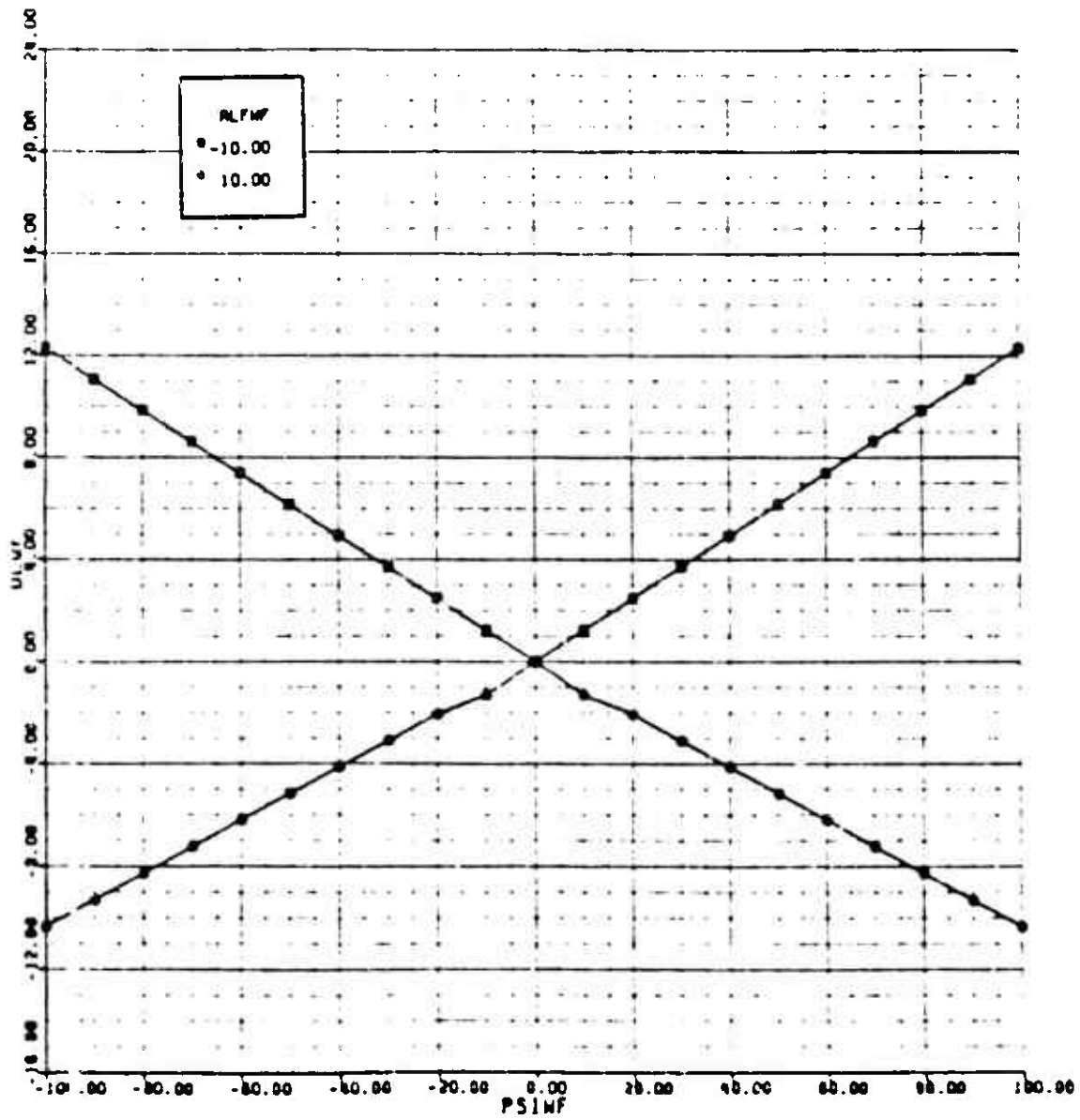


Figure F-11. AH-1S Fuselage Delta Lift Map

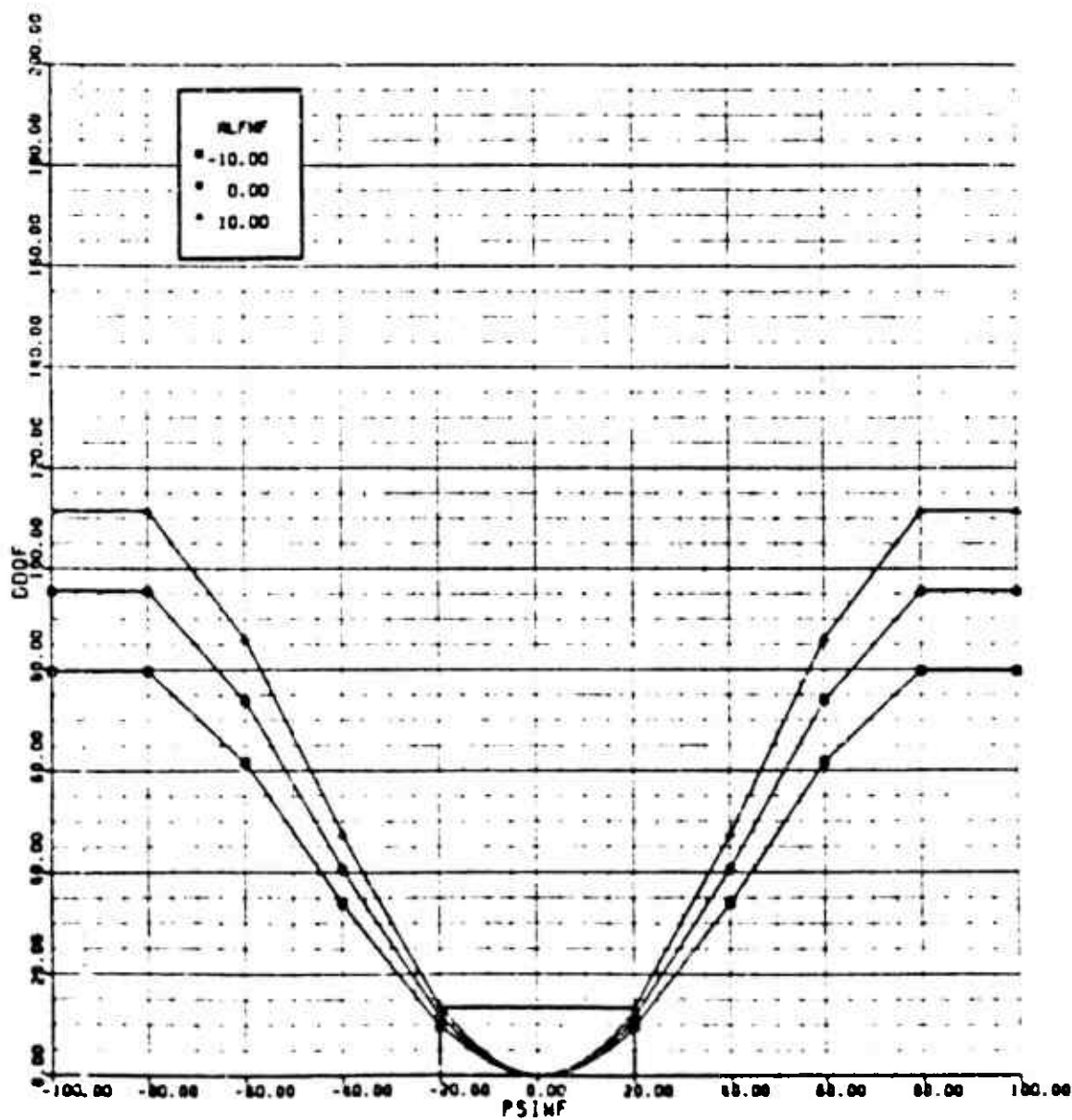


Figure F-12. AH-1S Fuselage Delta Drag Map

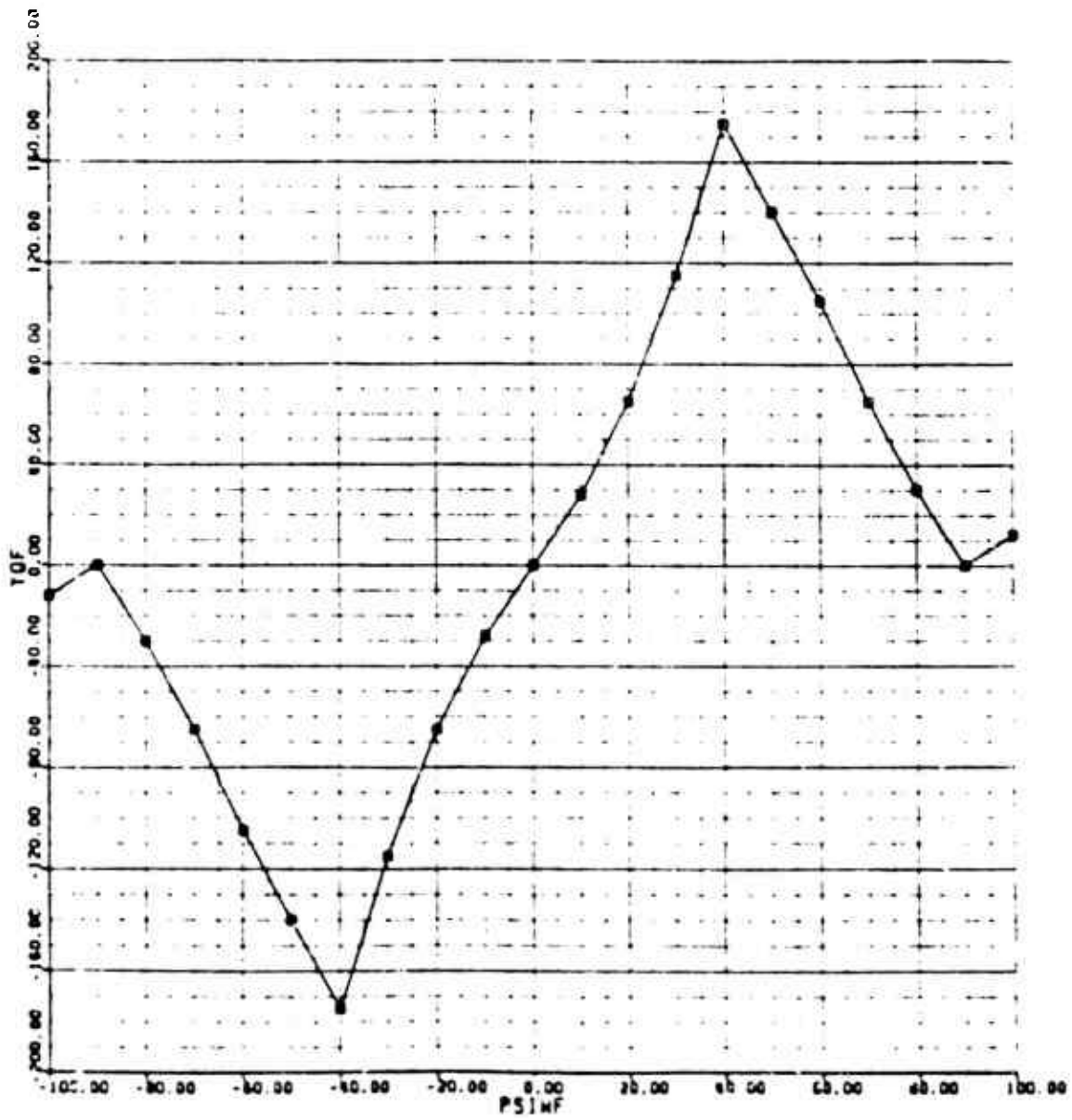


Figure F-13. AH-15 Fuselage Sideforce Map

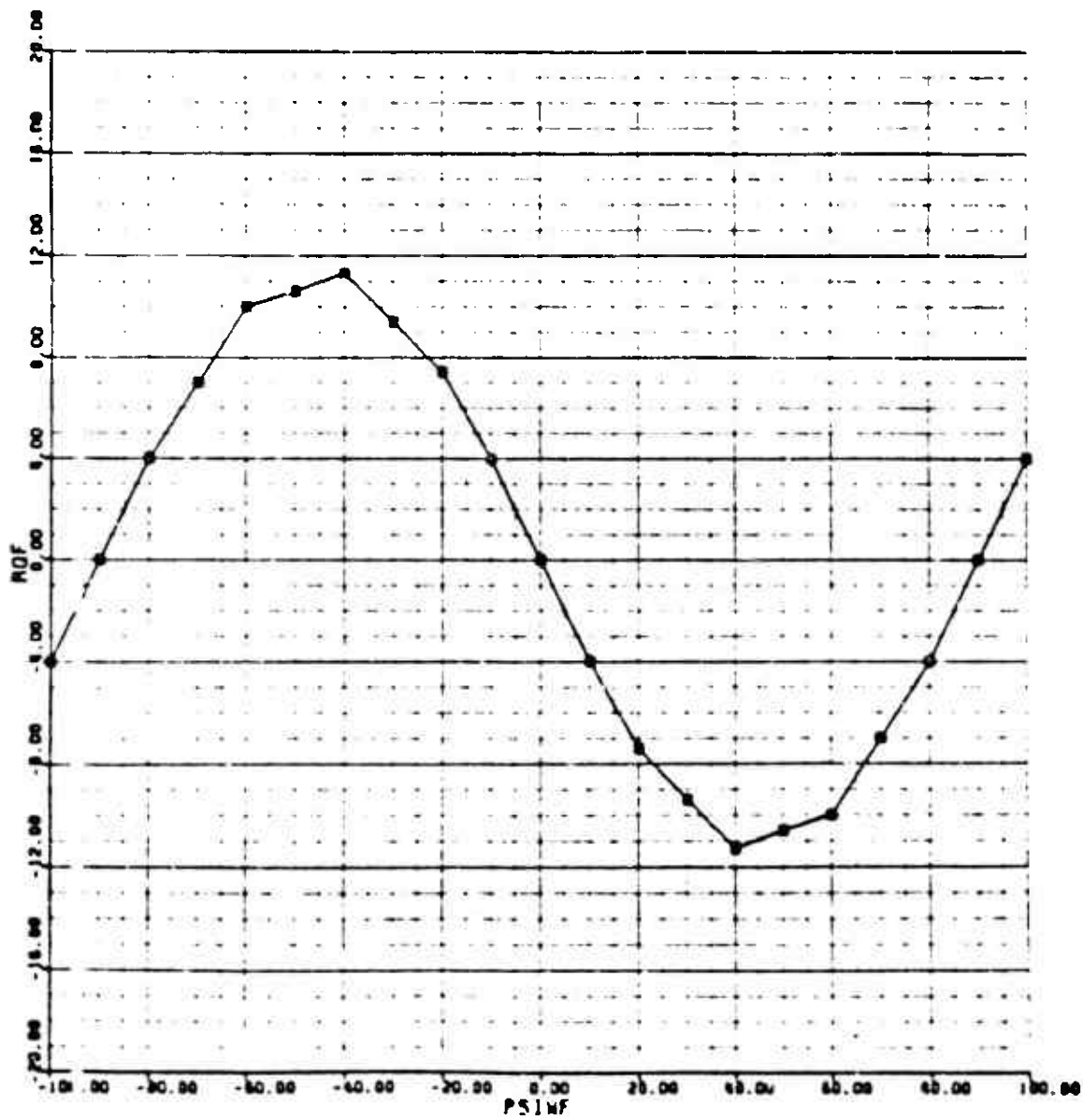


Figure F-14. AE-15 Fuselage Rolling Moment Map

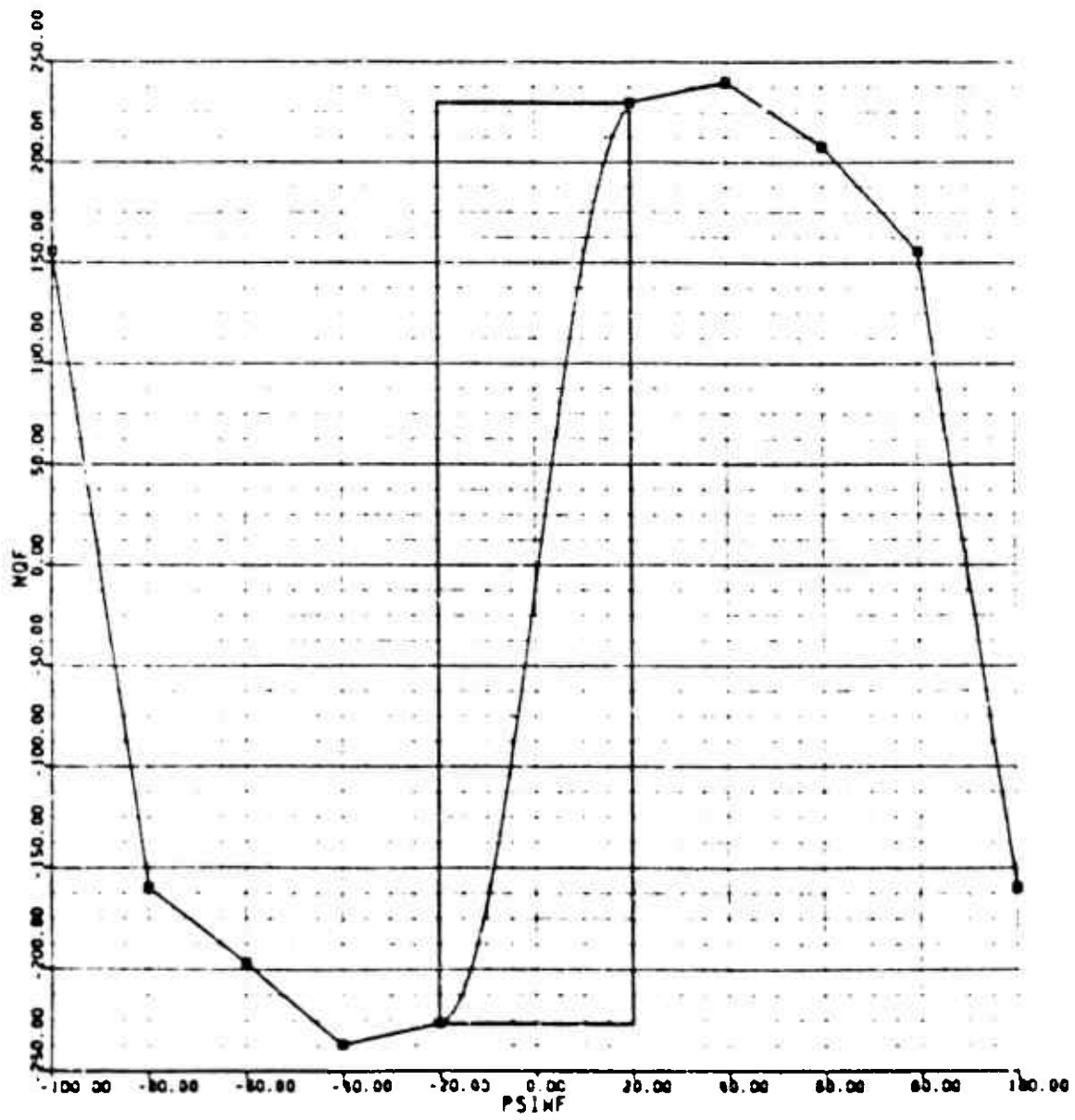


Figure F-15. AH-1S Pu lge Yewing Moment Map

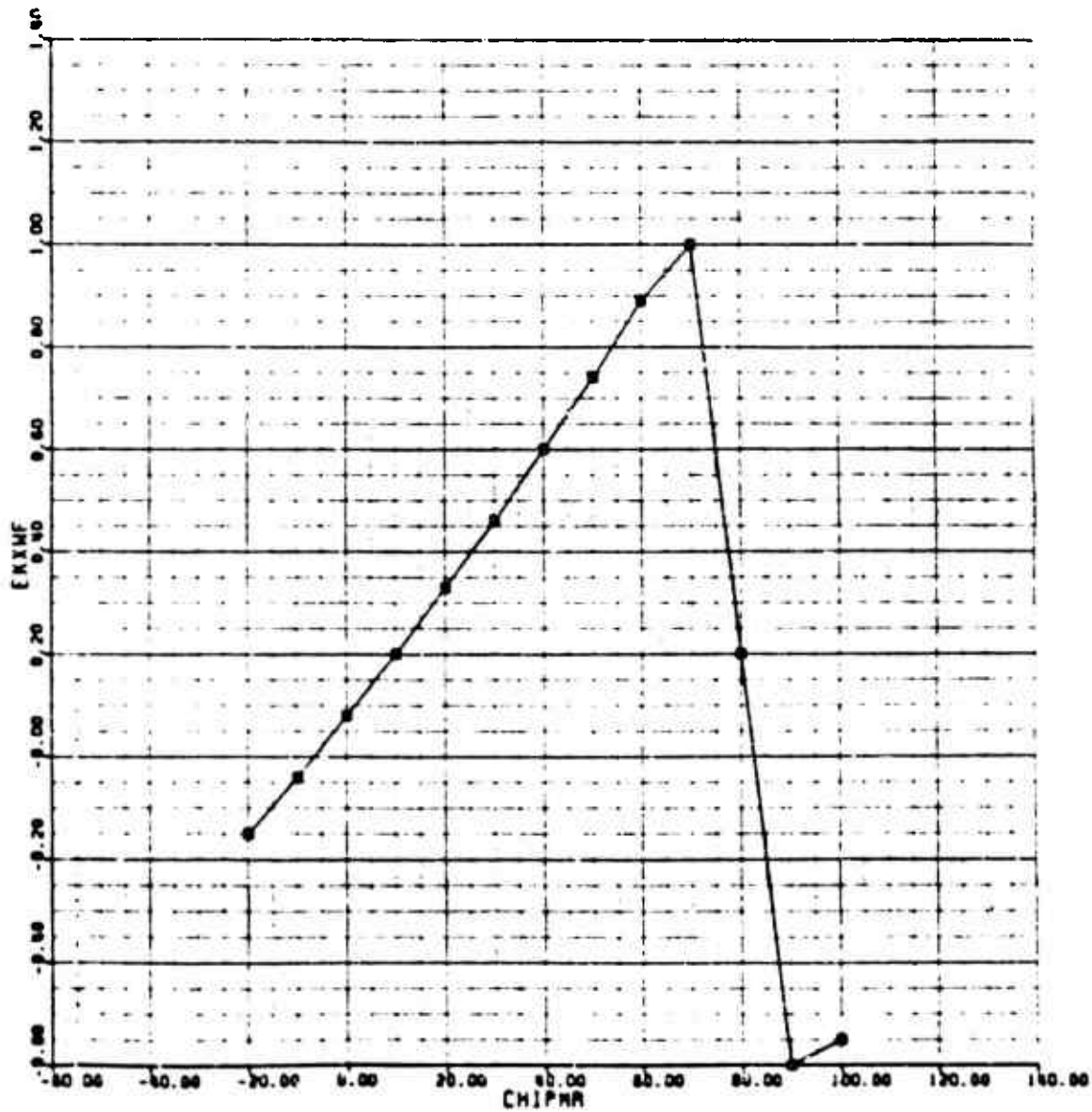


Figure F-16. AH-1S Main Rotor Downwash on Fuselage Map (x-direction)

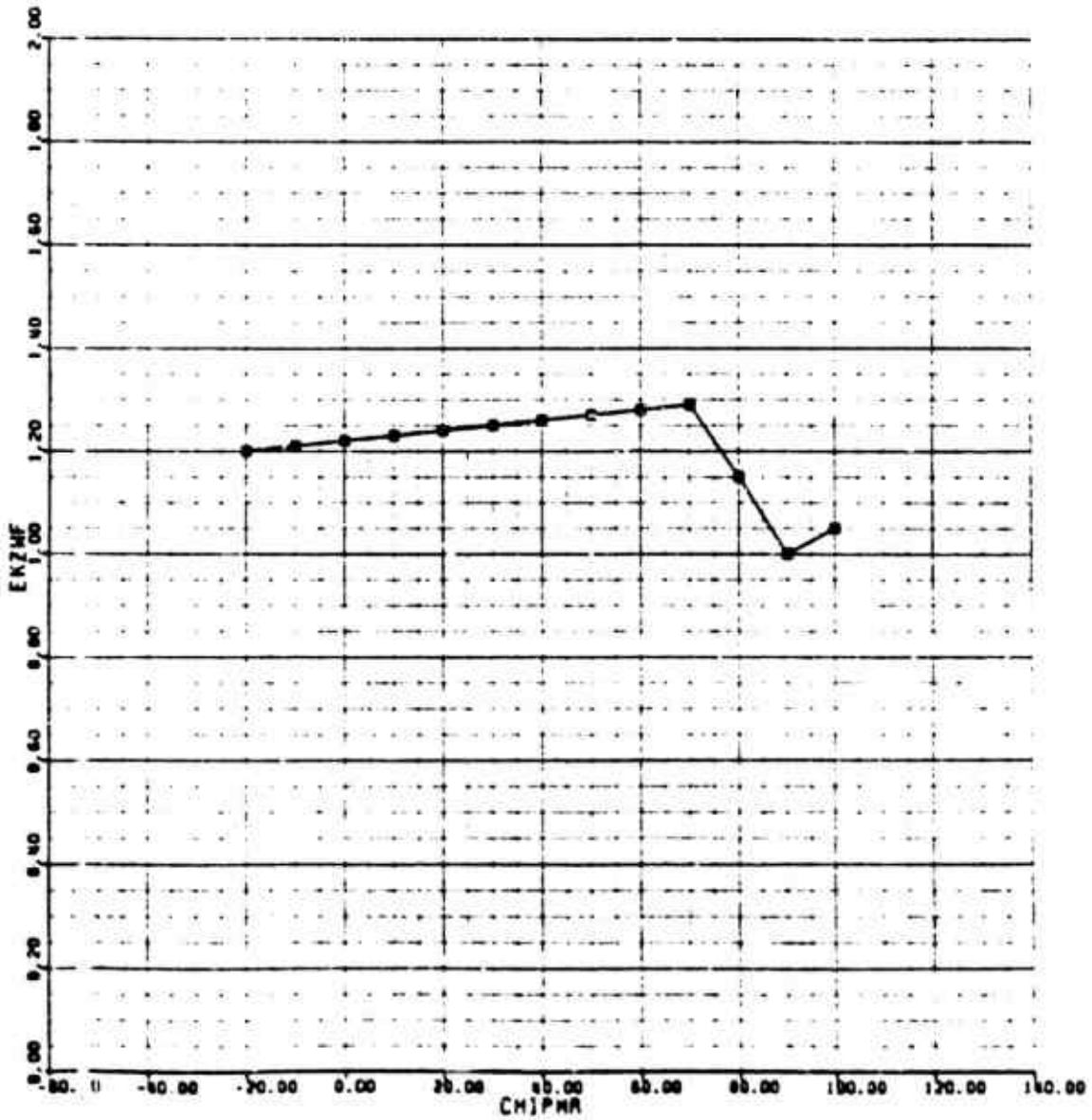


Figure F-17. AH-1S Main Rotor Downwash on Fuselage Map (z-direction)

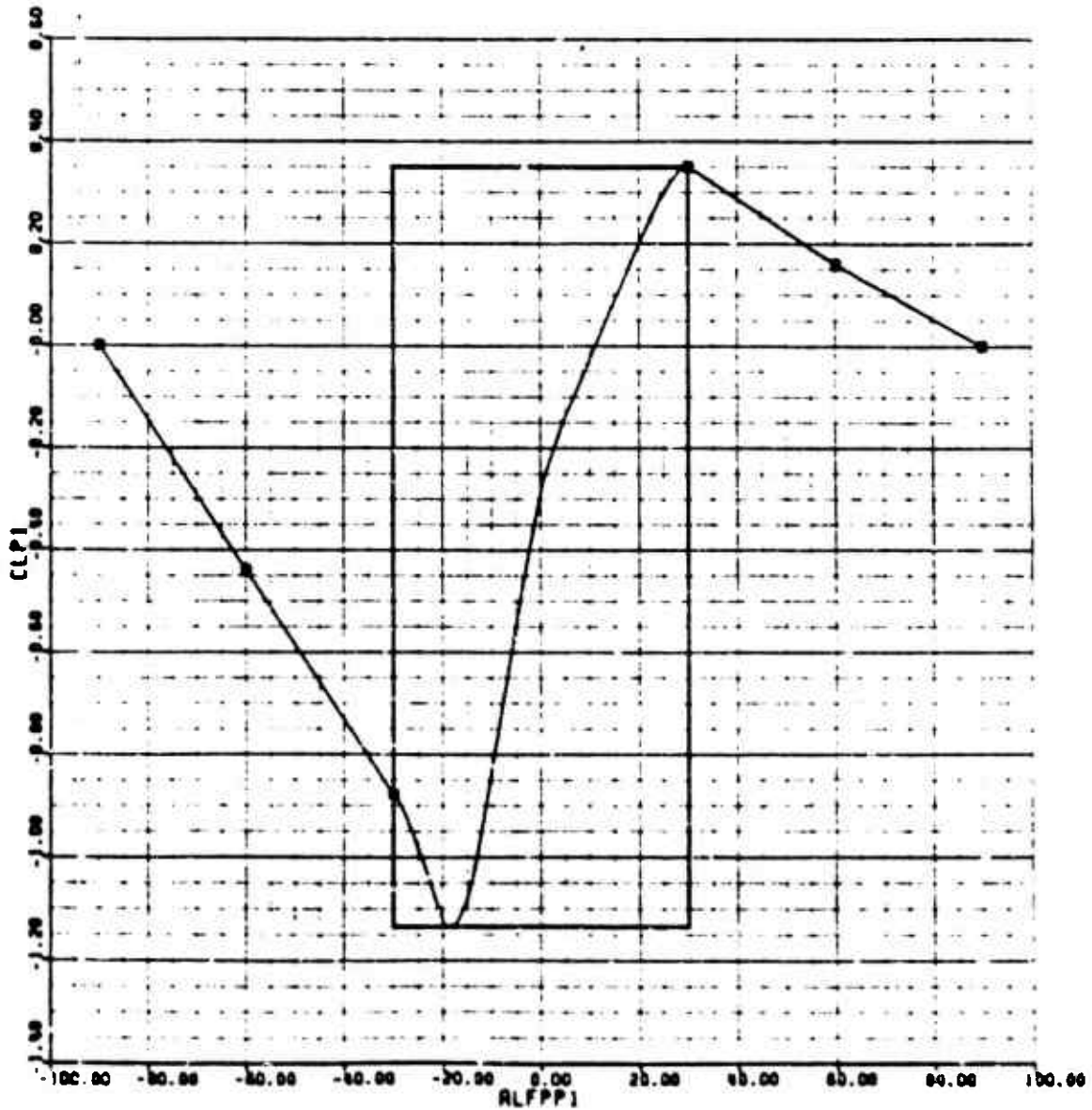


Figure F-18. AH-1S Horizontal Stabilizer Lift Map

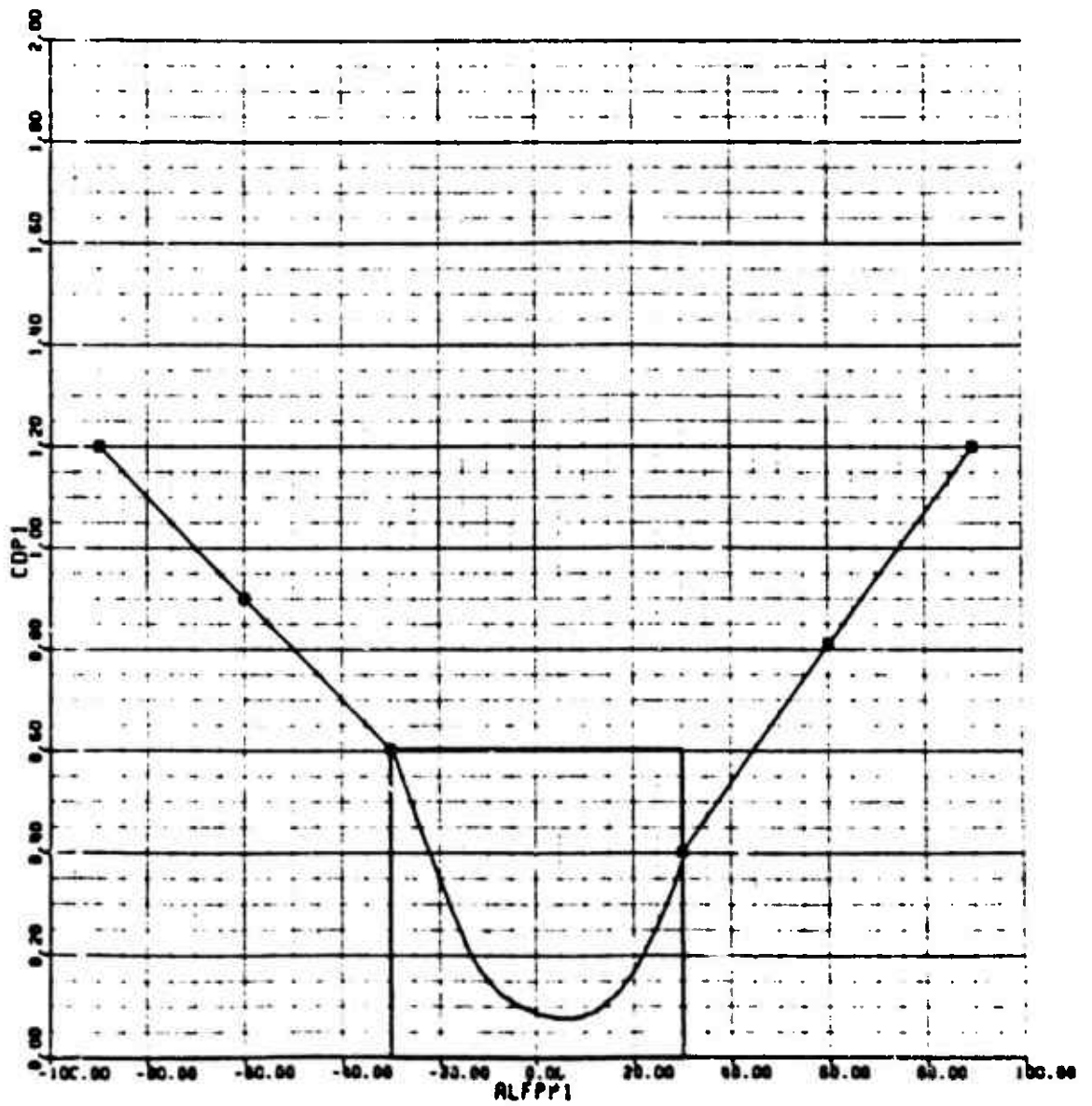


Figure F-19. AH-1S Horizontal Stabilizer Drag Map

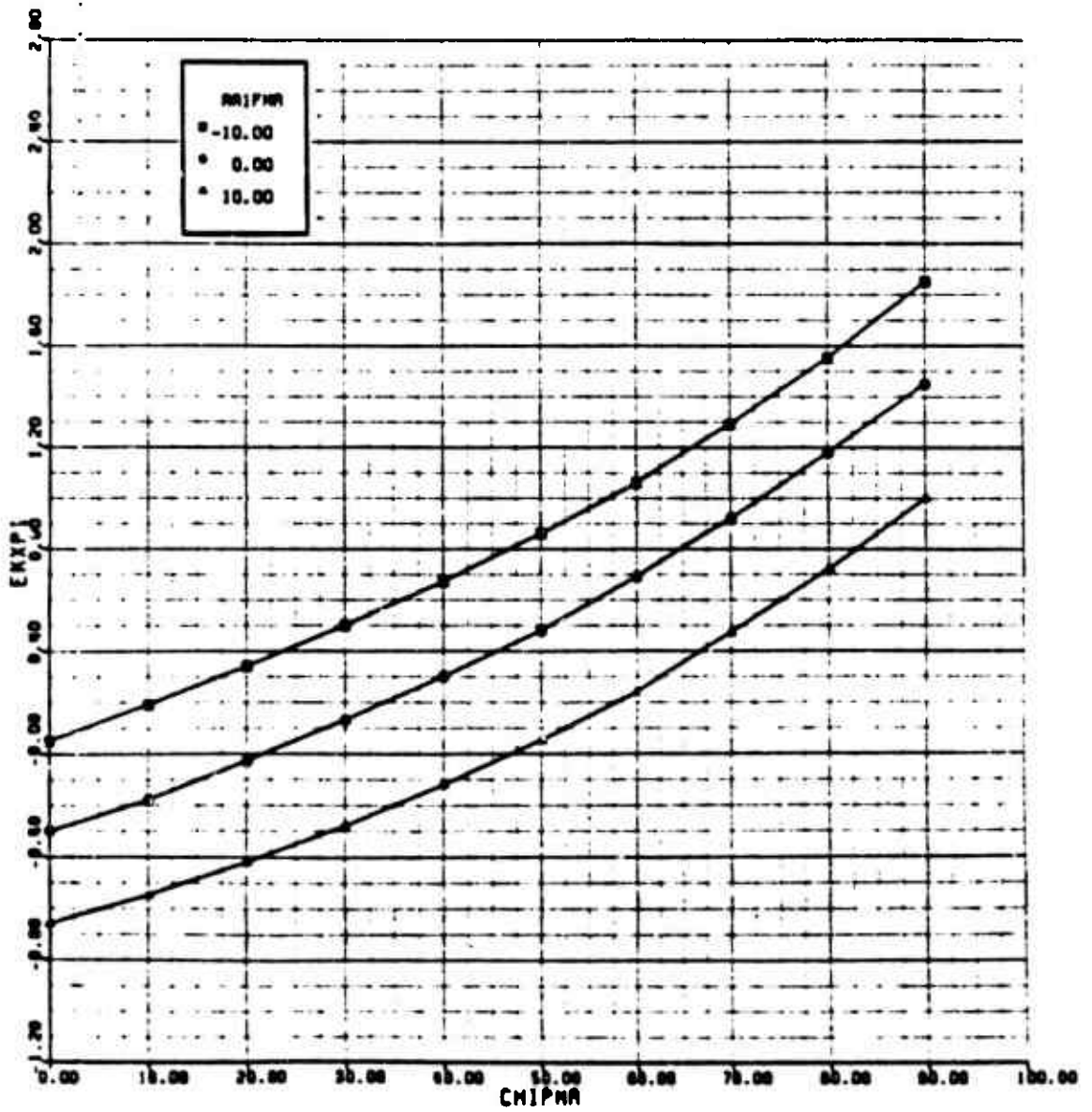


Figure F-20. AH-1S Main Rotor Downwash on Horizontal Stabilizer Map (x-direction)

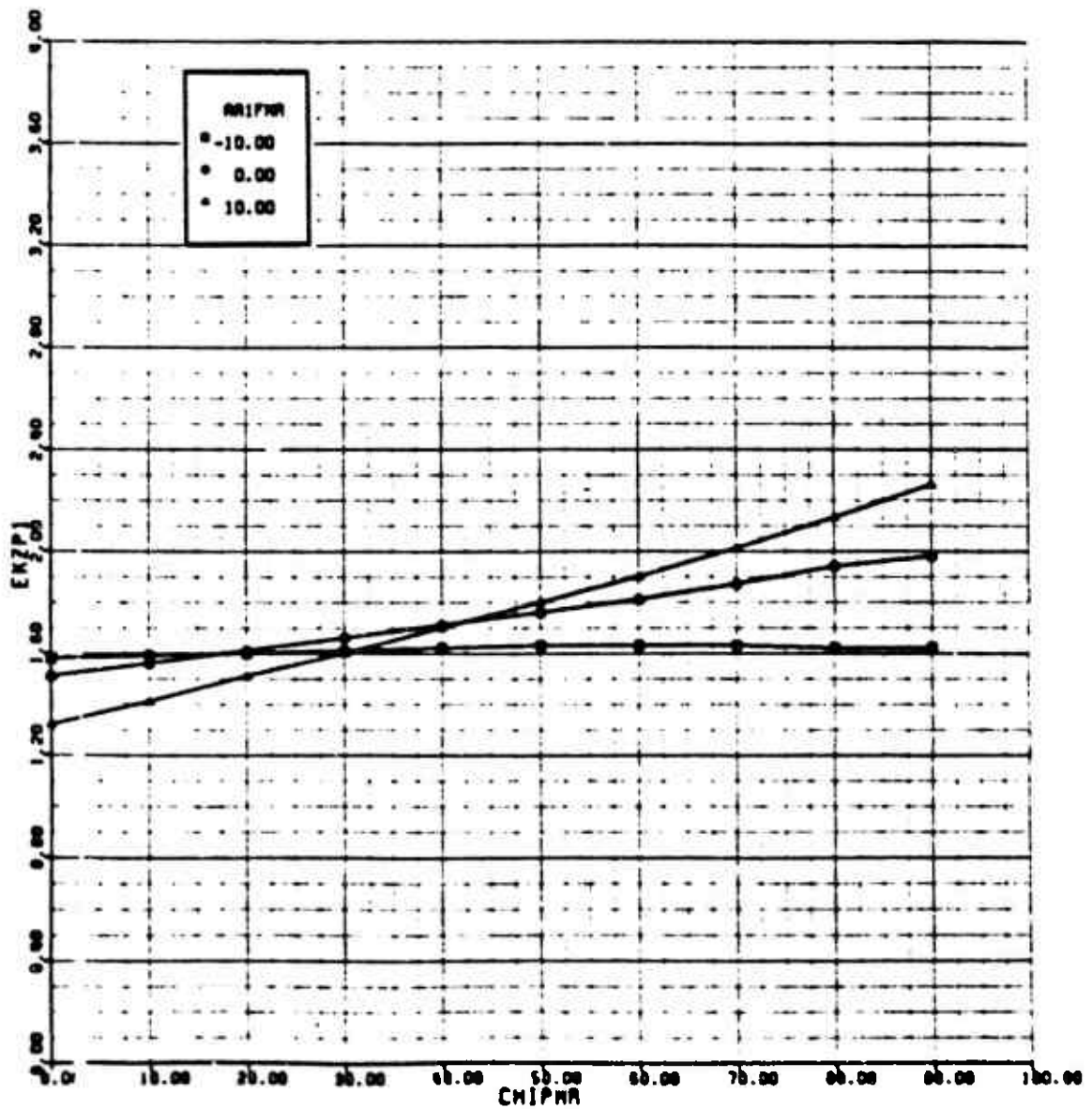


Figure F-21. AH-1S Main Rotor Downwash on Horizontal Stabilizer Map (z-direction)

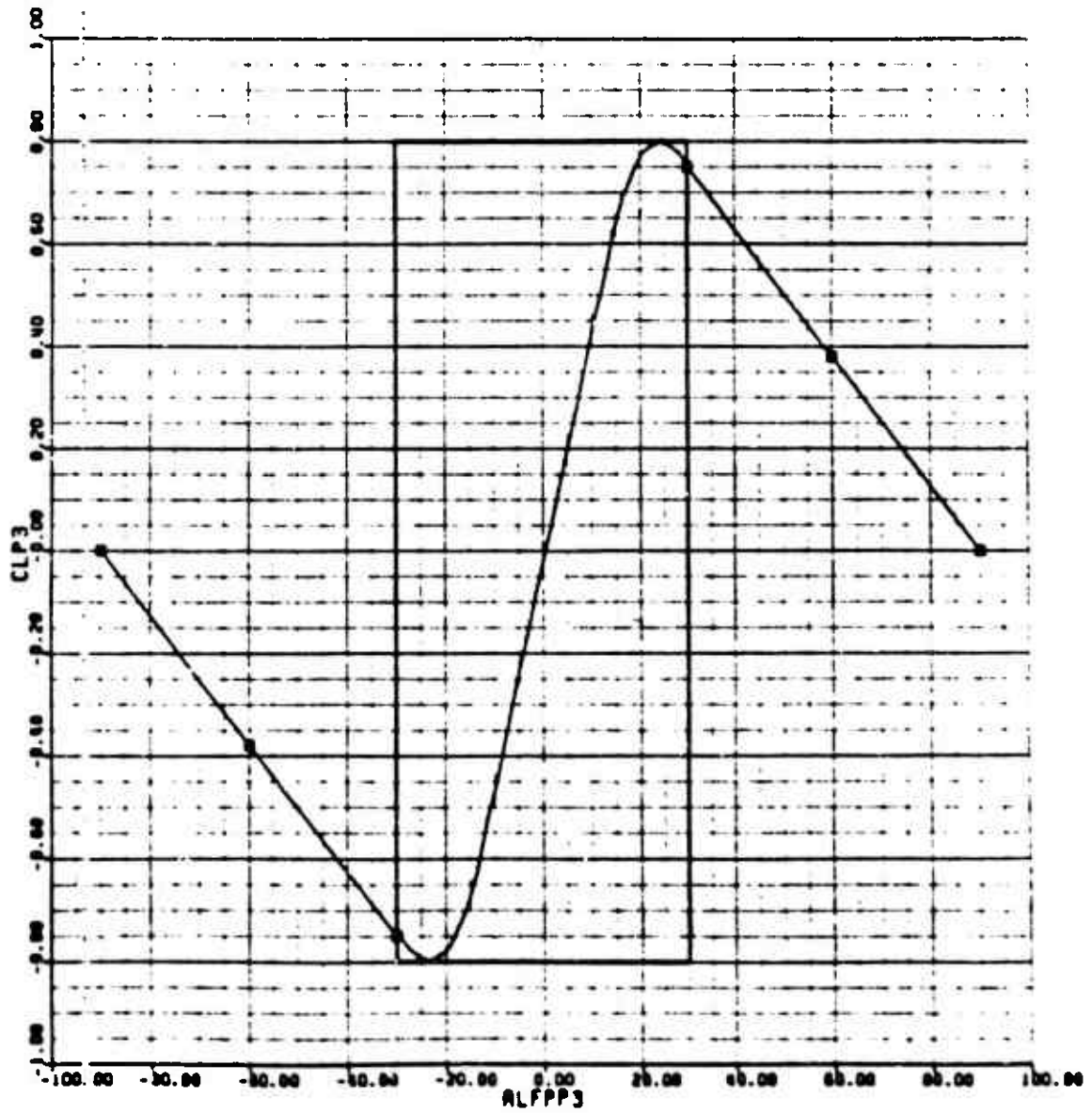


Figure F-22. AH-15 Vertical Stabilizer Lift Map

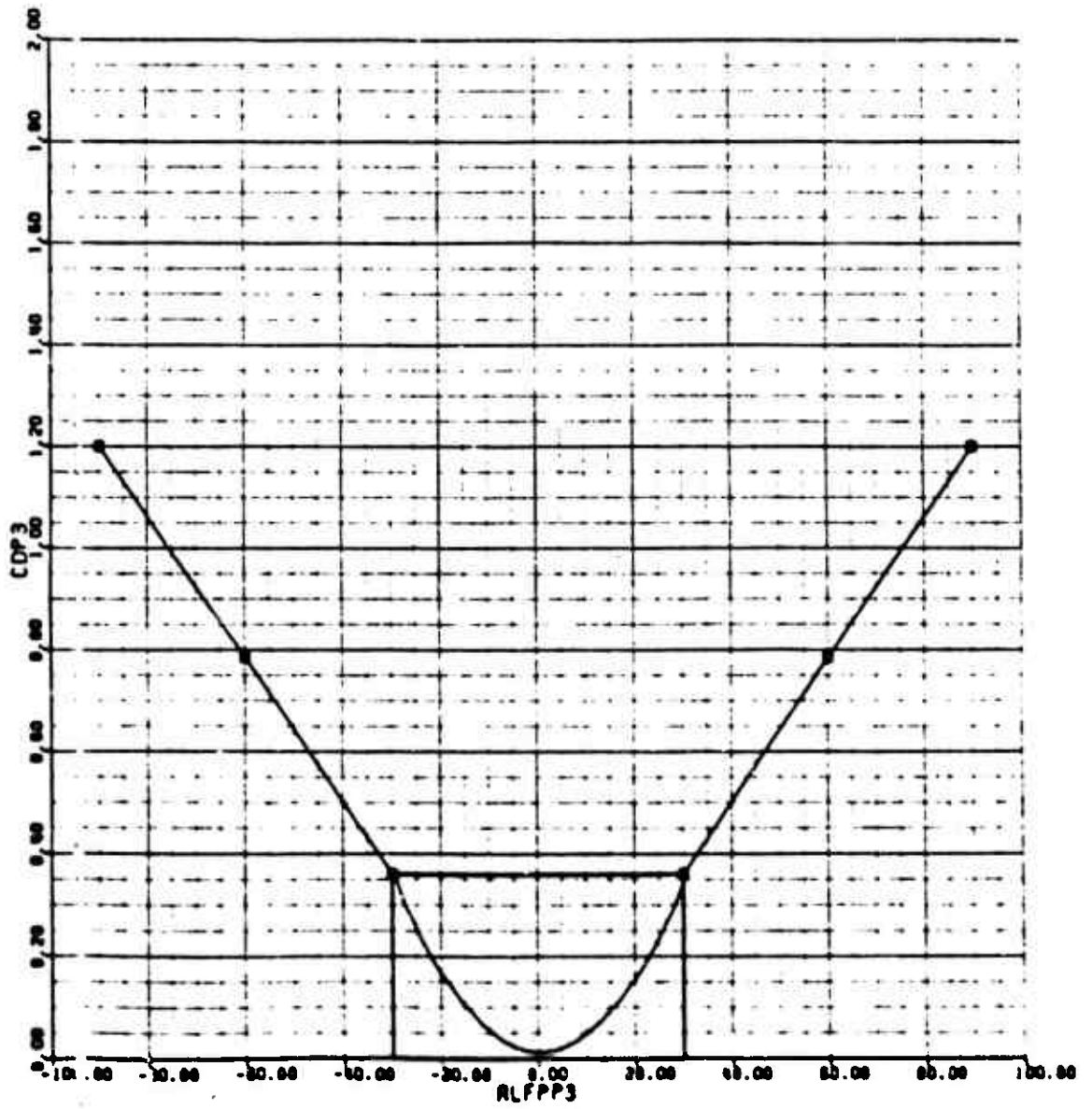


Figure F-23. AH-1S Vertical Stabilizer Drag Map

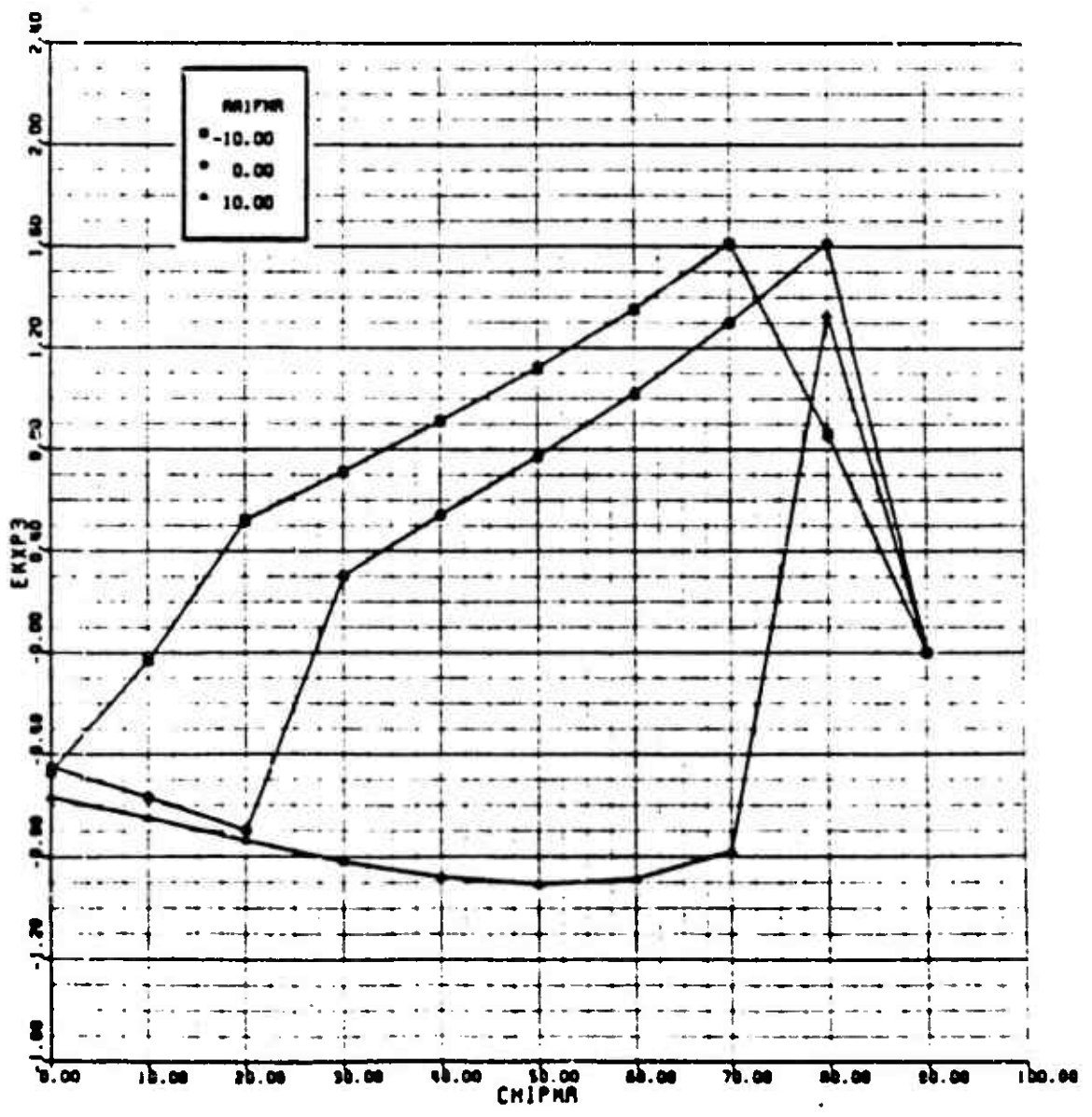


Figure F-24. AH-1S Main Rotor Downwash on Vertical Stabilizer Map (x-direction)

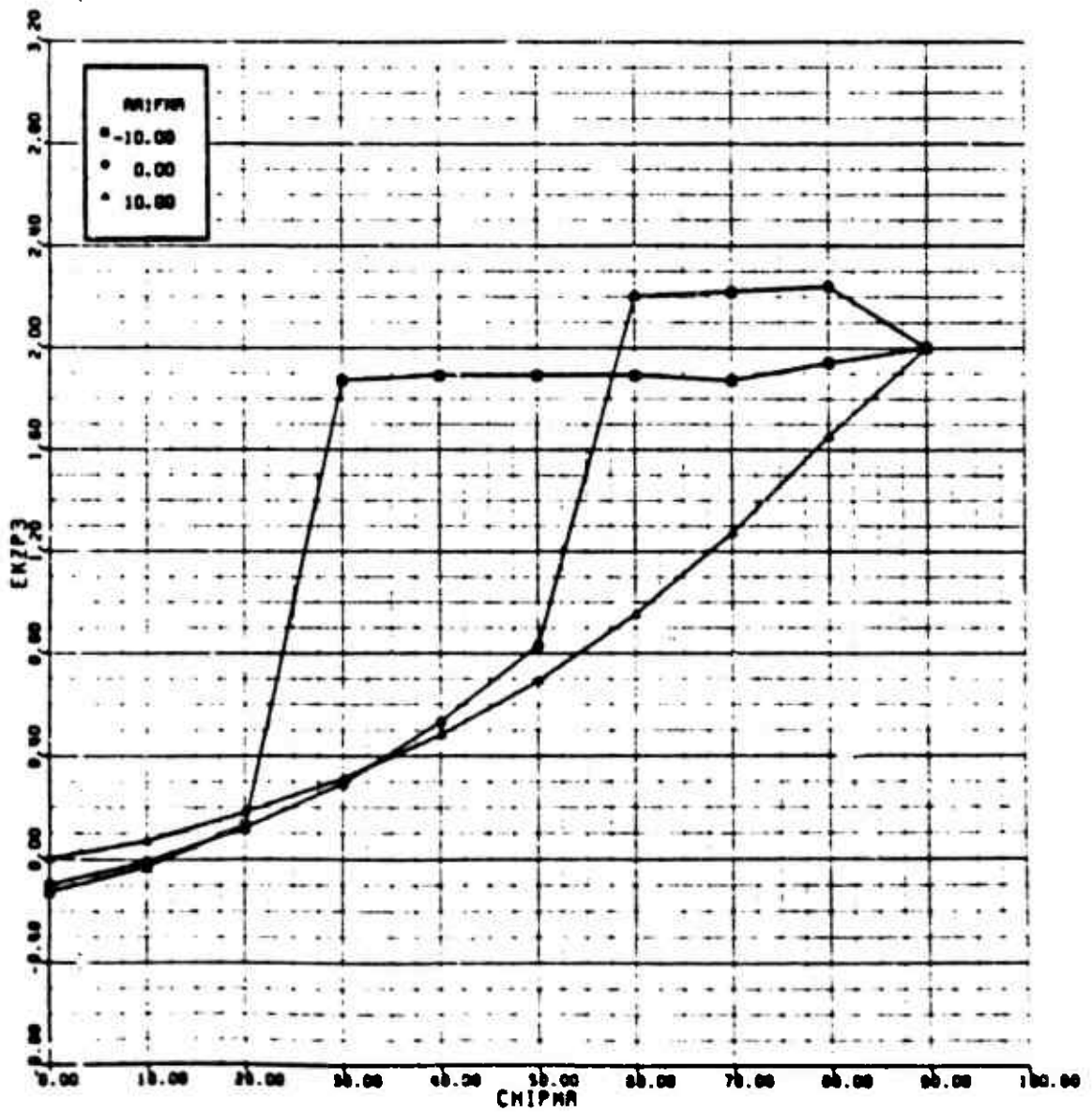


Figure F-25. AH-15 Main Rotor Downwash on Vertical Stabilizer Map (z-direction)

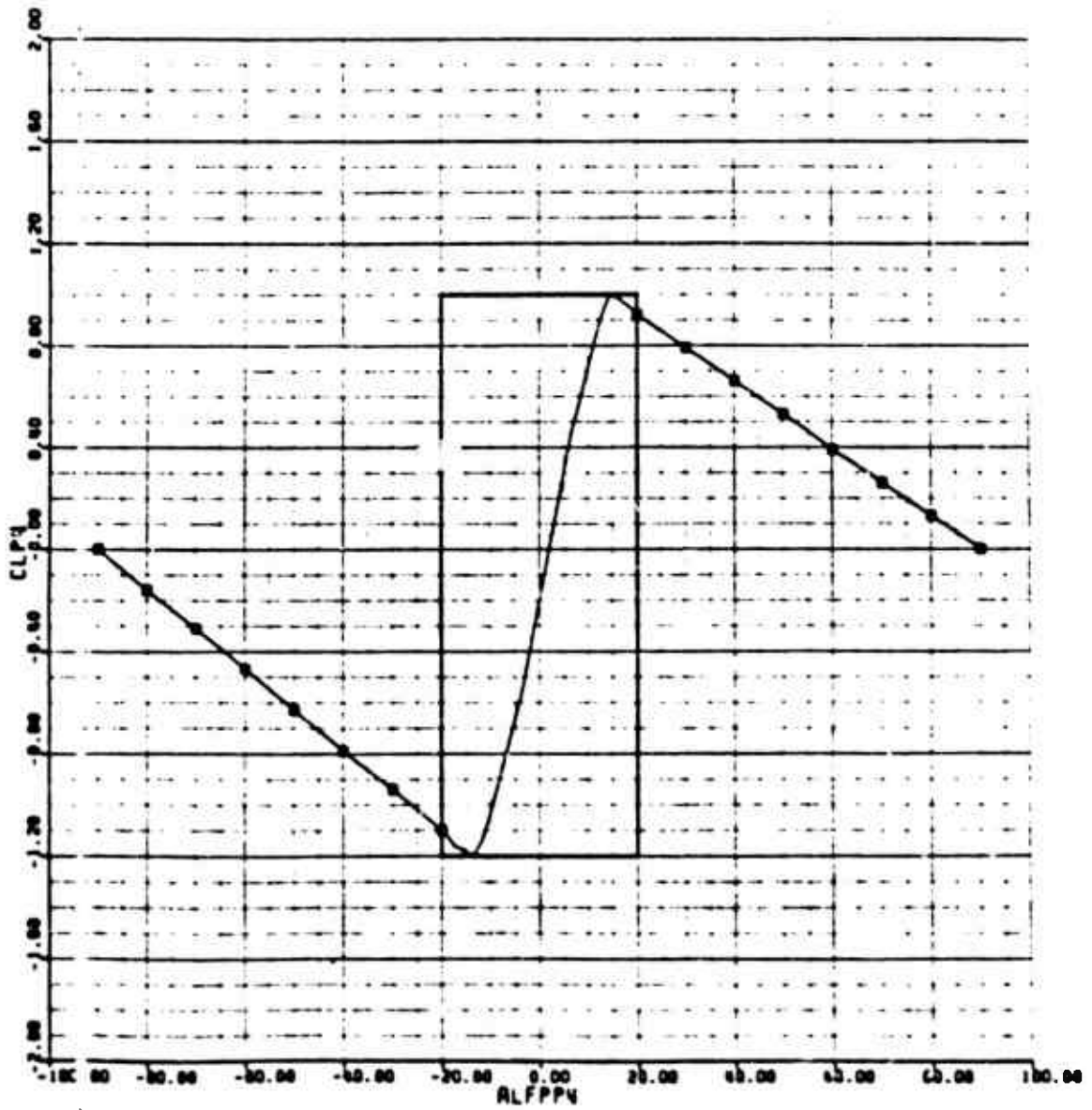


Figure F-26. AH-1S Wing Lift Map

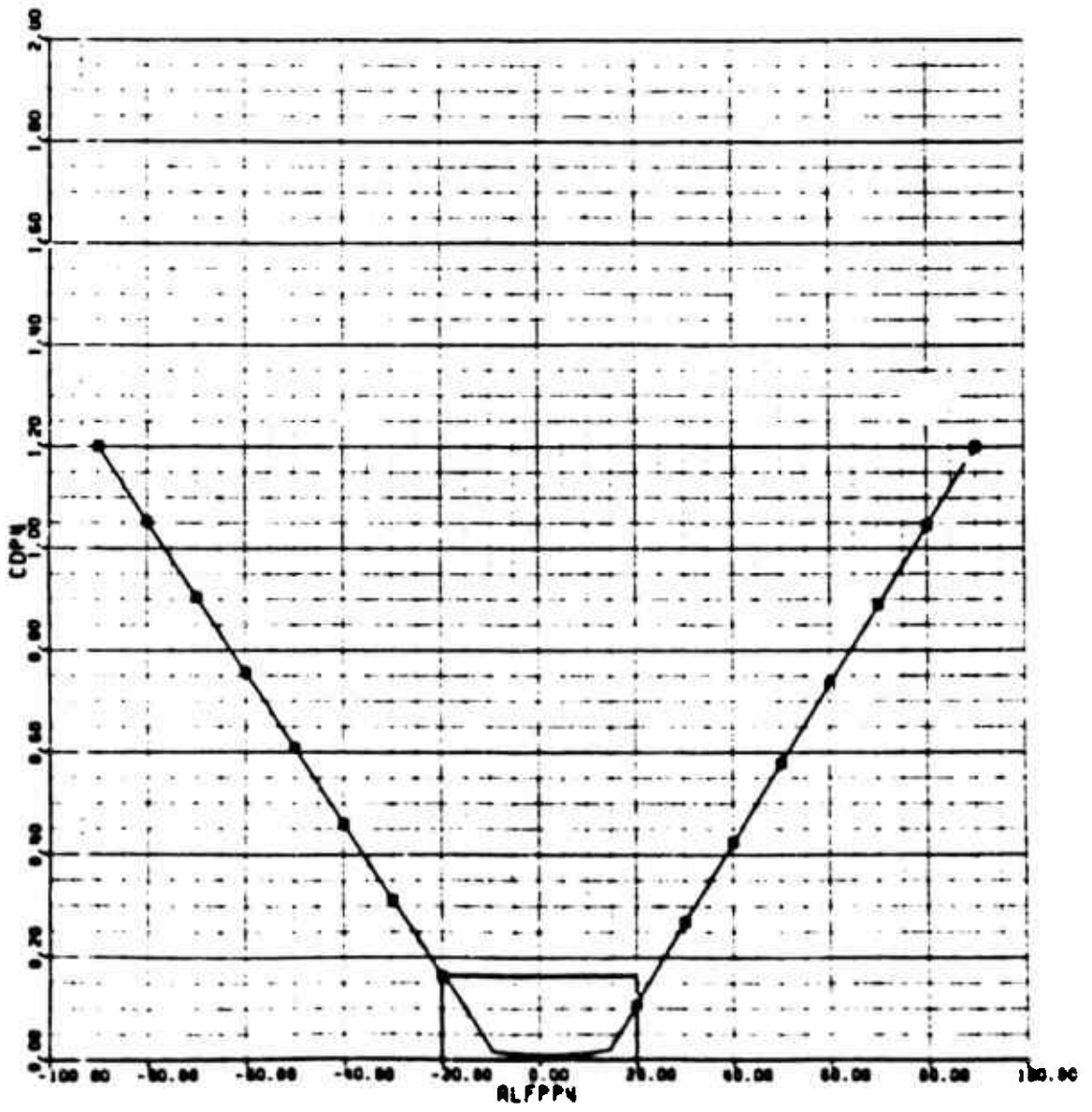


Figure F-27. AH-1S Wing Drag Map

APPENDIX G

SA-365N MODEL DATA

The SA-365N-1 Dauphin (Figure G-1) is the current production version of this French civil aircraft. Approximately 400 of these have been delivered. The most notable feature of the Dauphin is its use of a ducted fan, or Fenestron, instead of a tail rotor. In the N1 version, the Fenestron has an increased diameter of 1.1 meter (3 feet 7 inches) compared to the original value of 0.9 meter. The SA-365N has a maximum takeoff gross weight of 9,039 pounds, a rotor diameter of 39 feet 2 inches and is powered by two Turbomeca Ariel 1C turboshaft engines with an intermediate emergency power of 686 shp.

The main rotor is a four-blade unit using a hub that employs Aeroespatale's starflex design. The three conventional hinges for each blade are replaced by a single balljoint of rubber/steel sandwich construction. Blades use OA2 series airfoils, 12 percent thick inboard tapering to 7 percent at the tip. Blades are of all-composite construction utilizing fiberglass and graphite materials. The Fenestron is mounted in a duct or shroud at the base of the vertical fin and has eleven blades. A fixed horizontal stabilizer of 16 square feet is mounted on the tail boom just forward of the fin. The stabilizer is fitted with vertical endplates, each of 8.2 square feet. These endplates are canted nose-left to generate a right yawing moment to oppose main rotor torque at high speed. (Note-the rotor rotates with the advancing blade on the left side).

The SA-365N airframe is of mixed construction, primarily of aluminum semi-monocoque but making extensive use of composites in the nose and main rotor pylon. Retractable, tricycle landing gear is fitted.

Creation of a GenHel simulation model was difficult because of the lack of aerodynamic data for the fuselage and empennage and lack of inertia data. Attempts to work out a non-disclosure agreement between Aerospatiale and Sikorsky so that the data could be obtained from the manufacturer failed. As a consequence, the following approach to calculating these data was taken:

- fuselage aerodynamics - scaled from S-76
- tail aerodynamics - conventional data
- inertias - Sikorsky parameters
- fuselage aerodynamic interference on the tail - scaled from S-76A
- rotor interferences on fuselage and tail - use of existing Heyson program
- main rotor airfoils - use SC1095 data
- Fenestron - use existing Sikorsky Fan Tail model

The scaling method for the fuselage aerodynamics is discussed in detail in Appendix M. Geometry and weight data were available in Reference 18.

Inertias were estimated using Sikorsky parametrics. Data collected over the years on a variety of single rotor helicopters show that inertia can be estimated as:

$$I = (GW/K) \exp(x)$$

Where the coefficients are defined as:

Parameter	Ixx Roll	Iyy Pitch	Izz Yaw	Ixz
K	121.2	21.85	29.85	237.7
x	1.823	1.606	1.674	1.827

For a gross weight of 10,000 pounds, the pitch (Iyy) inertia would be

$$I_{yy} = \frac{10000}{21.85} \times 1.606 = 18,744 \text{ slug-ft}^2$$

The equivalent flapping hinge offset of the main rotor was set at 3.8 percent and SC1095 airfoils were used.

Trim data were available from a preliminary copy of a U.S. Army AEFA report on the SA-365N. GenHel correlation with these data are shown in Figures G-2 to G-7. The flight conditions for these data were:

GW = 7400 pounds
 FSCG = 159.2
 Density Altitude = 12,660 feet

Note that the Dauphin rotor rotates in a direction opposite to most American aircraft. The GenHel simulation was set up with conventional rotation. In presenting the correlation data, the lateral stick and pedal positions are shown with the original flight test data and with that data mirror imaged to account for rotation. Correlation for all controls and for main rotor power was very good, but the test data had 5 to 10 less horsepower required for the Fenestron than GenHel calculated.

All of the numerical data used to model the SA-365N are provided in this appendix. Table C-1 is a listing of all the input data. Figures G-8 through G-39 are plots of the map data for fuselage, vertical tail and horizontal tail aerodynamics along with plots of the rotor interference and fuselage interference data. The tabular data are provided with appropriate labels. Map data are identified with GenHel variables provided in the List of Symbols.

For the SA-365N model, the panel allocation was as follows:

1. Right horizontal tail
2. Left horizontal tail
3. Vertical tail
4. Feneatron shroud
5. Right vertical endplate
6. Left vertical endplate

TABLE G-1. SA-365N SPECIFIC FILE

```

***** INPUT PARAMETERS FOR MAIN ROTOR MODULES (8A) *****

FSMR:: 300.0 ; FUSELAGE STATION, INCHES
WLNR:: 200.0 ; WATERLINE STATION, INCHES
BLNR:: 0.0 ; BUTTLINE STATION, INCHES (+IVE TO PORT)
RRR:: 19.57 ; RADIUS, FT.
ONGTRR:: 36.65 ; TRIM ROTATIONAL SPEED, RAD/SEC
BNR:: 4.0 ; ACTUAL NUMBER OF BLADES
ISRR:: -4.0 ; LONGITUDINAL SHAFT TILT, (POS. BACKWARDS), DEG
ILNR:: 0.0 ; LATERAL SHAFT TILT, (POS. STARBOARD), DEG
DELSMR:: 0.0 ; SWASHPLATE PHASE ANGLE, DEG
OEL3RR:: 0.0 ; FLAPPING HINGE OFFSET ANGLE, DEG.
KAP1MM:: 0.0 ; LAGGING HINGE OFFSET COEF. (FUNC(LG))
KAP2MM:: 0.0 ; LAGGING HINGE OFFSET COEF. (FUNC(LG**2))
CNDTRR:: 1.263 ; BLADE CHORD AT TIP, FT.
CHDRR:: 1.263 ; BLADE CHORD AT ROOT, FT.
OPSTRR:: 0.75 ; HINGE OFFSET, FT.
SPLRR:: 2.531 ; HINGE TO START OF BLADE, FT.
WTBDMR:: 123.9 ; WEIGHT OF ONE BLADE, LBS.
IBMR:: 322.46 ; BLADE MOMENT OF INERTIA ABOUT HINGE, SLUG-FT**2
MBRR:: 28.88 ; BLADE MASS MOMENT ABOUT HINGE, SLUG-FT**2
INRR:: 450.0 ; ROTOR POLAR MOMENT OF INERTIA (LESS BLADES), SLUG-FT**2
BTLMM:: .97 ; BLADE TIP CUT OFF RATIO
DCDMR:: .002 ; DELTA DRAG COEF. FOR EACH SEGMENT
MBSMR:: 4 ; NUMBER OF BLADES SIMULATED, FIX PDINT
NSSMM:: 5 ; NUMBER OF SEGMENTS SIMULATED, FIX PDINT

; ** MAIN ROTOR NON LINEAR TWIST MAP **
TWRMP:: UVR00 ; MAP LOOM UP NAME
        XSEGM00 ; INPUT VARIABLE NAME
        TWSTR00 ; OUTPUT VARIABLE NAME
        TWRLD ; MAP NAME
        EXP 0.18, 0.98, 0.10 ; LOWER LIMIT, UPPER LIMIT, DELTA

TWRLO: EXP 0.0, 0.0, -1.017, -2.034, -3.050
        EXP -4.067, -5.084, -6.101, -7.188

***** MAIN MOTOR DOWNWASH SUBMODULE (8A) *****

RCTMR:: 1.0 ; THRUST GAIN FOR UNIFORM DOWNWASH
MCMHM:: 0.0 ; FITCH. RDM. GAIN FOR DOWNWASH SIN. HARMONIC
MSLHM:: 0.0 ; ROLL RDM. GAIN FOR DOWNWASH CDS. HARMONIC
TDWOMM:: .01038 ; TIME CONST. FOR UNIFORM DOWNWASH FILTER, SEC
TDWCMH:: 0.0 ; TIME CONST. FOR DOWNWASH SIN. HARMON. FILTER, SEC.
TDWSMM:: 0.0 ; TIME CONST. FOR DOWNWASH CDS. HARMON. FILTER, SEC.

***** FLAPPING/LAGGING DAMPER (8C) *****

RBMHM:: 8053.0 ; FLAPPING HINGE SPRING CONST, FT-LBS/RAD
MBM.HM:: 0.0 ; FLAPPING HINGE DAMPER CONST, FT-LBS-SEC/RAD

; ** SET OF MOUNTING DIMENSIONS FOR LAG DAMPER, INCHES **
ALDMR:: 0.0 ;
BLDMR:: 0.0 ;
CLDMH:: 15.6 ;
OLDMR:: 6.64 ;
RLDMR:: 5.0 ;
LGDORR:: -7.5 ; ALIGNMENT OFFSET IN RELATION TO LAG, DEG
THLDMH:: 2.0 ; FIXED BLADE FITCH RELATIONSHIP BET. ARM AND THRUFF

***** INPUT PARAMETERS FOR FUSELAGE/WING (8A) *****
***** MOUNTING POINT OF MODEL IN WIND TUNNEL *****

```

TABLE G-1. SA-365N SPECIFIC FILE (Cont'd)

```

FSWF:: 300.0 ; FUSELAGE STATION, IN.
WLWF:: 140.0 ; WATERLINE STATION, IN.
BLWF:: 0.0 ; BUTTLINE STATION, IN. (+IVE TO PORT)
IWF:: 0.0 ; WING INCIDENT, DEG.

; ** FUSELAGE LIFT (TAIL-OFF) VS ALFWF MAP **
LQFMP:: UVRUVR00 ; MAP ARGUMENT: LOOK UP ROUTINE
        ALFWF00 ; INPUT VARIABLE
        LQF00 ; OUTPUT VARIABLE
        LQFLO ; LOW ANGLE MAP NAME
EXP -20.0, 20.0, 2.0 ; LOWER LIM, UPPER LIM, DELTA
        LQFHI ; HIGH ANGLE MAP NAME
EXP -100.0, 100.0, 20.0 ; LOWER LIM, UPPER LIM, DELTA

; LOW ANGLE MAP: ALFWF -20 TO 20, DELTA = 2
LQFLO: EXP -10.26, -9.61, -8.29, -6.65, -5.17
        EXP -3.86, -2.63, -1.64, -0.66, -0.08
        EXP 0.33, 1.02, 1.71, 2.40, 3.09
        EXP 3.78, 4.47, 5.16, 5.85, 6.54
        7.22

; HIGH ANGLE MAP: ALFWF -100 TO 100, DELTA = 20
LQFHI: EXP 0.82, -0.82, -4.02, -8.29, -10.26
        EXP 0.33, 7.22, 5.75, 2.87, 0.82
        -0.82

; ** FUSELAGE DRAG (TAIL-OFF) VS ALFWF MAP **
DQFMP:: UVRUVR00 ; MAP ARGUMENT: LOOK UP ROUTINE
        ALFWF00 ; INPUT VARIABLE
        DQF00 ; OUTPUT VARIABLE
        DQFLO ; LOW ANGLE MAP NAME
EXP -20.0, 20.0, 2.0 ; LOWER LIM, UPPER LIM, DELTA
        DQFHI ; HIGH ANGLE MAP NAME
EXP -100.0, 100.0, 20.0 ; LOWER LIM, UPPER LIM, DELTA

; LOW ANGLE MAP: ALFWF -20 TO 20; DELTA = 2
DQFLO: EXP 9.02, 8.07, 7.36, 6.77, 6.49
        EXP 6.19, 6.13, 6.06, 5.98, 5.98
        EXP 6.06, 6.13, 6.24, 6.36, 6.49
        EXP 6.70, 6.93, 7.14, 7.36, 7.57
        7.86

; HIGH ANGLE MAP, ALPHA FROM -100 DEG TO 100 DEG, DEL=20
DQFHI: EXP 147.0, 138.0, 92.0, 35.7, 9.02
        EXP 6.06, 7.86, 34.1, 91.2, 137.0
        148.0

; ** FUSELAGE PITCH MOM (TAIL-OFF) VS ALFWF MAP **
MQFMP:: UVRUVR00 ; MAP ARGUMENT: LOOK UP ROUTINE
        ALFWF00 ; INPUT VARIABLE
        MQF00 ; OUTPUT VARIABLE
        MQFLO ; LOW ANGLE MAP NAME
EXP -20.0, 20.0, 2.0 ; LOWER LIM, UPPER LIM, DELTA
        MQFHI ; HIGH ANGLE MAP NAME
EXP -100.0, 100.0, 20.0 ; LOWER LIM, UPPER LIM, DELTA

; LOW ANGLE MAP: ALPHA FROM -20 DEG TO 20 DEG, DELTA = 2
MQFLO: EXP -272.0, -266.0, -257.0, -246.0, -231.0
        EXP -214.0, -194.0, -173.0, -145.0, -117.0
        EXP -89.3, -61.4, -33.5, -5.59, 22.4
        EXP 50.2, 78.1, 104.0, 129.0, 149.0
        168.0

; HIGH ANGLE MAP: ALPHA FROM -100 DEG TO 100 DEG, DEL=20
MQFHI: EXP 13.7, -13.7, -106.0, -220.0, -272.0
        EXP -89.3, 168.0, 137.0, 64.6, 8.2
        -8.2
    
```


TABLE G-1. SA-365N SPECIFIC FILE (Cont'd)

```

DLQFMP::UVR00      ;**FUSELAGE DELTA LYFT (TAIL-OPP) VS PSWPF MAP**
EXP  PSWPF00      ;MAP ARGUMENT:LOOK UP ROUTINE
      DLQF00      ;INPUT VARIABLE
      DLQFLO      ;OUTPUT VARIABLE
      EXP -20.0,20.0,2.0 ;MAP NAME
                          ;LOWER LIM,UPPER LIM,DELTA

                          ;PRIMARY MAP  PSWPF -20 TO 20 DEG, DELTA=2 DEG
DLQFLO: EXP  -4.43,  -4.06,  -3.53,  -2.79,  -2.13
EXP      -1.52,  -0.99,  -0.57,  -0.25,  -0.04
EXP      0.0,    -0.04,  -0.25,  -0.57,  -0.99
EXP      -1.52,  -2.11,  -2.79,  -3.53,  -4.06
EXP      -4.43

DDQFMP::UVRUVR00  ;** FUSELAGE DELTA DRAG VS PSWPF MAP **
EXP  PSWPF00      ;MAP ARGUMENT:LOOK UP ROUTINE
      DDQF00      ;INPUT VARIABLE
      DDQFLO      ;OUTPUT VARIABLE
      EXP -20.0,20.0,2.0 ;LOW ANGLE MAP NAME
                          ;LOWER LIM,UPPER LIM,DELTA
      DDQFHI      ;HIGH ANGLE MAP NAME
      EXP -100.0,100.0,20.0 ;LOWER LIM,UPPER LIM,DELTA

                          ;PRIMARY MAP - PSWPF FROM -20 TO 20 DEGREES, DELTA = 2
DDQFLO: EXP  15.0,  11.7,  9.2,  7.0,  5.1
EXP      3.6,  2.3,  1.6,  0.8,  0.5
EXP      0.0,  0.5,  0.8,  1.6,  2.3
EXP      3.6,  5.1,  7.0,  9.2,  11.7
EXP      15.0

DDQFHI: EXP  134.0,  129.0,  98.2,  49.1,  15.0
EXP      0.0,  15.0,  49.1,  98.2,  129.0
EXP      134.0

DMQFMP::UVRUVR00  ;** FUS. DELTA PITCH MOMENT VS PSWPF MAP **
EXP  PSWPF00      ;MAP ARGUMENT:LOOK UP ROUTINE
      DMQF00      ;INPUT VARIABLE
      DMQFLD      ;OUTPUT VARIABLE
      EXP -20.0,20.0,2.0 ;LOW ANGLE MAP NAME
                          ;LOWER LIM,UPPER LIM,DELTA
      DMQFHI      ;HIGH ANGLE MAP NAME
      EXP -100.0,100.0,20.0 ;LOWER LIM,UPPER LIM,DELTA

                          ;PRIMARY MAP - PSWPF -20 TO 20 DEG, DELTA=2 DEG
DMQFLD: EXP  61.0,  55.8,  49.1,  39.0,  29.8
EXP      20.9,  13.4,  8.2,  4.1,  1.5
EXP      0.0,  1.5,  4.1,  8.2,  13.4
EXP      20.9,  29.8,  39.0,  49.1,  55.8
EXP      61.0

DMQFHI: EXP  -3.0,  3.0,  23.9,  49.8,  61.0
EXP      0.0,  61.0,  49.8,  23.9,  3.0
EXP      -3.0

YQFMP::UVRUVR00   ;** FUSELAGE SIDEFORCE VS PSWPF MAP **
EXP  PSWPF00      ;MAP ARGUMENT:LOOK UP ROUTINE
      YQF00      ;INPUT VARIABLE
      YQFLO      ;OUTPUT VARIABLE
      EXP -20.0,20.0,2.0 ;LOW ANGLE MAP NAME
                          ;LOWER LIM,UPPER LIM,DELTA
      YQFHI      ;HIGH ANGLE MAP NAME
      EXP -100.0,100.0,20.0 ;LOWER LIM,UPPER LIM,DELTA

```

TABLE G-1. SA-365H SPECIFIC FILE (Cont'd)

```

;LOW ANGLE MAP;PSI -20 TO 20 DEG
YQFLO: EXP -34.7, -29.6, -25.7, -21.7, -17.7
        EXP -14.6, -11.5, -8.4, -5.5, -2.7
        EXP 0.0, 2.7, 5.5, 8.4, 11.5
        EXP 14.6, 17.7, 21.7, 25.7, 29.6
        34.7

; HIGH ANGLE MAP; PSI -100 TO 100 DEG
YQFHI: EXP -3.9, -55.3, -103.0, -78.9, -34.7
        EXP 0.0, 34.7, 78.9, 103.0, 55.3
        3.9

; ** FUSELAGE ROLLING MOMENT VS PSIWF MAP **
RQFRP:: UVRUVR00 ;MAP ARGUMENT:LOOK UP ROUTINE
EX° PSIWF00 ;INPUT VARIABLE
      RQF00 ;OUTPUT VARIABLE
      RQFLO ;LOW ANGLE MAP NAME
EXP -20.0,20.0,2.0 ;LOWER LIM,UPPER LIM,DELTA
      RQFHI ;HIGH ANGLE MAP NAME
EXP-100.0,100.0,20.0 ;LOWER LIM,UPPER LIM,DELTA

;LOW ANGLE MAP:PSIWF FROM -20 TO 20 DEG
RQFLO: EXP -13.3, -12.6, -11.6, -10.2, -9.1
        EXP -7.9, -6.3, -4.9, -3.5, -1.8
        EXP 0.0, 1.8, 3.5, 4.9, 6.3
        EXP 7.9, 9.1, 10.2, 11.6, 12.6
        13.3

;HIGH ANGLE MAP:PSIWF FROM -100 TO 100 DEG
RQFHI: EXP 280.0, 280.0, 210.0, 0.0, -13.3
        EXP 0.0, 13.3, 0.0, -210.0, -280.0
        -280.0

; ** FUSELAGE YAWING MOMENT VS PSIWF MAP **
NQFRP:: UVRUVR00 ;MAP ARGUMENT:LOOK UP ROUTINE
EXP PSIWF00 ;INPUT VARIABLE
      NQF00 ;OUTPUT VARIABLE
      NQFLO ;LOW ANGLE MAP NAME
EXP -20.0,20.0,2.0 ;LOWER LIM,UPPER LIM,DELTA
      NQFHI ;HIGH ANGLE MAP NAME
EXP-100.0,100.0,20.0 ;LOWER LIM,UPPER LIM,DELTA

;LOW ANGLE MAP:PSIWF -20 TO 20 DEG
NQFLO: EXP -85.5, -101.0, -108.0, -107.0, -104.0
        EXP -95.3, -81.3, -63.1, -42.1, -21.7
        EXP 0.0, 21.7, 42.1, 63.1, 81.3
        EXP 95.3, 104.0, 107.0, 108.0, 101.0
        80.5

;HIGH ANGLE MAP:PSIWF -100 TO 100 DEG
NQFHI: EXP 771.0, 421.0, 280.0, 210.0, -85.5
        EXP 0.0, 85.5, -210.0, -280.0, -421.0
        -771.0

;***** ROTOR INTERFERENCE ON THE FUSELAGE (RIPA) *****

; ** ROTOR X-FACTOR ON FUSELAGE MAP **
EXWFMP:: BIV00 ;MAP ARGUMENT:LOOK UP ROUTINE
EXP CHIPR00,AAIPR00 ;INPUT VARIABLE01,INPUT VARIABLE02
      EKWF00 ;OUTPUT VARIABLE
      EXWFLO ;PRIMARY MAP NAME
EXP 0.0,90.0,10.0,^D10 ;LOWER LIM,UPPER LIM,DELTA,0 ITEMS
EXP -10.0,10.0,10.0 ;LOWER LIM,UPPER LIM,DELTA - AAIPR

;CHIPR 0 TO 90 DEG FOR AAIPR -10.0,10 DEG

```

TABLE C-1. SA-365N SPECIFIC FILE (Cont'd)

```

;AA1FMR = -10 OEG
EKWFLO: EXP 0.34, 0.43, 0.54, 0.64, 0.76
        EXP 0.88, 1.01, 1.15, 1.30, 1.50

;AA1FMR = 0 OEG
        EXP 0.11, 0.20, 0.31, 0.43, 0.55
        EXP 0.67, 0.81, 0.96, 1.15, 1.30

;AA1FMR = 10 OEG
        EXP -0.13, -0.03, 0.08, 0.19, 0.31
        EXP 0.44, 0.58, 0.73, 0.90, 1.10

```

```

; ** ROTOR Z-FACTOR ON FUSELAGE MAP **
EZWFMP: BIV88 ;MAP ARGUMENT:LOOK UP ROUTINE
EXP CNIPMR88,AA1FMR88 ;INPUT VARIABLE#1,INPUT VARIABLE#2
      EKZWF88 ;OUTPUT VARIABLE
      EZWFLO ;PRIMARY MAP NAME
EXP 0.0,90.0,10.0,0.0 ;LOWER LIM,UPPER LIM,DELTA,#ITEMS
EXP -10.0,10.0,10.0 ;LOWER LIM,UPPER LIM,DELTA - AA1FMR

```

```

;CHIPMR 0 TO 90 OEG FOR AA1FMR -10,0,10 OEG
;AA1FMR = -10 OEG
EZWFLO: EXP 1.19, 1.17, 1.14, 1.10, 1.07
        EXP 1.03, 0.99, 0.95, 0.89, 0.84

;AA1FMR = 0 OEG
        EXP 1.24, 1.23, 1.23, 1.22, 1.21
        EXP 1.20, 1.18, 1.17, 1.16, 1.14

;AA1FMR = 10 OEG
        EXP 1.24, 1.25, 1.27, 1.28, 1.29
        EXP 1.31, 1.33, 1.35, 1.37, 1.39

```

;***** INPUT PARAMETERS FOR PANEL #1 (RT HORIZONTAL) *****

```

FSP1: 494.0 ; FUSELAGE STATION,INCH
WLP1: 126.0 ; WATERLINE STATION,INCH
HLP1: -30.0 ; BUTTLINE STATION,INCH (+IVE TO PORT)
SAP1: 8.0 ; SURFACE AREA,FT**2
GAMP1: 0.0 ; PANEL ORIENTATION,DEG
IOP1: -1.5 ; PANEL INCIDENCE,DEG
CPI1: 1.0 ; PANEL MEAN AERO CHORD,FT

```

```

; ** HORIZONTAL STABILIZER (RT PANEL) LIFT VS ALFPP1 MAP **
; ** S=8.0 FT**2, AR=5.5, 4412 INVERTED AIRFOIL
CLPIMP: UVRVVR88 ;MAP ARGUMENT:LOOK UP ROUTINE
        ALFPP188 ;INPUT VARIABLE
        CLP188 ;OUTPUT VARIABLE
        CLP1LO ;LOW ANGLE MAP NAME
EXP -24.0,24.0,2.0 ;LOWER LIM,UPPER LIM,DELTA
        CLP1HI ;HIGH ANGLE MAP NAME
EXP -90.0,90.0,15.0 ;LOWER LIM,UPPER LIM,DELTA

```

```

;LOW ANGLE MAP:ALFPP1 -24 TO 24 OEG, DELTA = 2 DEG
CLP1LO: EXP -0.76, -0.90, -1.15, -1.19, -1.17
        EXP -1.13, -1.07, -1.00, -0.86, -0.71
        EXP -0.57, -0.42, -0.27, -0.12, 0.03
        EXP 0.17, 0.30, 0.39, 0.45, 0.49
        EXP 0.51, 0.46, 0.50, 0.55, 0.60

```

```

;HIGH ANGLE MAP:ALFPP1 -90 TO 90 OEG, DELTA = 15 DEG
CLP1HI: EXP 0.0, -0.35, -0.70, -0.80, -0.75
        EXP -0.775, -0.27, 0.45, 0.70, 0.80
        EXP 0.70, 0.35, 0.0

```

; ** HORIZONTAL STABILIZER (RT PANEL) DRAG VS ALFPP1 MAP **

TABLE G-1. SA-365N SPECIFIC FILE (Cont'd)

```

CDPIMP:;UVRUVR44 ;MAP ARGUMENT:LOOK UP ROUTINE
        ALPPP160 ;INPUT VARIABLE
        CDP104 ;OUTPUT VARIABLE
        CDP1LO ;LOW ANGLE MAP NAME
EXP -24.0,24.0,2.0 ;LOWER LIM,UPPER LIM,DELTA
        CDP1HI ;HIGH ANGLE MAP NAME
EXP -90.0,90.0,15.0 ;LOWER LIM,UPPER LIM,DELTA

;LOW ANGLE MAP:ALPPP1 -24 TO 24 DEG, DELTA = 2 DEG
CDP1LO: EXP 0.36, 0.35, 0.34, 0.32, 0.29
        EXP 0.21, 0.13, 0.08, 0.06, 0.045
        EXP 0.03, 0.02, 0.013, 0.009, 0.009
        EXP 0.012, 0.016, 0.022, 0.03, 0.065
        EXP 0.11, 0.15, 0.18, 0.22, 0.26

;HIGH ANGLE MAP:ALPPP1 -90 TO 90 DEG, DELTA = 15 DEG
CDP1HI: EXP 1.20, 1.12, 0.91, 0.65, 0.41
        EXP 0.285, 0.013, 0.185, 0.31, 0.58
        EXP 0.89, 1.12, 1.20

;***** INPUT PARAMETER FOR ROTOR INTERFERENCE ON THE HORIZ.TAIL 41 (MRPA)

EXPIMP:;BIV44 ;** ROTOR X-FACTOR ON HORIZONTAL TAIL MAP **
        ;MAP ARGUMENT:LOOK UP ROUTINE
EXP CHIPMR44,AAIPMR44 ;INPUT VARIABLE#1,INPUT VARIABLE#2
        EKXP104 ;OUTPUT VARIABLE
        EXP1LO ;MAP NAME
EXP 0.0,90.0,10.0,"D10 ;LOWER LIM,UPPER LIM,DELTA,#ITEMS
EXP -10.0,10.0,10.0 ;LOWER LIM,UPPER LIM,DELTA - AAIPMR

;CHIPMR 0 TO 90 DEG FOR AAIPMR -10,0,10 DEG
;AAIPMR = -10 DEG
EXP1LC: EXP 0.14, 0.27, 0.43, 0.60, 0.77
        EXP 0.96, 1.17, 1.41, 1.69, 2.05

;AAIPMR = 0 DEG
EXP 0.24, 0.11, 0.05, 0.21, 0.39
EXP 0.58, 0.80, 1.04, 1.32, 1.62

;AAIPMR = 10 DEG
EXP 0.64, 0.52, 0.39, 0.23, 0.07
EXP 0.11, 0.32, 0.56, 0.84, 1.16

;** ROTOR Z-FACTOR ON HORIZONTAL TAIL MAP **
EZPIMP:;BIV00 ;MAP ARGUMENT:LOOK UP ROUTINE
        ;MAP ARGUMENT:LOOK UP ROUTINE
EXP CHIPMR40,AAIPMR00 ;INPUT VARIABLE#1,INPUT VARIABLE#2
        EKZP100 ;OUTPUT VARIABLE
        EZP1LO ;PRIMARY MAP NAME
EXP 0.0,90.0,10.0,"D10 ;LOWER LIM,UPPER LIM,DELTA,4ITEMS
EXP -10.0,10.0,10.0 ;LOWER LIM,UPPER LIM,DELTA - AAIPMR

;CHIPMR 0 TO 90 DEG FOR AAIPMR -10,0,10 DEG
;AAIPMR = -10 DEG
EZP1LO: EXP 1.58, 1.59, 1.60, 1.60, 1.60
        EXP 1.59, 1.59, 1.57, 1.54, 1.51

;AAIPMR = 0 DEG
EXP 1.53, 1.58, 1.63, 1.67, 1.72
EXP 1.76, 1.80, 1.84, 1.87, 1.90

;AAIPMR = 10 DEG
EXP 1.35, 1.44, 1.53, 1.63, 1.73
EXP 1.83, 1.93, 2.04, 2.15, 2.26

;***** FUSELAGE INTERFERENCE ON THE HORIZ.TAIL 01 (WPPA) *****

```

TABLE G-1. SA-365N SPECIFIC FILE (Cont'd)

```

; ** HORIZONTAL TAIL DYNAMIC PRESSURE RATIO MAP **
QP1RP::UVR00 ;MAP ARGUMENT:LOOK UP ROUTINE
        ALFWF40 ;INPUT VARIABLE
        QP1QWF00 ;OUTPUT VARIABLE
        QP1LO ;MAP NAME
        EXP -20.0,20.0,4.0 ;LOWER LIN,UPPER LIN,DELTA

;ALFWF -20 TO 20 DEG, DELTA = 4 DEG

QP1LO: EXP 1.00, .96, .82, .76, .76
        EXP .76, .79, .82, .85, .96
        EXP 1.00

; ** BOOY DOWNWASH ON HORIZONTAL TAIL MAP **
EPPIRP::UVR00 ;MAP ARGUMENT:LOOK UP ROUTINE
        ALFWF00 ;INPUT VARIABLE
        EPSP100 ;OUTPUT VARIABLE
        EPPILO ;MAP NAME
        EXP -40.0,40.0,5.0 ;LOWER LIN,UPPER LIN,DELTA

;LOW ANGLE MAP:ALFWF -40 TO 40 DEG, DELTA = 5 DEG
EPPILO: EXP 0.0, 1.0, 2.0, 3.0, 4.0
        EXP 3.6, 3.1, 2.6, 2.1, 1.55
        EXP 1.0, 0.5, 0.0, 0.0, 0.0
        EXP 0.0, 0.0

;***** INPUT PARAMETERS FOR PANEL #2 (LT HORIZONTAL) *****
FSP2:: 494.0 ; FUSELAGE STATION, INCH
WLP2:: 126.0 ; WATERLINE STATION, INCH
BLP2:: 30.0 ; BUTLINE STATION, INCH (+IVE TO PORT)
SAP2:: 8.0 ; SURFACE AREA FT**2
GAMP2:: 0.0 ; PANEL ORIENTATION, DEG
IOP2:: -1.5 ; TAIL INCIDENCE, DEG
CP2:: 1.0 ; PANEL MEAN AERO CHORD, FT

; ** HORIZONTAL STABILIZER (LT PANEL) LIFT VS ALPPP2 MAP **
; ** S=5.0 FT**2, AR=5.5, 4412 INVERTEO AIRFOIL
CLP2NP::UVRUVR00 ;MAP ARGUMENT:LOOK UP ROUTINE
        ALPPP200 ;INPUT VARIABLE
        CLP200 ;OUTPUT VARIABLE
        CLP1LO ;LOW ANGLE MAP NAME
        EXP -24.0,24.0,2.0 ;LOWER LIN,UPPER LIN,DELTA
        CLP1RI ;HIGH ANGLE MAP NAME
        EXP -90.0,90.0,15.0 ;LOWER LIN,UPPER LIN,DELTA

; ** HORIZONTAL STABILIZER (LT PANEL) DRAG VS ALPPP2 MAP **
COP2NP::UVRUVR00 ;MAP ARGUMENT:LOOK UP ROUTINE
        ALPPP200 ;INPUT VARIABLE
        COP200 ;OUTPUT VARIABLE
        COP1LO ;LOW ANGLE MAP NAME
        EXP -24.0,24.0,2.0 ;LOWER LIN,UPPER LIN,DELTA
        COP1RI ;HIGH ANGLE MAP NAME
        EXP -90.0,90.0,15.0 ;LOWER LIN,UPPER LIN,DELTA

;***** INPUT PARAMETER FOR ROTOR INTERFERENCE ON THE HORIZ.TAIL #2 (NRPA)

EXP2NP::BIV60 ; ** ROTOR X-FACTOR ON HORIZONTAL TAIL MAP **
        EXP CRIPNR00, AALFNR00 ;MAP ARGUMENT:LOOK UP ROUTINE
        ERXP200 ;INPUT VARIABLE#01, INPUT VARIABLE#02
        EXP1LO ;OUTPUT VARIABLE
        EXP1LO ;MAP NAME
        EXP 0.0,90.0,10.0,0.010 ;LOWER LIN,UPPER LIN,DELTA, #ITENS
        EXP -10.0,10.0,10.0 ;LOWER LIN,UPPER LIN,DELTA - AALFNR

; ** ROTOR B-FACTOR ON HORIZONTAL TAIL MAP **

```

TABLE G-1. SA-365N SPECIFIC FILE (Cont'd)

```

EZP2MP::BIV00 ;MAP ARGUMENT:LOOK UP ROUTINE
EXP CHIPMR00,AAIPMR00 ;INPUT VARIABLE#1,INPUT VARIABLE#2
EKZP200 ;OUTPUT VARIABLE
EZPILO ;MAP NAME
ERP 0.0,90.0,10.0,"D10 ;LOWER LIM,UPPER LIM,DELTA,#ITEMS
ERP -10.0,10.0,10.0 ;LOWER LIM,UPPER LIM,DELTA - AAIPMR

;***** FUSELAGE INTERPERNCE ON THE HORIZ.TAIL #2 (NPPA) *****

QP2MP::UVR00 ;** HORIZONTAL TAIL DYNAMIC PRESSURE RATIO MAP**
ALPWF00 ;MAP ARGUMENT:LOOK UP ROUTINE
QP2QWF00 ;INPUT VARIABLE
QPILO ;OUTPUT VARIABLE
;MAP NAME
EXP -20.0,20.0,4.0 ;LOWER LIM,UPPER LIM,DELTA

EPI2MP::UVR00 ;** BODY DOWNWASH ON HORIZONTAL TAIL MAP **
ALPWF00 ;MAP ARGUMENT:LOOK UP ROUTINE
EPSP200 ;INPUT VARIABLE
EPILO ;OUTPUT VARIABLE
;MAP NAME
EXP -40.0,40.0,5.0 ;LOWER LIM,UPPER LIM,DELTA

;***** INPUT PARAMETERS FOR PANEL #3 (VERTICAL TAIL) *****

PSP3:: 550.0 ; FUSELAGE STATION,INCH
WLP3:: 184.0 ; WATERLINE STATION,INCH
BLP3:: 0.0 ; BUTTLINE STATION,INCH (+IVE TO PORT)
SAP3:: 20.0 ; SURFACE AREA,FT**2
GAMP3:: -90.0 ; PANEL ORIENTATION,DEG
IOP3:: -3.5 ; PANEL INCIDENCE,DEG
CP3:: 1.0 ; PANEL MEAN AERO CHORD,FT

;** S-76 VERTICAL STABILIZER LIPT VS ALPPP3 MAP **
CLP3MP::UVRUVR00 ;MAP ARGUMENT:LOOK UP ROUTINE
ALPPP300 ;INPUT VARIABLE
CLP300 ;OUTPUT VARIABLE
CLP3LO ;PRIMARY (BASIC) MAP NAME
ERP -24.0,24.0,2.0 ;LOWER LIM,UPPER LIM,DELTA
CLP3HI ;HIGH ANGLE MAP NAME
ERP -90.0,90.0,15.0 ;LOWER LIM,UPPER LIM,DELTA

;LOW ANGLE MAP:ALPPP3 -24 TO 24 DEG, DELTA = 2 DEG
CLP3LO: ERP -0.76, -0.95, -0.89, -0.82, -0.75
ERP -0.68, -0.60, -0.52, -0.44, -0.36
ERP -0.28, -0.20, -0.12, -0.04, 0.04
ERP 0.12, 0.195, 0.27, 0.35, 0.43
ERP 0.51, 0.59, 0.66, 0.73, 0.66

;HIGH ANGLE MAP:ALPPP3 -90 TO 90 DEG, DELTA = 15 DEG
CLP3HI: ERP 0.0, -0.35, -0.70, -0.77, -0.70
ERP -0.85, -0.12, 0.60, 0.70, 0.77
ERP 0.70, 0.35, 0.0

;** S-76 VERTICAL STABILIZER DRAG VS ALPPP3 MAP
CDP3MP::UVRUVR00 ;MAP ARGUMENT:LOOK UP ROUTINE
ALPPP300 ;INPUT VARIABLE
CDP300 ;OUTPUT VARIABLE
CDP3LO ;LOW ANGLE MAP NAME
EXP -24.0,24.0,2.0 ;LOWER LIM,UPPER LIM,DELTA
CDP3HI ;HIGH ANGLE MAP NAME
EXP -90.0,90.0,15.0 ;LOWER LIM,UPPER LIM,DELTA

;LOW ANGLE MAP:ALPPP3 -24 TO 24 DEG, DELTA = 2 DEG
CDP3LO: ERP 0.260, 0.215, 0.175, 0.145, 0.119
EXP 0.077, 0.077, 0.061, 0.048, 0.034

```

TABLE G-1. SA-365N SPECIFIC FILE (Cont'd)

```

EXP      0.023,    0.016,    0.011,    0.009,    0.009
EXP      0.012,    0.017,    0.024,    0.034,    0.047
EXP      0.063,    0.080,    0.110,    0.150,    0.210

;HIGH ANGLE MAP:ALPPP3 -90 TO 90 DEG, DELTA = 15 DEG
CDP3HI: EXP      1.20,    1.12,    0.89,    0.58,    0.31
EXP      0.185,    0.011,    0.135,    0.26,    0.54
EXP      0.06,    1.12,    1.20

;***** MOTOR INTERPERENCE ON THE VERTICAL TAIL #3 (MRPA) *****

; ** MOTOR X-FACTDR ON VERTICAL TAIL MAP **
EXP3NP::BIV00 ;MAP ARGUMENT:LOOK UP ROUTINE
EXP      CHIPMR00,AAIPMR00 ;INPUT VARIABLE#1,INPUT VARIABLE#2
EKXP300 ;OUTPUT VARIABLE
EXP3 ;MAP NAME
EXP 0.0,90.0,10.0,^D10 ;LOWER LIM,UPPER LIM,DELTA,#ITEMS
EXP -10.0,10.0,10.0 ;LOWEN LIM,UPPER LIM,DELTA - AAIPMR

;CHIPMR -20 TO 100 DEG PDM AAIPMR -10,0,10 DEG
;AAIPMR = -10 DEG
EXP3: EXP      -0.47,    0.20,    0.38,    0.57,    0.78
EXP      1.00,    1.24,    1.50,    1.82,    2.20

;AAIPMR = 0 DEG
EXP      -0.65,    -0.78,    -0.93,    0.11,    0.34
EXP      0.59,    0.86,    1.15,    1.49,    1.86

;AAIPMR = 10 DEG
EXP      -0.84,    -0.88,    -0.92,    -0.94,    -0.94
EXP      -0.90,    -0.81,    -0.66,    -0.43,    -0.10

; ** RDTOR I-FACTOR ON VERTICAL TAIL MAP **
E2P3NP::BIV00 ;MAP ARGUMENT:LOOK UP ROUTINE
EXP      CHIPMR00,AAIPMR00 ;INPUT VARIABLE#1,INPUT VARIABLE#2
EK2P300 ;DUTPUT VARIABLE
E2P3LO ;MAP NAME
EXP 0.0,90.0,10.0,^D10 ;LOWER LIM,UPPER LIM,DELTA,#ITEMS
EXP -10.0,10.0,10.0 ;LOWEN LIM,UPPER LIM,DELTA - AAIPMR

;CHIPMR 0 TO 90 DEG PDR AAIPMR -10,0,10 DEG
;AAIPMR = -10 DEG
E2P3LD: EXP      -0.15,    1.75,    1.77,    1.78,    1.78
EXP      1.78,    1.77,    1.76,    1.75,    1.74

;AAIPMR = 0 DEG
EXP      -0.24,    -0.10,    0.03,    1.97,    2.04
EXP      2.09,    2.14,    2.18,    2.20,    2.20

;AAIPMR = 10 DEG
EXP      0.08,    0.22,    0.39,    0.59,    0.82
EXP      1.08,    1.38,    1.71,    2.07,    2.43

;***** FUSELAGE INTERPERENCE ON THE VERTICAL TAIL #3 (WPPA) *****

; ** S-76 VERTICAL TAIL DYNAMIC PRESSURE RATIO MAP **
OP3AP::RIV00 ;MAP ARGUMENT:LOOK UP ROUTINE
EXP      PSINP00,ALFNP00 ;INPUT VARIABLE#1,INPUT VARIABLE#2
OP3QNP00 ;OUTPUT VARIABLE
OP3LO ;MAP NAME
EXP -20.0,20.0,4.0,13 ;LOWER LIM,UPPER LIM,DELTA,#ITEMS
EXP -10.0,10.0,5.0 ;LOWEN LIM,UPPER LIM,DELTA - ALFNP

;LOW ANGLE MAP:PSINP -20 TO 20 DEG PDR ALFNP -10,0,10
;ALFNP = -10 DEG
OP3LO: EXP      1.000,    0.980,    0.950,    0.920,    0.880

```

TABLE G-1. SA-365W SPECIFIC FILE (Cont'd)

EXP	0.825, 1.00	0.880,	0.920,	0.950,	0.980
	;ALFMP = -5 DEG				
EXP	1.000,	0.970,	0.910,	0.880,	0.810
EXP	0.786, 1.000	0.810,	0.880,	0.910,	0.970
	;ALFMP = 0 DEG				
EXP	1.000,	0.960,	0.890,	0.850,	0.770
EXP	0.750, 1.00	0.770,	0.850,	0.890,	0.960
	;ALFMP = 5 DEG				
EXP	1.000,	0.940,	0.850,	0.790,	0.720
EXP	0.710, 1.000	0.720,	0.790,	0.850,	0.940
	;ALFMP = 10 DEG				
EXP	1.000,	0.910,	0.820,	0.730,	0.680
EXP	0.670, 1.00	0.680,	0.730,	0.820,	0.910

;***** INPUT PARAMETERS FOR PANEL #4 (PAN BASE) *****

```

PBP4:: 554.7 ; FUSELAGE STATION, INCH
WLP4:: 136.1 ; WATERLINE STATION, INCH
RLP4:: 0.0 ; RUTTLINE STATION, INCH (+IVE TO PORT)
SAP4:: 17.13 ; SURFACE AREA, FT**2
GAMP4:: -90.0 ; PANEL ORIENTATION, DEG
IOP4:: 2 ; PANEL INCIDENCE, DEG
CP4:: 1.0 ; PANEL MEAN AERO CHORD, PT
    
```

```

CLP4NP:: UVRUVR00 ;** PAN BASE LIFT VS ALPPP4 MAP **
ALPPP400 ;MAP ARGUMENT: LOOK UP ROUTINE
CLP4LO ;INPUT VARIABLE
CLP4HI ;OUTPUT VARIABLE
EXP -20.0,20.0,2.0 ;LOW ANGLE MAP NAME
EXP-100.0,100.0,20.0 ;HIGH ANGLE MAP NAME
    
```

```

;LOW ANGLE MAP:ALPPP4 -20 TO 20 DEG, DELTA = 2 DEG
CLP4LO: EXP -0.165, -0.160, -0.154, -0.146, -0.125
EXP -0.104, -0.082, -0.061, -0.040, -0.019
EXP 0.003, 0.024, 0.045, 0.066, 0.088
EXP 0.109, 0.130, 0.118, 0.146, 0.157
EXP 0.165
    
```

```

;HIGH ANGLE MAP:ALPPP4 -100 TO 100 DEG, DELTA = 20 DEG
CLP4HI: EXP 0.024, -0.024, -0.071, -0.118, -0.165
EXP 0.003, 0.165, 0.118, 0.071, 0.024
EXP -0.024
    
```

```

;** PAN BASE DRAG VS ALPPP4 MAP
CDP4NP:: UVRUVR00 ;MAP ARGUMENT: LOOK UP ROUTINE
ALPPP400 ;INPUT VARIABLE
CDP4LO ;OUTPUT VARIABLE
CDP4HI ;LOW ANGLE MAP NAME
EXP -20.0,20.0,2.0 ;LOWER LIN, UPPER LIN, DELTA
EXP-100.0,100.0,20.0 ;HIGH ANGLE MAP NAME
    
```

```

;LOW ANGLE MAP:ALPPP4 -24 TO 24 DEG, DELTA = 2 DEG
CDP4LO: EXP 0.160, 0.141, 0.130, 0.124, 0.119
EXP 0.115, 0.112, 0.109, 0.107, 0.106
    
```


TABLE G-1. SA-365N SPECIFIC FILE

EXP	0.105,	0.106,	0.107,	0.109,	0.112
EXP	0.115,	0.119,	0.124,	0.130,	0.141
EXP	0.160				

CDP4HI: EXP HIGH ANGLE MAP:ALFPP4 -100 TO 100 DEG, DELTA = 20 DEG
EXP .596, .532, .476, .286, .160
EXP .105, .160, .286, .476, .532
EXP .596

;***** ROTOR INTERFERENCE ON THE FAN BASE 84 (MRPA) *****

;** ROTOR X-FACTOR ON FAN BASE MAP **
EXP4MP: BIV88 ;MAP ARGUMENT:LOOK UP ROUTINE
EXP CHIPMR88,AAIFMR88 ;INPUT VARIABLE#1,INPUT VARIABLE#2
EXP488 ;OUTPUT VARIABLE
EXP4 ;LOW ANGLE MAP NAME
EXP 0.0,90.0,10.0,"D10 ;LOWER LIM,UPPER LIM,DELTA,#ITEMS
EXP -10.0,10.0,10.0 ;LOWER LIM,UPPER LIM,DELTA - AAIFMR

;CHIPMR 0 TO 90 DEG FOR AAIFMR -10,0,10 DEG
;AAIFMR = -10 DEG

EXP4: EXP	0.17,	0.32,	0.50,	0.68,	0.87
EXP	1.08,	1.30,	1.55,	1.84,	2.20

;AAIFMR = 0 DEG

EXP	-0.41,	-0.34,	0.11,	0.30,	0.50
EXP	0.72,	0.96,	1.22,	1.49,	1.75

;AAIFMR = 10 DEG

EXP	-0.54,	-0.66,	-0.81,	-0.93,	0.06
EXP	0.30,	0.56,	0.84,	1.16,	1.47

;** ROTOR Z-FACTOR ON FAN BASE MAP **
EXP4MP: BIV88 ;MAP ARGUMENT:LOOK UP ROUTINE
EXP CHIPMR88,AAIFMR88 ;INPUT VARIABLE#1,INPUT VARIABLE#2
EXP488 ;OUTPUT VARIABLE
EXP4LO ;LOW ANGLE MAP NAME
EXP 0.0,90.0,10.0,"D10 ;LOWER LIM,UPPER LIM,DELTA,#ITEMS
EXP -10.0,10.0,10.0 ;LOWER LIM,UPPER LIM,DELTA - AAIFMR

;CHIPMR 0 TO 90 DEG FOR AAIFMR -10,0,10 DEG
;AAIFMR = -10 DEG

EXP4LO: EXP	1.72,	1.74,	1.74,	1.73,	1.72
EXP	1.71,	1.69,	1.66,	1.63,	1.60

;AAIFMR = 0 DEG

EXP	-0.24,	0.71,	1.84,	1.88,	1.91
EXP	1.94,	1.97,	1.99,	2.01,	2.03

;AAIFMR = 10 DEG

EXP	-0.27,	-0.18,	-0.03,	0.22,	2.08
EXP	2.18,	2.26,	2.33,	2.41,	2.49

;***** FUSELAGE INTERFERENCE ON THE FAN BASE 84 (MPPA) *****

;** FAN BASE DYNAMIC PRESSURE RATIO MAP **
EXP4MP: UVR88 ;MAP ARGUMENT:LOOK UP ROUTINE
EXP PSIMF88 ;INPUT VARIABLE
EXP4QMF88 ;OUTPUT VARIABLE
EXP4LO ;PRIMARY MAP NAME
EXP -20.0,20.0,4.0 ;LOWER LIM,UPPER LIM,DELTA

;LOW ANGLE MAP:PSIMF -20 TO 20 DEG, DELTA=4 DEG

EXP4LO: EXP	1.00,	0.9	0.85,	0.82,	0.71
EXP	0.70,	0.71,	0.81,	0.85,	0.95
	1.00				

TABLE G-1. SA-365N SPECIFIC FILE (Cont'd)

```

***** INPUT PARAMETERS FOR PANEL #5 (RT ENDPLATE) *****

FSP5:: 495.0 ; FUSELAGE STATION, INCH
WLP5:: 126.0 ; WATERLINE STATION, INCH
BLP5:: -63.2 ; BUTTLINE STATION, INCH (+IVE TO PORT)
SAP5:: 1.0 ; SURFACE AREA, FT**2
GAMP5:: 90.0 ; PANEL ORIENTATION, DEG
IOP5:: 6.0 ; PANEL INCIDENCE, DEG
CP5:: 1.0 ; PANEL MEAN AERO CHORD, FT

; ** ENDPLATE (RT PANEL) LIFT VS ALFPP5 MAP **
CLPSMP:: UVRUVR## ; MAP ARGUMENT: LOOR UP ROUTINE
ALFPP5## ; INPUT VARIABLE
CLPS## ; OUTPUT VARIABLE
CLPSLO ; LOW ANGLE MAP NAME
EXP -30.0, 30.0, 5.0 ; LOWER LIM, UPPER LIM, DELTA
CLPSHI ; HIGH ANGLE MAP NAME
EXP -90.0, 90.0, 30.0 ; LOWER LIM, UPPER LIM, DELTA

; LOW ANGLE MAP: ALFPP5 -30 TO 30 DEG, DELTA = 5 DEG
CLPSLO: EXP -0.65, -0.93, -1.01, -0.91, -0.65
EXP -0.33, 0.0, 0.33, 0.65, 0.91
EXP 1.01, 0.93, 0.65

; HIGH ANGLE MAP: ALFPP5 -90 TO 90 DEG, DELTA = 15 DEG
CLPSHI: EXP 0.0, -0.33, -0.65, 0.0, 0.65
EXP 0.33, 0.0

; ** ENDPLATE (RT PANEL) DRAG VS ALFPP5 MAP **
CDPSMP:: UVRUVR## ; MAP ARGUMENT: LOOR UP ROUTINE
ALFPP5## ; INPUT VARIABLE
CDPS## ; OUTPUT VARIABLE
CDPSLO ; LOW ANGLE MAP NAME
EXP -30.0, 30.0, 5.0 ; LOWER LIM, UPPER LIM, DELTA
CDPSHI ; HIGH ANGLE MAP NAME
EXP -90.0, 90.0, 15.0 ; LOWER LIM, UPPER LIM, DELTA

; LOW ANGLE MAP: ALFPP5 -30 TO 30 DEG, DELTA = 5 DEG
CDPSLO: EXP 0.49, 0.37, 0.29, 0.19, 0.06
EXP 0.023, 0.013, 0.023, 0.06, 0.19
EXP 0.29, 0.37, 0.49

; HIGH ANGLE MAP: ALFPP5 -90 TO 90 DEG, DELTA = 30 DEG
CDPSHI: EXP 1.20, 1.16, 1.04, 0.85, 0.4
EXP 0.19, 0.013, 0.19, 0.49, 0.85
EXP 1.04, 1.16, 1.20

***** INPUT PARAMETER FOR ROTOR INTERFERENCE ON THE ENDPLATE #5 (MRPA)

; ** ROTOR R-FACTOR ON ENDPLATE MAP **
ZXP5MP:: BIV## ; MAP ARGUMENT: LOOK UP ROUTINE
EXP CHIPMR##, AAIFMR## ; INPUT VARIABLE#1, INPUT VARIABLE#2
EKXP5## ; OUTPUT VARIABLE
EXP1LO ; MAP NAME
EXP 0.0, 90.0, 10.0, 'D10 ; LOWER LIM, UPPER LIM, DELTA, #ITERS
EXP -10.0, 10.0, 10.0 ; LOWER LIM, UPPER LIM, DELTA - AAIFMR

; ** ROTOR L-FACTOR ON ENDPLATE MAP **
LZXP5MP:: BIV## ; MAP ARGUMENT: LOOK UP ROUTINE
EXP CNIPMR##, AAIFMR## ; INPUT VARIABLE#1, INPUT VARIABLE#2
EKLP5## ; OUTPUT VARIABLE
EXP1LO ; PRIMARY (BASIC) MAP NAME
EXP 0.0, 90.0, 10.0, 'D10 ; LOWER LIM, UPPER LIM, DELTA, #ITERS
EXP -10.0, 10.0, 10.0 ; LOWER LIM, UPPER LIM, DELTA - AAIFMR

```

TABLE G-1. SA-365N SPECIFIC FILE (Cont'd)

```

;***** FUSELAGE INTERFERANCE ON DE ENDPLATE 85 (WPPA) *****

QPSMP:: UVR00          ;** ENDPLATE DYNAMIC PRESSURE RATIO MAP**
        PSIMF00       ;MAP ARGUMENT:LOOK UP ROUTINE
        QPSQMF00     ;INPUT VARIABLE
        QP5LO        ;OUTPUT VARIABLE
        EXP -30.0,30.0,5.0 ;PRIMARY MAP NAME
        ;LOWER LIM,UPPER LIM,DELTA

QPSLO: EXP          ;PSIMF -30 TO 30 DEG, DELTA = 5 DEG
        EXP          1.00, 1.00, 1.00, 1.00, 1.00
        EXP          1.00, 1.00, 1.00, 0.87, 0.75
        EXP          0.65, 0.57, 0.52

;***** INPUT PARAMETERS FOR PANEL 06 (LT ENDPLATE) *****

PSP6:: 495.0          ; FUSELAGE STATION,INCR
WLP6:: 126.0          ; WATERLINE STATION,INCH
BLP6:: 63.2           ; BUTTLINE STATION,INCH (+IVE TO PORT)
SAP6:: 10.0           ; SURFACE AREA FT**2
GAMP6:: 90.0          ; PANEL ORIENTATION,DEG
IOP6:: 6.0            ; TAIL INCIDENCE,DEG
CP6:: 1.0             ; PANEL MEAN AERO CHORD,FT

;** ENDPLATE (LT PANEL) LIFT VS ALFPP6 MAP **
;** S=8.0 FT**2, AR=5.5, 4412 INVERTED AIRFOIL
CLP6MP::UVRUVR00     ;MAP ARGUMENT:LOOK UP ROUTINE
        ALFPP600     ;INPUT VARIABLE
        CLP600       ;OUTPUT VARIABLE
        CLP5LO       ;PRIMARY (BASIC) MAP NAME
        EXP -30.0,30.0,5.0 ;LOWER LIMIT, UPPER LIMIT,DELTA - LOW ANGLE MAP
        CLP5RI       ;SECONDARY (HIGH ANGLE) MAP NAME
        EXP -90.0 90.0,30.0 ;LOWER LIMIT, UPPER LIMIT, DELTA - HI ANGLE MAP

;** ENDPLATE (LT PANEL) DRAG VS ALFPP6 MAP **
CDP6MP::UVRUVR00     ;MAP ARGUMENT:LOOK UP ROUTINE
        ALFPP600     ;INPUT VARIABLE
        CDP600       ;OUTPUT VARIABLE
        CDP5LO       ;PRIMARY (BASIC) MAP NAME
        EXP -30.0,30.0,5.0 ;LOWER LIMIT, UPPER LIMIT, DELTA - LOW ANGLE MAP
        CDP5HI       ;SECONDARY (HIGH ANGLE) MAP NAME
        EXP -90.0,90.0,15.0 ;LOWER LIMIT, UPPER LIMIT, DELTA - RI ANGLE MAP

;***** INPUT PARAMETER FOR ROTOR INTERFERENCE ON ENDPLATE 06 (MRPA)

EXP6MP::CONST00      ;** ROTOR X-FACTOR ON ENDPLATE MAP **
        ERXP100     ;MAP ARGUMENT:LOOK UP ROUTINE
        ERXP600     ;INPUT VARIABLE
        ;OUTPUT VARIABLE

EZP6MP::CONST00      ;** ROTOR Z-FACTOR ON ENDPLATE MAP **
        ERZP100     ;MAP ARGUMENT:LOOK UP ROUTINE
        ERZP600     ;INPUT VARIABLE
        ;OUTPUT VARIABLE

;***** FUSELAGE INTERFERANCE ON ENDPLATE 06 (WPPA) *****

QP6MP:: UVR00          ;** ENDPLATE DYNAMIC PRESSURE RATIO MAP**
        PSIMF00       ;MAP ARGUMENT:LOOK UP ROUTINE
        QP6QMF00     ;INPUT VARIABLE
        QP0LO        ;OUTPUT VARIABLE
        EXP -30.0,30.0,5.0 ;PRIMARY (BASIC) MAP NAME
        ;LOWER LIMIT, UPPER LIMIT, DELTA

QP6LO: EXP          ;PSIMF -30 TO 30 DEG, DELTA = 5 DEG
        EXP          0.52, 0.57, 0.65, 0.75, 0.87

```

TABLE G-1. SA-365N SPECIFIC FILE (Cont'd)

```

EXP      1.00,      1.00,      1.00,      1.00,      1.00
EXP      1.00,      1.00,      1.00
;***** INPUT PARAMETERS FOR TAIL ROTOR (#E) - (FENESTRON) *****
RTR:: 1.805 ;RAIUS,PT
OMEGTR::383.8 ;TRIM ROTATIONAL RATE,RAD/SEC (100% NR)
BTR:: 11.0 ;ACTUAL NUMBER OF BLADES
FSTR:: 554.7 ;FUSELAGE STATION,IN
WLTR:: 136.1 ;WATERLINE STATION,IN
BLTR:: 0.0 ;OUTLINE STATION,IN (+IVE TO PORT)
TWSTR::-13.2 ;BLADE TWIST,ORIGIN CENTER OF ROTATION,OEG
BIASRTR:: 5.87 ;BLADE PITCH CORRECTION FOR N.L.TWIST(NEG REDUCES PITCH)
GAMTR:: -90.0 ;TAIL ROTOR CANT ANGLE,DEG
CHROTR::.1641 ;BLADE CHORD,FT
ATR:: 5.73 ;BLADE LIFT CURVE SLOPE,1/RAD
BTLTR:: .99 ;BLADE TIP LOSS FACTOR
COTR:: 0.0 ;TAIL ROTOR HEAD DRAG,FT**2 ( GOES NOWHERE IN TRE )
ETR:: 0.4889 ;RATIO OF FAN TO HUB DIAMETERS
CTMXTR::0.0896 ;ISOLATED FAN MAXIMUM THRUST COEFFICIENT
CTMNRTR::-0.0378 ;ISOLATED FAN MINIMUM THRUST COEFFICIENT
TAUDTR:: 0.1 ;TIME CONSTANT FOR LAGGED TAIL ROTOR DOWNWASH
ORO0TR::.0012 ;BLADE SECTION DRAG COEFFICIENTS WHERE:
ORD1TR::-0.0169 ; CO=ORD0TR+ORD1TR*ALPHA+OPD2TR*ALPHA**2
ORO2TR::0.3096 ; (ALPHA IS IN RADIANS)
SWRLTR:: 0.0 ;1.=INCLUDE SWIRL EFFECT, 0.=NEGLECT IT
IBTR:: 1.0 ;FAN POLAR MOMENT OF INERTIA (SLUGS-FT**2)
RINSW:: 0.5 ; SOME SORT OF SWITCH (SET TO 0.5 IN FIF5A.MAC{67,160})
RAMREC:: 0.45 ; PERCENT RAM RECOVERY
SDUCTX:: 7.785 ; DUCT EXIT AREA
RMU:: 0.0 ; FACTOR ON THE MU EFFECT IN BAILEY COEFFICIENTS
OQTR:: 1.5 ; EQUIVALENT FLAT PLATE RAM DRAG IN FORWARD FLIGHT(FT**2)
;*****
;
; R C O L M P ... INLET CENTER OF LIFT/FAN RAD @ MAX MACH
;
RCOLMP::UVR## ; UNIVARIATE MAP TYPE
VTR## ; INPUT: VTR, FT/SEC
RCOL## ; OUTPUT
RCOLO ; LABEL OF MAP DATA START
EXP 0.0,300.0,100.0 ; LOWER LIM,UPPER LIM,DELTA VTR RANGE
;
; DATA FOR KCOL = CVR( VTR )
;
RCOLO: .P 0.0, 0.75, .25, 0.75
;***** ROTOR INTERFERENCE ON TAIL ROTOR (MRFA) *****
;
; ** ROTOR X-FACTOR ON TAIL ROTOR MAP **
EXTRMP::CONST## ;MAP ARGUMENT:LOOK UP ROUTINE
EKXP4## ;INPUT VARIABLE
ERXTR## ;OUTPUT VARIABLE
;
EZTRMP::CONST## ;MAP ARGUMENT:LOOK UP ROUTINE
EKZP4## ;INPUT VARIABLE
ERZTR## ;OUTPUT VARIABLE
;***** FUSELAGE INTERFERENCE ON THE TAIL ROTOR (MPPA) *****
;
; ** TAIL ROTOR DYNAMIC PRESSURE RATIO MAP **
QTRMP:: CONST## ;MAP ARGUMENT:LOOK UP ROUTINE
QP4QWF ;INPUT VARIABLE
QTRQWF## ;OUTPUT VARIABLE
;***** VERTICAL TAIL INTERFERENCE ON TAIL ROTOR INFLOW *****

```

TABLE G-1. SA-365N SPECIFIC FILE (Cont'd)

```

; ** TAIL ROTOR BLOCKAGE NOT USED FOR FANTAIL
VBVTTR: 0.0 ; AIRSPEED BREAK PT. - NO BLOCKAGE ABOVE, RT.
KBVTTR: 1.0 ; TAIL ROTOR BLOCKAGE COEF. AT HOVER

; ***** INPUT PARAMETERS FOR EQUATIONS OF MOTION (#A) *****

PSCG: 300.0 ; FUSELAGE STATION, OF C.G., INCH
WLCC: 140.0 ; WATERLINE STATION OF C.G., INCH
BLCC: 0.0 ; BUTTLINE STATION OF C.G., INCH (+IVE TO PORT)

WEIGHT: 8750.0 ; AIRCRAFT GROSS WEIGHT, LBS.
IX: 2444.0 ; INERTIA ABOUT BODY X-AXIS, SLUG-FT**2
IY: 15130.0 ; INERTIA ABOUT BODY Y-AXIS, SLUG-FT**2
IZ: 13490.0 ; INERTIA ABOUT BODY Z-AXIS, SLUG-FT**2
IXZ: 726.0 ; CROSS COUPLING INERTIA, SLUG-FT**2
IYZ: 0.0
IXY: 0.0

```

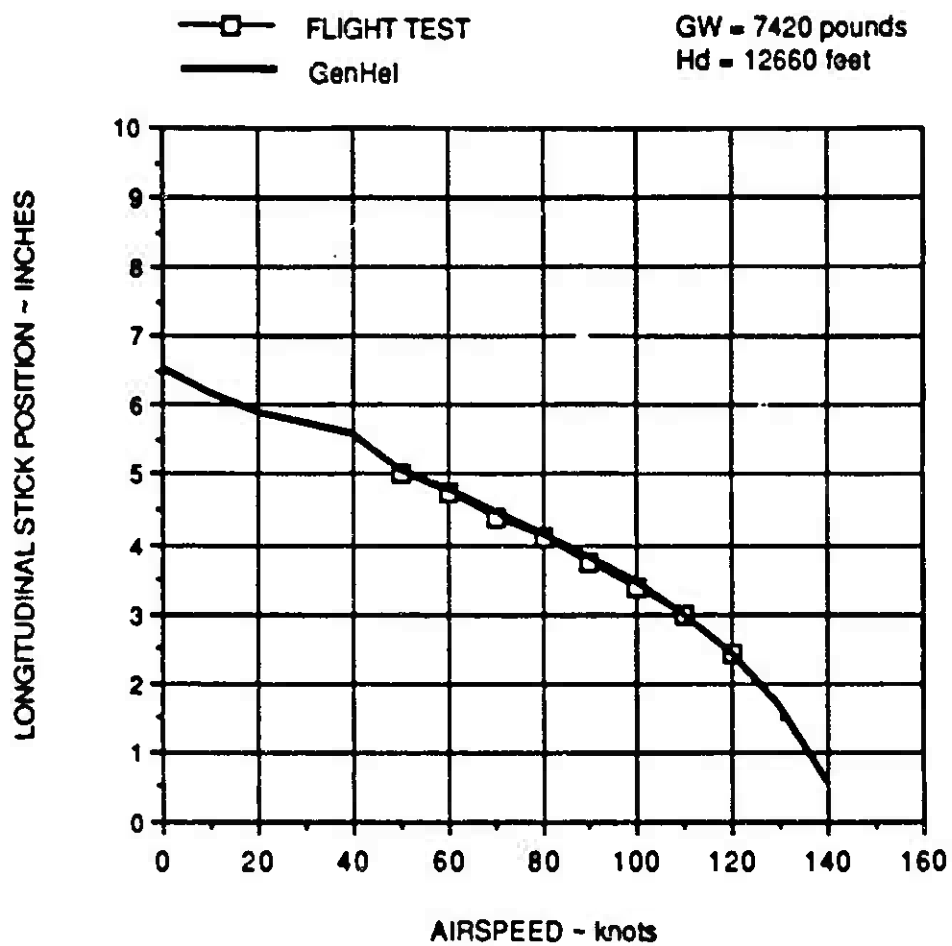



Figure C-2. SA-365N Longitudinal Stick Correlation

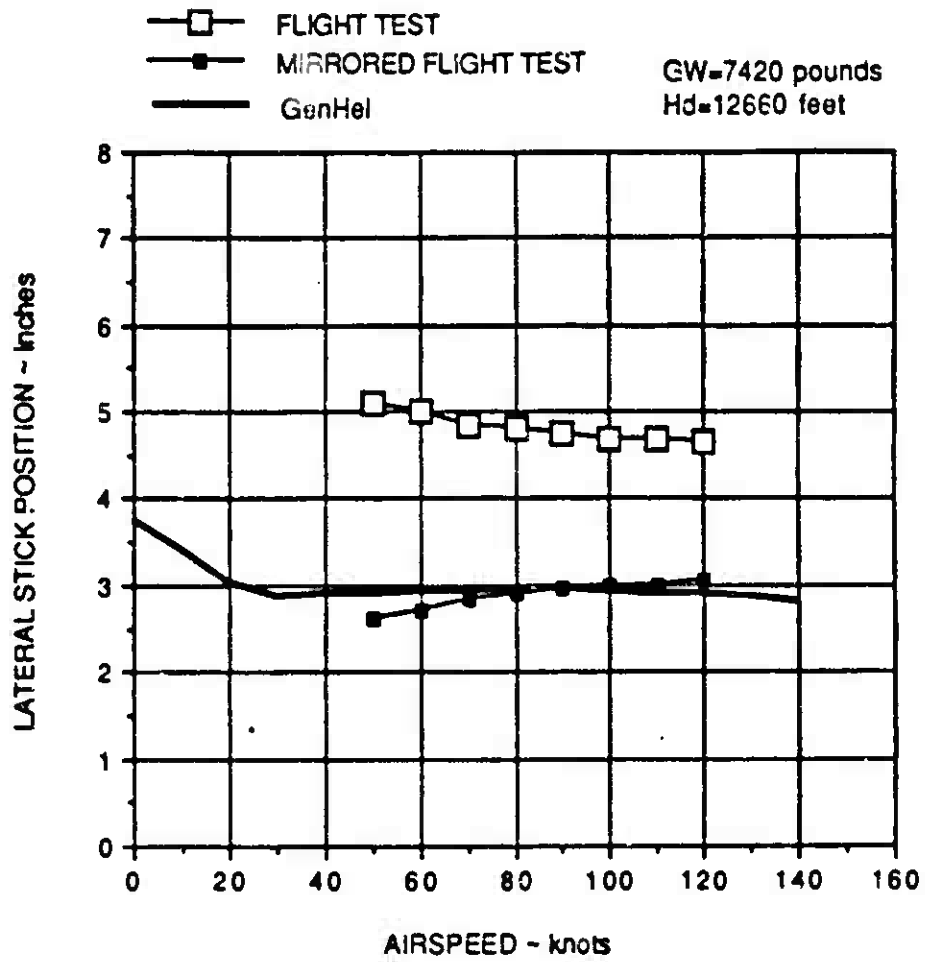


Figure C-3. SA-365N Lateral Stick Correlation

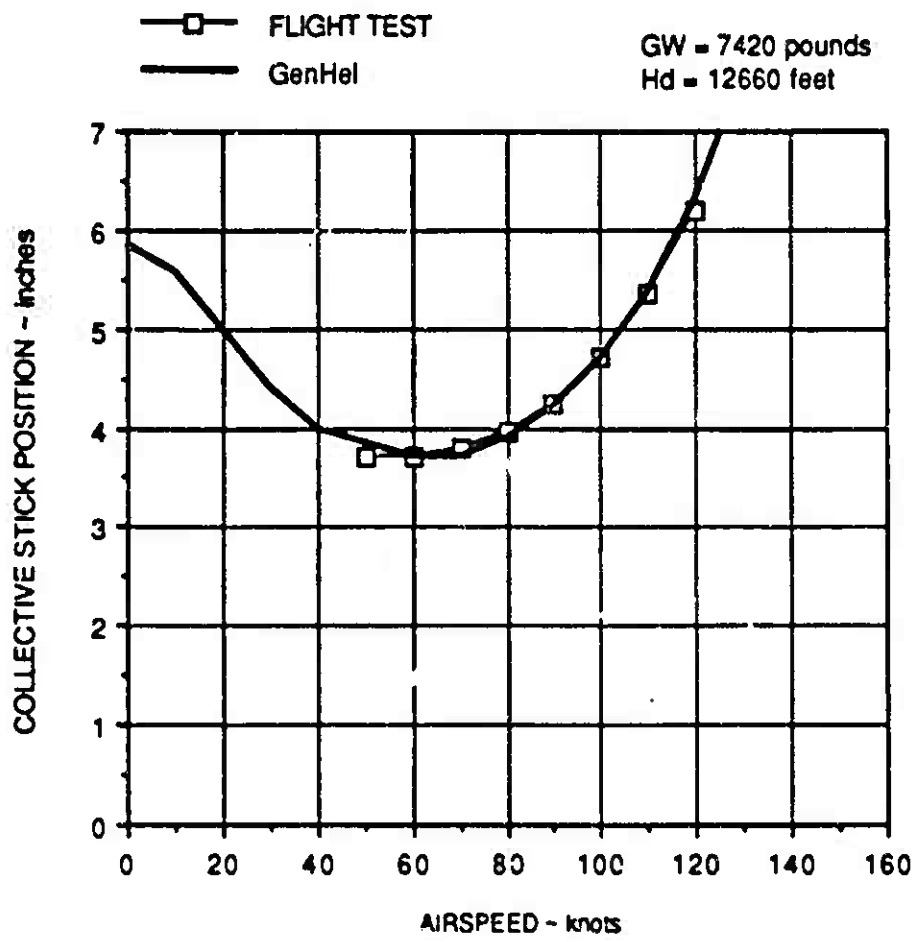


Figure G-4. SA-365H Collective Stick Correlation

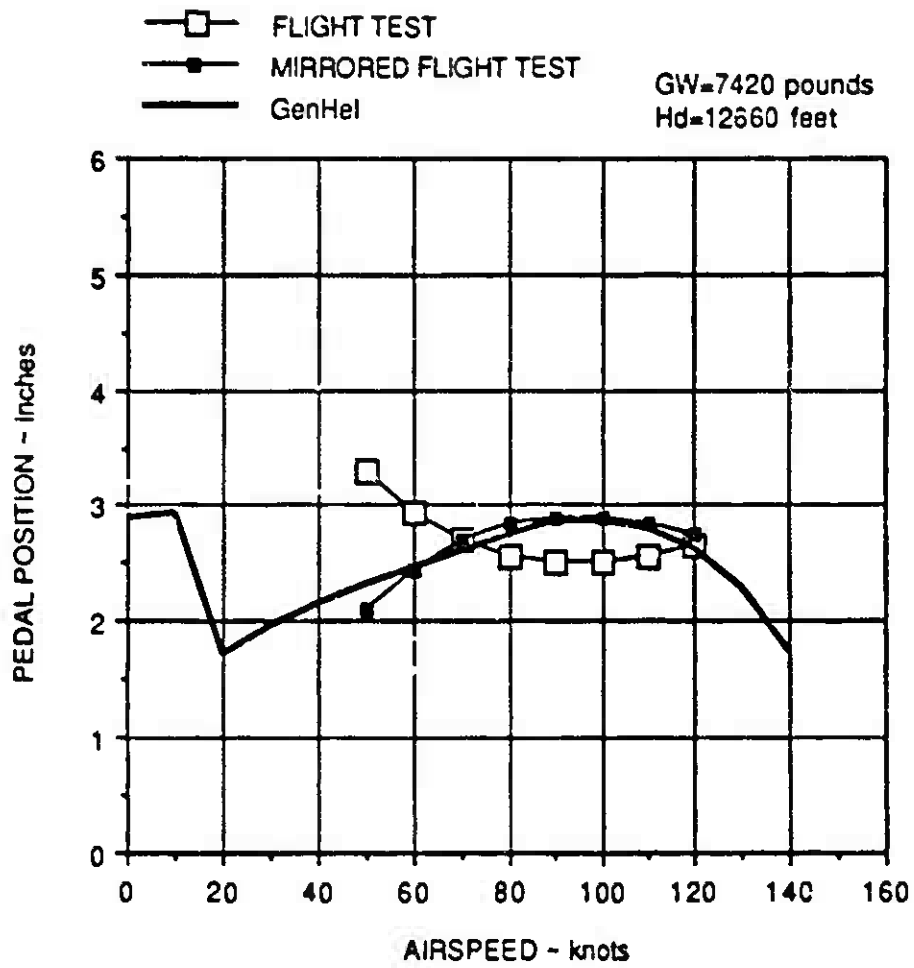


Figure C-5. SA-365N Pedal Correlation

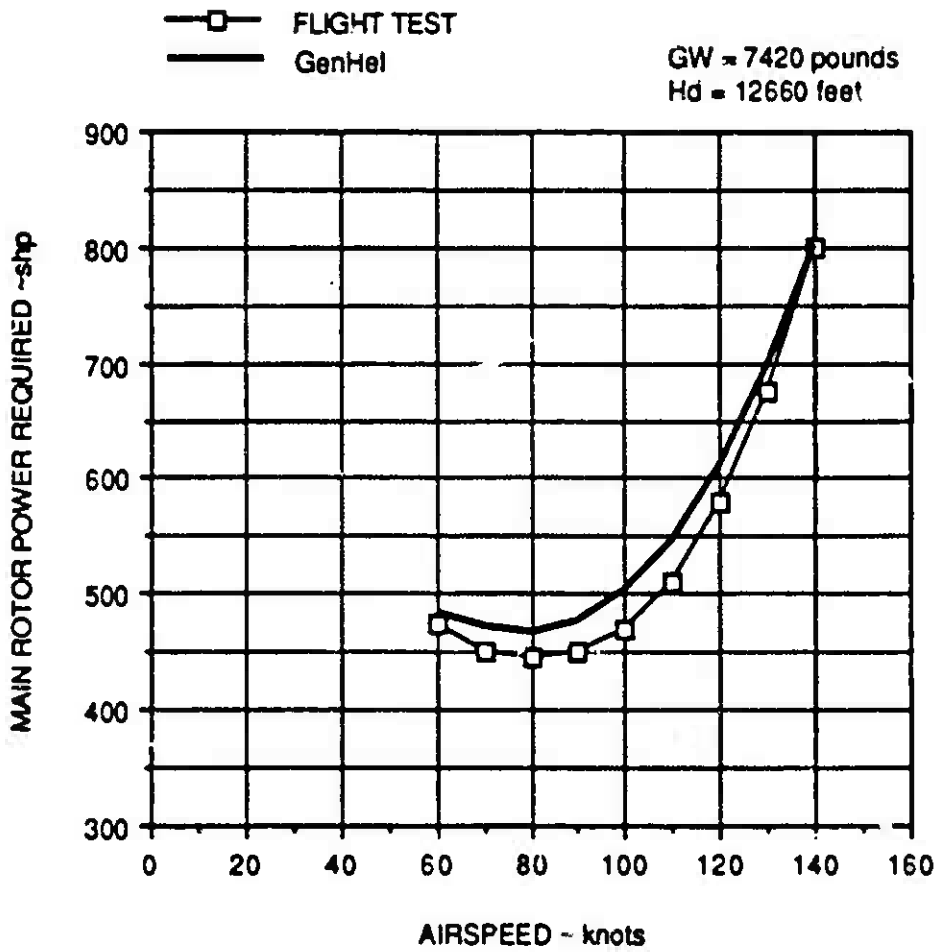


Figure C-6. SA-365N Main Rotor Power Required Correlation

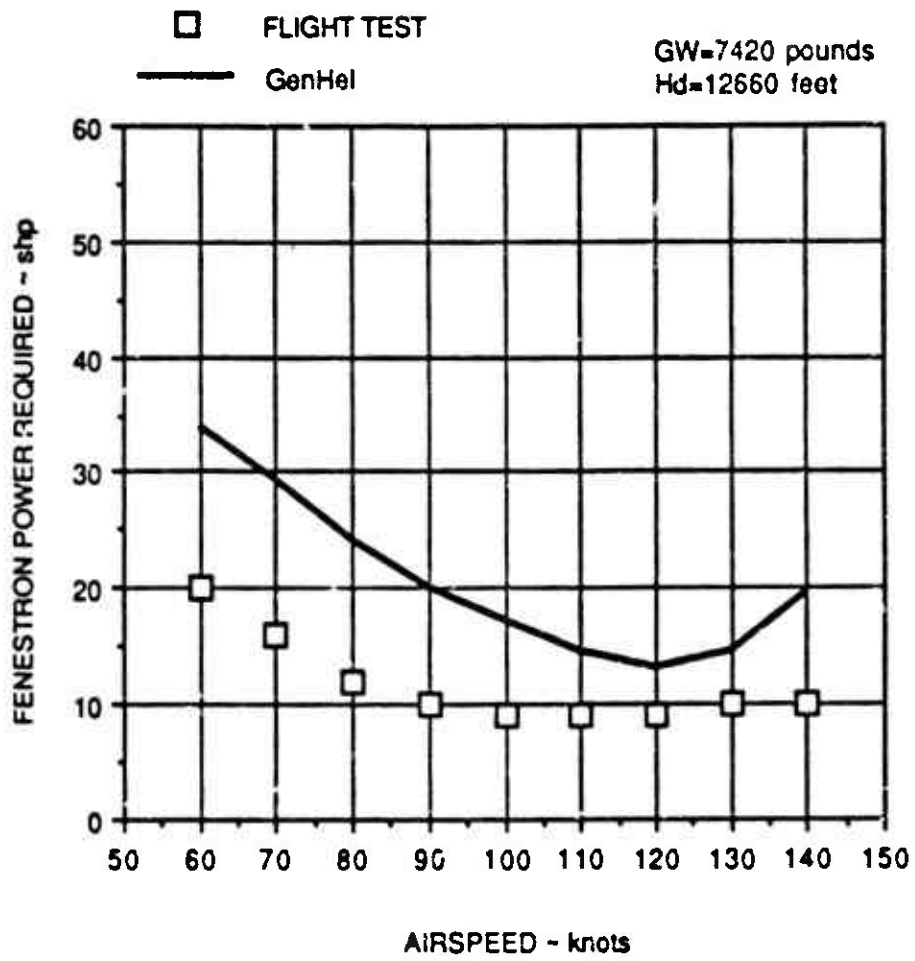


Figure G-7. SA-365N Fenestron Power Required Correlation

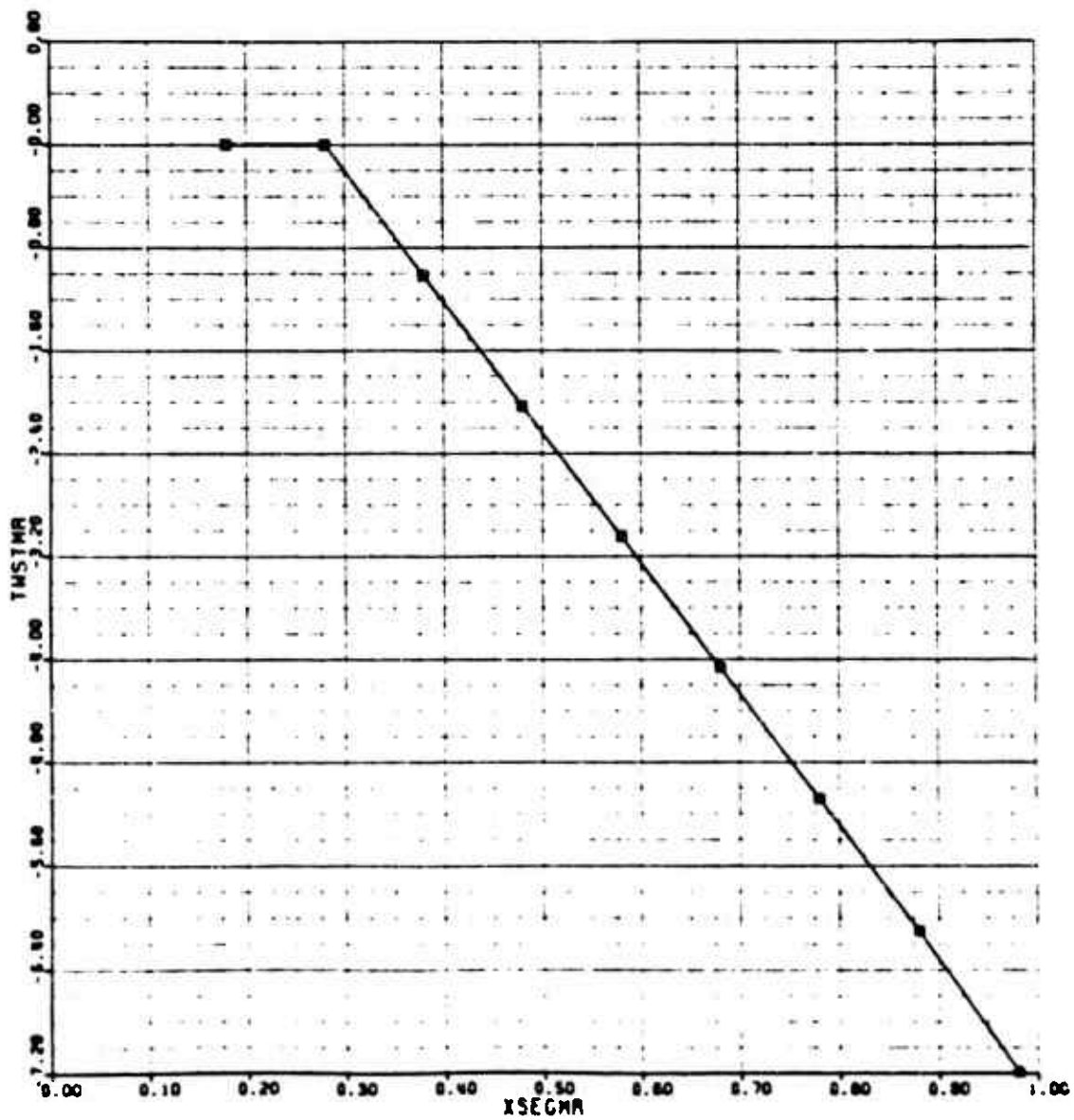


Figure G-8. SA-365N Main Rotor Blade Twist Map

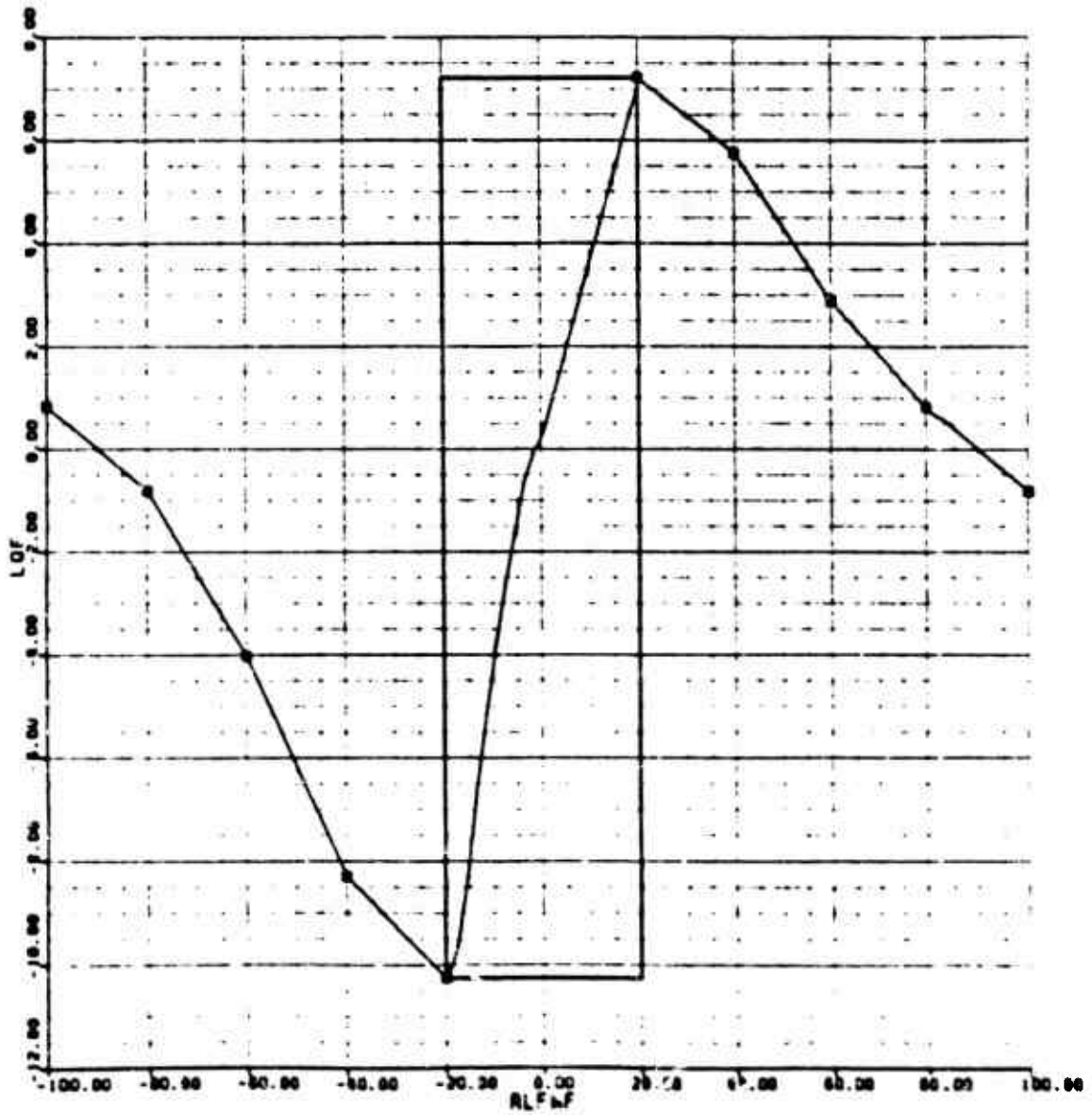


Figure G-9. SA-365N Fuselage Lift Map

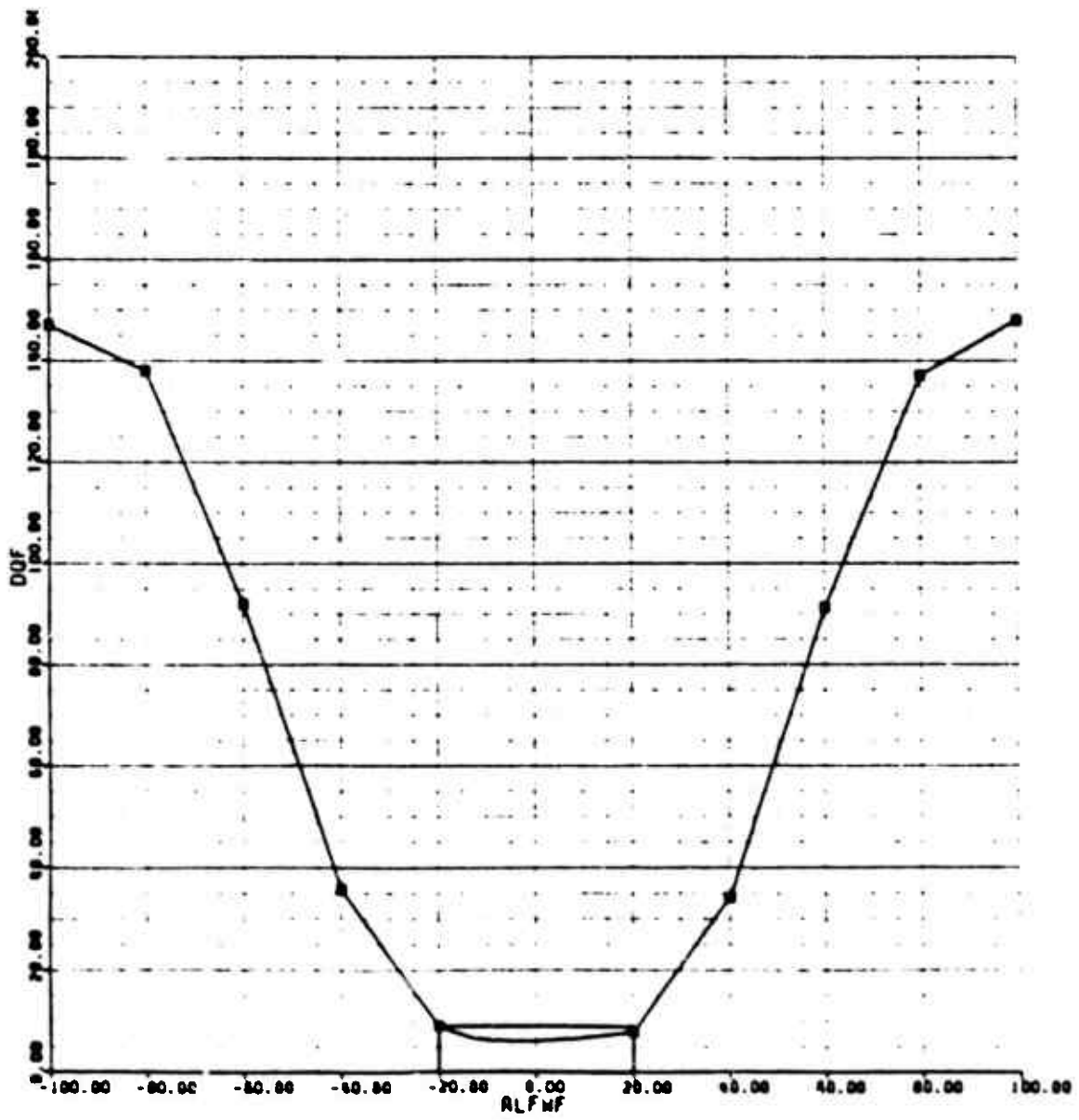


Figure C-10. SA-365N Fuselage Drag Map

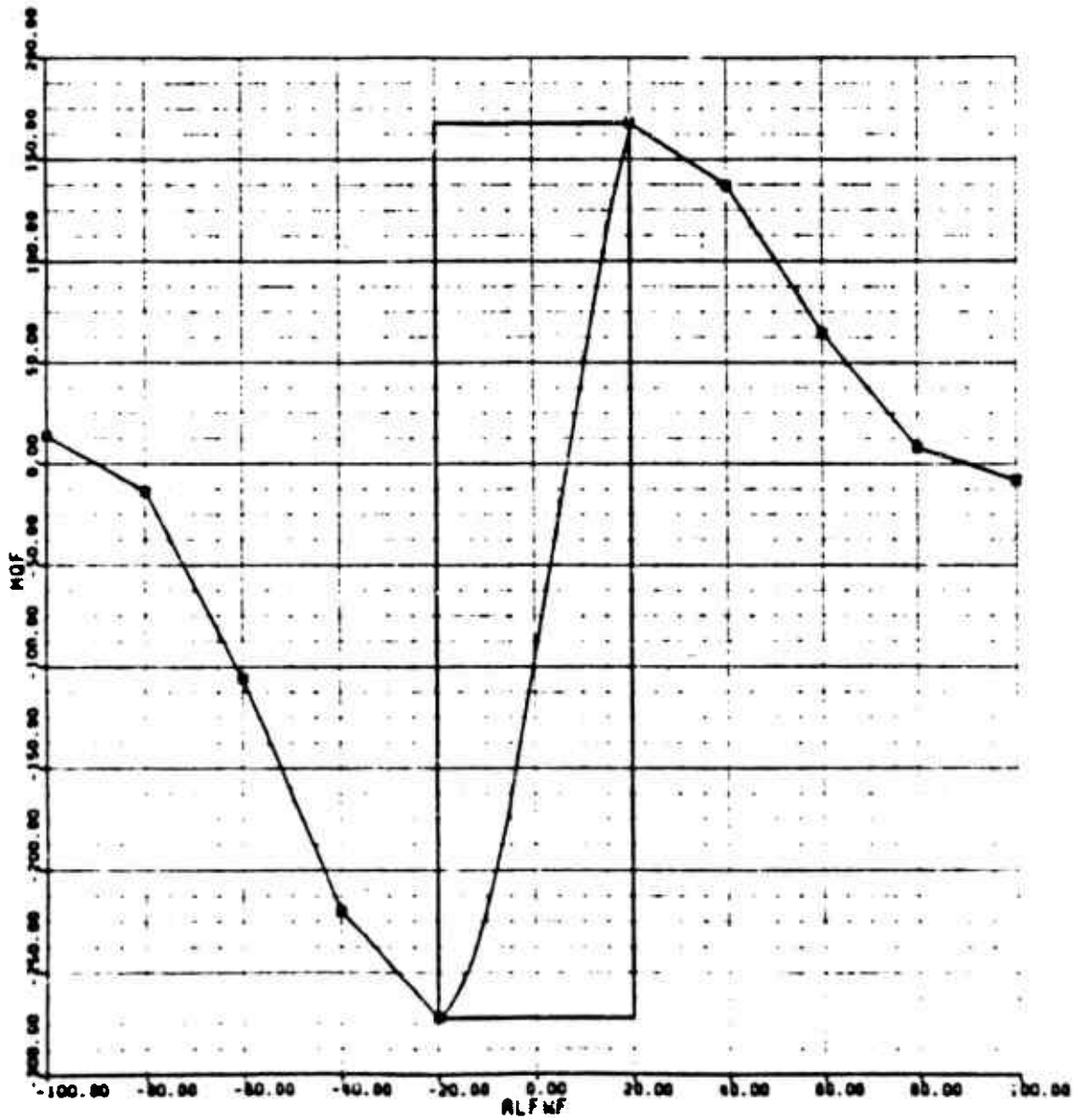


Figure C-11. SA-365N Fuselage Pitching Moment Map

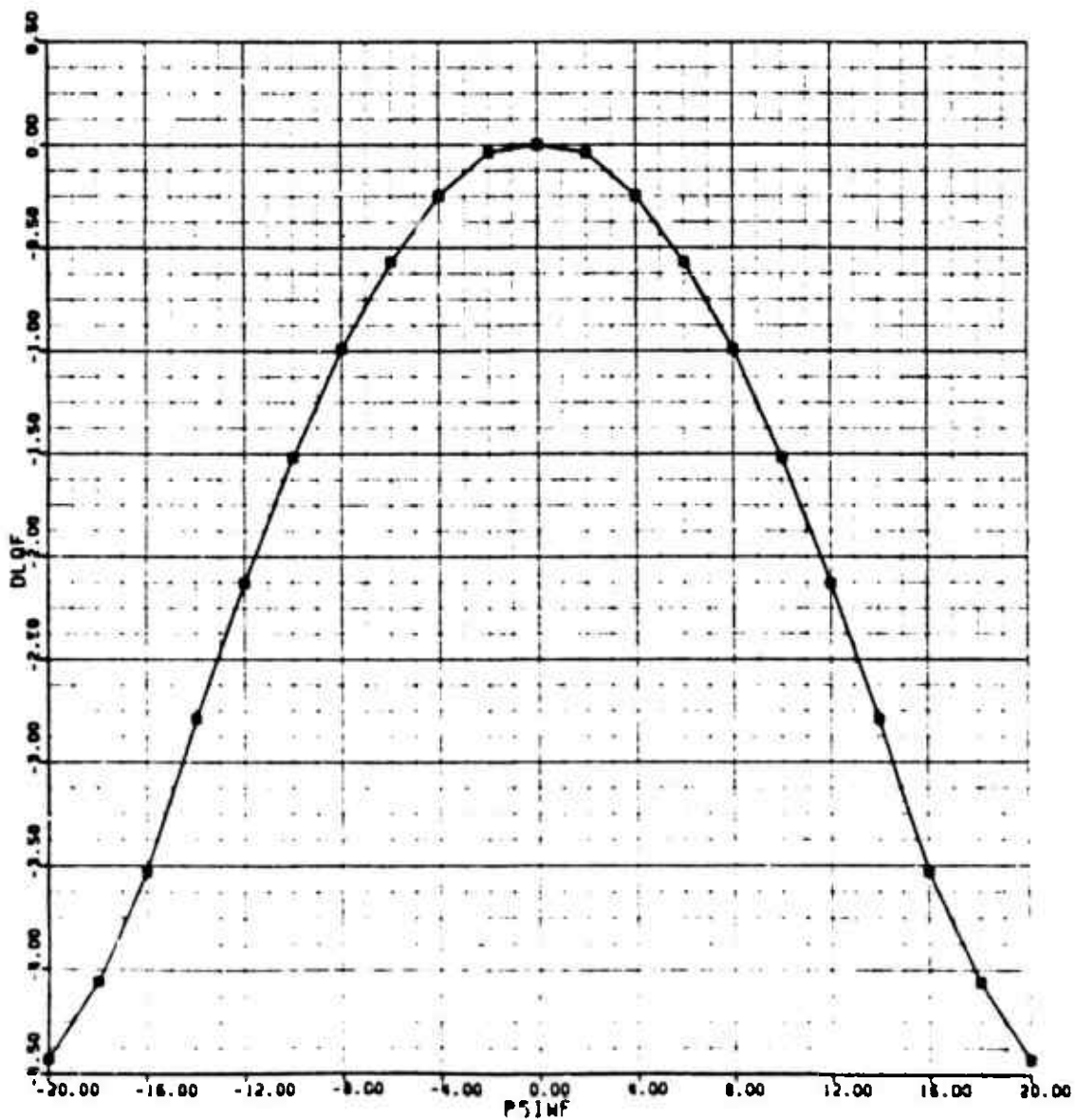


Figure G-12. SA-365N Fuselage Delta Lift Map

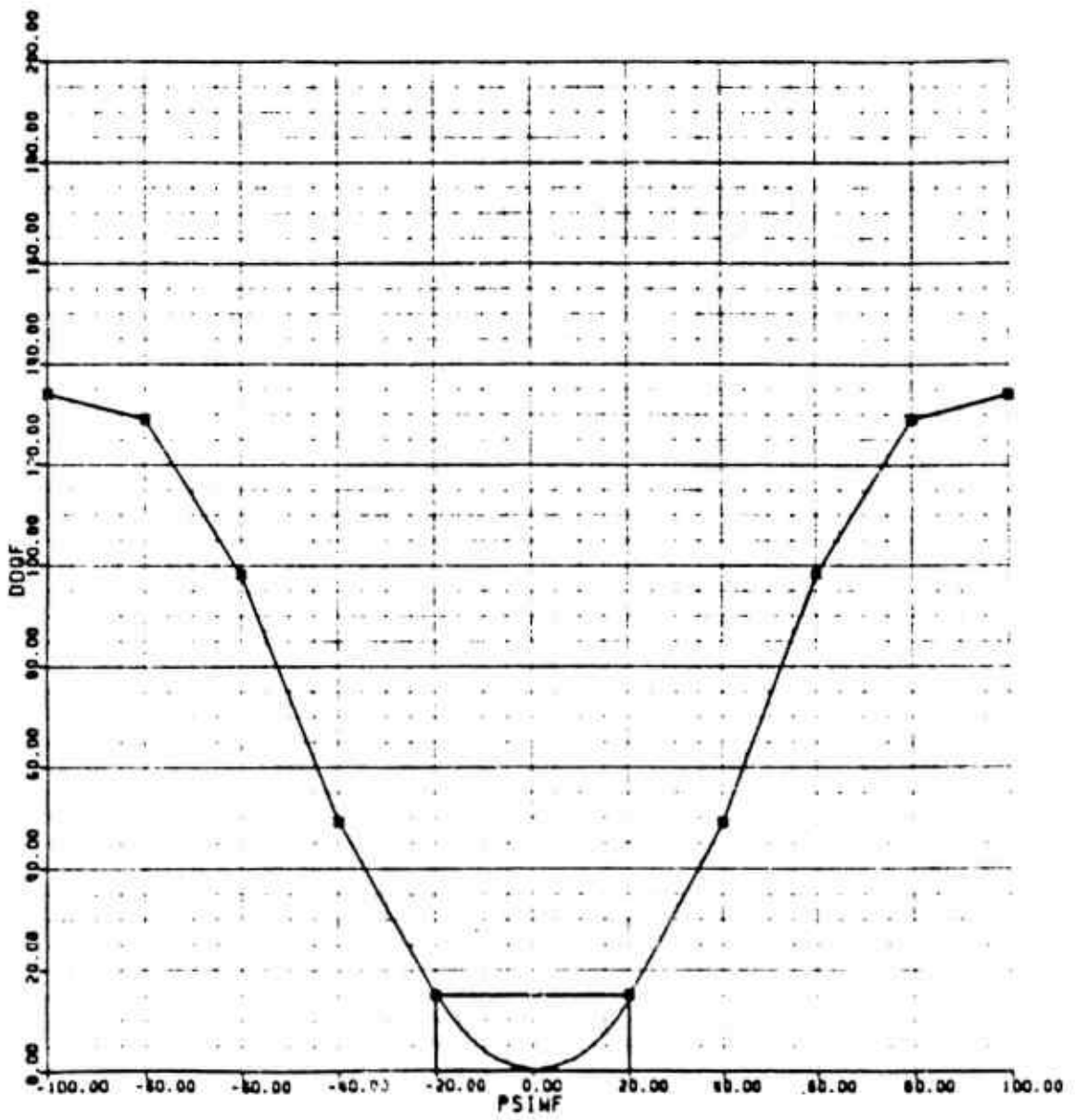


Figure G-13. SA-365N Fuselage Delta Drag Map

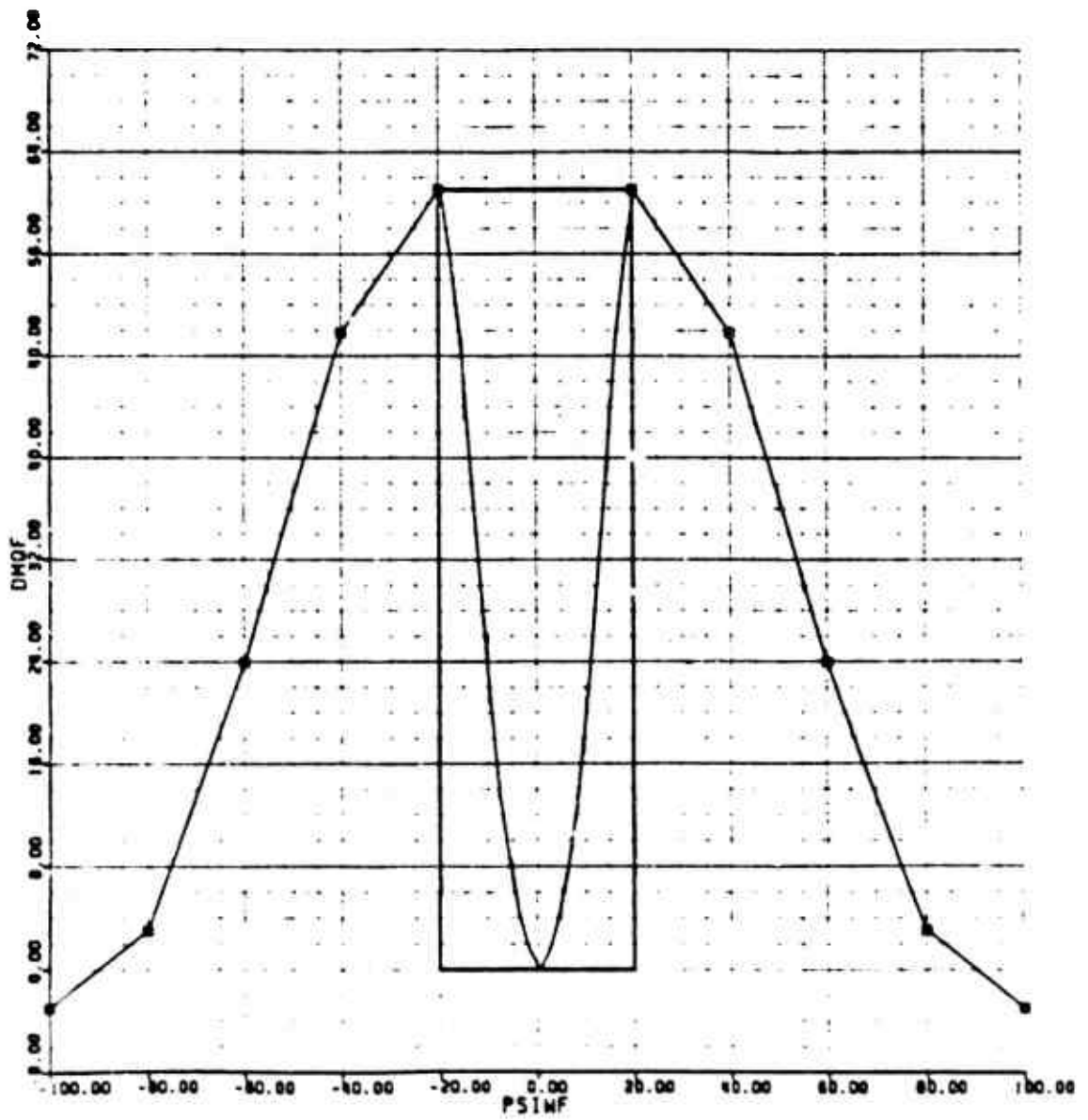


Figure G-14. SA-365N Fuselage Delta Pitching Moment Map

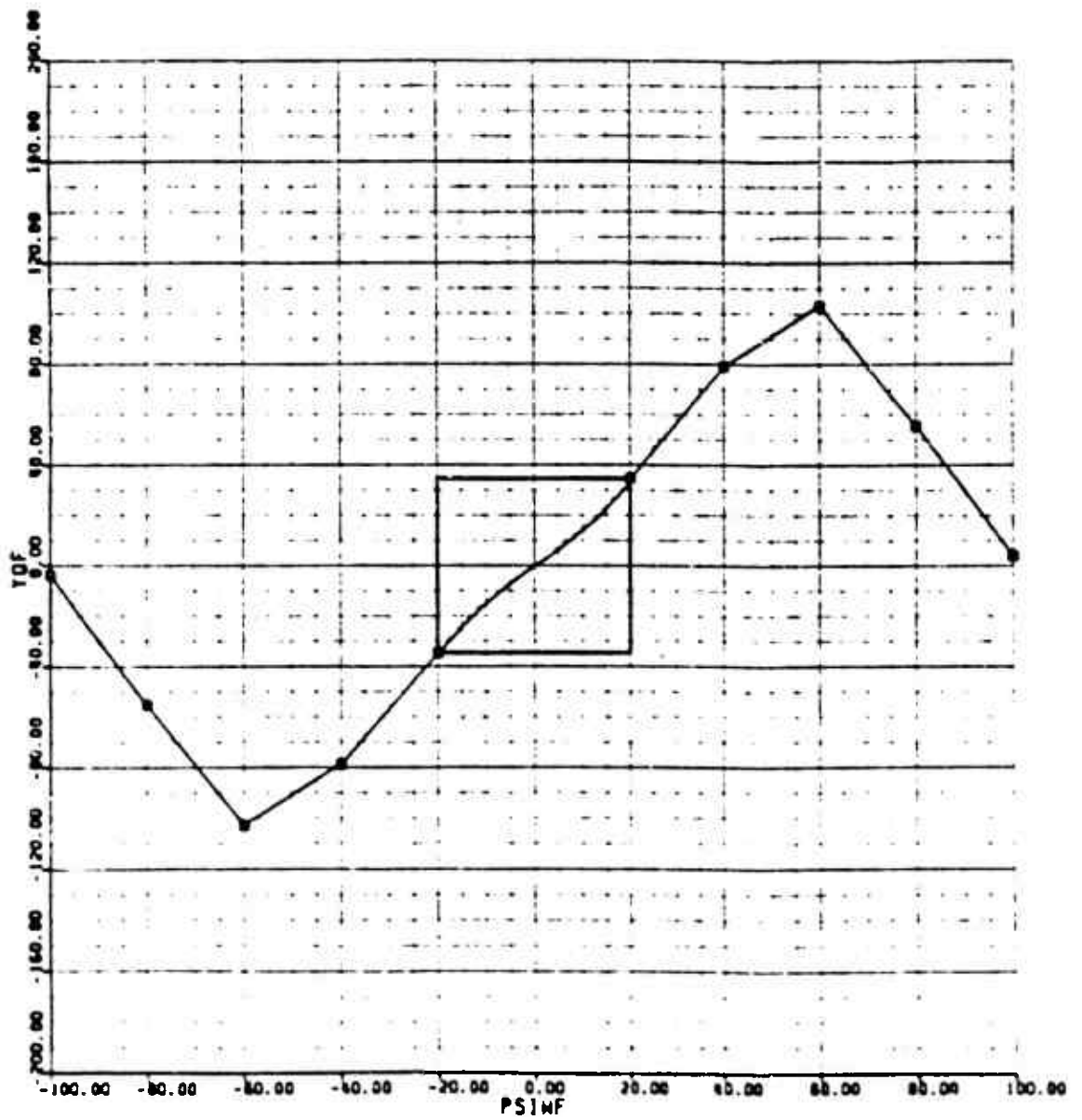


Figure G-15. SA-365N Fuselage Sideforce Map

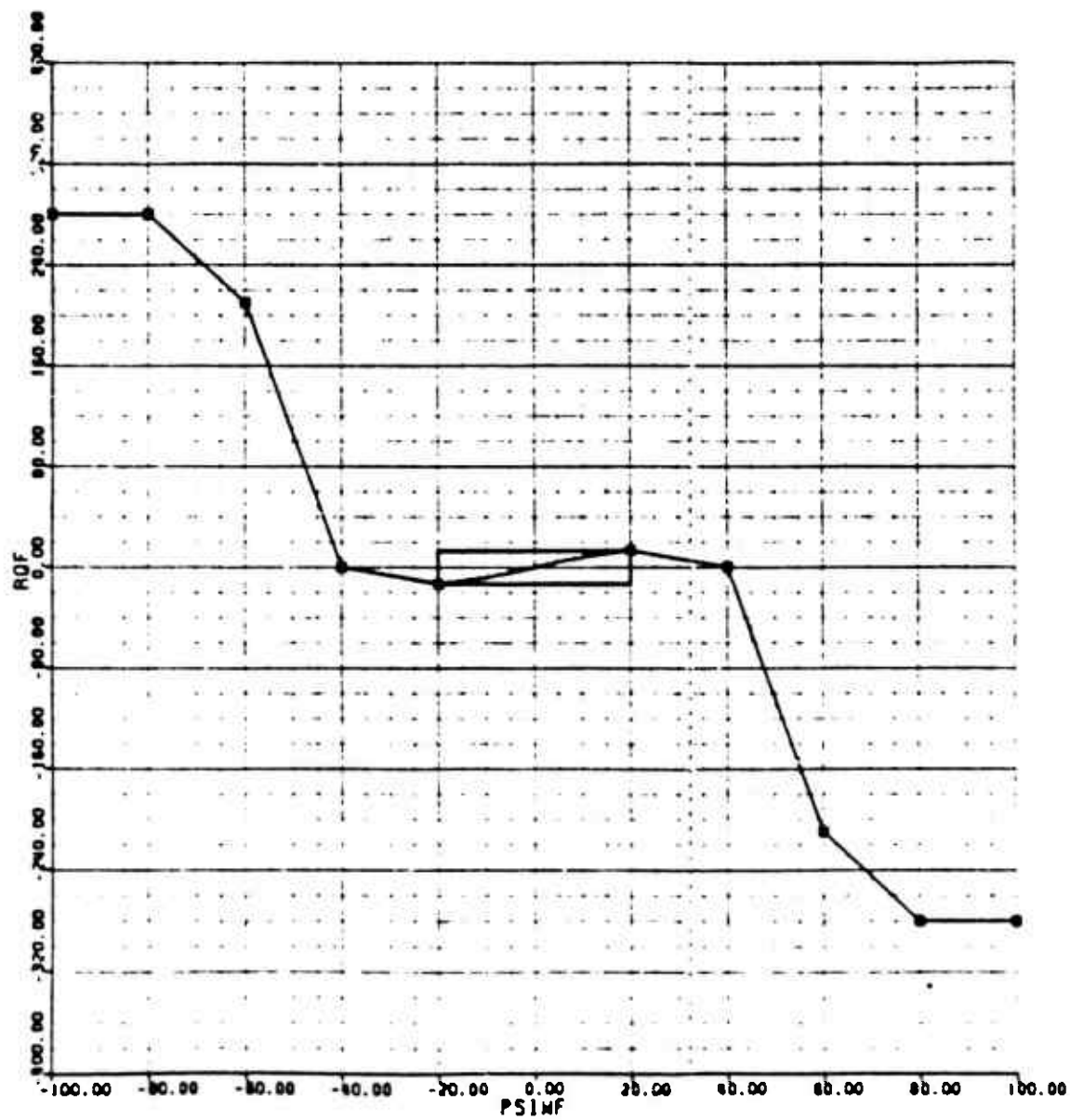


Figure C-16. SA-365N Fuselage Rolling Moment Map

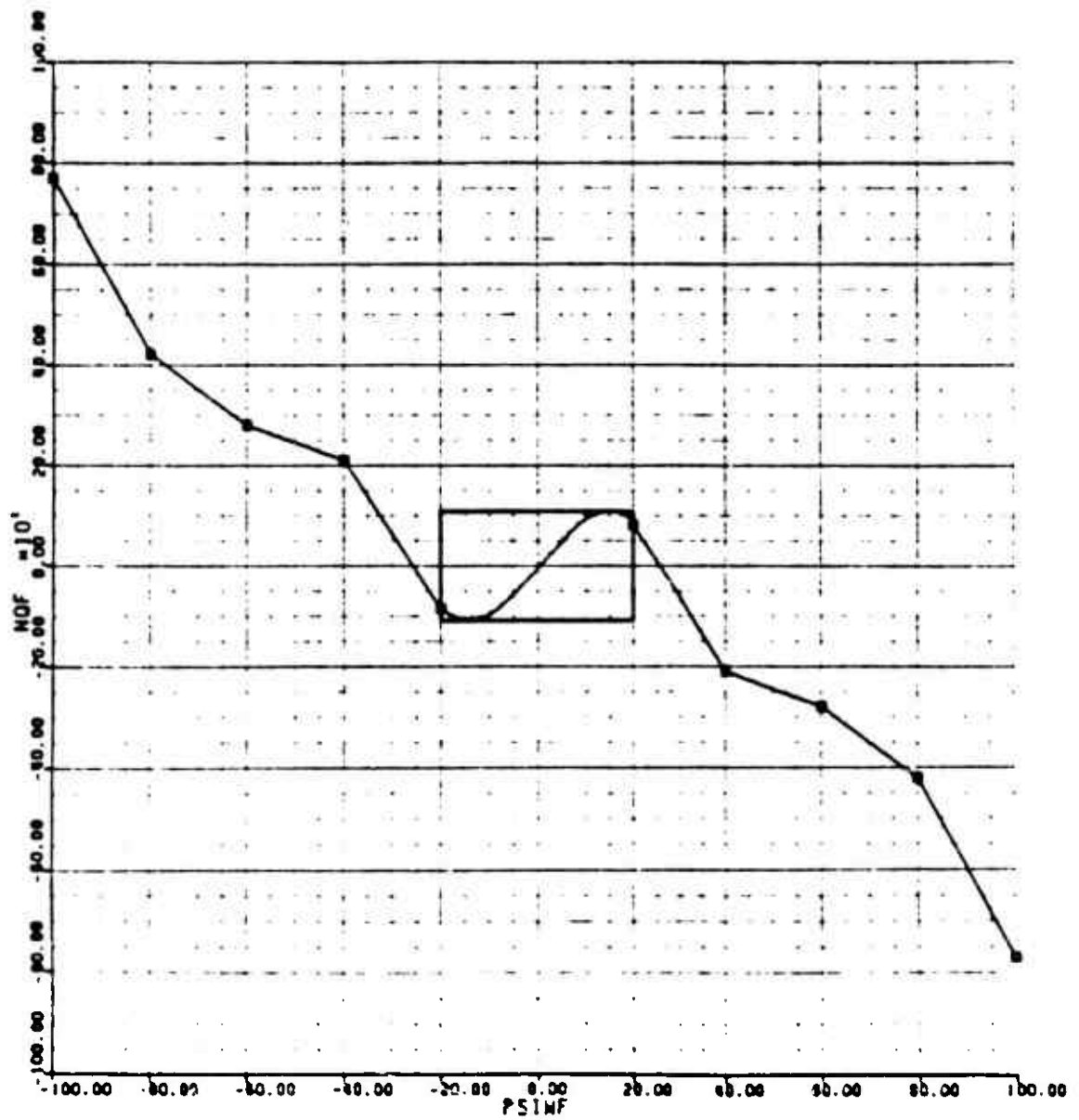


Figure C-17. SA-365N Fuselage Yawing Moment Map

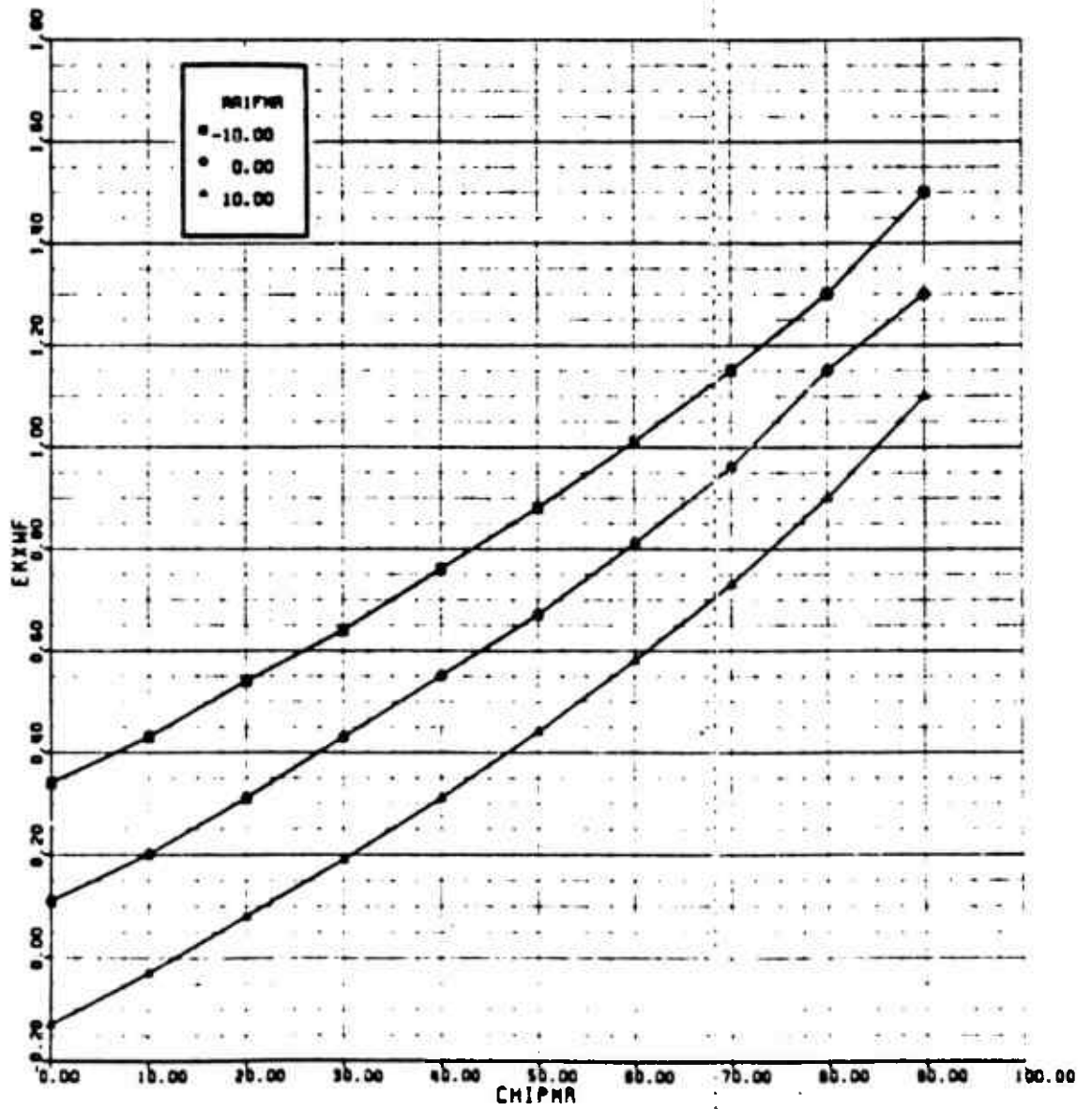


Figure G-18. SA-365N Main Rotor Downwash on Fuselage Map (x-direction)

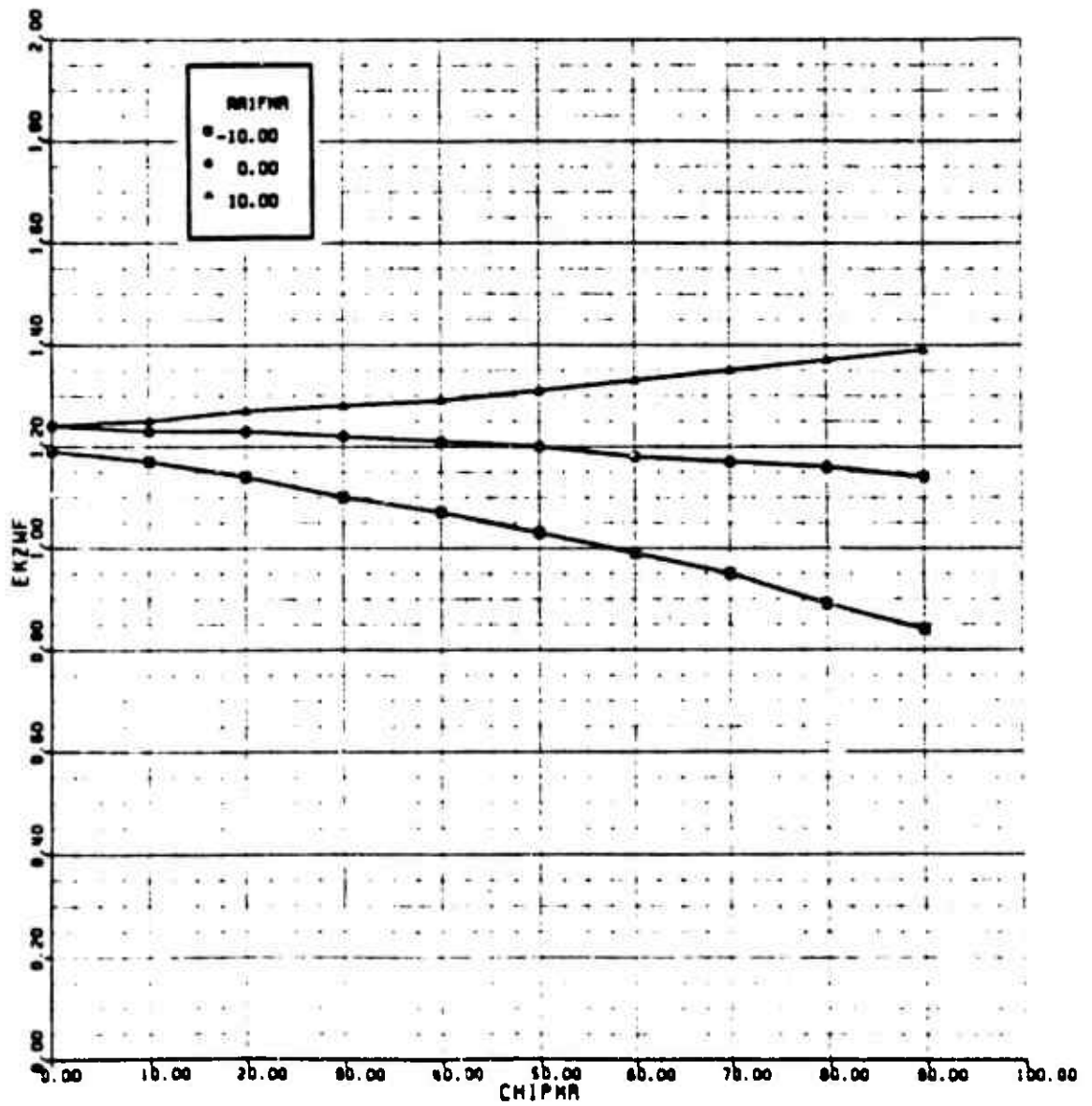


Figure C-19. SA-365N Main Inlet or Downwash on Fuselage Map (z-direction)

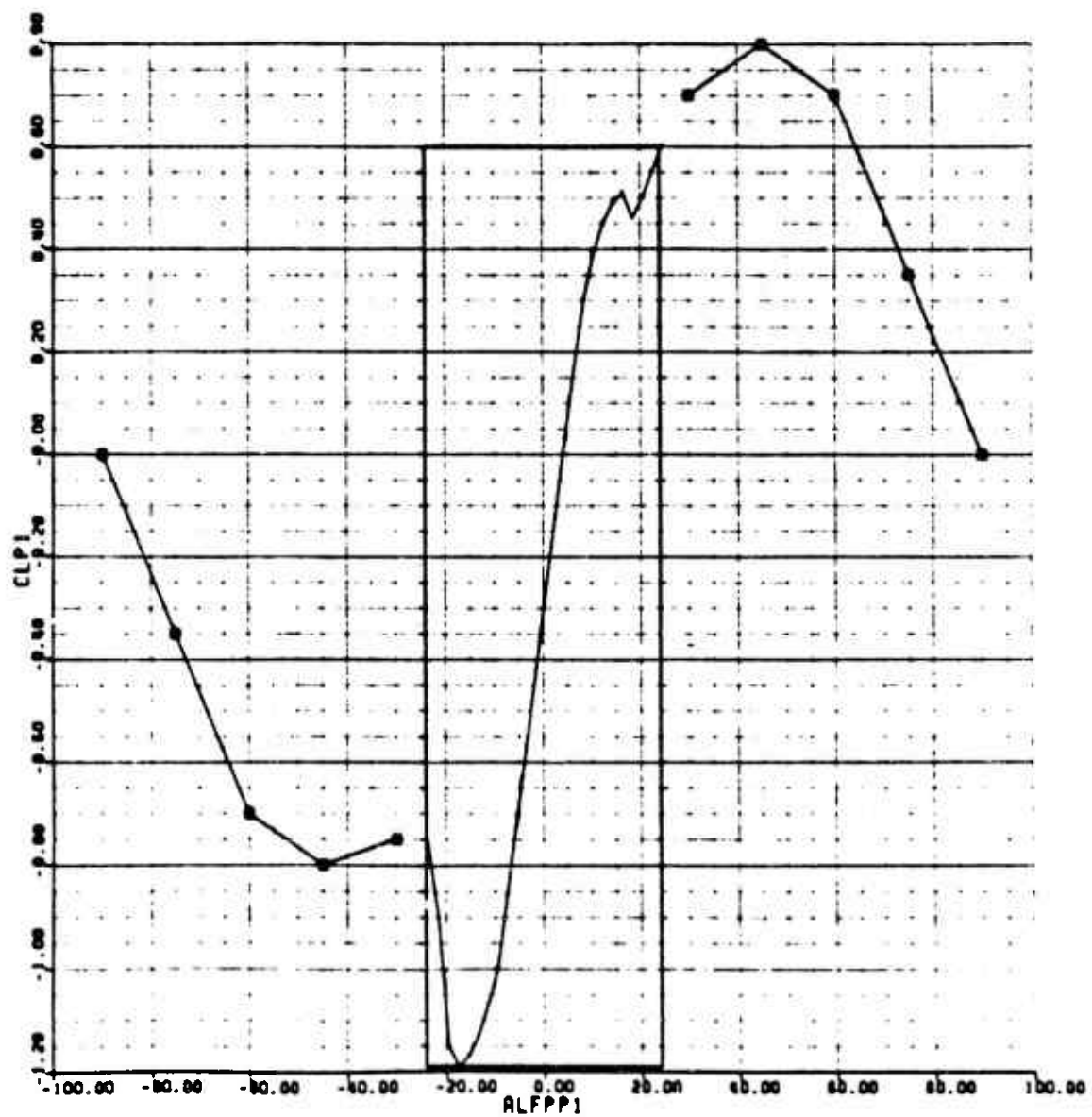


Figure G-20. SA-365N Horizontal Stabilizer Lift Map

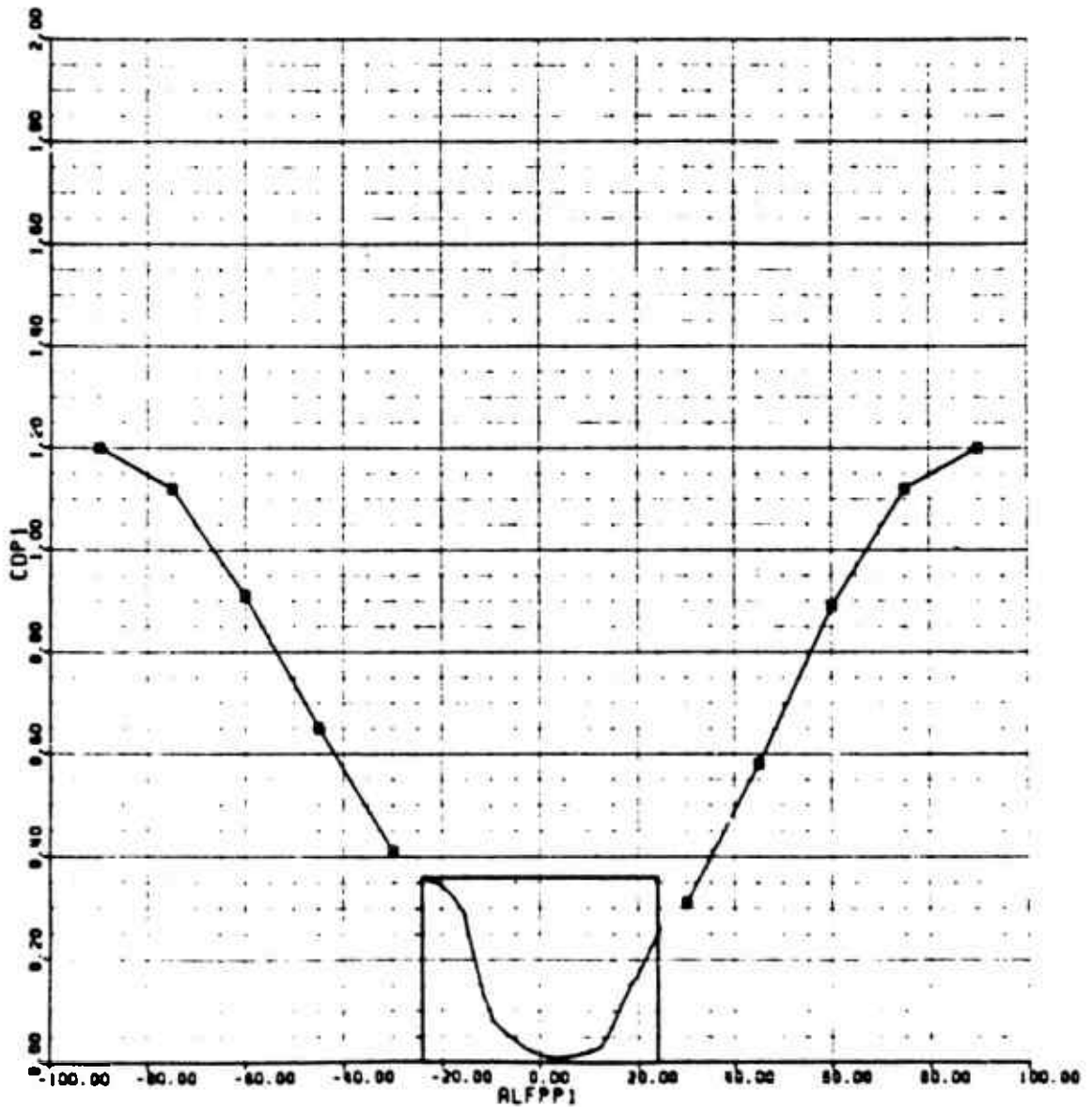


Figure G-21. SA-365N Horizontal Stabilizer Drag Map

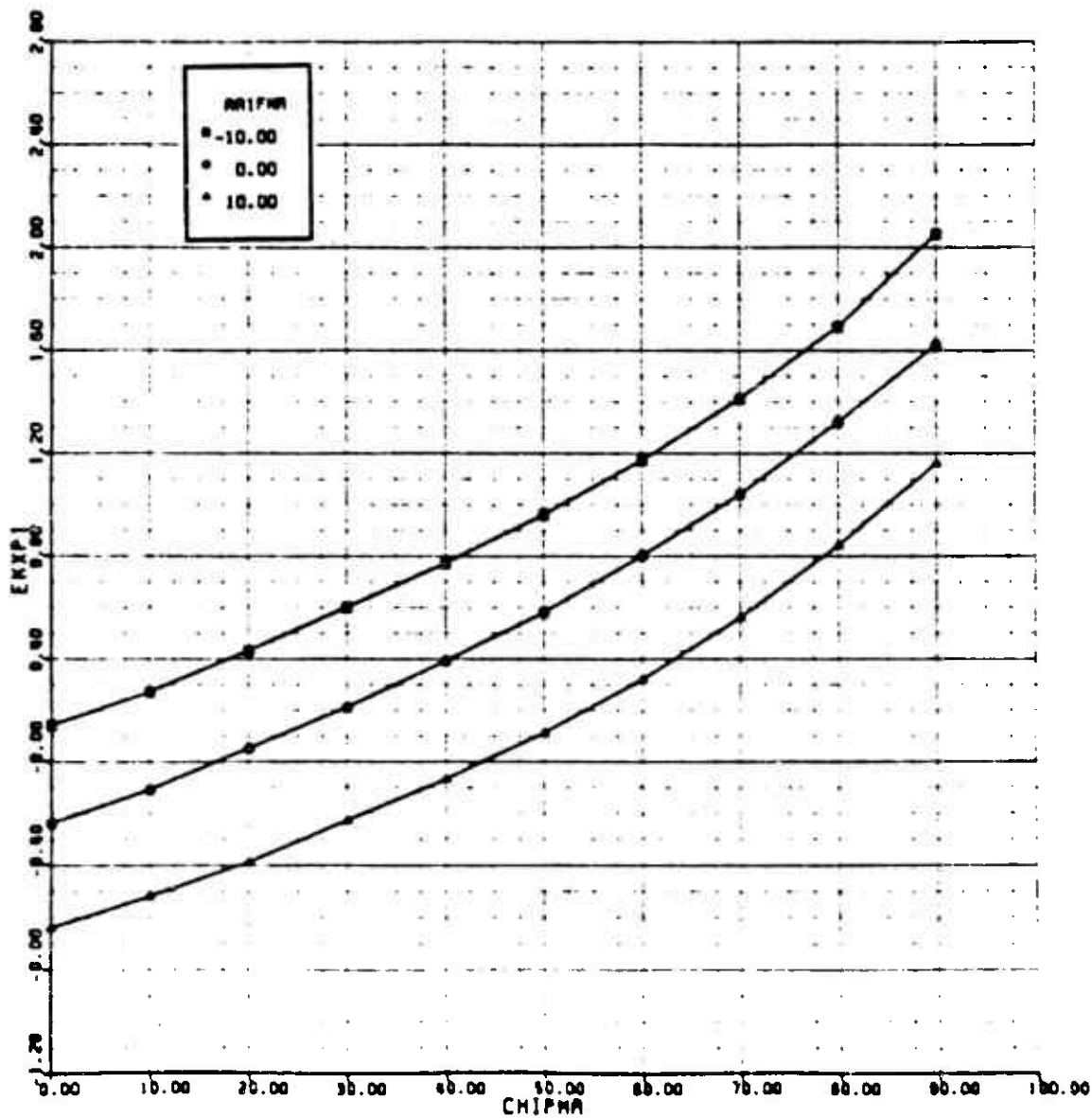


Figure C-22. SA-365N Main Rotor Downwash on Horizontal Stabilizer Map (x-direction)

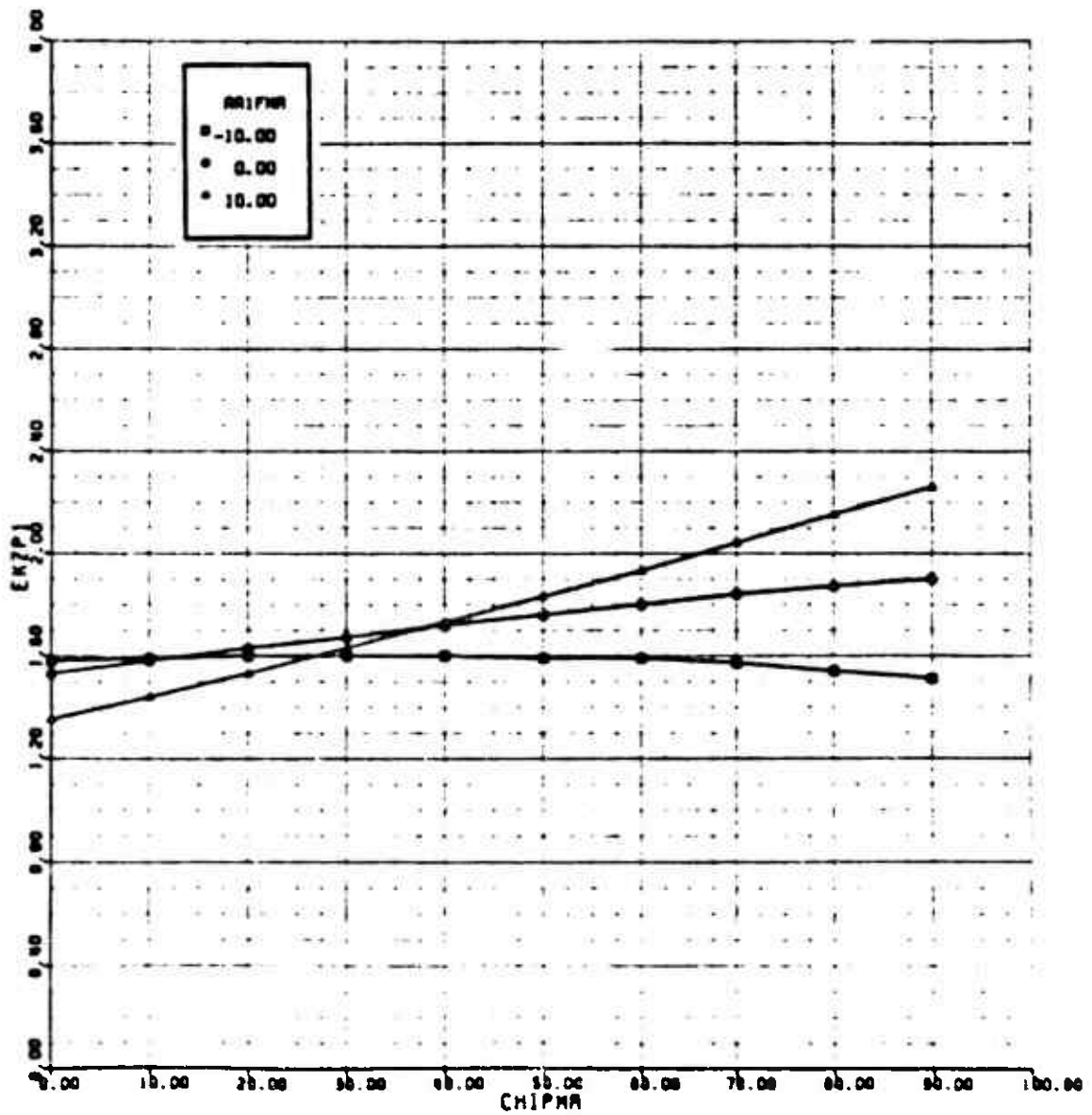


Figure C-23. SA-365H Main Rotor Downwash on Horizontal Stabilizer Map (x-direction)

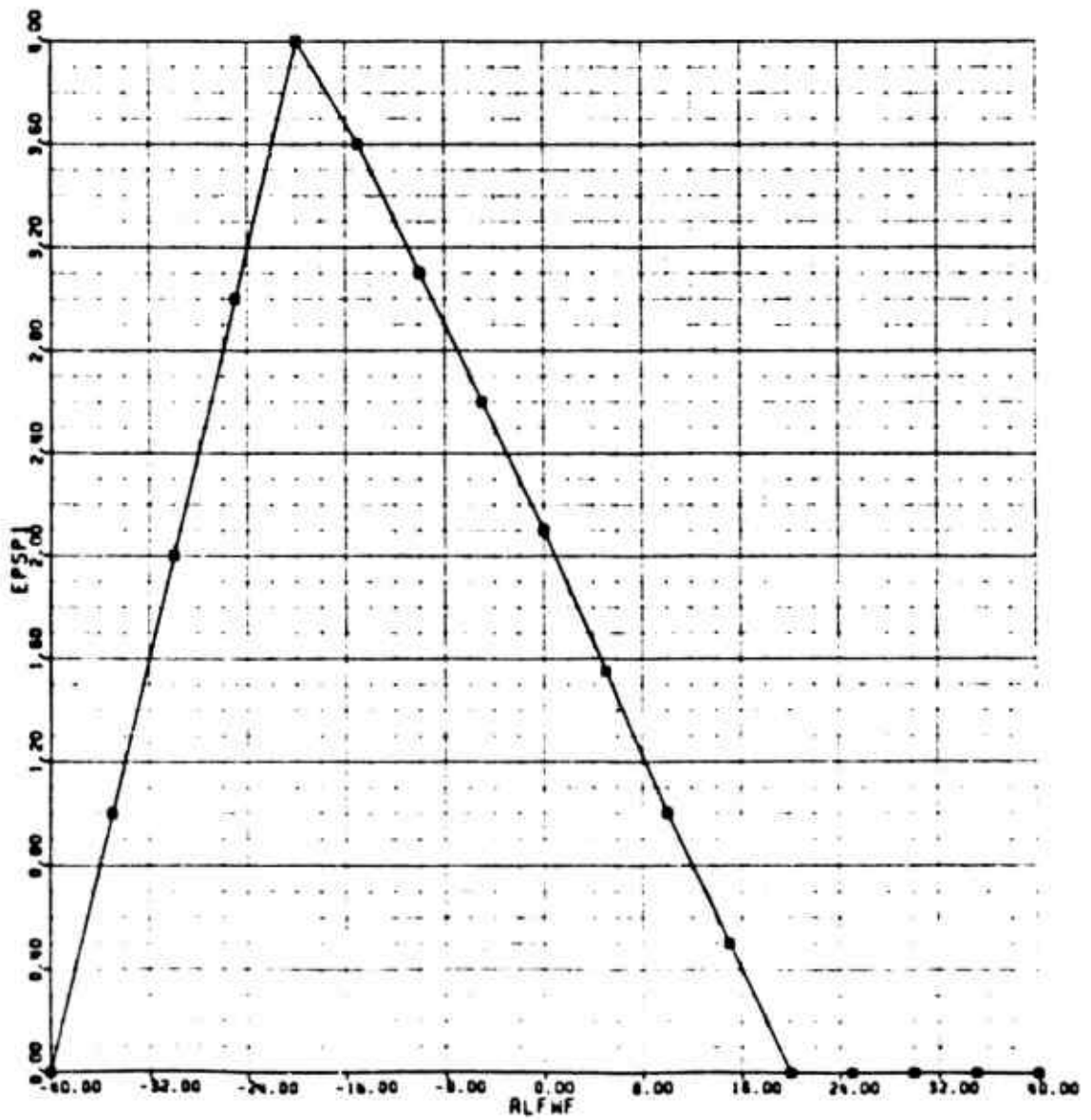


Figure G-24. SA-365N Fuselage Downwash on Horizontal Stabilizer Map

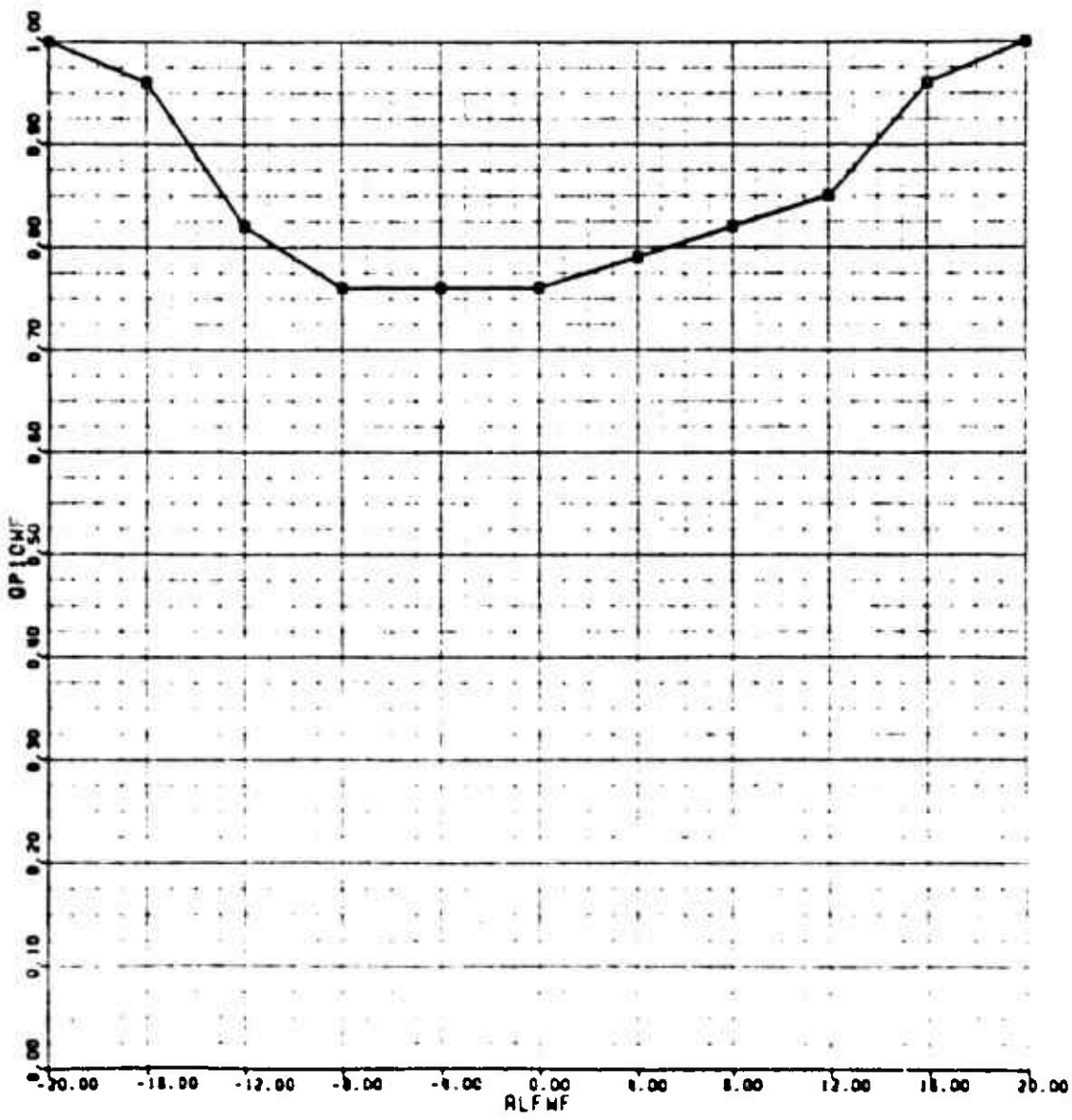


Figure G-25. SA-365N Dynamic Pressure Ratio at Horizontal Stabilizer Map

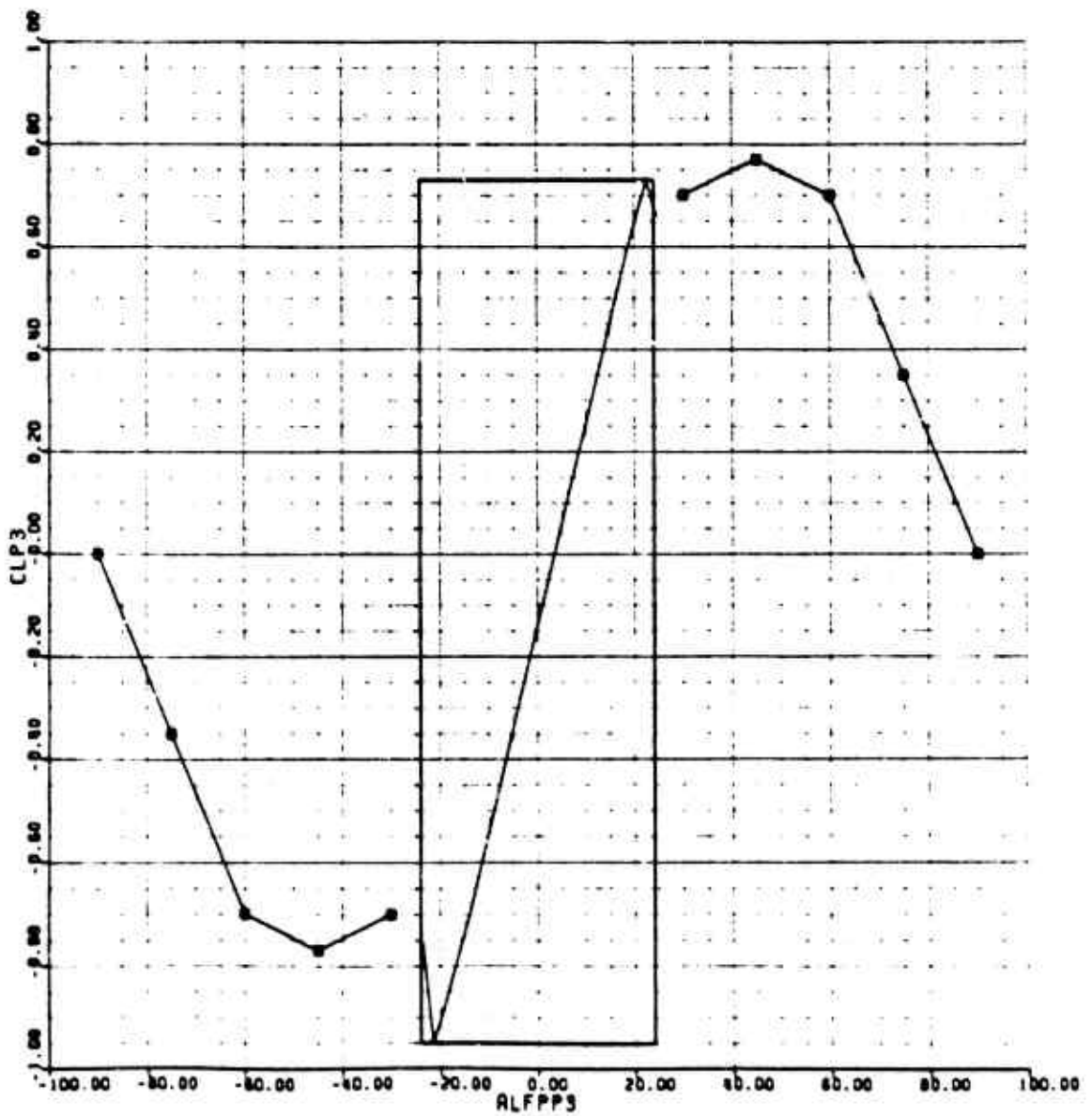


Figure G-26. SA-365N Vertical Stabilizer Lift Map

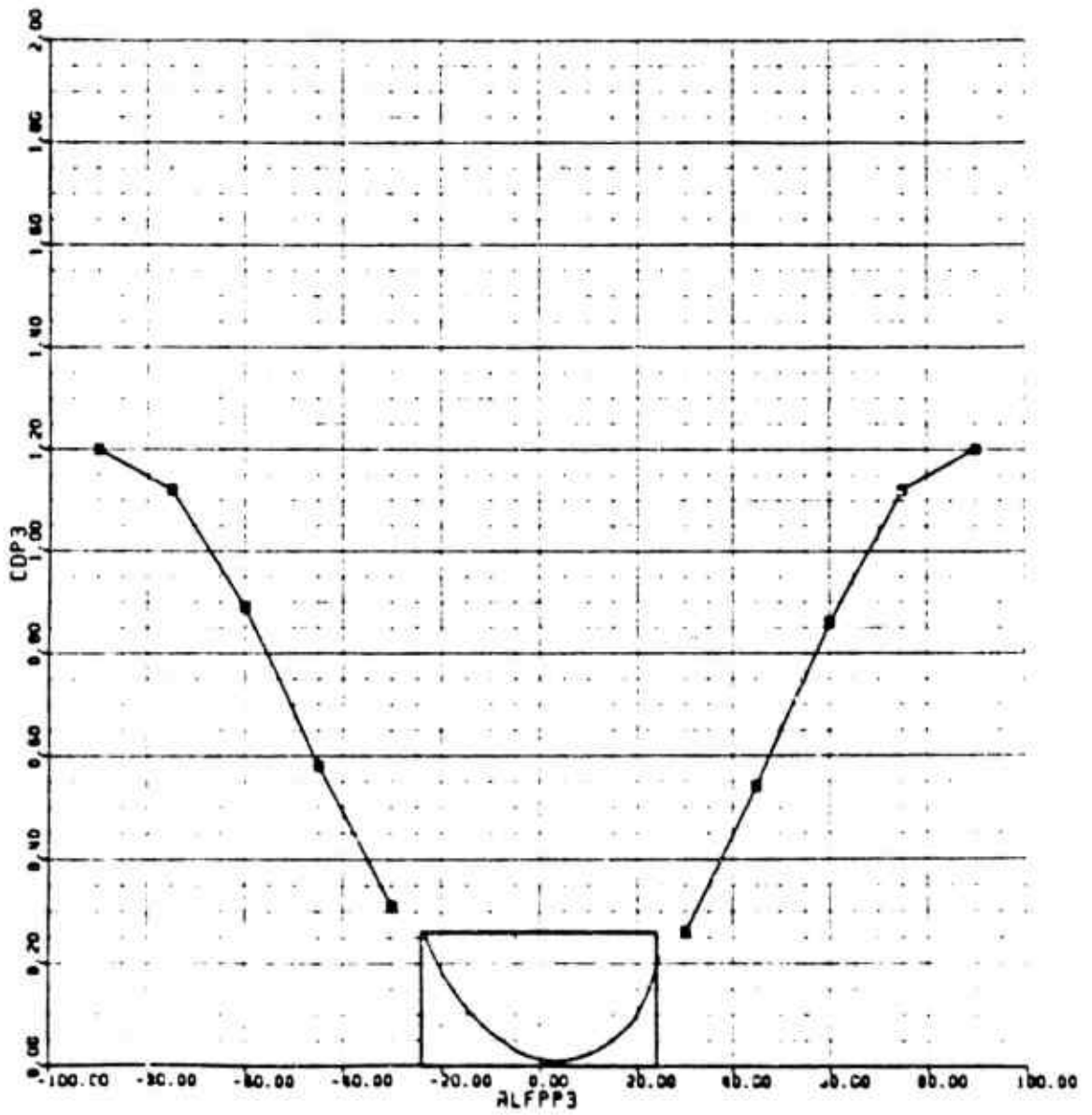


Figure C-27. SA-365N Vertical Stabilizer Drag Map

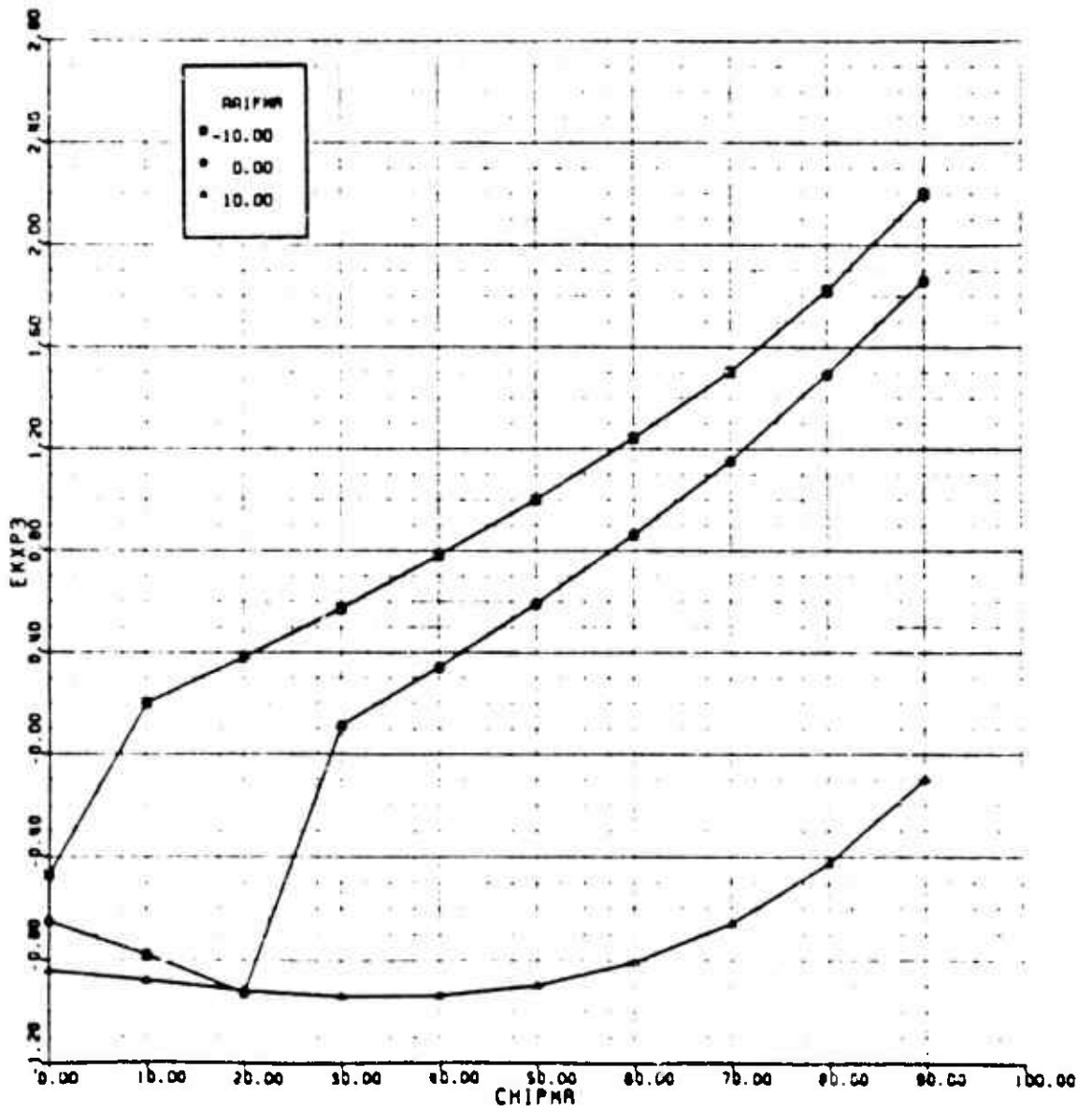


Figure G-28. SA-365N Main Fotor Downwash on Vertical Stabilizer Map (x-direction)

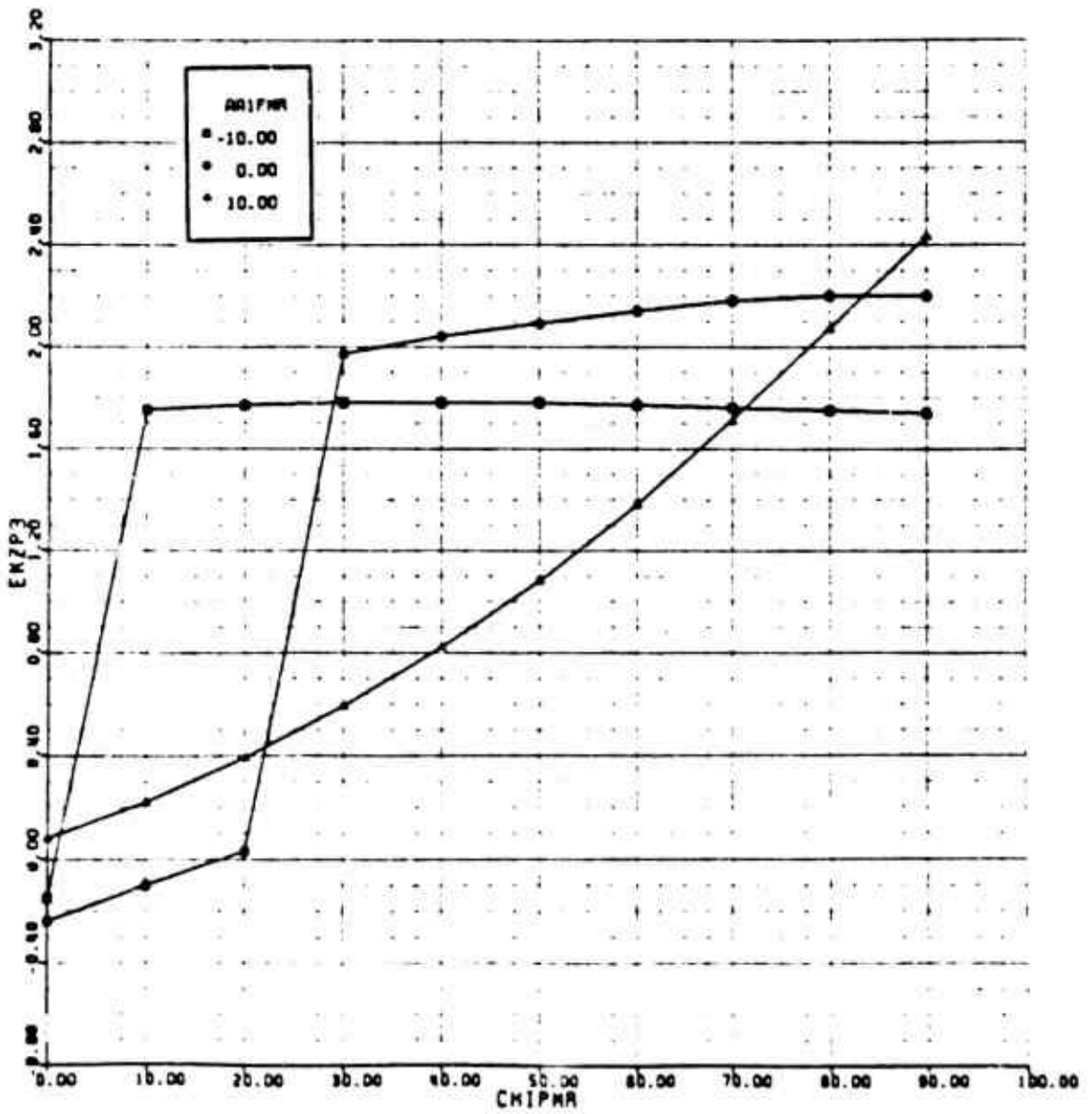


Figure G-29. SA-365N Main Rotor Downwash on Vertical Stabilizer Map (z-direction)

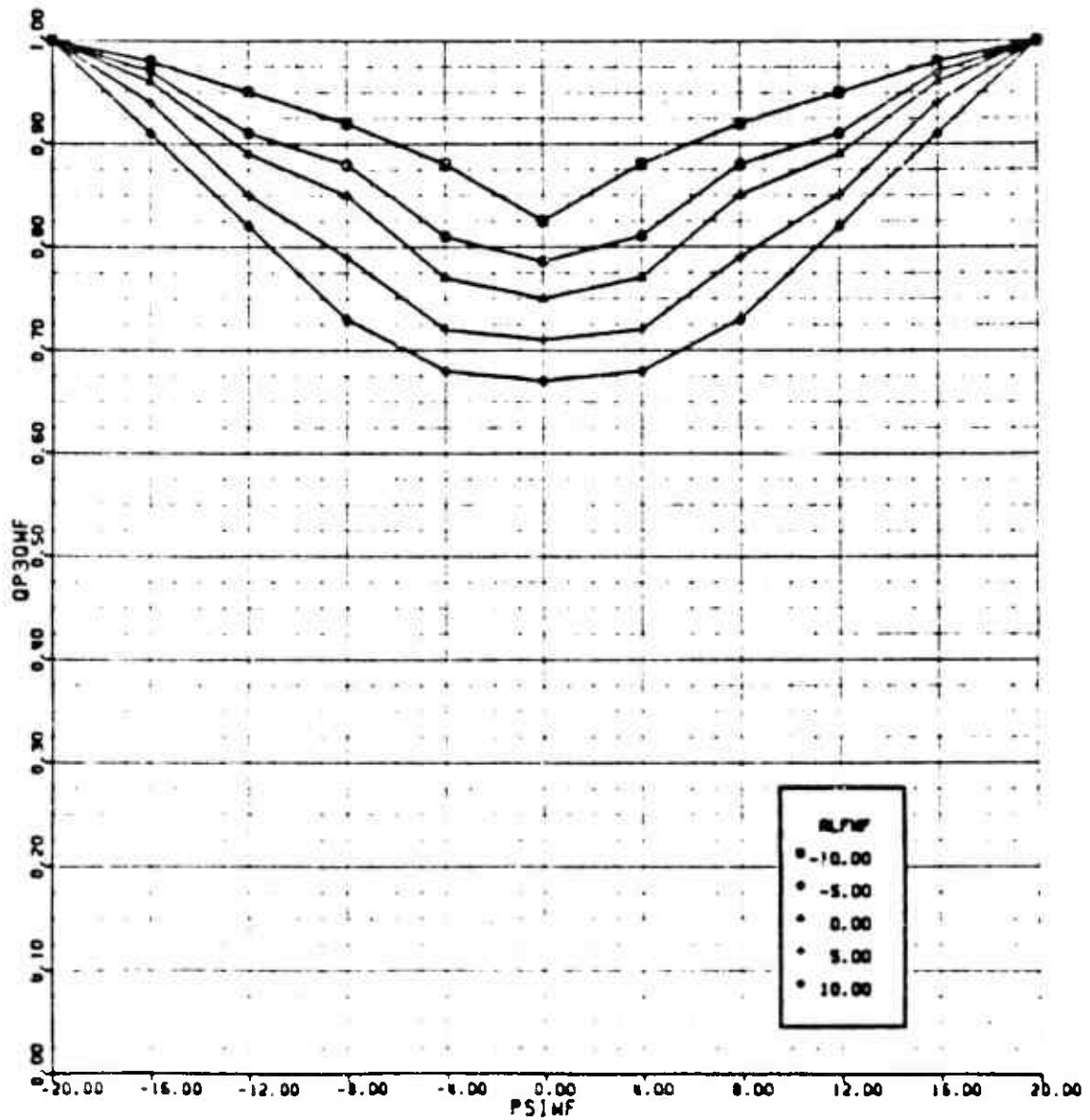


Figure C-30. SA-365N Dynamic Pressure Ratio at Vertical Stabilizer Map

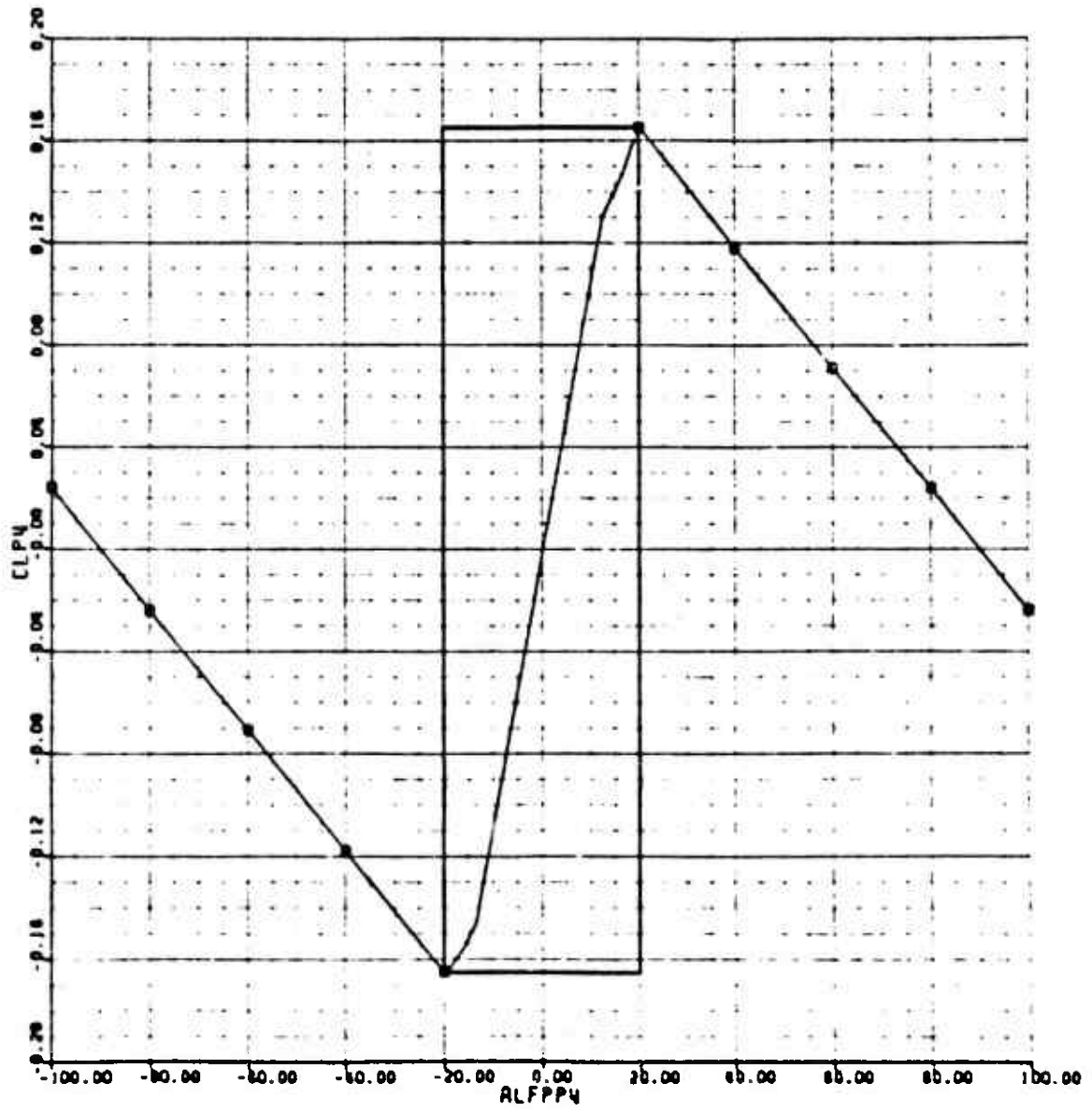


Figure G-31. SA-365N Fan Shroud Lift Map

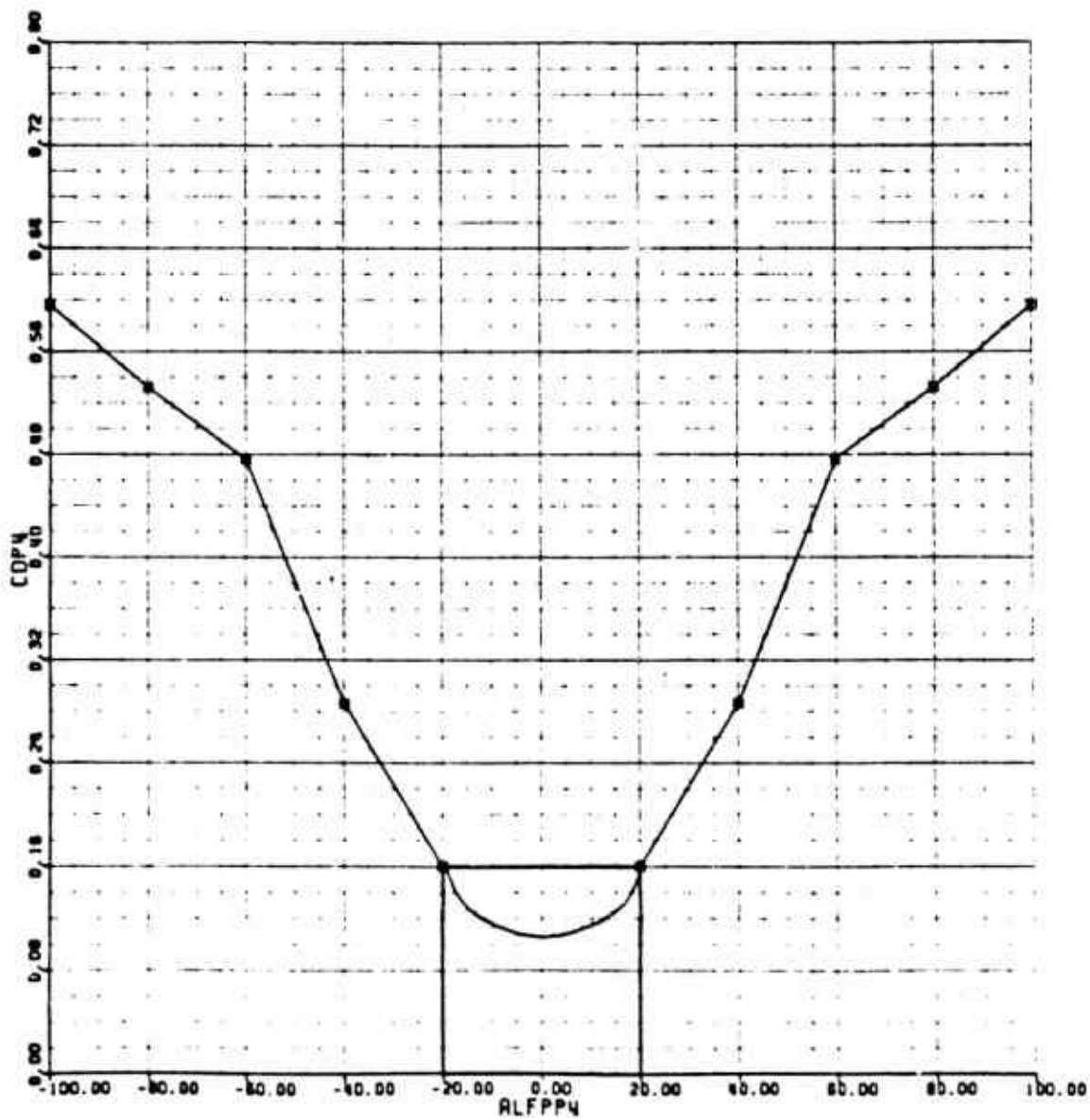


Figure C-32. SA-365N Fan Shroud Drag Map

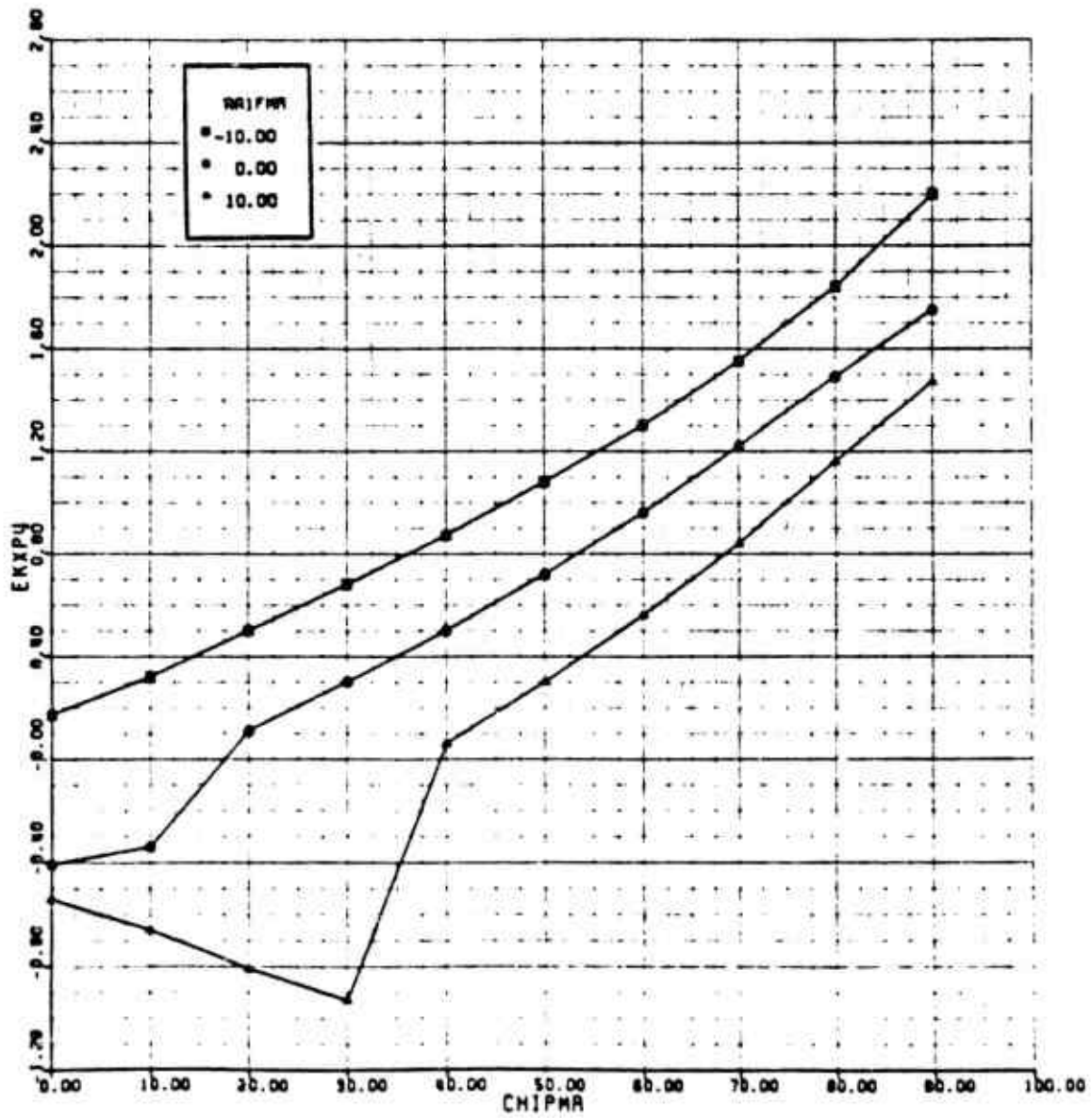


Figure G-33. SA-365N Main Rotor Downwash on Fan Shroud Map (x-direction)

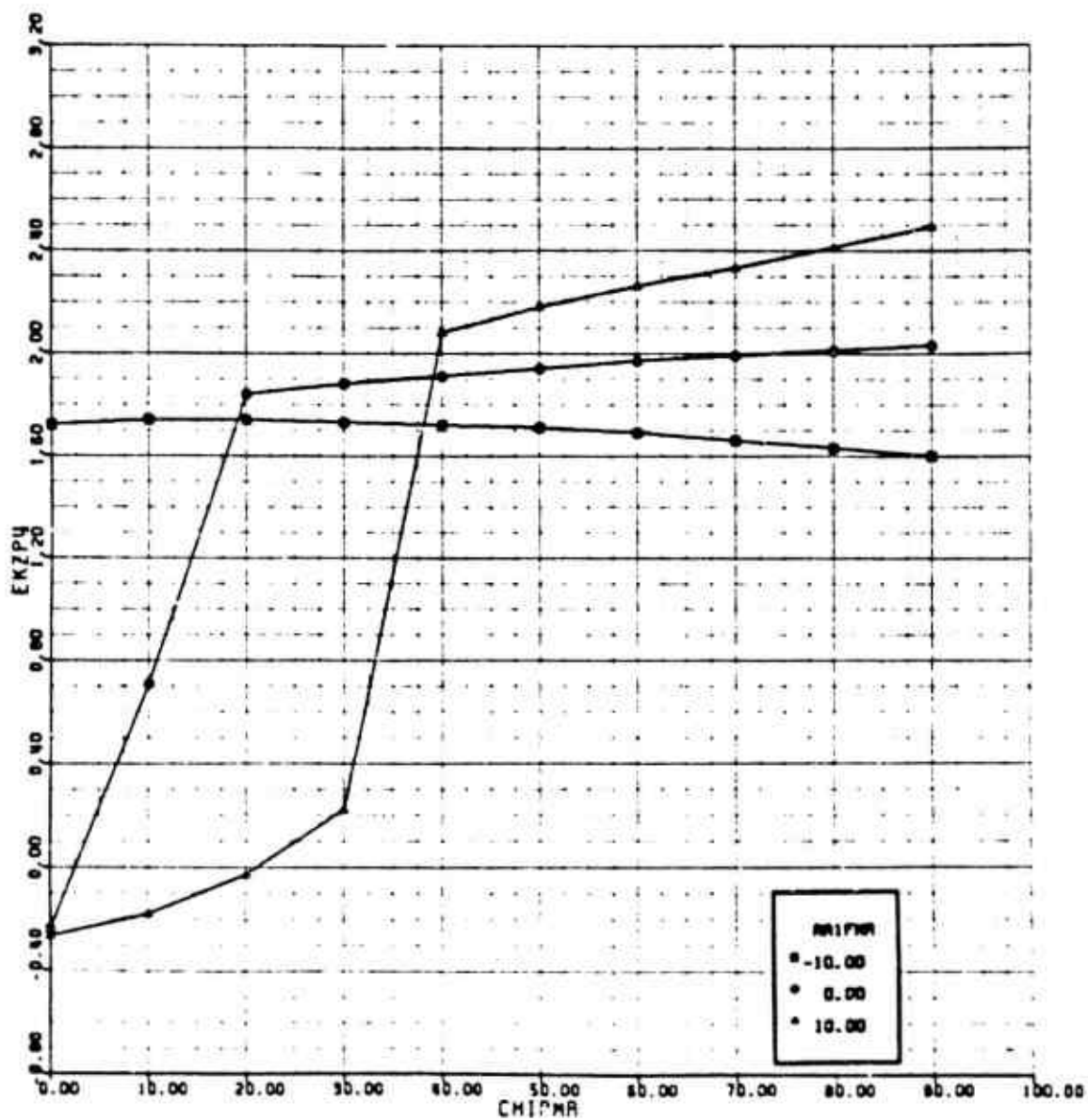


Figure C-34. SA-365N Main Rotor Downwash on Fan Shroud Map (z-direction)

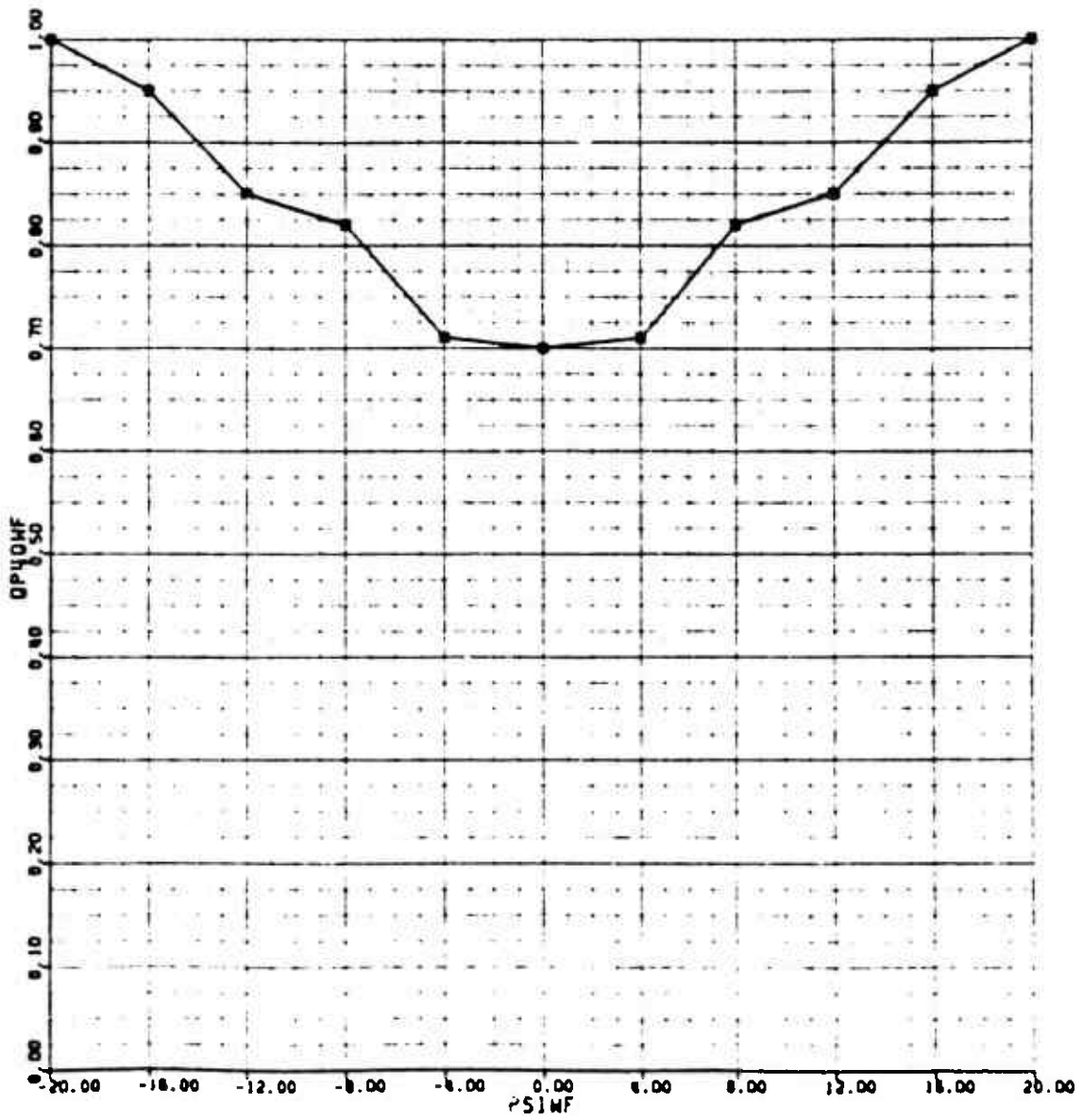


Figure G-35. SA-365N Dynamic Pressure Ratio on Fan Shroud Map

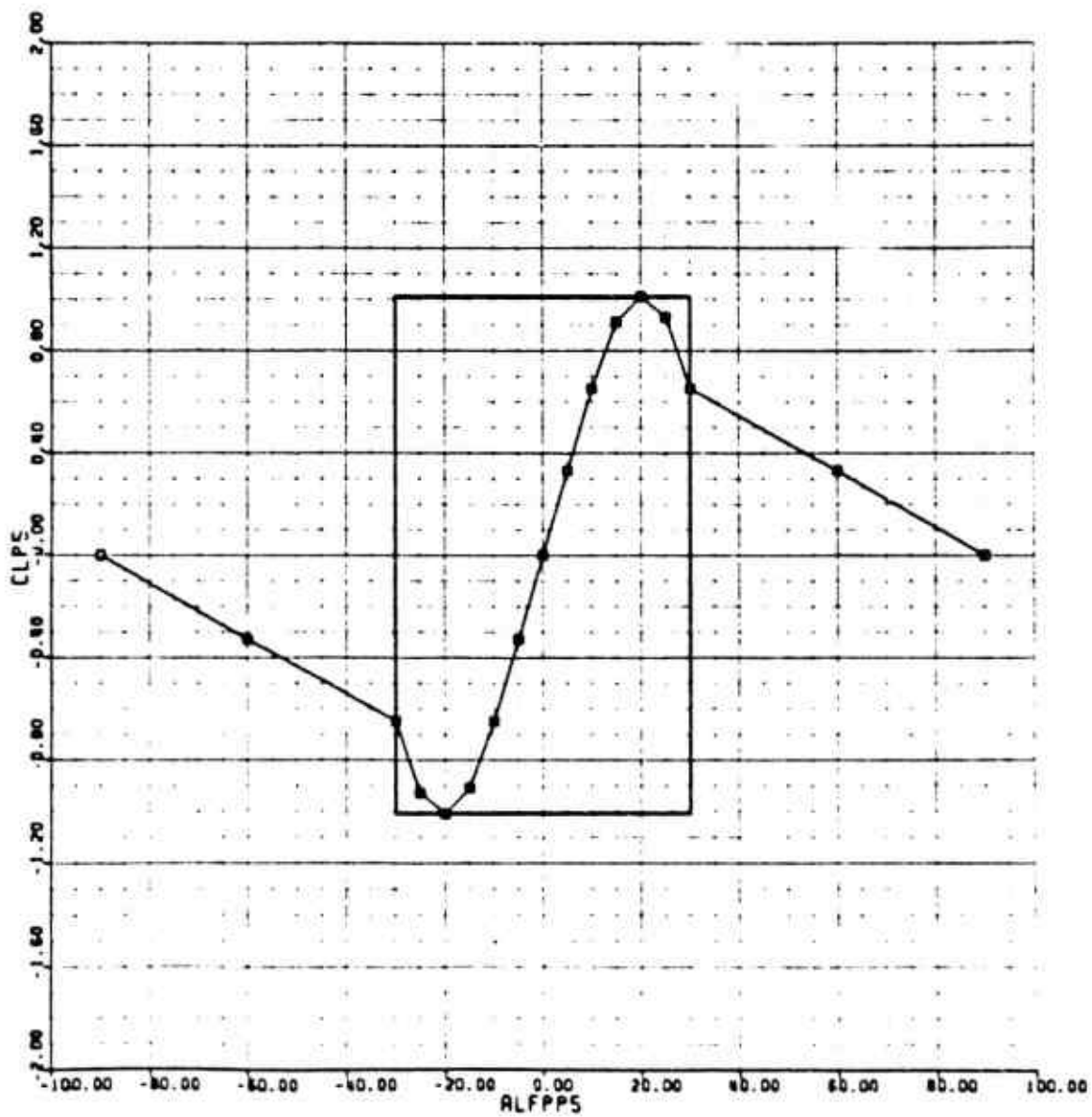


Figure G-36. SA-365N Endplate Lift Map

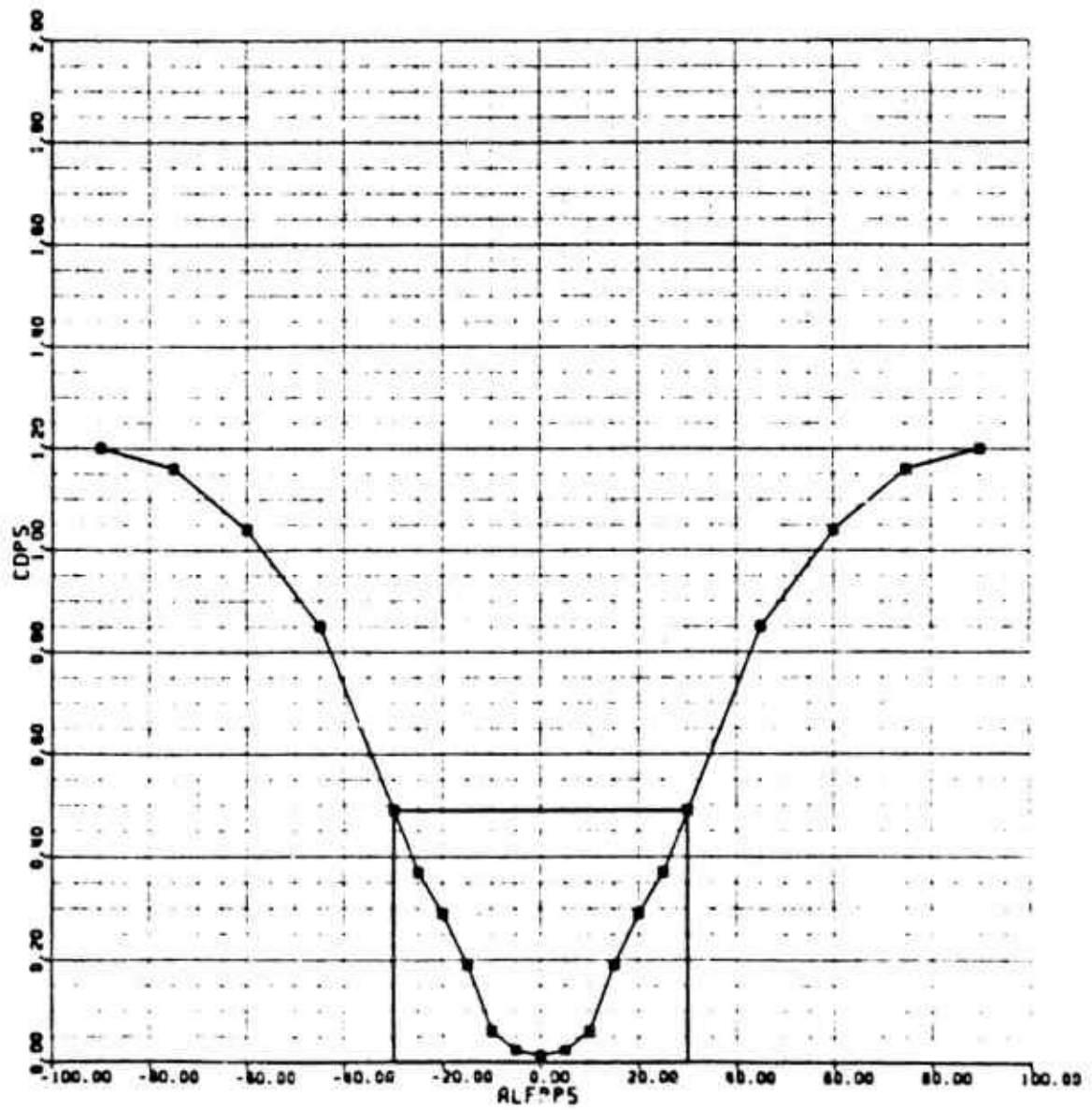


Figure G-37. SA-365N Endplate Drag Map

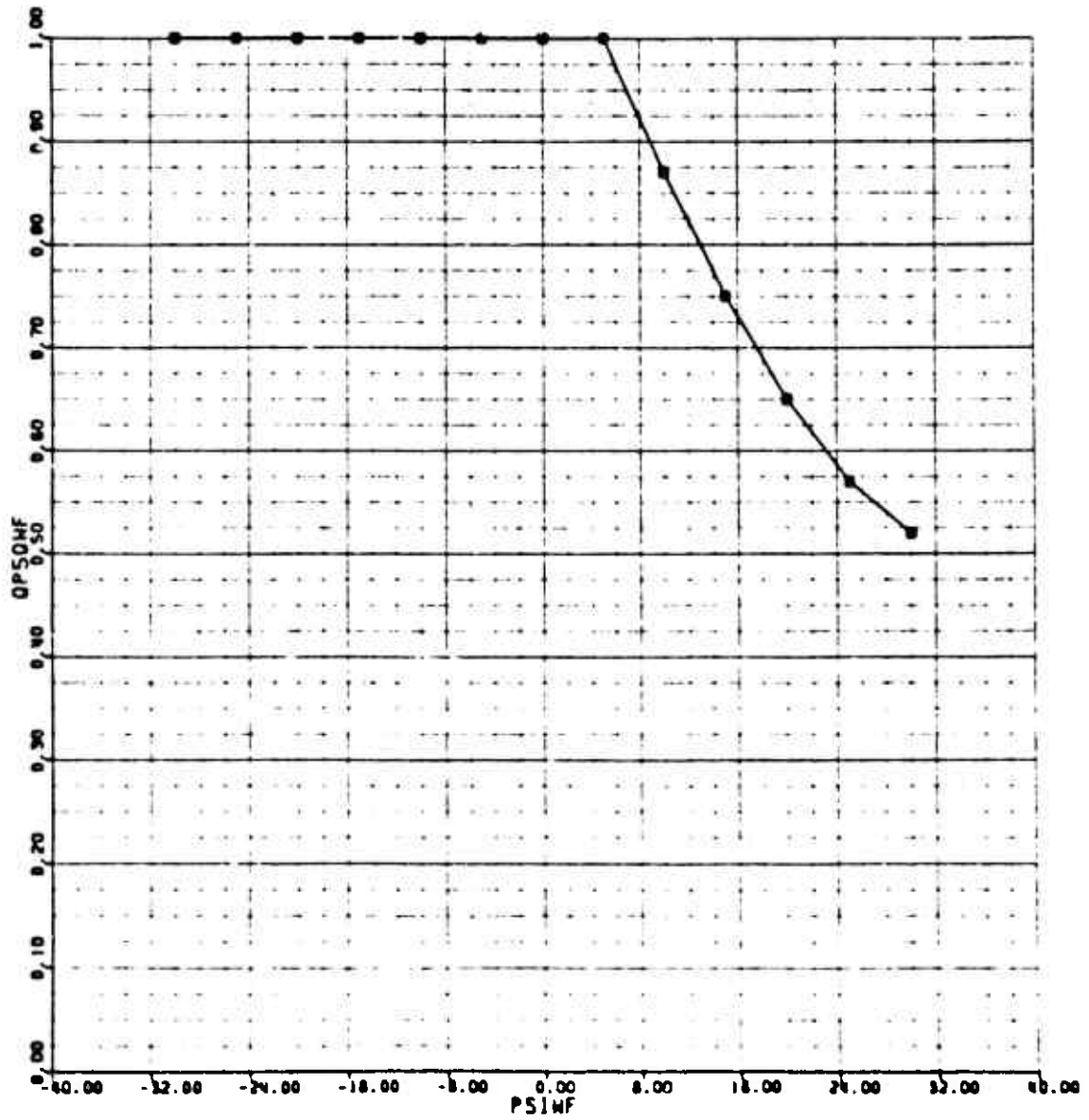


Figure G-38. SA-365N Dynamic Pressure Ratio on Left Endplate Map

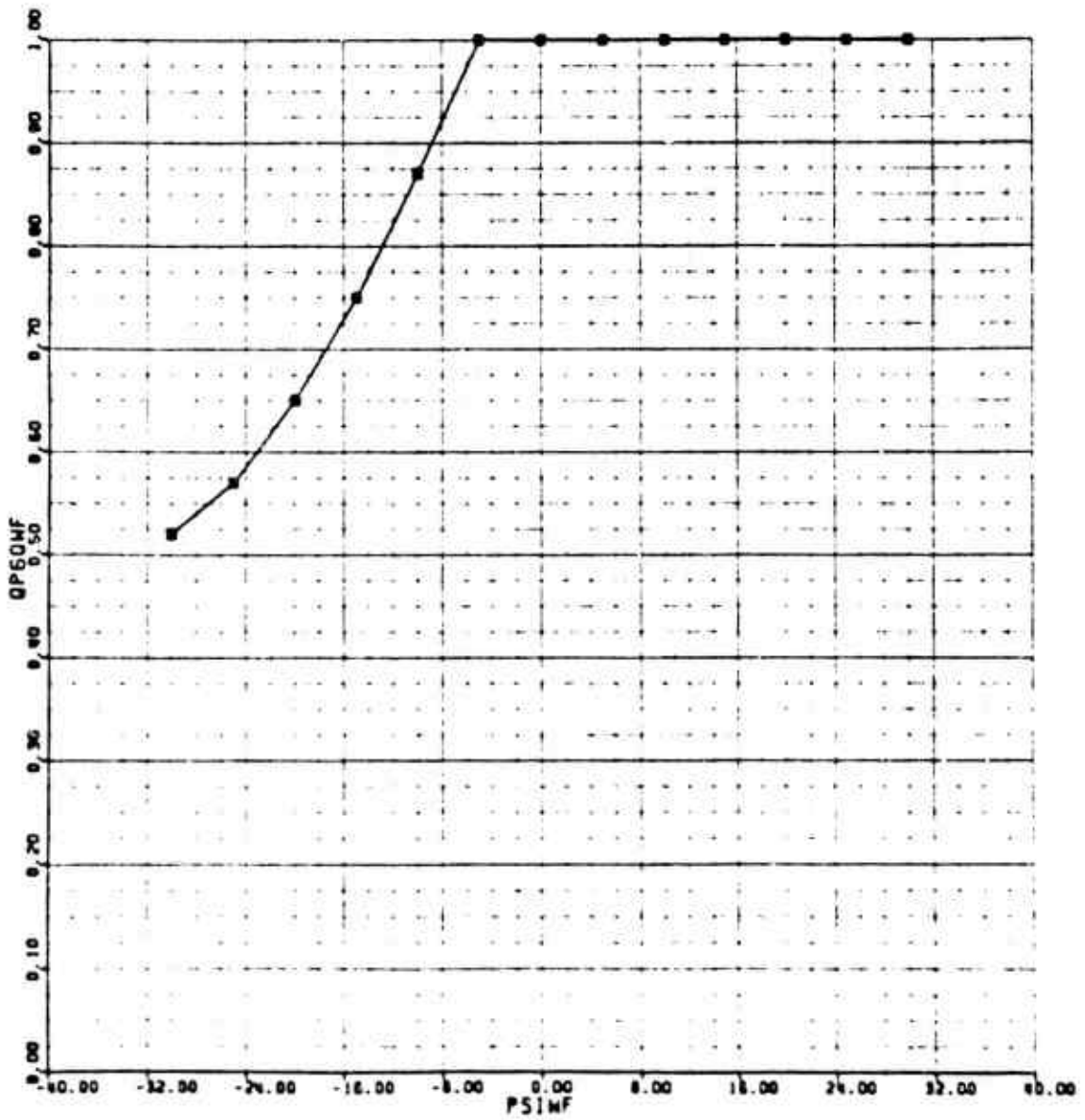


Figure G-39. SA-365N Dynamic Pressure Ratio on Right Endplate Map

APPENDIX H

Mi-28 MODEL DATA

The Mi-28 HAVOC (Figure H-1) is a large attack helicopter that has been under development since 1980 by the Mil Design Bureau in the Soviet Union. It is very large compared to Western attack helicopters as shown in the profile comparison of Figure H-2. Gross weight is estimated to be 22,984 pounds for a typical ground attack mission. The main rotor is 56 feet 5 inches in diameter and power is supplied by two Isotov TV3-117 turboshaft engines flat-rated to 2200 shp at 2000 meters (density altitude of 6561 feet).

The five-bladed main rotor is of conventional articulated design with an estimated flapping hinge offset of 5.5 percent. The rotor blades are of composite construction employing cambered airfoils. The four-bladed tail rotor is 12 feet 7 inches in diameter and consists of two coaxially-mounted two-bladed teetering rotors. These blades are "scissored" with a 35/145 degree spacing. A small horizontal tail is fitted to the top of the vertical fin opposite the tail rotor. Although strut-braced, this surface has an actuator to provide limited incidence variation.

The cockpit is a tandem configuration and is heavily armored. A 30mm gun is fitted to a chin turret under the nose. Stub wings protrude from the bottom of the engine nacelles to provide for carriage of external stores.

The GenHel simulation model for the Mi-28 was based on several unclassified sources. First, numerous photographs of the aircraft taken at the 1980 Paris Airshow were used to create a three-view drawing. This was possible because certain key dimensions were known. This provided the geometry for the location of components along with areas and incidences of the aerodynamic surfaces. Second, the Soviet delegates provided information on weights, rotor speed and engine performance. Finally, other parameters were estimated using existing Sikorsky techniques. For example, the fuselage aerodynamics were scaled-up from Apache data as noted in Appendix M. Inertias were estimated using the parametric equations in Appendix G. Rotor interference velocities on fuselage and empennage were calculated using an existing Heyson downwash program.

No flight test data were available for correlation, but Mi-28 trim characteristics were compared to those of the UH-60A and AH-64A as illustrated in Figures H-3 to H-9. Note that the GenHel Mi-28 model employed the "conventional" direction for rotor rotation, i.e., advancing blade on the right side. The actual aircraft has the opposite rotation, so the trim stick positions for lateral cyclic and pedal would be mirror-imaged for the actual helicopter.

The dominating factor in the Mi-28 trim data is the small size of the horizontal tail. In a helicopter, the horizontal tail makes a major contribution to longitudinal characteristics. In addition to providing pitch stability and pitch damping, the stabilizer tends to hold the fuselage at a level attitude. If the rotor has a strong hub moment capability, the forward inclination of the disk to provide propulsive force generates a strong nose down pitching moment. If the fuselage pitches down to large angles, the drag increases significantly and increases the required disk tilt even more. A large horizontal tail holds the body at a more level attitude, but does increase the bending moment on the main rotor shaft.

As noted earlier, the horizontal tail on the HAVOC appears to be very small, around 14 square feet. The Sikorsky design approach would yield a tail of at least twice this area. Looking at the pitch attitude data of Figure H-3, note that the Mi-28 trims out at more than ten degrees nose-down at 160 knots while the BLACK HAWK and Apache trim at minus four degrees. Sikorsky experience indicates that a nose-down pitch attitude of more than five degrees is uncomfortable to the pilots.

The longitudinal stick position versus airspeed is somewhat less forward than the Apache and BLACK HAWK, while the lateral stick is relatively well centered, as expected. The increased drag caused by the nose-down attitude of the Mi-28 causes the gradient of collective stick position with airspeed to be steeper at high airspeeds than the BLACK HAWK. The increased power required also tends to drive the simulation pedal left at high speeds (right on the actual aircraft) in spite of the cambered vertical fin. The power required comparison plot in Figure H-9 shows a very steep rise at high speed due to the excessive nose-down attitude.

Both the UH-60A and AH-64A are equipped with stabilators. The Mi-28 is also fitted with an all-moving tailplane but the configuration is unusual. The horizontal tail is mounted on top of the vertical fin opposite the tail rotor. Although strut braced, the tail can move over a limited incidence range, estimated to be plus or minus ten degrees. According to the Soviets, the tail servo was coupled to the longitudinal stick and could also be manually "beeped". The variable incidence can compensate for the area deficiency to some extent and a schedule of incidence versus airspeed is shown in Figure 54. Note that increasing the incidence range will not help since the combination of incidence and pitch attitude results in stall of the tail.

All of the numerical data used to model the Mi-28 are provided in this appendix. Table H-1 is a listing of all the input data. The second section presents plots of the map data for fuselage, vertical tail, horizontal tail and wing/stores support aerodynamics along with plots of the rotor interference and fuselage interference data (Figures H-10 through H-30). The tabular data are provided with appropriate labels. Map data are identified with GenHel acronyms provided in the List of Symbols.

For the Mi-28 model, the panel allocation was as follows:

1. Right horizontal tail
2. Left horizontal tail
3. Vertical tail
4. Right wing/stores support
5. Left wing/stores support

TABLE H-1. MI-28 SPECIFIC FILE DATA

```

;***** INPUT PARAMETERS FOR MAIN ROTOR MODULES (#A.) *****

FSMR:: 400.0 ; PUSELAGE STATION, INCHES
WLMR:: 300.0 ; WATERLINE STATION, INCHES
BLMR:: 0.0 ; BUTTLINE STATION, INCHES (+IVE TO PORT)
RMR:: 28.21 ; RADIUS, FT.
OMGTR:: 25.34 ; TRIM ROTATIONAL SPEED, RAD/SEC
BMR:: 5.0 ; ACTUAL NUMBER OF BLADES
ISMTR:: -5.0 ; LONGITUDINAL SHAFT TILT, (POS. BACKWARDS), DEG
ILMR:: 0.0 ; LATERAL SHAFT TILT, (POS. STARBOARD), DEG
DELSMR:: -5.0 ; SWASHPLATE PHASE ANGLE, DEG
DELSMR:: 0.0 ; FLAPPING HINGE OFFSET ANGLE, DEG.
KAP1MR:: 0.0 ; LAGGING HINGE OFFSET COEF. (FUNC(LG))
KAP2MR:: 0.0 ; LAGGING HINGE OFFSET COEF. (FUNC(LG**2))
CHDTR:: 2.0 ; BLADE CHORD AT TIP, FT.
CHDRMR:: 2.0 ; BLADE CHORD AT ROOT, FT.
OPSTR:: 1.552 ; HINGE OFFSET, FT.
SPRLMR:: 6.04 ; HINGE TO START OF BLADE, FT.
WTBDMR:: 244.1 ; WEIGHT OF ONE BLADE, LBS.
IBMR:: 1336.0 ; BLADE MOMENT OF INERTIA ABOUT HINGE, SLUG-FT**2
MBMR:: 77.08 ; BLADE MASS MOMENT ABOUT HINGE, SLUG-FT
IRMR:: 943.9 ; INERTIA OF DRIVE TRAIN: (LESS 2 ENGINES & ROTOR BLADES)
; (DUAL ENGINE FAILURE). SLUG-FT**2

BTLMR:: .97 ; BLADE TIP CUT OFF RATIO
DCDMR:: .002 ; DELTA DRAG COEF. FOR EACH SEGMENT
NBSMR:: 5 ; NUMBER OF BLADES SIMULATED, FIX POINT
NSSMR:: 5 ; NUMBER OF SEGMENTS SIMULATED, FIX POINT

; ** MAIN ROTOR NON-LINEAR TWIST MAP (FROM B/H) **
TWMRMP:: UVR## ; MAP ARGUMENT: LOOP UP ROUTINE
; XSEGR## ; INPUT VARIABLE
; TWSTMR## ; OUTPUT VARIABLE
; TWMRLO ; MAP NAME
EXP 0.0, 1.0, 0.05 ; LOWER LIMIT, UPPER LIMIT, DELTA

TWMRLO: EXP 0.00, 0.00, 0.00, 0.00, -0.15
EXP -0.95, -1.80, -2.75, -3.55, -4.40
EXP -5.30, -6.15, -7.10, -7.90, -8.80
EXP -9.65, -10.30, -10.75, -12.30, -13.10
EXP -10.90

;***** MAIN ROTOR DOWNWASH SUBMODULE (#A) *****

RCTMR:: 1.0 ; THRUST GAIN FOR UNIFORM DOWNWASH
RCMR:: 0.0 ; PITCH MOM. GAIN FOR DOWNWASH SIN. HARMONIC
RSLMR:: 0.0 ; ROLL MOM. GAIN FOR DOWNWASH COS. HARMONIC
TDWOMR:: 0.01038 ; TIME CONST. FOR UNIFORM DOWNWASH FILTER, SEC
TDWCHR:: 0.0 ; TIME CONST. FOR DOWNWASH SIN. HARMON. FILTER, SEC.
TDWSMR:: 0.0 ; TIME CONST. FOR DOWNWASH COS. HARMON. FILTER, SEC.

;***** FLAPPING/LAGGING DAMPER CALCULATIONS (#C) *****

RBRMR:: 0.0 ; FLAPPING HINGE SPRING CONST, FT-LBS/RAD
RBRMR:: 0.0 ; FLAPPING HINGE DAMPER CONST, FT-LBS-SEC/RAD

; **SE** OF MOUNTING DIMENSIONS FOR LAG DAMPER, INCHES**
ALDMR:: 0.227 ;
BLDMR:: 3.242 ;
CLDMR:: 12.040 ;
DLDMR:: 10.0102 ;
RLDMR:: 6.898 ;
LGDTR:: 7.0 ; ALIGNMENT OFFSET IN RELATION TO LAG, DEG
TLDMR:: 17.481 ; FIXED BLADE PITCH RELATIONSHIP BET. ARM AND TBCUFF

```

TABLE H-1. MI-28 SPECIFIC FILE DATA (Cont'd)

```

; ** BLACK HAWK LAG DAMPER FORCE VS LAG DAMPER ARM RATE
LDMRMP: :UVSUVS00 ;MAP ARGUMENT:LOOK UP ROUTINE
        LD.MR00(A16) ;INPUT VARIABLE
        PLD.MR00(A16) ;OUTPUT VARIABLE
        LDMRLO ;LOW RANGE MAP NAME
        EXP 0.0,2.0,0.1 ;LOWER LIMIT,UPPER LIMIT,DELTA
        LDMRHI ;HIGH RANGE MAP NAME
        EXP 2.0,7.0,1.0 ;LOWER LIMIT,UPPER LIMIT,DELTA

; LOW ANGLE MAP: LD.MR 0 TO 2.0 , DELTA = .1
LDMRLO: EXP 0.0, 30.0, 90.0, 160.0, 280.0
        EXP 490.0, 720.0, 950.0, 1190.0, 1400.0
        EXP 1630.0, 1860.0, 2090.0, 2310.0, 2530.0
        EXP 2770.0, 2980.0, 3200.0, 3310.0, 3370.0
        EXP 3410.0

; HIGH ANGLE MAP: LD.MR 2.0 TO 7.0 , DELTA=1.0
LDMRHI: EXP 3410.0, 3550.0, 3615.0, 3680.0, 3745.0
        EXP 3815.0

;***** INPUT PARAMETERS FOR FUSELAGE/WING (4A) *****
;***** MOUNTING POINT FOR MODEL IN WIND TUNNEL *****
PSWF:: 400.0 ; FUSELAGE STATION,IN.
WLWF:: 205.8 ; WATERLINE STATION,IN.
BLWF:: 0.0 ; BUTTLINE STATION,IN. (+IVE TO POFT)
IWF:: 0.0 ; WING INCIDENCE,DEG.

; ** MI-28 FUSELAGE LIFT (TAIL OFF) VS ALFWF
LQFMP: :UVPVVR04 ;MAP ARGUMENT:LOOK UP ROUTINE
        ALFWF04 ;INPUT VARIABLE
        LQF40 ;OUTPUT VARIABLE
        LQFLO ;LOW ANGLE MAP NAME
        EXP -30.0,30.0,5.0 ;LOWER LIMIT,UPPER LIMIT,DELTA-LOW ANGLE
        LQFHI ;HIGH ANGLE MAP NAME
        EXP -90.0,90.0,10.0 ;LOWER LIMIT,UPPER LIMIT,DELTA-HIGH ANGLE

; LOW ANGLE MAP: ALFWF -30 TO 30 , DELTA=5
LQFLO: EXP -83.9, -74.6, -63.4, -52.2, -37.3
        EXP -20.5, -1.9, 22.4, 46.6, 76.5
        EXP 104.4, 121.2, 132.4

; HIGH ANGLE MAP: ALFWF -90 TO 90 , DELTA=10
LQFHI: EXP 0.0, -35.4, -63.4, -82.1, -93.3
        EXP -95.1, -83.9, -63.4, -37.3, -1.9
        EXP 46.6, 104.4, 132.4, 141.7, 138.0
        EXP 119.4, 93.3, 56.0, 0.0

; ** MI-28 FUSELAGE DRAG (TAIL OFF) VS ALFWF
DQFMP: :BIVBIV00 ;MAP ARGUMENT:LOOK UP ROUTINE
        EXP ALFWF04,PSINWF44 ;INPUT VARIABLE #1, INPUT VARIABLE #2
        DQF04 ;OUTPUT VARIABLE
        DQFLO ;LOW ANGLE MAP NAME
        EXP -30.0,30.0,5.0,15 ;LOWER LIMIT,UPPER LIMIT,DELTA, # ITEMS
        EXP -20.0,20.0,10.0 ;LOWER LIMIT,UPPER LIMIT,DELTA,PSINWF
        DQFHI ;HIGH ANGLE MAP NAME
        EXP -90.0,90.0,10.0,23 ;LOWER LIMIT,UPPER LIMIT,DELTA,4 ITEMS
        EXP -20.0,20.0,10.0 ;LOWER LIMIT,UPPER LIMIT,DELTA,PSINWF

; LOW ANGLE MAP: ALFWF -30 TO 30, DELTA=5,PSINWF=-20 TO +20
; PSINWF = -20
DQFLO: EXP 144.1, 139.0, 133.9, 125.8, 118.7
        EXP 115.7, 113.6, 115.7, 118.7, 124.8
        EXP 131.9, 38.08, 42.09

; PSINWF = -10
EXP 133.9, 125.8, 109.6, 91.3, 80.1

```


TABLE H-1. MI-28 SPECIFIC FILE DATA (Cont'd)

	EXP	73.0,	71.0,	71.0,	77.1,	87.3
	EXP	105.5,	121.7,	133.9		
		; PSIMF = 0				
	EXP	123.8,	111.7,	88.0,	68.1,	56.4
	EXP	48.6,	45.0,	45.0,	50.9,	63.1
	EXP	87.3,	111.6,	125.8		
		; PSIMF = +10				
	EXP	133.9,	125.8,	109.6,	91.3,	80.2
	EXP	73.0,	71.0,	71.0,	77.1,	87.3
	EXP	105.5,	121.7,	133.9		
		; PSIMF = +20				
	EXP	144.1,	139.0,	133.9,	125.8,	118.7
	EXP	115.7,	113.6,	115.7,	118.7,	124.8
	EXP	131.9,	138.0,	142.0		
		; HIGH ANGLE MAP: ALFWF -90 TO 90, DELTA-10, PSIMF--20 TO +20				
		; PSIMF = -20				
DQFMI:	EXP	170.4,	166.4,	162.3,	160.3,	156.2
	EXP	151.2,	144.1,	133.9,	118.7,	113.6
	EXP	118.7,	131.9,	142.0,	150.1,	156.2
	EXP	160.3,	164.3,	166.4,	168.4	
		; PSIMF = -10				
	EXP	170.4,	166.4,	162.3,	158.3,	152.2
	EXP	145.1,	133.9,	109.6,	80.2,	71.0
	EXP	77.1,	105.5,	133.9,	146.1,	154.2
	EXP	159.3,	164.3,	166.4,	168.4	
		; PSIMF = 0				
	EXP	170.4,	166.4,	162.3,	156.2,	148.1
	EXP	140.0,	123.8,	91.3,	62.9,	54.8
	EXP	58.8,	91.3,	125.8,	143.0,	152.2
	EXP	158.3,	164.3,	166.4,	168.4	
		; PSIMF = +10				
	EXP	170.4,	166.4,	162.3,	158.3,	152.2
	EXP	145.1,	133.9,	109.6,	80.2,	71.0
	EXP	77.1,	105.5,	133.9,	146.1,	154.2
	EXP	159.3,	164.3,	166.4,	168.4	
		; PSIMF = +20				
	EXP	170.4,	166.4,	162.3,	160.3,	156.2
	EXP	151.2,	144.1,	133.9,	118.7,	113.6
	EXP	118.7,	131.9,	142.0,	150.1,	156.2
	EXP	160.3,	164.3,	166.4,	168.4	
		; ** MI-28 FUSELAGE FITCH MOMENT (TAIL OFF) VS ALFWF				
MOFNF:	UVRUVR00	;MAP ARGUMENT:LOOK UP ROUTINE				
	ALFWF00	;INPUT VARIABLE				
	MOF00	;OUTPUT VARIABLE				
	MOFLO	;LOW ANGLE MAP NAME				
EXP	-30.0,30.0,5.0	;LOWER LIMIT,UPPER LIMIT,DELTA-LOW ANGLE				
	MOFHI	;HIGH ANGLE MAP NAME				
EXP	-90.0,90.0,10.0	;LOWER LIMIT,UPPER LIMIT,DELTA-HIGH ANGLE				
		; LOW ANGLE MAP: ALFWF -30 TO 30 , DELTA-5				
MOFLO:	EXP	-665.8,	-633.1,	-571.9,	-447.5,	-331.8
	EXP	-222.7,	-135.3,	-54.6,	15.3,	76.4
	EXP	135.3,	189.9,	240.1		
		; HIGH ANGLE MAP: ALFWF -90 TO 90 , DELTA-10				
MOFHI:	EXP	0.0,	-207.4,	-392.9,	-534.8,	-622.2
	EXP	-670.2,	-665.8,	-571.9,	-331.8,	-135.3

TABLE H-1. MI-28 SPECIFIC FILE DATA (Cont'd)

EXP	15.3,	135.3,	240.1,	334.0,	355.8
EXP	327.5,	262.0,	131.0,	0.0	

; ** MI-28 FUSELAGE SIDE FORCE (TAIL OFF) VS PSIWF
YQFMP: :UVRUVR## ;MAP ARGUMENT:LOOK UP ROUTINE
PSIWF## ;INPUT VARIABLE
YQF## ;OUTPUT VARIABLE
YQFLO ;LOW ANGLE MAP NAME
EXP -30.0,30.0,5.0 ;LOWER LIMIT,UPPER LIMIT,DELTA-LOW ANGLE
YQFHI ;HIGH ANGLE MAP NAME
EXP -90.0,90.0,10.0 ;LOWER LIMIT,UPPER LIMIT,DELTA-HIGH ANGLE

; LOW ANGLE MAP: PSIWF -30 TO 30, DELTA=5
YQFLO: EXP -125.2, -108.8, -89.5, -67.1, -44.7
EXP -22.4, 0.0, 22.4, 44.7, 67.1
EXP 89.5, 108.8, 125.1

; HIGH ANGLE MAP: PSIWF -90 TO 90, DELTA=10
YQFHI: EXP 0.0, -58.2, -102.3, -131.2, -146.1
EXP -146.1, -125.2, -89.5, -44.7, 0.0
EXP 44.7, 89.5, 125.2, 146.1, 146.1
EXP 135.7, 111.8, 65.6, 0.0

; ** MI-28 FUSELAGE YAWING MOMENT (TAIL OFF) VS PSIWF
NQFMP: :UVRUVR## ;MAP ARGUMENT:LOOK UP ROUTINE
PSIWF## ;INPUT VARIABLE
NQF## ;OUTPUT VARIABLE
NQFLO ;LOW ANGLE MAP NAME
EXP -30.0,30.0,5.0 ;LOWER LIMIT,UPPER LIMIT,DELTA-LOW ANGLE
NQFHI ;HIGH ANGLE MAP NAME
EXP -90.0,90.0,10.0 ;LOWER LIMIT,UPPER LIMIT,DELTA-HIGH ANGLE

; LOW ANGLE MAP: PSIWF -30 TO 30, DELTA=5
NQFLO: EXP -890.5, -803.2, -680.9, -567.5, -410.3
EXP -218.3, -17.5, 157.1, 323.0, 457.5
EXP 567.5, 663.5, 724.6

; HIGH ANGLE MAP: PSIWF -90 TO 90, DELTA=10
NQFHI: EXP 0.0, -349.2, -637.3, -838.1, -942.8
EXP -960.3, -890.5, -680.9, -410.3, -17.5
EXP 323.0, 567.5, 724.6, 803.2, 768.2
EXP 663.5, 488.9, 261.9, 0.0

;***** ROTOR INTERFERENCE ON THE FUSELAGE (MRPA) *****

; ** MI-28 FORE/AFT M.R. DOWNWASH AT FUSELAGE
EXWFMP: :BIV## ;MAP ARGUMENT:LOOK UP ROUTINE
EXP CHIPMR##,AAIFMR## ;INPUT VARIABLE#1,INPUT VARIABLE#2
ERXWF## ;OUTPUT VARIABLE
EXWFLO ;LOW ANGLE MAP NAME
EXP 0.0,90.0,10.0,'D10 ;LOW LIM,UPPER LIM,DELTA-CHIPMR
EXP -10.0,10.0,10.0 ;LOW LIM,UPPER LIM,DELTA-AAIFMR

; LOW ANGLE MAP CHIPMR 0 TO 90 (DEL=10) AAIFMR -10.0,10
; AAIFMR=-10
EXWFLO: EXP 0.37, 0.46, 0.57, 0.68, 0.79
EXP 0.91, 1.04, 1.18, 1.32, 1.32

; AAIFMR=0
EXP 0.13, 0.23, 0.34, 0.46, 0.58
EXP 0.70, 0.82, 1.00, 1.17, 1.17

; AAIFMR=10
EXP -0.11, -0.01, 0.10, 0.22, 0.34
EXP 0.47, 0.61, 0.77, 0.93, 0.93

TABLE H-1. MI-28 SPECIFIC FILE DATA (Cont'd)

```

; ** MI-28 VERTICAL M.R. DOWNWASH AT FUSELAGE
EZWMP::NIV## ;MAP ARGUMENT:LOOK UP ROUTINE
EXP CHIPMR##,AAIFMR## ;INPUT VARIABLE#1,INPUT VARIABLE#2
EZWF## ;OUTPUT VARIABLE
EZWFLO ;LOW ANGLE MAP NAME
EXP 0.0,90.0,10.0,^O10 ;LOW LIM,UPPER LIM,DELTA-CHIPMR
EXP -10.0,10.0,10.0 ;LOW LIM,UPPER LIM,DELTA-AAIFMR

; LOW ANGLE MAP CHIPMR 0 TO 90 (OEL=10) AAIFMR -10,0,10
; AAIFMR=-10
EZWFO:EXP 1.11, 1.09, 1.08, 1.065, 1.05
EXP 1.04, 1.02, 1.01, 1.0, 0.88
0.6

; AAIFMR=0
EXP 1.12, 1.12, 1.12, 1.12, 1.12
EXP 1.12, 1.12, 1.12, 1.11, 0.96
0.6

; AAIFMR=10
EXP 1.15, 1.15, 1.15, 1.15, 1.16
EXP 1.17, 1.18, 1.22, 1.16, 0.98
0.6

;***** INPUT PARAMETERS FOR PANEL #2 (#A) *****
FSP2:: 825.0 ; FUSELAGE STATION, INCH
WLP2:: 312.5 ; WATERLINE STATION, INCH
BLP2:: 25.6 ; BUTTLINE STATION, INCH (+IVE TO PORT)
SAP2:: 14.0 ; SURFACE AREA OF PANEL, FT**2
GAMP2:: 0.0 ; PANEL ORIENTATION, DEG
IOP2:: 0.0 ; PANEL INCIDENCE, DEG
CP2:: 1.0 ; PANEL MEAN AERO CHORD, FT

CLP2MP::UVRUVR## ;MAP ARGUMENT:LOOK UP, ROUTINE
ALFPP2## ;INPUT VARIABLE
CLP2## ;OUTPUT VARIABLE
CLP2LO ;LOW ANGLE MAP NAME
EXP -30.0,30.0,5.0 ;LOWER LIMIT,UPPER LIMIT,DELTA-LOW ANGLE
CLP2HI ;HIGH ANGLE MAP NAME
EXP -90.0,90.0,10.0 ;LOWER LIMIT,UPPER LIMIT,DELTA-HIGH ANGLE

; LOW ANGLE MAP ALFPP2 -30 TO 30,DELTA=5
CLP2LO: EXP -0.80, -0.87, -0.93, -0.88, -0.58
EXP -0.29, 0.00, 0.29, 0.58, 0.88
EXP 0.93, 0.87, 0.80

; HIGH ANGLE MAP ALFPP2 -90 TO 90,DELTA=10
CLP2HI: EXP 0.00, -0.14, -0.28, -0.40, -0.53
EXP -0.68, -0.80, -0.93, -0.58, 0.00
EXP 0.58, 0.93, 0.80, 0.68, 0.53
EXP 0.40, 0.28, 0.14, 0.00

; ** HORIZONTAL STABILIZER ORAG VS ALFPP2
CDP2MP::UVRUVR## ;MAP ARGUMENT:LOOK UP ROUTINE
ALFPP2## ;INPUT VARIABLE
CDP2## ;OUTPUT VARIABLE
CDP2LO ;LDW ANGLE MAP NAME
EXP -30.0,30.0,5.0 ;LDWER LIMIT,UPPER LIMIT,DELTA
CDP2HI ;HIGH ANGLE MAP NAME
EXP -90.0,90.0,10.0 ;LOWER LIMIT,UPPER LIMIT,DELTA

; LDW ANGLE MAP ALFPP2 -30 TO 30,DELTA=5
CDP2LO: EXP 0.343, 0.271, 0.200, 0.105, 0.050
EXP 0.020, 0.010, 0.020, 0.050, 0.105
EXP 0.200, 0.271, 0.343

```

TABLE H-1. M1-28 SPECIFIC FILE DATA (Cont'd)

```

; HIGH ANGLE MAP ALPPP2 -90 TO 90, DELTA-10
CDP2BI: EXP 1.200, 1.057, 0.914, 0.771, 0.629
        EXP 0.486, 0.343, 0.200, 0.050, 0.010
        EXP 0.050, 0.200, 0.343, 0.486, 0.629
        EXP 0.771, 0.914, 1.057, 1.200
    
```

;***** INPUT PARAMETERS FOR ROTOR INTERFERENCE ON THE HORIZ.TAIL #1

```

; ** FORE/AFT H.R. DOWNWASH AT HORIZONTAL TAIL
EXP2MP: BIV#4 ;MAP ARGUMENT:LOOK UP ROUTINE
        EXP CHIPMR#4, AALFMR#4 ;INPUT VARIABLE #1, INPUT VARIABLE #2
        ERXP2#4 ;OUTPUT VARIABLE
        EXP2LO ;LOW ANGLE MAP NAME
        EXP 0.0,90.0,10.0,"D10 ;LOW LIM,UPPER LIM,DELTA-CHIPMR
        EXP -10.0,10.0,10.0 ;LOW LIM,UPPER LIM,DELTA-AALFMR
    
```

```

; LOW ANGLE MAP CHIPMR 0 TO 90 (DEL-10) AALFMR -10,0,10
; AALFMR=-10
EXP2LO: EXP -0.40, -0.48, -0.57, -0.65, -0.92
        EXP 1.17, 1.42, 1.69, 1.95, 2.20

; AALFMR=0
        EXP -0.45, -0.51, -0.57, -0.62, -0.66
        EXP -0.66, -0.61, -0.45, 1.76, 2.00

; AALFMR=10
        EXP -0.43, -0.46, -0.49, -0.52, -0.54
        EXP -0.54, -0.51, -0.44, -0.31, -0.87
    
```

```

; ** VERTICAL H.R. DOWNWASH AT HORIZONTAL TAIL
EXP2MP: BIV#4 ;MAP ARGUMENT:LOOK UP ROUTINE
        EXP CHIPMR#4, AALFMR#4 ;INPUT VARIABLE #1, INPUT VARIABLE #2
        ERXP2#4 ;OUTPUT VARIABLE
        EXP2LO ;LOW ANGLE MAP NAME
        EXP 0.0,90.0,10.0,"D10 ;LOW LIM,UPPER LIM,DELTA-CHIPMR
        EXP -10.0,10.0,10.0 ;LOW LIM,UPPER LIM,DELTA-AALFMR
    
```

```

; LOW ANGLE MAP CHIPMR 0 TO 90 (DEL-10) AALFMR -10,0,10
; AALFMR=-10
EXP2LO: EXP -0.06, 0.04, 0.20, 0.42, 1.83
        EXP 1.82, 1.79, 1.75, 1.69, 1.65

; AALFMR=0
        EXP -0.01, 0.08, 0.21, 0.37, 0.58
        EXP 0.85, 1.18, 1.57, 2.10, 2.70

; AALFMR=10
        EXP 0.07, 0.14, 0.24, 0.35, 0.59
        EXP 0.68, 0.91, 1.19, 1.54, 1.90
    
```

;***** FUSELAGE INTERFERENCE ON THE HORIZ.TAIL #1 (WFFA) *****

```

; ** S-61A DYNAMIC PRESSURE RATIO AT HORIZONTAL TAIL
QP2MP: UVR#4 ;MAP ARGUMENT:LOOK UP ROUTINE
        ALPWF#4 ;INPUT VARIABLE
        QP2QWF#4 ;OUTPUT VARIABLE
        QP2LO ;LOW ANGLE MAP NAME
        EXP -30.0,30.0,5.0 ;LOWER LIM,UPPER LIM,DELTA
    
```

```

; LOW ANGLE MAP ALPWF -30 TO 30 DELTA=5
QP2LO: EXP 1.00, 1.00, 1.00, 1.00, 0.85, 0.70, 0.70
        EXP 0.70, 0.65, 0.70, 0.85, 1.00, 1.00
    
```

;** S-61A FUSELAGE DOWNWASH ON HORIZ. TAIL **

TABLE H-1. MI-28 SPECIFIC FILE DATA (Cont'd)

```

EPP2M: :UVR00 ;MAP ARGUMENT:LOOK UP ROUTINE
        ALFWF00 ;INPUT VARIABLE
        EPSP200 ;OUTPUT VARIABLE
        EPP2LO ;LOW ANGLE MAP NAME
        EXP -30.0,30.0,5.0 ;LOWER LIR,UPPER LIR,DELTA
                ;LOW ANGLE MAP ALFWF -30 TO 30 DELTA=5
EPP2LO: EXP 0.0, -5.0, -3.0, -1.0, 1.0, 1.0, 1.0
        EXP 1.0, 3.7, 6.4, 9.0, 4.5, 0.0

;***** INPUT PARAMETERS FOR PANEL #3 (#A) *****

FSP3: : 790.0 ; FUSELAGE STATION,INCH
WLP3: : 267.5 ; WATERLINE STATION,INCH
BLP3: : 0.0 ; BUTTLINE STATION,INCH
SAP3: : 21.88 ; SURFACE AREA OF PANEL IF NOT INCLUDE IN MAP
GAMP3: : 90.0 ; PANEL ORIENTATION, DEG
IOP3: : 0.0 ; PANEL INCIDENCE,DEG
CP3: : 1.0 ; PANEL MEAN AREA CHORD,FT

; ** AN-64A VERTICAL STABILIZER LIFT COEFFICIENT VS ALPPP3
; ** S=21.9 FT**2,ASPECT RATIO =1.56,4415 RDD RODT,4416 TIP AIRFOIL
CLP3M: :UVRUVR00 ;MAP ARGUMENT:LDDK UP ROUTINE
        ALPPP300 ;INPUT VARIABLE
        CLP300 ;OUTPUT VARIABLE
        CLP3LO ;LOW ANGLE MAP NAME
        EXP -30.0,30.0,5.0 ;LOWER LIMIT,UPPER LIRIT,DELTA-LOW ANGLE
        CLP3HI ;HIGH ANGLE MAP NAME
        EXP -90.0,90.0,10.0 ;LDWER LIRIT,UPPER LIRIT,DELTA-HIGH ANGLE
                ; LOW ANGLE MAP ALPPP3 -30 TO 30,DELTA=5
CLP3LD:EXP -1.06, -0.81, -0.57, -0.31, -0.05
        EXP 0.20, 0.45, 0.71, 0.97, 1.19
        EXP 1.34, 1.40, 1.34
                ; HIGH ANGLE MAP ALPPP3 -90 TO 90,DELTA=10
CLP3HI:EXP 0.00, -0.22, -0.45, -0.68, -0.90
        EXP -1.13, -1.06, -0.57, -0.05, 0.45
        EXP 0.97, 1.34, 1.34, 1.12, 0.93
        EXP 0.68, 0.45, 0.23, 0.00

; ** AN-64A VERTICAL STABILIZER DRAG COEFFICIENT VS ALPPP3
CDF3M: :UVRUVR00 ;MAP ARGUMENT:LOOK UP ROUTINE
        ALPPP300 ;INPUT VARIABLE
        CDF300 ;OUTPUT VARIABLE
        CDF3LO ;LOW ANGLE MAP NAME
        EXP -30.0,30.0,5.0 ;LOWER LIMIT,UPPER LIMIT,DELTA-LOW ANGLE
        CDF3HI ;HIGH ANGLE MAP NAME
        EXP -90.0,90.0,10.0 ;LOWER LIRIT,UPPER LIMIT,DELTA-HIGH ANGLE
                ; LDW ANGLE MAP ALPPP3 -30 TD 30,DELTA=5
CDF3LD: EXP 0.559, 0.505, 0.310, 0.180, 0.130
        EXP 0.100, 0.090, 0.100, 0.130, 0.180
        EXP 0.310, 0.505, 0.559
                ; NIGN ANGLE MAP ALPPP3 -90 TD 90,DELTA=10
CDF3HI: EXP 1.200, 1.093, 0.986, 0.879, 0.772
        EXP 0.665, 0.559, 0.310, 0.130, 0.090
        EXP 0.130, 0.310, 0.559, 0.665, 0.772
        EXP 0.879, 0.986, 1.093, 1.200

;***** ROTOR INTERFERENCE ON THE VERTICAL TAIL (MRPA) *****
; ** ROTOR EKX-FACTOR ON VERTICAL TAIL MAP **
EXP3RF: :BIV00 ;MAP ARGUMENT:LOOK UP ROUTINE

```

TABLE H-1. M1-28 SPECIFIC FILE DATA (Cont'd)

```

EXP CHIPMR00,AA1FMR00 ;INPUT VARIABLE #1, INPUT VARIABLE #2
ERXP300 ;OUTPUT VARIABLE
EXP3LO ;LOW ANGLE MAP NAME
EXP 0.0,90.0,10.0,'D10 ;LOW LIM,UPPER LIM,DELTA-CHIPMR
EXP -10.0,10.0,10.0 ;LOW LIM,UPPER LIM,DELTA-AA1FMR

; LOW ANGLE MAP CHIPMR 0 TO 90 (DEL-10) AA1FMR -10,0,10
; AA1FMR--10
EXP3LO:EXP -0.41, -0.52, 0.49, 0.69, 0.89
EXP 1.11, 1.34, 1.60, 1.85, 2.20

; AA1FMR-0
EXP -0.50, -0.61, -0.72, -0.83, 0.51
EXP 0.76, 1.02, 1.30, 1.62, 1.96

; AA1FMR-10
EXP -0.60, -0.67, -0.74, -0.79, -0.83
EXP -0.84, -0.80, -0.70, -0.51, -0.25

; ** ROTOR ERZ-FACTOR ON VERTICAL TAIL MAP **

EZP3MP::BIV00 ;MAP ARGUMENT:LOOK UP ROUTINE
EXP CHIPMR00,AA1FMR00 ;INPUT VARIABLE #1, INPUT VARIABLE #2
ERZP300 ;OUTPUT VARIABLE
EZP3LO ;LOW ANGLE MAP NAME
EXP 0.0,90.0,10.0,'D10 ;LOW LIM,UPPER LIM,DELTA-CHIPMR
EXP -10.0,10.0,10.0 ;LOW LIM,UPPER LIM,DELTA-AA1FMR

; LOW ANGLE MAP CHIPMR 0 TO 90 (DEL-10) AA1FMR -10,0,10
; AA1FMR--10
EZP3LO:EXP -0.15, -0.01, 1.79, 1.79, 1.78
EXP 1.76, 1.74, 1.71, 1.65, 1.60

; AA1FMR-0
EXP -0.15, -0.05, 0.12, 0.35, 2.01
EXP 2.05, 2.07, 2.09, 2.09, 2.09

; AA1FMR-10
EXP -0.04, 0.07, 0.20, 0.38, 0.59
EXP 0.85, 1.16, 1.52, 1.92, 2.45

;***** FUSELAGE INTERFERENCE ON THE VERTICAL TAIL (WFWP) *****

; ** BLACK HAWK DYNAMIC PRESSURE RATIO AT VERTICAL TAIL VS PSIWFP
QP3MP:: BIV00 ;MAP ARGUMENT:LOOK UP ROUTINE
EXP PSABWFP00,ALPWF00 ;INPUT VARIABLE #1, INPUT VARIABLE #2
QP3QWFP00 ;OUTPUT VARIABLE
QP3LO ;LOW ANGLE MAP NAME
EXP 0.0,30.0,5.0,7 ;LOWER LIM,UPPER LIM,DELTA,#ITEMS (PSABWFP)
EXP -10.0,10.0,10.0 ;LOWER LIM,UPPER LIM,DELTA (ALPWF)

; LOW ANGLE MAP PSI(ABS) 0 TO 30 DELTA-5
;ALPWF- -10 DEG
QP3LO: EXP 0.62, 0.66, 0.66, 0.72, 0.79
EXP 0.88, 1.00

;ALPWF- 0 DEG
EXP 0.62, 0.64, 0.66, 0.72, 0.79
EXP 0.88, 1.00

;ALPWF- 10 DEG
EXP 0.62, 0.64, 0.66, 0.72, 0.79
EXP 0.88, 1.00

; ** BLACK HAWK SIDEWASH ON VERTICAL TAIL VS PSIWFP DUE TO BODY

SGP3MP::UVSUVS00 ;MAP ARGUMENT:LOOK UP ROUTINE
PSIWFP00 ;INPUT VARIABLE

```

TABLE K-1. NI-28 SPECIFIC FILE DATA (Cont'd)

```

SIGP300          ;OUTPUT VARIABLE
SGP3LO          ;LOW ANGLE MAP NAME
EXP 0.0,30.0,5.0 ;LDWER LIMIT, UPPER LIMIT, DELTA-LOW ANGLE
SGP3HI          ;HIGH ANGLE MAP NAME
EXP 0.0,90.0,30.0 ;LOWER LIMIT, UPPER LIMIT, DELTA-HIGH ANGLE

; LOW ANGLE MAP PSIWF 0 TO 30 DELTA=5
SGP3LO: EXP 0.0, -0.4, -0.6, 0.8, 1.4
        EXP 0.6, 0.2

; HIGH ANGLE MAP PSIWF 0 TO 90 DELTA=30
SGP3HI: EXP 0.0, 0.2, 0.0, 0.0
        PAGE

;***** INPUT PARAMETERS PDR PANEL #4 (#A) *****
PSP4:: 417.5      ; FUSELAGE STATION, INCH
WLP4:: 228.8      ; WATERLINE STATION, INCH
BLP4:: -73.8      ; BUTTLINE STATION, INCH (+IVE TO PORT)
SAP4:: 16.41      ; SURFACE AREA OF PANEL IF NOT INCLUDE IN MAP
GAMP4:: 0.0       ; PANEL ORIENTATION, DEG
IOP4:: 10.0       ; PANEL INCIDENCE, DEG
CP4:: 1.0         ; PANEL MEAN AERO CHORD, FT

; ** AH-15 WING LIFT COEFFICIENT VS ALPPP4
; ** S=16.41 FT**2 ,ASPECT RATIO=1.17,
CLP4MP:::UVRUVR04 ;MAP LDDK UP ROUTINE
ALPPP444         ;INPUT VARIABLE
CLP400          ;OUTPUT VARIABLE
CLP4LO          ;LOW ANGLE MAP NAME
EXP -20.0,20.0,2.0 ;LOWER LIM,UPPER LIM,DELTA
CLP4HI          ;HIGH ANGLE MAP NAME
EXP -90.0,90.0,10.0 ;LDWER LIM,UPPER LIM,DELTA

; LOW ANGLE MAP ALPPP4 -20 TO 20, DELTA = 2 DEG
CLP4LO: EXP -1.10, -1.16, -1.18, -1.20, -1.13
        EXP -1.00, -0.85, -0.70, -0.55, -0.35
        EXP -0.15, 0.05, 0.25, 0.45, 0.60
        EXP 0.75, 0.90, 1.00, 0.98, 0.95
        EXP 0.92

; HIGH ANGLE MAP ALPPP4 -90 TO 90 ,DELTA = 10 DEG
CLP4HI: EXP 0.00, -0.16, -0.31, -0.47, -0.63
        EXP -0.79, -0.94, -1.10, -1.00, 0.15
        EXP 0.75, 0.92, 0.79, 0.66, 0.53
        EXP 0.39, 0.26, 0.13, 0.00

; ** AH-15 WING DRAG VS ALPPP4
CDP4MP:::UVRUVR04 ;MAP LOOK UP ROUTINE
ALPPP444         ;INPUT VARIABLE
CDF440          ;OUTPUT VARIABLE
CDP4LO          ;LDW ANGLE MAP NAME
EXP -20.0,20.0,2.0 ;LDWER LIM,UPPER LIM,DELTA
CDP4HI          ;HIGH ANGLE MAP NAME
EXP -90.0,90.0,10.0 ;LOWER LIM,UPPER LIM,DELTA

; LOW ANGLE MAP ALPPP4 -20 TO 20, DELTA = 2 DEG
CDP4LO: EXP 0.164, 0.134, 0.105, 0.075, 0.046
        EXP 0.016, 0.013, 0.011, 0.010, 0.009
        EXP 0.008, 0.008, 0.009, 0.010, 0.011
        EXP 0.012, 0.015, 0.019, 0.050, 0.081
        EXP 0.112

; HIGH ANGLE MAP ALPPP4 -90 TO 90, DELTA = 10 DEG
CDP4HI: EXP 1.200, 1.052, 0.904, 0.756, 0.608
        EXP 0.460, 0.312, 0.164, 0.016, 0.008

```

TABLE H-1. MI-28 SPECIFIC FILE DATA (Cont'd)

```

EXP      0.012,    0.112,    0.268,    0.423,    0.578
EXP      0.734,    0.889,    1.045,    1.200

;***** INPUT PARAMETERS FOR POTCR INTERFERENCE ON THE RIGHT WING *****

      ; ** MI-28 FORE/AFT H.R. DOWNWASH AT RIGHT WING
EXP4MP::BIV03      ;MAP ARGUMENT:LOOK UP ROUTINE
EXP CHIPMR00,AA1FMR00 ;INPUT VARIABLE#1,INPUT VARIABLE#2
      EKP400      ;OUTPUT VARIABLE
EXP4LO      ;LOW ANGLE MAP NAME
EXP 0.0,90.0,10.0,'D10 ;LOW LIM UPPER LIM,DELTA-CHIPMR
EXP -10.0,10.0,10.0 ;LOW LIM,UPPER LIM,DELTA-AA1FMR

      ; LOW ANGLE MAP CHIPMR 0 TO 90 (DEL=10) AA1FMR -10,0,10
      ; AA1FMR=-10
EXP4LO:EXP      0.33,    0.42,    0.52,    0.63,    0.74
EXP      0.86,    0.99,    1.13,    -0.73,    -0.73

      ; AA1FMR=0
EXP      0.10,    0.20,    0.30,    0.41,    0.53
EXP      0.66,    0.79,    0.94,    -0.87,    -0.87

      ; AA1FMR=10
EXP      -0.13,    -0.03,    0.07,    0.18,    0.30
EXP      0.43,    0.56,    0.71,    -1.01,    -1.01

      ; ** MI-28 VERTICAL H.R. DOWNWASH AT RIGHT WING
EXP4MP::BIV03      ;MAP ARGUMENT:LOOK UP ROUTINE
EXP CHIPMR00,AA1FMR00 ;INPUT VARIABLE#1,INPUT VARIABLE#2
      EKP400      ;OUTPUT VARIABLE
EXP4LO      ;LOW ANGLE MAP NAME
EXP 0.0,90.0,10.0,'D10 ;LOW LIM,UPPER LIM,DELTA-CHIPMR
EXP -10.0,10.0,10.0 ;LOW LIM,UPPER LIM,DELTA-AA1FMR

      ; LOW ANGLE MAP CHIPMR 0 TO 90 (DEL=10) AA1FMR -10,0,10
      ; AA1FMR=-10
EXP4LO:EXP      1.17,    1.14,    1.11,    1.08,    1.05
EXP      1.02,    0.99,    0.95,    0.95,    0.95

      ; AA1FMR=0
EXP      1.21,    1.20,    1.19,    1.19,    1.18
EXP      1.17,    1.16,    1.15,    0.91,    0.91

      ; AA1FMR=10
EXP      1.20,    1.21,    1.22,    1.24,    1.26
EXP      1.27,    1.29,    1.31,    0.80,    0.80

;***** FUSELAGE INTERFERENCE ON THE RIGHT WING (WPPA) *****

      ; ** MI-28 DYNAMIC PRESSURE RATIO AT RIGHT WING VS ALFW
QP4MP::CONST00      ;MAP ARGUMENT:LOOK UP ROUTINE
      (1.0)
QP4QWF00      ;OUTPUT VARIABLE

;***** INPUT PARAMETERS FOR PANEL 85 (8A) *****

PSP5:: 417.5      ; FUSELAGE STATION,INCH
WLP5:: 228.8      ; WATERLINE STATION,INCH
BLP5:: 73.9      ; BUTTLINE STATION,INCH (+IVE TO FORT)
BAPS:: 16.41     ; SURFACE AREA OF PANEL IF NOT INCLUDE IN MAP
GAMP5:: 0.0      ; PANEL ORIENTATION, DEG
IOP5:: 10.0      ; PANEL INCIDENCE,DEG
CP5:: 1.0        ; PANEL MEAN AERO CHORD, FT

```


TABLE H-1. MI-28 SPECIFIC FILE DATA (Cont'd)

```

; ** AH-1S LEFT WING LIFT COEFFICIENT VS ALPPP5
; ** S=16.41 FT**2 ,ASPECT RATIO=1.17,

CLPSNP::UVRUVR00 ;MAP ARGUMENT:LOOK UP ROUTINE
ALPPP500 ;INPUT VARIABLE
CLP500 ;OUTPUT VARIABLE
CLP4LO ;LOW ANGLE MAP NAME
EXP -20.0,20.0,2.0 ;LOWER LIMIT,UPPER LIMIT,DELTA-LOW ANGLE
CLP4HI ;HIGH ANGLE MAP NAME
EXP -90.0,90.0,10.0 ;LOWER LIMIT,UPPER LIMIT,DELTA-HIGH ANGLE

; ** AH-1S LEFT WING DRAG VS ALPPP5
COP5NP::UYRUVR00 ;MAP ARGUMENT:LOOK UP ROUTINE
ALPPP500 ;INPUT VARIABLE
COP500 ;OUTPUT VARIABLE
COP4LO ;LOW ANGLE MAP NAME
EXP -20.0,20.0,2.0 ;LOWER LIMIT,UPPER LIMIT,DELTA
COP4HI ;HIGH ANGLE MAP NAME
EXP -90.0,90.0,10.0 ;LOWER LIMIT,UPPER LIMIT,DELTA

;***** INPUT PARAMETERS FOR ROTOR INTERFERENCE ON THE LEFT WING *****

; ** NI-28 FORE/AFT N.R. DOWNWASH AT LEFT WING
EXP5MP::CONST00 ;MAP ARGUMENT:LOOK UP ROUTINE
EKXP400 ;INPUT VARIABLE
EKXP500 ;OUTPUT VARIABLE

; ** NI-28 VERTICAL N.R. DOWNWASH AT LEFT WING
EZP5MP::CONST00 ;MAP ARGUMENT:LOOK UP ROUTINE
EKZP400 ;INPUT VARIABLE
EKZP500 ;OUTPUT VARIABLE

;***** FUSELAGE INTERFERENCE ON THE LEFT WING. (WPPA) *****

; ** NI-28 DYNAMIC PRESSURE RATIO AT LEFT WING VS ALPWF
QP5NP::CONST00 ;MAP ARGUMENT:LOOK UP ROUTINE
QP4QWF00 ;INPUT VARIABLE
QP5QWF00 ;OUTPUT VARIABLE

;***** INPUT PARAMETERS FOR TAIL ROTOR (BA) - (BAILEY) *****

RTR:: 6.3 ;RADIUS,FT
OMEGIR::113.5 ;TRIM ROTATIONAL RATE, RAO/SEC
OTR:: 4.0 ;ACTUAL NUMBER OF BLAOES
FSTR:: 817.5 ;FUSELAGE STATION,IN
WLTR:: 308.7 ;WATERLINE STATION,IN
BLTR:: -32.5 ;BUTTLINE STATION, IN (+IVE TO PORT)
TWSTTR::-10.0 ;BLAOE TWIST, OATUN CENTER OF ROTATION, OEG
BIASTR:: 1.5 ;BLAOE PITCH CORRECTION FOR N.L.TWIST
GAMTR:: 90.0 ;TAIL ROTOR CANT ANGLE, OEG
OEL3TR::35.0 ;FLAPPING NINGE OFFSET ANGLE, OEG
OELTTR::.001455 ;RATE OF CHANGE OF CONE ANGLE WITH THRUST, OEG/LB
CNRDTR::.792 ;BLAOE CHORD, FT
ATR:: 5.873 ;BLADE LIFT CURVE SLOPE, I/RAD
BTLTR:: .92 ;BLADE TIP LOSS FACTOR
COTR:: 0.0 ;TAIL ROTOR NEAD DRAG, FT**2
IBTR:: 4.0 ;T.R. BLADE SECOND MOMENT SLUGS-FT**2
DRO0TR::0.0087 ;T.R. BLAOE SECTION DRAG COEFF, CD0
DRO1TR::-0.0216 ;T.R. BLADE SECTION DRAG COEFF, CD1
DRO2TR::0.4 ;T.R. BLADE SECTION DRAG COEFF, CD2
OROTTR::-1.0 ;T.R. ROTATION +1.0 MEANS COUNTER CLOCKWISE
; WHEN VIEWED FROM PORT SIDE

```

TABLE H-1. MI-28 SPECIFIC FILE DATA (Cont'd)

```

***** ROTOR INTERFERENCE ON TAIL ROTOR (MRPA) *****

; ** ROTOR X-FACTOR ON TAIL ROTOR MAP **
EXTRMP::BIV## ;MAP ARGUMENT:LOOK UP ROUTINE
EXP CHIPR##,AA1PFR## ;INPUT VARIABLE #1, INPUT VARIABLE #2
EKXTR## ;OUTPUT VARIABLE
EXTRLO ;LOW ANGLE MAP NAME
EXP 0.0,90.0,10.0,"D10 ;LOW LIM,UPPER LIM,DELTA-CHIPRR
EXP -10.0,10.0,10.0 ;LOW LIM,UPPER LIM,DELTA-AA1PFR

; LOW ANGLE MAP CHIPMR 0 TO 90 (DEL=10) AA1PFR -10,0,10
; AA1PFR=-10
EXTRLO:EXP -0.41, -0.50, -0.59, -0.66, 0.93
EXP 1.16, 1.40, 1.67, 1.90, 2.20

; AA1PFR=0
EXP -0.48, -0.54, -0.60, -0.66, -0.70
EXP -0.70, -0.64, 0.34, 1.75, 2.30

; AA1PFR=10
EXP -0.46, -0.49, -0.52, -0.55, -0.57
EXP -0.57, -0.54, -0.46, -0.32, -0.75

; ** ROTOR Z-FACTOR ON TAIL ROTOR MAP **
EXTRMP::BIV## ;MAP ARGUMENT:LOOK UP ROUTINE
EXP CHIPR##,AA1PFR## ;INPUT VARIABLE #1, INPUT VARIABLE #2
EKZTR## ;OUTPUT VARIABLE
EXTRLO ;LOW ANGLE MAP NAME
EXP 0.0,90.0,10.0,"D10 ;LOW LIM,UPPER LIM,DELTA-CHIPRR
EXP -10.0,10.0,10.0 ;LOW LIM,UPPER LIM,DELTA-AA1PFR

; LOW ANGLE MAP CHIPMR 0 TO 90 (DEL=10) AA1PFR -10,0,10
; AA1PFR=-10
EXTRLO:EXP -0.87, 0.03, 0.20, 0.43, 1.84
EXP 1.92, 1.79, 1.75, 1.70, 1.65

; AA1PFR=0
EXP -0.02, 0.07, 0.21, 0.38, 0.60
EXP 0.88, 1.22, 1.83, 2.11, 2.25

; AA1PFR=10
EXP 0.07, 0.15, 0.25, 0.37, 0.52
EXP 0.71, 0.95, 1.24, 1.59, 2.10

```

TABLE H-1. MI-28 SPECIFIC FILE DATA (Cont'd)

```

;***** FUSELAGE INTERFERENCE ON THE TAIL ROTOR (WPPA) *****

QTRMP:: CONST00      ;** TAIL ROTOR DYNAMIC PRESSURE RATIO MAP **
QP3QWF      ;MAP ARGUMENT:LOOK UP ROUTINE
QTRQWF00    ;INPUT VARIABLE
              ;OUTPUT VARIABLE

EPTTMP::CONST00      ;** BODY DOWNWASH ON TAIL ROTOR MAP **
EPSP200     ;MAP ARGUMENT:LOOK UP ROUTINE
EPSTR00     ;INPUT VARIABLE
              ;OUTPUT VARIABLE

SGTRMP::CONST00      ;** BODY SIDEWASH ON TAIL ROTOR MAP **
SIGP300     ;MAP ARGUMENT:LOOK UP ROUTINE
SIGTR00     ;INPUT VARIABLE
              ;OUTPUT VARIABLE

;***** INPUT PARAMETERS FOR EQUATIONS OF MOTION (IB) *****

FSCG:: 400.0         ; FUSELAGE STATION,OF C.G.,INCH
WLCCG:: 205.8       ; WATERLINE STATION OF C.G.,INCH
BLCCG:: 0.0         ; BUTTLINE STATION OF C.G.,INCH (+IVE TO PORT)

WEIGHT::22984.0     ; AIRCRAFT GROSS WEIGHT,LBS.
IX:: 14084.6        ; INERTIA ABOUT BODY X-AXIS,SLUG-FT**2
IY:: 71333.0        ; INERTIA ABOUT BODY Y-AXIS,SLUG-FT**2
IZ:: 67915.6        ; INERTIA ABOUT BODY Z-AXIS,SLUG-FT**2
IXZ:: 4239.5        ; CROSS COUPLING INERTIA,SLUG-FT**2
IXY:: 0.0
IYZ:: 0.0

;***** INPUT PARAMETERS FOR NOASE (IA) *****

AISUL:: 7.0         ; AIS UPPER LIMIT
AISLL::-10.5        ; AIS LOWER LIMIT
BISUL:: 20.0        ; BIS UPPER LIMIT
BISLL::-10.0        ; BIS LOWER LIMIT
THOUL:: 25.9        ; THETA 0 UPPER LIMIT
THOLL:: 9.9         ; THETA 0 LOWER LIMIT
THRUL:: 36.5        ; THETA UPPER LIMIT
THRLL:: 4.5         ; THETA LOWER LIMIT

KAUL:: 9.0          ; LAT STICK UPPER LIMIT
KALL:: 0.0          ; LAT STICK LOWER LIMIT
XBUL:: 10.0         ; LONG STCK UPPER LIMIT
XBLL:: 0.0          ; LONG STCK LOWER LIMIT
XCUL:: 12.0         ; COLL STCK UPPER LIMIT
XCLL:: 0.0          ; COLL STCK LOWER LIMIT
XPUL:: 4.8          ; PEAL UPPER LIMIT
XPLL:: 0.0          ; PEAL LOWER LIMIT

```

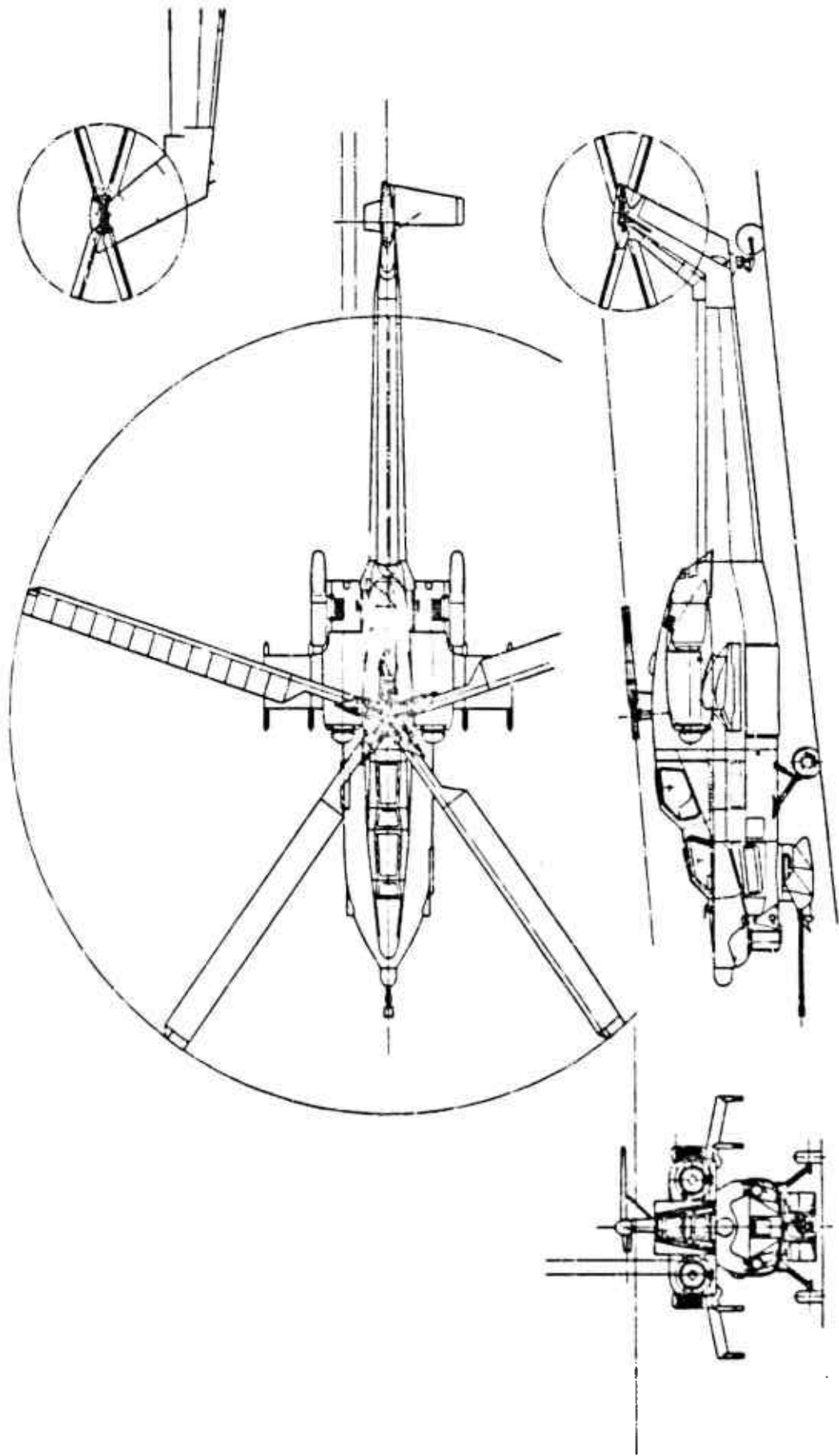


Figure H-1. MI-28 Three-View Drawing

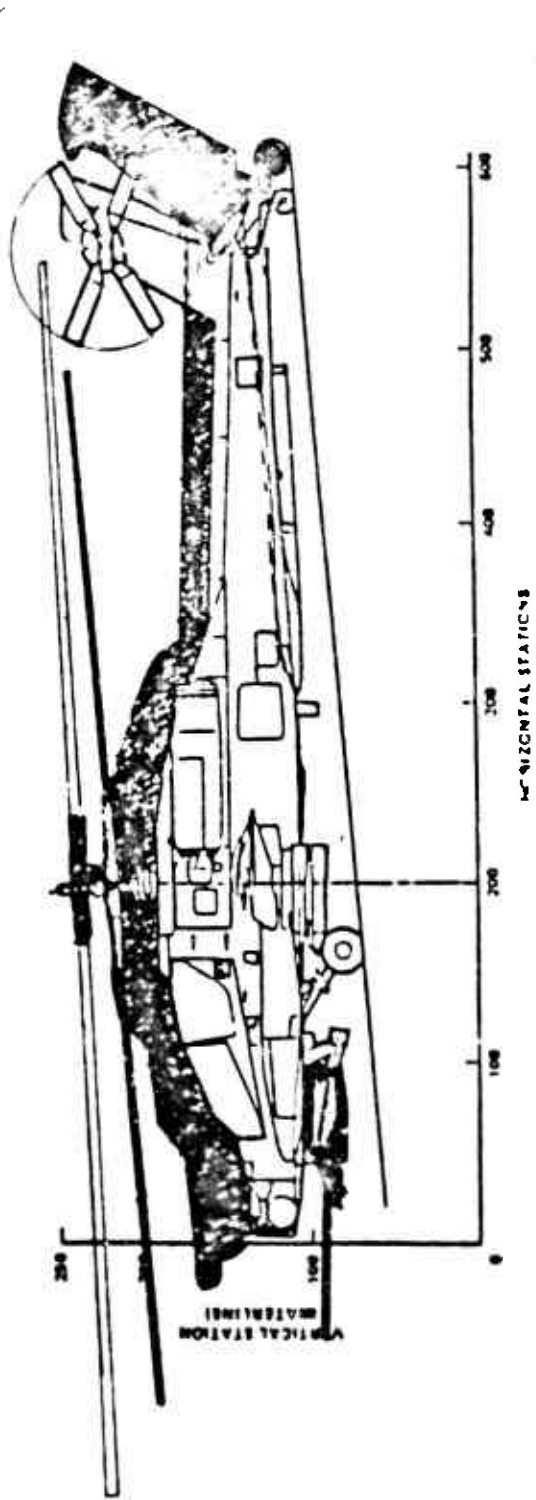


Figure H-2. MI-28/AH-64A Profile Comparison

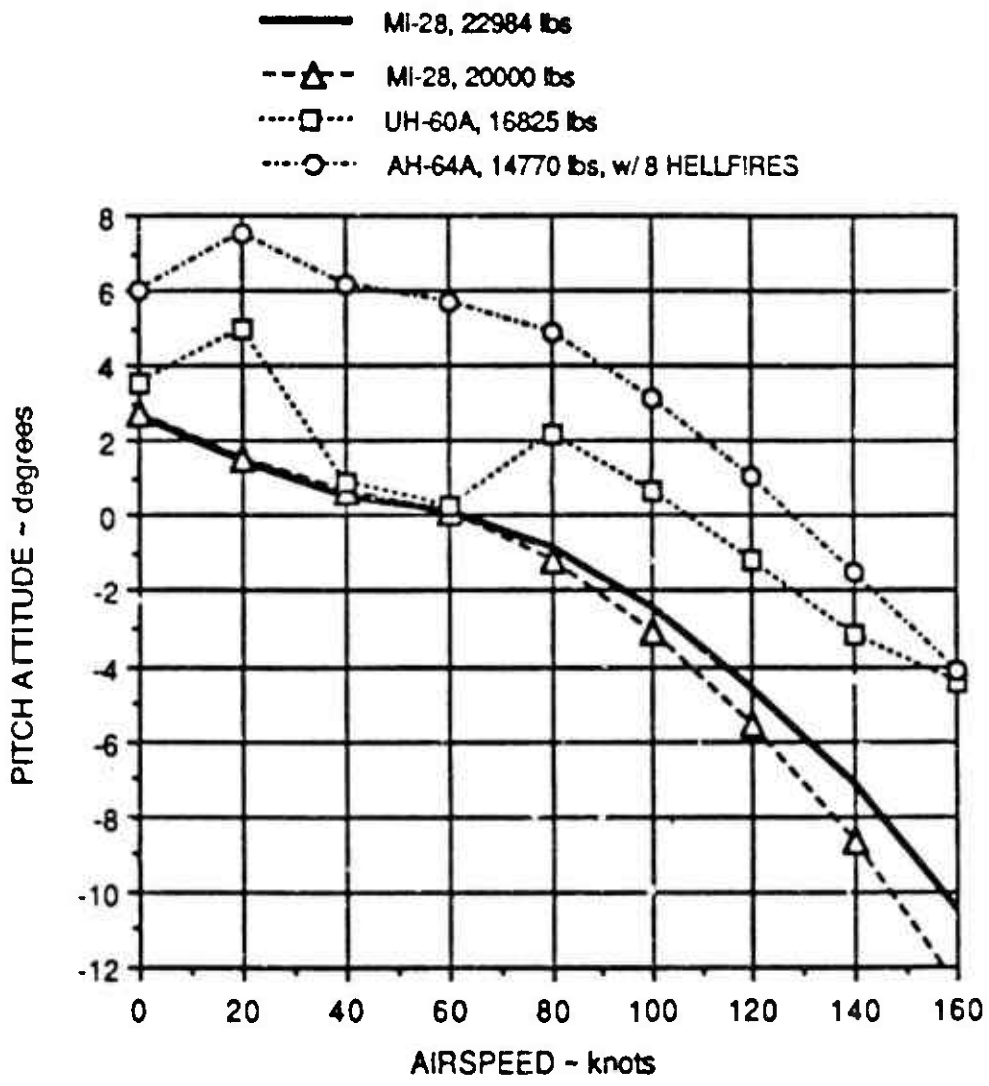


Figure H-3. MI-28 Pitch Attitude Comparison

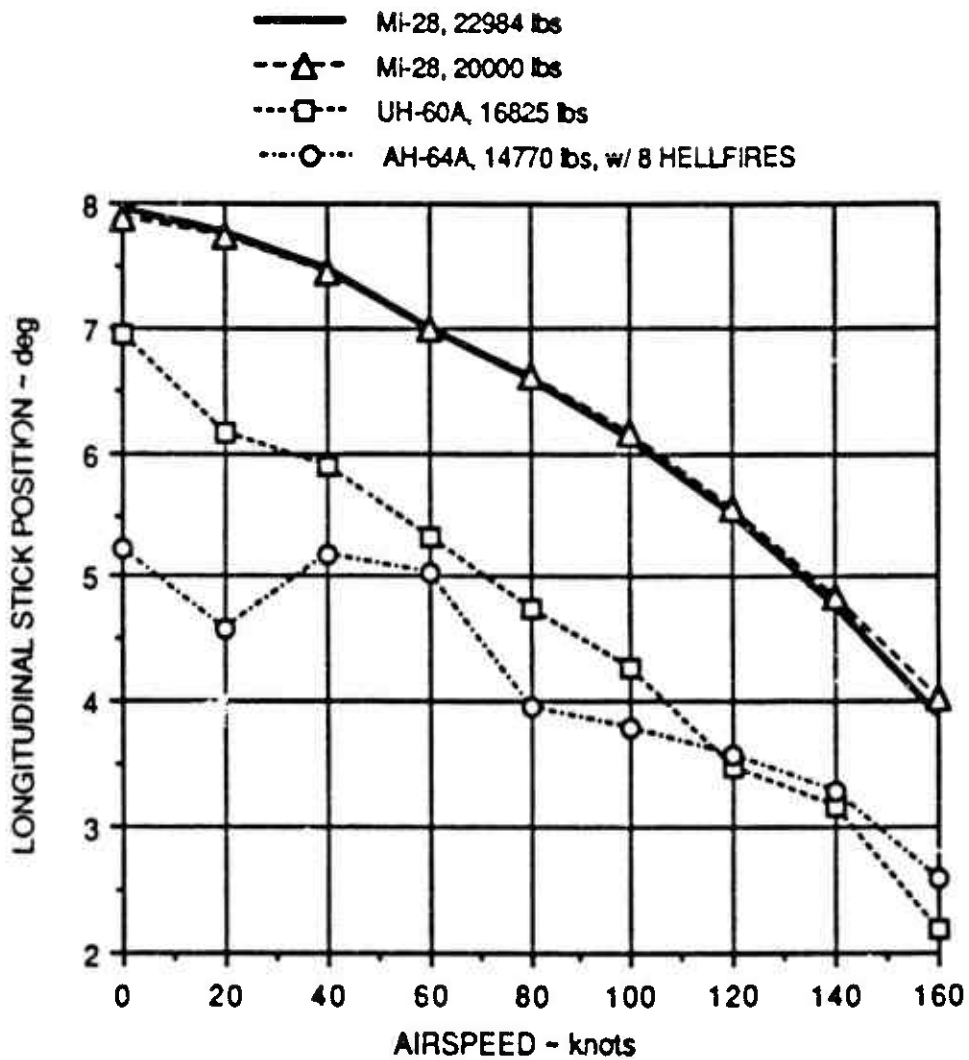


Figure H-4. MI-28 Longitudinal Stick Comparison

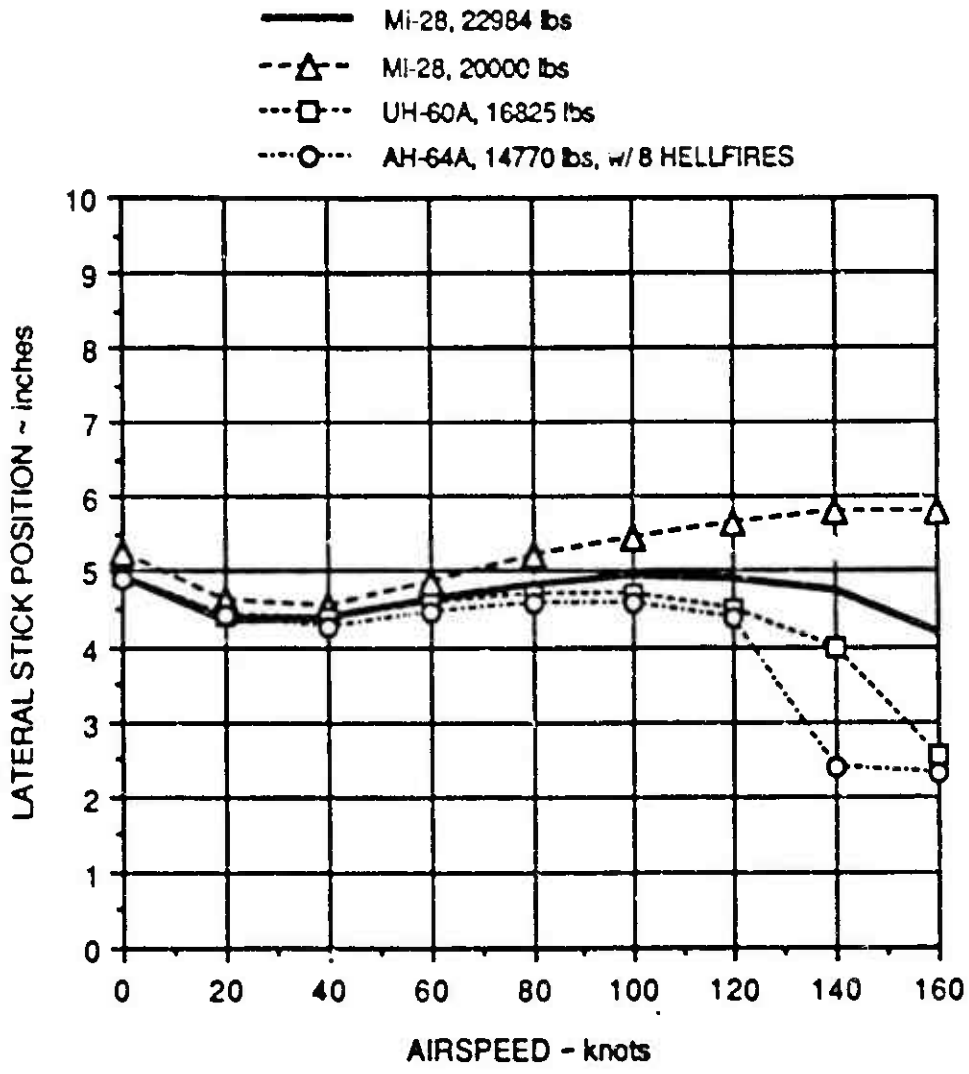


Figure H-5. Mi-28 Lateral Stick Comparison

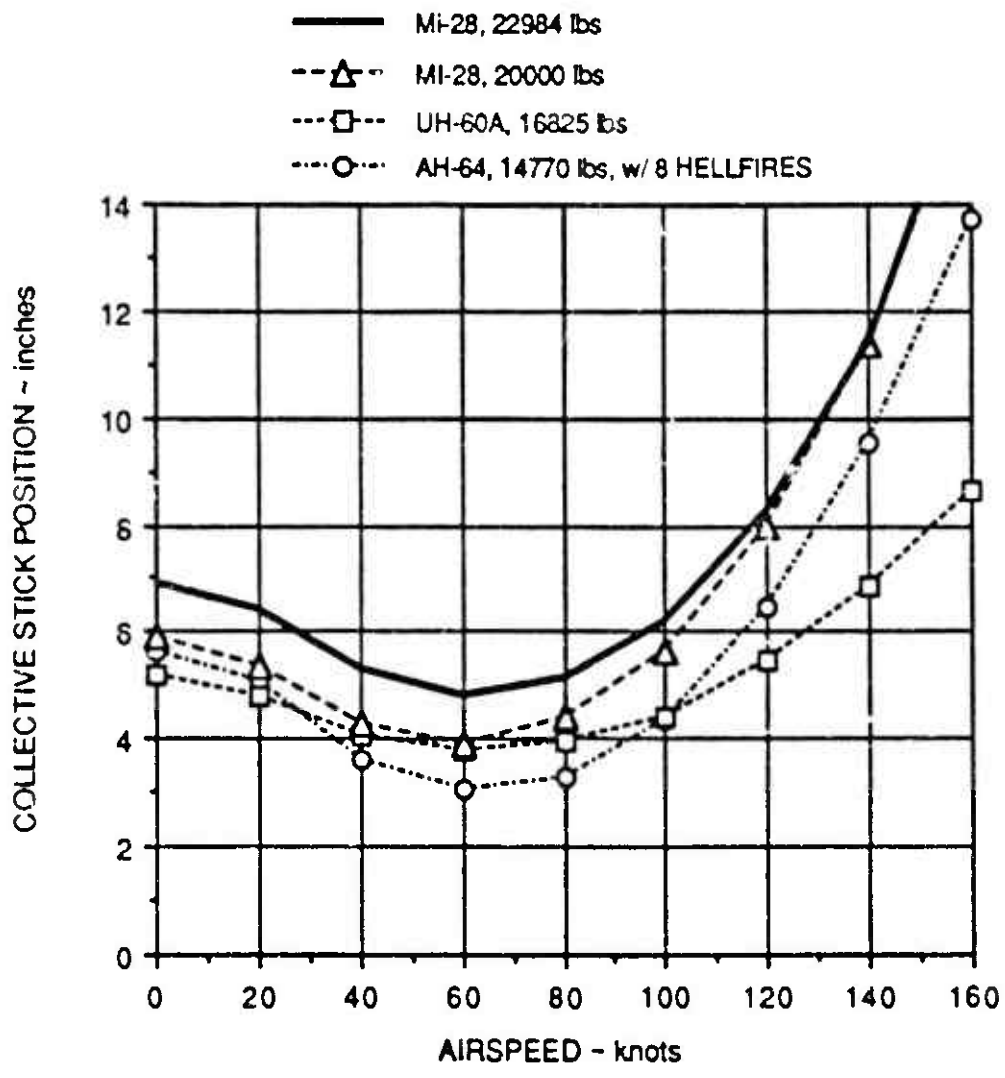


Figure H-6. Mi-28 Collective Stick Comparison

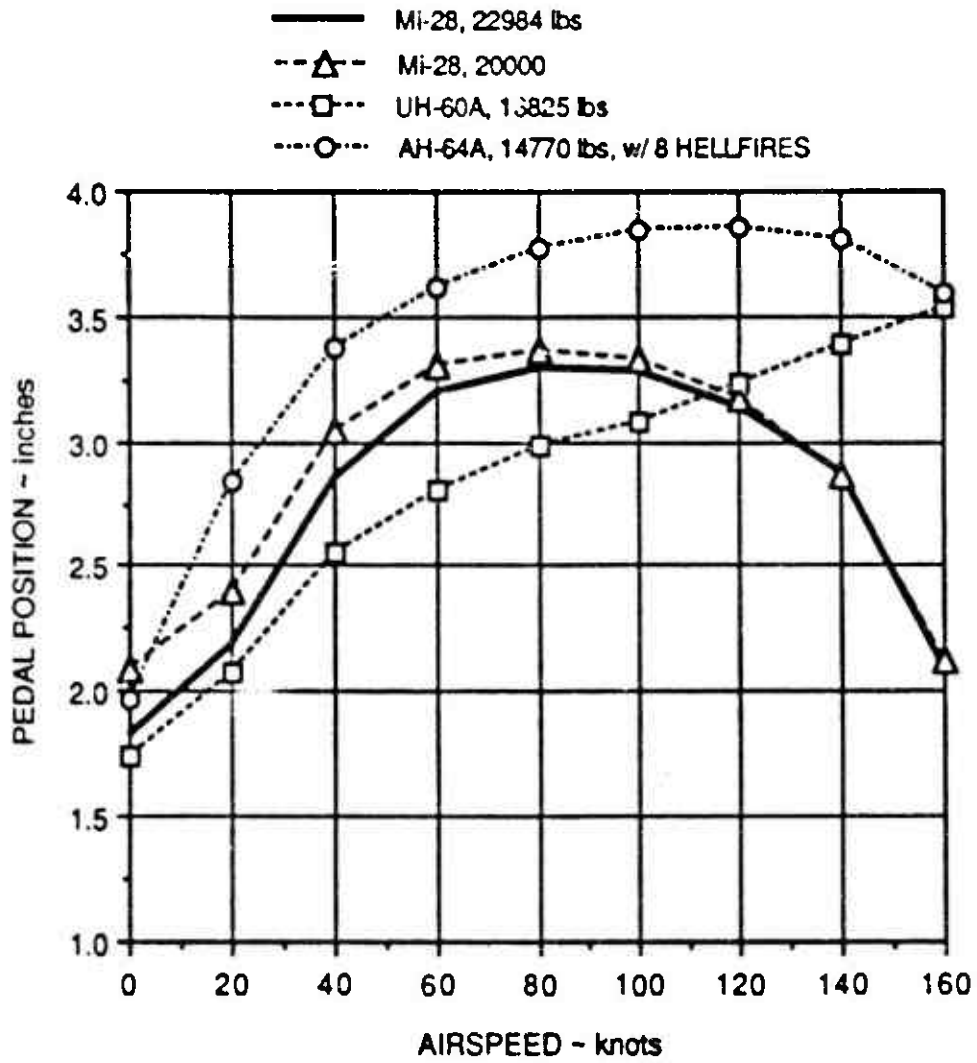


Figure H-7. Mi-28 Pedal Comparison

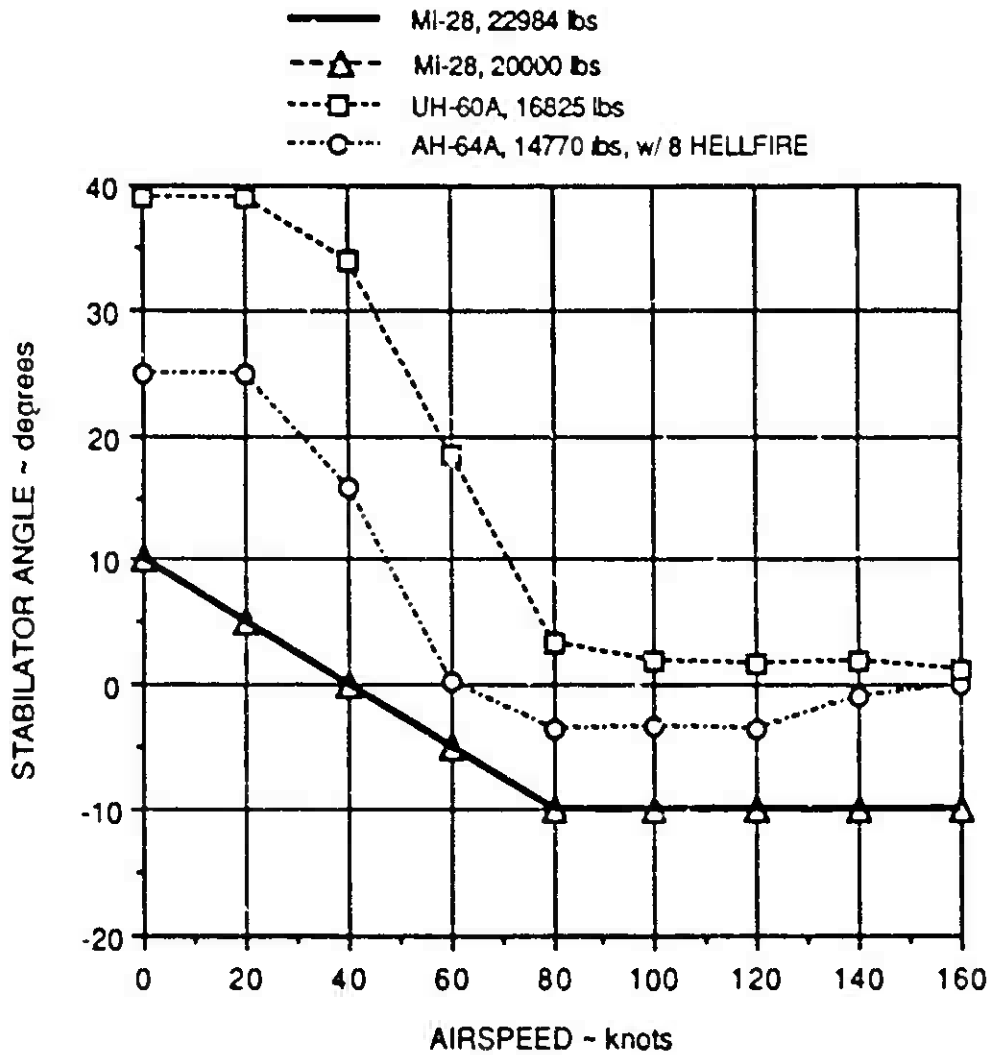


Figure H-8. MI-28 Stabilator Comparison

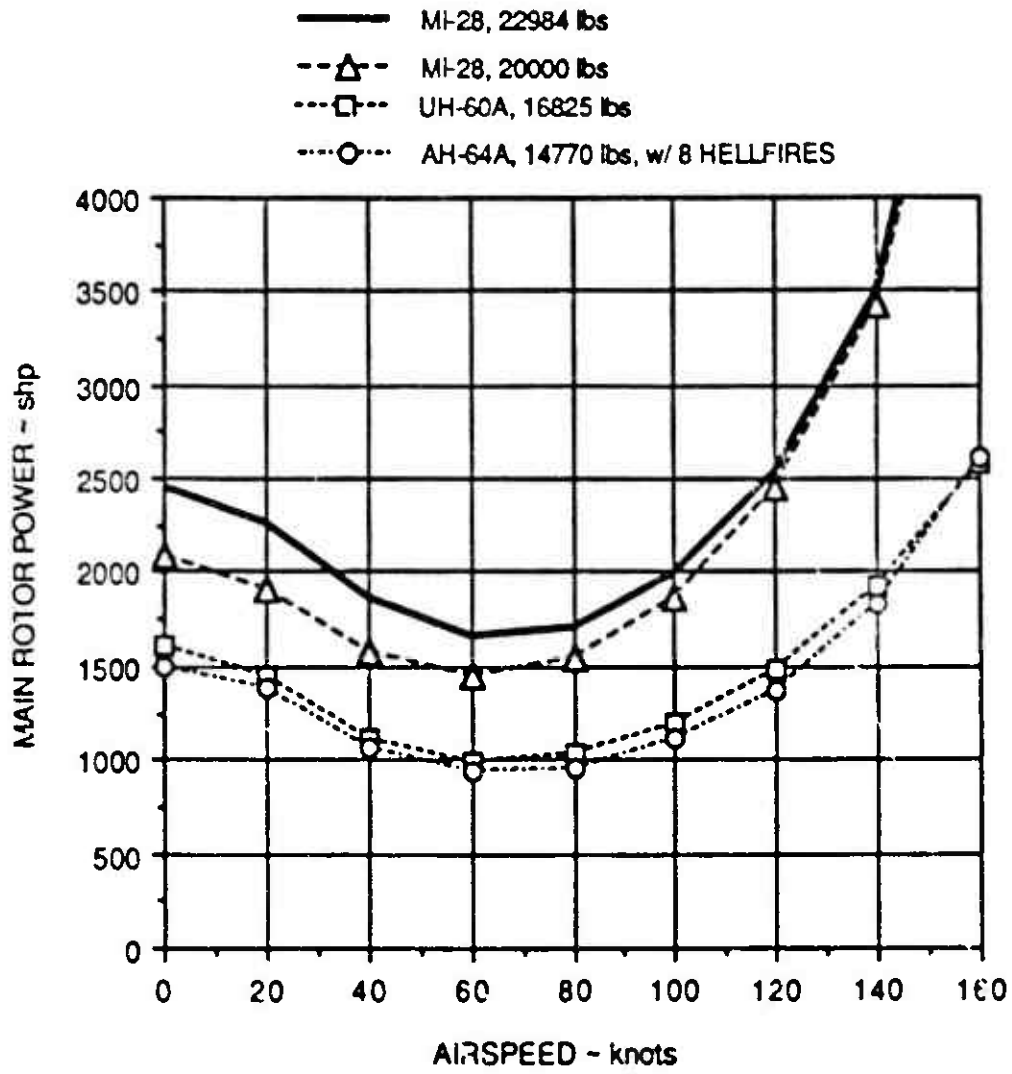


Figure H-9. MI-28 Power Required Comparison

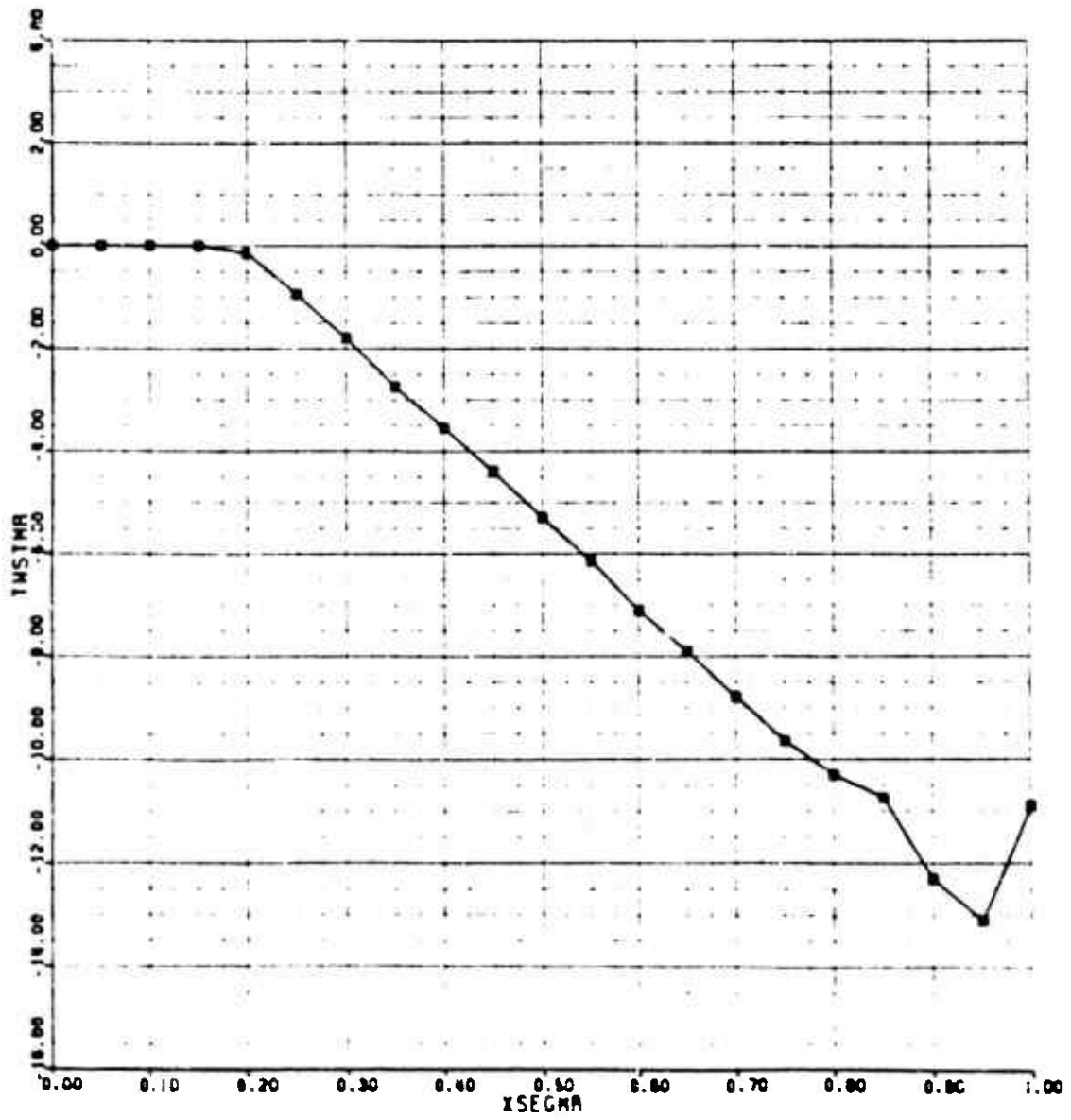


Figure H-10. MI-28 Main Rotor Blade Twist Map

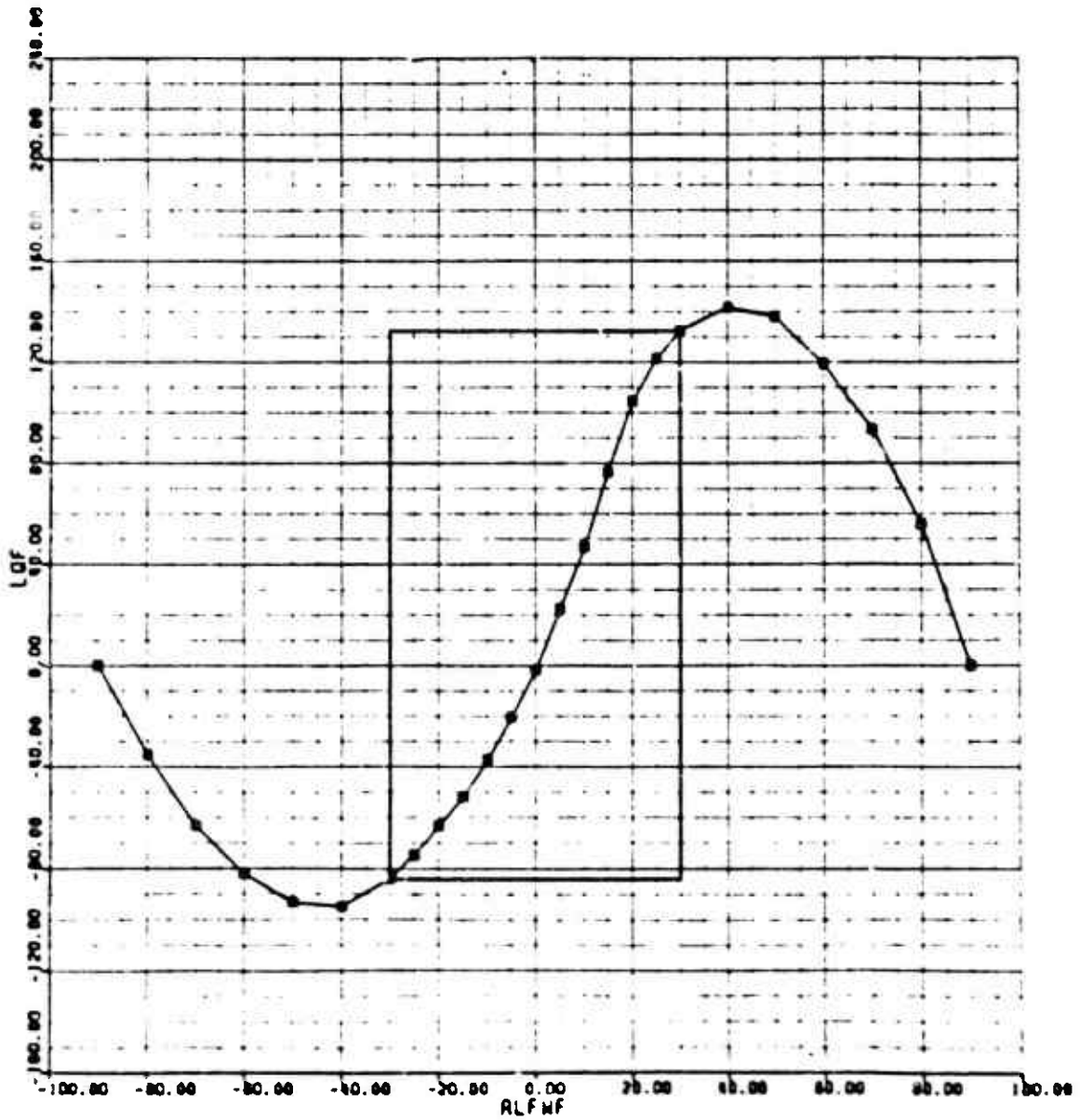


Figure H-11. Mi-28 Fuselage Lift Map

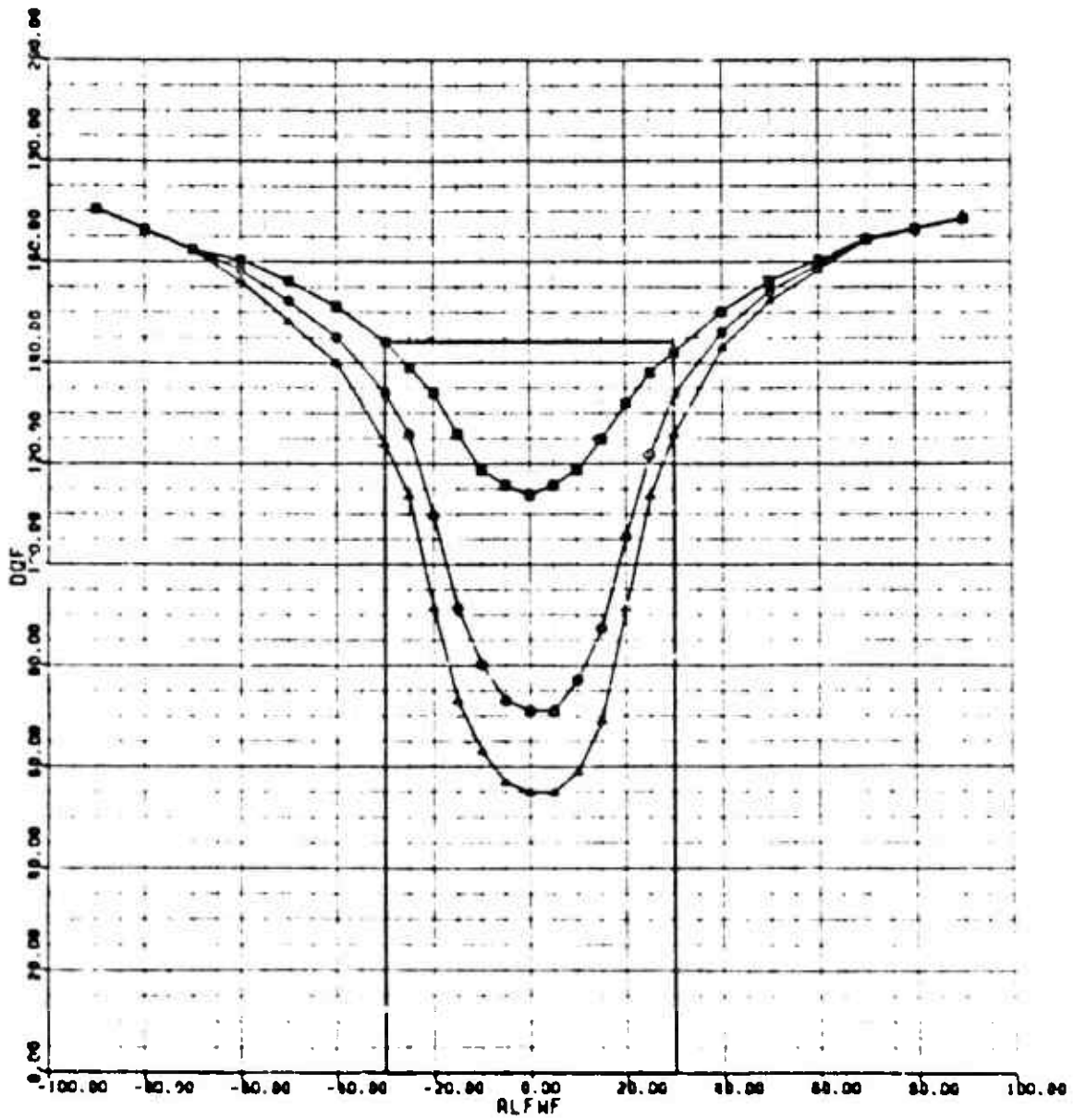


Figure H-12. Mi-28 Fuselage Drag Map

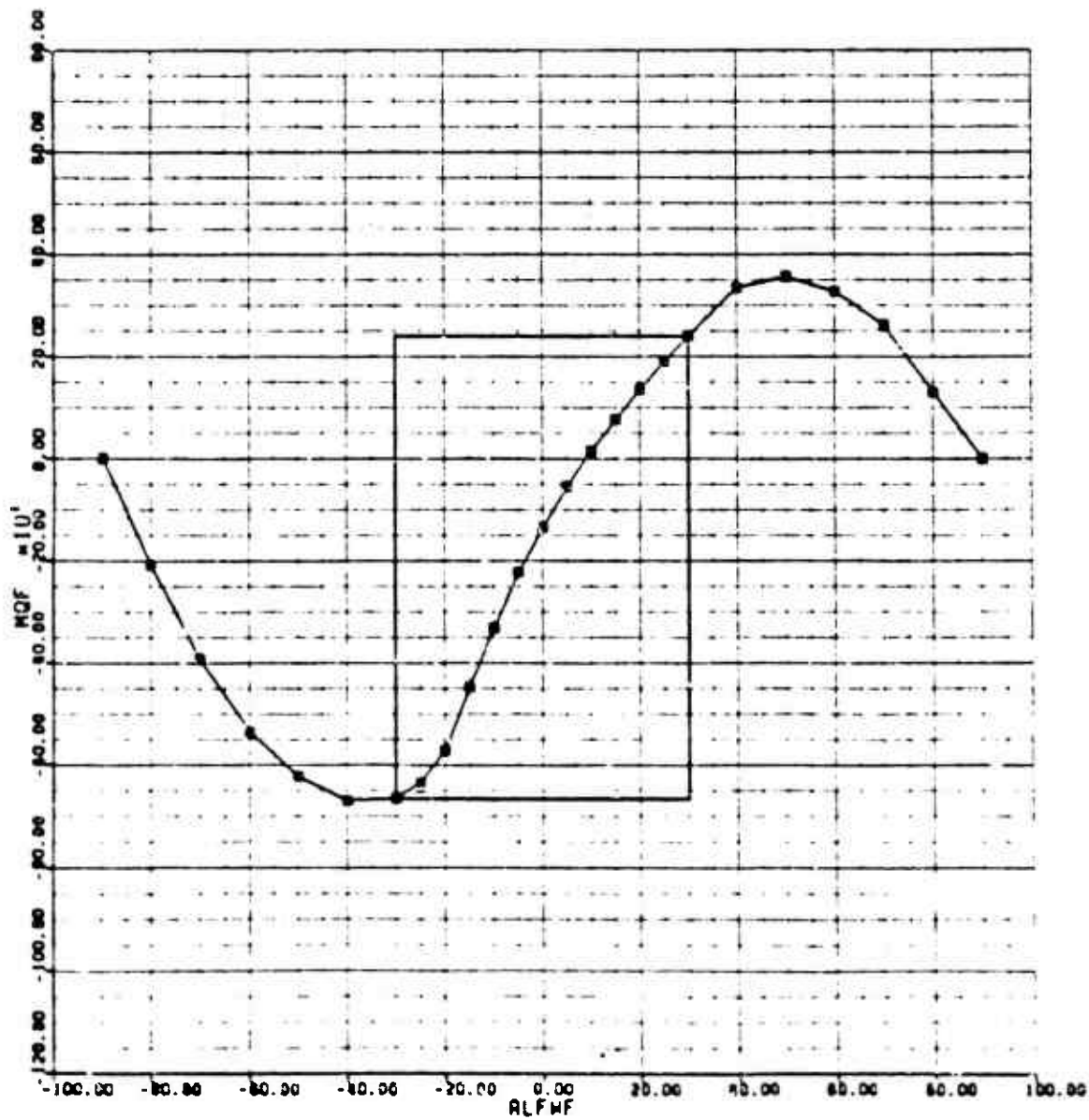


Figure H-13. Mi-28 Fuselage Pitching Moment M_a ,

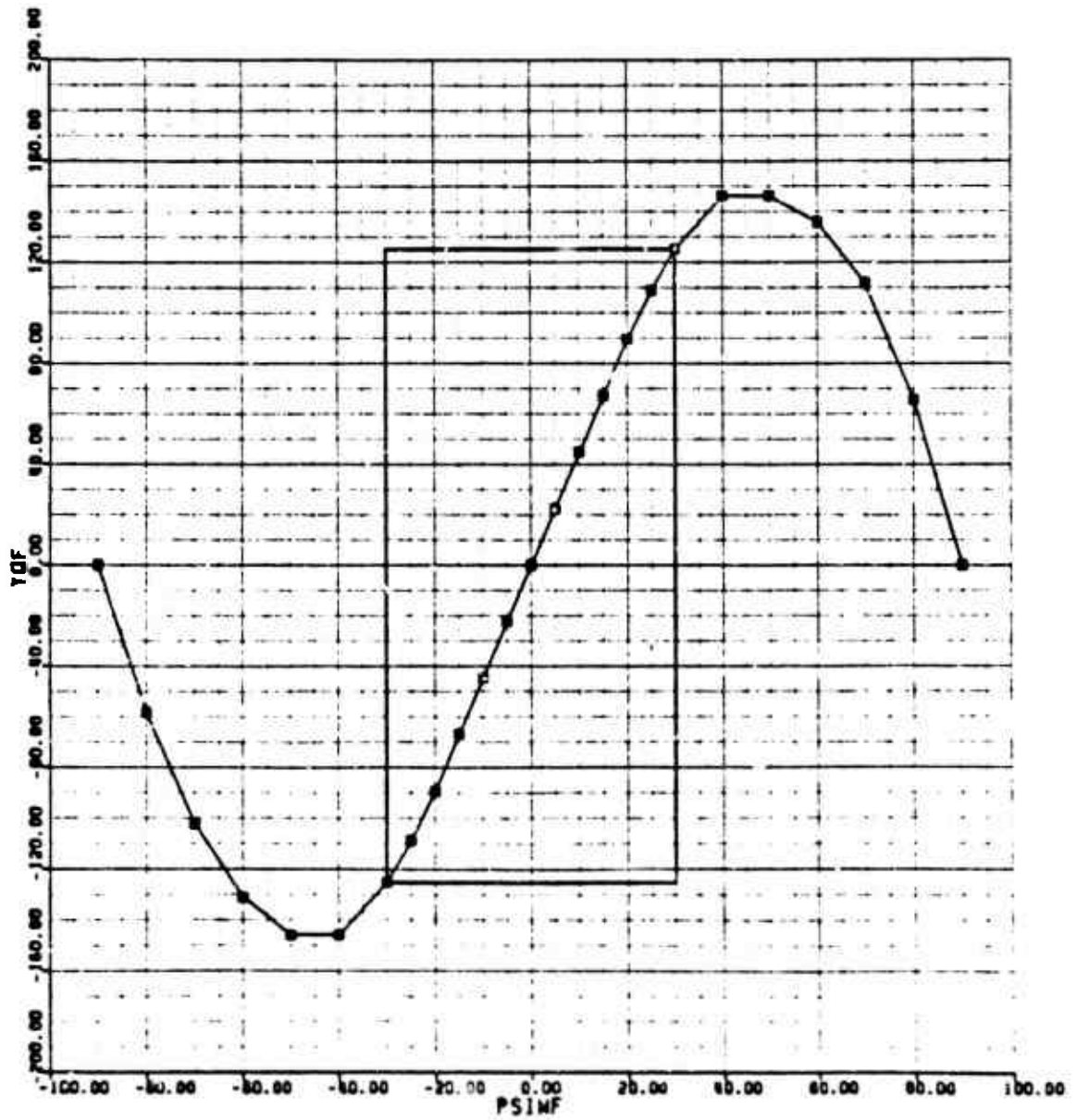


Figure H-14. Mi-28 Fuselage Sideforce Map

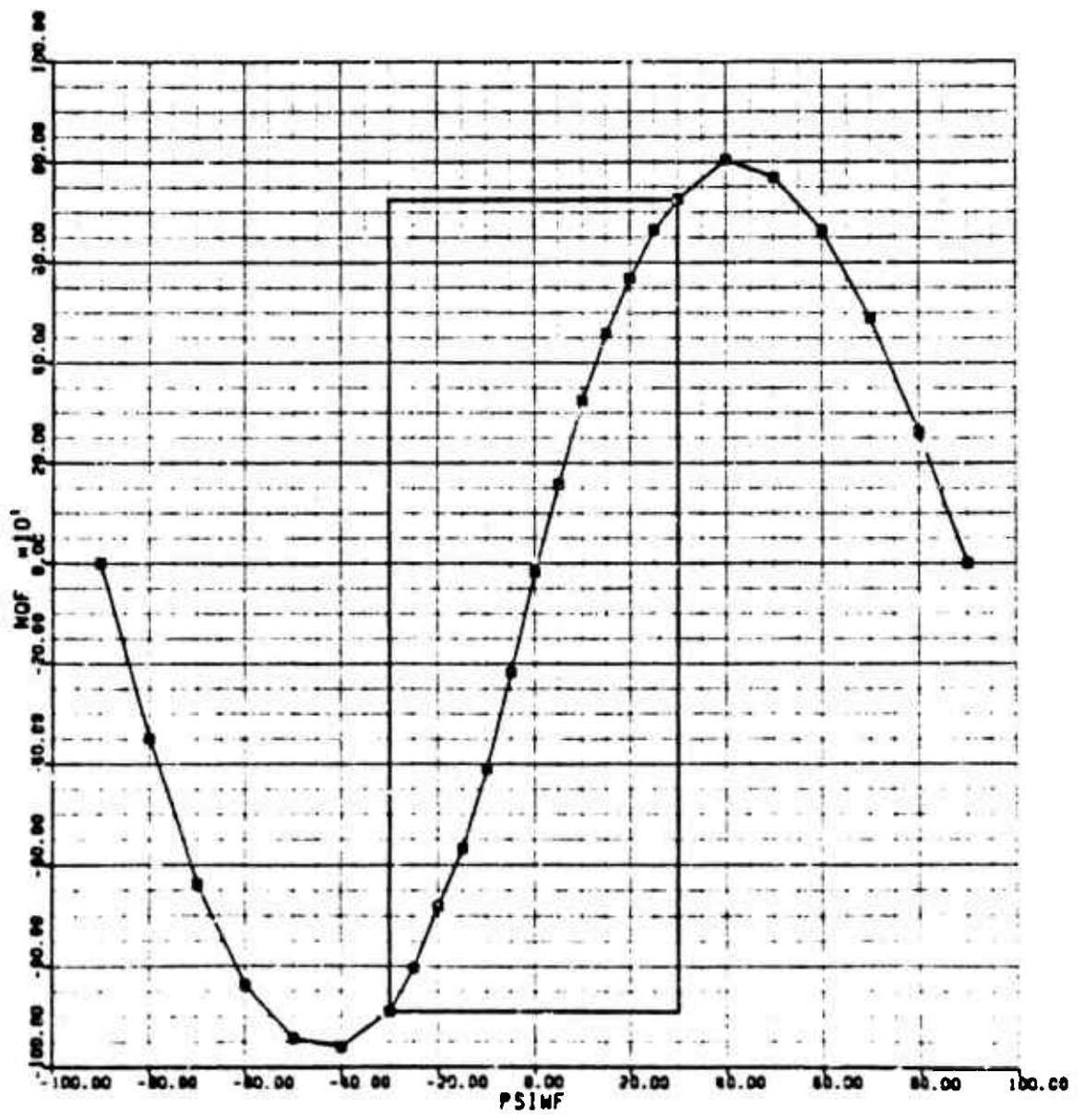


Figure B-15. Mi-28 Fuselage Yawing Moment Map

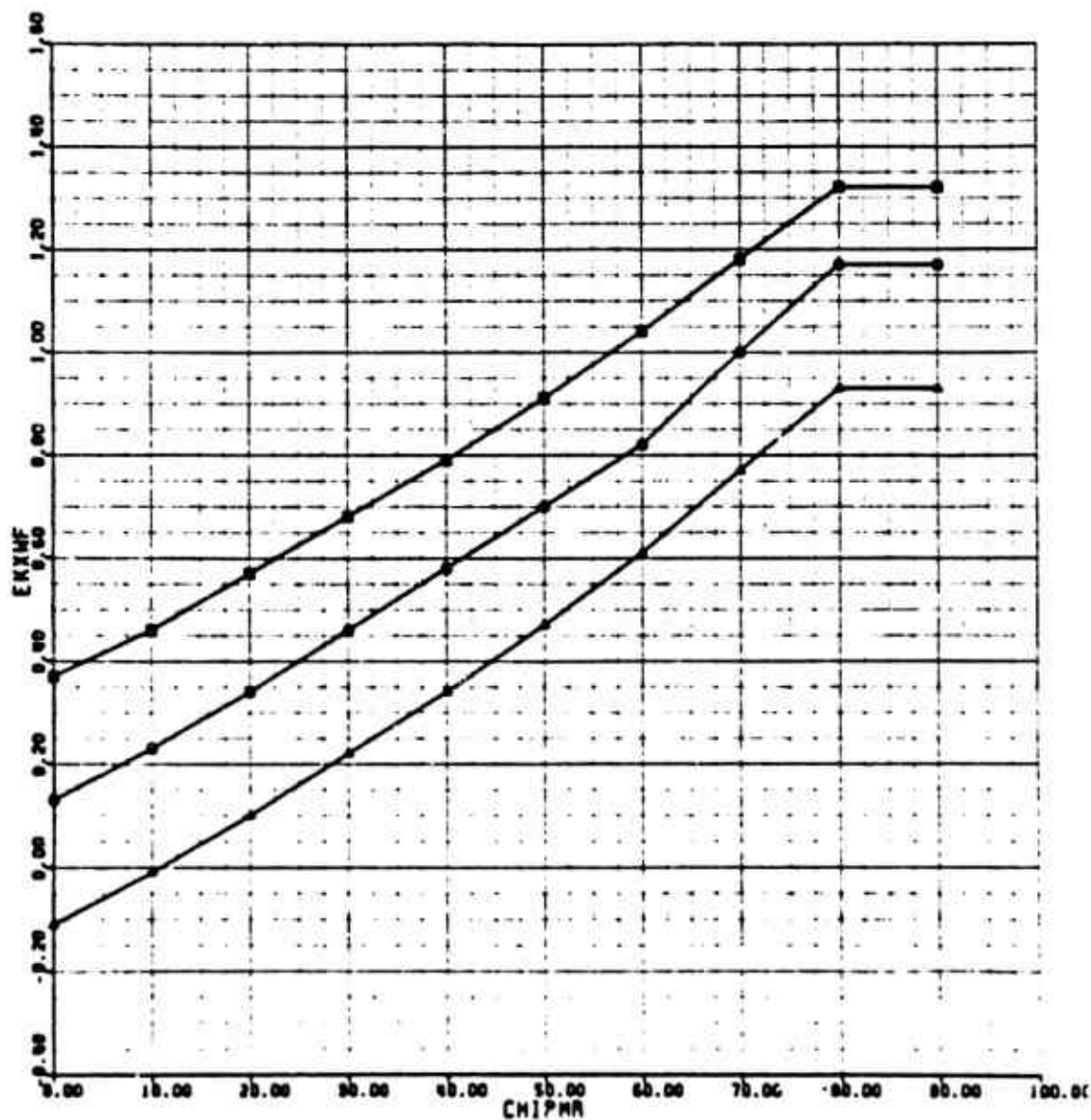


Figure H-16. Mi-28 Main Rotor Downwash on Fuselage Map (x-direction)

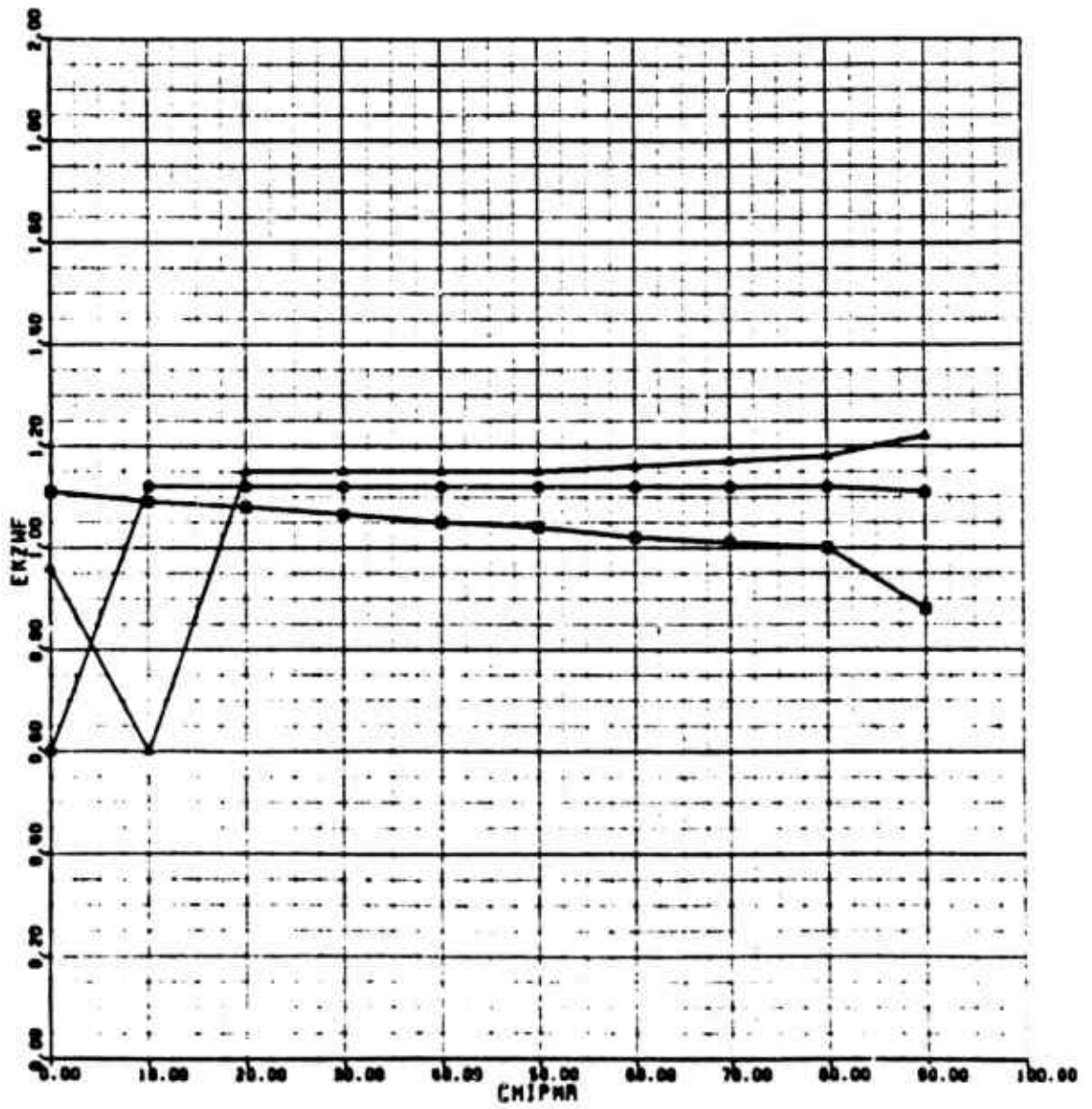


Figure H-17. Mi-28 Main Rotor Downwash on Fuselage Map (z-direction)

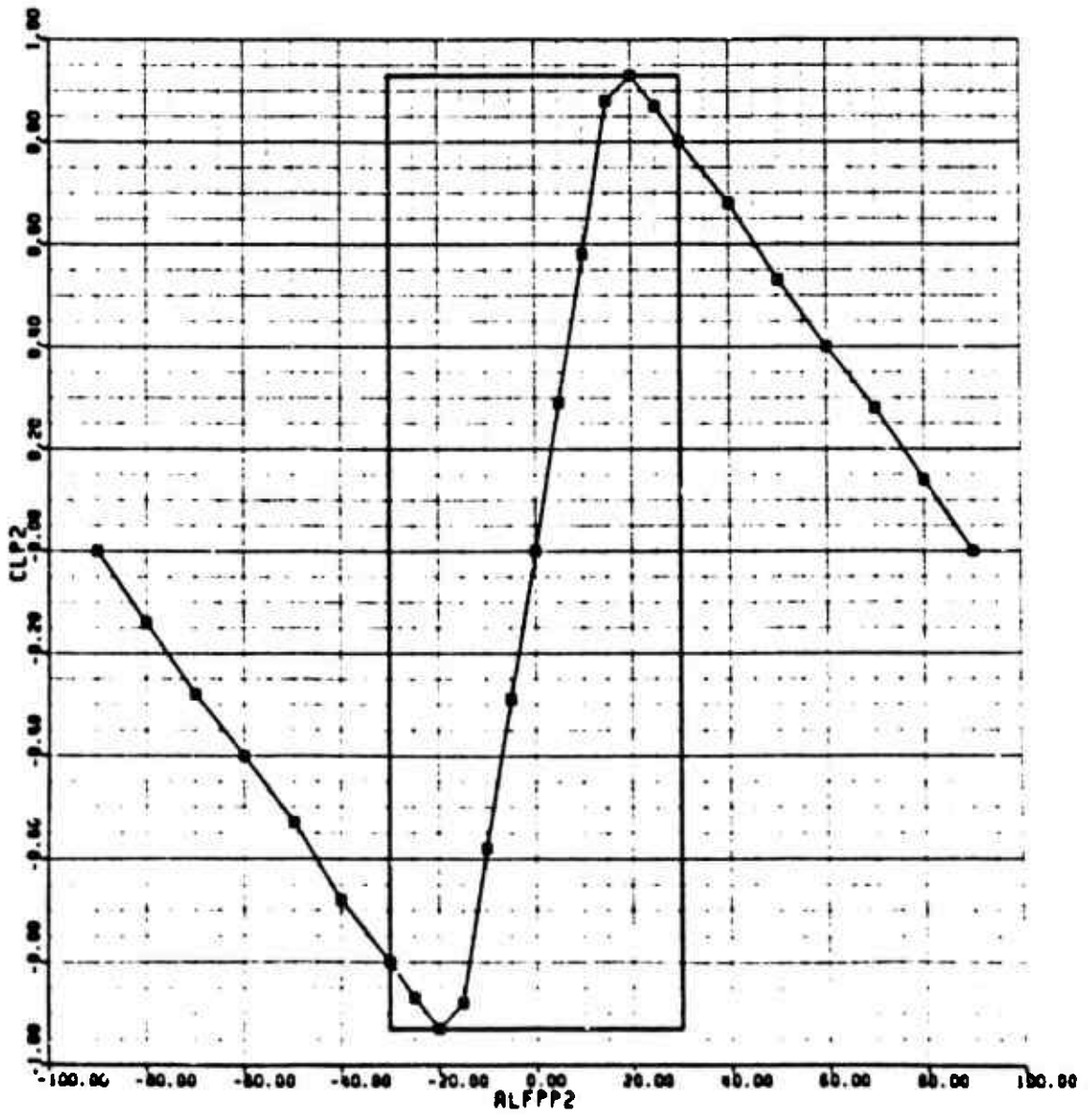


Figure H-18. Mi-28 Horizontal Stabilizer Lift Map

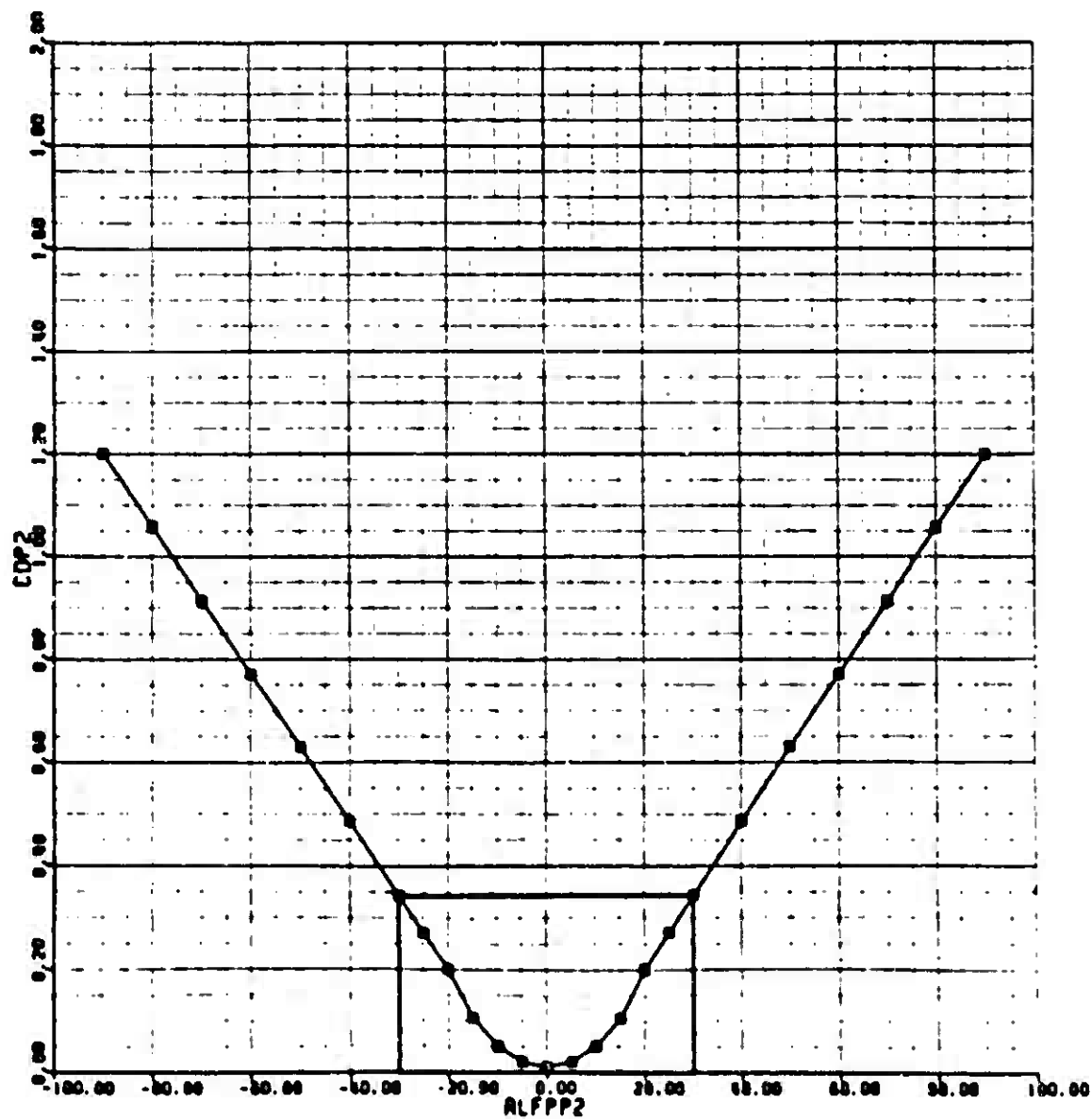


Figure E-19. Mi-28 Horizontal Stabilizer Drag Map

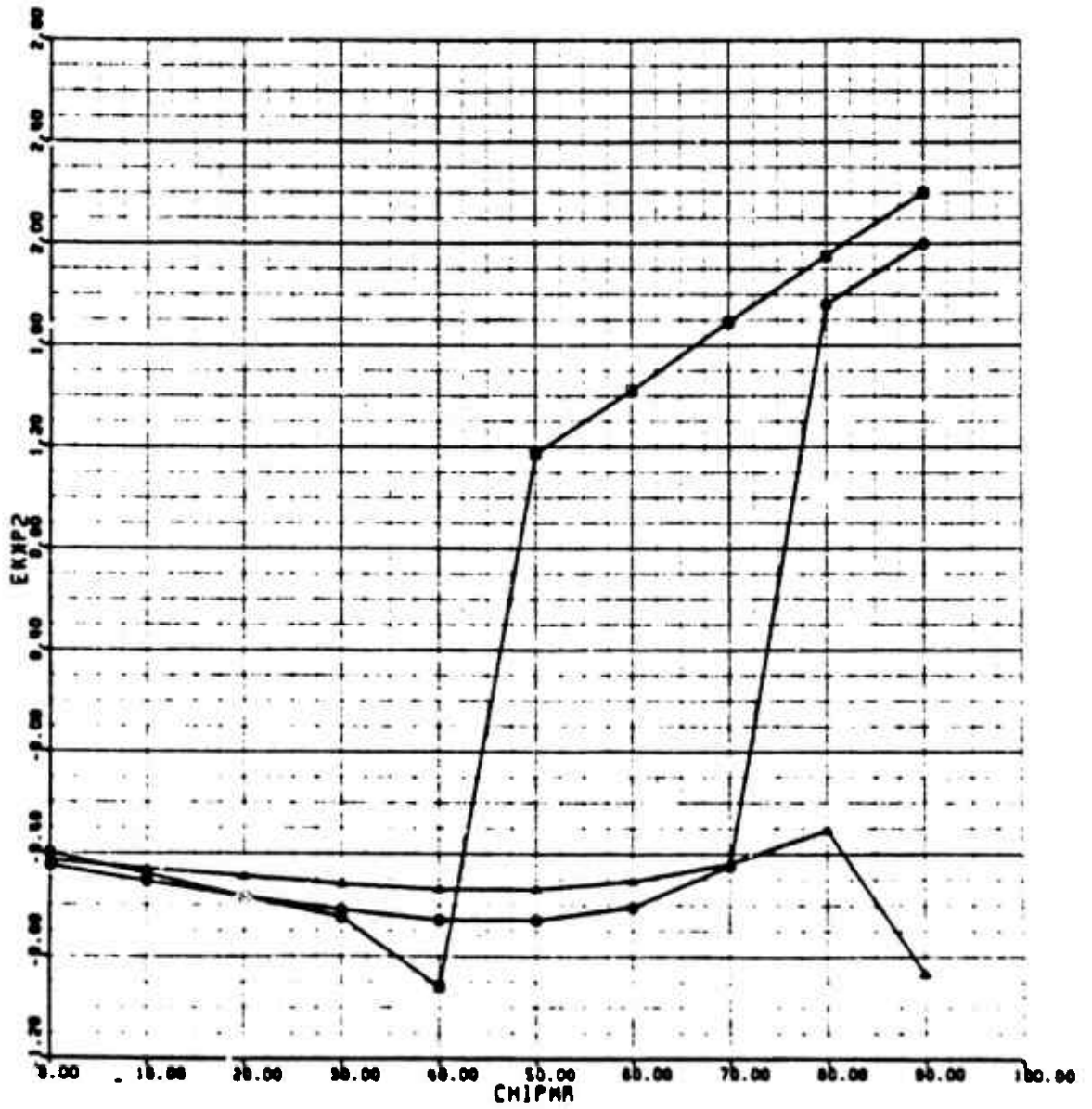


Figure H-20. Mi-28 Main Rotor Downwash on Horizontal Stabilizer Map (x-direction)

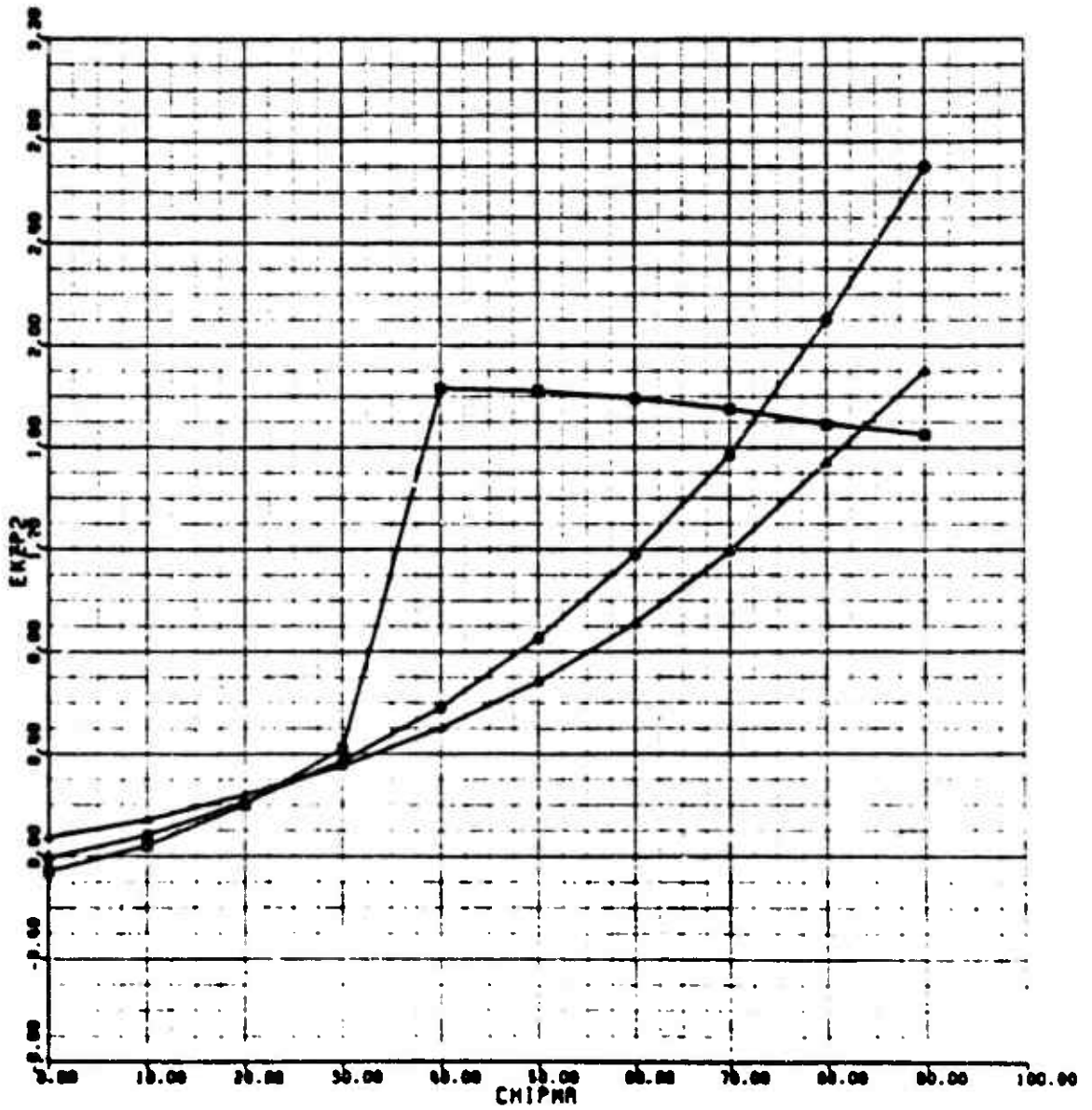


Figure B-21. MI-28 Main Rotor Downwash on Horizontal Stabilizer Map (z-direction)

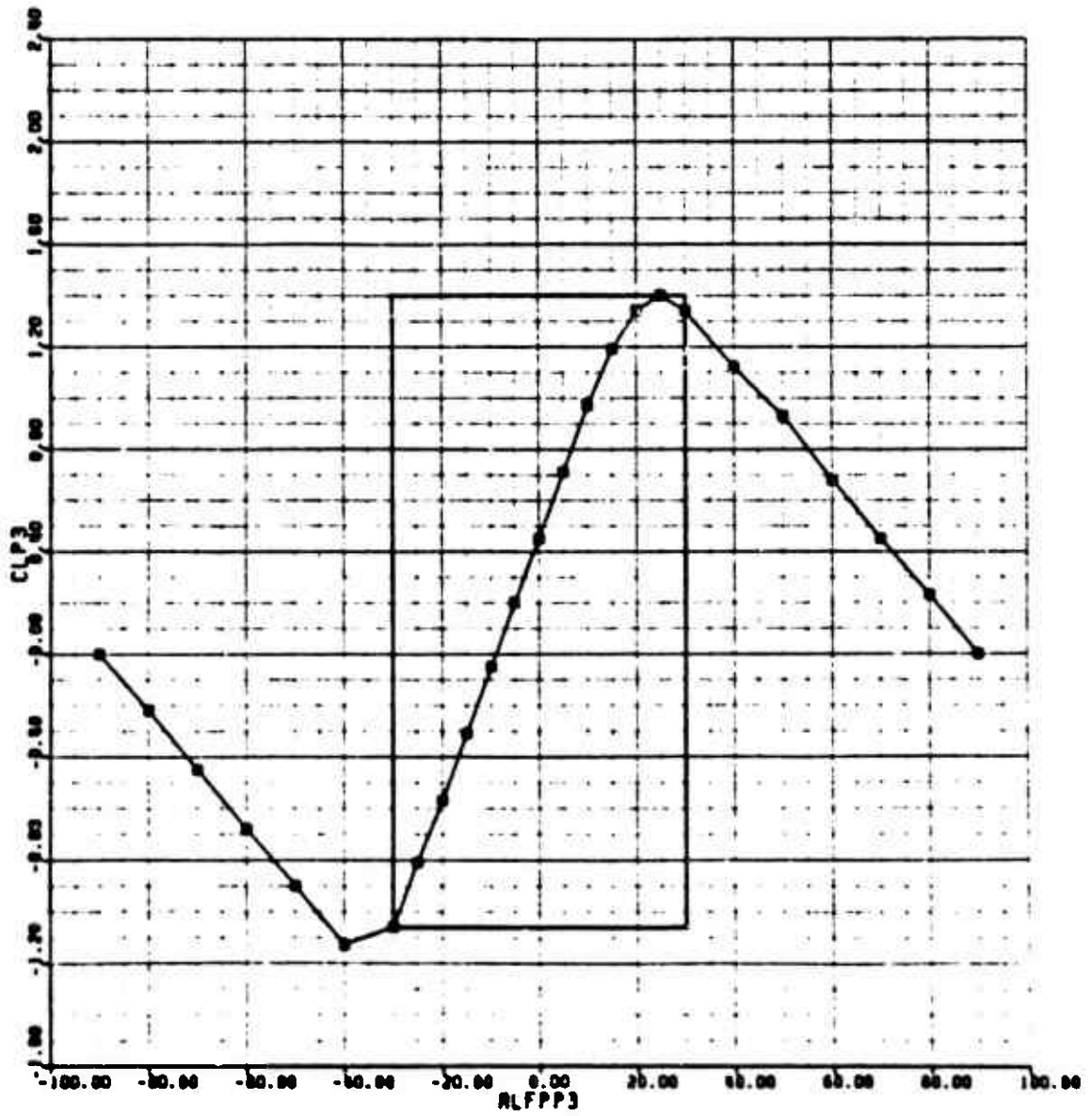


Figure M-22. Mi-28 Vertical Stabilizer Lift Map

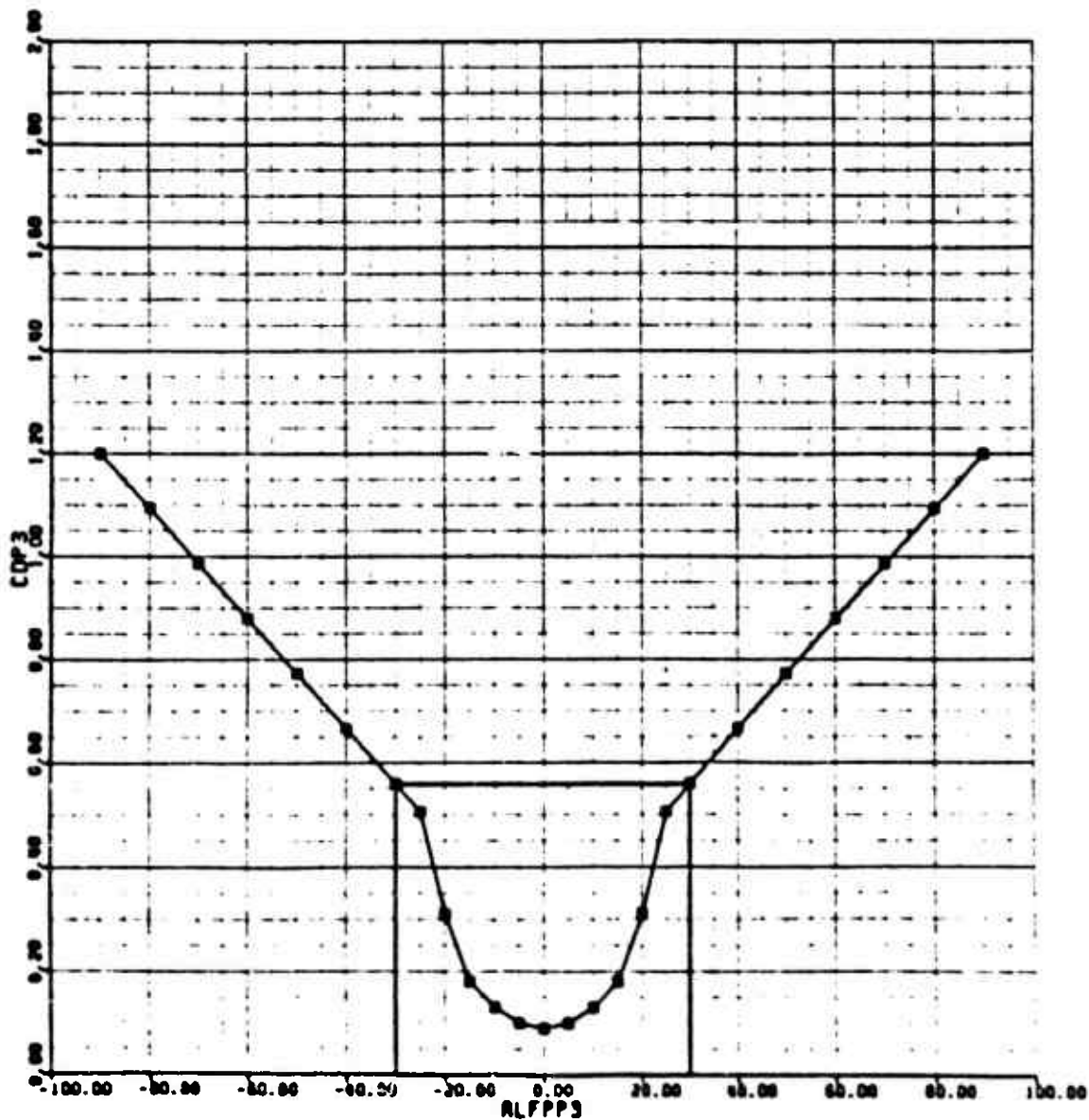


Figure B-23. H-28 Vertical Stabilizer Drag Map

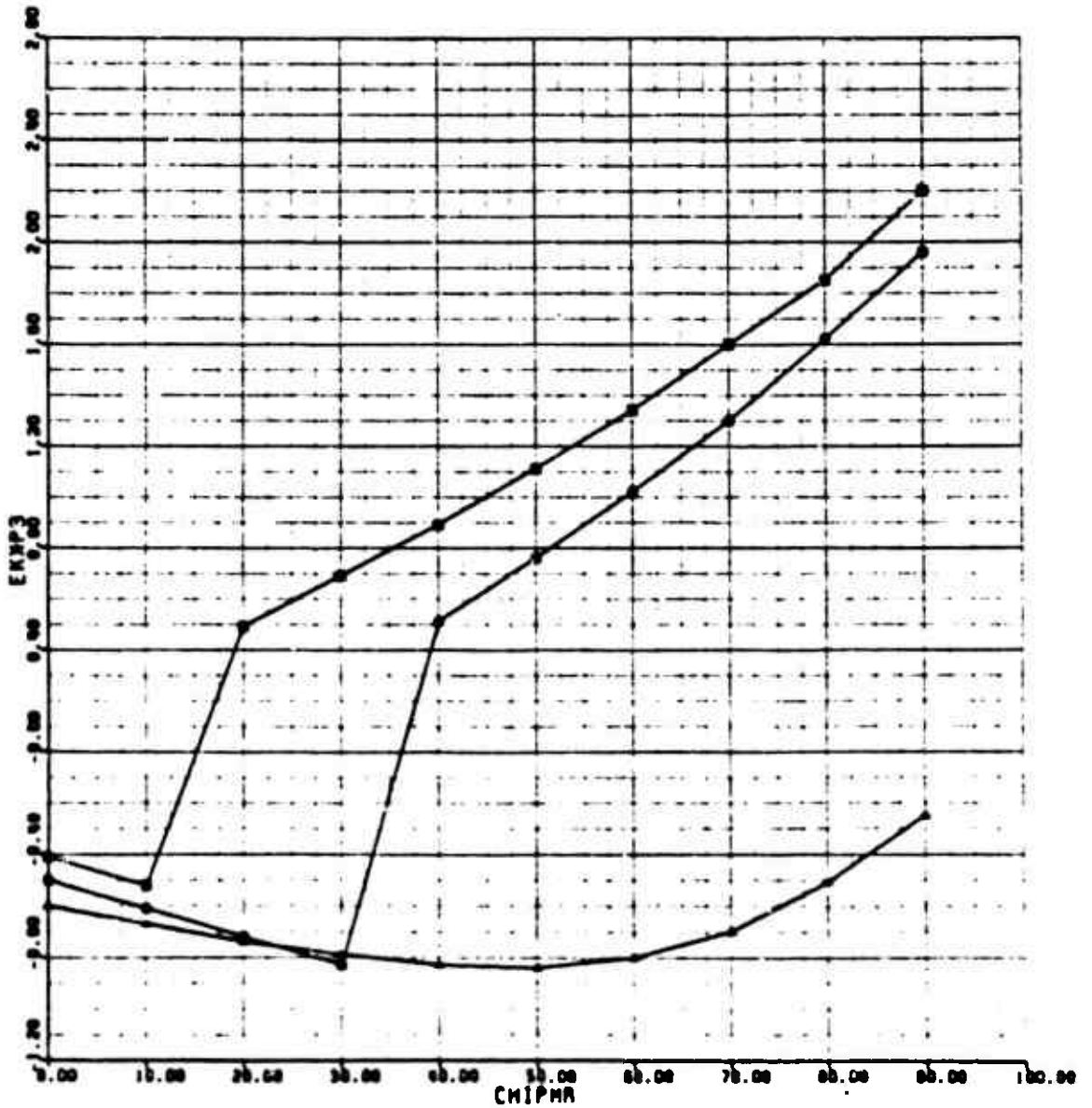


Figure N-24. Mi-28 Main Rotor Downwash on Vertical Stabilizer Map (z-direction)

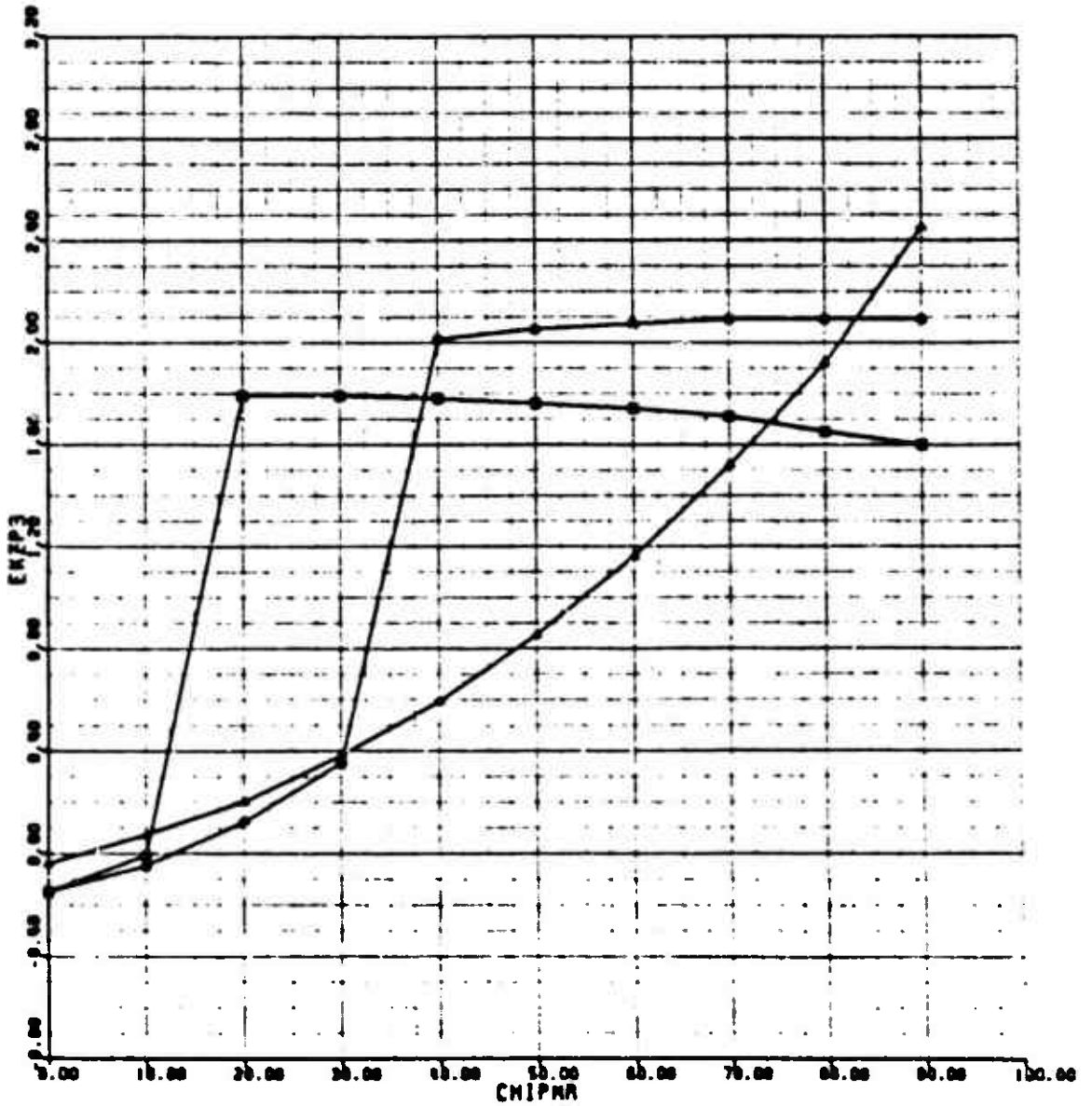


Figure H-25. MI-28 Main Rotor Downwash on Vertical Stabilizer Map (z-direction)

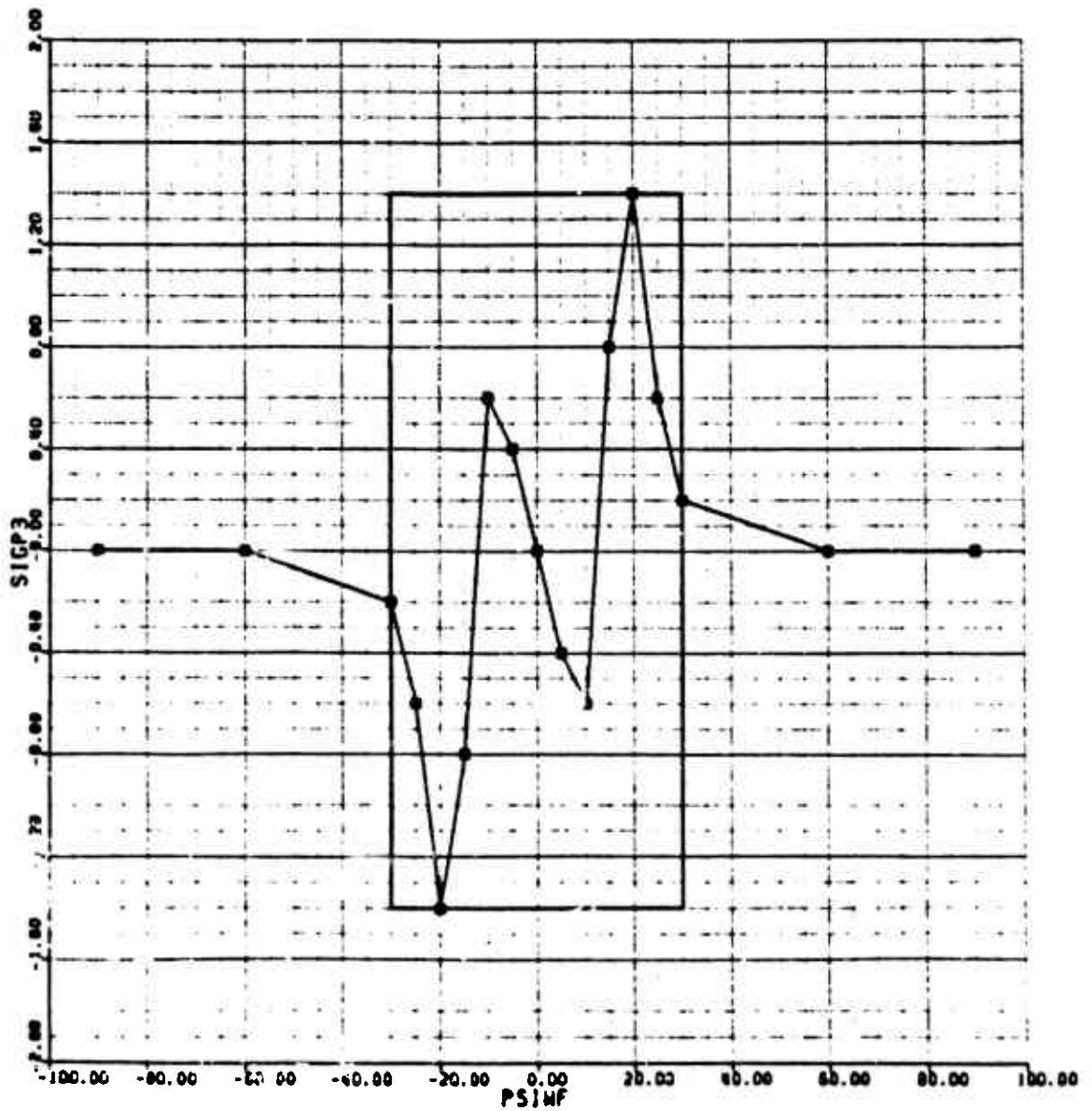


Figure H-26. Mi-28 Fuselage Sidewash on Vertical Stabilizer Map

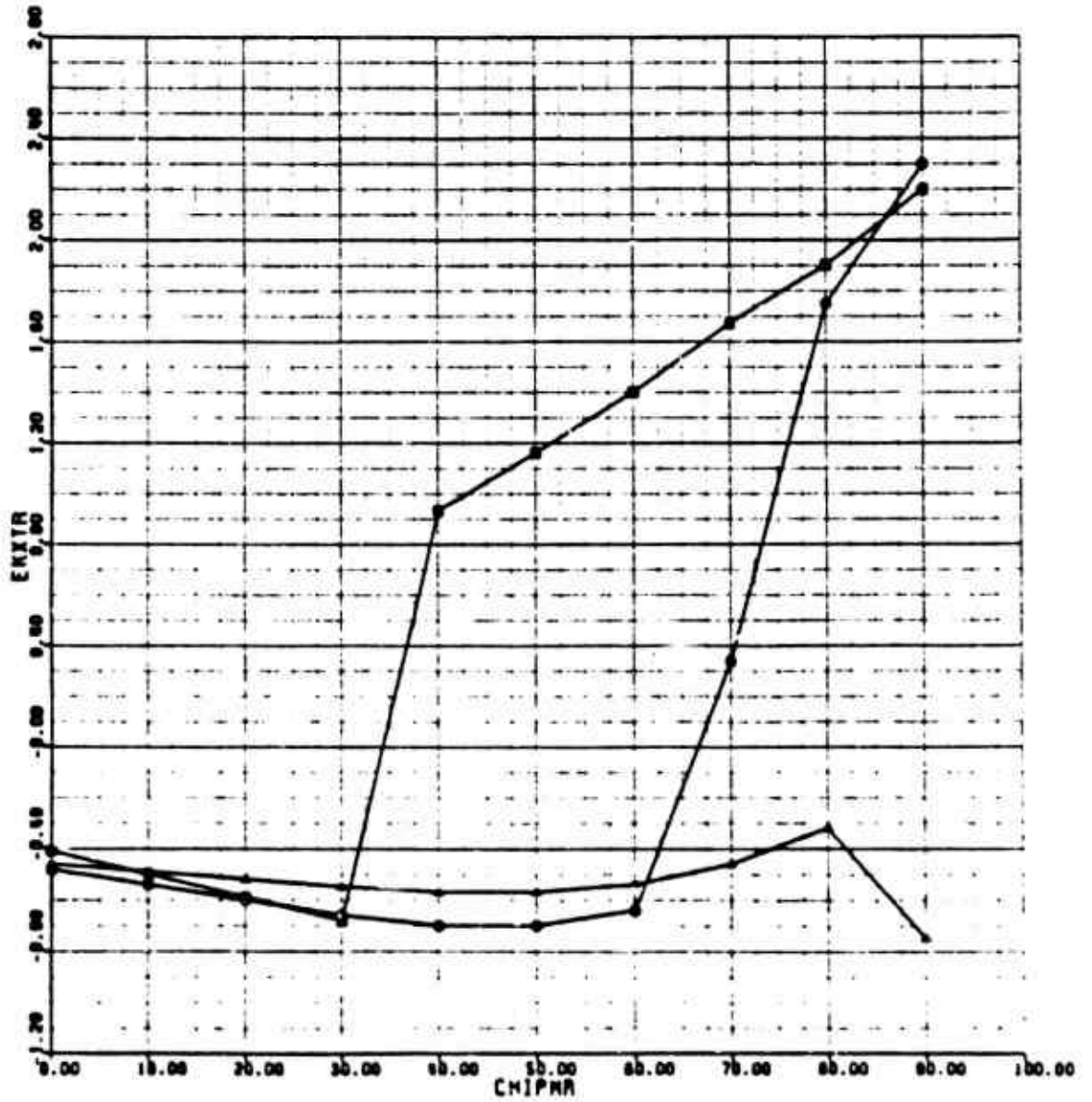


Figure H-27. MI-28 Main Rotor Downwash on Tail Rotor Map (x-direction)

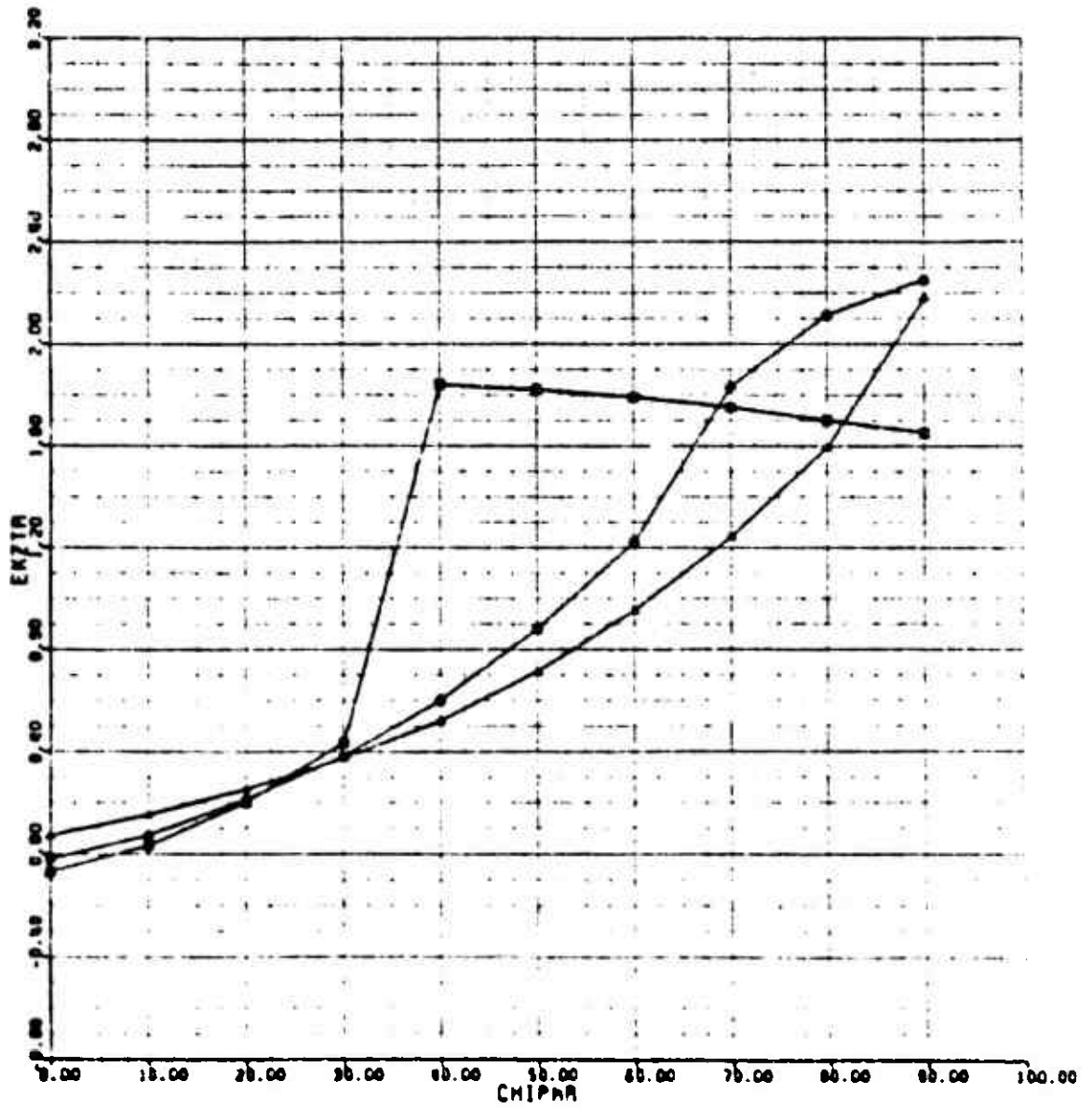


Figure H-28. Mi-28 Main Rotor Downwash on Tail Rotor Map (z-direction)

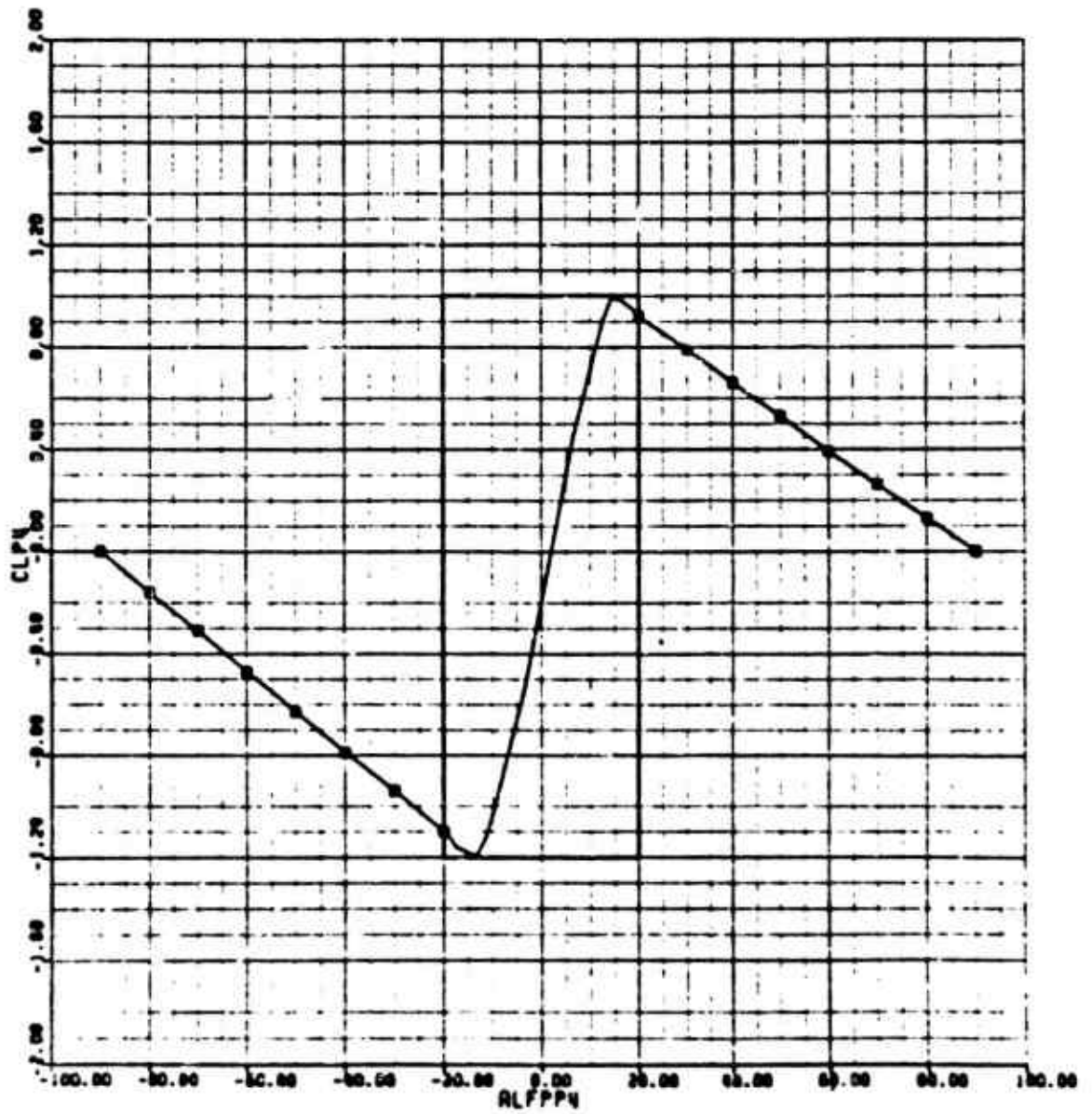


Figure H-29. Mi-28 Wing Lift Map

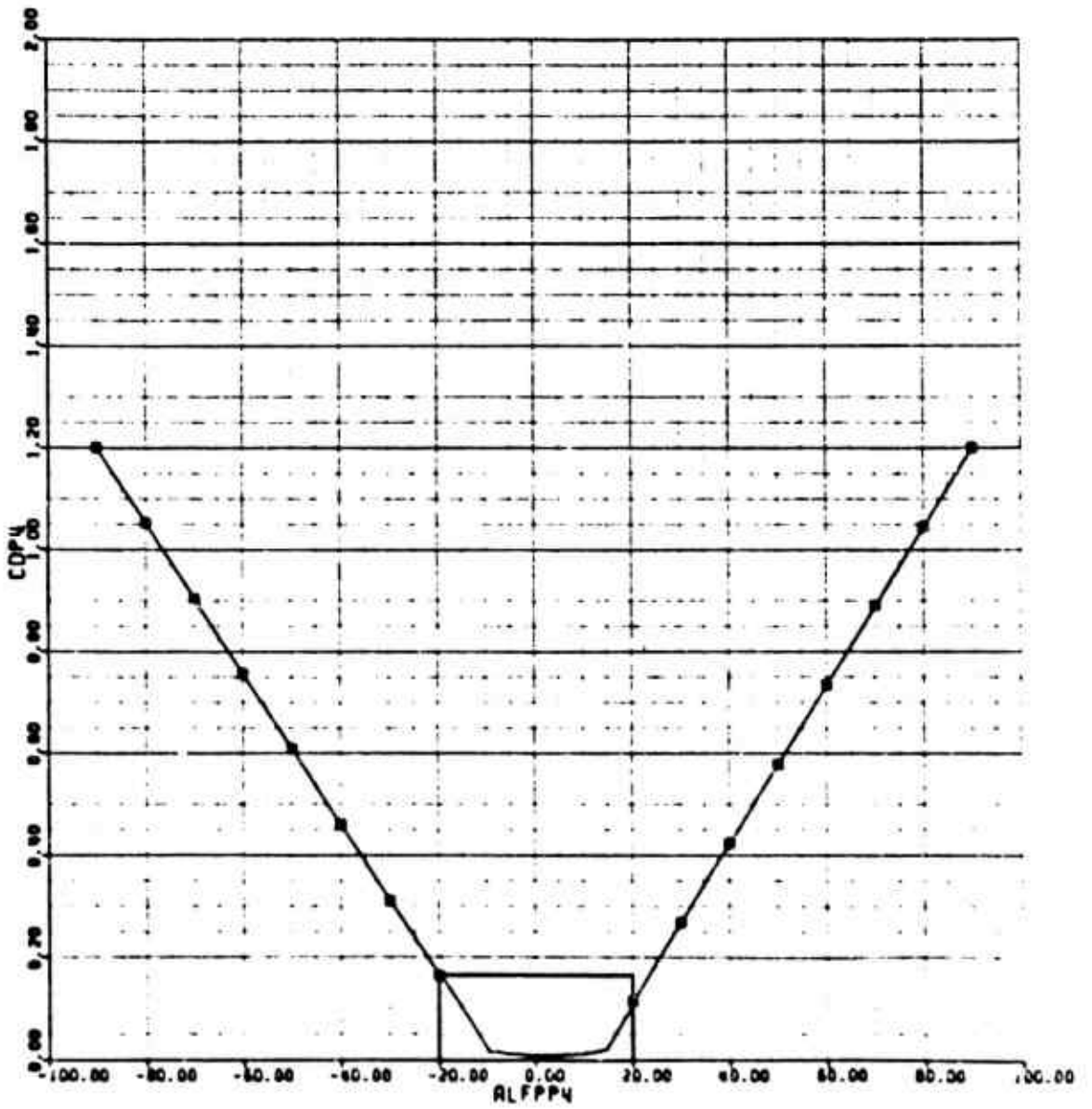


Figure H-30. MI-28 Wing Drag Map

APPENDIX I

AACT MANEUVER TIME HISTORY DATA

This appendix contains selected time history plots from the AACT data that were analyzed. These time histories represent the cases where a ± 3 -degree firing window was achieved. Data provided are:

S-76A vs UH-60A
Counters 208019 to 208027

AH-1S vs OH-58A
Counters 302014 to 302019

AH-64A vs SA-365N (AH-64A turreted gun)
Counters 417003 to 417009

AH-64A vs SA-365N (AH-64A fixed gun)
Counters 411011 to 411023

S-76A vs OH-58A
Counters 23020 to 23038

UH-60A vs OH-58A
Counters 27026 to 27043

The data presented shows the range between the helicopters in meters and the azimuth and elevation angles of each helicopter, as seen from the body axis of the other. The time scale is the time data recorded during the encounter. This is the same time used as a reference in column 5.3 of Table 6. The discontinuities in the angular data are caused by 180 degree phase shifts to keep the angles within plus or minus 180 degrees.

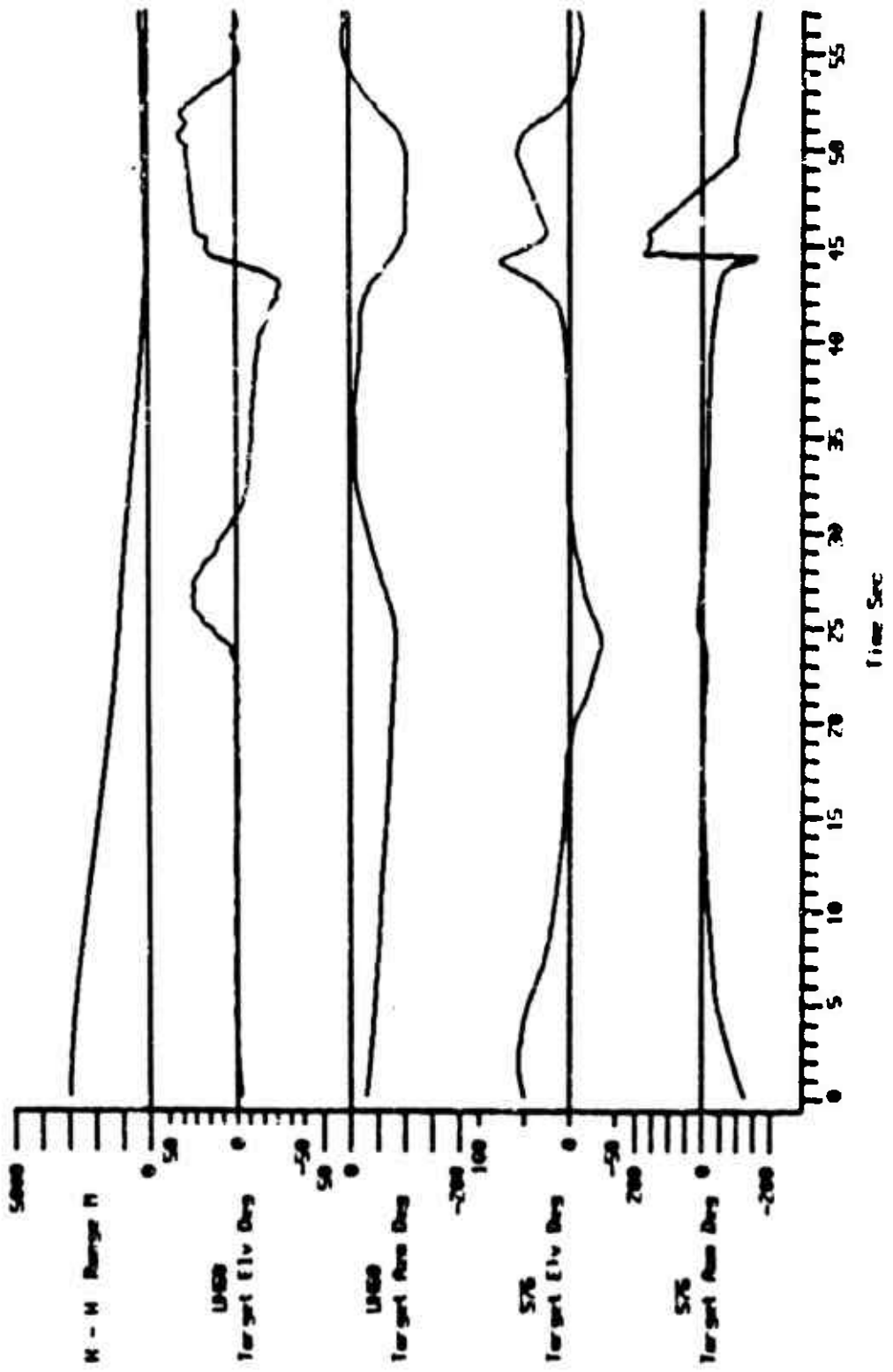


Figure I-2. Time History Data, Counter 208019

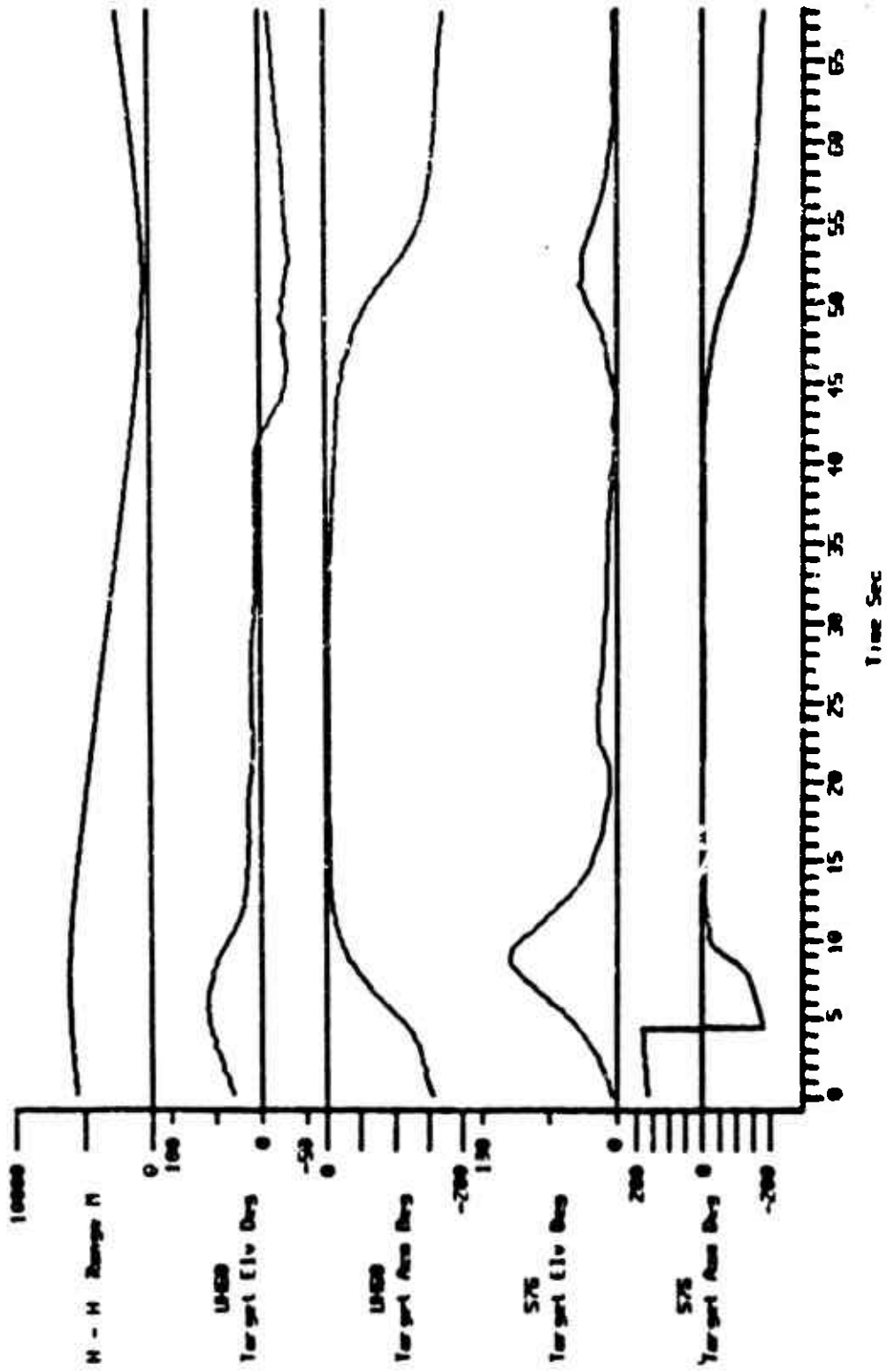


Figure I-1. Time History Data, Counter 206025

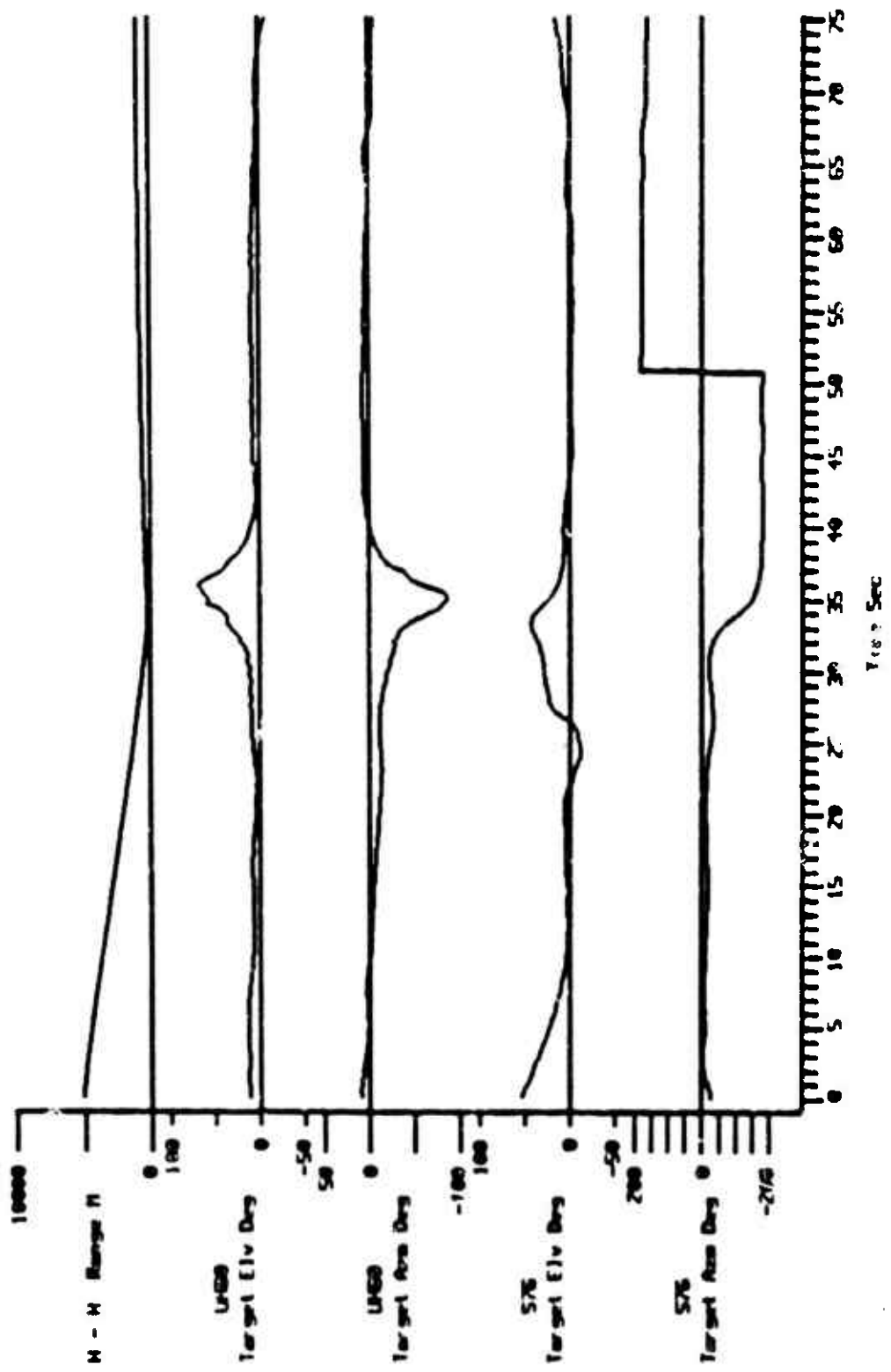


Figure I-3. Time History Data, Counter 208026

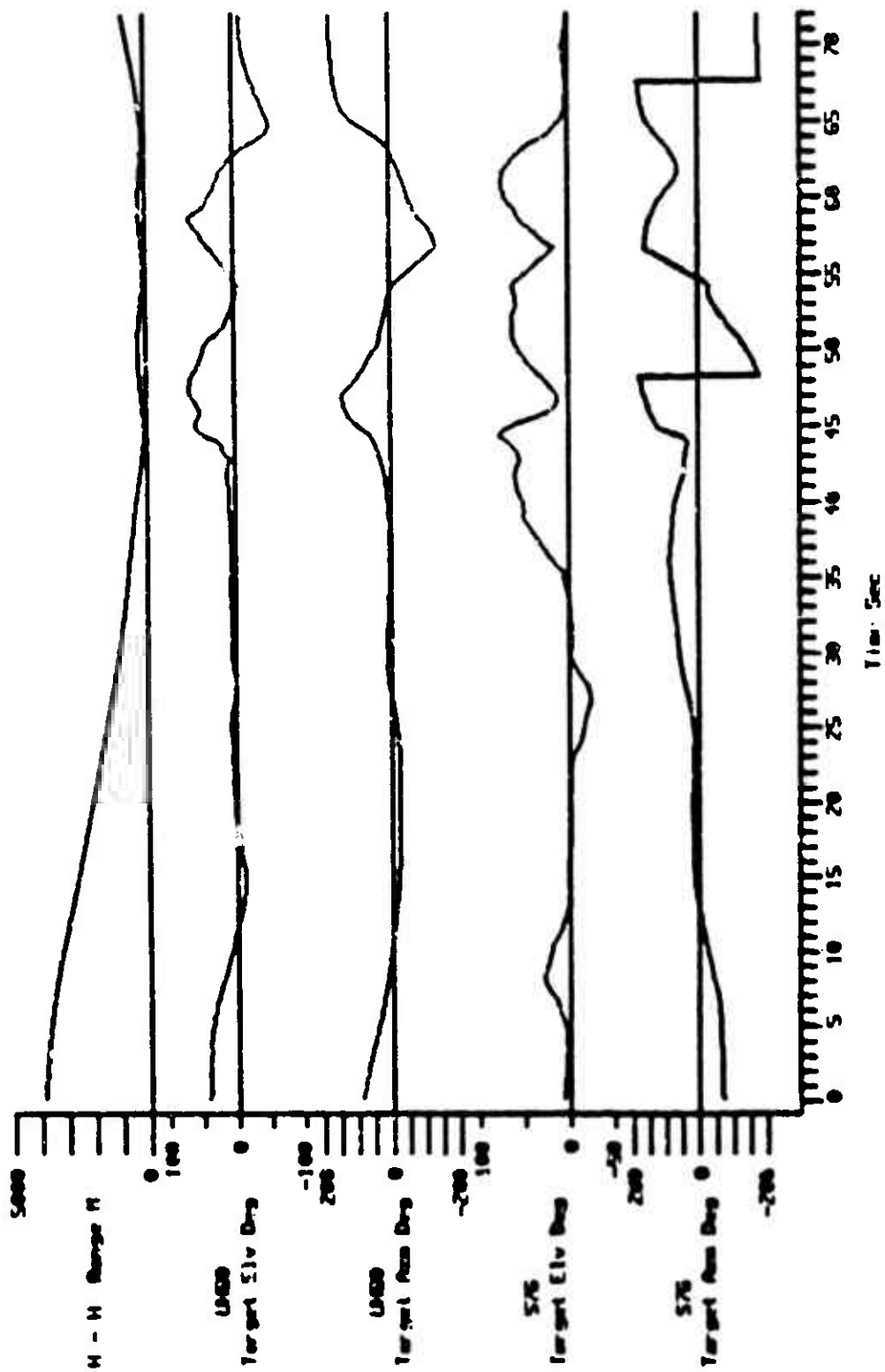


Figure I-4. Time History Data, Counter 208027

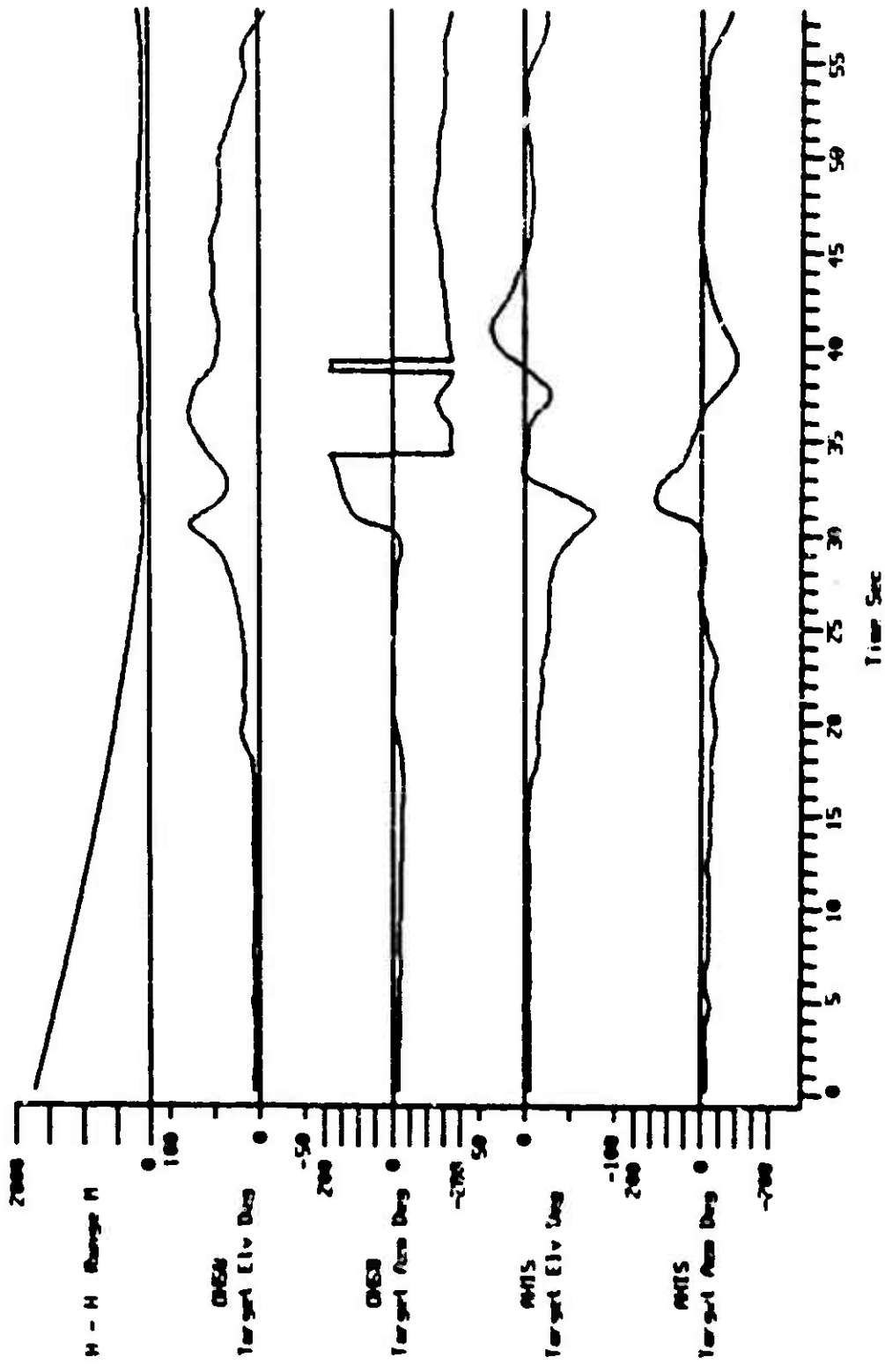


Figure I-5. Time History Data, Counter 302014

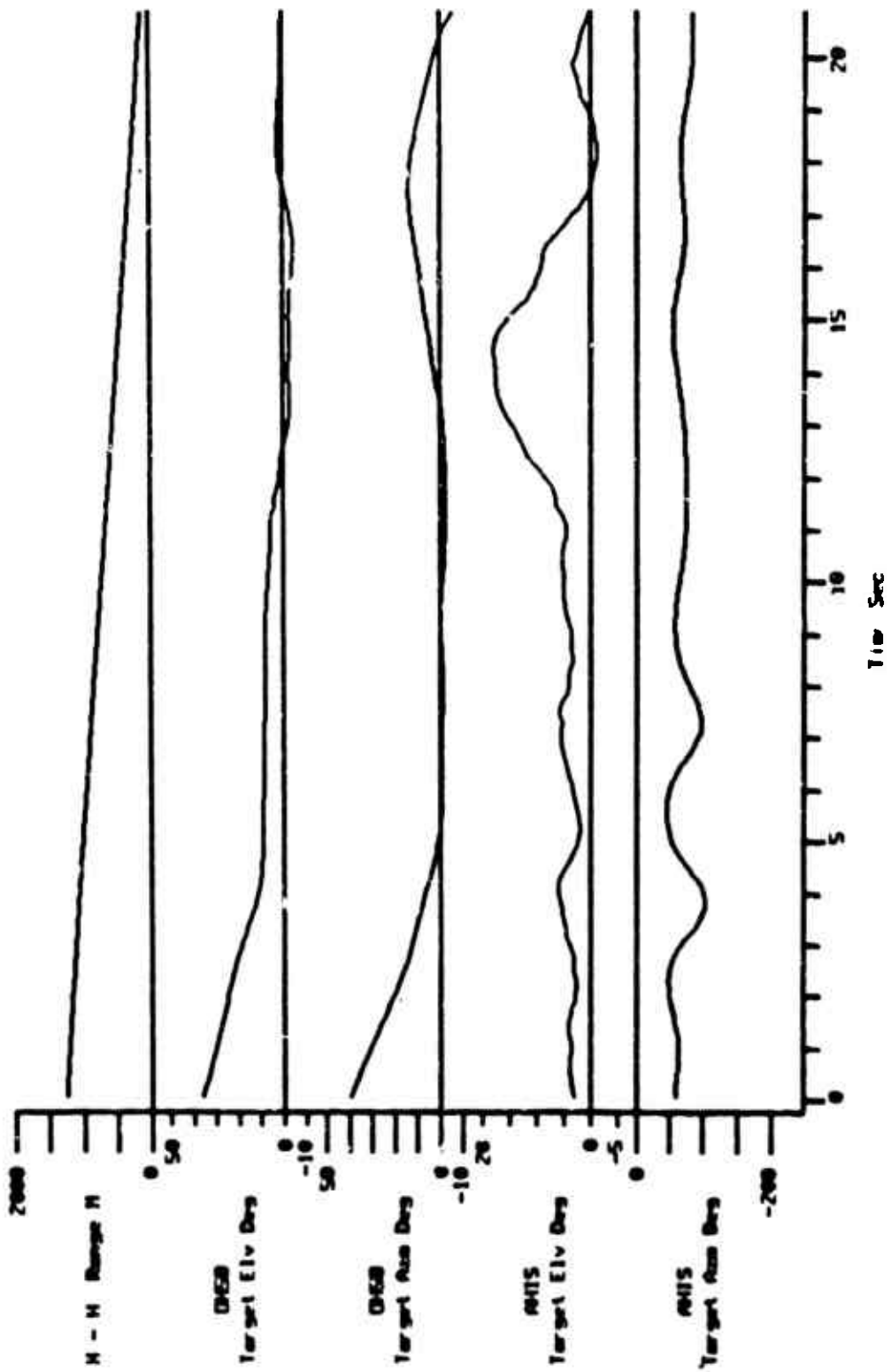


Figure I-6. Time History Data, Counter 302018

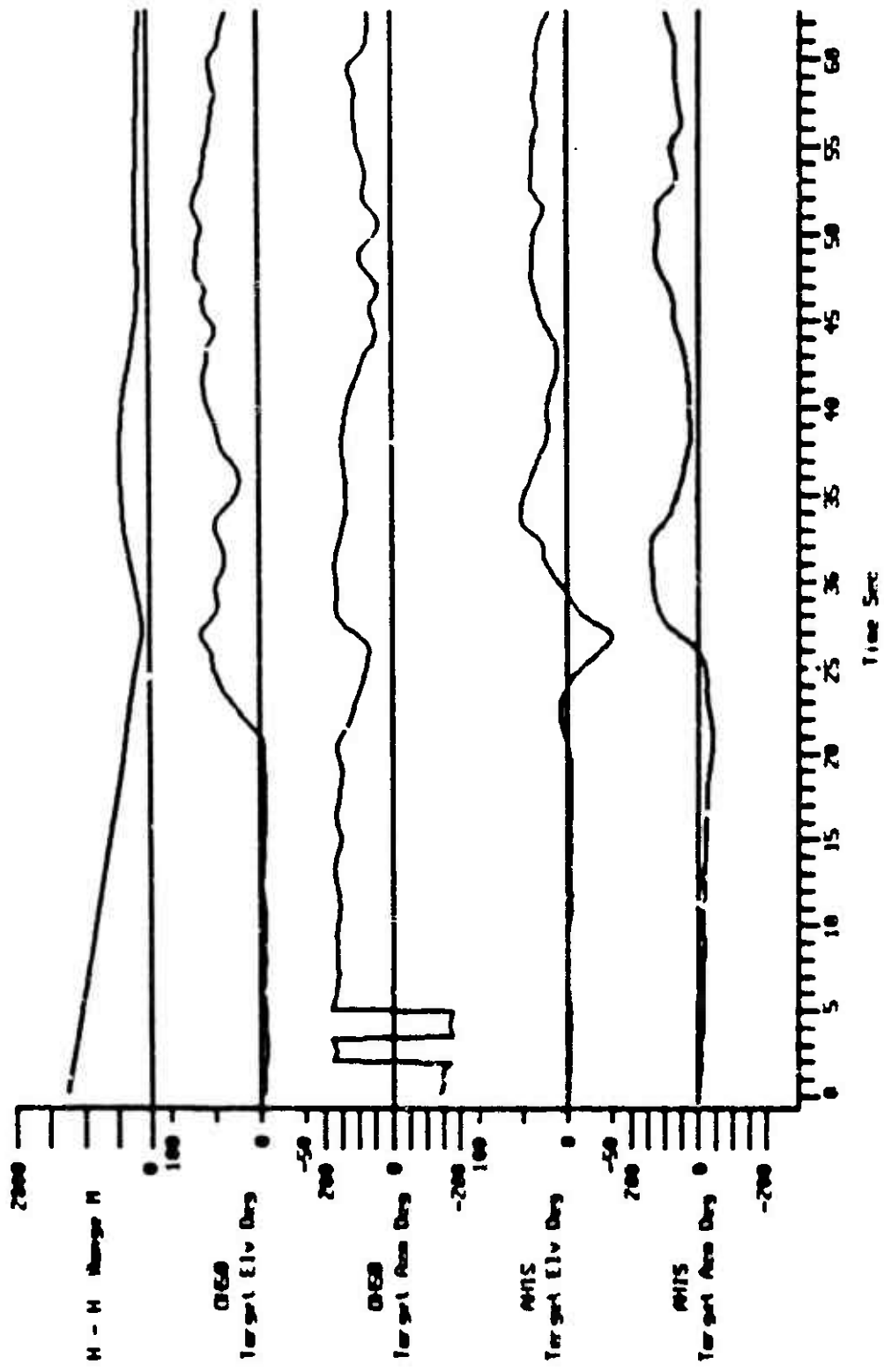


Figure 1-7. Time History Data, Counter 302019

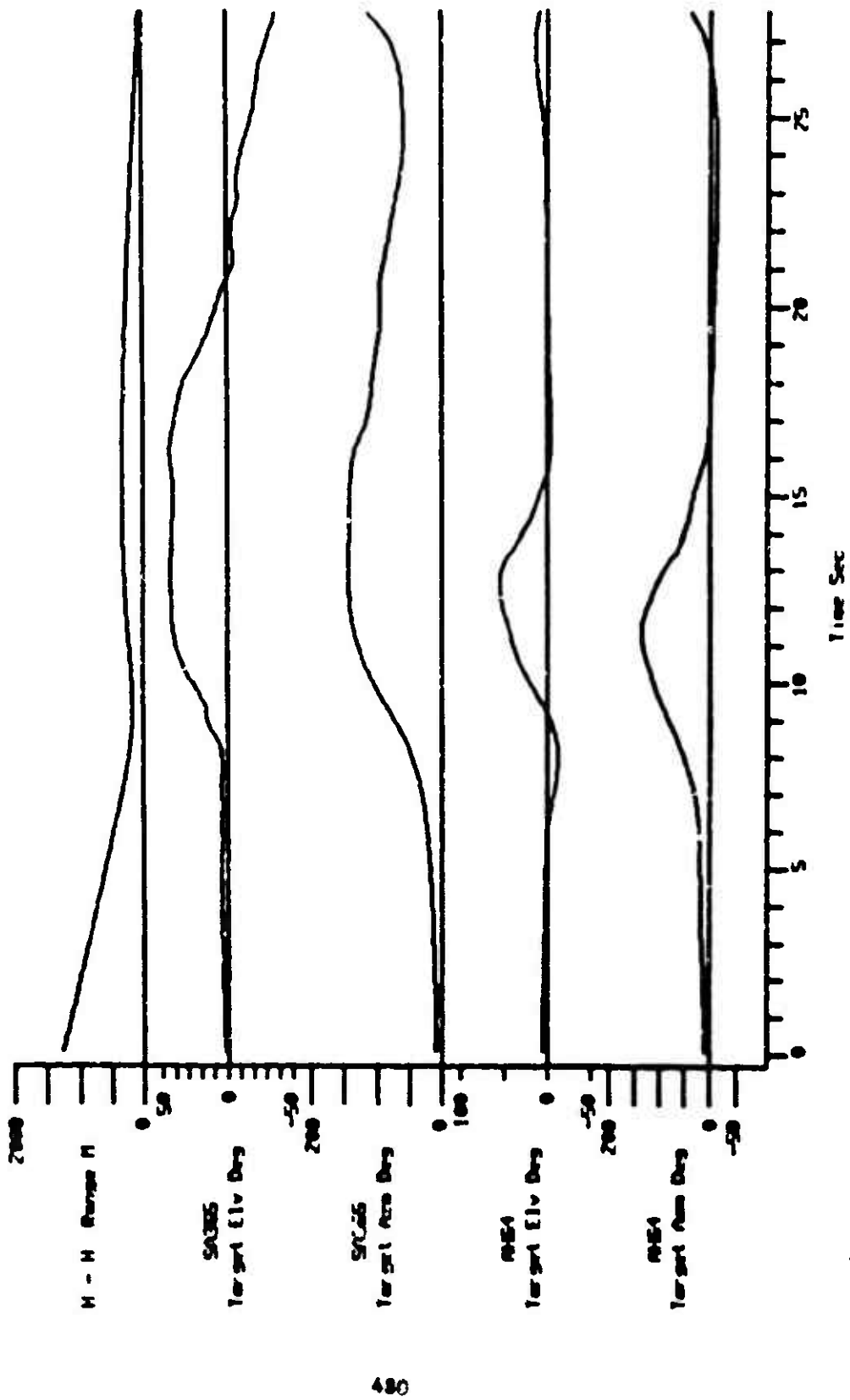


Figure I-8. Time History Data, Counter 417003

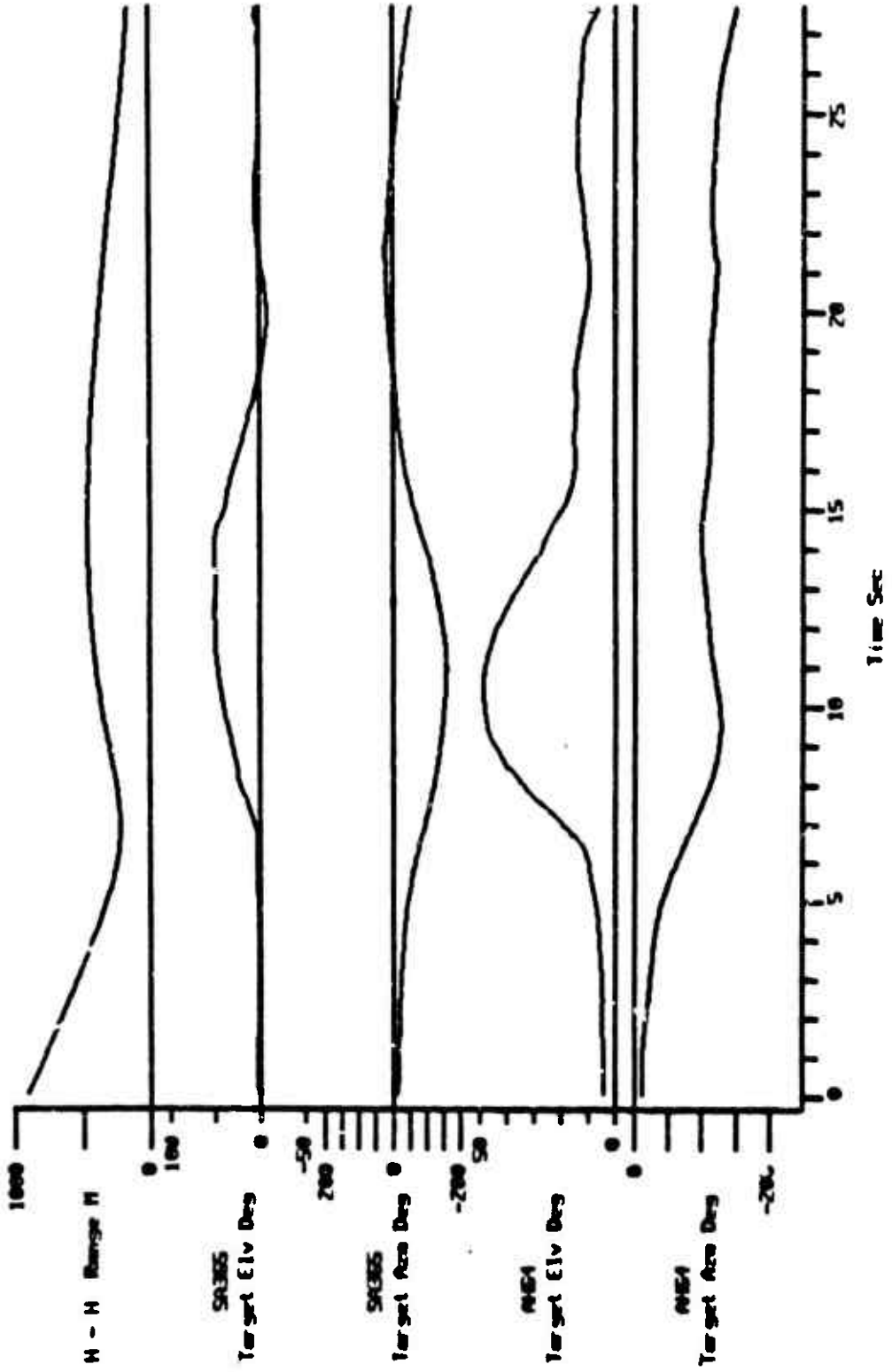


Figure I-9. Time History Data, Counter 417005

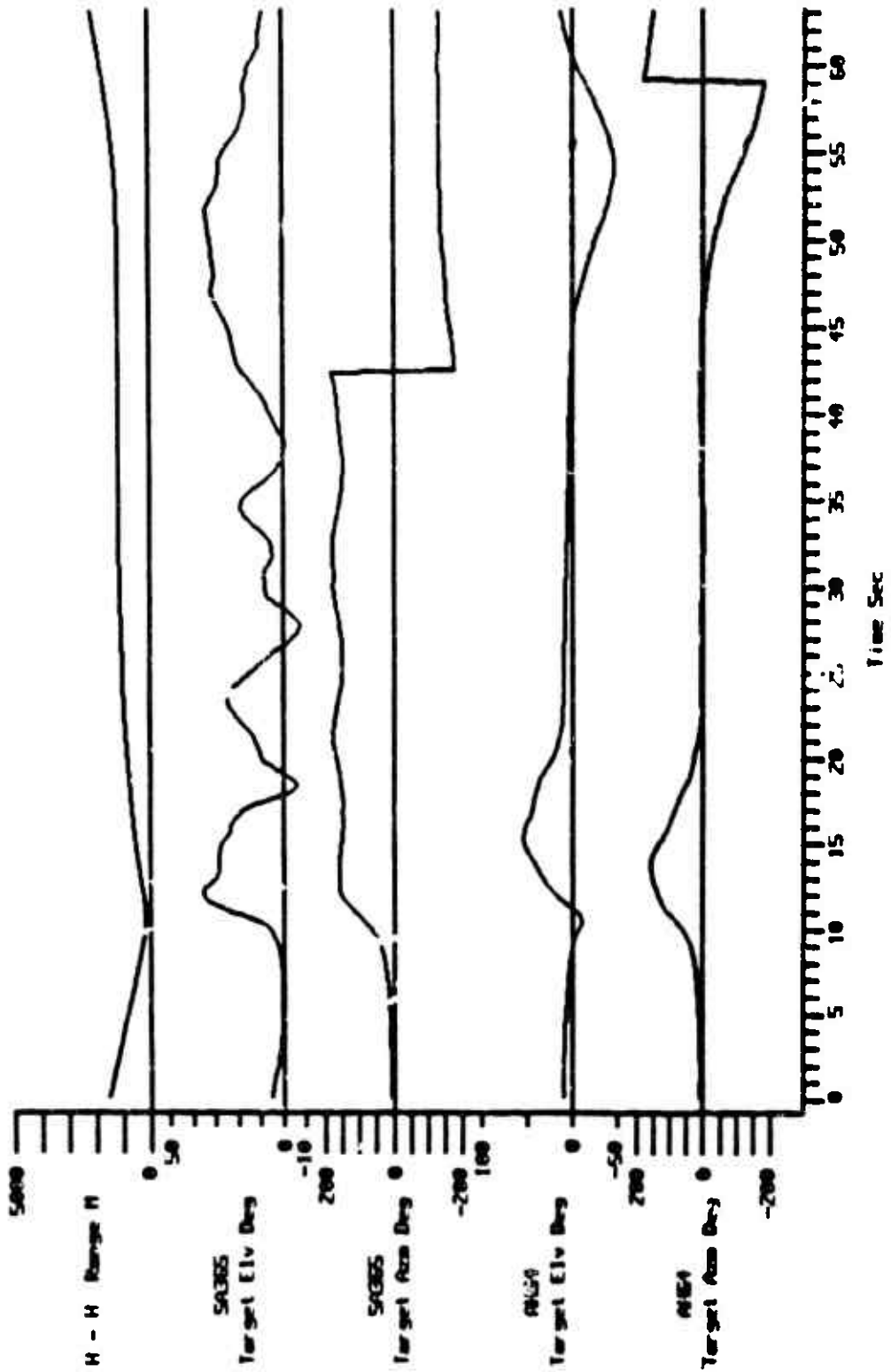


Figure I-10. Time History Data, Counter 417006

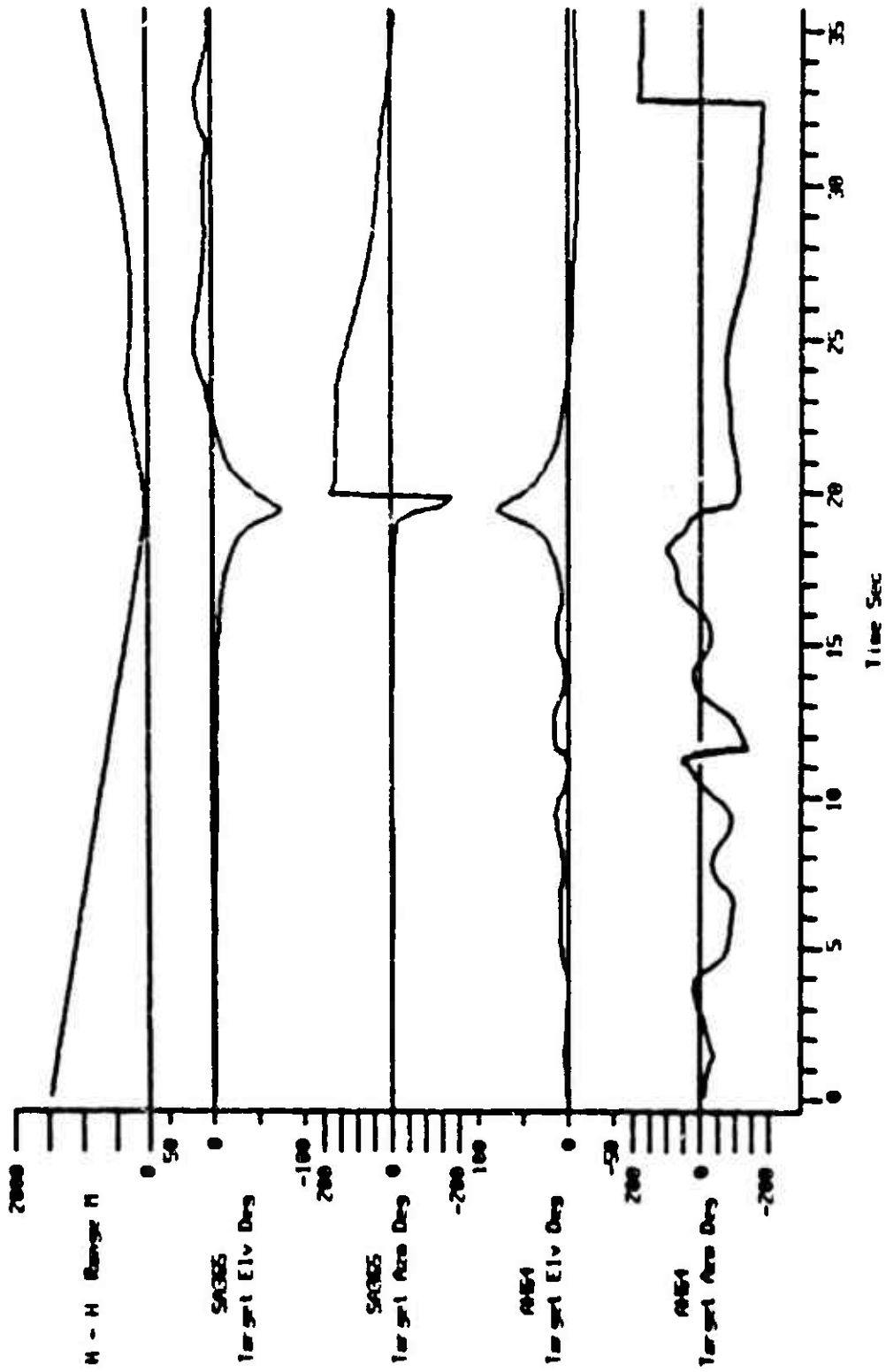


Figure I-11. Time History Data, Counter 417008

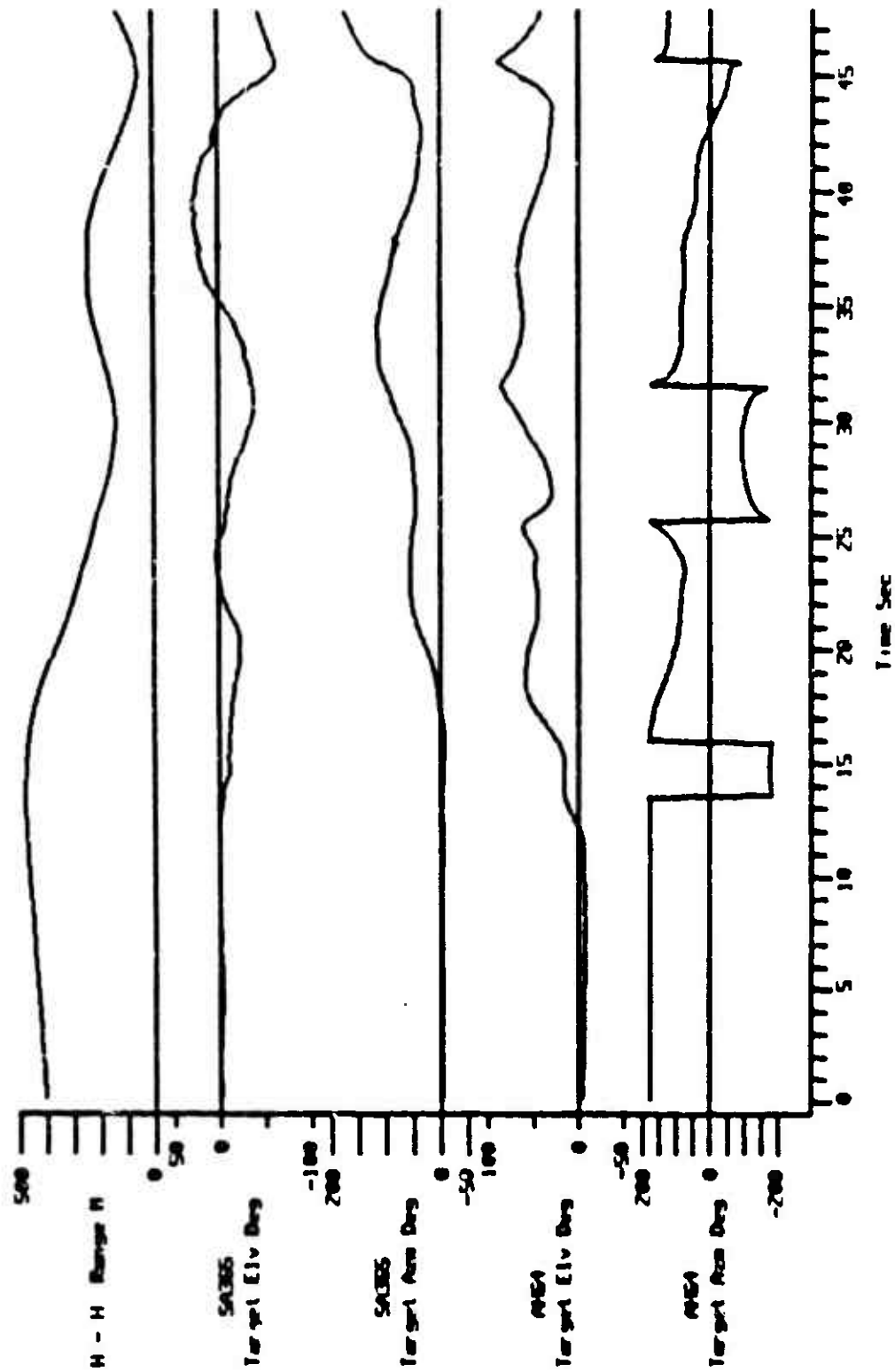


Figure I-12. Time History Data, Counter 417009

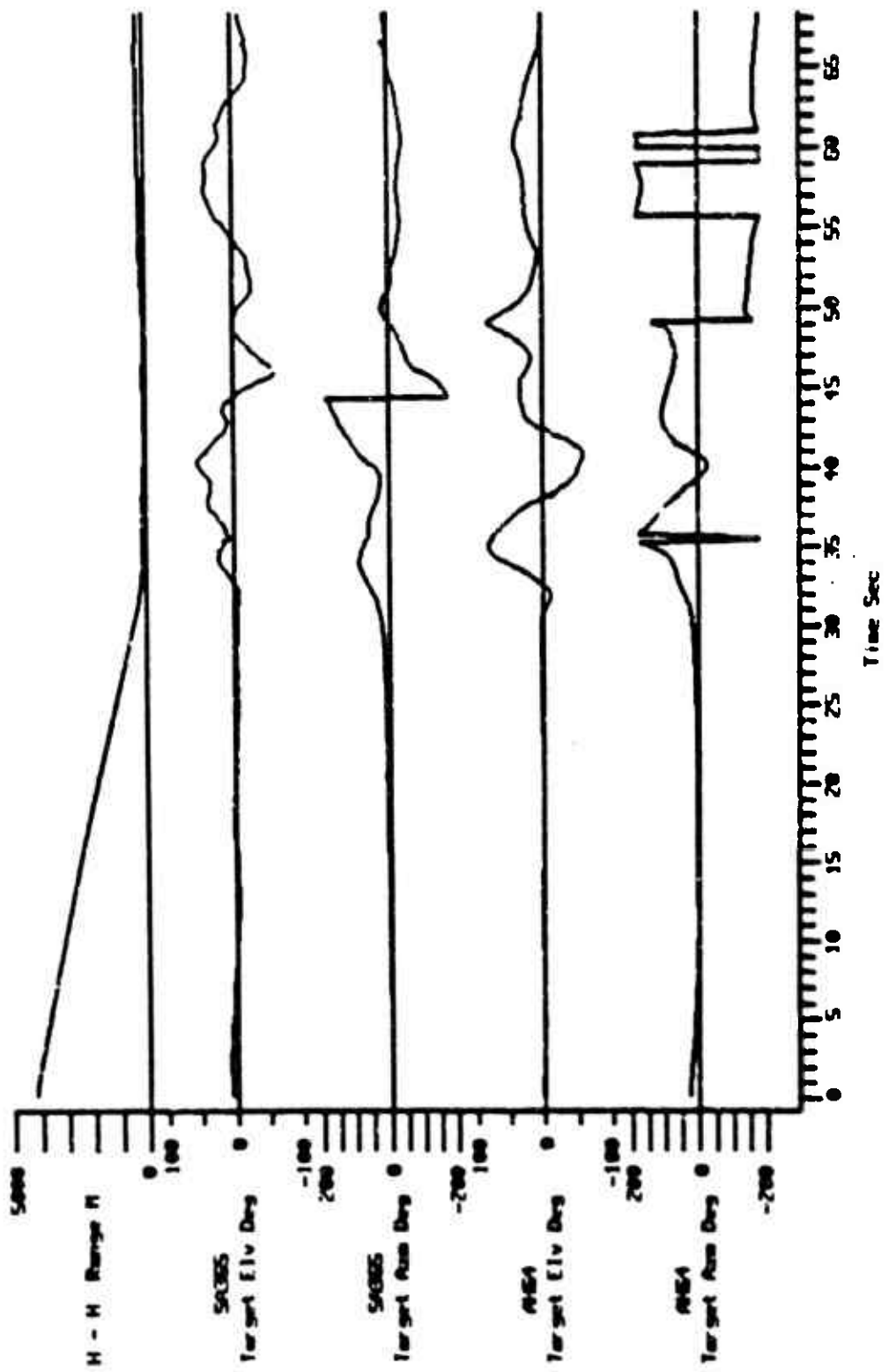


Figure I-13. Time History Data, Counter 411011

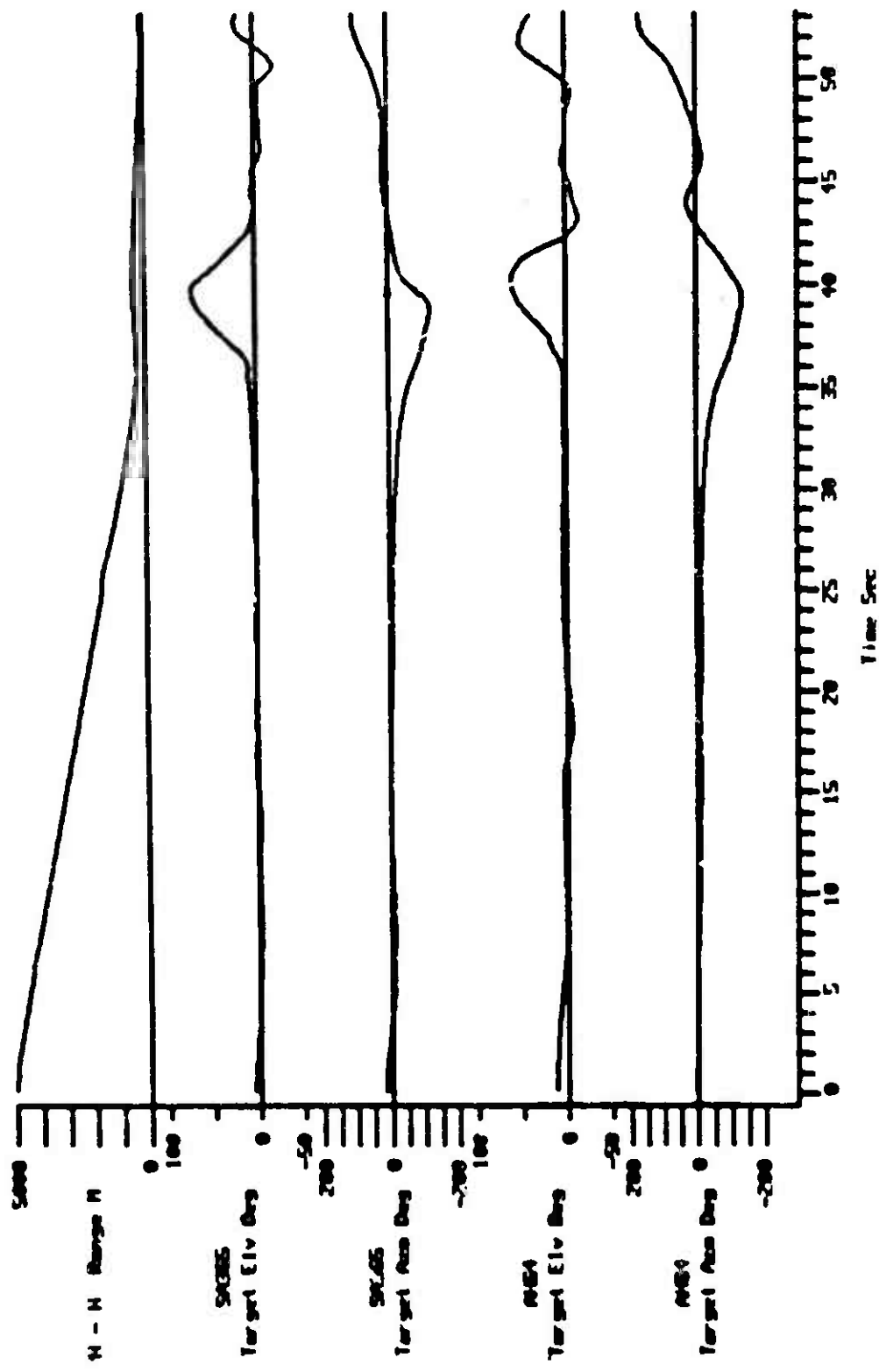


Figure 1-14. Time History Data, Counter 411013

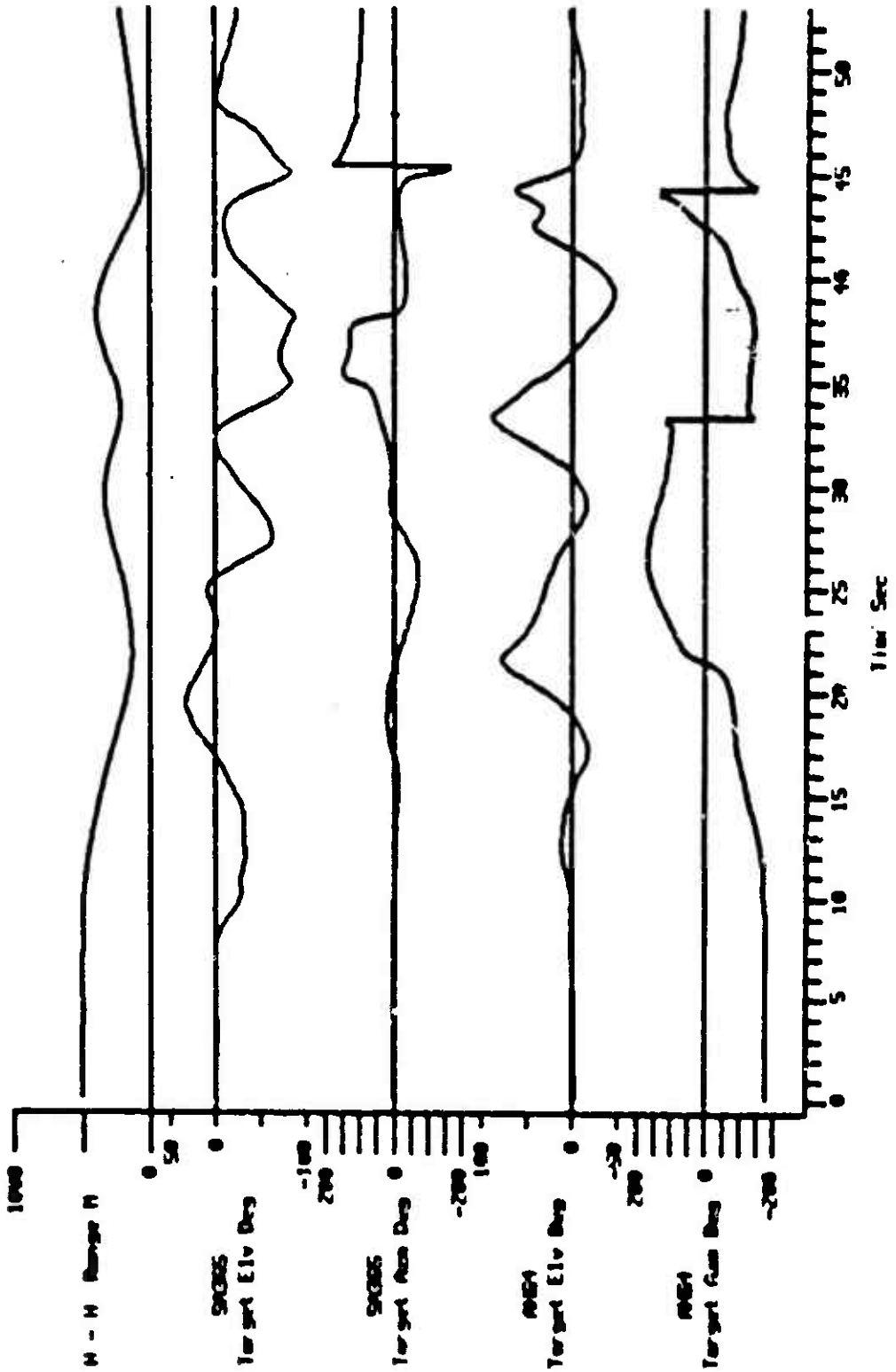


Figure I-15. Time History Data, Counter 411023

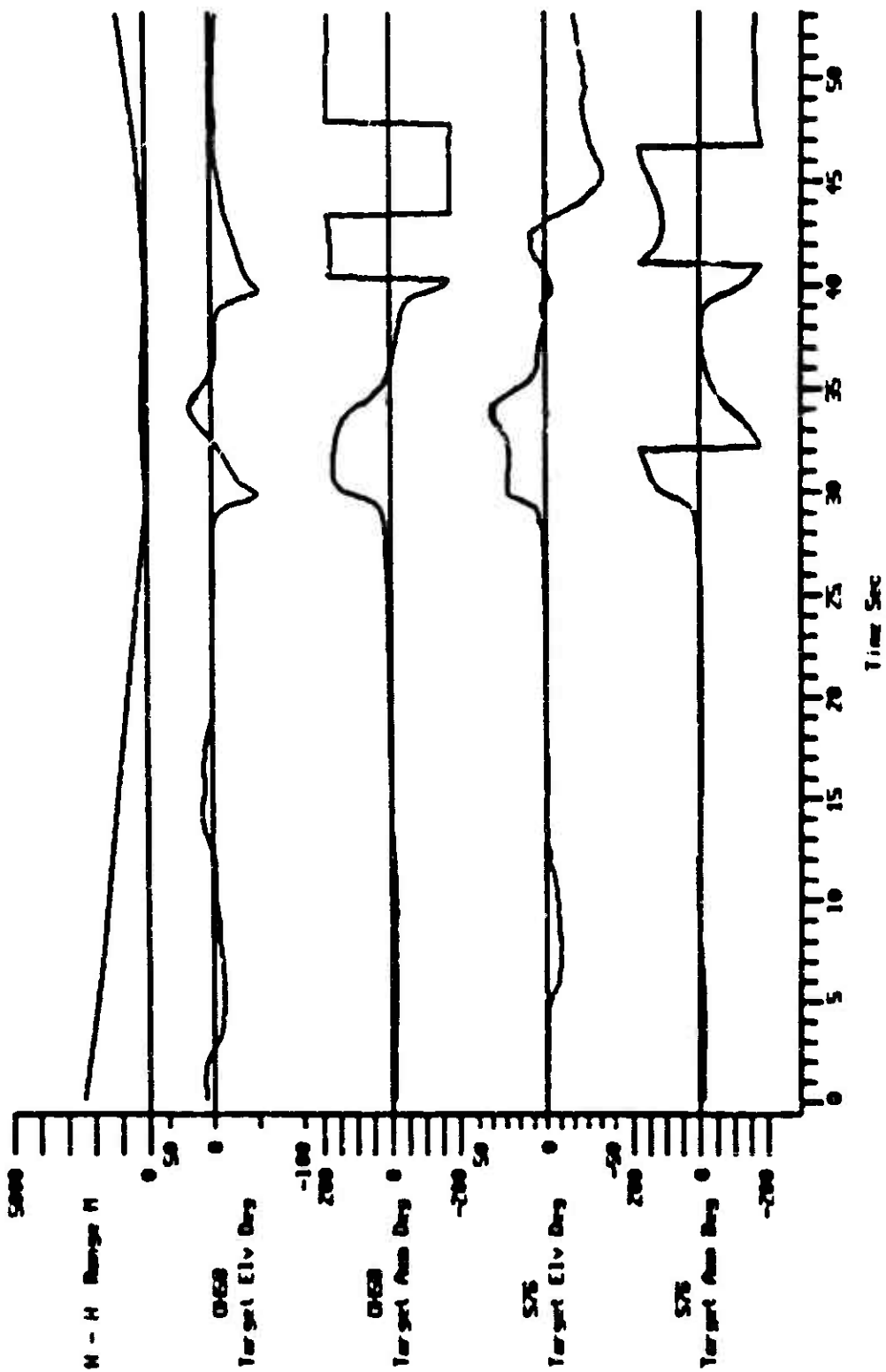


Figure I-16. Time History Data, Counter 23020

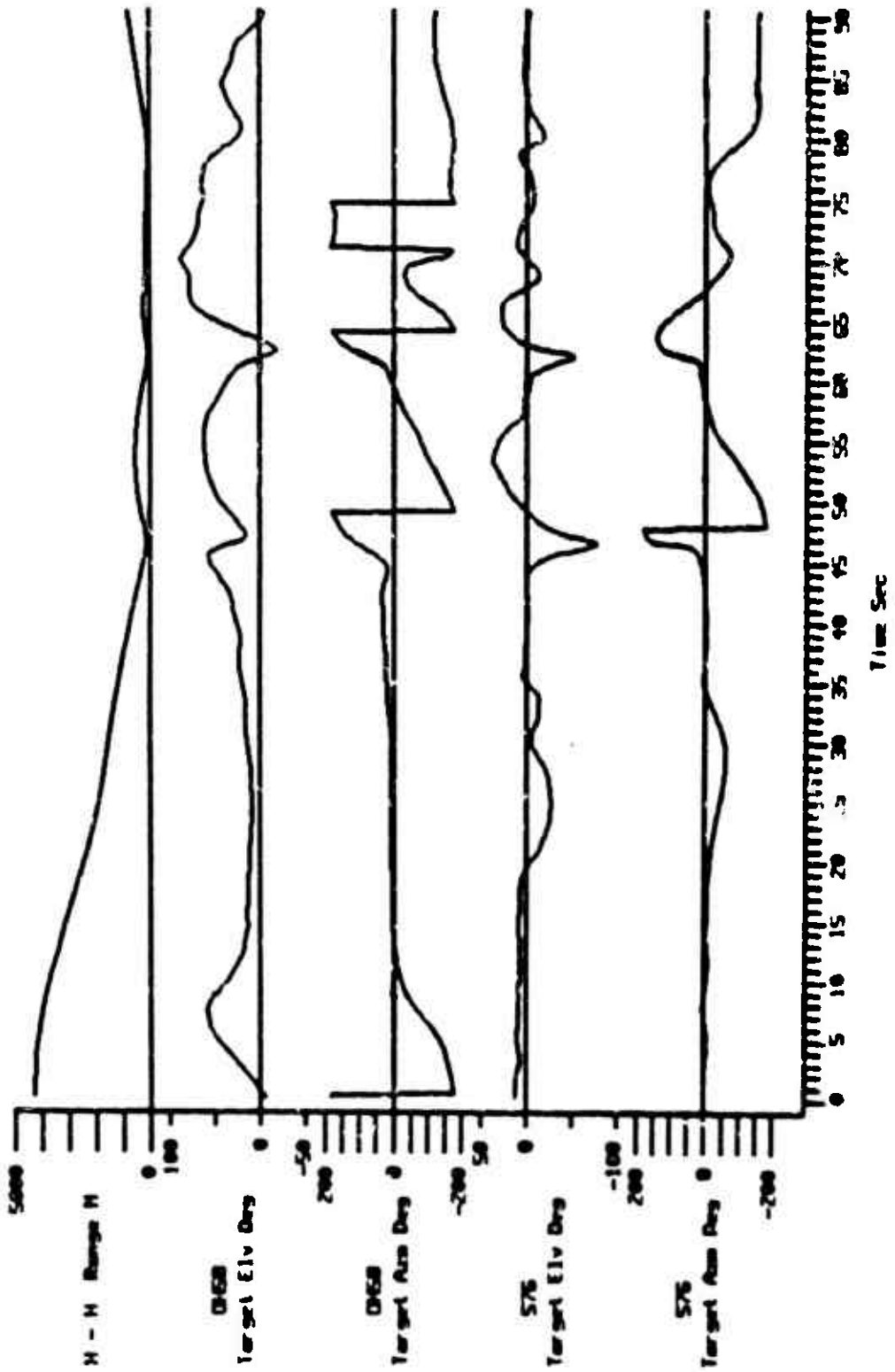


Figure I-17. Time History Data, Counter 23021

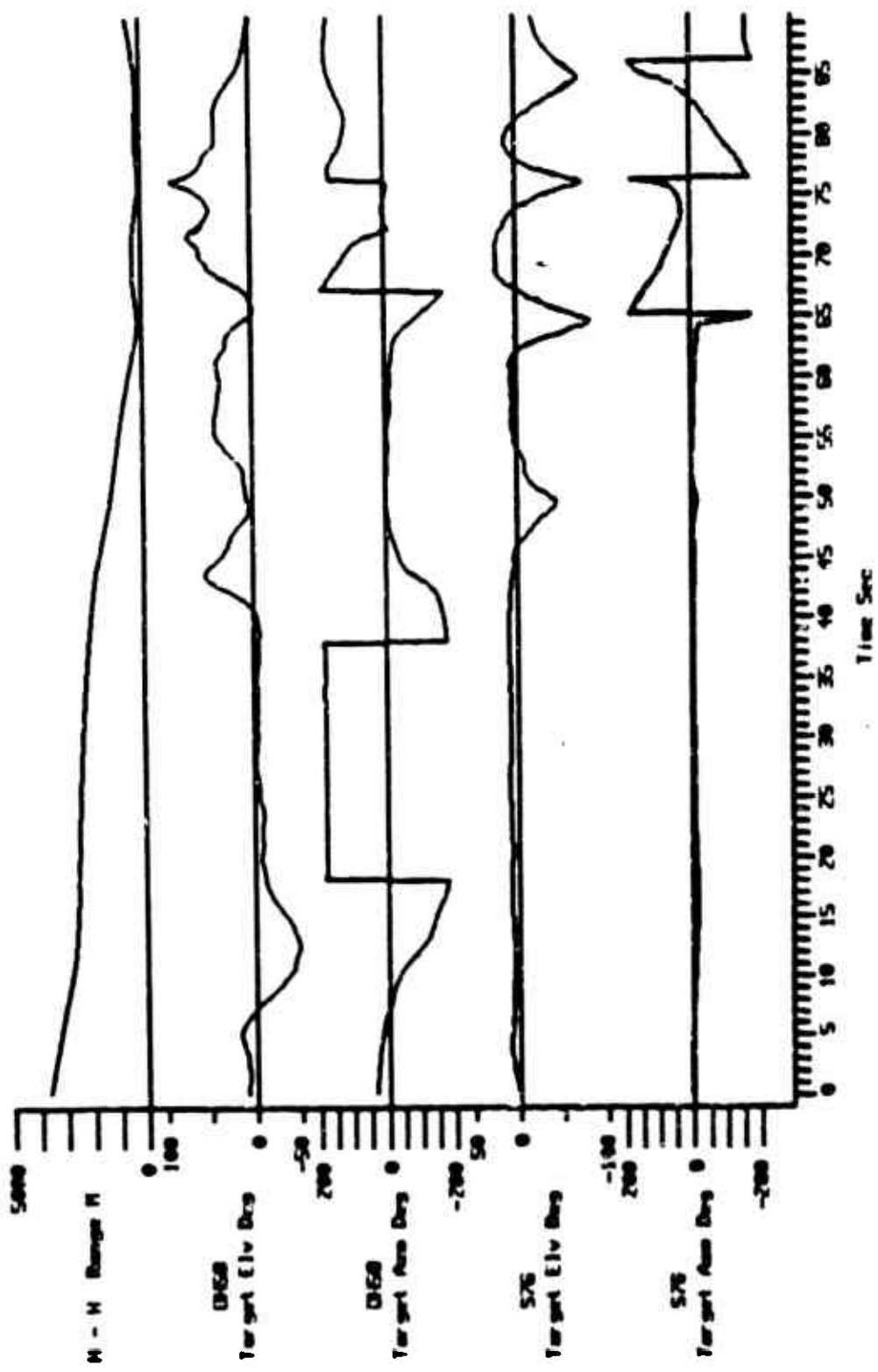


Figure I-18. Time History Data, Counter 23025

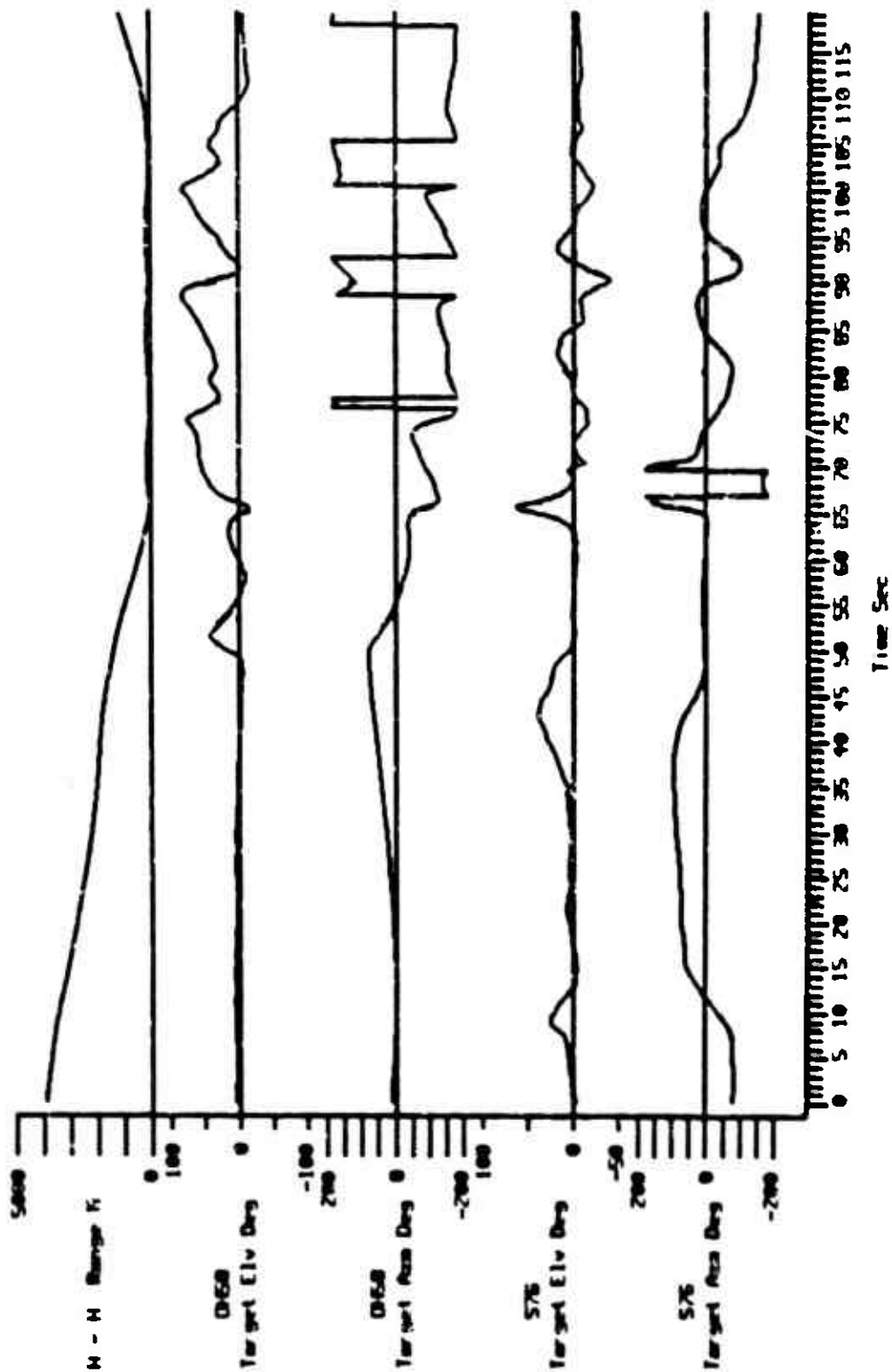


Figure 1-19. Time History Data, Counter 23026

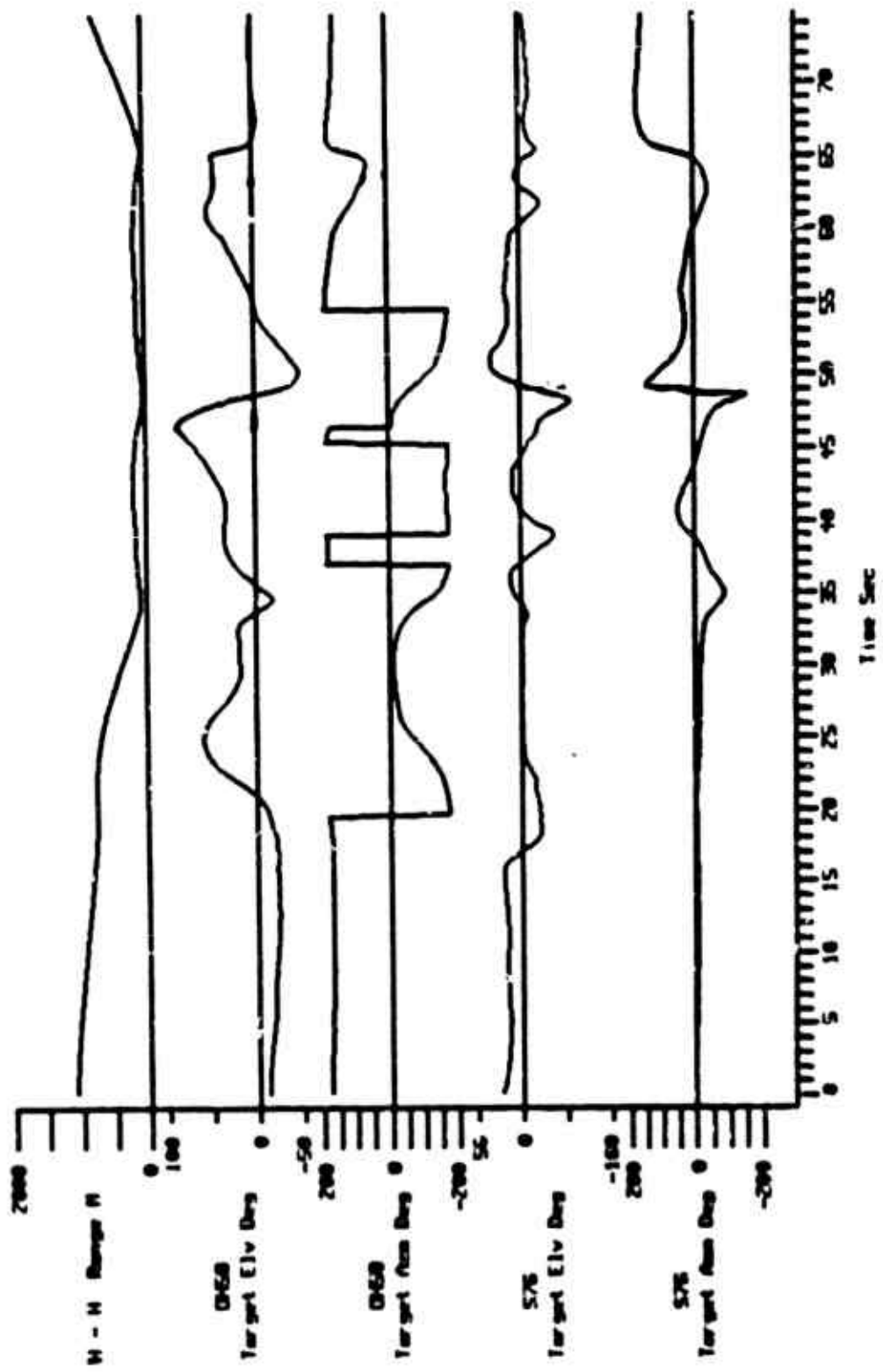


Figure 1-20. Time History Data, Counter 23032

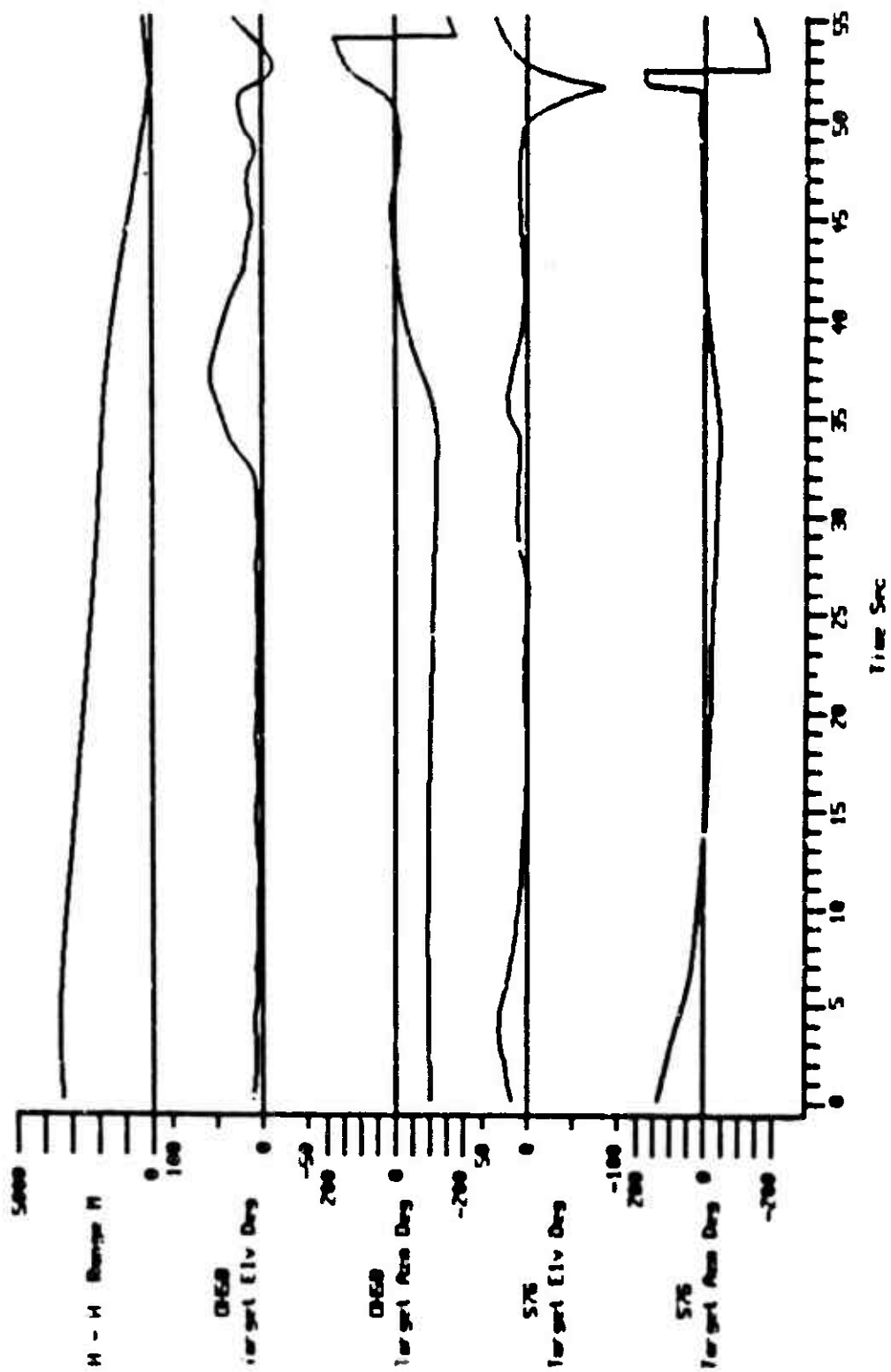


Figure I-21. Time History Data, Counter 23034

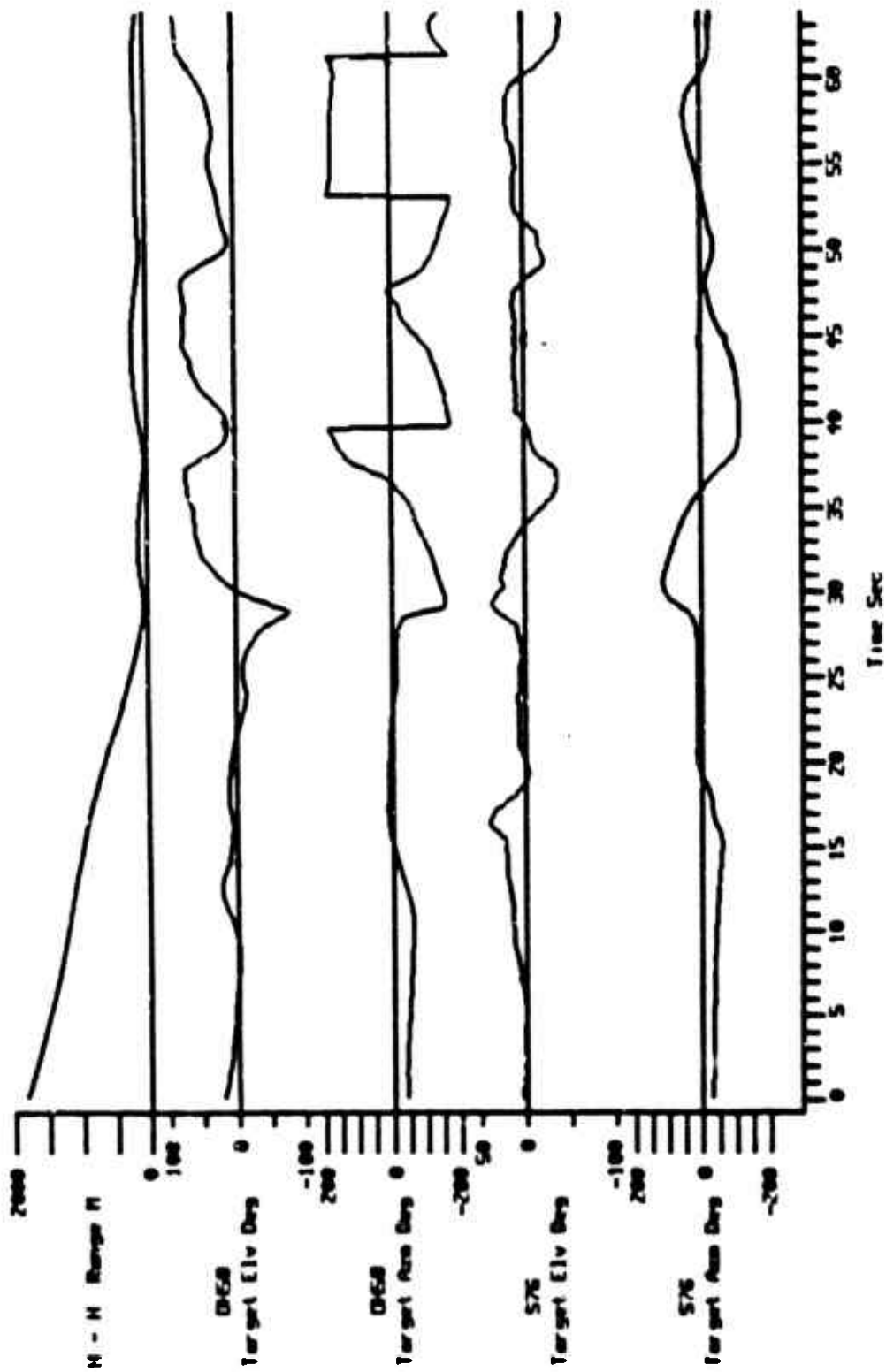


Figure 1-22. Time History Data, Counter 23035

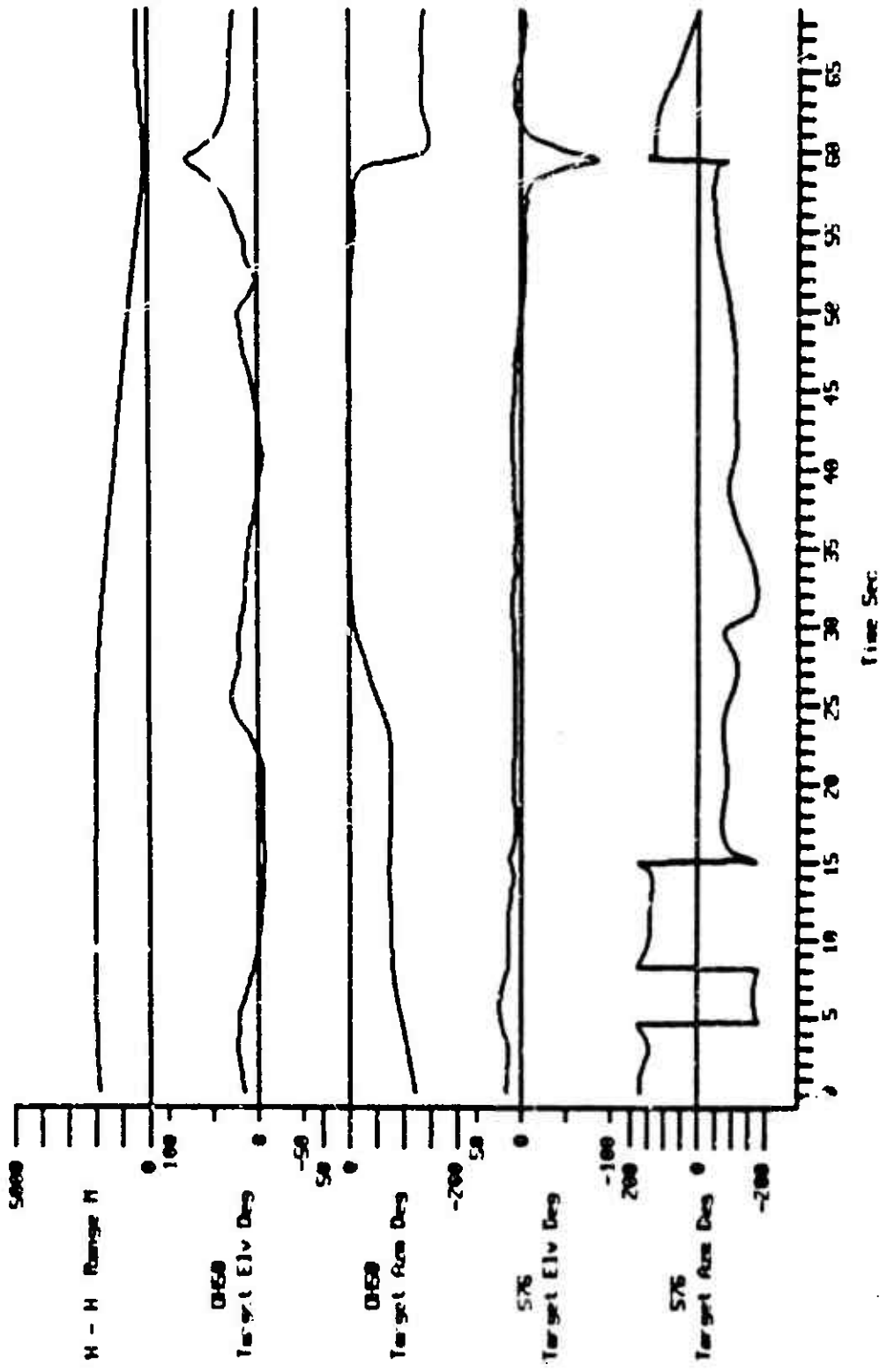


Figure I-23. Time History Data, Counter 23037

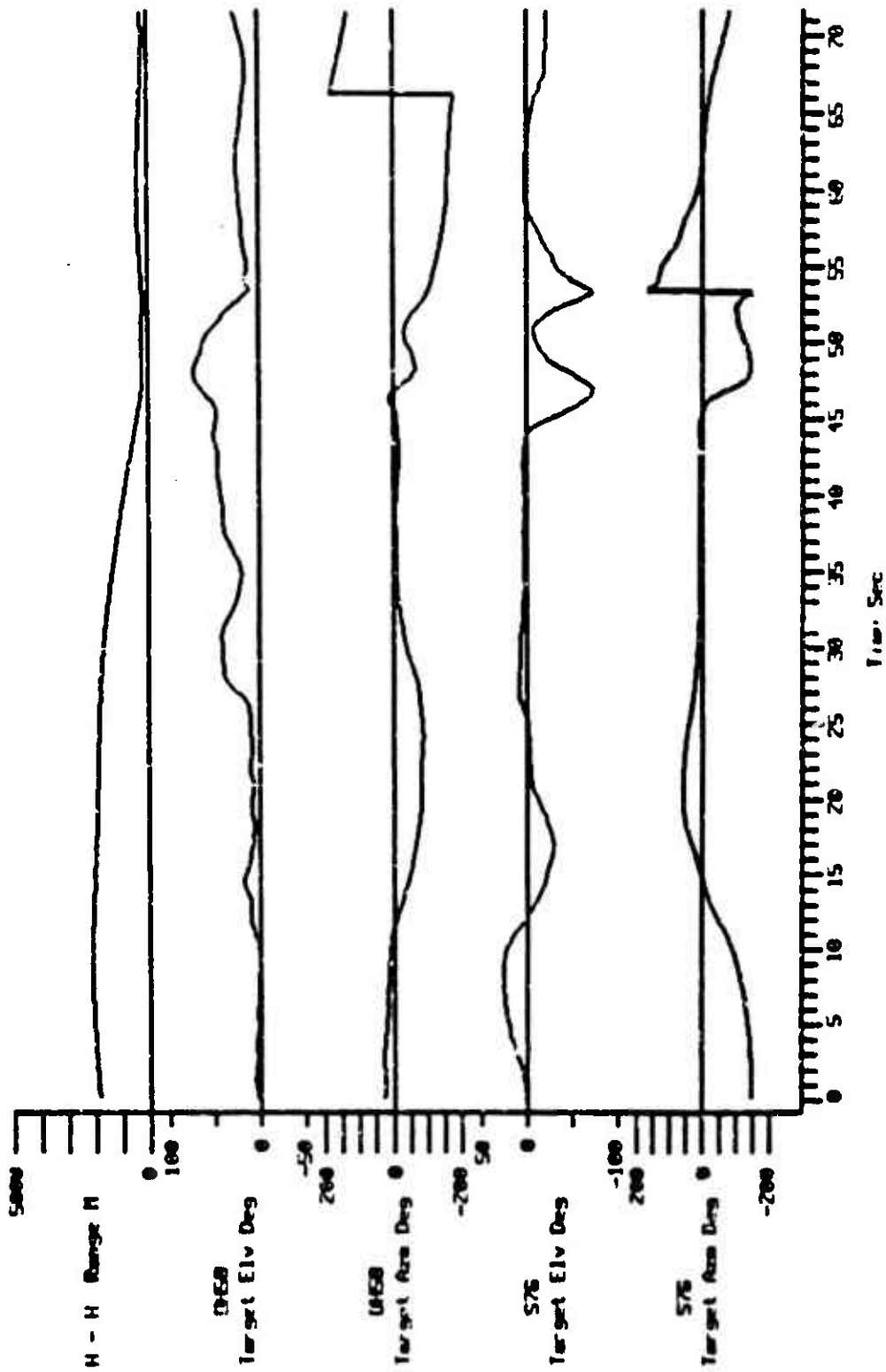


Figure I-24. Time History Data, Counter 23038

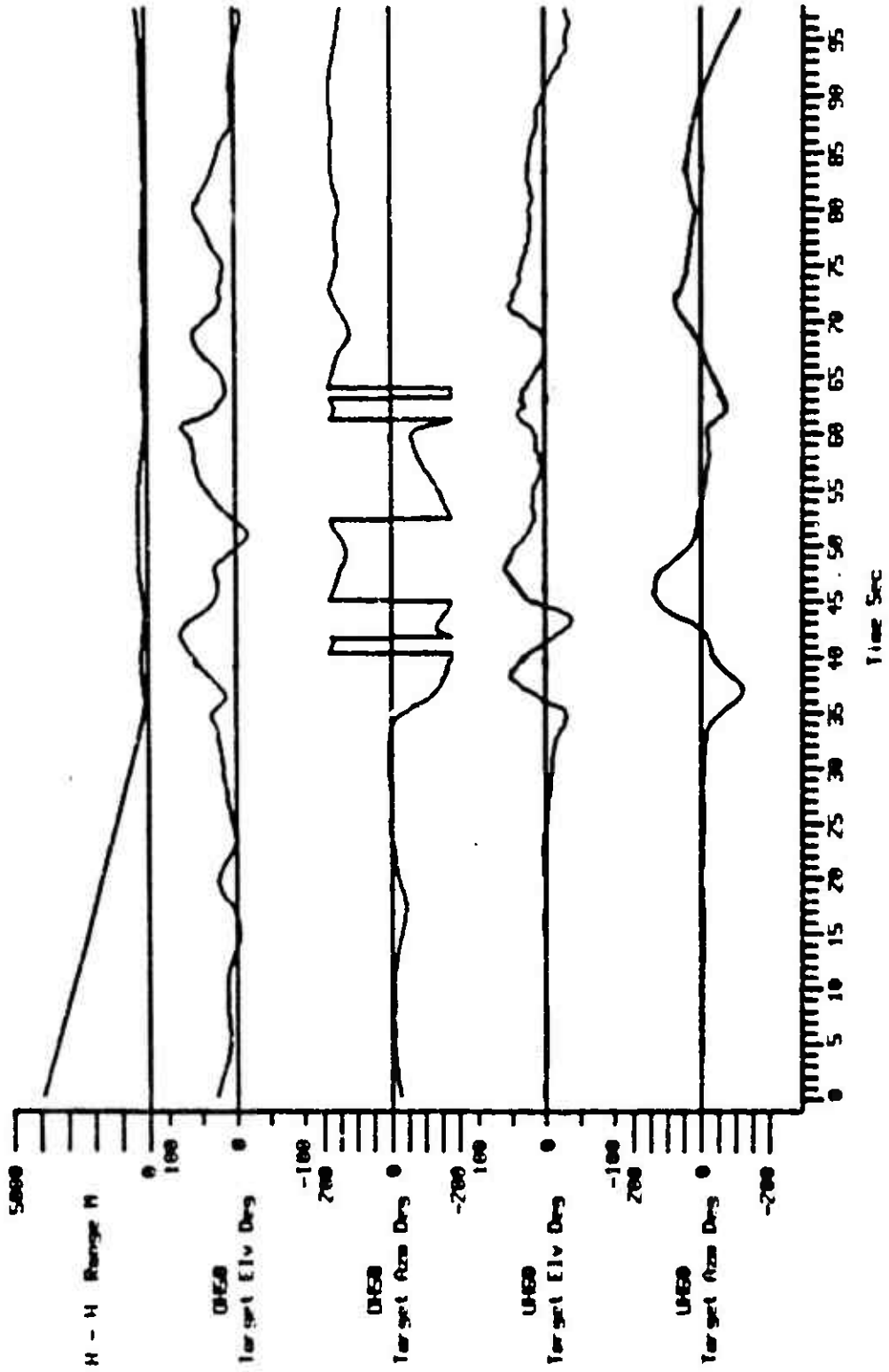


Figure I-25. Time History Data, Counter 27026

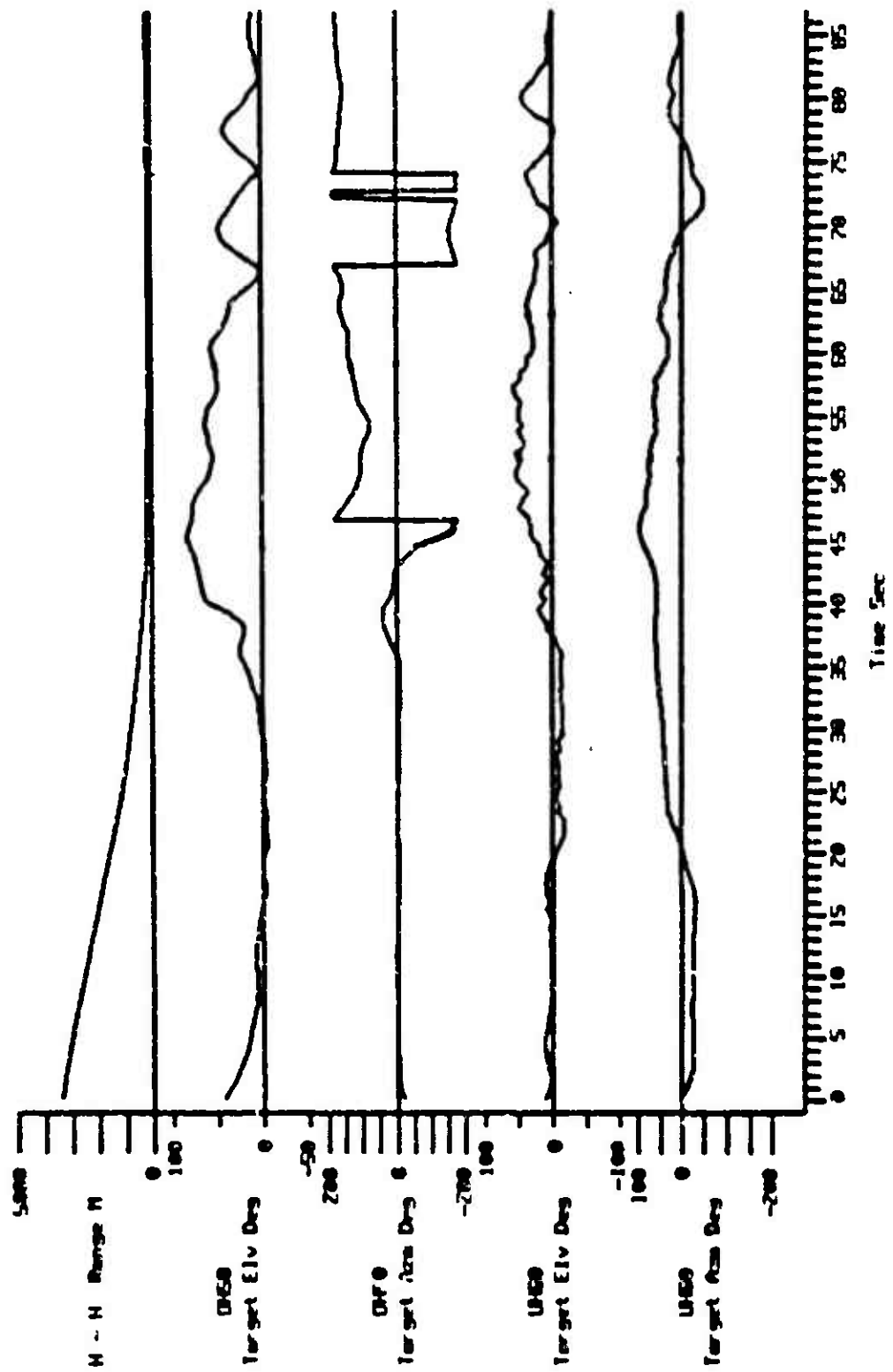


Figure I-26. Time History Data, Course 27027

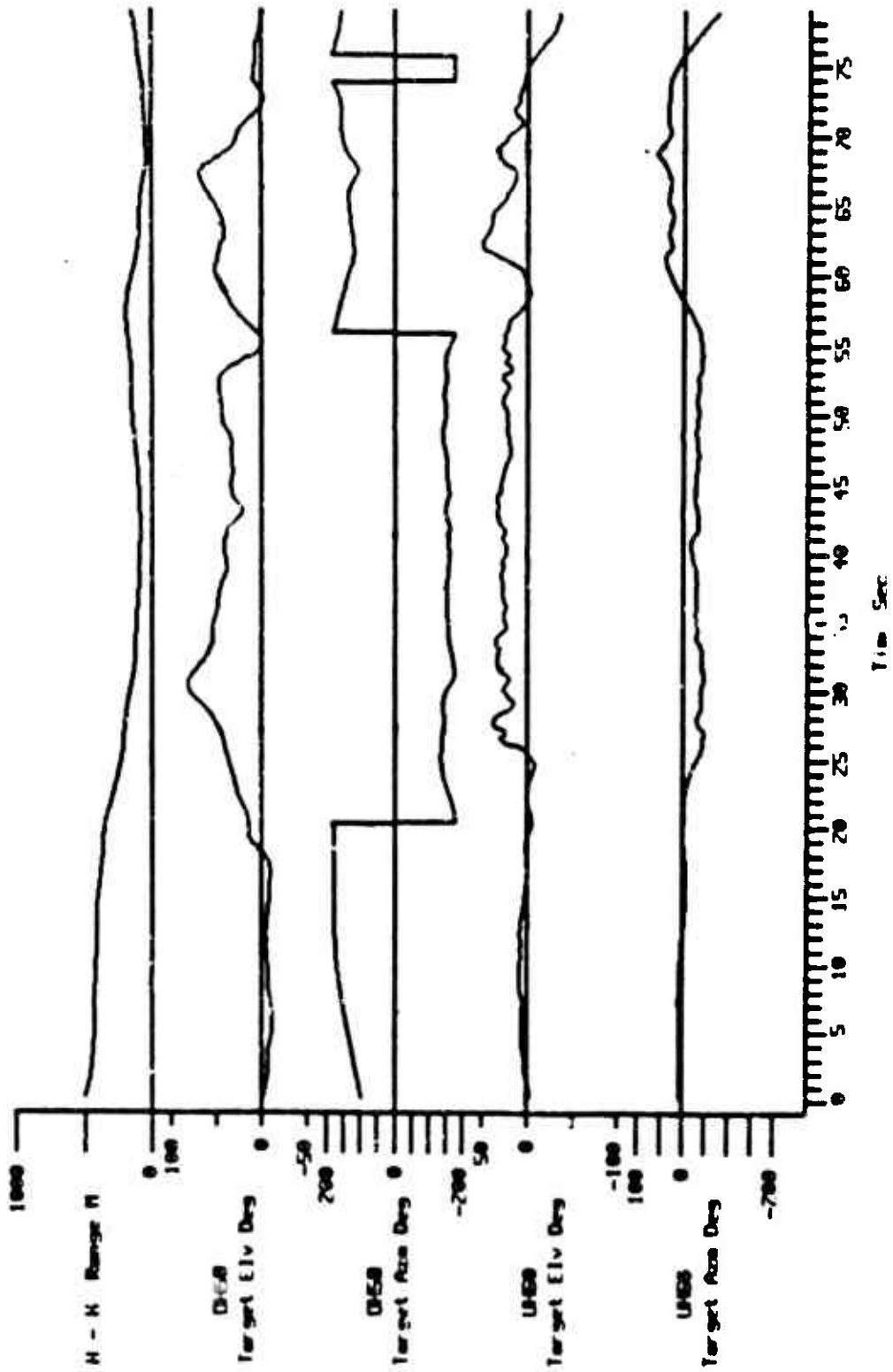


Figure 1-27. Time History Data, Course 27029

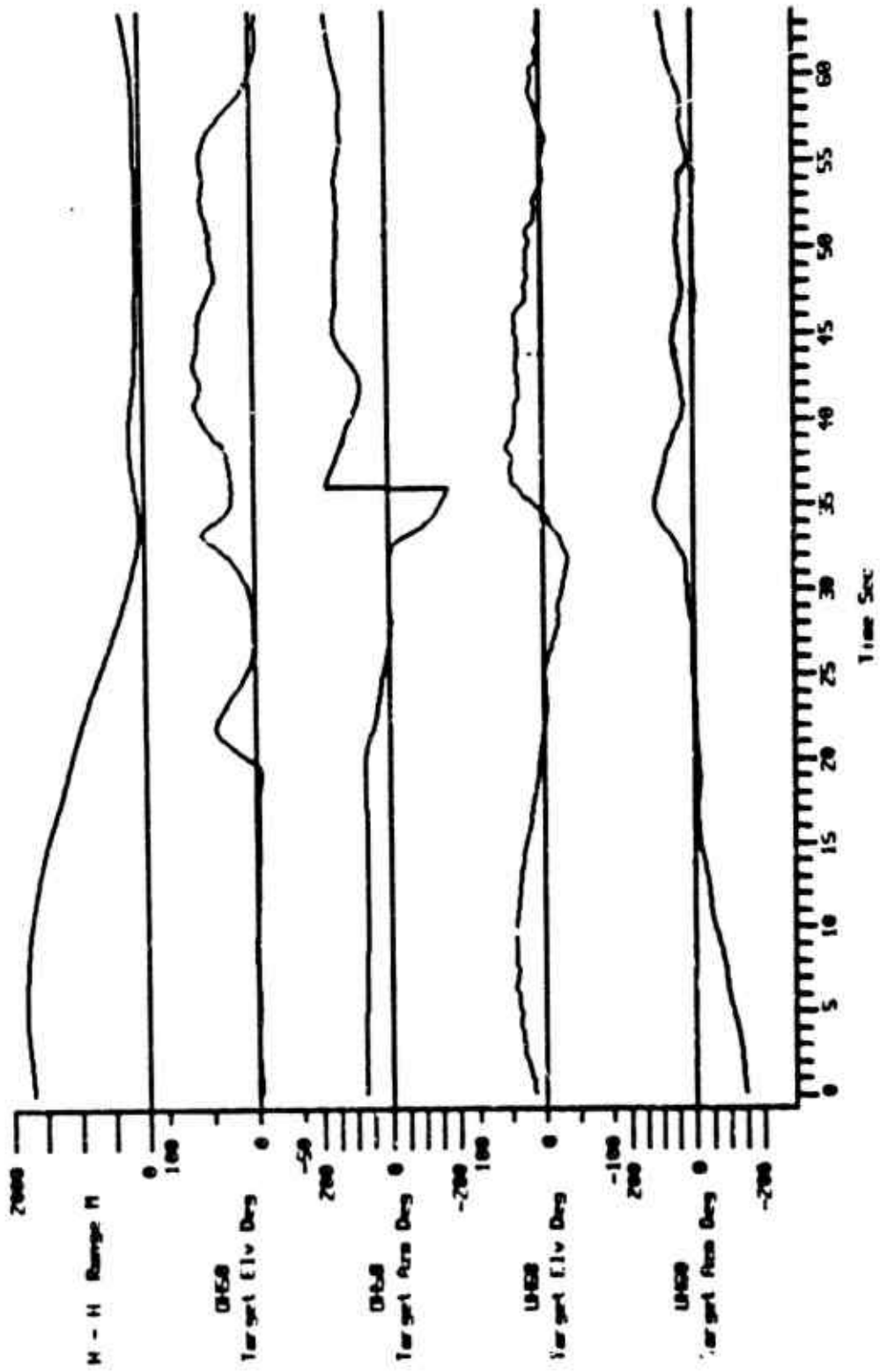


Figure I-28. Time History Data, Course 27031

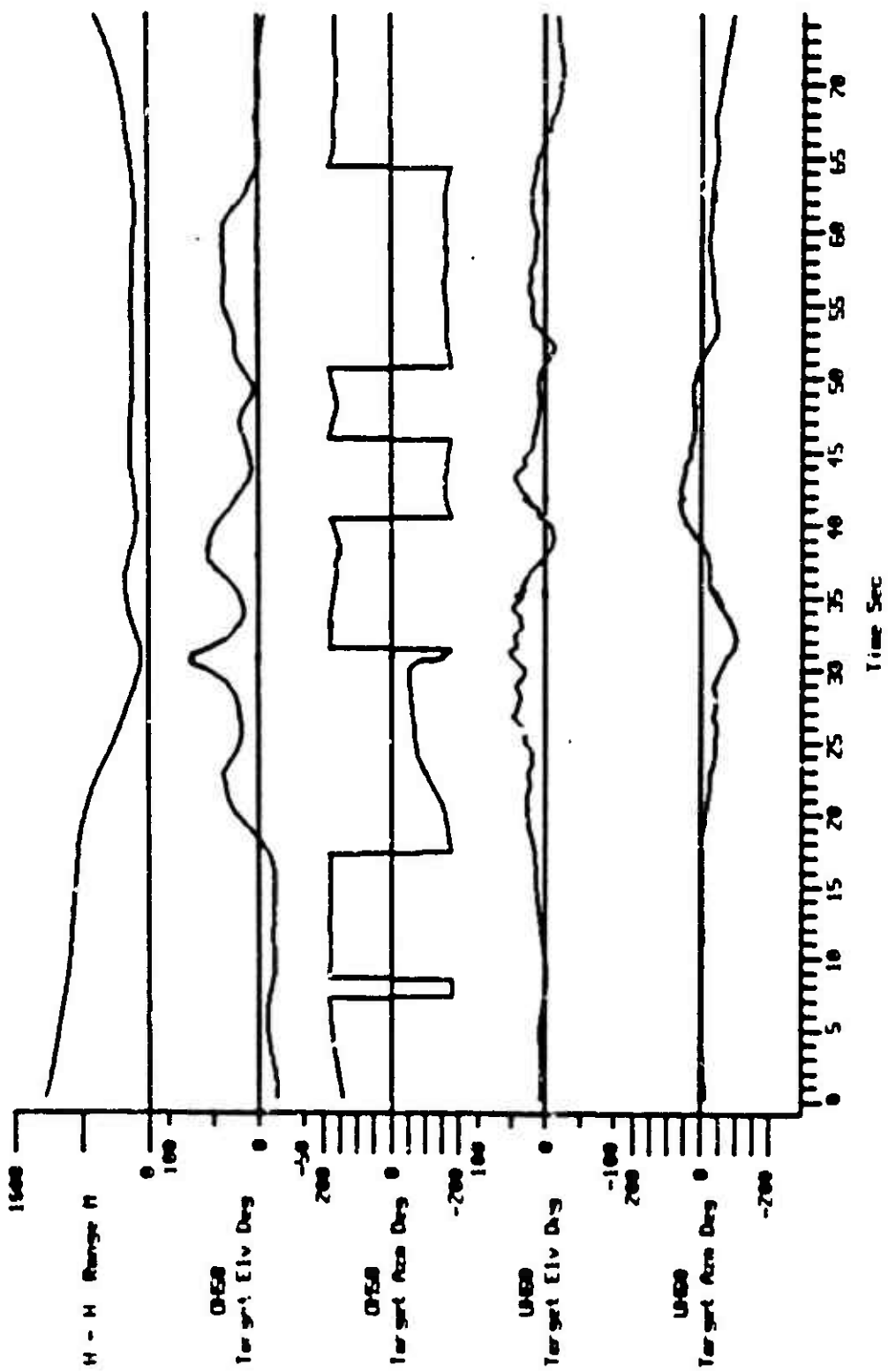


Figure I-29. Time History Data, Course 2703A

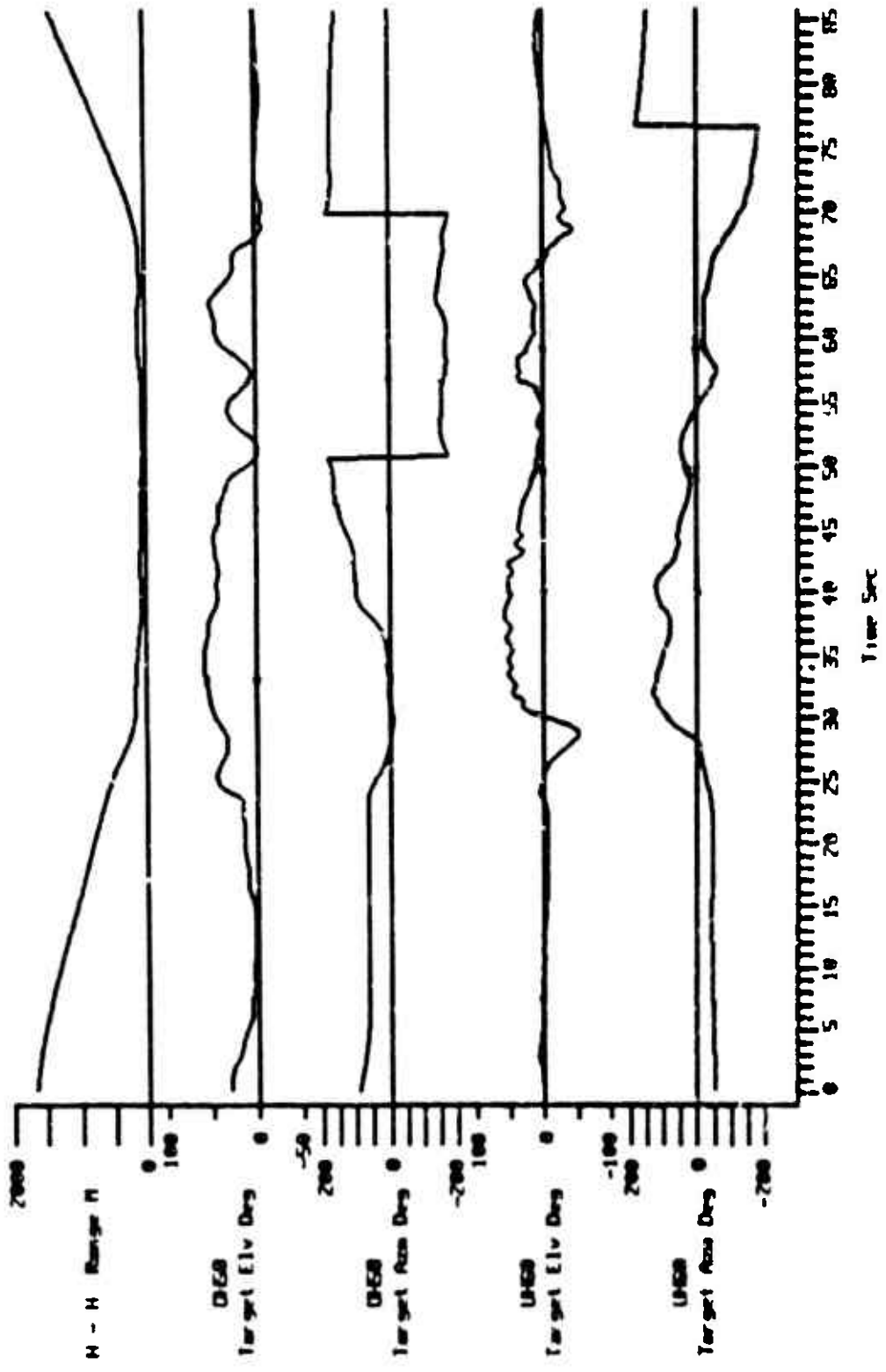


Figure I-30. Time History Data, Course 27036

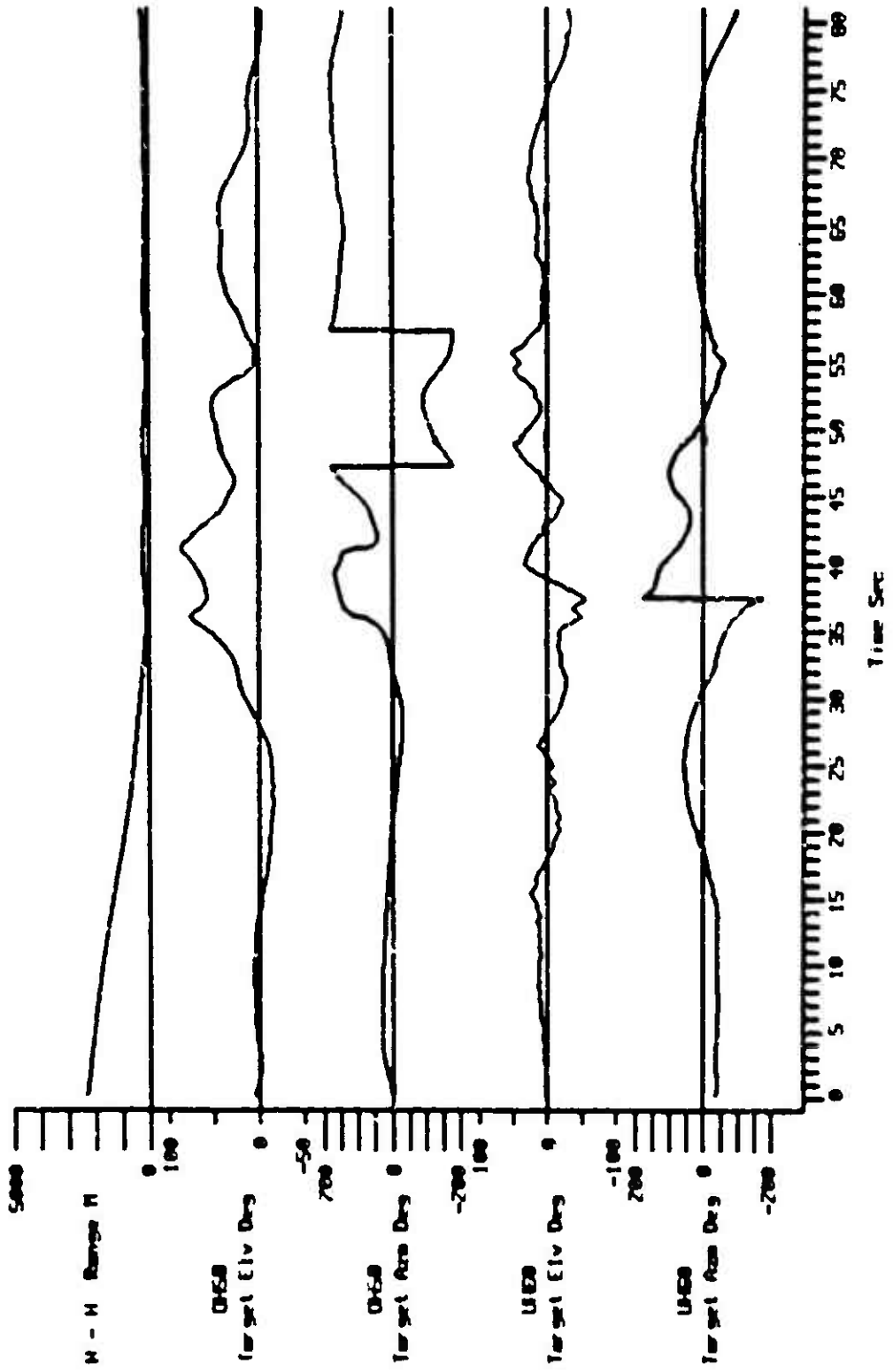


Figure I-31. Time History Data, Counter 27037

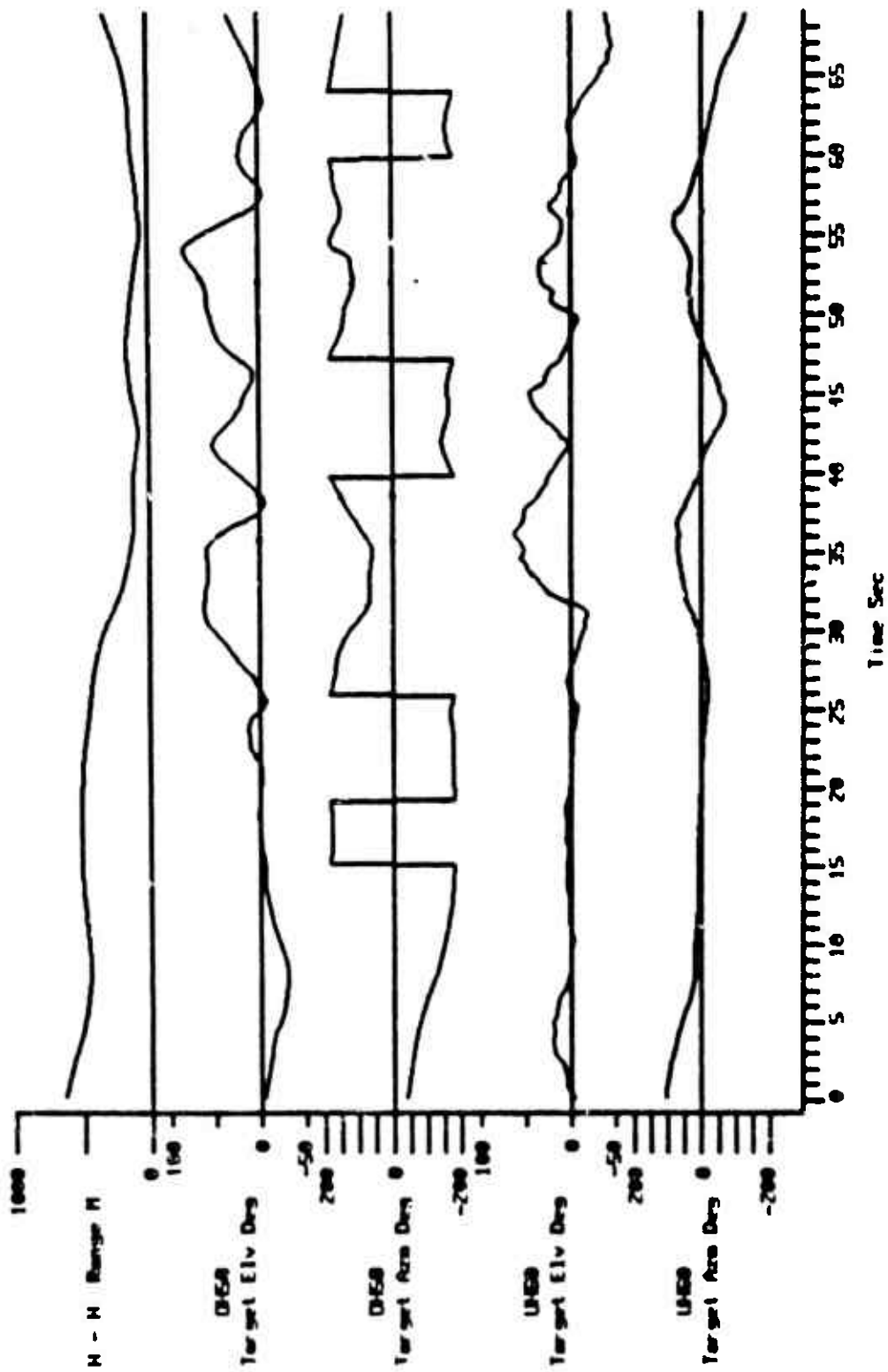


Figure I-32. Time History Data, Counter 27038

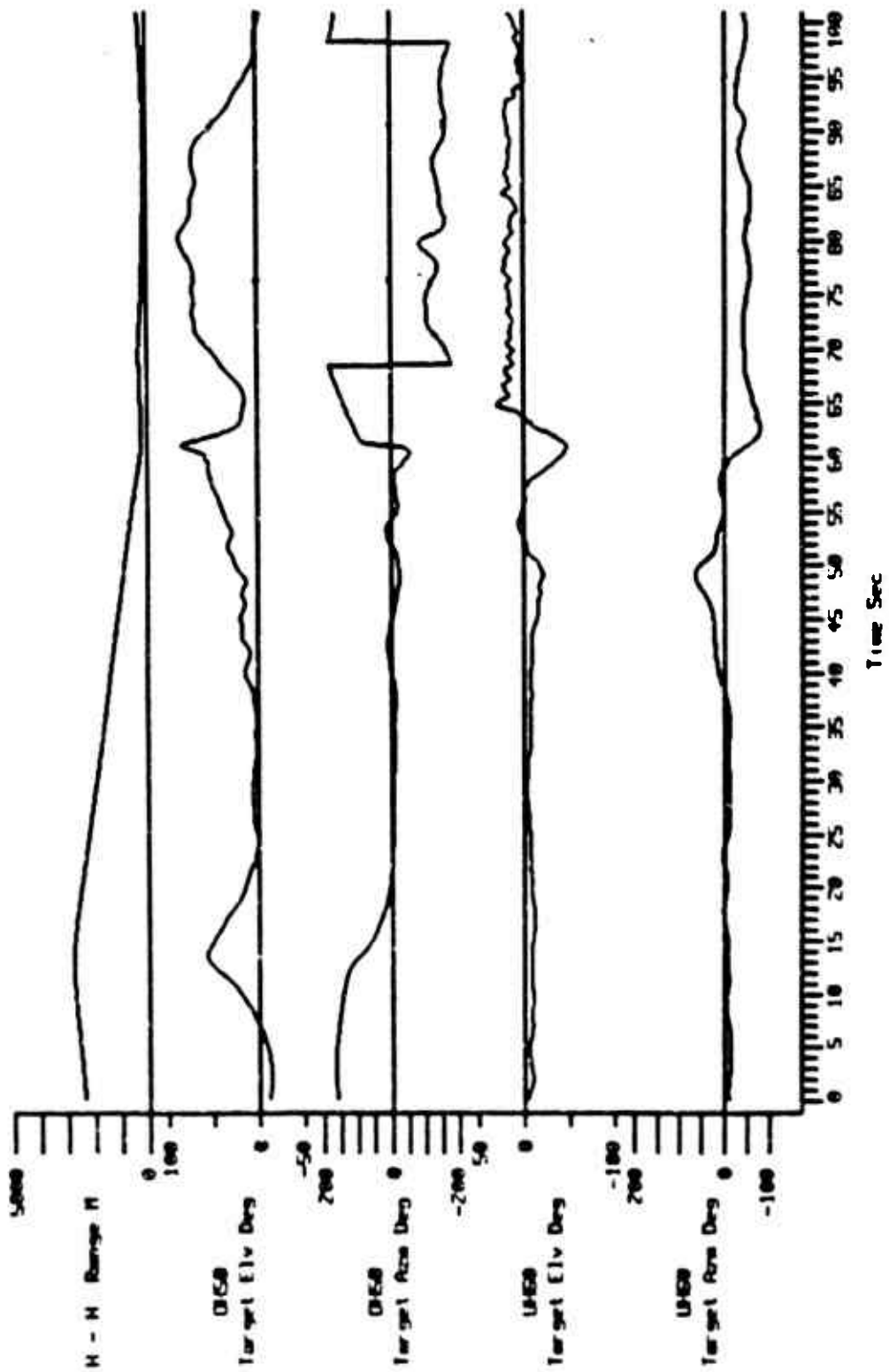


Figure I-33. Time History Data, Counter 27041

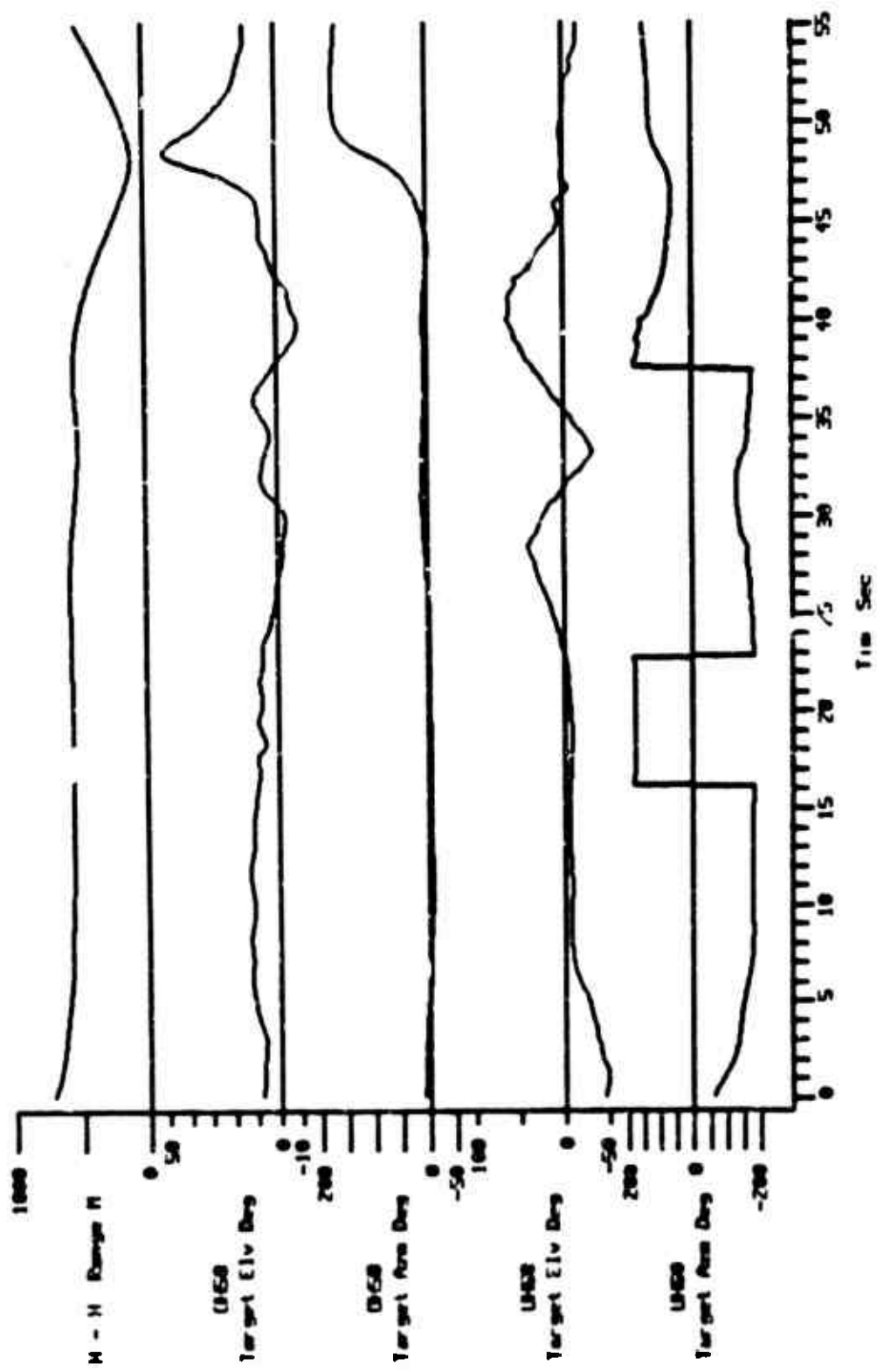


Figure I-34. Time History Data, Counter 27043

APPENDIX J

AACT MANEUVER ANALYSES

This appendix contains a summary of all the AACT encounters that were analyzed. They are arranged by counter number and are in the same order as Table 6. The initial conditions for each of the encounters are summarized in Table J-1.

COUNTERS 208018 - 208028
S-76 Vs UH-60A

208018

The S-76 performs a right yaw maneuver of 242 degrees in 6 seconds from a left banked initial condition. Although the S-76 did not achieve a 3-degree firing window, this flight sequence is an interesting one because of the high performance maneuver being executed.

208019

The 3-degree firing opportunity of the S-76 was achieved during the closure or set up of initial conditions of the flight sequence and not during the maneuvering. The maneuvering portion of the scenario was basically a tail chase with the UH-60A acquiring the 3-degree firing opportunity by performing a pedal turn at low airspeed.

208020

This scenario involves both helicopters making opposite spiral turns at different altitudes that produce differences in altitudes of from 400 to 700 feet. This delta altitude between the two helicopters may be the main reason why there are no significant firing windows.

208021

The S-76 performs a couple of highly banked high rate turns and holds the tail position of the UH-60A for the majority of the flight sequence.

208024

This scenario involved a tail chase with the UH-60A slowing down near the end of the flight sequence, executing a high rate turn and achieving the 4.8 degree resultant firing opportunity.

208025

There is essentially no maneuvering in this flight sequence and the 3-degree firing window opportunity by the S-76 is accomplished during the initial closure of the two helicopters.

208026

After the initial fly-by of the two helicopters, the S-76 never maneuvers while the UH-60A turns and achieves the 3-degree firing opportunity.

208027

The two helicopters perform a series of S-turns with the UH-60A developing two good firing opportunities. One of the firing opportunities is 3 degrees but for only one time step. The other 3-degree firing opportunity of the UH-60A was during the closures of the two helicopters for set up of the initial conditions.

208028

After the initial fly-by, the UH-60A slows to 14 kts and executes a 190-degree high rate turn in .7 second to develop an excellent firing opportunity on the S-76. Although no 3-degree firing windows are achieved, seven time steps with 3.4 degrees in azimuth and elevation combined are achieved.

COUNTERS 302013 - 302021
AH-1S Ve OH-58A

302013

This scenario consists of a sequence of several tail chases that are separated by S-turn maneuvers. The AH-1S maintains the greatest percentage of time on the tail position of the OH-58A.

302014

In this flight sequence the two helicopters are in a tail chase but the AH-1S maintains an advantage by slowing down and pedal-turning to track the OH-58A and achieving the 3-degree firing opportunity.

302015

After the initial pass the OH-58A slows down and performs a pedal-turn to achieve a short firing window on the right side of the AH-1S. The flight sequence ends at these conditions. If the scenario had continued the OH-58A might possibly have obtained a better firing opportunity.

302017

In this scenario the maneuvering consists of a tail chase with the AH-1S achieving the best firing window during the chase. The firing window data recorded for the OH-58A for this flight sequence occurred before the initial pass.

302018

The AH-1S maximum airspeed in this flight sequence is 48 knots and is in a hover for the majority of the scenario. The OH-58A achieves the long 2.9-second 3-degree firing opportunity because the AH-1S is in a hover. The fact that the OH-58A achieves such a successful firing opportunity when the AH-1S remains in a hover makes this flight sequence a good control test, but the data were not used for scoring.

302019

The 3-degree firing window is achieved by the AH-1S immediately after the scenario begins and before any maneuvering occurs, thus it is not a significant window. No other 3-degree firing windows were achieved.

302020

In this scenario the OH-58A is approaching a hovering AH-1S. When the OH-58A passes the AH-1S, the AH-1S executes a series of pedal turns to track the OH-58A. The maximum airspeed of the OH-58A during this scenario is 41 kts.

302021

There are some erroneous instrumentation parameters in this scenario since both helicopters perform impossible attitude and translation maneuver combinations.

AH-64A vs SA-365N

Two sets of engagements are discussed for the AH-64A/SA-365N combination. The first set (counters 417001 to 417012) were the data originally provided by the Army and inadvertently were those with the AH-64A simulating use of a turreted gun. The second set (counters 411009 to 411023) were subsequently provided near the end of the contract and represent the AH-64A using a fixed gun. For completeness, since both sets of data were analyzed, all of the scenarios are discussed below.

COUNTERS 417001 - 417012 AH-64A vs SA-365N (AH-64A in turreted gun mode)

417001

The minimum firing windows listed occur at the very beginning of the scenario before the maneuvering begins. During the maneuvering, the helicopters are 500 feet apart in altitude, which is why there are no good firing windows. The maneuvering flight sequences after the initial fly-by consists of turns and a second fly-by

417003

This flight sequence involves a fly-by and turns by both helicopters. The AH-64A slows down more than the SA-365N and executes a pedal turn to achieve the 3-degree firing window.

417004

After the initial fly-by, the AH-64A slows down and executes a high rate turn to achieve the advantage position behind the SA-365N. The data file ends just when the AH-64A has positioned itself for a possibly good firing window.

417005

In this scenario both helicopters slow down after the initial fly-by. The SA-365N then performs a high rate turn to achieve the 3-degree firing window. The AH-64A for some reason does not pedal turn toward the SA-365N; possibly because it was not within the field of view of the AH-64A or it was simulating use of a turreted gun.

417006

After the initial pass of the two helicopters in this scenario the SA-365N attempts an escape by running away from the AH-64A. The AH-64A follows and achieves the 3-degree firing opportunity on the tail position of the retreating SA-365N.

417008

Beginning at time step 23.5 seconds, the translation data for the SA-365N is erroneous since it tracks the helicopter reversing direction at constant airspeed and heading. The 3-degree firing windows were achieved before the maneuvering began while the SA-365N was approaching a hovering AH-64A.

417009

The SA-365N achieves the 3-degree firing window at the beginning of the flight sequence when, as set up in the initial conditions, the SA-365N is chasing the AH-64A. During the maneuvering segment of the scenario the AH-64A slows down to execute a high rate turn but the SA-365N eludes him by maintaining an altitude advantage.

417012

In this scenario the AH-64A tracks the SA-365N, which is at a higher altitude, by pedal turning. The AH-64A then accelerates to attempt to gain the tail position on the SA-365N. The AH-64A is unable to attain the advantage position but the SA-365N makes a high rate turn and ends up at the tail position of the AH-64A but is too high to achieve a good firing window.

COUNTERS 411009 - 411023

AH-64A Vs SA-365N
(AH-64A in fixed gun mode)

411009

The initial conditions of this scenario position the Apache and Dauphin in a head-on approach along offset parallel paths. After the initial pass, both aircraft turn in on the other and then the SA-365N slows down and pedal turns on the AH-64A. The ensuing maneuvers consist of S-turns where the Dauphin has the advantageous position more often than the Apache, but no firing opportunities are recorded.

411010

In this engagement, the initial conditions are the same as 411009. After the initial pass, the aircraft again turn towards each other. The SA-365N passes 170 feet over the Apache and then the two helicopters diverge without any further encounters.

411011

The AH-64A and SA-365N approach each other head-on as in 411009. Subsequent maneuvering develops into a series of S-turns and pedal turns by both aircraft. The firing window was achieved by the Dauphin after it acquired the Apache with a pedal turn.

411012

Similar initial conditions to 411009 start this engagement, but the AH-64A gains more altitude as the helicopters turn into each other after the initial pass. The Apache slows as the Dauphin passes underneath, and then the AH-64A executes a pedal turn and pursues the SA-365N for a short time until the scenario ends.

411013

After the two helicopters pass each other on offset, parallel courses, they turn in on each other. The AH-64A executes a lower airspeed pedal turn than the SA-365N. The firing windows were achieved as the two helicopters approached each other with the Dauphin achieving its window 2 seconds before the Apache.

411014

Initial conditions are as in the previous engagement where both helicopters perform pedal turns towards each other after the first pass. The Dauphin is quicker in executing its turn while the Apache stops turning before attack position is reached. This suggests the AH-64A may have lost sight of the SA-365N.

411016

This engagement starts with both aircraft on a parallel course in the same direction. They then turn in on each other with the SA-365N gaining an altitude advantage. The scenario then develops into a number of opposite spiral turns by the two helicopters with 200- to 350-foot differences in altitude with the Dauphin maintaining its advantage. This altitude offset prevents any achievement of firing windows.

411017

This encounter starts in the same manner as 411016. Again, the Dauphin gains an altitude advantage during the initial turn-in. By executing a sideslipping turn, the SA-365N gains the tail position on the AH-64A for a significant duration of this sequence.

411022

The two helicopters are initialized with the Apache on the tail of the Dauphin. The AH-64A gains altitude as the Dauphin tries to turn-in on its attacker. The remainder of the encounter is a series of spiral turns and pedal turns with neither aircraft able to get a firing window.

411023

This engagement starts out the opposite of 411022, with the SA-365N on the tail of the AH-64A. The Dauphin gets a firing window as the Apache is broadside to it, attempting to turn-in on the SA-365N. The remainder of the engagement is a series of S-turns by both vehicles.

COUNTERS 23020 - 23038
S-76 Vs OH-58A

23020

Both helicopters achieve their first 3-degree firing windows during the initial head on pass. The helicopters each perform pedal turns to achieve the second set of 3-degree firing windows. The OH-58A is about 1.8 seconds faster in achieving this second firing window than the S-76.

23021

The first 3-degree firing window by the S-76 was during the initial approach of the two helicopters. The maneuvering sequence of the scenario is a series of S-turns which ends in a tight turn tail chase. The last two 3-degree firing windows achieved by the S-76 were due to it slowing down and performing high rate turns.

23025

The S-76 3-degree firing window was achieved during the initial approach of the two helicopters. During the "fights-on" maneuvering, which consists of a series of S-turns, no 3-degree firing windows were scored.

23026

By performing a 100-degree pedal turn, the S-76 gains the tail position on the OH-58A and maintains it throughout the majority of the scenario. The 3-degree firing window of the S-76 is achieved during the initial approach of the flight sequence.

23027

This scenario ends before the two helicopters initially pass each other.

23032

The S-76 achieves the tail position on the OH-58A after the first turn of the maneuvering sequence and maintains the advantage position throughout the scenario. The maneuver that positions the S-76 on the tail of the OH-58A is a 49-degree banked left turn with a 162-degree heading change in 7.9 seconds performed at airspeed as low as 54 knots.

23033

The S-76 performs a high rate turn to gain the tail position of the OH-58A and maintains it throughout the majority of the scenario. The S-76 has a number of firing opportunities that are less than 10 degrees but none that are less than 3 degrees.

23034

The S-76 achieves its 3-degree firing window before the initial pass of the tow helicopters. The data file ends shortly after the first fly-by of the two helicopters.

23035

The 3-degree firing window by the S-76 was achieved before the initial pass of the two helicopters. The maneuvering sequence consisted of a couple of S-turn maneuvers and then the S-76 gains the tail position of the OH-58A for about 13 seconds but is unable to acquire a 3-degree firing window.

23037

In this flight sequence the OH-58A achieves a 3-degree firing opportunity while approaching a hovering S-76. After the initial pass the S-76 turns toward the OH-58A and the flight scenario ends.

23038

This scenario is a little different in that the S-76 achieves a 3-degree firing window while the two helicopters are at different altitudes. The S-76 enjoyed the 695 foot altitude advantage. The 3-degree firing window was achieved by the S-76 performing a 59-knot average airspeed, 200-degree turn in 11.4 seconds to gain the tail position of the OH-58A.

COUNTERS 27026 - 27043
UH-60A Vs OH-58A

27026

The OH-58A achieves the 3-degree firing window before the initial pass. After the first pass the two helicopters make S-turns then the UH-60A out-turns the OH-58A to acquire the tail position of the OH-58A and maintains it throughout the remainder of the scenario, during which time it scores a 2-degree firing window.

27027

The OH-58A scores a 3-degree window during the initial approach of the two helicopters. The maneuvering segment of the scenario is a tail chase with the UH-60A on the tail of the OH-58A throughout the flight sequence. The two 3-degree windows achieved by the UH-60A were during this tail chase segment.

27029

This scenario begins with the UH-60A on the tail position of the OH-58A at a range of 507 meters. The UH-60A maintains the tail position on the OH-58A throughout the flight sequence, scoring two 3-degree firing opportunities. The maneuvering consisted mostly of circling tail chases with a couple of S-turns.

27031

Both helicopters achieve 3-degree firing opportunities before the first pass of the two helicopters. The UH-60A has the best firing opportunities during the spiral tail chases that develop after the initial pass but no 3-degree firing windows are achieved in the maneuvering sequence.

27033

In this scenario the maneuvering segments consist of alternating S-turns and tail chases with the UH-60A achieving the tail position to the OH-58A most often. No 3-degree firing windows are achieved in this flight scenario by either aircraft.

27034

The first of the two 3-degree firing windows of the UH-60A on the OH-58A was achieved before the initial pass of the two helicopters. The remainder of the scenario was a series of tail chases, straight runs, and S-turns with the UH-60A achieving the best firing opportunities. The UH-60A achieves the second 3-degree firing window when the OH-58A performs a reversal while the UH-60A is on the tail of the OH-58A. The OH-58A achieved no firing opportunities.

27035

The initial conditions of this scenario have the OH-58A on the tail position of the UH-60A. A 92-degree left bank by the UH-60A is performed early in the scenario and reverses the position to where the UH-60A achieves the tail position on the OH-58A. However, no 3-degree windows are scored in this flight sequence.

27036

This scenario consists of spiral tail chases separated by an S-turn. The UH-60A acquires the tail position of the OH-58A and holds this position throughout the majority of the flight sequence. The 3-degree firing window was achieved by the UH-60A while on the tail position of the OH-58A which was performing a reversal at the time of the score.

27037

In this scenario the two helicopters perform S-turns after the initial fly-by that results in the UH-60A achieving the tail position on the OH-58A. The 3-degree firing window was acquired by the UH-60A during the last turn before the helicopters broke from their maneuvering sequence.

27038

This scenario begins with the UH-60A in a tail chase on the OH-58A and maintains the advantage position throughout the scenario. The maneuvering sequence consists of a series of S-turns by the OH-58A in an attempt to deny the UH-60A a firing solution. The first 3-degree firing window by the UH-60A was made during the initial approach of the two helicopters while the second one was acquired while the UH-60A was on the tail of the OH-58A.

27041

The UH-60A achieves the 3-degree firing window before the first pass of the two helicopters. The initial pass occurs at the 64-second mark of the scenario. The maneuvering segment of the scenario consists of a spiral tail chase with the UH-60A on the tail position of the OH-58A.

27042

The initial condition of this scenario positions the OH-58A on the tail of the UH-60A, and the OH-58A holds this position throughout the maneuvering sequence as evident by the minimum firing window resultant of 5.2 degrees for the OH-58A versus 87.9 degrees for the UH-60A. No 3-degree firing windows were scored.

27043

The initial conditions of this scenario place the OH-58A on the tail position of the UH-60A. The only maneuvering in this scenario consists of the UH-60A making a turn back toward the OH-58A and the subsequent fly-by. The two 3-degree firing window achieved by OH-58A were before the UH-60A made its turn back toward the OH-58A.

TABLE J-1. AACT ENGAGEMENT INITIAL CONDITIONS

COUNTER	INITIAL CONDITIONS
208018	Abeam level attack, S-76A bogey
208019	Abeam level attack, UH-60A bogey
208020	Abeam climbing attack, S-76A low
208021	Abeam climbing attack, UH-60A low
208024	Head-to-head attack, 80 kts
208025	Head-to-head attack, 120 kts
208026	Head-to-head attack, 120 kts
208027	Abeam level attack, S-76A bogey
208028	Abeam level attack, UH-60A bogey
302013	Head-to-head attack, AH-1S 120 kts, OH-58A 100 kts
302014	Head-to-head attack, 60 kts
302015	Head-to-head attack, AH-1S 120 kts, OH-58A 60 kts
302017	Abeam level attack, AH-1S 120 kts, OH-58A hover
302018	Abeam level attack, AH-1S hover, OH-58A 100 kts
302019	NOE, AH-1S 120 kts, OH-58A hover
302020	NOE, AH-1S hover, OH-58A 100 kts
302021	Tail chase
417001	Head-to-head attack, 120 kts
417003	Head-to-head attack, 120 kts
417004	Head-to-head attack, 120 kts
417005	Head-to-head attack, 120 kts
417006	Head-to-head attack, 120 kts
417009	NOE abeam flyover, AH-64A hover, SA-365N 120 kts

TABLE J-1. AACT ENGAGEMENT INITIAL CONDITIONS (Cont'd)

COUNTER	INITIAL CONDITIONS
417009	Tail chase
417012	NOE abeam flyover, AH-64A hover, SA-355N 120 kts
411009	Head-to-head attack, 120 kts
411010	Head-to-head attack, 120 kts
411011	Head-to-head attack, 120 kts
411012	Head-to-head attack, 120 kts
411013	Head-to-head attack, 120 kts
411014	Head-to-head attack, 120 kts
411016	Side-by-side attack, 120 kts
411017	Side-by-side attack, 120 kts
411022	Tail chase
411023	Tail chase
23020	Head-to-head attack
23021	Head-to-head attack
23025	Aft quarter attack
23026	Abeam climbing attack, S-76A low
23027	Abeam climbing attack, OH-58A low
23032	Tail climbing attack, S-76 low
23033	Tail climbing attack, OH-58A low
23034	Abeam descending attack, S-76A high
23035	Abeam descending attack, OH-58A high
23037	NOE S-76A hover, OH-58A attack
23038	NOE OH-58A hover, S-76A attack

TABLE J-1. AACT ENGAGEMENT INITIAL CONDITIONS (Cont'd)

COUNTER	INITIAL CONDITIONS
27026	Head-to-head
27027	Forward quarter attack
27029	Aft quarter attack, OH-58A bogey
27031	Tail quarter attack, UH-60A bogey
27033	Abeam climbing attack, OH-58A low
27034	Tail climbing attack, UH-60A low
27035	Tail climbing attack, OH-58A low
27036	Abeam descending attack, UH-60A high
27037	Abeam descending attack, OH-58A high
27038	Tail descending attack, UH-60A high
27041	NOE UH-60A hover, OH-58A attacker
27042	Vertical jink in tail chase
27043	Vertical jink in tail chase

APPENDIX K

MI-28 DESIGN ANALYSIS

INTRODUCTION

The Mil Mi-28 (NATO code name HAVOC) is the latest Soviet attack helicopter. It is clearly a new design which embodies the lessons learned in Afghanistan, such as the UH-60A and AH-64A reflect the American experience in Vietnam. In 1989, the HAVOC was shown at the Paris Air Show, both on static display and in flight demonstrations. This represented an unusual circumstance where Western observers had a close-up look at a current, frontline Soviet aircraft. In the spirit of glasnost, viewers were allowed to take photographs and the Soviet delegates were very open in their discussion of the aircraft. The helicopter has been in development since 1980 with its first flight in 1982 and the Paris vehicle was said to be the third developmental aircraft. Evidently, series production had not started at that time.

Since a large amount of information on the Mi-28 was available, it was possible to create a GenHel simulation of the aircraft and include it in the M/A analysis of this report. Because of the uncertainty in some of the data, parametric variations were also conducted. Since the HAVOC is of great interest, a detailed technical description, design analysis and performance evaluation are provided below.

AIRCRAFT DESCRIPTION

The Mi-28 is a large, single-rotor attack helicopter. It follows the conventional plan for such an aircraft in having a relatively narrow fuselage with tandem seating for pilot and navigator/gunner and in utilizing stub wings/stores pylons. Fixed, tail-wheel type landing gear are fitted with a 15 meter/second (49 feet/second) sink speed capability. A detailed three-view drawing is presented in Figure H-1. The main rotor has five blades while the tail rotor uses four blades in a scissored arrangement like the Apache. The cockpit is well armored with a tub of steel/ceramic armor and thick, armored glass. The HAVOC is quite large, as shown in the profile in Figure H-2 comparing the Apache and Mi-28. A large 30mm turreted gun is fitted below the nose. This is a high velocity weapon and appears to be the same as that used on the BMP-2 armored fighting vehicle, SU-25 Frogfoot ground attack aircraft and the new 2S6 mobile anti-aircraft weapon. Ballistically, the Soviet 30mm round is similar to the 30mm round used on the U.S. Air Force A-10 ground attack aircraft. This is significantly more potent than any other attack helicopter weapon, including the low-velocity 30mm chain gun on the AH-64A. Looking at the major components, a descriptive breakdown is as follows:

Main Rotor	Diameter	56.42 feet
	Chord	2.0 feet
	No. of Blades	5
	Hinge Offset	5.5 percent
	Tip Speed	715 fps
	Solidity	0.112
	Twist	-4 degree (spar)
		-10 degree (blade)

Shaft Incidence 5 degree forward
 Delta-3 0 degree
 Rotation Advancing blade on left side

Rotor Head - Well finished hub and spoke titanium head with blade yokes attached via elastomeric, spherical bearings. Conventional hydraulic lag dampers with individual reservoirs. Design similar to Sikorsky elastomeric hub for CH-53D.

Rotor Blades - Filament-wound fiberglass D-spar with composite blade pockets approximately 24 inches wide. Metal grips and conventional feathering bearings. The tip outboard of 98 percent radius has a leading edge sweep of 32 degrees. Since the trailing edge is straight, this generates quarter-chord sweep as well as taper. Modern, cambered airfoils are used.

1311 Rotor

Type	Pusher
Diameter	12.6 feet
Chord	0.792 foot
No. of Blades	4
Hinge Offset	0 (teetering)
Tip Speed	715 fpm (estimated)
Solidity	0.160
Twist	-10 degrees

Rotor Heads - Two teetering hubs, independently mounted with elastomeric snubbers. Little delta-3 noted.

Rotor Blades - Full composite blades with metal grips and conventional feathering bearings.

Fuselage

Length	55.3 feet
Width	18.4 feet (engines) 9.7 feet (basic fuselage)
Height	13.7 feet (to rotor head)
Length Overall	69.4 feet (rotors turning)

Surface Areas:

Wing	32.8 square feet
H. Tail	14.0 square feet
V. Tail	21.9 square feet

Construction - The fuselage is of conventional aluminum semi-monocoque design. The cockpit and other important areas are protected by titanium/ceramic armor plate. Cockpit transparencies are

one-inch thick with the characteristic green tint of Soviet armored glass.

The wing, horizontal tail and vertical tail are of mixed construction. They have aluminum torsion box spars with composite leading and trailing edges. The wing is a stores support with four hardpoints and is attached to the bottom of the engine nacelles. The vertical fin has 36 degrees of leading edge sweep. The horizontal tail is clearly too small, with an area of only 14 square feet. The stabilizer does have limited variable incidence even though it is strut-braced.

Engines

Type Isotov TV3-117 turboshaft
(free power turbine)

Configuration Rear Drive

Ratings

2000 Meters 2200 shp
SLS 2650 shp (T700 lapse rate)

The TV3-117 is assumably a development of the TV2-117 used on the Mi-8 and Mi-24 Hind. If it is flat rated to 2200 shp at 2000 meters (6600 feet) then the sea level rating would have to be about 2650 shp. This is a very significant increase over the 1700 shp of the TV2. The TV3 may be closer to the TV7-117 front drive engine being developed for the civil Mi-38 which has a 3200 shp rating. A rudimentary infrared suppression system is fitted to the engine. This consists of a downward facing exhaust duct that is trifurcated. Inlets on the side of the engine nacelle allow cooling air to flow between these exhaust ducts. This system would work in forward flight, but it would not be very effective in hover.

Weapons

Turreted Gun - The 30mm gun is the 2A42 unit from the BMP-2 armored fighting vehicle. Two rates of fire are available, 300 rpm and 900 rpm.

Ammunition is carried in two 150-round boxes on each side of the gun mount on the turret. Muzzle velocity is estimated to be 3200 fps. Range of turret motion is ± 110 degrees in azimuth -40 and $+13$ degrees in elevation. Turret trunnions and mount ring structure are magnesium.

Wing Stores - Four wet hardpoints are available on the wing, two per side. Pylons are rated at 500 Kg each, even the outboard stations. Typical war load of 16 AT-6 (NATO code name Spiral) anti-tank missiles in two eight-round packs on the outboard pylons and 40 280mm rockets in two 20-round pods on the inboard stations.

Avionics

Extensive MEP for a Soviet aircraft. Paris vehicle was "clearsed" for export. Basic systems include a nose radome for missile guidance and side blisters for IR and TV search and track equipment (but not used for pilotage). Optical weapons sight and laser range finder in double-glazed nose turret above the gun. Avionics turret azimuth range ± 110 degrees to match gun turret. Typical UHF/VHF NAV/COM and IFF equipment. Provisions for radar warning gear and chaff and flare dispensers.

Crashworthiness

Dual stroke landing gear designed to 49 feet-per-second.

Striking pilot seats designed for 17 g's.

Pyrotechnic system activated by impact to tighten shoulder straps, snap cyclic stick forward and open doors.

Bailout Provisions

Unlike Western helicopters, the Mi-28 has extensive bailout provisions. These are manually activated by a D-ring under the seat. On activation, the aft-hinged doors are opened, the entire stub wing assemblies are jettisoned, and bags under the doors are inflated to protect the crew from striking the fuselage.

DESIGN ANALYSIS

The Mi-28 is not merely a skinny fuselage version of the Hind, but clearly a new design. It represents a major step forward in the areas of survivability and sensor systems while maintaining classic Soviet virtues of simplicity and robustness. This design brings the Soviets up to the western standards of the BLACK HAWK and Apache, but is clearly still a generation behind in terms of the Mission Equipment Package (MEP) and low observability. The HAVOC is certainly large and powerful, but the very size which enables it to carry a formidable war load also hinders its maneuverability and agility. The effect of Stinger missiles on the Mi-24s in Afghanistan was obviously traumatic to the attack helicopter community. The HAVOC then is the result of these lessons learned. Looking at the design more closely, we see the following features:

Main rotor - The main rotor is a thoroughly modern design with elastomeric bearings and composite blades. Use of a 5.5-percent hinge-offset shows a clear acknowledgement of the need for increased maneuverability, as does the use of five blades. Rotor airfoils are modern, high camber types assumed to be equivalent to Sikorsky SC1095 in performance.

Tail rotor - The original Mi-28 aircraft were fitted with a three-bladed tail rotor but the Paris Air Show HAVOC had a four-bladed unit. The three-bladed unit would clearly be inadequate based on Sikorsky standards while the four-blade unit is better but still marginal. Adding an extra blade to the tail rotor is difficult since the increased hub moment causes a need to beef-up the gearbox and its attachments. The HAVOC designers have clearly solved this problem by fitting two teetering rotors. This increases the tail rotor effectiveness (by adding an extra blade) while reducing gearbox loads (by using teetering hubs). In addition, the scissoring of the rotors by an extreme 35/145 degrees allows for use of a slightly modified pitch change mechanism while deriving some acoustic benefits like the AH-64A.

Engines - The Isotov TV3-117 are probably upgraded versions of the TV2, but are still rear drive. The large 30mm gun turret, armored cockpit and nose sensors must present a significant center-of-gravity problem in the design. Location of the engines alongside the main gearbox is a good design solution. It separates the engines and improves survivability since it is unlikely one round could disable both engines. (A similar layout is used on the UH-60A and AH-64A). In addition, the aft location helps with the c.g. problem. However, the engines now require 135-degree tail gearboxes to route the power forward to the main gearbox. This adds clutter to the aft end of the gearbox which already has a tail rotor driveshaft. The Soviet designers indicated that they would very much like to have had front-drive turboshaft engines. Infrared (IR) suppression is provided by downward facing exhaust ducts that have external ram air inlets. The outlet is trifurcated to provide mixing. The Soviet delegates indicated that they had looked at both upward and downward facing ducts. U.S. experience is that upward facing ducts bathe the blade roots in hot air and can have a noticeable negative impact on performance. Since the HAVOC system uses ram air, it would not be very effective at low speed. This appears to be a very primitive IR suppression approach compared to the HIRSS of the UH-60A and the "Black Hole" of the AH-64A.

Airframe - The HAVOC airframe is of both conventional design and configuration. The choice of tail-wheel-type landing gear (as opposed to the tricycle gear of the Hind) mirrors the American preference for this configuration for Army aircraft. The Mi-28 was designed to carry an extensive set of sensors in the nose, showing that the Soviets continue to make progress in the MEP area. The 30mm gun is very large and presumably heavy, although some of the structure evidently uses magnesium. While not the first choice of an aircraft designer, the commonality of the 2A42 is certainly desirable. The heavy nose gun, extensive sensor set, and substantial cockpit armor plate must generate a significant forward center-of-gravity problem. Aft mounting of the engines

clearly improves this condition, but is very clumsy with rear-drive turbo-shaft. Several other interesting features are evident, like the individual, a/c-hinged doors for the cockpit and the separate tail compartment. This unventilated space, without windows, seems a direct result of Afghanistan experience. It allows downed helicopter crew to be rescued by their comrades. Interestingly, the Hinds were updated (in the D versions and after) to move the tail rotor to the port side of the fin and make it into a tractor while the HAVOC retains a starboard-side pusher configuration. Attempts to make the nose as short as possible has led to the pilot's seat being in very close proximity to the rotor. It is not obvious if this would restrict maneuverability by restricting flapping limits.

The horizontal tail is only about 14 square feet in area and appears to be too small by Sikorsky standards. The Sikorsky S-61 (H-3) of a similar size started with a 20-square-foot tail and was upgraded to a 27-square-foot unit. The Mi-28 designers have probably already encountered this problem. The HAVOC stabilizer has a limited range of incidence travel (± 10 degrees) which appears to be linked to the longitudinal stick and also manually beeped. The first function is used to help trim pitch attitude in forward flight while the second aids in targeting.

PERFORMANCE EVALUATION

A performance evaluation of the Mi-28 was conducted using existing Sikorsky methodology. Where empirical correction factors were needed, those of the UH-60A were employed since the HAVOC is assumed to have a similar technology level. The performance evaluation covered the following areas:

- 1) Estimated power capability of the Isotov TV3-117 engines.
- 2) Estimated weight breakdown based on Sikorsky parametric and information from the Soviets.
- 3) OGE hover gross weight capability for various altitudes/temperatures.
- 4) Effect of ground proximity on hover GW capability.
- 5) Estimates of power required versus airspeed for different gross weights and density altitudes.

While this performance evaluation is certainly not all inclusive, it does give a picture of the HAVOC's capabilities.

Power Available - Power available data are summarized in Table K-1. This shows the total power available (two engines) as a function of pressure altitude and temperature. Three cases are presented. The first assumes the engines are flat rated to 2200 shp at 2000 meters (6562 feet). Using T700 engine lapse rates, calculations show a capability of 2650 shp for sea level standard (SLS)

conditions. This is a very significant growth over the 1700 shp of the TV2-117. Case 2 shows the same data for an engine with a 2200 shp SLS rating. Case 3 is the same as Case 1 except that a 4400 shp main gearbox (MGB) limits has been imposed.

Weight Breakdown - An estimated weight breakdown for the Mi-28 is provided in Table K-2. Two configurations are presented, one for an air-to-ground mission typical of the HAVOC and the other for a hypothetical air-to-air mission. The empty weight of 15,470 pounds is derived from Sikorsky parametric data and agrees with Soviet data. The air-to-ground mission weight of 22,984 pounds includes a warload of 300 rounds of 30mm ammunition, 16 AT-6 SPIRAL missiles and 40 rockets. This was the configuration analyzed for M/A characteristics. An air-to-air configuration with 300 rounds of ammunition, eight AA-8 APHID missiles and a reduced fuel load is estimated to weigh 19,769 pounds.

Hover GW Capability - OGE hover GW data are provided in Table K-3 and plotted in Figures K-1 and K-2. Since power available is a function of both density and temperature, data are shown as a function of pressure altitude and temperature increments over the International Standard Atmosphere (ISA). Two cases are presented, one for 2650 shp engines and one for 2200 shp engines, both constrained by a 4400 shp MGB limit.

With the big engine, SLS OGE hover at 29,272 pounds is possible. This decreases to 27,938 pounds for an ISA +30 degree Celsius day. At 8,000 feet on a standard day, the hover GW capability is still a very significant 25,900 pounds. Obviously, the smaller 2200 shp engines cannot support such high GWs. SLS, the GW is the same since it is MGB limited, but there is a 3,500 pound reduction for ISA +30 at sea level and a 3,200 pound reduction for 8,000 feet on a standard day.

The effect of ground proximity is presented in Table K-4. The same cases are presented as those for the OGE data. A five-foot wheel height increases GW capability by about 21 percent while a two-foot wheel height yields a 28 percent improvement.

Power Required - Power required curves are presented in Figures K-3 to K-6. These show data for a clean aircraft (no external stores) and an air-to-ground configured aircraft, both at gross weight of 20,000 pounds and 24,000 pounds. Two ambient conditions were used, SLS and the Army hot day of 4,000 feet/95 degrees Fahrenheit.

TABLE K-1. MI-28 POWER AVAILABLE SUMMARY

CASE 1: 2 X 2650 SHP Engines

ALTITUDE (ft)	ISA	ISA+10°C	ISA+20	ISA+30
0	5300	5061	4733	4300
2000	4981	4791	4541	4225
4000	4695	4523	4300	4016
6000	4398	4240	4043	3810
8000	4123	3988	3822	3604

CASE 2: 2 X 2200 SHP Engines

ALTITUDE (ft)	ISA	ISA+10	ISA+20	ISA+30
0	4400	4202	3929	3570
2000	4135	3977	3770	3508
4000	3898	3755	3570	3334
6000	3651	3520	3356	3163
8000	3423	3309	3173	2992

CASE 3: 2 X 2650 SHP Engines with 4400 HP MGB Limit

ALTITUDE (ft)	ISA	ISA+10	ISA+20	ISA+30
0	4400	4400	4400	4300
2000	4400	4400	4400	4225
4000	4400	4400	4300	4016
6000	4398	4240	4043	3810
8000	4123	3988	2822	3604

TABLE K-2. Mi-28 WEIGHT BREAKDOWN

ITEM	WEIGHT	
	Air-to-Ground	Air-to-Air
Weight Empty	15,470 pounds	15,470 pounds
Crew	500	500
30mm Gun	300	300
Trapped Fluids	<u>85</u>	<u>85</u>
BASIC WEIGHT	16,355	16,355
Ammunition, 300 rounds	231	231
Missile Racks	575 (16)	288 (8)
Missiles, Anti-tank (AT-6)	1750 (16)	
Missiles, Air-to-air (AA-8)		950 (8)
Rocket Pylons (2)	120	
Rocket Pods (2)	220	
Rockets (40)	<u>1130</u>	<u> </u>
WARLOAD	4026	1469
FUEL	<u>2593 (400 gal.)</u>	<u>1945 (300 gal.)</u>
GROSS WEIGHT	22,984 pounds	19,769 pounds

TABLE K-3. M1-28 OGE HOVER GROSS WEIGHT CAPABILITY

CASE 1: 2 X 2650 SHP Engines. MGB Limit = 4400 SHP

ALTITUDE (ft)	ISA	ISA+10	ISA+20	ISA+30
0	29272	28973	28679	27938
2000	28752	28439	28130	27067
4000	28206	27878	27134	25618
6000	27635	26628	25487	24207
8000	25900	25006	24019	22818

SLS = 29272 [4400 shp, MGB limit]
 2K/70 = 28439 [4400 shp, MGB limit]
 4K/95 = 25933 [4075 shp]

CASE 2: 2 X 2200 SHP Engines. MGB Limit = 4400 SHP

ALTITUDE (ft)	ISA	ISA+10	ISA+20	ISA+30
0	29272	28031	26435	24394
2000	27505	26470	25213	23688
4000	25896	24945	23807	22425
6000	24259	23378	22352	21194
8000	22733	21946	21068	19980

SLS = 29272 [4400 shp]
 2K/70 = 26470 [3977 shp]
 4K/95 = 22712 [3383 shp]

Accessory load = 100 HP

Configuration: Stub Wings with 16 missiles and 2 rocket pods
 Vertical drag = 4.7% GW

TABLE X-4. MI-28 ICE HOVER CROSS WEIGHT CAPABILITY

CASE 1: 2 X 2650 SHP Engines. MGB Limit = 4400 SHP

WHEEL HEIGHT	SLS	2K/70	4K/95
OGE	29,272	28,439	25,933
5 ft	35,428	34,254	31,171
2 ft	37,331	36,053	32,792

CASE 2: 2 X 2200 SHP Engines. MGB Limit = 4400 SHP

WHEEL HEIGHT	SLS	2K/70	4K/95
OGE	29,272	26,470	22,712
5 ft	35,428	32,051	27,566
2 ft	37,331	33,776	29,065

@ 5 ft wheel height, $h_{rotor} = 13.5$ feet, $(GW_{IGE}/GW_{OGE}) = 1.21$

@ 2 ft wheel height, $h_{rotor} = 15.5$ feet, $(GW_{IGE}/GW_{OGE}) = 1.28$

Accessory load = 100 HP

Configuration: Stub Wings with 16 missiles and 2 rocket pods
Vertical drag = 4.7% GW

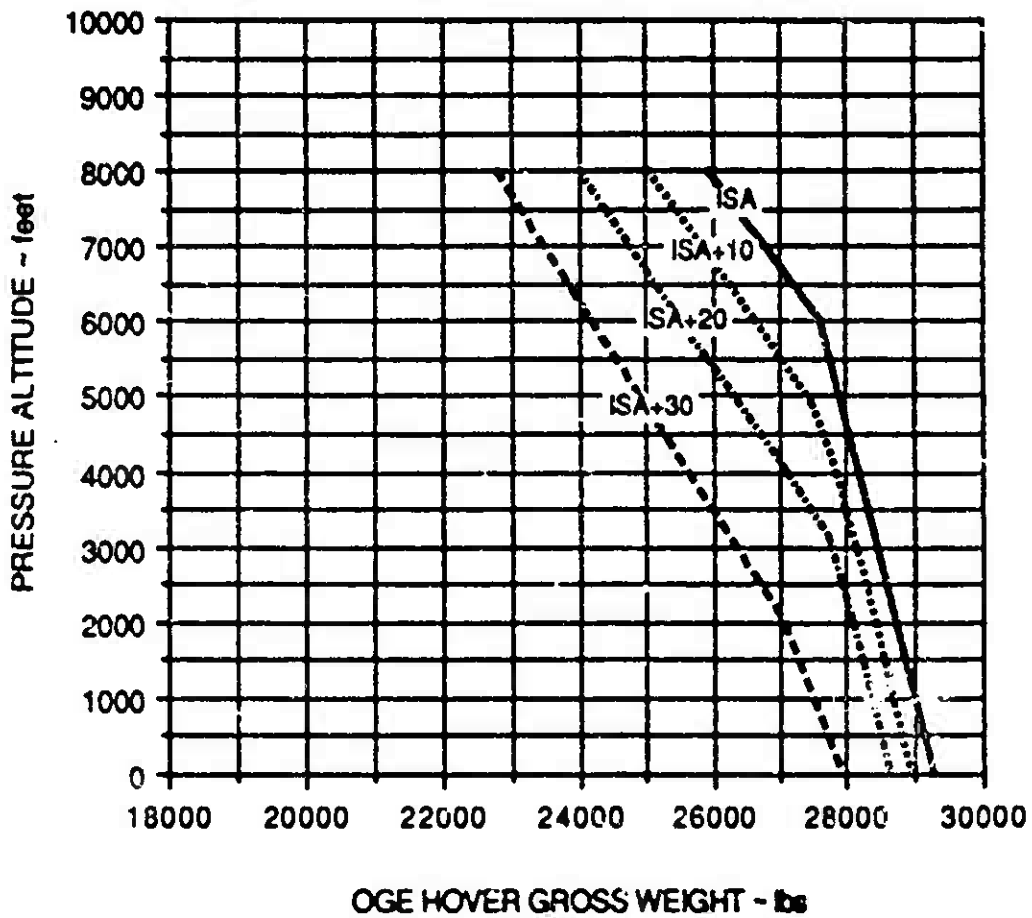


Figure K-1. MI-28 OGE Hover GW Capability with Two 2650-Shp Engines and 4400-Shp MCB Limit

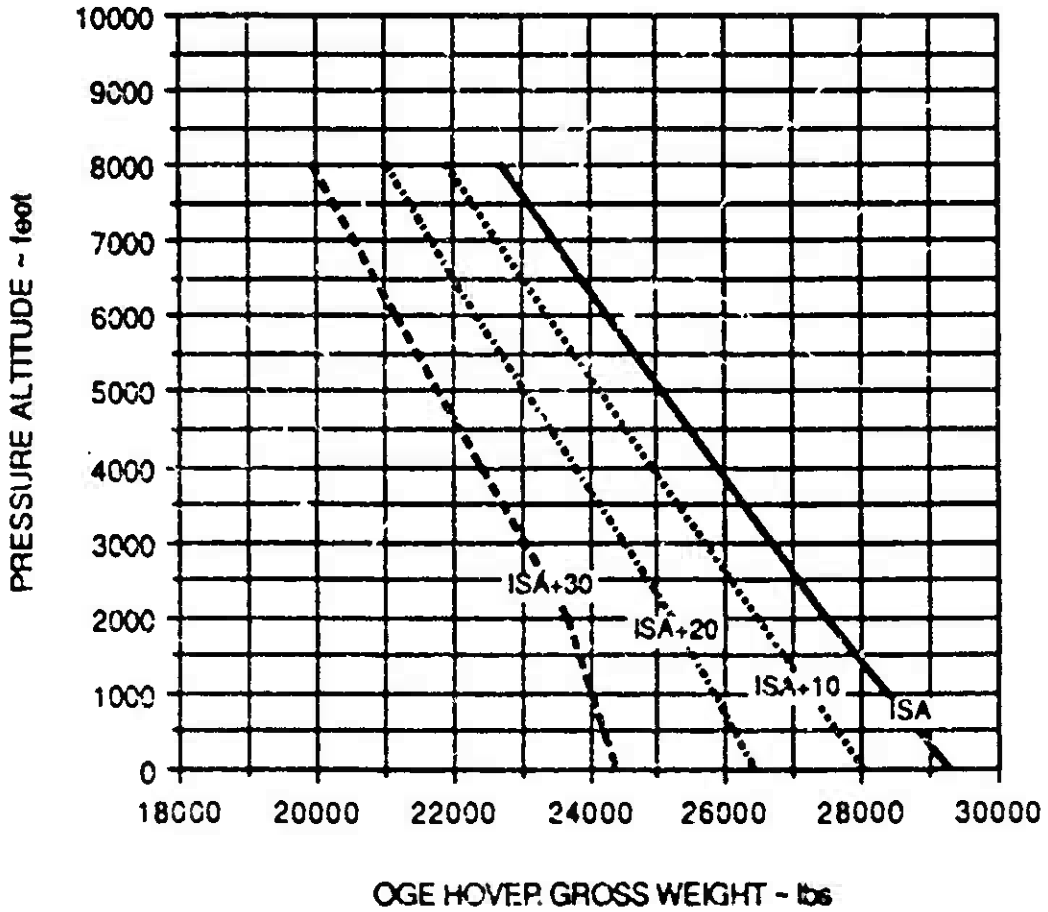


Figure K-2. MI-28 OGE Hover Cd Capability with Two 2200-Shp Engines

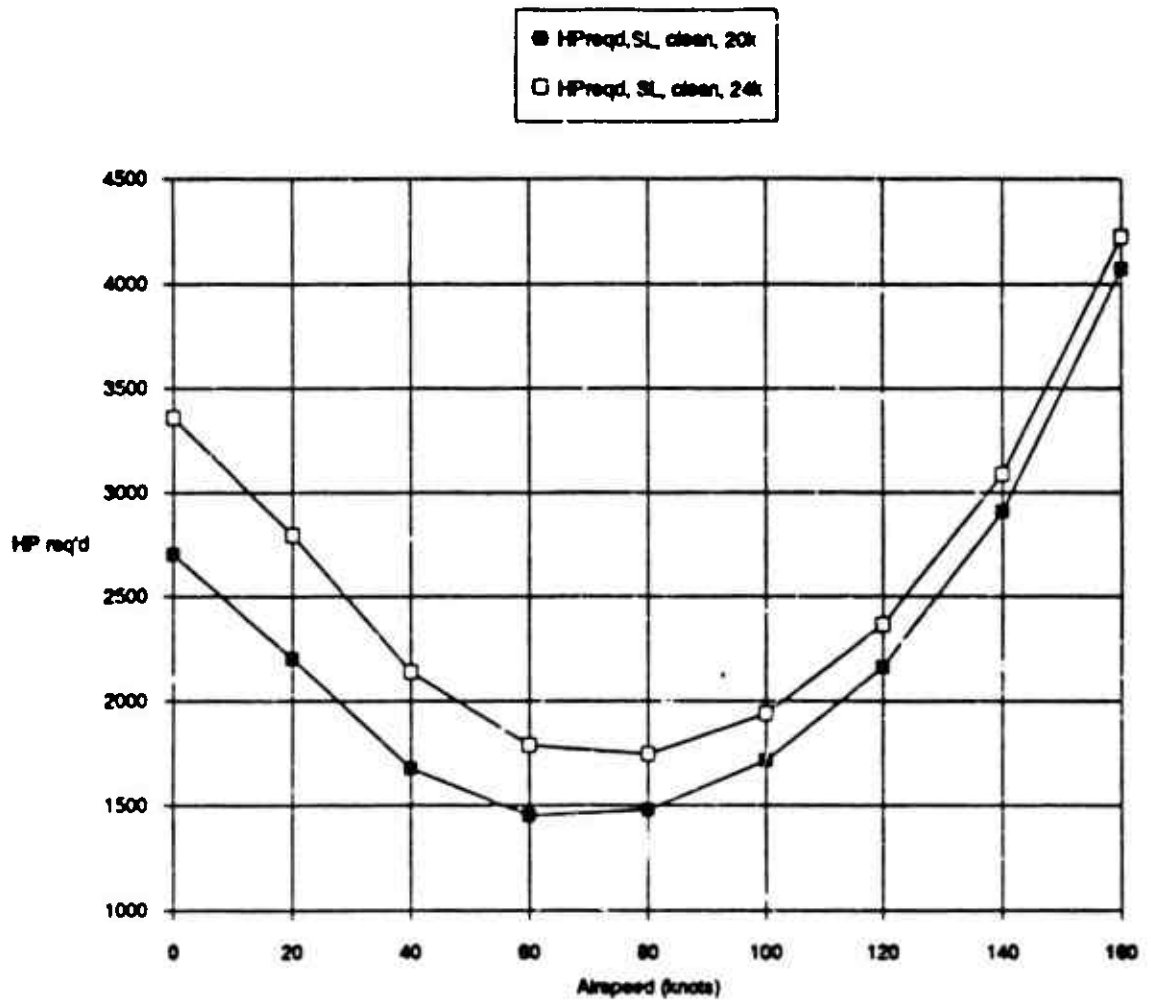


Figure K-3. Mi-28 Power Required, SLS Conditions, Clean

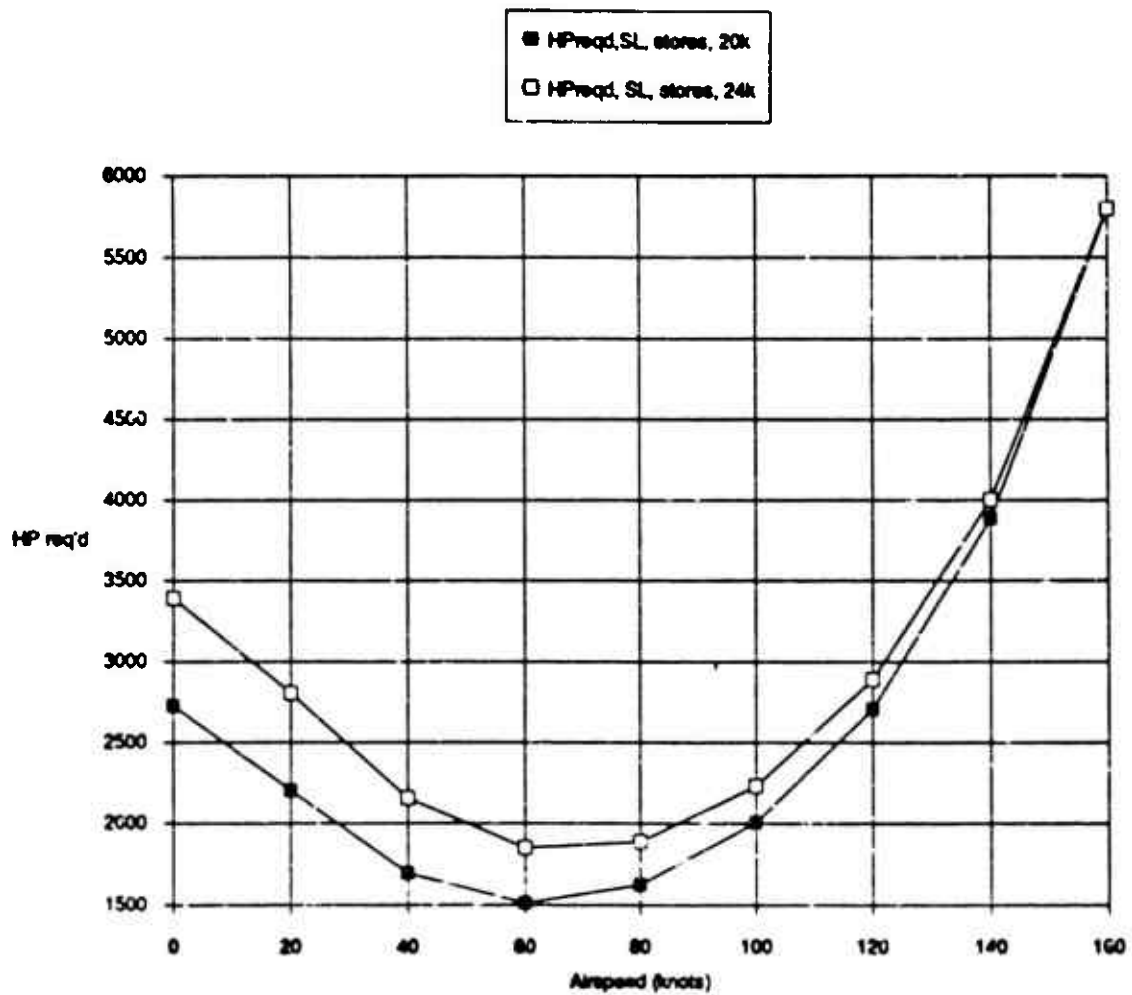


Figure K-4. Mi-28 Power Required, SLS Conditions, with External Stores

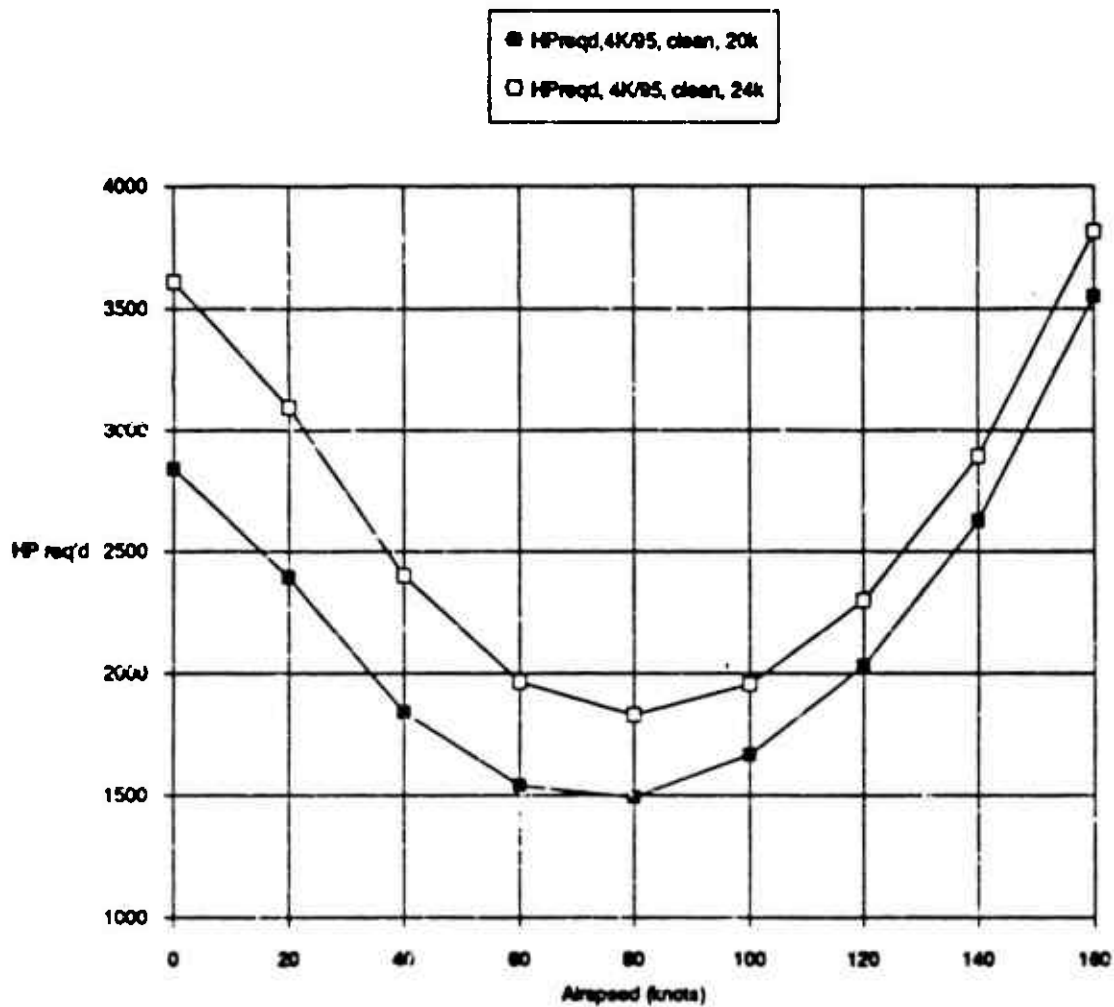


Figure K-5. MI-28 Power Required, 4000-foot/95°F Conditions, Clean

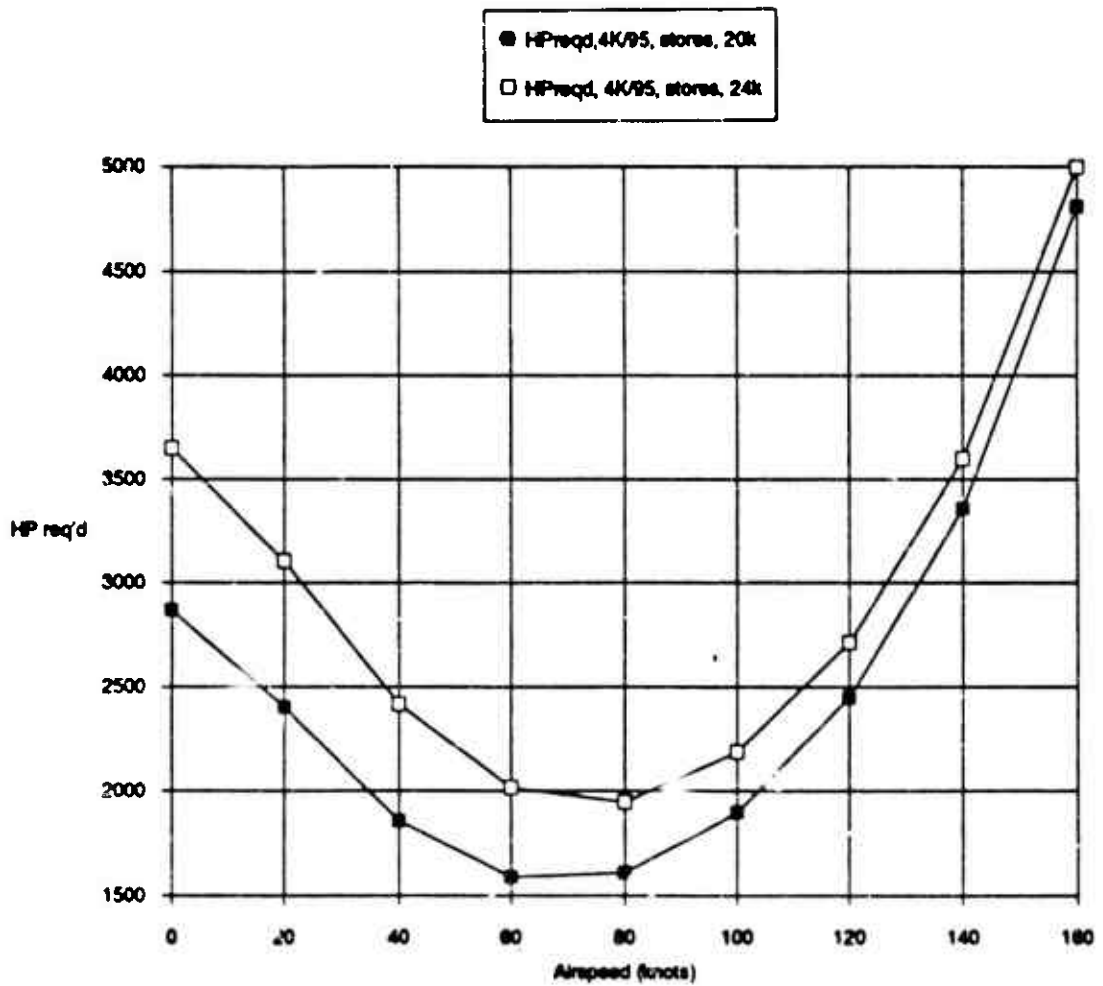


Figure K-6. MI-28 Power Required, 4000-foot/95'V Conditions, with External Stores

APPENDIX L

MATHEMATICAL CURVE FITS TO MANEUVER DATA

INTRODUCTION

This report shows that a M/A rating can be calculated based on the results of running a GenHel simulation model through nine different maneuvers. The maneuver results can be scored and the average score used as the M/A rating. If the maneuver results from a variety of helicopters are plotted against a previously defined fundamental parameter for each maneuver, they tend to cluster along a single line. Any single aircraft/maneuver combination may be off the line, but overall the data trend very well. This suggests that the maneuver results can be predicted by use of mathematical curve fits to the fundamental parameter plots. Obviously, the best method of calculating the maneuver results is to use the GenHel simulation or a math model with equivalent capabilities. This is the only way that the full flight dynamic and the effects of operational limitations can be evaluated. However, in the preliminary design processes, a method of estimating the M/A rating would be valuable for trade-off studies where parameters like gross weight, number of blades, tip speed, solidity, etc., are being evaluated. This appendix describes the results of generating mathematical curve fits to the fundamental parameter plots and of using them to predict the M/A ratings. In addition, the characteristics of the Mi-2E HAVOC at a 20,000-pound gross weight were estimated as an example of this technique.

METHODOLOGY

The basic curve fit approach was to take the fundamental parameter plot for a given maneuver and delete those points that were well off the basic trend. An existing curve fit routine was then used to fit a line through the data. The type of curve fit was based on the shape of the data and on the physics of the maneuver. For example, the steady climb data were fitted to a straight line with no offset at the origin since a zero fundamental parameter meant that all the helicopter's power is required for level flight and none is available for climb. On the other hand, a logarithmic fit was used for the hover turn data. If the helicopter has no residual yaw acceleration capability in hover (a fundamental parameter of zero), then it would take an infinite time to make the hover turn.

The resulting curve fit equations are shown in Figure L-1. Each predicted maneuver result is defined as a function of the fundamental parameter (FP). Most of the mathematical fits were linear or quadratic polynomials. The resulting curve fits are superimposed over the fundamental parameter plots in Figures L-2 to L-10. A brief discussion of each maneuver is given below:

Hover Bob-Up - These data were fit to a second order polynomial as shown in Figure L-2. The curve fit is very good because the data were well collapsed. However, this equation would obviously be erroneous at high I/W values where the negative square term would dominate and show decreasing ROC with increasing thrust capability.

1. Hover Bob-up

$$FP = \text{MAX HOVER THRUST} / \text{GW}$$

$$\text{ROC (fpm)} = -6320 + 8290 (FP) - 1970 (FP)^2$$
2. Acceleration to 80 knots

$$FP = [\text{HP (AVAIL)} - \text{HP (HOV)}] / \text{HP (HOV)}$$

$$T (\text{sec}) = 7.537 - 8.5841 * \text{LOG}_{10} (FP)$$
3. Deceleration 80 knots to Hover

$$FP = \text{HF (HOV)} / \text{GW}$$

$$T (\text{sec}) = -15.715 * \text{LOG}_{10} (FP)$$
4. 80 knot Steady Climb

$$FP = [\text{HP (AVAIL)} - \text{HP (80 TRIM)}] / \text{GW}$$

$$\text{ROC (fpm)} = 29,484 * FP$$
5. 80 knot Steady Turn

$$FP = \text{POWER LOADING} / \text{BLADE LOADING}$$

$$N_z (\text{n.d.}) = 0.955 + 0.8917 (FP)$$
6. 80 knot Decelerating Turn

$$FP = [C_l/\sigma (\text{max}) - C_l/\sigma (80)] / C_l/\sigma (80)$$

$$\text{Psidot (deg/sec)} = 34.649 (FP) - 6.1648 (FP)^2$$
7. 130 knot Decelerating Turn

$$FP = [C_l/\sigma (\text{max}) - C_l/\sigma (130)] / C_l/\sigma (130)$$

$$\text{Psidot (deg/sec)} = 23.21 (FP) - 5.36 (FP)^2$$
8. 140 knot Pull-up

$$FP = [C_l/\sigma (\text{max}) - C_l/\sigma (140)] / C_l/\sigma (140)$$

$$N_z (\text{n.d.}) = 1.0 + 1.2242 (FP)$$
9. Hover Turn

$$FP = \text{delta yaw acceleration}$$

$$T (\text{sec}) = 4.977 - 2.299 \text{ LOG}_{10} (FP)$$

Figure L-1. Empirical Maneuver Prediction Equations

Sea Level Standard Conditions

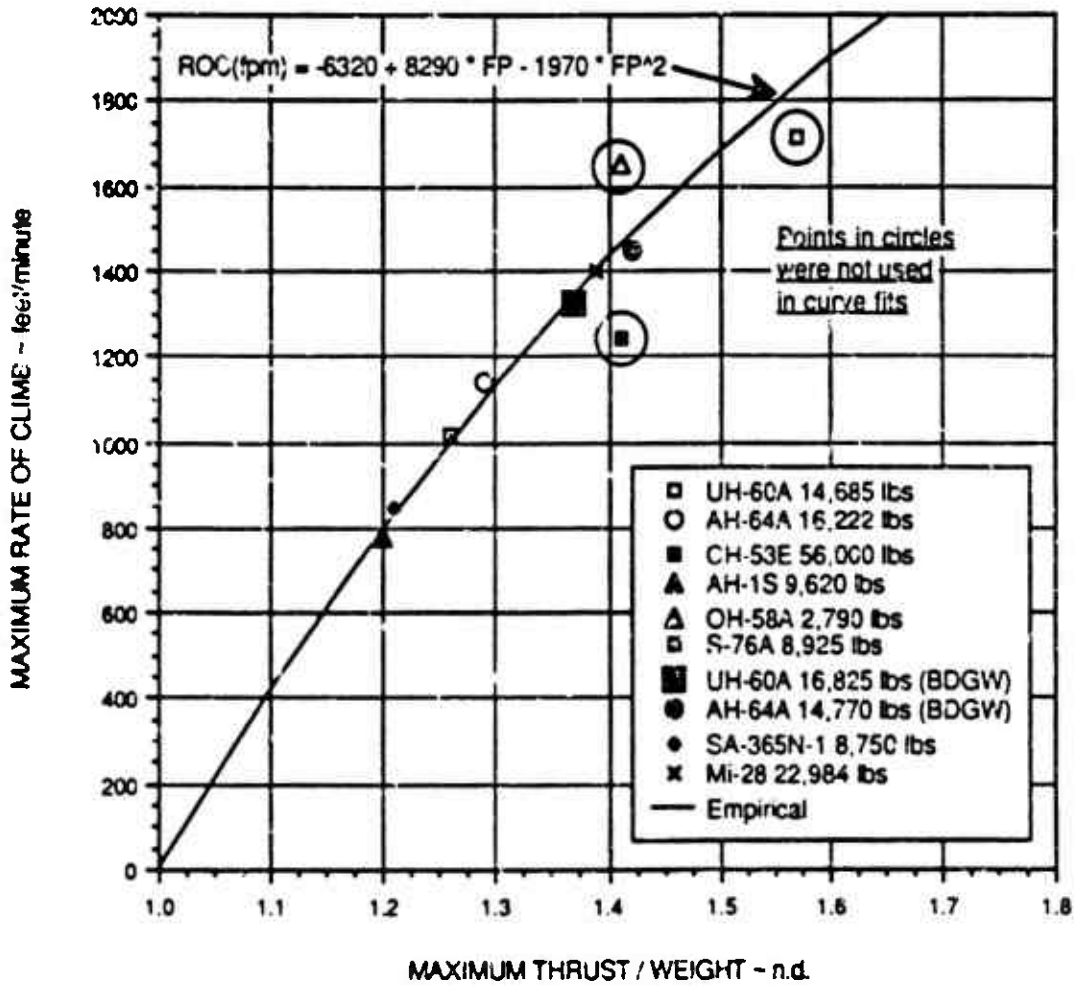


Figure L-2. Empirical Hover Rob-Up Comparison

Acceleration to 80 knots - A logarithmic fit was used for these data as illustrated in Figure L-3. This provided a good fit since the data points were well collapsed.

Deceleration to Hover - Figure L-4 shows the logarithmic fit imposed on the more scattered data of this maneuver. Note that this fit uses a multiplier times the logarithm of the fundamental parameter.

80-Knot Climb - A simple linear fit with zero offset at the origin works well for this maneuver (Figure L-5). This fit was selected because of the simple physics of the climb.

80-Knot Steady Turn - Figure L-6 shows that a linear fit works well to match these data, but some helicopters are well off the basic trend.

80-Knot Decelerating Turn - A second order polynomial was chosen to predict these data and is a good fit as shown in Figure L-7. This polynomial was constrained to have a zero constant term so a zero fundamental parameter (blade loading margin) would result in a zero turn rate. Only the CH-53E and AH-1S are well off this prediction.

130-Knot Decelerating Turn - This maneuver was handled in the same way as the 80-knot case. Different coefficients were required, of course, and the GenHel data were more scattered than the 80-knot maneuver (Figure L-8).

140-Knot Pull-Up - A simple straight line matched these data well as shown in Figure L-9. This line was selected to give a load factor capability of one (level flight) if the fundamental parameter was zero.

Hover Turn - The results for this maneuver (Figure L-10) were perhaps the most difficult to fit because the yaw rate constraint tends to yield constant turn times for high yaw acceleration capabilities. A logarithmic expression was used since it predicts an infinite time to turn if the yaw acceleration capability is zero.

ESTIMATED MANEUVER RESULTS AND NOTES

Once these mathematical curve fits were available, the estimated maneuver results could be calculated for each helicopter. These were then scored (using the previously defined scoring equations in Table 7) and the M/A ratings calculated. The results are shown in Figures L-11 to L-15 as bar graphs comparing the GenHel derived results to the empirical ones.

In general, the empirically derived M/A ratings are similar to ones from GenHel, typically agreeing within five points. There is no obvious trend, with the empirical results sometimes higher and sometimes lower than the GenHel values. Some predictions, however, were significantly in error. For example, the CH-53E empirical NOE rating is 13 points higher than the GenHel value while the OH-58A NOE rating is 10 points higher.

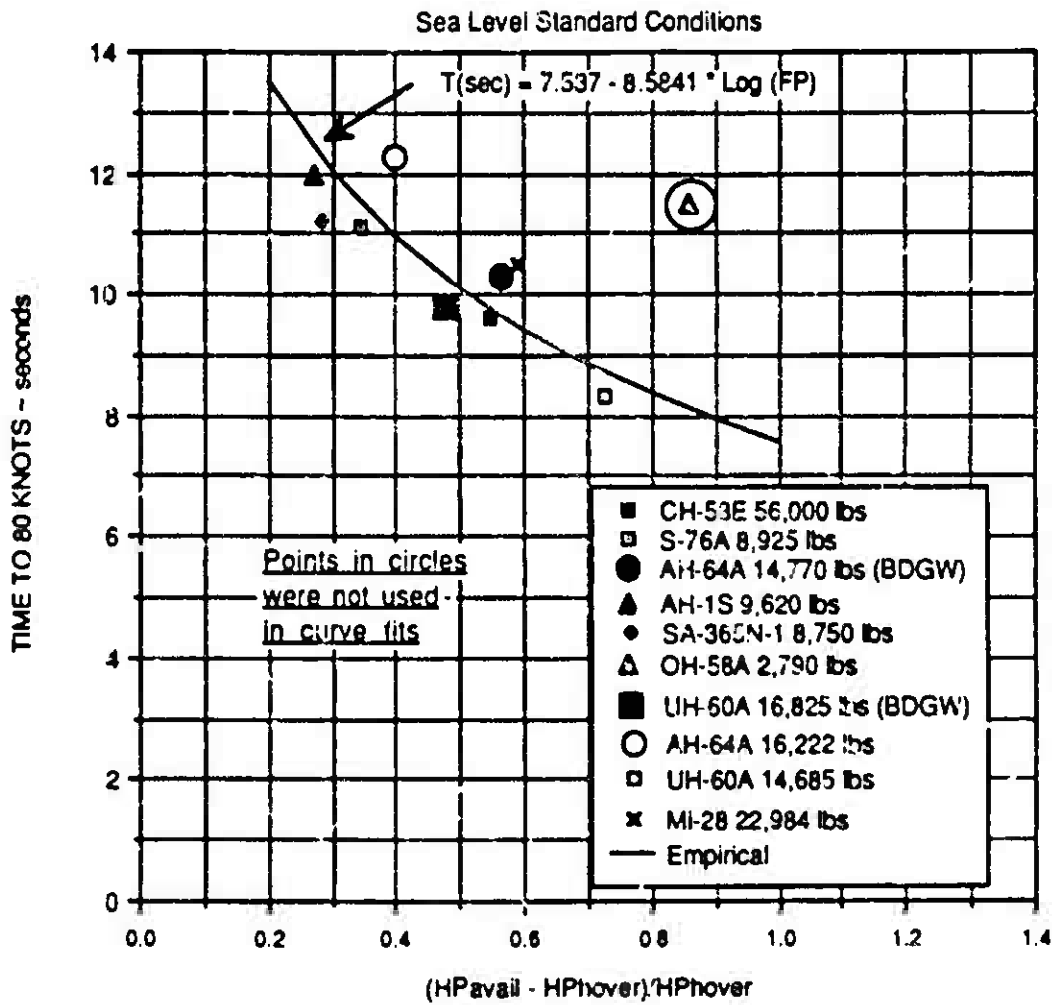


Figure L-3. Empirical Acceleration from Hover to 80 Knots Comparison

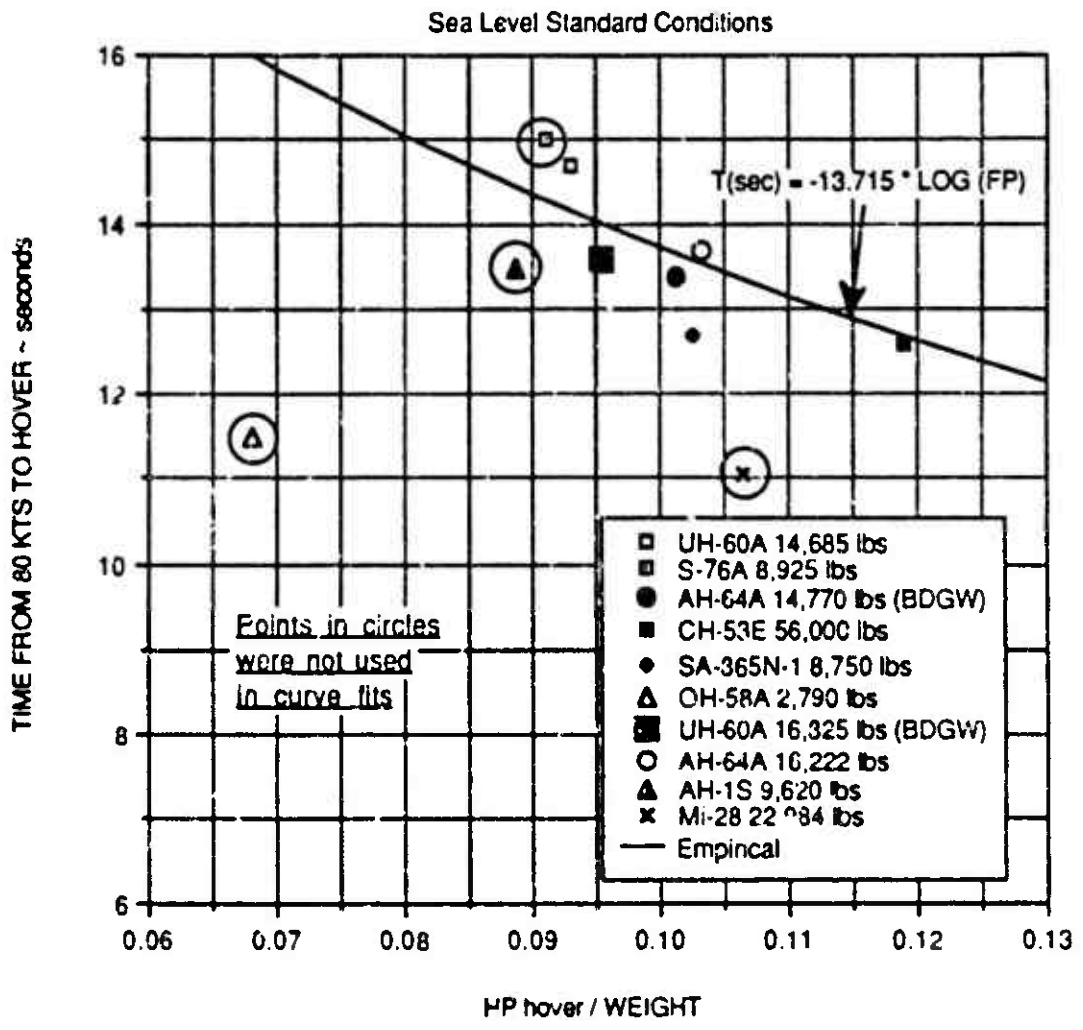


Figure L-4. Empirical Deceleration from 80 Knots to Hover Comparison

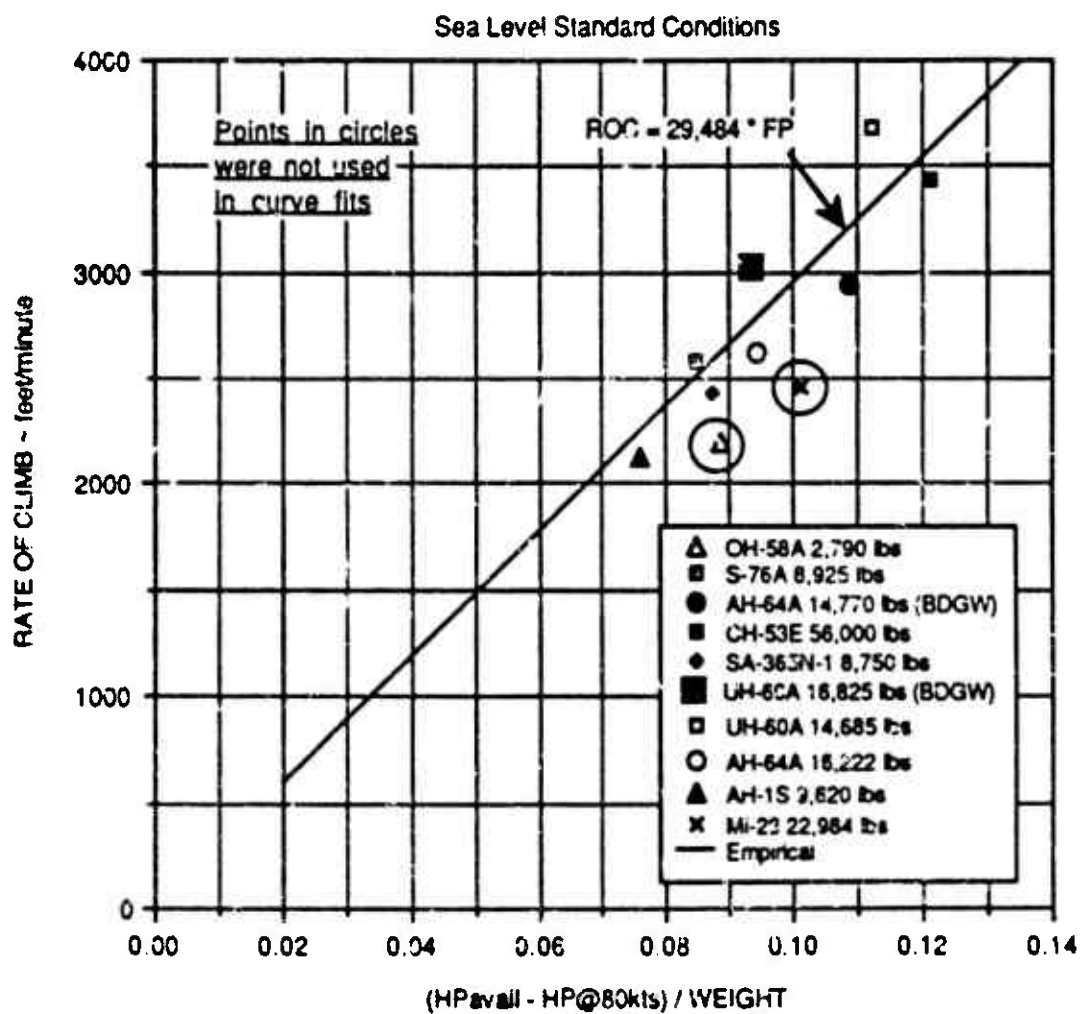


Figure L-5. Empirical 80-Knot Climb Comparison

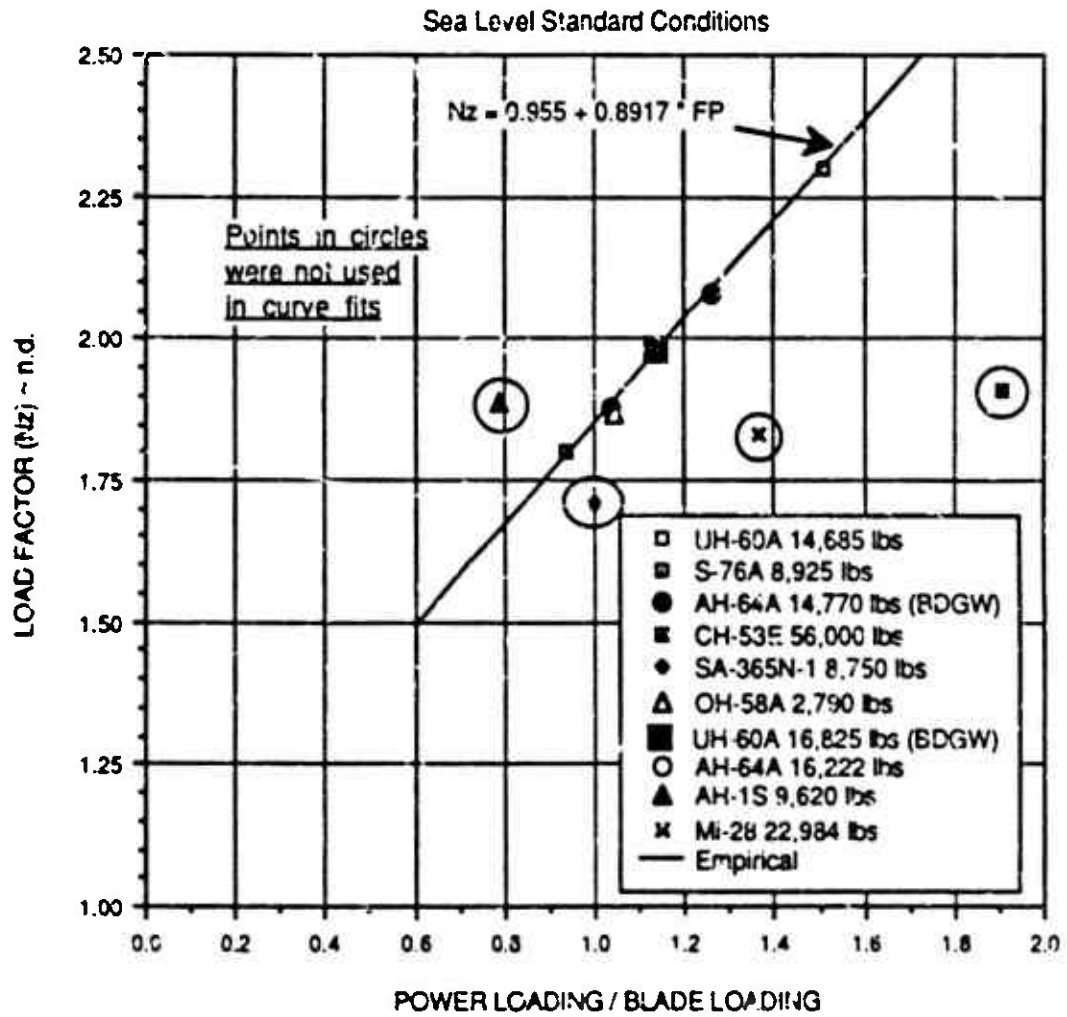


Figure L-6. Empirical 80-Knot Steady Turn Comparison

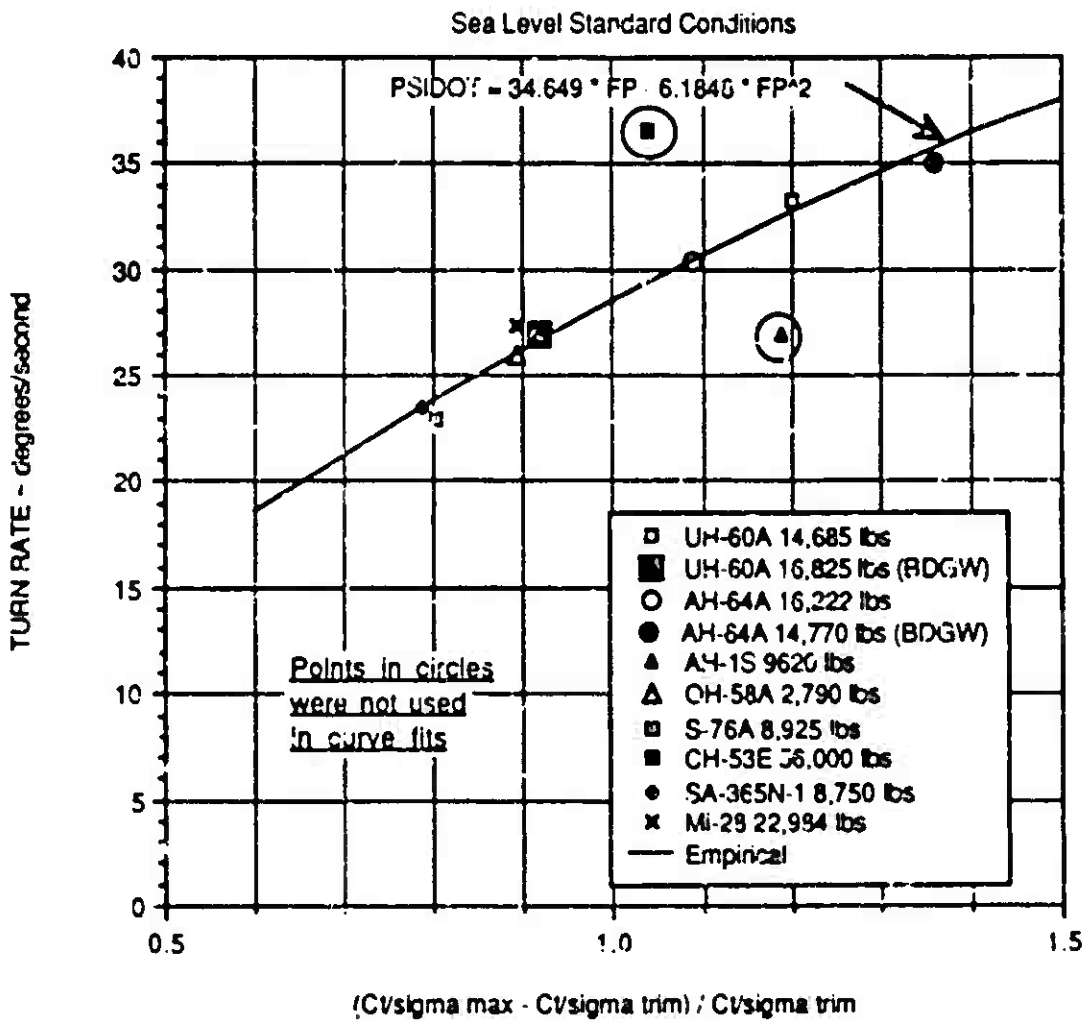


Figure L-7. Empirical 80-Knot Decelerating Turn Comparison

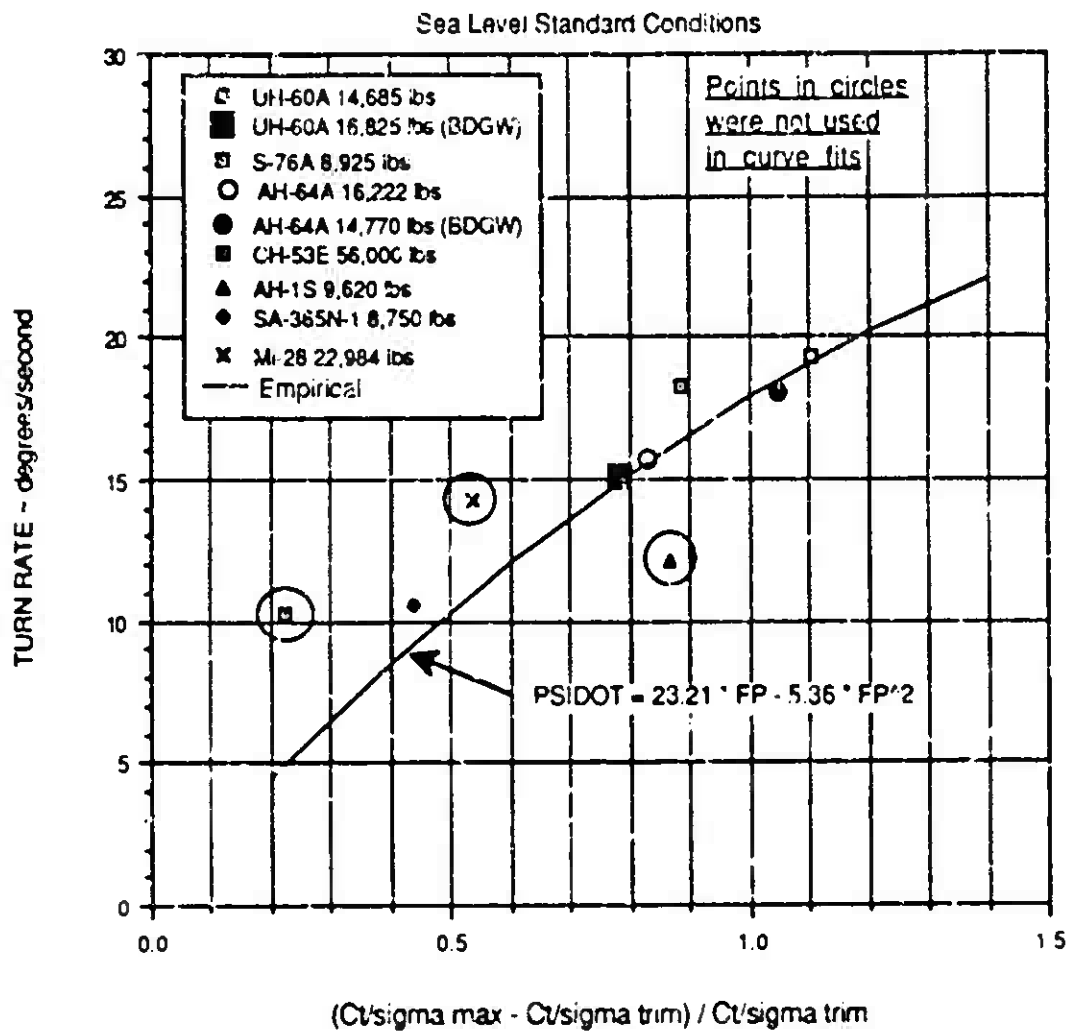


Figure L-8. Empirical 130-Knot Decelerating Turn Comparison

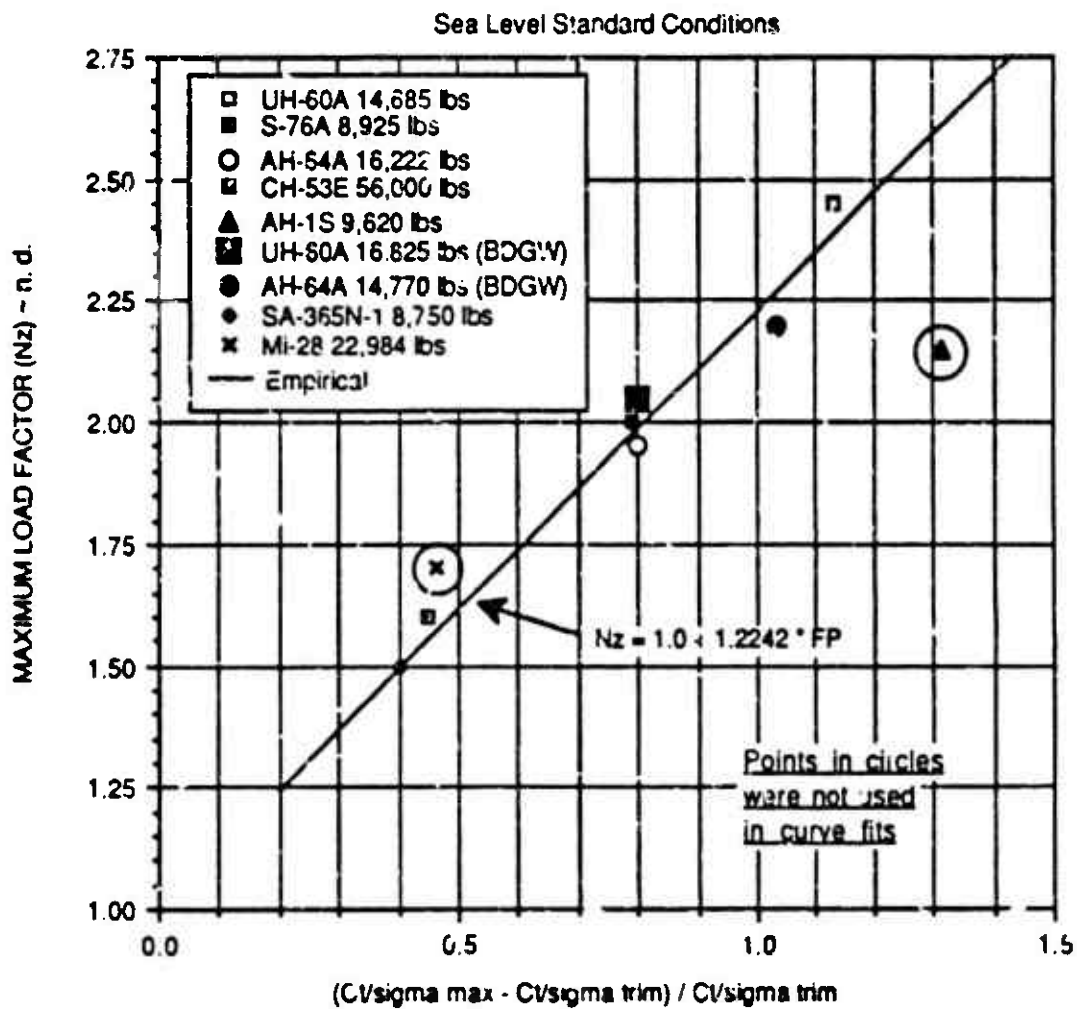


Figure L-9. Empirical 140-Knot Full-up Comparison

Sea Level Standard Conditions

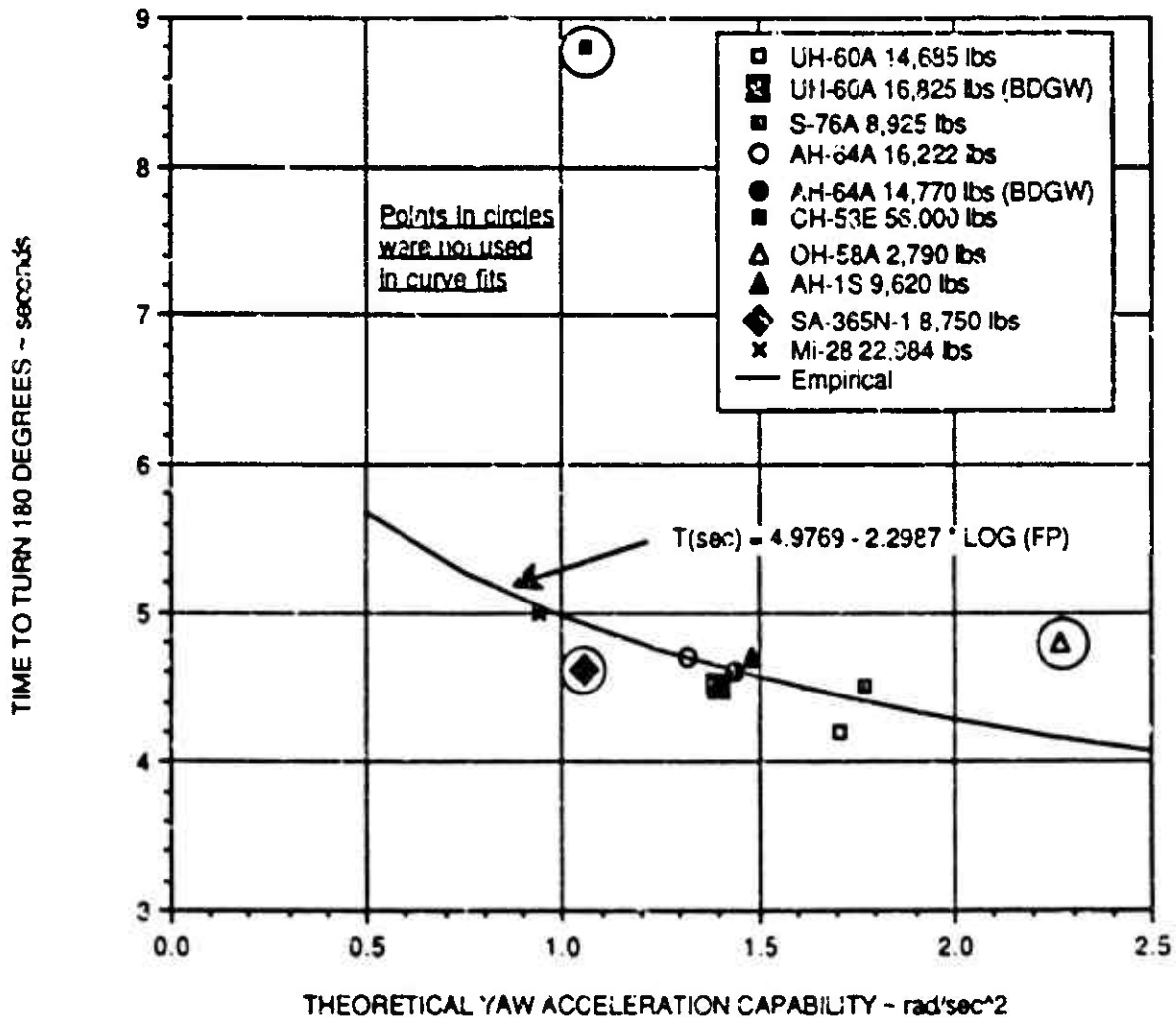


Figure L-10. Empirical 180-Degree Hover Turn Comparison

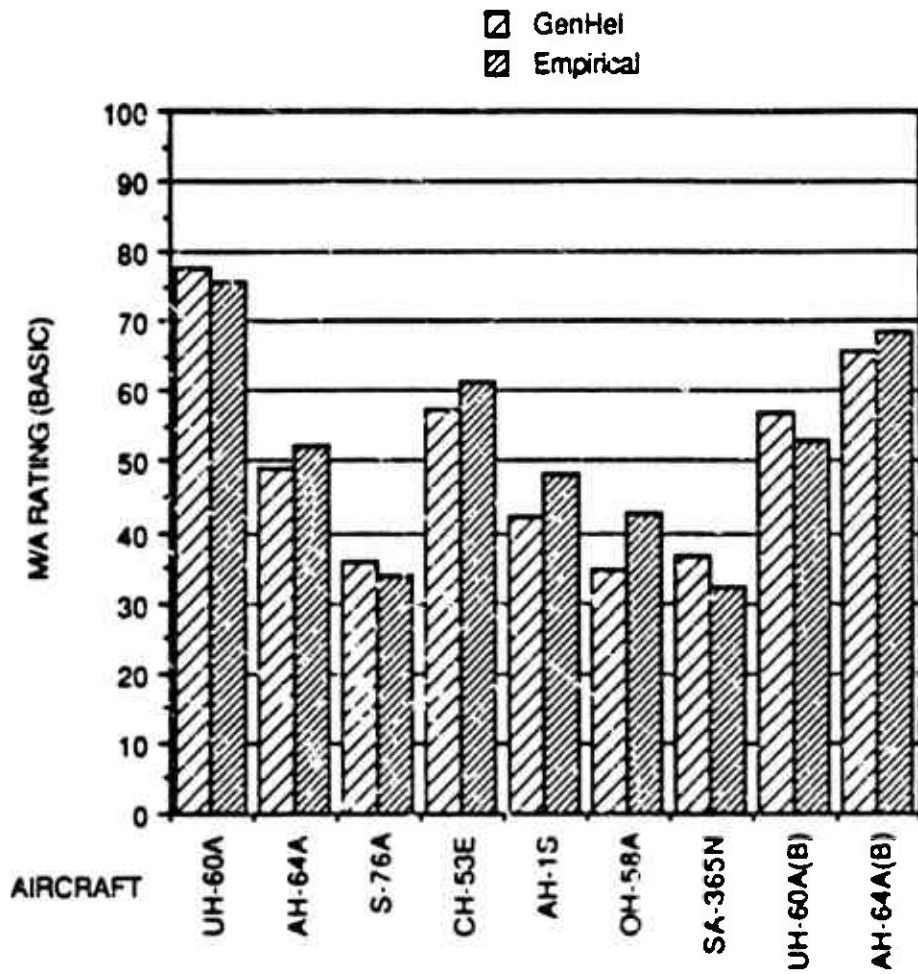


Figure L-11. Comparison of GenHel and Empirical Basic N/A Ratings

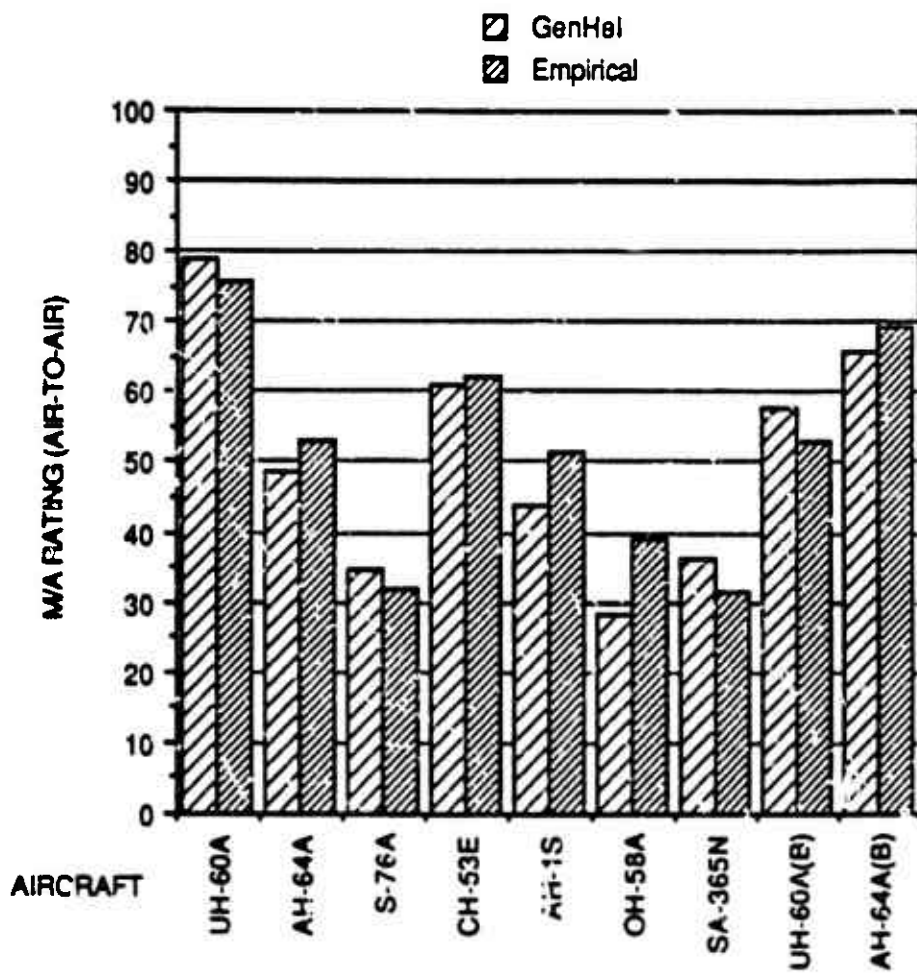


Figure L-12. Comparison of GenHel and Empirical ATA N/A Ratings

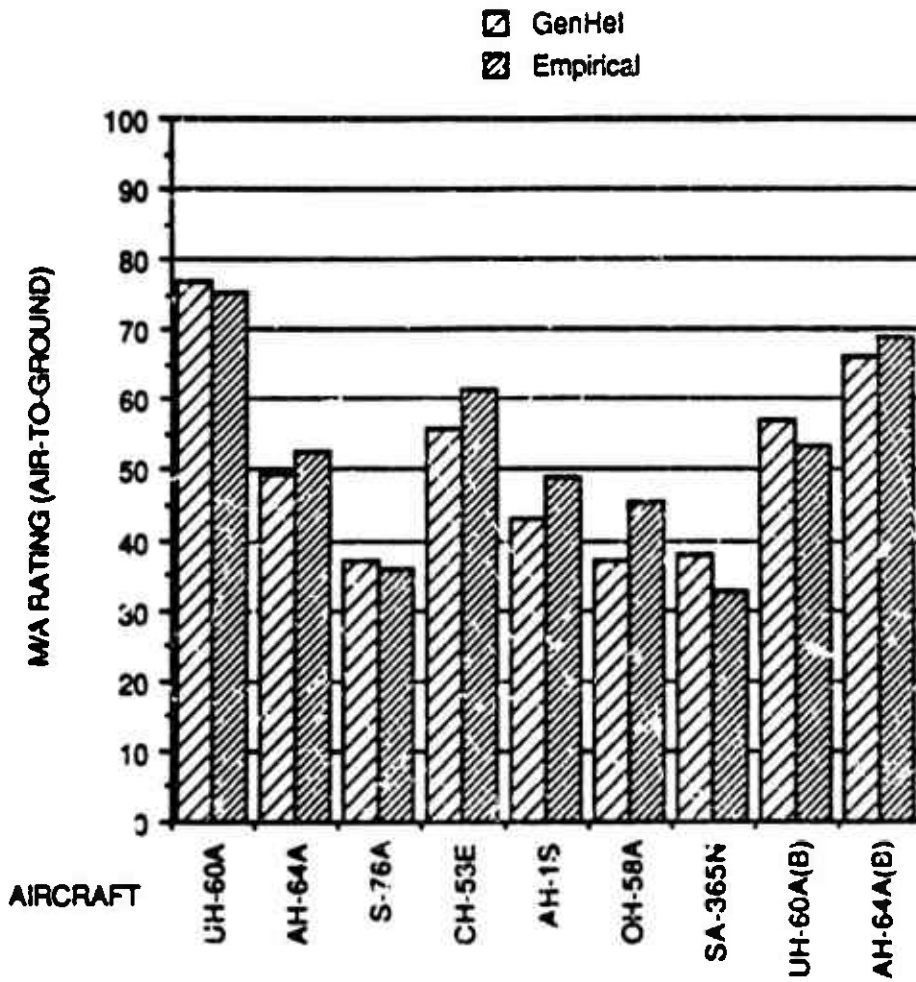


Figure L-13. Comparison of GenHel and Empirical ATC M/A Ratings

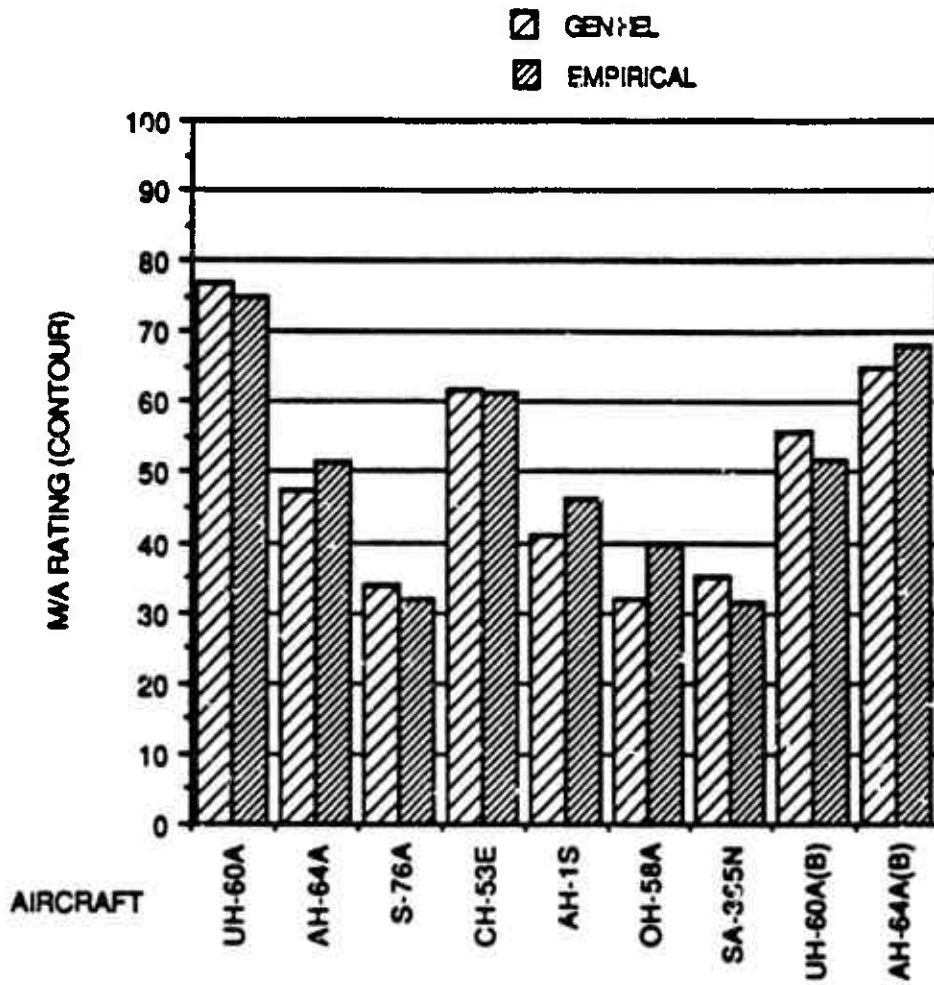


Figure L-15. Comparison of Geniel and Empirical Contour M/A Ratings

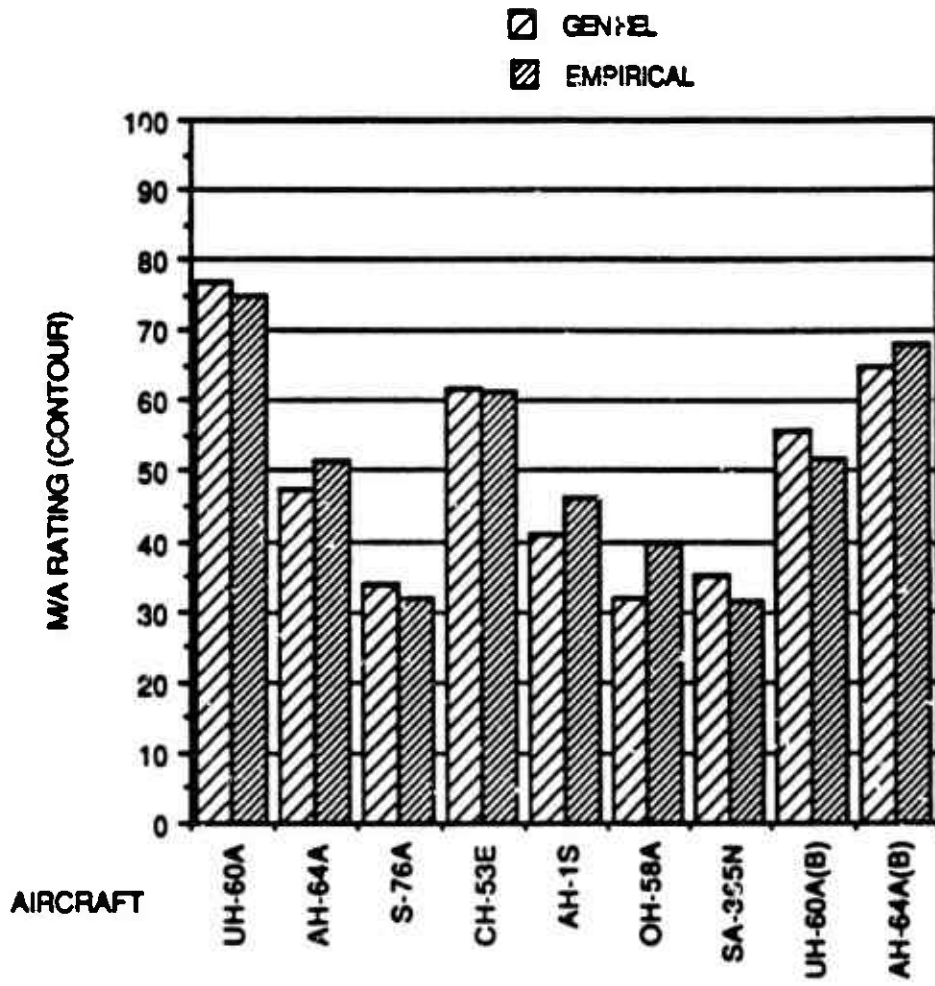


Figure L-15. Comparison of Genbel and Empirical Contour M/A Ratings

20,000-POUND Mi-28 EVALUATION

To evaluate the use of the empirical maneuver equations, predictions of the characteristics of the Mi-28 at a gross weight of 20,000 pounds were made, using the static data of Table 4 and the maneuver prediction equations in Figure L-1.

The empirical maneuver predictions can be used in one of two ways. First, the maneuver results can be predicted directly and then scored and averaged to obtain a M/A rating. Alternately, if GenHel results for a certain configuration of the aircraft are known, the empirical equations can be used to predict both the GenHel case and the case of interest. The difference between them is then added to the original GenHel data as a delta.

The second approach was taken with the "lightweight" HAVOC. The results are shown in Table L-1. This shows the original GenHel data for the 22,894 pound aircraft, the empirical predictions for the 22,894 pound and 20,000 pound versions and the final estimate generated by adding the difference to the original GenHel value.

The final 20,000 pound gross weight estimates for each maneuver were then scored using the scoring equations in Table 7 and the mission weighting factors in Figure 50. The M/A ratings were then derived by dividing the total of the maneuver scores for a given mission element (e.g., ATA = 453.5) by the total of the maneuver weighting factors for that mission element (e.g., ATA = 6.15) to get the final rating. The final results are shown in Table L-2.

These results show that the Mi-28 in a 20,000-pound air-to-air configuration would have good intrinsic M/A characteristics. However, the large differences between some of the predicted maneuver results and the actual GenHel values for the 22,984 pound vehicle indicate that the results should be considered tentative and a full-up GenHel evaluation at the lighter weight should be conducted.

TABLE L-1. 20K MI-28 MANEUVER PREDICTIONS

MANEUVER	GENHEL 22.9K	EMPIRICAL 22.9K	EMPIRICAL 20K	ESTIMATED 20K
1. HOVER BOB-UP	1400 fpm	1396	1896	1900
2. 0 TO 80 KT ACCEL	10.5 sec	9.49	7.65	8.66
3. 80 TO 0 KT DECEL	11.05 sec	13.33	13.77	11.49
4. 80-KNOT CLIMB	2467 fpm	2983	3797	3282
5. 80-KNOT STEADY TURN	1.83 g's	2.17	2.56	2.22
6. 80-KNOT DECEL TURN	27.3 deg/sec	26.0	32.2	33.5
7. 130-KNOT DECEL TURN	14.3 deg/sec	10.9	14.6	18.0
8. 140-KNOT PULL-UP	1.70 g's	1.57	1.84	1.97
9. HOVER TURN	5.0 sec	5.58	5.19	4.61

TABLE L-2. 20K MI-28 SCORES AND RATINGS

MANEUVER	BASIC	ATA	SCORES		
			ATC	NOE	CON
1. HOVER BOB-UP	93.3	9.3	56.0	93.3	42.0
2. 0 TO 80 KT ACCEL	89.0	80.1	57.9	71.2	57.9
3. 80 TO 0 KT DECEL	108.5	76.0	59.7	86.8	70.5
4. 80-KNOT CLIMB	76.1	64.7	34.2	26.6	57.1
5. 80-KNOT STEADY TURN	62.0	43.4	27.9	15.5	43.4
6. 80-KNOT DECEL TURN	53.9	29.6	40.4	35.0	35.0
7. 130-KNOT DECEL TURN	83.7	75.3	41.9	8.4	50.2
8. 140-KNOT PULL-UP	37.4	33.7	18.7	1.9	20.6
9. HOVER TURN	75.3	41.4	56.5	75.3	22.6
Total	679.2	453.5	393.2	414.0	399.3
Average Factor	9.0	6.15	5.20	5.00	5.30
Rating	75.5	73.7	75.6	82.8	75.3

CONCLUSIONS

In conclusion, the empirical maneuver estimation methodology presented in this appendix is a useful tool for predicting M/A scores and ratings when a GenHel or equivalent simulation evaluation is not practicable. This could be during preliminary design, evaluation of a design where only basic data were available, or for estimation of the effect of changes on an existing design. Obviously, a full-up GenHel-type evaluation should be conducted whenever possible. This will correctly capture all of the characteristics of the particular helicopter and their interaction with the operational constraints.

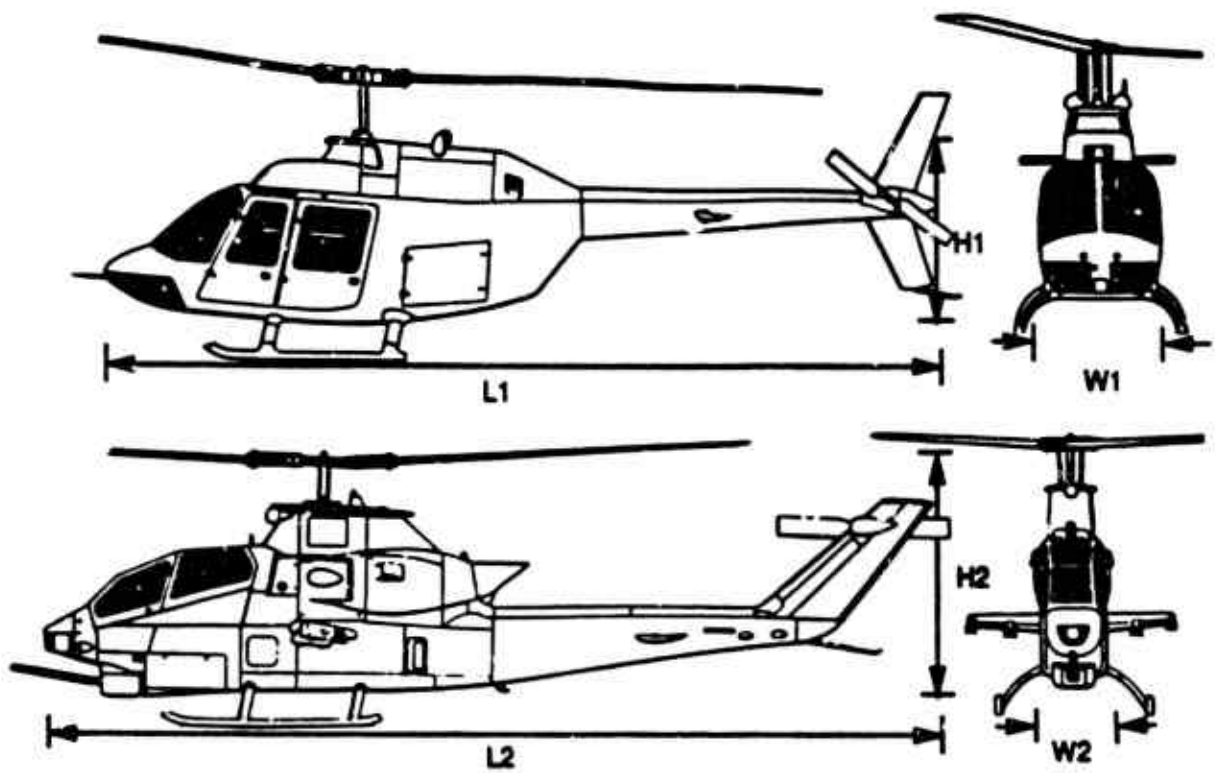
APPENDIX M

AERODYNAMIC SCALING METHOD

Aerodynamic data for most of the aircraft in this study were taken from existing sources. The Sikorsky helicopters already had GenHel data files, derived from wind tunnel tests. The other U.S. Army inventory aircraft (AH-64A, OH-58A, AH-1S) were modeled using data taken from C-81 computer code input listings that had been provided as Government Furnished Information (GFI). However, no aerodynamic data were available for the SA-365N or the Mi-28. Aerodynamic modeling for these vehicles can be broken into three areas. One is the main rotor blade airfoil data, another is the basic aerodynamics of the fuselage, and the third is aerodynamic modeling of the empennage and wings.

Main rotor blade airfoils were modeled using Sikorsky SC1095 airfoil data for both the Dauphin and HAVOC. Characteristics of the empennage surfaces and the wings were calculated using conventional techniques based on the airfoil, aspect ratio, sweep and area of the surface. Fuselage characteristics were derived by scaling of aerodynamic data from other helicopters of similar shape. The Mi-28 data were calculated by scaling up Apache fuselage aerodynamics while the Dauphin values were scaled down S-76A numbers.

The method used for scaling is shown in Figure M-1. Forces vary with the square of the scale factor while moments vary with the cube. Scaling factors for each aerodynamic load (lift, drag, etc.) are based on ratios of the appropriate principal dimensions. For example, lift is scaled by the ratios of fuselage lengths and fuselage widths. Pitching moment is scaled by the ratios of length, squared, and of the width. Obviously, this technique is only appropriate for airframes of similar shape and size.



LIFT $\left(\frac{L}{q}\right)_2 = \left(\frac{L}{q}\right)_1 \cdot \left(\frac{L2 W2}{L1 W1}\right)$

DRAG $\left(\frac{D}{q}\right)_2 = \left(\frac{D}{q}\right)_1 \cdot \left(\frac{W2 H2}{W1 H1}\right)$

SIDEFORCE $\left(\frac{Y}{q}\right)_2 = \left(\frac{Y}{q}\right)_1 \cdot \left(\frac{L2 H2}{L1 H1}\right)$

PITCH MOMENT $\left(\frac{M}{q}\right)_2 = \left(\frac{M}{q}\right)_1 \cdot \left(\frac{L2^2 W2}{L1^2 W1}\right)$

ROLL MOMENT $\left(\frac{R}{q}\right)_2 = \left(\frac{R}{q}\right)_1 \cdot \left(\frac{L2 H2^2}{L1 H1^2}\right)$

YAW MOMENT $\left(\frac{N}{q}\right)_2 = \left(\frac{N}{q}\right)_1 \cdot \left(\frac{L2^2 H2}{L1^2 H1}\right)$

Figure N-1. Aerodynamic Scaling Method

APPENDIX N

AIRCRAFT DRAG DATA

A summary of the drag data for each of the eight basic airframes evaluated in this report is provided in Table N-1. These data should be used with some care since the method for allocating drag amongst the various components of the airframe differs from manufacturer to manufacturer. For purposes of these data, the stub wings have been accounted for separately from the fuselage and the tail rotor hub drag is broken out separately from the vertical fin. The SA-365N has large vertical endplates on the ends of the horizontal tail which are shown separately. On the other hand, the 650-gallon drop tanks and their pylons are included in the CH-53E fuselage data as are the Engine Air Particle Separators (EAPS). The drag of the strut, bracing the horizontal tail on the Super Stallion, has been lumped into the vertical tail.

For all of these data, no accounting of external stores or their pylons has been made (except for the CH-53E as noted above).

TABLE N-1. DRAG BREAKDOWN SUMMARY

ITEM	AIRCRAFT			
	UH-60A	S-76A	CH-53E	AH-64A
Fuselage D/q	26.9	8.4	58.0*	22.0
H.T. Area, ft ²	45.0	18.5	58.0	33.36
H.T. Cd	.012	.013	.050	.010
H.T. D/q	0.54	0.24	2.90	0.33
V.T. Area, ft ²	32.3	19.7	74.0	32.2
V.T. Cd	.018	.016	.090	.016
V.T. D/q	0.58	0.32	6.66	0.52
Wing Area, ft ²	----	----	----	35.0
Wing Cd	----	----	----	.016
Wing D/q	----	----	----	0.56
Endplate Area, ft ²	----	----	----	----
Endplate Cd	----	----	----	----
Endplate D/q	----	----	----	----
T.R. Hub D/q	2.0	1.45	3.63	1.66
Total D/q	30.02	10.41	71.19	25.07

*Includes external tanks and their pylons

TABLE N-1. DRAG BREAKDOWN SUMMARY (Cont'd)

ITEM	AIRCRAFT			
	OH-58A	AH-1S	SA-365N	Mi-28
Fuselage D/q	6.0	5.5	7.86	37.0
H.T. Area, ft ²	9.65	15.14	16.0	11.94
H.T. Cd	.085	.085	.013	.010
H.T. D/q	0.82	1.29	0.21	0.12
V.T. Area, ft ²	9.18	18.87	20.0	21.88
V.T. Cd	.012	.012	.016	.012
V.T. D/q	0.11	0.23	0.32	0.26
Wing Area, ft ²	----	28.15	----	32.32
Wing Cd	----	.015	----	.015
Wing D/q	----	0.42	----	0.49
Endplate Area, ft ²	----	----	20.0	----
Endplate Cd	----	----	0.13	----
Endplate D/q	----	----	0.26	----
T.R. Hub D/q	0.94	1.54	----	2.3
Total D/q	7.87	8.98	8.65	40.17